Biomaterials Plenary Session
Room A120-121 - Session BP-SuA

Biomaterials Interfaces Plenary (ALL INVITED SESSION)
Moderator: Caitlin Howell, University of Maine

3:00pm **BP-SuA-1 Microbial Electron Conduits: Adventures at the Biotic-Abiotic Interface**, *Mohamed El-Naggar,* University of Southern California
INVITED

Electron Transfer (ET) is the stuff of life. The stepwise movement of electrons within and between molecules dictates all biological energy conversion strategies. With such a universal role across all domains of life, the fundamentals of ET and its precise impact on bioenergetics have received considerable attention, and the broad mechanisms allowing ET over small length scales in biomolecules are now well appreciated.

In what has become an established pattern, however, our planet's oldest and most versatile organisms are now challenging our current state of knowledge. With the discovery of bacterial nanowires, conductive biofilms, and multicellular bacterial cables, the length scales of microbial ET observations have jumped by 7 orders of magnitude, from nanometers to centimeters, during the last decade alone! This talk will take stock of where we are and where we are heading as we come to grips with the basic mechanisms and immense implications of microbial long-distance electron transport. We will focus on the biophysical and structural basis of long-distance, fast, extracellular electron transport by metal-reducing bacteria. These remarkable organisms have evolved direct charge transfer mechanisms to abiotic surfaces, allowing them to use abundant minerals as electron acceptors for respiration, instead of oxygen or other soluble oxidants that would normally diffuse inside cells. From a technological perspective, microbial extracellular electron transport is heavily pursued for interfacing redox reactions to electrodes in renewable energy technologies.

But how can an organism transfer electrons to a surface many cell lengths away? What molecules mediate this transport? And, from a physics standpoint, what are the relevant length, time, and energy scales? We will describe new experimental and computational approaches that revealed how bacteria organize heme networks on outer cell membranes, and along quasi-one-dimensional filaments known as bacterial nanowires, to facilitate long-range charge transport. Using electron cryo-tomography, *in vivo* fluorescent microscopy, and single molecule tracking, we are gaining new insight into the distribution of multiheme cytochromes along membranes. In addition, we will examine the fundamental limits of extracellular electron transport, down to single molecules and energy acquisition by individual cells. These findings are shedding light on one of the earliest forms of respiration on Earth while unraveling surprising biotic-abiotic interactions.

3:40pm **BP-SuA-3 Conductive Biofilms As Living Electronic Materials**, *Sarah Glaven,* U.S. Naval Research Laboratory*; L Bird, E Onderko,* National Research Council*; D Phillips, R Mickol,* American Society for Engineering Education*; A Malanoski, M Yates, B Eddie,* U.S. Naval Research Laboratory
INVITED

Natural living conductive biofilms transport electrons between electrodes and cells, as well as among cells fixed within the film, catalyzing an array of reactions from acetate oxidation to CO_2 reduction. Synthetic biology offers tools to modify or improve electron transport through biofilms, creating a new class of engineered living conductive materials. However, these applications are currently limited by a lack of understanding of the physiological constraints of the host bacterium (chassis) to properly and predictably express and orient electron transfer (ET) proteins (e.g. *c*-type cytochromes) in the cell membrane, the ability to rapidly screen a large number of constructs for different ET pathways, and a library of operationally relevant chassis strains. In this talk I will describe results demonstrating the use of a suite of highly-optimized small molecule sensors (Marionette) developed for control over *E. coli* cellular processes and used here to control expression of the *Shewanella* MtrCAB pathway, and accessory electron carriers, in *Marinobacter atlanticus*. Marionette sensors were transformed into *M. atlanticus* and assessed for expression of yellow fluorescent protein (YFP) after the addition of 7 different small molecules (choline, vanillin, naringenin, DAPG, cumate, tetracycline, and IPTG) during both planktonic growth and in biofilms. A broad dynamic range of YFP expression was observed similar to that demonstrated with *E. coli.* When YFP was replaced with ET proteins, expression of MtrCAB led to an increase in current compared to the wild type strain when induced prior to inoculation into a bioelectrochemical system (BES). However, the effect was not robust. Moving the MtrCAB pathway from a plasmid construct to the chromosome enabled more control over the quantity of protein expressed, however, no improvement in current was observed. Based on these results, we conclude that the MtrCAB pathway can be successfully expressed in *M. atlanticus* and requires further optimization for reliable biofilm based ET. Engineered living conductive materials could be used in a range of applications for which traditional conducting polymers are not appropriate including improved catalytic coatings for microbial fuel cell electrodes, self-powered sensors for austere environments, and next-generation living components of bioelectronic devices that interact with the human microbiome.

2D Materials
Room A216 - Session 2D+EM+MI+NS-MoM

Properties of 2D Materials including Electronic, Magnetic, Mechanical, Optical, and Thermal Properties I

Moderator: Jeehwan Kim, Massachusetts Institute of Technology

8:20am 2D+EM+MI+NS-MoM-1 Extreme Fatigue Life of Graphene, *Teng Cui, S Mukherjee, P Sudeep, G Colas, J Tam,* University of Toronto, Canada*; P Ajayan,* Rice University*; C Singh, Y Sun, T Filleter,* University of Toronto, Canada

Materials can fail when subjected to cyclic loading at stress levels much lower than the ultimate tensile strength or yielding limit, which is known as mechanical fatigue. Understanding the fatigue behavior is critical for any emerging material in order to evaluate its long-term dynamic reliability. Two-dimensional (2D) materials have been widely applied to mechanical and electronic applications, where they are commonly subjected to cyclic stress. However, the fatigue life and underlying damage mechanisms of these atomically thin, nearly defect-free, materials are unknown. Here we show the first fatigue study of freestanding 2D materials, in particular graphene and graphene oxide (GO). Monolayer and few layer graphene and GO were found to all exhibit ultrahigh fatigue life of more than one billion cycles at large stress level in the GPa range. Such a remarkable fatigue life is higher than that of any material reported to date at similar stress levels. Graphene exhibits global and catastrophic fatigue failure preceded by bond reconfiguration near the defective site due to inhomogeneous charge distribution and higher potential energy. Graphene can fracture under cyclic loading but without progressive damage, which is distinct from the fatigue failure mechanism of any other materials. The presence of functional groups on GO imparts a local and progressive fatigue damage mechanism, which fits the macroscopic fatigue convention. The extraordinary fatigue life was found to diminish significantly when the material is scaled up in thickness (10s of layers). This work not only provides new fundamental insights into the widely observed fatigue enhancement behavior of graphene-embedded nanocomposites, but also serves as a starting point for the mechanical dynamic reliability evaluation of other 2D materials.

8:40am 2D+EM+MI+NS-MoM-2 Epitaxial Growth and Thermal Degradation of Monolayer MoS_2 on $SrTiO_3$ Single Crystal Substrates, *Peiyu Chen, W Xu, Y Gao, P Holdway, J Warner, M Castell,* University of Oxford, UK

Monolayer MoS_2 crystals grown on amorphous substrates such as SiO_2 are randomly oriented. However, when MoS_2 is grown on crystalline substrates, the crystal shapes and orientations are also influenced by their epitaxial interaction with the substrate. In the first part of this talk, we present the results from chemical vapor deposition growth of MoS_2 on three different terminations of single crystal strontium titanate ($SrTiO_3$) substrates: (111), (110), and (001). On all three terminations of $SrTiO_3$, the monolayer MoS_2 crystals try to align their <2 -1 -1 0>-type directions (i.e., the sulfur-terminated edge directions) with the <1 -1 0>-type directions on $SrTiO_3$. This arrangement allows near-perfect coincidence epitaxy between seven MoS_2 unit cells and four $SrTiO_3$ unit cells. On $SrTiO_3$(110), this even distorts the crystal shapes and introduces an additional strain detectable by photoluminescence (PL). Our observations can be explained if the interfacial van der Waals (vdW) bonding between MoS_2 monolayers and $SrTiO_3$ is greatest when maximum commensuration between the lattices is achieved. Therefore, a key finding of this study is that the vdW interaction between MoS_2 and $SrTiO_3$ substrates determines the supported crystal shapes and orientations by epitaxial relations.

Monolayer MoS_2 is also a wide-bandgap semiconductor suitable for use in high-temperature electronics. It is therefore important to understand its thermal stability. In the second part, we uncover the thermal degradation behavior of monolayer MoS_2 supported on $SrTiO_3$ in ultrahigh vacuum (UHV) because of sulfur loss. MoS_2 was found to degrade on the (111), (110), and (001) terminations of $SrTiO_3$ substrates in a similar way. The sulfur loss begins at 700 °C, at which point triangular etch trenches appear along the sulfur-terminated edge directions of the MoS_2 crystals (in scanning tunneling microscopy). The sulfur vacancies can be filled byannealing the crystals in a hot sulfur atmosphere, and the optical properties (by Raman spectroscopy and PL) of monolayer MoS_2 can nearly be fully recovered. At higher UHV annealing temperatures, the remaining Mo is oxidized by the $SrTiO_3$ substrates into MoO_2 and MoO_3. The initial sulfur loss and the formation of MoO_x are confirmed by X-ray photoelectron spectroscopy. The sulfur annealing no longer takes effect

when all the Mo has been oxidized, which happens at a temperature between 800 °C and 900 °C in UHV. The MoS_2 crystal shapes are stable upon annealing until the residual MoO_3 particles evaporate at above 1000 °C. This infers that any triangular crystals that look intact under low-magnification optical microscopy and SEM may not mean pristine MoS_2.

9:00am 2D+EM+MI+NS-MoM-3 3D Printed and Injection Molded Polymer Matrix Composites with 2D Layered Materials, *Sangram Mazumder,* University of North Texas*; J Catalan,* University of Texas at El Paso*; N Hnatchuk, I Chen,* University of North Texas*; P Perez,* University of Texas at El Paso*; W Brostow, A Kaul,* University of North Texas

The two-dimensional layered materials (2DLMs), MoS_2 and WS_2, as well as three-dimensional (3D) graphite were infused in thermoplastic polymer matrices, specifically acrylonitrile butadiene styrene (ABS) and polyethylene terephthalate glycol (PETG). Two techniques were explored for the production of these composites into dog-bone structures for mechanical testing, which included 3D printing and injection molding. The ductility of the composites was generally seen to decrease with the addition of the fillers compared to the otherwise ductile polymer matrix counterparts. Also, changes in Young's modulus, yield and tensile strengths, as well as percent strain at fracture, were analyzed as a function of filler loadings. The effect of processing technique on microstructures was also investigated by scanning electron microscopy of the fracture surfaces which revealed the presence of microstructural defects in the form of voids in the injection molded samples, which act as stress concentrators in the composite samples. Additionally, dynamic friction data of the composites was measured in an attempt to exploit the traditional, inherent solid phase lubricating properties of the 2DLMs. Graphite was indeed seen to lower dynamic friction in case of 3D printed PETG and injection molded ABS. Also, MoS_2 and WS_2 were found to reduce friction in 3D printed PETG and ABS. Graphite being an intrinsically good conductor, while the other 2DLMs explored, specifically MoS_2 and WS_2 given their semiconducting nature, can also be used as avenues for introducing electrical conductivity within these otherwise insulating parent polymer matrices. Thermal conductivity was also found to increase in both ABS and PETG composites containing graphite, MoS_2 and WS_2, irrespective of their processing routes. The use of 2DLM-based polymer composites remains an area that is bound to open up avenues for a wide range of applications in the future related to wearable electronics and sensors with low-cost additive manufacturing approaches.

9:20am 2D+EM+MI+NS-MoM-4 Semiconducting WS_2 and h-BN Inks for Printing Optically-active Nanodevices, *Jay A. Desai,* University of Texas at El Paso*; S Mazumder, A Kaul,* University of North Texas

We present our work on dispersions of WS_2 and h-BN using cyclohexanone and terpineol (C/T) as the solvent to subsequently print prototype nanodevices. Current-voltage measurements, Raman spectroscopy, and photoluminescence spectroscopy were used to characterize the properties of these inks produced by various sonication techniques such as horn tip sonication, magnetic stirring and shear mixing. Both photodetector and capactive heterostructure devices were formed with these materials. From this analysis, the photoresponsivity and detectivity of the graphene-WS_2-graphene heterostructure devices were calculated to be ~ 0.86 A/W and ~ 10^{13} J, respectively. Capacitance-voltage (C-V) and C-frequency (f) measurements were also conducted, where the V was swept from − 6 V to + 6 V, while the change in C was measured from f ~ 20 kHz up to 3 MHz to gain insights into the nature of the graphene-WS_2 interface. An all-inkjet-printed graphene-h-BN-graphene capacitors were fabricated and leakage current density, $J_{Leakage}$, of up to ~ 0.072 μA/mm² and *capacitance density* of up to ~ 2.4 μF/cm² is reported. Finally, the influence of temperature, frequency, and LED illumination on the performance of the graphene-h-BN-based capacitor is explored with the help of *capacitance density*-voltage measurements at different parameters to promote the all-inkjet-printed capacitor for photosensitive detector applications.

9:40am 2D+EM+MI+NS-MoM-5 Transparent PEDOT:PSS Based Electro-Chromic/Thermal Devices With Excellent Durability For Applications In Smart Electronics, *Hossein Sojoudi, S Nemani,* University of Toledo

Thin-film electro-thermal/chromic devices were fabricated by utilizing PEDOT:PSS as the active conductive electrode thin-film and a compliant flexible polyurethane/ glass substrate as the building block. PEDOT:PSS exhibits electrochromic properties by undergoing an electrochemical redox reaction when an external stimulus in the form of electric potential is induced across the film. One major advantage of this technology is that it requires significantly lesser power per unit area and the color switching can be bi-stable in either transparent (oxidation) or dark blue (reduction)

states. This low powered, controlled tuning in transparency of PEDOT:PSS was achieved by coupling doped PEDOT:PSS films with graphene as counter electrode, sandwiched between a solid-state electrolytic medium while maintaining high level of transparencies ~85% at peak oxidation levels. A high color contrast and improved coloration efficiency of 75% coupled with low power densities of 0.96 W/m^2, envisions its used in smart windows and visors. The mechanical self-assembly approach of graphene can be regulated by controlling the wavelength of wrinkles generated by inducing measured pre-strain conditions and regulating the modulus contrast of the materials used, which control the level of transparency, conductivity, and hydrophobic nature of the electrode(s). The transparency of wrinkled few layered graphene with an induced biaxial pre-strain = 0.36 was found to be 95% at 550 nm. We have also harnessed the electrothermal nature of PEDOT:PSS to achieve significant thermal responses at the expense of low power inputs to achieve temperatures as high as ~100°C due to joule heating in the doped PEDOT:PSS thin films. The absorbance and transmittance spectra for PEDOT:PSS were studied using a UV-VIS spectrometer at various oxidation and reduction states by applying biased voltage in the range of 2-5 Volts in varying cycles to determine electrochromic/thermal reversibility under induced strains, and electrothermal nature at various additive concentrations. These exceptional properties of the polymer, coupled with high work-function graphene electrodes can be envisioned to develop in-tandem smart electronic windows with tunable transmittances and heating responses for applications in automobile, aerospace, and service industries.

10:00am **2D+EM+MI+NS-MoM-6 Edge Dominated Graphene/h-BN Lateral Hybrid Nanostructures for Electronic and Spintronic Applications**, *Gour P. Das,* IIT Kharagpur India, India

For hybrid 2D nanostructures, the prime challenge is to control the electronic structure of edges that play a dominant role in tuning their structural, electronic, magnetic and other properties. Such heterostructures have been fabricated in-plane as well as perpendicular to the 2D plane, the latter constituting a class known as van der Waals heterosturctures. We have studied, using first principles approach, the electronic structure as well as transport properties of graphene/h-BN lateral hetero-nanoribbons of finite width, in order to probe the role of edge atoms and edge geometry on the resulting device behavior. For example, edge B doped zigzag graphene nanoribbons (ZGNRs) leads to spin filter based device [1]. We have investigated the origin of the spin filtering property in edge B-doped zigzag graphene nanoribbons (ZGNRs) and provide a guide to preparing a graphene based next-generation spin filter based device. While 100% edge B doping in ZGNR results in semiconductor to metal transition, 50% edge B doping shows half-metallicity when doped edge is unpassivated. Zero-bias transmission function of the other configurations shows asymmetric behavior for the up and down spin channels, thereby indicating their possible application potential in nano-spintronics.

In another related study [2], we have systematically varied the number of C-C or B-N units present in the graphene/*h*-BN hetero nanoribbon (G/BNNR), and have investigated their electronic as well as magnetic properties. Systems with both N or B terminated edges, undergo a semiconductor-to-semimetal-to-metal transition with the increase in the number of C-C units for a fixed ribbon width. The spin density distribution indicates significant localization of the magnetic moments at the edge carbon atoms, that gets manifested when the number of C-C units is greater than 2 for most of the structures.

* Work done in collaboration with Soubhik Chakrabarty, Tisita Das, Ranjit Thapa and Yoshiyuki Kawazoe.

References :

[1] "Origin of spin polarization in an edge boron doped zigzag grapheme nanoribbon: a potential spin filter", Soubhik Chakrabarty, A H M Abdul Wasey, Ranjit Thapa and G. P. Das, Nanotechnology **29**, 345203 (2018).

[2] "Tuning the electronic and magnetic properties of graphene/h-BN hetero nanoribbon: A first-principles investigation", Tisita Das, Soubhik Chakrabarty, Y. Kawazoe and G. P. Das, AIP Advances **8**, 65111 (2018)

10:40am **2D+EM+MI+NS-MoM-8 Engineering Interfaces in the Atomically-Thin Limit**, *Deep Jariwala,* University of Pennsylvania **INVITED**
The isolation of a growing number of two-dimensional (2D) materials has inspired worldwide efforts to integrate distinct 2D materials into van der Waals (vdW) heterostructures. While a tremendous amount of research activity has occurred in assembling disparate 2D materials into "all-2D" van der Waals heterostructures, this concept is not limited to 2D materials

alone. Given that any passivated, dangling bond-free surface will interact with another via vdW forces, the vdW heterostructure concept can be extended to include the integration of 2D materials with non-2D materials that adhere primarily through noncovalent interactions. I will present our work on emerging mixed-dimensional (2D + nD, where n is 0, 1 or 3) heterostructure devices. Two distinct examples of gate-tunable p-n heterojunctions with anti-ambipolar field efect will be presented. The anti-ambipolar field effect observed in the above systems is also shown generalized to other semiconducting heterojunction systems and extended over large areas with practical applications in wireless communication circuits. Recent work on high performance 2D/3D triodes will also be presented.

The second part of talk will focus on engineering interfaces on photovoltaic devices from 2D semiconductors such as transition metal dichalcogenides (TMDCs).High efficiency inorganic photovoltaic materials (e.g., Si, GaAs and GaInP) can achieve maximum above-bandgap absorption as well as carrier-selective charge collection at the cell operating point. Experimental demonstration of light confinement in ultrathin (< 15 nm) Van der Waals semiconductors (MoS_2, WS_2 and WSe_2) leading to nearly perfect absorption will be demonstrated concurrently with record high quantum efficiencies. Ongoing work on addressing the key remaining challenges for application of 2D materials and their heterostructures in high efficiency photovoltaics which entails engineering of interfaces and open-circuit voltage will be presented in addition to on going work on probing of buried metal/semiconductor interfaces with sub 50 nm resolutions as well as near field luminescence spectroscopy. I will conclude by giving a broad perspective of future work on 2D materials from fundamental science to applications.

11:20am **2D+EM+MI+NS-MoM-10 Ultrasoft Slip-mediated Bending in Few-layer Graphene**, *Jaehyung Yu, E Han, E Annevelink, J Son, E Ertekin, P Huang, A van der Zande,* University of Illinois at Urbana-Champaign
A challenge and opportunity in nanotechnology is to understand and take advantage of the breakdown in continuum mechanics scaling laws as systems and devices approach atomic length scales. Such challenges are particularly evident in two-dimensional (2D) materials, which represent the ultimate limit of mechanical atomic membranes as well as molecular electronics. For example, after more than a decade of study, there is no consensus on the bending modulus of few layer graphene, with measured and predicted values ranging over two orders of magnitude, and with different scaling laws. However, comparing these studies is challenging because they probe very different and often fixed curvatures or magnitudes of deformation. To unravel the discrepancy, a systematic measurement of bending stiffness versus deformation is needed. The results have practical implications on predicting and designing the stiffness of many 2D mechanical systems like origami/kirigami nanomachines, stretchable electronics from 2D heterostructures, and resonant nanoelectromechanical systems.

In this study, we combine atomistic simulation and atomic scale imaging to theoretically and experimentally examine the bending behavior of few-layer graphene. First, we experimentally probe the nanoscale bending by laminating few-layer graphene over atomically sharp steps in boron nitride and imaging the cross-sectional profile using aberration-corrected STEM. Second, we use DFT simulations to examine the bending of few-layer graphene under compression. By measuring the nanoscale curvatures, we extract the simulated and experimental bending modulus while varying both the number of layers and the degree of nanoscale curvature.

We find remarkable agreement between the theory and experiment and observe an unexpected curvature dependent bending stiffness of few-layer graphene that deviates from continuum scale bending mechanisms. We find that the bending stiffness of few layer graphene versus curvature corresponds with a gradual change in scaling power with thickness from cubic to linear. We find that the transition in scaling behavior originates from a transition from shear, slip and the onset in superlubricity between the graphene layers at the van der Waals interface, verified by a simple Frenkel-Kontorova model. Our results provide a unified model for the bending of 2D materials and show that their multilayers can be orders of magnitude softer than previously thought, among the most flexible electronic materials currently known.

11:40am 2D+EM+MI+NS-MoM-11 Experimental Study on Vanadium Oxides Films by Sputtering, *Chuan Li,* National Yang Ming University, Taiwan, Republic of China*; J Hsieh,* Ming Chi University of Technology, Taiwan, Republic of China*; C Su,* National Yang Ming University, Taiwan, Republic of China

Vanadium is noteworthy for its multivalence states of the four adjacent oxidation states 2–5. The oxides of vanadium(II-V) presents various colors in aqueous solution as $[V(H_2O)_6]^{2+}$ (lilac), $[V(H_2O)_6]^{3+}$ (green), $[VO(H_2O)_5]^{2+}$ (blue) and $[VO(H_2O)_5]^{3+}$ (yellow). Because of the broad range of oxidation states, vanadium oxides can be both an amphoteric oxide and an oxidizing/reducing agent. Thus vanadium oxides are used as precursors and catalysts as well in many industrial processes.

By its nature of multivalence, vanadium oxides have been widely used in devices for memory, photonics, and optoelectronics. Through articulately harnessing on phase transitions between metal and compound, vanadium oxides can be produced with specific properties for targeted functions. For example, one of the stoichiometric oxides, VO_2, vanadium dioxide is thermochromic which a phase change occurs at a temperature above 68°C from the semiconducting monoclinic microstructure to the almost conductive tetragonal structure. Correspondingly the high optical transmittance in the range of near-infrared also switches to high reflectance.

In this study, we fabricate vanadium oxide thin films by sputtering using vanadium targets by adjusting the oxygen flow rate to have amorphous vanadium oxides. The temperature during deposition is room temperature. To monitor the chamber condition, optical emission spectrometer is employed to record the optical spectra change following different oxygen flow rates fed into the chamber. To have a crystalline phase of as-deposited films, a rapid thermal annealing process is set up and the time and temperature of annealing shall be investigated to determine the appropriate operational range.

Actinides and Rare Earths Focus Topic
Room A215 - Session AC+LS+MI-MoM

Magnetism, Complexity, Superconductivity, and Electron Correlations in the Actinides and Rare Earths
Moderators: Krzysztof Gofryk, Idaho National Laboratory, Ladislav Havela, Charles University, Prague, Czech Republic

8:20am AC+LS+MI-MoM-1 Possible Structural Quantum Phase Transition in UCr2Si2 Accessed Through Cr → Ru Chemical Substitution, *Ryan Baumbach,* Florida State Universityy **INVITED**
Materials with intertwined magnetic, electronic, and structural degrees of freedom often can be tuned (e.g., using pressure or chemical substitution) to induce novel behavior, including unconventional superconductivity. Examples include the cuprates, iron based superconductors, and lanthanide/actinide-based compounds, and despite the their diversity of structure, chemistry and interaction mechanisms, their individual phase diagrams often conform to a semi-universal format that features a quantum phase transition. As a result, there have been prolonged efforts to develop new families of materials based on this paradigm. Even so, there still are few examples of f-electron intermetallics that combine both magnetic and structural quantum phase transitions. In this talk, we will present results from recent efforts to tune the ordered states of UCr_2Si_2, which is a Kondo lattice metal with antiferromagnetic ordering near $T_N \approx 24$ K and a structural phase transition near $T_S \approx 200$ K. In particular, we will focus on the influence of Cr to Ru chemical substitution, where we find that both T_N and T_S are rapidly suppressed towards separate quantum phase transitions. The impact of the quantum phase transitions on the structural, magnetic, and electronic properties will be examined in detail.

9:00am AC+LS+MI-MoM-3 Dynamic Spin Transport in Antiferromagnetic Insulators: Angular Dependent Spin Pumping in Y₃Fe₅O₁₂/NiO/Pt Trilayers, *Fengyuan Yang,* The Ohio State University **INVITED**
In recent years, pure spin transport driven by ferromagnetic resonance (FMR) spin pumping or a thermal gradient has attracted intense interest and become one of the most active frontiers in condensed matter and materials physics. Extensive research efforts have demonstrated pure spin currents in a broad range of materials, which enrich our understanding of dynamically-driven spin transport and open new paradigms for energy-efficient, spin-based technologies. Antiferromagnetic (AF) insulators possess various desired attributes, such as low loss and high speed up to THz frequencies, for future spintronic applications.

To probe the dynamic spin transport phenomena and the underlying mechanisms in AF insulators, we use high-quality $Y_3Fe_5O_{12}$ (YIG) epitaxial thin films excited by FMR as a source to inject spins into AF insulator NiO layers and detect the transmitted spin current using inverse spin Hall effect (ISHE) signals in YIG/NiO/Pt trilayers [1, 2]. We observed robust spin currents from YIG to Pt across AF insulators, which initially enhances the ISHE signals and can transmit spin currents up to 100 nm thickness, demonstrating highly efficient spin transport through an AF insulator carried by magnetic excitations. Recently, we studied the angular dependence of spin pumping in a series of YIG/NiO/Pt trilayers as the orientation of the applied magnetic field is rotated out of plane [3]. A simple sinusoidal angular dependence of V_{ISHE} has been viewed as a signature of spin pumping. Surprisingly, we observe an extensive plateau in the V_{ISHE} vs. ϑ_H plots with a pronounced peak feature at an out-of-plane angle of 45° to 60° when the measurement temperature is close to the Néel temperature (T_N) of NiO. This phenomenon can be understood as arising from the competition between the exchange coupling at the YIG/NiO interface, the easy-plane and in-plane easy-axis anisotropies of NiO, and the effect of the applied magnetic field. While insulating antiferromagnetic films can efficiently transmit spin currents and show promise for integration in spintronic devices, the underlying physics of spin ordering and dynamics is richer than currently understood.

References:

1. H. L. Wang, *et al.PRB* **91**, 220410(R) (2015).

2. H. L. Wang, *et al.PRL***113**, 097202 (2014).

3. Y. Cheng, *et al.PRB* 99, 060405(R) (2019)

9:40am AC+LS+MI-MoM-5 Pressure Studies of Strongly Correlated Phases in Rare Earth Compounds, *Rena Zieve,* University of California, Davis **INVITED**
Various strongly correlated materials have complex low-temperature phase diagrams, exhibiting magnetism and superconductivity as well as spin glass, non-Fermi liquid, and other behaviors. Since each material has its own quirks, determining the underlying universal influences has been challenging. Pressure is a key tool in these efforts, since pressure can tune the interactions within a material without changing its chemical composition or impurities. I will discuss how hydrostatic or uniaxial pressure can probe strongly correlated materials by changing valence, breaking crystal symmetry, or altering the dimensionality of the electron system. I will draw examples from various rare earth compounds. Finally, I will mention recent pressure application techniques that expand the range of possible characterization measurements.

10:40am AC+LS+MI-MoM-8 Fermi Surface Reconstructions and Transport Properties in Heavy-fermion Materials, *Gertrud Zwicknagl,* Institut f. Mathemat. Physics, TU Braunschweig, Germany
The search for new types of exotic topological orders has recently rekindled the interest in Fermi surface reconstructions. Of particular interest are Electronic Topological (Lifshitz) transitions where the number of FS sheets changes abruptly under the influence of external parameters like chemical doping, pressure, or magnetic field. Lifshitz transitions (LTs) are generally associated with the presence of critical points in the electronic band structure, i. e., maxima, minima, or saddle points whose presence follows directly from lattice periodicity. As their separation from the Fermi energy is of the order of the bandwidth the critical points usually do not a ect the low temperature behavior. In heavy-fermion materials, however, magnetic fields can drive LTs which are reflected in pronounced anomalies in thermodynamic and transport properties. Here we demonstrate that the magnetic field-dependent anomalies in the Seebeck coefficient provide detailed information not only on the critical points, i. e., their character and position relative to the Fermi energy but also on the quasi-particle dispersion in the vicinity of the critical points, i. e., the effective mass tensor. For lanthanide-based HFS, the theoretical analysis is based on Renormalized Band (RB) structure calculations assuming that the heavy quasiparticles result from a Kondo effect. For U-based HFS, on the other hand, we adopt the "dual nature" model which allows for a microscopic description of the heavy bands. The calculated Lifshitz transitions reproduce the observed positions of anomalies in the Seebeck coecients surprisingly well.

11:00am AC+LS+MI-MoM-9 Direct Measurement the 5 $f_{5/2}$ and 5 $f_{7/2}$ Unoccupied Density of States of UO₂, *James G. Tobin,* University of Wisconsin-Oshkosh*; S Nowak,* SLAC National Accelerator Laboratory*; C Booth,* Lawrence Berkeley National Laboratory*; E Bauer,* Los Alamos National Laboratory*; S Yu,* Lawrence Livermore National Laboratory*; R Alonso-Mori, T Kroll, D Nordlund, T Weng, D Sokaras,* SLAC National Accelerator Laboratory

In a world of ever increasing population and diminishing resources, the need for abundant and inexpensive energy remains critical. [1] Despite the problems associated with radioactive contamination/disposal and nuclear proliferation, electricity generated by nuclear power remains immensely important, [2] providing for 20% of the electrical grid of the USA and 50% or more for several European nations. [3-6] Uranium Dioxide (UO2) is by far the widely used nuclear fuel for the generation of electricity. [7] Thus, a fundamental understanding of the electronic structure of UO2 is crucial, if only to provide the best theoretical models for its disposal and storage. [7, 8]

Using High Energy Resolution Fluorescence Detection (HERFD) in a Resonant Inelastic Scattering (RIXS) experiment and electric dipole selection rules, the U 5f5/2 and U 5f7/2 Unoccupied Densities of States (UDOS) were determined. Significant changes were observed in going from UF4 (localized, 2 5f electrons) to UCd11 (localized, 3 5f electrons), consistent with the predictions of the Intermediate Coupling Model. The results for UO2 were experimentally confirmed by direct comparison with the Bremstrahlung Isochromat Spectroscopy for Uranium Dioxide.

References

1. "Reasons for increase in demand for energy," BBC News, https://www.bbc.com/bitesize/guides/zpmmmp3/revision/1

2. Y. Guerin, G.S. Was, S.J. Zinkle, MRS Bull. 34, 10 (2009).

3. Nuclear Energy Institute, Nuclear shares of electricity generation, http://www.world-nuclear.org/info/nshare.html

4. Eleanor Beardsley, France presses ahead with nuclear power, Nat'l Pub. Radio, http://www.npr.org/templates/story/story.php?storyId=5369610

5. Nuclear energy, Environmental Protection Agency, USA, http://www.epa.gov/cleanenergy/energy-and-you/affect/nuclear.html

6. Energy, electricity, and nuclear power: developments and projections-25 years past and future, International Atomic Energy Agency, Vienna, 2007,www-ub.iaea.org/mtcd/publications/pdf/pub1304

7. F. Gupta, A. Pasturel, G. Brillant, Phys. Rev. B 81, 014110(2010).

8. J.G. Tobin and S.-W. Yu, Phys. Rev. Lett, 107, 167406 (2011).

11:20am AC+LS+MI-MoM-10 Optimizing the Magnetic Performance of Tetragonal ReFe₁₂₋ₓMₓ Phases by First Principles Computational Simulations, *Heike Christine Herper,* O Vekilova, P Thunström, O Eriksson, Uppsala University, Sweden

The increase of environmentally friendly energy production is coupled to an increasing demand for new magnetic materials. Especially, new Rare earth (Re) lean permanent magnets are highly sought after as possible replacement for high-performance magnets based on Nd-Fe-B and Dy to limit costs and supply risk. In this context the tetragonal 1:12 phase (TmMn₁₂) which contains 35% less Re than commercial Nd-Fe-B magnets are rediscovered. To stabilize this phase with light Re and Fe instead of Mn a nonmagnetic phase stabilizing element is needed but this degrades the magnetic performance.

To identify new 1:12 phases being suitable for permanent magnet applications materials design based on computational simulations has become an important tool. Here we focus on ReFe₁₂₋ₓMₓ. with Re = Y, Ce, Nd, Sm and M = Ti and V. We use state of the art density functional theory methods (VASP; full potential LMTO (RSPt)). The phase stability and the magnetic properties were calculated depending on the M concentration. Aiming to reduce the Re amount we monitor the performance depending on the Nd/Y ratio.

The key quantities are the magnetocrystalline anisotropy (MAE) and the magnetization. To capture the correct magnetic behavior, it is crucial to describe the localization of the 4f electron properly for each Re. While for Sm-based systems the spin-polarized core approximation is sufficient to describe the localized 4f electrons, it fails for Nd, e.g. the low temperature MAE of NdFe₁₁Ti would be uniaxial instead of conic. Using a DFT+U approach with U = 5 eV, J = 1.1 eV for NdFe₁₁Ti reproduces the experimentally observed behavior. Ce is special since the uniaxial MAE of CeFe₁₁Ti is obtained independent from the treatment of the 4f electron. However, an analysis of the hybridization function analogue to [1] shows

that a spin polarized core approximation is more appropriate for Ce-based 1:12 phases. For a deeper insight additional studies are carried out to examine the crystal field splitting.

With SmFe₁₁V system a new phase was found leading to an increase of the magnetization by 17% compared to the commonly used concentrations of V. In view of the MAE a replacement of Nd by Y turned out to be preferable over a reduction of Ti. MAE values of 1.3 MJ/m³ ((NdY)Fe₁₁Ti) and 1.7 MJ/m³ (SmFe₁₁V) are predicted [2]. The latter could already be verified in recent experiments [2].

[1] H.C.Herper et al., Phys. Rev. Materials**1**, 033802 (2017)

[2] A. M. Schönhöbel et al., JALCOM **786**, 969 (2019)

11:40am AC+LS+MI-MoM-11 Optical Excitation Effect on Magnetodielectric and Photodielectric Properties of Rare Earth doped ZnO:Na Nanoparticles, *W Jadwisienczak, Mohammed Bsatee, F Inbanathan,* Ohio University*; R Martínez,* University of Puerto Rico*; H Huhtinen,* University of Turku, Finland*; R Palai,* University of Puerto Rico

There have been ongoing efforts in developing rare earth (RE) ions doped semiconductors responsive to optical and magnetic stimuli for developing multifunctional devices. ZnO is considered as a promising semiconductor with wide range of applications in optoelectronics and spintronics due to its optical properties (*i.e.* direct band gap, high electron mobility, high thermal stability, strong absorption of UV), and at the same time being an attractive host for RE doping resulting in enhanced spin polarization in ZnO:RE matrix [1]. In this project, undoped and RE ions (Er and Yb) doped and co-doped ZnO:Na nanoparticles were studied with an aim to understand recently reported magnetodielectric and photodielectric effects stimulated by magnetic field and UV excitation stimuli [2]. After synthesizing well-defined Er and Yb-co-doped ZnO:Na by sol-gel route, evaluation of structural, optical, magnetic and electrical characteristics of synthesized nanoparticles was performed. Structure, morphology, and composition of the samples were analyzed by XRD and SEM showing high quality hexagonal crystal structure. The absence of secondary phases was confirmed by Raman spectroscopy and XPS analysis of all elements in ZnO:NaErYb compound. Optical properties were investigated by optical reflectance spectroscopy, photoluminescence (PL), PL excitation, and PL kinetics with photons excitation energy corresponding to above and below bandgap energy. PL spectra were investigated under magnetic field of up to 2 Tesla in 7 K – 400 K temperature range. It was observed that PL spectra exhibit broad green-yellow defects emission band without NBE excitonic peak. PLE spectra revealed that both Er^{3+} and Yb^{3+} ions are optically active and involved in complex energy transfer between ZnO:Na host and 4f-shall levels of RE^{3+} ions dopants. PL spectra show features related to intra-shell 4f-4f transitions of the Er^{3+} ion (at 522 nm) and Yb^{3+} ion (at 980 nm). It was observed that luminescence decay of the ZnO defect band is unexpectedly long (> tens of 10^{-3} second), strongly affected by RE^{3+} ions doping and depends on the magnetic field strength when excited at 3.814 eV. In the presentation we will attempt to correlate reported magnetodielectric and photodielectric properties of the Er,Yb-co-doped ZnO:Na [2] with observed optical characteristics.

References

[1] A.G. El Hachimi, H. Zaari, A. Benyoussef, M. El Yadari, A. El Kenz, J. Rare Earths, 32, p.715 (2014).[2] R. Martinez Valdes, N. Kumar, H. Huhtinen, W. M. Jadwisienczak, R Palai, MRS Adv. (2019), DOI: 10.1557/adv.2019. 66.

Atomic Scale Processing Focus Topic
Room A214 - Session AP+2D+EM+PS+TF-MoM

Area Selective Deposition and Selective-Area Patterning

Moderators: Satoshi Hamaguchi, Osaka University, Japan, Eric A. Joseph, IBM Research Division, T.J. Watson Research Center

8:40am AP+2D+EM+PS+TF-MoM-2 Surface Pre-functionalization of SiNₓ and SiO₂ to Enhance Selectivity in Plasma–Assisted Atomic Layer Etching, *Ryan Gasvoda,* Colorado School of Mines*; Z Zhang, S Wang, E Hudson,* Lam Research Corporation*; S Agarwal,* Colorado School of Mines

To manufacture semiconductor devices in the current sub-7-nm node, stringent processing windows are placed on all aspects in manufacturing including plasma-etching. In recent years, atomic layer etching (ALE) has emerged as a patterning technique that can provide high etch fidelity, directionality, layer–by–layer removal, and selectivity to meet the tight

processing windows. Plasma–assisted ALE of SiO_2 and SiN_x is of particular interest since Si-based dielectrics are commonly used throughout the entire fabrication process. Typically, these materials are etched in a cyclic ALE process consisting of two sequential half–cycles: fluorocarbon (CF_x) deposition from a fluorocarbon plasma followed by an Ar plasma activation step. Etch selectivity can be achieved through careful manipulation of the plasma and processing parameters. To further increase overall etch selectivity, we have proposed a methodology that selectively pre–functionalizes the SiO_2 or SiN_x surface with hydrocarbons prior to ALE. Recently, we showed that an etch blocking graphitic hydrofluorocarbon film will readily accumulate on a pre–functionalized SiO_2 surface.

In this study, we used *in situ* attenuated total reflection Fourier transform infrared (ATR–FTIR) spectroscopy and *in situ* 4–wavelength ellipsometry to monitor the surface reactions, film composition, and net film thickness during the entire ALE process. We show that aldehydes can be used to functionalize SiN_x with extremely high selectivity to SiO_2 surfaces. During ALE on bare SiN_x, a thick graphitic fluorocarbon film accumulates on the surface and can stop all etching after cycle 5. This is attributed to inefficient removal of both the C and N from the surface. To enhance removal and prevent graphitic carbon accumulation, we graft a branched hydrocarbon aldehyde to the SiN_x surface. This branched hydrocarbon provides an abundance of $-CH_3$ groups which allows for greater C and N removal possibly via HCN formation, thus lowering overall graphitic carbon formation. This retardation of the graphitic hydrofluorocarbon film formation leads to both an overall increase in the etch per cycle and the number of ALE cycles that can be run before an etch stop is observed.

9:00am AP+2D+EM+PS+TF-MoM-3 Area-selective Atmospheric-pressure Spatial ALD of SiO₂ using Interleaved Back-etch steps Yielding Selectivity > 10 nm, *A Mameli,* Holst Centre / TNO, The Netherlands*; F Roozeboom, **Paul Poodt**,* Holst Centre / TNO, The Netherlands, Netherlands

Area-selective atomic layer deposition (AS-ALD) has great potential in reducing cost by maskless device manufacturing of patterned layers. Still, in this new *bottom-up* approach the selectivities currently obtained for film growth on patterned growth areas vs. that on the non-growth areas are often very limited. Also the substrate throughput values for conventional low-pressure ALD is too low for industrial acceptance.(1,2) In this work we present a process for AS-ALD of SiO_2 using intermittent plasma etch-back steps to increase the selectivity above 10 nm film thickness.(3) In addition, the deposition process itself is performed in a spatial ALD reactor at atmospheric pressure which allows for achieving high throughput.(4)

AS-ALD of SiO_2 on a substrate with pre-patterned SiO_2 and ZnO areas was demonstrated using a highly chemo-selective inhibitor that chemisorbs preferentially on the non-growth area (ZnO) while allowing the deposition of SiO_2 on the growth area (SiO_2). In order to maximize the process selectivity, a blanket fluorocarbon plasma etch-back step was interleaved after every 110 ALD cycles. This way, selective SiO_2 deposition up to ~ 30 nm film thickness was demonstrated. Furthermore, X-ray Photoelectron Spectroscopy was carried out to verify the selectivity of the process: no Si was detected (detection limit 0.3 at. %) on the non-growth area, demonstrating the high selectivity of the process.

The process presented here combines selective inhibitor chemisorption, plasma-based spatial ALD with high deposition rates and plasma etch-back steps to correct for selectivity loss. This approach is compatible with *roll-to-roll* and *sheet-to-sheet* concepts and can therefore enable high-throughput AS-ALD on large-area and flexible substrates.

[1] A. Mameli, *et al.*, *ACS Nano*, **11**, 9303 (2017).

[2] F.S.M. Hashemi, *et al.*, *ACS Nano*, **9**, 8710 (2015).

[3] R. Vallat, *et al.*, *J. Vac Sc. Technol. A*, **35**, 01B104 (2017).

[4] P. Poodt, *et al.*, *Adv. Mater.*, **22**, 3564 (2010).

9:20am AP+2D+EM+PS+TF-MoM-4 Mechanisms of Precursor Blocking during Area-selective Atomic Layer Deposition using Inhibitors in ABC-type Cycles, *M Merkx,* Eindhoven University of Technology, The Netherlands*; D Hausmann,* Lam Research Corporation*; E Kessels,* Eindhoven University of Technology, The Netherlands, Netherlands*; T Sandoval,* Universidad Técnica Federico Santa María, Chile*; **Adrie Mackus**[1],* Eindhoven University of Technology, The Netherlands, Nederland

The development of new processes for area-selective atomic layer deposition (ALD) is currently motivated by the need for self-aligned fabrication schemes in semiconductor processing. For example, area-selective ALD processes for dielectric-on-dielectric deposition are being considered for fully self-aligned via (FSAV) fabrication schemes in advanced interconnect technology.

Instead of solely relying on surface functionalization prior to ALD, an novel strategy to area-selective ALD involves the dosing of inhibitor molecules during every cycle in an ABC-type recipe.[1,2] By using small molecules that can be dosed in vapor-phase as inhibitor, this approach is compatible with industrial process flows. Moreover, the reapplication of the inhibitor molecules during every cycle allows for the use of a plasma as the co-reactant, which broadens the range of materials that can be deposited selectively. In contrast to conventional approaches to area-selective ALD based on self-assembled monolayers (SAMs), very little is known about how small inhibitor molecules can block the ALD growth.

In this contribution, insight into the mechanisms of precursor blocking by inhibitor molecules as obtained from in-situ Fourier transform infrared spectroscopy (FTIR) and density functional theory (DFT) calculations will be discussed. Area-selective ALD of SiO_2 using acetylacetone (Hacac) as inhibitor will be described as a model system, illustrating various mechanisms that can contribute to the loss of selectivity. It was found that at saturation, Hacac adsorbs through a mixture of chelate and monodentate bonding configurations. Hacac in monodentate configuration is displaced from the surface when exposed to bis(diethylamino)silane precursor molecules, which limits the selectivity. Strategies for improving the selectivity based on the understanding from these studies will be discussed.

[1] A. Mameli, M.J.M. Merkx, B. Karasulu, F. Roozeboom, W.M.M. Kessels, and A.J.M. Mackus, ACS Nano **11**, 9303 (2017).

[2] A.J.M. Mackus, M.J.M. Merkx, and W.M.M. Kessels, Chem. Mater. **31**, 2 (2019).

9:40am AP+2D+EM+PS+TF-MoM-5 Area-Selective Deposition of TiO₂ using Isothermal Integrated Atomic Layer Deposition and Atomic Layer Etching in a Single Reaction Chamber*, **Gregory Parsons**, S Song, H Saare,* North Carolina State University **INVITED**

Several new approaches are emerging where chemical etching is being coupled with atomic layer deposition to achieve area-selective deposition of dielectrics and metals. During ALD, selectivity is generally lost when undesired nuclei form on the targeted non-growth surface. These undesired nuclei can sometimes be removed by periodic etching, improving the overall selectivity. However, it is not known to what extent these coupled deposition/etching sequences can proceed while maintaining good selectivity. As desirable deposition and etching reactions proceed, other changes in the process can occur to enhance unwanted nucleation and/or impede desired etching, thereby limiting the net selectivity. Recent experiments in our lab have used in-situ probes to explore coupled thermal ALD and ALE super-cycles, performed sequentially under isothermal conditions in a single reaction chamber, to achieve area selective deposition of TiO_2 on SiO_2 with hydrogen-terminated silicon (100) as the desired non-growth surface. We find that as ALD/ALE super-cycles proceed, small changes occur in the ALD and ALE reactions, particularly during the transition from ALD to ALE, or from ALE to ALD. Also, modeling studies allow us to quantitatively analyze the ASD results and compare our findings to other known approaches. These insights will be helpful to understand opportunities and challenges in advanced atomic scale reactions and process implementation.

10:40am AP+2D+EM+PS+TF-MoM-8 Area-Selective Atomic Layer Deposition of Metal Oxides on an Inhibitor-Functionalized SiO₂ Surface, ***Wanxing Xu,*** Colorado School of Mines*; P Lemaire, K Sharma, D Hausmann,* Lam Research Corporation*; S Agarwal,* Colorado School of Mines

The continued downscaling of modern semiconductor devices together with the incorporation of 3D architectures places new constrains on conventional lithography techniques. To enable further advances in patterning process, new techniques will be required for next-generation devices to overcome the challenges of limiting the growth of desired materials in a specific area. One method to address these issues is area-selective atomic layer deposition (ALD), which provides the opportunity to build defined patterns from the bottom-up at the atomic-level accuracy. In this study, we will focus on area-selective ALD of metal oxides including ZrO_2 and Al_2O_3 with a metal as the growth surface and inhibitor-functionalized SiO_2 as the non-growth surface. To inhibit ALD, the SiO_2 surfaces were functionalized with aminosilane inhibitors through the vapor phase or with a solution-based method. The functionalized SiO_2 surfaces were characterized by transmission Fourier transform infrared (FTIR) spectroscopy, ellipsometry, and water contact angle measurements. Metal oxides including ZrO_2 and Al_2O_3 were deposited by ALD using metal

---

[1] **Paul Holloway Award Winner**

precursors and H_2O over a temperature range of 150-250 °C. *In situ* attenuated total reflection FTIR spectroscopy was utilized to identify the surface reactions sites and absorbed surface species during ALD. In addition, the corresponding film growth was measured using *in situ* four-wavelength ellipsometry.

Using *in situ* optical diagnostics, we show the mechanism for the breakdown in selectivity during area-selective ALD on a SiO_2 surface that is functionalized with aminosilanes. The infrared spectra show that aminosilane inhibitors react with almost all of the surface –SiOH groups forming Si–O–Si–R bonds on the surface (see Figure 1). After repeated exposure of the functionalized SiO_2 surface to TEMAZ and ZTB, these precursors react with Si–O–Si bonds without surface –SiOH groups (see Figure 2). Although small growth in the first few ALD cycles is not detected by *in situ* ellipsometry, growth inhibition breaks down after an increased number of ALD cycles. These results suggest that it is an additional requirement to suppress other reactions with a higher activation energy barrier during ALD expect removing main surface reactive sites through surface functionalization. To further impede growth of metal oxides on functionalized SiO_2 surface, a two-step functionalization method was developed to passivate the SiO_2 surface while providing additional steric blocking for the underlying substrates. Comparative studies were carried out to evaluate the effect of different functionalization methods on suppressing the nucleation during ALD.

11:00am **AP+2D+EM+PS+TF-MoM-9 Area-selective Deposition Achieved in a Continuous Process using Competitive Adsorption**, *Taewon Suh, Y Yang, K Lao, R DiStasio, Jr., J Engstrom,* Cornell University
A significant challenge for single-nm fabrication technologies is the development of area selective deposition (ASD) processes, particularly for device structures with exposed metallic and dielectric surfaces on patterned, often three dimensional, substrates. A number of techniques have been proposed and examined for ASD processes, particularly with respect to ALD, and these include the use of "permanent" blocking layers in the form of SAMs, and repetitive deposition/etch cycles. Some success has been reported with these techniques, but they possess potential drawbacks. An ideal ASD process should be fast, preferably vapor phase, and leave no residue on the non-growth surface. One technique that can possibly provide this is the use of competitive adsorption to induce area selective deposition, where a co-adsorbate is chosen that will bind much more strongly to one surface vs. another. A significant challenge concerning this approach is avoiding direct reactions between the co-adsorbate and the thin film precursor in the case of ALD, and also the co-reactant in the case of CVD. We are coupling quantum mechanical calculations of co-adsorbate/thin-film precursor/substrate interactions with experiments using our coupled micro-reactor/UHV surface analysis system. We have examined the effect of a class of unsaturated hydrocarbons as co-adsorbates on the CVD growth of ZrO_2 thin films using a Zr amido-coordination complex as the thin film precursor and O_2 as the co-reactant. The substrates were SiO_2 and Cu, and we examined the effects of both temperature, T_s = 120-240 °C, and the partial pressure of the co-adsorbate hydrocarbon. DFT calculations predict that the binding energies of these hydrocarbons are at least a factor of two larger on Cu vs. those on SiO_2. For CVD growth of ZrO_2 thin films as thick as 22 nm (growth rates of ~ 1 nm-s^{-1}), we find that the co-introduction of the hydrocarbon results in linear growth with time on a SiO_2 substrate, with no apparent incubation time, while essentially no growth is observed on Cu. *In situ*, post-deposition analysis with XPS reveals ZrO_2 thin films on SiO_2, and only adventitious carbon and less than a monolayer of Zr on the Cu surface. Consistent with a model based on competitive adsorption, we find that selectivity is eventually lost at sufficiently high substrate temperatures or sufficiently low partial pressures of the hydrocarbon co-adsorbate. Finally, we will report on the CVD growth on patterned Cu/SiO_2 substrates where we observe deposition only on those areas covered by SiO_2. We will conclude with a discussion of the promise and challenges of this approach for ASD concerning both ALD and CVD processes.

11:20am **AP+2D+EM+PS+TF-MoM-10 Surface Chemistry during Plasma-Assisted ALE: What Can We Learn from ALD?**, *Sumit Agarwal,* Colorado School of Mines **INVITED**
Due to ever decreasing device dimensions and the introduction of 3D device architectures, it is challenging to operate within a narrow processing window using conventional plasma etching. One method to address the demands of the next-generation of devices is atomic layer etching (ALE) which provides high fidelity, selectivity, and directionality, and layer-by-layer removal. Plasma-assisted ALE has been extensively studied for a variety of materials, including Al_2O_3, HfO_2, Si, and Si–based dielectrics. Plasma-assisted ALE of SiO_2 or SiN_x typically uses two sequential steps in a cyclic fashion: CF_x deposition from a C_4F_8/Ar plasma followed by an Ar plasma activation step. However, the surface chemistry during plasma ALE is not well understood. In this study, we used *in situ* attenuated total reflection Fourier transform infrared (ATR–FTIR) spectroscopy and *in situ* four-wavelength ellipsometry during ALE to monitor the surface reactions, film composition, as well as the net film thickness. Similar to area-selective atomic layer deposition, we show that surface functionalization prior to ALE can be used to alter the etch per cycle. Using this methodology, I will discuss how selective functionalization of SiO_2 or SiN_x can be used to alter the selectivity during plasma-assisted ALE.

Applied Surface Science Division
Room A211 - Session AS+BI+RA-MoM

Quantitative Surface Analysis I/Reproducibility Issues in Quantitative XPS

Moderators: Donald Baer, Pacific Northwest National Laboratory, Mark Engelhard, EMSL, Environmental Molecular Sciences Laboratory

8:20am **AS+BI+RA-MoM-1 Improving Accuracy in Quantitation by XPS: Standards, Cross-sections, Satellite Structure**, *C. Richard Brundle,* C.R.Brundle & Associates*; P Bagus,* University of North Texas*; B Crist,* XPS International LLC **INVITED**
Determining elemental composition by XPS requires determining relative peak intensities from the elements concerned, and then normalizing using Relative Sensitivity Factors (RSF's). Such RSF's are usually generated from standard materials using the intensity from the "main" peak only and ignoring any associated satellite structure (shake-up, shake-off, and multiplet splitting components) intensity. In the seminal paper by Wagner, et al, (1) this resulted in a conclusion that the calculated Li(1s) photoionization cross-section, σ, (2) was too low by ~40%, relative to F(1s). This apparent discrepancy cast doubt on the claimed 5% accuracy of the calculated σ values for low Z elements (2). We show that this is incorrect. The discrepancy is due, primarily, to the fact that Li(1s) loses almost zero intensity from the main peak into associated satellites, whereas for F1s it is substantial, *spreading over 100ev to lower KE*. A calculated σ always refers to the *total* intensity of photoemission from the orbital concerned, including any intrinsic satellite structure. In addition, the experimental Li(1s) peak intensity in Wagner, et al. (1) was actually *overestimated*, owing to inclusion of overlapping satellite structure spreading from the nearby F(2s) peak. For the 1s intensities of the first row elements, a crude theoretical approximation predicts the total intensity lost from the "main" peak to satellites quite well. It involves an exponential dependence on the number of valence shell electrons present, which for Li+ of LiF, is zero, and for F- is 6 (the filled 2p shell), yielding values of zero loss for Li+ and 20-30% for F-. Full a*b initio* quantum calculations for these ions support the crude estimate (calculated Li+ losses are 1.4%; F- losses are 22.7%). In contrast to earlier claims to the contrary(3), satellite losses, for elements across the periodic table, vary widely from core-level to core level, element to element, *and most critically with the bonding situation of an element (see, for example ref 4)*. Thus any "universal" element RSF's, using main peak intensities only, though semi-quantitatively useful, are inherently limited in potential accuracy achievable, sometimes by up to a factor of 2. What is needed, for improved accuracy, are sets of RSF's appropriate to different bonding situations. Such sets would be particularly useful for the current large inexperienced XPS user base. We attempt to give guidelines.

C.D. Wagner, et al, Surf. Interface Anal. **3**, 211, 1981

J.H. Scofield, J. Elec. Spec. **8**, 129, 1976

V.G. Yarzhemsky, et al, J. Elec. Spec. **123**, 1, 2001

P. S. Bagus, E. Ilton, and C. J. Nelin, Catalysis Letters, **148**, 1785, 2018

9:00am **AS+BI+RA-MoM-3 A Rigorous Approach to the Calculation of the Uncertainties in XPS Analysis**, *A Herrera-Gomez,* CINVESTAV-Unidad Queretaro, México*; Orlando Cortazar-Martinez,* CINVESTAV-Unidad Queretaro, Mexico
One of the most important applications of X-ray photoelectron spectroscopy (XPS) is the characterization of the chemical composition of solids near the surface. However, the proper assessment of the associated uncertainties has remained an elusive problem. One of the issues is that the total uncertainty comes from various sources: the experimental data (peak intensities), parameters theoretically calculated (cross-section,

mean-free-path), and parameters associated to the XPS equipment (angular and kinetic energy transmission functions).

The uncertainty on most of these parameters should be treated as systematic errors. The most important non-systematic uncertainty comes from the peak intensities [1]. It is a common practice in XPS data peak fitting to first subtract the background and then peak-fit the backgroundless data (*static* approach [2]). This approach prevents the use of the covariance matrix to calculate uncertainties because the covariance with the parameters defining the background cannot be accounted. It is only under the *active* approach [2] that it is possible to account for the covariance with the background parameters because the background is optimized in conjunction with the peak parameters. In this paper, the assessment of the uncertainty on the peak intensities will be treated in detail, as well as the total uncertainty on the composition.

[1] A. Herrera-Gomez, A rigorous approach to the calculation of the uncertainties in XPS analysis (Internal Report), Internal Report, Internal Report. CINVESTAV-Unidad Queretaro, n.d. http://www.qro.cinvestav.mx/~aherrera/reportesInternos/uncertaintiesXPS.pdf.

[2] A. Herrera-Gomez, M. Bravo-Sanchez, O. Ceballos-Sanchez, M.O.O. Vazquez-Lepe, Practical methods for background subtraction in photoemission spectra, Surf. Interface Anal. 46 (2014) 897–905. doi:10.1002/sia.5453.

9:20am AS+BI+RA-MoM-4 Gross Errors in XPS Peak Fitting, *Matthew Linford, V Jain, G Major,* Brigham Young University

X-ray photoelectron spectroscopy (XPS) is the most important method for chemically analyzing surfaces. It is widely used in numerous areas of research and technology. Many research groups and individuals are skilled at analyzing XPS data. However, too much of what has appeared and continues to appear in the literature is of at best questionable value and accuracy. In this talk, I will discuss some of the all too common gross errors. Both correct and incorrect examples of each of the following will be shown. (i) Not plotting the data according to international convention of binding energy increasing to the left. (ii) Fitting and interpreting data that are far too noisy to be interpreted. (iii) Labeling noise as chemical components. (iv) Not showing the original data – only showing the synthetic (fit) peaks and their sum. (v) Not plotting the sum of the fit components with the original data. (vi) Having widely varying peak widths in a fit. (vii) Having the baseline completely miss the noise on either side of the peak. (viii) Not collecting data over a wide enough energy window to see a reasonable amount of baseline on both sides of the peak envelope. (ix) In a C 1s spectrum, reversing the labeling on the C-O and C=O peaks, and other mislabeling issues. The C 1s peak envelope is well understood so there shouldn't be huge mistakes here. (x) Not taking into account spin-orbit splitting when it is necessary. (xi) In a comparison of spectra, having widely differing peaks and peak positions for components that are supposed to be the same between the spectra.

9:40am AS+BI+RA-MoM-5 Improved Energy Referencing in XPS, *Hagai Cohen,* Weizmann Institute of Science, Israel

Basically, energy referencing in XPS relies on an absolute reference provided at the back contact of the sample: the electrical ground. If poor connectivity is encountered between the studied surface and ground, reference signals may be used to derive correction terms for the energy scale, such as to get the proper binding energies for elements of interest. Unfortunately, in many cases this procedure fails to accurately address differential charging effects, namely local and temporal variations in the surface charge and the related electrostatic potential.

In the present work, a method for introducing a second absolute/external reference is described. The technical improvement is proven to be mandatory. It enables advanced analyses of binding energies, which refines the chemical analysis significantly. The method further reveals intriguing cases in which the x-ray induced charging does not follow the trivially expected behavior. On top of that, an access to rich electrical information is realized as soon as a second reference is introduced, thus expanding the XPS capabilities into new areas. Measurements of the inherent inner fields in semiconductors and the reliable derivation of device band diagrams, free of the beam-induced artifacts, are just a few examples to be mentioned.

10:00am AS+BI+RA-MoM-6 How to Avoid Errors in the Interpretation of XPS Data?, *Andreas Thissen, P Dietrich,* SPECS Surface Nano Analysis GmbH, Germany; *W Unger,* Bundesanstalt für Materialforschung und -prüfung - Berlin (Germany), Germany

Over the last fifty years significant developments have been done in photoelectron spectroscopy instrumentation and thus opened new fields of application. Especially XPS or ESCA developed into a standard analytical method in many labs for surface and material characterization. The number of users and the number of publications using XPS data has tremendously increased. But as a side effect it is a challenge to keep the level of knowledge about the method and correct data interpretation at a high level for all users of these data.

To avoid errors in the interpretation of XPS data instrument manufacturers put efforts inside their instruments and software packages to help and guide the user through data acquisition, data quantification and interpretation and finally also through data reporting. By this data can be made compatible with existing ISO and other community standards. But even more, data quality becomes transparent also in times of open source publications and open data repositories.

This paper summarizes the challenges of data handling, data treatment, data storage, parameter-data correlation, expert systems for data acquisition, reporting assistance and tracking and authorization tools for sensitive data. In summary future perspectives and suggestions are discusses for improved data repeatability and data reliability.

10:40am AS+BI+RA-MoM-8 Misinterpretations in the Spectroscopic Analysis of Heterogeneous Materials and Defected Structures, *Lisa Swartz, K Artyushkova, J Mann, B Schmidt, J Newman,* Physical Electronics

Analysis of samples where lateral heterogeneities can be present at a variety of scales poses a challenging spectroscopic task. In routine applications of XPS spectroscopy, the analyst is usually acquiring spectra over a large area from multiple positions on the sample and derives conclusions on "representative" chemical composition from average atomic concentrations and standard deviations. However, if lateral heterogeneities existing at the surface have smaller physical dimensions as the analysis area, the conclusions on "representative" chemical composition derived from large area spectroscopy will be erroneous. For accurate structural analysis of heterogeneous materials, it is very important to understand the scale of heterogeneity beforehand, so that the analysis areas and the size of the X-ray probe used for analysis are chosen appropriately. Often, complimentary microscopic techniques, such as SEM, are performed before XPS analysis which addresses some of this challenge but does not allow analysis over the same area.

The ability to perform small area spectroscopy for studying the heterogeneity and physical dimensions of samples is critical for obtaining accurate information on sample structure. In this talk, we will show examples of inaccurate use of large area spectroscopy and discuss the experimental approach towards selecting the relationship between the X-ray size and physical scale of defects and heterogeneities at the surface required to obtain an accurate representation of heterogeneous sample structure.

11:00am AS+BI+RA-MoM-9 Current Issues and Solutions for Reliable, Robust and Reproducible XPS Spectral Acquisition and Data Reporting, *J Counsell, C Blomfield,* Kratos Analytical Limited, UK; *Christopher Moffitt,* Kratos Analytical Limited; *N Gerrard, S Coultas,* Kratos Analytical Limited, UK

XPS is now a truly interdisciplinary technique used in a wide variety of fields including catalysis, tribology, bioremediation and nuclear energy. With more than 1000 instruments currently in use, the ubiquitous nature of XPS means there is a greater requirement than ever for clarity regarding spectral acquisition, analysis and interpretation. The XPS user base has changed significantly – no longer the field of dedicated "technical experts" and spectroscopists – requiring instruments to be simple to use with a higher degree of automation in all parts of operation and analysis.

Here we will discuss the overall procedure for the technique specifying the critical steps in generating sound data and conclusions. Pitfalls and perils in the following steps will be briefly discussed: surface charging, beam damage, contamination, peak identification, energy calibration, quantification, peak-fitting, database usage, chemical state assignment and error reporting as will the latest methods implemented in mitigating against these issues. Worked examples and user studies will be presented to illustrate common inconsistencies.

11:20am AS+BI+RA-MoM-10 Intensity Calibration and Sensitivity Factors for XPS Instruments with Monochromatic Ag Lα and Al Kα Sources, *Alexander Shard,* National Physical Laboratory, UK; *J Counsell, C Blomfield,* Kratos Analytical Limited, UK; *D Cant,* National Physical Laboratory, UK; *E Smith,* University of Nottingham, UK; *P Navabpour,* Teer Coatings Ltd, UK

The use of monochromated Ag La X-ray has been described previously.[1, 2] These sources have now become more widely available on commercial instruments and easier to use due to automation and the superior collection efficiency of modern analysers. To enable direct comparison between data acquired using both sources it is essential to be able have a common calibration scheme and a set of useful sensitivity factors. We employ the calibration method developed by the National Physical Laboratory for Al Kα sources[3] and extend this for Ag Lα sources.[4] Sensitivity factors for Ag Lα and Al Kα are calculated from photoionisation cross sections and electron effective attenuation lengths. These compare well to previous experimental values and data acquired from ionic liquids. The intensity of the Ag Lα source is found to be approximately 50 times lower than the Al Kα source. This, coupled with generally lower photoemission efficiencies, results in noisier data or extended acquisition times. However, there are clear advantages to using the Ag Lα source to analyse certain elements where additional core levels can be accessed and for many technologically important elements where interference from Auger electron peaks can be eliminated. The combination of calibrated data from both sources provides direct and easily interpreted insight into the depth distribution of chemical species. This could be particularly important for topographic samples, where angle resolved experiments are not always helpful. We also demonstrate, using thin coatings of chromium and carbon, that the inelastic background in Ag Lα wide-scan spectra has a significantly increased information depth compared to Al Kα.

References

1. Yates, K.; West, R. *Surf. Interface Anal.* **1983,**5 (4), 133-138.

2. Edgell, M.; Paynter, R.; Castle. *J. Electron Spectr. Rel. Phenom.* **1985,**37 (2), 241-256

3. Seah, M. P.. *J. Electron Spectr. Rel. Phenom.* **1995,**71 (3), 191-204.

4. Shard, A. G. *et al.* *Surf. Interface Anal.* **2019**https://doi.org/10.1002/sia.6647

11:40am AS+BI+RA-MoM-11 Reporting XPS Measurements and How Can We Do Better to Minimize Reproducibility Problems, *Karen Gaskell,* University of Maryland, College Park

The level of detail and information provided in the average scientific article reporting XPS measurement and analysis varies widely. In some cases journal page limitations limit the inclusion of information such as experimental details, instrumental parameters and data sets that are required to fully describe the data collection and subsequent analysis so that it can be adequately reproduced by others. In other cases important information is simply left out. What are the minimum and preferable types of information we should include when reporting XPS results?

Biomaterial Interfaces Division
Room A120-121 - Session BI+AS+NS-MoM

Biofabrication, Bioanalytics, Biosensors, Diagnostics, Biolubrication and Wear

Moderators: Joe Baio, Oregon State University, Caitlin Howell, University of Maine

8:20am BI+AS+NS-MoM-1 Bio-inspired Peptide-polymer Hybrid Mucin Analogues: Applications in Osteoarthritis and Kidney Stone Disease, *Daniel L. French, L Navarro, S Zauscher,* Duke University

Mucins play diverse and crucial roles in the body. These functions range from lubrication of articular joints and the eye, to protection of stomach endothelium, to modulation of oral and gut microflora populations. Despite their diversity, these functions commonly stem from modifications in a general structure shared by all mucins: a blocky polypeptide backbone comprised of terminal moieties for binding surfaces or crosslinking and a characteristic glycosylated bottlebrush. Inspired by this adaptable structure, we have created a mucin analogue platform which engenders key structural features preserved among native mucins. We have emulated the mucinous bottlebrush with a lysine-rich elastin-like polypeptide backbone, which provides primary amines for conjugation of synthetic polymer "bristles." Binding modules target surfaces of interest, to facilitate intramolecular associations, or to direct surface conformation of our

construct. To demonstrate the application of our platform to clinically-relevant problems, we have tailored our mucin analogues to osteoarthritis and kidney stone disease, conditions infamous for profound morbidity and high prevalence. We will demonstrate that collagen-targeted mucin analogues adsorb to model surfaces and prevent protein fouling. This recapitulates the function of lubricin, a mucin downregulated in osteoarthritis. Similarly, we will show that we can target mineral surfaces relevant in kidney stone disease by exchanging the binding module of our analogue mucins. We will show that these altered analogues also inhibit protein-fouling, which is implicated in stone growth. In this platform technology, we have been inspired by the diverse functions of native mucins. By harnessing the general structure which gives rise to these properties, we endeavor not only to replicate the in vivo function of mucins, but also to harness the properties of natural mucins and apply them to systems not naturally protected by mucinous coatings, such as inhibiting the growth of kidney stones.

8:40am BI+AS+NS-MoM-2 Investigation of the Mechanical and Dielectric Properties of Bone Scaffolds, *Kimberly Cook-Chennault,* Rutgers University

Despite the vast number of biomaterials and synthesis technologies available to treat bone defects and disease, few are readily employed for clinical use due in part to challenges in the development of materials that functionally mimic and facilitate the hierarchal processes of bone healing and regeneration. Calcium phosphate based bone replacement materials have been developed over the years for bioengineered bone structures due to their ability to mimic the general properties of mineralized bone. These bone replacement materials have mainly be fabricated in the form of hydroxyapatite (Hap), which can suffer from premature fracture when subjected to typical human load conditions. On the other hand, it is well known that enhanced osteobonding and bone growth results from the exposure of the bone to polarized Hap, which presents a negatively charged surface. Composite hydroxyapatite (Hap) – barium titanate scaffold materials are compared and contrasted with hydroxyapatite (Hap) samples for mechanical elastic moduli, compression strength and dielectric properties. Composite structures were observed to present better mechanical and dielectric properties when compared to HaP samples. For example, the elastic modulus of the HaP and composite samples were 2655.4 MPa and 3559.1 MPa, respectively. Understanding the interrelationship between scaffold architecture/material composition and mechano-transduction will improve our ability to realize patient specific solutions that eliminate hindrances to bone healing such as, lack of vascularization and lack of adequate mechanical stability.

9:00am BI+AS+NS-MoM-3 Bioelectronics with Graphene and Graphene-Based Hybrid-Nanomaterials – From Transparent to Fuzzy Interfaces, *Tzahi Cohen-Karni,* Carnegie Mellon University **INVITED**

We focus on developing a new class of nanoscale materials and novel strategies for the investigation of biological entities at multiple length scales, from the molecular level to complex cellular networks. Our highly flexible bottom-up nanomaterials synthesis capabilities allow us to form unique hybrid-nanomaterials. Recently, we have demonstrated highly-controlled synthesis of 3D out-of-plane single- to few-layer fuzzy graphene (3DFG) on a Si nanowire (SiNW) mesh template. By varying graphene growth conditions, we control the size, density, and electrical properties of the NW templated 3DFG (NT-3DFG). This flexible synthesis inspires formation of complex hybrid-nanomaterials with tailored optical and electrical properties to be used in future applications such as biosensing, and bioelectronics. Currently, we target the limits of cell-device interfaces using out-of-plane grown 3DFG, aiming at electrical recordings with subcellular resolution (<5μm). Moreover, NT-3DFG unique optical properties allows formation of remote interfaces with tissue and cells. We demonstrate photostimulation of tissue and cells by using the photothermal effect of NT-3DFG. Last, we have developed a unique transparent graphene-based electrical platform that enables concurrent electrical and optical investigation of ES-derived cardiomyocytes' intracellular processes and intercellular communication. In summary, the exceptional synthetic control and flexible assembly of nanomaterials provide powerful tools for fundamental studies and applications in life science, and open up the potential to seamlessly merge either nanomaterials-based platforms or unique nanosensor geometries and topologies with cells, fusing nonliving and living systems together.

9:40am BI+AS+NS-MoM-5 Experimental Observation of Multiple Plasmon Induced Transparency and Fano Resonance in Titanium Nitride Based Devices, *J Asencios, Arturo Talledo, R Moro, C Luyo,* Facultad De Ciencias Universidad Nacional De Ingeniería, Perú

Abstract: We built three types of plasmonic structures based on titanium nitride thin films by using the technique dc magnetron sputtering and D-shaped prisms as substrates. The prisms were made of glass or sapphire. Devices with structure Prism/TiN, Prism/TiN/SiO_2 and Prism/TiN/SiO_2/Nb_2O_5 were called devices type 1, type 2 and type 3, respectively. Attenuated Total Reflection in the Kretschmann configuration was studied in the three types of devices. Experimental angular spectra were fitted by using a calculation program based on the solutions to Maxwell equations. ATR spectra of devices type 1 show a wide absorption band. The main feature for ATR spectra of devices type 2 was a series of maxima and minima of reflectance within a wide absorption band. ATR spectra of devices type 3 are identified with a very sharp window within the absorption band. The spectra of devices type 2 and type 3 were associated with the phenomena of Multiple Plasmon Induced Transparency (MPIT) and Fano Resonance, respectively. Based on calculations of the square of the electric fields in the involved media, we proposed some simple phenomenological explanations for the phenomena of MPIT and Fano resonance. Potential use of these structures as refractive-index sensors was also discussed.

10:00am BI+AS+NS-MoM-6 Breaking the Mass Resolution Limit of Shear Wave Resonators in Liquid through Integrated Microfluidic Channels, *Z Parlak, S Zhao, D French, Stefan Zauscher,* Duke University

Acoustic shear wave resonator sensors (SWRS), e.g., quartz crystal microbalance, are widely used in applications (e.g., thin film deposition) where their high quality factor in air or vacuum provides exquisite mass resolution. SWRS are also used as biosensors in liquid environments; however, they have not yet found widespread use outside the research environment despite their simple and robust detection modality. This is because current SWRS suffer from viscous contributions to shifts in resonance frequency, which inherently leads to low mass resolution. Furthermore, current SWRS require accurate temperature control and use large liquid volumes (~ml). Together these limitations prohibit accurate and economic measurement of surface bound mass, e.g., in protein binding assays. We show through experiments and simulations that by confining fluid into small, rigid channels oriented perpendicularly to the shear direction of the SWRS, we can manipulate liquid to behave as a lossless layer and thus perform precise mass measurements of the confined liquid. Canceling viscous effects in μ-fluidic SWRS not only enhances their mass resolution in liquid to levels observed in air/vacuum, but also enables efficient device miniaturization. Combined with the extremely small volume requirements for sensing (~nL), we show that μ-fluidic SWRS can overcome current barriers for their widespread use in diagnostic sensing and point of care applications.

10:40am BI+AS+NS-MoM-8 Designing Anti-Fouling Lubricious Surfaces Based on Modular Approaches, *T Galhenage, C Khatri, A Vena, A Labak, T Banks, G Tremelling, Philseok Kim,* Adaptive Surface Technologies, Inc.
INVITED

Biofouling, the growth of marine organisms on man-made structures, poses numerous challenges including >$15 billion additional fuel costs to vessel operators worldwide, cost and time for cleaning, corrosion issues, and negative environmental impacts. Anti-fouling coatings are the primary method of protection against this persistent problem, yet the widespread use of toxic, biocide-based coating products is causing even greater concerns for our environment and sustainability. Therefore, a groundbreaking coating solution is sought to protect both the environment and our properties.

Adaptive Surface Technologies has been developing a modular additive approach to address this problem. The SLIPS (Slippery Liquid Infused Porous Surfaces) effect (Physical module) has been successfully integrated with novel library of Surface Active Polymers (SAPs, Chemical module) to form what we call Active Performance Ingredients (APIs) that could be easily introduced as an additive in a conventional binder matrix to yield a coating formulation. I will discuss the synergistic effect of customized lubricant and SAPs in controlling biofouling without using biocides along with promising results in both laboratory and field tests. This new additive route can open up a new avenue in developing environmentally friendly, non-toxic functional additives and formulation strategies for industrial, architectural, interior, and medical coatings applications.

11:20am BI+AS+NS-MoM-10 All Inkjet Printed Biosensor for Easy and Rapid Detection of Immunoglobulin G (IgG) Protein, *Ridwan Fayaz Hossain, A Kaul,* University of North Texas

Protein detection biosensors are interesting tools for detecting and measuring the levels of specific proteins in biological and environmental samples, offering certain operational advantages over standard photometric methods, notably with respect to rapidity, ease-of-use, cost, simplicity, portability, and ease of mass manufacture. Although inkjet printed electrode based sensor is widely reported, the number of fully inkjet printed biosensors is still limited [1,2]. Here, we report the design, fabrication, and evaluation of a flexible field-effect transistor (FET) for biosensing based on the inkjet printing technique, where the insulator layer is uniquely functionalized for Immunoglobulin G (IgG) protein detection. IgG is a plasma-cell protein that is produced within the lymph nodes, spleen, bone marrow, respiratory tract mucosa, tissue, etc. Since IgG protein is produced as part of the body's response to bacteria, viruses, and tissue antigens, measurement of blood IgG levels can reveal any of the body's abnormal conditions. Until now, proteins are detected mostly by antibodies in analytical formats like ELISA, immunobead assay, western blotting, and microarrays, etc. but their performance is limited by low sensitivity. This new generation biosensor is more stable and well adapted to the conditions of real samples. The protein detection biosensor reported here represents an important starting point for the design and fabrication of flexible, rapid detection biosensing devices by inkjet printing. This work shows a promising aspect of protein detection that will pave the way for the development of a fully functional device for point-of-care diagnosis.

Reference:

[1] Jensen, G. C., Krause, C. E., Sotzing, G. A., & Rusling, J. F. (2011). Inkjet-printed gold nanoparticle electrochemical arrays on plastic. Application to immunodetection of a cancer biomarker protein. Physical Chemistry Chemical Physics, 13(11), 4888-4894.

[2] Carvajal, S., Fera, S. N., Jones, A. L., Baldo, T. A., Mosa, I. M., Rusling, J. F., & Krause, C. E. (2018). Disposable inkjet-printed electrochemical platform for detection of clinically relevant HER-2 breast cancer biomarker. Biosensors and Bioelectronics, 104, 158-162.

11:40am BI+AS+NS-MoM-11 Biosensing Applications of Silver Nanorods Array Fabricated by Glancing Angle Deposition (GLAD), *Shashank Gahlaut,* Indian Institute of Technology Delhi, India

Silver being most widely used material due to its unique electrical and optical properties. Here we have investigated biosensing properties of silver nanorods array (AgNRs) fabricated by glancing angle deposition. GLAD grown silver nanorods are found to be highly sensitive and selective for hydrogen sulfide (H_2S) gas. Color and water wetting (contact angle) of AgNRs array are parameters affected in the presence of this gas. H_2S is one the major gaseous products evolved in bacterial metabolic process. On the basic of H_2S production, we have shown the detection of viability as well as antibiotic resistance in different strains of bacteria.

Another potential application of as synthesized AgNRs array in Surface enhanced Raman scattering (SERS) based detection. The dengue is a viral disease and a serious global health concern. About 2.5 billion of world's population has been living at the risk of dengue infection. It causes a spectrum of illness ranges from acute febrile illness called dengue fever (DF) to more severe life threatening forms dengue hemorrhagic fever (DHF) and dengue shock syndrome (DSS) causing vascular leakage that may lead to death. So far, neither specific treatment nor effective vaccine available for the prevention and treatment. Therefore, early detection is the key of the survival of the patients. The earlier symptom starts with mild dengue fever, at this stage the concentration of the biomarkers are very less which pose a problem in early detection. In the present study, we have demonstrated the detection of dengue from clinical blood samples employing AgNRs array as SERS substrates with hand held Raman spectrometer. A notable change in SERS spectral signature observed in the blood of dengue infected patients in comparison to that of healthy subject. This change was further confirmed using the statistical tool principal component analysis (PCA) and the samples were differentiated as healthy, dengue positive and dengue negative. All the blood samples were also dually verified with Antigen (NS1) as well as Antibody (IgM) ELISA kit. This method provides a field deployable, rapid diagnosis of dengue at its early stage.

Fundamental Discoveries in Heterogeneous Catalysis Focus Topic
Room A212 - Session HC+SS-MoM

Utilization of Theoretical Models, Machine Learning, and Artificial Intelligence for Heterogeneously-Catalyzed Reactions

Moderators: Liney Arnadottir, Oregon State University, Sharani Roy, University of Tennessee Knoxville

8:40am **HC+SS-MoM-2 Theoretical Study of Acetic Acid Decomposition on Pd (111) using Density Functional Theory**, *Kingsley Chukwu, L Arnadottir,* Oregon State University

Acetic acid decomposition on Pd (111) and the effects of water on the decomposition are good model systems for the study of solvent effects on small oxygenates. Numerous studies have found that solvents influence the selectivity and rate of heterogenous catalytic reactions, so fundamental understanding of how water affects OC-O, C-OH, CO-H, C-H and C-C bond cleavages will give us valuable insight into how water influences selectivity of oxygenates decomposition, further enabling bottom up design of effective catalyst and catalyst system. Here we present density functional theory calculations of the decomposition of acetic acid on Pd (111) and the effects of water on the reaction mechanism. Our results suggest that the most favorable decarboxylation (DCX) and decarbonylation (DCN) mechanisms in vacuum proceed through dehydrogenation of acetic acid (CH_3COOH) to acetate (CH_3COO), followed by dehydrogenation of CH_3COO to CH_2COO. The competition between the most favorable DCN and DCX pathway depends on two endothermic elementary steps, the deoxygenation of CH_2COO to ketene (CH_2CO) and dehydrogenation of the carboxylmethylidene (CH_2COO) to carboxylmethylidyne (CHCOO). Water can affect the different elementary steps by changing the stability of the initial, transition and/or final state or by providing new reaction paths such as through hydrogen shuttling, which can lead to changes in the selectivity of a complex reaction network as presented herein. Here we will discuss how water influences different critical reaction steps and how that effects the overall reaction network.

9:00am **HC+SS-MoM-3 Towards a Chemically Accurate Description of Reactions of Molecules with Transition Metal Surfaces**, *Geert-Jan Kroes,* Leiden University, Netherlands **INVITED**

Heterogeneously catalyzed processes consist of several elementary reactions. Accurately calculating their rates requires the availability of accurate barriers for the rate controlling steps. Unfortunately, currently no first principles methods can be relied upon to deliver the required accuracy. To solve this problem, in 2009 we came up with a novel implementation of the specific reaction parameter approach to density functional theory (SRP-DFT). This allowed us to reproduce experiments for H_2 reacting on copper surfaces, and to determine barrier heights for H_2-Cu systems, with chemical accuracy. The original procedure used was not extendable to reactions of molecules heavier than H_2 with surfaces, because the metal surface was treated as static. This problem has been solved by combining SRP-DFT with Ab Initio Molecular Dynamics (AIMD). This method was applied to the dissociative chemisorption of methane on a Ni surface, a rate-limiting step in the steam reforming reaction. We were able to reproduce experiments on CHD_3 + Ni(111) with chemical accuracy, and have predicted a value of the reaction barrier height that we claim to be chemically accurate. We have new results for CHD_3 + Pt(111) that are even better, and which show that the SRP density functional for methane interacting with Ni(111) is transferable to methane interacting with another group X metal surface, i.e., Pt(111). Even more interestingly for applications to catalysis, the SRP functional derived for methane reacting with Ni(111) also gives a very accurate description of molecular beam sticking experiments on CHD_3 + Pt(211). Finally, thanks to a collaboration with Jörg Behler (University of Göttingen) we are now able to develop potential energy surfaces also depending on the degrees of freedom associated with the surface phonons, for polyatomic molecules interacting with metals. This has enabled us to compute statistically accurate reaction probabilities for highly activated reactions not open to investigation with AIMD, for which reaction probabilities are less than 0.01.

9:40am **HC+SS-MoM-5 The Apparent Activation Energy for Complex Mechanisms: A Simple Relationship via Degrees of Rate Control**, *Zhongtian Mao[1,2], C Campbell,* University of Washington

Reactions on surface usually consists of several elementary steps. It is known that the observed reaction kinetics often represents a composite of the contribution from each of these elementary steps. The "rate-determining step" (RDS) assumption is a common approach for dealing with multistep mechanisms, where a single step is assumed to dominate the reaction kinetic behaviors and the kinetic parameters of this RDS (e.g., net rate, activation energy) are good estimation for those of the overall reaction. However, RDS is not a rigorous concept in mathematics and there is no universal definition for RDS. Efforts have been made to clarify the actual physical meaning behind RDS, and the "Degree of Rate Control" (DRC) was raised as a rigorous mathematical approach to quantify to what extent the change of the Gibbs free energy of a species in the reaction scheme can affect the rate of the overall reaction. DRC analysis to reaction kinetics elucidates that there are only rate-determining species with non-negligible DRCs instead of rate-determining steps.

The apparent activation energy E_{app} is determined by fitting the temperature dependence of the reaction rate to the Arrhenius law. It is believed that E_{app} is a direct measurement of energy information in the RDS, which has been challenged by DRC analysis. A general and accurate elaboration of the microscopic origin of E_{app} has not been reported except in cases where there is an analytical rate expression. Here a simple but general mathematical expression of E_{app} in terms of the enthalpies of species in the reaction and their DRCs is derived. To verify the accuracy of this equation, microkinetic modelling of methanol synthesis through CO_2 hydrogenation on Cu-based model catalysts under three different conditions was carried out based on previously-published DFT energetics. On pure Cu(211) at 450 K, there are only one transition state and only one intermediate with non-negligible DRCs, and E_{app} estimated using our equation is within 1 kJ/mol of the true value. When the temperature is raised to 570 K, the surface sites are mostly unoccupied; and, when the model catalyst is promoted by Zn, there are four transition states with non-negligible DRCs, which means the single RDS assumption is not true. In both these complicated cases, the error of the estimated value for E_{app} is still <1 kJ/mol.

10:00am **HC+SS-MoM-6 First-Principles Kinetic Monte Carlo Simulation of CO Oxidation on PdO(101): Role of Oxygen Vacancies**, *Minkyu Kim, A Asthagiri,* The Ohio State University

CO oxidation on transition metal (TM) oxide surfaces has been widely studied both experimentally and theoretically; however, a healthy debate continues on the coupling between changes in oxide phase and surface reactivity. In this study, we investigated CO oxidation over PdO(101) surface, which has been proposed to be important in Pd oxidation catalysis. In contrast to earlier studies of CO oxidation on TM oxide surfaces, we incorporate neighbor effects of oxygen vacancies on all the elementary surface processes. We employ density functional theory (DFT) to map out the kinetics of 50 elementary surface processes. We find that barriers for elementary steps such as O vacancy, O_2 dissociation, and CO_2 formation can be decreased by 20-40% in the presence of O vacancies, while O_2 desorption is increased by 70%. Using the DFT-derived rate constants, we have developed a lattice-based kinetic Monte Carlo (kMC) framework that can simulate CO oxidation under both ultra-high vacuum (UHV) and reaction conditions.

Initially, the kMC simulations were performed under UHV conditions (low CO partial pressure, no O_2 pressure) as a function of increasing surface temperature. As the CO oxidation proceeds and the surface lattice O atom coverage is depleted, the CO oxidation rate decreases rapidly at 400 K; however, the rate sharply increases at temperatures above 450 K. At 450 K, we find a new complex pathway to CO_2 formation that is activated in the presence of O vacancies and is the source of the increased CO oxidation rate despite the depletion of surface oxygen atoms. These kMC results match UHV isothermal experiments under similar conditions. KMC simulations at steady state conditions of low CO and O_2 pressures (P_{CO}: 5×10^{-9} Torr / P_{O2}: 1.5×10^{-8} Torr), show that the rate-limiting step is O_2 dissociation and this elementary step requires the presence of adjacent oxygen vacancies to be activated at temperatures below 500 K. Without the addition of O vacancy neighbor effects to the kMC model, the PdO(101) surface would be inactive to CO oxidation because surface oxygens cannot

---

[1] **Heterogeneous Catalysis Graduate Student Presentation Award Finalist**
[2] **Morton S. Traum Award Finalist**

be healed by gaseous O_2. In addition, we will discuss kMC simulations under reaction conditions at varying CO/O_2 partial pressures.

10:40am HC+SS-MoM-8 Accelerating *ab initio* Simulations using Surrogate Machine Learning Models, *Jose A. Garrido Torres*, *P Jennings, M Hansen,* Stanford University; *T Bligaard,* SLAC National Accelerator Laboratory

Typically, first-principle calculations are computationally expensive. This problem is usually accentuated when modeling materials due to the large number of atoms involved in the models. Therefore, the development and implementation of robust and fast optimizers have always been a hot topic in this field. The desired algorithms must minimize the number of *ab initio* function calls as much as possible without compromising the accuracy of the simulated properties. Our approach is based on a surrogate machine learning model which allows to substantially reduce the number of function calls in the search of the optimal solution. Here, we present the evidence of the aforementioned acceleration for two of the most commonly encountered optimizations problems in computational catalysis: structural relaxations and transition-state search, such as energy minimization and Nudged Elastic Band (NEB) calculations.

11:00am HC+SS-MoM-9 Integrating Materials Databases and Autonomous Workflows for the Discovery of New Heterogeneous Catalysts, *Kirsten Winther*, *T Bligaard,* SLAC National Accelerator Laboratory

With the accelerating amount of electronic structure data being generated in materials research, data-driven approaches have a huge potential to guide the discovery of new materials and catalysts. This paradigm relies on the development of sophisticated tools and software for storing, sharing and generating calculational results.

Several open materials databases, including Materials Project and the Open Quantum Materials Database (OQMD), have been successful in making the results of electronic structure calculations openly available, where vast amount of crystalline materials data has been generated. Recently, we developed the Catalysis-Hub.org database platform[1], which is suited to handle the complexity of computational catalysis.

In my talk I will present the Catalysis-Hub platform, which consists of a database for surface reactions containing 105,000+ reaction energies from more than 50 publications, as well as several in-browser apps, such as atomistic machine learning predictions for adsorption energies [2] and generation of crystal [3] and surface-adsorbate geometries[4]. Next, I will discuss how these efforts can be integrated into computational workflows for generating atomic geometries and calculations. This includes how machine learning predictions in an active learning framework can be used for an autonomous exploration of new catalytic materials.

[1] K.T. Winther, M.J. Hofmann, O. Mamun, J. R. Boes, M. Bajdich, T. Bligaard. Scientific Data, Accepted (2019).

[2] M.H. Hansen et al. https://arxiv.org/abs/1904.00904 (2019).

[3] A. Jain, T. Bligaard Phys. Rev. B 98, 214112 (2018).

[4] J.R. Boes, O. Mamun, K. T. Winther and T. Bligaard. JPCA 123, 2281–2285 (2019).

11:20am HC+SS-MoM-10 Knowledge-Based Approaches in Catalysis and Energy Modelling, *Karsten Reuter*, Technical University of Munich, Germany **INVITED**

Reflecting the general data revolution, knowledge-based methods are now also entering theoretical catalysis and energy related research with full might. Automatized workflows and the training of machine learning approaches with first-principles data generate predictive-quality insight into elementary processes and process energetics at undreamed-of pace. Computational screening and data mining allows to explore these data bases for promising materials and extract correlations like structure-property relationships. At present, these efforts are still largely based on highly reductionist models that break down the complex interdependencies of working catalysts and energy conversion systems into a tractable number of so-called descriptors, i.e. microscopic parameters that are believed to govern the macroscopic function. For certain classes of materials like transition metal catalysts, corresponding human-designed models have indeed established trend understanding and spurred a targeted materials design. Future efforts will concentrate on using artificial intelligence also in the actual generation and reinforced improvement of the reductionist models. This is expected to better capture complexities

like incomplete understanding or operando changes of interfacial morphology, to provide access to structured and compound materials classes, or ultimately to even fulfill the dream of an inverse (de novo) design from function to structure. In this talk, I will briefly survey these developments, providing examples from our own research, in particular on adsorption energetics at bimetallic catalysts and data mining for the design of organic semiconductors.

MEMS and NEMS Group
Room A210 - Session MN-MoM

MEMS, BioMEMS, and MEMS for Energy: Processes, Materials, and Devices I

Moderators: B. Robert Ilic, National Institute for Science and Technology (NIST), Zenghui Wang, Case Western Reserve University

8:20am MN-MoM-1 Piezoelectrics Meets Photonics – Acousto-Optic Microsystems, *Gianluca Piazza*, Carnegie Mellon University **INVITED**

Advancements in thin film piezoelectric technology and the ability to define and pattern acousto-electric devices that support micron and sub-micron acoustic wavelengths have opened up new opportunities to integrate acoustic functionalities into photonic circuits. The field of opto-mechanics has grown from fundamental physics investigation into device applications. Acousto-optic interactions are equally interesting and will have immediate applications in facilitating miniaturization and power efficiency for radio/microwave communication, inertial sensing, photonic signal processing, optical phased arrays, and new displays for virtual/augmented/mixed reality.

In this talk, I will present preliminary work towards the demonstration of integrated acousto-optic microsystems that take advantage of the unique properties of micro-patterned piezoelectric thin films such as sputtered aluminum nitride and single crystalline lithium niobate. The talk will focus on a couple of microsystem examples and will detail the design, fabrication and experimental demonstration of high frequency acousto-optic devices that are used for the synthesis of integrated RF oscillators or high precision and high stability gyroscope sensors.

9:00am MN-MoM-3 On-chip Silicon Photonics Radiation Sensors, *Nikolai Klimov*, *Z Ahmed, R Fitzgerald, L Cumberland, I Pazos, R Tosh,* National Institute of Standards and Technology (NIST)

The last few decades have witnessed an exponential growth in photonics, driven in part by improvements in micro-electronics fabrication techniques and by increasing adoption of photonics components by the telecommunications industry. As a result, a wide variety of photonics-based devices have been recently proposed and developed [1-4]. These photonic sensors are particularly valuable due to their micro-/nanoscale footprint, ultra-high sensitivity, low power consumption, and tolerance to harsh environmental variables. One potential application of photonic sensors is ionizing radiation dosimetry. At present, primary standards for absorbed dose are based on large (m^3) water calorimeters used to link the absorbed energy from a large uniform radiation beam to the temperature rise in a ~0.5-mm sized thermistor probe. The realization of this standard requires radiation-beam uniformity on the order of centimeters. On the other hand, rapidly evolving medical and industrial applications are demanding a deployable solution capable of detecting ionizing radiation on a millimeter to micrometer scale. To address industry demand, National Institute of Standards and Technology (NIST) has recently started a program to develop the next generation radiation dose primary standards. The new proposed standard, built on a nano-photonic chip, will leverage nano-photonics and frequency metrology to provide a field-deployable solution. Our radiation sensors are based on high-Q silicon photonic resonators such as ring resonators and photonic crystal cavities. We have recently demonstrated [5] that these sensors can withstand 1 MGy (1 Gy = 100 Rad) absorbed dose in ca. 1 MeV gamma- and electron-beam irradiations with negligible degradation to device performance. In this presentation we will give an overview of the NIST photonic dosimetry program and its most recent developments. We will explain design, nanofabrication, packaging and interrogation of our devices. We will also show our preliminary results on real-time photonic calorimetry measurements in on/off cycles of the electron beam provided by a Van de Graaff accelerator at nominal dose rate of kGy/s. Comparison of the device response with the output of finite-element modelling of heat transport and dose measurements obtained by co-irradiated alanine pellets (analyzed via EPR) will also be discussed.

[1] B. Guha et al., Opt. Lett. 37 (212) 2253–2255.

[2] Oates, L.W. Burgess, Anal. Chem. 84 (2012) 7713–7720.

[3] H. Xu, et al., Opt. Express. 22 (214) 3098–3104.

[4] N.N. Klimov, et al., Sensor ad Actuators A, 269 (2018) 308-312.

[5] Z. Ahmed, et al. , Sci. Rep. 8 (2018) 13007.

9:20am MN-MoM-4 Synthesis and Characterization of Nanoscale 3 dimensional Plasmonic Architectures, *Grace Pakeltis, E Mutunga,* University of Tennessee Knoxville*; Z Hu, D Masiello,* University of Washington*; J Idrobo,* Oak Ridge National Laboratory*; H Plank,* Graz University of Technology, Austria*; J Fowlkes,* Oak Ridge National Laboratory*; P Rack,* University of Tennessee Knoxville

New breakthroughs and better understanding in the underlying theory of plasmonics has led to an increased demand for advanced design, synthesis and device integration strategies for plasmonic nanomaterials. Three-dimensional plasmonic nanostructures have the ability to advance applications such as ultra-fast communication, high density memories, and sensing while enabling further investigation into plasmonic physical phenomena. In this study, we illustrate a nanoscale synthesis process which utilizes a hybrid of direct-write 3D nanoprinting and thin film deposition to fabricate complex, free-standing plasmonic nanostructures for the investigation of 3D plasmonics. Focused electron beam induced deposition is used to deposit non-plasmonic 3D scaffolds, which are subsequently isolated with a conformal SiO_2 layer and coated with a plasmonic materials, specifically Au, to create functional 3D plasmonic nanostructures. A variety of single and dimer structures were fabricated and low-loss electron energy loss spectroscopy was utilized to characterize their full plasmonic spectra with nanoscale resolution. Complementary electron discrete dipole approximation simulations were performed to elucidate the resultant consequent electric and magnetic field distributions. This work demonstrates the flexibility FEBID scaffolds offer for the advancement of new 3D devices for applications and fundamental studies of plasmonic nanomaterials.

9:40am MN-MoM-5 2D Raman Imaging and Characterization of Surface Acoustic Waves on GaAs Substrates, *Brian Douglas Rummel, G Heileman,* University of New Mexico*; M Henry,* Sandia National Laboratories*; S Han,* University of New Mexico

We have fabricated Surface Acoustic Wave (SAW) devices on a GaAs (110) substrate to demonstrate the capability of 2D Raman microscopy to image and characterize acoustic waves traveling on the surface of a piezoelectric substrate. SAW devices are typically utilized in sensors and rf filters, and developing a facile technique to image the transmitted signal would be useful in characterizing device operation and optimization. SAWs are generated using a two-port interdigital transducer (IDT) platform, modified to produce free surface standing waves. These standing waves provide a means to differentiate nodes and antinodes of the acoustic wave. The frequency of SAWs does not easily allow *in situ*, real-time imaging of the waves. However, we make use of Raman peak broadening that corresponds to an averaging of the peak shifts over the integration time of the spectrometer. We have derived an analytical model to fit the peak broadening and effectively calculate the maximum strain induced by the acoustic waves, thus allowing one to characterize the SAWs and measure surface displacements on the order of picometers. The application of this research for the strain-induced fabrication of highly ordered nano/micro structures in III-V semiconductors will also be discussed.

10:00am MN-MoM-6 Impacts of Stress and Dissipation in van der Waals Interfaces on 2D Material Nanoelectromechanical Systems, *SunPhil Kim, A van der Zande,* University of Illinois at Urbana-Champaign

Two-dimensional materials such as graphene and MoS_2 represent the ultimate limit of both nanoelectronic and nanoelectromechanical systems due to their intrinsic molecular scale thickness. While 2D materials exhibit many useful properties, many of the most exciting phenomena and applications arise at the van der Waals interface. Electrically, the van der Waals interface enables the constructing of heterostructures and molecular scale electronics. Mechanically, the van der Waals interface displays superlubricity[1] or solitons[2] depending on whether the interface is aligned. A fascinating question is how the van der Waals interface affects the mechanical properties of 2D membranes. Answering this question is important to incorporating 2D heterostructure electronics into diverse applications such as highly tunable nanoelectromechanical systems from suspended 2D membranes, stretchable electronics from crumpled 2D materials, and origami/kirigami nano-machines.

In this study, we explore the impact of the van der Waals interface by comparing mechanical resonance of electrostatically contacted circular drumhead resonators made from atomic membranes of monolayer graphene to commensurate (Bernal stacked) bilayers, incommensurate (twisted) bilayer, and graphene-MoS_2 heterostructures (2D bimorph).

For Bernal stacked bilayer, we observe the creation and destruction of individual solitons manifesting as stochastic jumps in the mechanical resonance frequency tuning. We find individual dislocation creation and destruction of single solitons lead to shifts in membrane stress of < 7 mN/m or an in-plane interlayer slip distance of < 0.7 Å. We observe similar jumps in the few layer graphene and heterostructure, but not in the twisted bilayer.

For twisted bilayer, temperature and amplitude dependent studies reveal that the resonators show a factor of 3 higher dissipation rate, leading to different nonlinear behaviors compared to monolayer graphene and Bernal stacked bilayer resonators.

These results show that van der Waals interfaces strongly affect stress and dissipation of many multilayer 2D atomic membranes; an important consideration in engineering 2D nanomechanical devices.

[1]Dienwiebel, M.; Verhoeven, G. S.; Pradeep, N.; Frenken, J. W. M.; Heimberg, J. A.; Zandbergen, H. W., Superlubricity of graphite. *Phys Rev Lett* **2004,***92*(12).

[2]Alden, J. S.; Tsen, A. W.; Huang, P. Y.; Hovden, R.; Brown, L.; Park, J.; Muller, D. A.; McEuen, P. L., Strain solitons and topological defects in bilayer graphene. *P Natl Acad Sci USA* **2013,***110*(28), 11256-11260.

10:40am MN-MoM-8 Nanomechanical Sensing for the Life Sciences, *Montserrat Calleja,* IMN-CSIC, Spain **INVITED**

Physical and, among them, mechanical properties of biological entities as cells, bacteria, viruses and biomolecules are valuable cues to better understand human diseases. Still, this has remained an underexplored route for the development of novel biosensing and diagnostic strategies. Biosensors based on nanomechanical systems are best suited to respond to the demand for accurate physical characterization of biofilms, biomolecules and single cells. The continuous downscaling of such devices from micro- to nano- scale is providing a drastic improvement in their mass resolution, while the robustness of nanomechanical biosensors for high throughput immunodetection has reached the demands of clinical applications. Interestingly, other physical parameters than the added mass of the biological targets are at reach for nanomechanical systems. We have recently observed that thin films of DNA demonstrate a Young's modulus tuning range of about 10 GPa, by simply varying the environment relative humidity from 0% up to 70%; while upon hybridization with the complementary strand, the DNA self-assembled monolayers significantly soften by one order of magnitude. Thus, we have demonstrated direct detection without prior purification or amplification of DNA sequences for gene-based identification of pathogens and antibiotic resistances. Also, the mass, position and stiffness of analytes arriving the resonator can be extracted from the adsorption-induced eigenfrequency jumps. We have proposed that this approach serves for identification of large biological complexes near their native conformation, a goal that is beyond the capabilities of conventional mass spectrometers. The capability to describe the analytes that arrive to the resonator by two orthogonal coordinates, the mass and the stiffness, clearly enhances the selectivity of nanomechanical spectrometry and it opens the door to relevant biomedical applications, as now the important role of mechanical properties in biological processes and in pathogenic disorders is becoming increasingly clear. In this talk, several avenues to advance nanoresonators for multiparameter fingerprinting of single proteins, cells, viruses and bacteria will be reviewed.

11:20am MN-MoM-10 Neutral Mass Spectrometry of Metallic Nanoparticles with Optomechanical Resonators, *Marc Sansa, M Defoort, M Hermouet, L Banniard, A Fafin, M Gely,* Université Grenoble Alpes, CEA, LETI, France*; I Favero,* Centre de Nanosciences et de Nanotechnologies, CNRS, Université Paris-Sud, Université Paris-Saclay, France*; G Jourdan,* Université Grenoble Alpes, CEA, LETI, France*; A Brenac,* Université Grenoble Alpes, CEA, CNRS, Grenoble INP, INAC-Spintec, France*; S Hentz,* Université Grenoble Alpes, CEA, LETI, France

Nanomechanical resonators have shown record performance in mass or force sensing thanks to their miniature sizes. Pioneering works have shown single protein mass spectrometry (MS) could be performed with nanoresonators (1). It was recently demonstrated that they are particularly well suited for the analysis of high-mass species like virus capsids (~100MDa), out of reach for any commercial instrument as of today (2). In parallel, cavity-based nano-optomechanical resonators have shown

exceptional displacement sensitivities (3), opening new avenues to improve the limit of detection of nanomechanical sensors (4). Here we report the first proof of concept of mass spectrometry with a nano-optomechanical resonator, made possible by a novel resonator geometry, the combination of optomechanics with electrical actuation and advances in fabrication and assembly of the sensor.

Taking advantage of the optomechanical detection, we use an ultra-thin planar sensor geometry. It displays several advantages compared to commonly used 1D-like resonators: the capture area is increased threefold while maintaining a similar mass resolution. Additionally, this planar membrane resonator is designed to be insensitive to particle position, shape or stiffness, avoiding the need for multi-mode operation (5). The resonators are fabricated using the first Very Large Scale Integration process for optomechanics, which allows the combination of standard photonic components (grating couplers, waveguides, optical cavities), electrical actuation of the resonator and a protection layer covering the optical and electrical features.

Our process and design also allow optical packaging in order for our sensor to be portable and usable in any vacuum system with optical and electrical input/outputs, such as a sputtering system containing a standard Time-of-Flight (TOF) mass spectrometer (6). This set-up allows the generation of particles of controllable mass, and the comparison of optomechanical and TOF mass spectrometry in situ. We show that the measured mass is equivalent with both techniques, while optomechanical detection is more performant at higher masses (>5 MDa), where TOF becomes less efficient. This work represents the first step towards the optomechanical addressing of large sensor arrays, which combine the advantages of nanomechanical sensors with reduced analysis times comparable to those of conventional MS.

1. M.S. Hanay et al. Nat. Nanotechnol. (2012)

2. S. Dominguez-Medinaet al. Science (2018)

3. A. Schliesser et al. New J. Phys. (2008)

4. A. Venkatasubramanian et al. Nano Lett. (2016)

5. E. Gil-Santos et al. Nat. Nanotechnol. (2010)

6. E. Sage et al. Nature Communications (2018)

11:40am MN-MoM-11 Mass Calibration of Nanomechanical Resonators from Electrical Measurements for Mass Spectrometry Applications, *Bogdan Vysotskyi,* CEA/LETI-University Grenoble Alpes, France*; S Lai,* CEA/IRIG-University Grenoble Alpes, France*; M Defoort, M Sansa,* CEA/LETI-University Grenoble Alpes, France*; K Clement,* CEA/IRIG-University Grenoble Alpes, France*; M Gely,* CEA/LETI-University Grenoble Alpes, France*; C Masselon,* CEA/IRIG-University Grenoble Alpes, France*; S Hentz,* CEA/LETI-University Grenoble Alpes, France

Nanomechanical resonators have recently shown their potential to extend mass spectrometry towards a mass range inaccessible to commercial spectrometers [1]. The frequency shift-to-particle mass conversion requires precise knowledge of the resonator's effective mass. When using a single resonator, uncertainty on the effective mass translates into a shift into central mass of the measured mass profile. If this resonator can be used for a large amount of time, time and effort can be spent into proper morphological characterization such as scanning electronic microscopy or local stress measurement. While these techniques can be suitable for MEMS-type devices [2], they prove much more complex and less effective in the case of nanomechanical resonators due to limited precision (*c.a.* 5 to 10nm). Moreover, the issue becomes way more acute when using arrays of resonators [3]: in this case, effective mass uncertainty and variability within the array leads to shifts in central mass, but also changes in mass profile. Lastly, routine particle measurements demand frequent changes in devices and time-effective calibration techniques are required. This crucial issue for mass spectrometry applications is very little discussed in the literature, or is addressed with complex procedures [4]. FEM simulations show that two main parameters impact effective mass assessment in the case of our monocrystalline silicon resonators (160nm thickness, 300nm width and *c.a.* 10um long): width and residual plane stress. The resonance frequencies of all resonators in the array are measured, thus both deviation from the theoretical frequency spacing and absolute frequency of our 20 resonators in the array are used for calibration of effective mass. A two-step optimization routine is used in conjunction with a physical model and internal stress and beam width are deduced. With this method an extremely low absolute mass error (<1%) is demonstrated to be reached. This non-destructive technique based on electrical measurement is amenable to the future use of very large arrays (>1000 resonators) for very

short analysis time. This method can be extended for non-destructive characterization of nanomechanical resonators for different applications.

[1] S. Dominguez-Medina et al., Science 362, 918-922 (2018)

[2] A. Brenes et al., Mechanical Systems and Signal Processing 112, 10-21 (2018)

[3] E. Sage et al., Nature Communications 9 : 3283 (2018)

[4] O. Malvar et al., Nature Communications 7 : 13452 (2016).

Plasma Science and Technology Division
Room B131 - Session PS1+SE-MoM

Atmospheric-Pressure Plasmas
Moderators: Michael Gordon, University of California at Santa Barbara, François Reniers, Université Libre de Bruxelles

8:20am **PS1+SE-MoM-1 On the Versatility of Atmospheric Non-equilibrium Plasmas: Material Synthesis, Packaging Sanitation and Oncological Applications**, *Matteo Gherardi, V Colombo, F Barletta, A Bisag, C Bucci, F Capelli, R Laurita,* Alma Mater Studiorum-University of Bologna, Italy*; E Mezzofanti,* AlmaPlasma srl*; T Gallingani,* Alma Mater Studiorum-University of Bologna, Italy, Italia*; G Girolimetti, S Coluccelli, L Amato, G Gasparre,* S.Orsola-Malpighi Hospital, Bologna, Italy*; M Perrone,* S. Orsola-Malpighi Hospital, Bologna, Italy*; A Porcelli,* Alma Mater Studiorum-University of Bologna, Italy*; P De Iaco,* S. Orsola-Malpighi Hospital, Bologna, Italy **INVITED**

Non-equilibrium atmospheric pressure plasmas (APPs) are an extremely versatile sources of reactive species, UV radiation, radicals and electrons, showing the promise of new medical therapies and offering innovative means to induce chemical reactions and synthesize materials. Trying to capture the versatility of this technology and to depict the current challenges, the presentation will deal with three different technological applications of APPs.

In the first part of the talk, APP biocidal potential is discussed in the industrial perspective of producers of food/beverage packaging and packaging machines. In this field, a fast and economic packaging sanitation is required in order to guarantee a sufficient shelf life to the product. Advantages and limitations of APPs with respect to conventional technologies, as well as the challenges of scaling plasma equipment up to the dimensions required by the industrial production volumes will be discussed.

In the second part of the talk, recent findings on the oncological applications of APPs will be presented. The discussion will focus in particular on Epithelial Ovarian Cancer (EOC), the fifth leading cause of cancer-related death among women and a disease characterised by the diffusion of nodules or plaques from the ovary to the peritoneal surfaces (carcinosis), with a poor prognosis at diagnosis (15-20% within 5 years) in advanced stages (III-IV). Due to the limitations of the currently available therapeutic options, the use of APPs is envisioned to produce plasma activated liquids (PALs) containing reactive oxygen and nitrogen species (RONS) to wash the intraperitoneal cavity with the aim of selectively provoking apoptosis in cancer cells without damaging the healthy ones.

Finally, the use of APPs for the synthesis of materials will be discussed in the frame of the development of an innovative multi-layer coating able to reduce biofilm proliferation onto a biomedical device, while at the same time preserving its bio- and hemo-compatibility, avoiding blood clots formation. An APP assisted process is here used to deposit all the different layers of the coating, composed by silver nanoparticles (AgNPs) embedded in a plasma polymerized HMDSO (ppHMDSO) matrix. The coating characteristics will be discussed in light of the results provided by chemo-morphological analysis and cellular and anti-biofilm assays.

9:00am **PS1+SE-MoM-3 Spectroscopic Characterization of a Multi-pins Plasma System**, *M Gulan, R Muddiman, Vladimir Milosavljevic,* Technological University Dublin, Ireland

The generation of high-energetic species in plasma in plasma using electrical discharge in ambient air renders possible applications such as material functionalization or water treatment. In atmospheric pressure, to get a stable and reproducible plasma discharge, additional to the electrodes, a dielectric would be required. The function of this dielectric is to spread the electrical charge throughout the entire electrode in order to create multiple conducting paths for the discharges to occur. This is the foundation of the Dielectric-barrier discharge (DBD). One or both electrodes in DBD could be covered by a dielectric material which serves as

an electric polarizer, and helps maintain a low gas temperature. Over the course of its life, for any DBD system, the biggest disadvantage is the dielectric contamination. In most cases, this dielectric is a polymer, and polymers are very fragile materials, which cannot be sterilised or cleaned. This work presents research of pulsing plasma systems (PPS) which can run at atmospheric pressure under various external parameters. The system has a planar electrode configuration with a bottom (grounded) flat electrode and a top pin array electrode (high voltage). The design of PPS allows setting several parameters such as: discharge frequency (30-125 kHz), duty cycle (1-100%), pulse frequency (100-3000 Hz), peak-to-peak voltage (up 60 kV), power (up to 700 W), distance between electrodes (up to 55mm), and treatment time (unlimited). The new plasma system allows an increase in the surface-plasma interaction selectivity and reduces plasma induced damages to the surface.

In this work, the study and diagnostics of plasma includes: optical emission spectroscopy (OES), optical absorption spectroscopy (OAS), and phase resolved optical emission spectroscopy (PROES). These optical diagnostic methods are applied to study the temporal and spatial characteristics of the reactive species produced. Due to its simplicity, optical spectroscopy is commonly used for the measurement and real time monitoring of plasma radicals and plasma kinetic processes. For comparison purposes, the absolute spectral intensity measurement of the atomic lines and molecular bands associated with helium, argon, oxygen, and nitrogen are included.

9:20am PS1+SE-MoM-4 Breaching Debye Law by Coupling of Y2O3 Vapor Carrying Focused Atmospheric ICP Beam Penetrating Showernead's Holes with Opposite CCP Discharge during Chemical Corrosion Barrier Coating in Open Air, *Yuri Glukhoy,* Nanocoating Plasma Systems Inc

Debye screening is considering as a dielectric phenomenon associated with plasma-solid state interaction and redistribution of space charge in the front of the wall. It prevents penetration into the plasma bulk by an external electric field. On the other hand, Debye screening characterized by the Debye length prevents penetration of plasma inside the holes with the size that is less than this length. This is the main obstacle in plasma chemical corrosion protective coating of the inner walls of the gas holes of showerheads used in the wafer etching processors. Such holes having diameter 0.5 mm and 10 mm depth believed to be not penetrable using the conventional PVD and CVD methods of deposition of the corrosion-resistant films. However, breaching the Debye Law was achieved in our open-air nanocoating process with a focused Atmospheric Pressure Inductively Coupled Plasma (AP-ICP) beam. Such beam having 0.1 mm crossover could deliver inside the holes chemicals for cleaning the inner surface and YSZ vapor droplets created by preliminary melting and vaporization of commercial nanoparticles in the high-temperature atmospheric plasma discharge, from which such beam was originated. As a focused heat source, this beam can provide inside the hole three consecutive processes like chemical cleaning, Y2O3 deposition and final annealing for the transition of deposited amorphous nanolayer to nanocrystalline. However, the Debye layer in the entrance of the gas hole may obstruct such penetration in this case, also. In order to neutralize this layer, the vacuum chuck holding the showerhead was supplied by the means for the generation of CCP discharge in the vicinity of the outlets of the holes in the backside of the showerhead. Due to a small number of neutrals of the beam breaking-through the Debye layer and penetrate the hole, as well as the bottom CCP discharge, this discharge ionizing such neutrals established capacitive coupling with this layer in spite of its remoteness. Finally, the Debye layer is neutralized by displacement current from the RF generator sustaining the CCP discharge. The released AP-ICP beam. receiving access to the inlet and propagating along the hole this beam beside delivering the Y2O3 vapor for deposition and heat for annealing has the ability to neutralize the Debye layer without the additional help of the auxiliary CCP discharge investing own positive plasma species. Uniformity of thickness of the Y2O3 layers inside the holes can be achieved by deposition from both sides of the showerhead. Cross-sectional SEM images recording interface morphology and thickness of the nanolayer deposited on the inner walls of the hole will be demonstrated.

9:40am PS1+SE-MoM-5 Streamers Effects in Cold Atmospheric Plasma Applications: Coatings, Gas Conversion, Surface Chemistries, *A Ozkan, J Mertens, François Reniers,* Université Libre de Bruxelles, Belgium

For a long time, research in atmospheric plasma dielectric barrier discharges (DBDs) focused on homogeneous discharges. However, most of the DBDs present inhomogeneities in the form of streamers.

In this presentation, we aim at showing the drastic effect of these streamers on the chemical reactivity of the discharges. Consequences can

be found for instance on the chemistry and on the roughness of plasma deposited coatings, on the deposition rates, or on the conversion of gases inside the discharge. These streamers can be studied through a high speed/high sensitivity camera, and by recording the current – voltage curves with a Rogowski coil on an oscilloscope. The chemistry in the plasma phase is studied using mass spectrometry, optical emission spectroscopy and gas chromatography. Roughness can be measured using profilometry or AFM, and the surface chemistry is analyzed by XPS.

The effect of the streamers will be demonstrated using the following examples :

- the plasma polymerization of CFx coatings, in Argon or Helium leads to different coatings chemistriess and roughnesses, induced by the streamers. This leads to coatings with contact angle varying from 110° (PTFE like) to more than 140°.

- the plasma polymerization of anhydrides shows that the number of streamers depends on the nature of the anhydride injected, and more specifically on the presence of double bonds, and their location. This affects the final chemistry of the coatings, but also the deposition rate.

- the conversion of CO_2 by a DBD is a highly filamentary discharge. Although this is due to the electronegative nature of CO_2, we show that, by changing the dielectric, and by playing with the plasma parameters, one can significantly vary the number of streamers. We also show that this number of streamers seems to be a key factor for the gas conversion.

10:00am PS1+SE-MoM-6 Improved Water Intrusion Resistance on Adhesive Bonded Metals using Atmospheric CVD SiO2 Barrier Coatings, *Zachary Jeckell,* D Patel, T Choi, M Schmid, L Bónová, D Barlaz, D Ruzic, University of Illinois at Urbana-Champaign; *I Shchelkanov, B Jurczyk,* Starfire Industries LLC

Lightweight manufacturing, specifically the bonding of dissimilar metals is gaining traction lately as the automobile industry looks for new ways to reduce the weight of their vehicles without compromising the safety or performance. However, current technologies such as spot welding can either be difficult, as is the case for aluminum and magnesium, or impossible as is the case for carbon fiber reinforced polymers. The Center for Plasma Material Interactions (CPMI) has developed a scalable method for performing atmospheric plasma enhanced chemical vapor deposition (AP-CVD) using a 2.45 GHz microwave power supply and a torch design that allows for inline precursor delivery to the plasma. Atmospheric plasmas offer unique advantages for manufacturing, such as the potential to be directly integrated into an assembly line, as well as the ability to deposit on complex geometries. This research investigates the feasibility of depositing SiO2, using hexamethyldisiloxane (HMDSO) as the chemical precursor, onto materials commonly used in lightweight manufacturing and then applying an automotive adhesive to bond the materials together. The silica layer is intended to function as both an adhesion promoter as well as a water barrier coating. The composition of the film is verified using XPS, and the film morphology and thickness are observed using cross-sectional SEM to verify that the deposited film is dense and in the range of 10-100 nm. The robustness of these films is determined by adhesion testing following deposition of silica, as well as after water soak testing which are used to simulate prolonged exposure to realistic environments. Preliminary water soak testing on aluminum has shown a decrease in max stress of 2.5% after 168 hours of water soak at 55 °C, which is a significant improvement over the 25% benchmark currently used in the automotive industry.

10:40am PS1+SE-MoM-8 OES Imaging and Double Langmuir Probe Studies of Flow-through, Supersonic Microplasma Jet Sources, *K Mackie, Michael Gordon,* University of California at Santa Barbara

Spatially-resolved OES imaging and double Langmuir probe (DLP) measurements were carried out on flow-through supersonic microplasma jets to highlight how plasma operating conditions (e.g., pressure, current, presence of growth precursors/O_2, distance from the nozzle) affect the local gas (T_{rot} and T_{trans}) and electron (T_e) temperatures in the plasma jet plume. T_{rot} and T_{vib} were estimated using semi-empirical and rigorous quantum mechanical fits to OES spectra of the first positive group of N_2 ($B^3\Pi$ --> $A^3\Sigma_u^+$), and T_e was obtained via fits to DLP IV curves. Experiments on Ar jets with downstream pressures in the 10-200 Torr regime yielded estimates of $T_{rot} = T_g$ and T_{vib} of 500-700 K and 5000-6000 K, respectively, using two independent methods. DLP data gave estimates of T_e in the 1-3 eV range, which depended on the exact location in the expanding jet plume. The transition between a pre-discharge-like operating regime at low plasma currents to true hollow cathode operation at high currents was also observed in the plasma IV characteristic and companion OES measurements. The talk will highlight OES imaging and DLP results, as well

as the effect of gas additives, i.e., the presence of film deposition precursors and/or oxidants in the jet feed vs. background gas, on jet operating characteristics (T_e, T_{gas}, etc.).

11:00am PS1+SE-MoM-9 Time-resolved Optical Emission Spectroscopy of an Atmospheric Pressure Plasma Jet – Surface Interaction, *Michael Johnson, D Boris, T Petrova, S Walton,* U.S. Naval Research Laboratory

Atmospheric pressure plasma jets (APPJs) have become a valuable tool for the modification of surfaces. One of the large benefits of APPJs is their ability to generate a chemically-rich environment in open air, allowing for the modification of a board range of surfaces including metals, polymers, ceramics, and biological materials. However, when an APPJ interacts with a surface, the surface will influence the structure of the plasma jet and thereby alter the chemistry of the jet. This is particularly vital because different chemical species important for surface modification will form in different quantities depending on the surface. Because of this, two different surfaces treated by the same plasma jet will undergo exposure to slightly different conditions. In this work, time-resolved measurements of the optical emission of a pulsed-DC plasma jet impinging on different surface is measured to investigate how the structure and chemistry of the plasma on the surface evolve in time. Initially, the plasma source emits a streamer which propagates out from the jet nozzle into the open air and eventually collides the surface. With a metal surface, a 'secondary stroke' forms on the surface and extends back towards the jet outlet. The formation, extension, and duration of the stroke are functions of the pulse width and frequency of the voltage waveform used to generate the plasma jet. The metal surface allows for the formation of a long-lived, surface plasma that exists for the duration of the pulse. If a dielectric surface is impinged with the APPJ, the streamer will strike the surface and produces an ionization wave that extends along the surface. The ionization wave is short-lived and not significantly affected by the length of the pulse. This work is supported by the Naval Research Laboratory base program.

11:20am PS1+SE-MoM-10 Atmospheric-Pressure Plasmas As Ionization Sources For Atomic, Molecular, And Biological Mass Spectrometry, *Jacob Shelley, S Badal, C Walton, G MacLean,* Rensselaer Polytechnic Institute*; I Ayodeji,* University of South Florida*; G Chan,* Lawrence Berkeley National Laboratory*; T Evans-Nguyen,* University of South Florida **INVITED**

Analytical plasmas that operate at ambient pressures and mass spectrometry (MS) have been in a symbiotic relationship since the near-coincident advent of the inductively coupled plasma (ICP) ionization source and atmospheric-pressure (AP) inlets for mass spectrometers. Preceding that discovery by only a few years, it was shown that low-power plasmas could be used for soft ionization of intact molecules through chemical ionization pathways. More recently, analytical plasma source development has seen a resurgence with the realization of a variety of low-power AP plasma designs useful as MS ionization sources. AP plasmas are unique in that they have the ability to create a wide-range of energetic species useful for desorption and/or ionization processes.

Plasmas produce highly energetic species (e.g., ions, metastable neutrals, fast electrons, etc.), which can lead to high-energy physical or chemical processes to fragment and ionize molecules. This fragmentation can be so extensive that molecules are broken down into bare elemental constituents. In addition, low-energy ionization reactions can also occur due to the abundance of collisional cooling that can take place at ambient pressures. For instance, the helium-based flowing atmospheric-pressure afterglow (FAPA) source has been shown to produce intact molecular ions of molecular species with quite high ionization efficiencies.

This presentation will demonstrate the broad utility and range of applications of low-power AP glow discharges, specifically the FAPA discharge, and the solution-cathode glow discharge (SCGD). The possibilities of these devices extend well beyond conventional atomic and small molecule detection. By tuning the chemistry of the discharge, we can alter conventional ionization modes to encompass elemental analysis to biomolecular detection to polymer analysis. For instance, our group has developed a method to detect elemental ions with FAPA-MS via online complexation reactions with volatile ligands. But, the open-air nature of FAPA can produce isobaric interferences from ambient species. To overcome this issue, differential mobility spectrometry was used as a post-ionization filter to remove background ions. Ultimately, FAPA-DMS may dramatically improve selectivity and sensitivity in fieldable MS applications. Meanwhile, it was found that SCGD-MS could be used for the detection of atomic, molecular, and biological species directly from solutions. Furthermore, it was found that peptides could be tunably fragmented at

atmospheric pressure, which led to 100% sequence coverage for many of the peptides examined.

Plasma Science and Technology Division
Room B130 - Session PS2-MoM

Plasma Modeling

Moderators: Mingmei Wang, TEL Technology Center, America, LLC, Nathan Marchack, IBM T.J. Watson Research Center

8:20am PS2-MoM-1 Computational Modeling of Capacitively Coupled Plasmas at Moderate Pressures in gases of Argon, Helium and Nitrogen, *Wei Tian,* Applied Materials*; D Peterson, S Shannon,* North Carolina State University*; S Rauf,* Applied Materials

Shrinking features and 3D structures in integrated circuits are pushing the semiconductor manufacturing processes to a new level of complexity. Processes that combine etching and deposition steps including rapid cycling between them have become important to achieve the desired features and structures. A plasma source design which enables etching and deposition in the same chamber is desirable. In this paper, we report on a computational investigation of capacitively coupled plasmas in the same reactor with pressure ranging from 0.1 Torr to 4.0 Torr in Ar, He and N_2, respectively. The pressure range covers typical etching and deposition conditions. Spatio-temporal profiles of plasma properties along with voltage and current characteristics are compared with experimental results. In this reactor, the plasma is formed in the gap between the top powered electrode and bottom grounded electrode. Electron density peaks at the chamber center at lower pressure, < 0.5 Torr, and becomes concentrated near the top edge when pressure is increased. In He plasma, electrons are produced mainly through electron impact ionization at lower pressure; at higher pressure, Penning ionization starts to dominate. In Ar plasma, electron impact ionization always dominates electron production due to lower Ar ionization threshold. Both in He and Ar plasma, the rf voltage decreases with the pressure. In contrast to the atomic gases, the N_2 plasma exhibits a more localized plasma density profile. The rf voltage does not monotonically change with the pressure. The rf voltage decreases from 0.1 Torr to 0.75 Torr in N_2 plasma and increases with higher pressure.

8:40am PS2-MoM-2 Relation between Atomic Interaction Parameters of a Surface Material and its Physical Sputtering Yield; How to Predict the Etching Rate based on the Surface Material Properties, *Nicolas Mauchamp, M Isobe, S Hamaguchi,* Osaka University, Japan

Since the invention of a transistor in the last century, the typical dimensions of semiconductor devices have diminished and are now reaching the atomic sizes. Plasma etching techniques have been widely used to manufacture semiconductor devices. However, as the device dimensions decrease and a wider variety of materials are used to form highly advanced devices, the precise control of device structures during the etching process has become extremely challenging. A better understanding of plasma-surface interactions during the etching process is expected to help one obtain the desired device structures and avoid unwanted effects such as damage formation during the etching processes. Plasma-surface interaction with surface chemical reactions and collision cascade due to energetic ion impact have been widely studied both experimentally and theoretically. Such interaction should be determined from atomic interactions among atoms and ions involved in the process, so that once the material properties of the surface and physical properties of incident ions and radicals are known, macroscopic surface reaction properties such as the etching rate and resulting surface chemical compositions should be predictable. However, the relation between such atomic properties and macroscopic process parameters are so complex that few (empirical) formulas exist that relate material properties and process properties (e.g., etching rate) and are valid under wide process conditions.

In this study, we consider a Lennard-Jones (LJ) solid, which is an FCC crystalline solid made of particles interacting through a simple two-body LJ potential function, and analyze its physical sputtering properties using Molecular Dynamics (MD) simulation. The goal of this study is to understand the dependency of the physical sputtering yield, a macroscopic and non-thermodynamic property of the material, on the interatomic potential functions [1]. In this presentation, we focus our discussion on the sputtering yields at high incident ion energies, where the sputtering yield depends sensitively on the repulsive potential of the surface atoms and incident ions. We also compare the simulation results with experimental sputtering yield data archived in Ref. [2], in an attempt to relate

thermodynamical properties of the surface material and atomic properties of incident ions to the observed sputtering yield, based on an analogy to the sputtering properties of the LJ system that we analyze in detail in this study.

[1]N. A. Mauchamp, et al., AVS 65th International Symposium and Exhibition, PS-FrM05 (2018).

[2]Y. Yamamura and H. Tawara, Atomic Data and Nuclear Data Tables 62, 149-253 (1996).

9:00am **PS2-MoM-3 Investigation on the Uniformity Control of the Electron and the Ion Kinetics in a Capacitively Coupled Plasma Reactor using a Parallelized Particle-in-Cell Simulation**, *Hae June Lee,* Pusan National University, Republic of Korea*; H Kim,* Dong A Uiversity, Republic of Korea*; J Kim,* Tokyo Electron Technology Solutions Limited, Japan   **INVITED**
The radially non-uniform power absorption in a capacitively coupled plasma (CCP) causes non-uniform plasma density and temperature which results in the spatial variations of etching or deposition profiles. In this study, we investigate the electron energy probability function (EEPF) in the bulk plasma and the ion energy and angle distribution function (IEADF) on the substrate using a two-dimensional particle-in-cell simulation. The spatial variation of the EEPFs and the IEADFs are observed with the variation of the electrode structure and the gas pressure. The non-uniform transition of the heating mode from stochastic heating to Ohmic heating was observed to be enhanced with the side wall effect in CCP deposition reactors. While the ionization rate is affected by the heating mode transition and the electron density, the IEADFs are mainly affected by the time-average potential profiles for a single high-frequency CCP. However, the dual frequency CCP has more variety for the control of the IEADF uniformity.

9:40am **PS2-MoM-5 Capacitively Coupled Plasma Uniformity Improvement Using Phase and Amplitude Control of Electrode Potential**, *Xiaopu Li, K Bera, S Rauf,* Applied Materials
Capacitively coupled plasmas (CCPs) are widely used for semiconductor material processing to provide uniform active neutral and ion fluxes and their energies that lead to on-wafer process uniformity. High density discharge at Very High Frequency (VHF) is required to produce enough reactive radicals for Plasma Enhanced- Chemical Vapor Deposition (PE-CVD), Atomic Layer Deposition (PE-ALD) and Atomic Layer Etching (PE-ALE). However, the uniformity of discharge profile is strongly affected by both electrostatic coupling and electromagnetic standing wave effects that depend on reactor design and operating conditions. Consequently, it is challenging to achieve adequate on-wafer uniformity using high-density discharge that utilizes high power density. Electric potential modulation has been proposed for the uniformity control of VHF CCPs using external circuits [1], and separate power sources [2]. In the present work, a compact size reactor is modeled with parallel plate electrodes and grounded chamber walls at moderately high pressure driven by power in kWs. The amplitudes and phases of electrode potentials are modulated by external circuits or two separate power sources. The discharge profile is systematically investigated by a fluid-based plasma model using Ar discharge [3]. This study demonstrates a tunable plasma profile using phase and amplitude control of electrode potential, which is important to achieve flexible uniformity control in high-density VHF CCPs.

1. Bera, K., et al. IEEE Transactions on Plasma Science 38.11 (2010): 3241-3248.

2. Bera, K., et al. Journal of Applied Physics 106.3 (2009): 033301.

3. Agarwal, A., et al. J. Phys. D: Appl. Phys. 50 (2017): 424001 (13pp).

10:00am **PS2-MoM-6 Kinetic Modeling of Non-Equilibrium Plasmas for Modern Applications**, *Igor Kaganovich, A Khrabrov, A Powis,* Princeton Plasma Physics Laboratory
We have studied several non-equilibrium plasma devices where kinetic effects determine plasma self-organization: neutralization of ion beams and electron cloud effects in accelerators, negative hydrogen Ion Sources, ExB discharges (plasma switch and Penning discharge), thermoelectric converters.

Neutralization of positive ion beam space-charge by electrons is important for many accelerator applications, i.e., heavy ion inertial fusion, and ion beam-based surface engineering. Past experimental studies showed poorer ion beam neutralization by electron-emitting filaments, compared with neutralization by plasmas. Now researchers have found that reduced neutralization may be related to the generation of electrostatic solitary

waves (ESWs) during the neutralization process, as the ion beam passes through the electron-emitting filaments. [1].

We have also developed a Global Model Code for Negative Hydrogen Ion Sources, GMNIS [2]. The codes ultimate goal is to aid developing optimized negative ion beams for ITER. The code solves volume-averaged equations: continuity for plasma species and electron energy equation for the electron temperature, and include more than 1000 volumetric and surface reactions for interactions of electrons, ground-state atomic and molecular hydrogen, molecular ions and atomic ions, negative ions, 14 vibrationally-excited states of molecular hydrogen, and excited atoms. Results of the code are benchmarked against another code [2]. Convenient analytical solution for vibrational spectrum of H_2 was also derived.

We have studied the low-pressure (left-hand) branch of the Paschen curve at very high voltage when electrons are in the runaway regime and charge exchange/ionization avalanche by ions and fast neutral atoms becomes important for plasma switch application, which operates at 100-500KV range. For these voltages, a multi valued Pashen curve was observed. We performed particle-in-cell simulations and developed analytical model that can explain experimentally observed Pashen curve .[3]

We have also preformed studies of rotating spoke in a Penning discharge and proposed analytical scaling law for its frequency [4].

Efficient thermal electric converter is proposed in Ref.[5].

References

[1] C. Lan and I. D. Kaganovich, arXiv:1810.04655 and accepted Phys. Plasmas (2019) - feature article.

[2] W. Yang, et al, Phys. Plasmas **25**, 113509 (2018).

[3] Liang Xu, et al, Plasma Sources Sci. Technol. **27**, 104004 (2018).

[4] Andrew T. Powis, et al., Physics of Plasmas **25**, 072110 (2018).

[5] A. S. Mustafaev, et al, Journal of Applied Physics **124**, 123304 (2018).

10:40am **PS2-MoM-8 Automated Reduction of Plasma Chemistry Sets**, *Sebastian Mohr,* Quantemol Ltd., UK*; M Hanicinec,* University College London, UK*; A Dzarasova,* Quantemol Ltd., UK*; J Tennyson,* University College London, UK
Simulating plasma reactors in multi-gas mixtures easily leads to chemistry sets comprising dozens of species and many hundreds of reactions. Including such complex chemistry sets in spatially resolved plasma models quickly becomes infeasible due to the high computational cost. Hence, it is desirable to keep a chemistry set simple while preserving the behavior of the plasma with regards to the density etc. of key species such as the radicals interacting with the surface. We are developing an algorithm within the Quantemol Database (QDB) [1] to automate this simplification for specified process parameters such as pressure, power, and gas mixture [2]. The algorithm will select a minimum set of species and reactions from the entirety of the database, which produce the same results with regards to user-specified species and the desired accuracy.

The challenge here is to find a reduction method, which can be automated reliably with minimum human input and is computationally cheap enough to run within the QDB framework. One method, which satisfies the need for quick calculation times is to run a 0D model with the full set of reactions and species, identify species with negligible densities, and remove these and associated reactions from the chemistry set. This requires only one run of the 0D model and a check of the species densities with the set threshold density. However, there are a few pitfalls concerning reliable automation. For example, a specie might have a low density in the steady state solution but act as a precursor for a more numerous specie, which would be missed by such an algorithm.

On the other side of the spectrum is the Morris method [3] based on Monte Carlo techniques. Here, the rate coefficients for the specific reactions are randomly changed for each run of the model. The effect of each reaction on the plasma system can be evaluated by the perturbations of, for example, densities of specified species caused by the variation in the rate coefficients. Reactions with low impact can be removed as well as species whose reactions showed no significant effect. This method is much more reliable without additional human input but requires a large number of simulation runs to gather enough data. Hence, it might be unfeasible to be used within the QDB infrastructure.

Given this, we require a method between these two extremes. Here, we will present our assessment of different methods, the current stage of development, and examples for chemistry reduction for specific process parameters.

[1] Tennyson J et al. Plasma Sources Sci. Technol. 26 (2017) 055014

[2] Ayilaran A, J Plasma Sci. Tech., 21 (2019) 064006

[2] Morris M D Technometrics 33 (1991) 161

11:00am PS2-MoM-9 Prediction of Etch Rates for New Materials by Machine Learning - Case Study for Physical Sputtering, *Kazumasa Ikuse,* Osaka University, Japan*; H Kino,* National Institute for Materials Science (NIMS), Japan*; S Hamaguchi,* Osaka University, Japan

Due to the latest development of new chip designs, various non-conventional materials, such as ferromagnetic metals for magnetoresistive random access memories (MRAMs) and perovskite-type oxides for resistive random access memories (ReRAMs), have been introduced to microelectronics devices and required to be processed together with conventional Si based materials in the chip manufacturing processes. Furthermore, as the device dimensions are approaching the atomic scale, new process technologies, such as atomic-layer deposition (ALD) and atomic-layer etching (ALE), have been introduced to the surface processing, where the interactions between the processed surface and newly introduced gaseous species are not necessarily well understood. Having a variety of choices for surface materials and process conditions increases the complexity of process development because of our insufficient knowledge on surface reactions in the new processes. With a large number of possible choices of process conditions, exhaustive search for process optimization by experiments is prohibitively expensive. One of the possible solutions to this problem is to use machine learning (ML) to predict certain characteristics of the surface reactions such as the etching/deposition rates and surface chemical compositions, based on the existing knowledge of materials and gas-phase molecules involved in the new processes.

As the first step to develop such technologies based on data driven science, we have developed a system to predict the physical sputtering yields of single-element materials under single-species ion bombardment [1,2], based on the experimental sputtering yield data provided in Ref. [3]. Identification of the material/ion properties, which we call "descriptors," that the sputtering yield strongly depends on is the key for the successful prediction of sputtering yields under unknown conditions. In this study, the selection of descriptors was performed by the sparse modeling with the exhaustive search method [4] and the subgroup relevance method [5].

[1] H. Kino, K. Ikuse, H. C. Dam, and S. Hamaguchi, 2nd International Conference on Data Drive Plasma Science (Marseille, 2019).

[2] K. Ikuse, K. Kino, and S. Hamaguchi, ibid.

[3] Y. Yamamura and H. Tawara, Atomic Data and Nuclear Data Tables 62, 149-253 (1996).

[4] K. Nagata, J. Kitazono, S. Nakajima, S. Eifuku, R. Tamura and M. Okada, IPSJ Online Transactions 8, 25 (2015).

[5] H. C. Dam, V. C. Nguyen, T. L.Pham, A.T. Nguyen, K. Terakura, T. Miyake and H. Kino, J. Phys. Soc. Jpn 87, 113801 (2018).

11:20am PS2-MoM-10 Maskless and Contactless Patterned Silicon Deposition using a Localized PECVD Process, *Ronan Leal, B Bruneau, P Bulkin, T Novikova, F Silva,* LPICM, CNRS, Ecole Polytechnique, Institut Polytechnique de Paris, France*; N Habka,* TOTAL GRP - New Energies, France*; E Johnson,* LPICM, CNRS, Ecole Polytechnique, Institut Polytechnique de Paris, France

We present a novel technique to perform contactless and mask-free patterned plasma enhanced chemical vapor deposition (PECVD) and etching. When a powered electrode with narrow slits is placed very close to the substrate, plasma is selectively ignited within the slits due to the hollow cathode effect, and so deposition or etching occurs only within an area smaller than the size of the slit. This technique is demonstrated through the deposition of hydrogenated amorphous silicon using a gas mixture of hydrogen and silane. Slits as small as 1 mm generate a plasma, and for this width, the lines deposited are about 750 μm wide, homogenous over their length (60 mm), and are deposited at a rate of 50 nm/min. The phenomenon is studied using Particle In Cell (PIC) modelling. The electron localization observed in the PIC modelling provides an explanation of why the deposition is narrower than the slit. In addition, an excellent correlation between results of modeled ion flux profile and experimental etching profile is observed.

This technique offers several advantages as it allows the lithographic function to be performed (i) directly, including for high quality semiconductor layers that can be deposited using PECVD, and (ii) in a contactless fashion, as the technique does not require a mask to be in contact with the substrate, (iii) at high rates without depositing powder, and (iv) in a reactor chamber that can be also used to deposit homogenous blanket layers simply by backing the electrode away from the surface.

Materials and Processes for Quantum Information, Computing and Science Focus Topic
Room B231-232 - Session QS+EM+MN+NS-MoM

High Coherence Qubits for Quantum Computing

Moderators: Vivekananda Adiga, IBM, T.J. Watson Research Center, Martina Esposito, Oxford University, UK

8:20am QS+EM+MN+NS-MoM-1 Measurement of a Two-Level-System Dipole Distribution in a Nanoscale Aluminum Oxide Barrier, *Chih-Chiao Hung, N Foroozani, K Osborn,* University of Maryland

Random atomic-sized material defects, identified as two-level systems (TLS), have garnered wide interest because they cause decoherence in superconducting qubits. TLSs often arise in the nonlinear element, the Josephson junction, which is typically made of amorphous aluminum oxide. This material is a clear concern in qubits due to a substantial loss tangent in bulk: large area JJs. However, detail on the dipole moments of individual TLSs is generally lacking but is fundamental to defect-qubit coupling. We have recently developed a method to study individual dipole moments in thin dielectric films with a quantum regime resonator using an electrical bridge of capacitors. We have now extended this technique to a different material, aluminum oxide, using a smaller nanoscale thicknesses and barrier volume. The geometry of the device allows extraction of the individual dipole moments within the central layer of a superconductor-aluminum oxide-superconductor trilayer. This new study also produced a greater statistical sample of TLS dipoles than previous work. Preliminary analysis allows us to extract a dipole moment distribution with a clear mean value. This information on aluminum oxide can be used in the future modeling of qubits and the future characterization of qubit materials.

8:40am QS+EM+MN+NS-MoM-2 Mapping Quantum Systems to Quantum Computers using Symmetry, *Daniel Gunlycke, S Fischer, S Hellberg, S Policastro, S Tafur,* U.S. Naval Research Laboratory

Quantum entanglement is a natural phenomenon in quantum mechanics that has enormous significance in quantum information science, including quantum computing. It enters quantum states in quantum algorithms through the application of multi-qubit quantum logic operations such as the CNOT and Ising gates. While deliberate entanglement adds power and efficiency to algorithms, unintentional entanglement can be undesirable for a variety of reasons. Unintentional entanglement adds complexity, making the outcome of a given algorithm more difficult to understand, as well as more sensitive to errors. Furthermore, it can be an indication that an algorithm has not been optimized. If we could transfer entanglement from our algorithms into the bases that define our systems, then we could potentially reduce our algorithms, including the qubit requirement. Such algorithm reductions will be of outmost importance for resource-limited, noisy intermediate-scale quantum (NISQ) computers.

In this presentation, we will demonstrate how such a reduction could be achieved for the simulation of quantum systems using symmetry. In addition to reducing the needed resources, our quantum computer calculations show a significant improvement in accuracy.

9:00am QS+EM+MN+NS-MoM-3 History of Superconducting Qubit Coherence and the Current Challenges, *Hanhee Paik,* IBM T.J. Watson Research Center **INVITED**

Since the first demonstration of a few nanoseconds of coherent oscillations in 1999, a tremendous amount of effort has been put in to improve coherence of superconducting qubits. A modern day superconducting qubits show typically 100 microseconds of coherence times which allowed us to demonstrate a few simple quantum computing applications that led rapid growth of quantum computing industry. To build a full fault-tolerant universal quantum computing system, however, we still need a couple more orders of magnitude improvement in the superconducting qubit coherence, the solution to which, we believe, is in the qubit materials. In this talk, I will review the history of the superconducting qubit coherence research and what we learned about the materials for quantum computing at milli-kelvin temperatures, and I will discuss the current challenges of the coherence studies in the conjunction with the challenges in material science research.

9:40am QS+EM+MN+NS-MoM-5 Loss and Decoherence Benchmarking of Superconducting Transmon Qubits, *Jonas Bylander,* Chalmers University of Technology, Sweden **INVITED**

We are engineering a superconducting quantum processor within the Wallenberg Center for Quantum Technology [1] in Sweden and the project OpenSuperQ [2] of the European Union's Flagship on Quantum Technology.

Here we will present our engineering approach for high-coherence superconducting quantum hardware. We have studied the temporal stability of relaxation and dephasing in transmon qubits [3]. Our qubits are made of aluminum on silicon; they have reached average T_1 relaxation times of about 70 us. The T_2^* decoherence time, as measured in a Ramsey fringe, is practically relaxation-limited. By collecting statistics during measurements spanning several days, we reveal large fluctuations of qubit lifetimes – the standard deviation of T_1 is about 15 us – and find that the cause of fluctuations is parasitic, near-resonant two-level-systems (TLS). Our statistical analysis shows consistency with an interacting-TLS model. Interacting TLS also cause low-frequency capacitance fluctuations, ultimately leading to frequency noise and dephasing of the qubit state. These discoveries are important for creating stable superconducting circuits suitable for high-fidelity quantum gates in quantum computing applications.

[1] www.wacqt.se

[2] www.opensuperq.eu

[3] J. J. Burnett, A. Bengtsson, M. Scigliuzzo, D. Niepce, M. Kudra, P. Delsing, and J. Bylander, "Decoherence benchmarking of superconducting qubits" arXiv:1901.04417

10:40am QS+EM+MN+NS-MoM-8 Towards PAMBE Grown Nitride Superconductors for Epitaxial Josephson Junctions and Quantum Circuits, *Christopher Richardson, A Alexander, C Weddle,* Laboratory for Physical Sciences*; M Olszta, B Arey,* Pacific Northwest National Laboratory **INVITED**

Low microwave loss superconducting circuit components are a necessity of fabricating high-fidelity superconducting qubits. Accordingly, significant research has focused on making high-quality planar resonators from elemental and nitride superconductors. Josephson junctions are the nonlinear component of superconducting qubits, that also need to be high performance. Interestingly, superconducting qubits all use Josephson junctions fabricated from aluminum and aluminum oxide using the double angle evaporation process. Details of this alternative design will be presented.

Plasma assisted Molecular beam epitaxy (PAMBE) is used to grow niobium titanium nitride alloys ($Nb_xTi_{1-x}N$) and wide bandgap nitride (AlN) superconductors directly on sapphire wafers. This combination of nitride materials provides sufficient degrees of freedom that synthesis of an epitaxial Josephson junction may be possible. Using a structure first approach to design optimization, the structural, surface topology, chemical characteristics, and superconducting critical temperature of these films are used for optimization of the growth conditions before resonators are fabricated and tested.

Growth results of NbTiN and AlN films, bi-layer insulator-superconductor structures and trilayer superconductor-insulator-superconductor structures will be presented along with superconducting properties.

11:20am QS+EM+MN+NS-MoM-10 Josephson Junction Metrology for Superconducting Quantum Device Design, *Ruichen Zhao, M Bal, J Long, R Lake, X Wu, C Rae McRae, H Ku, H Wang, D Pappas,* National Institute of Standards and Technology (NIST)

Josephson junctions (JJs) are the power horses that drive the development of superconducting quantum technologies in the past decades. The non-linear inductance of JJs turns superconducting circuitry into a high-coherence two-level system that forms the foundation for quantum information processing [1]. They also enable Josephson parametric amplification that significantly improves the measurement of the fragile quantum state of superconducting qubits, mechanical oscillators or spins [2]. Consequently, the characterization of junction inductance becomes essential for the design and fabrication of these superconducting quantum devices.

Here, we present a systematic approach to characterize the micron-size JJs made from a new process. This new recipe extends from our previous work on nanoscale overlapping qubit junctions [1]. First, we collect statistics of the normal-state resistance over 2000 JJs through the room-temperature automated probing test. Second, we use Ambegaokar-baratoff formula to map the normal-state junction resistance into Josephson inductance [3]. Then we extract and investigate the process bias of our JJs. Based on this

new information of JJs variation, we proposed a new JJ process which could potentially provide better control over the Junction inductance and therefore, deliver more reliable parameters for the device design.

[1] X. Wu, et al. "Overlap junctions for high coherence superconducting qubits." Applied Physics Letters 111.3: 032602 (2017).

[2] M. Malnou, et al. Optimal operation of a Josephson parametric amplifier for vacuum squeezing. Physical Review Applied, 9(4), 044023 (2018).

[3] V. Ambegaokar, & A. Baratoff, "Tunneling between superconductors." Physical Review Letters, 10(11), 486 (1963).

11:40am QS+EM+MN+NS-MoM-11 Superconducting Metamaterial Resonator Spectrum and Interaction with Qubit, *Haozhi Wang, S Indrajeet, M Hutchings, M LaHaye, B Plourde,* Syracuse University*; B Taketani, F Wilhelm,* Saarland University

Metamaterial transmission line resonators fabricated from superconducting thin films can be designed to exhibit novel mode spectra like a high density of modes in the same frequency range where superconducting qubits are typically operated. We demonstrate the mode spectrum of a metamaterial resonator made of single layer of Nb and the coupling quality factor of the modes. We also present a series of low-temperature measurements of such a superconducting metamaterial resonator coupled to a flux-tunable transmon qubit. We observe Rabi vacuum crossing when performing transmission measurement of the metamaterial resonator as we tune the qubit frequency through many of the metamaterial resonances and we are able to track the qubit using a separate conventional resonator to read out the qubit state.

Thin Films Division
Room A122-123 - Session TF+EM+MI+MN+OX+PS-MoM

Functional Thin Films: Ferroelectric, Multiferroics, and Magnetic Materials

Moderators: Christophe Vallee, LTM - MINATEC - CEA/LETI, France, Jessica Kachian, Intel Corporation

8:20am TF+EM+MI+MN+OX+PS-MoM-1 A Room-Temperature Magnetoelectric Multiferroic made by Thin Film Alchemy, *D Schlom, Megan Holtz,* Cornell University **INVITED**

Materials that couple strong ferroelectric and ferromagnetic order hold tremendous promise for next-generation memory devices. Meticulous engineering has produced novel ferroelectric and multiferroic materials, although known single-phase multiferroics remain limited by antiferromagnetic or weak ferromagnetic alignments, by a lack of coupling between the order parameters, or by having properties that emerge only well below room temperature. Here we construct single-phase multiferroic materials in which ferroelectricity and strong magnetic ordering are coupled near room temperature. Starting with hexagonal $LuFeO_3$—a geometric ferroelectric with planar rumpling—we introduce individual monolayers of ferrimagnetic $LuFe_2O_4$ within the $LuFeO_3$ matrix, that is, $(LuFeO_3)_m/(LuFe_2O_4)_1$ superlattices. The rumpling of the $LuFeO_3$ drives the ferrimagnetic $LuFe_2O_4$ into a ferroelectric state, reducing the $LuFe_2O_4$ spin frustration. This increases the magnetic transition temperature to 281K for m=9. Moreover, the ferroelectric order couples to the ferrimagnetism, enabling direct electric-field control of magnetism at 200 kelvin. Further, charged ferroelectric domain walls align at $LuFe_2O_4$ layers, resulting in charge transfer which increases the magnetic moment. We are currently pursuing higher temperature multiferroics by incorporating cubic spinels with high magnetic ordering temperatures, such as $CoFe_2O_4$, into the $LuFeO_3$ matrix. Our results demonstrate a design methodology for creating higher-temperature magnetoelectric multiferroics through epitaxial engineering.

9:00am TF+EM+MI+MN+OX+PS-MoM-3 Magnetic Losses in FeGa/NiFe/Al₂O₃ Laminates for Strain-Mediated Multiferroic Micro-Antenna Applications, *Kevin Fitzell, A Acosta, C Rementer, D Schneider, Z Yao,* University of California, Los Angeles*; C Dong,* Northeastern University*; M Jamer, D Gopman, J Borchers, B Kirby,* National Institute of Standards and Technology (NIST)*; N Sun,* Northeastern University*; Y Wang, G Carman, J Chang,* University of California, Los Angeles

The ability to reduce the size of antennae would enable a revolution in wearable and implantable electronic devices. Multiferroic antennae, composed of individual ferromagnetic and piezoelectric phases, could reduce antenna size by up to five orders of magnitude through the efficient

coupling of magnetization and electric polarization via strain. This strategy requires a material with strong magnetoelastic coupling and acceptable magnetic losses at high frequency.

Galfenol ($Fe_{84}Ga_{16}$ or FeGa) is a promising candidate material due to its large magnetostriction (200 $\mu\varepsilon$), large piezomagnetic coefficient (5 ppm/Oe), and high stiffness (60 GPa), but it is highly lossy in the GHz regime. On the other hand, Permalloy ($Ni_{81}Fe_{19}$ or NiFe) is a soft magnetic material that has very low loss in the GHz regime, with a ferromagnetic resonance (FMR) linewidth of 10 Oe, but almost no magnetostriction. In this work, nanoscale laminates containing alternating layers of FeGa and NiFe were fabricated via DC magnetron sputtering to combine the complementary properties of the two magnetic phases, resulting in a composite material with a small coercive field, narrow FMR linewidth, and high permeability (Rementer et al., 2017). Optical magnetostriction measurements confirmed that these laminates retain the large saturation magnetostriction of FeGa (200 $\mu\varepsilon$) while enhancing the piezomagnetic coefficient (7 ppm/Oe), allowing for optimal piezomagnetic actuation at substantially reduced magnetic bias fields. Furthermore, multiferroic composites incorporating these magnetic laminates were studied via polarized neutron reflectometry, demonstrating uniform rotation of the individual layers' magnetization with an applied electric field across distances much larger than the exchange length of either material.

Due to the metallic nature of these FeGa/NiFe multilayer composites, however, resulting devices would be inefficient due to the generation of eddy currents at high frequency. To mitigate these losses, ultrathin layers of Al_2O_3 were incorporated into the multilayer materials to reduce the conductivity and mitigate the generation of eddy currents. The effect of Al_2O_3 thickness, FeGa:NiFe volume ratio, and multilayer architecture on the soft magnetic properties was also studied, resulting in a 50% reduction in the FMR linewidth. Optimized magnetic laminates were shown to exhibit a small coercive field (<20 Oe), narrow ferromagnetic resonance linewidth (<50 Oe), and high relative permeability (>500) while maintaining excellent magnetoelastic coupling, showing great promise for the use of FeGa/NiFe/Al_2O_3 laminates in strain-mediated micro-scale communications systems.

9:20am **TF+EM+MI+MN+OX+PS-MoM-4 Multiferroic Gd-substituted HfO₂Thin Films**, *John Hayden, F Scurti, J Schwartz, J Maria,* Pennsylvania State University

Modern ferroelectric technologies utilize perovskite structured materials, which have limited Si compatibility and modest bandgaps requiring thick films to reduce leakage current, hindering their implementation in realizable thin film devices. HfO_2 has been extensively researched as a gate dielectric thin film with excellent Si processing compatibility and has recently been found to exhibit ferroelectricity induced by a combination of impurity substitution, mechanical confinement by capping, intergranular surface area, and film thickness effects. This work investigates the microstructural characteristics, the ferroelectric response, and the potential for concomitant magnetic properties in sputtered Gd:HfO_2 thin films.

Gd-substituted HfO_2 thin films are a promising candidate as a multiferroic material, due to the presence of the magnetically active Gd^{3+} ion. Though substituting with Gd is known to induce ferroelectricity in HfO_2, the magnetic properties of Gd:HfO_2 have yet to be studied in depth. In this study, Gd:HfO_2 films are fabricated on TaN substrates by radio frequency sputtering of a composite Gd metal and HfO_2 oxide target in a mixed Ar and O_2 atmosphere. Grazing incidence x-ray diffraction is used to evaluate the suppression of the paraelectric monoclinic phase and stabilization of the ferroelectric orthorhombic phase. Electrical polarization measurements are used to study the room temperature spontaneous polarization in TaN/Gd:HfO_2/TaN metal-insulator-metal capacitors. Surface morphology of the films is characterized using atomic force microscopy, while magnetic properties are measured by variable temperature magnetometry. Initial magnetometry shows that Gd-substituted HfO_2 exhibits remnant magnetization at room temperature.

The scalability and simplicity of Gd:HfO_2, if it exhibits magnetoelectric coupling, make it an attractive model system for future developments in thin film multiferroics, having potential impacts for spintronics and other magnetoelectronic devices.

9:40am **TF+EM+MI+MN+OX+PS-MoM-5 Epitaxial Growth of Antiferromagnetic NiO Films by Off-axis Sputtering for Spintronic Devices**, *A Churikova, G Beach,* Massachusetts Institute of Technology; **Larry Scipioni**, *A Shepard, J Greer, T Newhouse-Illige,* PVD Products, Inc.

High-quality epitaxial growth of antiferromagnetic thin films is essential for future spintronic devices, as it allows small antiferromagnetic domain sizes and efficient electrical manipulation of domain walls via reading and writing currents. Antiferromagnetic materials are candidates for ultrafast operation due to THz antiferromagnetic spin dynamics, high packing densities due to the absence of stray magnetic fields, and stability due to insensitivity to external magnetic fields [1,2]. Meanwhile, the long spin diffusion lengths [3] and theoretically predicted superfluid transport of spin currents [4] in antiferromagnetic insulators are crucial for low-power device operation. The electrical control of magnetic spin textures has been thus far realized in epitaxially grown NiO on MgO substrates [5] and ferrimagnetic maghemite (γ–Fe2O3) and magnetite (Fe3O4) thin films [6].

We report the preparation of antiferromagnetic NiO thin films with (111) orientation on *c*-plane sapphire (1000) substrates by off-axis RF magnetron sputtering from a NiO target. The off-axis angle was 45°, and the sputtering pressure was 5 mTorr. Samples were grown with thicknesses ranging from 5 – 50 nm, and with growth temperatures from room temperature to 600°C, to determine optimum conditions. Structural characterization by x-ray diffraction demonstrates a high degree of epitaxy across a range of deposition temperatures and thicknesses. The deposition temperature and thickness dependence of epitaxial quality is investigated, with a characterization of the strain state, mosaicity, and crystallographic relationship between substrate and film. Evidence for antiferromagnetic order forming domains in NiO is provided via magnetic characterization of the films. Our results are essential for the optimization of the fabrication of high quality epitaxial antiferromagnetic films for practical spintronics devices.

[1] J. Železný, P. Wadley, K. Olejník, A. Hoffmann, and H. Ohno, Nat. Phys. 14, 220 (2018)

[2] V. Baltz, A. Manchon, M. Tsoi, T. Moriyama, T. Ono, and Y. Tserkovnyak, Rev. Mod. Phys. 90, 015005 (2018).

[3] R. Lebrun, A. Ross, S. A. Bender, A. Qaiumzadeh, L. Baldrati, J. Cramer, A. Brataas, R. A. Duine, and M. Kläui, Nature 561, 222 (2018).

[4] S. Takei, B. I. Halperin, A. Yacoby, and Y. Tserkovnyak, Phys. Rev. B 90, 094408 (2014).

[5] T. Moriyama, K. Oda, T. Ono, Sci. Rep. 8, 14167 (2018).

[6] L. Baldrati, A. Ross, T. Niizeki, C. Schneider, R. Ramos, J. Cramer, O. Gomonay, M. Filianina, T. Savchenko, D. Heinze, A. Kleibert, E. Saitoh, J. Sinova, and M. Kläui, Phys. Rev. B 98, 024422 (2018).

10:00am **TF+EM+MI+MN+OX+PS-MoM-6 Structural and Magnetic Properties of CoPd Alloys for Non-Volatile Memory Applications**, *S Gupta, J Abugri, B Clark,* University of Alabama; *P Komninou,* Aristotle University of Thessaloniki; **Sujan Budhathoki**, *A Hauser, P Visscher,* University of Alabama

A study of perpendicular magnetic anisotropy (PMA) CoPd alloys is presented as a simple means of pinning MgO-based perpendicular magnetic tunnel junctions (pMTJs) for spin transfer torque magnetic tunnel junction (STT-MRAM) applications. A compositional study of the Co_xPd_{100-x} alloys at 50 nm thickness showed that the maximum coercivity and anisotropy was found for $Co_{25}Pd_{75}$. Perpendicular magnetic tunnel junction stacks were deposited using different compositions of CoPd. Current-in-plane tunneling measurements indicated that the TMR values roughly correlated with the coercivity and anisotropy of the single layers. A thickness study indicated that the alloy was fully perpendicular for thicknesses as low as 20 nm. Various seed layers were employed to optimize the coercivity of the $Co_{25}Pd_{75}$ layer. Magnetometry, X-ray diffraction (XRD), scanning electron microscopy (SEM) and high resolution transmission electron microscopy studies were carried out to relate the magnetic and structural properties of these layers. These studies showed that the highest coercivity $Co_{25}Pd_{75}$ was achieved on a seed layer of Ta/Pd which helped to crystallize the CoPd layer in an fcc (111) orientation.

10:40am **TF+EM+MI+MN+OX+PS-MoM-8 Size Effects of the Electromechanical Response in Ferroic Thin Films: Phase Transitions to the Rescue**, *Nazanin Bassiri-Gharb,* Georgia Institute of Technology
INVITED

Silicon-integrated ferroelectric thin films have been leveraged over the last two decades for fabrication of high performance piezoelectric microelectromechanical systems (MEMS) devices. Ceramic $Pb(Zr_xTi_{1-}$

$_x$)O$_3$(PZT) thin films have been often the material of choice, due to their large electromechanical response, especially at morphotropic phase boundary compositions (MPB at x ~0.52), where co-existence of multiple crystallographic distortions can enhance extrinsic electromechanical contributions. However, ferroelectric thin films suffer from extrinsic size effects that lead to deteriorated piezoelectric properties in thin and ultra-thin films. Here we report on different strategies for processing of thin films with enhanced piezoelectric response with respect to traditionally processed PZT thin films.

Specifically, we will discuss preparation of superlattice-like polycrystalline PZT thin films through chemical solution depositions, polycrystalline relaxor-ferroelectric thin films (PMN-PT), and finally alternative non-ferroelectric compositions, where the electric field-induced phase transitions can result in substantial enhancement in thinner films, even where traditional

11:20am TF+EM+MI+MN+OX+PS-MoM-10 Ferroelectrics Meet Ionics in the Land of van der Waals, *S Neumayer,* Center for Nanophase Materials Sciences, Oak Ridge National Laboratory*; J Brehm,* Vanderbilt University*; M McGuire,* Oak Ridge National Laboratory*; M Susner,* Air Force Research Laboratory*; E Eliseev,* National Academy of Sciences of Ukraine*; S Jesse, S Kalinin,* Center for Nanophase Materials Sciences, Oak Ridge National Laboratory*; A Morozovska,* National Academy of Sciences of Ukraine*; S Pantelides,* Vanderbilt University*; N Balke, **Petro Maksymovych,** Center for Nanophase Materials Sciences, Oak Ridge National Laboratory

Van der Waals crystals of metal thiophosphates can be thought of as derivatives of transition metal dichalcogenides where 1/3 of metal atoms is replaced with diphosphorous, thereby stabilizing the remaining 2/3 of metal ions in low oxidation states.1 Consequently, thiophosphates enable ultrathin magnetic, ferroelectric and Mott insulating materials, in q2D materials while also providing new opportunities for multifunctional interfaces .

Of particular interest is CuInP$_2$S$_6$, where ferroelectricity emerges out of ionically conducting state .2,3 In this work, we discuss unusual and perhaps anomalous properties observed in CuInP$_2$S$_6$ in both states.

CuInP$_2$S$_6$ exhibits giant negative electrostriction (Q$_{33}$ = -3.2 m^4/C^2), which leads to large piezoelectric coefficients despite small polarization values and increase of Tc with applied pressure. It's the only material other than polymer PVDF for which such behavior is experimentally confirmed. Density functional theory reveals that the reason for negative electrostriction is a slight movement of Cu ions into the van der Waals gap due to anharmonicity of the potential well.4 Moreover, under high compressive strain, Cu starts to form interlayer bonds with sulfur across the van der Waals gap, leading to an additional phase of high polarization. Consequently, the potential distribution exhibits 4 instead of the usual two minima - a quadruple well, that is precisely tunable by strain. In the paraelectric state above ~70°C, Cu ion mobility drastically increases. Intriguingly, Cu can be reversibly extracted out of the lattice without visible damage. Finally, the selenide sibling CuInP$_2$Se$_6$, exhibits a lower transition temperature and propensity toward antiferroelectric ordering under the effect of depolarizing fields. In this material, we have for the first time observed piezoelectric response confined to domain walls (opposite to ferroelectrics), fulfilling the long-standing predictions for polar antiferroelectric domain walls and providing a new model system for emergent properties of topological defects in ferroic order parameter fields.

Research sponsored by Division of Materials Science and Engineering, Basic Energy Sciences, US Department of Energy. Microscopy was conducted at the Center for Nanophase Materials Sciences, which is a DOE Office of Science User Facility.

1Susner et al, Adv. Mater. 29,1602852 (2018)

2Neumayer et al, Phys. Rev. Materials **3**, 024401 (2019)

3Balke et al, ACS Appl. Mater. Interfaces 10, 27188 (2018)

4Brehm et al, in review

11:40am TF+EM+MI+MN+OX+PS-MoM-11 Adsorption-controlled Epitaxial Growth of the Hyperferroelectric Candidate LiZnSb on GaSb (111), *D Du, P Strohbeen,* University of Wisconsin - Madison*; H Paik,* Cornell University*; C Zhang, P Voyles, **Jason Kawasaki,** University of Wisconsin - Madison

A major challenge for ferroelectric devices is the depolarizing field, which competes with and often destroys long-range polar order in the limit of ultrathin films. Recent theoretical predictions suggest a new class of materials, termed hyperferroelectics [1], should be immune to the depolarizing field and enable ferroelectric devices down to the monolayer limit. Here we demonstrate the epitaxial growth of hexagonal LiZnSb, one of the hyperferroelectric candidate materials, on GaSb (111) substrates. Due to the high volatility of all three atomic species, we find that stoichiometric films can be grown in a thermodynamically adsorption-controlled window, using an excess zinc flux. Outstanding challenges remain in controlling the point defects of LiZnSb and in controlling polytypism. While the films primarily grow in a hexagonal "stuffed wurtzite" phase (space group *P6$_3$mc*), which is has the desired polar structure, there exists a competing cubic "stuffed zincblende" polymorph that is nonpolar (*F-43m*). We will discuss our strategy towards controlling defects and polytypism in LiZnSb, which is based in large part on the wurtzite – zincblende polytypism observed in InAs. We will also present preliminary electrical measurements on phase pure ferroelectric capacitor structures.

This work was supported by the Army Research office (W911NF-17-1-0254) and the National Science Foundation (DMR-1752797).

[1] K. F. Garrity, K. M. Rabe, and D. Vanderbilt, Phys. Rev. Lett. **112**, 127601(2014).

Thin Films Division
Room A124-125 - Session TF-MoM

Thin Films for Electrochemistry and Energy Storage
Moderators: Parag Banerjee, University of Central Florida, Jason Avila, U.S. Naval Research Laboratory

8:20am TF-MoM-1 Enabling Energy Dense Lithium Batteries Using Thin Film Technology, *Wyatt Tenhaeff,* University of Rochester **INVITED**
As new materials and electrochemical cell compositions are developed to meet the ever-increasing demand for high capacity, long-life lithium batteries, thin film deposition technology provides critical capabilities for engineering key interfaces within these batteries. This presentation will present our efforts to address challenges in lithium metal and silicon anodes. Thin films are integrated as ultrathin solid electrolytes in Li metal batteries and as protective coatings on Si anodes to limit undesirable side reactions.

Key requirements for electrolytes in solid-state lithium metal batteries are a large electrochemical stability window and low area-specific resistance (ASR). Solid electrolytes must also possess robust mechanical properties to accommodate large-scale production and integration into conventional lithium battery cell designs. To realize these properties, 50 nm-thick films of lithium phosphate oxynitride (Lipon) were deposited onto microporous polymer separators (Celgard) using RF magnetron sputtering. These separators provide a low ASR due to the thin, dense Lipon film; the total resistance of the separator was determined to be 40 Ω cm^2 in alkyl carbonate electrolytes, which is much lower than traditional ceramic electrolytes membranes, such as those fabricated from Garnet and NASICON-class of solid electrolytes. Furthermore, these composite separators inhibit chemical cross-diffusion and reaction between anode and cathode in both Li-S and Li-LiMn$_2$O$_4$ cells.

Silicon is also an intriguing next-generation anode offering charge capacities comparable to lithium metal, yet significant challenges arise from the >300% volume expansion of Si during lithiation. To address continual electrochemical reduction of lithium ion battery electrolyte on Si anodes, nanoscale, conformal polymer films were synthesized as artificial solid electrolyte interface (SEI) layers. Initiated chemical vapor deposition (iCVD) was employed to deposit poly(1,3,5,7-tetravinyl-1,3,5,7-tetramethylcyclotetrasiloxane) (pV4D4) onto silicon thin film electrodes. 25 nm-thick pV4D4 films on Si electrodes improved initial coulombic efficiency by 12.9% and capacity retention over 100 cycles by 64.9% relative to untreated electrodes. PV4D4 coatings also improved rate capabilities, enabling higher lithiation capacity at all current densities. Post-cycling FTIR and XPS showed that pV4D4 inhibited electrolyte reduction and altered the SEI composition, with LiF formation being favored. This work will guide further development of polymeric artificial SEIs to mitigate electrolyte reduction and enhance capacity retention in Si electrodes.

9:00am TF-MoM-3 Molecular Layer Deposition of Organic Li-containing Thin Film for Li Ion Solid-state Batteries, *Haotian Wang,* University of Maryland, College Park

High performance 3D solid-state Li ion batteries require uniform and conformal coating of solid electrolytes with high mechanical compliance, to enable the usage of high energy density anodes, such as Si, and maintain a good electrode-electrolyte contact during cycling. Molecular layer deposition (MLD) is a vapor phase deposition technique that deposits thin films in a layer by layer manner. The incorporation of organic moieties into the resulting MLD thin films potentially provides enhanced mechanical flexibility while retaining the high uniformity and conformality, making this technique promising for applications in the next generation 3D solid state batteries.

In this work, we are presenting a fundamental study of organic Li-containing thin film by MLD. A comprehensive understanding of the organic-inorganic reaction and growth mechanism was obtained based on a model chemistry with Li tertbutoxide (LiO^{t}Bu) and propanediol (PPD). The ALD-like growth temperature window, linear growth and the self-limiting behavior were observed by employing in-situ ellipsometry during deposition. Chemical structure of the film grown by LiO^{t}Bu and PPD was characterized by X-ray photoelectron spectroscopy (XPS) and simulated by ab-initio calculation. Based on both the experimental characterization and theoretical calculation, a hybrid inorganic-organic Li-containing material, Li propane oxide, with well-defined stoichiometry ($Li_{1.6}C_3H_6O_{2.2}$) was successfully synthesized via MLD.

Additionally, nucleation delay during film growth was observed, indicating an island growth and crystal formation. Single crystal nucleus with cubic crystal structure at early growth stage was observed by transmission electron microscopy (TEM), while at later growth stage, nucleus coalesced and formed polycrystalline thin film with high surface roughness. To reduce the surface roughness and enhance the applicability of the MLD film in high aspect ratio geometries, we applied nitrogen plasma to the Li propane oxide MLD process. The nitrogen plasma modified MLD process showed no nucleation delay and was later used as seeding for Li propane oxide growth. A significant attenuation of surface roughness of Li propane oxide MLD films grown on this seeding layer was observed. The understanding of the inorganic-organic reaction and the development of the seeding layers for the Li-containing thin film will benefit directly to the flexible and three-dimensional solid state battery research.

9:20am TF-MoM-4 Organic/Inorganic Solid Electrolytes and Electrode Coatings for 3D Lithium-ion Microbatteries, *Ryan Sheil[1], J Lau,* University of California, Los Angeles*; K Jungjohann,* Sandia National Laboratories*; J Yoo,* Los Alamos National Laboratory*; B Dunn, J Chang,* University of California, Los Angeles

Lithium-ion batteries have been an enabling factor in the success of consumer electronics and have the potential to offer energy storage solutions for microelectromechanical systems (MEMS), such as sensors for IoT and biomedical applications. Three-dimensional battery architectures allow for an effective decoupling of the areal energy and power density resulting in improved areal footprint utilization required of these small devices. In 3D battery designs, the short distances between the anode and cathode improve the transport properties allowing for high areal power densities and the high aspect-ratio nature of the electrodes promotes high areal energy densities. One requirement in the utilization of 3D based electrodes is the incorporation of a solid electrolyte that can be coated pinhole free and conformally on high aspect ratio structures. The solid electrolyte material must be ionically conductive, electronically insulating, and be flexible to withstand the volume expansion and contraction of the electrode during charge and discharge.

The self-limiting nature of atomic layer deposition allows for precise thickness control across high aspect ratio structures. ALD $Li_xAl_ySi_zO$ was synthesized utilizing lithium tert-butoxide (LTB), trimethyl aluminum (TMA), and tris(tert-butoxy) silanol (TTBS). ALD $Li_xAl_ySi_zO$ was integrated with high aspect ratio SiGe nanowires for in-situ TEM characterization, where the chemical, structural, and morphological changes of the electrode/electrolyte system were characterized in-situ during lithiation and delithiation. An ALD $Li_xAl_ySi_zO$-coated $Si_{0.4}Ge_{0.6}$ nanowire demonstrates lithiation and delithiation with an intact solid state electrolyte layer with ~39% radial expansion observed upon lithiation. To further improve the mechanical properties for integration on high capacity/large volume expansion anodes, an MLD process was explored to synthesize lithium

alkoxide and aluminum alkoxide utilizing trimethyl aluminum and lithium tert-butoxide coupled with glycerol. Incorporation of the MLD, ALD, and MLD/ALD coatings were integrated with Si and Co_3O_4 elecrodes, where improvements to cycling stability and coulombic efficiency were observed. $Li_xAl_ySi_zO$ coated Co_3O_4 thin films exhibited improved coulombic efficiency (99.5% (coated), 90.5% (uncoated)) and capacity retention (2458 mAh/cm^3 (coated), 2038 mAh/cm^3 (uncoated)) after 100 cycles at 2C.

9:40am TF-MoM-5 Structural Rearrangement in $Li_xV_2O_5$ Thin Films, a **Cathode Material for All-solid-state Batteries**, *Angelique Jarry,* University of Maryland, College Park*; N Pronin, M Walker,* The Ohio State University*; J Ballard,* University of Maryland*; D Stewart,* University of Maryland, College Park*; L Brillson,* The Ohio State University*; G Rubloff,* University of Maryland, College Park

The requirements to enable all-solid-state batteries (SSBs) are extremely stringent and necessitate control of the chemistry and interfaces over a wide structural length and long-time scales. Investigations using multi-probe approaches have confirmed that surface composition, defects, structure, and morphology of the electrodes/electrolyte themselves has a strong impact on interfacial processes. Therefore, to understand how to overcome the barriers related to the implementation of SSBs, it is necessary to start with pure, well-defined models systems such as cathode thin films. V_2O_5 is of particular interest due to the large interlayer spacing of its metastable varieties that allows a topochemical de-intercalation of various cation ($M_xV_2O_5$ withM = Li, Na, Mg). However this cation de-insertion leads to structural distortion/surface reconstruction that impedes the cathode performance. A detailed understanding of these degradation mechanisms is needed to identify the appropriate remedies.

In this work, V_2O_5 thin films of ~500 nm were produced by atomic layer deposition (ALD) on sputtered gold on silicon substrate. The films were subsequently electrochemically lithiated in liquid electrolytes by galvanostatic cycling i.e, $Li_xV_2O_5$ with x < 2. We investigated the effects of lithiation on the structural characteristics and surface morphology of $Li_xV_2O_5$ thin films as a function of depth through multiple methods. Change in the crystallinity and local atomic structure were probed with Raman spectroscopy (RS), X-ray photoelectron spectroscopy (XPS), optical/scanning electron microscopy and, atomic force microscopy (AFM). We demonstrated that partial lithiation of V_2O_5 results in reduction of the vanadium that is accompanied by a progressive surface hydroxylation and amorphization of the films. At high lithium content, significant non reversible structural rearrangements associated with the destabilization of the V-O framework are observed. The correlation between the lithium content, structural stability, electrode's surface activity and electrochemical performance will be presented and discussed.

Acknowledgement

10:00am TF-MoM-6 Atomic Layer Deposition and Performance of Sodium and Potassium Electrolytes for Conformal Solid State Batteries, *Blake Nuwayhid, A Jarry, G Rubloff, K Gregorczyk,* University of Maryland, College Park

Solid-state batteries (SSBs) provide significant advantages over conventional liquid electrolyte based batteries, such as their non-flammable nature and improved chemical stability. Specifically, thin film SSBs possess the ability to provide high power densities due to a shorter transport pathway and are compatible with semiconductor device manufacturing. The fabrication of 3D thin film SSBs through conformal deposition processes is extremely promising due to the dramatic enhancement in both energy and power densities compared to planar cells. Our group recently demonstrated the fabrication of the first fully conformal 3D Li-based thin film SSBs, in which all battery components were deposited by Atomic Layer Deposition (ALD).[1] This was made possible through the development of a new lithium phosphazene (Li_2PO_2N) solid electrolyte. Sodium and potassium ion batteries are interesting as well for SSB applications due to the lower cost and higher abundance of the alkali metals compared to lithium. However, few such efforts have been put into solid state systems, and none in 3D thin film SSBs. In this presentation, we will discuss the development of conformal sodium phosphorous oxynitride (NaPON) and potassium phosphate (KPO) ion-conductors, and their potential in 3D thin film SSBs. Similar to our previously published LiPON ALD process[2], NaPON and KPO processes use the thermal reaction of sodium tert-butoxide or potassium tert-butoxide, with diethyl

---

phosphoramidate. The growth behavior of NaPON and KPO were very similar, exhibiting a linearly increasing growth rate of 0.1-1.0 Å/cycle at 250-400 °C, but no temperature window was observed. An ultra-high vacuum chamber coupled the ALD reactor to a X-ray Photoelectron Spectrometer, allowing for sensitive film characterization as a function of temperature. Characterization was also complemented by Raman and IR spectroscopy to reveal differences in the phosphorus oxynitride bonding networks. The structure of NaPON resembled that of LiPON, containing similar atomic ratios (P/N = 1) and 2 nitrogen species (=N– and >N–), whereas KPO films contained only 1% nitrogen and a considerable amount of carbon incorporation. We will also highlight the electrochemical behavior of the films in planar solid-state cells and 3D systems in high aspect ratio substrates.

1. Pearse, A.; Schmitt, T.; Sahadeo, E.; Stewart, D. M.; Kozen, A.; Gerasopoulos, K.; Talin, A. A.; Lee, S. B.; Rubloff, G. W.; Gregorczyk, K. E. *ACS Nano* **2018**, *12*, 4286-4294.

2. Pearse, A.; Schmitt, T. E.; Fuller, E. J.; El-Gabaly, F.; Lin, C. F.; Gerasopoulos, K.; Kozen, A. C.; Talin, A. A.; Rubloff, G.; Gregorczyk, K. E. *Chemistry of Materials* **2017**, *29*, 3740-3753.

10:40am TF-MoM-8 ALD as Tool for Bottom-up Synthesis of Catalyst Powders, *Frank Rosowski,* BASF Se, Germany   **INVITED**
Atomic Layer Deposition is mainly applied in microelectronics as a thin film deposition technique. In academic research, ALD is also applied for synthesis of battery materials and catalysts. The main challenge for ALD in these research fields is the morphology of the substrate materials, usually small particles with high specific surface areas, e.g. up to 1000 m^2/g for zeolites. Catalytic reactors can hold packed beds of several cubic meters of catalyst. The high specific surface areas and the amounts in which such catalysts are needed require safe and efficient ways of dosing ALD precursors without bypass and waste. And while mass and heat transport limitations play only a minor role in the case of flat substrates, these phenomena need to be considered when coating large amounts of powder.

At BasCat, ALD is used in several projects to synthesize and modify catalysts. Some research is done along well-established lines of work in the field of supported metal catalysts, e.g. modifying supported metal catalysts with metal oxide layers, but the focus lies on catalysts used for selective oxidation reactions, typically consisting of mixed metal oxides or phosphates. Catalysts are usually prepared in two batch sizes. For establishing suitable ALD process conditions, a sample size of about 1 cm^3 is used. In a second step, catalyst amounts of 10–25 cm^3 are prepared. It is important that process conditions established on the small scale are easily transferrable to the large scale.

For this purpose, a new and unique test facility was installed at BasCat equipped with a thermogravimetric balance as analytical small scale ALD reactor and a second reactor for catalyst synthesis on a large scale via ALD.[1] Based on our first ALD results, a fixed bed was chosen as reactor geometry for the analytical reactor and the synthesis reactor.

In order to check the feasibility of our new in situ method and the ALD performance of our fixed bed reactor, first studies covered the deposition of alumina on a typical catalyst support, a silica with high surface area (Davisil 636). It was shown that the fixed bed geometry is suitable for ALD, that the substrate is homogeneously covered, and that scaling-up from 1 cm^3 to 10 cm^3 is possible.[2]

The combination of analytical reactor and synthesis reactor was then successfully used for modifying supported metal catalysts with layers of alumina, alucone, and zinc oxide. Other works included the deposition of rhenium on silver and phosphorus on vanadia.[3]

[1] Strempel et al., *Rev. Sci. Instrum.*, 074102. 2017

[2] Strempel et al., F.,*Nanomaterials*, 365. 2018

[3] Strempel et al., *J. Vac. Sci. Technol. A Vacuum, Surfaces, Film.*, 01A135. 2016

11:20am TF-MoM-10 Strategies for the Stabilization of Metal Anodes for Li and Na Metal Batteries, *Yang Zhao[1], X Sun,* University of Western Ontario, Canada
Li-metal batteries (LMBs) and Na-metal batteries (NMBs) are considered as the promising candidates to replace the conventional Li-ion batteries due to their high theoretical energy density. Li metal and Na metal are the ultimate choices as anodes to achieve their high energy density due to the high specific capacity, low electrochemical potential and lightweight [1].

However, as alkali metals, both Li and Na metal anodes suffer from serious challenges including 1) dendrite formations and short circuits; 2) Low Coulombic efficiency (CE) and poor cycling performance; and 3) Infinite volume changes. This presentation mainly focuses on the design of multiple strategies for the stabilization of Li and Na metal anode for LMBs and NMBs.

Solid electrolyte interphase (SEI) layer is one of the key factors for the Li and Na deposition behaviors [2]. We developed different approaches to fabricate the artificial SEI with significantly improved electrochemical performances. Firstly, we have demonstrated different ultra-thin protective layers for Li and Na metal anodes by atomic layer deposition (ALD) and molecular layer deposition (MLD) techniques, including Al_2O_3, alucone, and polyurea, et al [3]. More recently, we designed a dual-protective layer for Li metal anode with precisely controlled thicknesses, compositions and mechanical properties [4]. Secondly, we developed the in-situ solution-based methods to fabricate the Li_3PS_4 and Na_3PS_4 as protective layers for both Li and Na metal anodes with enhanced performances and reduced dendrite growth [5].

To address another challenge of volume change, 3D conductive interlayers and hosts have been designed for Li and Na metal anodes. Carbon paper (CP) and modified CP with carbon nanotubes have been used as host/interlayer with excellent electrochemical performance under high current density and high capacity [6].

In conclusion, we developed the different approaches, including protective layers fabricated by ALD/MLD and solution methods, interlayers, and 3D skeleton design, for Li and Na metal anodes with enhanced electrochemical performances and reduced dendrite growth. Meanwhile, the ideas have been also applied to solve the practical issues for testing Li and Na metal batteries.

[1] *Energy & Environmental Science*, 2018, 11, 2673

[2] *Joule*, 2018, 2, 2583

[3] *ACS Energy Letters*, 2018, 3, 899; *Small Methods*, 2018, 2, 1700417; *Advanced Materials*, 2017, 29, 1606663; *Nano Letters*, 2017, 17, 5653; *Advanced Materials*, 2019, 31, 201806541

[4] *Matter*, 2019, in press

[5] *Journal of Materials Chemistry A*, 2019, 7, 4119

[6] *Nano Energy*, 2018, 43, 368; *Energy Storage Materials*, 2018, 15, 415; *Small*, 2018, 14, 1703717

11:40am TF-MoM-11 Competition Between Incorporation and Desorption of Nitrogen in Plasma-Enhanced Atomic Layer Deposition of Cobalt and Cobalt Nitride Catalysts, *Gerben van Straaten,* Eindhoven University of Technology, The Netherlands, Netherlands*; H Fredriksson,* Syngaschem BV, Netherlands*; R Deckers,* Eindhoven University of Technology, Netherlands*; M Vos,* Eindhoven University of Technology, The Netherlands, Netherlands*; K Weststrate,* Syngaschem BV, Netherlands*; E Kessels,* Eindhoven University of Technology, The Netherlands, Netherlands*; A Creatore,* Eindhoven University of Technology, Netherlands
Cobalt catalysts have various applications in the chemical industry. Most prominently, metallic Co is used in the production of synthetic fuels via the Fischer-Tropsch process, while cobalt nitrides (with the general formula CoN_x) are being explored as noble-metal free electro-catalysts for the oxygen evolution reaction. Atomic Layer Deposition (ALD) of Co and CoN_x thin films and nanoparticles can be achieved using a variety of Co precursors with NH_3- plasma[1]. Moreover, the precursors $Co(CO)_8$ and $CoCp_2$ can yield either metallic Co or CoN_x, depending on temperature[2]. We will demonstrate here that this is due to the metastable nature of CoN_x.

We have found that film deposition below 350°C onto thermally grown SiO_2 using $CoCp_2$ and an inductively coupled NH_3 plasma yielded Co_2N, while deposition at higher temperatures resulted in Co with traces of N. To gain insight into the incorporation of N into the films, Spectroscopic Ellipsometry (SE) and X-ray photoelectron spectroscopy (XPS) were performed on 20 nm Co films exposed to NH_3 plasma. These measurements revealed that at 150°C, 30 min of plasma exposure resulted into the formation of a 5 nm thick N-enriched diffusion layer at the film surface. However, the nitridation process is temperature-dependent: at 350°C and above, no N incorporation into the bulk of the layer was observed. The origin of this temperature dependence was analyzed using Temperature-Programmed Desorption (TPD), which showed that N could be released from the low temperature plasma-treated layers in two stages. Around 270°C, N desorbed from the surface, but no loss of N from the bulk of the Co layer was observed. Subsequently, starting at 350°C, complete

effusion of bulk N took place, allowing the film to relax back to its original thickness.

These results show that at low temperatures N is incorporated into the growing film from the NH_3 plasma, leading to the formation of homogeneous CoN_x films, but at elevated temperatures, N desorption outpaces incorporation and metallic Co is formed instead. Thus, it is possible to deposit Co and CoN_x catalysts with controlled stoichiometry by balancing N incorporation and desorption. Preliminary measurements show that Co nanoparticles and thin films deposited in this way are capable of catalyzing the methanation reaction; further characterization of their activity is currently ongoing.

[1] M. F. J. Vos, G. van Straaten, W. M. M. Kessels, and A. J. M. Mackus, *J. Phys. Chem. C*, p. acs.jpcc.8b06342, Sep. 2018.

[2] H.-B.-R. Lee and H. Kim, *Electrochem. Solid-State Lett.*, vol. 9, no. 11, p. G323, Nov. 2006.

Vacuum Technology Division
Room A213 - Session VT-MoM

Pumping, Outgassing, leaks, and Vacuum Pressure Measurement

Moderators: Scott Heinbuch, MKS Granville-Phillips Division, Longmont, Giulia Lanza, SLAC National Accelerator Laboratory

8:20am **VT-MoM-1 Operational Experiences of Compact Non-Evaporable Getter Pumps in CHESS-U and CBETA**, *Yulin Li*, Y Lushtak, L Ying, Cornell University

In two recently commissioned accelerator projects at Cornell Laboratory of Accelerator-based Sciences and Education (CLASSE), a large number of high pumping capacity, compact non-evaporable getter (NEG) pumps were implemented to fulfill the required vacuum performances with very tight space constraint. In the Cornell Brookhaven ERL Test Accelerator (CBETA), NEGs are the only installed pumps. At a maximum electron beam energy of 150-MeV, no beam-induced gas load is expected in normal beam operations. We have demonstrated that adequate level of vacuum ($P<10^{-8}$ torr) can be achieved quickly after a ultra-dry nitrogen venting without in situ bakeout, which provide required flexibility in the CBETA vacuum system for various beam test configurations. In contrast, very high dynamic gas-load due to synchrotron radiation induced desorption (SRID) is expected in the vacuum system for the CHESS-U Upgrade, a major upgrade project for the Cornell High Energy Synchrotron Source (CHESS). During the commissioning phase of the CHESS-U, an extremely high SRID gas load may not only cause rapid NEG saturation (thus requiring frequent NEG re-activations), but also may potentially damage the small sputtering ion pumps (SIPs) of the NexTorr® (a NEG-SIP combination pump from SAES Getters). Protective control program is developed to prevent the potential damage to these SIPs, while keeping monitoring. In this paper, we will present our operational experiences of these compact NEGs in both CBETA and CHESS-U projects.

8:40am **VT-MoM-2 Al_2O_3 Coated Stainless Steel Vacuum Chamber and Parts**, *Martin Wüest*, Y Kuzminykh, G Mata Osoro, W Fuchs, J Gabathuler, L Ospelt, INFICON Ltd., Liechtenstein

We built a vacuum system for calibration of total pressure sensors in the conventional way. We made initial performance measurements such as pumpdown times and achieved base pressure. This system was then taken apart and the stainless steel parts (chamber and fittings) were then coated with an Al_2O_3 layer using an ALD process. To do this we cleaned the parts with ozone, heated them to 300 °C and then finally coated them with an Al_2O_3 ALD process. We rebuilt the vacuum system using those coated parts and performed the performance test again. The result is that we can achieve a lower base pressure in shorter time. The achieved base pressure is approximately a factor 3 lower in the coated version compared to the uncoated version.

9:00am **VT-MoM-3 Comparative Outgassing Study of Identical Vacuum Chambers**, *James Fedchak*, National Institute of Sandards and Technology (NIST)

We have measured and compared the H_2 and water outgassing rates for 7 identical vacuum chambers constructed of common vacuum materials and heat treatments: 304L, 316L, 316LN-ESR (electro-slag remelt), titanium, aluminum vacuum-fired 316L, and vacuum-fired 316LN-ESR. These chambers are of identical geometry and are from the same manufacturer. Comparison studies of outgassing from a large selection of chambers has

the advantage over those of single samples or chambers in that the influence of chamber geometry in minimized. Much of the motivation for NIST to conduct this study is to identify ultralow outgassing materials for UHV and XHV vacuum systems, common candidate materials include aluminum, titanium, and vacuum-fired 316L or 316LN-ESR stainless steel. Obtaining these low pressures usually requires vacuum chambers with outgassing rates much less than 10^{-9} Pa L s^{-1} cm^{-2}. In addition, vacuum chambers constructed from materials with ultra-low outgassing rates can help reduce the cost of large vacuum systems by requiring fewer pumps (with the associated cost of operation and maintenance) to obtain the desired ultimate pressure. Other considerations in the selection of vacuum materials include the material cost, strength, machinability, weldability, and chemical resistance. One of our aims of this study is to put outgassing rates into the engineering tool kit. In addition to the above materials, we intend to present data on post process of some of the chambers, including electropolishing and a light air-bake, and on mild steel chambers.

9:20am **VT-MoM-4 The NIST VAcuum LEaks System (VALES): a new system for the primary and comparison calibration of small gas flows.**, *Julia Scherschligt*, J Fedchak, R Vest, National Institute of Sandards and Technology (NIST)

Helium leak standards for low molecular flow rates are critical to the calibration of leak detectors, gas analyzers, and other equipment used in vacuum, aerospace, and space industries. Since 1984, the National Institute of Standards and Technology (NIST) has provided calibration services for the calibration of vacuum leak standards using two independent systems: The Primary Leak System (PLS), which calibrates leak artifacts against a flow meter, and the Leak Comparison Standard (LCS) which compares a customer leak to a NIST owned leak artifact as a function of temperature. The PLS system has recently been upgraded with a new mass-sensitive detector (a quadupole mass analyzer or QMA). The LCS has been retired from service but its functionality has been efficiently replicated on PLS. In this talk, we will describe the new calibration system, VALES, present recent results on the characterization of the new PLS detector and discus the on-going upgrade and automation of the entire calibration system

9:40am **VT-MoM-5 Creating a Controlled Gas Environment for Lifetime Testing of EUV Optics**, *Timo Huijser*, M van Putten, M van der Lans, TNO, Netherlands

Optics used in Extreme ultra-violet (EUV) lithography typically operate in an environment of 0.01 to 0.1 mbar hydrogen. Since EUV machines cannot receive a bake out after installation it is difficult to reduce background outgassing such as for water, oxygen, nitrogen and hydrocarbons. Although the partial pressures of these contaminants are orders of magnitude lower, their presence in combination with EUV irradiation induces oxidation, etching, deposition and other processes that affect the lifetime of EUV optics.

At TNO these processes are studied using an EUV beam line facility (EBL2). To enable this type of research a method was developed to create a well-controlled environment of multiple gases with defined and stable partial pressures.

The gas environment typically consists of hydrogen (10^{-2} to 10^{-1} mbar) with added oxygen, water, nitrogen and/or hydrocarbons (10^{-8} to 10^{-4} mbar). The strategy for controlling the gas environment is to start by setting the pressures of the additives prior to adding hydrogen. For accuracy, the pressure values are chosen such that the pump speed drop after adding hydrogen is taken into account. In order to do this, the pump speed of all gases needs to be known for both (ultra) high vacuum conditions as well as medium vacuum conditions (after addition of hydrogen). The procedure for setting the gas environment comprises 4 steps:

1. Determine the pump speed at HV conditions of relevant additives such as oxygen, water, nitrogen and/or hydrocarbons
2. Calibrate the differentially pumped RGA system with a gas mixture of hydrogen with defined, small fractions of additives.
3. Inject this mixture in the exposure chamber at nominal operating conditions. Using the RGA calibration data, the individual pump speed of each species in hydrogen is now calculated.
4. Set the partial pressures of additives prior to adding hydrogen, taking into account the calculated drop of pump speed.

Once step 1 to 3 have been carried out for all additives the resulting pump speed values can be applied for each exposure as long as the vacuum

system and its geometry are not altered. As a result the partial pressures can be set quickly using common ion gauges.

The method developed to create a well-controlled environment of multiple gases along with its corresponding procedures and results will be presented.

10:00am VT-MoM-6 Sampling System Design to Predict Mixture Composition at a Quadrupole Mass Spectrometer Ion Source, *Robert Ellefson,* REVac Consulting

The use of gas mixtures to measure the sensitivity and fragmentation ratios for calibration of a quadrupole mass spectrometer (QMS) simplifies the process and enables *insitu* calibrations. A necessary factor in a mixture calibration method is knowledge of the composition present in the QMS ion source and at the reference ion gauge. Under the conditions of molecular flow of the mixture into the ion source and molecular pumping of the outlet flow, the composition at the ion source is equal to the stated values of the mixture. This knowledge enables a composition-weighted correction of the ion gauge reading to get the true ion source pressure due to different gauge sensitivities of each species. The partial pressures of components in the ion source are calculated using the mole fraction of the mixture's species times the corrected ion gauge pressure. The sensitivity for a specific gas species is the ratio of the ion current representing the species to the calculated partial pressure at a common time.

The gas dynamics of very low flow rate gas into the ion source from an end crimped capillary or small pore size frit from a high-pressure mixture is presented. The low flow rate produces molecular effusion and the stated mixture composition is established in the ion source. Another model for low pressure (< 10 Torr) gas introduction through an orifice predicts molecular flow into the ion source and a (correctable) species dependence of the mixture composition as a function of time as the species deplete from the sample volume. Results of QMS calibrations using these gas sources and methods are presented together with composition analyses of unknown gas samples.

10:40am VT-MoM-8 Quantum Pressure Standard in the range 200 Pa to 20 kPa using Superconducting Microwave Cavity, *Laurent Pitre,* LNE Cnam-LCM, France*; P Gambette,* LNE-Cnam LCM, France*; R Gavioso, D Ripa,* INRiM, Italy*; M Plimmer,* LNE-Cnam LCM, France   **INVITED**

An LNE-INRiM collaboration is conducting proof-of-principle tests of a primary pressure standard operating at pressures 200 Pa< p < 20 kPa at temperatures 4.6 K < T < 5.8 K. The proposed standard is based on precise measurements of the microwave resonance frequencies of a quasi-spherical, helium-filled, superconducting cavity maintained at cryogenic temperatures. Ultimately, the accuracy of this standard will be competitive with the present standard at LNE over the whole pressure range. The proposed standard exploits 4 theoretical and technological advances: (1) recent *ab-initio* calculations of the microwave-frequency refractive index of helium $n(p, T)$ near 6 K with an uncertainty corresponding to a relative pressure uncertainty $u_r(p) < 1.10^{-5}$ (at a 68% confidence level); (2) the commercial availability of cryogen-free, low-cost, pulsed-tube refrigerators, (3) the ability to manufacture superconducting microwave cavities with resonance quality factors on the order of 5 million (4) and the impending change of the SI that fixes the value of the Boltzmann constant, thereby reducing the uncertainty of thermodynamic temperature determinations in the cryogenic range. A crucial requirement for microwave pressure standards is maintaining the purity of the ^{4}He sample under test. For the proposed standard, this is facilitated by cryogenic cold traps that effectively remove all impurities except ^{3}He.

The first experimental result will be present with a 2.5 cm radius and with Nobium coated quasi sphere. A particular focus on the hydrostatic head correction and the thermomolecular effect will be presented during the presentation.

11:20am VT-MoM-10 Progress Toward Primary Pressure Measurements based on Refractive Index, *Kevin Douglass, J Ricker, J Hendricks,* National Institute of Standards and Technology (NIST)

Towards the goal of quantum-based traceability of the Pascal, NIST has developed an optical pressure measurement system where traceability is achieved through accurate quantum mechanical calculations of the refractivity virial coefficients. Extremely accurate measurements of refractive index are possible; however, traceability is currently through the mercury manometer. Primary traceability for the NIST Fixed Length Optical Cavity (FLOC) will require an independent approach, relying solely on refractive index type measurements. A critical step in achieving primary traceability for the FLOC is determining the pressure dependent distortion terms. This is a major challenge because the pressure and the distortion term need to be determined simultaneously. A dual-wavelength approach can provide two measurements in-order to solve for the two unknown variables. The operational wavelengths for this measurement are at 633 nm and 1542 nm. The dual-wavelength approach and current results will be presented.

11:40am VT-MoM-11 Application of Porous Conductance Element for High Vacuum Gauge Calibration, *Martin-Viktor Johansson,* Aix Marseille University, France*; M Wüest,* INFICON Ltd., Liechtenstein*; P Perrier,* Aix Marseille University, France*; I Graur,* Aix-Marseille University, France

It is well known that the sensitivity of high vacuum gauges, such as ionization gauges (IG), drift in time [1] and need to be periodically recalibrated. Removal of the sensors from in-situ is time-consuming, and calibration by direct comparison with calibrated IGs has limited accuracy.

The permeability and conductance of the micro sintered stainless-steel membranes with pores varying from 0.2 μm to 0.5 μm was investigated for a wide range of pressure and several gases, from continuum to free molecular regime using a previously developed method [2]. The conductance of this kind of membranes was found constant for low pressures. This property makes the studied membranes particularly suitable as a leak element, by taking advantage of the constancy of conductance in the free molecular regime.

Effective pumping speed of a turbo molecular pump and the conductance of the fabricated microporous conductance element tend to a constant value as the pressure decreases [3], which is still in the measurement range of a 10 mTorr CDG. With the measured constant value, we can use a CDG and the sintered porous stainless steel to calibrate high vacuum sensors. The proposed configuration can be put on the user's high vacuum system for calibration on site. This calibration method is based on absolute pressure sensors and was found to be robust and easy to use.

References:

[1] H.Yoshida, K.Arai, H. Akimichi, M. Hirata, Stability tests of ionization gauges using two-stage flow-dividing system, Vacuum, 84, 705-708, 2009

[2] M.V. Johansson, F. Testa, I. Zaier, P. Perrier, J.P. Bonnet, P. Moulin, I. Graur, Mass flow rate and permeability measurements in microporous media, Vacuum, 158, 75-85, 2018

[3] H. Yoshida, K. Arai, M. Hirata, H.Akimichi, New leak element using sintered stainless steel filter for in-situ calibration of ionization gauges and quadrupole mass spectrometers, Vacuum, 86, 838-842, 2012

2D Materials
Room A226 - Session 2D+AP+EM+MI+MN+NS+PS+TF-MoA

Nanostructures including Heterostructures and Patterning of 2D Materials

Moderator: Deep Jariwala, University of Pennsylvania

1:40pm 2D+AP+EM+MI+MN+NS+PS+TF-MoA-1 Tailoring and Patterning 2D Material Interfaces Through Chemical Functionalization, *Arend van der Zande,* University of Illinois at Urbana-Champaign **INVITED**
Two-dimensional materials are all surface, so any change in the surface chemistry affects the entire material. This offers a challenge and an opportunity to engineering the material properties and new device behavior. There are many strategies to altering the chemical structure of 2D materials, yet one of the most successful is the chemical functionalization with low energy plasmas such as hydrogen and fluorine. Functionalization enables phase changes within materials to dramatically alter their properties, can be applied post synthesis and device fabrication, and is compatible with lithography for spatial patterning. Most studies of chemical functionalization focus on single functionalization of single 2D materials, yet there are many opportunities when applying the principles of chemical functionalization to spatially engineer the properties though in plane interfaces or out of plane in heterostructures.

First, we will examine selective etching with XeF_2 to pattern heterostructures using graphene etch stops. These techniques are self-limiting, yet scalable, and enable the patterning of 2D heterostructures into 3D multilayer circuitry. Moreover, devices like encapsulated graphene transistors fabricated with these techniques have exceptionally low contact resistances and mobilities which approach theoretical limits.

Second we will present a new strategy for tailoring the stoichiometry of functionalized graphene compounds through the systematic control of the ratio between adatoms. We demonstrate new ternary HFG compounds and reversible switching of material stoichiometry via the sequential exposure of graphene to low energy H plasma and XeF_2 gas. By patterning regions of different functionalization on a single chip, we perform direct comparisons and show spatially controlled tuning of the relative surface properties such as wettability, friction, electronic conductivity and molecular adhesion. Taken together, these studies show that chemical functionalization offers new atomically precise nanofabrication and materials engineering techniques for scalable engineering of circuitry along all three dimensions.

2:20pm 2D+AP+EM+MI+MN+NS+PS+TF-MoA-3 Dual-Route Hydrogenation of the Graphene/Ni Interface, *Rosanna Larciprete,* CNR-Institute for Complex Systems, Roma, Italy*; D Lizzit,* Elettra - Sincrotrone Trieste, Trieste, Italy*; M Trioni,* CNR-Institute of Molecular Science and Technologies, Milano, Italy*; P Lacovig, L Bignardi, S Lizzit,* Elettra - Sincrotrone Trieste, Trieste, Italy*; R Martinazzo,* Università degli Studi di Milano, Milano, Italy
Although the high surface-to-weight ratio would make graphene (Gr) one of the most promising material for hydrogen accumulation, up to now only moderate gravimetric density values of 1-2% have been obtained at room temperature (RT). The ultimate H coverage is limited by the competition between the adsorption and desorption/abstraction processes and by the elastic energy that accumulates in the C lattice once puckered by the local sp3rehybridization of the C atoms binding hydrogen. Moreover, for epitaxial Gr on metals, the substrate-induced Gr corrugation might modulates periodically H adsorption. In this respect, the Gr/Ni(111) interface appears much more favorable than other graphene/metal systems, as the limitations due to the presence of the moirè supercell vanish due to commensurate relation between the Gr and Ni(111) lattices. Moreover, hydrogenation might be favored by the peculiar reactivity of Gr/Ni(111).This issues motivated a re-investigation of the interaction of this particular interface with hydrogen.

In this study [1]we used x-ray photoelectron spectroscopy (XPS) and near edge x-ray absorption fine structure spectroscopy (NEXAFS) to follow the RT hydrogenation of Gr/Ni(111) and determined the configuration of the hydrogenated interface by scanning tunneling microscopy (STM). We found that hydrogenation proceeds through a dual path that includes hydrogen chemisorption on top of the graphene followed by a slow but continuous intercalation below graphene. At low coverage H atoms predominantly adsorb as monomers and chemisorption saturates when ≈ 25% of the surface is hydrogenated. The formation of C–H bonds determines new

components in the C 1s core level spectrum that are attributed by DFT calculations to C atoms directly bonded to H and to their first neighbors. In parallel with chemisorption, with a much lower rate, H atoms intercalate below Gr and bind to Ni surface sites. Thermal programmed desorption measurements showed that chemisorbed hydrogen is released around 600 K, whereas the intercalated phase desorbs abruptly below 400 K. Then the Gr cover, besides offering a storage volume for the intercalated H, stabilizes it above room temperature rising by a few tens of kelvins the H2 release temperature with respect to the bare Ni(111) surface.

The effectiveness of these results can be expanded by using Ni substrates with large specific surface, as nanoparticles or nanostructured foils, which, when covered with Gr, might become media where hydrogen can be loaded and stored above room temperature.

[1] D. Lizzit et al. ACS Nano 13 (2019) 1828

2:40pm 2D+AP+EM+MI+MN+NS+PS+TF-MoA-4 Assembly of Arrays of Predefined Monolayer Features into vdW Heterostructure by a Continuous Exfoliate-align-Release Process, *Vu Nguyen,* H Taylor, University of California at Berkeley
One of the major challenges of van der Waals (vdW) integration of 2D materials is the high-yield and -throughput assembly of pre-defined sequence of monolayers into heterostructure arrays. Although a variety of techniques have been developed to exfoliate the 2D materials from the source and deterministically place them onto a target substrate, they typically can transfer only either a wafer-scale blanket or a small flake at a time with uncontrolled size and shape. Here we present a method to exfoliate arrays of lithographically defined monolayer MoS_2 and WS_2 features from multilayer sources and directly transfer them in a deterministic manner onto target substrates. The continuous exfoliate-align-release process, without the need of an intermediate carrier substrate, was enabled by a new transfer medium fabricated by spin-coating a low-crosslinked and transparent adhesive on a transparent, electrostatically active backing material with low surface energy. MoS_2/WS_2 vdW heterostructure arrays produced by this method were characterized, showing coupled photoluminescence between the monolayers. Light-emitting devices using WS_2 monolayer were also demonstrated, proving the functionality of the fabricated materials. This method promises to produce large-area monolayer and multiplex heterostructure arrays with capability to integrate with existing semiconductor manufacturing equipment.

3:00pm 2D+AP+EM+MI+MN+NS+PS+TF-MoA-5 van der Waals Heterojunction Photothermoelectric Effect in MoS_2/Graphene Monolayers, *Yunqiu Kelly Luo,* The Ohio State University*; T Zhou,* University at Buffalo, State University of New York*; M Newburger,* The Ohio State Univesity*; R Bailey-Crandell, I Lyalin,* The Ohio State University*; M Neupane,* U.S. Army Research Laboratory*; A Matos-Abiague,* Wayne State University*; I Zutic,* University at Buffalo, State University of New York*; R Kawakami,* The Ohio State University
Two-dimensional (2D) van der Waals (vdW) heterostructures provide a vast playground for exploring new phenomena due to its unique ability to tailor and combine dissimilar materials with atomic precision. In particular, the combination of graphene and transition metal dichalcogenides (TMDC) garners immense interest due to their novel optoelectronic, valleytronic and spintronic properties. Here, we report the observation of a highly tunable vdW heterojunction photothermoelectric effect (HPTE) in dual-gated MoS_2/graphene heterostructures, identified by a signature six-fold photocurrent pattern as a function of heterojunction bias and carrier density. In stark contrast to photovoltaic and photothermionic effects, we discover a new mechanism arising from photoexcitation of hot electrons in graphene and subsequent thermoelectric transport across the vdW junction. While analogous to lateral photothermoelectric effects at quasi-1D junctions in single layers, the vertical geometry of HPTE offers area scaling of 2D active regions and establishes, for the first time, the photothermoelectric response in vdW heterostructures. Operating at both low (18 K) and room temperatures, the discovery of HPTE creates new

possibilities for electrically-tunable broadband photodetectors and atomically-thin spin caloritronic devices.

3:20pm 2D+AP+EM+MI+MN+NS+PS+TF-MoA-6 Formation of Edge-bonded MoS₂-graphene Nanoribbons by On-surface Synthesis, *Mark Haastrup, M Mammen, J Rodríguez-Fernández, J Lauritsen,* Aarhus University, Denmark

2D materials exhibiting unique material properties have the potential for a huge impact on our future. Graphene, as the first discovered truly 2D material, has been extensively studied. However, the lack of an intrinsic band gap makes it inadequate for electronic and optical devices. MoS_2 from the family of transition metal dichalcogenides has been intensively investigated for its possibility to be used in future applications. The vision is to integrate various 2D materials to realise an actual device. However, the actual assembly of these materials with high controllability remains a challenge. Vertical heterostructures, supported by Van der Waals interactions, have already been realised by manually stacking 2D materials on top of each other[1]. An ultimate thin device can be realised by creating lateral heterostructures with atomically sharp interfaces where each material is directly bonded to another. Currently, methods for in-plane bonding of MoS_2 to other materials (e.g. graphene) are limited due to poor structural match. One possible solution is to develop selective bottom-up methods for synthesis of molecular nanostructures by self-assembly.

This study aim to investigate the fundamental nature of bonding of graphene nanoribbons (GNRs) to the edges of MoS_2 nanoparticles by scanning tunnelling microscopy (STM). The aim is to synthesise GNRs from precursor molecules through a thermally activated Ullmann reaction already used elsewhere[2,3]. After initial growth of MoS_2, it is necessary to anneal in a hydrogen atmosphere to activate the edges to facilitate the attachment of an intermediate structure of poly(para-phenylene) (PPP) wires. STM reveals the PPP wires have an affinity for the corners of the MoS_2 nanoparticles with a distance, obtained from line scans across the adsorption site, consistent with a covalent C-S bond.

[1]: Pant et al., Nanoscale, 2016, 8, 7, 3870-3887

[2]: Cai et al., Nature, 2010, 466, 7305, 470–473

[3]: Basagni et al., J. Am. Chem. Soc., 2015, 137, 5, 1802-1808

4:00pm 2D+AP+EM+MI+MN+NS+PS+TF-MoA-8 The Effects of Metal-modification and Two Dimensional (2D) Lamellar Structure on Catalytic Performance of MFI Zeolite for Ethylene Conversion into Liquid Aromatics, *Laleh Emdadi, L Mahoney, D Tran, I Lee,* US Army Research Laboratory

The effects of two dimensional (2D) meso-/microporous structure and metal modification with gallium or zinc on catalytic performances of lamellar MFI zeolites in ethylene conversion reaction to liquid aromatics were investigated. Dual template technique was used to synthesize the 2D zeolite and metal modification of the zeolite was carried out by wet impregnation method. The results of multiple analysis techniques such as TEM, XRD, Ar adsorption-desorption, UV-Visible spectroscopy, and H_2-TPR showed that the zeolite structure is a pivotal factor for controlling the type of metal dopant species forming on zeolite, their size, and their distribution. Adding metal dopants to 2D zeolite structures improved the yield of liquid aromatics and selectivity for mono-benzene alkylated aromatics compared to their microporous commercial MFI analogies while decreased the coke formation rate. Zinc loaded lamellar MFI had the most efficient catalytic performance among all studied catalysts with lowest amount of total coke and highest fraction of light coke including mono-benzene alkylated aromatics determined by combination of different techniques such as FTIR, UV-Vis, MS-temperature programmed oxidation (TPO), FTIR-TPO, and GC-MS. This can be explained by higher accessibility of reactants to active sites and facilitated transport of products and coke precursors from lamellar structure of this zeolite and the lower Brønsted/Lewis acid site ratio of this catalyst provided by metal modification which is more suitable for ethylene aromatization and suppresses the formation of heavy coke species. The catalytic performance of zeolite catalyst can be tuned by modulating both the textural and acidity properties of the zeolite structure. The metal modified 2D lamellar MFI zeolites as bifunctional catalysts open an avenue for converting large reactant molecules to desired products by designing a catalyst with an optimal structure, acidity, and dispersion of metal dopants.

4:20pm 2D+AP+EM+MI+MN+NS+PS+TF-MoA-9 Structural Stability of Graphene Nanoflakes:From the View Point of Aromaticity, *M Ushirozako, H Matsuyama, A Akaishi,* **Jun Nakamura,** The University of Electro-Communications (UEC-Tokyo), Japan

Recently, nano-scale graphene nanoflakes (GNFs) have attracted great attention as one of the promising materials for electronics and spintronics. Kim *et al*. have successfully fabricated GNFs with various sizes up to 35 nm and have reported that the photoluminescence property of GNFs depends on the size and the edge shape [1]. From the view point of the structural stability of GNFs, we have not yet acquired the systematic comprehension with regard to effects of shapes and sizes of GNFs on the stability. In the present study, we have examined how the stability of GNFs is dominated by the edge shape and the size of GNFs, using first-principles calculations within the density functional theory.

In order to evaluate the stability of GNFs, we calculated the edge formation energy. First, we consider GNFs with the six-fold symmetry (D_{6h}) and classify them into zigzag GNFs (ZZGNFs) and armchair GNFs (ACGNFs). ACGNFs have two subtypes, AC(1) and AC(2), depending on whether carbon atoms are just at the corner of the outermost envelope hexagon of GNFs. We define the edge purity as the ratio of the number of carbon atoms at the edge unambiguously regarded as the armchair to the total number of edge atoms. The purity of AC(1) is higher than that of AC(2). The chemical formulae associated with ZZ, AC(1), and AC(2) are $C_{6n^2}H_{6n}$, $C_{18n^2-18n+6}H_{12n-6}$, $C_{18n^2-30n+12}H_{12n-12}$, respectively. In addition, we also evaluate the structural stabilities of triangular and rhombus GNFs.

We calculated the edge formation energy of the GNFs having up to 1200 carbon atoms as a function of the number of edge carbon atoms [3]. The formation energy of ZZGNFs is higher than that of ACGNFs irrespective of the size of GNFs. This instability of ZZGNFs is attributed to the presence of the so-called edge state. Indeed, it has also been shown that the formation energy of the zigzag graphene nanoribbon is higher than that of the armchair one [4]. It is noted that AC(2) is slightly more stable than AC(1), whereas the purity of AC(2) is lower than that of AC(1). Such peculiar stabilization can be reasonably explained in terms of the aromaticity of GNFs. The Nucleus Independent Chemical Shifts (NICS) values, which is averaged for the six-membered rings in GNFs, for AC(2) are lower than those for AC(1). This means AC(2) is more aromatic than AC(1). We will discuss the quantitative relationship between the stability and the aromaticity of GNFS.

[1] S. Kim et al., ACS Nano, **6**, 9, 8203 (2012)

[2] W. Hu *et al*., J. Chem. Phys. **141**, 214704 (2014)

[3] A. Akaishi, M. Ushirozako, H.Matsuyama, andJ.Nakamura, Jpn.J.Appl.Phys. **57**, 0102BA(2018)

[4] S. Okada. Phys. Rev. B, **77**, 041408 (2008)

4:40pm 2D+AP+EM+MI+MN+NS+PS+TF-MoA-10 Wafer-scale 2D-3D Mixed Heterostructures Enabled by Remote Epitaxy through Graphene, *Jeehwan Kim,* Massachusetts Institute of Technology **INVITED**

The current electronics industry has been completely dominated by Si-based devices due to its exceptionally low materials cost. However, demand for non-Si electronics is becoming substantially high because current/next generation electronics requires novel functionalities that can never be achieved by Si-based materials. Unfortunately, the extremely high cost of non-Si semiconductor materials prohibits the progress in this field. Recently our team has invented a new crystalline growth concept, termed as "remote epitaxy", which can copy/paste crystalline information of the wafer remotely through graphene, thus generating single-crystalline films on graphene [1,2]. These single-crystalline films are easily released from the slippery graphene surface and the graphene-coated substrates can be infinitely reused to generate single-crystalline films. Thus, the remote epitaxy technique can cost-efficiently produce freestanding single-crystalline films including III-V, III-N, and complex oxides. This allows unprecedented functionality of flexible device functionality required for current ubiquitous electronics. I will also present detailed mechanism behind remote atomic interaction through graphene [2]. In addition, we have recently demonstrated a manufacturing method to manipulate wafer-scale 2D materials with atomic precision to form monolayer-by-monolayer stacks of wafer-scale 2D material heterostructures [3]. In this talk, I will discuss the implication of this new technology for revolutionary design of next generation electronic/photonic devices with combination of 3D/2D mixed heterostructures.

[1] Y. Kim, et al, and J. Kim, "Remote epitaxy through graphene enables two-dimensional material based layer transfer" **Nature**, Vol. 544, 340 (2017)

[2] W. Kong, et al, and J. Kim, "Polarity govern atomic interaction through two-dimensional materials", **Nature Materials**, Vol. 17, 999 (2018)

[3] J. Shim, S. Bae, et al, and J. Kim, "Controlled crack propagation for atomic precision handling of wafer-scale two-dimensional materials" **Science**, 362, 665 (2018)

2D Materials
Room A216 - Session 2D+AP+EM+MI+NS+PS+TF-MoA

2D Materials Growth and Fabrication
Moderator: Sarah Haigh, University of Manchester, UK

1:40pm **2D+AP+EM+MI+NS+PS+TF-MoA-1 Two-dimensional Non-layered Indium Sulfide for Electronic and Optical Applications**, *Jian Zhen Ou, A Jannat, K Xu,* RMIT University, Australia

Tetragonal indium sulfide (In_2S_3) is a n-type semiconductor enabled by a unique ordered vacancy structure, which have interesting electronic and optical properties. However, its non-layered nature results in the challenge to realize its two-dimensional (2D) form. Here, we demonstrate two approaches to synthesize 2D In_2S_3. In the first approach, we grow 2D In_2S_3 with the thickness of single unit cell in wafer-scale using liquid metal as the reactant medium. The first principle calculation reveals that the 2D $InsS_3$ has highly dispersive conduction band with low effective electron mass, forming multiple band-like electronic transport channels. The field effect mobility of the material is measured to be ~60 cm2 V−1 s−1 with a high degree of reproducibility. In the second approaches, we synthesize 2D In_2S_3 with the thickness of a few unit cells using the liquid phase exfoliation of the bulk powder. It is found that there is an ultra-thin layer of 2D hexagonal indium oxide (In_2O_3) formed during the exfoliation process, hence forming an inherent 2D In_2O_3/In_2S_3 heterostructure. The photoluminescent life time is enhanced compared to In_2S_3 alone and the NO_2 gas sensing performance of the heterojunction is assessed under the illumination of visible light at room temperature. Excellent response and recovery kinetics are observed with the NO_2 detection of limit of <0.5 ppb. These two representative examples demonstrate that 2D In_2S_3 can be a suitable candidate for high performance electronic and sensing devices.

2:00pm **2D+AP+EM+MI+NS+PS+TF-MoA-2 Synthesis of High Quality Monolayer Transition Metal Dichalcogenides using Direct Liquid Injection**, *Kathleen M. McCreary, E Cobas, A Hanbicki, M Rosenberger, H Chuang, B Jonker,* U.S. Naval Research Laboratory

In recent years, interest in monolayer transition metal dichalcogenides (TMDs) has rapidly increased, spurred by the possibility for integration into a variety of technologies such as photodetection, flexible electronics, and chemical sensing. While fundamental investigations can be performed on exfoliated flakes or chemical vapor deposition synthesized isolated islands, the limited size resulting from these techniques poses a significant barrier forimplementation of TMDs in technological applications. To overcome these obstacles, new synthesis avenues should be explored. Here, we outline a novel technique that utilizes a commercially available Anneal Sys growth chamber equipped with direct liquid injection (DLI) heads for all precursors. The use of liquid, rather than solid precursors, provides fine control of both metal and chalcogen precursors leading to the synthesis of monolayer MoS_2 across cm^2 areas. Photoluminescence, Raman, XPS, and conductive AFM are used to evaluate DLI grown MoS_2, and indicate high quality material having low defect density, with metrics comparable to or better than exfoliated and chemical vapor deposition grown MoS_2.

2:20pm **2D+AP+EM+MI+NS+PS+TF-MoA-3 Understanding and Controlling the Growth of 2D Materials with Non-Equilibrium Methods and in situ Diagnostics**, *David Geohegan, Y Lin, Y Yu,* Oak Ridge National Laboratory; *C Liu, G Duscher,* University of Tennessee Knoxville; *A Strasser,* University of Texas at Dallas; *A Puretzky,* Oak Ridge National Laboratory; *K Wang,* Intel Corporation, USA; *M Yoon, C Rouleau,* Oak Ridge National Laboratory; *S Canulescu,* DTU Nanolab, Technical University of Denmark; *P Rack,* University of Tennessee Knoxville; *L Liang, W Zhang, H Cai, Y Gu, G Eres, K Xiao,* Oak Ridge National Laboratory **INVITED**

Atomically-thin two-dimensional (2D) materials, including layered 2D transition metal dichalcogenide (TMD) semiconductors and their heterostructures, exhibit remarkable quantum properties that are envisioned for energy-efficient photovoltaics, flexible optoelectronics,

catalysis, and quantum information science. However, significant synthesis and processing challenges currently limit the technologic development of these "all-surface" materials, including wafer-scale, bottom-up synthesis of uniform layers of crystalline 2D materials that are comparable in quality to exfoliated flakes of bulk materials. As-synthesized crystals of 2D TMDs display remarkable heterogeneity on both the atomistic level (e.g., vacancies, dopants, and edge terminations) and on the mesoscopic length scale (e.g., misoriented grains, layer orientations, and interactions with substrates and adsorbates) that can strongly influence the structure and electronic properties in 2D materials. This heterogeneity offers a serious challenge for synthesis and processing, yet offers a tremendous opportunity to tailor functionality.

Here we describe several approaches that are being developed for in situ diagnostic analysis and control of synthesis and heterogeneity. In addition to conventional vapor transport techniques, progress in laser-based approaches for 2D synthesis and modification, such as pulsed laser deposition (PLD) and pulsed laser conversion of precursors, are presented that permit control of the growth environment using time-resolved in situ diagnostics. The non-equilibrium advantages of PLD to form alloys and vertical heterojunctions are demonstrated using the tunable kinetic energy and digital nature of the process. Correlated atomic-resolution electron microscopy and atomistic theory are used to understand the size and stoichiometry of the "building blocks" deposited for synthesis and the forces that guide assembly. 2D crystals are grown directly on TEM grids within custom chambers and transmission electron microscopes where the ability to 'see' every atom in these atomically-thin crystals permits a unique opportunity to understand the forces governing their synthesis and functionality. In situ optical spectroscopy techniques are described to characterize the material's evolving structure and properties, offering the opportunity to 'close the loop' between synthesis and optoelectronic functionality of 2D materials and heterostructures.

3:00pm **2D+AP+EM+MI+NS+PS+TF-MoA-5 Area-Selective Atomic Layer Deposition of 2D WS_2 Nanolayers**, *Shashank Balasubramanyam* [1] , Eindhoven University of Technology, The Netherlands, Noord Brabant; *M Merkx,* Eindhoven University of Technology, The Netherlands, Netherlands; *E Kessels,* Eindhoven University of Technology, The Netherlands, Netherlands; *A Mackus,* Eindhoven University of Technology, The Netherlands, Nederland; *A Bol,* Eindhoven University of Technology, The Netherlands, Netherlands

With continued downscaling of device dimensions, ultra-thin two dimensional (2D) semiconductors like WS_2 are considered as promising materials for future applications in nanoelectronics. At these nanoscale regimes, device fabrication with precise patterning of critical features is challenging using current top-down processing techniques. In this regard, area-selective atomic layer deposition (AS-ALD) has emerged as a promising candidate for bottom-up processing to address the complexities of nanopatterning. Till date, AS-ALD of metals[1] and dielectrics[2] have been successfully demonstrated. However, AS-ALD of 2D materials has remained elusive. In this contribution, we demonstrate area-selective deposition of 2D WS_2 nanolayers by using a three-step (ABC-type) plasma-enhanced ALD process.

AS-ALD of WS_2 was achieved by using acetylacetone (Hacac) inhibitor (A), bis(tertbutylimido)-bis(dimethylamido)-tungsten precursor (B), and H_2S plasma (C) pulses. This process resulted in immediate growth on SiO_2 while a significant nucleation delay was observed on Al_2O_3, as determined from *in-situ* spectroscopic ellipsometry (SE) and *ex-situ* X-ray photoelectron spectroscopy (XPS) measurements. The surface chemistry of this selective process was analysed by *in-situ* Fourier transform infrared spectroscopy (FTIR). The analyses revealed that the inhibitor adsorbed on the Al_2O_3 surface, blocking precursor adsorption, while little or no inhibitor adsorption was detected on the SiO_2 surface where WS_2 was readily deposited. Furthermore, the area-selective growth was demonstrated on SiO_2 samples with patterned Al_2O_3 on top. On SiO_2, WS_2 could be deposited with angstrom-level thickness control.

To improve the crystallinity, the AS-ALD WS_2 films were annealed at temperatures within the thermal budget of industrial semiconductor processing (≤ 450°C). The annealed films exhibited sharp Raman peaks, which is a fingerprint of highly crystalline WS_2. Furthermore, Raman line scans over the patterns showed very sharp peak intensity transitions at the

---

[1] **TFD James Harper Award Finalist**

SiO_2-Al_2O_3 interface which confirmed that annealing had no impact on selectivity.

To summarize, this work pioneered the combination of two key avenues in atomic-scale processing: area-selective growth and ALD of 2D materials. It is expected that the results of this work will lay the foundation for area-selective ALD of other 2D materials.

[1] R. Chen and S.F. Bent, *Adv. Mater.* (2006).

[2] A. Mameli, M.J.M. Merkx, B. Karasulu, F. Roozeboom, W.M.M. Kessels and A.J.M. Mackus, *ACS Nano* (2017).

3:20pm 2D+AP+EM+MI+NS+PS+TF-MoA-6 Growth Behavior of Hexagonal Boron Nitride on Cu-Ni Binary Alloys, *Karthik Sridhara,* Texas A&M University*; J Wollmershauser,* U.S. Naval Research Laboratory*; L Nyakiti,* Texas A&M University*; B Feigelson,* U.S. Naval Research Laboratory

Controlled growth of large area n-layered chemical vapor deposited (CVD) hexagonal boron nitride (h-BN) is of great interest as a tunnel dielectric, and substrate for graphene and transition metal dichalcogenides (TMDs). The CVD growth of h-BN has been demonstrated on various transition metal catalytic substrates such as Cu, Ni, Pt and Fe. Of these metal substrates, Cu and Ni are frequently used due to their relative abundance and low cost. However, h-BN growth on Cu leads to monolayer films, and growth on Ni yields thicker, substrate grain-dependent films. Therefore, a cost-effective transition metal substrate is needed that will facilitate controlled n-layered h-BN growth.

In this work, we prepare isomorphous Cu-Ni binary alloys from 10-90 wt.% Ni by creating Ni-rich (Ni-Cu) and Cu-rich (Cu-Ni) alloys using electroplating of Cu on Ni foils and Ni on Cu foils, respectively. The electroplated foils are then annealed at ~1030° C for >5 hours to create Ni-Cu and Cu-Ni alloys. The alloys are subsequently polished mechanically to create a planarized surface suitable for h-BN growth. The surface morphology before and after polishing is assessed using a scanning electron microscope (SEM). Energy dispersive spectroscopy (EDS) characterization of the alloys confirms a designed stoichiometry at every weight percent. h-BN is grown on the alloys using atmospheric pressure chemical vapor deposition (APCVD) at 1030° C, with ammonia borane as the precursor, and H_2/N_2 as the carrier gas flowing at ~200 sccm. Cu and Ni foils are used as control samples for this study. Fourier transform infrared reflection absorption spectroscopy (FT-IRRAS) is used to confirm and characterize h-BN growth directly on Cu, Ni and alloy substrates. SEM is performed to evaluate the h-BN film and crystal morphology. The results indicate that the h-BN growth behavior on Ni-Cu is different than on Cu-Ni alloys. A trend of decreasing h-BN amount with reducing Ni concentration is observed on Ni-Cu alloys while no such trend is observed on Cu-Ni alloys. Additionally, there are large (~20 μm) multilayer and monolayer single crystals of h-BN on Ni-Cu alloys, and predominantly monolayer crystals and films of h-BN on Cu-Ni alloys. The difference in growth behavior is studied using x-ray photoelectron spectroscopy (XPS) and electron backscattering diffraction (EBSD), which reveal that the alloy surface composition determines the h-BN growth. This work demonstrates how Cu-Ni alloy substrate of different compositions, along with CVD growth conditions, can be used to control h-BN growth.

4:00pm 2D+AP+EM+MI+NS+PS+TF-MoA-8 Chemical Deposition of Vanadium Disulfide on Silicon for Optoelectronic Applications, *Mathias Fraccaroli, R Gassilloud, S Cadot,* CEA-LETI, France*; B Pelissier,* LTM, Univ. Grenoble Alpes, CNRS, France*; C Vallée,* LTM, Univ. Grenoble Alpes, CEA-LETI, France*; A Sylvestre,* G2Elab, Univ. Grenoble Alpes, France

In recent years, the search for alternative substrates to standard semiconductors (Si, Ge, SiGe, III-V, II-VI, etc.) has intensified. In this context, the transition metal dichalcogenides (TMDs) have recently emerged as candidates for the realization of original devices in a context of diversification of functionality (more than Moore). Indeed, these lamellar materials, structurally similar to graphene, have a great diversity of electrical behaviors, from the semiconductor to the metal, as well as many interesting properties (piezoelectricity and photoluminescence for MoS_2 and WS_2, even ferromagnetism by the addition of a dopant, temperature resistive transition for TaS_2, ...). The interest of the scientific community for this family of materials is growing, mainly for the most famous of them: MoS_2 and WS_2. Among this family, vanadium disulfide (VS_2)remains little studied and the development of a transferable synthesis method to an industrial scale remains a real challenge.

In this context, the development of a method of synthesis by atomic layer deposition could allow to consider future application for this material in microelectronics. In fact, due to its inherent uniformity and conformity,

atomic layer deposition (ALD) is currently envisaged as a solution to grow these sulfides on 200/300mm silicon wafers.

This presentation will describe for the first time the process developed for VS_2 synthesis on a 300mm silicon wafer. The different growth mechanisms involved with this film were first analyzed by *quasi-insitu* X-ray Photoelectron Spectroscopy (XPS) without airbreak. Also, the compositions were extracted to assess the growth rate and the incubation time and compared to other standard technics such as X-ray reflectometry. Subsequently, the physico-chemical properties of the film obtained by different will be presented. A focus on the optoelectronic properties of the film will be presented. Indeed, this film is transparent and conductive, an 8nm film has a transmittance of 78% and a resistivity of 784 μOhm.cm.

This work has been partially supported by the program EquipEx IMPACT (ANR-10-EQPX-33)

Keyword: *Quasi-insitu* XPS, Transition Metal Dichalcogenides, CVD.

4:20pm 2D+AP+EM+MI+NS+PS+TF-MoA-9 Controlled Growth of Transition Metal Dichalcogenide Monolayers for Applications in Nanoelectronic and Nanophotonic Devices, *A George, C Neumann, D Kaiser, R Mupparapu,* Friedrich Schiller University Jena, Germany*; U Hübner,* Leibniz Institute of Photonic Technology, Jena, Germany*; Z Tang, A Winter, I Staude,* **Andrey Turchanin,** Friedrich Schiller University Jena, Germany

Controlling the flow rate of precursors is highly essential for the growth of high quality monolayer crystals of transition metal dichalcogenides (TMDs) by chemical vapor deposition. Thus, introduction of an excess quantity of precursors affects the reproducibility of the growth process and results in the multilayer growth. Here, we demonstrate the use of Knudsen-type effusion cells for controlled delivery of sulfur precursor for the large area, high density, size-controlled and highly reproducible growth of monolayer TMD crystals [1]. The size of the grown crystals can be tuned between 10 - 200 μm. We grow MoS_2, WS_2, $MoSe_2$ and WSe_2 monolayer crystals as well as $MoSe_2$-WSe_2 lateral heterostructures and characterize them by optical microscopy, atomic force microscopy, Raman spectroscopy, photoluminescence spectroscopy and electrical transport measurements. It has been found that they possess a high crystalline, optical and electrical quality based on their single crystalline nature. We demonstrate their implementation in novel field-effect and nanophotonic devices and discusse an influence of the point defect density on their functional characteristics [2-3]. Moreover, we present a novel synthetic route for the integration of TMDs into lateral heterostructures with other 2D materials [4].

[1] A. George et al., *J. Phys.: Mater.* 2 (2019) 016001.

[2] T. Bucher et al., *ACS Photonics* 6 (2019) 1002.

[3] R. Meyer et al., *ACS Photonics* 6 (2019) DOI: 10.1021/acsphotonics.8b01716

[4] A. Winter et al., *Carbon* 128 (2018)106.

4:40pm 2D+AP+EM+MI+NS+PS+TF-MoA-10 Atomic Layer Deposition of BN as a Novel Capping Barrier for B_2O_3, *Aparna Pilli, J Jones, J Kelber,* University of North Texas*; A LaVoie, F Pasquale,* Lam Research Corporation

The deposition of boron oxide (B_2O_3) films on Si and SiO_2 substrates by atomic layer deposition (ALD) is of growing interest in microelectronics for shallow doping of high aspect ratio transistor structures. B_2O_3, however, forms volatile boric acid (H_3BO_3) upon ambient exposure, requiring a passivation barrier, for which BN was investigated as a possible candidate. Here, we demonstrate, deposition of BN by sequential BCl /NH reactions at 600 K on two different oxidized boron substrates: (a) B O deposited using BCl /H O ALD on Si at 300 K ("B O /Si"); and (b) a boron-silicon oxide formed by sequential BCl /O reactions at 650 K on SiO followed by annealing to 1000 K ("B-Si-oxide"). X-ray photoelectron spectroscopy (XPS) data demonstrate layer-by-layer growth of BN on B_2O_3/Si with an average growth rate of ~1.4 Å/cycle, accompanied by some B_2O_3 removal during the first BN cycle. In contrast, continuous BN growth was observed on B-Si-oxide without any reaction with the substrate. XPS data also indicate that the oxide/nitride heterostructures are stable upon annealing in ultrahigh vacuum to >1000 K. XPS data, after the exposure of these heterostructures to ambient, indicate a small amount of BN oxidation at the surface NH species, with no observable hydroxylation of the underlying oxide films. These results demonstrate that BN films, as thin as 13 Å, are potential candidates for passivating boron oxide films prepared for shallow doping applications.

5:00pm 2D+AP+EM+MI+NS+PS+TF-MoA-11 Atomic Layer Deposition of SiO₂ on Group VIII Metals: Towards Formation of a 2D Dielectric, *T Suh, R Yalisove, James Engstrom,* Cornell University

The atomic layer deposition (ALD) of many metals, particularly Group VIII (now known as Groups 8, 9 and 10), on SiO$_2$ has been an active area of research in many fields, which include microelectronics and heterogeneous catalysis. There have been many fewer studies of the inverse—the deposition of SiO$_2$ on many of these same metals. One possible reason to explore the ALD growth of SiO$_2$ on transition metals is that it might provide a route to an atomically thick SiO$_2$ dielectric, *silicatene*. Silicatene is a 2D material that consists of a bilayer of Si$_2$O$_3$ linked to each other by bridging oxygen atoms (giving SiO$_2$), where there are no dangling bonds or covalent bonds to the underlying substrate on which it is grown. For example, an established route to form silicatene involves deposition of elemental Si in UHV and subsequent high-temperature annealing on various single-crystalline metal surfaces including, but not limited to, Ru(0001), Pt(111), and Pd(100). Such a process, unfortunately, is likely not compatible with high-volume manufacturing. With this motivation we embarked on a study of the plasma-assisted ALD of SiO$_2$ on e-beam deposited polycrystalline thin films of Ru, Pt and Pd using a commercial ALD reactor. We analyzed both the thin films and the starting substrates using a combination of techniques including contact angle, spectroscopic ellipsometry (SE) and X-ray photoelectron spectroscopy. Thin films of SiO$_2$ were deposited using tris(dimethylamido)silane and an oxygen plasma at a substrate temperature of 200 °C, and we examined growth for 5, 10, 20, 50 and 100 cycles. Contact angle measurements showed immediate evidence for SiO$_2$ deposition on all metal surfaces, and the contact angle decreased and remained constant and < 10° from 5 to 100 cycles of ALD. From SE we found little evidence of an incubation period, and growth was linear for the range of sample examined and the thickness deposited per cycle was remarkably constant at a value of 0.76-0.78 Å-cycle^{-1}. Analysis of these films using angle-resolved XPS was consistent with the formation of a thin film of SiO$_2$ with uniform thickness. Having characterized the thin film thickness-ALD cycle relationship we subjected SiO$_2$ thin films with thickness of ~ 7-15 Å to post-deposition high-temperature anneals in oxygen furnace. Initial attempts to form silicatene with an anneal at 800 °C, produced a structure suggesting possible interfacial reaction between the SiO$_2$ and Ru, perhaps involving silicide formation. We will end our presentation with a discussion of recent work involving a more extensive examination of the post-deposition annealing step, and deposition on patterned wafers.

Actinides and Rare Earths Focus Topic
Room A215 - Session AC-MoA

Early Career Scientists

Moderators: Art Nelson, Lawrence Livermore National Laboratory, David Shuh, Lawrence Berkeley National Laboratory, Evgeniya Tereshina-Chitrova, Charles University, Prague, Czech Republic

1:40pm AC-MoA-1 Advanced Characterization of Nuclear Fuels, *Lingfeng He, T Yao,* Idaho National Laboratory; *V Chauhan,* The Ohio State University; *A Sen,* Purdue University; *Z Hua, M Bachhav,* Idaho National Laboratory; *M Khafizov,* The Ohio State University; *J Wharry,* Purdue University; *M Mann,* Air Force Research Laboratory; *T Wiss,* European Commission, Joint Research Centre (JRC); *J Gan, D Hurley,* Idaho National Laboratory **INVITED**

Oxide nuclear fuels have been widely used in light water reactors. The thermal conductivity of nuclear fuels is closely related to energy conversion efficiency as well as reactor safety. Understanding the mechanisms that cause the degradation in thermal conductivity in a high radiation environment is important for the design and development of new high-burnup fuels. For oxide nuclear fuels, phonon scattering by point defects, extended defects such as dislocation loops and bubbles, and grain boundaries plays a significant role in limiting the thermal transport properties. In this work, detailed microstructural characterization of pristine and ion irradiated ThO$_2$ and UO$_2$ has been performed by using electron backscatter diffraction (EBSD), atomic-resolution scanning transmission electron microscope (S/TEM), atom probe tomography (APT) and time-domain Brillouin scattering (TDBS) techniques. The thermal conductivity before and after irradiation has been determined using laser-based modulated thermoreflectance (MTR) technique. This work is partially supported by the Center for Thermal Energy Transport under Irradiation, an Energy Frontier Research Center funded by the U.S. Department of Energy Office of Sciences.

2:20pm AC-MoA-3 The Influence of Relative Humidity on the Oxidation of δ-Pu, *Scott Donald, J Stanford, A Nelson, B McLean,* Lawrence Livermore National Laboratory **INVITED**

The evolution of delta stabilized plutonium aged under a controlled environment composed of laboratory air and a range of relative humidities up to 95% was studied using Auger electron spectroscopy (AES). Linear-least squares analysis was performed on AES spectra acquired during Ar$^+$ sputter depth profiles to gain insight on the thickness and any variation in the chemical speciation of the oxide. Sputter rates were calibrated from depth profiles obtained from an oxide of a known thickness from FIB/SEM measurements. At all relative humidities, the initial oxide layer was found to grow logarithmically, indicative of a diffusion-controlled process. The rate of oxide growth was also found to be independent of oxygen partial pressure (for pO$_2$ > 31.5 Torr) for all conditions studied.

The work was performed under the auspices of the U.S. Department of Energy by Lawrence Livermore National Laboratory under Contract DE-AC52-07NA27344.

3:00pm AC-MoA-5 Magnetization and Transport Properties of Delta Phase Uranium, *Xiaxin Ding, N Poudel, T Yao, J Harp, K Gofryk,* Idaho National Laboratory

At room temperature, uranium metal is in its alpha form, the most common structural form of the element. It consists of corrugated sheets of atoms in an asymmetrical orthorhombic structure. However, the room temperature stabilized delta phase can be formed by alloying uranium with zirconium, which is known to have hexagonal crystal structure. It is important to know the physical properties of U-Zr alloys due to their technological importance. In this talk, we will present the first-time results of magnetization, transport and thermodynamic measurements of delta phase uranium at low temperatures and under high magnetic fields. The results obtained help us to understand the 5f ground state properties in different phases of U. We will discuss implications of these results.

3:20pm AC-MoA-6 Using Fused Filament Fabrication to Develop Customized Materials which Attenuate Ionizing Radiation, *Zachary Brounstein, E Murphy, J Dumont, S Talley, K Lee, A Labouriau,* Los Alamos National Laboratory

Ionizing radiation is of serious consideration in the nuclear industry because protecting workers and instrumentation is of utmost concern when operating equipment that emits potentially hazardous radiation. Currently, commercial products are readily used as protective barriers, but there are circumstances when these are less than ideal at providing optimal shielding against neutrons and gamma rays[1],[2]. As innovations to nuclear energy technologies continue to progress, developing new materials for radiation shielding grows in importance and need.

In the present work, we used an additive manufacturing (AM) technique known as Fused Filament Fabrication (FFF) to create novel 3D printed materials for radiation shielding. FFF is a layered AM process whereby thermoplastic filaments are heated up to their melting point and extruded into cross-sections of the end product[3],[4]. Because FFF has the capability to create prototypes and end-use parts with fine resolution details and excellent strength-to-weight ratios, the technology is used throughout aerospace, automotive, and medical industries.

Difficulties in creating filaments for FFF arise from fabricating a homogeneous wire that has uniform thickness and a smooth surface. If a filament does not have these initial properties, then either the FFF process will not work or the end product will not be as desired. Creating a homogeneous wire proves more difficult when different base and filler materials are used in the fabrication process, however, this can be solved if the different materials are combined in a liquid solution. Creating a wire of uniform thickness relies heavily on the extrusion process, whereby the temperature and extrusion speed are controlled.

In this study, we have prepared homogeneous filaments with varying processing conditions such as the contribution of additives and the control of extrusion temperature and speed. Thus, we used FFF to create novel filaments to print sheets of customized materials for attenuating ionizing radiation. Irradiating the printed samples was performed at the Los Alamos Neutron Science Center and the Gamma Irradiation Facility by bombarding the customized materials with neutrons and gamma rays, respectively.

References

1. McAlister, D.R., *Gamma Ray Attenuation Properties of Common Shielding Materials.* PG Research Foundation, Inc., 2018. Revision 6.1.

2. Shin, J.W., *et al, Thermochimica Acta*, 2014. **585**: p. 5-9.

3. Guo, N. and M.C. Leu, *Frontiers of Mechanical Engineering*, 2013. **8**(3): p. 215-243.

4. Srivatsan, T.S. *et al*, *Additive Manufacturing: Innovations, Advances, and Applications*. CRC Press. 2016. p. 1-48.

4:00pm AC-MoA-8 Thermodynamic and Thermal Transport Properties of Thorium Dioxide single crystals, *Narayan Poudel, X Ding,* Idaho National Laboratory; *J Mann,* Air Force Research Laboratory; *K Gofryk,* Idaho National Laboratory

Thorium dioxide (ThO_2) crystalizes into CaF_2-type (fluorite) cubic structure, similar to other members of AnO_2 (An = Th-Am) family. Thorium dioxide forms stoichiometrically and is a wide-gap transparent insulator (E_g~5-6 eV). This material is used as nuclear fuel in certain types of nuclear reactors (CANDU) that might have more advantages than conventional UO_2 based nuclear reactors. It is because of its higher thermal conductivity, higher corrosion resistance, and higher melting point. Despite its importance in nuclear technology, the thermodynamic and thermal transport properties of ThO_2 single crystals have not been studied extensively, especially at low temperatures where many different scattering mechanisms such as boundary, defects, and/or phonon-phonon dominate the heat transport. In this talk, we will present our recent measurements of the heat capacity and thermal conductivity of ThO_2 single crystals, obtained from room temperature down to 2 K. Large and good quality single crystals of ThO_2 have been synthesized by hydrothermal method for this study. We will also compare the result obtained on ThO_2 to UO_2, especially in the context of impact of 5*f*-electrons on thermodynamic and transport behavior in these materials.

4:20pm AC-MoA-9 Magnetic Nanoparticles for Biomedical Applications, *Iliana Medina-Ramirez, A Diaz de Leon Olmos,* Universidad Autonoma de Aguascalientes, Mexico; *J Zapien,* City University of Hong Kong

Magnetic nanostructured materials (MNMs) are attractive candidates for biomedical applications because of the highly desirable advantages of magnetic-guided targeting. Furthermore, MNMs can be produced by simple fabrication processes that enable flexibility to modulate their properties and desired bio-activity.

The simultaneous optimization of the bio-activity of interest while simultaneously preventing, or at least minimizing, deleterious side effects is of the outmost importance for critical applications such as the development of magnetic hyperthermia cancer treatment. However, this requires more complex multi-criteria optimization studies. We use Fe_3O_4 and $CoFe_2O_4$ MNMs prepared by microwave solvothermal method and a citrate surface modification, to modulate their toxicity and stability, as model systems to develop protocols for optimization of therapeutic MNMs. The interaction of surface-modified MNMs with HepG2 cells is evaluated by colorimetric, optical microscopy and Atomic Force Microscopy (AFM) studies for dose. We show that AFM presents important advantages over conventional techniques including information on the potential internalization of MNMs by the cells as function of surface modification. The optimized MNMs in this study present morphological, colloidal, biocompatibility and magnetic properties that make them promising candidates for the development of efficient therapeutic agents for hyperthermia cancer treatment applications.

Biomaterial Interfaces Division
Room A120-121 - Session BI+AS-MoA

Cutting Edge Bio: Bio-Nano, Bio-Energy, 3D Bio

Moderators: Heather Canavan, University of New Mexico, Jordan Lerach, ImaBiotech Corp.

1:40pm BI+AS-MoA-1 Emulsion-templated Asymmetric Vesicles, *Laura Arriaga*, University of Madrid, Spain   **INVITED**

A vesicle is a naturally existing or an artificially prepared aqueous droplet stabilized by an amphiphilic membrane that ensures retention of hydrophilic ingredients within its core. This amphiphilic membrane typically comprises two leaflets, which have either identical or different compositions. While membranes comprising two compositionally identical leaflets exhibit lateral asymmetries or domains if prepared from mixtures of amphiphilic molecules capable of phase separation, membranes comprising compositionally different leaflets are asymmetric in the transversal direction. Moreover, internal vesicle asymmetries can be induced through the phase separation of sufficiently concentrated polymer solutions encapsulated in the vesicle cores. All these types of asymmetry dictate vesicle properties, making them more suitable than symmetric vesicles for a wide range of applications, especially to appropriately mimic biological cells. However, the utility of these vesicles depends critically on the degree of control achieved over their properties in the fabrication process. Here, we address the adequacy of emulsion droplets with well-controlled topologies, fabricated with exquisite control by microfluidic technologies, as vesicle templates. In particular, we describe a first strategy to fabricate vesicles with symmetric membranes exhibiting lateral domains and internal asymmetries using double emulsion drops as templates [1,2], and a second strategy to form vesicles with asymmetric membranes using triple emulsion drops as templates [3]. These strategies efficiently encapsulate ingredients within the core of the vesicles or their membranes and yield vesicles with monodisperse sizes and controlled degrees of asymmetry.

[1] L.R. Arriaga, S. Datta, S.-H. Kim, E. Amstad, T. Kodger, F. Monroy, D.A. Weitz. Ultra-thin shell double emulsion templated giant unilamellar lipid vesicles with controlled microdomain formation. Small 10, 950-956 (2014).

[2] J. Perrotton, R. Ahijado-Guzman, L.H. Moleiro, B. Tinao, A. Guerrero-Martinez, E. Amstad, F. Monroy, L.R. Arriaga. Microfluidic fabrication of vesicles with hybrid lipid/nanoparticle bilayer membranes. Soft Matter 15, 1388-1395 (2019).

[3] L.R. Arriaga, Y. Huang, S.-H. Kim, J.L. Aragones, R. Ziblat, S.A. Koehler, D.A. Weitz. Single-step assembly of asymmetric vesicles. Lab Chip 19, 749-756 (2019).

2:20pm BI+AS-MoA-3 Antimicrobial Cyclic Peptide Polymer Nanopores, *Kenan Fears, L Estrella,* US Naval Research Laboratory

We present a new class of bioinspired nanomaterials that are stabilized by a combination of covalent and hydrogen bonds. Prior work by others has shown that cyclic peptides can self-assemble to form supramolecular assemblies through backbone-backbone hydrogen bonding. To improve upon this molecular architecture, we develop a synthesis route to polymerize cyclic peptides and form a linear polymer chain that can transition between a rigid nanorod and a "soft" unfolded conformation. For a cyclic peptide polymer containing amine-terminated side chains on each ring, we demonstrate self-assembly can be triggered in aqueous solutions by varying the pH. We measure the elastic modulus of the rigid nanorods to be ca. 50 GPa, which is comparable to our molecular dynamics (MD) prediction (ca. 64 GPa). Our results highlight the uniqueness of our molecular architecture, namely their exemplary toughness (up to 3 GJ m^{-3}), in comparison to other cyclic peptide-based assemblies. Finally, we demonstrate the amphiphilic cyclic peptide nanopores are capable of inserting into the membrane of both gram-negative and gram-positive bacteria, and causing their deaths by disrupting their osmotic pressure.

2:40pm BI+AS-MoA-4 ToF-SIMS Analysis of the Distribution of *p*-Hydroxybenzoate in Wood, *Robyn E. Goacher,* Niagara University; *Y Mottiar,* University of British Columbia, Canada

The progress towards a green bio-based economy depends in part on our ability to chemically modify lignocellulosic plant matter. Possible targets for such chemical modifications include ester-linked pendant groups that occur on lignin in some plant species. The lignin in poplar and willow is known to contain 1-10% of *p*-hydroxybenzoate (-*p*HB) moieties, although little is known about the function of these -*p*HB groups. To understand the function of -*p*HB, it is important to understand the distribution of -*p*HB among different cell types. Previous work with ultraviolet microscopy suggests that -*p*HB is present only in fibers and not in vessels. The goal of this work is to provide a more specific analysis of the spatial distribution of -*p*HB in wood by using surface-sensitive chemical imaging. Time-of-flight secondary ion mass spectrometry (ToF-SIMS) was used to image cross-sections of mature Lombardy poplar, juvenile (greenhouse-grown) Lombardy poplar and mature DUKE-5 willow. Lombardy poplar is known to contain higher levels of -*p*HB than the DUKE-5 willow. Samples were analyzed prior to and after solvent extraction to remove spectral interferences from small molecule extractives, which have similar chemical composition to -*p*HB and lignin. A milk alkaline hydrolysis was also performed to cleave ester-linked -*p*HB from lignin in order to confirm identification of certain peaks within the mass spectra as characteristic of -*p*HB. Multivariate statistical analysis was used to aid in the data interpretation. The process of identifying peaks that arise from -*p*HB will be discussed, and chemical images of the localization of -*p*HB will be presented. This data contributes to our understanding of how -*p*HB is distributed in wood. These insights may shed light on the role of ester-linked moieties in lignin and will hopefully advance the use of -*p*HB as a biotech target.

3:00pm BI+AS-MoA-5 Feeling the Force; Probing the Cues that Influence Stem Cell Behaviour, *Stephanie Allen*, School of Pharmacy, The University of Nottingham, UK **INVITED**

There is considerable research activity directed towards understanding the basic biology of stem cells and controlling their mechanisms of self-renewal and differentiation into functional tissue types. Much of the current research involves genetic and/or biochemical approaches to control proliferation and differentiation. Over the last decade, studies using biophysical approaches, including our own, have begun to impact on this understanding, revealing that physical signals and cues elaborated by neighbouring cells and the surrounding extra-cellular matrix, are also fundamental to controlling stem cell fate (1-4). For many emerging approaches/applications, including those that aim to create functioning tissues through the 3D patterning of stem cells, an understanding of such physical cues is therefore vital.

Despite this importance relatively few studies have still attempted to investigate and quantify the physical interactions between stem cells and/or the effects of applied stimuli. This talk aims to provide an overview of our recent research in this area, that aims to address this knowledge gap by utilizing force measurement approaches (including optical tweezers and atomic force microscopy). The presentation will include results from a current project where we are employing AFM-based single molecule force measurement approaches to provide new insights into the role of cadherins on mouse embryonic stem cells (mESCs).

(1) Discher *et al Science* 324 :1673-1677 (2009)

(2) Lanniel *et alSoft Matter.* 7, 6501-6514 (2011)

(3) Lanniel *et alThin Solid Films* 519, 2003-2010 (2011)

(4) Kirkham *et alScientific Reports*, 5, No. 8577 (2015)

4:20pm BI+AS-MoA-9 Angstrom-Resolved Characterization of Electrochemical Interfaces in Real Time during Polarization, *Markus Valtiner*, Vienna University of Technology, Austria

Electrochemical solid|liquid interfaces are critically important for energy conversion, biosensing and biodegradation processes. Yet, a real-time visualization of dynamic charging processes at electrified solid|liquid interfaces with close to atomic resolution is extremely challenging.

I will discuss a unique real-time atomistic view into dynamic charging processes at electrochemically active metal interfaces using white light interferometry in an electrochemical surface forces apparatus. This method allows simultaneous deciphering of both sides of an electrochemical interface; the solution and the metal side; with microsecond resolution under dynamically evolving reactive conditions that are inherent to technological systems in operando. The real-time capability of this approach reveals significant time lags between electron transfer, oxide reduction/oxidation, and solution side reaction during a progressing electrode process. In addition, the developed approach provides detailed insight into the structure of the electric double layer under varying charging conditions. I will also discuss how we can complementary use high resolution in-situ AFM imaging to further characterize ion layering at charged surfaces.

The presented work may have important implications for designing emerging materials utilizing electrified interfaces and may apply to bio-electrochemical processes, signal transmission and pore charging.

4:40pm BI+AS-MoA-10 New Electrochemical Methods for Probing Metalloenzymes, *Alison Parkin*, University of York, UK **INVITED**

Large amplitude Fourier transform alternating current voltammetry (FTacV) is being developed as a new tool for probing electron-transfer processes in metalloenzymes. We can probe non-innocent active site ligand chemistry in molybdenum enzymes and based on our new insight into the rates and energetics of electrons entering/exiting an iron sulfur cluster we have been to rationally re-design a hydrogen enzyme to increase the catalytic efficiency and hydrogen production. This talk will describe these studies and detail our solutions to the challenges in efficient data analysis and protein-electrode wiring.

Electronic Materials and Photonics Division
Room A214 - Session EM+PS+TF-MoA

New Devices and Materials for Logic and Memory

Moderators: Rehan Kapadia, University of Southern California, Nicholas Strandwitz, Lehigh University

1:40pm EM+PS+TF-MoA-1 Short-term Plasticity to Long-term Plasticity Transition Mimicked by High Mobility InP FETs with TiO_2 Trapping Layer, *Jun Tao, R Kapadia,* University of Southern California

Memory is widely believed to be encoded and stored in the central nervous system by altering the synapse strength via activity-dependent synaptic plasticity between millions of neurons in vertebrates. Consolidations from short-term plasticity (STP) to long-term plasticity (LTP) not only transform the important external stimuli to permanently stored information but release storage space for accepting new coming signals. Although memristor technology (e.g. RRAM) has been reported to mimic the STP and LTP characteristics and exhibited its merit in density comparing to traditional CMOS based SRAM technology, some conventional memristors suffer non-ideal operation speed, small dynamic range, and high resistance variation.

In our work, the single crystal Indium Phosphide (InP) based synaptic devices demonstrated its advantages not only in the emulation of the synaptic functions for both STP and LTP characteristics but also in the controllability of transition from STP to LTP. Since we interpret gate voltage pulses as the pre-synaptic action potentials, the source-drain current as post-synaptic current, and the channel conductance as synaptic weight, the consolidations from STP to LTP are elaborately demonstrated through mediating multiple action potential parameters like pulse numbers, pulse intervals (or rates), and pulse durations. The synaptic devices we demonstrated here are essentially single crystal channel InP Field Effect Transistors (FETs) fabricated on Si/SiO_2 substrates with the templated liquid-phase (TLP) method. In addition, TiO_2 trapping layer is inserted into the gate dielectric layer to provide extra deeper trap states. The 'ratchet' mechanism is utilized to have the charges 'fall' into the TiO_2 well and implement the transition from STP to LTP effectively.

2:00pm EM+PS+TF-MoA-2 Magnetic Domain Wall Devices for Artificial Neural Network, *Saima Siddiqui, S Dutta, A Tang, L Liu, M Baldo, C Ross,* MIT

Magnetic domain wall devices are promising candidates for logic [1] and storage class memory [2]. Due to the non-volatility and energy-efficient switching, this type of device is one of the prime candidates for in memory computing and brain-inspired computing. In-memory computing is a non-von-Neumann architecture where data computation and storage are done locally to reduce the data movement between the processor and the storage memory [3]. The layer-by-layer operations of data require synapses (i.e. variable resistors whose resistance vary linearly with the input) and activation function generators between layers (i.e. variable resistors whose resistance vary non-linearly with the input current).

Domain walls' motion in a magnetic wire is a function of applied current due to spin-orbit torque from an adjacent heavy metal (Fig. 1). The current density and spin orbit torque can be modified along the wire by adjusting the width of the heavy metal. The spin orbit torque then becomes a function of the domain wall position, which makes the domain wall motion a nonlinear function of the applied current (Fig. 2). Linear and nonlinear domain wall motion can be detected via magnetoresistance by using a magnetic tunnel junction in which the magnetic wire forms the free layer. The electrical detection is necessary for the analog matrix multiplication in neuromorphic accelerator. However, domain walls are pinned due to the magnetostatic energy minima on the sides of the MTJ. The synaptic (Fig. 3) and activation function (Fig 4) like magnetoresistive behavior can still be generated by using multiple MTJs in parallel. In this study, we demonstrate linear and nonlinear domain wall motion in magnetic wires and modify the design of magnetic tunnel junctions to convert these motions into magnetoresistance. The experimental observations of the device characteristics agree with both analytical and micromagnetic modeling.

[1] J. A. Currivan-Incorvia, S. Siddiqui, S. Dutta, E. R. Evarts, J. Zhang, D. Bono, C. A. Ross, and M. A. Baldo, Nat Commun., 7, 10275 (2016).

[2] Stuart S. P. Parkin, Masamitsu Hayashi, and Luc Thomas, Science, Vol. 320, Issue 5873, pp. 190-194 (2008)

[3] Jacob Torrejon, Mathieu Riou, Flavio Abreu Araujo, Sumito Tsunegi, Guru Khalsa, Damien Querlioz, Paolo Bortolotti, Vincent Cros, Kay Yakushiji,

Akio Fukushima, Hitoshi Kubota, Shinji Yuasa, Mark D. Stiles & Julie Grollier, Nature volume 547, pp. 428–431 (2017).

2:20pm EM+PS+TF-MoA-3 Ferroelectric Devices for Non-von Neumann Computing, *Z Wang, Asif Khan,* Georgia Institute of Technology **INVITED**
Excitation and inhibition go hand in hand in neuronal circuits in biological brains. For example, neurons in the visual and the auditory cortices provide excitatory responses to visual and auditory stimuli, respectively. On the other hand, interneurons in the central nervous system provide inhibitory signals to downstream neurons thereby imparting regulation and control in neuronal circuits—the loss of which often causes neurodegenerative disorders. These neuro-biological facts have inspired the bio-mimetic computational perspective that artificial, excitatory neurons need to be paired with inhibitory connections for functional correctness and efficient compute models such as spiking neural networks.

In this talk, we will introduce a ferroelectric neuromorphic transistor platform [1,2] which can (1) efficiently incorporate both excitatory and inhibitory inputs in the simple two transistor topology of an artificial, ferroelectric spiking neuron, and (2) emulate several classes of biological spiking dynamics (such as regular, fast, Thalamo-Cortical spiking and so on). We will discuss the recent experimental demonstrations of ferroelectric spiking neurons. The talk will end with a simulation experiment where a full-scale spiking neural network was implemented using experimentally calibrated ferroelectric circuit models and the network was benchmarked analog CMOS and other emerging device technologies.

References:

[1] Z. Wang, B. Crafton, J. Gomez, R. Xu, A. Luo, Z. Krivokapic, L. Martin, S. Datta, A. Raychowdhury, A. I. Khan, "Experimental Demonstration of Ferroelectric Spiking Neurons for Unsupervised Clustering," *The 64th International Electron Devices Meeting (IEDM 2018)*, 2018.

[2] Z. Wang, S. Khandelwal & A. I. Khan, "Ferroelectric oscillators and their coupled networks," IEEE Electron Dev. Lett. 38, 1614 (2017).

3:00pm EM+PS+TF-MoA-5 Ultrafast Measurement of Nanoseconds Polarization Switching in Ferroelectric Hafnium Zirconium Oxide, *Mengwei Si, P Ye,* Purdue University
Ferroelectric (FE) hafnium oxides (HfO_2) such as hafnium zirconium oxide (HZO) is the promising thin film ferroelectric material for non-volatile memory applications. The ultrafast measurements of polarization switching dynamics on ferroelectric (FE) and anti-ferroelectric (AFE) hafnium zirconium oxide (HZO) are studied, with the shortest electrical pulse width down to as low as 100 ps. The transient current during the polarization switching process is probed directly. The switching time is determined to be as fast as 10 ns to reach fully switched polarization with characteristic switching time of 5.4 ns for 15 nm thick FE HZO and 4.5 ns for 15 nm thick AFE HZO by Kolmogorov–Avrami–Ishibashi (KAI) model. The limitation by parasitic effect on capacitor charging is found to be critical in the correct and accurate measurements of intrinsic polarization switching speed of HZO. The work is in close collaborations with Xiao Lyu, Wonil Chung, Pragya R. Shrestha, Jason P. Campbell, Kin P. Cheung, Haiyan Wang, Mike A. Capano and was in part supported by SRC and DARPA.

3:20pm EM+PS+TF-MoA-6 Interfacial Charge Engineering in Ferroelectric-Gated Mott Transistors, *X Chen, Y Hao, L Zhang, Xia Hong,* University of Nebraska-Lincoln
Ferroelectric field effect transistors (FeFETs) built upon Mott insulator channel materials have been intensively investigated over the last two decades for developing nonvolatile memory and logic applications with sub-nanometer size scaling limit. However, the intrinsically high carrier density of the Mott channel (10^{22}-10^{23}/cm³) also imposes significant challenges in achieving substantial modulation of the channel conduction. In this work, we exploit the intricate interplay between interfacial charge screening and transfer effects in epitaxial heterostructures composed of two strongly correlated oxide layers, one layer of rare earth nickelate $RNiO_3$ (R = La, Nd, Sm) and one layer of (La,Sr)MnO₃ (LSMO), to realize a giant enhancement of the ferroelectric field effect in Mott-FeFETs with a Pb(Zr,Ti)O₃ gate. For devices with 1-5 nm single layer $RNiO_3$ channels, the room temperature resistance switching ratio (R_{off}-R_{on})/R_{on} increases with decreasing channel thickness till it reaches the electrical dead layer thickness. For devices built upon $RNiO_3$/LSMO bilayer channels, the resistance switching ratio is enhanced by up to two orders of magnitude compared with the single layer channel devices with the same channel thickness. Systematic studies of the layer thickness dependence of the field effect show that the LSMO buffer layer not only tailors the carrier density profile in $RNiO_3$ through interfacial charge transfer, but also provides an extended screening layer that reduces the depolarization effect in the ferroelectric gate. Our study points to an effective strategy for building high density nanoelectronic and spintronic applications via functional complex oxide heterointerfaces.

4:00pm EM+PS+TF-MoA-8 The Interface of Transition Metal Dichalcogenides and Ferroelectric Oxides, *Maria Gabriela Sales, S Jaszewski, S Fields, R Christopher, N Shukla, J Ihlefeld, S McDonnell,* University of Virginia
Transition metal dichalcogenides (TMDs) are an interesting class of materials because of their unique properties owing to their 2D nature, wherein layers that are covalently bonded in-plane are held together by van der Waals forces in the out-of-plane direction, similar to graphene. However, unlike graphene, semiconducting TMDs have a band gap that is tunable with layer thickness, allowing control over its properties depending on specific applications. One such application is in ferroelectric-based transistors, which have high potential for use in memory and logic, but whose major drawback in integration when using silicon as the semiconducting channel is the poor semiconductor-ferroelectric interface, due to issues such as interdiffusion across the interface. Thus, a promising alternative route is using a TMD as the channel with a ferroelectric material as the gate dielectric. This is expected to have an improved interface quality because of the fact that TMDs have no dangling bonds at the surface and are highly stable in-plane. In this study, we focus on a mixture of hafnium oxide and zirconium oxide as our ferroelectric material, with zirconium stabilizing the ferroelectric phase in hafnia. We explore the TMD/ferroelectric structure, addressing certain integration issues in growth, and looking at their interface chemistry and thermal stability. Specifically, we look at commercially available geological MoS₂ and molecular beam epitaxy-grown WSe₂ interfaced with an atomic layer deposited Hf$_x$Zr$_{1-x}$O₂ ferroelectric. Our report will focus on the results of our investigations of this interface carried out using a combination of X-ray photoelectron spectroscopy (XPS) and X-ray diffraction (XRD) techniques.

4:20pm EM+PS+TF-MoA-9 Electronic and Thermal Properties of 2D Materials, *Connor McClellan, E Yalon, K Smithe, C English, S Vaziri, C Bailey, A Sood, M Chen, E Pop,* Stanford University
This talk will present recent highlights from our research on two-dimensional (2D) materials and devices including graphene, and transition metal dichalcogenides (TMDs). The results span from fundamental measurements and simulations, to devices, to system-oriented applications which take advantage of unusual 2D material properties.

Using the low cross-plane thermal conductance, we found unexpected applications of graphene as an ultra-thin electrode to reduce power consumption in phase-change memory [1]. We have also demonstrated wafer-scale graphene systems for analog dot product computation [2]. We have grown monolayer 2D semiconductors by chemical vapor deposition over cm² scales on amorphous oxides, including MoS₂ with low device variability [3], WSe₂, and MoSe₂.

Using a self-aligned process, we demonstrated 10 nm gate-length monolayer MoS₂ transistors with excellent switching characteristics and approaching ballistic limits [4]. Using sub-stochiometric oxides, we achieved high electron doping to reduce electrical contact resistance down to 480 Ω·μm and increase on-current up to a record of 700 μA/μm in monolayer MoS₂ [5]. We also directly measured the saturation velocity in monolayer MoS₂, finding it is thermally-limited (i.e. by device self-heating and phonon scattering) to about one-third that of silicon and about one-tenth that of graphene [6]. Using Raman thermometry, we uncovered low thermal boundary conductance (~15 MW/m²/K) between MoS₂ and SiO₂, which could limit heat dissipation in 2D electronics [7]. We are presently exploring unconventional applications including thermal transistors [8], which could enable nanoscale control of heat in "thermal circuits" analogous with electrical circuits. These studies reveal fundamental limits and new applications of 2D materials, taking advantage of their unique properties.

References: [1] A. Behnam et al., Appl. Phys. Letters. 107, 123508 (2015). [2] N. Wang et al., IEEE VLSI Tech. Symp., Jun 2016, Honolulu HI. [3] K. Smithe et al., ACS Nano 11, 8456 (2017). [4] C. English et al., IEEE Intl. Electron Devices Meeting (IEDM), Dec 2016. [5] C. J. McClellan et al., IEEE Device Research Conference (DRC), June 2017. [6] K. Smithe et al., Nano Lett. 18, 4516 (2018). [7] E. Yalon, E. Pop, et al., Nano Lett. 17, 3429 (2017). [8] A. Sood, E. Pop et al. Nature Comm. 9, 4510 (2018).

4:40pm EM+PS+TF-MoA-10 Electronics in Flatland, *Sanjay Banerjee*, University of Texas at Austin INVITED
2D materials such as graphene, transition metal dichalcogenides and topological insulators have opened up avenues in beyond-CMOS device concepts. We will discuss our work involving single or many-particle 2D-2D tunneling, leading to transistors with negative differential resistance. We also explore spintronics in these systems for novel logic and memory devices. We will also discuss the use of these materials in less esoteric, but more practical high frequency, mechanically flexible FETs for IoT applications.

MEMS and NEMS Group
Room A210 - Session MN-MoA

Microfabricated Systems for Gas Chromatography and Nanomechanical Mass Sensing

Moderators: Robert Davis, Brigham Young University, Christian Zorman, Case Western Reserve University

1:40pm MN-MoA-1 Micromachined Silicon Micro-pillar Arrays for Liquid and Gas Chromatography, *Gert Desmet*, Vrije Universiteit Brussel, Belgium INVITED
The present contribution aims at illustrating and demonstrating how micro-machining technology can give a boost to High Performance Liquid Chromatography (HPLC). Currently, HPLC is routinely used in nearly every chemical analysis lab. Despite its high degree of maturity, the technique however suffers from serious performance limitations when faced to the complex samples that need to be separated to solve the current state-of-the-art problems in the biological and pharmaceutical research (e.g., proteomics and metabolomics), the food and environmental analysis, etc.

The currently used packed bed HPLC columns are clearly underachieving because of the packing disorder and the concomitant large degree of band broadening. To solve this packing disorder problem, the present contribution will focus on the possibilities of advanced photolithographic etching techniques such as the Bosch-process to produce perfectly ordered porous support columns with optimized hydrodynamic shape and optimized external porosity.

At the conference, we will demonstrate the possibility of rapid multi-component separations and the possibility to achieve very high separation efficiencies with a microfabricated column in pressure-driven liquid chromatography. In addition, we have also extended the concept to gas chromatography (GC), where the micromachining allows to make designs that combine fast separation kinetics with a high mass loadability, two factors with opposite requirements in the current commercial format for GC.

2:20pm MN-MoA-3 An Integrated Passive µPreconcentrator with Progressively-Heated µInjector for µGC, *R Hower, C Zhan, M Akbar, N Nuñovero, J Wang, J Potkay, Edward Zellers*, University of Michigan INVITED
We report on a new device designed to serve as a universal 'front-end' for gas chromatographic microsystems (µGC) for remote, long-term monitoring of vapor-phase chemical threats or environmental pollution. This small, low-power, Si/glass-micromachined device, dubbed a micro-collector/injector (µCOIN), combines a passive micro-preconcentrator (µPP) with a progressively heated micro-injector (µPHI). The µPP samples vapors at known rates by molecular diffusion and transfers them under active flow via thermal desorption to the µPHI, which, in turn, injects them to a downstream (µGC) separation column via progressive (sequential) heating. Most testing to date was performed with discrete devices, both of which contain tandem cavities packed with granular carbon-based adsorbents of different specific surface areas. Carbopack B (CB, 100 m^2/g) and Carbopack X (CX, 240 m^2/g) were used for most compounds. But CX was used with Carboxen 1003 (C3, 1000 m^2/g) for more volatile compounds. Using a conventional GC for downstream analyses, we have found that the µPP (CX/CB) can collect vapors of widely different volatility at a nearly constant effective sampling rate for up to 24 hrs (low concentrations) and over a 2,500-fold concentration range (0.25-hr samples). Effective (compound-specific) sampling rates ranged from ~0.25 to 0.69 mL/min, most of which agreed with theoretical predictions. Desorption/transfer efficiencies from the µPP were > 87% (most > 94%) at 5 mL/min and 250 °C for 60 sec. For the µPHI (CX/CB) bolus challenges of compounds at 5mL/min, mimicking transfer from the µPP, resulted in > 90% capture efficiency for up to 3.6 µg of lower volatility compounds. More

volatile or highly polar compounds required the CX/C3-loaded device. Back-flushed progressive heating of the µPHI produced injection bands < 250 ms wide at flow rates < 0.5 mL/min. In separate tests, remarkable selectivity for polar compounds was achieved by applying an ionic-liquid surface modifier to the carbon adsorbents (tests in the µPP and µPHI are pending). The monolithically integrated µCOIN (0.23 cm^3) has not yet been tested. But, a hybrid-integrated µCOIN (capillary connections) provided good preliminary performance, including efficient sampling, transfer, and injection of multi-component mixtures. Valveless flow modulation was implemented to avoid backflow to the µPP. Using typical power levels for each device, two valves, a pump, an interconnect heater, and supporting electronics, the energy consumption was only 320 J per cycle for the hybrid µCOIN. Thus, the µCOIN shows promise as a component in future ultra-low-power µGC systems for analyzing complex vapor mixtures.

3:00pm MN-MoA-5 Developments and Challenges in Full-range Microchip Gas Chromatography, *Abhijit Ghosh*, Honeywell UOP, Des Plaines, IL, USA.; *M Lee*, Brigham Young University
This year (2019) marks the 40th anniversary of microchip gas chromatography (GC). In these four decades of investigations, many avenues, as well as challenges, have been encountered by researchers to produce microchip columns that are as efficient as fused silica open tubular columns in GC. Although there are exciting theoretical possibilities, in reality many practical constraints remain that limit their widespread commercialization and use. The main challenges are difficulty in static coating, unwanted dead volumes and inadequate interfacing technologies, which all affect both column performance and range of applications. This presentation emphasizes some of the challenges and key developments in the field of microchip gas chromatography, as well as novel approaches that are currently being investigated

3:20pm MN-MoA-6 Fabrication of Thermally Isolated micro-Column for Gas Chromatography, *James Harkness, H Davis, A Davis, R Davis, B Jensen, R Vanfleet*, Brigham Young University
Micro gas chromatography (GC) has suffered from poor separations due to short column length and stationary phase pooling, however introducing a thermal gradient along a GC micro-column has been shown to enhance separations. We will present a thermally isolated micro-column for thermal gradient GC, fabricated using a two-wafer deep silicon etch/bond/etch process. Desired thermal isolation was achieved by forming suspended micro-columns that enable low-power thermal control using passive and active elements.

4:00pm MN-MoA-8 Control of Surface Geometry and Chemistry to enable integration of Microfabricated Structures into High Performance Microscale Gas Chromatography Systems, *Henry Davis, D McKenna, J Harkness, D Kane, R Vanfleet, R Davis*, Brigham Young University
There are a variety of microfabricated structures, materials and devices that could enable high performance microscale gas chromatography systems, such as micro pillar arrays and porous resonant mass detectors. However, integration of these structures into microscale gas chromatography systems will require a high degree of control over surface geometry and surface chemical functionalization. Here we will describe processes using liquid deposition of silsesquioxanes and oxide atomic later deposition for control of surface chemistry and geometry of micro and nanoscale structures.

4:20pm MN-MoA-9 Constructive Utilization of Nonlinear Dynamics in MEMS/NEMS, *Hanna Cho*, The Ohio State University INVITED
During the last decades, we have witnessed that MEMS/NEMS revolutionized fundamental and applied science. However, due to small size and low damping, these devices often exhibit significant nonlinearity and thus the operational range of these impressive applications shrinks. Therefore, understanding the mechanisms leading to nonlinearity in such systems will eliminate obstacles to their further development and significantly enhance their performance. Motivated by the need to advance current capabilities of MEMS/NEMS, our research has been focused on the implementation of intentional intrinsic nonlinearity in the design of MEMS/NEMS resonators and proved that harnessing intentional strong nonlinearity enables exploiting various nonlinear phenomena, not attainable in linear settings, such as broadband resonances, dynamic instabilities, nonlinear hysteresis, and passive targeted energy transfers. We developed a comprehensive analytical, numerical, and experimental methodology to consider structural nonlinearity as a main design factor enabling to tailor mechanical resonances and achieve targeted performance. We investigated the mechanism of geometric nonlinearity in

a non-prismatic microresonator and suggested strategies to tailor the various types of nonlinear resonance. Our recent works focus on exploiting nonlinearity and multimodality simultaneously by internally coupling two or more modes through the mechanism of internal resonance or combination resonance. This talk will introduce various types of nonlinearity realized in micro/nanomechanical systems and discuss their unique behavioral features that can be exploited in the field of MEMS/NEMS.

5:00pm MN-MoA-11 Frequency Stabilization in a MEMS Oscillator Via Tunable Internal Resonance, *Jun Yu, H Cho,* The Ohio State University

Micro-Electro-Mechanical Systems (MEMS) oscillators are being considered as substitutes of quartz oscillators since these microscale oscillators are easier to be integrated in electronics. As a timing device, one of the most important functionalities of MEMS oscillators is to provide a reference frequency with a minimal frequency fluctuation. The mechanism of internal resonance (IR) was proposed to stabilize the frequency by Antonio et al. in 2012 [1]. Here, we report a MEMS resonator that is specifically optimized to provide 1:2 relationship between its modal frequencies and, thus, implement 1:2 IR in its dynamic response. We also tune the frequency ratio precisely by adjusting the applied DC voltage to achieve an ideal IR characteristic for frequency stabilization.

In this study, a clamped-clamped silicon microbeam resonator shown was designed and fabricated to enforce a 1:2 ratio between its second and third flexural modes. We first characterized the thermal-mechanical noise of the resonator under different DC biases using a Laser Doppler Vibrometer. Its modal frequencies can be tuned with DC bias, because the DC bias influences the mid-plane stretching of the microbeam structure. Thereby, the ratio between second and third flexural modes can be finely adjusted around the 1:2 commensurate condition and eventually achieve exact 1:2 ratio when the DC bias is 21V. Under this IR condition, a well-documented M-shape, typically occurring in a 1:2 IR system. The externally resonated (ER) curve represents the oscillation amplitude at the excitation frequency, while the internally resonated (IR) curve represents the oscillation amplitude at the twice of the excitation frequency. We further studied the frequency stabilization by exploiting the energy transfer mechanism of internal resonance. We measured the frequency fluctuations from the MEMS oscillator implementing this resonator in the cases without and with IR. When IR was triggered, the frequency fluctuation was diminished by more than 20 times to be 5.72 ppm. The Allan deviations is also reduced by about 30 times when the IR is activated.

[1] D. Antonio, D. H. Zanette, and D. López, "Frequency stabilization in nonlinear micromechanical oscillators," *Nat. Commun.*, vol. 3, no. 1, Jan. 2012.

Plasma Science and Technology Division
Room B130 - Session PS+AS+EM+SS+TF-MoA

Plasma-Surface Interactions

Moderators: Sebastian Engelmann, IBM T.J. Watson Research Center, Sumit Agarwal, Colorado School of Mines

1:40pm PS+AS+EM+SS+TF-MoA-1 Cleaning Chamber Walls after ITO Plasma Etching Process, *Salma Younesy,* *C Petit-Etienne,* LTM/CNRS, France; *S Barnola,* CEA-LETI, France; *P Gouraud,* ST Microelectronics, France; *G Cunge,* LTM/CNRS, France

Controlling the reactor walls in plasma etching is a key to avoid process drifts. In fact, the deposition of plasma generated species on the reactor walls during etching changes their chemical nature, thereby affecting plasma characteristics such as the radical concentration and the ion flux, which eventually leads to etch rates, anisotropy and selectivity variations. To overcome this issue, the chemical nature of the deposit formed on the chamber walls during etching must be determined to be able to develop efficient plasma chamber cleaning strategies. For new optoelectronic devices, the integration of materials with low volatility etch products such as ITO renders the dry cleaning processes long and laborious. Therefore, we have investigated several plasma chemistries to find out the most efficient reactor cleaning strategy after ITO etching.

The chemical nature of the reactor walls is analyzed quasi in situ by XPS using the "floating sample" technique [1], in which an Al_2O_3 sample representing the reactor walls is fixed on the 200 mm diameter wafer, but separated from it by a 4 mm gap (which forces the sample to be electrically floating even when the holding wafer is RF-biased). After the process, the wafer and sample can be transported under vacuum to the XPS analyzer

and the coating formed on the walls can be analyzed (along with the cleaning efficiency).

The results show that after ITO etching the walls are contaminated by indium. At low temperature, BCl_3/Cl_2 plasma is ineffective to remove this deposit while HBr/Ar and CH_4/Cl_2 chemistries provide promising results. More particularly, an Ar-rich mixture of HBr/Ar is the most efficient strategy, which suggests that Ar^+ ions play an important role in the removal of ITO etching deposit.

[1] O. Joubert, G. Cunge, B. Pelissier, L. Vallier, M. Kogelschatz, and E. Pargon, "Monitoring chamber walls coating deposited during plasma processes: Application to silicon gate etch processes," *J. Vac. Sci. Technol. A Vacuum, Surfaces, Film.*, vol. 22, no. 3, p. 553, 2004.

2:00pm PS+AS+EM+SS+TF-MoA-2 Plasma Resistance of Sintered Yttrium Oxyfluoride (YOF) with Various Y, O, and F Composition Ratios, *Tetsuya Goto,* *Y Shiba, A Teramoto,* Tohoku University, Japan; *Y Kishi,* Nippon Yttrium Co., Ltd, Japan; *S Sugawa,* Tohoku University, Japan

Yttrium oxyfluoride (YOF) has been received much attention as the material for various functional components used in the plasma process chamber for semiconductor manufacturing. This is because, as compared to the widely used Y_2O_3, YOF is stable against various corrosive plasmas using halogen gases which is frequently used in the etching processes and/or chamber cleaning processes. We have reported that YOF (1:1:1) film has the higher resistance to various plasma conditions (N_2/Ar, H_2/Ar, NH_3/Ar, NF_3/Ar, O_2/Ar) than the Y_2O_3 and YF_3 films [1, 2]. In this presentation, we report the effect of ion bombardment on the surface structure of sintered yttrium oxyfluoride (YOF) with various Y, O, and F composition ratios. By combining the starting materials of YOF, $Y_5O_4F_7$, and YF_3 in sintering, the YOF samples with different Y, O, and F composition ratios were prepared. In these samples, the oxygen composition ratio was changed from 33 at% to 7at%. According to this, the fluorine composition ratio was changed from 33at% to 66at%, and thus, the samples became from Y_2O_3 rich to YF_3 rich. Ar ion beam with 500 eV was irradiated to these YOF samples. It was found that the sputtering etching rate was monotonically decreased as the oxygen composition ratio was decreased. It was also found that the surface roughness was relatively smaller for the samples with the composition ratios of Y:O:F=1:1:1 and 5:4:7 (both correspond to the stable composition) than those with other composition ratios. The results indicated that the atomic composition ratio is an important parameter to obtain YOF with good stability against plasmas.

Acknowledgement

The plasma irradiation and inspection were carried out in Fluctuation-Free-Facility in Tohoku University.

1. Y. Shiba, A. Teramoto, T. Goto, Y. Kishi, Y. Shirai and S. Sugawa, J. Vac. Sci. Technol. A, 35 (2), 021405 (2017).

2. A. Teramoto, Y. Shiba, T. Goto, Y. Kishi and S. Sugawa p. 16, AVS 65th International Symp., Long Beach, 2019.

2:20pm PS+AS+EM+SS+TF-MoA-3 Understanding Atomic Layer Etching: Thermodynamics, Kinetics and Surface Chemistry, *Jane P. Chang* [1], University of California, Los Angeles   **INVITED**

The introduction of new and functionally improved materials into silicon based integrated circuits is a major driver to enable the continued down-scaling of circuit density and performance enhancement in analog, logic, and memory devices. The top-down plasma enhanced reactive ion etching has enabled the advances in integrated circuits over the past five decades; however, as more etch-resistive materials are being introduced into these devices with more complex structures and smaller features, atomic level control and precision is needed in selective removal of these materials. These challenges point to the growing needs of identifying and developing viable etch chemicals and processes that are more effective in patterning complex materials and material systems such as multiferroics, magnetic materials and phase change materials, with tailored anisotropy and selectivity.

In this talk, a universal chemical approach is presented, combining thermodynamic assessment and kinetic validation to identify and validate the efficacy of various plasma chemistries. Specifically, potential reactions between the dominant vapor phase/condensed species at the surface are considered at various temperatures and reactant partial pressures. The volatility of etch product was determined to aid the selection of viable etch chemistry leading to improved etch rate of reactive ion etching process. Based on the thermodynamic screening, viable chemistries are tested

---

[1] **PSTD Plasma Prize Winner**

experimentally to corroborate the theoretical prediction. Some of the above mentioned material systems such as complex oxides and metallic material systems used in logic and memory devices are used as examples to demonstrate the broad applicability of this approach.

3:00pm PS+AS+EM+SS+TF-MoA-5 Comparison of Silicon Surface Chemistry between Photo-Assisted Etching and Ion-Assisted Etching, *Emilia Hirsch, L Du, V Donnelly, D Economou,* University of Houston

Etching of p-Si in 60 mTorr Cl_2/Ar Faraday-shielded inductively coupled plasmas was investigated under both ion-assisted etching (IAE) and photo-assisted etching (PAE) conditions. Real-time etching rate and after-etch Si surface chemical composition were characterized by laser interferometry and vacuum-transfer X-ray photoelectron spectroscopy (XPS), respectively. By varying the duty cycle of a pulsed negative DC bias applied to the sample stage, it was found that the IAE rate scaled with the ion current integrated over the bias period, and the total etching rate was simply the sum of PAE and IAE rates. Consequently, little or no synergism occurred between VUV photon- and ion-bombardment stimulated etching. The PAE rate was ~ 210 nm/min at 60 mTorr. Above the 25 eV threshold, the IAE etching rate increased with the square root of the ion energy. Compared to RF bias, a more monoenergetic IED was obtained by applying pulsed DC bias, allowing precise control of ion energy near the low-energy IAE threshold. XPS spectra showed that, when compared to IAE, the chlorinated layer on the surface of samples etched under PAE conditions had significantly lower chlorine content, and it was composed of SiCl only. Under IAE conditions, however, Si· dangling bonds, $SiCl_2$, and $SiCl_3$ were found, in addition to SiCl, with relative abundance of $SiCl>SiCl_2>SiCl_3$. The absence of higher chlorides and Si· dangling bonds under PAE conditions suggested that VUV photons and ions are interacting with the Si surface very differently. When PAE and IAE occurred simultaneously, energetic ion bombardment dictated the surface chemistry that resulted in the formation of higher chlorides.

3:20pm PS+AS+EM+SS+TF-MoA-6 Chemical Reaction Probabilities in the Etching of Si by Fluorine Atoms Produced in a Mixture of NF₃/SF₆ Plasma, *Priyanka Arora[1], T Nguyen,* University of Houston*; S Nam,* Samsung Electronic Company, Republic of Korea*; V Donnelly,* University of Houston

Reaction probabilities in the absence of ion bombardment, defined as the number of silicon atoms removed per incident fluorine atom, have been investigated in mixtures of NF_3 and SF_6 plasmas in an inductively-coupled plasma reactor. Fluorine atom densities were measured by optical emission actinometry, and isotropic etching rates were measured by the degree of undercutting of SiO_2-masked silicon, using cross-sectional scanning electron microscopy (SEM). In addition, atomic force microscopy (AFM) was used to examine surface roughness after etching. The F atom reaction probabilities derived from these measurements indicate ~30-fold higher reaction probability in SF_6 plasma compared with values in NF_3 plasma. Surfaces etched in SF_6 plasma were much smoother than those etched in NF_3 plasma. Addition of only 10% SF_6 to an NF_3 plasma produced a much higher reaction probability (~10-fold) than in a pure NF_3 plasma. This surprising enhancement of reaction probabilities for F with Si in SF_6 plasma will be shown to be due to adsorbed sulfur acting as a catalyst to greatly enhance the etching rate of Si. By allowing sulfur in isopropyl alcohol to evaporate on the masked Si samples, sulfur could be preferentially deposited in relatively high concentrations near mask edges in ~2 mm diameter periodic "strings of beads". When this sample is placed side by side with one not exposed to sulfur, the sulfur dosed sample etched several times faster at the center of each bead, while sulfur-free surface exhibited the expected slower rate.

4:00pm PS+AS+EM+SS+TF-MoA-8 John Thornton Memorial Award Lecture: Low Temperature Plasma-Materials Interactions: Foundations of Nanofabrication And Emerging Novel Applications At Atmospheric Pressure, *Gottlieb S. Oehrlein[2],* University of Maryland, College Park **INVITED**

Our ability to understand and control the interactions of non-equilibrium plasma with surfaces of materials has been an exciting frontline and enabled the realization of new applications and technologies. The plasma-surface interactions (PSI) field has grown rapidly because of a number of reasons. First, plasma-assisted etching (PE) is one of the foundations of micro- and nanofabrication where increasingly atomistic precision in materials processing is required. By enabling the realization of intricate material features that semiconductor circuits and microstructures consist

of, PE makes possible our technological tools that form modern society. This exceedingly complex procedure begins with the transfer of a resist mask in a directional and chemically selective fashion into various materials. Controlling profile shape, critical dimensions, surface roughness, and electrical integrity are crucial, and determined by PSI. Second, development of novel low temperature plasma sources operating at atmospheric pressure has enabled advances in areas where use of PSI has historically been limited, e.g. biology. In this talk I will present a brief review of contributions that I and my collaborators have been honored to make to our understanding of PSI, in particular in the areas of surface processes that are essential for achieving the objectives of plasma etching processes in current semiconductor fabrication that are approaching the atomic scale, and interaction of low temperature atmospheric pressure plasma sources with model polymers and biomolecules aimed at disinfection and sanitation of biological materials.

4:40pm PS+AS+EM+SS+TF-MoA-10 Determining Surface Recombination Probabilities during Plasma-enhanced ALD using Lateral High Aspect Ratio Structures, *Karsten Arts,* Eindhoven University of Technology, The Netherlands, Netherlands*; M Utriainen,* VTT Technical Research Centre of Finland, Finland*; R Puurunen,* Aalto University School of Chemical Engineering, Finland*; E Kessels,* Eindhoven University of Technology, The Netherlands, Netherlands*; H Knoops,* Eindhoven University of Technology, The Netherlands

In this work we measure surface recombination probabilities r of plasma radicals, which is essential for the modeling and understanding of radical-driven plasma processes. Such quantitative information on r is scarcely reported in the literature and typically obtained by difficult and indirect measurement techniques. Here, we determine r using plasma-enhanced atomic layer deposition (ALD) on high aspect ratio (AR) structures, where the AR up to which film growth is obtained gives direct insight into r corresponding to the growth surface. This is demonstrated by measuring the recombination probabilities of O atoms on SiO_2, TiO_2, Al_2O_3 and HfO_2, revealing a surprisingly strong material-dependence. Aside from studying different materials, our method can for instance be used to investigate the impact of pressure and temperature on r. This can provide valuable information for e.g., device fabrication, plasma source design and simulations, in the context of plasma-enhanced ALD but also relevant outside this field.

For this study, we use microscopic lateral-high-aspect-ratio (LHAR) structures[1] supplied by VTT (PillarHall® LHAR4). These chips have extremely high AR trenches (AR<10000) such that film growth is limited up to a certain penetration depth for even the most conformal processes. In the case of plasma ALD, where the film conformality is typically limited by surface recombination,[2] we show that the achieved penetration depth can be used to determine r. Furthermore, the LHAR structures allow for comparison of growth behavior with and without an ion component.

These opportunities are demonstrated by plasma ALD of SiO_2, TiO_2, Al_2O_3 and HfO_2, using an O_2/Ar plasma and $SiH_2(N(C_2H_5)_2)_2$, $Ti(N(CH_3)_2)_4$, $Al(CH_3)_3$ and $HfCp(N(CH_3)_2)_3$, respectively, as precursors. It is observed that an exponential increase in plasma exposure time is required to linearly increase the film penetration depth. This relation, which solely depends on r, has been used to determine $r=(6\pm2)\cdot10^{-5}$, $(6\pm3)\cdot10^{-5}$, $(1-10)\cdot10^{-3}$ and $(0.1-10)\cdot10^{-2}$ for oxygen radicals on SiO_2, TiO_2, Al_2O_3 and HfO_2, respectively. Corresponding to these large differences in r, growth of SiO_2 and TiO_2 penetrated extremely deep up to AR~900, while deposition of Al_2O_3 and HfO_2 was achieved up to AR~90 and AR~40, respectively. This strong material-dependence illustrates the importance of our quantitative research on surface recombination of plasma radicals.

5. Arts, Vandalon, Puurunen, Utriainen, Gao, Kessels and Knoops, J. Vac. Sci. Technol. A **37**, 030908 (2019)
6. Knoops, Langereis, van de Sanden and Kessels, J. Electrochem. Soc. **157**, G241 (2010)

5:00pm PS+AS+EM+SS+TF-MoA-11 Study of Plasma-Photoresist Interactions for Atomic Layer Etching Processes, *Adam Pranda[3], K Lin, G Oehrlein,* University of Maryland, College Park

The emergence of atomic layer etching (ALE) processes has enabled improved control of surface profiles. Whereas the implementation of ALE processes on hard mask materials has been well established, the effects of these processes on photoresist materials is not well known. With the

---

advent of next generation extreme ultraviolet (EUV) photoresists, there is the potential to utilize ALE processes with photoresist materials for fabrication of sub-10 nm feature sizes.

The plasma processing of photoresist materials induces several key physical and chemical modifications which affect material properties such as the etching behavior and surface roughness. In this work, we utilize in-situ ellipsometry, atomic force microscopy (AFM), x-ray photoelectron spectroscopy (XPS), and Fourier transform infrared (FTIR) spectroscopy to interpret the relationships between the aforementioned material properties, the photoresist chemical composition, and plasma ALE parameters such as ion energy and precursor gas type. By comparing these relationships between baseline continuous plasma etching processes and ALE processes, which include the introduction of chemically reactive surface passivation, we elucidate the intrinsic photoresist behaviors under plasma exposure and how an ALE process specifically impacts these behaviors.

Under nonreactive plasma chemistries, a universal response among photoresist materials is the development of a surface dense amorphous carbon (DAC) layer due to energetic ion bombardment. We have found that the photoresist etch rate is inversely proportional to the DAC layer thickness.[1] However, photoresists with UV sensitive pendant groups, such as 193 nm photoresists, develop a greater surface roughness due to the stresses in the surface generated by synergistic ion and UV photon interactions.

With depositing fluorocarbon (FC)-based ALE gas chemistries, the deposited FC layer reacts with the DAC layer and converts it into a mixed layer. This incorporation of FC into the DAC layer reduces the surface roughness without impacting the etch rate of the underlying photoresist as long as a sufficient DAC layer thickness remains.[2] This behavior is potentially advantageous for maximizing the photoresist to SiO_2 selectivity while maintaining an adequate surface roughness.

[1] A. Pranda et al., J. Vac. Sci. Technol. A **36**, 021304 (2018).

[2] A. Pranda et al., Plasma Process. Polym. e1900026 (2019).

Plasma Science and Technology Division
Room B131 - Session PS1-MoA

Plasma-Liquid Interactions, Medicine, and Agriculture

Moderators: Kazunori Koga, Kyushu University, Japan, Deborah O'Connell, University of York, UK

1:40pm PS1-MoA-1 Peroxynitric acid (HOONO₂) Chemistry in Plasma-treated Water for Effective and Safety Disinfection, *Katsuhisa Kitano,* Osaka University, Japan*; S Ikawa, Y Nakashima,* Osaka Research Institute of Industrial Science and Technology, Japan*; T Yokoyama,* Osaka University, Japan*; A Tani,* Kobe University, Japan **INVITED**

Plasma medicine is one of attractive research areas in the area of plasma application. By the exposure of low temperature atmospheric plasma to living organism (human body, bacteria, and so on), positive effect is expected. As biological environment is wet condition, plasma induced chemical reactions in liquid should be considered.

For the plasma disinfection of human body, we have developed the reduced-pH method with direct plasma exposure, which brings stronger bactericidal activity in the liquid at lower pH condition, where the threshold is pH 4.8. The enhancement is thought to be due to hydroperoxy radical (HOO•) generated from superoxide anion radical (O_2^-•) by acid dissociation equilibrium (pKa 4.8). Electrically neutral HOO• could easily penetrate into cell to bring intracellular oxidative stress. In addition, we found that the plasma-treated water (PTW) also has strong bactericidal activity under acidic condition in the same manner. Physicochemical properties of PTW are discussed based on chemical kinetics. Lower temperature brings longer half-life, and the bactericidal activity of PTW can be kept by cryo-preservation. This means that PTW with higher bactericidal activity could be obtained by longer plasma treatment under enough low temperature. High performance PTW, corresponding to the disinfection activity of 22 log reduction (against Bacillus subtilis spore), can be obtained by special plasma system equipped with cooling device. The bactericidal activity of our PTW is much stronger than others.

Many researchers are interested in this area of PTW, where the waters are treated / activated by their original devices. For scientific understanding, we should discuss based on chemical species. Although PTW has many chemical components, respective chemical components in PTW were isolated by ion chromatography. Active ingredient of PTW was successfully purified to be confirmed to be HOONO₂ (PNA: peroxynitric acid). Although the existence of PNA has been known since 100 years ago, sterilization by PNA has never been reported in past papers. PNA is known to release HOO• by radical cleavage. So we conclude that PNA is a key chemical species of cryo-preserved PTW with the reduced-pH method.

From the experimental results of chemical synthesis, PNA is effectively generated from HNO_2 and H_2O_2 under extremely acid condition (pH < 2). Although averaged pH of PTW is about 3~4, pH at the surface of PTW (limited area of interface between plasma and liquid) during plasma treatment is thought to be enough low that PNA can be synthesized from HNO_2 and H_2O_2 supplied from plasma. In the presentation, peroxynitric acid chemistry in PTW will be discussed in detail.

2:20pm PS1-MoA-3 Impact of Solution Properties on Plasma Formation in DC Plasma Electrolysis, *Hernan E. Delgado*[1]*, D Bartels, P Rumbach, D Go,* University of Notre Dame

A common configuration used in plasma-liquid interactions is that in which a direct current (DC) gas discharge is generated between a liquid and a metal. Under this configuration, known as plasma electrolysis or glow-discharge electrolysis, the liquid itself functions as a plasma cathode or anode, for a positive or negative DC bias, respectively. However, it is not clear exactly how the liquid participates in the formation and sustaining of the plasma, including charge transfer at the plasma-liquid interface. This is especially true when the liquid is acting as a cathode, and secondary emission from the liquid is ostensibly required to sustain the plasma. In this work, we use measurements of the breakdown and discharge voltages to understand this process. Voltage measurements for an argon plasma in contact with an aqueous solution are conducted in an electrochemical H-cell reactor to test for conditions that would facilitate secondary emission from the liquid. Voltage measurements across the plasma show a strong dependence on ionic strength, and no dependence on pH (from pH = 0 to 14) while controlling for ionic strength. The voltage was also found to be strongly dependent on the temperature of the liquid. Free radical scavengers nitrite and nitrate had no significant effect on the plasma voltage even at 1.0 M concentration, suggesting that the solvated electron, the pre-solvated electron, and the hydrogen atom do not play a crucial role in secondary emission as previously proposed.

2:40pm PS1-MoA-4 Plasma Reactive Species Formation in Liquids, *Sylwia Ptasinska,* University of Notre Dame **INVITED**

Plasma reactive species which are directly originated in an atmospheric pressure plasma jet (APPJ) and/or indirectly produced in liquids can drive a plethora of chemical reactions. Despite the rapid growth in interest in this type of plasma, our fundamental and comprehensive knowledge of the chemistry which plasma induces in multiphase systems is still needed to be achieved. One of the approaches to obtain this goal is a development of sophisticated interrogation techniques to provide such characterization. In our laboratory, we developed in situ optical absorption technique, and used ferrous sulfate (Fricke) solution in which species were detected under plasma interaction to quantify the total yield of these species under different experimental conditions. A yield of ferric (Fe3+) ions measured using this technique was attributed to the formation of plasma reactive species provided and/or originated in the solution. The results indicated that the number of reactive species formed was proportional to plasma frequency and voltage. However, the Fe3+ yield per pulse decreased with increased frequency. To obtain a better understanding of the processes and species involved in the chemical reactions due to plasma exposure, Fe3+ yields were calculated and compared to the experimental data. At higher frequencies, there was insufficient time to complete all reactions before the next pulse reached the solution; at lower frequencies, the Fe3+ yield was higher because of the relatively longer time available for reactions to occur. It is also known that gas composition of APPJ as well as ambient conditions influence plasma chemistry and thus also reactions in liquids which are in contact with plasma. We performed systematic studies to probed changes in plasma electrical properties, by adjusting the fraction of oxygen and water vapor in the plasma jet environment and feed gas. While DNA was used to identify chemical changes that occurred in the plasma jet under these various experimental conditions. We determined

---

[1] **Coburn & Winters Student Award Finalist**

optimal conditions at which increase in the damage to the molecular probe was significant. This increase can be attributed primarily to the formation of reactive species caused by water and oxygen decomposition in the APPJ. At the same time, we observed no change in the plasma electrical power when oxygen or water vapor were added to the jet environment but decreased when these gases were introduced to the feed gas. This indicates that the effects of plasma chemistry supersede those due to the power applied for APPJ ignition.

3:20pm PS1-MoA-6 In-flight Synthesis and Online Characterization of Silver Nanoparticles from Aerosol Droplets Reacting in a Non-thermal Plasma, *Tommaso Gallingani*, Alma Mater Studiorum-University of Bologna, Italy, Italia; *N Abuyazid*, Case Western Reserve University; *M Gherardi, V Colombo*, Alma Mater Studiorum-University of Bologna, Italy; *C Hogan*, University of Minnesota, Minneapolis; *M Sankaran*, Case Western Reserve University

Because of their unique features and low-temperature chemistry, non-thermal, atmospheric-pressure (AP) plasmas have attracted interest for material synthesis in multiphase environments where the plasma is in contact with a liquid surface. In the most common configuration, the reaction interface is highly localized, leading to inhomogeneities and mass transport limitations. In light of these issues, liquid water jet and a liquid aerosol have been proposed as alternative strategies that allow continuous liquid flow and promote more controlled reaction. However, applications of these multiphase systems are complicated and limited by lack of knowledge of reaction mechanisms.

Here, we carried out a detailed study of a flow-through, liquid-droplet plasma system using an online ion mobility spectrometry (IMS) system to characterize precursor to particle conversion. IMS measures the electrical mobility of aerosol particles providing real time size distribution. The focus of our study was silver nitrate ($AgNO_3$) which has been well-studied in plasma-liquid synthesis and, thus, provides a straightforward chemistry to benchmark our results . Liquid droplets containing $AgNO_3$ were produced by a Venturi effect nebulizer and carried in by an argon flow into an AP dielectric barrier discharge (DBD). The DBD configuration was a quartz tube with two ring electrodes in parallel to avoid any metal in contact with the plasma and driven by an alternating current high voltage generator. The effluent of the reactor was diluted by a flow of nitrogen gas and coupled to the inlet of a commercial IMS system. For a given flow rate, precursor concentration, and plasma power, our results show that the mean particle diameter decreases from 38 to 26 nm when the plasma is on which could be ascribed to $AgNO_3$ reduction to silver (Ag). The synthesized Ag nanoparticles (NPs) were collected either by electrostatic precipitation or filtration for materials analysis. NPs size distribution and morphology were assessed by transmission electron microscopy and found to have good agreement with IMS data. Ultraviolet-visible absorbance showed the well-known localized surface plasmon resonance peak for Ag at approximately 400 nm, confirming a successful conversion. We also performed a control experiment with a diffusion dryer to remove the water and only introducing dried $AgNO_3$. The lack of any reduction to Ag NPs suggested that the mechanism involves water and plasma species alone cannot reduce $AgNO_3$. This study provides important insight into liquid-droplet-based multiphase plasma reactors which are a novel approach to synthesizing NPs from precursors that are not available as a vapor.

4:00pm PS1-MoA-8 Plasma-assisted Fabrication and Functionalization of Materials for Applications at the Nano-biointerface, *Cristina Satriano*, University of Catania, Italy **INVITED**

Surface tailored (nano)materials are of striking interest to better control protein/material and cell/material interactions at the sub-molecular level.

Current fabrication of nanomaterials is facing the following two challenges: high selectivity toward specific chemical compositions or morphologies and their scalable production. This usually requires new synthesis/functionalisation conditions beyond the conventional approaches.

Plasma chemistry presents an opportunity to explore these features and to potentially trigger new surface-driven biological effects. Indeed, the unique synergy of physical and chemical phenomena that occur in the low temperature plasmas has led to an ever-increasing effort to find solutions to currently problematic medical, agricultural, cosmetic and environmental problems by using multifaceted cold plasma environment.

In this paper, the latest progress in the plasma-assisted fabrication and/or functionalization of materials from nanoparticles to low-dimensional nanostructures, including graphene oxide, are briefly reviewed, with a special focus on discussing plasma properties responsible for the nanomaterial growth with high throughput, desired compositions and shapes, or narrow size distributions as well as for the surface functionalization with some control on the ageing processes.

Case studies on plasma-synthesized plasmonic nanogold and nanosilver with tunable optical and electrical properties and plasma surface-modified polymers and nanocarbons at the interface with peptides/proteins, extracellular matrix, supported lipid bilayers and cells are discussed. An outlook of challenges and opportunities for further advancement in this emerging field is given.

4:40pm PS1-MoA-10 Cold Plasma Jets, Liquids and Biomaterials for Bone Cancer Therapy, *Cristina Canal*, Universitat Politècnica de Catalunya, Spain **INVITED**

Over the last few years, significant attention has been paid to biomedical applications of Atmospheric Pressure Plasmas (APP), and especially to the involvement of reactive species (RONS) in selective cancer cell death [1] without damaging surrounding healthy tissues [2]. The anti-cancer properties of the APP have been described in many cancer cell lines, such as breast, skin, lung, pancreas, brain cancers among others and only more recently in bone cancer cells [3-4]. The biological effects of plasmas have been observed also in a wide variety of plasma activated liquids (PAM) [5], opening the door for minimally invasive therapies.

Despite being rare, Osteosarcoma (OS) is the most common primary bone tumorbeing the most common solid tumor in teenagers and the third most common malignancy in children. Our research focuses on the effects of plasmas on osteosarcoma.

We have investigated the effects of different plasma jets in the generation of RONS in liquids of biological interest. OS cells show higher sensitivity to PAM treatment than healthy cells, activating apoptosis, DNA damage and deregulating cellular pathways mediated by c-JUN, AKT, AMPK or STAT3 [6].

However, injection of a liquid in the body associates it being washed away by the blood flow, so development of efficient vehicles which allow location and delivery of RONS to the diseased site is lacking. Therefore, it is our interest to elucidate the potential of hydrogels to generate and store RONS generated by plasmas. Hydrogels are highly hydrated networks of cross-linked polymer chains whose features such as biocompatibility make them great candidates for the design of advanced biomaterials.

We will discuss different hydrogels; in general, their physic-chemical properties remain unchanged by the plasma treatment, while the hydrogels show several-fold larger capacity for generation of RONS than a typical PAM – the absolute amounts generated depending a lot on the chemistry of the hydrogel. The hydrogels show different capacity for release of RONS depending on their properties. The plasma-treated hydrogels show efficient killing of OS cells, related to the different RONS generated.

1. X. Lu et al, Physics Reports, 630, 1 (2016).

2. M. Keidar et al, Physics of Plasmas, 20, 57101 (2013)

3. C. Canal et al, Free Radical Biology and Medicine, 110, 72 (2017)

4. D. Gümbel et al, Anticancer Research, 36, 5915-5922 (2016)

5. A. Khlyustova et al, Frontiers Chem. Sci. Eng. (2019)

6. J. Tornin et al, Scientific Reports (Under revision 2019)

Materials and Processes for Quantum Information, Computing and Science Focus Topic
Room B231-232 - Session QS+EM+MN+NS+VT-MoA

Systems and Devices for Quantum Computing

Moderators: Jonas Bylander, Chalmers University of Technology, Sweden, Ruichen Zhao, National Institute of Standards and Technology (NIST)

1:40pm QS+EM+MN+NS+VT-MoA-1 DEMUXYZ Gate Using Single Microwave Drive Line for Multiple Qubits, *Matteo Mariantoni*, University of Waterloo, Canada; *C Earnest*, University atof Waterloo, Canada; *J Béjanin*, Unversity of Waterloo, Canada

Superconducting qubits have the potential to lead to large-scale quantum computers with 10^5 or more qubits in 2D arrays. As the number of qubits increases, finding methods to connect all the necessary control lines to

each qubit can become a serious challenge. In this talk, we introduce a new demultiplexed one-qubit gate: DEMUXYZ. This gate makes it possible to decrease the number of microwave control lines from N^2 to 1 by allowing multiple qubits to share a single microwave line. The shared line carries a continuous wave (CW) microwave tone, which is initially detuned from the qubits' idle frequency. When a qubit must undergo an arbitrary rotation on the Bloch sphere, the qubit is tuned on resonance with the CW tone and allowed to interact with the drive for the duration required to achieve the desired rotation. The rotation phase is tuned by detuning the qubit frequency away from the drive and idle frequency for the required time length. We demonstrate a first proof of concept for this gate performing experiments on Xmon transmon qubits. We characterize the gate ON/OFF ratio and perform quantum state tomography.

2:00pm QS+EM+MN+NS+VT-MoA-2 Structural and Electronic Characterization of a Novel Si/SiGe Heterostructure for Quantum Computing, *Thomas McJunkin*, *E MacQuarrie, S Neyens, B Thorgrimsson, J Corrigan, J Dodson, D Savage, M Lagally, R Joynt, M Friesen, S Coppersmith, M Eriksson,* University of Wisconsin - Madison

In recent years, silicon-based quantum dots have been shown to be a promising avenue for quantum computing. However, dots formed in silicon quantum wells exhibit a near-degeneracy of the two low-lying valley states. Motivated by a desire to increase the magnitude and tunability of this valley splitting, we report the characterization of a novel Si/SiGe heterostructure grown with a thin layer of SiGe embedded within the Si quantum well, near the top of the well. The Si/SiGe heterostructure is grown via UHV-CVD on a linearly graded SiGe alloy with a final Ge concentration of 29%. STEM measurements reveal the quantum well structure to consist of a ~10 nm Si layer, followed by a thin ~1 nm SiGe layer, and subsequent ~2 nm layer of pure Si. Above this quantum well, a ~35 nm layer of SiGe with 29% Ge is grown to separate the quantum well from the surface. The intent of this ~1 nm layer of SiGe, positioned just below the upper interface of the quantum well, is to modify the valley splitting of electrons in a 2-dimensional electron gas (2DEG) that reside near this interface. By modifying an external vertical electric field, the electron wavefunction can be moved on and off this spike in germanium concentration.

We report electronic measurements of both Hall bars and quantum dot devices that are fabricated on this heterostructure. Shubnikov-de Haas (SdH) and quantum Hall (QH) measurements reveal a peak transport mobility in excess of 100,000 cm^2/(V s) at 6 x 10^{11} cm^{-2} carrier density . We report SdH and QH measurements over a wide range of carrier density and magnetic field in the form of a fan diagram. Valley splitting values are measured in the quantum dot device by magnetospectroscopy, in which a few-electron dot transition is measured as the in-plane magnetic field is swept. Measuring at the second, third, and fourth electron transition in the quantum dot, we find valley splittings of 29, 48, and 65 ueV, respectively. To measure tunability of valley splitting, nearby gate voltages are changed to vary the vertical electric field at constant charge occupation. We find that both the lowest lying valley splitting and the valley splitting in the first excited orbital can be tuned over a factor of 2 by means of such changes in gate voltage.

2:20pm QS+EM+MN+NS+VT-MoA-3 Efficient Quantum Computation using Problem-specific Quantum Hardware and Algorithms, *Stefan Filipp,* IBM Research - Zurich, Switzerland **INVITED**

In recent years we have observed a rapid development of quantum technologies for the realization of quantum computers that promise to outperform conventional computers in certain types of problems. This includes problems in optimization, machine learning, finite element calculations, and in the computation of complex molecules. A key requirement to perform computations on current and near-term quantum processors is the design of quantum algorithms with short circuit depth that finish within the coherence time of the qubits. To this end, it is essential to implement a set of quantum gates that are tailored to the problem at hand and that can be directly implemented in hardware. To efficiently compute the ground and excited states of molecular hydrogen we utilize a parametrically driven tunable coupler to realize exchange-type gates that are configurable in amplitude and phase on two fixed-frequency superconducting qubits. Such gates are particularly well suited for quantum chemistry applications because they preserve the number of qubit excitations corresponding to the fixed number of electrons in the molecule. With gate fidelities around 95% we compute the eigenstates within an accuracy of 50 mHartree on average, an good starting point for the simulation of larger molecular systems.

3:00pm QS+EM+MN+NS+VT-MoA-5 Reconfigurable Magnetic Textures for Quantum Information Applications, *Alex Matos-Abiague,* Wayne State University **INVITED**

Spintronic devices such as spin valves have extensively been used for non-volatile memory applications. The magnetic fringe fields generated by spin valves strongly depend on the magnetic state of the device. Thus, an array of electrically switchable spin valves allows for the generation of reconfigurable magnetic textures whose specific form and properties can be controlled on the nanometer scale. When combined with materials with large g-factor, such magnetic textures can have sizable effects not only on the spin but also on the localization, exchange, and transport properties of carriers. We show how the local control of the fringe-field-generated magnetic texture provides a unique tool for creating effective reconfigurable nanostructures and how it can be used for various quantum information applications. In particular, we focus on the use of reconfigurable magnetic textures as a new path to the realization of fault-tolerant topological quantum computing by enabling the generation and manipulation of Majorana bound states (MBSs) in superconductor/semiconductor heterostructures [1-4]. MBSs are emergent quasiparticles that obey non-Abelian statistics and can store quantum information that is immune against smooth local perturbations. Magnetic textures can provide not only synthetic spin-orbit and Zeeman fields -two important ingredients for the creation of MBSs- but also spatial confinement by creating closed domains in the form of effective topological wires. The effective wires can be re-shaped and re-oriented by properly changing the magnetic texture, allowing for the transportation of the MBSs [1,3] and the realization of quantum gates through braiding operations [2]. Other platforms combining the use of reconfigurable magnetic textures and Josephson junctions, as well as the main experimental challenges regarding materials, scalability, and detection are also discussed.

[1] G. L. Fatin, A. Matos-Abiague, B. Scharf, I Žutić, Phys. Rev. Lett. **117**, 077002 (2016).

[2] A. Matos-Abiague, J. Shabani, A. D. Kent, G. L. Fatin, B. Scharf, I. Žutić, Solid State Commun. **262**, 1 (2017).

[3] T. Zhou, N. Mohanta, J. E. Han, A. Matos-Abiague, and I. Žutić, Phys. Rev. B **99**, 134505 (2019).

[4] N. Mohanta, T. Zhou, J. Xu, J. E. Han, A. D. Kent, J. Shabani, I. Žutić, and A. Matos-Abiague, arXiv:1903.07834

4:00pm QS+EM+MN+NS+VT-MoA-8 Coaxial Multilayer Superconducting Circuits for Quantum Computing, *Peter Leek,* University of Oxford, UK **INVITED**

Superconducting circuits are one of the leading candidates for the realization of quantum computers, in particular for near-term applications which may already be reached with circuits consisting of a few hundred qubits, provided they are operated at high fidelity. Until recently, the topology of superconducting circuits has typically been constrained to two dimensions, which becomes difficult to scale as the number of qubits increases and control and measurement wiring is needed for qubits in the middle of large arrays. It is natural to explore new circuit topologies that incorporate wiring in the third dimension to solve this problem. In this talk I will present an overview of an approach that builds on a coaxially-symmetric circuit QED unit cell with out-of-plane wiring [1] that provides a simple route to scaling to grids of many qubits. In this approach, arrays of qubits and resonators can be fabricated on opposing sides of a substrate and capacitively coupled, while control and readout are achieved via off-chip coaxial wires which run perpendicular to the chip plane and are built into a precision micro-machined enclosure that provides a high-quality microwave environment for the circuit.

[1] Rahamim et al., Applied Physics Letters **110**, 222602 (2017)

4:40pm QS+EM+MN+NS+VT-MoA-10 Josephson Parametric Amplifiers based on Micron Scale Overlap Junctions (O-JPA)*, Mustafa Bal, J Long, R Zhao, H Wang,* National Institute of Standards and Technology (NIST)*; C McRae,* National Institute of Standards and Technology (NIST) and University of Colorado Boulder*; R Lake, X Wu, H Ku, D Pappas,* National Institute of Standards and Technology (NIST)

Quantum limited amplifiers have become indispensable tools in superconducting quantum circuits. In recent years, quantum limited amplification has been demonstrated in parametric amplifiers based on high kinetic inductance superconductors as well as Josephson junctions. Previously, we have demonstrated submicron scale overlap Josephson junction fab process for qubits with long coherence times [1]. Here, we extend the overlap junction fab process to micron scale junctions to enable the realization of other superconducting quantum devices such as overlap junction-based Josephson parametric amplifiers (O-JPA). Our fab scheme yield frequency tunable O-JPAs with negligible insertion loss. We readily observe over 25 dB gain. Compared to other competing processes, overlap junction process for micron scale junctions allows the fabrication of O-JPAs with high yield and good device performance at a much lower infrastructure requirements. The fabrication details of overlap junction process as well as the results of O-JPA characterization will be presented. The metrology of overlap Josephson junctions will also be presented in this this symposium [2].

[1] X. Wu, J. L. Long, H. S. Ku, R. E. Lake, M. Bal, and D. P. Pappas, "Overlap junctions for high coherence superconducting qubits", Appl. Phys. Lett. **111**, 032602 (2017).

[2] R. Zhao *et al*., "Josephson Junction metrology for superconducting quantum device design", also presented at AVS 66th International Symposium & Exhibition.

5:00pm QS+EM+MN+NS+VT-MoA-11 Development and Characterization of a Flux-pumped Josephson Parametric Amplifier*, Martina Esposito,* University of Oxford, UK

Josephson parametric amplification is a tool of paramount importance in circuit quantum electrodynamics (circuit-QED), especially for the quantum-noise-limited single-shot readout of superconducting qubits. Here we present the development and characterization of a flux-pumped Josephson parametric amplifier (JPA) based on a lumped-element LC resonator, in which the inductance L is composed by a geometric inductance and an array of superconducting quantum interference devices (SQUIDs) [1]. In addition, we show preliminary experiments where the JPA is used as the first stage of amplification for the readout of a superconducting qubit based on a coaxial architecture recently developed in our lab in Oxford [2]. Finally, we will introduce future scientific direction based on using JPAs for generation and control of non-classical states in microwave photons.

[1] M. Esposito et al. EPJ Web of Conferences 198, 00008 (2019)

[2] J. Rahamim et al. Applied Physics Letters 110, 222602 (2017)

New Challenges to Reproducible Data and Analysis Focus Topic
Room A211 - Session RA+AS+NS+SS-MoA

Quantitative Surface Analysis II/Big Data, Theory and Reproducibility

Moderators: Kateryna Artyushkova, Physical Electronics, Donald Baer, Pacific Northwest National Laboratory

1:40pm RA+AS+NS+SS-MoA-1 A Data-Centric View of Reproducibility*, Anne Plant,* National Institute of Standards and Technology (NIST)*; J Elliott,* NIST*; R Hanisch,* National Institute of Standards and Technology (NIST) **INVITED**

Ideally, data should be shareable, interpretable, and understandable within the scientific community. There are many challenges to achieving this, including the need for high quality documentation and a shared vocabulary. In addition, there is a push for rigor and reproducibility that is driven by a desire for confidence in research results. We suggest a framework for a systematic process, based on consensus principles of measurement science, to guide researchers and reviewers in assessing, documenting, and mitigating the sources of uncertainty in a study. All study results have associated ambiguities that are not always clarified by simply establishing reproducibility. By explicitly considering sources of uncertainty, noting aspects of the experimental system that are difficult to characterize quantitatively, and proposing alternative interpretations, the researcher provides information that enhances comparability and reproducibility.

2:20pm RA+AS+NS+SS-MoA-3 Enhancing Data Reliability, Accessibility and Sharing using Stealthy Approaches for Metadata Capture*, Steven Wiley,* Pacific Northwest National Laboratory **INVITED**

Science is entering a data-driven era that promises to accelerate scientific advances to meet pressing societal needs in medicine, manufacturing, clean energy and environmental management. However, to be usable in big data applications, scientific data must be linked to sufficient metadata (data about the data) to establish its identity, source, quality and reliability. This has also driven funding agencies to require projects to use community-based data standards that support the FAIR principles: Findable, Accessible, Interoperable, and Reusable. Current concerns about data reproducibility and reliability have further reinforced these requirements. Truly reusable data, however, requires an enormous amount of associated metadata, some which is very discipline and sample-specific. In addition, this metadata is typically distributed across multiple data storage modalities (e.g. lab notebooks, electronic spreadsheets, instrumentation software) and is frequently generated by different people. Assessing and consolidating all of the relevant metadata has traditionally been extremely complex and laborious, requiring highly trained and motivated investigators as well as specialized curators and data management systems. This high price has led to poorly documented datasets that can rarely be reused. To simplify metadata capture and thus increase the probability it will indeed be captured, EMSL (Environmental Molecular Sciences Laboratory) has developed a general-purpose metadata capture and management system built around the popular ISA-Tab standard (Investigation-Study-Assay Tables). We have modified this framework by mapping it onto the EMSL workflow, organized as a series of "transactions". These transactions are natural points where metadata is generated, include specifying how samples will be generated and shipped, instrument scheduling, sample storage, and data analysis. Software tools have been built to facilitate these transactions, automatically capture the associated metadata and link it to the relevant primary data. This metadata capture system works in concert with automated instrument data downloaders and is compatible with commercial sample tracking and inventory management systems. By creating value-added tools that are naturally integrated into the normal scientific workflow, our system enhances scientific productivity, thus incentivizing adoption and use. The entire system is designed to be general purpose and extensible and thus should be a useful paradigm for other scientific projects that can be organized around a transactional model.

3:00pm RA+AS+NS+SS-MoA-5 From Electrons to X-rays: Tackling Big Data Problems through AI*, Mathew Cherukara, Y Liu, M Holt, H Liu, T Gage, J Wen, I Arslan,* Argonne National Laboratory **INVITED**

As microscopy methods and detectors have advanced, the rates of data acquisition and the complexity of the acquired data have increased, and these are projected to increase several hundred-fold in the near future. The unique electron and X-ray imaging capabilities at the Center for Nanoscale Materials (CNM) are in a position to shed light on some of the most challenging and pressing scientific problems we face today. To fully leverage the capability of these advanced instruments, we need to design and develop effective strategies to tackle the problem of analyzing the data generated by these imaging tools, especially following facility upgrades such as the upgrade to the Advanced Photon Source (APS-U) and the commissioning of the ultrafast electron microscope (UEM).

The data problem is especially acute in the context of coherent imaging methods, ultra-fast imaging and multi-modal imaging techniques. However, analysis methods have not kept pace. It is infeasible for a human to sort through the large, complex data sets being generated from imaging experiments today. At the CNM, we apply machine learning algorithms to our suite of electron and X-ray microscopy tools. Machine learning workflows are being developed to sort through data in real-time to retain only relevant information, to invert coherently scattered data to real-space structure and strain, to automatically identify features of interest such as the presence of defects, and even to automate decision making during an imaging experiment. Such methods have the potential not only to decrease the analysis burden on the scientist, but to also increase the effectiveness of the instruments, for instance by providing real-time experimental feedback to help guide the experiment.

Monday Afternoon, October 21, 2019

4:00pm RA+AS+NS+SS-MoA-8 Quantifying Shell Thicknesses of Core-Shell Nanoparticles by means of X-ray Photoelectron Spectroscopy, *Wolfgang Werner,* Vienna University of Technology, Austria **INVITED**
Determining shell thicknesses and chemistry of Core-Shell Nanoparticles (CSNPs) presently constitutes one of the most important challenges related to characterisation of nanoparticles. While for particlae number concentration various routine analysis techniques as well as methods providing reference measurements have been or are in the process of being developed, one of the most promising candidates for shell thickness determination is x-ray photoelectron spectroscopy (XPS).

Different approaches to quantify shell thicknesses will be presented and compared. These comprise: (1) The infinitesimal columns model (IC), (2) Shard's empirical formula (TNP-model) and (3) SESSA (Simulation of Electron Spectra for Surface Analysis) simulations with and (4) without elastic scattering.

CSNP XPS intensities simulated with SESSA for different combinations of core/shell-material combinations for a wide range of core and shell thicknesses have been evaluated with the TNP-model and the retrieved thicknesses are in good agreement with the nominal thickness, even when elastic scattering is turned on during the simulation, except for pathological cases. For organic shell materials these simulations fully confirm the validity of the (much simpler) TNP-method, which also coincides with the IC model.

Experimental data on of a round robin experiment of PMMA@PTFE CSNPs involving three research institutions were analysed with the aforementioned approaches and show a good consistency in that evaluations of the shell thicknesses among the institutions agree within 10% (and are in good agreement with the nominal shell thickness). This consistency is promising since it suggests that the error due to sample preparation can be controlled by following a strict protocol.

Use of the F1s signal leads to significant deviations in the retrieved shell thickness. Independent measurements using Transmission Electron Microscopy were also performed, which revealed that the core-shell structure is non-ideal, i.e. the particles are aspherical and the cores are acentric within the particles. SESSA simulations were employed to estimate the effect of various types of deviations of ideal NPs on the outcome of shell thickness determination.

The usefulness and importance of different kind of electron beam techniques for CSNP analysis and in particular shell thickness determination is discussed.

4:40pm RA+AS+NS+SS-MoA-10 Modeling the Inelastic Background in X-ray Photoemission Spectra for Finite Thickness Films, *Alberto Herrera-Gomez,* CINVESTAV-Unidad Queretaro, México
The background signal in photoemission spectra caused by inelastic scattering is usually calculated by convolving the total signal with the electron-energy loss-function. This method, which was proposed by Tougaard and Sigmund in their classic 1982 paper [1], only works (as clearly indicated in [1]) for homogeneous materials. However, the method is commonly applied to finite thickness films. In this paper it is going to be described the proper way to remove the inelastic background signal of spectra from thin-conformal layers including buried layers and delta-doping [2]. The method is based on the straight-line inelastic scattering path, which is expected to be a very good approximation for low energy losses (near-peak regime). It is also a common practice to use the parametric Tougaard Universal Cross Section [3] with the provision that, instead of using the theoretical values for the parameters valid for homogeneous materials, the B-parameter is allowed to vary until the experimental background signal ~ 50 to 100 eV below the peak is reproduced. This is equivalent to scale the loss-function, which partially compensates the error from using the convolution method [1]. The error compensation on the modeling of the background of finite-thickness layers by scaling the loss-function will be quantitatively described.

[1] S. Tougaard, P. Sigmund, Influence of elastic and inelastic scattering on energy spectra of electrons emitted from solids, Phys. Rev. B. 25 (1982) 4452–4466. doi:10.1103/PhysRevB.25.4452.

[2] A. Herrera-Gomez, The photoemission background signal due to inelastic scattering in conformal thin layers (Internal Report), 2019. http://www.qro.cinvestav.mx/~aherrera/reportesInternos/inelastic_background_thin_film.pdf.

[3] S. Tougaard, Universality Classes of Inelastic Electron Scattering Cross-sections, Surf. Interface Anal. 25 (1997) 137–154. doi:10.1002/(SICI)1096-9918(199703)25:3<137::AID-SIA230>3.0.CO;2-L.

5:00pm RA+AS+NS+SS-MoA-11 R2R(Raw-to-Repository) Characterization Data Conversion for Reproducible and Repeatable Measurements, *Mineharu Suzuki, H Nagao, H Shinotsuka,* National Institute for Materials Science (NIMS), Japan*; K Watanabe,* ULVAC-PHI Inc., Japan*; A Sasaki,* Rigaku Corp., Japan*; A Matsuda, K Kimoto, H Yoshikawa,* National Institute for Materials Science (NIMS), Japan
NIMS, Japan, has been developing a materials data platform linked with a materials data repository system for rapid new material searching by materials informatics. The data conversion from raw data to human-legible/machine-readable data file is one of the key preparation techniques prior to data analysis, where the converted data file should include meta-information. Our tools can convert raw data to a structured data package that consists of (1) characterization measurement metadata, (2) primary parameters which we will not call "metadata" to distinguish from (1), (3) raw parameters as written in original raw data, and (4) formatted numerical data. The formatted numerical data are expressed as matrix type with robust flexibility, not obeying a rigid definition. This flexibility can be realized by applying the data conversion style of Schema-on-Read type, not Schema-on-Write type based on *de jure* standards such as ISO documents. The primary parameters are carefully selected from raw parameters and their vocabularies are replaced from instrument-dependent terms to general ones that everyone can readily understand. These primary parameters with linked specimen information are useful for reproducible and repeatable instrument setup. By this R2R conversion flow, we have verified that we can generate and store interoperable data files of XPS spectra and depth profiles, powder XRD patterns, (S)TEM images, TED patterns, EELS spectra, AES spectra, EPMA spectra and elemental mapping, and theoretical electron IMFP data. We have also developed a system to allow semi-automatic data transfer from an instrument-controlling PC isolated from the network, by adopting a Wi·Fi-capable SD card's scripting capability, while keeping the PC offline. We are working on further software development for on-demand data manipulation after R2R data conversion. So far it has been possible to perform XPS peak separation using automated information compression technique. Using these components, high-throughput data conversion/accumulation and data analyses are realized, where human interaction is minimized. Using metadata extracted from raw data, other users can reproduce or repeat measurements even if they did not carry out the original measurement. Human-legible and machine-readable numerical data is utilized for statistical analyses in informatics.

Surface Science Division
Room A220-221 - Session SS+HC-MoA

CO2, CO, Water, and Small Molecule Chemistry at Surfaces
Moderators: Donna Chen, University of South Carolina, Omur E. Dagdeviren, Yale University

1:40pm SS+HC-MoA-1 Calculations of the Electrochemical Reduction of CO2 and the Competing Hydrogen Evolution Reaction, *Hannes Jónsson,* University of Iceland, Iceland **INVITED**
Calculations of electrochemical CO2 reduction to formate, alcohols and hydrocarbons will be presented. The mechanism for the formation of the various products is established, the rate evaluated and comparison made with experimental measurements. The rate of the main side reaction, the hydrogen evolution reaction, is also estimated. The calculations are based on a detailed atomistic model of the electrical double layer (metal slab and water layer) and density functional theory calculations to evaluate not only the free energy of intermediates as a function of applied voltage but also the activation energy for each elementary step, both Heyrovsky and Tafel reactions [1]. Comparison is also made with calculations using an implicit solvation model [2]. A range of close packed metal surfaces are compared, including Cu, Ag, Au, Ni, Fe, Rh, Ir and Pt. The resuls are in remarkably good agreement with the reported experimental measurements. A two parameter descriptor is established that can help identify improved catalysts for CO2 electrochemical reduction.

[1] J. Hussain, H. Jónsson and E. Skúlason, ACS Catalysis 8, 5240 (2018).

[2] M. Van den Bossche, E. Skúlason, C. Rose-Petruck and H. Jónsson, J. Phys. Chem. C 123, 4116 (2019).

2:20pm SS+HC-MoA-3 CO_2 Adsorption on the O-Cu(100) Surface Studied by STM and DFT, *S Tjung, Q Zhang, J Repicky, S Yuk,* The Ohio State University; *X Nie,* Dalian University of Technology; *Seth Shields,* The Ohio State University; *N Santagata,* University of Memphis; *A Asthagiri, J Gupta,* The Ohio State University

Copper oxide catalysts are promising candidates for reducing CO_2 into useful fuels, such as ethanol, but the mechanism remains obscure. Studying the O-Cu(100) surface, which represents the initial transition of the oxidation of copper to copper oxide, and the adsorption process of CO_2 has the potential to elucidate the CO_2 reduction mechanism.

We performed a DFT/STM theoretical and experimental probe of the properties of CO_2 adsorption on the O-Cu(100) surface. The Cu(100) surface was repeatedly sputtered with Ar^+ and annealed at 550°C in an ultra-high vacuum chamber, and subsequent Auger spectroscopy revealed the lack of surface contamination. The O-Cu(100) surface was obtained by exposing the Cu(100) face to 10^{-6} mbar of oxygen for 5 minutes at 300°C. The sample was then cooled and transferred into an attached low temperature (5K) ultra-high vacuum (10^{-11} mbar) STM chamber.

The atomic resolution STM revealed the $(2\sqrt{2} \times \sqrt{2})$ R45°O-Cu(100) reconstruction, in good agreement with the DFT calculations. The reconstruction consists of an O-Cu-O row structure separated by missing Cu rows. Additionally, there are two equivalent domains which result from nucleation along the [001] and [010] directions of the Cu(100). Differential conductance spectroscopy reveals an increase in the work function of the O-Cu(100) surface, and two additional unoccupied states generated by the oxygen atoms, in agreement with the DFT calculations.

CO_2 was adsorbed onto the O-Cu(100) surface via *in situ* dosing in the STM. The CO_2 adsorbed exclusively between two oxygen atoms in the missing row reconstruction, which has the largest predicted adsorption energy. The lack of point defects on the surface indicates that the CO_2 does not dissociate, and the CO_2 molecules are easily disturbed by the tip under all tunneling conditions, which is consistent with the theoretically predicted low diffusion barrier.

2:40pm SS+HC-MoA-4 Employing Carbon Monoxide and Carbon Dioxide Plasmas to Improve the Gas Sensing Performance of Tin(IV) Oxide, *Kimberly Hiyoto, E Fisher,* Colorado State University

Metal oxide semiconductors are commonly researched materials for solid-state gas sensors; however, several limitations (i.e., operating temperatures of ≥300 °C and poor selectivity) impede wide-spread commercialization of these devices. Plasma processing offers a desirable alternative route to traditional methods, such as doping, because of the tunability of treatment parameters and the ability to modify the surface of the material while maintaining bulk properties. Previous work using plasma modification to enhance tin dioxide (SnO_2) gas sensor performance has mainly focused on oxygen or oxygen/argon plasma systems because these systems are thought to etch oxygen from the SnO_2 lattice creating oxygen vacancies that can lead to lower operating temperatures and improved sensor selectivity. Thus, further work needs to be done with other precursor gases to determine an effective strategy for fabricating improved gas sensors.

Here, we present carbon monoxide (CO) and carbon dioxide (CO_2) plasma-treated SnO_2 nanoparticle gas sensors treated at various applied rf powers. After plasma processing, the sensors demonstrate higher response to CO, ethanol, and benzene at lower operating temperatures compared to untreated SnO_2. In addition, the response and recovery behavior of the treated and untreated sensors were also evaluated as a metric for improved performance. To elucidate how plasma modification resulted in these changes, optical emission spectroscopy measured during plasma treatment and material characterization post plasma processing (X-ray photoelectron spectroscopy and X-ray powder diffraction) will also be discussed. All of these data work toward better understanding the relationship between surface chemistry and gas sensing performance, ultimately to develop a targeted approach to designing improved gas sensors.

3:00pm SS+HC-MoA-5 The Role of Steps in the Dissociation of CO_2 on Cu, *Johan Gustafson, B Hagman,* Lund University, Sweden; *A Posada-Borbón, A Schaefer,* Chalmers University of Technology, Sweden; *M Shipilin,* Stockholm University, Sweden; *C Zhang,* Lund University, Sweden; *L Merte,* Malmö University, Sweden; *A Hellman,* Chalmers University of Technology, Sweden; *E Lundgren,* Lund University, Sweden; *H Grönbeck,* Chalmers University of Technology, Sweden **INVITED**

CO_2 chemistry has received significant attention recently, due to the greenhouse effect of CO_2 emissions and the resulting climate change. CO_2 reduction reactions, such as methanol synthesis and reverse water-gas shift, provide routes for recycling of CO_2 and thus limiting the CO_2 emissions. These reactions are commonly performed over Cu-based catalysts, making the interaction of CO_2 and Cu, on the atomic scale, of importance for a fundamental understanding and the development of new and more efficient catalysts.

We have previously studied the dissociative adsorption of CO_2 on Cu(100) using APXPS and DFT. In summary, exposure of the Cu surface to CO_2 in the mbar range at temperatures above room temperature results in dissociation of CO_2 into CO, that desorbs, and O that stays on the surface. The rate of the increase in O coverage, however, was not consistent with what one would expect from adsorption on the flat Cu(100) surface. Instead, we propose a model where the dissociation happen at atomic steps. The steps were found to both lower the activation barrier for the dissociation and separate the products, such that the probability for recombination is lowered.

As an obvious follow-up of this study, we have studied the dissociative adsorption of CO_2 on Cu(911), which exposes five atoms wide (100) terraces separated by monatomic steps. In contrast to what we expected, the O coverage did not increase significantly faster on this stepped surface. Our preliminary analysis suggests that diffusion of O from one step to another reduces the effect of the steps separating O and CO, but also that the steps facilitate O diffusion to the subsurface region and possibly stabilisation of CO_2 or CO_3 species on the surface.

In this presentation we will report how we conclude that the steps control the dissociation and, especially, the present status of the studies of Cu(911).

4:00pm SS+HC-MoA-8 Surface Temperature Dependence of Methane Dissociation on Ni(997), *Daniel Tinney, E High, L Joseph, A Utz,* Tufts University

Commercial steam reforming reactors operate at temperatures of 1000K or higher, and methane dissociation on the Ni catalyst is generally believed to be the rate-limiting step in this industrially important process. Despite the commercial importance of this reaction, nearly all studies probing the dynamics of methane dissociation have focused on surface temperatures of 600K or lower. Here, we use energy and vibrationally state selected methane molecules in a supersonic molecular beam to quantify the impact of surface temperature on methane activation over a wide range of surface temperatures. Our use of methane molecules with a precisely defined energy highlights provides a clear view of how surface temperature impacts reactivity.

Vibrationally state-resolved reactivity measurements reveal details of fundamental processes that impact reactivity in the field of heterogeneous catalysis. Non-statistical, mode-specific, and bond-selective enhancements observed for methane and its isotopologues on transition metal surfaces provide insights into energy flow during reactions. Reactive gas molecules with strictly-defined energy in well-defined energetic coordinates used in state-selective experiments have also proven to be valuable probes of how surface atom motion affects overall reactivity. For this work, vibrationally state-resolved data was collected via infrared (IR) laser excitation of the anti-symmetric stretch of supersonically-expanded methane (CH_4) gas molecules impinging on a lightly-stepped Ni(997) surface. Measurements on the single crystal were investigated over a broad range of surface temperatures (82 K ≤ T_S ≤ 1000 K) while utilizing varying incident energies (E_i = 20 kJ/mol to >140 kJ/mol). A comparison with prior data on Ni(111) surface reveals the role that steps may play in methane activation.

4:20pm SS+HC-MoA-9 Promotion and Inhibition of Methane Dissociation by Carbon on Ni Single Crystal Surfaces, *Arthur Utz, E High, D Tinney,* Tufts University

State-resolved beam-surface scattering measurements, when coupled with molecular beam reactivity modulation measurements, permit real-time measurement of methane dissociation on Ni(111) and Ni(997) surfaces. At surface temperatures above 550K, methyl reaction products

dehydrogenate to C atoms, and H atoms recombine and desorb, leaving C atoms behind. At higher surface temperatures, C atoms begin to aggregate on the surface and also absorb into the Ni subsurface region. We monitor how the presence of these C atoms on and beneath the surface impacts methane dissociation probability.

4:40pm SS+HC-MoA-10 Two-Dimensional Polymorphism as a Result of Non-Equilibrium Self-Assembly, *Angela Silski*[1], *J Petersen,* University of Notre Dame; *R Brown,* Clarkson University; *S Kandel,* University of Notre Dame

The challenge in the field of molecular self-assembly is that the outcome of these processes is not easily predicted a priori, rather, results of self-assembly processes are often rationalized after the fact. In this study, a systemic approach to self-assembly is taken; the chemical structure of the starting molecule is iteratively changed (adding, removing or substituting particular functional groups) and the resulting self-assembled structure is observed via scanning tunneling microscopy. The focus of this study is on the functional groups that can form directional interactions (hydrogen- and halogen-bonds). We observe a metastable cyclic pentamer for isatin (1H-indole-2,3-dione) with density functional theory providing support for a cyclic structure stabilized by both NH· · ·O and CH· · ·O hydrogen bonds between neighboring molecules. The CH· · ·O hydrogen bond is made between the 7-position proton acting as the hydrogen bond donor and the 3-position carbonyl as the hydrogen bond acceptor, and calculations indicate that the isatin pentamer structure is 17 kJ/mol more stable than the dimer on the per molecule basis. To probe the importance of the CH···O hydrogen bond in stabilizing the isatin pentamer, we compare to isatin derivatives: we replace the 3-position carbonyl with a methyl group (3-methyl 2-oxindole), the 7-position proton with a fluorine (7-fluoroisatin), systematically move the location of the hydrogen bond donor/acceptor by one position, (phthalimide), and remove of the primary hydrogen bond donor (1,2-indandione and 1,3-indandione). We show that cyclic pentamer formation is either altered or precluded as a result of these substitutions. To our surprise, substituting the 6-position with a bromine (6-bromoisatin) which is a position remote to the positions of the hydrogen-bond contacts, does not result in the formation of cyclic pentamers on the surface. A monolayer of 6-bromoisatin consists of almost entirely "zipper" dimer structures. Additionally, the importance of CH···O bonding in forming isatin pentamers is supported by electrospray ionization mass spectrometry (ESI-MS) measurements, which include a magic-number isatin pentamer peak. A mass spectrum of 6-bromoisatin also shows a relatively intense pentamer peak, whereas the other derivative molecules show little clustering under the same conditions. This work is significant in understanding the role that the position of the hydrogen- and halogen-bond donor/acceptor groups has on the resulting 2D supramolecular assemblies.

Thin Films Division
Room A124-125 - Session TF+2D+AP+EL+SS-MoA

ALD and CVD: Nucleation, Surface Reactions, Mechanisms, and Kinetics

Moderators: Adrie Mackus, Eindhoven University, Netherlands, Qing Peng, University of Alabama

1:40pm TF+2D+AP+EL+SS-MoA-1 ALD on Particles: What is Different from Wafers?, *Ruud van Ommen,* Delft University of Technology, Netherlands
INVITED

Advanced materials, often relying on nanostructured particles as building blocks, are crucial in meeting grand challenges in energy and health. Atomic layer deposition (ALD) is an excellent technique to make such nanostructured particles: particles of which the surface is either covered by an ultrathin film or by nanoclusters. Although the underlying mechanisms are similar, there are quite some differences between ALD processing of wafers and ALD processing of particles. This presentation will discuss recent developments and insights in the field of applying ALD to particles, with an emphasis on reactor technology, precursor utilization, operating conditions, and scaling up. I will show that ALD is suited to produce nanostructured particles with very high precision. Moreover, it is scalable such that large amounts of such particles can be produced.

2:20pm TF+2D+AP+EL+SS-MoA-3 Insights into Particle ALD Peculiarities from In- and Ex-Situ Characterization, *Benjamin Greenberg,* American Society for Engineering Education; *J Wollmershauser, B Feygelson,* U.S. Naval Research Laboratory

Particle atomic layer deposition (pALD) is an increasingly popular technique for mass production of core/shell nanoparticles (NPs). In a typical pALD process, NP powders are agitated in a fluidized bed or rotary reactor, and conformal coating of the entire powder surface—often > 100 m^2 in lab-scale reactors—is attempted via prolonged precursor exposures and purges. Over the past 2+ decades there have been many reports of highly encouraging results, including TEM images of NPs individually encapsulated by shells of uniform thickness. Nevertheless, several fundamental questions about pALD mechanisms and behavior remain challenging to answer. For example, how does the pALD growth per cycle (GPC) deviate from the corresponding ALD GPC on a flat substrate, and why? Or more importantly, what conditions are required to maximize the fraction of powder that attains an ideal core/shell structure (individual NP encapsulation) rather than a coated-agglomerate structure in which cores are glued together? In this work, using a commercial rotary pALD reactor to coat various NPs with oxide shells, we employ a wide array of characterization techniques to shed light on these issues and inform process optimization. In situ, we experiment with relatively uncommon techniques such as high-speed video analysis and pyrometry of the agitated NP powder, as well as conventional techniques such as mass spectrometry (RGA). High-speed videos in particular reveal aspects of the process often undiscussed (and sometimes difficult to convey) in the pALD literature, including changes in the powder motion as surface chemistry evolves. Ex situ, we characterize the coated NPs via TEM, XRD, SAXS, XPS, and N_2-adsorption surface area measurements (BET method).

2:40pm TF+2D+AP+EL+SS-MoA-4 Impact of Medium Energy Ions on HfO2 Nucleation Mechanisms on Si, SiO2,TiN Substrates in PEALD Processes Investigated by In situ Ellipsometry, Optical Emission Spectroscopy, AFM and XPS Analyses, *Marceline Bonvalot, S belahcen, A Bsiesy, C Vallée,* LTM, Univ. Grenoble Alpes, CEA-LETI, France

Area Selective Deposition (ASD) processes have recently attracted an increasing technological interest, as a very promising route for the development of bottom-up fabrication processes as an alternative to increasingly expensive thin layer patterning processes in advanced nanoscale devices. However, to achieve a high quality selective deposition, a deep understanding of the very initial stages of growth in Atomic Layer Deposition (ALD) processes is needed. This so-called nucleation step is strongly dependent upon growth conditions in ALD processes, namely pressure and temperature, but also on precursor types and susbtrate surfaces on which growth is carried out.

In this work, we have investigated the nucleation mechanism of HfO_2 with TEMAH precursor by plasma-enhanced ALD carried out in an Oxford FlexAL tool. This tool is equipped with an Atomic Layer Etching (ALE) system from Oxford Instruments, which consists of a continuous tunable bias power set-up applied in the back face of the chuck. When turned on during the plasma step of the PE-ALD cycle, medium energy ions (0 - 100 W) can be extracted from the inductive plasma source toward the sample surface. They may in turn contribute physically and chemically to the growth mechanism, and thus, a careful adjustment of this bias power allows a tuning of the physical properties of the layer under growth.

The nucleation behavior of HfO_2 on 3 types of substrates (H-terminated Si, SiO_2 and TiN) has been followed under applied bias power values between 0 and 100 W, by in situ spectroscopic ellipsometry assisted by Optical Emission Spectroscopy for the identification of plasma active species and desorbed by-products. The samples have then been analysed by means of Atomic Force Microscopy and X-ray Photoelectron Spectroscopy (XPS). Insights into Hf peak intensities allow an estimate of the coverage of HfO2 nuclei formed in the very first (typically 5) cycles of the PE-ALD process. A discussion will be presented on the role of medium energy ions in the observed nucleation mechanism, in view of potential applications to the development of ASD processes.

---

[1] **Morton S. Traum Award Finalist**

3:00pm TF+2D+AP+EL+SS-MoA-5 Controlling the Nucleation of CVD Cobalt Films on SiO₂ : Combining an Amido-based Nucleation Promotor with an Amine-based Growth Inhibitor to Afford Atomically-smooth Surfaces, *Zhejun Zhang, G Girolami, J Abelson,* University of Illinois at Urbana-Champaign

Cobalt films are of interest for the back-end metallization and transistor contact in microelectronics because cobalt has a greater electromigration resistance and a lower diffusion rate in dielectrics compared with copper. However, few-nanometer thick Co films deposited by CVD on dielectrics are usually non-continuous – they consist of islands with pinholes and significant roughness – which renders them unsuitable for nanoscale device fabrication. A nucleation layer, such as TiN, can be pre-deposited to improve the area density of Co nuclei; this approach eliminates the problem of islanding, but it subtracts cross-sectional area from the plug or line, thus increasing the electrical resistance.

Here, we solve the Co nucleation problem in CVD using a two-pronged approach. First we expose the SiO_2 surface to a tetrakis(dimethylamido)(transition metal) precursor at low temperature. This affords a self-limiting, submonolayer coverage of an intermediate, similar to the behavior of such molecules in ALD processes. The adsorbate layer then enhances the nucleation of cobalt from the $Co_2(CO)_8$ precursor, such that a large area density of nanoscale islands forms with essentially no nucleation delay. Using this approach, the rms surface roughness for a 1.5-nm-thick Co film decreases from 2.5 to 1.0 nm.

Second, we further improve the surface morphology by adding a co-flow of ammonia together with the carbonyl precursor; this serves as a growth inhibitor that reduces the steady-state growth rate of Co films by 50 %. The presence of the inhibitor does not alter the nucleation rate, however, the rms roughness of a 1.5-nm-thick film is further reduced to only 0.4 nm. We suggest that the roughness is due to a better valley-filling at low precursor reaction probability, consistent with the literature. In summary, our approach enables the use of CVD to afford excellent Co films for nanofabrication.

3:20pm TF+2D+AP+EL+SS-MoA-6 Plasma-assisted Atomic Layer Epitaxy of Indium Aluminum Nitride Studied Using *in situ* Grazing Incidence Small-angle X-ray Scattering, *Jeffrey M. Woodward,* ASEE (residing at US Naval Research Laboratory)*; S Rosenberg,* American Society for Engineering Education (residing at US Naval Research Laboratory)*; S Johnson, N Nepal,* U.S. Naval Research Laboratory*; Z Robinson,* SUNY Brockport*; K Ludwig,* Boston University*; C Eddy,* U.S. Naval Research Laboratory

Indium aluminum nitride (InAlN) is an attractive material for power electronic applications. However, conventional methods of epitaxial growth of InAlN are challenged by a large miscibility gap and the significant differences in optimal growth conditions for the constituent aluminum nitride (AlN) and indium nitride (InN) binary compounds. Despite these challenges, the epitaxial growth of InAlN alloys throughout the entire compositional range has been demonstrated using plasma-assisted atomic layer epitaxy (ALEp)[1], a variant of atomic layer deposition in which relatively higher temperatures are utilized. In the ALEp growth of InAlN, the desired alloy compositions are achieved by forming ultra-short period superlattices of alternating InN and AlN layers, referred to as digital alloys (DA). In order to further advance these empirical efforts, significant research is needed to better understand the nucleation and growth kinetics of ALEp DA growth. To this end, we employ *in situ* grazing incidence small angle X-ray scattering (GISAXS) for the real-time study of the evolving ternary InAlN surfaces as has been done previously for binary InN[2] and AlN[3].

Here we present *in situ* GISAXS studies of ALEp growth of InN, AlN, and a range of InAlN DAs on GaN (0001) substrates, which were performed at Brookhaven National Laboratory's NSLS-II using a custom reactor. The InAlN DAs studied include $In_{0.19}Al_{0.81}N$ (3 AlN cycles and 2 InN cycles per supercycle), $In_{0.5}Al_{0.5}N$ (1 AlN cycle and 3 InN cycles per supercycle), $In_{0.64}Al_{0.36}N$ (1 AlN cycle and 5 InN cycles per supercycle) and $In_{0.83}Al_{0.17}N$ (1 AlN cycle and 14 InN cycles per supercycle). Preliminary analysis of the data suggests that while the pure InN and AlN grew in 3D and 2D modes, respectively, the InAlN growth mode did not follow a simple trend as the nominal composition was tuned from InN to AlN. Instead, select compositions (50% and 83% In) exhibited predominantly 3D growth, while others (19% and 64% In) exhibited 2D growth. We also present complementary ALEp growth studies using a commercial Ultratech/Cambridge Nano Tech Fiji 200 and *ex situ* characterization methods, including high resolution X-ray diffraction, X-ray reflectivity, and atomic force microscopy.

[1] N. Nepal, V.R. Anderson, J.K. Hite, and C.R. Eddy, Thin Solid Films **589**, 47 (2015)

[2] J.M. Woodward, S.G. Rosenberg, A.C. Kozen, N. Nepal, S.D. Johnson, C. Wagenbach, A.H. Rowley, Z.R. Robinson, H. Joress, K.F. Ludwig Jr, C.R. Eddy Jr, J. Vac. Sci. Technol. A **37**, 030901 (2019)

[3] V.R. Anderson, N. Nepal, S.D. Johnson, Z.R. Robinson, A. Nath, A.C. Kozen, S.B. Qadri, A. DeMasi, J.K. Hite, K.F. Ludwig, and C.R. Eddy, J. Vac. Sci. Technol. A **35**, 031508 (2017)

4:00pm TF+2D+AP+EL+SS-MoA-8 Real-time Monitoring of the Surface Chemistry of Atomic Layer Deposition by Ambient Pressure X-ray Photoelectron Spectroscopy, *Joachim Schnadt, P Shayesteh,* Lund University, Sweden*; R Tsyshevskiy,* University of Maryland*; G Jean-Jacques, F Bournel,* Sorbonne Université, France*; R Timm,* Lund University, Sweden*; A Head,* Brookhaven National Laboratory*; G D'Acunto, F Rehman, S Chaudhary,* Lund University, Sweden*; R Sánchez-de-Armas,* Uppsala University, Sweden*; F Rochet,* Sorbonne Université, France*; B Brena,* Uppsala University, Sweden*; A Mikkelsen, S Urpelainen, A Troian, S Yngman, J Knudsen,* Lund University, Sweden   **INVITED**

Atomic layer deposition (ALD) and chemical vapour deposition (CVD) are very important methods that enable a highly controlled growth of thin films [1]. The surface chemis-try of the underlying processes remains, however, little understood. While idealised reac-tion mechanisms have been developed, they represent postulates rather than models based on the factual identification of surface species and kinetics [2]. New *in situ* and *operando* methods offer the prospect of gaining a much more thorough understanding of the involved molecular and atomic surface processes and (dynamic) structures, which, in turn, means that a much better knowledge basis can be achieved for the future improvement of materials and growth recipes (see, e.g. [3,4]). One such *operando* method, which can be applied to the investigation of ALD and CVD, is synchrotron-based ambient pressure x-ray photoelectron spectroscopy (APXPS). While conventional x-ray photoelectron spectroscopy (XPS) is limited to vacuum pressures of 10^{-5} mbar and below, APXPS can be carried out at realistic pressure. Today, most APXPS machines can operate at pressures up to the 10 mbar regime, which is an ideal match to the pressure regime used in standard ALD reactors.

Here, I will report on our recent efforts to apply density functional theory (DFT)-assisted synchrotron-based APXPS to the ALD/CVD of oxides (TiO_2, SiO_2, and HfO_2) on semiconductor (InAs and Si) and oxide surfaces (TiO_2, RuO_2) [3-5]. I will show that APXPS allows the identification of the surface species occurring during thin film growth and the real-time monitoring of their evolution with a time resolution of down into the millisecond regime. Here, DFT is an important tool for pinpointing the nature of the chemical species and for providing deeper insight in the surface chemical processes. I will also report on our efforts to further improve instrumentation with the goal of achieving a much closer match of the APXPS sample environment with the geometries used in conventional ALD reactors. The development will also open for the use of a wider range of precursors and growth protocols.

[1] V. Miikkulainen et al., J. Appl. Phys. 113 (2013) 021301.

[2] F. Zaera, Coord. Chem. Rev. 257 (2013) 3177.

[3] B. A. Sperling et al. Appl. Spectrosc. 67 (2013) 1003.

[4] K. Devloo-Casier et al., J. Vac. Sci. Technol. 32 (2014) 010801.

[3] S. Chaudhary et al. , J. Phys. Chem. C 119 (2015) 19149.

[4] A. R. Head et al. , J. Phys. Chem. C 120 (2016) 243.

[5] R. Timm et al., Nature Commun. 9 (2018) 412.

4:40pm TF+2D+AP+EL+SS-MoA-10 Kinetics during TMA-H₂O ALD: The Possible Role of Cooperative Surface Reactions, *Brent Sperling, B Kalanyan, J Maslar,* National Institute of Standards and Technology (NIST)

Until recently, the CH_3 groups produced by surface reactions of trimethylaluminum (TMA) during atomic layer deposition were widely believed to always be highly reactive toward H_2O, but *in situ* measurements have shown this is not the case below about 200 °C.[1] At these temperatures, some CH_3 groups react slowly, and a significant amount persists from cycle to cycle under typical growth conditions. Interestingly, these persistent CH_3 groups are not incorporated as carbon impurities. We have observed these CH_3 groups using *in situ* reflection infrared spectroscopy and have confirmed low carbon concentrations in our films using *ex situ* XPS. Furthermore, we have measured the kinetics of the reaction with H_2O and have found them to be well-described by a double-exponential decay function. A simple Monte Carlo simulation that

incorporates cooperative effects by clustered surface reactants (as suggested by DFT calculations[2]) reveals that a double-exponential decay of coverage can result even when only one species of reactant is present. Furthermore, the short-range distributions of coverage that result in the simulation differ from purely random ones. This difference implies that measurements sensitive to dipole-dipole interactions when combined with an independent measurement of surface coverage could be used to confirm or disprove the cooperative reaction model.

[1] V. Vandalon and W. M. M. Kessels, *J. Vac. Sci. Techol. A* **35** (2017) 05C313

[2] M. Shirazi and S. D. Elliott, *Nanoscale* **7** (2015) 6311.

5:00pm **TF+2D+AP+EL+SS-MoA-11 Atomic Layer Deposition of Metal Sulfides: Growth and Surface Chemistry**, *Xinwei Wang,* Shenzhen Graduate School, Peking University, China

Atomic layer deposition (ALD) of metal sulfides has recently aroused great interest, and many new sulfide ALD processes have emerged during the past several years. Surface chemistry plays a key role in ALD, but it remains yet to be investigated for many recently developed sulfide ALD processes. In this representation, I will report our study on the growth and surface chemistry of the ALD of nickel, iron, and cobalt sulfides, using various in situ characterization techniques of X-ray photoelectron spectroscopy (XPS), low-energy ion scattering (LEIS), quartz crystal microbalance (QCM), and quadrupole mass spectrometry (QMS). For instance, nickel sulfide (NiS) can be deposited from a Ni amidinate precursor ($Ni(amd)_2$) and H_2S by ALD (*Chem. Mater.* (2016) 28, 1155), but the surface chemistry of this process is found to deviate from the conventional ligand-exchange ALD scheme, and a formation of a nonvolatile acid-base complex from acidic surface sulfhydryl and basic amidine is suggested during the H_2S half-cycle (*J. Phys. Chem. C* (2018) 122, 21514). The initial ALD growth of NiS on a SiO_x surface is also intriguing, as the initial growth mechanism is found to be rather different from that in the later steady film growth. In the initial ALD cycles, the XPS results show a drastic cyclic variation of the signals for the Ni−O bonds, with prominently observable Ni−O signals after each $Ni(amd)_2$ dose but almost negligible after the subsequent H_2S dose. These results suggest that the Ni−O bonds are first formed on the surface in the $Ni(amd)_2$ half-cycles and then mostly converted to NiS in the following H_2S half-cycles. To describe this initial ALD growth process, a reaction-agglomeration mechanistic scheme is proposed (*Chem. Mater.* (2019) 31, 445). Surface thermolysis study of the Ni amidinate precursor further reveals the temperature-dependent behavior of the film growth.

Thin Films Division
Room A122-123 - Session TF+SE-MoA

HiPIMS and Reactive HiPIMS for Novel Thin Films

Moderators: Joe Becker, Kurt J. Lesker Company, Megan Holtz, Cornell University

1:40pm **TF+SE-MoA-1 The Influence of the Magnetic Field on the Deposition Rate and Ionized Flux Fraction in the HiPIMS Discharge**, *H Hajihoseini,* University of Iceland, Iceland; *M Cada, Z Hubicka,* Academy of Sciences of the Czech Republic, Czech Republic; *S Unaldi,* LPGP Université Paris-Sud, France; *M Raadu, N Brenning,* KTH Royal Institute of Technology, Sweden; *Jon Tomas Gudmundsson,* University of Iceland, Iceland; *D Lundin,* LPGP Université Paris-Sud, France

Three different ways to quantify the degree of ionization in sputtering magnetrons are discussed [1]. Then we move on to explored the effect of the magnetic field strength $|B|$ and geometry (degree of balancing) on the deposition rate and ionized flux fraction F_{flux} in dc magnetron sputtering (dcMS) and high power impulse magnetron sputtering (HiPIMS) when depositing titanium. The HiPIMS discharge was run in two different operating modes. The first one we refer to as 'fixed voltage mode' where the cathode voltage is kept fixed at 625 V while the pulse repetition frequency is varied to achieve the desired time average power (300 W). The second mode we refer to as 'fixed peak current mode' is carried out by adjusting the cathode voltage to maintain a fixed peak discharge current and by varying the frequency to archive the same average power. Our results indicate that the dcMS deposition rate is weakly sensitive to variations in the magnetic field while the deposition rate during HiPIMS operated in fixed voltage mode changes from 30% to 90% of the dcMS deposition rate as $|B|$ decreases [2]. In contrast, when operating the HiPIMS discharge in fixed peak current mode the deposition rate increases only slightly with decreasing $|B|$. In fixed voltage mode, for weaker $|B|$ the

higher the deposition rate, the lower the F_{flux}. The measured quantities, the deposition rate and ionized flux fraction, are then related to the ionization probability α_t and the back attraction probability of the sputtered species β_t. We show that the fraction of the ions of the sputtered material that escape back attraction increases by 30% when $|B|$ is reduced during operation in fixed peak current mode while the ionization probability of the sputtered species increases with increased discharge current when operating in fixed voltage mode.

[1] A. Butler, N. Brenning, M. A. Raadu, J. T. Gudmundsson, T. Minea and D. Lundin, *Plasma Sources Science and Technology*, **27**(10) (2018) 105005

[2] H. Hajihoseini, M. Čada, Z. Hubička, S. Unaldi, M. A. Raadu, N. Brenning, J. T. Gudmundsson and D. Lundin, *Plasma*, submitted for publication, April 2019

2:00pm **TF+SE-MoA-2 HIPIMS and Magnetron Sputtering of Niobium for use in Josephson Junctions**, *George Major, M Linford,* Brigham Young University

Niobium (Nb) is a technology-critical element with superconductive properties, and applications in electronics, superconductors, and particle accelerators. Thin film niobium is commonly deposited by magnetron sputtering. Properties of Nb thin films must be precisely tuned for applications, e.g., Josephson Junctions, as surface roughness, crystallite size, and apparent elastic modulus can affect superconducting film properties. To create a Josephson Junction, a thin film of Al (4 to 10 nm) is deposited on top of a smooth Nb film (ca. 100 nm). The functionality of this Al film is inversely related to its thickness. The smoother the film onto which the Al is deposited, the thinner it can be. High-power impulse magnetron sputtering (HIPIMS) is an emerging method for physically depositing thin films. HIPIMS produces a high degree of ionization of sputtered material and a high rate of molecular gas dissociation, which results in high density films. Various metals, including Ti and Ta, have been successfully deposited by HIPIMS, showing dense, smooth microstructures free of large-scale defects. Here, Nb thin films are deposited using magnetron sputtering and HIPIMS. These films are characterized by AFM, TEM, XPS, and SEM. Ellipsometry is used to study their optical properties and to determine their optical constants. HIPIMS should result in lower surface roughness compared to magnetron sputtering. The resulting films will lead to improved superconductive devices.

2:20pm **TF+SE-MoA-3 Thin Film Crystal Growth of Oxides, Nitrides and Carbides using High Impulse Magnetron Sputtering**, *Jon-Paul Maria,* The Pennsylvania State University **INVITED**

This presentation will discuss thin film crystal growth using reactive pulsed magnetron sputtering specifically in the region referred to as high power impulse magnetron sputtering, or HIPIMS. HIPIMS is characterized by duty cycles less than approximately 10%, and magnetron power densities in excess of 1 kW/cm². These intense impulses produce high ionization fractions of both the gas and sputtered species, they can be sustained in atmospheres containing substantial fractions of O_2 or N_2 with only modest re-sputtering, and they can be tuned so as to minimize target poisoning. Pulsed dc plasmas have been applied routinely to promote thin film adhesion, to achieve high deposition rates, and to produce extremely hard and wear resistant coatings. Their introduction to electronic materials has been much less rapid.

The intent of this presentation is to demonstrate the utility of pulsed dc plasmas, and specifically the HIPIMS regime, for electronic materials, including oxides, nitrides and carbides which require reactive environments that can in many cases can be challenging to realize. Three case studies will be presented: 1) epitaxial growth of CdO thin films for IR optoelectronic applications, 2) epitaxial growth of GaN thin films for wide bandgap applications, and 3) entropy-stabilized carbides for extreme environments. The basic instrumentation of this interesting plasma method will be discussed, and how it offers advantages for controlling defect chemistry, and this transport properties, in CdO, for enabling epitaxy at surprisingly low temperatures in GaN, with excellent control of surface morphology, and for achieving high carbon content in rocksalt carbides, and thus high hardness. In all cases the specific connections between plasma parameters, temperature, pressure, growth mode, and ultimately physical properties will be stressed. The intent is to demonstrate how this less-well explored region of plasma processing space offers possible advantages to crystal growth of electronic materials of contemporary interest.

Monday Afternoon, October 21, 2019

3:00pm TF+SE-MoA-5 Reactive Bipolar High Power Impulse Magnetron Sputtering (B-HiPIMS) for Deposition of High Entropy Carbides, *Trent Borman, M Hossain, J Maria,* The Pennsylvania State University

Sputtered carbide thin films frequently feature significant carbon sub-stoichiometry irrespective of the source materials, while amorphous-C or a-C:H secondary phases begin to precipitate with as many as 1/3 or more of the carbon sites vacant in the rock salt structure. In reactive sputtering it is often necessary to sputter in the compound regime in order to achieve a higher carbon stoichiometry, however this comes with the penalty of reduced sputter yield. Reactive HiPIMS can avoid carburization of the target through gas rarefaction and high target etch rates. While this is beneficial for process stability, carbide microstructural evolution is still limited by the low homologous temperature achievable in thin film deposition (0.25-$0.3 T_{melt}$). Recently, bipolar-HiPIMS has been discussed as a means of tailoring the bombardment in order to drive microstructural development through momentum transfer and thermalization of kinetic energy.

The authors will discuss the reactive synthesis of high entropy carbide films from metal alloy targets using Bipolar High-Power Impulse Magnetron Sputtering (B-HiPIMS) in a mixed Ar/CH_4 atmosphere. The effects of bipolar pulse voltages and lengths on microstructural, compositional, and phase development will be discussed. Additionally, the impacts of order of magnitude changes in sputter pulse length on the formation of carbide thin films will be reported. This work investigates a broad range of carbon stoichiometries: from metallic films and carbon deficient carbides to near stoichiometric carbides and carbide/amorphous-carbon nanocomposites. This enables investigation of the property trends as a function of carbon content, as it is presently unclear if the diverse trends observed in the binary carbides persist in a high entropy system or are overshadowed by the high entropy metal sublattice.

This material is based upon work supported by the National Science Foundation Graduate Research Fellowship (DGE-1252376) and the Office of Naval Research (N00014-15- 1-2863).

3:20pm TF+SE-MoA-6 High Density Titanium Oxide and Silicon Oxide Films Deposited by Current-Controlled High Power Impulse Magnetron Sputtering, *Arutiun P. Ehiasarian, P Hovsepian, D Loch,* Sheffield Hallam University, UK

High density transparent oxide layers on glass can improve the environmental viability of photovoltaics, displays, and low emissivity layers in glazing as well as aid the photocatalytic deactivation of organic contaminants. High Power Impulse Magnetron Sputtering (HIPIMS) produces high density microstructures and high hardness due to the delivery of an ionised metal and dissociated oxygen deposition flux to the substrates.

TiOx and SiOx films were produced in a cluster tool by reactive HIPIMS of a pair of metallic targets in an Ar-Oxygen atmosphere. The HIPIMS process was carried out by controlling the current within the pulse. This resulted in the elimination of stability issues associated with runaway currents for all target poisoning states from metallic to fully poisoned. TiOx was deposited by a fast plasma ignition and a constant current during pulses of up to 200 microseconds. Electron cooling and gas rarefaction were observed sequentially during the initial stages if the pulse. These were followed by a steady increase in metal ion emission at constant power input. SiOx was deposited using a current ramp and shorter pulses of up to 20 microseconds and a bipolar operation. In the transition mode oxygen was emitted mainly from the target whilst in the filly poisoned mode it was detected in the gas phase by time-resolved optical emission spectroscopy. TiOx films deposited without additional heating or substrate biasing had good transparency and a refractive index which increased continuously as the oxygen flow reduced from 45 to 13% reaching a maximum value of 2.55 at a wavelength of 550 nm. The films comprised a mixture of rutile and anatase phase with HIPIMS deposition producing higher fractions of rutile compared to bipolar pulsed DC operation. The HIPIMS films reached higher refractive index of 2.55 compared to 2.47 for bipolar pulsed DC. The hardness of the films and its relation to process conditions are discussed. The morphological density was extremely high as confirmed by a 2 orders of magnitude reduction in corrosion current in potentiodynamic polarisation tests on 304 stainless steel substrates. SiOx microstructural density, refractive index and hardness are discussed.

4:00pm TF+SE-MoA-8 Epitaxial Growth and Surface Morphology of Thin Film GaN via HiPIMS, *Kevin Ferri, E Runnerstrom,* Pennsylvania State University*; A Klump, Z Sitar, R Collazo,* North Carolina State University*; J Maria,* The Pennsylvania State University

GaN is a desirable wide bandgap semiconductor for applications as blue and UV emitters as well as high temperature, high power, and high frequency electronic devices. In order to overcome the low reactivity of gallium with nitrogen at low temperatures, thin film GaN deposition techniques such as Metal Organic Chemical Vapor Deposition often use high pressure growth at temperatures in excess of 1000 °C. While higher temperatures allow for high crystal quality thin film GaN with favorable morphology, this presents challenges to abrupt junction formation due to fast diffusion rates that cause dopant migration during deposition. It is thus advantageous to find avenues to lower the deposition temperature for GaN to a region where controlled doping can occur. While doing so, it is imperative to maintain epitaxy and growth morphology for device fabrication.

In this presentation, we demonstrate that reactive High-Power Impulse Magnetron Sputtering (HiPIMS) is an effective low temperature alternative for depositing high quality, epitaxial GaN thin films. In contrast to conventional direct current (DC) or radio frequency (RF) sputtering, pulsed DC provides the needed kinetic energy and ionization fraction to establish a sufficiently reactive environment to promote full nitridation. This can be challenging with many other Ga sources. More specifically, the low duty cycle regime of pulsed DC known as HiPIMS provides access to kW/cm^2 peak power densities without target degradation and thus dramatically increased gallium reactivity. In addition, adding an opposite polarity voltage pulse between the target bombarding events, known as a kick pulses, further allows one to tailor both the adatom landing energy on the substrate surface, and mitigate target poisoning.

This unique capability set enables us to prepare high crystal quality epitaxial GaN thin films with smooth surface morphologies characterized by c/2 steps and terraces at temperatures below 500 °C. The presentation will focus on the relationships between sputtering parameters including voltage, kick pulse, pulse length, and duty cycle, on GaN thin film crystal quality, surface morphology, and growth rate. Preliminary transport properties will be reported.

4:20pm TF+SE-MoA-9 Reactive HiPIMS Deposition of a Thick Cu:CuCNx Multilayered Nano-composite Coating Material for Improving Machining Process Performance in Rough Turning, *Md.Masud-Ur Rashid, C Nicolescu,* KTH Royal Institute of Technology, Plasmatrix Materials AB, Sweden*; A Archenti,* KTH Royal Institute of Technology, Sweden*; G Shuai,* KTH Royal Institute of Technology*; R Tomkowski,* KTH Royal Institute of Technology, Sweden

Vibrations in metal cutting process such as turning have detrimental effect on productivity, finished surface roughness of workpiece and cutting insert life. During machining process high frequency vibration (equal to or above 10000 Hz) causes micro cracks to the cutting insert, which facilitate the failure of cutting insert and consequently resulted in higher roughness on workpiece surface. In this study a reactive high power impulse magnetron sputtering (R-HiPIMS) deposition process was used to deposit a thick copper and copper-carbon nitride (Cu:CuCNx) multilayered nano-structured composite coating, with higher stiffness and damping properties, on the shim. This coated shim was then used to suppress the high frequency vibration during rough turning operation. Scanning electron microscopy (SEM) of the coating cross section as well as energy dispersive x-ray spectroscopy (EDS) mapping of the cross-section confirms the multilayered structure with the presence of different rations of copper (Cu), carbon (C), and nitrogen (N). The Cu:CNx coating thickness was measured to be approximately 100 μm. The average surface hardness (SH) and cross-sectional hardness (CSH), measured by Vickers-microhardness indention, were found to be 353.2 HV and 149.5 HV respectively. Insert wear measurement after 30 minutes of rough turning process, reveals that the studied 100 μm Cu:CuCNx multi-layered composite coating material can reduce the tool wear by 60.5%. The average roughness value (Ra) of the work piece material is also reduced by 8.76% in case of using Cu:CNx coated shim comparing to conventional shim.

4:40pm TF+SE-MoA-10 The Residual Stress Control in Hard Metal Films by Energetic Deposition, *Y.G. Li, Y Qu, Z Jiang, M Lei,* Dalian University of Technology, China

For energetic deposition, ion bombardment was an important factor independent of grain size for influencing the residual stress, and the energy and flux were critical parameters to determine the residual stress

evolution. In this work, modulated pulsed power magnetron sputtering (MPPMS) and deep oscillation magnetron sputtering (DOMS) were employed to control the energy and flux with or without bias to modulate the ion bombardment for intrinsic stress generation. The films thickness was selected at 0.2, 0.5, 1.5 and 3.0 μm to give a comparative study of the intrinsic stress, and thermal stress was not considered since the effect of thermal stress made no major influences. It was found that the thin films all showed compressive residual stress with thickness under 1 μm, and the residual stress of Cr thin film was lower than that of the Nb thin film under similar thickness. The residual stress of DOMS Nb thin film was always higher than MPPMS Nb thin film, however the residual stress of DOMS Cr thin film was equivalent to MPPMS Cr thin film. The ion irradiation effect should be the dominating effect responsible for the difference between Nb and Cr thin films, since Nb generated more Nb^{2+} ions than Cr in energetic deposition. For Cr thin films, the grain size and deposition rate were also important influencing factors, fine grain size and high deposition rate promoted the formation of compressive residual stress. For energy deposition, the effect of secondly charged ions in the film growing front should be concentrated to establish a proper kinetic model for intrinsic stress generation.

5:00pm TF+SE-MoA-11 Advanced HIPIMS Coatings Through Kick Pulse Technology, *Jason Hrebik,* Kurt J. Lesker Company
HIPIMS coating technology has been rapidly growing over the past few years due to the availability of R&D scale supply offerings. This has resulted in many new breakthroughs in application enhancement, production scalability, and efficiency. The number of applications where HIPIMS is now considered is also advancing. Breakthroughs in HIPIMS controllability have enabled researchers to find a variety of ideal operating parameter sets for various performance requirements. One of the most significant technical advances is a reverse positive kick pulse. This option provides a significant variable for driving out film stress in HIPIMS applications and increasing yield rates, which have been a major downside to HIPIMS in the past. These advances open up new possibilities for the technology and the enhancement of many thin film applications. This presentation will highlight examples of these applications along with the advantages associated with HIPIMS and the Kick pulse technology. It will show how these advances can be scaled to larger scale production applications and provide examples of what enhancements can be expected.

Energy Transition Focus Topic
Room A212 - Session TL+2D+HC+SS-MoA

Surface Reaction Mechanisms in Energy Conversion (ALL INVITED SESSION)

Moderators: Marie Turano, Loyola University Chicago, Sarah Zaccarine, Colorado School of Mines

1:40pm TL+2D+HC+SS-MoA-1 Selective Photo-driven Organic Reactions on the Surfaces of Colloidal Quantum Dots, *Y Jiang, K McClelland, C Rogers, Emily Weiss,* Northwestern University **INVITED**
Colloidal quantum dots present a unique opportunity not only to power chemical reactions with sunlight but to control those chemical reactions through various templating strategies. This talk will explore demonstrations of chemo-, regio-, and stereoselective reactions photocatalyzed by quantum dots.

2:20pm TL+2D+HC+SS-MoA-3 Single-Atom Alloy Catalysts: Born in a Vacuum, Tested in Reactors, and Understood In Silico, *Charles Sykes,* Tufts University **INVITED**
In this talk I will discuss a new class of metallic alloy catalysts called *Single Atom Alloys* in which precious, reactive metals are utilized at the ultimate limit of efficiency.[1-5] These catalysts were discovered by combining atomic-scale scanning probes with more traditional approaches to study surface-catalyzed chemical reactions. This research provided links between the atomic scale surface structure and reactivity which are key to understanding and ultimately controlling important catalytic processes. Over the last five years the concepts derived from our surface science and theoretical calculations have been used to design *Single Atom Alloy* nanoparticle catalysts that can perform industrially relevant reactions at realistic reaction conditions in collaboration with Maria Flytzani-Stephanopoulos at Tufts. For example, alloying elements like platinum and palladium with cheaper, less reactive host metals like copper enables 1) dramatic cost savings in catalyst manufacture, 2) more selective chemical reactions, 3) reduced susceptibility to CO poisoning, and 4) higher

resistance to deactivation by coking. I go on to describe very recent theory work by collaborators Stamatakis and Michaelides at UCL that predicts reactivity trends of 16 different *Single Atom Alloy* combinations for important reaction steps like activation of H-H, C-H, N-H, O-H and C=O bonds. This project illustrates that the field of surface science is now at the point where it plays a critical role in the design of new heterogeneous catalysts.

References:
[1] Kyriakou et al. Science **335**, 1209 (2012).
[2] Marcinkowski et al. Nature Materials **12**, 523 (2013).
[3] Lucci et al. Nature Communications **6**, 8550 (2015).
[4] Liu et al. JACS **138**, 6396 (2016).
[5] Marcinkowski et al. Nature Chemistry **10**, 325 (2018).

3:00pm TL+2D+HC+SS-MoA-5 Understanding Fundamental Energy Conversion Mechanisms: How Surface Science Can Help, *Ulrike Diebold,* Institute of Applied Physics, TU Wien, Austria **INVITED**
As we move to a more sustainable society, current energy conversion schemes need to be improved and novel ones designed. The relevant charge transfer processes and chemical transformations all occur at interfaces, so insights into fundamental mechanisms are needed to provide a scientific basis for these developments.

Using the frontier tools of surface science, I will discuss how we can directly inspect charge transfer to molecules, investigate the influence of the local environment on the reactivity of active sites, or probe the acidity of individual hydroxyls. Together with first-principles computations such experiments give crisp and clear insights into surface processes. I will also discuss the steps that are necessary to the transfer the knowledge gained from model systems to more complex environments.

4:00pm TL+2D+HC+SS-MoA-8 Atomically-defined Model Interfaces in Energy-related Catalysis, Electrochemistry, and Photoelectrochemistry, *Jörg Libuda,* University Erlangen-Nuremberg, Germany **INVITED**
The transformation between chemical energy, solar energy, and electrical energy occurs at interfaces. Therefore, functional interfaces are the key to the development of new materials in energy technology and energy-related catalysis. In our work, we explore model systems, which provide detailed insight into the chemistry and physics at such functional interfaces. Complex, yet atomically-defined model systems are studied both under 'ideal' surface science conditions and under 'real' conditions, i.e., in contact with gases, liquids, in electrochemical, and in photoelectrochemical environments. We illustrate the approach in three examples from our recent research.[1-5]

First, we consider new noble-metal-efficient catalysts for fuel cell applications.[1] We show that precious noble metals such as Pt can be anchored to nanostructured oxide supports. The resulting materials show very high noble metal efficiency and high stability. Surface science studies on model catalysts provide insight into the functionality of these systems. Electronic metal support interactions modify the reactivity of the catalytic surfaces but also stabilize sub-nanometer-sized Pt nanoparticles against sintering and deactivation.

Secondly, we report on the development of atomically defined model systems for oxide-based electrocatalysts, which can be studied under true operation conditions, i.e., in liquid environments and under potential control. We describe how such model electrodes are prepared by surface science methods and, subsequently, are studied in liquid electrolytes preserving their atomic structure. We investigate the role of particle size effects and identify the origin of metal-support interactions.

In the third part, we scrutinize the role of organic-oxide hybrid interfaces in energy transformation. Particularly fascinating are organic layers of molecular photoswitches, which provide an extremely simple solution for solar energy conversion and storage. We show that it is possible to assemble fully operational solar-energy-storing hybrid interfaces by anchoring tailor-made norbornadiene photoswitches to atomically defined oxides. Interestingly, the activation barrier for energy release in these systems is not affected by the anchoring reaction. Finally, we demonstrate that solar energy storage and release in such systems can also be controlled electrochemically with high reversibility.

[1] A. Bruix, et al., *Angew. Chem. Int. Ed.*, 53, 10525 (2014)
[2] Y. Lykhach, et al., *Nat. Mater.* 15, 284 (2016)
[3] O. Brummel et al., *ChemSusChem* 9, 1424 (2016)

[4] O. Brummel et al., *J. Phys. Chem. Lett.*, 8, 2819 (2017)

[5] F. Faisal et al., *Nat. Mater.*, 17 592 (2018)

4:40pm TL+2D+HC+SS-MoA-10 Controlling Ultrafast Photochemical Reactions in Photocatalysis, *Annemarie Huijser,* University of Twente,The Netherlands, The Netherlands **INVITED**

The transition from fossil to renewable energy is one of the most important challenges of our society. Solar devices are widely considered as a highly promising option, as the energy provided by the sun to the earth by far exceeds global needs. We are investigating the use of nanostructured materials for application in solar energy conversion. The overall efficiency relies on the complex interplay of many elementary process, occurring at different time scales and also dependent on the nanostructure. In this presentation I will show how a combination of methods for ultrafast spectroscopy can shed light on the nature of photoinduced processes and provide mechanistic information valuable for the design of novel materials.

Vacuum Technology Division
Room A213 - Session VT-MoA

Gas Dynamics, Surface Science for Accelerators, and Ultra-Clean Vacuum Systems

Moderators: Jason Carter, Argonne National Laboratory, James Fedchak, National Institute of Standards and Technology

1:40pm VT-MoA-1 Advancement in Transient Flow Simulations: Applications to Channel and Porous Media Conductance Modeling, *Irina Graur Martin,* Aix Marseille University, France **INVITED**

The gas flow through long channels of various and variable cross-sections is a practical problem in the MEMS and vacuum technology applications. As examples of such kind of flows the leakage through compressor valves and the flows in the micro bearing may be given. Among these applications, the gas flows through the low permeable membranes, which are also the flows at microscale, present also a great interest, especially in vacuum technology for filtering, separation process, protection and flow control. Recently some advancement in the transient flow simulation, based on the gas kinetic theory, was proposed in [1], [2]. Using this approach, the determination of the micro tube conductance is realized in [3]. The very similar approach is also proposed recently to characterize the permeability of the porous media like the low porous membranes [4]. Different examples of application of the proposed methodology will be shown for various type of porous media et different gases under isothermal and non-isothermal conditions.

References:

[1] F.Sharipov, I.Graur, General approach to transient flows of rarefied gases through long capillaries, Vacuum, v100, pp.22-25, 2014

[2] Graur, M.T. Ho, Rarefied gas flow through a long rectangular channel of variable cross-section, Vacuum, 101, 328-332, 2014.

[3] M. Rojas-Cardenas, E. Silva, M.-T. Ho, C. J. Deschamps, I. Graur, Time-dependent methodology for non-stationary mass flow rate measurements in a long micro-tube: Experimental and numerical analysis at arbitrary rarefaction conditions, I. Microfluid Nanofluid (2017) 21: 86.

[4] M.V. Johansson, F. Testa, I. Zaier, P. Perrier, J.P. Bonnet, P. Moulin, I. Graur, Mass flow rate and permeability measurements in microporous media, v 158, Vacuum, 2018, pp. 75-85

2:20pm VT-MoA-3 A Multiphysics Simulation Tool for Storage Ring Vacuum System Design and Optimization, *Nicholas Goldring, Z Wu, D Bruhwiler, B Nash,* RadiaSoft LLC*; J Carter, J Lerch, K Suthar,* Argonne National Laboratory*; R Nagler,* RadiaSoft LLC*; P Den Hartog,* Argonne National Laboratory

Fourth generation storage ring light sources are creating orders-of-magnitude brighter x-rays by reducing horizontal emittance via multi-bend achromats. This requires the bending magnet pole tips to be closer to the electron beam axis, which in turn requires smaller vacuum chambers. The resultant design challenges are dictated by complex and coupled physical phenomena including electromagnetic wake fields, high thermal stresses and photon stimulated desorption. To better analyze and optimize next-generation vacuum systems, the authors are developing and benchmarking a suite of COMSOL Multiphysics models, which include the production, propagation, and surface interactions of synchrotron x-rays, as well as the resulting physical phenomena specified above. These coupled physics models are benchmarked against the open source codes SynRad and

MolFlow. Finally, the models are embedded within a browser-based GUI, enabling scientists and engineers to execute simulations in the cloud.

2:40pm VT-MoA-4 Vacuum System Design and Modeling for the Jefferson Lab Electron Ion Collider Interaction Region, *Marcy Stutzman,* Jefferson Lab

Jefferson Lab and Brookhaven National Lab are both pursuing designs to build an electron ion collider in the United States following the 2015 US Nuclear Science Advisory Committee recommendations for such a facility. The design of the Jefferson Lab Electron Ion Collider (JLEIC) interaction region (IR) requires vacuum in the UHV regime to reduce background rates sufficiently in the detectors. Additionally, though the final bending magnets are far upstream from the IR in the electron line, the interaction between residual gas and the electron beam will produce synchrotron radiation and subsequent elevated gas load in the interaction region. Preliminary designs of the vacuum system for the JLEIC interaction region and the cryogenic final focusing quadrupoles will be presented using the Molflow+ software. Synchrotron radiation due to the finite beam envelope traveling through the quadrupoles will be also modelled using Molflow's complementary program SynRad. However, since the primary synchrotron radiation in this system may be from the beam-gas interactions in the long straight section upstream of the IR, synchrotron radiation distributions and their effect on the gas load will also be studied using an existing 2D radiation prediction code and GEANT4 beam-gas interaction cross section calculations.

3:00pm VT-MoA-5 Photocathode Growth and Diagnostic Systems for LCLS-II, *Xianghong Liu, T Vecchione, B Dunham,* SLAC National Accelerator Laboratory

We have designed and manufactured a multisource physical vapor deposition system for producing photocathodes to be used in the LCLS-II, a hard X-ray free electron laser accelerator facility at SLAC. The photocathodes currently produced are thin film Cs_2Te, but the system has the capability to integrate up to four independent sources permitting the future growth of ternary and quaternary compounds. The deposition system has a load-lock which permits photocathodes to be transferred into and out of the system without breaking vacuum. The geometry of the photocathode substrate is adopted from INFN, so photocathodes can be exchanged between systems and institutions that share the same design using a vacuum suitcase. We have also designed a diagnostic system for characterizing photocathode performance and are in the process of manufacturing this system. The system is capable of measuring the quantum efficiency and transverse momentum distributions of photoemitted electrons. The wavelength dependence of these measurements can be recorded as a function of temperature down to below 10 K. We will present the designs of these systems and report on their operational status and early results.

3:20pm VT-MoA-6 Characterization of NbTiN Thin Film Structures, *David Beverstock, A Valente-Feliciano,* Jefferson Lab*; V Smolyaninova,* Towson University*; M Kelley,* The College of William and Mary

Approaching the bulk Nb material RF performance limits has urged development of alternative superconducting materials for superconducting radio frequency (SRF) accelerator cavities for further performance enhancement. A promising theory has predicted that thin film structures of superconductor-insulator-superconductor (SIS) [1] can delay magnetic flux penetration in accelerator cavities to higher fields. A candidate superconductor for the SIS structures is NbTiN. A few key aspects of SIS structures development are high quality individual layers, sharp interfaces and optimum thickness for first flux penetration (H_{fp}) delay. High quality monocrystalline NbTiN films are deposited by reactive DC magnetron sputtering. In a parallel development, interface quality was assessed by depositing bilayers of 3 nm NbTiN with ~1 nm AlN repeated up to 16 times with no increase in roughness of the structure. The stacked layers form a metamaterial, which could exhibit T_c greater than bulk NbTiN [2]. This contribution presents the characterization of the surface, material and superconductivity of NbTiN with concentration on the H_{fp} enhancement for 200 to 5 nm films and multilayer nanostructures.

References:

[1] Gurevich, Alex. "Maximum screening fields of superconducting multilayer structures." *AIP Advances 5.1* (2015): 017112.

[2] Smolyaninova, Vera N., et al. "Enhanced superconductivity in aluminum-based hyperbolic metamaterials." *Scientific reports 6* (2016): 34140.

Acknowledgements:

Monday Afternoon, October 21, 2019

4:00pm VT-MoA-8 Future Laser Interferometer Gravitational Wave Observatories and their Vacuum Requirements, *Chandra Romel,* California Institute of Technology*; R Weiss,* Massachusetts Institute of Technology*; M Zucker,* California Institute of Technology*; H Dylla,* American Institute of Physics **INVITED**

The Laser Interferometer Gravitational Wave Observatory (LIGO) comprises a pair of large facility observatories in Washington and Louisiana dedicated to gravitational wave (GW) astronomy and astrophysics, funded by the U.S. National Science Foundation. A century after Einstein predicted the existence of gravitational waves, LIGO detected these ripples in the fabric of spacetime resulting from two massive binary black holes colliding almost 1.3 billion years away, birthing a new era of GW astronomy. For this achievement LIGO founders were awarded the 2017 Nobel Prize in Physics. Since the first detection in 2015, over a dozen black hole mergers have been recorded, in addition to neutron star collisions, marking a significant breakthrough for multi-messenger astronomy. Concepts of third generation GW instruments are undergoing research and development, with the promise to expand humanity's ability to listen to the cosmic symphony of gravitational waves out to the very edge of the universe.

An NSF workshop was held at the LIGO Livingston site in January to explore potential novel vacuum system solutions for 3G observatories. Cost effective solutions are required for the design, construction and operation of these large vacuum systems, proposed to be a factor of ten larger than the current systems in the U.S. (LIGO), Europe (Virgo) and Japan (KAGRA). Technologies developed and employed in the existing GW observatories have been shown to meet stringent requirements of vacuum integrity, low hydrogen and heavy molecule outgassing, minimal particulate generation, low vibration, and stray light optical absorbance for successful operation. However, extrapolating costs from current lengths to 40km/arm of vacuum beamtube indicates the need to investigate a wide range of technologies and materials that could significantly lower the final cost of 3G observatories such as the Cosmic Explorer in the U.S. and the Einstein Telescope in the E.U. Two classes of solutions for the vacuum enclosures were examined: 1) the first design concept is an extrapolation of the single-wall vacuum pipe in the present generation of detectors; 2) the second design concept involves double-walled or nested vacuum pipes that would separate the atmospheric load from the stringent UHV properties needed for the inner wall. Pumping solutions and surface treatments were examined for both concept designs with an emphasis on potential hardware and treatments that could lower total costs but still meet the stringent vacuum requirements.

4:40pm VT-MoA-10 Status Update on the New Space Calibration Facility at TNO, *Freek Molkenboer*, R Jansen, F Driessen, T Luijkx, TNO, The Netherlands

In 2018 TNO started with the conceptual design of a new Space calibration facility, called CSI. The CSI will be used for the performance verification and calibration of optical earth observation instruments on satellites. At the end of 2018, Angelantoni Test Technologies (ATT) from Italy was awarded a contract after completion of the European tendering procedure as the supplier of the Thermal Vacuum Chamber (TVC) and in January 2019 Symétrie, located in France was awarded a contract after completion of the European tendering procedure as the supplier for the hexapod on a rotation table that will be placed inside the vacuum chamber.

The TVC will be a vertically placed stainless steel cylinder with a diameter of 2.75 meter and a height of 2.5 meter. The chamber and thermal shrouds are sliced diagonally, resulting in a wedge shaped bottom half and top half, this reduces the total height (room and top half of the chamber) required for opening the chamber and loading a space instrument.

The thermal shroud of the TVC will be able to create an environment between 193K and 353K. Two thermal plates will be present to cool part(s) of the instrument down to 100K if required. The vacuum system consists of two turbomolecular pumps and two cryopumps to reach the ultimate pressure of 10e-7 mbar. The vacuum conditions in the TVC will be monitored with an RGA (Residual Gas Analyser) and a QCM (Quarts Cristal Microbalance).

During the calibration of a Space instrument, its position relative to the calibration light sources (Optical Ground Support Equipment or OGSE) has to be changed with an extremely high accuracy and reproducibility. To achieve this, TNO has selected a vacuum compatible hexapod on a rotation table that meets the stringent accuracy and stability requirements.

Additionally TNO has designed an active thermal system around the hexapod in order to locally create a thermal stable environment.

During this talk I will discuss the design and current manufacturing status of both the thermal vacuum chamber, including the vacuum lay-out and thermal lay-out, and the design of the hexapod on rotation table including the protective measures we have taken to keep the hexapod at stable temperature.

5:00pm VT-MoA-11 Advancements in Monitoring and Operating Thermal Vacuum Environmental Test Chambers for Next-Generation Space Exploration Hardware, *Maxwell Martin*, A Wong, W Hoey, J Alred, P Boeder, C Soares, Jet Propulsion Laboratory, California Institute of Technology

As space exploration missions continue to develop and implement increasingly sensitive instruments and incorporate advanced detection capabilities for organics, contamination control protocols have necessarily evolved in their sophistication and stringency. Monitoring spacecraft hardware as it undergoes environmental testing requires high-precision measurements in thermal vacuum chambers. With increased sensitivity of instruments and missions, the traditional use of witness plates and solvent swabs is insufficient to characterize both chamber background, and the induced environment of the system being tested and the associated ground-support equipment. Quartz crystal microbalances (QCMs) are required to conduct *in situ* monitoring of hardware outgassing rates. QCMs are sensitive to thermal and mechanical perturbations; therefore, within an environmental testing facility, as-collected QCM data requires post-processing for signal noise due to instrumentation sensitivity, and uncertainties in data analysis. Insertion and removal of hardware into chambers introduces ambient atmosphere to the vacuum systems, providing additional sources of measurement uncertainty, particularly as relates to the collection and interpretation of pre-test chamber backgrounds. In an effort to support the next generation of space exploration, the Contamination Control team at JPL is implementing upgrades in systematic data analysis, thermal vacuum chamber operations, and instrumentation selection for use in spacecraft hardware environmental testing. These advancements in environmental test chamber monitoring support JPL's current portfolio of space exploration missions, and challenging mission science objectives.

2D Materials
Room A216 - Session 2D+AS+MI+NS-TuM

2D Materials Characterization including Microscopy and Spectroscopy

Moderator: David Geohegan, Oak Ridge National Laboratory

8:00am **2D+AS+MI+NS-TuM-1 Near-field Infrared Spectroscopy of Single Layer MnPS₃**, *Sabine Neal,* University of Tennessee Knoxville*; H Kim,* Rutgers University*; K Smith, A Haglund, D Mandrus,* University of Tennessee Knoxville*; H Bechtel,* Advanced Light Source, Lawrence Berkeley National Laboratory*; L Carr,* National Synchrotoron Light Source II, Brookhaven National Lab*; K Haule, D Vanderbilt,* Rutgers University*; J Musfeldt,* University of Tennessee Knoxville

In order to explore the properties of a complex van der Waals material under confinement, we measured the near-field infrared response of the magnetic chalcogenide $MnPS_3$ in bulk, few-, and single-layer form and compared the results with traditional far field vibrational spectroscopy and complementary lattice dynamics calculations. Trends in the activated B_u mode near 450 cm^{-1} are particularly striking, with the disappearance of this structure in the thinnest sheets. Combined with the amplified response of the A_g mode and analysis of the $A_u + B_u$ features, we find that the symmetry is unexpectedly *increased* in single-sheet $MnPS_3$. The monoclinicity of this system is therefore a consequence of the long-range stacking pattern rather than local structure.

8:20am **2D+AS+MI+NS-TuM-2 Multi-parameter Analysis of Genesis and Evolution of Secondary Electrons produced in the Low Energy Regime**, *Alessandra Bellissimo,* ETH Zürich, Switzerland*; G Pierantozzi,* CNR - Istituto Officine Materiali, Italy*; A Ruocco, G Stefani,* Università degli Studi Roma Tre, Italy*; O Ridzel, V Astašauskas, W Werner,* Technische Universität Wien, Austria*; M Taborelli,* CERN, Switzerland*; G Bertolini, U Ramsperger,* ETH Zürich, Switzerland*; O Gürlü,* ETH Zürich, Switzerland, Turkey*; D Pescia,* ETH Zürich, Switzerland

The mechanisms responsible for electron-induced Secondary Electron Emission (SEE) generation of these ubiquitous Secondary Electrons (SEs) in a solid surface is not yet fully understood. In particular, the question *how many* "true secondary" electrons are generated and emitted from the target per incident primary electron awaits resolution and is of great fundamental as well as technological importance. The present work reports on a study of these and related questions by means of a variety of spectroscopic tools of increasing finesse. The interaction of Low-Energy Electrons with surfaces exhibiting different long-range order, was investigated by combining measurements of the Total Electron Yield in absolute units, single-electron as well as (e,2e)-coincidence spectroscopy. This investigation has led to the disentanglement of the elementary processes that need to be considered and comprehended for the understanding of the SE-generation probability, fully taking into account both energy and momentum conservation in the collision and the band structure of the solid. Single ionising scattering events, assisted by collective excitations, i.e. *plasmons*, constitute one of the fundamental ingredients leading to SEE. In the Low-Energy-regime the electron yield of a material is constituted by the interplay of reflectivity and SEE, both strongly dictated by the target band structure. The gathered information is further used in an attempt to interpret the signal generation mechanisms relevant in Scanning Field-Emission Microscopy (SFEM) [1].

Reference:

[1] A. Bellissimo, PhD Thesis, *"Multiparameter Analysis of Genesis and Evolution of Secondary Electrons produced in the Low Energy Regime"*, URL:

https://www.researchgate.net/publication/332684398_Multiparameter_Analysis_of_Genesis_and_Evolution_of_Secondary_Electrons_produced_in_the_Low_Energy_regime

8:40am **2D+AS+MI+NS-TuM-3 Probing Point Defects, Folds and Interfaces in 2D Material Heterostructures using Scanning Transmission Electron Microscopy**, *Sarah Haigh,* University of Manchester, UK   **INVITED**
Scanning Transmission Electron Microscopy (STEM) is one of the few techniques able to probe the structure and chemistry of 2D materials when these are stacked to form vertical heterostructures. By combining STEM with electron energy loss spectroscopy and energy dispersive X-ray spectroscopy it is possible to characterise individual point defects,[1] to measure interlayer distances for dissimilar materials [2] and to investigate the microstructure of mechanically deformed structures at the atomic scale [3]. We have extensively employed plan view and cross sectional STEM imaging to investigate complex 2D heterostructures. For example, we have

shown that protruding defects prevent the realisation of pristine interfaces between transition metal selenides (MoSe2, WSe2, NbSe2) and boron nitride, unless exfoliation is performed in an inert environment.[2]

We have analysed microstructures produced when 2D van der Waals materials (graphite, boron nitride, MoSe2) are subjected to mechanical deformation and find that the types of defect can be predicted from just the bend angle and thickness of the materials.[3] In particular we find that above a critical thickness the materials exhibit numerous twin boundaries and for large bend angles these can contain nanoscale regions of local delamination. Such features are proposed to be important in determining how easily the material can be thinned by mechanical or liquid exfoliation.[3]

2D material heterostructures are also enabling new STEM imaging capabilities. We show they can be used as a platform to study real time reactions in liquid environments with unprecedented spatial resolution and spectroscopic capabilities [4]. We further demonstrate that graphene encapsulation allows imaging of point defect dynamics, structural degradation and mechanically induced stacking faults in 2D monochalcogenides, GaSe and InSe [1].

References

[1] D G Hopkinson et al, ACS Nano, (2019) 10.1021/acsnano.8b08253

[2] A P Rooney et al. Nano Letters, (2017) 17, 5222.

[3] A P Rooney et al. Nature Communications (2018) 9, 3597

[4] D J Kelly et al Nano Letters, (2018) 18, 2, 1168

9:20am **2D+AS+MI+NS-TuM-5 Low-Energy Electron Induced Disordering and Decomposition of Self-assembled Monolayers on Au(111)**, *Jodi Grzeskowiak* [1]*,* University at Albany - SUNY*; C Ventrice, Jr.,* SUNY Polytechnic Institute
To study the interaction of low energy electrons with thin organic films, measurements have been performed on electron induced disordering and decomposition of 1-decanethiol molecules grown via vapor phase deposition on Au(111). Surface analysis techniques were used to characterize the monolayers before and after electron exposure. LEED was used to determine the structure of the SAM and the rate of disordering and decomposition. It was observed that the diffraction pattern of the lying down phase of the SAM, held near 100 K, almost completely disappears within about three minutes of exposure. However, when the temperature of the irradiated sample was raised to 300 K and then cooled back down to around 100 K, most of the intensity of the diffraction pattern returns, indicating that electron exposure is primarily inducing disorder. TPD was used to evaluate the thermal stability of the SAMs and the resulting desorption products after electron exposure. For the standing up phase SAM, two desorption features for the hydrocarbon fragments of the SAM are observed, one around 130 °C and a second near 220 °C. For the lying down phase, only the higher temperature desorption feature is observed, which indicates that the SAM is converting from the standing up phase to the lying down phase during the heating process. For both phases, desorption peaks for S and H_2S at around 250 °C were observed, suggesting that there is a high probability for the alkane chain of the decanethiol molecule to detach from the sulfur head group. After electron exposure of the standing up phase, a large reduction in the intensity of the two desorption peaks for the masses monitored for the hydrocarbon fragments was observed. However, the intensities of the peaks associated with S and H_2S were similar to those for the samples that were not irradiated with electrons. For the lying down phase, the intensities and positions of all of the desorption peaks were similar to the unexposed SAMs, which indicates that the cross-section for electron beam damage for the lying down phase is much lower than that for the standing up phase. Ex-situ XPS was used to monitor the decomposition of the SAMs. After irradiation with 80 eV electrons, an uptake of oxygen was observed in the XPS measurements for both samples. This oxygen uptake gives evidence that oxygen in the air is reacting with carbon and sulfur atoms whose bonds were broken during electron exposure.

9:40am **2D+AS+MI+NS-TuM-6 Continuous Silicene, Silicene Ribbons and Surface Reconstructions on h-MoSi₂**, *Anna Costine, C Volders,* University of Virginia*; M Fu,* Oak Ridge National Laboratory*; P Reinke,* University of Virginia

Silicene has emerged as a 2D material of interest because of its spin -orbit coupling, tunable electronic structure, and Dirac type behavior. Synthesis of silicene with preserved Dirac-type electronic structure has proven

---

[1] **ASSD Student Award Finalist**

challenging, but is critical to realizing theoretically predicted quantum states and devices. To date, Ag(111) remains the most popular substrate for silicene synthesis, but is discussed controversially due to its similarity with surface alloys. Silicene has also been synthesized on other substrates including Ir, IrSi₃, and ZrB₂. Silicene synthesis on a semiconducting substrate with a low buckling conformation to conserve the Dirac-type behavior would be ideal. The synthesis of silicene on new substrates that allow for direct device integration is an important next step.

We developed an alternate approach to silicene synthesis that allows for silicene synthesis on semiconducting silicides. The (0001) surface of h-MoSi2 has hexagonal symmetry and a lattice constant close to that of silicene. Our recent measurements support the assumption that silicene is electronically decoupled from the substrate. The h-MoSi2 crystallites, which are terminated by the (0001) plane are grown by depositing Mo onto a Si (001) or Si(111) surface. Upon annealing to ~800℃, the Si atoms decouple from the underlying surface and form a weakly buckled silicene layer with the √3 x√3 surface as seen by STM.

Our recent work expands this study and uses STM/S at 77 K to achieve a comprehensive description of silicene-on-silicide. The amount of Mo deposited (0.3 nm - 18 nm) and annealing temperature (700- 1000℃) were varied. All surface structures discussed here are on h-MoSi2 crystallites in the (0001) plane,. Three distinct surface structures coexist - silicene ribbons , a 4x4 reconstruction, and a complex reconstruction which is very sensitive to variations in the bias voltage. The electronic structure of silicene-ribbons shows a V-shaped density of states close to EF, indicative of Dirac-like behavior, while the other reconstructions are semiconducting. The surface and electronic structures observed on h-MoSi₂ crystallites as a function of the synthesis conditions will be discussed. The preference for silicene-ribbons in the low T STM/STS measurements is currently attributed to a faster post-deposition cooling rate, but the exact mechanism is still open to debate. We will present a detailed discussion of the electronic structure of silicene and silicene ribbons, and suggest mechanisms for the transition from the (0001) surface to silicene. Our goal is to develop synthesis approaches suitable for device integration of both silicene conformations.

11:00am **2D+AS+MI+NS-TuM-10 Epitaxial Growth and Characterization of Single-Orientation Single-Layer Transition Metal Dichalcogenides on Au(111)***, L Bignardi,* University of Trieste, Italy*; **Daniel Lizzit***, Elettra - Sincrotrone Trieste, Trieste, Italy*; *B Harsh, E Travaglia,* Department of Physics, University of Trieste, Italy*; *C Sanders,* iNANO, Aarhus University, Denmark, UK*; *M Dendzik,* Aarhus University, Denmark, Germany*; *P Lacovig,* Elettra-Sincrotrone Trieste, Italy*; *M Michiardi,* iNANO, Aarhus University, Denmark, Canada*; *M Bianchi,* Aarhus University, Denmark*; *R Larciprete,* CNR-Institute for Complex Systems, Roma, Italy*; *J Flege, J Falta,* University of Bremen, Germany*; *P Das,* Abdus Salam International Centre for Theoretical Physics, Trieste, Italy*; *J Fujii, I Vobornik,* IOM-CNR, Laboratorio TASC, Trieste, Italy*; *M Ewert, L Buß,* University of Bremen, Germany*; *A Baraldi,* University of Trieste, Italy*; *P Hofmann,* Aarhus University, Denmark*; *S Lizzit,* Elettra - Sincrotrone Trieste, Trieste, Italy*

It has been widely demonstrated that Transition Metal Dichalcogenides (TMDs), and in particular MoS₂ and WS₂ could be good candidates for future electronic devices because of their intrinsic electronic properties and their potential for ultimate device scaling. In the single layer (SL) form, the inversion symmetry breaking and the strong spin-orbit coupling of the heavy transition metals (Mo or W) open new possibilities for data storage and computing thanks to the spin and valley degrees of freedom. However, in order to investigate the fundamental physics behind these materials and to produce high quality electronic devices, SL TMDs with enough large area and high quality are demanded. In particular, single domain oriented layers, that are SLs without mirror domains, allow to strongly suppress defects due to the absence of grain boundaries which are known to degrade the overall performances.

We here present a successful synthesis method based on physical vapor deposition that consists in dosing W or Mo in H₂S atmosphere onto Au(111), and provide an in-depth characterization of the synthesized SL TMDs through different surface science techniques. Synchrotron radiation based photoelectron spectroscopy in the fast modality (fast-XPS) was used to carefully tune the growth parameters whereas high resolution (HR-XPS) was used for the characterization. In particular fast-XPS allowed to optimize the growth parameters which turned out to be different for MoS₂ [1] with respect to WS₂[2]. Then, photoelectron diffraction (XPD) was employed to find the structural parameters of the SLs and to unambiguously determine their single orientation character and the relative alignment with respect to the underlying substrate. Scanning Tunneling Microscopy (STM), Low Energy Electron Diffraction (LEED) and

Microscopy (LEEM) added further insight into the lateral extension of the SLs and the structural order at the atomic level.

[1] H. Bana, E. Travaglia, L. Bignardi, P. Lacovig, C. E. Sanders, M. Dendzik, M. Michiardi, M. Bianchi, D. Lizzit, F. Presel, D. D. Angelis, N. Apostol, P. K. Das, J. Fujii, I. Vobornik, R. Larciprete, A. Baraldi, P. Hofmann and S. Lizzit, 2D Materials, 2018, 5, 035012.

[2] L. Bignardi, D. Lizzit, H. Bana, E. Travaglia, P. Lacovig, C. E. Sanders, M. Dendzik, M. Michiardi, M. Bianchi, M. Ewert, L. Buss, J. Falta, J. I. Flege, A. Baraldi, R. Larciprete, P. Hofmann, and S. Lizzit, Physical Review Materials 3, 014003 (2019).

11:20am **2D+AS+MI+NS-TuM-11 Surface Reactivity of MoS₂ by ambient pressure X-ray Photoelectron Spectroscopy***, Rafik Addou, D Dardzinsky, G Herman,* Oregon State University*

Molybdenum disulfide (MoS₂) has potential applications as a low-cost catalyst for the hydrogen evolution reaction (HER). Defect sites in MoS₂ have been demonstrated to have high catalytic activities, where edge sites and sulfur vacancies are the major active sites for HER. Intentionally inducing defects offers a simple way to enhance the reactivity of MoS₂ and other 2D materials. In this study, we have characterized the surface reactivity and the catalytic activities of bulk MoS₂ samples using ambient pressure X-ray photoelectron spectroscopy (APXPS). The pristine surface was exposed to 1 mbar of H₂O vapor for temperatures ranging from 300 to 573 K. APXPS Mo 3d, S 2p, and O 1s core levels do not show any significant changes under these reaction conditions due to the inert nature of the MoS₂ surface. To activate the MoS₂ basal plane to improve surface reactivity, we have formed well-controlled densities of defects using Ar⁺ sputtering. The defective surfaces were exposed to 1 mbar of H₂O vapor for temperatures ranging from 300 to 600 K. Changes in the APXPS Mo 3d, S 2p, and O 1s core levels indicate that the surface is much more reactive to H₂O, with the formation of Mo-O bonds. These results are consistent with the reduction in the H₂O gas phase which was measured by operando mass spectrometry. We have found that the reactivity strongly depends on the temperature and the size and density of defects. Following this first report of APXPS on MoS₂ acquired at more realistic pressure, we will also report the HER activity and X-ray absorption spectroscopy (XAS) on the pristine surface and compare it with defective surfaces. Our findings demonstrate that the reactivity and the catalytic activity of MoS₂ are significantly improved through the formation of defects.

11:40am **2D+AS+MI+NS-TuM-12 Surface Characterization of 2D Materials and their 3D Analogues using XPS***, Jonathan Counsell, S Coultas, C Blomfield, N Gerrard,* Kratos Analytical Limited, UK*; *C Moffitt,* Kratos Analytical Limited*; *A Roberts,* Kratos Analytical Limited, UK*

Since the synthesis of Graphene in 2004 there has been significant interest in novel 2D materials. Indeed this area has produced an abundance of high impact publications and so far >$10bn has been committed globally to both fundamental research and commercialisation. This interest has been due to the unique properties exhibited such as mechanical strength and charge/heat transfer. The potential commercial possibilities are diverse with applications as varied as heat management and dissipation to increasing computer processing power. To fully understand the nature and potential of these materials a comprehensive surface characterisation is necessary.

Herein we illustrate how by applying conventional surface analysis techniques with novel methodologies it is possible to create a more complete picture of the chemical and physical nature of deposited 2D materials. Both organic and inorganic 2D materials will be explored to demonstrate the methods and capabilities. Dichalcogenide materials (sulphides and selenides) containing different metal centres were analysed with XPS, and angular resolved methods, to calculate layer thicknesses, stoichiometry and chemical states. The lateral distribution of CVD ultra-thin films was studied using both macro and micro area XPS imaging modes to distinguish uniformity and evenness. The application of UPS will explore the bonding structure, sensitivity of the materials and as a potential tool for identifying damage/defects in the surface lattice. The merits and pitfalls of ion etching will be discussed and a complete method and protocol will be proposed for limiting spectral artefacts and therefore misleading results. The effects of deposition and analysis on the 2D materials' structure and composition will be highlighted as will the characterisation of unwanted reduction/oxidation, contamination and structural defects. Utilising the complete surface analysis tool box allows the analyst to gain further insight and to fully understand the complex nature of these novel materials.

12:00pm 2D+AS+MI+NS-TuM-13 Characterization of Catalytic Active Sites on the Surface of MoS2 2-D Materials, *Miguel Jose Yacaman,* University of Texas at San Antonio*; T Zepeda, S Fuentes Moyado,* CNyN UNAM Ensenada, Mexico

Materials such as the MoS2 have been used in catalysis at industrial level for many decades mostly on the hydrodesulfurization of naftas.

However more stringent regulations about the sulfur amount in diesel has printed the need to improve the catalysts .In order to achieve that it is important to understand the nature of the active sites and ways to improve the activity.In this presentation we discuss the use of in-situ techniques to study the surfaces of MoS2 materials made of few layers and discuss the role of the sites on the crystal edges.We also demonstrate that during the reaction the MoS2 material becomes crumpled and changes from semiconductor to metallic.

2D Materials
Room A226 - Session 2D+EM+MI+MN+NS+QS-TuM

Novel Quantum Phenomena

Moderator: Arend van der Zande, University of Illinois at Urbana Champaign

8:00am 2D+EM+MI+MN+NS+QS-TuM-1 Charge Density-Wave States in Single-Layer Transition-Metal Dichalcogenides, *Phil King,* University of St Andrews, UK   **INVITED**

Control over materials thickness down to the single-atom scale has emerged as a powerful tuning parameter for manipulating not only the single-particle band structures of solids, but increasingly also their interacting electronic states and phases. A particularly attractive materials system in which to explore this is the transition-metal dichalcogenides, both because of their naturally-layered van der Waals structures as well as the wide variety of materials properties which they are known to host. Yet, how their interacting electronic states and phases evolve when thinned to the single-layer limit remains a key open question in many such systems. Here, we use angle-resolved photoemission to investigate the electronic structure and charge density wave (CDW) phases of monolayer $TiSe_2$, $TiTe_2$, and VSe_2. Three-dimensionality is a core feature of the electronic structure of all of these parent compounds, but we show how their CDW phases not only persist, but are strengthened, in the monolayer limit. In $TiSe_2$, we observe an orbital-selective CDW, necessarily without a k_z-selectivity in band hybridisation that is of key importance for the bulk instability,[1] while $TiTe_2$ is driven into a charge-ordered phase in the monolayer which is not stable in the bulk at all. In VSe_2, we show how the monolayer hosts a much stronger-coupling CDW instability than the bulk, which in turn drives a metal-insulator transition, removing a competing instability to ferromagnetism.[2] Together, these studies point to the delicate balance that can be realized between competing interacting states and phases in monolayer transition-metal dichalcogenides.

This work was performed in close collaboration with M.D. Watson, A. Rajan, J. Feng, D. Biswas, and colleagues from the Universities of St Andrews, Oxford, Keil, Diamond, Elettra, and SOLEIL.

[1]Watson *et al.*, Phys. Rev. Lett. 122 (2019) 076404.

[2]Feng *et al.,* Nano Lett. 18 (2018) 4493.

8:40am 2D+EM+MI+MN+NS+QS-TuM-3 Sublattice Symmetry Breaking and Kondo-effect Enhancement in Strained Graphene, *D Zhai,* Ohio University*; K Ingersent,* University of Florida*; S Ulloa,* *Nancy Sandler,* Ohio University

Kondo physics in doped monolayer graphene is predicted to exhibit unusual features due to the linear vanishing of the pristine material's density of states at the Dirac point. Despite several attempts, conclusive experimental observation of the phenomenon remains elusive. One likely obstacle to identification is a very small Kondo temperature scale TK in situations where the chemical potential lies near the Dirac point. We propose tailored mechanical deformations of monolayer graphene as a means of revealing unique fingerprints of the Kondo effect. Inhomogeneous strains are known to produce specific alternating changes in the local density of states (LDOS) away from the Dirac point that signal sublattice symmetry-breaking effects. Small LDOS changes can be amplified in an exponential increase or decrease of TK for magnetic impurities attached at different locations. We illustrate this behavior in two deformation geometries: a circular "bubble" and a long fold, both described by Gaussian displacement profiles. We calculate the LDOS

changes for modest strains and analyze the relevant Anderson impurity model describing a magnetic atom adsorbed in either a "top-site" or a "hollow-site" configuration. Numerical renormalization-group solutions of the impurity model suggest that higher expected TK values, combined with distinctive spatial patterns under variation of the point of graphene attachment, make the top-site configuration the more promising for experimental observation of signatures of the Kondo effect. The strong strain sensitivity of TK may lift top-site Kondo physics into the range experimentally accessible using local probes such as scanning tunneling microscopy.

9:00am 2D+EM+MI+MN+NS+QS-TuM-4 Indirect Transition and Opposite Circular Polarization of Interlayer Exciton in a MoSe2 WSe2 van der Waals Heterostructure, *Hsun-Jen Chuang,* A Hanbicki, M Rosenberger, C Hellberg, S Sivaram, K McCreary, I Mazin, B Jonker,* U.S. Naval Research Laboratory

An emerging class of heterostructures involves monolayer semiconductors such as many of the transition metal dichalcogenides (TMDs) which can be combined to form van der Waals heterostructures (vdWHs). One unique new optical property of heterostructure is an interlayer exciton (ILE), a spatially indirect, electron-hole pair with the electron in one TMD layer and the hole in the other. Here, we fabricated MoSe2/WSe2 hetero-bilayer encapsulated in h-BN with the alignment angle close to 60 degree between MoSe2 and WSe2. Followed by the state-of-the-art preparation techniques (Nano-squeegee) to ensure the optimal contact between the TMDs. The Strong ILE emission is observed with the emission energy around 1.35 eV at room temperature and resolve this emission into two distinct peaks (ILE1 and ILE2) separated by 24 meV at zero field at 5 K. Furthermore, we demonstrate that the two emission peaks have *opposite*circular polarizations with up to +20% for the ILE1 and -40% for ILE2 when excited by circularly polarized light. A*b initio* calculations provide an explanation of this unique and potentially useful property and indicate that it is a result of the indirect character of *both* electronictransitions. These peaks are *double*indirect excitons. *i.e.*indirect in both real and reciprocal space, split by relativistic effects.

This research was performed while H.-J.C. held an American Society for Engineering Education fellowship and M.R.R and S.V.S held a National Research Council fellowship at NRL. This work was supported by core programs at NRL and the NRL Nanoscience Institute. This work was also supported in part by a grant of computer time from the DoD High Performance Computing Modernization Program at the U.S. Army Research Laboratory Supercomputing Resource Center.

9:20am 2D+EM+MI+MN+NS+QS-TuM-5 Integrating 2D Magnet 1T-MnSe₂ with Topological Insulator Bi₂Se₃, *Tiancong Zhu,* The Ohio State University*; D O'Hara,* University of California, Riverside*; J Repicky, S Yu, M Zhu, B Noesges, T Liu, M Brenner, L Brillson, J Hwang, F Yang, J Gupta, R Kawakami,* The Ohio State University

Integrating two-dimensional(2D) magnet with topological insulator is an exciting topic. Other than the possible proximity induced magnetic ordering inside topological insulator, the 2D magnet/ topological insulator heterostructure can also lead to more efficient spin orbit torque switching, or the formation of magnetic skyrmions. The recent discovery of room temperature ferromagnetic ordering in 2D material MnSe and VSe further brings more potential in such heterostructure systems. In this talk, we report the synthesis and characterization of 2D magnet 1T-MnSe on topological insulator Bi Se . Monolayer of MnSe is grown on Bi Se with molecular beam epitaxy, and subsequently characterized with various techniques, including X-ray diffractometry (XRD), X-ray photoemission spectroscopy (XPS) and scanning tunneling microscopy (STM). STM measurement reveals the co-existence of monolayer a-MnSe(111) and 1T-MnSe₂ on Bi₂Se₃ surface. By performing spin-polarized STM measurement with Cr tip, we observed directly the magnetic signal from 1T-MnSe₂ on Bi₂Se₃. The growth of 1T-MnSe₂ on Bi₂Se₃ further leads to the MBE synthesis of magnetic topological insulator Bi₂MnSe₄, which also shows ferromagnetism down to the monolayer limit. The structural and magnetic characterization of the material will also be discussed in this talk.

9:40am 2D+EM+MI+MN+NS+QS-TuM-6 Effect of Exchange-correlation Functional and Structural Constraints on the Transition Temperature of Two- Dimensional Ferroelectrics, *Shiva P. Poudel*, J Villanova, B Miller, A Pandit, S Barraza-Lopez, University of Arkansas, Fayetteville

In this presentation, I will discuss two inconsistent models for obtaining the transition temperature (T_c) of two-dimensional (2D) ferroelectrics. It will be shown that the inconsistency arises from the choice of exchange-correlation functional and structural constraints [1-4] by obtaining T_c for a SnSe monolayer with PBE and vdW exchange-correlation functional, and with increased constraints. It has been found that vdW functional gives a larger T_c in comparison with PBE functional. Also, the increasing constraint raises T_c as well. Afterward, a complete analysis of the converged unit cell with seven different exchange-correlation functional will be provided. These results represent the most comprehensive theoretical benchmarks for these intriguing 2D ferroelectric materials.

References:

1. M. Mehboudi et al., Nano Lett. **16**, 1704 (2016).

2. M. Mehboudi, et al., Phys. Rev. Lett. **117**, 246802 (2016).

3. S. Barraza-Lopez, et al., PRB **97**, 024110 (2018).

4. R. Fei, et al., Phys. Rev. Lett. **117**, 097601 (2016).

11:00am 2D+EM+MI+MN+NS+QS-TuM-10 Sign-change Pairing Symmetry in Single Layer FeSe/SrTiO$_3$ Film, *Huimin Zhang*, West Virginia University; Z Ge, M Weinert, University of Wisconsin; L Li, West Virginia University

Single layer FeSe film epitaxially grown on SrTiO$_3$(001) substrate has drawn much interest for its novel interfacial effects, which have led to the highest superconducting temperature (T_c) to date amongst all Fe-based superconductors. While several paring states, such as sign-persevering s_{++}-wave, sign-changing nodeless d-wave and $s_\pm$-wave have been suggested, the pairing symmetry remains to be experimentally validated. Here we investigate the intrinsic impurity-induced in-gap bound states and quasiparticle interference (QPI) patterns in single layer FeSe/SrTiO$_3$ by scanning tunneling microscopy/spectroscopy. We observed bound states induced by nonmagnetic impurities, which strongly suggests a sign-changing order parameter. Through detailed analysis of the phase-sensitive QPI patterns, we further confirm that the order parameter indeed changes sign within the electron pockets. This identification of a sign change pairing symmetry in single layer FeSe/SrTiO$_3$ presents a critical step towards the understanding of its high T_c superconductivity.

11:20am 2D+EM+MI+MN+NS+QS-TuM-11 High Temperature Superconductivity in Epitaxial Single Layer FeTe$_{1-x}$Se$_x$/STO(001), *Qiang Zou*, Z Ge, C Yan, H Zhang, L Li, West Virginia University

Single crystal FeTe exhibits a distinct long-range bicollinear antiferromagnetic order that can be suppressed by alloying with Se, where superconductivity emerges at a critical Se concentration of 0.3 with a T_c of 10 K. In this work, we show that this phase transition can be further modulated by reducing the thickness of FeTe$_{1-x}$Se$_x$, downto the single atomic layer limit. High quality single layer FeTe$_{1-x}$Se$_x$ films are grown on SrTiO$_3$(001) substrate by molecular beam epitaxy and characterized by scanning tunneling microscopy/spectroscopy and angle-resolved photoemission spectroscopy. We find the electronic properties are strongly dependent on the Se content. For x < 0.1, hole-like bands cross the Fermi level and form a hole-pocket at the Γ point with no states observed around the M point, indicating no superconductivity. With increasing Se content, the top of the valence bands moves away from the Fermi level, accompanied by a decrease in effective mass at the Γ point. For x > 0.1, the hole pocket at Γ point moves below the Fermi level, and an electron-pocket emerges at M point where a superconducting gap opens with a T_c of ~50 K. These findings and their implications for the emergence and stabilization of superconductivity in Fe-based superconductors at reduced dimensions will be presented at the meeting.

11:40am 2D+EM+MI+MN+NS+QS-TuM-12 The Observation of Majorana Zero Mode and Conductance Plateau in an Iron-based Superconductor, *Hong-Jun Gao*, Institute of Physics, Chinese Academy of Sciences, China **INVITED**

Majorana zero-modes (MZMs) are spatially-localized zero-energy fractional quasiparticles with non-Abelian braiding statistics that hold great promise for topological quantum computing. Recently, by using scanning tunneling microscopy/spectroscopy (STM/STS), a new breakthrough of Majorana zero mode (MZM) was achieved in a single material platform of high-T_c iron-based superconductors, FeTe$_{0.55}$Se$_{0.45}$, which combined advantages of simple material, high-T_c, and large ratio of Δ/E_F [1]. A detail STM/STS study of a FeTe$_{0.55}$Se$_{0.45}$ single crystal, also revealed the mechanism of two distinct classes of vortices present in this system, which directly tied with the presence or absence of zero-bias peak [2]. To further investigated the MZM, it is still needed to find a "smoking-gun" type of evidence for the existence of MZM, and a quantized conductance plateau is widely believed to be one of them. Here we report an observation of the Majorana conductance plateau in vortices on the iron superconductor FeTe$_{0.55}$Se$_{0.45}$ surface by using STM/STS [3]. We found that both extrinsic instrumental convoluted broadening and intrinsic quasiparticle poisoning can reduce the conductance plateau value. When extrinsic instrumental broadening is removed by deconvolution, the plateau is found to nearly reach a $2e^2/h$ quantized value. The direct observation of a conductance plateau on a single zero-mode in a vortex strongly supports the existence and protection of MZMs in this iron-based superconductor, which can serve as a single-material platform for Majorana braiding at relatively high temperature.

* In collaboration with, D.F. Wang[1,2], L.Y. Kong[1,2], P. Fan[1,2], H. Chen[1], S.Y. Zhu[1,2], W.Y. Liu[1,2], L. Cao[1,2], Y.J. Sun[1,2], S.X. Du[1,2,3], J. Schneeloch[4], R.D. Zhong[4], G.D. Gu[4], Liang Fu[5], Hong Ding[1,2,3].

[1] Institute of Physics & University of Chinese Academy of Sciences, CAS, Beijing 100190

[2] CAS Center for Excellence in Topological Quantum Computation, UCAS, Beijing 100190

[3] Collaborative Innovation Center of Quantum Matter, Beijing 100190

[4] Brookhaven National Laboratory, Upton, New York 11973, USA

[5] Dept. of Physics, Massachusetts Institute of Technology, Cambridge, Massachusetts 02139, USA

References:

[1] D. F. Wang et al, *Science.***362**, 333 (2008).

[2] L. Y. Kong et al, arXiv:1901.02293 (submitted to *Nature Physics* on November 19, 2018)

[2] S. Y. Zhu et al, arXiv: 1904.06124 (submitted to *Science* on February 15, 2019)

Actinides and Rare Earths Focus Topic
Room A215 - Session AC+AS+LS-TuM

Chemistry and Physics of the Actinides and Rare Earths

Moderators: Melissa Denecke, University of Manchester, UK, James G. Tobin, University of Wisconsin-Oshkosh

8:00am AC+AS+LS-TuM-1 Study of the Early Actinide Oxides and Fluorides – Systematics of the Electronic Structure, *Thomas Gouder*, R Eloirdi, R Caciuffo, European Commission - Joint Research Centre, Germany **INVITED**
Oxidation properties of uranium have a great influence on the stability of nuclear waste. U^{VI} has

a 1000 times higher solubility in water than U^{IV}, and so the dissolution of UO$_2$ based spent fuel nuclear waste strongly depends on the oxidation state of the surface. Oxygen incorporation into the surface of UO$_2$ first results in the formation of U(V), found in UO$_{2+x}$ and mixed valent oxides, and then formation of U^{VI}. But despite early reports on the existence of a pure U(V) phase (U$_2$O$_5$) there are no spectroscopic data on pure U(V). This may be due to its position between the highly stable UO$_2$ and UO$_3$. Also, apparent mixed surface phases containing U^{IV}, U^V and U^{VI} may result from the strong redox gradient between the oxidizing environment and the reduced bulk, present in most corrosion experiments. Replacing bulk samples by thin films allows avoiding this problem, by confining the reaction to a thin region where final conditions are reached everywhere simultaneously, keeping the system homogeneous. This opened the path for a systematic study of the evolution of the electronic structure of

uranium upon oxidation and follow the outer shell configuration from $5f^2$ (U^{IV}), to $5f^1$ (U^V) to $5f^0$ (U^{VI}).

We will present electron spectroscopy (XPS, UPS and BIS) and Electron Energy Loss (ELS) study of U_2O_5 compare results to the neighbouring oxides (UO_2 and UO_3). U_2O_5 has been produced by exposing UO_2 successively to atomic oxygen, leading to UO_3, and to atomic hydrogen. Films have been deposited on polycrystalline gold foils (inert substrate). During gas exposure the samples were heated to 400°C to ensure fast diffusion and equilibrium conditions.

Determination of the U oxidation states was based on the characteristic U-4f core level satellites, separated from the main lines by 6, 8 and 10 eV for U^{IV}, U^V and U^{VI}, respectively. We managed producing films which showed exclusively a single 8 eV satellite, indicating the presence of pure U^V. The formation of U^V was confirmed by the intensity evolution of the $U5f$ valence emissions. Also the linewidth of the XPS $5f$ line decreases from UO_2, with the $5f^1$ final state multiplet, to U_2O_5, with a $5f^0$ final state singlet. The U-5d line also displays a multiplet structure due to interaction with the open 5f shell (U^{IV} and U^V). Evolution of the O2p/O1s intensity ratio indicates increasing covalence of the U-O bond in higher oxides.

U oxide spectra will be compared to spectra of ThO_2. Multiplet splitting and its dependence on the open shell was followed by comparing $5f^2$ (UO_2) and $5f^0$ (ThO_2) systems. Finally XPS/BIS of the valence region will be presented for various oxides (UO_2, U_2O_5, UO_3 and ThO_2) and fluorides (UF_4 and ThF_4).

8:40am AC+AS+LS-TuM-3 Broadening of the XPS Spectra of U Oxides, *Paul S. Bagus*, University of North Texas; *C Nelin*, Consultant **INVITED**

It is common to attempt to improve the energy resolution of XPS in order to obtain more information about the electronic structure. However, it may not be possible to improve the resolution because unresolved final states are present. When the energy separations of these states are less than or comparable to the lifetime of the core-hole, it will not be possible to resolve the states and there will only be a broadening, often quite significant, for the observed peak. The unresolved features may arise from closely spaced multiplets for the angular momentum coupling of the open shell electrons and from excitations to higher lying vibrational levels for the final ionic states; the later is especially important when bond distances for the core-ionized states are very different from those for the initial state; see, for example, Ref. [1] . Thus, for example, the $U(5f_{7/2})$ peak of UO_2 has a FWHM of 1.4 eV although the instrumental resolution was 0.3 eV. [2] Similar large FWHM have been observed for U in different oxidation states. [3-4] In order to be able to relate the widths of these broadened features to the chemical and physical interactions in the system, it is necessary to understand the separate contributions of the multiplet splittings and the vibrational excitations. It has been shown that, for U(IV) 4f XPS in UO_2, the contributions of the multiplet splitting and the vibrational excitations are comparable, each contributing ~0.5 eV to the FWHM. [2] In the present work, the contributions of these mechanisms are examined for U(IV), U(V), and U(VI) oxidation states. In addition, the broadening is examined for the XPS of different core levels where the relative importance of multiplet and vibrational broadening is different from that for the U(4f) XPS. Furthermore, the importance of temperature for the vibrational broadening is also examined. The theoretical predictions for these different parameters can be validated [4] paving the way to extract chemical information from the measured FWHM. [5] The theoretical framework for these predictions is based on wavefunctions for embedded cluster models of the oxides which allows for a balanced treatment of spin-orbit, angular momentum coupling, and covalent bonding.

1. C. J. Nelin et al. Angew. Chem. Int. Ed. 50, 10174 (2011).

2. P. S. Bagus, C. J. Nelin, S. Rennie, G. H. Lander, and R. Springel, (In preparation).

3. T. Gouder, R. Eloirdi, and R. Caciuffo, Scientific Reports 8, 8306 (2018).

4. T. Gouder, R. Eloirdi, R. Caciuffo, and P. S. Bagus, "XPS Broadening in U Oxides", (In preparation).

5. P. S. Bagus, E. S. Ilton, and C. J. Nelin, Catal. Lett. 148, 1785 (2018).

9:20am AC+AS+LS-TuM-5 Multiscale Characterization of Lanthanide and Actinide Nanoparticles Embedded in Porous Materials, *Stefan Minasian, S Alayoglu, S Aloni,* Lawrence Berkeley National Laboratory; *J Arnold,* University of California at Berkeley; *E Batista,* Los Alamos National Laboratory; *A Braun, C Booth, A Herve,* Lawrence Berkeley National Laboratory; *Y Liu,* University of California at Berkeley; *L Moreau,* Lawrence Berkeley National Laboratory; *T Lohrey, J Long, M Straub, S Robin, D Russo,* University of California at Berkeley; *D Shuh,* Lawrence Berkeley National Laboratory; *J Su, P Yang, X Zhang,* Los Alamos National Laboratory **INVITED**

Decades of synthetic work has shown that desirable physical properties can be obtained by tailoring the size and composition of main-group and transition metal nanoparticles. The origin of these phenomena can be traced to a variety of factors that are intrinsic to nanoparticles, including but not limited to (1) quantization of the electronic states and (2) increasing contributions from nanoparticle surfaces. Despite this progress, very few methods provide the level of synthetic control needed to prepare lanthanide and actinide nanoparticles with well-defined sizes and compositions. Furthermore, many conventional methods of characterization are unable to determine the relative roles of volume and surface chemistry on physical behavior involving the 4f- and 5f-electrons.

We established syntheses for lanthanide and actinide nanoparticles by adapting a conceptual approach employed previously by Fischer and Suh to form d-block transition metal and main-group element nanoparticles in metal organic frameworks (MOFs). Implantation of lanthanide and actinide precursor molecules in covalent organic frameworks (COFs) was achieved by sublimation, followed by decomposition to form nanoparticles via exposure to reactive gases and/or elevated temperatures. A multi-pronged imaging and spectroscopic strategy was developed to fully characterize the complex multi-component materials. The characterization techniques are complementary in that they provide atomic to micron-scale probes, element and bulk-level selectivity, and measurements that are individual and statistically significant (Figure 1). Transmission electron microscopy (TEM) showed that the COF-5 templates limited UO_2 nanoparticle growth to between 1-3 nm, which is similar to the COF-5 pore size (2.7 nm). In addition, small-angle X-ray scattering (SAXS) was used to determine the nanoparticle form factor (for size and polydispersity) in a globally-averaged manner. Scanning transmission X-ray microscopy (STXM) was used to probe micron-scale morphology and to evaluate composition with X-ray absorption spectroscopy at the B, C, and O K-edges. Finally, X-ray absorption fine structure (XAFS) spectroscopy was used to determine composition and structure because it does not require long-range crystallographic order, and because it is capable of probing the nanoparticles selectively despite the substantial background from the organic host. This presentation will also discuss our efforts to show how 4f and 5f-electron behavior changes with variations in size and composition at the nanometer level.

11:00am AC+AS+LS-TuM-10 Multiple Forms of Uranium Hydrides and their Electronic Properties, *Ladislav Havela, V Buturlim, E Chitrova, O Koloskova, P Minarik, M Cieslar, M Dopita, L Horak, M Divis, I Turek,* Charles University, Prague, Czech Republic; *D Legut,* VSB-Technical University of Ostrava, Czech Republic; *T Gouder,* European Commission - Joint Research Centre, Germany

Although the published U-H binary phase diagram contains only the UH_3 phase, a recent progress in sputter deposition synthesis led to the discovery of UH_2, which is with its CaF_2 structure type analogous to e.g. PuH_2 or YH_2 [1]. In addition, a high pressure synthesis yielded several U hyper-hydrides (as UH_8), which are predicted to be a high-temperature superconductors [2]. As both UH_3 (appearing in two structure modifications, α- and β-UH_3) and UH_2 allow alloying with selected transition metals, we have a whole spectrum of U-H hydrides and certain general features can be deduced, which have a serious implications for our understanding of actinides in general.

The striking fact that both UH_3 phases have, despite very different crystal structure, practically identical size of U moments and magnetic ordering temperature $T_C \approx 165$ K, which do not change even in the nanostructured state (grain size several nm) is underlined by the fact that both parameters only weakly depend on substantial alloying with Mo and other d-metals. UH_2 with substantially larger U-U spacing is a ferromagnet, as well, its $T_C \approx 125$ K. Structure of all those forms contains identical building blocks, H atoms inside U tetrahedra of invariable size, which are only set up into different patterns. The U-H bonding seems to be therefore an ingredient, which is more important than the conventional U-U spacing. The nature of the bonds is revealed by ab-initio calculations. One general feature is the U-$6d$ hybridization with the H-$1s$ states, which leads to an electron transfer

towards H. However, unlike rare-earth trihydrides, UH_3 remains metallic, UH_2 naturally, too. The $5f$ states largely released from the $5f$-$6d$ hybridization can therefore develop a strong ferromagnetism despite low U-U spacings. The transfer could be traced even in the real space using the Bader analysis.

The ab-initio techniques, which are successful in capturing the equilibrium volumes and U magnetic moments, are so far less successful in description of photoelectron spectra close to the Fermi level, which indicates importance of electron-electron correlations.

This work was supported by the Czech Science Foundation under the grant No. 18-02344S.

[1] L. Havela et al., Inorg. Chem. 57 (2018) 14727.

[2] I.A. Kruglov et al., Sci. Adv. 4 (2018) eaat9776.

11:20am AC+AS+LS-TuM-11 Hafnium L-Edge X-ray Absorption Near Edge Structure Spectra Reveals Crystal Field Splitting, *David Shuh*, *D Caulder*, Lawrence Berkeley National Laboratory; *L Davis*, Pacific Northwest National Laboratory; *M Mara*, University of California at Berkeley; *C Booth*, Lawrence Berkeley National Laboratory; *J Darab*, *J Icenhower*, *D Strachan*, Pacific Northwest National Laboratory

One method for the safe disposal of actinides currently under consideration by the U.S. Department of Energy is immobilization of radionuclides in a glass or ceramic wasteform that will subsequently be stored in a geological repository. To develop successful, stable wasteforms, it is necessary to acquire an understanding of the fundamental chemistry of the actinides (U, Pu, etc.) and neutron absorbers (B, Gd, Hf) that will be incorporated into the glass or ceramic matrix. The X-ray absorption near edge structure (XANES) at the hafnium L_3 and L_1 absorption edges has been investigated to elucidate the local structure of Hf in wasteform glasses that are currently being considered as candidates for the immobilization of radionuclides. During our investigations of the structure of Hf, a neutron absorber and potential Pu(IV) surrogate, we noted an unusual feature at the white line maximum at the L_3 absorption edge: The examination of a variety of Hf model compounds demonstrates that the second derivative of the Hf L_3 XANES displays structure characteristic of crystal field splitting of the empty d-manifold. The peralkaline glasses studied exhibit L_3 XANES spectra typical of Hf in an octahedral crystal field. The L_1 XANES data corroborate these results, as the L_1 spectra of the glasses also resemble that of an octahedral Hf siloxane model compound, distinct from spectra of other standards measured.

11:40am AC+AS+LS-TuM-12 Electrical Resistivity in Uranium-based Thin Films, *Evgeniya Tereshina-Chitrova*, *L Havela*, *M Paukov*, *M Dopita*, *L Horak*, *M Cieslar*, Charles University, Prague, Czech Republic; *Z Soban*, Institute of Physics, Academy of Sciences of the Czech Republic, Czech Republic; *T Gouder*, *F Huber*, *A Seibert*, Joint Research Center, European Commission, Germany

Metallic $5f$ materials have a very strong coupling of magnetic moments and electrons mediating electrical conduction. It is caused by strong spin-orbit interaction together with involvement of the $5f$ states in metallic bonding. In this work we investigate the electrical resistivity $\rho(T)$ of various uranium-based thin films using the Van der Pauw method. Thin film samples of U-Mo and their hydrides were prepared by reactive sputter deposition [1]. The basic in-situ diagnostics was performed using a photoelectron spectroscopy (XPS). The films were further characterized using x-ray diffraction (XRD) methods and Transmission Electron Microscopy (TEM). The $\rho(T)$ of the films studied correspond to known bulk systems of equivalent composition but provide much more variability of concentrations and geometries.

We studied superconductivity in the U-Mo films by measuring low-temperature resistivity down to 0.4 K. The 100 nm-thick $U_{0.79}Mo_{0.21}$ film shows a transition to the superconducting state at 0.55 K. The transition is wide and extends to 0.4 K. The upper critical field for the thin U-Mo film is ~1 T, i.e. much lower that for the bulk U-Mo obtained by splat cooling [2].

The hydrides of the U-Mo films had to be prepared using a cooled substrate (≈ 177 K). The study of the $(UH_3)_{0.74}Mo_{0.26}$ of estimated thickness 210 nm showed that it is a ferromagnet with the Curie temperature of ≈165 K, i.e. equivalent to bulk UH_3, which underlines the general insensitivity of U hydrides to structure modifications. Overall temperature dependence is very weak and the absolute value of 2 mΩcm, estimated from the nominal thickness, is very high for a metallic system.

The net negative resistivity slope in the U-Mo films and hydrides can be attributed to the randomness on atomic scale, yielding very strong

scattering of electrons and weak localization. In the hydrides it is supported also by random anisotropy, randomizing local directions of U moments.

[1] Gouder, R. Eloirdi, F. Wastin, E. Colineau, J. Rebizant, D. Kolberg, F. Huber, Phys.Rev. B **70**, 235108 (2004).

[2] N.-T. H. Kim-Ngan, S. Sowa, M. Krupska, M. Paukov, I. Tkach and L Havela, Adv. Nat. Sci: Nanosci. Nanotechnol. **6**, 015007 (2015).

Applied Surface Science Division
Room A211 - Session AS+BI+RA-TuM

Quantitative Surface Analysis III/Other Surface Analysis Methods

Moderators: Karen Gaskell, University of Maryland, College Park, Alexander Shard, National Physical Laboratory

8:00am AS+BI+RA-TuM-1 Oxygen Energy Filtering and Relative Sensitivity Factor Considerations for Making U and Pu Measurements by LG-SIMS, *Todd Williamson,* Los Alamos National Laboratory **INVITED**

During nuclear facility inspections, inspectors collect materials intended to show a history of the operations that have taken place within a facility. These materials can be particles obtained using cotton swipes, solid discarded or operationally related nuclear materials, or other items contaminated with nuclear materials. Analysis of these samples is an extremely powerful tool with which to determine facility operations and history. Uranium analysis by SIMS is a mature technique used by the IAEA and its Network of Analytical Laboratories for treaty verification. The analysis of mixed uranium-plutonium particles and solids is not as mature as a capability and has been identified by the IAEA as topic for increased R&D.

This presentation will cover two technical topics related to the analysis of mixed uranium-plutonium materials, relative sensitivity factors (RSF) and energy filtering to improve hydride correction. For a material that contains both U and Pu, while both elements will be sputtered and become ionized during SIMS analysis, they will do so with different efficiencies. This ionization difference tends to be sample-type (matrix) dependent. This phenomenon is known as the relative sensitivity factor (RSF). This presentation will discuss our investigations into determining accurate RSF values for U:Pu and U:Np inter-element measurements. With accurate RSF values, which should be universal for a given sample type, the measured inter-isotope ratios can be corrected to their true values. In a mixed actinide sample, there is ^{239}Pu present which will be unresolvable from $^{238}U^1H$. This will prevent a conventional hydride correction on measurements, and there are not other clean masses in a mixed actinide sample where a hydride signal can be easily measured. Without a hydride correction the measurement of smaller concentration isotopes will have poor accuracy due to interference from large hydride interferences from major isotopes, and ^{239}Pu measurements will be highly inaccurate. The presentation will discuss our use of energy filtering mediated by an intentionally introduced partial pressure of oxygen in the sample analysis chamber, which changes ionization behavior.

8:40am AS+BI+RA-TuM-3 Utilizing Large Geometry Secondary Ion Mass Spectrometry for Age-Dating of Individual Uranium Particles, *Christopher Szakal*, *D Simons*, *J Fassett*, National Institute of Standards and Technology (NIST); *A Fahey*, Corning Inc.

Secondary ion mass spectrometry (SIMS) is routinely utilized by the International Atomic Energy Agency (IAEA) and its global partner laboratories for the isotopic analysis of individual uranium particles as part of nuclear safeguards efforts. One additional isotopic analysis that has repeatedly been requested by the IAEA involves the development of a capability to perform single particle age-dating, which would provide information about the last time that the nuclear material was purified or enriched. Previously reported efforts in multiple countries have reported the ability to use SIMS and/or large geometry (LG)-SIMS for this purpose, but with the caveat that the measurement can only be viable if the particles are large enough, old enough, and/or enriched enough. We present a new methodology, complete with propagated uncertainties, that advances the individual uranium particle age-dating measurement to include smaller, younger, and lower enriched nuclear material than

previously envisioned. Additionally, we will provide insights into utility of this measurement advance within the aims of global nuclear safeguards objectives.

9:00am AS+BI+RA-TuM-4 Peak Shape Analysis in TOF SIMS: Best Practices and Limiting Precision in Accounting for Detector Saturation, *Lev Gelb, A Walker,* University of Texas at Dallas

We compare strategies for analyzing high-mass resolution TOF SIMS data sets affected by detector saturation. The detectors used in many instruments undercount ions due to saturation effects. If two or more ions arrive within a very short interval (the "dead time") only the first ion is recorded. This changes both the total number of ions collected and their statistical distribution. The dead time is typically short enough that only ions of the same nominal mass are affected, but a significant fraction of the total ions reaching the detector may still be missed.

We demonstrate an approach to correct for dead time errors in which a probability model for the detector behavior is developed and used in peak fitting of the "uncorrected" data. This approach has many advantages over previous methods which required an estimate of the variance, and it behaves better under conditions of poor data quality (low counts or high saturation.)

Using both synthetic and experimental data, we examine how saturation affects apparent peak shape, position and intensity, the effects of background on estimated peak position and shape, the dependence of peak-location precision on the total number of counts, how interference between satellite peaks is best accounted for, and the biases exhibited by different data analyses. Finally, we extend these methods to imaging data taken at high mass resolution and compare the results obtained with analyses performed at unit-mass resolution.

9:20am AS+BI+RA-TuM-5 Electronic Structure and Band Gaps of Industrially Relevant Materials Investigated by Photoelectron Spectroscopy and REELS (Reflection Electron Energy Loss Spectroscopy), *Paul Mack, T Nunney,* Thermo Fisher Scientific, UK*; H Meyer III,* Oak Ridge National Laboratory

Many inorganic and organic materials have been created and evaluated for use in a diverse range of applications, such as microelectronics, solar cells and TV displays. The electronic properties of these materials can be tuned by modifying their elemental or chemical state composition. Ideally, the analyst would like to characterize both the composition and electronic properties of a given material in a single experimental run, enabling correlation between electronic properties and composition to be established.

In this work thin films of industrially relevant materials, such as polydioctylfluorene, which is a polymer light emitting diode (PLED), and HfO_2 were analysed using a multi-modal approach. (Thermo Scientific ESCALAB Xi$^+$ and Nexsa tools, configured with multiple surface analysis techniques, were used for the analysis.)

X-ray photoelectron spectroscopy was used to measure elemental and chemical state composition (together with some electronic information) and ultraviolet photoelectron spectroscopy was used to measure ionization potentials and the energies of the highest occupied molecular orbitals (HOMOs). Information about the band gap and lowest unoccupied levels (LUMOs), which cannot be determined with XPS or UPS, was measured with REELS. Energy level diagrams for the materials could then be constructed using the information from the complementary spectroscopic techniques.

Due to the low kinetic energy of photoelectrons generated by the ultraviolet source, UPS is a particularly surface sensitive spectroscopy. When analyzing samples stored in the atmosphere, the resulting data is typically dominated by surface adventitious carbon. This carbon needs to be removed, but with care not to damage the underlying material being studied. The use of an argon cluster ion beam for this kind of careful sample preparation was demonstrated in this work.

9:40am AS+BI+RA-TuM-6 Practical References for Low Energy Ion Scattering by Ca and F, *S Průša, T Šikola,* Brno University of Technology, Czech Republic*; Hidde Brongersma,* IONTOF Technologies GmbH, Germany/Eindhoven University of Technology, Eindhoven, The Netherlands, Germany

Low-Energy Ion Scattering (LEIS) is known for its extreme surface sensitivity. It is just as well suited for the analysis of amorphous, isolating, extremely rough surfaces, as for flat single crystals. Thus LEIS is applicable to any type of sample that can be taken into vacuum. Since matrix effects are generally absent, or relatively small in LEIS, a quantitative analysis is straightforward. However, the theory to quantitatively predict the atomic sensitivities of the elements falls short. Therefore, an accurate quantification relies on well-defined reference materials. Practical references should be chemically inert, easy to clean and inexpensive. The powder of calcium fluoride, CaF_2, has been suggested as practical reference for Ca and F [1], while the powder of calcium carbonate, $CaCO_3$, has also been suggested for Ca [2].

A complication is that the composition of the outer atomic layer of a material is generally fundamentally and radically different from that of the atoms below this surface. Thus it is unlikely that the F/Ca ratio in the outer surface of CaF_2 will be 2. In fact, precisely this difference makes the LEIS information unique and complementary to that of analytic techniques such as XPS, Auger and (TOF-) SIMS which probe several to many atoms deep. The difference is also highly relevant, since the outer atoms of a surface largely control important processes as adhesion, catalysis, electron emission and growth

It will be shown how the F/Ca atomic ratio, the Ca and F atomic densities, as well as the roughness factors for CaF_2 and $CaCO_3$ have been determined.

[1] T. Gholian Avval, C.V. Cushman, P. Brüner, T. Grehl, H.H. Brongersma, M.R. Linford,

Surf. Sci. Spectra, to be published (2019)

[2] R.M. Almeida, R. Hickey, H. Jain, C.G. Pantano, J. Non-Cryst. Solids 385 (2014) 124

11:00am AS+BI+RA-TuM-10 Extreme-Ultraviolet-Assisted Atom Probe Tomography, *Norman Sanford, L Miaja Avila,* National Institute of Standards and Technology (NIST)*; P Blanchard,* National Institute of Sandards and Technology (NIST)*; D Diercks, B Gorman,* Colorado School of Mines*; A Chiaramonti,* National Institute of Sandards and Technology (NIST)

Laser-assisted atom probe tomography (L-APT) often returns compositional biases that deviate from a specimen's true chemical makeup [1]. In our L-APT studies of GaN, which utilize a 355 nm laser, we find stoichiometric composition (50% Ga, 50% N) only when the pulse fluence is roughly 2E-7 J/cm^2. Higher fluences return nonphysical, Ga-rich compositions; lower fluences give nonphysical N-rich compositions. L-APT of other materials, including SiO2, exhibit similar biases. L-APT is a thermally-activated mechanism. The specimen is subjected to a strong electric field that is held just below the threshold for field evaporation of ions; evaporation is triggered by thermal transients imparted by the incident laser pulses. Motivated by the need to improve the quantitative accuracy of atom probe tomography, we explored an alternative, photoionization-triggered pathway for field evaporation by replacing the conventional laser on an L-APT tool with a pulsed, extreme-ultraviolet (EUV) source—thus realizing the XAPT [2,3]. The tabletop EUV source is an ultrafast, amplified Ti:sapphire laser driving an Ar-filled capillary waveguide. Pulsed, coherent EUV is produced via high-harmonic generation [4]. The respective characteristics of EUV pulse width, repetition rate, wavelength (energy), and fluence, incident on a specimen tip are: 10 fs, 10 kHz, 30 nm (42 eV), and 2.5E-8 J/cm^2. Comparative XAPT and L-APT analyses were performed on specimens of GaN and SiO2 (amorphous fused silica). For SiO2, L-APT returned an off-stoichiometry composition of 41% Si and 59% O; XAPT yielded 33% Si and 66% O (stoichiometry). For GaN, XAPT found 49% Ga and 51% N; L-APT yielded laser-pulse-fluence-dependent composition and returned 68% Ga and 32% N for a fluence of roughly 2E-6 J/cm^2; L-APT conditions giving stoichiometric GaN appear above. The uncertainty of these measurements is 1—3 at. %. All specimens were examined at 50 K. XAPT-derived mass spectra show reduced occurrences of molecular ions and reduced "thermal tails" (persistent field emission following the laser pulse). Ongoing work for presentation at the meeting includes comparative studies of InGaN, Mg:GaN, and AlGaN. In all cases examined thus far, the XAPT approach offers measurable improvements over L-APT.

1. D. J. Larson, et al, Local Electrode Atom Probe Tomography (Springer, New York, 2013)

2. A. N. Chiarmonti, et al, MRS Advances (in press, 2019)

3. L. Miaja Avila, et al, Frontiers in Optic (FiO), Optical Society of America, Wash. DC, p. FTu5C. 3 (2018)

4. L. Miaja Avila, et al, Phys. Rev. Lett. 97, 113604 (2006)

11:20am AS+BI+RA-TuM-11 A Multi-Technique Approach for Complete Thin Film Characterisation, *Sarah Coultas, J Counsell, N Gerrard, C Blomfield,* Kratos Analytical Limited, UK*; C Moffitt,* Kratos Analytical Limited*; T Conard,* IMEC, Belgium

The application of thin film technology is of commercial importance across a range of industries and is commonly used to influence both the physical and chemical properties of bulk materials. Ranging in thickness from tens of Angstroms to microns, their applications are used across a broad range of disciplines including the semiconductor, biomaterial and energy harvesting industries. Herein, we provide a multi-technique investigation of layered thin film and ultra-thin film coatings using a model system for gate oxide structures. The combination of techniques allows one to build a complete picture of the chemistry of these materials and how subtle differences in chemistry and stoichiometry can influence the properties of a substrate to enhance its application specificity.

X-ray Photoelectron Spectroscopy (XPS) was used to characterize the surface chemistry of these layered thin film materials. Using monochromated Al-Kα (1486.6 eV) X-rays, it was possible to gain quantitative chemical information from the uppermost 10 nm of the surface. In this study, we illustrate how angle-resolved XPS (ARXPS) can be used as a more surface sensitive approach to probe only the topmost 1-3 nm, and how one can utilize maximum entropy modelling (MEMS) to recreate a concentration depth profile from the resulting data.

In contrast to increased surface sensitivity, high energy excitation sources can be used to extend the analysis depth of a material to >15 nm. Here, we describe the use of a monochromated Ag-Lα (2984.2 eV) X-rays to delve deeper into the bulk structure. In combination with ARXPS, the greater excitation energy and increased analysis depth allows one to measure elemental core levels which are not accessible using the conventional Al-Kα source. In light of this, one can build a more detailed description of the structure of these thin film materials and their use in relevant applications.

11:40am AS+BI+RA-TuM-12 Polymeric Barrier Coatings for Silicone Elastomer against Diffusion of Isocyanate in Vacuum Casting Processes, *Martin Wortmann, R Petkau,* Bielefeld University of Applied Sciences, Germany*; N Frese,* Bielefeld University, Germany*; E Moritzer,* Paderborn University, Germany*; A Gölzhäuser,* Bielefeld University, Germany*; B Hüsgen,* Bielefeld University of Applied Sciences, Germany

The vacuum casting process is used industrially to replicate prototypes of polyurethane (PUR). Due to the diffusion of 4,4'-methylene diphenyl diisocyanate (MDI), a PUR resin component, the silicone casting molds used in this process show a progressive degradation, which leads to the failure of the casting molds after a few casting cycles [1]. In this contribution, we present ways to protect the surface of the silicone elastomer by various thermoplastic polymer coatings. The polymers investigated were dissolved in different volatile solvents and coated on pretreated silicone surfaces. For this purpose, the compatibility of those polymer solutions with polydimethylsiloxane (PDMS) was investigated and their diffusion coefficients with respect to MDI were measured. Polymer coatings that have exhibited a high diffusion barrier have been used to drastically increase the output of the casting molds.

[1] M. Wortmann et al., *Polymer Plast Tech Eng* 57, 1524 (2018).

12:00pm AS+BI+RA-TuM-13 pARXPS Study of GeSbTe Surface Oxidation, *Ludovic Goffart,* ST Microelectronics/LTM/CEA-LETI, France*; C Vallée,* Laboratoire des Technologies de la Microélectronique (LTM), France*; B Pelissier,* LTM, Univ. Grenoble Alpes, CEA-LETI, France*; J Reynard, D Benoit,* ST Microelectronics, France*; G Navarro,* CEA-LETI, France

This work is focusing on the oxidation of the well-known GST material (Ge$_2$Sb$_2$Te$_5$, GST225) widely used in storage optics like CD, DVD and Blu-ray. This time, we use the GST for its electrical properties to create a non-volatile memory. The GST we use in this work is modified from the GST225 chemical composition to comply with the specifications needed in automotive applications, the most important being a good stability and cycling at high temperature environment.

This non stoichiometric GST composition leads to instability in its structure, therefore more aging and oxidation which conflict with the objectives of this new PCM cell. Added to this is some atomic segregation during crystallographic relaxation, which leads to low cycling durability of the cell and lower crystallization temperatures. To counter these effects, the GST material is doped but this makes more complex the chemical characterization of the material.

To understand and overcome these problems, different GST materials (from 225 to Ge rich) have been characterized using the pARXPS technique which is an angular resolved XPS. With this technique a very complete chemical characterization of the surface of these samples have been performed to gather useful information of atomic segregations and surface oxidation, by acquiring 8 simultaneous angles at the same time for different element windows. This is only possible by developing a complex fitting model for the large amount of spectra obtained. This model has to deal with the complex feature of the spectra obtained since some peaks were overlapping. Physical constraints are then necessary to obtain a realistic fit of the spectra. Once the model optimized, the aging of the samples have been studied by monitoring the evolution of specific XPS shapes with time. As a result, the oxidation kinetic and the thickness of the oxidized surfaces are quantified and finally a depth profile reconstruction of the different chemical bonds is performed. In addition to pARXPS, TEM-EDX analysis were performed to confirm the fitting model developed and profile depth reconstruction obtained with pARXPS technique.

Biomaterial Interfaces Division
Room A120-121 - Session BI+AS-TuM

Characterization of Biological and Biomaterial Surfaces

Moderators: Karyn Jarvis, Swinburne University of Technology, Sally McArthur, Swinburne University of Technology, Australia

8:00am BI+AS-TuM-1 Characterizing Protein Fiber Structures in Solution with Vibrational Sum-Frequency Scattering Spectroscopy, *David G. Castner, P Johansson,* University of Washington

Sum frequency generation vibrational spectroscopy has been developed as a powerful technique for investigating the structure of proteins at flat liquid-solution interfaces. However, many biological processes are regulated by interactions at the interface of 3D structures. Collagen forms large fibers that are responsible for the structural integrity of tissues. The structure, organization and interactions of these fibers are important for the survival, communication, migration, and proliferation of cells. Investigating protein fiber interactions is challenging, particularly under biological conditions. However, vibrational sum-frequency scattering (SFS) spectroscopy, with inherent contrast for local molecular ordering, can be utilized towards these important goals. We have applied SFS to collagen type I fiber networks self-assembled in aqueous environments. Signals were detected from the amide I band stretching vibrations (associated with the protein backbone structure) and signals from the C-H stretching and bending vibrations (associated with the protein side-chains). The angular scattering patterns for the backbone (amide I) and side-chain (C-H stretches and bends) signals are different, making the spectra dependent on the angle of detection. For randomly oriented fiber networks the amide I chiral signals are dominant in the phase-matched direction. In contrast, amide I achiral and chiral signal strengths are comparable at scattering angles above 6°. The backbone signal intensity decreases significantly as the scattering angle increases. In contrast, the side-chain signals remain high at large scattering angles. Distinctions in the organizational symmetry and the relative fiber surface contribution to the overall signal are probable reasons for these observations. The amide I band the spectra acquired at a scattering angle of 22 degrees provided good specificity to the surface region of the collagen fibers. This surface sensitivity was used to investigate how a dilute sodium dodecyl sulfate surfactant solution affects the spectra and scattering patterns of the SFS signals. The amide I SFS polarization ratios at a scattering angle of 22° provided insights to early changes to the collagen fiber structure. This shows the promise of SFS as an important technique for providing detailed information about the surface structure and chemistry of protein fibers, complementary to what can be obtained from other techniques such as SHG imaging or IR spectroscopy. Thus, SFS can provide a molecular level understanding of the changes to collagenous tissues during decellularization and help optimize the protocols for tissue engineered organs.

8:20am BI+AS-TuM-2 Near-Ambient Pressure XPS Surface Characterisation of Bacteria and Biofilms - Model Systems and Sample Preparation, *Marit Kjaervik,* Bundesanstalt für Materialforschung und -prüfung, Germany*; P Dietrich, A Thissen,* SPECS Surface Nano Analysis GmbH, Germany*; K Schwibbert, W Unger,* Bundesanstalt für Materialforschung und -prüfung, Germany

Bacterial samples are typically freeze dried or cryo-prepared prior to XPS analysis to allow for measurements in ultra-high vacuum (UHV). The sample environment in the near-ambient pressure (NAP) XPS instrument EnviroESCA allows for measurements in up to 15 mbar water vapor, thus, sample preparation is no longer restricted to UHV-compatible

techniques.[1] For instance, biofilms grown in medium can be transferred directly from the medium to the measurements chamber, maintaining a humid environment throughout the measurements.[2] Considering the complexity of bacterial samples, sample preparation must be carefully considered in order to obtain meaningful and reproducible results.

In this talk, various strategies for sample preparation of bacteria and biofilms for NAP-XPS measurements will be discussed. Model systems of planktonic bacteria, artificial biofilms resembling the exopolysaccharide matrix and biofilms have been characterised in various conditions. The stability and homogeneity of the samples were assessed by monitoring the C1s core-level peak at different sample locations. The quality of the XP spectra is also influenced by the gas environment, which will be exemplified by core level spectra of *P. Fluorescens* acquired in air, water vapor and ultra-high vacuum.

Furthermore initial results from iodine doped model biofilms will be presented. The in-depth chemcial compositon profile of these model films was obtained using an argon gas cluster ion gun.

Acknowledgements

[1] P. M. Dietrich, S. Bahr, T. Yamamoto, M. Meyer, and A. Thissen, "Chemical surface analysis on materials and devices under functional conditions – Environmental photoelectron spectroscopy as non-destructive tool for routine characterization," *J. Electron Spectros. Relat. Phenomena*, vol. 231, pp. 118–126, Feb. 2019.

[2] M. Kjaervik, K. Schwibbert, P. Dietrich, A. Thissen, and W. E. S. Unger, "Surface characterisation of *Escherichia coli* under various conditions by near-ambient pressure XPS," *Surf. Interface Anal.*, vol. 50, no. 11, pp. 996–1000, Nov. 2018.

8:40am BI+AS-TuM-3 ToF-SIMS Imaging of Plant seed Interactions with Plant-growth Promoting Bacteria, *Yuchen Zhang, X Yu,* Pacific Northwest National Laboratory

Presentation Summary:

This presentation aims to show that we have successfully used delayed image extraction in time-of-flight secondary ion mass spectrometry (ToF-SIMS) to study the interaction between Brachypodium seed and plant growth-promoting bacteria (PGPB) for the first time.

Abstract

The use of time-of-flight secondary ion mass spectrometry (ToF-SIMS) is a relatively unexplored in plant biology that is undergoing fast development [1]. The majority of existing research in plant biology that has utilized ToF-SIMS mostly involves the study of plant stems and leaves, and only a handful of studies apply it on the analysis of plant roots and/or seeds. Additionally, the use of Brachypodium distachyon (Brachypodium) as a model system for research has become more prominent in plant biology. Brachypodium, a C3 model, can provide more insight into the biological studies of other species including small grain crops such as wheat and barley [2], therefore it has a significant scientific impact in plant biology. To the best of our knowledge, this will be the first systematic ToF-SIMS imaging of Brachypodium. In this work, we obtained chemical mapping of the interaction of grains of Brachypodium with plant growth-promoting bacteria (PGPB) [3], namely, Pseudomonas and Arthrobacter, using ToF-SIMS. Specifically, the use of the delayed image extraction mode in ToF-SIMS provides chemical speciation of the Brachypodium seed surface and simultaneously captures the morphological features of the plant-bacteria interface. Our findings provide high resolution spatial distributions of fatty acids (e.g., palmitic acid, stearic acid, and arachidic acid) and phospholipid (e.g., cardiolipin) present on the Brachypodium seed surface. Spectral PCA results indicate that the biofilm and planktonic cells both have effects on the seed surfaces. In terms of seedling potentials, the seed brush is the most active after PGPB attachment on the biointerface.

Key words: ToF-SIMS, delayed image extraction, PGPB, Brachypodium, Pseudomonas, Arthrobacter

References:

1. Boughton, B.A., et al., Mass spectrometry imaging for plant biology: a review. Phytochem Rev, 2016. 15: p. 445-488.

2. Delaplace, P., et al., Influence of rhizobacterial volatiles on the root system architecture and the production and allocation of biomass in the model grass Brachypodium distachyon (L.) P. Beauv. BMC Plant Biol, 2015. 15: p. 195.

3. Scholthof, K.B.G., et al., Brachypodium: A Monocot Grass Model Genus for Plant Biology. Plant Cell, 2018. 30(8): p. 1673-1694.

9:00am BI+AS-TuM-4 Visualization of Signaling Molecules in Brain Tissue by Multimodal Imaging with Matrix Assisted Laser Desorption/Ionization Mass Spectrometry and Time-of-Flight Secondary Ion Mass Spectrometry, *Matthias Lorenz, S King, N Borodinov, C Steed, J Chae, A Ievlev, O Ovchinnikova,* Oak Ridge National Laboratory

Matrix Assisted Laser Desorption/Ionization (MALDI) is commonly used for the chemical imaging of biological tissue samples with mass spectrometry due to its capability to desorb and ionize large organic molecules with limited fragmentation, thus preserving a high degree of molecular information. MALDI is suitable to analyze species such as peptides and proteins, and the intact molecular ion is observable in many cases.[1] The achievable spatial resolution using MALDI mass spectrometry imaging (MSI) is limited to about 30 μm using standard matrix compounds, primarily due to the dimensions of matrix crystals and the stability of the matrix coating.[2] Time-of-Flight (ToF) Secondary Ion Mass Spectrometry (SIMS) is another mass spectrometry based chemical imaging technique that can achieve a spatial resolution below 100 nm.[3] The chemical information obtained from ToF-SIMS analyses is, however, limited to smaller organic molecules and elemental species due to a more significant fragmentation of intramolecular bonds and decreasing ion yields with increasing molecular weight. We present here a workflow comprising the consecutive application of ToF-SIMS and MALDI-ToF-MS MSI to combine the strength of both chemical imaging techniques. Even though mass spectrometry based surface analysis techniques are inherently destructive in nature, the volumes of sample material that the two imaging techniques extract at each sampling location differs significantly (~30 μm vs. ~100 nm craters). This difference enables the assumption of a non-destructive nature for the ToF-SIMS imaging cycle relative to the MALDI sampling volume and spatial resolution, leaving a virtually pristine sample surface for a subsequent MALDI imaging cycle of the same sample area. We showcase the application of our workflow for the multimodal imaging of a coronal mouse brain tissue section, with automated co-registration of the two imaging data sets. We demonstrate how the MALDI mass spectral data enable to complement the high spatial resolution ToF-SIMS MSI data set with an additional degree of molecular structural information and discuss our workflow based on the visualization of signaling molecules in the mouse brain tissue.

[1] Todd, P.J.; Schaaff, T.G.; Chaurand, P.; Caprioli, R.M. *J. Mass Spectrom.* **2001**, *36*, 355–369.

[2] Yang, J.; Norris, J.L.; Caprioli, R. *J. Mass Spectrom*. **2018**, *53*, 1005–1012.

[3] Kollmer, F.; Paul, W.; Krehl, M.; Niehuis, E. *Surf. Interface Anal.* **2013**, *45*, 312–314.

9:20am BI+AS-TuM-5 *In situ* Observation of Triacylglycerol (C39:0) and Acylceramide (C17) Colocalization in Lipid Droplets of Apoptotic Cells using ToF-SIMS, *Shohini Sen-Britain, N Li, G Atilla-Gokcumen, J Gardella Jr.,* State University of New York, Buffalo

The formation of phase segregated lipid droplets storing triacylglycerol containing polyunsaturated fatty acyl chains (PUFA-TAGs) during apoptosis, or programmed cell death, has been previously observed [1,2]. Polyunsaturated fatty acids are incorporated into PUFA-TAGs by diacylglycerol acyltransferases (DGATs) [1]. The acylation of ceramide by DGATs also produces acylceramide which has been found in lipid droplets as well [3]. The accumulation of ceramide and PUFA phospholipids sensitizes cells to cell death. Therefore, acylation of these molecules into phase segregated droplets is thought to have a protective effect [1,2].

Previous studies observing these acylated molecules in lipid droplets have utilized LC-MS of fractionated lipid droplets [1-3]. However, colocalization of these lipids has not been observed *in situ*. Previous imaging studies have been limited by the use of nonspecific lipid dyes, such as nile red, in observing lipid droplets.

In this study, we have utilized metal-assisted time-of-flight secondary ion mass spectrometry (ToF-SIMS) to image the colocalization of TAG (C39:0) and acylceramide (C17) in apoptotic HCT-116 human colorectal carcinoma cells. We maintained sample preparation conditions used in previous microscopy studies by cutting out squares of cell culture plates containing lyophilized apoptotic HCT-116 cells. Imaging of lipids within the cells was accomplished by milling off the top half of the cells using a focused ion beam-scanning electron microscope (FIB-SEM). Imaging of gold sputter coated samples in negative ion mode allowed for the observation of high molecular weight secondary ions (>1000 m/z) and of unique spectra of

both TAG (C39:0) and AC (C17). Colocalization of endogeneous TAG and AC were observed in apoptotic cells. TAG and AC fragmentations were determined by analyzing (1) gold sputter coated TAG and AC standards on cell culture plates and (2) standard additions of TAG and AC onto milled lyophilized apoptotic cells that were also gold sputter coated.

The work accomplished in this study illustrates the potential of identifying the spatial localization of large biomolecules in cells on insulating, high topography containing samples through the use of standard additions and high mass resolution, metal-assisted ToF-SIMS. The results are also the first reported *in situ* observation of TAG and AC colocalization in apoptotic cells.

[1] *Biochemistry* 2018, 57, 72-80

[2] *ACS Chemical Biology* 2016, 11, 2583-2587

[3] *Cell Metabolism* 2017, 25, 686–697

9:40am **BI+AS-TuM-6 Customizing Decellularized Biopolymer Matrices to Serve as Cell-instructive Microenvironments: A ToF-SIMS Study**, *Mirko Nitschke, V Magno, R Zimmermann, N Dennison,* Leibniz Institute of Polymer Research Dresden, Germany*; C Werner,* Leibniz Institute of Polymer Research Dresden, Germany, Deutschland, Germany
Decellularized extracellular matrix (ECM) preparations provide highly valuable options for the *in vitro* reconstitution of tissue-specific niches. In this approach, control over the ECM composition and structural assembly can be achieved through the modulation of cell culture conditions. We have previously demonstrated that adding ascorbic acid and using macromolecular crowding (MMC) allows for tuning the ECM deposition by human mesenchymal stem cells by boosting procollagen synthesis and enhanced complexation/deposition of soluble matrix components [Prewitz *et al. Biomaterials* **73** (2015) 60]. Combining both options, we now explored the fabrication of a large set of cell-derived ECM variants which were analyzed by time-of-flight secondary ion mass spectrometry (ToF-SIMS) and immunostaining. Principle component analysis (PCA) of the ToF-SIMS spectra and quantitative immunofluorescence data revealed distinct differences and trends in the complex ECM composition. The introduced methodology is validated by cell culture experiments using the decellularized matrix variants and concluded to provide a new level of control in tailoring matrix properties for tissue and organoid models (authors MN and VM contributed equally).

11:00am **BI+AS-TuM-10 Hierarchical Changes in Protein Structure: from Surface Influence to Cell Control**, *Sapun Parekh,* University of Texas at Austin **INVITED**
Protein structure, not just identity, is now appreciated as a critical variable that determines downstream biochemical reactivity. In biomaterials research, proteins are often coated onto materials to make them biocompatible; however, the structure of particular proteins on the material surface is often unknown or not taken into account, leading to inconsistent biological responses. The same protein on different biomaterial surfaces can take on distinct structures that can, for example, lead to differential receptor activation or stem cell differentiation into specific lineages. In this work, we demonstrate how both chemical and physical stimuli modulate protein structure and ultimately direct cell response. In the first part of this talk, I will show how graphene materials, with their unique physico-chemical properties and potential applications in tissue engineering, can strongly modulate fibronectin structure, cellular integrin binding, and stem cell differentiation. In the second part, I will show how physical forces on protein-based fibrin hydrogels can modulate protein structure, modifying enzymatic and integrin binding sites and drastically reducing platelet adhesion. The work presented here shows that physical and chemical properties of materials strongly influence protein structure and downstream biological responses, showing that biomaterial design should include considerations to control protein structure in addition to protein capture.

11:40am **BI+AS-TuM-12 The Role of Cr-N phases Prepared by Plasma Processes on 316L Stainless Steel and the Potential Use in Biocompatible Systems**, *Diana Galeano-Osorio, S Vargas-Giraldo, C Castano,* Virginia Commonwealth University
The corrosion performance of chromium nitride (CrN) phases obtained by two different plasma-based techniques on 316L stainless steel was investigated by electrochemical testing in simulated body fluid, SBF. One method consisted of the surface treatment of 316L stainless steel by plasma nitriding. The other approach comprised the deposition of Cr-N thin film layers on 316L stainless steel substrates by reactive sputtering

technique. The structural analysis of the Cr-N phases on the plasma nitrided samples by X-ray diffraction (XRD) showed an expanded austenite phase (S-Phase), while X-ray photoelectron spectroscopy (XPS) analysis revealed the presence of both the S-Phase and CrN. In the case of thin films, the XRD and XPS characterization predominantly showed a CrN phase. The different topographical characteristics of both approaches coupled with the surface energy characteristics and the electrochemical behavior in SBF provided valuable information for the potential use of these materials in biocompatible applications.

12:00pm **BI+AS-TuM-13 Direct Interspecies Electron Transfer (DIET) in Syntrophic Microbes**, *Cuiyun Yang, X Yu,* Pacific Northwest National Laboratory
Presentation Summary:
This presentation will show our recent results of metabolic performance of direct interspecies electron transfer between syntrophic *Geobacter* species by using *in situ* liquid time-of-flight secondary ion mass spectrometry (ToF-SIMS).

Abstract

Direct interspecies electron transfer (DIET) is deemed important and effective for electron exchange among syntrophic Geobacter species. DIET facilitates coupling of carbon, nitrogen, phosphorus biogeochemical cycles in the natural anaerobic environment [1]. In this presentation, Geobacter sulfurreducens and Geobacter metallireducens were employed to investigate the metabolic behavior of a syntrophic community cultured in a SALVI microfluidic reactor and analyzed by *in situ* liquid time-of-flight secondary ion mass spectrometry (ToF-SIMS). More types of molecules that facilitate metallic-like electron conductivity pilis or cellular outer-membrane cytochrome (e.g., OmcS) formation in the *Geobacter* co-culture community were observed than the planktonic cells. Characteristic peaks observed include aromatic acids m/z$^+$ 82 ($C_4H_6N_2^+$, histidine), 120 ($C_8H_{10}N^+$, phenylalanine), and 166 ($C_9H_{12}NO_2^+$, phenylalanine), benzene polymers m/z$^-$ 93 ($C_6H_5O^-$), 94 ($C_6H_6O^-$), and 133 ($C_9H_9O^-$) in the co-cultured aggregate. The compositions of specific fatty acid also changed according to the culture condition when comparing the single population vs. co-cultured community. Abundance of water clusters were observed in this work and the water cluster differences observed among the cultured community, single population biofilms, or planktonic cells also suggest that other living activities of cells is possible, for instance, moderation of the solvation spheres when forming the aggregates due to IET and/or DIET. Alternatively, we hypothesize that proton-coupled electron transfer (PCET) may play a role in the syntrophic community besides DIET based on *in vivo* spectral comparisons. Our *in situ* molecular imaging results lead to the following conclusions: 1) interspecies electron transfer in co-cultured planktonic states may be mainly mediated by reduced molecular hydrogen; and 2) DIET in co-cultured aggregates functions via direct contact or microbial nanowire. Our findings improve the understanding of the electron transfer in syntrophic communities based on *in vivo* molecular imaging.

Key words: direct interspecies electron transfer (DIET), interspecies electron transfer, *Geobacter sulfurreducens*, *Geobacter metallireducens*, *in situ* liquid TOF-SIMS

References:

1. D.R. Lovley, et al., *Geobacter*: the microbe electric's physiology, ecology, and practical applications. Adv. Microbiol. Physiol., 59, 1-100, 2011.

Electronic Materials and Photonics Division
Room A214 - Session EM+2D+AP+NS+PS-TuM

New Devices and Materials for Electronics and Photonics
Moderators: Sean W. King, Intel Corporation, Michelle M. Paquette, University of Missouri-Kansas City

8:00am **EM+2D+AP+NS+PS-TuM-1 Performance Modeling and Design for Spintronic Logic and Memory Devices**, *Azad Naeemi,* Georgia Institute of Technology **INVITED**
As scaling conventional logic and memory devices becomes more and more challenging, there is a global search for novel materials and devices that can augment mainstream technologies used for data storage and processing. To this end, spintronic materials and devices are promising candidates as they provide dense non-volatile storing elements that enable novel computing paradigms such as in memory-computing and neural networks.

This talk will present physical models for various read and write spintronic mechanisms and quantifies the potential performances of Boolean circuits based on various spintronic logic devices. It will be shown that without major breakthroughs such circuits will not be able to compete with their CMOS counterparts. However, novel circuit paradigms that take advantage of the physics of these devices can potentially provide significant benefits. For example, cellular neural networks based on spintronic devices are projected to perform better compared to their analog CMOS implementation.

While spin-transfer-torque random access memory (STT-RAM) is becoming commercially available, it suffers from relatively large switching currents that limits its density and causes reliability challenges. Novel read and write mechanisms such as spin-orbit torque or magneto-electric effects can potentially address or partially mitigate some of these challenges. In this talk, the array-level potential performance of various magnetic memory devices will be quantified and benchmarked.

8:40am EM+2D+AP+NS+PS-TuM-3 High Yield, Low Variability HfO₂ 1T1R Cells Fabricated in 65nm CMOS, *Jubin Hazra, M Liehr, K Beckmann, N Cady,* SUNY Polytechnic Institute

Hafnium Oxide (HfO$_2$) based Resistive Random Access Memory (ReRAM) devices are promising candidates for non-volatile memory, having a wide variety of applications in neuromorphic computing, artificial intelligence and future memory solutions. Stochastic conductive filament (CF) generation and rupture processes, however, contribute to high variability resistive switching in these devices. In order to address this issue, an extensive characterization of HfO$_2$ 1 transistor 1 RRAM (1T1R) cells was performed to investigate switching yield and cell-to cell variability. 1T1R devices were integrated into a 300mm wafer platform utilizing the IBM 65nm 10LPe process technology, in which the memristor device stack is implemented between the M1 and M2 metallization layers, using a custom designed FEOL compatible process flow. The ReRAM device stack is comprised of a TiN bottom electrode followed by conformal deposition of the HfO$_2$ switching layer, Ti oxygen scavenging layer and TiN top electrode. The HfO$_2$ switching layer was deposited using an atomic layer deposition (ALD) process with an organic precursor. For statistical significance, the performance of 50 different 1T1R cells was compared for cell-to-cell variability in operating voltage and resistance in the on and off state. An impressive 100% switching yield and low cell-to-cell switching variability were observed for these devices. 1T1R cells were also investigated for long term endurance and high temperature retention, exhibiting excellent endurance of up to 1 billion switching cycles with an average R_{off}/R_{on} ratio of 10:1. As compared to 1T1R cells that we have fabricated with alternative ALD precursors/methods, these devices show superior yield and performance. We are currently performing compositional and structural comparisons between these sets of devices, to elucidate the impact of ALD precursor choice and processing methods on yield and electrical performance.

9:00am EM+2D+AP+NS+PS-TuM-4 Heat Transfer Proximity Effects in Resistive Memory Crossbar Arrays, *Marius Orlowski, M Al-Mamun,* Virginia Tech

Evidence for thermal cross talk in resistive RAM memory arrays is presented. Frequent switching of a resistive memory cell (Cu/TaO$_x$/Pt) may lead to a considerable local accumulation of Joules heat. The heat generated in a stressed device spreads via common electrode lines to the neighboring cells impacting their switching behavior. As a probe into degraded performance of the neighbor cells we choose the cell itself set into the on-state under specific conditions. The cell is set at a critical compliance current I_{cc} that allows repeated switching for no more than ~15 cycles. After the maximum number of cycles the on-state becomes volatile. For a lower I_{cc}, the cell produces a volatile on-state, and for higher I_{cc} the cell switches for hundred of times with a stable on-state. We find that the cells in close proximity of the heated device display various degrees of degradation indicated by a reduced number of cycles of the probed cell. The 1st neighbor cell experiences the greatest, and the 4th neighbor cell the smallest degradation. This indicates the spread of the heat from the heated device to its neighbors. After a sufficient cooling off period (10 minutes or longer), all the neighboring cells and the heated device display again the maximum number of cycles i.e. 15, when set under the critical compliance current and reset, repeatedly. Also cells that don't share any of the common electrode metal lines with the heated source cell, may degrade provided that the intermediate cells are set to on-state, thus enabling a continuous thermal conduction path between the heated cell and the probed cell. The heat dissipation from the heated device is slower for narrow and thin metal electrode lines than for wide and thick metal lines. However, in case of wide and thick metal lines more distant neighbor cells are affected by the parasitic cell-to-cell heat transfer.

We have performed the characterization o the neighboring cells along the Cu and Pt electrode lines. We find that the performance degradation of the neighboring cells along the Cu line is significantly stronger than along the Pt metal line. This observation is consistent with the much better heat conductivity of Cu lines (385W/(mK) and 150nm thick) than the Pt (72W/(mK) and 50nm thick) lines, but is at odds with the assumption of the standard electro-chemical metallization model postulating a conical shape of the Cu filament with a broad base of the cone at the Pt electrode and a tip at the Cu electrode. We discuss the extant controversial experimental evidence and models for the filament's shape and propose an hour-glass shape for the filament reconciling the extant findings and our thermal results.

9:20am EM+2D+AP+NS+PS-TuM-5 High Performance Memristive Action in Methylammonium Bismuth Iodide([MA]3Bi2I9) Films, *P Cheng,* Vanderbilt University*; G Luo,* Washington University in St. Louis*; Z Gao,* University of Central Florida*; A Thind, R Mishra,* Washington University in St. Louis*; Parag Banerjee,* University of Central Florida

We demonstrate high performance (ON/OFF ~ 2.4x10^5) resistive switching in methylammonium bismuth iodide ((CH$_3$NH$_3$)$_3$Bi$_2$I$_9$ or, MBI) thin films.[1] MBI has a post-perovskite structure and consists of 2D layers of face-shared

BiI$_6$ octahedra. This talk focuses on the structure, composition and associated defect chemistry that is critical for memristive behavior in MBI films.

Memristors are formed by contacting MBI films with aluminum electrodes. The switching for a 200 nm film is observed at voltages ~ 0.5 V. High frequency performance of these memristors shows a peak ON/OFF ratio 2.4x10^5 at 50 KHz. The ON state retention is maintained at 50C for > 10^6 seconds. Stable room temperature endurance is noted for up to 1000 cycles. Energy dispersive x-ray spectroscopy on planar memristor devices show that, postswitching,

a detectable change in the I- concentration is observed closer to the anode side. Density-functional theory (DFT) calculations show low activation barrier for iodine migration in agreement with the experimental results. The DFT calculations also provide insights about the migration pathway and strategies to control this behavior.

From a synthesis perspective, MBI films can be deposited using solution as well as low temperature (< 200C), atmospheric CVD technique.[2] The compounds are air stable. This family of ternary compounds offers a large compositional and structural tunability; unlike binary metal oxides commonly used for memristors. As opposed to recent 2D MoS$_2$ based planar, tunneling RAM devices[3], the vertical stack of the 2-terminal memristor bodes well for scalability. Thus, we propose that hybrid organic-inorganic thin films may offer strategic materials and design advantages together with seamless process integration into current Si-based devices.

References:

1. Cheng, P., Thind, A., Gao, Z., Luo, G., Mishra, R., Banerjee, P., "High performance memristors from methylammonium bismuth iodide thin films", Submitted.

2. Chen, X.; Myung, Y.; Thind, A. S.; Gao, Z.; Yin, B.; Shen, M.; Cho, S. B.; Cheng, P.; Sadtler, B.; Mishra, R.; Banerjee, P., "Atmospheric pressure chemical vapor deposition of methylammonium bismuth iodide thin films", J. Mater. Chem. A, 2017, 5, 24728 - 24739.

3. Vu et al., "Two-terminal floating-gate memory with van der Waals heterostructures for ultrahigh on/off ratio", Nat. Comm., 2016, DOI: 10.1038/ncomms12725.

9:40am EM+2D+AP+NS+PS-TuM-6 Mechanism of Chalcogen Passivation of GaAs Surfaces, *Takayuki Suga, S Goto,* UEC-Tokyo, Japan*; A Ohtake,* NIMS, Japan*; J Nakamura,* UEC-Tokyo, Japan

GaAs surfaces are stabilized by surface treatments with Se or S through the reduction of the dangling bond density [1,2]. It has long been thought that the Se- or S-treated GaAs(111)B-(1x1) surface has a simple structure; the outermost As atoms of the ideal (111)B surface are completely replaced by Se or S atoms, the Se- or S-terminated model [3]. In general, the structural stability of compound semiconductor surfaces can be explained in terms of the so-called electron-counting rule (ECR) [4]. The Se- or S-terminated model, however does not satisfy ECR. Recently, the atomic structure of the Se-treated GaAs(111)B surface has been revisited [5] and another structure

model has been proposed, where the Se atoms substitute 3/4 of the topmost surface As atoms in a (2x2) unit [6]. This mixed Se/As-terminated model satisfies ECR, being electronically stable [6]. We have depicted phase diagrams of Se- or S- treated GaAs(111)B surface at 0K as functions of the chemical potentials of Se ($\Delta\mu_{Se(S)}$) and As ($\Delta\mu_{As}$). The (2x2) As-trimer and the mixed Se(S)/As-terminated surfaces appear under Se poor condition. It is noted that the Se- or S-terminated surface also becomes stable as $\Delta\mu_{Se}$ or $\Delta\mu_S$ increases, respectively, even though these surfaces are not qualified for ECR.

The Se(S)-treated GaAs(111)B surface is prepared experimentally by molecular beam epitaxy under a finite temperature and a gas pressure. Therefore, it is necessary to consider the free energy of a molecule in vapor phase. In this study, we investigate the stabilization of the Se- or S-treated GaAs(111)B surface structures by considering the beam equivalent pressure of As and Se(S) in a growth temperature using the first-principles calculations within the density functional theory. The chemical potentials of molecules are derived from the partition functions for the translation, the rotation, and the vibrational motions.

In the phase diagram for the actual experiment condition, T=800K, the mixed Se/As terminated surface appears in the Se pressure of 10^{-15}-10^{-5} Torr, being consistent with the recent experiment [5]. Surprisingly, the Se-terminated surface also becomes stable as the Se pressure increases. We will discuss the stabilization mechanism of the chalcogen-treated GaAs surfaces.

[1]J. Fan, H. Oigawa and Y. Nannichi, Jpn. J. Appl. Phys. **27**, L2125 (1998).

[2]T. Scimeca, Y. Watanabe, R. Berrigan, and M. Oshima, Phys. Rev. B **46**, 10201 (1992).

[3]V. N. Bessolov and M.V. Lebedev, Semiconductors **32**, 11 (1998).

[4]M.D. Pashley, Phys. Rev. B **40**, 10481 (1989).

[5]A. Ohtake and Y. Sakuma, Cryst. Growth Des. **17**, 363 (2017).

[6]A. Ohtake, S. Goto and J. Nakamura, Sci. Rep. **8**, 1220 (2018).

11:00am EM+2D+AP+NS+PS-TuM-10 Combining 2D and 1D Atomic Scale Tailored Nanowire Surfaces for Novel Electronics and Photonics, *Anders Mikkelsen,* Lund University, Sweden **INVITED**

The III-V nanowire (NW) technology platform has reached a level of advancement that allows atomic scale control of crystal structure and surface morphology as well as flexible device integration. In particular, controlled axial stacking of Wurtzite (Wz) and Zincblende (Zb) crystal phases is uniquely possible in the NWs. We explore how this can be used to affect electronic, optical and surface chemistry with atomic scale precision opening up for 1D, 2D and 3D structures with designed local properties.

We have previously demonstrated atomically resolved Scanning Tunneling Microscopy/Spectroscopy (STM/S) on a wide variety of these III-V NWs and on operational NW devices[1-4]. We now use these methods for studying atomic scale crystal phase changes, the impact on local electronic properties and demonstrating full atomic resolution STM during device operation[5-7]. We explore the surface alloying of Sb into GaAs NWs with controlled axial stacking of Wz and Zb crystal phases[5] demonstrating a simple processing-free route to 1D and 2D compositional control at the monolayer level. Further we show how Bi can form unique 1D and 2D structures in particular on the unique Wz GaAs NW segments. Using 5K STM/S we measure local density of states of Zb crystal segments in Wz InAs NWs down to the smallest possible atomic scale crystal lattice change [6], which is effectively a small 2D material segment in a 1D structure. We find that the general Zb electronic structure is preserved locally in even the smallest segments and signatures of confined states in them.

Characterization to the atomic scale during electrical and optical operation is necesarry to understand and develop the functionality of structures as discussed above. We demonstrate a novel device platform allowing STM/S with atomic scale resolution across a III-V NW device simultaneously with full electrical operation and high temperature processing in reactive gases[7].Using 5-15 femtosecond laser pulses combined with PhotoEmission Electron Microscopy (PEEM) we explore local dynamic response of carriers in the 1D Wz and Zb crystal phases down to a few femtoseconds temporally and a few tens of nanometer spatially[8].

[1] E. Hilner et al., Nano Lett., 8 (2008) 3978; M. Hjort et al., ACS Nano 6 (2012) 9679

[2] M. Hjort et al., Nano Lett., 13 (2013) 4492; M. Hjort et al., ACS Nano, 8 (2014) 12346

[3] J.L. Webb, et al Nano Lett. 15 (2015) 4865

[4] O. Persson et al., Nano Lett. 15 (2015) 3684

[5] M. Hjort et al Nano Lett., 17 (2017) 3634

[6] J.V. Knutsson e tal ACS Nano, 11 (2017) 10519

[7] J.L. Webb et al, Sci. Rep. 7 (2017) 12790

[8] E. Mårsell et al, Nano Lett. 18 (2018) 907

11:40am EM+2D+AP+NS+PS-TuM-12 Nanoflower Decorated GaN and AlGaN/GaN based Catalyst-free CO Sensors*, Monu Mishra, G Gupta,* National Physical Laboratory, India

III-Nitride semiconductors owing unique material properties have proven their potential in the detection of light, chemical, biomolecules and toxic/explosive gases. Despite of numerous advantages *viz.* biocompatibility, high temperature/frequency tolerance and harsh/adverse environmental condition sustainability, the use of expensive catalysts (e.g. platinum) and higher operation temperature (>250°C) for gas sensing has plagued the development of GaN based cost-effective sensing technology. Upto the best of our knowledge, literature lacks any scientific report on the development of catalyst-free CO sensors operating at room-temperature using GaN or AlGaN/GaN structures indicating the necessity of dedicated scientific attention in this area. Therefore, we report the fabrication of nanoflowers-decorated GaN and AlGaN/GaN heterostructure based catalyst-free CO sensors operating at lower (including room) temperature. Planar as well as nanostructured GaN & AlGaN/GaN thin films were employed for sensors fabrication which exhibited significant CO sensing associated with its superior surface and interface properties. For in-depth understanding, the obtained results were thoroughly analyzed and correlated to investigate the underlying science/phenomenon which revealed that CO sensing on GaN (and AlGaN/GaN) is governed by the chemical nature of ambient-oxidation induced amorphous oxide (O_2^-, O^{2-} orOH$^-$ species) layer grown on the surface and acting as a donor/acceptor state. Besides, electron accumulation at AlGaN/GaN interface influenced the critical parameters like schottky barrier height, ideality factor etc. perturbed the effective carrier transport and ultimately the device performance. The study demonstrate that development of catalyst-free room temperature operating GaN based CO sensors is feasible using nanostructured surfaces, though further research is required for optimization of device performance.

12:00pm EM+2D+AP+NS+PS-TuM-13 Surface Transfer Doping of Diamond by Complex Metal Oxides for Power Electronics: A Combined Experimental and Simulation Study*, Vihar Georgiev, D Moran, J McGhee,* University of Glasgow, UK

Diamond has unique properties that make it an attractive wide band-gap material to produce future high-performance electronic devices. With a wide band-gap of 5.5eV, a thermal conductivity 5 times greater than 4H-SiC, a high breakdown field and high hole and electron carrier velocities, diamond is a clear stand out candidate for high frequency and high power devices. However, the lack of a suitable doping mechanism has hindered the application of diamond in electronic devices. Conventional substitutional doping techniques are limited as it is difficult to substitute atoms into the diamond crystal lattice.

Surface Transfer Doping (STD) gives the use of diamond for such applications more promise. For STD to occur there are typically two prerequisites: hydrogen terminated diamond (H-diamond) and an electron accepting material in intimate contact with the H-diamond surface. The hydrogen termination gives the diamond a negative electron affinity which facilitates the transfer of electrons from the diamond to the electron-accepting material, creating a shallow, quasi two-dimensional hole gas (2DHG) in the diamond. This doping process traditionally relies upon interfacial electron transfer between the diamond valence band and favourable energy states provided by atmospheric molecules dissolved in a water layer naturally adsorbed on the diamond surface. However, the stability of this atmospheric layer, upon which the transfer doping process relies, has been a significant limiting factor in the production of high-power handling and robust operation devices.

One of the materials that can improve the performance and stability of STD in diamond are the metal oxides such as MoO_3 which acts as an alternative electron acceptor medium on the H-diamond surface. In order to validate and understand the physical and the chemical process in such STD, in this work we have combined experimental and simulation studies. The electrical characterisation is done by high temperature Hall measurements. Those experimental results are compared to numerical simulation based on the first principle methods such as Density Functional Theory. Comparing the simulation and experimental results revealed that the electrons are

transferred from the diamond to the metal oxides, leading to formation of a sub-surface 2DHG in the diamond. Due to this transfer of electrons to the oxide the hole carrier concentration increases in comparison to the air-exposed H-diamond. Our work shows the potential to improve the stability and performance of hydrogen-terminated diamond electronics devices through incorporation of high electron affinity transition metal oxides.

Exhibitor Technology Spotlight Workshops
Room Hall A - Session EW-TuM

Exhibitor Technology Spotlight I
Moderator: Christopher Moffitt, Kratos Analytical Inc

10:40am **EW-TuM-9 eSpectra: The Data Analysis Resource for You, or for Your Customers**, *Jessica Hoy*, AIPP/AVS
Are you looking for an easier way to analyze spectral data and share your results with your collaborators? Or perhaps this is this a question you are trying to answer for your customers? Learn more about eSpectra, the new online platform where you can plot, compare and share your data in just a few clicks. Brought to you by AVS and AIP Publishing, eSpectra is the only interactive tool of its kind that lets you easily plot your data against peer-reviewed data, public data, or your team's data to better understand, analyze, and validate your results. Download and print plotted graphs, or save, share, and store your graphs and data in a secure environment. eSpectra includes XPS, AES, UPS, and now UV-Vis experimental techniques, with additional techniques under consideration. Our Free Access and our Individual or Team Premium Access options support a range of research needs from academic labs to industry partnerships. You can sign up anytime for free at eSpectra.aip.org and when you register, you receive a 30-day free trial of Premium Access. If you're unable to attend the session and have partnership questions, please email espectrasurfsci@aip.org.

MEMS and NEMS Group
Room A210 - Session MN-TuM

MEMS, BioMEMS, and MEMS For Energy: Processes, Materials, and Devices II
Moderators: Robert Davis, Brigham Young University, Zenghui Wang, Case Western Reserve University

8:00am **MN-TuM-1 Near-Zero Power Integrated Microsystems for the IoT**, *Matteo Rinaldi*, Northeastern University **INVITED**
The recent advancements in terms of sensor miniaturization, low power consumption and low cost allow envisioning a new era for sensing in which the data collected from multiple individual smart sensor systems are combined to get information about the environment that is more accurate and reliable than the individual sensor data. By leveraging such sensor fusion, it will be possible to acquire complete and accurate information about the context in which human beings live, which has huge potential for the development of the Internet of Things (IoT). To address the growing demand of such large wireless sensor networks, there is a need for wireless sensors with dimensions and power consumption that are orders of magnitude smaller than the state-of-the-art. Energy is the key challenge. Batteries have limited capacity, and existing sensors are not "smart" enough to identify targets of interest. Therefore, they consume power continuously to monitor the environment even when there is no relevant data to be detected. This talk presents a new class of zero-power microsystems that fundamentally brake this paradigm, remaining dormant, with zero-power consumption, until awakened by a specific physical signature associated with an event of interest. In particular, a zero-power infrared (IR) digitizing sensor microsystem consisting of plasmonically-enhanced micromechanical photoswitches is presented. Such a passive IR digitizer is capable of producing a wake-up bit when exposed to a specific IR spectral signature associated to a target of interest (such as the exhaust plume of a car, a forest fire, or a human body) while rejecting background interference. The capability of these zero-power sensors of consuming power only when useful information is present results in a nearly unlimited duration of operation, with a groundbreaking impact on the proliferation of the IoT.

8:40am **MN-TuM-3 Development of Inorganic Metal Salt Inks for Printable Sensor Applications**, *Y Sui*, Case Western Reserve University; *A Hess-Dunning*, Louis Stokes Cleveland VA Medical Center; *M Sankaran*, **Christian Zorman**, Case Western Reserve University
The rapid advancement of flexible and stretchable electronics has stimulated the development of printing approaches as a means to fabricate metallic interconnects, antenna and other essential conducting structures. Unfortunately, metal inks have been limited to silver, copper, and gold, due to the complexity of nanoparticle synthesis and metallo-organic compound design. While sufficient for interconnects, the development of printed sensors is significantly limited by the small selection of printable metals. Recently, we reported a new class of inks that are based on inorganic metal salts that are converted to metallic structures by exposure to a low-temperature inert gas plasma. This approach to ink design opens up a much wider range of printable metals than currently available from conventional inks. We found that chemical, biological and mechanical sensors fabricated using this printing approach significantly outperformed the same sensors fabricated using conventional approaches, presumably due to the surface morphology of the printed sensors.

In this paper, we describe a method of controlling the surface morphology for metal structures fabricated using plasma activation of inorganic metal salt-based inks. We have found that the ink solvent plays a key role in the nucleation and crystal growth of metal nanostructures during the plasma reduction process. Using solvents of different vapor pressures, we were able to control the duration of plasma-induced liquid-phase nucleation and crystallization, thereby tuning the surface morphology, conversion depth, and resistivity of the printed metal structures. Silver nitrate-based ink was used for this study and the ink solvents in order of decreasing vapor pressure were ethylene glycol (EG), di-ethylene glycol (di-EG), and tri-ethylene glycol (tri-EG). The structural, morphological, and electrical properties of metals printed with different ink solvents were characterized by cross-sectional scanning electron microscopy (SEM), optical profilometry, and sheet resistance measurements, respectively. To show that the tunable morphology can be used to enhance the sensitivity of printed sensors, we fabricated and tested a silver-based hydrogen peroxide sensor using inks made from the three solvents.

9:00am **MN-TuM-4 Void-Free Copper Electrodeposition in Full Wafer Thickness Through-Silicon Vias with 10:1 Aspect Ratios**, *Rebecca Schmitt*, *L Menk, C Sadler, E Baca, A Hollowell*, Sandia National Laboratories
Copper-filled through-silicon vias (TSVs) are incorporated in microelectronic devices as a 3D integration technique to increase I/O per unit volume. Industry has incentivized thinning wafers to increase TSV density, but certain MEMS applications require full thickness substrates, thus creating a demand for mesoscale TSVs. Using a full thickness silicon wafer helps preserve wafer flatness during multi-layer device fabrication and conserves mass, often required in MEMS applications. Traditionally, a three-additive Cu deposition chemistry is used for TSV filling; however, in this work, a single-additive chemistry has been established to achieve bottom-up superfilling in high-aspect ratio features. This electroplating chemistry involves a mixture of $CuSO_4$, CH_4O_3S or H_2SO_4, chloride, and a poloxamine suppressor additive. Cyclic voltammetry (CV) can be used to characterize the electrolyte and identify a hysteretic region, which is caused by suppressor breakdown at the cathode surface. This hysteresis corresponds to an operating window where void-free Cu filling of high-aspect ratio features can be achieved.

Previously, potentiostatic and galvanostatic deposition conditions for void-free filling were developed for nominally 100 μm diameter and 600 μm deep vias. Copper electrodeposition in TSVs with a 10:1 aspect ratio is currently under investigation. These TSVs have a 62.5 μm diameter etched into a 625 μm thick silicon-on-insulator (SOI) wafer. However, the conditions that resulted in void-free, bottom-up filling in 100 μm diameter TSVs have not translated to fill 62.5 μm geometries. In this work, electrolyte constituent concentrations, applied potential, and applied current were varied to analyze their effect on fill profile in 62.5 μm TSVs. Fill profiles were analyzed through cross sectioning and optical microscopy, as well as through X-ray CT scans. This work details the experimental approach associated with determining electrodeposition conditions for 62.5 μm diameter TSVs and presents the resulting fill profiles of copper in these vias.

Sandia National Laboratories is a multimission laboratory managed and operated by National Technology and Engineering Solutions of Sandia, LLC., a wholly owned subsidiary of Honeywell International, Inc., for the U.S.

Tuesday Morning, October 22, 2019

9:20am MN-TuM-5 Ion-Conducting Materials and Devices for Cold Atom Microsystems, *Christopher Roper*, HRL Laboratories, LLC; *S Kang*, NIST; *R Mott, A Mis*, HRL Laboratories, LLC; *E Donley, J Kitching*, NIST

Atomic instruments using laser-cooled atoms in ultra-high vacuum enable highly precise measurements of time, acceleration, and rotation [1]. Use of such devices outside the laboratory requires control of the atomic vapor density to prevent warm atoms from prematurely disturbing the cold atoms prior to measurement. Portable, miniature cold atom devices require a low-power, scalable method for controlling atomic vapor density.

Recently, solid-state electrochemical devices based on the solid electrolyte beta"-alumina have been used to change Rb vapor density on the scale of first 100s [2] and then 10s [3] of seconds. Reduction in vapor density up to 7X has been reported. Furthermore, these devices have been used to stabilize Rb vapor density using a feedback loop [4].

We present a solid-state electrochemical device consisting of a fine Pt grid top-electrode with submicron lithographically patterned features, beta"-alumina solid electrolyte, patterned Pt bottom electrode, and graphite reservoir. For relatively slow actuation cycle frequencies (17 mHz), this device exhibits a 100X increase in Rb vapor density with -30 V sourcing voltage and 20X decrease in the Rb vapor density with +30V sinking voltage. Rb vapor density can be modulated at up to 50 Hz, although at lower Rb vapor density dynamic range. An inverse relationship is found between Rb vapor density dynamic range and actuation cycle frequency. The high vapor density dynamic range and fast cycling rates demonstrated with this device are attributed to the fine, submicron top electrode features compared to coarse top electrode features (>100 μm) used in prior works. These devices are expected to be key components in future cold atom microsystems.

[1] J. Kitching, et al., IEEE Sensors J 11 (9), 1749 (2011).

[2] J. Bernstein, et al., Hilton Head 2016, pp. 180-184.

[3] S. Kang et al., Applied Physics Letters 110, 244101 (2017).

[4] S. Kang et al., Optics Express 26 (3) pp. 3696-3701 (2018).

9:40am MN-TuM-6 Determining the Material Properties of Carbon Nanotube Structures Through Cantilever Resonances, *Richard Cass*, Brigham Young University; *E Eion Hindsman-Curry*, University of Alabama; *R Vanfleet, R Davis, D Allred, B Anderson, R Vanfleet*, Brigham Young University

Nanotube Templated Microfabrication (CNT-M) processes use nanotube forest growth from a 2-D pattern to form 3-D structures. The resulting structure is then infiltrated with a second material to form the final device. Materials properties of these structures with different infiltration materials and varying degrees of infiltration is of interest.

We have used force-displacement data (in fixed-free and 3-point bending configurations) to determine the Ultimate Strength, the Young's Modulus, and the Maximum Strain of CNT-M structures using various infiltration materials. However, in the case of tungsten infiltration processes and typical test beams (~250 um in width), the infiltration was not sufficiently uniform for high confidence results. Smaller beams (< 50 um width) are difficult to handle using the conventional 3-point bending processes. We report resonance frequency testing, using a Laser Doppler Vibrometer (LDV), of thin CNT-M cantilevers to find the Young's Modulus of these CNT structures.

11:00am MN-TuM-10 Nanoporous Titanium Nitride Electrodes for Biosensing, *Mark Ming-Cheng Cheng*, *G Chen*, Wayne State University

We report corrosion-resistant and high-capacity implantable nanoporous titanium nitride (TiN) electrodes for neural probes applications Traditionally, the TiN electrodes are prepared using reactive sputtering techniques and have limited surface areas. To research smaller electrodes to minimize tissue damage, high aspect ratio TiN nanotube structures were fabricated using electrochemical anodization of Ti wires followed by high-temperature nitration. The specific charge capacity of nanoporous TiN correlates proportional with the surface area and pore size.

According to Shannon criteria, an empirical rule in neural engineering for possibility of tissue damage from electrical stimulation, the recommended limit density of a stimulation pulse is 30μCcm^{-2}for a geometric surface area of 0.06cm^2. Nevertheless, the charge injection capacity of chronically implanted electrodes has shown degraded over the time (within one month to a year), including sputtered iridium oxide (SIROF), porous platinum and tungsten. One of the challenges for these implantable electrodes involves irreversible reduction and oxidation reactions occurring at the electrode surface through faradic or pseudocapacitive charge transfer. On the other hand, TiN has different mechanism of charge injection (through capacitive double layers). TiN has been shown promising electrode material in neural implants thanks to its super electrical conductivity, biocompatibility and chemical stability. TiN is also known for physiologically inert and corrosion resistant. To increase the spatial resolution of neural stimulation, small electrodes with high surface areas are more desirable. To the best of our knowledge, TiN nanotubes electrodes have not been studied in the literature for neural implants. Compared to tungsten electrode, the impedance and morphology of nanoporous TiN was found stable over a long-term in stress tests (at an elevated temperatures in phosphorous buffered solution).

11:20am MN-TuM-11 Toward a Simple Process for Fabricating Multi-channel Neural Probes on Optical Fiber Substrates, *Md Ashiqur Khan*, *M Gheewala, V Jonnalagadda, T Tisa, M Rao, A Awale, P Motwani, N Randhawa, H Sajedi, W Shih, J Wolfe*, University of Houston; *J Dani*, University of Pennsylvania; *P Mauger*, No Matching Affiliation

Electrical probes are used to stimulate spiking activity within a target population of neurons and monitor how these electrical signals propagate through the brain. This paper describes a simple fabrication process for multi-electrode neural probes on optical fiber substrates. It relies on neutral particle proximity lithography to achieve the required depth-of-field and freedom from charging artifacts but circumvents the complexity of membrane masks (complementary exposures, radiation resistant coatings, and fragility) and on-fiber alignment.

Fig. 1 of the supplementary document shows, conceptually, a probe with 4-channel thin-film sensor, a tetrode, on each of four sides of a fiber. It requires two masks; the first for the interconnect traces. The other for vias in the dielectric overcoat where the metal lines contact the brain.

As shown in Fig. 2, optical fibers are held in V-grooves etched into the top surface of a (100) Si wafer. A second set of V-grooves, etched from the opposite side of the wafer, forms open windows at the bottom of the upper grooves. When this *mask* is illuminated by 50 keV He atoms, transmitted beamlets transfer the stencil pattern to resist on the fibers. A negative--tone, plasma-deposited, resist is used to mask the gold interconnects. The vias are similar, but require a tone-reversal step. Rotational alignment of the 2 masks uses a high precision cubic bead glued to the end of the fiber to reference the rotational angle of the fibers to a precision-ground aluminum platform on the jig. Longitudinal alignment is achieved using a fiber-stop. These are high precision (Grade 5) 440C stainless steel ball bearings which are held in an anisotropically etched pocket at the tip-end of a V-groove by a rare earth magnet. Longitudinal and transverse positional errors of 1.0 ± 0.6 mm and $0.3\pm.15$ mm, respectively. A single-interconnect mask can be printed multiple times to build the probe of Fig.1. The offset is produced by tilting the mask relative to the beam. Fig. 3 shows two lines printed on a 300 mm fiber with 21.5 and 29.5 mm offsets in the longitudinal and transverse directions, respectively.

Fig. 4 is an in-vitro recording from a brain slice (mouse) after a battery of bench tests, including a) a 3-week soak phosphate buffered, b) repeated insertion in agar and a stainless steel cannula, d) disinfection in MetriCide-2.6% glutaraldehyde, and a 6 hour implantation in mouse brain). Impedance spectra were the same within the measurement error of the impedance bridge before and after these bench tests.

At this time the tone reversal process has not been fully optimized.

11:40am MN-TuM-12 A Low-Temperature Packaging Process for Mechanically-Adaptive Neural Interfaces for Microfluidic-Aided Drug Delivery, *E Szabo, L Greenwood*, Case Western Reserve University; *Allison Hess-Dunning*, Louis Stokes Cleveland VA Medical Center

Advances in polymer-based materials development have led to an array of environmentally-responsive materials that are uniquely suited for biomedical implant applications. Compatible microfabrication processes

continue to be developed to integrate these responsive materials into biomedical microdevices. Progressing beyond proof-of-concept devices into functional implants for long-term use requires additional development of compatible and reliable packaging strategies to facilitate interfacing the microdevices with peripheral components. Our group has previously developed a mechanically-adaptive, polymer nanocomposite-based (NC) intracortical implant with a microfluidic channel for diffusion-based drug delivery. Interfacing the device with fluid pumps requires a means for secure attachment of polyethylene tubing to the inlet and outlet ports of the neural microdevice that will remain stable under physiological conditions. Packaging process considerations include incompatibilities of NC with organic solvents and temperatures exceeding 80°C. Additionally, out-of-plane forces on the devices must be minimized in order to maintain the integrity of the microfluidic channels.

We designed connectors to interface polyethylene tubing with the NC-based neural microdevices, to be built using a multi-jet 3D printer. Components produced using multi-jet printers typically have a plastic structural material and a wax-based support material that is removed during post-processing operations. However, our approach involves using a controlled, thin layer of the wax support material as a functional adhesive between the plastic connector and the NC device. With a melting point of 60°C, the wax is stable at body temperature (37°C) and can be melted and reformed at temperatures below the processing limit for the device. Because the wax is printed as part of the connector, the tubing ports can be aligned to the microfluidic inlet and outlet in a single step. Through this approach, we established a leak-free connector design and packaging process to facilitate a fluidic connection between syringe or osmotic pumps and NC-based microdevices. The adhesive bonding strength provided by the wax to the NC exceeded 37 MPa, much higher than the 0.75 MPa required to pump fluid through the connector and microfluidic channel. Packaged devices remained functional in phosphate buffered saline heated to 37°C, even after soaking for 24 hours. The potential for scaling the packaging process and for applying to other materials will also be discussed.

12:00pm **MN-TuM-13 Vascular Graft Pressure-Flow Monitoring Using Nanocomposite Carbon Black/PDMS Based Strain Sensors**, *Hao Chong*, Case Western Reserve University; *S Majerus*, Louis Stokes Cleveland VA Medical Center; *J Liu, C Zorman*, Case Western Reserve University

A vascular graft is commonly used to bypass damaged blood vessels or to form an arteriovenous shunt for vascular access (e.g. for hemodialysis). Real-time monitoring of blood flow in synthetic grafts would provide early warning of graft failure to permit interventions such as angioplasty or graft replacement to avoid catastrophic failure. Based on biocompatible materials, we have developed a new type of flexible pulsation sensor (FPS) which is wrapped around a graft to monitor blood pressure and flow. The FPS uses Carbon Black (CB) dispersed in polydimethylsiloxane (PDMS) as a piezoresistive sensor layer, which is stencil printed on a structural PDMS layer. In this study, we analyze the strain transducer mechanisms on a vascular graft and show the linear and stable strain response of CB-PDMS composites from 0-50% strain. The material has a broader strain range than graft materials and a gauge factor of 5. In vitro testing of the FPS on a vascular graft phantom showed a robust, linear sensor output to pulsatile flows and pressures. The composite material shows excellent potential in biologic strain sensing applications where a flexible sensor with large maximum strain range is needed.

Plasma Science and Technology Division
Room B131 - Session PS+EM-TuM

Advanced FEOL

Moderators: Keren Kanarik, Lam Research Corporation, Alok Ranjan, TEL Technology Center, America, LLC

8:00am **PS+EM-TuM-1 Investigation on Plasma Etch Technology Enabling Si/SiGe MOSFET Process Integration**, *Yohei Ishii,* Hitachi High Technologies America Inc.; *Y Lee, W Wu,* Taiwan Semiconductor Research Institute, Taiwan, Republic of China; *R Sugano,* Hitachi, Ltd., Japan; *K Maeda,* Hitachi High Technologies America Inc.; *H Ishimura,* Hitachi High-Technologies Taiwan Corp., Taiwan, Republic of China; *M Miura,* Hitachi High Technologies, Japan **INVITED**

Many challenges have emerged due to down-scaling of device structure in order to follow Moore's law. By modifying the transistor structure from planar to Fin-type Field Effect transistors (FinFETs), transistor electro-statics were improved, which led to overcoming short-channel effects. However, the change is no longer sufficient, and the semiconductor industry faces difficulty to further improve the transistor performance. One of the promising candidates for the improvement in sub-10nm process is to utilize Silicon/Silicon-germanium (Si/SiGe) dual channel FinFETs (Si in n-FETs and SiGe in p-FETs). In this case, simultaneous etching of Si and SiGe is required [1]. However, etch rate of SiGe is greater than Si for halogen chemistries commonly used in Si etch. Therefore, it is required to develop selective Si etch over SiGe for etch rate control between these two materials.

In order to maximize electrical performance of SiGe, modifying the SiGe surface composition into Si-rich surface at SiGe/gate-oxide interface is critical to reduce interface state density due to the impact on sub-threshold characteristics [2]. Traditional methods to produce Si-rich surface are epitaxial growth of Si cap over SiGe fin [3] and GeOx-scavenging process [4]. However, thermal budgets of these methods are relatively high, and there are concerns of strain relaxation in SiGe channel and Ge diffusion into Si substrate, both of which deteriorate the FET characteristics. Hence, a low-temperature process to produce Si-rich surface is required.

In this presentation, we will present two phenomena; one is Si-SiGe selective etch control, and the other is SiGe surface composition modification of SiGe into Si-rich surface by low temperature plasma. We will first present a plasma process, which etches Si selective to SiGe for Si-SiGe etching control, and will discuss the etching mechanism of the selective etching. We will then present the composition modification into Si-rich surface by utilizing Si segregation from the low temperature plasma process. This plasma etch technique can solve the etch rate control and surface composition challenges, which can be a promising scheme for realizing well-controlled SiGe finFETs with improved characteristics.

[1]. Y. Ishii et. al., Jpn. J. Appl. Phys. **57**, 06JC04 (2018).

[2]. C. H. Lee et. al., IEDM Tech. Dig., p.31.1.1., 2016

[3]. H. Mertens, et al., VLSI Tech. Dig., p.58, 2014

[4] C.H. Lee, et. al., VLSI Tech. Dig., p. 36, 2016

8:40am **PS+EM-TuM-3 Etching of Sub-10 nm Half-pitch High Chi Block Copolymers for Directed Self-Assembly (DSA) Application**, *Maria Gabriela Gusmão Cacho*, *P Pimenta-Barros, K Benotmane, A Gharbi, M Argoud,* CEA-LETI, France; *C Navarro,* Arkema France, France; *K Sakavuyi,* Brewer Science Inc.; *R Tiron, N Possémé, S Barnola,* CEA-LETI, France

As the semiconductor industry approaches the smaller technologic nodes such as the sub-10 nm, conventional lithography technologies have reached their limit. Among the different approaches investigated to continue pattern scaling, Directed Self-Assembly (DSA) of Block Copolymers (BCP) is one of the most promising due to its simplicity, low manufacturing cost and capability to design high density cylindrical or line/space patterns. For the last few years, PS-*b*-PMMA has been the most used BCP for this application. However, since the minimum feature size for the PS-*b*-PMMA system is limited to ~13 nm due to its low interaction parameter (also known as "chi"), new systems have been developed to achieve higher resolution by improving its microphase separation strength, thus obtaining the so called "high chi" BCPs.

In this paper, the high chi BCP system investigated is a modified PS-*b*-PMMA that presents a pitch of 18 nm, which will be referred to as "L18". One critical step for its integration is the PMMA removal selectively to the PS. The results obtained with both dry and wet etching of the L18 BCP are presented, highlighting the challenges encountered due to its smaller dimensions.

A wet PMMA removal process based on UV exposure followed by IPA rinse will be presented. An Ar/O_2 dry etch step for the brush layer opening was developed and the transfer of the line/space pattern into the SiO_2 and Si underlayers was demonstrated for the L18 BCP. However, this wet development is expected to cause pattern collapse when the BCP will be guided by chemoepitaxy due to capillary forces.

Therefore a complete PMMA removal by dry etching alone was also investigated. Different etching chemistries based on $CH_3F/Ar/SO_2$, CH_4/N_2 or cyclic $CO + CO/H_2$ were applied to the modified PS-*b*-PMMA BCPs with a 30 nm pitch and with an 18nm pitch (L18). For the 30 nm-pitch BCP, all three plasma chemistries allow the complete PMMA and brush layer removal by dry etching and the subsequent pattern transfer into the SiO_2 layer. In contrary, for the L18 BCP, the $CH_3F/Ar/SO_2$ plasma does not present enough PS budget for pattern transfer due to its low selectivity and the small thickness of the BCP. For the more passivating chemistries such as CH_4/N_2 and cyclic $CO + CO/H_2$, which have higher selectivity, we observe

the formation of bridges that prevent complete pattern transfer. We used *ex-situ* X-ray Photoelectron Spectroscopy (XPS) to investigate the origin of these bridges and to understand the etching mechanisms present.

9:00am PS+EM-TuM-4 Mechanism of Highly Selective SiCN Etchings Using NF₃/Ar-based Gases, *Miyako Matsui,* Hitachi Ltd., Japan*; K Kuwahara,* Hitachi High-Technologies Corp., Japan

Highly selective etchings over various other materials are increasingly required to achieve self-aligned processes, which provide higher density devices without shrinkage of the pattern dimensions in three-dimensional devices, such as fin-based field-effect transistors. In a self-aligned process, SiCN etching is required to achieve high selectivity to both SiO_2 and Si_3N_4. However, it had been difficult to achieve high selectivities to both SiO_2 and Si_3N_4 using fluorocarbon gas chemistries. For example, selectivity to SiO_2 increased using a hydrofluorocarbon plasma, while selectivity to Si_3N_4 decreased. So, it is important to investigate gas chemistries to simultaneously control selectivities to various materials.

In this study, mechanisms for highly selective SiCN etchings with microwave ECR plasma using NF₃/Ar-based gases were investigated over various materials. The rate of SiCN etching using NF₃/Ar plasma was higher than that of other materials, which were TiN, poly-Si, SiO_2, and Si_3N_4. The SiCN was etched with NF₃/Ar plasma, which formed SiF_x and FCN. On the other hand, other materials were etched with low rates. To achieve higher selectivities, the effects of adding gases to NF₃/Ar plasma on various materials to inhibit etching were analyzed by X-ray photoelectron spectroscopy (XPS).

Firstly, a highly selective SiCN etching over poly-Si was achieved by adding O_2 to NF₃/Ar plasma. This was because poly-Si etching was inhibited by the formation of a 1.0 nm-thick oxidized layer, which protected the poly-Si surface from the etching reaction with F radicals. The SiCN etch rate also decreased when the poly-Si etching was stopped. However, C atoms contained in the SiCN layer reacted with O radicals and controlled oxidization of the SiCN surface.

Next, highly selective SiCN etchings over SiO_2 and Si_3N_4 were achieved by using a NF₃/Ar-based plasma by which deposited layers were formed on the surfaces. The deposited layers formed on the SiO_2 and Si_3N_4 protected the surfaces from being etched by reacting with F radicals. On the other hand, the deposited layer was thought to be more difficult to be formed on the SiCN.

Lastly, highly selective etching over TiN was achieved by using H₂-added plasma. XPS result showed that a thin protective layer containing TiF_x and ammonium fluoride, which is decomposed over 673K, had been formed on the TiN surface. The protective layer formed on the TiN surface was very effective at protecting the TiN from being etched by F radicals.

In conclusion, we achieved extremely highly selective SiCN etchings over various materials by forming protective layers, which were formed on non-etched materials by adding gases to NF₃/Ar plasma.

9:20am PS+EM-TuM-5 Impact of Plasma Process on Source/Drain Epitaxy Film, *Yun Han, B Messer, M Sapel, H Kim, Y Shi, M Wang, Y Trickett, K Maekawa,* TEL Technology Center, America, LLC*; K Taniguchi, S Morikita,* Tokyo Electron Miyagi Ltd., Japan*; A Metz, P Biolsi,* TEL Technology Center, America, LLC

Middle-of-Line (MOL) contact open by plasma etching is a very critical step in logic IC fabrication. Source/Drain Epitaxy (S/D Epi) film as a key element in device transistors controls device performance in various aspects. S/D Epi film damage induced by plasma etch processes have been one of the challenges in MOL integration. Epi film damage includes surface roughening and oxidation, crystal structure relaxation and elemental doping, all of which could lead to uncontrolled variation and degradation in electrical performance of the devices. In this paper, SiGe (known pMOS S/D material) film damage post varying CCP plasma conditions have been studied by utilizing different characterization techniques including X-ray photoelectron spectroscopy (XPS), Transmission Electron Microscope (TEM) / Energy-dispersive X-ray spectroscopy (EDS), Rutherford backscattering spectrometry (RBS) and Secondary ion mass spectroscopy (SIMS). Various CCP plasma conditions include changes in gas chemistries (N/H/O/C/F/Ar), plasma source/bias power and chamber configurations. Electrical response on short loop device wafers have been collected and correlated with observed physical/chemical changes in S/D Epi film post plasma processes. We also performed molecular dynamics, quantum chemistry and chamber scale simulation to understand the fundamental chemical behavior and characterize the surface/chemical properties between provided plasma and SiGe film at various ion energy and

ion/radical flux in an atomic/molecular level. The study provides a comprehensive understanding in plasma damage to S/D Epi film and a fundamental guideline in optimizing plasma processes to achieve ideal contact open etch with minimal damage on source/drain Epi film.

9:40am PS+EM-TuM-6 CCP Dry Clean Process Development Using Quadrupole Mass Spectrometer and Optical Emission Spectroscopy, *Harutyun Melikyan, A Martinez, S Pandey, M Koltonski, G Sandhu,* Micron Technology

Dual frequency capacitive coupled plasmas provide flexible control of ion energy distributions, enabling high selectivity for etching of different materials, and flexibility to develop more efficient dry clean processes for higher productivity. It is common for each patterned wafer etch to have pre and post dry clean steps, with and without wafer, respectively. The primary focus of dry etch engineers is to design high etch rate processes, with minimized process time, and without changing the critical dimensions. Additionally, significant gains can be achieved by optimizing the dry clean recipes because they contribute significantly to the raw process time. In some cases, it can take a long time to achieve proper pre and post conditioning of the chamber.

In this work, we show that real-time monitoring techniques can be used to provide insight into the etch process byproducts, enabling intelligent development of the dry clean recipes. Integrating quadrupole mass spectrometry and optical emission spectroscopy with the capacitive coupled plasma reactor, and monitoring in parallel, we were able to identify 99% of the patterned wafer etch byproduct species with high confidence. Knowing the etch byproducts provides a clear path to an optimized dry clean process. We were then able to develop the dry clean recipe with appropriate precursor gases to increase volatile byproducts significantly (e.g. SiF4 at 33%) and minimize non-volatile byproducts (e.g. ammonium salts at <1%), resulting in a 70% reduction of dry clean process time.

11:00am PS+EM-TuM-10 Surface Reaction of Atomic Hydrogen with SiGe Surface Compared with Si Through Ab-initio Calculations, *Ryoko Sugano,* Hitachi, Ltd., Japan*; Y Ishii, K Maeda,* Hitachi High Technologies America Inc.*; M Miura, K Kuwahara,* Hitachi High Technologies, Japan

Simultaneous etching of Si and SiGe is an indispensable process for high throughput in the fabrication of Si/SiGe dual-channel FinFETs. SiGe etch rate is higher than Si etch rate by typical halogen chemistries used for Si etching [1]. Therefore, to control the etch rate between Si and SiGe, it is necessary to develop the chemistry that gives a higher Si etch rate than SiGe etch rate. Recently Ishii et al. have reported that hydrogen plasma selectively etched Si over SiGe, showing the selective Si removal over Ge [2]. In spite of selective Si etching over Ge, the Si-rich surface was observed after the hydrogen plasma exposure. They have attributed the Si-rich surface to hydrogen-induced Si surface segregation [2].

To understand the mechanism of the experimental phenomena on SiGe film described above, we performed ab-initio calculations that combined geometry optimizations and Nudged Elastic Band calculations. In the hydrogen-terminated SiGe surface system, we assumed the reacted states of SiGe were single dimer, in which three hydrogen atoms adsorbed on one of the dimer atoms (SiH3, GeH3) and a single hydrogen atom adsorbed on another of the dimer atoms. We found that the formation with SiH3 was energetically stable and was easy to desorb with a lower activation energy than that with GeH3. We considered that the selective Si removal over Ge was caused by both the selective formation and selective desorption of SiH3. We also calculated the formation energy of the SiGe surface immediately after selective Si removal, which originated from dimer breaking. It was found that the site exchange between the Ge atom in the first layer and the Si atom in the second layer was energetically favorable when another dimer atom left on the surface was terminated with a hydrogen atom. In conclusion, we confirmed experimental results of both selective Si etching over SiGe and Si surface segregation under the condition of hydrogen plasma by performing ab-initio calculations.

[1] G. S. Oehrlein, et al., Appl. Phys. Lett. 58, 2252 (1991).

[2] Y. Ishii et al., Jpn. J. Appl. Phys. 57, 06JC04 (2018).

11:20am PS+EM-TuM-11 Nanopantography with Reusable Membrane-based Electrostatic Lens Arrays, *Ryan Sawadichai, Y Chen, P Basu, V Donnelly, P Ruchhoeft, D Economou,* University of Houston

Nanopantography is a method for massively parallel writing of nano-sized patterns using an ion beam in combination with a reactive gas. In this process, a broad area, collimated, nearly-monoenergetic ion beam is directed towards an array of micron-scale electrostatic lenses in direct

contact with a substrate. By applying an appropriate DC voltage to the lens array with respect to the substrate, the ion beamlet entering each lens converges to a fine spot that can be 100 times smaller than the diameter of each lens. Previously, lenses fabricated directly on the silicon substrate were used to etch 3 nm diameter holes in silicon by exposure to a monoenergetic Ar^+ ion beam and chlorine gas. This work reports on the development of removable and reusable free-standing membrane-based electrostatic lens arrays that are designed to pattern any conducting surface. The lens arrays were fabricated on a silicon wafer coated with PMGI, SU-8, gold, copper, and PMMA. Lens openings were lithographically defined, and an acrylic frame was placed over the array. The lens patterns were etched through the SU-8 and the membrane was released by dissolution of the PMGI layer. The applied voltage used to focus the ion beamlets also served to electrostatically clamp the lens array to a conducting substrate, which was observed as a flattening of the membrane against the substrate surface and an increasing capacitance measured between the lens array and the substrate. An array with lens diameters between 0.8 μm and 1.5 μm and dielectric thickness of 1 μm was used to pattern nanoscale features on a silicon substrate using a 70 eV Ar^+ ion beam and chlorine gas. Ion trajectory simulations were performed to understand the sensitivity of minimum feature size to the variation of lens potential, lens aspect ratio, and lens size. Simulations agreed with the experimentally observed patterns when chromatic and spherical aberrations were considered. With a thinner dielectric and higher lens voltage, it should be possible to print sub 10-nm features in a step and repeat nanopantography process.

Plasma Science and Technology Division
Room B130 - Session PS-TuM

Plasma Diagnostics and Sources I

Moderators: Tetsuya Tatsumi, Sony Semiconductor Solutions Corporation, Geun Young Yeom, Sungkyunkwan University, Korea

8:00am **PS-TuM-1 Optimizing Power Delivery in a Pulsed Inductively Coupled Plasma Using Set-Point Impedance Match and Frequency Tuning**, *Chenhui Qu*, University of Michigan; *J Brandon, C Smith, S Shannon*, North Carolina State University; *D Coumou, S White*, MKS Instruments; *M Kushner*, University of Michigan

During pulsed operation of inductively coupled plasmas (ICPs) using radio frequency (RF) power, the resistance of the plasma can change by factors of 10-100 while the reactance can change sign (from negative to positive during an E-H transition). These changes in impedance add to the intrinsic impedance of the reactor. The components in the impedance matching network (IMN) hat interface the reactor to the power supply typically cannot be changed rapidly enough to track the plasma transients and maintain a match. The IMN is then tuned to match at a specified time during the plasma pulse, a process called set-point-matching. With feedback control systems and wideband amplifiers, it is possible to make a real-time adjustment of the frequency of the RF oscillator to provide a real-time impedance matching.

In this work, impedance matching to a pulsed ICP plasma was computationally and experimentally investigated using set-point-matching and frequency tuning. The Hybrid Plasma Equipment Model (HPEM) was used for the computational investigation with results compared to experiments performed on the ICAROS reactor, consisting of a four-turn solenoidal coil powering a cylindrical ICP having a 5 cm radius and 15 cm height. The ICPs were operated in Ar at pressures of 1-50 mTorr. The RF power (frequencies from 10-14 MHz) was pulsed modulated at 10 kHz pulsed power with 50 W amplitude and 50% duty cycle.

Set-point-matching early during the pulsed cycle produces more rapid rise in the plasma density while having high reflective power late in the pulse. Set-point-matching late during the pulsed cycle produces a slow rise in the plasma density while having low reflective power late in the pulse. Frequency tuning is able to functionally match during the entire pulsed cycle. For example, when the IMN was set to match in the early period during the pulse, frequency tuning within a range of ±2 MHz is able to maintain reflected power to be less than 10%, and functionally zero late in the pulse. Combinations of set-point-matching and frequency tuning are able to match pulsed-operation over a wide range of power, pressure, pulse repetition frequency and duty cycle.

8:20am **PS-TuM-2 Compact Surface Wave Plasma Source**, *G Panici, David Ruzic, D Qerimi, D Barlaz,* University of Illinois at Urbana-Champaign; *B Jurczyk,* Starfire Industries LLC

Surface wave plasmas have been used increasingly in industrial applications due to their high electron densities (10^{11-12} cm^{-3}), high radical densities (10^{13-14} cm^{-3}), and low electron temperatures (1-5 eV). Typical radical creation systems generate radicals at a distance from where they are needed. A compact surface wave plasma source can generate and deliver the radicals at the surface where etching is desired. The source is microwave driven, operating in the hundreds of megahertz. At these frequencies, the wave reflects at the plasma sheath boundary due to the cutoff frequency of electrons once the plasma reaches critical density (typically a microsecond). The power is then largely deposited in the sheath, creating a plasma along the surface. In addition to local radical delivery, they can operate from fractions of millitorr to 10 torr and utilize a variety of antenna geometries (lines, arcs, plates).

A compact surface wave plasma source was characterized over a large range of pressures. The electron densities, electron temperatures and radical densities were measured as a function of distance from the plasma source. Multiple gas species were used to investigate the influence on plasma and radical parameters. These results will be presented.

8:40am **PS-TuM-3 Overview of Linear Plasma Sources as Applied to Ribbon ion and Plasma Beam Processing of Scanned Substrates**, *Peter Kurunczi,* Applied Materials, Varian Semiconductor Equipment **INVITED**
Ribbon beams of ions and plasmas offer unique capabilities within scanned substrate processing techniques such as ion implantation, physical and chemical surface modification, etching and deposition. This talk will cover an overview of ribbon beam technology used across a range of applications, with examples from processing of silicon, glass, and flexible plastic substrates used within semiconductor, display and roll to roll web industries. Various types of linear plasma sources and methods of ion beam generation will be discussed. Of note are the very different types of plasma ion sources used, from magnetized dc discharges driven by thermionic cathodes to rf generated plasmas. The audience is encouraged to extrapolate to how ribbon beams can be used for their specific material processing needs, for example as applied to this year's symposium theme of "Materials, Technologies and Processes for Energy Transition"

9:20am **PS-TuM-5 Online Diagnostics of Non-Thermal Plasma Nanoparticle-Laden Systems by Ion Mobility Spectrometry**, *Xiaoshuang Chen, S Ghosh, D Buckley,* University of Minnesota, Minneapolis; *M Sankaran,* Case Western Reserve University; *T Seto,* Kanazawa University, Japan; *U Kortshagen, C Hogan,* University of Minnesota, Minneapolis
Non-thermal plasmas (NTPs) have been shown to be capable of producing chemically-pure, size-controlled, low polydispersity, crystalline nanoparticles (NPs). Vapor-phase precursors are dissociated in the NTP reactor, typically by high electron energy impact, leading to nucleation and NP growth in the gas phase. A prevailing thought is that the NPs are unipolarly charged negative in the plasma, which mitigates coagulation and promotes surface growth, yielding low polydispersity NPs. In this study, we apply ion mobility spectrometry (IMS) as an online diagnostic to NTPs to address particle charging and coagulation.

In the first part of the study, we present an IMS system developed for low pressure to characterize Si nanocrystals synthesized in a radio-frequency (RF), capacitively-coupled NTP operating at 2 Torr. A uniquely designed low-pressure differential mobility analyzer (LPDMA) coupled with an electrical detector was utilized to measure NP size distributions in real time. Via the Twomey-Markowsi inversion approach, we have demonstrated, for the first time, that DMAs can be utilized to analyze NPs synthesized in low-pressure NTPs. Excellent agreement was found between the size distributions measured and inverted by LPDMA system and inferred from TEM images. Importantly, we found that at the outlet of the NTP flow tube reactor, Si NPs are bipolarly charged with nearly identical size distribution functions for both negatively and positively charged NPs. Furthermore, NPs are modestly aggregated, implying that the decharging of NPs exiting the plasma reactor from highly negative charge states to a bipolar charge distribution likely drives aggregation on the plasma boundary.

In the second part, ion-mobility mass-spectrometry (IM-MS) method was implemented to study the morphology of as-synthesized carbon-coated Ni NPs generated in an atmospheric-pressure DC microplasma. Sequentially, NPs were sampled by a DMA that classifies NPs by their mobilities, and an aerosol particle mass analyzer (APM), which separates NPs by masses. The concentration of size-mass classified NPs was measured by a condensation

particle counter (CPC) downstream of the DMA-APM system, yielding two-dimensional (2D) size-mass distribution function. The shape and location of the sampled NPs on the 2D contour plot reveal their morphologies and extent of aggregation. Utilizing fractal theory to describe particle mobility, particle morphologies were described quantitatively. Our results demonstrate that Ni NPs leaving the plasma reactor are aggregated in chain-like, low fractal dimension aggregates, which are also verified by TEM images.

9:40am PS-TuM-6 Experiment-Model Comparisons in Capacitively Coupled Plasmas at Moderate Pressures for Argon, Helium and Nitrogen, *David J. Peterson,* North Carolina State University*; T Koh, T Chua, W Tian, K Bera, S Rauf, P Kraus,* Applied Materials, Inc.*; S Shannon,* North Carolina State University

Discharge parameters including electron density, effective collision frequency, effective electron temperature, voltage & current characteristics and sheath thickness around the probe are measured over different pressures and powers ranging from 0.01-4.0 Torr and 10-100 W in Ar, He and N2 plasmas. Fully floating hairpin resonator probes are used in a parallel plate capacitively coupled radiofrequency (rf) discharge driven at 13.56 MHz with a gap distance of 1 inch. Probe measurements are made in the axial and radial directions. Effective collision frequency is measured using the resonance full width half max. Effective electron temperature can determined from the effective collision frequency through the plasma conductivity equation but must assume an electron energy distribution function (EEDF). Probe sheath thickness is measured using a time resolved measurement system capable of ~5 ns time resolution. High temporal resolution is utilized to measure rf phase resolved electron density and effective collision frequency. Measurements indicate the presence of enhanced ionization rates near the powered sheath edge in the collisional regime. Electron density peaks at the discharge center at lower pressures, <100 mTorr, and begins to shift towards the powered electrode at higher pressures due to a measurable DC self bias that is known to occur for geometrically asymmetric discharges. The influence of axial probe spatial resolution and approaches for providing sufficient probe isolation from ground are discussed. Spatial profiles of plasma parameters along with voltage & current characteristics are compared with 2-dimensional fluid plasma simulation results. Detailed model-experiment comparisons play an important role in understanding plasma chemistry mechanisms for these low temperature plasmas at moderately high pressure. All analysis and data acquisition is done with python scripts which are freely available to the public.

11:00am PS-TuM-10 Optical and Mass Spectrometric Measurements of O_2 and NF_3 Dissociation in a Low Frequency, High Density, Remote Plasma, *Hanyang Li, Y Zhou, V Donnelly,* University of Houston*; J Chiu, X Chen,* MKS Plasma & Reactive Gas Solutions

Remote plasma sources are widely used in many applications, such as chamber cleaning and flowable chemical vapor deposition (FCVD). Processes using remote plasmas are purely chemical in nature, since there are no ions present. In such processes, it is desirable that the dissociation rate of the feed gases in the plasma source be as high as possible, while recombination rates of reactive species on the way to a downstream chamber should be minimized. Only a few studies have been reported on low frequency, high pressure, very high density remote plasma sources. In this paper we present results on radical densities and gas dissociation fractions for a 400 kHz toroidal transformer-coupled plasma source (MKS Instruments), operating at a power density of $5 - 50$ W/cm^3 with feed gases mixtures of O_2 or NF_3 with Ar, and pressures of 0.4 or 2.0 Torr. The radical densities and feed gas dissociation percentages in the plasma were measured by optical emission spectroscopy (OES), combined with Ar actinometry. Plasma products flow into an anodized Al downstream chamber that is probed by vacuum ultraviolet (VUV) absorption spectroscopy and line-of-sight molecular beam mass spectrometry, allowing radical and stable species number densities to be determined in the plasma source as well as in the downstream chamber. The dissociation of O_2 and NF_3 was found to be roughly from 60% to 10% with the rise O_2% in plasma and >95% in the plasma source (via Ar actinometry with O and F) and not very dependent of flow rate. Midway across the downstream chamber, substantial recombination of O to form O_2 (via VUV O_2 absorption) occurred; the O/O_2 ratio was a strongly increasing function of increasing flow rate. At the back wall of the downstream chamber, O has nearly completely recombined to O_2 (mass spectrometry), even at the highest flow rate. NF_3 is completely dissociated and does not reform in the downstream chamber; no NF or NF_2 was detected. F was found to be mostly recombined to for F_2 at the back of the downstream chamber. The F_2, F and N_2 product absolute number densities confirmed the 3:1 F:N mass balance of the NF_3 feed gas. The gas temperature at the back downstream chamber was also measured by mass spectrometry, and was found to be 450K for 95% NF_3/Ar at a flow rate from 200 sccm to 600 sccm and 2.0 Torr.

11:20am PS-TuM-11 A Combined Experimental and Modeling Study of Reactive Vapor-nanoparticle-plasma Interactions in a Dusty Atmospheric-pressure Plasma, *Nabiel Abuyazid,* Case Western Reserve University*; X Chen,* University of Minnesota, Minneapolis*; D Mariotti, P Maguire,* University of Ulster, UK*; C Hogan,* University of Minnesota, Minneapolis*; M Sankaran,* Case Western Reserve University

Low-temperature (non-thermal), atmospheric pressure plasmas are characterized by several important fundamental and technological advantages for the gas-phase synthesis of nanoparticle materials. However, the effect of the particles on these plasmas remains poorly understood. It is generally accepted that nanoparticles acquire charge, typically negative, which leads to a reduction in the electron (plasma) density. The degree of reduction is not known and experimental measurements are challenged by several issues. One, plasmas operated at atmospheric pressure are small in size (~1 mm) and probes cannot be easily introduced into the plasma volume. Two, there are strong gradients in the plasma volume as the precursor vapor is dissociated and nanoparticles nucleate and grow, and the effect of particles on the plasma must be decoupled. Three, the material could have other effects on the plasma, for example by undergoing further reactions or by vaporizing after particle formation, that must also be isolated or avoided.

We present a tandem, atmospheric-pressure plasma system that separates a first "reactive" plasma, where the precursor vapor is dissociated leading to particle growth, from a second "dusty" plasma, where the effect of particles on the plasma can be studied. Two non-contact methods, an external electrical conductivity probe (Impedans Octiv Poly) and spectroscopy are applied on the dusty plasma to monitor changes in the electron density. We focused our study on carbon which has a relatively high boiling point and should be chemically stable within the plasma environment. The measurements show that electron densities decrease as expected upon the introduction of the nanoparticles into the second plasma at all powers. For example, at a power of 50 W, the electron density decreased from 4.0×10^{14} cm^{-3} for a pure Ar plasma to 3.6×10^{14} cm^{-3} for a dusty Ar plasma with a total particle concentration of about 4.0×10^6 particles/cm^3. Monte Carlo simulations were carried out in support of experiments and showed that by preferential negative charging, particles in plasmas can reduce bulk electron concentrations. We will also discuss the effect of residual hexane vapor and possible particle evaporation on plasma properties.

Materials and Processes for Quantum Information, Computing and Science Focus Topic
Room B231-232 - Session QS-TuM

AVS Quantum Science (ALL INVITED SESSION)
Moderators: Eray Aydil, New York University, Ivan Petrov, University of Illinois at Urbana-Champaign

8:00am QS-TuM-1 Quantum Technologies from Cold Atoms to Matter-waves, *Philippe Bouyer,* CNRS, France   **INVITED**
The remarkable success of atom coherent manipulation techniques has motivated competitive research and development in precision metrology as well as quantum simulation.

Our ability to cool down atoms to temperature near absolute zero lead to the production of new state of matter e.g. dilute atomic Bose-Einstein condensates (BEC) and degenerate Fermi gases (DFG) where the single or collective quantum behaviour of the particles takes over their classical properties. At these temperatures, atoms can be described by matter waves which behaviour can help understanding quantum properties of conduction, or with which we can create matter-wave sensors that are sensitive to rotation, acceleration or gravitation.

Quantum transport (eg the conduction of electrons in an imperfect crystal) is today widely investigated by using atoms in controlled potentials that mimic the properties of a solid or a semiconductor. While the ideal case is when no defects exist in the periodic potentials used to reproduce the solid matrix, it is also possible to introduce controlled disordered that will lead to peculiar quantum conduction properties. Semi-classical theories, such as those based on the Boltzmann equation, often fail to fully describe the transport properties and the ultra-cold atoms provide a "quantum

simulator" to investigate such properties. These properties extend from Anderson localization, percolation, disorder-driven quantum phase transitions and the corresponding Bose-glass or spin-glass phases.

Matter-wave inertial sensors – accelerometers, gyrometers, gravimeters – use our exquisite control of the matter-wave resulting form cooling atoms near absolute zero. They are today all at the forefront of their respective measurement classes. Atom inertial sensors provide nowadays about the best accelerometers and gravimeters and allow, for instance, to make the most precise monitoring of gravity or to device precise tests of general relativity. The outstanding developments of laser-cooling techniques and related technologies allowed the demonstration of matter-wave interferometers in micro-gravity. Using two atomic species (for instance ^{39}K and ^{87}Rb) allows to verify that two massive bodies will undergo the same gravitational acceleration regardless of their mass or composition, allowing a test of the Weak Equivalence Principle (WEP). New concepts of matter-wave interferometry are also currently developed to study sub Hertz variations of the strain tensor of space-time and gravitation, providing a new window of observation for gravitational waves detectors.

I present here some recent advances in theses fields

8:40am QS-TuM-3 Generating Maximal Entanglement Between Spectrally Distinct Solid-state Emitters, *D Hurst,* University of Sheffield, UK*; K Joanesarson,* University of Sheffield, UK, Tech. University of Denmark*; J Iles-Smith,* University of Sheffield, UK*; J Mork,* University of Denmark*; Pieter Kok,* University of Sheffield, UK **INVITED**
We show how to create maximal entanglement between two spectrally distinct solid-state emitters embedded in a waveguide Mach-Zehnder interferometer. By tailoring the input to the interferometer, we optimise the concurrence of the emitter qubits states and show that a two-photon input state can generate deterministic maximal entanglement even for emitters with significantly different transition energies and line-widths. The optimal frequency is determined by two competing processes: which-path erasure and interaction strength. Smaller spectral overlap can be overcome with higher photon numbers, and quasi-monochromatic photons are optimal for entanglement generation. Our work reveals a rich underlying structure in multi-photon scattering from two non-identical emitters, and provides a new methodology for solid-state entanglement generation, where the requirement for perfectly matched emitters can be relaxed in favour of optical state optimisation.

9:20am QS-TuM-5 From Quantum Atom Optics to Living Cells with Sculpted Light, *Halina Rubinsztein-Dunlop, T Neely, G Gauthier, T Bell, A Pritchard, K Goddard-Lee, A Stilgo, I Favre-Bulle, S Zhang, T Nieminen, I Lenton,* University of Queensland, Australia **INVITED**
Spatial light modulators (SLM) or Digital Micromirror Devices (DMD) give us a great flexibility in sculpting light. What is means is that we have perfect tools that can be used for production of configurable and flexible confining potentials and utilise them to confine atoms as well as lager scale objects and conduct novel experiments outlining light –matter interaction in these systems. In general, we divide the techniques that are used to sculpt light to those based on time average methods and those utilising SLMs in either Fourier plane or direct imaging plane. A Gaussian beam can be modulated using two-axis acousto-optic modulator (AOM) to create highly configurable time-averaged traps. SLMs in Fourier plane control the phase and /or amplitude of an input Gaussian beam, with the pattern representing the spatial Fourier transform of the desired amplitude pattern. The optical system then focuses this sculpted light pattern to the plane containing the system of interests, performing a Fourier transform and recovering the desired pattern. The optical system then focuses this sculpted light pattern to the plane containing the system of interests, performing a Fourier transform and recovering the desired pattern. DMD can configure the amplitude of an input beam either in the Fourier plane or in a direct imaging configuration. Sculptured light produced using these methods promises high flexibility and an opportunity for trapping and driving systems ranging from studies of quantum thermodynamics using ultra cold atoms to trapping and manipulating nano and micron-size objects or even making measurements *in-vivo* inside a biological cell.

In this talk, I will present techniques and results that open up new avenues for the study of quantum fluids, be it by providing a concise atomtronic model for predicting superfluid transport or expanding the accessible parameters space available to fundamental studies of turbulence. The results from our studies of Onsager vortices will be also presented. The realization of negative temperature vortex distributions, long predicted by Onsager, open up the experimental study of the full phase-diagram of 2D vortex matter.

Finally I will demonstrate how carefully sculpted light can be used in microsystems including microthermodynamics and heat engines at that scale.

11:00am QS-TuM-10 Spin-helical Particles: An Enabling Platform for Quantum Matter and Quantum Technologies, *Yong P. Chen,* Purdue University **INVITED**
Spin is one of the most fundamental quantum properties of particles. In this talk I will describe our experimental studies of "spin-helical" particles (analogous to neutrinos with spin locked to the momentum, but for electrons and atoms) as a powerful platform to realize novel quantum matter and enable new applications in quantum technologies --- such asquantum information, quantum energy, and even quantum chemistry. In particular, we have demonstrated spin-helical electrons [1,2] on the surface of "topological insulators" (TI) and discovered a "topological spin battery" [3], opening the possibility to electrically induce and readout a nuclear and electronic spin polarization with exceptionally long lifetime --- which we present as a remarkable demonstration of the "topological protection" unique to TI. We further observe unusual behaviors in superconducting Josephson junctions and SQUIDs made out of our TIs [4,5,6], paving the way for using such spin-helical electrons to realize "topological superconductor" proposed to harbor "majorana fermions" that could enable scalable, topologically-protected quantum computing. Time permits, I may also describe an experiment on spin-helical (bosonic) atoms, realized using light-matter interaction to engineer "synthetic" spin orbit coupling and gauge fields on laser-cooled ^{87}Rb atoms in a Bose-Einstein condensate (BEC). We demonstrate a new "interferometric" approach for quantum control of chemical reactions (in our case photoassociation of two atoms into a molecule) by preparing reactants in spin superpositions [7]. It would be interesting to extend such ideas and explore such "quantum beam" experiments the context of surface chemistry and catalysis for example.

Refs: [1] J.Tian et al. Sci. Rep. 5, 14293 (2015); [2] J. Tian et al., Nature Comm. 10, 1461 (2019); [3] J.Tian et al., Science Advances 3, e1602531 (2017); [4] Luis A. Jauregui et al., APL 112, 093105 (2018); [5] M.Kayyalha et al., PRL 122, 047003 (2019); [6] M.Kayyalha et al., arXiv:1812.00499; [7] D.Blasing et al., PRL 121, 073202 (2018)

Surface Science Division
Room A220-221 - Session SS+2D+HC-TuM

Atom Manipulation and Synthesis/Oxide Surface Reactions & Flash Session

Moderators: Liney Arnadottir, Oregon State University, Stephen McDonnell, University of Virginia, Martin Setvin, TU Wien, Austria

8:00am SS+2D+HC-TuM-1 Angstrom Scale Chemical Analysis of Metal Supported *Trans*- and *Cis*-Regioisomers by Ultrahigh Vacuum Tip-Enhanced Raman Mapping, *S Mahapatra, J Schultz, L Li, Nan Jiang,* University of Illinois at Chicago
Real space chemical analysis of two structurally very similar components i.e. regioisomers lies at the heart of heterogeneous catalysis reactions, modern-age electronic devices and various other surface related problems in surface science and nanotechnology. One of the big challenges in surface chemistry is to identify different surface adsorbed molecules and analyze their chemical properties individually. Herein, we report a topological and chemical analysis of two regioisomers, *trans-* and *cis-*tetrakispentafluorophenylporphodilactone (*trans-* and *cis-*H_2F_{20}TPPDL) molecules by high resolution scanning tunneling microscopy (STM), and ultrahigh vacuum tip-enhanced Raman spectroscopy (UHV-TERS). Both isomeric structures are investigated individually on Ag(100) at liquid nitrogen temperature. Following that, we have successfully distinguished these two regioisomeric molecules simultaneously through TERS with an angstrom scale (8 Å) spatial resolution. Also, the two-component organic heterojunction has been characterized at large scale using high resolution two-dimensional (2D) mapping. Combined with time-dependent density functional theory (TDDFT) simulations, we explain the TERS spectral discrepancies for both isomers in the fingerprint region.

8:20am SS+2D+HC-TuM-2 Theoretical Modeling of Metal Release from Complex Oxide Surfaces, *Sara Mason,* University of Iowa
Nanoscale complex metal oxides have transformed how technology is used worldwide. The most widespread examples are the electroactive components of Li-ion batteries found in portable electronic devices. As the

number of portable devices is projected to increase, so too will the inadvertent release of complex metal oxide nanomaterials into the environment. There is a fundamental knowledge gap in developing sustainable nanotechnology because there is not yet a systematic method to predict how the properties of a complex metal oxide will change with changes in chemical environment. Our studies have shown that the oxidation states of the metals in these types of materials with adjust according to the chemical environment. The oxidation states also determine the stability of that metal in the lattice of the material, and can facilitate dissolution of the potentially toxic ions into aqueous environments. We have developed an analysis, based on Hess's Law, which combines DFT-computed total energies and experimentally adjustable reaction conditions to compute the surface dissolution of complex metal oxides. We focus on the materials found in a Li-ion battery cathode, namely $LiCoO_2$ (LCO) and compositionally tuned variants with general chemical formula $Li(Ni_xMn_yCo_z)O_2$ (NMC). We find that adjusting surface terminations, compositions and pH will change the oxidation states of the metals. These changes in oxidation state alters the dissolution properties of this family of materials. We track the changes in oxidation state with respect to changes in the environment with electronic structure calculations such as, band structure and projected density of states. Our confirms the incongruent dissolution trend seen by our experimental collaborators. Our further investigations show that increasing the amount of Mn in the lattice will facilitate dissolution from all the metals and increasing the amount of Ni will stabilize the lattice and have similar dissolution to the equistoichiometric NMC. Since the release of Ni, Mn, and Co has shown to have adverse biological effects, we employ database mining to generate a new set of materials where we have replaced Ni, Co, and Mn with metals that will keep the same functionality while reducing biological impact. We then predict the thermodynamics of metal release to give insight on tailorable properties that can be used to formulate sustainable design principles for future generations of functional CMO materials.

8:40am SS+2D+HC-TuM-3 On-surface Synthesis by Atom Manipulation Studied with Atomic Force Microscopy, *Leo Gross,* IBM Research - Zurich, Switzerland **INVITED**

Elusive molecules are created using atomic manipulation with a combined atomic force/scanning tunneling microscope (AFM/STM). Employing high-resolution AFM with functionalized tips provides insights into the structure, geometry, aromaticity, charge states and bond-order relations of the molecules created and into the reactions performed [1].

We created radicals, diradicals [2], non-Kekulé molecules [3] and polyynes [4] and studied their structural and electronic properties. We recently showed that the reorganization energy of a molecule on an insulator can be determined [5]. In addition, we expanded the toolbox for the synthesis of molecules by atomic manipulation, demonstrating reversible cyclisation reactions [2], skeletal rearrangements [4] and controlled reactions on insulating substrates by electron attachment/detachment [6].

On insulating substrates we can control the charge state of molecules and resolve changes within molecular geometry, adsorption and aromaticity related to the oxidation state.

References:

[1] L. Gross *et al. Angew. Chem Int. Ed* **57**, 3888(2018)

[2] B. Schuler *et al. Nat. Chem.***8**, 220 (2016)

[3] N. Pavliček *et al. Nat. Nano.***12**, 308 (2017)

[4] N. Pavliček *et al. Nat. Chem.***10**, 853 (2018)

[5] S. Fatayer *et al. Nat. Nano.***13**, 376 (2018)

[6] S. Fatayer *et al. Phys. Rev. Lett.***121**, 226101 (2018)

9:20am SS+2D+HC-TuM-5 The Large Effect of Solvents on Heats of Adsorption versus Gas Phase Explained with a Simple Bond-additivity Model: A Case Study with Phenol on Pt(111) in Water, *Charles T. Campbell,* University of Washington*; N Singh,* University of Michigan*; J Rumptz,* University of Washington

The low-coverage heat of adsorption of phenol on Pt(111) facets of a Pt wire in aqueous phase is approximately 21 kJ/mol (relative to aqueous phenol)[1], much smaller than the heat for gas phase phenol adsorption at this same low coverage on single-crystal Pt(111) in ultrahigh vacuum (200 kJ/mol from adsorption calorimetry[2]). Here we quantitatively analyze the individual contributions that give rise to this large solvent effect using a simple pairwise bond-additivity model, taking advantage of experimental data from the literature to estimate the bond energies. The dominant contribution to the lowering in heat when adsorbing phenol in water is the energy cost to break the strong bond of liquid water to Pt(111) ($E_{adhesion}$ = ~116 kJ per mole of phenol area). The water-phenol bonding is lost on one face of the phenol and this costs ~50 kJ/mol, but this is nearly compensated by the new water-water bonding (~53 kJ/mol of phenol area). The results indicate that the intrinsic bond energy between phenol and Pt(111) is not very different when in gas versus aqueous phase, provided one takes into consideration the expectation that water forces phenol into 2D islands of high local coverage even at low average coverage (for the same reason that oil and water don't mix). This also explains the lack of a strong coverage dependence in the heat of adsorption when measured in aqueous phase, whereas it decreases by ~60 kJ/mol with coverage when measured in gas phase. This bond-additivity analysis can be extended to other surfaces and solvents for any flat adsorbate. It clarifies why catalysis with molecules like phenol which have very strong bonding to Pt group metals can proceed rapidly at room temperature in liquid solvents like water, but would never proceed in the gas phase at room temperature due to irreversible site poisoning. We also present many new measurements of solvent / metal adhesion energies that will aid future analyses of solvent effects in adsorption.

(1) Singh, N.; Sanyal, U.; Fulton, J. L.; Gutiérrez, O. Y.; Lercher, J. A.; Campbell, C. T. Quantifying Adsorption of Organic Molecules on Platinum in Aqueous Phase by Hydrogen Site Blocking and in Situ X-Ray Absorption Spectroscopy. *Submitted***2019**.

(2) Carey, S.; Zhao, W.; Mao, Z.; Campbell, C. T. Energetics of Adsorbed Phenol on Ni(111) and Pt(111) by Calorimetry. *J. Phys. Chem. C***2019**, *123*, 7627–7632.

9:40am SS+2D+HC-TuM-6 Atomic-Scale Growth Mechanisms of Niobium Hydrides on Hydrogen Infused Nb(100), *Rachael Farber, D Veit, S Sibener,* The University of Chicago

Particle accelerator technology and science, while commonly associated with fundamental high-energy physics applications, is also a crucial component in biological, chemical, and industrial scientific technologies. In order to increase the accessibility and applicability of accelerator-based technologies in multiple sectors, it is imperative to develop technologies that will enable the production of a more intense particle beam at a lower price point. As such, it is essential to identify structural and chemical features that inhibit beam intensity and develop methods to suppress such surface features.

Niobium (Nb) is the current standard for superconducting radio frequency (SRF) accelerator cavities due to its ultra-low surface resistance (R_s) and high cavity quality factor (Q) at operating temperatures of ~ 2 K. It is known that SRF cavity surface composition and contaminant incorporation is directly related to Q, and much work has been done to understand factors influencing SRF cavity performance for the clean and oxidized Nb surface. Hydrogen incorporation, which results in the formation of Nb hydrides, has been identified as a major source of decreased Q. There is not, however, a fundamental understanding of the growth mechanism for Nb hydrides. In this work, we have investigated the atomic-scale growth mechanism of Nb hydrides on oxidized Nb(100) under ultra-high vacuum (UHV) conditions using temperature programmed desorption (TPD), low-temperature scanning tunneling spectroscopy (LT-STM), and scanning tunneling spectroscopy (STS). The incorporation of relevant concentrations of hydrogen into the Nb(100) crystal was confirmed using TPD, LT-STM experiments revealed novel, real space information regarding the atomic-scale growth mechanism of Nb hydrides, and STS was used to elucidate the relationship between Nb hydride formation and the surface density of states.

11:00am SS+2D+HC-TuM-10 Water induced restructuring of Vanadium oxide clusters, *Kræn Christoffer Adamsen, J Lauritsen, S Chiriki, B Hammer,* Aarhus University, Denmark

Fundamental knowledge of catalytic processes for NO_x removal (Selective Catalytic reaction, SCR) is important for improving existing catalysts and developing new. In the SCR cycle, NO_x is known to react from gas-phase on adsorbed ammonia on a VO_x/TiO_2 based catalysts. It is well established that vanadium in the V^{+5}-state is most catalytic active state, though is still debated whether it is a hydroxylated- or an unhydroxylated- species that is most active species. Here we investigate the structure of vanadium oxide (V_2O_5) before, under and after exposure of water.

By evaporation of Vanadium in an oxygen-rich atmosphere (10^{-6} mBar) on an anatase-TiO_2 (101) substrate, we can create well-dispersed single V_2O_5 – clusters. Confirm the oxidation state of vanadium with X-ray Photo electron Spectroscopy (XPS) and image the size and structure ~5 with high resolution

Scanning Tunneling Microscopy (STM). Prior to water exposure V_2O_5 – clusters appear predominately as elongated features extending across two bridging oxygen rows of the anatase-TiO_2 (101) substrate. Utilizing the high scanning speed of the Aarhus STM we can follow the water induced restructuring of the clusters in situ. We observe a clear change in appearance of the vanadium oxide cluster, where a vanadium atom moves across on of the bridging oxygen rows of the a-TiO_2 substrate. Removal of water causes another change in appearance, but re-exposure of water the previous appearance is restored. We therefor observe a reversible reaction with exposure and removal of water, however with several hour of pumping we cannot return to the initial state directly after evaporation.

Together with Theoreticians, we are able to suggest structure models of the interactions between the vanadium oxide and water. We are able to explain both the irreversible restructuring in the first water exposure and the reversible restructuring with re-exposure of water. Understanding the structure and it dynamical behavior under water exposure bring us closer to understand the catalyst under working conditions.

11:20am SS+2D+HC-TuM-11 Hydrogenation of Titanium Doxide with Low-energy Hydrogen Ions and Atomic Hydrogen, *N Nagatsuka, Y Ohashi*, Institute of Industrial Science, The University of Tokyo, Japan*; M Fujimoto, M Matsumoto*, Tokyo Gakugei University, Japan*; **Katsuyuki Fukutani**, Institute of Industrial Science, The University of Tokyo, Japan

Interaction of hydrogen with TiO_2 surfaces is of interest and importance in view of photocatalytic H_2 generation and hydrogen sensors. Furthermore, hydrogenated TiO_2 has recently acquired much attention due to its excellent photocatalytic activity [1]. In our previous study, we have investigated the interaction of hydrogen with the rutile TiO_2(110) surface with nuclear reaction analysis (NRA) and ultraviolet photoemission (UPS) [2]. Whereas the former allows us to quantify hydrogen in the sample in a depth-resolved manner [3], the latter provides us with the information on the electronic states. In the present study, we have studied interaction of low-energy hydrogen ions with TiO_2 single-crystal surfaces, where the hydrogen ion penetrates the surface being distributed in the near-surface region [4]. We also report atomic hydrogen interaction with TiO_2 nanoparticles in relation with hydrogenation of TiO_2.

When the rutile TiO_2(110) and anatase TiO_2(101) surfaces are exposed to atomic hydrogen, NRA shows adsorption of hydrogen on the surfaces with a coverage of about 0.5 monolayer [2]. When the rutile TiO_2(110) surface is exposed to a hydrogen ion beam at 500 eV, on the other hand, NRA reveals a maximum at a depth of about 1 nm extending to $\sim$30 nm with an average concentration of 5.6 at. % and UPS shows an in-gap state (IGS) at $\sim$0.8 eV below the Fermi level with a downward band-bending by 0.5 eV. The IGS intensity is about ten times as large as that of the H-adsorbed surface. Upon annealing at 673 K, the IGS intensity is reduced by about 40 % and H with a coverage of 1.4 monolayer remains in the near-surface region, which suggests stable H occupation of subsurface sites. When the H-ion-irradiated surface is exposed to oxygen molecules, on the hand, the hydrogen distribution remains unchanged although the IGS intensity is substantially reduced. The effect of hydrogen in the near-surface region on the surface electronic state is discussed.

[1] Z. Wang et al., Adv. Func. Mater. 23, 5444 (2013).

[2] K. Fukada et al., J. Phys. Soc. Jpn. 84, 064716 (2015); N. Nagatsuka et al., in preparation.

[3] M. Wilde, K. Fukutani, Surf. Sci. Rep. 69, 196 (2014).

[4] Y. Ohashi et al., J. Phys. Chem. C in press.

11:40am SS+2D+HC-TuM-12 Direct Observation of Atomic Exchange during Surface Self-diffusion, *Matthew Koppa, P Schwoebel, D Dunlap*, University of New Mexico

The growth of crystals from the vapor phase is widely used in many technological applications, ranging from the microfabrication of microprocessors to the development of biological sensors. The dynamics of processes such as the surface diffusion of adatoms are key phenomena governing mass transport and the resulting crystal growth. Atomic exchange with substrate atoms during surface self-diffusion has been inferred from previous field ion microscope(FIM)-based experiments by mapping adatom visitation sites. Here iridium enriched to >93% ^{191}Ir was deposited onto an atomically clean and smooth *Ir(100)* plane as observed in an atom-probe field ion microscope. Following thermally activated surface self-diffusion the adatom was field desorbed and mass analyzed. Observation of the ^{193}Ir isotope in one-half of the cases demonstrates conclusively that atomic exchange can occur during surface self-diffusion.

Thin Films Division
Room A124-125 - Session TF+AP-TuM

ALD and CVD: Precursors and Process Development
Moderators: Paul Poodt, Holst Centre / TNO, Erwin Kessels, Eindhoven University of Technology, the Netherlands

8:00am TF+AP-TuM-1 Mechanism-Based Precursor Design for CVD of Metal Oxides and Sulfides, *Lisa McElwee-White*, University of Florida
INVITED

Aerosol-assisted chemical vapor deposition (AACVD) of WO_x was demonstrated using the oxo tungsten(VI) fluoroalkoxo single-source precursors, $WO[OC(CF_3)_2CH_3]_4$ (**1**) and $WO[OC(CH_3)_2CF_3]_4$ (**2**). Mechanistic studies of the decomposition of **1** and **2** were consistent with gas phase decomposition to yield tungsten (VI) dioxo intermediates during growth of WO_x materials. The dioxo tungsten alkoxide precursors $WO_2[OC(CF_3)_2CH_3](DME)$ (**3**) and $WO_2[OC(CF_3)_3](DME)$ (**4**) were then prepared as a means of independently generating intermediates involved in deposition of WO_x materials from **1** and **2**. Further experimental and computational mechanistic studies have led to synthesis of related precursors with other O-bound ligand types, including β-diketonates, β-ketoesterates, β-ketoiminates, and β-diketiminates, which have been used for deposition of WO_x films and nanostructures. Similar mechanism-based design strategies using S-bound ligands have been extended to precursors for deposition of MoS_2 and WS_2. Precursor syntheses, mechanistic studies, deposition of films under AACVD and CVD conditions, and characterization of the resulting materials will be discussed.

8:40am TF+AP-TuM-3 Improved Control of Atomic Scale Processing: Characterization and Optimization of Precursor Mass Delivery Utilizing a Novel Thermal Sensor, *Daniel Alvarez, J Spiegelman, C Ramos, Z Shamsi*, RASIRC

ALD precursor utilization is a long-standing problem in semiconductor manufacturing. In general, precursors are quite expensive ($5-$25/gram), particularly where utilization is estimated as low as 5-10%. Thus far, chip manufacturers have been burdened by precursor costs and low wafer throughput. A non-optimized process consumes excess material and requires longer purge time.

For Area Selective Deposition (ASD), control of precursor mass delivery is even more critical to process viability. Here, excessive precursor material can initiate growth on "Non-growth" surfaces, leading to a need for intermittent etch steps.

More process control may make problematic processes viable for semiconductor manufacturing. Recently RASIRC introduced a novel dry hydrogen peroxide (H_2O_2) precursor. A novel H_2O_2 mass flow sensor was developed to aid in product characterization. This thermal sensor accurately measures heat of decomposition for minute amounts of H_2O_2:

$H_2O_2 \rightarrow \frac{1}{2} O_2 + H_2O + heat$
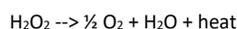
Our work uses this device to characterize H_2O_2 delivery parameters to:

- Minimize total precursor mass required
- Maximize precursor mass delivered in shortest time
- Limit purge time for increased throughput
- Minimize nucleation of "Non-growth" surfaces

Quantitative experimental methods are used to understand the effects of:

- Ampoule headspace pressure
- Carrier gas flow rate
- Liquid precursor temperature
- Precursor pulse time
- Saturation efficiency of carrier gas with precursor vapor
- Binary interactions for multicomponent liquids
- System heat transfer
- Ampoule design

An ALD simulation manifold was built to re-create typical ALD conditions. An automated test program controls valves and sensors to simulate process recipes. Initial results indicate highly variable mass delivery w.r.t. pressure. An ampoule outlet pressure of 20 torr results in 33.22 mg/min H_2O_2 mass delivery, vs 15.11 mg/min at 70 torr and 1.22 mg/min at 760 torr. Results are less affected by flow rate, where 0.5 slm at 22 torr leads to 33mg/min H_2O_2 vs 1.0 slm at 34 torr leads to 42 mg/min, and 2.0 slm at 57 torr leads to 44 mg/min. Here, increased mass delivery from higher flow rate is offset by a corresponding increase in pressure. In addition, while increased flow rate does not result in significant mass delivery increase for 2 slm, there is a significant decrease in precursor concentration, where the molar ratio of H_2O_2/N_2 is decreased by 70% vs 0.5 slm. Concentration

effects are significant to film uniformity in ALD and have ramifications in ASD.

Mass delivery vs pulse time was also examined. Data will be presented for 3s, 1s, 0.3 sec, and 0.1s pulses. Application to process optimization will also be discussed.

9:00am TF+AP-TuM-4 Effect of Co-Reactant on the Atomic Layer Deposition of Copper Oxide, *Jason Avila, N Nepal, V Wheeler,* U.S. Naval Research Laboratory

Atomic layer deposition (ALD) of copper oxide presents a powerful opportunity to grow p-type semiconductor material for a wide variety of applications such as transparent conducting oxide, solar fuels catalysis, and power devices. There are, however, very few ALD processes to facilitate the growth of copper oxide. Cu(II) bis(dmiethylamino-2-propoxide) (Cudmap) has previously been used to grow copper metal using a reducing source such as tertiary butyl hydrazine.[1,2] Cudmap has also been demonstrated to grow Cu_2O using water as a co-reactant, self-reducing from Cu(II) to Cu(I) in the presence of water.[3] This study will examine the effect of ALD co-reactants, ozone and water, on the copper oxidation state of copper oxide films grown using Cudmap.

Copper oxide films were grown in a Veeco Savannah ALD reactor using Cudmap and ozone or water at 150 °C on Si and c-plane sapphire. This is the first experimental demonstration of CuO films using Cudmap and ozone. Using ozone, a growth rate of 0.18 Å/cycle was achieved at 150 °C, far higher than the measured growth rate of 0.04 Å/cycle when using water. Since growth rates are still quite slow, a vapor assisted precursor delivery system for the Cudmap was implemented and its ability to achieve higher growth rates will be presented.

XPS was able to confirm the presence of only the Cu(II) oxidation state with a Cu/O ratio of 1, verifying the deposition of CuO films. For comparison, films grown with water show the presence of only Cu(I) oxidation state and have a nearly stoichiometric with a Cu/O ratio of 2:1, confirming the deposition of Cu_2O films. AFM also indicated uniform, continuous film growth, independent of co-reactant, for films as thin as 2 nm. However, for a similar thickness, CuO films deposited with ozone were rougher than Cu_2O films grown with water. In addition to these initial results, comparison of the optical and electrical properties of the different copper oxide films for p-type semiconductor applications will be presented.

References

(1) Väyrynen, K.; Mizohata, K.; Räisänen, J.; Peeters, D.; Devi, A.; Ritala, M.; Leskelä, M. Chemistry of Materials 2017, 29, 6502.

(2) Kalutarage, L. C.; Clendenning, S. B.; Winter, C. H. Chemistry of Materials 2014, 26, 3731.

(3) Avila, J. R.; Peters, A. W.; Li, Z.; Ortuno, M. A.; Martinson, a. B. F.; Cramer, C. J.; Hupp, J. T.; Farha, O. Dalton Transactions 2017, 46, 5790.

9:20am TF+AP-TuM-5 Electron Enhanced Atomic Layer Deposition (EE-ALD) of Cobalt Films and Development of New Hollow Cathode Plasma Electron Source, *Zachary Sobell,* CU Boulder*; A Cavanagh, S George,* University of Colorado at Boulder

Cobalt films were grown with electron enhanced atomic layer deposition (EE-ALD) at room temperature using sequential surface reactions. The Co film growth was performed using sequential cobalt tricarbonyl nitrosyl (CTN, $Co(CO)_3NO$) exposures and low energy (75-175 eV) electrons. A hot filament electron flood gun was used as the electron source. The electrons desorb the CO and NO ligands from CTN on the surface and produce active sites for additional CTN adsorption. The maximum growth rate was 0.5 Å per cycle at an electron energy of 125 eV. Cobalt is important as an advanced interconnect material to replace copper or tungsten. Because the electron flux is normal to the substrate, Co EE-ALD may be used to facilitate bottom-up-fill of trenches and vias.

One difficulty with Co EE-ALD using the electron flood gun is the long cycle times of 540 seconds. Much of this cycle time is consumed protecting the flood gun filament from precursor exposures and the long duration of the electron exposure due to the limited current of the gun. 42% of the cycle time is needed for the warm up and cool down of the filament of the electron flood gun between CTN exposures. Another 44% of the cycle time is required for the electron exposures. An additional 14% of the cycle time is needed to reduce the precursor pressure in the chamber following CTN exposures. The cycle time could be reduced significantly using a more robust and higher flux electron source.

A new hollow cathode plasma electron source (HC-PES) has been developed to reduce the cycle time during EE-ALD. The HC-PES has a >100X

increase in electron flux compared with the electron flood gun. The HC-PES also eliminates the warm-up and cool-down time of the filament of the electron flood gun. The electron current from the HC-PES can be switched from nanoamps to miliamps in < 10 ms. The HC-PES is also chemically insensitive and reduces the need for pumping out the chamber following CTN exposures. This presentation will report on the characterization of this new HC-PES and its use for Co EE-ALD.

9:40am TF+AP-TuM-6 Surface Science Studies of GaN Substrates Subjected to Plasma-Assisted Atomic Level Processes, *Samantha G. Rosenberg,* American Society for Engineering Education (residing at U.S. Naval Research Laboratory)*; D Pennachio, E Young, Y Chang, H Inbar,* University of California at Santa Barbara*; J Woodward,* U.S. Naval Research Laboratory*; Z Robinson,* SUNY Brockport*; J Grzeskowiak,* University at Albany - SUNY*; C Ventrice, Jr.,* SUNY Polytechnic Institute*; C Palmstrøm,* University of California at Santa Barbara*; C Eddy, Jr.,* U.S. Naval Research Laboratory

III-N semiconductors are well suited for applications in several important technological areas, including high current, normally-off power switches.[1,2] Such devices require heterostructures not readily achievable by conventional growth methods. Therefore, we have developed a technique adapted from atomic layer deposition (ALD), called plasma-assisted atomic layer epitaxy (ALEp).[2] Using surface science techniques, we strive to develop not only a fundamental understanding of the ALEp growth process but also complimentary atomic level processes (ALPs) that will result in the best preparation method for a pristine GaN starting surface for ALEp.

Here we employ *in-situ* and *in-vacuo* surface science studies of GaN substrate preparation to advance fundamental understanding of the ALEp process. Having optimized our GaN surface preparation (gallium flash off ALP),[3] we conduct *in-vacuo* X-ray photoelectron spectroscopy (XPS), reflection high-energy electron diffraction (RHEED), and scanning tunneling microscopy (STM) studies in the Palmstrøm Lab at UCSB to further refine both our process and our understanding. Preliminary XPS results show that a GFO ALP conducted at 250°C for 12 cycles reduces the oxygen content by 5% but shows no reduction in the carbon content, while a GFO ALP conducted at 400°C for 30 cycles reduces the carbon content by 60% but shows no reduction in the oxygen content. Other XPS results show that our previously reported optimal GFO ALP results in a ~25% reduction of carbon, while a similar 25% reduction of oxygen was achieved using a GFO ALP with or without TMG. We have also conducted comparable temperature program desorption (TPD) and low energy electron diffraction (LEED) experiments at SUNY Polytechnic Institute to correlate structural and chemical changes that occur on GaN surfaces treated with our GFO ALP. TPD shows that NH_3 is released from GaN surfaces not subjected to GFO ALP as it is heated past 150°C, while GFO ALP GaN surfaces show no NH_3 release upon subsequent TPD experiments. Both GaN surfaces, before and after TPD, show an unreconstructed 1x1 diffraction pattern in LEED.

1. N. Nepal, et al., Appl. Phys. Lett. 103, 082110 (2013)

2. C. R. Eddy, Jr, et al., J. Vac. Sci. Technol. A 31(5), 058501 (2013)

3. S. Rosenberg, et. al., J. Vac. Sci. Technol. A 37, 020908 (2019)

11:00am TF+AP-TuM-10 Reaction Pathways in Photolytic CVD of Platinum on Organic Thin Films, *Bryan G. Salazar,* University of Texas at Dallas*; H Liu, L McElwee-White,* University of Florida*; A Walker,* University of Texas at Dallas

Chemical vapor deposition (CVD) is widely used to deposit materials including metals, oxides, and sulfides. However, CVD is generally unsuitable for use on organic substrates because it often requires high temperatures (> 200 °C). In this work we investigate photolysis as an alternative to thermal activation for CVD of metals on organic thin films. To study the role of precursor chemistry on the Pt CVD process we use three different precursors: $(COD)Pt(CH_3)_2$, $(COD)PtCl(CH_3)$, and $(COD)PtCl_2$. We also investigate the role of substrate functionality on the CVD process using three different self-assembled monolayers (SAMs) with carboxylic acid-, hydroxyl-, and methyl- terminal groups to model organic thin films. Solution-phase photochemistry studies and residual gas analysis indicate that the photolytic activation of $(COD)Pt(CH_3)_2$ and $(COD)PtCl(CH_3)$ occurs via the loss of a methyl radical, while the $(COD)PtCl_2$ occurs via the loss of a chlorine. Subsequently these radicals abstract ligands from the gas phase precursor and the organic surface leading to the formation of methane, chloromethane, chlorine and ethane. Using X-ray photoelectron spectroscopy and time-of-flight secondary ion mass spectrometry (TOF SIMS), we also investigated the reaction pathways involved on the organic surfaces. The data indicates that the deposition is highly dependent on the wavelength of light, the Pt precursor, and the SAM terminal group. Using

(COD)Pt(CH$_3$)$_2$, we observe a small amount of Pt deposition on –OH and –COOH terminated SAM surfaces. In TOF SIMS we observe Pt- and O-containing ions indicating that Pt has inserted into the terminal group. Little, or no, deposition is observed on the –CH$_3$ terminated SAMs. In agreement with previous studies, the data also shows that the neutral polyhapto ligand, COD, is difficult to remove; there are Pt- and COD-containing species present on the surface. Further, the data indicates that there is some SAM decomposition during the deposition. In contrast, for (COD)PtCl(CH$_3$) and (COD)PtCl$_2$ little, or no, Pt deposition is observed and the data indicates that the SAM layers decompose to form polyaromatic hydrocarbons. The damage appears to be caused by the formation of chlorine radicals during the photolysis, which can penetrate through and react with the SAM. In contrast, the methyl radical is larger leading to less SAM damage because it cannot penetrate through the SAM layer. These studies provide insight into the reaction pathways involved in photolytic CVD and the role of radicals in the subsequent deposition and interaction with organic layers. Such studies therefore aid in the rational design of photolytic CVD on organic substrates.

11:20am TF+AP-TuM-11 Process Development and Mechanism Analysis of Low Temperature ALD TiN with TiCl$_4$/Monomethylhydrazine, *Taiki Kato, Z Ni, M Matsukuma, H Nakamura, Y Ideno, Y Serizawa,* Tokyo Electron Technology Solutions Limited, Japan

TiN is an important barrier metal for semiconductor devices. Nevertheless, it is difficult to form low-electrical-resistance TiN films at low temperature with existing thermal TiCl$_4$/NH$_3$ ALD processes. To overcome this difficulty, we tried a new azotizing gas MMH (Monomethylhydrazine: CH$_3$NHNH$_2$) instead of NH$_3$ and achieved low electrical resistance TiN (~1 mW.cm) under 300 deg C deposition temperature. XPS and AFM observations revealed that the film deposited with TiCl$_4$/MMH has smaller Cl concentration and is smoother than the one deposited with TiCl$_4$/NH$_3$. In this study, we analyzed the TiCl$_4$/MMH ALD reactions to clarify the process improvement mechanism when using MMH. Furthermore, we also analyzed the reactivity of TiCl$_4$ with NH$_3$ and with novel azotizing gases HZ (Hydrazine: H$_2$NNH$_2$) and UDMH (Unsymmetrical dimethylhydrazine: (CH$_3$)$_2$NNH$_2$) for future process development.

To analyze surface azotizing reactions, we used density functional theory calculation software, DMol^3. Surface reaction analysis of TiCl$_2$ termination revealed that the azotizing reactions removed Cl from the substrate by HCl gas generation and MMH was more reactive as an azotizing gas than NH$_3$. These results explained the experimental phenomenon in which MMH can remove Cl from a TiN film more efficiently than NH$_3$ and improve the film's roughness and electrical resistance. HZ and UDMH are also more reactive than NH$_3$ and are candidates for future azotizing gases.

Next, we analyzed gas phase decomposition reactivity of these agents for clarification of ALD process windows. This analysis is conducted by GRRM (Global Reaction Route Mapping) program which can search for reaction paths automatically. Gas decomposition reaction paths search revealed that ALD processes of TiCl$_4$ / HZ, MMH and UDMH are feasible under 400 deg C.

Furthermore, we analyzed azotizing gas chain reactivity for safe conservation estimation. This analysis is calculated by a molecular dynamics simulator, ADF ReaxFF. We inspected the chain reactivity of HZ, MMH, and UDMH densely packed in a tight container at high temperature. Reaction MD simulations showed that UDMH is the safest, followed by MMH then HZ.

In summary, we developed a new thermal TiN ALD process with TiCl$_4$/MMH instead of existing NH$_3$. Our simulation studies suggest that MMH, HZ and UDMH can remove Cl from TiN film more efficiently than NH$_3$ and improve the film roughness and the electrical resistance. Other reaction paths analyses show that the novel azotizing agents also have ALD temperature process windows under 400 degC and that the safe conservation trend HZ < MMH < UDMH. These hydrazine-like agents are promising azotizing precursors for low temperature ALD.

11:40am TF+AP-TuM-12 Atomic Layer Deposition of Aluminum, Hafnium and Zirconium Oxyfluoride Films with Tunable Stoichiometry, *Neha Mahuli, J Wallas, S George,* University of Colorado at Boulder

Metal oxyfluoride films are chemically robust and resistant to plasma corrosion. This study explored the atomic layer deposition (ALD) of various metal oxyfluorides including aluminum oxyfluoride (AlO$_x$F$_y$), hafnium oxyfluoride (HfO$_x$F$_y$) and zirconium oxyfluoride (ZrO$_x$F$_y$). Different deposition techniques were developed to obtain tunable stoichiometry of these metal oxyfluoride films. The complicating factor was fluorine/oxygen exchange and the diffusion of fluorine in the oxyfluoride film.

For the metal oxyfluoride deposition, H$_2$O and HF were used as the oxygen and fluorine sources. Al(CH$_3$)$_3$ was used as the Al source. Hf and Zr alkylamide precursors were used as the Hf and Zr sources. The metal oxyfluorides were deposited using either (1) the halide-exchange method or (2) the nanolaminate method. These two methods gave rise to tunable stoichiometry from pristine metal oxide to adjustable oxyfluoride to pristine metal fluoride.Both methods were evaluated using *in situ* quartz crystal microbalance (QCM) measurements and *ex situ* X-ray photoelectron spectroscopy (XPS) analysis.

The halide-exchange method is based on the facile exchange of oxygen by fluorine from HFbased on following equation (MO$_x$ + yHFàMF$_y$ + xH$_2$O). HF exposures after deposition of the metal oxide easily replaced oxygen with fluorine. The fluorine also diffused into the underlying metal oxide film as a function of time and temperature. The compositional control is achieved either using metal oxide layers of various thicknesses or different HF pressures. The rate of fluorine diffusion determined by *in-situ* QCM as well as *ex-situ* XPS was assigned as AlO$_x$F$_y$>ZrO$_x$F$_y$>HfO$_x$F$_y$.

The stoichiometry was also tuned using the nanolaminate method with different numbers of metal oxide ALD and metal fluoride ALD cycles. One supercycle (of ratio n:m) here consists of 'n' layers of metal oxide followed by 'm' layers of metal fluoride. The F:O ratios in the metal oxyfluoride films using this mechanism could be controlled over the full range of compositional ratios. The rate of fluorine diffusion in these systems was also found to be AlO$_x$F$_y$>ZrO$_x$F$_y$>HfO$_x$F$_y$.

12:00pm TF+AP-TuM-13 ALD on Thermally and Chemically Treated Fused Silica and Glass Surfaces, *Tahereh Gholian Avval, G Hodges, V Carver, M Linford,* Brigham Young University

Silanol (SiOH) and surface hydroxyl (OH) groups strongly affect the absorption behavior of species onto silica (SiO$_2$) surfaces. The density of hydroxyl (OH) groups on these surfaces are important for initiating and producing conformal thin films by atomic layer deposition (ALD). The combination of chemical and thermal treatments of surfaces in ALD increases insight into their chemistry. Different chemical treatments, including cleaning solutions of industrial importance, affect surface silanol density and consequently subsequent thin film growth by ALD. In this work, we describe the density of hydroxyl (OH) groups on fused silica surfaces and their effect on ALD. In particular, we hydroxylated pieces of fused silica with hydrofluoric acid (HF) and then heat treated it at 200, 500, 700 and 900 °C. The samples then underwent different numbers of ALD cycles to produce thin films of Al$_2$O$_3$. As expected, analysis of these surfaces by X-ray photoelectron spectroscopy (XPS) showed that higher temperatures lead to lower aluminum loading/deposition. As a result, heat-treated samples at 900 °C appear to be significantly depleted in surface silanols and lagged behind in thickness compared to the other samples. Other chemical treatments of industrial relevance for silica and glass were also considered in this study, including hydrochloric acid (HCl), tetramethylammonium hydroxide (TMAH), and a detergent. This information is important for ALD deposition of this important material.

Thin Films Division
Room A122-123 - Session TF+EM+MI-TuM

Thin Films for Microelectronics, Photonics, and Optoelectronic Applications
Moderators: John F. Conley, Jr., Oregon State University, Halil Akyildiz, Uludag University, Turkey

8:00am **TF+EM+MI-TuM-1 Monolithic Integration of III-Vs on Si for Electronic and Photonic Applications**, *P Staudinger, S Mauthe, N Vico Trivino, M Sousa, C Convertino, Y Baumgartner, P Tiwari, H Schmid,* **Kirsten Moselund,** IBM Research Zurich, Switzerland **INVITED**

For more than half a century researcher have been working on monolithic integration of III-V materials on Si in order to achieve seamless integration of III-V with Si CMOS. Progress has been made in recent years for example on nanowires [1], aspect ratio trapping (ART) [2] and other selective growth techniques suitable for III-V device integration. Here, I will discuss our work on Template-Assisted Selective Epitaxy (TASE) [3], as a novel epitaxial technique where III-V nanostructures are grown within an oxide template.

In this method we first use a combination of lithography and etching to define our structures in Si. These might be vertical or lateral nanowires, or more exotic shapes such as hall-bars, rings and disks. The Si features are covered by an oxide, which is opened locally, and the Si is partially etched exposing a Si nucleation seed within a hollow oxide cavity (template). The

template is subsequently filled by metal-organic chemical vapor deposition (MOCVD) grown III-V material. The geometries of the III-V features are lithographically defined by the shape of the hollow template and to a large extent independent of growth conditions.

The versatility of this technique will be shown through several experimentally demonstrated devices, such as InGaAs MOSFETs [4], heterojunction tunnel FETs [5] and monolithically integrated room temperature optically pumped GaAs [6] and InP microdisk lasers [7].

The quality of the TASE-grown material is assessed by high-resolution scanning transmission electron microscopy (HR-STEM). Devices are free from propagating defects and dislocations, but stacking faults are present as expected for selective epitaxy. By controlling the twinning, we were successful in demonstrating pure wurtzite InP micro-substrates for the first time. We also compare lasing performance to that of devices based on defect-free bonded material, which currently represents the state-of-the-art in terms of photonic integration.

1. B. Mayer et al., Nano Lett., vol. 16, no. 1, pp. 152–156, 2016.

2. Z. Wang et al., Nat. Photonics, vol. 9, pp. 837–842, 2015.

3. H. Schmid et al. Appl. Phys. Lett. 2015, *106* (23), 233101.

4. L. Czornomaz et al., Symp. VLSI Tech., 2015, pp. T172–T173, 2015.

5. Cutaia, D. et al., Symp. VLSI Tech., pp. 403-407, (2016).

6. S. Wirths et al., ACS Nano 12 (3), pp. 2169, 2018.

7. S. Mauthe et al., submitted to IEEE J. Sel. Top. Quantum Electron. (2019).

8. M. Sousa et al. , 2018 IEEE Nano, DOI: 10.1109/NANO.2018.8626223

9. P. Staudinger et al., Nano Letters, vol. 18 (12), 7856, 2018.

8:40am TF+EM+MI-TuM-3 A Scheme for Better Future Technology by developing AlGaN based Highly Responsive Photosensing Devices, *Neha Aggarwal, S Krishna, L Goswami, G Gupta,* CSIR-National Physical Laboratory, India

All species on Earth are affected by UV radiation, from environment-to-humans, industrial-to-residential, defense-to-technology; a number of current & futuristic applications of detecting UV radiation exist. For fabricating UV photodetectors (PDs), III-Nitrides are promising candidates due to their superior material properties such as wide-direct bandgap, high thermal conductivity, good radiation hardness, etc. Also, III-nitrides are intrinsically blind to the visible region of EM spectrum; thus, do not require expensive optical filters unlike existing Si-based UV PDs. Among nitrides, AlGaN based heterostructures have gained huge interest in optoelectronic applications due to their ability to tune the bandgap by modulating Al concentration which allows them to select the cut-off wavelength depending upon the application. Further, to facilitate the integration of AlGaN based devices with existing Si technology, Si substrates were utilized for growing AlGaN heterostructures. However, large lattice mismatch between AlGaN & Si may restrict the growth of defect-free AlGaN, thus a nucleation layer is needed to avoid cracking due to tensile strain. Incorporation of AlN as interlayer reforms the tensile stress in AlGaN layer directly grown on Si into compressive stress which yields the desired crack-free epitaxial structure. In this work, extensive efforts are employed to grow AlN on Si (111) substrate via PAMBE & successfully accomplished best quality AlN with lowest HRXRD FWHM of 15 arcmin having screw dislocation density of 8.5×10^8 cm^{-2}. Then, we have performed hetero-epitaxial growth of $Al_xGa_{1-x}N$ on AlN buffered Si (111) for x in 0.30-0.45 range & discusses the compositional fluctuations associated with changes in buffer growth parameters. As the buffer growth conditions changes, Al composition varies from 0.30-0.45 & FWHM is reduced from 55.6 to 36.4 arcmin. To realize a highly responsive UV PD, uniformly oriented AlGaN nano-islands are grown aimed to efficiently absorb photons due to increased surface-to-volume ratio. On this, we also implemented interdigitated (ID) electrode configuration to collect higher photo-generated charge carriers. The fabricated AlGaN UV PDs having cut-off wavelength of 284 nm yielded a significant enhancement in responsivity from 36.4 to 140.5 A/W at 2 V bias upon changing electrodes from non-ID to ID. However, the developed UV detection device exhibit high response towards UV with responsivity value of 182 mA/W under 2.5 V bias which is better than the commercially available UV detectors. Conclusively, the highly responsive AlGaN UV-PD on Si displays potential application in the development of advanced optoelectronic devices.

9:00am TF+EM+MI-TuM-4 Correlating the Optical Property Evolution in the Au-Ni Binary Thin Films: From Metastable Solid Solution to Phase Separated Alloy, *Robyn Collette, Y Wu, P Rack,* University of Tennessee Knoxville

Surface plasmon resonances can be sustained by metallic nanostructures and have been explored for potential optoelectronic device applications. Metallic alloys provide a pathway to tune the plasmonic response of a material. Additionally, alloying may allow for multifunctional materials to be realized. For example, Au-Ni alloys may combine the magnetic properties of ferromagnetic Ni with the plasmonic properties of Au. However, limited studies have been conducted on Au-Ni alloys for use in plasmonic devices. Since the behavior of the alloys depends on the structure, it is first critical to understand the relationship between the structure and the optical properties of the alloy.

In this study, the optical properties of $Au_{1-x}Ni_x$ alloy thin films are investigated by employing a combinatorial sputtering approach. The dielectric function is measured using spectroscopic ellipsometry and is correlated to the composition (energy dispersive x-ray spectroscopy), and phases present (x-ray diffraction). As-deposited alloys form a metastable solid solution, however, annealed alloys exhibited phase separation into Au-rich and Ni-rich phases due to the large miscibility gap in the Au-Ni material system. The optical properties are then rationalized by modeling the dielectric function of the solid solution alloys with a Drude-Critical Point analytical model. Lastly, the efficacy of the model is demonstrated which shows that the dielectric function of the phase separated alloys may be approximated using a composition-weighted average of two solid solution dielectric functions.

9:20am TF+EM+MI-TuM-5 Integration of Electro-optically Active BaTiO₃ and BaₓSr₁₋ₓTiO₃ with Buffered Si (001) by Chemical Methods, *John G. Ekerdt, B Edmondson, E Lin,* University of Texas at Austin*; S Kwon,* University of Texas at Dallas*; A Demkov,* University of Texas at Austin*; M Kim,* University of Texas at Dallas

Recent investigations into thin film $BaTiO_3$ (BTO) show it is a promising candidate for on-chip photonic devices due to its large linear electro-optic (EO) coefficient (r > 100-1000 pm/V) relative to more conventional photonic materials such as $LiNbO_3$ (~30 pm/V) or strained Si (~2 pm/V). However, such high coefficients are achieved only by costly and inherently un-scalable physical vapor deposition techniques. In recent studies, we have investigated chemical routes to the integration of electro-optically active BTO thin films with Si, which offer faster and more scalable methods of deposition. Specifically, atomic layer deposition (ALD) of 40 nm BTO films and chemical solution deposition (CSD) of 85 nm BTO films on $SrTiO_3$ (STO) templates on Si (001) prepared by molecular beam epitaxy (MBE) yield epitaxial BTO films with microstructure and defect nature markedly different from physical deposition techniques. Furthermore, we explored CSD of *c*-axis in-plane $Ba_xSr_{1-x}TiO_3$, which is difficult to achieve by physical methods and offers unique insight into the EO behavior of this highly tunable dielectric. X-ray diffraction and scanning transmission electron microscopy confirmed epitaxial, distorted tetragonal structures with a range of structural defects, and electrical and electro-optical measurements showed diminished ferroelectricity and EO response compared to MBE-grown thin films or bulk BTO. ALD-grown films exhibited optical hysteresis with coercivity of ~10 kV/cm, an effective linear EO coefficient of 26 pm/V for 40 nm films, and leakage currents caused by oxygen vacancies. CSD-grown films did not show evidence of ferroelectric hysteresis but maintained EO response with a coefficient of 25 pm/V and had very low leakage current. Past reports of chemical vapor deposited films yielded an EO coefficient of 7 pm/V. These results provide further understanding into the relationship between film structure and linear EO behavior.

9:40am TF+EM+MI-TuM-6 Nonlinear Optical Properties of TiO₂-based ALD Thin Films, *Theodosia Gougousi, R Kuis, I Basaldua, P Burkins, J Kropp, A Johnson,* University of Maryland, Baltimore County

Nonlinear materials in thin film form are highly desirable for the development of ultrafast all-optical system on-a-chip platforms, optical frequency converters and optical limiting applications. Conventional nonlinear optical (NLO) materials are usually cut from bulk crystals or are liquids that are not suitable for integration with the contemporary semiconductor industry process flow. The third order nonlinear response of ALD TiO_2-based films is investigated using thermally managed Z-scan technique. Some of the as-deposited films exhibit very high nonlinear response which is orders of magnitude higher than conventional nonlinear optical materials such as silica fibers and CS_2. Thermal treatment of the

films at 450°C for 3 hours in an oxygen rich atmosphere affects the films' optical properties and results in the loss of the high nonlinear optical response. TiO_2 films deposited by Physical Vapor Deposition (PVD) from a 99.9% TiO_2 target at room temperature are used as control samples and their nonlinear optical response is found below the detection limit of the Z-scan setup. This extraordinary nonlinear optical behavior of the TiO_2 ALD films is linked to the presence of a very small at. % of TiN bonding in the film. We will present detailed characterization of these films by x-ray photoelectron spectroscopy, x-ray diffraction and UV-Vis absorption. The high level of control of the nonlinear index of refraction, n_2, using the deposition process coupled with the ability of ALD to coat nonplanar geometries with atomic level precision and the fact that these processes are CMOS compatible have the potential to provide a breakthrough in optical device design and applications.

11:00am TF+EM+MI-TuM-10 Atomic Layer Deposition on Hexagonal Ge and SiGe Nanowires for Surface Passivation, *Willem-Jan Berghuis,* Department of Applied Physics, Eindhoven University of Technology, Postbus 513, 5600 MB Eindhoven, The Netherlands*; E Kessels,* Eindhoven University of Technology, The Netherlands, Netherlands*; J Haverkort, E Bakkers, A Dijkstra, E Fadaly, M Verheijen,* Eindhoven University of Technology, The Netherlands

Semiconductor nanowires (NWs) are nanoscale rods with a typical length of a few microns. They are made of materials such as Ge, Si, InP, GaAs. Due to their high aspect ratio, nanowires have a very high surface-to-volume-ratio, which leads to a large influence of the surface on their electronic and optical properties. Surface states facilitate recombination of electron-hole pairs, which reduces the photovoltaic conversion efficiency of NW solar cells [1] or which decreases the output of NW based LEDs or lasers. The surface can also induce space charge regions in the nanowires, which greatly affects their conductivity and which can be critical in for example sensing applications [2]. To reach the desired performance of nanowires in their applications, it is important to control the surface effects.

Atomic layer deposition (ALD) is a deposition technique that allows for preparation of ultrathin films with sub-nanometer thickness control and with an excellent conformality on high aspect ratio structures such as nanowire arrays. For these reasons ALD is a suitable technique to cover nanowires with thin films to control the surface properties.

Recently, nanowires have enabled the growth of Ge and SiGe in the hexagonal diamond crystal phase [3]. In contrast to the cubic crystal phase of these materials, the hexagonal crystal phase leads to a direct bandgap. The latter makes this material an interesting candidate to realize solid-state lasers that are compatible with the current silicon-based electronics. One of the important steps to accomplish this is to reduce the surface recombination losses; i.e. to passivate the surface.

The aim of this work is to explore the surface passivation of these hexagonal Ge and SiGe nanowires. We do so by covering the nanowires with ultrathin films of Al_2O_3 prepared by thermal and plasma-assisted ALD (PE-ALD). Secondly, we cover the wires with a stack of PO_x/Al_2O_3. The latter is a relatively new passivation scheme that has proven very successful for the surface passivation of InP nanowires [4] and Si wafers [5]. The change in photoluminescence (PL) of the nanowires as a function of the ALD films has been studied to assess the surface passivation and the influence of various pre- and post-treatments. Conformal coating of hexagonal Ge nanowires has been realized and we have observed an improvement of the photoluminescence for NWs covered with PE-ALD Al_2O_3 and PO_x/Al_2O_3.

11:20am TF+EM+MI-TuM-11 Oxidation Studies of Silicon Germanium (SiGe) using In-Situ Steam Generated (ISSG) and Plasma Enhanced Atomic Layer Deposited (PEALD) Oxides, *Yi Song, S Siddiqui, C Durfee, A Pana, J Li, M Belyansky, S Naczas, E Stuckert, L Jiang, J Demarest, V Basker, D Guo, H Bu,* IBM Research Division, Albany, NY

SiGe is a versatile material for the semiconductor industry for sub-7 nm node technology development; it can be used as a high mobility channel material in FinFET, and as multiple sacrificial layers to form channel regions in gate all around (GAA) nanosheet device architecture. Understanding SiGe film oxidation is important for matching oxidation rates between SiGe layers with different Ge% in nanosheet applications [1]. In this paper, a study of ISSG (800 °C) and PEALD (room temperature to 300 °C) oxidation processes is performed on blanket $Si_{1-x}Ge_x$ films ranging from x = 0.25 to 0.80. We establish the boundaries of three distinct regions of oxidation behavior for the ISSG process (Region I: $0 < x < 0.5$, Region II: $0.5 < x < 0.67$, and Region III: $x > 0.67$). Historically, low Ge oxidation has been extensively studied [2-4]. Here, we show for Region I, the ISSG oxidation rate is very small (1.7 nm of oxide growth in 5 sec). The oxidation rate rapidly increases in Region II as x increases, where it reaches a maximum (13.8 nm in 5 sec) at the Region II/Region III boundary, then abruptly drops in Region III as x increases due to complete sublimation of Ge (see Figure 1). The abrupt increase in the ISSG oxidation rate between Regions I and II makes it difficult to match oxide thicknesses for the wide range of Ge% utilized by nanosheet device architecture. Therefore, we studied a lower temperature oxidation process (PEALD) which has a lower oxidation rate. We found that PEALD oxidation rates are unchanged across the Region I/II boundary, even for higher temperatures up to 300 °C as shown in Figure 2. This enables oxide thickness matching for a wide range of Ge%. These results are applicable to the development of various nanotechnologies such as nanosheet and high mobility channel FinFET devices.

11:40am TF+EM+MI-TuM-12 Precision Defect Engineering of Metal/Insulator/Metal (MIM) Diodes using Localized ALD Transition Metal Impurities in Al_2O_3 Tunnel Barriers, *Konner Holden[1], Y Qi, J Conley, Jr.,* Oregon State University

Thin film MIM tunnel diodes are receiving increased interest for high-speed applications such as THz detection and rectenna based energy harvesting. Traditionally, current density vs. field (J-$\mathcal{E}$) asymmetry ($f_{asym} = J^-/J^+$) with MIM diodes has been achieved through metal work function differences ($\Delta\Phi_M$). Recently, nanolaminate insulator tunnel barrier MIIM diodes enabled by ALD showed improved f_{asym}, non-linearity, and responsivity at low voltage by step tunneling through the wider bandgap (E_G) insulator to the conduction band of the narrow E_G insulator.[1] *Intrinsic defects* present in narrow E_G insulators were later demonstrated to further improve low $\mathcal{E}$ asymmetry via defect enhanced direct tunneling, when paired with an insulator dominated by tunneling.[2,3] In this work, we investigate the impact of localized *extrinsic defects* by using ALD to intentionally introduce Ni at precise intervals in an Al_2O_3 tunnel barrier.

ALD of Al_2O_3 on TiN was performed at 200 °C using TMA and H_2O. Five samples were prepared in which a 100 cycle Al_2O_3 ALD sequence was interrupted by two cycles (c) of $Ni(^{tBu2}DAD)_2$ and O_3 after 25, 50, 75, and every 25 c of Al_2O_3. As-deposited MIM devices were tested with bias applied to an Al top electrode (Fig. 1).

DC J-$\mathcal{E}$ sweeps of the 100 c device show Fowler-Nordheim tunneling (FNT) at high $\mathcal{E}$, with $f_{asym} > 1$ due to $\Delta\Phi_M \approx 0.2$ eV (Fig. 1). The addition of Ni cycles in all cases leads to an increase in J at low $\mathcal{E}$ vs. the 100 c Al_2O_3 device, suggesting defect related conduction. At high $\mathcal{E}$, however, J of all Ni devices is lower than the 100 c device, suggesting suppression of FNT. The 25/2/75 and 75/2/25 ($Al_2O_3/Ni/Al_2O_3$) devices show f_{asym} *opposite* of the 100 c device, while the 50/2/50 and 25/(2/25)x3 devices are roughly symmetric (Fig. 1). The greater reduction in J at large negative $\mathcal{E}$, f_{asym} reversal, and reduced J-$\mathcal{E}$ slope for the 25/2/75 and 75/2/25 devices suggest that FNT is suppressed more for emission from the smaller Φ_M electrode (Al) than for TiN. FNT suppression appears greatest for the 75/2/25 device in which Ni is closest to the Al, pointing to an increase in effective barrier height, likely due to negative charge in the Al_2O_3. Capacitance (C) *vs.* $\mathcal{E}$ sweeps (Fig. 2) reveal a positive voltage shift in C_{min} for all Ni devices, consistent with negative charge.

The asymmetry reversal demonstrates the possibility of precision defect engineering of MIM tunnel devices using ALD. An in-depth discussion of J-$\mathcal{E}$ and C-$\mathcal{E}$, temperature-IV, frequency-CV, other impurities, and annealing will be presented.

1. Alimardani et al., APL 102 143501 (2013).

2. Alimardani et al., JAP 116, 024508 (2014).

3. Alimardani and Conley, Jr., APL 105, 082902 (2014).

12:00pm TF+EM+MI-TuM-13 Improvement in the Electrical Characteristics of a-ZTO based TFTs *via* Microwave Assisted Annealing of Channel Layer, *Sunil Uprety, M Khanal, H Lee, S Sarwar,* Auburn University*; A Subramanian,* Stony Brook University*; E Hassani, T Oh, X Zhang,* Auburn University*; C Nam,* Brookhaven National Laboratory*; M Park,* Auburn University

In this research, we have investigated the effect of microwave-assisted annealing of amorphous zinc tin oxide (a-ZTO) channel layers on the electrical characteristics of the thin film transistors (TFTs). A multi-stacked a-ZTO layer was deposited on the oxidized Si wafer using sol-gel process. The precursor solution was prepared by dissolving zinc acetate dihydrate and tin chloride dihydrate into methoxyethanol. The solution was spin coated and calcined in a hot plate at 285°C. The as-calcined a-ZTO wafers

---

[1] **TFD James Harper Award Finalist**

were microwave annealed. The microwave (MW) annealing was carried on a commercial microwave oven at different power levels with the sample placed in a kiln which acts as a susceptor. The films remained amorphous even after MW annealing, which was evidenced by X-ray diffraction. The devices were fabricated using the microwave-annealed and as-calcined samples. Hall measurement is being carried out to study the concentration and mobility of charge carries. The performance of the TFTs with as-calcined and MW annealed channel layers were compared. Improvement in the electrical characteristics of the TFTs with MW annealed films were noted. It is believed that the microwave irradiation may promote the enhancement of the electrical characteristics of TFTs. Further research is being pursued to elucidate the role of microwave annealing in improvement of the device performance.

Energy Transition Focus Topic
Room A212 - Session TL+MS+VT-TuM

Implications of Implementation: Making Energy Transition a Reality (ALL INVITED SESSION)

Moderators: Margaret Fitzgerald, Colorado School of Mines, Natalie Seitzman, Colorado School of Mines

8:00am **TL+MS+VT-TuM-1 The Energy Transition: Science and Technology Development Aspects**, *Richard M.C.M. van de Sanden*, DIFFER, Eindhoven University, The Netherlands, Netherlands   **INVITED**
The Paris climate agreement requires a decarbonization of our energy infrastructure leading to a CO_2 neutrality by 2050. Therefore renewable energy generation by means of wind or from solar radiation through photovoltaics or concentrated solar power will continue to increase its share in the energy mix. Intermittency (due to e.g. day/night cycle), the regional variation of these energy sources, and penetration of renewable energy into other sectors than electricity (e.g. the chemical industry) requires means to store, transport and convert energy on a large scale. A promising option is the synthesis of chemicals and synthetic fuels (easily deployable within the present fossil fuels infrastructure) from raw feedstock using renewable energy. A truly circular economy requires that the raw materials are the thermodynamically most stable molecules such as water (H_2O), carbondioxide (CO_2) and nitrogen (N_2) to produce base chemical feedstock, such as e.g. hydrogen, hydrocarbons and ammonia. In this talk I will discuss the opportunities this transformation of the chemical industry provides. Furthermore, I will highlight the science and technology challenges, the catalytic materials, processes and systems developments needed that can provide compatibility of renewable energy driven chemistry with e.g. intermittency and localized production.

8:40am **TL+MS+VT-TuM-3 Electrochemical CO2 Reduction Across Scales: From Fundamental Mechanisms to Practical Applications**, *Wilson Smith*, Delft University of Technology The Netherlands, The Netherlands   **INVITED**
Electrocatalytic CO_2 reduction has the dual-promise of neutralizing carbon emissions in the near future, while providing a long-term pathway to create energy-dense chemicals and fuels from atmospheric CO_2. The field has advanced immensely in recent years, taking significant strides towards commercial realization. While catalyst innovations have played a pivotal role in increasing the product selectivity and activity of both C1 and C2 products, slowing advancements indicate that electrocatalytic performance may be approaching a hard cap. Meanwhile, innovations at the systems level have resulted in the intensification of CO_2 reduction processes to industrially–relevant current densities by using pressurized electrolytes, gas-diffusion electrodes and membrane-electrode assemblies to provide ample CO_2 to the catalyst. The immediate gains in performance metrics offered by operating under excess CO_2 conditions goes beyond a reduction of system losses and high current densities, however, with even simple catalysts outperforming many of their H-cell counterparts. Using recent literature as a guidepost, this talk will focus on some of the underlying reasons for the observed changes in catalytic activity, and proposes that further advances can be made by shifting additional efforts in catalyst discovery and fundamental studies to system-integrated testing platforms.

9:20am **TL+MS+VT-TuM-5 Perspectives on the Research and Development of Nanomaterials for Hydrogen Production**, *Marcelo Carmo*, Forschungszentrum Jülich, Germany   **INVITED**
Hydrogen is often considered the best means by which to store energy coming from renewable and intermittent power sources. With the growing capacity of localized renewable energy sources surpassing the gigawatt range, a storage system of equal magnitude is required, such as the production of electrolytic hydrogen by water electrolysis. Despite of more than 100 years of experience in alkaline electrolysis systems, and thousands of plants installed all over the world, only a few systems or industries remain, providing the state-of-the-art of this technology today. This is due to the fact that the cost of electrical energy has always remained as an uncomfortable barrier, with electrolytic hydrogen costs not being able to compete with the costs for the production of hydrogen by conventional steam reforming of fossil fuels. Nevertheless, today, increased interest can be observed for PEM water electrolysis technology, and over the past 20 years, new companies and projects have appeared, with new leaders being consequently established in this growing niche. The reason is that PEM electrolysis provides a sustainable solution for the production of hydrogen, and is well suited to couple with energy sources such as wind and solar. The advantages of PEM electrolysis over alkaline electrolysis together with novel R&D approaches can potentially reduce the investment costs of PEM electrolysers. We expect that in the following years, frontier advancements on PEM electrolysis systems will appear, demonstrating a true capacity to ultimately establish hydrogen as a key player in the energy market, and contribute to a future hydrogen economy.

11:00am **TL+MS+VT-TuM-10 Impacts and Adaptation Strategies in Ethiopia**, *Aschale Dagnachew Siyoum*, Xavier University of Louisiana
This paper highlights climate change and variability and its impact and adaptation strategies in Ethiopia. Due to low adaptive capacity and high sensitivity of socio economic systems, climate vulnerability is worsening over the last few decades in Ethiopia. Available evidences showed that since 1960, the mean annual temperature of the country has risen by about 1.3°C with an average rate of 0.28°C per decade imposing a significant challenge on food security, water availability, energy supply, poverty reduction and sustainable development efforts of the nation. Ethiopia has responded to the increasing impact of climate change and variability through developing relevant adaptation strategies, plans and policies largely focused on decreasing vulnerability in many different sectors including agriculture and food security, water resources, forestry, and health. To tackle the impact of climate change, the government has approved the National Adaptation Program of Action (NAPA) in 2007 which includes projects that focused on promoting drought insurance program, strengthening drought and flood early warning systems, developing small-scale irrigation and water harvesting schemes in arid, semi-arid, and dry sub-humid areas, and realizing food security through a multi-purpose large-scale water development project. Results, however, shows that although some progress has been made in addressing the impacts of climate change and variability, adaptation measures implemented over the last few decades were generally ineffective resulting in increasing losses as more and more people occupy vulnerable areas. This requires a sustained effort to further plan and implement the right mix of climate change adaptation strategies to address vulnerability to biodiversity and humanity to the increasing impacts of climate change. Addressing the impact of climate change requires a good understanding of the nexus between climate change adaptation measures and sustainable development as well as knowledge of climate change adaptation tools and techniques, which when used properly can minimize the total damage to life and property.

11:20am **TL+MS+VT-TuM-11 Developing and Scaling Up the Manufacturing of Thin Film Materials for the Future of Energy Production, Storage, and Reduction**, *Ken Nauman*, Von Ardenne North America   **INVITED**
The world, and thus the economy, are clearly dependent on energy and in particular electricity. Production of electricity is ever increasing while the desire to create cleaner sources becomes a higher priority to reduce the environmental impact. The transition to electricity for mobility in transportation and communication relies on new technology to improve market penetration. Thus, the three key aspects of electricity in our modern society are: generation, storage, and saving. In order to make the energy transition a profitable reality, companies that develop technology will have to reduce the cost of energy production and storage while also considering how to lower energy usage. This talk will cover these key aspects from the perspective of an equipment and process technology company. Companies such as Von Ardenne that develop thin film materials have focused on these topics to reduce the CapEx and CoO for our customer's factories. This includes processes for Thin Film Photovoltaics and Crystalline Photovoltaics, along with emerging cell architectures, to reduce the cost of electricity generation while reducing overall CO2 production. Our company also works on leading material science in battery and fuel cell technology to increase storage capacity and cost of storing energy. Finally, other technology development is focused on saving energy

with low-e coatings for glass and plastics. This presentation will review the history of the technological development as well as the latest trends, economics, and status of market leading performance in manufacturing products related to generating, storing, and saving electricity.

Vacuum Technology Division
Room A213 - Session VT-TuM

Accelerators and Large Vacuum Systems
Moderators: Yulin Li, Cornell University, Marcy Stutzman, Jefferson Lab

8:00am **VT-TuM-1 Vacuum Operation and Future Upgrade of the LHC Accelerator Complex**, *Giuseppe Bregliozzi,* CERN, Switzerland **INVITED**
The LHC accelerator complex returned in operation in April 2015, after almost 2 years of long shutdown (LS1) for various upgrades and consolidation programs. During Run2 of operation (2015-2018), the entire accelerator complex has shown remarkable reliability and in particular, the LHC operated for more than 3600 fills reaching a total integrated luminosity of more than 150 fb−1.

In 2019, the entire LHC accelerator complex will stop again for 2 years (Long Shutdown 2 - LS2). This period will be dedicated to the LHC Injector Upgrade (LIU) and will prepare the CERN injector complex for the final upgrade of the LHC to High-Luminosity (HL-LHC) foresee during the LS3 (2024-2025).

This paper summarizes the vacuum related major issues happened during last 3 years of operation in the entire LHC accelerator complex and a summary of the most important vacuum observations along the LHC during the physics runs are presented. In addition, an overview of the planned activities during the LS2 will be presented and an outlook on the technical challenges for the HL-LHC upgrade is given.

8:40am **VT-TuM-3 Final Design into Production for the APS-Upgrade Storage Ring Vacuum System**, *Jason Carter,* Argonne National Laboratory
The Advanced Photon Source Upgrade (APS-U) project is progressing from its final design phase into production for the future 6 GeV, 200 mA, multi-bend achromat upgrade of the existing APS and so too is the storage ring vacuum system design. The vacuum system will include over 2500 custom vacuum chambers ranging from 50 mm up to 2.5 meters in length and typically featuring APS-U's standard narrow 22 mm inner diameter aperture. The vacuum system must maintain UHV for the circulating electron beam while the water-cooled vacuum components intercept significant synchrotron radiation loads. The scope of NEG coatings was increased to 50% of the length of the vacuum system to ensure the vacuum system conditions quickly and pressure requirements can be met.

Vacuum chamber locations, lengths, and materials were settled in the preliminary design phase but significant effort was required to work through local and system level design challenges. Local challenges include detailing robust welds and brazes on the thin-walled vacuum chambers and performing detailed FEA thermal/stress analysis for vacuum components which intercept large synchrotron radiation heat loads. System level challenges include using CAD to design within the complex machine assembly, networking components to utilities, and planning for installation and alignment. This presentation will highlight the major design challenges and solutions for the storage ring vacuum system and also plans for production and installation.

9:00am **VT-TuM-4 The Design of the Advanced Photon Source Upgrade (APSU) Insertion Device (ID) Straight Section Vacuum Systems**, *Jason Lerch*, M Szubert, E Anliker, T Bender, Argonne National Laboratory
There are 35 straight sections in the APS-U, requiring 30 planar vacuum chambers (IDVC) and 5 superconducting vacuum systems (SCU VC). These vacuum systems provide Ultra-High Vacuum (UHV) continuity between storage ring (SR) sectors. The IDVC, nominally 5.363 meters long, requires bake-out before operation and expands 10mm on both ends. The SCU vacuum chambers, nominally 5.383 meters long, are cooled cryogenically and contract 14 mm on both ends. The APS-U straight sections are identical around the SR but require bellows on both ends to accommodate the change in length of both systems. The aluminum planar vacuum chamber operates in UHV with a 600 thick wall over a length of 5050 mm and requires the use of 1 ion pump and 7 NEG cartridges for pumping down the system. The SCU is comprised of two copper "warm" vacuum systems, operating at room temperature outside the cryostat, and one aluminum "cold" vacuum system (4.8m long), operating at 20K inside the cryostat. The "warm" chambers have a minimum wall thickness of 1 mm and

operate as photon absorbers at either end of the system, one protecting the cryogenically pumped chamber and one protecting downstream equipment. The "cold" chamber has a minimum wall thickness of 400 and operates at UHV at 20 Kelvin. The internal geometries of these various systems are optimized to reduce dissipated heat on the chamber walls where possible and allow for seamless transitions for various apertures. Both vacuum systems require the ability to align the apertures ±50 microns along their lengths.

9:20am **VT-TuM-5 The Vacuum Commissioning and Simulation of Non-Evaporable Getter Dominated Cornell High Energy Synchrotron Source Upgrade.**, *Yevgeniy Lushtak,* Y Li, X Liu, Cornell University
The Cornell High Energy Synchrotron Source Upgrade (CHESS-U) converts the Cornell Electron Storage Ring (CESR) from dual-beam to single-beam operation while significantly reducing the beam emittance, increasing the beam energy to 6 GeV, and improving the facility's X-Ray beamline brightness.

The CHESS-U vacuum system was completed in the fall of 2018 and the initial beam current and energy targets were met in the spring of 2019. The majority of the CHESS-U vacuum system consists of narrow gap aluminum chambers. With pre-installation 150 C bake followed by in situ 95 C hot-water bake and relying on the high pumping speed of distributed and lumped Non-Evaporable Getters (NEGs), a low 10^{-9} Torr base pressure was quickly achieved.

Since the CHESS-U vacuum pumping system is NEG-dominated and NEGs are prone to surface saturation at high synchrotron radiation (SR) induced gas loads, the vacuum conditions during the CHESS-U accelerator commissioning were carefully monitored and periodical vacuum simulations using MolFlow were performed to ascertain the status of the NEGs. The SR-induced vacuum conditioning has proceeded very well, with the dynamic pressure holding in the low 10^{-9} range with 100 mA stored positron beam current, after an accumulated beam dose of 20 A-hr. With the moderate initial beam conditioning, a beam lifetime allowing X-ray beam operation to commence has already been achieved. Further gradual improvements in the dynamic pressure and beam lifetime are expected during the course of X-ray user operations.

In this paper, we describe the CHESS-U vacuum system, report on the SR-induced vacuum conditioning status, and detail the computational model developed to accurately simulate the vacuum conditions while taking into account the NEG saturation and the radiation-induced cleaning of the chambers.

9:40am **VT-TuM-6 Advanced Light Source Upgrade Vacuum Controls and Instrumentation Design**, *Sol Omolayo,* Lawrence Berkeley Lab, University of California, Berkeley
A project is underway to upgrade the existing Advanced Light Source (ALS) synchrotron. The goal of the project is to lower the horizontal emmitance to <75pm resulting in a 2 orders of magnitude increase in soft x-ray brightness. The design features two new accelerators: the accumulator ring and the storage ring. Both rings are also connected by transfer lines. The preliminary design for the vacuum systems for these rings and transfer lines in underway. With over 400m long electron beam vacuum pipe, the control and instrumentation required for the vacuum system is complex. We present the design specification and solution the project has adopted.

11:00am **VT-TuM-10 Vacuum Electronics Community Pioneers Additive Manufacturing of Copper**, *Diana Gamzina,* SLAC National Accelerator Laboratory*; T Horn, C Ledford,* North Carolina State University*; C Nantista,* SLAC National Accelerator Laboratory*; P Frigola,* Radiabeam **INVITED**
Even though there are many players in the world of additive manufacturing (AM), vacuum electronic devices (VED) community made a significant impact on AM of copper specifically, with recognition by industrial partners and government agencies. Copper is a challenging material to print because of its high reflectivity and high thermal conductivity; material purity is also hard to achieve due to the lack of high quality precursors. VED community has the most stringent requirements for copper. The successful implementation of copper AM for VEDs will support a wide range of applications, including thermal management, power electronics, and nuclear. Many critical to VED manufacture properties have been achieved (density, ultra-high vacuum compatibility, electrical and thermal properties), but few still remain to be challenging (reduction of oxygen content and surface roughness). A variety of components relevant to VED community have been manufactured; more interesting examples include: high efficiency klystron output cavity with micro cooling channels and weight reducing web support structure; one inch long sections of WR-10

waveguide demonstrating post-polishing techniques to reduce surface roughness to 2 microns in enclosed envelopes, coupled cavity travelling wave tube amplifier circuit structures demonstrating over 50% cost reduction capability. Most of the benefits that AM can offer still lie ahead to be explored: predesigning material properties local to specific design features while varying physical, electronic, or chemical properties locally.

11:40am **VT-TuM-12 Particle-Free Manufacturing and Installation for LCLS-II Vacuum Systems**, *Arnela Gamzina,* SLAC National Accelerator Laboratory

SLAC National Accelerator Laboratory, a multipurpose laboratory for astrophysics, photon science, accelerator and particle physics, is currently building an upgrade to the World's First X-ray Free-Electron Laser (LCLS-II). In the past years, SLAC Vacuum Laboratory has prepared, tested, and assembled many of the beamline components and the activity is still in progress.

This presentation will go through the manufacturing and quality check processes, documentation and installation check lists that were developed to meet the LCLS-II UHV and Particle Free requirements. Especially, in order to meet Particle Free requirements new equipment and facilities were acquired. The vacuum group worked to establish new procedures and made sure that selected personnel developed the requested skills, best practices, and gained the experience necessary to complete a successful installation.

12:00pm **VT-TuM-13 Development of Remote Handleable Axially Decoupled Radiation Resistant Vacuum Seal**, *Geoff Hodgson,* TRIUMF, Canada

Advanced Rare IsotopE Laboratory (ARIEL) facility is a major expansion of TRIUMF's rare isotope research program.

Aiming to triple the production of rare isotopes, ARIEL facility includes the new electron linac driver and

two target stations for electron and proton beams [1]. Particularities of ARIEL target stations design define the requirements for vacuum interfaces with both primary electron and proton beamlines and rare-isotope beamlines. None of the existing products fully met the requirements, driving the development of custom vacuum interfaces. The design of new vacuum seals is driven both by unique design specifications (limited amount of allowed axial forces, extreme radiation

resistance, remote handleability and high repeatability) as well as limitations of the proposed design of beamline nfrastructure in the target hall (limited available space and the choice of materials for certain components). This paper discusses preliminary results of the vacuum seal development and presents first results of prototype testing.

Tuesday Afternoon, October 22, 2019

Exhibitor Technology Spotlight Workshops
Room Hall A - Session EW-TuL

Exhibitor Technology Spotlight Workshop II
Moderator: Christopher Moffitt, Kratos Analytical Inc

12:20pm **EW-TuL-2 New Developments from Thermo Fisher Scientific**, *Timothy Nunney*, *P Mack, R Simpson, A Bushell,* Thermo Fisher Scientific, UK

In this presentation we will highlight the latest developments in surface analysis and materials analysis instrumentation from Thermo Fisher Scientific.

12:40pm **EW-TuL-3 New Trends in Photoelectron Spectroscopy: Momentum Resolved Photoelectron Spectroscopy, Spin-resolved ARPES, Small Spot and Hard X-ray XPS**, *A Thissen,* SPECS Surface Nano Analysis GmbH, Germany; *Thomas Stempel Pereira,* SPECS Surface Nano Analysis GmbH

Over the last two decades, significant developments have been done in Photoelectron Spectroscopy instrumentation. The significant expansion of XPS into near ambient pressure environments (NAP-XPS), especially new concepts for electron optics, new concepts for X-ray sources, and new type of detectors have opened the field for new applications.

New electron optical concepts have been introduced, allowing for K-resolving lenses in Angle resolved Photoelectron Spectroscopy and Small Spot Momentum Spectroscopy and Microscopy. The brand new ASTRAIOS 150 is a consequently k-resolving hemispherical analyzer for cutting-edge ARPES with large acceptance angles at ultimate energy and k- (or angle) resolutions. For limiting the acceptance areas to μm-ranges or momentum microscopy applications k-resolving immersion lenses have to be used. The KREIOS 150 series demonstrates perfectly the applications to small and/or inhomogeneous samples.

On the detector field the 2D-CMOS detector has proven to be the perfect choice for ultimate resolution and highest linearity at significant time resolution. Especially for momentum microscopy the direct imaging spin detector DISpin allow for highest sensitivities and uncompromising energy and k-resolutions.

Switching gears, on the XPS field the above mentioned new analyzers also can make a significant contribution to small spot-XPS. On the other hand still a high power small spot monochromatic X-ray source is needed. Thus the μFOCUS 195 is presented for the first time, being a Al Ka and Ag La dual anode monochromator source is presented, with a spot diameter smaller than 10μm.

For higher information depth the μFOCUS 730 HE is presented, a Cr Ka monochromator source with a 100μm spot size for laboratory HAXPES and NAP-HAXPES.

1:00pm **EW-TuL-4 Latest Trends and Instrumentation for TOF-SIMS**, *Nathan Havercroft*, IONTOF USA, Inc.

During the last 30 years IONTOF has continuously made significant development efforts to further improve the instrumentation for Time-of-Flight Secondary Ion Mass Spectrometry (TOF-SIMS) and related techniques. Some of the most recent achievements include in-situ sample preparation and tomography by FIB, enhancement of maximum count rates and dynamic range in conventional depth profiling of inorganic materials, the design of a TOF-SIMS / SPM combination instrument, as well as the integration of an OrbitrapTM mass spectrometer with unrivalled mass resolution and mass accuracy into the TOF.SIMS 5 instrument.

In this spotlight session we will showcase the latest TOF-SIMS developments from IONTOF.

1:40pm **EW-TuL-6 Kratos Analytical – 50 Years of XPS**, *Christopher Blomfield*, Kratos Analytical Limited, UK

In 1969 Kratos, then AEI, shipped the first commercially available X-ray photoelectron spectrometer to Dr David Clark at the University of Durham. In this presentation we will outline the developments from the first ES-100 to the state-of-the-art AXIS Supra+ and have established Kratos Analytical as a leader in the design and manufacture of XPS instruments.

We will detail the development of the Aberration Compensated Input Lens (ACIL) in the early 1980's. Importantly the nature of the ACIL provided the analyst with an easy to use microprobe-like capability, enabling exact correlation of classic spectroscopic analysis with XPS and physical images – the advent of spatially keyed spectroscopy. A further significant development came with the AXIS series of spectrometers which were the first to incorporate a magnetic immersion (snorkel) lens. The combination of magnetic and electrostatic lenses lead to much greater collection efficiency of photoelectrons when compared to previous instruments, providing a step-change in performance specifications.

Another Kratos innovation, launched in the late 1990's, was the incorporation of the spherical mirror analyser (SMA) with the hemispherical analyser in the AXIS Ultra. The SMA allowed fast, high spatial resolution parallel imaging, where an image of the sample is projected onto a 2D detector. This technology is still used today and allows us to define 1um imaging spatial resolution.

There have been a number of other momentous advances including software, automation and accessories. Probably the most significant of these recent developments is the gas cluster ion source (GCIS). This accessory has allowed the successful depth profiling of organic polymers and inorganic samples with retention of chemistry throughout the profile.

It is hoped that in reviewing milestones in Kratos' development of XPS over the previous 50 years we will trigger discussion on requirements for the technique in the next 50 years.

2:00pm **EW-TuL-7 What's New at PHI**, *K Artyushkova, J Mann, B Schmidt, L Swartz, John Newman,* Physical Electronics

PHI has multiple exciting projects currently underway in our XPS product line. This presentation will provide updates on:

•The PHI Quantes, laboratory based, XPS/HAXPES instrument

•Some new analytical options for complete characterization of electronic band structures on the PHI VersaProbe

•New features for XPS data acquisition and data reduction.

2D Materials

Room A216 - Session 2D+EM+MI+NS-TuA

Properties of 2D Materials including Electronic, Magnetic, Mechanical, Optical, and Thermal Properties II

Moderator: Roland Wiesendanger, University of Hamburg, Germany

2:20pm **2D+EM+MI+NS-TuA-1 Boundary Conditions for a Continuum Model of Lateral Interfaces in Transition Metal Dichalcogenides**, *Kaelyn Ferris,* Ohio University

Tight-binding models of in-plane, lateral heterostructures of commensurate transition-metal dichalcogenides (TMD), such as MoS_2-WS_2 and $MoSe_2$-WSe_2 have demonstrated the appearance of laterally localized effective one-dimensional interfacial and edge states with unique features. These states lie within the band gap of the bulk structure and may provide a stable, tunable one-dimensional platform for possible use in exploring Majorana fermions, plasma excitations, and potential spintronics applications [1]. Motivated by the possible versatility of these modes in a variety of 2D systems, we now explore their appearance in continuum model descriptions of effective massive Dirac systems at low energy. We use different k*p models to characterize TMD nanoribbons and analyze proposals for the appropriate boundary conditions at lateral interfaces with various terminations. In particular we examine an *M*-Matrix approach [2] and envelope function approximation to obtain suitable boundary conditions.

[1] O. Avalos-Ovando et al., J. Phys.: Cond. Matt. **31**, 213001 (2019).

[2] C. G. Peterfalvi et al., Phys. Rev. B **92**, 245443 (2015).

2:40pm **2D+EM+MI+NS-TuA-2 Resolving the Structural and Electronic Properties of Graphene/Ge(110)**, *Luca Camilli,* Technical University of Denmark, Denmark*; M Galbiati,* Technical University of Denmark*; L Persichetti, M De Seta,* Università degli Studi Roma Tre, Italy*; F Fabbri,* Italian Institute of Technology, Italy*; A Scaparro,* Università degli Studi Roma Tre, Italy*; A Notargiacomo,* Centro Nazionale di Ricerca, Italy*; V Miseikis, C Coletti,* Italian Institute of Technology, Italy*; L Di Gaspare,* Università degli Studi Roma Tre, Italy

Unraveling the structural and electronic properties of the interface between graphene and conventional semiconductors is critical to enable novel graphene-based applications [1].

In this framework, the graphene/Ge(110) system has since last year received unprecedented attention [2-6]. Notably, graphene can be grown via chemical vapor deposition directly on the surface of germanium, similarly to the case of graphene grown on metals [7]. From a structural point of view, the graphene/Ge system is very dynamic, and the Ge surface has been shown by scanning tunneling microscopy (STM) studies to undergo a number of changes (i.e., reconstructions). However, the conclusions drawn in those studies do not always agree, probably also due to the strong dependence of the STM images on the applied voltage bias that makes comparison between different images rather difficult. In Ref. [6], for instance, the authors report three different surface reconstructions that are driven by thermal annealing, while the authors in Ref. [4] find only the unreconstructed surface and a (6x2) reconstruction, which again can reversibly change to unreconstructed surface after annealing at high temperature in hydrogen.

In this study, we aim at resolving the rich phase diagram of the Ge surface protected by graphene. We carry out annealing of the sample at different temperatures, and use a low-temperature STM to investigate the surface structure with atomic precision. At each stage, images at different applied biases are collected in order to allow a more straightforward comparison of the results.

Moreover, we perform electron energy loss spectroscopy (EELS) and scanning tunneling spectroscopy (STS) at temperature below 10 K to shed light on the electronic properties of the graphene/Ge interface, and to get more insights into their interaction.

Finally, we also show through a combination of STM and Raman spectroscopy that graphene can protect the germanium surface from oxidation even after continuous exposure to ambient conditions for more than 12 months, which is surprisingly a far more efficient protection than that offered by graphene on metals [8, 9].

References

[1] J.-H. Lee et al. Science 344, 286 (2014)

[2] G. Campbell et al. Physical Review Materials 2, 044004 (2018)

[3] J. Tesch et al. Nanoscale 10, 6068 (2018)

[4] D. Zhou et al. Journal of Physical Chemistry C 122, 21874 (2019)

[5] H.W. Kim et al. Journal of Physical Chemistry Letters 9, 7059 (2018)

[6] B. Kiraly et al. Applied Physics Letters 113, 213103 (2018)

[7] X. Li et al. Science 324, 5932 (2009)

[8] F. Zhou et al. ACS Nano 7, 6939 (2013)

[9] X. Zhang et al. Physical Chemistry Chemical Physics 18, 17081 (2016)

3:00pm **2D+EM+MI+NS-TuA-3 Array of Strain Induced Quantum Dots in Graphene**, *Md Tareq Mahmud, N Sandler,* Ohio University

Local Gaussian-shaped deformations induce strain fields that are represented by scalar and vector potentials in a continuum model description of electron dynamics in graphene. The ubiquitous strain changes the charge distribution in a very peculiar way, introducing a sublattice symmetry breaking, as has been reported in the literature. This feature can be exploited to design specific charge profiles by combining several deformations. Naturally, a combination of two or more is expected to introduce interference effects that can enhance charge accumulation in specific regions. We have investigated the effects of two overlapping deformations with different separations on the local density of states (LDOS). We showed that the overlap term can enhance the LDOS leading to stronger charge confinement in certain regions. Motivated by the work of Mason et. al (2018) we have extended these studies to a closed pack structure with a unit cell of 3 distinct deformations. This arrangement can be extended by symmetry to a lattice superstructure, thus creating a periodic array of confined charge regions, i.e, quantum dots. This array can be tailored by appropriately choosing the parameters of the deformations and their distances. The total charge distribution in these systems is similar to those observed in twisted bilayer systems, known as 'Moire patterns'. We discuss optimal tuning of deformations to control the physical properties of these graphene devices.

3:20pm **2D+EM+MI+NS-TuA-4 Ultrafast Spin and Charge Dynamics in Monolayer WSe₂-Graphene Heterostructure Devices**, *Michael Newburger, K Luo,* The Ohio State University*; K McCreary,* U.S. Naval Research Laboratory*; I Martin, E McCormick,* The Ohio State University*; B Jonker,* U.S. Naval Research Laboratory*; R Kawakami,* The Ohio State University

Monolayer transition metal dichalcogenides (TMDs) have attracted attention due to their long spin/valley lifetimes and ability to couple the helicity of light to spin/valley polarization. Additionally, a strength of TMDs lies in their ability to complement other materials, such as graphene, by acting as a means of optical spin injection or proximity coupling. Recently, multiple groups have demonstrated proximity mediated charge transfer and optical spin injection in TMD/graphene heterostructures. However, the spin transfer dynamics across a TMD/graphene interface remain largely unexplored.

Here we utilize time-resolved Kerr rotation (TRKR) microscopy to image the spatial dependence of spin/valley dynamics in monolayer WSe_2/graphene heterostructure devices. Spatial maps demonstrate long-lived spin/valley lifetimes on the bare WSe_2 but reveal a quenching of spin-valley signal at the WSe_2/graphene interfaces. Time delay scans show these interface lifetimes to be quenched up to 3 orders of magnitude in comparison to bare WSe_2. Furthermore, photoluminescence mapping exhibits quenching at the interfaces while photoconductivity is enhanced in these regions, demonstrating efficient charge transfer from WSe_2 to graphene. Consequently, we attribute the ultrafast spin/valley quenching to the transfer of spin information by conducted charge carriers.

4:20pm **2D+EM+MI+NS-TuA-7 Spatially Selective Enhancement of Photoluminescence in MoS by Exciton-Mediated Adsorption and Defect Passivation**, *Saujan V. Sivaram, A Hanbicki, M Rosenberger, G Jernigan, H Chuang, K McCreary, B Jonker,* U.S. Naval Research Laboratory

Monolayers of transition metal dichalcogenides (TMDs) are promising components for flexible optoelectronic devices due to their direct band gap and atomically thin nature. The photoluminescence (PL) from these materials is often strongly suppressed by non-radiative recombination mediated by mid-gap defect states. Here, we demonstrate up to a 200-fold increase in PL intensity from monolayer MoS_2 synthesized by chemical vapor deposition (CVD) by controlled exposure to laser light in ambient. This spatially resolved passivation treatment is air and vacuum stable. Regions unexposed to laser light remain dark in fluorescence despite continuous impingement of ambient gas molecules. A wavelength dependent study confirms that PL brightening is concomitant with exciton generation in the MoS_2; laser light below the optical band gap fails to

produce any enhancement in the PL. We highlight the photo-sensitive nature of the process by successfully brightening with a low power broadband white light source (< 10 nW). We decouple changes in absorption from defect passivation by examining the degree of circularly polarized PL. This measurement, which is independent of exciton generation, confirms that laser brightening reduces the rate of non-radiative recombination in the MoS_2. A series of gas exposure studies demonstrate a clear correlation between PL brightening and the presence of water. We propose that H_2O molecules passivate sulfur vacancies in the CVD-grown MoS_2, but require photo-generated excitons to overcome a large adsorption barrier. This work represents an important step in understanding the passivation of CVD-synthesized TMDs and demonstrates the interplay between adsorption and exciton generation.

This research was performed while S.V.S and M.R.R held a National Research Council fellowship and H.-J.C. held an American Society for Engineering Education fellowship at NRL.

4:40pm **2D+EM+MI+NS-TuA-8 Strained Graphene in the Quantum Hall Regime: Valley Splitting and Extra Conducting Channels**, *Daiara Faria,* Ohio University / Universidade do Estado do Rio de Janeiro*; C León,* Brigham Young University*; L Lima,* Universidade Rural do Rio de Janeiro, Brazil*; A Latgé,* Universidade Federal Fluminense, Brazil*; N Sandler,* Ohio University

The coupling between electronic and mechanical properties in 2D materials has become an important tool to control valleytronics. Graphene experiments have been reported with common deformations such as membrane bending that induces strain in the samples [1]. It has also been shown that strain affects charge distributions and graphene transport properties. Motivated by these responses, we have studied the effect of folds and wrinkles in graphene. New 'edge'-like states along the graphene folded region, that are valley polarized, were found and explored [2]. To take advantage of the existence of these new states, it would be desirable to separate their contribution from the continuum extended states that make graphene a semimetal.

Here we present a theoretical study of folds effects on a graphene membrane in the quantum Hall regime. We show that the addition of an external magnetic field allows the isolation of the valley polarized edge states in energy and in real space. Local density of state calculations in the deformation region predict the valley split peaks, as observed in recent experimental [3]. Using recursive Green's function method, we are able to reveal new extra conducting channels due to the "new edges" at the deformation region. These extra conducting channels could be detected in transport measurements.

A discussion is presented to bring attention on the role of the deformation parameters on the graphene quantum Hall regime and their relations with the magnetic lengths. With this in mind, we perform an analytic study based on the continuum (Dirac) description of electrons in graphene. In this model, the deformation is considered as a perturbation to the Landau Level states. The results show the existence of two different regimes, characterized by the ratio between the magnetic length and the deformation width ($\gamma = l_B/b$). For $\gamma < 1$ the magnetic confinement allows the electrons to follow the strain potential profile. In this regime, the spatial separation between the polarized currents is larger. This could encourage the design of devices where contacts can efficiently detect these polarized currents.

[1] Y. Jiang et al., Nano Lett. 17, 2839 (2017).

[2] R. Carrillo-Bastos et al., PRB 94, 125422 (2016).

[3] S. Li, arXiv:1812.04344.

5:00pm **2D+EM+MI+NS-TuA-9 Unraveling the Novel Quantum Phenomena in Two-dimensional Materials using Transport and Photoemission Spectroscopy**, *Jyoti Katoch,* Carnegie Mellon University
INVITED

The extreme surface sensitivity of two-dimensional (2D) materials provides an unprecedented opportunity to engineer the physical properties of these materials via changes to their surroundings, including substrate, adsorbates, defects, etc. In addition, 2D materials can be mechanically assembled layer-by-layer to form vertical or lateral heterostructures, making it possible to create new material properties merely by the choice of the constituting 2D layers and the relative twist angle between them. In this talk, I will discuss our recent transport [1] and photoemission [2, 3] results that shed light on the intricate relationship between controlled external perturbations, substrate, and electronic properties of 2D materials. I will show that the decoration of the 2D materials with adatoms,

such as sub-lattice selective atomic hydrogenation of graphene and alkali metal doping of single layer WS_2 can be utilized to tailor electronic properties and induce novel quantum phenomena in 2D landscape.

[1] Katoch et. al., Physical Review Letters 121, 136801 (2018).

[2] Katoch et. al., Nature Physics 14, 355-359 (2018).

[3] Søren Ulstrup, et. al., arXiv:1904.06681 (2019).

5:40pm **2D+EM+MI+NS-TuA-11 Electronic Properties and Charge Density Wave Transition in Single-layer VSe₂**, *Kien Nguyen-Cong, P Neto, M Batzill, I Oleynik,* University of South Florida

Single-layer VSe_2 has been recently attracted attention due to experimental observations of ferromagnetism and charge density wave (CDW) transition. There are controversies from both theory and experiment concerning ferromagnetism in both bulk and single layer VSe_2.In addition, CDW transition in VSe_2 is not well understood. In this work, structural, electronic, magnetic and CDW properties of this system are investigated using first-principle calculations. The calculated electronic structure is compared with recent APPRES measurements and conclusions concerning its magnetic state are made. The calculated phonon spectra are used in investigation of CDW transition mechanism. Crystal structure of the CDW state is determined using the evolutionary crystal structure prediction combined with lattice dynamics.

6:00pm **2D+EM+MI+NS-TuA-12 Tunable Band Gap and Thermal Conductivity Measurements of Monolayer MoSe₂ by S Incorporation**, *Shyama Rath, V Singh,* University of Delhi, India

Monolayer $MoSe_2$ was grown on insulating SiO2/Si substrates by chemical vapor deposition. Scanning electron microscopy and optical contrast images were used to determine the domain size, morphology, and the number of layers. The crystallinity, and thickness of the synthesized domains were determined by Raman spectroscopy. The band gap was determined from Photoluminescence (PL) spectroscopy. The PL emission was absent for more than 4 layers, and the peak position varied from 1.48 eV for 4 layers to 1.55 eV in the monolayer limit. Sulphur incorporation was done to obtain MoS_xSe_{2-x} so as to obtain a further tunability of the bandgap. The band gap changes from 1.55 eV for monlayer $MoSe_2$ to 1.64 eV for monolayer $MoS_{0.32}Se_{0.68}$. Further, larger area domains were achieved in the alloy as compared to binary. The thermal conductivity of the monolayer $MoSe_2$ and MoS_xSe_{2-x} were determined from temperature-dependant Raman spectroscopy.

Actinides and Rare Earths Focus Topic
Room A215 - Session AC+AS+LS-TuA

Forensics, Science and Processing for Nuclear Energy

Moderators: Paul S. Bagus, University of North Texas, Tomasz Durakiewicz, National Science Foundation, David Geeson, AWE

2:20pm **AC+AS+LS-TuA-1 Helium Implantation Studies in Metals and Ceramics for Nuclear Energy Applications, Microstructure and Properties**, *Peter Hosemann, M Balooch, S Stevenson, A Scott,* University of California, Berkeley*; Y Yang,* Lawrence Berkeley Lab, University of California, Berkeley
INVITED

Helium damage in materials is a concern for fission and fusion materials. The development of Helium bubbles in a solid can lead to fundamental property changes ranging from embrittlement to surface blistering. Especially shallow ion beam implantation is of interest to the fusion community since the surface degradation of materials is one of the main materials degradation mechanism. This work features a rapid Helium implantation and screening method based on nanometer precise helium implantation using the helium ion beam microscope (HIM). This tool allows multiple doses in the same grain with subsequent rapid materials examination. We evaluate single and polycrystalline SiC, W, Cu, and Ti in this work and find interesting channelling phenomena which have been fit to modelling results from the literature. Further we evaluate mechanical and microstructural property changes using TEM, nanoindentation, AFM and micropillar compression testing on these alloys.

3:00pm AC+AS+LS-TuA-3 Origin of Element Selectivity during Solvent Extraction of Rare Earths: Studies of Model Interfaces using Synchrotron Radiation, *M Miller, Y Liang, H Li, M Chu, S Yoo,* Northwestern University; *W Bu,* University of Chicago; *M Olvera de la Cruz,* **Pulak Dutta,** Northwestern University **INVITED**

Solvent extraction, commonly used to remove lathanides from aqueous solutions, is known to preferentially extract heavier lanthanides. To understand the underlying nanoscale mechanisms, we studied a model system: extractant monolayers floating on an aqueous solution containing lanthanide ions. X-ray fluorescence near Total Reflection (XFNTR) was used to detect interfacial cations, using synchrotron radiation at the ChemMatCARS facility, Advanced Photon Source.

We found that the interfacial density of adsorbed cations increases very sharply as the solution concentration is increased, reminiscent of a first-order phase transition. The threshold concentration is an order of magnitude lower for erbium (Z=68) compared to neodymium (Z=68). When the solution contains both ions equally, only erbium is found at the extractant interface, and the bulk erbium concentration must be decreased by one order of magnitude relative to neodymium before both species appear equally at the interface.

These results indicate that element selectivity during liquid-liquid extraction occurs at the extractant-laden interface. Electrostatic effects arising from the dielectric mismatch, ionic correlations, and the sizes of the cations can be used to theoretically model the observed behaviors.

4:20pm AC+AS+LS-TuA-7 Analysis of Aged of Uranium Particles via X-ray Xpectromicroscopy, *Andrew Duffin, J Ward,* Pacific Northwest National Laboratory **INVITED**

Uranyl fluoride (UO_2F_2) particles are a common by-product when uranium hexafluoride (UF_6), a volatile form of uranium used in industry, is released into air. Uranyl fluoride particles continue to react in the environment, eventually moving towards uranium oxide. Understanding the chemical changes uranyl fluoride takes is important as the chemical state affects how this contaminant is transported in the environment. We employed scanning transmission X-ray microscopy (STXM) to map the chemical changes that occur in single particles of uranyl fluoride, aged under controlled conditions. We have shown that ligand K-edge X-ray absorption spectroscopy can fingerprint uranium chemical species at the nm spatial scale and we have used this specificity to gain insight into the transformation of uranyl fluoride to uranium oxide.

5:00pm AC+AS+LS-TuA-9 Heat Transfer and Phase Stability of Early Actinides and Actinide Compounds, *Dominik Legut, L Kývala, U Wdowik, G Jaglo, P Piekarz,* Technical University of Ostrava, Ostrava, Czechia; *L Havela,* Charles University, Prague, Czechia **INVITED**

Actinides and especially their carbides as prospective nuclear fuel materials for the generation IV reactors were investigated using the density functional theory. We demonstrate that their electronic, magnetic, elastic, and thermal properties can be at present well described if the spin-orbit interaction and partial delocalization 5f electrons is properly included in the computational approaches. One can well reproduce not only basic electronic structure but also elastic constants, phonon dispersions, and their density of states, provided by XPS, UPS, BIS, and inelastic neutron scattering data [1-4]. The localization of the 5f electrons could be captured using a moderate value of the on-site Coulomb interaction parameter. The case studies include a realistic description of the ground-state properties of elemental metals as Th, U and their monocarbides ThC and UC. The realistic description of the electronic structure and lattice dynamics (phonons) explains much higher thermal expansion and heat capacity in pure actinides (as Th) comparing with respective actinide monocarbides. The modelling also gives an insight up to which temperature the heat transport depends on lattice vibrations and where the electron transport starts to dominate. We can identify the vibration modes influencing the heat transport most. Carbides are compared with actinide oxides, where the major role is played by optical phonon branches [3]. The phase stability and elastic properties have been explored in a cascade of uranium hydrides [5], for which the requirement to reproduce the ferromagnetic moments gives an important feedback for the choice of on-site Coulomb U and Hund's exchange J.

1. U. D. Wdowik, P. Piekarz, D. Legut, and G. Jaglo, Phys. Rev. B 94, 054303 (2016).

2. L. Kyvala and D. Legut (submitted to PRB April 2019)

3. P. Maldonado, L. Paolasini, P. M. Oppeneer, T. R. Forrest, A. Prodi, N. Magnani, A. Bosak, G. H. Lander, and R. Caciuffo, Phys. Rev. B 93, 144301 (2016).

4. Y. Yun, D. Legut and P. M. Oppeneer, J. Nucl. Mat. 426, 109 (2012).

5. L. Havela, M. Paukov, M. Dopita, L. Horak, D. Drozdenko, M. Divis, I. Turek, D. Legut, L. Kyvala, T. Gouder, A. Seibert, F. Huber, Inorg. Chem. 57, 14727 (2018).

5:40pm AC+AS+LS-TuA-11 Reactivity of Potential TRISO Fuel Barrier Layers (SiC and ZrN) with H_2O Probed with Ambient Pressure Photoelectron Spectroscopy, *Jeff Terry, M Warren,* Illinois Institute of Technology; *R Addou, G Herman,* Oregon State University

While the use of TRISO fuels has been long postulated within High Temperature Gas Reactors, another potential use for the TRISO fuels is as an accident tolerant fuel in Light Water Reactors (LWRs). Before TRISO fuels can be used in LWRs, the corrosion properties of the different layers of TRISO fuels must be well understood. Photoelectron Spectroscopy (PES) has long been utilized to study the oxidation behavior of materials due to its sensitivity to both element and chemical state. The problem with PES has been that it has historically been a technique that required Ultrahigh Vacuum conditions for measurements. This made it difficult to study corrosion in situ. New instruments have expanded the capabilities of PES. It is now possible to measure photoemission spectra at ambient pressure. We have measured the in situ corrosion of a SiC layer grown as a TRISO simulant at a pressure of 1 mbar of H_2O at temperatures up to 500 C using an ambient pressure photoemission system. We see no oxidation of the SiC layer by water at temperatures up to 350 C. Above 350 C, the SiC begins to oxidize with the formation of SiO_2. In contrast, ZrN reacts at a pressure of 1 mbar of H_2O at room temperature. As the temperature increases, the ZrN layer is completely converted to ZrO_2. In the TRISO fuel, the barrier layer is surrounded by pyrolytic carbon. We model the protective ability of the outer carbon layer by making multilayers SiC/C and ZrN/C and measuring these under the same conditions. We find that a 2 nm carbon layer prevents the underlying barrier layers from reacting with water.

Atomic Scale Processing Focus Topic
Room B130 - Session AP+EL+MS+PS+SS+TF-TuA

Advancing Metrology and Characterization to enable Atomic Layer Processing

Moderators: Eric A. Joseph, IBM Research Division, T.J. Watson Research Center, Jessica Kachian, Intel Corporation

2:20pm AP+EL+MS+PS+SS+TF-TuA-1 In Situ Ellipsometry Characterization Of Atomic Layer Processes: A Review, *James Hilfiker, G Pribil, J VanDerslice,* J.A. Woollam Co., Inc. **INVITED**

Atomic layer processes such as atomic layer deposition (ALD) and atomic layer etch (ALE) provide monolayer-level thin film deposition or etch. Spectroscopic ellipsometry (SE) is ideally suited for the characterization requirements of such very thin layers. In situ SE provides real-time feedback, which is invaluable for establishing new atomic layer processes. In situ SE characterization has been adopted by many researchers due to its versatility. SE measurements are sensitive to deposition or etch at the (sub)monolayer level. The real-time evolution of film thickness provides details on nucleation periods or delays, the growth or etch rates per cycle, and verifies the self-limiting nature of a process. Multiple experiments can be performed within a single run by modifying the process conditions, allowing quick qualification of deposition temperatures, chemical exposure times, plasma influences, and purge times. In this paper, we will review the areas where in situ SE has been applied to both atomic layer deposition and etch.

We will also discuss the applications of in situ SE that benefit from a broad wavelength range. SE is best known for determining film thickness and optical constants. This characterization can be accomplished for many types of materials – dielectrics, semiconductors, organics, and even metals – provided the layer remains semi-transparent. Other material properties affect the optical constants and can be determined via this relationship. In situ SE has been used to estimate the crystal structure, composition, and even conductivity of thin films. We will discuss the advantages and limitations of in situ SE, which in many ways has proven to be an ideal partner for atomic layer processes.

3:00pm AP+EL+MS+PS+SS+TF-TuA-3 Elucidating the Mechanisms for Atomic Layer Growth through In Situ Studies, *Jeffrey Elam,* Argonne National Laboratory **INVITED**

Atomic Layer Deposition (ALD) provides exquisite control over film thickness and composition and yields excellent conformality over large areas and within nanostructures. These desirable attributes derive from self-limiting surface chemistry, and can disappear if the self-limitation is removed. Understanding the surface chemical reactions, i.e. the ALD mechanism, can provide insight into the limits of self-limitation allowing better control, successful scale up, and the invention of new processes. In situ measurements are very effective for elucidating ALD growth mechanisms. In this presentation, I will describe our recent investigations into the growth mechanisms of ALD nanocomposite films comprised of conducting (e.g. W, Mo and Re) and insulating (e.g. Al_2O_3, ZrO_2 and TiO_2) components using in situ measurements. These ALD nanocomposites have applications in particle detection, energy storage, and solar power. We have performed extensive in situ studies using quartz crystal microbalance (QCM), quadrupole mass spectrometry (QMS), Fourier transform infrared (FTIR) absorption spectroscopy, and current-voltage measurements. These measurements reveal unusual ALD chemistry occurring upon transitioning between the ALD processes for the two components. This results in unique reaction products that affect the properties of the films in beneficial ways. The knowledge gained from our in situ studies of the ALD nanocomposite films has helped us to solve problems encountered when we scaled up the ALD processes to large area substrates.

4:20pm AP+EL+MS+PS+SS+TF-TuA-7 Surface, Interface, or Film: A Discussion of the Metrology of ALD Materials in Semiconductor Applications, *G. Andrew Antonelli, N Keller,* Nanometrics **INVITED**

Atomic layer deposition, etching, and interface engineering are enabling technologies for semiconductor manufacturing. These processes have led to an explosion in the use of laboratory techniques such as transmission electron microscopy and the need to bring such instruments closer to or into the fab itself. However, there remains a need for in-line, non-destructive, non-contact metrology capable of quickly characterizing and monitoring these extremely thin films on test structures, on product, or in device as these data are the only meaningful method for monitoring of ultimate device performance. Indeed, in cases such as the use of selective deposition or etching, no test vehicle other than the ultimate product may be relevant. A variety of measurement techniques with a focus on x-ray and optical probes as applied to this class of problems will be reviewed. Examples will be provided on relevant logic such as the Gat-All-Around FET and memory devices such as 3D NAND.

5:00pm AP+EL+MS+PS+SS+TF-TuA-9 In Line and Ex Situ Metrology and Characterization to Enable Area Selective Deposition, *Christophe Vallee, M Bonvalot, B Pelissier, J Tortai, S David, S belahcen, V Pesce, M Jaffal, A Bsiesy,* LTM, Univ. Grenoble Alpes, CEA-LETI, France*; R Gassilloud, N Posseme,* CEA-LETI, France*; T Grehl, P Bruner,* IONTOF GmbH, Germany*; A Uedono,* University of Tsukuba, Japan

Innovation in materials, architectures (3D), gap filling technologies, lithography and etch processes are mandatory at every node of CMOS or memory devices. These challenging integration issues can be facilitated by the use of an integration scheme currently being intensively investigated known as area selective deposition (ASD). Criteria for an adequate area selective deposition process are: growth only on specific regions, high throughput compatible with industrial demands, no so-called mushroom profiles into adjacent features as well as no nuclei defectivity on undesired sites. Several routes can be developed to achieve an ASD process with ALD. The one discussed here concerns the deposition/etch approach which takes benefit from an *in situ* etching step inserted in a standard ALD cycle [1]. By incorporation of anisotropic or isotropic etching steps in the ALD process, "surface" selective deposition, as well as topographically selective deposition (TSD) have been obtained [2, 3]. The major current shortcoming of this approach lies in the deep insight which is required regarding elementary atomic-scale reaction mechanisms. Indeed, in the case of an ALD/ALE Area Selective Deposition process, a highly precise control of etching and its selectivity at the atomic scale is needed. Controlling the nature and density of defects induced by etching or passivation steps and understanding their impact on the physical and electrical properties of selectively deposited films are of course also required. Moreover, in order to optimize these processes, an accurate understanding of the underlying reasons why passivation after a low number of ALD cycles, is no more effective. Thus, *in situ* as well as *ex situ* monitoring and metrology are mandatory.

In this presentation, we will discuss how to optimize and understand atomic-scale reaction mechanisms in an ALD/ALE ASD process using combined *in situ* or *ex situ* measurements, such as ellipsometry, XPS, XRR, LEIS, FIB-STEM, and positron annihilation. We will show that when crosslinked, these technics are very effective to perform atomic scale metrology and characterization. As an example, we will discuss F atom localization and density in selectively deposited oxides thanks to a F-based ALE chemistry incorporated in the ALD process. In the case of a topographically selective deposition (TSD) process attempts will be presented to understand ion/surface interactions when low energetic ions are extracted from the plasma of the PEALD reactor both during deposition and plasma-ALE steps.

[1] R. Vallat et al, JVSTA **35** (2017) 01B104

[2] R. Vallat et al, JVSTA **37** (2019) 020918

[3] A. Chacker et al, APL **114** (2019)

5:20pm AP+EL+MS+PS+SS+TF-TuA-10 Recent Progress in Thin Film Conformality Analysis with Microscopic Lateral High-aspect-ratio Test Structures, *Riikka Puurunen,* Aalto University, Finland **INVITED**

Conformal thin films which cover complex 3D shapes with a film of uniform properties (thickness, composition, etc.) are increasingly demanded applications such as semiconductor devices, microelectromechanical systems, energy conversion/storage and catalysis. Atomic layer deposition (ALD) and its counterpart atomic layer etching (ALE) [together known as atomic layer processing (ALP)], are increasing in usage largely thanks to their known conformal character.

A question that needs to be asked in the R&D of 3D applications using conformal ALD/ALE processes is: how conformal is conformal; is the conformality sufficient to meet the specs? In semicon industry, vertical vias and cross-sectional transmission electron microscopy (TEM) are standardly used for conformality analysis. Recently, microscopic lateral high-aspect-ratio (LHAR) test structures have been developed to improve the conformality analytics capabilities. LHAR structures e.g. enable detailed conformality analysis at arbitrarily high aspect ratios (e.g., >5000:1), where no film can coat the 3D structure fully, thereby exposing the saturation profile characteristic for the process. This, in turn enables the kinetic analysis of the process and e.g. extraction of the sticking coefficients related to the growth reactions.

This invited talk will address recent progress related to the fabrication and the use of microscopic LHAR conformality test structures. After the breakthrough with the first prototypes (PillarHall LHAR1; Gao et al. 2015, Mattinen et al. 2016; reviewed in Cremers et al., 2019), third and fourth generation prototypes have been developed (PillarHall LHAR3 and LHAR4). This work will review the conformality analysis progress enabled by the microscopic LHAR structures and discuss the benefits and challenges of this approach. Recent published progress includes the conformality modelling by Ylilammi et al. (2018) and experimental extraction of sticking coefficient by Arts et al. (2019). In addition, several other ongoing conformality analysis cases will be presented.

References

Arts, Vandalon, Puurunen, Utriainen, Gao, Kessels, Knoops, J. Vac. Sci. Technol. A 37, 030908 (2019); https://doi.org/10.1116/1.5093620

Cremers, Puurunen, Dendooven, Appl. Phys. Rev. 6, 021302 (2019); https://doi.org/10.1063/1.5060967

Gao, Arpiainen, Puurunen, J. Vac. Sci. Technol. A 33, 010601 (2015); https://doi.org/10.1116/1.4903941

Mattinen, Hämäläinen, Gao, Jalkanen, Mizohata, Räisänen, Puurunen, Ritala, Leskelä, Langmuir, 32, 10559 (2016); http://doi.org/10.1021/acs.langmuir.6b03007

Ylilammi, Ylivaara, Puurunen, J. Appl. Phys. 123, 205301 (2018); https://doi.org/10.1063/1.5028178

6:00pm AP+EL+MS+PS+SS+TF-TuA-12 *In operando* XPS Study on Atomic Layer Etching of Fe and Co Using Cl_2 and Acetylacetone or Hexafluoroacetylacetone, *Zijian Wang, O Melton, D Angel, B Yuan, R Opila,* University of Delaware

Etching of transition metals is one of the major challenges in magnetoresistive random-access memory (MRAM) device fabrication. In this work, atomic layer etching of iron and cobalt surfaces with halogen and an organic molecule was studied. We successfully performed etching of Fe and Co thin films via forming volatile metal complexes at low temperature with cyclic sequential reactions of Cl_2 and acetylacetone (acac)

or hexafluoroacetylacetone (hfac) . The etching reaction mechanism of acac and hfac reacting with Clorine-modified Fe and Co surfaces was investigated: the surface was first activated with Cl_2 gas, and subsequently, the top layer of chlorinated metal was removed by reaction with a diketone (acac/hfac). The extent of Cl_2 reaction determines the etching rate of the metal. At substrate temperatures lower than 135°C, acac could remove the chlorinated Fe metal layer from Fe surfaces, but not chlorinated Co from Co surfaces. In-operando x-ray photoelectron spectroscopy (XPS) and density functional theory (DFT) simulation shows that the reaction of acac or hfac with Chlorinated Fe or Co surfaces is likely following a complex reaction pathway instead of simple diketone substitution for the metal chloride. Diketone decomposition may play an important role in the etching process.

Applied Surface Science Division
Room A211 - Session AS+BI+CA+LS-TuA

Beyond Traditional Surface Analysis

Moderators: Michaeleen Pacholski, The Dow Chemical Company, Xiao-Ying Yu, Pacific Northwest National Laboratory

2:20pm AS+BI+CA+LS-TuA-1 Nanotechnology as a Driver for Going Beyond Traditional Surface Analysis, *Olivier Renault,* CEA-LETI, France   **INVITED**
In the last 10 years, the progress of analytical methods has been more and more strongly connected to the pressing needs from materials and processing developments in the nanoelectronics industry. The field of materials analysis is now expanding as more and more complementary information are needed to tailor new materials for particular applications. Time-consuming techniques in the past (e.g, ARPES) are now accessible with increasing throughput, whereas the reliability of others, such as depth profiling, is improving. Finally, techniques like HAXPES implemented in the past only at synchrotron facilities, are now entering into laboratories.

In this talk I will illustrate by a series of examples in the field of device technology this evolution of surface analysis getting beyond traditional methods, driven by technological developments.

3:00pm AS+BI+CA+LS-TuA-3 Core Levels Sub-shell Photo-ionization Cross-sections of Au, Ag, Cu in the Hard X-ray Photon Energy Range of 7-26 keV, *Germán Rafael Castro, J Rubio Zuazo,* Spanich CRG BM25-SpLine Beamline at the ESRF, France
Hard X-ray Photo-electron spectroscopy (HAXPES)[1] has been developed in the last 10-15 years as a unique tool for retrieving accurate non-destructive[2] compositional and electronic bulk property of materials in the tens of nano-meters depth-scale with nano-meter resolution. Furthermore, the ability to tune the excitation energy in the hard X-ray regime enables tuning the sampling depth, i.e. depth profile analysis, but also enables the discrimination between bulk and surface effects, especially if combined with variable incident and exit angle.

However, an important drawback is the lack of knowledge of the photo-ionization cross-section at the HAXPES photon energy and in special for now accessible deeper core levels. Recently theoretical data has been reported [6] concerning the photo-ionization cross sections and parameters of the photo-electron angular distribution for atomic subshells but for binding energies lower than 1.5 keV of all elements with $1 \leq Z \leq 100$ in the photon energy range 1.5–10 keV. Unfortunately, these calculations do not contain information for deep orbitals accessible in HAXPES, even more there are scarce experimental results reported for both depth core levels and hard x-ray excitation energies.[3,4]

In the present work we will show the experimentally obtained relative sub-shell photo-ionization cross sections for 2s, 2p, 3s, 3p, 3d, 4s, 4p, 4d, 4f, 5s, 5p, 5d core levels of gold (Au), 2s, 2p, 3s, 3p, 3d, 4s, 4p, 4d core levels of silver (Ag) and 1s, 2s, 2p, 3s, 3p, 3d core levels of Cooper (Cu) in the X-ray photon energy range of 7–26 keV. In the case of Au, cross sections have been corrected with experimental obtained angular anisotropy parameter. A comparison with theoretical sub-shell photo-ionization cross sections, and angular anisotropy photo-inionization parameters [5,6] will be also presented.

References

1. J. Rubio-Zuazo, G.R. Castro, *Nucl. Instrum. Methods Phys. Res. A, 547, 64-72 (2005).*

2. J. Rubio-Zuazo, P. Ferrer, G.R. Castro, *J. Electron Spectrosc. Relat. Phenom., 180, 27-33 (2010).*

3. M. Gorgoi, F.Schäfers, S.Svensson, N.Mårtensson," J. Electron Spectrosc. Relat. Phenom.,, 190, 153-158 (2013)

4. C. Kunz, S. Thiess, B. Cowie, T.-L. Lee, J. Zegenhagen, *Instrum. Methods Phys. Res. A, 547,* 73-86 (2005).

5. J.H. Scofield, J. Electron Spectrosc. Relat. Phenom. 8 129–137 (1976).

6. M.B. Trzhaskovskaya, and V.G. Yarzhemsky, At. Data and Nucl. Data Tables,119 (2018) 99–174

3:20pm AS+BI+CA+LS-TuA-4 Interfacial Photochemistry of Pyruvic Acid in Atmospheric Chemistry, *Yanjie Shen, Y Fu,* Pacific Northwest National Laboratory*; X Yao,* Ocean University of China*; Z Zhu,* Pacific Northwest National Laboratory*; X Yu,* Earth and Biological Sciences Directorate
Presentation Summary:

This presentation will show our latest results of pyruvic acid photochemical aging in dry and liquid surface analysis s using time-of-flight secondary ion mass spectrometry.

Abstract

Pyruvic acid is widespread in fogs, aerosols, and clouds. The sunlight driven reaction pathways of pyruvic acid in the air-liquid interface are more elusive compared to its well-known gas and bulk phase chemistry in the atmosphere. We investigated photochemical aging products from pyruvic acid after different UV photolysis times up to 8 hours in dry and liquid samples using time-of-flight secondary ion mass spectrometry (ToF-SIMS). Both ToF-SIMS spectral and spectral principal component analysis (PCA) were used to study the surface photochemical aging products among various photochemical aging samples. A number of aging products were observed in dry samples indicating the importance of interfacial reactions[1]; however, the dry sample analysis cannot fully represent the air-liquid interfacial chemistry of pyruvic acid. Therefore, we used our unique liquid surface molecular imaging approach enabled by the SALVI microfluidic reactor to study the air-liquid interface. The in situ liquid SIMS observations show photochemical products of pyruvic acid at the air-liquid interface including oxidation products (i.e., acetic acid, oxalic acid, formic acid, lactic acid), oligomers (i.e., dimethyltartaric acid), and water clusters (i.e., $(H_2O)_nH^+$, $(H_2O)_nOH^-$) with submicrometer spatial resolution. In addition, SIMS three-dimensional chemical mapping provides visualization of the surface mixing state at the molecular level. For example, oligomers and oxidation products become more significant as illustrated in the chemical spatial mapping with increased photolysis time. Our study of the pyruvic acid aqueous surface provides new understanding of complex photochemical reactions as an important source of aqueous secondary organic aerosols (SOAs) in atmospheric chemistry.

Key Words: pyruvic acid, photochemical, dry SIMS, liquid SIMS, air-liquid interface, oligomer, water cluster, SOA.

References:

1.Fu, Y.; Zhang, Y.; Zhang, F.; Chen, J.; Zhu, Z.; Yu, X.-Y., Does interfacial photochemistry play a role in the photolysis of pyruvic acid in water? *Atmospheric Environment* **2018,***191*, 36-45.

4:20pm AS+BI+CA+LS-TuA-7 Nanoscale Tomographic Mapping the Liquid-Solid Interface with Cryo-APT, *Daniel Perea, D Schreiber, J Evans, J Ryan,* Pacific Northwest National Laboratory   **INVITED**
The liquid-solid interface plays an essential role in many phenomena encountered in biological, chemical, and physical processes relevant to both fundamental and applied science. However, study of the liquid/solid interface at the nanoscale is challenging as liquids are generally incompatible with many analytical techniques that require high to ultrahigh vacuum conditions. One strategy to probe the liquid-solid interface is to cryogenically freeze the liquid into solid form to preserve local ionic chemistry gradients and surface composition within a solid structure, making it more amendable to vacuum-based analyses such as Atom Probe Tomography (APT). However, the regular application of APT to hydrated materials is lacking due to challenges in preparing the necessary nanoscale needle-shaped specimens using a FIB-SEM and the subsequent environmentally-protected transfer of the frozen specimens to the APT instrument for analysis. In this presentation, I will discuss the development of a FIB-based site-specific liftout and attachment scheme of cryogenically cooled specimens involving a combination of redeposition and overcoating of organic and organometallic molecules. A modified commercially-available specimen suitcase shuttle device and an environmental transfer hub vacuum chamber at PNNL is used to facilitate environmentally-protected specimen transfer between the cryo FIB and the APT tool, allowing for the first time, APT analysis of a water/solid interface in 3D to reveal the complex nanoscale water-filled porous network of corroded

glass. Application of this unique specimen preparation approach to biological specimens will also be discussed.

5:00pm AS+BI+CA+LS-TuA-9 Characterization of Electronic Materials using Low Energy Inverse Photoemission Spectroscopy, *Benjamin Schmidt, J Newman, J Mann, K Artyushkova, L Swartz,* Physical Electronics*; M Terashima, T Miyayama,* ULVAC-PHI Inc., Japan

The development of complex electronic materials in areas such as batteries, solar cells, and flexible display panels require a detailed knowledge of the electronic band structure in order to achieve desired performance. A few of the material properties of interest are electron affinity, work function, ionization potential, and bandgap. Photoemission spectroscopic techniques such as Ultraviolet Photoelectron Spectroscopy (UPS) and Inverse Photoemission Spectroscopy (IPES) have traditionally been used to measure these values.

Organic electronic materials are growing in popularity due to lower costs of production and the ability to create interesting mechanical structures. However, they are susceptible to chemical damage with prolonged exposure to high-energy electron beams during analyses, which can affect the measured properties.

Low Energy Inverse Photoemission Spectroscopy (LEIPS) is a variant of IPES but uses an incident electron beam at lower energy than traditional IPES (< 5 eV vs. ~10 eV, respectively), making it less damaging for organic materials. In this talk, the operating principles of LEIPS will be discussed. Several material system examples will be shown, including films of C60 and copper phthalocyanine (CuPc).

5:20pm AS+BI+CA+LS-TuA-10 Deconvolution of Atom Probe Tomography on Nanomaterials for Renewable Energy, *Margaret Fitzgerald, M Dzara, D Diercks,* Colorado School of Mines*; N Leick, S Christensen,* National Renewable Energy Laboratory*; T Gennett, S Pylypenko,* Colorado School of Mines

Technologies for hydrogen-based economy rely heavily on advancements in development of nano-structured materials. Nano-materials used in applications for energy conversion, storage and production have unique, desirable properties because of their intricate chemistries and morphologies, however this makes them difficult to characterize using traditional techniques. Of specific interest is elucidation of the surface properties and identification of differences between surface and bulk composition. This work features Atom Probe Tomography (APT) paired with other techniques that enable multi-scale characterization in 2D and 3D as a promising approach to create a more complete picture of the complexities of nano-structured materials.

APT is an incredibly powerful tool that has been used to render sub-nanometer-resolution, 3D reconstructions of metallic and, more recently, ceramic samples to enhance the understanding of local composition variations, such as around grain-boundaries and precipitates. This presentation outlines the procedures and considerations for expansion of APT towards analysis of nano-structured materials used for catalysis and hydrogen storage. Challenges related to both APT specimen preparation, APT analysis, and data reconstructions will be discussed. Specific considerations that will be addressed include sample pre-screening for mass spectrometry peak overlap, substrate and encapsulation material selection based on field evaporation compatibility, and prevention of sample damage for air- and beam-sensitive materials. In order to produce accurate 3D reconstructions of the APT data for these samples, initial assessment of a two-dimensional morphology of these materials is made using scanning transmission electron microscopy (STEM) and elemental distributions are acquired with energy dispersive x-ray spectroscopy (EDS). Surface chemistry of the sample is determined using X-ray Photoelectron Spectroscopy (XPS) in order to correlate surface chemistry between APT data and quantified XPS chemical ratios. This talk will provide evidence of cross-correlation across multiple techniques and integration of 2D and 3D data to provide a pathway for understanding these complex materials beyond traditional capabilities.

5:40pm AS+BI+CA+LS-TuA-11 Mass Spectrometric Investigation of Ion Solvation in Liquids, a Comparison of *in situ* Liquid SIMS to Regular ESI-MS, *Yanyan Zhang,* Institute of Chemistry, Chinese Academy of Sciences, China*; D Baer, Z Zhu,* Pacific Northwest National Laboratory

Ion solvation plays very important roles in many important biological and environmental processes. Mass spectrometry (MS)-based methods have been used to investigate this topic with molecular insights. To study ion solvation, ionization processes should be as soft as possible in order to retain solvation structures. An *in situ* liquid secondary ion MS (SIMS)

approach developed in our group has been recently utilized in investigations of Li ion solvation in nonaqueous solution, and it detected a series of solvated Li ions.[1] As traditionally SIMS has long been recognized as a hard ionization process with strong damage occurring at the sputtering interface, it is very interesting to study further how soft *in situ* liquid SIMS can be. In this work, we used halide ion hydration as a model system to compare the ionization performance of the *in situ* liquid SIMS approach with regular electrospray ionization MS (ESI-MS). Results show that, although ESI has been recognized as a soft ionization method, nearly no solvated halide ions were detected by regular ESI-MS analysis, and only strong signals of salt ion clusters were seen. As a comparison, in liquid SIMS spectra, a series of obvious hydrated halide ion compositions could be observed.[2] Our findings demonstrated that the *in situ* liquid SIMS approach is surprisingly soft, and it is expected to have very broad applications on investigation of various weak interactions and many other interesting chemical processes (e.g., the initial nucleation of nanoparticle formation) in liquid environment.

References:

[1] Zhang, Y.; Baer, D.; Zhu, Z.*, et al., "Investigation of Ion-Solvent Interactions in Non-Aqueous Electrolytes Using *in situ* Liquid SIMS", *Anal. Chem.*, **2018**, *90*, 3341–3348.

[2] Zhang, Y.; Zhu, Z.*, et al., "*In Situ* Liquid SIMS: A Surprisingly Soft Ionization Process for Investigation of Halide Ion Hydration", *Anal. Chem.***2019**, *published online,* DOI: 10.1021/acs.analchem.8b05804.

6:00pm AS+BI+CA+LS-TuA-12 Characterizing the Thickness and Physical Properties of Nearly Ideal Zirconium Oxide Surfaces Using Ellipsometry, ESCA, Profilometry and FIB, *Edward Gillman,* Naval Nuclear Laboratory

Zirconium alloys are used in nuclear reactor cores due to their small neutron scattering cross-section and corrosion resistance. Corrosion of zirconium alloys results in the formation of a protective oxide layer that the corrosion species must travel through in order to continue the corrosion process. This oxide prevents further oxidation of the metal, slowing down the reaction rate. Characterizing this important oxide film on a metal is difficult. A number of analytical techniques are used to better understand the properties and growth of this oxide film. To insure that reliable information is reported, the thickness and physical properties of zirconium oxide deposited on a single-crystal silicon wafer by magnetron sputtering has been investigated. Data obtained from Electron Spectroscopy for Chemical Analysis (ESCA), profilometry, ellipsometry and Focused Ion Beam (FIB) experiments are all self-consistent with each other. This validates the utility of these measurements for the characterization of the oxide observed on metallic surfaces.

Biomaterial Interfaces Division
Room A120-121 - Session BI+AS-TuA

Biomolecules and Biophysics and Interfaces & Flash Session

Moderators: Markus Valtiner, Vienna University of Technology, Austria, Tobias Weidner, Aarhus University, Denmark

2:20pm BI+AS-TuA-1 Electrochemical Surface Reactivity of Catechol Derivatives: Competitive Adsorption and Ion Effects, *Laila Moreno Ostertag, L Mears, D Dworschak, M Valtiner,* Vienna University of Technology, Austria

Catechols are molecules well known for their participation in important biological processes such as neurotransmission and bioadhesion. Their adhesive properties are of great interest for the development of biocompatible glues and coatings. In particular, L-3,4-dihydroxyphenylalanine (L-DOPA) has been found to play a defining role in the attachment of mussel feet to organic and inorganic surfaces in wet environments. Its electrochemistry has been widely studied, but the possibilities of many other catechols in this field remain largely unexplored, as is the effect of diverse ionic media in which their properties could be improved.

By using several electrochemical techniques and comparing to a well-known model system, we have obtained an understanding of the redox mechanisms involved in the interaction of these molecules at a metallic interface. Reaction parameters such as diffusion coefficients and reaction constants have been determined in different ionic media.

This fundamental insight allows us to set catechols in the context of their role within interfacial phenomena. Our approach enables the elucidation of

free energies that characterize the energy landscape of adhesion processes at electrified interfaces, which can then bridge the gap between bulk electrochemistry and single-molecular surface-force analysis techniques. Full energy pathways can be drawn based on combined results and lead to a wide range of possibilities in the development of catechols for specific applications.

2:40pm BI+AS-TuA-2 Direct Observation of Lysozyme Interaction with a Curved Lipid Membrane Surface by Sum Frequency Scattering Vibrational Spectroscopy, *Thaddeus Golbek,* Aarhus University, Denmark, Denmark*; H Okur, S Kulik, J Dedic, S Roke,* École Polytechnique Fédérale de Lausanne (EPFL), Switzerland*; T Weidner,* Aarhus University, Denmark

Highly ordered protein aggregates play a large role in many neurodegenerative and non-neuropathic disorders including type II diabetes, Alzheimer's, Parkinson's, prion, and Huntington's disease. Even though a causative link between the formation of protein aggregates and server diseases has been established, the molecular level-details of protein aggregation and cell membrane disruption are still underdeveloped. One of the most characterized proteins that has been used to model protein aggregation is hen egg-white lysozyme. While lysozyme has been extensively studied at model surfaces, it has not been well studied on curved, more realistic, surfaces. In order to observe lysozyme at a curved surface we applied sum frequency scattering (SFS) vibrational spectroscopy to probe the interface between the protein and the curved lipid model cell membrane surface. The model cell membrane was built upon 10% 1,2-dimyristoyl-*sn*-glycero-3-phospho-(1'-rac-glycerol) (DMPG) and 90% 1,2-dipalmitoyl-*sn*-glycero-3-phosphocholine (DPPC) lipid nanodroplet emulsions, were the oil is *n*-hexadecane. SFS studies at the protein-lipid interface demonstrate that binding of lysozyme induces increased lipid monolayer order. An increase in acyl chain order determined by the ratio of the CH_3 symmetric and CH_2 asymmetric peak amplitudes and lipid head group orientation change from about 0° to greater than 60°, determined by the increase is phosphate head group signal, suggests that lysozyme inserts into the lipid layer causing lipid dehydration and reorientation. The amide I SFS spectrum lysozyme interacting with the model cell lipid monolayer is also studied to observe the folding and ordering of the protein. Altogether, we demonstrate the use of lipid monolayer nanodroplet emulsions as a platform to study protein membrane interactions in solution, which excludes air form the model further increasing biomimetic modeling potential using SFS.

3:00pm BI+AS-TuA-3 Iron Speciation at Aqueous Surfaces, *Heather Allen,* Ohio State University **INVITED**

Ion pairing and speciation in the condensed phase and at the aqueous surface is presented for mono and multi-valent ions including iron and phosphate systems. We present new evidence of iron (III) surface prevalence at both the water and glycerol surfaces. Understanding surface water solvation structure using polarized Raman and vibrational sum frequency generation spectroscopy are also discussed.

4:20pm BI+AS-TuA-7 Identifying the Molecular Mechanisms that Mediate Cell Membrane Repair by Sum Frequency Generation Spectroscopy, *T Golbek,* Oregon State University*; S Roeters, T Weidner,* Aarhus University, Denmark*; C Johnson,* **Joe Baio,** Oregon State University

Movement in everyday life places stress on sarcolemma which creates small tears in the muscle cell membrane. Mutations in this multi-domain dysferlin protein render it unable to repair the membrane and this phenomena is related to diseases such as specific forms of muscular dystrophy. Of particular importance is the moment after the release of calcium from tears in the muscle cell membrane, whereby the release of calcium triggers the C2A domain of dysferlin to dock with a lipid vesicle. Mutations mapped to this domain cause loss of binding ability of the C2A domain. This is the first step of muscle cell membrane repair, therefore there is a crucial need to understand the geometry of dysferlin C2A at a membrane interface as well as cell membrane lipid reorientation when compared to a variant. Here we describe a comparison between the wild type dysferlin C2A and a mutation to the conserved aspartic acids on the domains binding loops. To identify both the geometry and the cell membrane lipid reorientation, we applied sum frequency generation (SFG) vibrational spectroscopy and coupled it with simulated SFG spectra to observe and quantify the interaction. A model cell membrane was built with phosphotidylserine and phosphotidylcholine. Observed changes in surface pressure demonstrate that calcium bridged electrostatic interactions govern the initial interaction of the C2A domains docking with a lipid membrane. SFG spectra taken from the amide I region for wild type and variant contain features near 1642 cm^{-1}, 1663 cm^{-1}, and 1675 cm^{-1}

related to the C2A domains beta-sandwich secondary structure indicates that the domain binds in a specific orientation. Mapping simulated SFG spectra to the experimentally collected spectra indicated that both wild type and variant domains have nearly the same orientation to the membrane surface. However, examining the ordering of the lipids that make up a model membrane using SFG, we find that the wild type clusters the lipids as seen by the ratio of the CD3 and CD2 symmetric intensities increases by 170% for the wild type and by 120% for the variant. This study demonstrates and highlights the capabilities of SFG to probe with great detail biological mutations in proteins at cell membrane interfaces.

4:40pm BI+AS-TuA-8 Fishing Manganese out from Cellulose: Impact of Coupling Desferrioxamine B to Stainless Steel Beads on the Circular Economy of Paper and Pulp Industry, *Jeff Wilkesman,* Mannheim University of Applied Sciences, Germany*; K Mörtter, I Sommer, P Kunz,* Mannheim University of Applied Sciences, Deutschland

Important as an essential trace element with abundant applications, manganese (Mn) is rising attention due to its aesthetic, operational and health problems at higher concentration in the paper and water industry. When oxygen-containing paper bleaching chemicals (O_2, O_3, H_2O_2 or peracids) are used, the presence of heavy metals like Mn causes problems in the pulp processing, increasing the consumption of the bleaching chemicals and deteriorating pulp quality, including pulp darkening. An effective way to remove Mn from pulp is employing chelators, although its effectiveness is influenced by the overall water chemistry and concomitant contaminants. Successful chelation of Mn usually occurs at pH<8, otherwise highly oxidized species would form, precipitating insoluble Mn(III/IV) oxide minerals, and binding strongly to the pulp. Though the environmentally critical EDTA is used in the paper industry to chelate heavy metals, friendlier and greener alternatives are sought, like desferrioxamine B (DFOB) or E (DFOE), which are linear trihydroxamic acid siderophores produced by bacteria to acquire primarily Fe(III), but also Mn(II/III). Advantages of employing siderophores are its commercial availability, high solubility and stability over a wide pH range. The coupling of DFOB to ~3-4 mm stainless steel beads as solid support was performed. The beads were incubated overnight with several cellulose suspensions to allow formation of the Mn-DFOB complex (log K ~29.9). Control assays were performed using EDTA. After treatment, cellulose suspensions originally containing ~30–40 mg Mn/kg, were submitted for Mn(II), Mn(III) analysis, employing the TCPP [Tetrakis(4-carboxyphenyl)porphyrin] method. Total Mn content was also determined by Inductively Coupled Plasma (ICP). Preliminary results show an approximate 80% reduction of Mn content from the cellulose suspension, though experimentation is still carried on; DFOE is planned to be also analyzed. Mn was recovered by decoupling from DFOB by metal exchange and the beads were reused for further activation with DFOB. This removal alternative resulted in a feasible, easy, greener and economical procedure, leading for improvement in the paper industry. Still, the most expedient option comprising circular economy statements based on sustainable management parameters (cost-effectiveness, performance, simplicity) must be deeper explored. Clearly, further research regarding Mn(II/III) formation and removal will help the water and paper industry, by developing better methods to diminish Mn oxide deposits in pipe networks and optimizing the paper bleaching process, ultimately reducing significant operational costs.

5:00pm BI+AS-TuA-9 The Hybrid Nano-biointerfaces Between Gold, Graphene Oxide and Angiogenin for Wound Repair, *Diego La Mendola,* University of Pisa, Italy*; L Cucci, G Villaggio, C Satriano,* University of Catania, Italy

Angiogenin (ANG) is a member of the ribonuclease family and a physiological constituent of the human plasma. Ang is a potent angiogenic factor regulating a wide range of responses, such as angiogenesis, cell proliferation, cell migration, and pro-survival effects. ANG has been shown related to many pathophysiological processes, including cancers, neurodegeneration, inflammation and regeneration of damaged tissues. In this work, we investigated a hybrid obtained by the assembly of ANG to gold nanoparticles and graphene oxide nanosheets, to exploit the synergic effects of antioxidant AuNP and antimicrobial GO, respectively. Au-GO-ANG were characterized by UV-visible spectroscopy, to correlate the changes in the plasmonic peak as well as in the π-->π* transitions to the protein interaction with Au and GO, respectively. QCM-D measurements on supported lipid bilayers, as model of cell membranes, pointed to a stronger interaction of the AuNP-Ang systems in comparison with the uncoated nanoparticles. The developed systems promoted fibroblasts migration and wound closure. Confocal microscopy cell imaging evidenced dynamic processes at the level of cytoskeleton and sub-cellular compartments. The

results reveal a promising multifunctional platform for wound care treatment and tissue regeneration.

5:20pm BI+AS-TuA-10 Improved Antibacterial Sandwich system for Urological Purposes, *Sara Bröskamp, G Franz,* Munich University of Applied Sciences, Germany; *D Jocham,* University Hospital of Schleswig-Holstein, Germany

In the anaerobic environment of kidneys and bladder which even lack the permanent presence of weak but always toxic oxidative reagents (like ClO_2^-) it is obvious that no Ag^+ ions can be generated by oxidation of a metallic silver film. However, it is well known that the antibacterial impact of Ag^+ ions which can act as a single ion is much higher than the effect of neutral silver nanoparticles [1]. In our efforts to define an effective membrane which is deposited on the interior and exterior surfaces of tubes which exhibit an aspect ratio of more than 100 (balloon catheters) we introduce a significantly improved coating which makes use of the soft oxidation of already deposited silver layers by a microwave or RF plasma [2]. This procedure not only improves the antibacterial effect but also extends the active time of the catheters. The silver oxide on top of the base silver layer which is deposited on an originally hydrophobic surface of an organic polymer by a well-known process is eventually topped by an organic layer of comparable thickness [3,4]. This coating with even thickness on the interior of the tubes has been extensively improved by a device which counteracts the decreasing vapor density of the film-building species by a well-definded temperature gradient [5]. In the case of ureteral stents, we make use of the series of drainage holes along the catheter which act as adjacent sources for the film-building monomer. This layer controls the antibacterial activity which can be effectively tuned by its porosity [6]. The oxidation of the silver also effectively prevents sulfidation by S-containing amino acids (cysteine) which can be present in the kidneys of patients. The silver release rate has been measured by atomic absorption spectroscopy (AAS).

[1] Heidari Zare, V. Juhart, A. Vass, G. Franz, and D. Jocham; Biointerphases 12, 011001 (2017).

[2] G. Franz, S. Bröskamp, K. Resch, W. Hiemeyer, D. Jocham; German patent disclosure DE 10 2019 001 994.6, Mar 26, 2019.

[3] G. Franz, F. Schamberger, A. Kutschera, S. Seyedi, D. Jocham, German patent disclosure DE 102012023349.3, Nov. 29, 2012.

[4] G. Franz, F. Schamberger, H. Heidari Zare, S.F. Bröskamp, and D. Jocham; Beilstein J. Nanotechn. 8, 1982 (2017). [5] S. Bröskamp, D. Redka, A. Möhlmann, G. Franz, and D. Jocham; AIP Advances 7, 075005(2017).

[6] F. Schamberger, A. Ziegler, and G. Franz, J. Vac. Sci. Technol. B30, 01801 (2012).

5:40pm BI+AS-TuA-11 Quantitative Characterization of Piezoelectric Property in Biological System via Piezoresponse Force Microscopy, *Jinha Kwon, D Kim, H Cho,* The Ohio State University

Piezoresponse force microscopy (PFM) is a variant of scanning probe microscopic technique based on atomic force microscopy (AFM) that allows imaging of piezoelectric material domains with high resolution. This is achieved by keeping a sharp conductive probe in contact with a piezoelectric material and applying an alternating current (AC) directly to the sample through the probe, which results in deflection of the probe detected through photodiode detector. PFM has been successfully applied to many biological materials such as teeth [1], bone [2], seashell [3], and collagen fibrils [4]. Although biological samples are commonly vulnerable to high voltage input, previous studies used a high voltage input more than 10V to induce a piezoelectric strain large enough to be captured by an AFM tip [5]. Moreover, previous works did not carefully scrutinize the effect of substrate's conductivity and the contribution of parasitic electrostatic forces between the tip and sample, which should be precisely examined to obtain the quantitative piezoelectric properties of sample. In this study, we used type I collagen fibril which has weak piezoelectricity around 1 pm/V. The collagen fibril was aligned to the probe perpendicularly and AC voltage was applied to the fibril through the conductive AFM tip which was carefully calibrated in both vertical and lateral directions. In order to amplify its piezoresponse signal with a small electrical input, we utilized the contact resonance of an AFM cantilever. We also carefully examined the effect of substrate's conductivity by comparing piezoelectric response of the collagen on bare and gold-coated glass slides. Moreover, the contribution of electrostatic forces to the PFM results were investigated while they are varied by applying different DC offsets simultaneously to compensate the electrostatic force. Finally, the piezoelectric property of the collagen was calculated by fitting the measured piezoresponse vs.

applied voltage graph. As a result, the piezoelectric properties of a single collagen fibril were precisely characterized in both vertical and shear directions and its heterogeneous nature within a fibril was revealed.

[1] S.V. Kalinin, B.J. Rodriguez, J. Shin, S. Jesse, V. Grichko, T. Thundat, A.P. Baddorf, A. Gruverman, Bioelectromechanical imaging by scanning probe microscopy: Galvani's experiment at the nanoscale, Ultramicroscopy. 106 (2006) 334–340.

[2] M. Minary-Jolandan, M.-F. Yu, Shear piezoelectricity in bone at the nanoscale, Appl. Phys. Lett. 97 (2010) 153127.

[3] T. Li, K. Zeng, Nanoscale piezoelectric and ferroelectric behaviors of seashell by piezoresponse force microscopy, J. Appl. Phys. 113 (2013) 187202.

[4] M. Minary-Jolandan, M.-F. Yu, Nanoscale characterization of isolated individual type I collagen fibrils: polarization and piezoelectricity, Nanotechnology. 20 (2009) 085706.

[5] D. Denning, J.I. Kilpatrick, E. Fukada, N. Zhang, S. Habelitz, A. Fertala, M.D. Gilchrist, Y. Zhang, S.A.M. Tofail, B.J. Rodriguez, Piezoelectric Tensor of Collagen Fibrils Determined at the Nanoscale, ACS Biomater. Sci. Eng. 3 (2017) 929–935.

Electronic Materials and Photonics Division
Room A214 - Session EM+OX+TF-TuA

Nikolaus Dietz Memorial Session: Wide and Ultra-wide Band Gap Materials and Devices

Moderators: Seth King, University of Wisconsin - La Crosse, David Aspnes, North Carolina State University

2:20pm EM+OX+TF-TuA-1 Nitride-Based Semiconducting Materials: A Long Pathway to Advanced Nuclear Detection Capabilities, *Vincent Woods, L Hubbard,* Pacific Northwest National Laboratory; *Z Sitar,* North Carolina State University; *A Kozhanov,* Georgia State University **INVITED**

This energetic talk will focus primarily on the development of advanced nitride-based avalanche photodiode devices but will also highlight the many contributions that Nikolaus Dietz made to the field of real-time optical characterization, materials development and advanced growth techniques. Iterative development and advances in growth techniques and characterization have allowed sufficient improvement in materials quality to show demonstrable g ain in Avalanche Photodiode Detector (APD) device structures currently being produced for nuclear detection applications. This contribution will present the structural and optoelectronic properties of GaN/AlGaN heterostructures grown by Metal Organic Chemical Vapor Deposition (MOCVD) on AlN, GaN and sapphire templates/substrates. The target parameters for the materials heterostructures have been modeled for utilization in APD structures operating in the UV region. Optical modeling has improved absorption within the heterojunction as well as maximized light trapping within the device. Electronic modeling has determined the optimal dopant concentrations for maximum impact ionization rate, as well as tolerance to defects and unintentional doping. This application required advances in the defect densities, surface morphology, and interfaces. Surface morphological and structural properties of the GaN/AlGaN heterostructures are analyzed by Atomic Force Microscopy (AFM), and high resolution transmission electron microscopy (TEM). Recent results related to the gain of the final APD device will be presented.

3:00pm EM+OX+TF-TuA-3 New Mg-based Ternary Nitrides for Wide Band Gap Device Applications, *K York, R Makin III, Steven Durbin,* Western Michigan University; *R Reeves,* University of Canterbury, New Zealand; *N Senabulya, R Clarke,* University of Michigan

There continues to be significant interest in discovering viable alternatives to the traditional indium- and gallium-containing semiconductors, especially the nitrides, given the cost of the metallic constituents. The general family of ternary heterovalent semiconductors provides a number of interesting candidates, and considerable progress with a number of them has been made in the last several years. In addition to realizing $ZnSnN_2$ in thin film form using plasma-assisted molecular beam epitaxy (PA-MBE), we have recently demonstrated for the first time that the previously hypothetical wide band gap semiconductors $MgSnN_2$ (Eg ~ 3.4 eV) and $MgGeN_2$ (Eg ~ 5.1 eV) can also be grown. Zinc tin nitride ($ZnSnN_2$) has received considerable interest recently as a potential earth-abundant element based compound semiconductor for photovoltaic device applications. Its constituent elements are inexpensive, readily available in

high-purity form, non-toxic, and both zinc and tin benefit from mature recycling infrastructure. We have studied the growth of crystalline thin films of all three ternary heterovalent compounds with a view to understand their optical and electronic properties. We have demonstrated that the optical band gap energy exhibits a strong correlation with the ordering of the cation sublattice, and used this to determine the full range of possible band gap energies. Cation ordering is quantified through the long-range order parameter, which can be measured by x-ray diffraction, Raman spectroscopy, or in-situ reflection high-energy electron diffraction. All three materials can be successfully grown on (111) YSZ substrates, which represents a nontrivial lattice mismatch. We are able to control the cation ordering over essentially the entire range of possible long-range order parameter values through systematic variation of PA-MBE growth parameters, and have demonstrated reproducibility of a few percent.

3:20pm EM+OX+TF-TuA-4 Low Temperature Growth of InN by Atomic Layer Epitaxy, *Charles R. Eddy, Jr.,* U.S. Naval Research Laboratory*; S Rosenberg, J Woodward,* American Society for Engineering Education (residing at U.S. Naval Research Laboratory)*; K Ludwig,* Boston University*; N Nepal,* U.S. Naval Research Laboratory

Wurtzite indium nitride (InN) has direct bandgap of about 0.7 eV with large phonon gap and is an attractive semiconductor material for application in various areas, e.g. optical, electrical, optoelectronic, and spintronic device technologies [1]. InN and its alloys with GaN and AlN (III-N) have therefore found application in a variety of technologies such as high power transistors, emitters, detectors, and solar-cells. The relatively high growth temperature of common III-N synthesis techniques has impeded further development and application of the materials due to challenges with miscibility gaps and strain related to thermal expansion mismatch with non-native substrates. To address these challenges, plasma assisted atomic layer epitaxy (PA-ALEp) offers a new approach to low temperature III-N growth and can be used to epitaxially grow InN by using alternative pulses of trimethylindium and nitrogen plasma [2]. We report on development of the PA-ALEp process for InN growth on sapphire and gallium nitride substrates demonstrating the self-limited growth windows as a function of temperature and pulse durations in the process. We benchmark the quality of our films compare to those grown by Dietz et al. by high pressure CVD [3]. The process produces quality, crystalline semiconductor films with properties comparable to those grown by conventional methods at temperatures roughly 2X higher. Beyond that, the PA-ALEp process affords realization of InN containing ternary nitrides with aluminum and gallium that are not possible with conventional growth methods. Further, the unique, non-thermal equilibrium process enables realization of cubic (rock salt) phases on InN. In order to better understand nucleation and growth mechanisms involved in the PA-ALEp process, we employ in situ X-ray scattering methods using synchrotron radiation. We have determined that the growth proceeds largely by a Stranski-Krastinov process on either sapphire or gallium nitride. Further, we have investigated the impact of components of the PA-ALEp cycle on the growth process [4], in particular the plasma pulse time. Here we see that pulse time can affect the nature of nucleation from bimodal nucleation to single mode nucleation to degraded growth as pulse time increases from 15 seconds to 30 seconds. These and other nucleation and growth behaviors will be highlighted.

[1] O. Ambacher, J. Phys. D: Appl. Phys. 31, 2653 (1998).

[2] N. Nepal, et al., Cryst. Growth Design 13, 1485 (2013).

[3] N. Dietz, et al., Phys. Status Solidi B 242, 2985 (2005).

[4] N. Nepal, et al., J. Vac. Sci. Technol. A 37, 020910 (2019).

4:20pm EM+OX+TF-TuA-7 Stochiometry- and Orientation-Dependent Native Point Defects of MOCVD-Grown ZnGeN$_2$ Films, *Micah Haseman, D Ramdin, R Karim,* The Ohio State University*; D Jayatunga,* Case Western Reserve University*; H Zhao,* The Ohio State University*; K Kash,* Case Western Reserve University*; L Brillson,* The Ohio State University

Heterovalent ternary II-IV-nitrides like ZnGeN$_2$ are attracting increased interest due to their close relation to technologically important III-nitrides such as GaN. Unlike many III-nitrides, the constituents of ZnGeN$_2$ are more earth-abundant with potential for more versatile optoelectronic lattice matching. Essential to II-IV-nitride device application is the control of native point defects and subsequent manipulation of doping and carrier compensation. In many wide band gap binary semiconductors such as GaN or ZnO the most thermodynamically stable defects are cation or anion vacancies whereas stable defects in ternary alloys may include antisites, interstitials, and their complexes as well as H interstitials and complexes. Thus identification of native point defects in ZnGeN$_2$ and other ternaries can be challenging. Using depth-resolved cathodoluminescence

spectroscopy (DRCLS), we have observed multiple deep level defects in MOCVD-grown ZnGeN$_2$ films. Excitation depths obtained via Monte Carlo simulations for varying incident electron beam energies provide depth-resolution for the cathodoluminescence spectra which reveal defects that extend throughout the deposited ZnGeN$_2$ film and are not localized near the free surface nor the film-substrate interface, therefore, unless these defects are unintentional impurities, they must be native point defects. Density functional theory (DFT) predicts the most thermodynamically stable native point defects are in fact Zn$_{Ge}$ and Ge$_{Zn}$ antisites and the n-type nature of the films studied suggests that Zn$_{Ge}$ acceptor is the most favorable defect to form [1]. We used off-stoichiometric films to identify luminescence features due to gap state transitions from specific defects. For Zn-rich films (Zn/Ge = 1.15), we observe an additional defect feature at 2.4 eV corresponding to a near mid-gap state. DFT band structures for ZnGeN$_2$ show that Zn$_{Ge}$ antisites create gap states just below mid-gap, consistent with the n-type Fermi level and with the Zn-rich films. In addition, we observe strong variation in these mid-gap states with Al$_2$O$_3$ vs GaN substrate growths as well as an Al$_2$O$_3$ orientation dependence. DRCLS's ability to probe electronic structure on a near-nanometer scale enables us to probe defect variations with stoichiometry as growth conditions are varied within the outer tens of nanometers - a nanoscale testbed to identify defects. Identifying and controlling such defects using growth processes can enable advances in ZnGeN$_2$ for next generation electronic device applications. The authors gratefully acknowledge support from NSF grants DMR-18-00130 and DMREF 1533957.

[1]Skachkov et. al. Phys. Rev. B 93, 155202 (2016)

4:40pm EM+OX+TF-TuA-8 Low-temperature Growth of Wide Bandgap Nitride and Oxide Thin Films via Plasma-assisted Atomic Layer Deposition: Influence of rf-plasma Source and Plasma Power, *Necmi Biyikli, S Ilhom, A Mohammad, D Shukla,* University of Connecticut

Plasma-assisted atomic layer deposition (PA-ALD) provides an alternative way to grow wide bandgap materials at substantially reduced substrate temperatures (lower than 400°C) when compared to conventional epitaxial growth techniques. While majority of the published literature indicate polycrystalline or amorphous films, recent results depict preferred crystal orientation and even single crystalline nitride and oxide films obtained mainly by delicate substrate in-situ cleaning and careful plasma condition tuning and optimization.

In this talk, we will give an overview of the current state-of-the-art in PA-ALD research on wide and ultra-wide bandgap semiconductors, focusing mainly on wide bandgap III-nitrides (AlN, GaN) and III-oxides (Ga$_2$O$_3$). Subsequently, we'll share our recent research efforts on growing crystalline GaN and Ga$_2$O$_3$ thin films via PA-ALD utilizing two different plasma sources: inductively coupled plasma (ICP) and capacitively-coupled hollow-cathode plasma (CCHCP) source. We show that for III-nitride films, CCHCP source provides significant improvement in terms of oxygen impurity incorporation and structural film quality, while using a compact vacuum reactor with reduced source-to-substrate distance leads to reduced plasma power levels needed for self-limiting growth saturation curves. Both sources will also be compared in terms of film quality for ultra-wide bandgap Ga$_2$O$_3$.

We will present how the choice of plasma source and rf-plasma power affects the structural, chemical, optical, and electrical properties of the grown wide bandgap nitride and oxide films. Detailed x-ray diffraction (XRD), x-ray photoelectron spectroscopy (XPS), transmission electron microscopy (TEM), spectroscopic ellipsometer (SE), Hall measurements (HM) results and analyses will be presented. In addition to these ex-situ characterization results, we'll provide our real-time in-situ ellipsometric film growth monitoring results which provide valuable information about the single chemisorption, ligand-exchange/removal, and nitrogen/oxygen incorporation reactions.

We'll present proof-of-concept electronic and opto-electronic device demonstration based on GaN and Ga2O3 films grown via PA-ALD and will conclude with a future outlook in terms of how to further improve material quality and device performances.

5:00pm EM+OX+TF-TuA-9 Wide Bandgap Dilute Magnetic Semiconductors for Room Temperature Spintronic Applications, *V Saravade, A Ghods,* Missouri University of Science and Technology, Rolla, MO, USA*; N Ben Sedrine,* Universidade de Aveiro, Portugal*; C Zhou, Ian Ferguson,* Missouri University of Science and Technology **INVITED**

Wide bandgap dilute magnetic semiconductors (DMS) are promising materials for spintronic applications due to their theoretically predicted and experimentally observed ferromagnetic properties at room

temperature (RT) [1]. Spintronics is an enabling technology for devices that will meet current and future computing needs through quantum computing, neuromorphic applications, and artificial intelligence.

Gallium nitride doped with rare earth or transition metals have exhibited ferromagnetic behavior for spintronic applications although its mechanism is still not well understood [1]. In order to build spin-based devices, it is necessary to understand, control, and manipulate their magnetic properties. MOCVD-grown GaGdN shows RT ferromagnetism as evidenced in vibrating sample magnetometry and anomalous Hall Effect (AHE) measurements. Also, AHE measurement showed that the mechanism for the ferromagnetism is intrinsic and likely mediated by free carriers, which is conducive for spintronic applications [2]. However, ferromagnetism is only observed with a Gd precursor, $(TMHD)_3Gd$, which contains oxygen in its organic ligand that appears to be incorporated into the GaGdN. As per density functional theory calculations, oxygen and carbon could introduce deep localized states close to the Fermi level in GaGdN that couple with Gd states to render ferromagnetism [3, 4]. To achieve a clarity and control of this phenomenon, O and C are intentionally implanted into GaGdN grown using oxygen-free Cp_3Gd source. In this case, as-grown GaGdN is not ferromagnetic, but post-implantation with O or C does result in ferromagnetism. X-ray diffraction exhibits low damage and good crystal quality for the implanted GaGdN with peak shifts as compared to the GaGdN before implantation, showing signs of O or C incorporation. Annealing the implanted GaGdN activates the dopant, improves the crystal quality, and shows clear signs of AHE. This indicates that the intrinsic and potentially free carrier-mediated RT ferromagnetism in GaGdN is activated by band states introduced by O or C. A better understanding of the mechanism for RT ferromagnetism will enable using these materials to build spintronic devices, and processors for high speed computing applications.

References

1. M. Kane, S. Gupta and I. Ferguson, "Transition metal and rare earth doping in GaN", Woodhead publishing, 2016

2. V. Saravade, C. Ferguson, A. Ghods, C. Zhou, and I. Ferguson, MRS Adv. 3 (3), p. 159, 2018

3. Z. Liu, X. Yi, J. Wang, J. Kang, A. Melton, Y. Shi, N. Lu, J. Wang, J. Li, and I. Ferguson, Appl. Phys. Lett. 100 (23), 232408, 2012

4. R. Xie, H. Xing, Y. Zeng, Y. Liang, Y. Huang and X. Chen, AIP Adv. 7, 115003, 2017

5:40pm **EM+OX+TF-TuA-11 Processing and Characterization of Schottky and Ohmic contacts on (100) β-Ga₂O₃**, *Luke Lyle, K Jiang, E Favela, D Moody, T Lin, P Chung,* Carnegie Mellon University*; K Das,* North Carolina State University*; Z Galazka, A Popp, G Wagner,* Leibniz-Institut für Kristallzüchtung, Germany*; L Porter,* Carnegie Mellon University

Over the past decade beta-gallium oxide (β-Ga₂O₃) has accrued increased interest due to its ultrawide bandgap of around 4.6 eV, superior figures of merit for numerous electronic and optoelectronic applications, and the ability to produce single-crystal melt-grown substrates. Considering these factors, β-Ga₂O₃ has been primarily pursued for applications as high-power electronics, of which the understanding and development of Schottky and ohmic metal contacts is critical. In this study we characterized the electrical properties of electron-beam evaporated Ni, Mo, Au and other metal Schottky contacts to (100) β-Ga₂O₃ substrates. Prior to deposition of the metals, the Ga₂O₃ surface was cleaned via a 10% HCl solution followed by a clean in boiling 30% H₂O₂ solution at 85°C. Ti/Au was deposited via electron-beam evaporation and annealed at 400°C in an Ar atmosphere for use as ohmic contacts. The ideality factors, barrier heights, and doping densities were calculated from I-V and C-V measurements, which showed excellent agreement in most cases; I-V-T measurements are also planned as a complementary method to determine electrical transport behavior as a function of temperature. From our measurements it was observed that the Schottky barrier heights tended to increase as a function of the metal workfunction. These results are in contrast to our prior measurements of Schottky contacts on (-201) β-Ga₂O₃, which showed little to no correlation between Schottky barrier height and metal workfunction. In this presentation we will compare the electrical behavior of the various metal contacts on (100) β-Ga₂O₃, including the extracted ideality factors (~1.05–1.2) and Schottky barrier heights (~0.9–2 eV). The results will be discussed in the context of important processing conditions, as well as structural, optical, and morphological characteristics of (100) and (-201) -Ga₂O₃ substrates as determined from x-ray diffraction, UV-visible spectroscopy, atomic force microscopy, and other techniques.

6:00pm **EM+OX+TF-TuA-12 III-Nitrides: Enabling Applications with Wide to Ultra-Wide Bandgap Materials and Devices**, *Erica Douglas, A Baca, B Klein, A Allerman, A Armstrong, A Colon, C Stephenson, R Kaplar,* Sandia National Laboratories

Though now commercially available, wide band gap semiconductors (WBG) such as GaN were pursued due to immense potential for high frequency, light-emission, and power electronic applications. Due to high breakdown voltages, which have been achieved due in part to intrinsic material properties and device engineering, as well as low on-state resistance, wide bandgap semiconductors have found significant success in the commercial application regime. The critical electric field that a material can withstand can be significantly increased through bandgap engineering due to critical field scaling as $E_g^{2.5}$ [1]. Thus, moving from WBG materials with bandgaps ~3 eV, to UWBG with bandgaps above 3.4 eV, alloying GaN with Al can increase the bandgap from 3.4 eV (GaN) to 6.2 eV (AlN) and result in a critical electric field approaching 5X that of GaN.

Since the first AlGaN-channel transistor was reported in 2008 [2], development and progress on devices with increasing Al content has been pursued, including high electron mobility transistors with channel concentrations as high as 85% Al [3]. Though a corollary can be drawn to GaN, there are still a significant number of challenges to overcome for AlGaN-channel devices, ranging from epitaxial growth to fabrication. This talk will describe the latest results at Sandia National Laboratories in AlGaN-channel HEMTs, including recent advances in: enhancement-mode operation, current density, device performance over temperature, and RF operation.

[1] R. J. Kaplar, *et al.*, *ECS J. Solid State Science and Technology*, vol. 6, p. Q3061 (2017).

[2] T. Nanjo, *et al.*, *Appl. Phys. Lett.***92**, 263502 (2008).

[3] A.G. Baca, *et al.*,*Appl. Phys. Lett.***109**, 033509 (2016).

MEMS and NEMS Group
Room A210 - Session MN+QS-TuA

Devices for Quantum Information and Quantum Nanomechanics

Moderators: Sebastian Hentz, CEA-LETI, France, Matthew Jordan, Sandia National Laboratories

2:20pm **MN+QS-TuA-1 Fabrication Challenges in Quantum Optomechanics**, *Simon Groeblacher,* Delft University of Technology, The Netherlands, Netherlands **INVITED**

Mechanical systems have recently attracted significant attention for their potential use in quantum information processing tasks, for example, as compact quantum memories or as transducers between different types of quantum systems. Recent advances have allowed to demonstrate non-classical behavior of mechanical motion by coupling a micro-fabricated acoustic resonator to single optical photons. These experiments include the heralded generation and on-demand readout of single phononic excitations, as well as entanglement between two mechanical modes.

Here we would like to discuss how we fabricate the optomechanical crystals used in these quantum experiments, which feature engineered mechanical resonances in the Gigahertz regime that can be addressed optically from the conventional telecom band. We will also show some of the challenges that need to be overcome in order to realize useful devices for real-world quantum information processing applications.

3:00pm **MN+QS-TuA-3 Floquet Dynamics and Time Symmetry Breaking in Arrays of Driven Nanoresonators**, *Mark Dykman,* Michigan State University **INVITED**
Periodically driven modes of nanomechanical resonators and electromagnetic cavities allow one to study peculiar features of quantum dynamics related to the discrete time translation symmetry imposed by the driving. For modes with high quality factors, which are typically studied in the experiment, these features become pronounced already for

Tuesday Afternoon, October 22, 2019

comparatively weak driving, provided it is resonant. Quantum dynamics of driven modes is described in terms of the Floquet states. Generally, if the system is in a Floquet state, its dynamical variables oscillate with the period of the driving. However, the discrete time-translation symmetry can be broken, leading to what is called the time crystal effect. For arrays of coupled vibrational modes, the symmetry breaking can occur both in the coherent and dissipative regimes. In the both regimes the transitions are induced by quantum fluctuations, making them nonequilibrium quantum phase transitions. However, the coherent and dissipative transitions are very different. The structure of the emerging states strongly depends on the disorder in the resonator arrays. We will discuss the transitions for the modes driven parametrically close to twice their eigenfrequency and also for the modes driven close to triple the eigenfrequency. Along with the theory we will discuss the ways of observing the vibrational time crystals in the experiment.

4:20pm MN+QS-TuA-7 Engineering Quantum Signal Transduction in Atomic Layer 2D Devices, *Philip Feng*, Case Western Reserve University **INVITED**

An essential theme of the ongoing 'second quantum revolution' is to realize human-made structures and devices where 'quantum phenomena' can be sustained and harnessed to enable radically new approaches to information processing. These require exquisite creation and scalable fabrication of atom-like devices, design and engineering of new information carriers and transduction schemes. Atomic layer crystals have emerged as attractive enablers for creating atomically thin 2D devices that can support signal transduction and information processing functions in the regime where classical meets quantum. In this presentation, we will report on our latest effort and results on developing novel 2D devices (including nanomechanical and photonic resonators, phononic waveguides, photodetectors, etc.), investigating quantum emitters and coupling effects on relevant 2D device platforms, and engineering both classical and quantum signal transduction schemes in such 2D devices and systems.

5:00pm MN+QS-TuA-9 Superconducting Resonators as Diagnostics for Qubit Fabrication, *Rupert Lewis*, Sandia National Laboratories **INVITED**
Quantum bits (qubits) fashioned from superconducting thin films and Josephson junctions

require different fabrication approaches than back-end-of-the-line semiconductor fab. This

point is driven home most clearly by the realization that the qubit as an anharmonic singlephoton

microwave resonator. The presence of single photon in the qubit represents a one, the

absence represents a zero, thus if the photon is lost, the quantum state is also lost. In

consequence, fabricators of qubits go to extremes to provide low microwave loss environments

for their qubits. Planar microwave resonators—of the multiphoton variety—are an invaluable

diagnostic tool for assessing loss mechanisms in qubit fabrication and the quality of processes

used. This presentation will give a general overview of superconducting qubits and fabrication

techniques and how microwave resonators improve qubits.

Supported by the Laboratory Directed Research and Development program at Sandia National

Laboratories, a multi-mission laboratory managed and operated by National Technology and

Engineering Solutions of Sandia, LLC., a wholly owned subsidiary of Honeywell International,

Inc., for the U.S. Department of Energy's National Nuclear Security Administration under

contract DE-NA-0003525.

5:40pm MN+QS-TuA-11 Surface Ion Trap Device Fabrication for Experiments in Quantum Information Science, *Matthew Blain*, Sandia National Laboratories **INVITED**
Radio-frequency (rf) surface ion traps offer important advantages for realizing precise control of the spatial positioning, as well as motional and electronic states, of trapped ions. The control of ions provided by micro-fabricating planar trap electrodes on a silicon device surface has allowed

ion trapping to be at the forefront of experiments in quantum sensing, simulation, and information processing. Engineered surface traps offer the ability to extend the performance of their macroscopic equivalents and can even allow new concepts to be explored in both classical and quantum trapped-ion physics and chemistry. T he ability to fabricate complex and arbitrarily arranged 2-D and 2.5-D trap electrode geometries is critical for numerous trapped ion quantum information science experiments. Surface electrode ion traps [1] have enabled the Kielpinski ion trap CCD (charge coupled device) architecture [2], whereby ions can be shuttled between linear trapping regions via junctions, as well as trap designs, for example triangles [3] or rings [4], optimized for different experimental objectives. The ability to design and fabricate precision through-chip holes for ion loading and photon collection/delivery and to arbitrarily shape trap chips for increased optical access to ions is also critical for rendering a highly evolved ion trap chip technology. As well, micro ion trap chip technologies are beginning to integrate passive and active electronic and photonic capabilities for enhanced performance, including trench capacitors, optical waveguides, and avalanche photodiodes. Aspects of the "micro-systems" approach to the design and integration of surface electrode ion trap devices will be presented.

Sandia National Laboratories is a multimission laboratory managed and operated by National Technology & Engineering Solutions of Sandia, LLC, a wholly owned subsidiary of Honeywell International Inc., for the U.S. Department of Energy's National Nuclear Security Administration under contract DE-NA0003525.

[1] D L Moehring, *et al.*, *New Journal of Physics*, 13 (2011) 075018

[2] D Kielpinski, *et al.*, *Nature*, 709, 417(2002)

[3] M Mielenz, *et al.*, *Nature Communications*, 7 (2016) 11839

[4] B Tabakov, *et al.*, *Physical Review Applied*, 4 (2015) 31001

Nanometer-scale Science and Technology Division
Room A222 - Session NS-TuA

Recent Advances in Nanoscale Probing and Fabrication
Moderator: Jay Mody, GLOBALFOUNDRIES Inc.

4:20pm NS-TuA-7 Electrical, Photovoltaic, and Nano-Optical Characterization of TMD Lateral Heterostructures, *Marudachalam Shanmugasundaram*, HORIBA Scientific; *A Elias, M Terrones*, The Pennsylvania State University; *H Terrones*, Rensselaer Polytechnic Institute
The growth of lateral heterostructures of transition metal dichalcogenides (TMDs) was recently demonstrated, which has created the potential for fabricating semiconductor devices with novel electronic properties. Specifically, it would combine distinct properties of materials derived from different sources into one device. It has been shown that under well-controlled growth conditions, MoS_2-WS_2 lateral heterostructures with atomically sharp interfaces can be synthesized. While the growth of such materials can be challenging, the development of analytical methods with the capability of providing chemical information, in addition to morphological information, with nanometer-scale spatial resolution is equally challenging.

Raman spectroscopy is used to study chemical composition of materials with high specificity, but it lacks sensitivity due to the inherent weakness of the Raman scattering phenomenon. Besides, its spatial resolution is diffraction-limited to ~0.5 λ. These drawbacks can be overcome by combining Raman spectroscopy with Scanning Probe Microscopy (SPM) in which certain metal particles placed at the end of the SPM tip act as plasmonic substrate. This technique is referred to as tip-enhanced Raman spectroscopy (TERS). This combination provides not only the benefits of both SPM and Raman microscopy at the same time, but also enables Raman mapping with spatial resolution proportional to the size of the coated SPM tip (well below the diffraction limit) due to plasmonic enhancement of Raman signal.

In this work, we present characterization of MoS_2-WS_2 lateral heterostructures based on morphology, electrical properties, photovoltaic properties, and chemical composition, using a single platform. Scanning Kelvin imaging was used to map the surface potential as well as electro-mechanical contrast proportional to capacitance from the heterostructures. Their surface potential and capacitance change dramatically in a reversible manner when the heterostructures are illuminated by a laser, highlighting their photovoltaic properties. Raman and photoluminescence (PL) maps were recorded with 532 nm excitation,

Tuesday Afternoon, October 22, 2019 89 2:20 PM

which enabled collection of Raman and PL bands from both materials simultaneously with reasonable separation. In addition, tip-enhanced Raman and PL maps were collected across the interface, with sub-diffraction limited spatial resolution. In summary, a unique collection of characterization techniques were used based on AFM-Raman instrumentation to study morphological, electrical, photovoltaic properties, and chemical composition of MoS_2–WS_2 lateral heterostructures.

4:40pm NS-TuA-8 Development of Near-Field Electrospinning for 3D Nanofabrication for tissue engineering applications, *Alex Nagle,* University of Wollongong, Australia

The major goal in this work was to mimic the nanofibrous proteins found in the neural extracellular matrix (nECM). NFES is a versatile nanofiber patterning technique, utilising additive layer-by-layer deposition to create nanofibrous microstructures. However, high volume can be a difficult to achieve due to inhibition of the ejection process by polymer build-up. To mimic the 3D nECM, led to the development of a new technique: Suspension Near-Field Electrospinning (SNFES).

Suspended, aligned fibres can be printed across void space between electrodes and so a strategy of using free standing electrode pillars to support distributed PEO fibres within space was investigated. This strategy relied on a high accuracy, software integrated NFES system as well as 3D printed pillar electrodes, fabricated by Selective laser melt (SLM). Interpillar motion of the emitter, drew fibers between four-pillar electrodes, demonstrating SNFES.

The process parameters, working distance, maximum stage speed, voltage, PEO solution concentration, and pattern iteration effects of SNFES through orthogonal experiments. The need for more complex structures in TE, led to the development of further pattern types, working around the simple four-pillar structure, to produce crossing arrays. Alignment of the arrays was accurate to ± 5°; diameter was modulated by the process parameters; while density exponentially decayed at high iteration by the electrostatic inhibitory effects.

Finally, ultrafine polycaprolactone (PCL) fiber arrays prepared using SNFES, then encapsulated into a biocompatible gellan gum methacrylate (GGMA) hydrogel matrix, to mimic the nanofibrous proteins of the nECM. Parametric studies varying fiber diameter, as well as electrode pillar design and pattern iteration; elucidated the encapsulated array effects. It was found that fiber encapsulation led to dramatic improvements in the constructs mechanical properties, raising the storage modulus from 0.17 up to 1.28 kPa, (native tissue 0.5 -1kPa) upon minimising the fiber diameter below 1 micron.

The findings of this research are significant as it creates for the first time a suspended polymer nanoarray, in a directed manner, which can be extended across multiple working 3D planes in situ. The hybrid fiber-gel systems can be mechanically tailored based on the findings of the parametric experiments. The increase in nanoarray volume and density achieved here is expected to address challenges of producing hierarchical tissue constructs in 3D.

Acknowledgements

5:00pm NS-TuA-9 The Fundamentals of Silica Nanoparticle-based Hydrophilic Antifouling Coating, *Dan Yang,* University of wollongong, Australia*; P Molino,* University of Wollongong, Australia*; M Higgins,* University of Wollongong

Biological fouling of artificial surfaces has led to enormous problems for many industries including biomedical devices and maritime shipping. One of the strategies is using environmentally benign antifouling coatings, in particular, hydrophilic coating to prevent the adhesion of microbes. From an industry perspective, the silica nanoparticles (SiNP) synthesis can be easily scaled up and applied by different fabrication techniques, making the use of hydrophilic SiNPs a promising strategy to address the challenges of biofouling.

A commercially available Glycidoxypropyltrimethoxysilane (GPS) modified SiNPs hydrophilic coating system was firstly discovered to have an excellent antifouling performance by our research group, after tests against protein, bacteria and fungal spore. To elucidate the underlying antifouling mechanisms of GPS-SiNPs coating, static AFM force measurements were undertaken to compare the nanoscale surface forces of Unmodified versus GPS modified SiNPs coatings in liquid as a function of salt concentration and pH, and 3D Scanning Force Microscopy (3D-SFM) was employed to

visualize the interfacial structures at the molecular and atomic level above single nanoparticles. These studies showed that the presence of a GPS/hydration layer on the GPS-SiNPs surface was attributed to the antifouling properties and suggested to arise from the presence of hydration/steric forces.

In the current work, Single Cell Force Spectroscopy (SCFS) was employed to reveal the biological interactions between the above antifouling coatings and single live fungal spores of *Epicoccum nigrum*. A main finding is that the GPS-SiNPs surfaces can prevent the fungal spore adhesion through both the long-range EDL repulsion, as well as the short-range hydration/steric repulsion. Furthermore, the latter short-range hydration/steric effect upon spore contact is stable at all salt concentrations, and hence shows remarkable ability of the GPS/hydration layer to prevent the spore adhesion given the known sophisticated surface structures and diversity of biomolecules of these microbial organisms. This study reveals the fungal spore interactions on surfaces at the molecular level upon approach to and during the detachment process by using a single-cell method to quantify the antifouling performance of coatings against biofoulants, i.e. fungal spore, and give insights about future coating design.

5:20pm NS-TuA-10 The Effects of Atomic-Scale Strain Relaxation on the Electronic Properties of Monolayer MoS₂, *Daniel Trainer, Y Zhang,* Argonne National Laboratory*; F Bobba,* University of Salerno, Italy*; X Xi,* Temple University*; S Hla,* Argonne National Laboratory*; M Iavarone,* Temple University

The ability to control nanoscale electronic properties by introducing macroscopic strain is of critical importance for the implementation of two-dimensional (2D) materials into flexible electronics and next-generation strain engineering devices. In this work, we correlate the atomic-scale lattice deformation with a systematic macroscopic bending of monolayer molybdenum disulfide films by using scanning tunneling microscopy and spectroscopy implemented with a custom-built sample holder to control the strain. Using this technique, we are able to induce strains of up to 3% before slipping effects take place and relaxation mechanisms prevail. We find a reduction of the quasiparticle bandgap of about 400 meV per percent local strain measured with a minimum gap of 1.2 eV. Furthermore, unintentional nanoscale strain relaxation of van der Waals monolayer sheets can negatively impact strain engineered device performance. Here we investigate such strain relaxation mechanisms that include one-dimensional ripples and 2D wrinkles which alter the spatial electronic density of states and strain distribution on the atomic scale.

5:40pm NS-TuA-11 Understanding Tip-induced Nanoscale Wear for Tomographic Atomic Force Microscopy, *Umberto Celano,* IMEC, Belgium*; X Hu,* University of California-Merced*; L Wouters, K Paredis, T Hatschel, P van der Heide,* IMEC, Belgium*; A Martini,* University of California-Merced

The ability of contact-mode atomic force microscopy (AFM) to remove material while scanning has repeatedly been used for surface modification and small-scale tip-induced nanofabrication.[1] In the simplest form, the physical removal of material can be achieved by scanning the nanosized probe against the surface at high enough pressure.[2] More recently, tomographic capability has been explored for various electrical AFM modes by leveraging the same concept and alternating tip-induced removal and probing, in what is often referred to as Scalpel AFM.[3] Here, high-pressure AFM scans (i.e., high load force) are used for a controlled material removal and alternated with conventional contact-mode scans (i.e., standard load force). The alternation of scanning conditions delivers a slice-and-view methodology that generates three-dimensional (3D) datasets, with nm-precision in depth. This method has found wide application in the analysis of ultra-scaled nanoelectronics, where 3D architectures are currently dominating and the probing of confined volumes is mandatory.[4] However, for complex nanostructures such as integrated electronic devices, a detailed comprehension of the tip-sample interaction it's required for the precise control of the removal process in heterogenous materials. In this work, we combine experimental AFM data with molecular dynamics (MD) simulations that study the fundamentals of high-pressure tip-induced material removal for heterogenous nanostructures. Metal-oxide nanopillars (80 -120 nm diameter) embedded in SiO_2 are experimentally probed using high pressure sliding contacts (i.e., diamond probes). We select a regime whereby tens of nm^3 are removed targeting a controllable removal rate below 3 nm/scan. The impact of the tip-sample interaction inside the worn regions is investigated in order to generate understanding on the physical wear mechanisms. The experimental results are compared with MD simulations that allow us to study the removal

processes as a function of different parameters of the AFM scan, including removal rate and the quality of the machined area. As such, this work paves the way for the development of accurate models to improve the quality of tip-induced material removal in complex nanostructures, with great scientific and technological interest for tomographic probing using AFM.

References

[1] A.A. Tseng, Small. 7 (2011), 3409–3427.

[2] A. A. Tseng, et al., J. Vac. Sci. Technol. B, (2005), 23, 877.

[3] U. Celano, et al., Nano Lett., (2015), 15, 7970–5.

[4] W. Vandervorst, et al., Mater. Sci. Semicond. Process., (2017), 62, 31.

6:00pm **NS-TuA-12 Probing the Viscoelastic Properties of Polymer Composites with AFM-based Dynamic Mechanical Analysis**, *Bede Pittenger, S Osechinskiy, J Thornton, S Loire, T Mueller,* Bruker Corporation
The mechanical performance and function of polymer composites and thin films are controlled by the properties of the components as well as the microstructure of the material. As confinement effects and interphase formation can alter properties of the microphases, only measurements performed directly on the composite can provide the needed local property distribution. Mechanical properties of polymers are generally time dependent, so a full understanding requires measurements over a range of frequencies and temperatures. Ideally, one would like to observe the mechanical behavior of these microscopic domains while they pass through their glass transitions to appreciate the influence of size effects and confinement on time dependent mechanical properties.

With its proven ability to map mechanical properties at the nanometer level [1], Atomic Force Microscopy (AFM) has the resolution and mechanical sensitivity needed to investigate these domains. Unfortunately, established AFM measurement modes do not yield results that allow direct comparison to established rheological techniques like Dynamic Mechanical Analysis (DMA). Contact resonance [2] provides mechanical property maps at well-defined frequencies, but cantilever resonances are many orders of magnitude higher than DMA, making comparisons indirect at best. Intermittent contact methods like TappingMode [3], force volume, and PeakForce Tapping [4] face challenges in calculating intrinsic mechanical properties like storage and loss modulus (or tan delta) due to the non-linear process of making and breaking contact [5].

AFM based nano-DMA (AFM-nDMA) provides viscoelastic results that can be directly compared with bulk DMA. Like bulk DMA, it provides spectra of storage and loss modulus across frequency and temperature allowing construction of master curves through Time Temperature Superposition (TTS) [6]. In addition, it allows high resolution measurements localized to the microscopic structures within heterogeneous samples. This presentation will examine the capabilities of this new mode with examples in a wide range of polymers and composites.

[1] F. Rico, C. Su, and S. Scheuring, Nano Lett. 11, 3983 (2011).

[2] U. Rabe, S. Amelio, E. Kester, V. Scherer, S. Hirsekorn, and W. Arnold, Ultrasonics, 2000, 38, 430.

[3] O. Sahin, C. Quate, O. Solgaard, and A. Atalar, Phys. Rev. B, 2004, 69, 1.

[4] B. Pittenger and D. G. Yablon, Bruker Application Note, 2017, AN149, 1. doi: 10.13140/RG.2.2.15272.67844

[5] M. Chyasnavichyus, S. L. Young, and V. V Tsukruk, Langmuir, 2014, 30, 10566.

[6] M. L. Williams, R. F. Landel, and J. D. Ferry, J. Am. Chem. Soc.,1955, 77, 3701.

Complex Oxides: Fundamental Properties and Applications Focus Topic
Room A220-221 - Session OX+EM+HC+MI+NS+SS+TF-TuA

Complex Oxides: Catalysis, Dielectric Properties and Memory Applications

Moderators: Alexander Demkov, University of Texas at Austin, Jeffry Kelber, University of North Texas

2:20pm **OX+EM+HC+MI+NS+SS+TF-TuA-1 Novel Multiferroic and Ferroelectric Ferrite Thin Films**, *Peter A. Dowben, C Binek, X Xu,* University of Nebraska-Lincoln **INVITED**
Ferroelectricity and ferromagnetism are foundational to numerous technologies, yet the combination of ferroelectricity and ferromagnetism, namely multiferroicity, may be even more desirable. Multiferroic materials are believed to be a route to voltage controlled spintronic devices. Yet very few single phase materials are known to be ferroelectric and ferromagnetic at the same time, i.e. multiferroic. Even fewer materials are fewer materials are magneto-electric, that is to say materials with magneto-electric coupling, i.e. voltage control of magnetization, but without separate order parameters for magnetism (or antiferromagnetism) and ferroelectricity. This talk will review the electronic structure of the tri-rutile magneto-electric antiferromagnets, like Fe_2TeO_6, as well as rare earth ferrites like $ReFeO_3$ (Re = rare earth) stabilized in the hexagonal phase. Both types of materials are frequently antiferromagnetic, and, in principle, both can exhibit magneto-electric coupling. The surface termination affects the measured spin polarization of the surface and the interface with other materials. This will have a significant influence on the voltage control of magnetization. We have investigated the structural and electronic properties at the surface of these more unusual multiferroic materials using angle-resolved x-ray photoemission spectroscopy (ARXPS), complemented by x-ray diffraction (XRD), x-ray photoemission electron microscopy (X-PEEM), and X-ray circular dichroism. We find that the low local symmetry, especially at surfaces, will split the electronic states, via spin–orbit coupling. In some cases, the result is a net spin polarization at the surface, under electric field cooling. Because of the strongly preferential surface termination of these types of materials, the boundary polarization is roughness insensitive, in some cases making spintronic device applications plausible.

3:00pm **OX+EM+HC+MI+NS+SS+TF-TuA-3 Potential Applications and Challenges for Complex Oxides in Advanced Memory and Computing Applications**, *Sebastian Engelmann, T Ando, V Narayanan,* IBM T.J. Watson Research Center **INVITED**
As the semiconductor industry continues to push for and develop higher performance computing systems, there is also a growing trend of redeveloping or optimizing fundamental computing approaches to be more energy efficient. The development of hardware for novel AI systems is no exception. New integration schemes, novel materials, multi-component materials or even nanoscale materials and the ability to integrate all of these approaches together becomes the compounded challenge. Deposition and etch technologies that offer differentiating solutions to these issues therefore need to meet somewhat conflicting demands, such as low damage processing as well as high rate processing beside many other issues.

Novel thin films, thin film laminates and alloys promising unprecedented performance are very interesting candidates to enable such computing paradigm shifts. In particular the class of complex oxides is a very interesting area of research as they offer new phenomena such as ferroelectricity, ferromagnetism or high temperature conductivity. While new phenomena are being discovered, unraveling the fundamental physics behind these properties is a critical element for an industrial exploitation of these properties.

In addition, these new and complex materials are growing the need for the ultimate process solution: atomic layer precision processing. Atomic layer etching is a promising path to answer the processing demands of new devices at the Angstrom scale. Self-limiting reactions, discrete reaction and activation steps or extremely low ion energy plasmas are some of the pathways being pursued for precise material removal control and maintaining the original film performance. Depending on the nature of the material, the etch response may be either too much or not enough chemical modifications of the material. Resulting modifications of the films is an important variable to consider in the readiness of material systems. In particular synergy to deposition approaches such as atomic layer deposition has been proposed as a solution, but more work is needed.

4:20pm **OX+EM+HC+MI+NS+SS+TF-TuA-7 Epitaxial Design of Complex Oxides for Catalysis and Electrocatalysis**, *Yingge Du,* Pacific Northwest National Laboratory **INVITED**

Predictive synthesis of highly active and cost-effective catalysts and electrocatalysts for energy conversion and storage is critical for leveraging intermittently available energy sources. Transition metal oxides with perovskite (ABO3) and perovskite-related structures (e.g., Brownmillerite and Ruddlesden-Popper) have been identified as robust catalysts with high oxygen reduction reaction (ORR) and/or oxygen evolution reaction (OER) activities that rival the performance of noble metals and their compounds. The study of perovskites as epitaxial thin films enables measurement of their intrinsic catalytic activity, deconvolved from the effects of surface roughness and polycrystalline defects (e.g., grain boundaries and edges between facets). In addition, epitaxial growth facilitates accurate control over the composition, crystallographic orientation, and strain in thin films.

In this talk, our recent efforts in the design of epitaxial complex oxides for catalysis and electrocatalysis will be highlighted. Using LaNiO₃, a bi-functional electrocatalyst, as an example, I will show how isovalent substitution, alliovalent substitution, and interfacial strain can be used to tune the structural, electronic, and optical properties of the resultant films, and how these observed changes correlate with their (electro)catalytic performance. The use of complex oxide thin films as support or anti-corrosion layers during catalytic reactions will also be discussed.

5:00pm **OX+EM+HC+MI+NS+SS+TF-TuA-9 Manipulate the Electronic Structures of Complex (Ni, Co) Oxides by Hole Doping for Oxygen Evolution Reaction**, *Kelvin Zhang,* Xiamen University, China

This talk reports a fundmanetal study on the correlation of the composition and electronic structures of complex oxides with their electrocatalytic activity for oxygen evolution reaction (OER). In particular, we modulated the electronic states of complex oxides using hole doping strategy, e.g., Li doped NiO, Sr doped LaFeO₃ and Ni doped Co₃O₄. Photoemission spectroscopy and x-ray absorption spectroscopy (XAS) were used to study both the occupied and unoccupied density of states around the Fermi level. The electronic structures determines the adsorption strength of reaction intermediates for OER. Our results reveal two important change in the electronic structures induced by hole doping are crucial for improving OER activity: (1) upshift of the occupied valence band center to enhance the surface absorption; (2) creation of a new hole (unoccupied) state just above the Fermi level to reduces the energy barrier for electron transfer. Our results supplemented with DFT calculations established a direct correlation between the enhancement of activity with electronic structure, providing guideline for design of highly active electrocatalysts.

5:20pm **OX+EM+HC+MI+NS+SS+TF-TuA-10 Vanadia/Tungsten Oxide on Anatase TiO2(101): a Model Catalyst Study by STM and XPS**, *Tao Xu, J Lauritsen, K Adamsen,* Aarhus University, Denmark*; S Wendt,* iNANO, Aarhus University, Denmark

Nitrogen oxides (NOX) from flue gas are in concern as major sources of air pollution. Increasingly stricter NOX emission control policies (e.g. Euro VI) demand innovation and better performance of NOX reduction technology. The Selective Catalytic Reduction (SCR) of NOX by vanadia supported on anatase titania, with tungsten oxide (WO3) as promoter, has been widely used for this service and attracted much research attention. However, many aspects of the SCR catalysis process remain poorly understood at the atomic level. Particularly, the synergistic effect of tungsten oxide and vanadia remain elusive in literature, despite intensive RAMAN and infrared spectroscopy studies.

In this work, we use mineral a-TiO2 single crystals exposing the (101) facets as the model surface and deposit V2O5 and WO3 in our ultrahigh vacuum chamber (UHV) chamber by e-beam evaporation in oxygen. Combining Scanning Tunneling Microscope (STM) and X-ray photon-electron Spectroscopy (XPS), we systematically investigated the morphology and oxidation state changes of the model catalyst upon heating and reactant adsorption.

The STM results illustrate the distribution of V2O5 and WO3 on anatase TiO2(101) at the atomic level. It is found that both species are highly dispersed in the sub-monolayer region. For the deposition of surface oxide species, we explored different methods to achieve the highest oxidation state of vanadium (5+) and tungsten (6+). The thermal stability of the as-deposited V2O5 and WO3 are investigated by XPS and STM systematically. We found that when V2O5 and WO3 co-exist on the a- TiO2 surface the stability of V2O5 is improved. This work provides atomic level understanding on the V2O5/WO3/TiO2 SCR catalyst and new insights into

the synergistic interactions between vanadia and tungsten oxide on the a-TiO2 surface.

5:40pm **OX+EM+HC+MI+NS+SS+TF-TuA-11 Observation of Memory Effect and Fractal Surface in SrRuO₃ Epitaxial Thin Films**, *Ratnakar Palai,* University of Puerto Rico*; H Huhtinen,* University of Turku, Finland

Integration of multifunctional oxide materials (ferroelectrics and multiferroics) into silicon technology is of great technological and scientific interests. The current interest in functional oxides is largely based on engineered epitaxial thin films because of their superior properties compared to the bulk and polycrystalline thin films and their technological applications in dynamic random access memories, magnetic recording, spintronics, and sensors. Most of these applications require bottom and top electrodes to exploit the electronic properties of the functional materials.

SrRuO3 (SRO) has been found to be very useful for electrodes and junctions in microelectronic devices because of its good electrical and thermal conductivities, better surface stability, and high resistance to chemical corrosion, which could minimize interface electrochemical reactions, charge injection in oxide, and other detrimental processes, thus improving retention, fatigue resistance, and imprint. It also has good work function to produce the required large Schottky barrier on most ferroelectric oxide capacitors.

The bulk SRO exhibits several useful properties, such as extraordinary Hall effect, strong magnetocrystalline anisotropy, itinerant ferromagnetism, and spin-glass behavior. Spin-glass materials are currently frontier field of research and the most complex kind of condensed state of matter encountered so far in solid-state physics. Despite of the enormous importance of spin-glass models in neural networks, our knowledge of the underlying mechanistic processes involved is extremely limited. Although memory effect has been reported in bulk SRO, to our knowledge, the behavior is not well understood and there was no such report in thin films.

In this work, we report on the observation of memory effect and strong magnetic anisotropy in extremely smooth 1–3 Å roughness epitaxial (110) and (010) SrRuO3 thin films. The observation of non-zero imaginary susceptibility and frequency dependent cusp at freezing temperatures confirms the spin-glass behavior, which agrees well with the dc magnetization measurement. The origin of memory effect can be attributed to the magnetic frustration and random interaction, which is affected by dynamics of cooling and will be discussed in details.

6:00pm **OX+EM+HC+MI+NS+SS+TF-TuA-12 *In situ* Auger Electron Spectroscopy of Complex Oxide Thin Film Surfaces Grown by Pulsed Laser Deposition**, *Thomas Orvis, M Surendran, Y Liu, A Cunniff, J Ravichandran,* University of Southern California

Complex oxides can enhance the functionality of electronic and photonic devices by supplementing them with interesting properties such as ferroelectricity, superconductivity, and magnetoresistivity. Furthermore, low dimensionality in these materials can result in additional useful properties, inspiring the continued study of complex oxides in thin film form. However, the deposition of these materials is typically governed by notoriously complex growth mechanisms, revealing the need for *in situ* probes to observe and understand their precise nature. To this end, we report the *in situ* observation of chemical composition of complex oxide thin film surfaces with Auger electron microscopy during growth by pulsed laser deposition. Our implementation of real-time monitoring techniques for complex oxide thin films sheds an important light on the intricacies of the relationships between processing conditions and resulting composition.

Plasma Science and Technology Division
Room B131 - Session PS+EM-TuA

Advanced BEOL/Interconnect Etching and Advanced Memory and Patterning

Moderators: Hisataka Hayashi, Toshiba, Japan, Kenji Maeda, Hitachi High Technologies America Inc.

2:20pm **PS+EM-TuA-1 BEOL Etch Challenges and Solutions for Advanced Process Nodes**, *Angélique Raley, K Lutker-Lee, X Sun, Y Lu, Q Lou, N Joy, M Edley,* TEL Technology Center, America, LLC*; K Taniguchi, M Honda,* TEL Miyagi Limited, Japan*; P Biolsi,* TEL Technology Center, America, LLC **INVITED**

As logic nodes continue to scale below 7 nm, the back-end-of-line (BEOL) critical pitch has moved to sub-40 nm and is forecasted to scale down to 14

nm according to the latest International Roadmap for Devices and System (IRDS). This aggressive scaling has led to an industry wide effort in terms of materials research to manage interconnect resistance, patterning innovations to control for process variation impact and an increased focus on self-limited or highly selective processes.

In addition to the patterning and integration complexities that arise with scaling, pitch reduction has a direct impact on the plasma etch-processing window. Conventional continuous wave processes can no longer achieve stringent aspect ratio dependent etching (ARDE), selectivity and profile control requirements and have gradually given way to pulsed plasma processes, decoupled process sequence plasmas or remote plasmas to widen the process space.

In this talk, we will give an overview of plasma etching challenges and solutions for the BEOL in terms of patterning integration, dielectric etch and new materials introduction.

3:00pm PS+EM-TuA-3 Enabling Fully Aligned Via for Advanced BEOL Nodes Scaling -Etch and Film Co-optimization*, Xinghua Sun, A Raley,* TEL Technology Center, America, LLC*; J Lee, J Arnold,* IBM Research Division, Albany, NY*; K Taniguchi,* TEL Miyagi Limited, Japan*; M Edley, K Lutker-Lee,* TEL Technology Center, America, LLC*; D O'Meara,* Tokyo Electron America, Inc.*; K Tapily, Y Lu, P Biolsi,* TEL Technology Center, America, LLC

Aggressive metal pitch scaling of back end of line (BEOL) interconnect for future nodes leads to increased sensitivity to via overlay and critical dimension (CD) errors, resulting in yield loss. Spacing between top and bottom metal layers in via chain macros are reaching the limits of current materials, such that device reliability may become compromised due to metal shorting or dielectric breakdown. The technique of 1-D self-aligned via (SAV) constrained by top metal hard mask (MHM) is widely used to control one direction of via CD. 2-D fully aligned via (FAV) was recently introduced to mitigate the drawbacks of SAV at via bottom. In FAV, vias are constrained with spacers resulting from recessed metal in the orthogonal direction to the MHM, thereby increasing the margin of error allowed due to CD variations and overlay shifts. However, one of the biggest challenges in successfully integration of FAV in the BEOL is maintaining the integrity of these spacers during via etch. Etch selectivity, landing on conformably deposited Nblok based cap layers, is far from sufficient to maintain good self-confinement that demonstrates adequate FAV behavior. High selectivity etch stop layers (ESL) along with compatible etches that promote soft landing on these films are required.

In this presentation, we demonstrate that etch and film can collaboratively work to make FAV a competitive solution for sub-7nm nodes. Different ESL materials and film properties are investigated in conjunction with unique via and trench etch processes to achieve optimized FAV corner shape. This work shows a multifaceted approach to successful implementation of FAV as a valuable scaling booster for advanced BEOL nodes.

3:20pm PS+EM-TuA-4 Non-selective Silicon Oxide and Nitride Etch in Oxygen/Nitrogen-containing Fluorocarbon Plasmas*, Yu-Hao Tsai, D Zhang, Y Han, J Baillargeon, Y Shi, H Kim, M Wang,* TEL Technology Center, America, LLC*; T Yokoyama, M Iwata, Y Kihara, M Honda, W Sakamoto,* Tokyo Electron Miyagi Ltd., Japan*; A Mosden, A Metz, P Biolsi,* TEL Technology Center, America, LLC

Performing an all-in-one etch process for 3D-NAND fabrication requires comparable and high etch rates (E/R) for SiO_2 and Si_3N_4; the goal remains challenging. As the discrepancy of E/R largely results from the different nature of materials, surface modifications of SiO_2 and Si_3N_4 to achieve comparable composition during etch can improve the desired non-selectivity. In the presented work, we study the conversion of SiO_2 [*Submitted*] and Si_3N_4 [*J. Micro. Manuf.***1**, 20180102 (2018)] to oxynitride (SiO_xN_y) via the nitridation and oxidation-etch reactions, respectively. We computationally identify the etching mechanism of SiO_2/Si_3N_4 in the N/O-containing fluorocarbon plasmas using both quantum chemistry (QC) and molecule dynamics (MD) simulations; the surface conversion to SiO_xN_y is predicted. The results are further validated by the plasma etching of blanket SiO_2 and Si_3N_4 films in a Capacitively Coupled Plasma (CCP) chamber; both E/R trends and surface analysis on validation of oxinitride and/or nitrioxide (SiO_xN_y) formation using methods such as XPS, EDS etc. are discussed. We detail the etch reaction pathway, in which the elimination of O/N atom forming nitric oxide (NO) species is predicted. Along with that, the synergy of having F species in the process is justified. Finally, we discuss the impact of fluorocarbon to N/O ratio on the preference of either high E/R or active SiO_xN_y formation. The research builds a foundation for future development work on pursuing robust all-in-one non-selective SiO_2/Si_3N_4 etch processes.

4:20pm PS+EM-TuA-7 Challenges in High-aspect-ratio Hole Etching for 3D Flash Memory*, Mitsuhiro Omura, J Hashimoto, T Adachi, Y Kondo, M Ishikawa, J Abe, I Sakai, H Hayashi,* Toshiba Memory Corporation, Japan
INVITED

Memory devices with higher bit density are required for effective use of big data in the internet of things era, and 3D memory architecture is required. 3D flash memory encompasses numerous pillars that punch through control gate plates, and cells are arranged along the pillars [1]. We refer to each pillar as a memory hole. Memory holes are fabricated by dry etching of stacked films, which are generally constructed of dozens to several hundred pairs of SiO2/Si or SiO2/Si3N4 films. Therefore, the aspect ratio of a memory hole reaches several tens. Moreover, the critical dimension and profile of a memory hole must be strictly controlled because these features at each control gate plate directly affect the characteristics of memory cell. Therefore, the key technology of 3D flash memory is a high aspect ratio (HAR) hole etching process. However, the dry etching process of HAR holes has a variety of profile issues, including bowing, shape distortion, twisting of the hole profile, and striation.

In this study, sidewall striation formation in a HAR hole was investigated. In spite of the smooth morphology of the mask, sidewall striation was observed on dielectric films. Results from the carbon mask sample treated with several gas plasmas implies that ion irradiation can increase the degree of striation on the carbon mask, and striation tends to be suppressed by deposition of a fluorocarbon film from fluorocarbon radicals. An ion beam experiment with a simulated hole sidewall using blanket films shows that striation tends to form on the fluorocarbon film rather than on SiO2 and Si3N4 films. In connection with this result, the shallower region with striation had thicker fluorocarbon film than the deeper region with smooth sidewall. Therefore, the possible of sidewall striation formation mechanism is as follows. When the etching depth of the HAR holes reaches a certain depth, striation forms on the deposited fluorocarbon film and is transferred to the dielectric films laterally as the hole diameter increases. The region with striation depends on the aspect ratio, defined as the depth divided by the neck width of the carbon mask. Consequently, as etching progresses, the mask thickness decreases and striation forms in a deeper region, depending on the aspect ratio.

References

[1] H. Tanaka et al., Symposium on VLSI Technical Digest, 14 (2007).

5:00pm PS+EM-TuA-9 Plasma Processing of Phase Change Materials*, Ernest Chen, N Altieri,* University of California, Los Angeles*; C Neumann, S Fong, H Wong,* Stanford University*; M Shen, T Lill,* Lam Research Corporation*; J Chang,* University of California, Los Angeles

The manipulation of the amorphous to crystalline phase transition observed in chalcogenide glasses for non-volatile memory applications has been studied for many years since its initial conception. However, only recently has innovation in both materials development and memory device architecture enabled phase change random access memory (PCRAM) to become a promising candidate for applications such as neuromorphic computing. Ternary chalcogenide glasses consisting of germanium, antimony, and tellurium are widely used in PCRAM applications, and $Ge_2Sb_2Te_5$ (GST-225) will be the focus of this study.

Understanding the effects of plasma processing on the phase change material (PCM) utilized in PCRAM is crucial to ensuring proper device performance. The studies presented in this talk utilize a custom-built integrated system equipped with ion beam processing, downstream plasma processing, quadrupole mass spectrometry, optical emission spectroscopy, and x-ray photoelectron spectroscopy capabilities. The samples are prepared by sputtering from a stoichiometric GST-225 target. Prior studies have examined the behavior of GST-225 when exposed to different components of ambient exposure (N_2, O_2, and H_2O) as well as H_2 and CH_4 discharges and identified H_2 and CH_4 as capable GST etchants.

It is known that ambient exposure will cause a GST-225 layer to be oxidized in the first several nanometers, and this oxidized layer has different properties from the bulk of the GST-225 film and may also behave differently from the bulk material when exposed to plasma processing. Initial studies with *ex-situ-* XPS analysis indicate that H_2 can etch GST-225 with approximately 5% change in composition (5% increase in Ge, 5% decrease in Sb, approximately 0% change in Te) and a significant change in the ratio of 0+ to X+ (non-oxidized to oxidized) bonding states between the oxidized surface and the etched surface. In order to distinguish the effects of plasma processing on the oxidized layer and the bulk material, a custom-built downstream plasma processing chamber integrated with an XPS chamber is used. This system allows for the study of the surface states of

GST-225 post-processing without any inadvertent effects from ambient conditions that may complicate *ex-situ* XPS analysis.

5:20pm PS+EM-TuA-10 Meeting the Challenges in Patterning Phase Change Material for Next Generation Memory Devices, *Meihua Shen, L Thorsten, J Hoang, S Chiou, D Qian, A Routzahn, J Chen, A Dulkin, J Sims, A McKerrow, R Dylewicz,* Lam Research Corporation **INVITED**
Phase change materials (PCM) have emerged as the leading candidate for next generation non-volatile memory device with unique characteristics that significant differ from conventional DRAM and NAND flash memory. Recently, 3-D Cross point PCRAM, for example, has transitioned into high volume production, demonstrating a non-volatile memory product exhibiting faster speed, low voltage operation and high density.

Phase change materials are typically chalcogenide alloys containing elements such as Ge, Sb, Se, Te with various dopants. The materials exhibited phase change between amorphous insulating state and the crystalline conductive state under thermal/electric heating. To ensure electric device performance, it is critically important to maintaining the PCM elemental composition and structure integrity during patterning. The challenges of patterning PCM come from the soft nature of the material and the damages that can easily occur during plasma dry etch, ambient exposure, wet clean and encapsulation process. To meet the challenges, we developed an integrated system combining dry etch, wet clean and ALD encapsulation modules together. In this paper, we will present the comprehensive studies on each module as well as the interactions of the modules in successful patterning of the phase change materials. The discussions will be focused key learnings on how to maintain the feature fidelity and the integrity of the materials during etch and encapsulation.

6:00pm PS+EM-TuA-12 Utilizing Photosensitive Polymers to Estimate UV Radiation Exposures in Different Plasma Chamber Configurations, *Luxherta Buzi, M Sagianis, S Engelmann,* IBM T.J. Watson Research Center
Monitoring vacuum ultraviolet (UV/VUV) emission in plasma systems is challenging as it requires specialized diagnostic systems or sensors to be compatible with reactive ion etch (RIE) tooling. This study is mapping different reactor configurations with various levels of UV emission and its effect on a known set of polymers.

Photon-induced modifications on polymers can help decouple ion and photon effects on materials therefore, the impact of inductively coupled and microwave plasma configurations on etch rates and chemical properties of photoresists were investigated. Poly(methyl methacrylate) and Poly(4-hydroxystyrene)-based photoresists were deposited on Si wafers and exposed to argon (Ar) and nitrogen (N_2) plasmas which generate different levels of UV irradiation. X-ray Photoelectron Spectroscopy (XPS) and Fourier Transform Infrared (FTIR) were used to analyze the polymer composition and molecular structure and the surface roughness was analyzed with an atomic force microscope (AFM).

FTIR and XPS confirmed that N_2 plasma effects on chemical modifications were more pronounced on the Poly(methyl methacrylate). Roughness and etch rate was significantly higher for Poly(methyl methacrylate) compared to Poly(4-hydroxystyrene)-based photoresists. Detailed elemental and molecular structure analysis of polymers showed relatively higher damage caused from the inductively coupled plasma, which is ultimately correlated to a higher UV emission.

Materials and Processes for Quantum Information, Computing and Science Focus Topic
Room B231-232 - Session QS+2D+EM+MN+NS-TuA

Materials for Quantum Sciences
Moderators: Matthew R. Rosenberger, U.S. Naval Research Laboratory, Robert Walko, The Ohio State University

2:20pm QS+2D+EM+MN+NS-TuA-1 Electrically Detected Electron Nuclear Double Resonance Study of Defects in 4H-SiC Bipolar Junction Transistors, *Ryan Waskiewicz, B Manning, D McCrory, P Lenahan,* Pennsylvania State University
There is growing interest in the possibilities of SiC in spin-based quantum computation. The development of such spin-based quantum computation will require a fundamental understanding of spin physics of paramagnetic defects in SiC including both electron and nuclear paramagnetism. We utilize electrically detected magnetic resonance (EDMR) detection through spin dependent recombination (SDR). In this study we demonstrate relatively high signal to noise electron nuclear double resonance (ENDOR)

in a single fully processed SiC pn junction at room temperature. The electrically detected ENDOR (EDENDOR) involves nitrogen nuclei in close proximity to deep level centers within the depletion region of the pn junction; the deep levels are almost certainly silicon vacancies.

We believe these observations are of importance for at least two reasons: (1) they demonstrate that the enormous analytical power of ENDOR can be extended to the study of problems in conventional solid-state electronics and (2) the results demonstrate a way to directly monitor small numbers of nuclear spins through the measure of electronic currents.

In our EDMR measurements, a slowly varying magnetic field and an oscillating microwave frequency magnetic field are applied to the sample inside a microwave cavity. As in conventional EPR, energy is absorbed by paramagnetic sites when the resonance condition is met. For a simple case, this resonance condition is $h\nu = g\mu_B B \pm \Sigma m_i A_i$, where h is Planck's constant, g is an orientation dependent number typically expressed in a g-tensor, μ_B is the Bohr magneton, B is the magnetic field, m_i is the spin quantum number of the ith nucleus, and A_i is the hyperfine interaction of the ith magnetic nucleus. In EDMR, the EPR response is detected through a change in device current, in our case due to SDR.

The devices in this study are 4H-SiC BJTs. The EDMR response obtained on these BJTs is very similar to an EDMR spectrum that has been linked to a silicon vacancy in 4H-SiC MOSFETs. To perform the EDENDOR measurement, the magnetic field is held constant and an NMR frequency sweep is applied to the device. The device current is measured and a large response is measured at what is unambiguously the nuclear frequency of nitrogen. These results demonstrate the analytical power of the EDENDOR measurement, measuring nitrogen in the vicinity of the silicon vacancy defect centers that are measured with EDMR.

2:40pm QS+2D+EM+MN+NS-TuA-2 Scanning Tunneling Microscopy Studies of Er Adatoms on GaAs (110), *Rebekah Smith, A Benjamin, J Gupta,* The Ohio State University
Rare earth dopants in III-V semiconductors are of interest as high quality optical sources due to the preservation of sharp intra-*f*-shell transitions. The long optical coherence lifetime and narrow energy width of these transitions, at 1.54 um, make them a candidate for quantum communication. Here we investigate Er interactions with host GaAs (110) surface with atomic resolution using STM. Er atoms were deposited via electron beam evaporation onto the GaAs surface at 5 K. We find three different Er_{ad} configurations with varying abundance upon deposition, each with a different surface site location. All three configurations exhibit long-range depressions in STM topographic images, attributed to band bending associated with a positive adatom charge state. Individual Er adatoms can be switched between these states by applying a positive voltage pulse with the STM tip. Tunneling spectroscopy on Er adsorbed at the interstitial sites reveals prominent states within the GaAs bandgap, but no evidence of sharp *f*-shell transitions inferred from bulk optical studies. We also form substitutional Er_{Ga} by applying a larger positive voltage pulse. Substitutional Er appears neutral, which we attribute to it being isoelectronic with Ga. This work acknowledges funding from the DOE (DE-SC0016379).

3:00pm QS+2D+EM+MN+NS-TuA-3 Defect-based Quantum Systems in Hexagonal Boron Nitride, *Trong Toan Tran,* University of Technology Sydney, Australia **INVITED**
Engineering solid state quantum systems is amongst grand challenges in realizing integrated quantum photonic circuitry. While several 3D systems (such as diamond, silicon carbide, zinc oxide) have been thoroughly studied, solid state emitters in two dimensional (2D) materials are still in their infancy. In this talk I will introduce hexagonal boron nitride (hBN) as a promising layered material that hosts ultra bright quantum emitters. I will present several avenues to engineer these emitters in large area hBN multilayers and monolayers using chemical vapour deposition techniques. I will then show unique tuning expeirments and promising results for controlling the emission wavelength of these quantum emitters. At the second part of my talk, I will discuss promising avenues to integrate the emitters with plasmonic and photonic cavities to achieve improved collection efficiency and Purcell enhancement. These are fundamental experiments to realize integrated quantum photonics with 2D materials. I will summarize by outlning challenges and promising directions in the field of quantum emitters and nanophotonics with 2D materials and other wide band gap materials.

4:20pm QS+2D+EM+MN+NS-TuA-7 Specific Placement of V_{Si} in 4H-SiC for Quantum Technologies using Li+ Implantation, *S Pavunny, Rachael L. Myers-Ward, D Gaskill,* U.S. Naval Research Laboratory; *E Bielejec,* Sandia National Laboratories; *H Banks, A Yeats,* U.S. Naval Research Laboratory; *M DeJarld,* Raytheon; *S Carter,* U.S. Naval Research Laboratory

Silicon carbide has been a material of interest in the quantum technology field for future applications in communication and sensing due in part to the long spin (S = 3/2) coherent lifetime of the Si vacancies (V_{Si}). Additional benefits to using SiC for quantum technologies is wafer scalability and fabrication capability using standard processing techniques, making it a favorable material. To improve emission rates of photoluminescence from the vacancies, exact placement of the V_{Si} within microcavities is necessary. Here we show implanted Li+ into Si-face, 4H-SiC homoepitaxy creates V_{Si} in desired locations. The epitaxial material had no measurable V_{Si} prior to Li+ implantation. The dose of 100 keV Li+ ranged from $10^{12} - 10^{15}$ cm^{-2} and was directed using a maskless focused ion beam technique with a positional accuracy of ~25 nm. The arrays were characterized with high-resolution scanning confocal fluorescence microscopy. Using a 745 nm excitation source, the photoluminescence ranging from 860 − 975 nm produced the characteristic V1', V1 and V2 lines, with the V1' zero-phonon line being consistent for all measurements. In addition, the V1' intensity showed a linear dependence with implantation dose. Moreover, near single photon emission is obtained from V_{Si} at the lowest doses.

4:40pm QS+2D+EM+MN+NS-TuA-8 Silicon Vacancy Point Defect in High-quality Nanobeam Photonic Crystal Cavities in 4H Silicon Carbide, *Mena Gadalla, X Zhang, A Greenspon,* Harvard University; *D Bracher,* Harvard GSAS; *R Defo, E Hu,* Harvard University

Silicon carbide (SiC) has recently found promise and applications in the quantum world, because of various fluorescent point defects that serve as an intriguing platform for solid-state quantum information and quantum sensing technologies. One such native point defect is the negatively charged silicon vacancy (V_{Si^-})in the 4H polytype of SiC. This color center can occupy two inequivalent lattice sites, resulting in two distinct zero-phonon-lines (ZPL) at 862nm and 916nm. V_{Si^-} possesses good spin coherence properties, with spin states that can be initialized and read out optically. Unfortunately, low branching ratio is a characteristic of the V_{Si^-} spectrum where a small fraction of the total emission is coupled into the ZPL and the rest is emitted into the phonon sideband. This low emission fraction limits the ability to employ V_{Si^-} in various quantum information schemes. To increase the fraction of light emitted into the ZPL and increase the defect emission rate, we fabricated high-quality factor nanophotonic crystal cavities designed to match the ZPL frequency. Through tuning of the cavity into resonance with the ZPLs, we have demonstrated a 75-fold Purcell enhancement at 4K. This talk will describe the fabrication process for 1D nanobeam photonic crystal cavities, leading to quality factors in excess of 10^4. The highest cavity-defect interactions depend on resonance in frequency and high spatial overlap of the defect with the maximum electric field within the cavity. Using the cavity as a "nanoscope", revealing defect position, we used laser irradiation annealing at varying times and different laser frequencies to infer the diffusive motion of defects within the cavity. We showed that a systematic and controlled laser annealing can increase the ZPL of the implanted cavity mode by a factor of 4.

5:00pm QS+2D+EM+MN+NS-TuA-9 Tailoring the Heterogeneities in 2D Materials by Controlled Synthesis and Processing, *Kai Xiao, X Li, K Wang, A Oyedele, M Yoon, S Xia, M Mahjouri-Samani, C Rouleau, A Puretzky, L Liang, R Unocic, D Geohegan,* Oak Ridge National Laboratory

Two-dimensional (2D) materials are intrinsically heterogeneous, thereforecontrolling defects, understanding the impact of boundaries and interfaces and developing means to exploit these heterogeneities is a transformative opportunity that could underpin future technologies and energy applications. In this talk, I will discuss the fundamental understanding of the roles of heterogeneities including defects, dopants, edges, strain, and phases in 2D materials on their optoelectronic properties. Through isoelectronic doping in monolayer of $MoSe_2$, the Se vacancies are effectively suppressed and photoluminescence is significantly enhanced. In addition, we demonstrate the non-equilibrium, bottom-up growth approach not only can tailor the defect density far beyond intrinsic levels in monolayers of 2D $MoSe_{2-x}$ but also create new antisite defects in

monolayers of WS_2during the synthesis. The build-in localized strain in 2D crystals directly grown on patterned curved surface can tune the bandgap of 2D crystals for possible quantum emitting applications. The bottom up synthesis of 2D materials discussed here provides excellent control over the heterogeneity in 2D materials, which can modulate the optical and electrical properties in 2D materials and their heterostructures for ultra-thin and flexible electronics.

5:20pm QS+2D+EM+MN+NS-TuA-10 Epitaxial Al Films for Plasmonic and Quantum Computing Applications, *Ka Ming Law, S Budhathoki, S Ranjit, F Martin, A Hauser,* The University of Alabama

Superconducting resonators are important for application in quantum computing but require high quality factors. Much work has been done on superconducting resonators fabricated from aluminum thin films on sapphire, and superconducting Josephson tunnel junctions made from aluminum are used as the basis for quantum bit designs. In addition, epitaxial aluminum films has attracted attention in plasmonics due to their superior performance in the UV regime compared to Au and Ag, and their compatibility with current CMOS technology. Sapphire substrates are chemically stable and have low lattice mismatch with aluminum, allowing higher film quality without the need for elaborate substrate preparation and time-consuming growth procedures.

Epitaxial aluminum films were successfully grown by off-axis magnetron sputtering on c-plane sapphire. This study assessed the effects of varying both substrate preparation conditions and growth and prebake temperatures on crystallinity and smoothness. X-ray diffraction and reflectivity measurements demonstrate superior crystallinity and surface smoothness for films grown at 200℃ in15mTorr Ar. An additional substrate preparation procedure which involves 1) a modified RCA procedure and 2) prebake in oxygen environment is shown by atomic force microscopy to be highly effective in reducing void density and depth.

5:40pm QS+2D+EM+MN+NS-TuA-11 Minimizing Coulomb Oscillation Linewidth on Silicon Quantum Dots, *Yanxue Hong, A Ramanayaka, M Stewart, Jr., X Wang, R Kashid, P Namboodiri, R Silver, J Pomeroy,* National Institute of Standards and Technology (NIST)

In quantum science research, both cryogenic temperatures and low measurement noise are required for high fidelity. For silicon quantum dot devices, an increase in either one causes broadening of Coulomb blockade peaks, which is usually referred to as a high electron temperature. Here we report on temperature-dependent (T-dependent) conductance measurements and evaluation of effective electron temperature (T_{eff}) using an STM-patterned atom-scale silicon single-electron transistor (SET). Measurements are made in various cryogenic systems over temperatures varying from 10 mK to 25 K. The effective electron temperature is extracted by fitting the experimental data using a theoretical model. We initially find that the measured peak width has a linear dependence on the bath temperature above 1 K and saturates below 1 K. In addition, a considerable mismatch (> 2 K) between the lattice (thermometer) temperature and the carrier temperature (T_{eff}) is observed. Therefore, the Coulomb resonance is not only thermally broadened by T_{eff} but also broadened by other T-independent sources such as gate noise, triboelectric noise, etc. We study the origins of the saturation at low temperature regime and analyze factors inducing high T_{eff}. We report on progress to reduce the noise and reach an effective temperature of < 300 mK. Since our silicon SETs have high charging energies and large energy level spacings, we also seek to measure the transition from classical (multilevel) regime to quantum (single-level) regime by manipulating the bath temperature.

6:00pm QS+2D+EM+MN+NS-TuA-12 Micro-magnetic Simulations of Correlated Switching in Touching Nano-magnetic Elements, *Tejumade Durowade, V Metlushko,* University of Illinois at Chicago

Nanomagnets hold significant potential for use as building blocks for room temperature quantum computers. Bistability based on stable ground magnetization states means power dissipation can be extremely low and their small size allows magnetization to be maintained for a long period time [1]. With packing density on the order of 10^{10} /cm^2 and switching frequency in the terahertz range, nanomagnets are a promising replacement for current state of art metal oxide semiconductor processes that are already at the limits of continued scaling. In this work, we present

the results of simulations of touching nanomagnetic disks that can be used for room operable quantum computing. Like gears in a mechanical system, the chirality of the magnetization in each disk is determined through interaction with its neighbors. These simulations offer insight into the switching dynamics within the disks as current experimental techniques lack the combined temporal and spatial resolution needed to observe the formation and annihilation of the magnetic domains that facilitate the switching process. The switching of touching symmetric disks can be achieved at zero applied field as the disks settle into a remanent vortex state, meaning minimal energy loss during the process. Due to the quantum exchange force, at the point of contact between disks, the magnetization vectors rotate in the same direction giving rise to opposite chiralities in the disks. Since logic states can be represented using the chirality of the in-plane magnetization, configurations of touching disks can potentially be used to implement basic or complex logic functions. Maintaining coherence of opposite chirality in chains of disks was achieved with the introduction of a biasing element to eliminate the bidirectionality of interaction between disks.

[1] A. Orlov *et al.*, Nano. & Optoelec. vol. 33, p. 55, (2008).

[2] A. Imre *et al.*, *IEEE Conf. Nanotech.*, vol. 15, p. 137, (2004).

[3] G.H. Bernstein *et al.*, *Microelec. Journ.,* vol. 36, p. 619, (2005).

[4] T. Shinjo *et al.*, *Science.*, vol. 289 p. 930, (2000).

[5] A. Hirohata *et al.*, *IEEE Transc. on Magnetics.*, vol. 35, p. 3886 (1999).

[6] L. Fumagalli *et al.*, *Conf. Electromag in Adv. App..*, p. 617, (2007)

[7] M. Donahue *et al.*, *OOMMF, NIST, US Depart. Commerce*

Thin Films Division
Room A124-125 - Session TF+PS-TuA

Epitaxial Thin Films
Moderator: Robert Grubbs, Sandia National Laboratories

2:20pm **TF+PS-TuA-1 In-situ Epitaxy of Ultrathin Ni Ferrite Films Studied by Surface Sensitive Time-resolved High Energy X-ray Diffraction**, *Joachim Wollschläger, M Hoppe, T Pohlmann,* University Osnabrück, Germany*; F Bertram,* DESY, Hamburg, Germany
Ultrathin films of transition metal ferrites show a large variety of electronic and magnetic properties due to their inverse spinel structure. Therefore, they are of large interest in different fields as catalysis, spintronic and spincaloritronic. The performance of ultrathin ferrite films for devices, however, is strongly coupled to their structure and to their interface properties which are determined by the details during film growth. Therefore, we developed an experimental setup to study the structure of ultrathin films during deposition using surface sensitive time-resolved high energy x-ray diffraction (tr-HEXRD). Here, a large area detector is used to record large parts of reciprocal space while the sample is rotated during growth. The setup offers good time resolution within the range of seconds. Thus, it is possible to record both evolving Bragg peaks of the film and crystal truncation rods (CTRs) while the film is formed and to analyse the diffraction data with respect to evolving film structure.

Here, we present studies performed during growth of Ni ferrite films on $SrTiO_3(001)$ at various temperatures. This epitactical system is characterized by a lattice mismatch of 7.5% taking into account the doubled lattice constant of the perovskite $SrTiO_3$. Recording simultaneously several CTRs and evolving Bragg peaks, we could follow the temporal evolution of the film structure in detail. Having past the initial stages of growth, the temporal evolution of the lattice constants depends on the growth temperature. Following the standard model of relaxation of epitactical films, we expected that the strained films show lateral compressive and vertical tensile strain. Our experiments, however, show the opposite relaxation behaviour. This unusual relaxation is attributed to the interface between spinel film and perovskite substrate.

2:40pm **TF+PS-TuA-2 Van der Waals Layer Promoted Heteroepitaxy in Sputter-deposited Transition-metal Carbide and Sulfide Thin Films**, *Koichi Tanaka*[1], *P Arias, M Liao, Y Wang, H Zaid, A Aleman,* University of California, Los Angeles*; K Hojo,* Nagoya University, Japan*; A Deshpande, M Goorsky, S Kodambaka,* University of California, Los Angeles
Over the past decade, two-dimensional (2D) layered materials such as graphene, MoS_2, etc., have attracted considerable attention for a variety of

applications, primarily in nanoelectronics and optoelectronics. An exciting and relatively little explored application of these van der Waals (vdW) layered materials is their use as templates for crystal growth. In the recent years, vdW layers present at the substrate-film interface have been shown to promote 'remote epitaxy', by relaying the epitaxial registry between the film and the substrate.

Here, we demonstrate that the crystallinity of sputter-deposited thin films can be significantly improved using vdW layered materials as buffer layers on growth substrates. Using 2D hexagonal boron nitride (hBN, $a = 0.250$ nm and $c = 0.667$ nm) as the buffer layer, we grow hexagonal-MoS_2 ($a = 0.315$ nm and $c = 1.23$ nm), trigonal-structured Ta_2C ($a = 0.310$ nm and $c = 0.494$ nm), and NaCl-structured TaC ($a = 0.446$ nm) of desired thickness on $Al_2O_3(0001)$ substrates via ultra-high vacuum direct current magnetron sputtering of Mo and TaC targets respectively, in Ar/C_2H_4 and Ar/H_2S gas mixtures. hBN layers are deposited in the same system via pyrolytic cracking of borazine (~600 L) onto the substrates at prior to the growth of the thin films. The as-deposited films are characterized using a combination of *in situ* using Auger electron spectroscopy and low-energy electron diffraction and *ex situ* X-ray diffraction (XRD), X-ray photoelectron and Raman spectroscopies, and transmission electron microscopy (TEM) based techniques.

We find notable differences in the layers deposited on hBN-covered $Al_2O_3(0001)$ compared to those grown on bare substrates: significantly stronger 0002 (or 111 in case of TaC) reflection intensities and observation of Laue oscillations in ω-2θ XRD scans and higher intensity of MoS_2 characteristic peaks in Raman spectrum. Furthermore, we show that inserting hBN layers at regular intervals results in highly-0002-oriented growth and suppression of polycrystallinity in thicker Ta_2C films. Our results indicate that hBN layers enhance the crystallinity, irrespective of the crystal structure, of sputter-deposited thin films.

3:00pm **TF+PS-TuA-3 Molecular Beam Epitaxy Applied to Tensile-Strained Quantum Dots for Quantum Optics and Band-Structure Engineering**, *Paul Simmonds,* Boise State University   **INVITED**
Since the early 1990s, solid-state self-assembled quantum dots (QDs) have been the subject of intensive research for devices and technologies ranging from high-stability lasers, to intermediate band solar cells. Driven by compressive strain, semiconductor QDs form spontaneously on the (001) surfaces of both III-V and group IV materials during growth by molecular beam epitaxy (MBE). But several years ago, I became interested in the question of why QD self-assembly seemed to be limited to materials with this specific combination of compressive strain, and a (001) surface orientation. For example, why could we not grow QDs under *tensile* rather than compressive strain or on non-(001) surfaces, especially since QDs with these characteristics are predicted to be highly desirable for certain applications. The low fine-structure splitting of (111) QDs should make them ideal entangled photon sources; tensile-strained QDs would have dramatically reduced semiconductor band gaps, with implications for infrared optoelectronics and nanoscale band structure engineering.

The first step towards answering this question was to understand how the competition between plastic and elastic strain relief mechanisms made it enormously challenging to synthesize non-(001) or tensile-strained QDs without the formation of crystallographic defects. The outcome of this analysis was the discovery of a robust new approach to QD self-assembly based on MBE that overcomes these difficulties, and enables the reliable, controllable growth of defect-free, tensile-strained QDs on (111) and (110) surfaces.

I will describe the model upon which tensile-strained QD self-assembly is founded, and then discuss the application of this novel growth mode to several different material systems. I will present data confirming that the (111)-oriented QDs we can now grow do indeed show promise as entangled photon sources. I will highlight the possibilities for band structure engineering that are now available with tensile-strained QDs, using the example of transforming germanium into a direct band gap semiconductor.

In summary, I hope to demonstrate that tensile-strained self-assembly represents a powerful new tool for heterogeneous materials integration, and nanomaterial development.

---

[1] **National Student Award Finalist**

5:00pm **TF+PS-TuA-9 Low-temperature Homoepitaxial Growth of N-type Superlattices for Ultrastable, Ultrafast X-Ray and Charged Particle Detectors**, *April Jewell,* Jet Propulsion Laboratory, California Institute of Technology; *M Hoenk,* Jet Propulsion Laboratory; *Q Looker, M Sanchez, B Tierney,* Sandia National Laboratories; *A Carver,* Jet Propulsion Laboratory; *S Nikzad,* Jet Propulsion Laboratory, California Institute of Technology

We present a low-temperature process for the homoepitaxial growth of antimony superlattices in silicon. The all low temperature superlattice doping process is compatible as a post-fabrication step for device passivation. We have used low-temperature molecular beam epitaxy (MBE) to embed atomically thin (2D), highly concentrated layers of dopant atoms within nanometers of the surface. This process allows for dopant densities on the order of 10^{13}-10^{14} cm^{-2} (10^{20}-10^{21} cm^{-3}); higher than can be achieved with three-dimensional (3D) doping techniques. This effort builds on our prior work with n-type delta doping; we have optimized our growth processes to achieve delta layers with sharp dopant profiles. By transitioning from a standard effusion cell to a valved cracker cell for antimony evaporation, we have achieved carrier densities approaching 10^{21} cm^{-3} with peak distribution at ~10 Å FWHM for single delta layers. We will discuss details related to growth optimization, and show results from in situ monitoring by electron diffraction. We will also report on elemental and electrical characterization of our films.

The performance of our low-temperature 2D-doping processes has been validated by applying both p-type and n-type superlattice-doping to fully depleted photodiodes. The superlattice-doped devices show significantly higher responsivity than the equivalent ion-implanted devices. Additionally, when exposed to pulsed X-rays the superlattice-doped devices exhibit fast response and recovery times required for use in pulsed power experiments.

5:20pm **TF+PS-TuA-10 Epitaxial Growth of Ultrathin Molybedenum Nitrides on Ru(0001) and Ag(100)**, *Asim Khaniya, M Sajid, A Kara, W Kaden,* University of Central Florida

Molybdenum-nitrides are known to possess interesting mechanical, electronic, and catalytic properties. For example, (i) hexagonal δ-MoN exhibits mechanical elasticity and hardness values comparable to cubic BN and diamond, (ii) both hexaganol and cubic phases of molybdeumn nitrides are known to be superconducting, and (iii) mixed-phase structures have been shown to outperform commercial hydrotreatment catalysts for selective nitrogen removal from heterocyclic organic feedstocks. To better understand these properties, many groups have worked to create improved recipes to grow different phase-pure crystallographic phases of the material. To-date, the most successful procedures have leveraged epitaxy to improve long-range bulk order, but have lacked the well-defined, planar terminations suitable for controlled surface-science investigations. To establish such samples, our group has opted to use low energy nitrogen ions in tandem with molybdenum physical vapor deposition to grow and characterize molybdenum-nitride films on Ru(0001) and Ag(100) supports, which have been chosen to template the growth of hexaganol and cubic phases of the nitride. At the time of this abstract submission, we have succeeded in the growth of a δ-MoN-like film that appears to grow layer-by-layer and in registry with the Ru(0001) support, and are now in the early stages of repeating the process to create γ-Mo$_2$N on Ag via an analogous process. This talk will focus on the interesting aspects of these materials (particularly those relevant to catalysis), our approach to film preparation, and a thorough analysis of the physical properties of the resultant films and growth modes via: XPS, LEED, He$^+$ Ion Scattering Spectroscopy, STM, and DFT.

5:40pm **TF+PS-TuA-11 Using Time and Temperature of the Purge Step to Control Crystallinity, Phase Assemblage, and Epitaxy in Atomic Layer Deposited (ALD) Thin Films**, *Mark Losego, B Piercy, R Petrie,* Georgia Institute of Technology

The purge step between precursor and co-reactant doses in an atomic layer deposition (ALD) process is often viewed as a process liability. The goal for most manufacturing processes is to make this purge step as short as possible without disrupting the quintessential self-limited growth of ALD. In our lab, we have instead viewed this purge step as a potential opportunity to influence the crystallinity and phase assemblage of our materials. In actuality, each of these purge steps are an opportunity to allow surface diffusion to rapidly reform the film's microstructure before the next layer is deposited. Throughout the literature are interesting, but often conflicting reports of how ALD films crystallize with temperature and thickness. In our recent work, we have asked some simple questions, like how does the onset of such crystallinity change with purge time? We have found, for

example, that the onset of anatase formation in the TiCl$_4$-H$_2$O ALD system can be reduced by more than 40 °C by simply extending the purge time between each cycle. While potentially time intensive, these results have implications for depositing crystalline materials on temperature-sensitive substrates, like polymers. We also find that often an initial seeding of the crystallinity can lead to accelerated growth of crystalline phases with subsequent cycles. In a second paradigm to be discussed, we have introduced a high-temperature pulsed heating source to an ALD system to intentionally crystallize materials and drive epitaxial growth. As proof-of-concept, we have studied epitaxial growth of ZnO on c-plane sapphire using a diethylzinc (DEZ) / water chemistry. DEZ is known to decompose above about 180˚C, and the DEZ-H$_2$O system cannot be grown epitaxially on c-sapphire with traditional thermal ALD approaches. Here, we show that heating pulses up to 900˚C can be used to drive epitaxy. Interestingly, we find that a template layer of only 20 pulsed heating ALD cycles is sufficient to template ZnO epitaxy with subsequent low temperature ALD growth (180 °C) to film thicknesses of up to 100 nm.

6:00pm **TF+PS-TuA-12 The Role of Template Layers in Heteroepitaxial ALD Growth of Crystalline La$_2$O$_3$ on GaN(0001)**, *Pei-Yu Chen, T Hadamek,* University of Texas at Austin; *S Kwon,* University of Texas at Dallas; *F Al-Quaiti, A Posadas,* University of Texas at Austin; *M Kim,* University of Texas at Dallas; *A Demkov, J Ekerdt,* University of Texas at Austin

The high switching frequency, operating temperatures and voltages make GaN the material of choice for higher power applications and instrumental to reducing power consumption. In many of these applications, there is a need for a high quality gate dielectric. Lanthanum sesquioxide, La$_2$O$_3$, is one of the promising gate insulator candidates. In this work, we compare La$_2$O$_3$ thin films grown by atomic layer deposition (ALD) and molecular beam epitaxy (MBE), and explore the formation of ALD-La$_2$O$_3$ films on GaN(0001). An island growth mode (Volmer-Weber growth) was observed when La$_2$O$_3$ films were deposited directly on GaN(0001) at 250 °C by ALD using tris(N,N'-diisopropylformamidinato)-lanthanum as the precursor and H$_2$O as the co-reactant. Only with use of a thin template layer, 2 nm-thick hexagonal La$_2$O$_3$ grown by MBE or 3 nm-thick cubic Er$_2$O$_3$ grown by ALD, can a 2-dimensional ALD-La$_2$O$_3$ thin film be formed. The 2-dimensional ALD-La$_2$O$_3$ growth on templated-GaN(0001) was confirmed by RHEED and AFM. The macrostructure and microstructure of ALD-La$_2$O$_3$ films were verified with XRD, STEM, and atomic structure modeling. The ALD-La$_2$O$_3$ film retains a cubic structure on ALD-Er$_2$O$_3$ templated-GaN(0001) while it transforms from the cubic phase to mixture of cubic and hexagonal phases on MBE-La$_2$O$_3$ templated-GaN(0001) when the film is thicker than 15 nm. Hexagonal La$_2$O$_3$ is more thermodynamically stable than cubic bixbyite La$_2$O$_3$; the stabilization of cubic ALD-La$_2$O$_3$ on ALD-Er$_2$O$_3$ templated-GaN(0001) can be attributed to the use of the cubic ALD-Er$_2$O$_3$ template and relatively low growth temperature. Analogies are presented for the In$_2$O$_3$ system, which has similar cubic bixbyite and hexagonal structures as La$_2$O$_3$, except the phases are reversed in In$_2$O$_3$. We calculate the surface energy of hexagonal In$_2$O$_3$ and compare the result with reported cubic In$_2$O$_3$ values to explore the relative contribution of bulk and surface energies in stabilizing the structure of thin crystalline films. Stabilization of thin cubic ALD-La$_2$O$_3$ on hexagonal MBE-La$_2$O$_3$ templated-GaN(0001) is attributed to likely surface energy differences between cubic and hexagonal La$_2$O$_3$.

Thin Films Division
Room A122-123 - Session TF-TuA

Emerging Applications for Thin Films

Moderators: Emily McGuinness, Georgia Institute of Technology, Jesse Jur, North Carolina State University

2:20pm **TF-TuA-1 Flexible Hybrid Electronics Process Maturation using Printed Inks**, *John D. Williams,* The Boeing Company   **INVITED**

Flexible hybrid electronics (FHE) are at the intersection of additive electronics and printed electronics. This is achieved through the utilization of additive methods on flexible and/or stretchable substrates. FHE leverages the low manufacturing cost of additive manufacturing due to fast processing time and low material waste. There are many applications that benefit from small low-cost sensor arrays and wireless networks, including new data collection devices on both manufacturing floors and aerospace systems to enable big data analytic capabilities.

In 2016, Boeing joined the NextFlex Manufacturing Innovation Institute established by U.S. Department of Defense Manufacturing Technology Program to support industry-wide improvements in the manufacturing

readiness level (MRL) of Flexible Hybrid Electronics. Boeing's Radio Frequency Manufacturing and Sensing Technologies (RFMaST) laboratory in Huntsville, AL is working in concert with a dozen companies and university partners on seven different NextFlex efforts to improve manufacturing processes and produce industrially relevant technology demonstrators.

The results to date, document an MRL 6 or higher capability for flexible hybrid electronics technologies. Current and previous work has improved the design interface for the nScrypt additive liquid dispense tool, and pushed the industrial supply chain for thinned Integrated Circuits. Additionally, we have documented repeatable printing processes multilayer passive elements on 2D and 3D surfaces, generated Flexible Antenna Array Technologies (FAAT) for GHz frequency applications, and developed in-situ monitoring approach for FHE print processes. Most recently, Boeing and its partners have shown a demonstrator for the Condition Monitoring Sensor Array (CMSA) project that combines a flexible battery, Bluetooth Low Energy, edge processing, and four sensors onto a single flex circuit. Over the next two years, our team will widen these efforts to include UAV flight applications, composite health monitoring, multilayer flexible PCBs and dozens of other sensing applications.

Coupling these achievements with materials characterization, in-situ process monitoring, and large area digital printing will provide Boeing and the US industrial base with MRL 7 small-scale production capabilities for the next generation of electronic sensors. Today, our company has the manufacturing readiness to vertically implement new FHE products and help establish the supply chain required for utilization in commercial and military products.

3:00pm TF-TuA-3 Large-Area Atmospheric Pressure Spatial ALD for Flexible OLED Display Applications, *C Frijters, J Smeltink, **Huib Heezen**, P Poodt,* SALDtech B.V., Netherlands

Atmospheric pressure Spatial ALD (sALD) is able to deliver high deposition rates while maintaining the advantages of conventional ALD, such as low defect density, high conformality and thickness uniformity. First industrial applications of Spatial ALD include passivation of c-Si solar cells and roll-to-roll manufacturing of flexible barrier foils. An emerging application for Spatial ALD is flat panel (OLED) displays. Examples include semiconducting and dielectric layers for use in thin-film transistors, and thin-film encapsulation for flexible OLED displays. As today's displays are fabricated using glass panels in the order of several square meters, a remaining challenge is the development of large-area Spatial ALD deposition technology that is able to combine high throughput with uniform performance across very large areas.

We are developing large-area Spatial ALD technology, and as a first step between the lab and the display fab, we have installed a large area Spatial ALD sheet-to-sheet tool which can handle up to 400x325 mm^2 sized substrates. With this tool we are able to deposit uniform films across a deposition width of 400 mm. The whole tool is operated under an atmospheric pressure but inert N$_2$ environment. The tool can be used to deposit a variety of materials using both thermal and plasma-enhanced Spatial ALD.

We will present the basic deposition performance of the tool in terms of thickness- and compositional uniformity. Large-area thickness non-uniformities of less than 1% are achieved for several oxide materials. Next, we will focus on two display-related applications: thin-film encapsulation of OLED devices, and high mobility InZnO and InGaZnO semiconductors for thin-film transistors. We will explain the requirements, the deposition process and the performance of the deposited films. Finally, the challenges in up-scaling Spatial ALD to plate sizes of 1.5 m and beyond will be discussed.

3:20pm TF-TuA-4 Printed Polymer Heat Sinks for High-Power, Flexible Electronics, *Katherine Burzynski,* University of Dayton; *N Glavin, E Heckman,* Air Force Research Laboratory; *C Muratore,* University of Dayton

Consumers and military personnel alike are demanding ubiquitous electronic devices which require enhanced flexibility and conformality of electronic materials and packaging, while maintaining device performance. Whether it be high-power devices for faster data speeds, such as fifth generation (5G) wireless communication technology or wearable sensors to facilitate the Internet of Things (IoT), the age of flexible, high performance electronic devices has begun. Managing the heat from flexible electronics is a fundamental challenge. Even on rigid substrates with significantly higher thermal conductivity than polymeric and other flexible substrates, the full potential of semiconducting materials is often thermally limited. The flexible gallium nitride (GaN) high electron mobility transistors (HEMTs) employed in this work are conventionally processed devices that can be released from their growth substrate and transferred to a variety of rigid and flexible substrates. Characterization of the GaN device behavior on the as-grown sapphire wafers (prior to transfer) provide a baseline for evaluation of the thermal performance of engineered interfaces and substrates. With conventional substrates, device performance (specifically, the saturation current) is reduced when the device is transferred to polymeric substrates. The thermal dissipation is further restricted due to the addition of an adhesive layer to the substrate. Thermal imaging of devices in operation reveals that the current passing through an as-grown GaN transistor on a sapphire wafer reaches the target operating temperature at approximately five times the power of the same device transferred to a flexible substrate. Printable, thermally conductive nanocomposites integrating 1D, 2D, and 3D forms of carbon in a flexible polymer matrix, as well as metal nanoparticles, were developed to maximize heat transfer from electronic devices. The thermal conductivity of the candidate substrate materials was measured experimentally to have more than a 900 percent increase in thermal conductivity (from 0.2 to 1.7 W/mK), while maintaining desirable mechanical properties. The performance of devices transferred to these novel flexible composite substrates was characterized and used in computational simulations to predict flexible substrate architectures that effectively promote point-to-volume heat transfer to further improve device performance. Additive manufacturing for engineered architectures of the flexible, thermally conductive substrate materials was demonstrated to substantially reduce the thermal limitation of high-power flexible electronics.

4:20pm TF-TuA-7 Selective Deposition by Fast-ALD of Transparent Conductive Metal Oxides for Application in Organic (opto)electronic Devices, *M Granados, D Munoz-Rojas,* LMGP, France; *c fontelaye, G Nonglaton, **Tony Maindron**,* CEA-LETI, France

Future's demands for new TCOs are driven by new developments made toward the realization of displays onto temperature-sensitive plastic substrates, transparent displays, as well as sensor arrays for bio-healthcare applications. With regard to the realization of TCOs, the Atomic Layer Deposition (ALD) technology is well adapted since it allows the realization of high quality materials at low temperatures, together with a digital control of thickness. In the meantime, multicomponent film growth can be reproducible and highly controllable even on large substrates, with the self-limiting reaction of ALD offering great benefits to many materials. The mainstream TCO deposited by ALD today is by far ZnO, as well as its derivatives (ZnO:Al; ZnO:Sn; ZnO: In…). Unfortunately, the ALD of ZnO suffers from two major drawbacks: (i) ALD is a very low throughput technique and (ii) ZnO-based materials are very sensitive to moisture (environmental and during microfabrication processes). Fast-ALD is an alternative new generation high-throughput process that will be approached in this work to make TCO films, to solve issue (i). In the meantime, Area Selective Deposition (ASD) strategies based on the use of vapor-deposited SAMS (Self Assembled Monolayers) will be investigated to selectively deposit the materials. Doing so, this work will leverage the use of intensive photolithography/etching processes of ZnO, to solve issue (ii). A future perspective of this work is to provide innovative fast-ASD deposited TCO-based TFT architectures.

4:40pm TF-TuA-8 Photocatalytic Antibacterial Activity of ALD Thin Films on Fibrous Materials, *Halil Akyildiz, S Diler,* Uludag University, Turkey

Semiconductor metal oxide thin film materials show photocatalytic properties, which can achieve various reactions for a variety of applications such as degradation of organic pollutants. Using similar mechanism, elimination of bacteria is also presented in the literature mostly on planar substrates. Since increase in the photocatalytic performance is expected with increasing surface area, thin films of ZnO and TiO$_2$ were deposited onto fibrous Nylon 66 surfaces via Atomic layer deposition (ALD) were tested for the elimination of bacteria. Tests were conducted at various thicknesses of ALD films for both types of materials. Formation and morphology of the films were investigated via electron microscope techniques TEM, FTIR, and SEM. Furthermore the structural analysis of the films were conducted via XRD and AFM while optical properties of the films were investigated via UV-Vis and PL spectrophotometers. Photocatalytic activity of the coated fiber materials was investigated by measuring methylene blue degradation. Antibacterial performance of the ALD films on fibers was tested using standard methods ISO 20645 and AATCC 100 against S. Aureus (ATCC 6538) and E. Coli (ATCC 35218) bacteria. As deposited ZnO samples showed better antibacterial performance compared to the TiO$_2$ films which is attributed the higher crystallinity of ZnO films.

5:00pm TF-TuA-9 A Kinetic and Thermodynamic Study of Aromatic Compounds Interacting with Metal-Organic Framework Thin Films, *J Shankwitz, D Speed, D Sinanan, Greg Szulczewski,* University of Alabama
Metal-organic frameworks (MOFs) are a class of highly porous materials that can be synthesized using a variety of inorganic nodes and organic linkers, which enables MOFs for emerging application in gas sensing, gas storage and gas separations. In this talk, we will describe the synthesis of MOF thin films of the UiO-66-X type, where X = H, NH_2 and NO_2 grown on Au-coated Si wafers and Au-coated quartz microbalance crystals using a vapor-assisted conversion method. The thin films were characterized by XPS, XRD, RAIRS and SEM. The thin films were activated by heating under high vacuum and exposed to a saturation pressure of benzene, toluene, ethyl benzene and xylene isomers (BTEX family) while recording the frequency change of the crystal at different temperatures. The Sauerbrey equation was used to convert the frequency change to accumulated mass, followed by calculation of the Henry's constant at each temperature for the BTEX family of compounds. The results show that $UiO-66-NO_2$ had the highest affinity for all of the aromatic compounds studied. In addition, the kinetics of adsorption have been modeling by a Fickian diffusion process to estimate the diffusion coefficients of the molecules in the MOFs.

5:20pm TF-TuA-10 Carbon's Role in Reducing Alumina's Resistivity Through Catalytic Carbon Nanotube Growth, *Berg Dodson, R Davis, R Vanfleet,* Brigham Young University
Alumina is used as a diffusion barrier in the catalytic synthesis of carbon nanotubes (CNTs). Prior to CNT growth, the alumina film is electrically insulating, but becomes conductive following a CNT growth process. Electrical resistance measurements show how this change in conductivity correlates principally with a carbon CVD process. Low resistances are observed even when no iron is present for the CNT growth and when deposited carbon layers are etched off. TEM (and SIMS) data demonstrate that both iron and carbon can diffuse into the alumina layer during processing. Additionally, I will discuss at how predicted doping levels compare to the observed conductivity of the samples.

5:40pm TF-TuA-11 Ferroelectricity in Hafnia-Zirconia based Thin Films: Characterization and Applications, *Vineetha Mukundan,* SUNY Polytechnic Institute*; S Consiglio, D Triyoso, K Tapily, R Clark, G Leusink,* TEL Technology Center, America, LLC*; J Hazra, K Beckmann, N Cady, A Diebold,* SUNY Polytechnic Institute, Albany
Hafnia-based materials have tremendous potential to replace perovskites in FeRAM applications due to their unique ferroelectric properties and potential for scalability [1]. Implementation of hafnia-based thin films in FeRAM has recently been demonstrated by Mikalojick *et al* [1]. With hafnia's high coercive field, enhanced endurance and memory window achieved by encapsulation with different electrodes, it is advantageous to also integrate it into a FET device [2]. For use in neuromorphic computing, Jerry *et al.*have employed electric-field controlled partial polarization switching in atomic layer deposited ferroelectric hafnia-zirconia films to demonstrate a FeFET based analog synapse [3]. Ferroelectricity in hafnia doped with Si was recently discovered by Böscke e*t al* [4] and it has been well established that the orthorhombic Pca21 is responsible for its ferroelectric properties. The factors leading to the formation and stabilization of this metastable phase are unclear. Structural modification and stabilization of different metastable states are being investigated by alloying hafnia with ZrO_2, doping with Si and Al, various annealing schemes and different processing schemes including different semiconductor substrates. We study the long range structure of hafnia-zirconia films by grazing incidence in-plane x-ray diffraction (GI-I-XRD) and local structure by extended x-ray absorption fine structure spectroscopy (EXAFS) along with polarization measurements to study their electrical properties. An important part for advancing these ultra-thin films for application as both FeRAM and NCFET devices necessitates studying capacitive stacks in the form of metal-insulator-metal (MIM) and metal-insulator-semiconductor (MIS) [5]. Further, we estimate the percentage content of the different phases including the non-centrosymmetric orthorhombic phases in these stacks varying in composition and thickness. With increasing zirconia content in these stacks, the monoclinic phase decreases and it exhibits anti-ferroelectric property. With increasing thicknesses, it is found that the monoclinic phase increases in content, which should give rise to a decrease in the polarization of these stacks. We observed no change in the structure with annealing after it has been encapsulated by the TiN electrode, even up to 1000°C suggesting the confinement plays an active role in its structural evolution. Additional studies are underway to understand the influence of processing conditions, electrical cycling, annealing temperature, types of

electrodes, and substrates on the structure and electrical properties of Hafnia-zirconia based thin films [6].

6:00pm TF-TuA-12 Atomic Layer Deposition-enabled Formation of Laser-Induced Graphene for Charged Membrane Applications, *David Bergsman, B Getachew, J Grossman,* Massachusetts Institute of Technology
Membrane-based processes are becoming increasingly popular for water treatment due to their relatively high energy efficiency and low cost compared to other treatment methods. However, the advantages of membranes are mitigated by the need for additional pre-treatment steps that are required to maintain their effective operation. The treatment and prevention of membrane fouling, in particular, constitutes a large fraction of typical membrane operational costs. One potential approach to combat fouling is to design conductive membrane coatings that can prevent the attachment and growth of biofoulants both electrostatically and via electrochemical generation of reactive oxygen species. Despite their potential, these conductive membrane coatings are often expensive, requiring additional chemicals and non-scalable methods to produce, e.g. carbon nanotube mats or other graphitic coatings deposited by vacuum filtration.

In this work, we explore the use of laser-induced graphene (LIG) for the creation of conductive ultrafiltration membranes. Porous polyethersulfone (PES) membranes are first coated in a thin layer of alumina using atomic layer deposition (ALD) before being irradiated with an infrared laser. We show that this alumina film, which can be scalably produced using spacial ALD, can localize LIG formation to the surface of the membrane, preventing the buried, un-lased areas of PES from melting and losing their porosity during the lasing process. This allows the top-most layer of the PES to be a conductive coating that can be used to charge the membrane surface and used to improve membrane performance (e.g. fouling mitigation). The formation of LIG is verified by scanning electron microscopy and Raman spectroscopy. The conductive layer is also shown to possesses relatively high conductivity, which is important for reducing power consumption in devices. Insight into the mechanism behind the improved stability to melting provided by ALD is provided by thermogravimetric analysis, differential scanning calorimetry, and Fourier-transform infrared spectroscopy. The effect of ALD film thickness and the use of sequential infiltration synthesis will also be explored. These insights are used to discuss the potential application of this approach to creating conductive coatings on other polymers using ALD-based approaches.

Energy Transition Focus Topic
Room A226 - Session TL+AS+SS+TF-TuA

Breakthroughs and Challenges in Applied Materials for Energy Transition (ALL INVITED SESSION) & Panel Discussion
Moderators: Jason Avila, U.S. Naval Research Laboratory, Devika Choudhury, Argonne National Laboratory

2:20pm TL+AS+SS+TF-TuA-1 Interface Science and Engineering for Energy-Water Systems, *Seth Darling,* Argonne National Laboratory   **INVITED**
Driven by climate change, population growth, development, urbanization, and other factors, water crises represent the greatest global risk in the coming decades. Advances in materials represent a powerful tool to address many of these challenges. Understanding—and ultimately controlling—interfaces between materials and water are pivotal [1]. In this presentation, we will lay out the challenges and present several examples based on materials science strategies for addressing applications in water. In each instance, manipulation of interfacial properties provides novel functionality, ranging from selective transport to energy transduction to pollution mitigation.

[1] J. Appl. Phys. 124 (2018) 030901

3:00pm TL+AS+SS+TF-TuA-3 Atomic Dynamics of Noble Metal Surface in Gases Revealed by Time Resolved Environmental Transmission Electron Microscopy, *Seiji Takeda, N Kamiuchi, R Aso, H Yoshida, T Tamaoka,* Osaka University, Japan   **INVITED**
The surface of noble metals in gas has been extensively studied in the field of surface science. The surface has been investigated in both ultra high vacuum and various gases of high pressure and under various stimuli, for instance the illumination of intense light, the electric and/or magnetic field and the irradiation of charged particles. A microscopy study is potentially useful to provide us with the imaging data on the surface in real space and

time at the resolution that is available in a microscopy apparatus to use. Among various methodologies for microscopy, atomic resolution environmental transmission electron microscopy has advanced greatly in the time resolution recently, allowing us to explore the dynamic surface and to elucidate the mechanism of the dynamic phenomena that are related to various energy transition processes. We show recent our studies, including the self-activated surface dynamics of gold catalysts in reaction environments [1] and the unexpected gas (nitrogen) -solid (palladium) transition [2] that is occurring on the surface under a strong electrostatic field. We demonstrate that the surface dynamics that is associated with the energy transition processes needs to be visualized at atomic scale for understanding the electronic excitations behind the surface dynamics.

References

[1] N. Kamiuchi et al., Nat. Commun. **9** (2018) 2060.

[2] T. Tamaoka, R. Aso et al., Nanoscale (2019) .

4:20pm TL+AS+SS+TF-TuA-7 Totally Organic and Organic-Inorganic Hybrid Batteries, *Burak Esat,* Fatih University, Turkey, Rutgers University*; S Bahceci, S Akay,* Fatih University, Turkey*; A Momchilov,* Bulgarian Academy of Science, Bulgaria

We hereby represent novel polymers and reduced graphene oxide with pendant electro-active groups such as TEMPO and quinones.

The first example of polymers with pendant anode-active groups studied in our group is a polymethacrylate derivative carrying anthraquinone moieties (pMAntrq). This anthraquinone based anode-active material has proven to show a quite good reversible electrochemical reduction behavior in both aqueous and non-aqueous electrolytes in our studies. pMAntrq|1M LiClO$_4$ in EC:DEC=1:1|Li battery system has been constructed. The initial discharge capacity of the cell obtained was 151 mAh/g when cycled between 4.2 and 1.2V at 0.25C rate and 79.2 mAh/g when cycled between 4.0 and 1.5V at 0.3C rate during subsequent cycles.

This material was also used in an aqueous battery, pMAntrq |5M KOH aq.|LiMn$_2$O$_4$. Although an initial discharge capacity of 37.7 mAh/g was obtained, it deteriorated quickly due to the solubility of the reduced form of the polymer in this electrolyte system. This is the first reported example of such organic-inorganic hybrid battery.

An anode material based on reduced graphene oxide (RGO) functionalized with anthraquinone is also investigated and a battery against Li metal revealed a quite reversible capacity of 200 mAh/g based on the weight of electro-active anthraquinone moieties when cycled between 3.2 and 1.8 V at 0.3C rate. The energy density was found to be around 450 mWh/g.

We have also synthesized and characterized polyacetylene polymers with pendant TEMPO radicals which are electrochemically oxidizable in a reversible manner at around 3.5-3.6V vs. Li. These materials have been proven to be cathode-active materials for rechargeable batteries. We have demonstrated that a mixture of Tempo radical polymer with LiMn$_2$O$_4$ (1:1) can be used as a hybrid cathode material. Typically, this polymer may be expected to act as a polymeric electro-active binder and a stability improver for the inorganic cathode-active material.

Studies toward construction of all organic batteries using these anode and cathode materials are currently in progress.

4:40pm TL+AS+SS+TF-TuA-8 Electrochemical Strategies for Designing Interfaces of Battery Materials, *Betar Gallant,* Massachusetts Institute of Technology **INVITED**

Future generations of energy-storage devices require advances beyond state-of-the-art materials and redox systems. Rechargeable batteries, specifically today's Li-ion batteries, have largely been dominated by transition metal oxide cathodes; advanced conversion systems with higher theoretical energy densities, such as Li-S and Li-O$_2$, have received significant attention as "beyond Li-ion" batteries, but have their own challenges and limitations. Looking at the periodic table invites one to wonder, "Is there more beyond sulfur and O$_2$?" This talk will focus on challenges and opportunities related to a different chemical family: fluorine, or more specifically, active fluoride. Fluoride-containing additives, electrolytes, solid electrolyte interphases (SEI), and intercalation materials represent a recurring motif in many proposed next-generation battery chemistries, but current understanding of the behavior of fluorinated interfaces and materials remains largely phenomenological. In addition, controlling the incorporation of fluoride into materials still remains a major challenge owing to safety issues of fluorine and the intransigence of fluoride-containing precursors, hindering design in this space.

In this talk, I describe our group's exploration of several applications where fluoride-forming reactions can be harnessed and tailored for benefit in advanced batteries. First, I describe our efforts to develop high-energy density redox systems based on the electrochemical reduction of fluorinated gases. We show that fundamental knowledge and the experimental framework developed in the field of Li-O$_2$ batteries in recent years can be successfully translated to the development of new gas-to-solid conversion reactions with high energy densities. Next, I will discuss the opportunities presented by the ability to generate fluoride *in situ* in working batteries from these reactions, creating new possibilities to fluorinate interfaces in tailorable and precise ways. I will present our findings relevant to two examples where fluoride has been suggested to play a critical and enabling role: Li anode interfaces, and oxyfluoride-based intercalation cathodes. Using our gas-based fluoridation architecture, we explore the fundamental role that fluoride plays in each of these applications. Finally, I will highlight future challenges and opportunities in the characterization of fluoridated materials.

Vacuum Technology Division
Room A213 - Session VT-TuA

Advanced Applications of Vacuum Technology
Moderators: Julia Scherschligt, NIST, Alan Van Drie, TAE Technologies

2:20pm VT-TuA-1 Single Atom and Single Electron Transistors for Quantum Technologies, *Richard Silver,* X Wang, R Kashid, J Wyrick, P Namboodiri, K Liu, M Stewart, G Bryant, National Institute of Standards and Technology (NIST) **INVITED**

Atomically precise fabrication has an important role to play in developing atom-based electronic devices for use in quantum information processing, quantum materials research and quantum sensing. Atom by atom fabrication has the potential to enable precise control over tunnel coupling, exchange coupling, on-site charging energies, and other key properties of basic devices needed for solid state quantum computing and analog quantum simulation. Using hydrogen-based scanning probe lithography we deterministically place individual dopant atoms with atomically aligned contacts and gates to build single electron transistors and single or few atom transistors.

We have developed robust lithography, device relocation, and contact processes that enable routine electrical measurement of atomically precise devices with an emphasis on minimizing process-induced dopant movement. Our low temperature palladium silicide contact process provides low-resistance ohmic contacts with yield better than 98%. Fabrication at the atomic scale requires exceptional vacuum and sample cleanliness. Our STM and sample preparation vacuum systems operate in the low 1×10^{-11} torr regime and we are implementing several hardware upgrades to achieve $< 10^{-12}$ torr vacuum.

This presentation will cover the design, fabrication, and characterization of multiple STM patterned single electron transistors that demonstrate stable coulomb blockade oscillations. We will report measurements of the electronic properties and tunnel coupling in single electron transistors where the tunnel gap is varied at the dimer row scale. Shrinking single electron transistors to the atomic limit, we demonstrate single dopant atom and few dopant cluster devices - essential building blocks in silicon-based donor dot qubits and proposed solid state analog quantum simulators. This presentation will include spectroscopic transport measurements and modeling of atomically precise single and few atom transistors.

3:00pm VT-TuA-3 Turbomolecular Pump for Achieving Ultra-high Vacuum in a High-power Proton Accelerator Vacuum System, *Junichiro Kamiya,* M Kinsho, Japan Atomic Energy Agency, Japan*; N Ogiwara,* KEK, Japan*; M Sakurai, T Mabuchi,* Osaka Vacuum, Ltd., Japan*; K Wada,* Tokyo Electronics Co., Ltd., Japan

Challenges for achieving an ultrahigh vacuum (UHV) region in J-PARC 3 GeV rapid cycling synchrotron (RCS), which produces proton beam with 1 MW power, come from the large static and dynamic outgassing. In the RCS vacuum system, turbomolecular pumps (TMP) have been used as main pump because it can evacuate such continuous and additional outgassing with a large pumping speed in the wide pressure range. TMP also has the advantage of not causing pressure instabilities like ion pumps. The more than 10 years operation of the RCS vacuum system showed that the UHV was rapidly obtained from the atmospheric pressure. It was also shown that the large additional outgassing during the high-power beam operation

was promptly evacuated by the TMP due to its constant pumping speed in the wide pressure rage. The future operation with more high-beam power requires the vacuum system for the lower pressure region. The pumping speed and compression ratio of the standard TMP is limited by the rotational speed of the rotor. We have developed a TMP with the rotor of titanium alloy, which have much higher mechanical strength than aluminum alloy for the normal rotter. When the rotational speed increase by a factor of 1.3, the pumping speed and compression ratio increase by a factor of 1.3 and 12.5, respectively. The increase of the compression ratio is especially effective for hydrogen, which is the main outgas component in the UHV region. Challenges in the development comes from the difficulty of the machining performance and the weightiness of the titanium alloy comparing with the aluminum alloy. We report the signification and the status of the development of the TMP with titanium alloy.

3:20pm **VT-TuA-4 US Contributions to ITER Vacuum Auxiliary System**, *Charles Smith*, Us Iter
This paper gives an overview of the ITER Tokamak Vacuum Auxiliary System (VAS) with a focus on the design challenges, solutions, and validation unique to a reactor-scale fusion vacuum system.

US ITER, the United States Domestic Agency for US contributions to the ITER project, is responsible for the final design, procurement, and acceptance testing for the Vacuum Auxiliary System (VAS) to be used in support of over 5000 clients of the ITER machine. The VAS system consists of more than six kilometers of pipework used in the vacuum roughing headers, more than 100 high-vacuum stations to support specific plant needs, and the Service Vacuum System (SVS) which is used to connect the roughing system to the end-use clients. VAS is a key element to the world's first vacuum system rated for a licensed nuclear fusion facility.

ITER received a nuclear construction authorization decree from the French Ministry of Environment in 2012, as its goal is to demonstrate the feasibility of fusion energy and produce a reactor-scale deuterium/tritium fueled plasma. ITER's VAS will utilize ASME B31.3 piping with a minimum schedule 10 wall thickness. In most large vacuum systems, commercially available vacuum fittings, flanges, and other standard components are designed around tubing. The requirement for schedule 10 piping and B31.3 design criteria has resulted in US ITER designing and certifying the components as opposed to procuring commercial off-the-shelf (COTS) items. These components must then be integrated into the overall VAS system in a way that meets all seismic and safety requirements needed to maintain tritium confinement. In addition to developing safety-critical double-gasket vacuum flanges, the certification of standard CF flanges to B31.3 has been required.

The VAS system's interfaces and location through the tokamak building have created another set of challenges to the use of standard vacuum equipment. The tokamak building will be subjected to radiation and high magnetic fields during plasma operations. The proximity of vacuum systems to high power RF systems and tritium containment are all design inputs for VAS design. The SVS portion of VAS, in addition to its role of interfacing between clients and the roughing header, acts as an integral part of plant safety systems. The interspaces between the gaskets on safety related flanges are actively monitored by SVS to detect any change in pressure which could indicate a leak. As an example, the SVS is used to verify the integrity of diamond vacuum windows used in high-powered RF plasma heating systems.

The work detailed in this paper, shall illustrate the progress being made to reach the first plasma milestone.

4:20pm **VT-TuA-7 Importance of Advanced Vacuum Technology to the Present Thin Film Photovoltaics Industry**, *Timothy Gessert*, Gessert Consulting, LLC **INVITED**
World use of photovoltaic (PV) solar electricity has been increasing at an average annual exponential growth rate >35% since about 2000. Not surprisingly, during this same time, the percentage of US-consumed energy (~100 Quadrillion BTUs total) derived from PV has increased from ~0.003% in 2004, to >1% at the end of 2018. Indeed, if these trends continue, PV could produce >50% of all energy consumed in the US by as early as 2030. Combining this with the rapidly decreasing energy costs for large grid-tied PV systems (presently <2.5¢/kWh for long-term power purchase agreements) largely explains why PV-derived energy is – even now – a main source of *new* US and world energy. Although the majority of this PV-derived energy is presently generated by crystalline-based Si module technologies, because of combined efficiency, production, cost, and other advantages, an ever-increasing amount of PV energy is being produced from polycrystalline thin-film (TF) materials. These TF PV technologies owe

much of their rapidly advancing success to improved understanding in related materials synthesis, while applying these advancements to industry, in turn, has relied on design innovations of related vacuum-process equipment. This talk will briefly overview the present state of TF PV technologies, taking into consideration both the present dominance of crystalline Si PV, and evolving trends in TF PV. Several examples where keen understanding of vacuum processes in laboratory-scale devices has fostered successful utilization of advanced vacuum technology in the commercial TF PV industry will be presented. The talk will also suggest some areas where further advancements in vacuum-process and equipment innovation could yield potentially even lower-cost TF PV technologies.

5:00pm **VT-TuA-9 Enabling Hydrogen as an Energy Carrier through Analytical Electron Microscopy**, *David Cullen, K More,* Oak Ridge National Laboratory **INVITED**
Hydrogen is an important energy carrier which can be produced from renewable or intermittent energy sources for use in markets ranging from metal refining to transportation. Polymer electrolyte membrane fuel cells (PEMFCs) are a key technology for converting the chemical potential energy of hydrogen in electrical energy and driving down the cost of these systems is important towards enabling a hydrogen economy. At the heart of the matter is the membrane electron assembly (MEA), which consists of an anode and cathode separated by a proton-conducting membrane. Pt-based catalysts are typically used to drive the sluggish oxygen reduction reaction (ORR) at the cathode and are responsible for much of the cost of the MEA. Near term approaches to reduce Pt loading and hence cost involve the development of Pt-alloy catalysts which show exceptionally high mass activity but require improvements in durability. Long-term solutions will require the development of stable platinum group metal-free (PGM-free) catalysts, with current best-in-class candidates being derived from transition metal doped metal organic frameworks (MOFs). In both approaches, accelerated materials discovery and development is required to keep pace with increasing market and performance demands.

To this end, scanning transmission electron microscopy (STEM) has been employed to study MEAs from the atomic to micron scale. The application of atomic-resolution spectroscopic techniques to assess the quality and durability of Pt-alloy and PGM-free electrocatalysts will be presented. At a wider scale, the impact of particle dispersion, hierarchal porosity and proton-conducting ionomer distribution will be linked to electrochemical performance limitations through quantitative STEM imaging and energy dispersive X-ray spectroscopy (EDS). Finally, the movement of dissolved species across the membrane and gaseous diffusion layer will be explored to explain durability losses during fuel cell cycling. The synergy between electron microscopy and other characterization techniques such as X-ray photoelectron spectroscopy, X-ray absorption spectroscopy, and Mossbauer spectroscopy will also be discussed

5:40pm **VT-TuA-11 Defect Manipulation to Control Energy Processes in Electronic Materials**, *Leonard Brillson,* The Ohio State University **INVITED**
The control of native point defects in advanced electronic materials and device architectures is critical to a wide array of energy intensive processes including generation, transport, storage, switching, and display. AVS research in electronic materials surfaces and interfaces at the nanoscale has played an important role in this arena. Defect control of transparent conducting oxides such as ZnO for smart windows and heads-up displays have revealed how to create homojunctions with high electron mobility 2-dimensional interfaces.[1] Surface/interface techniques enable identification and control of native defects in Ga_2O_3,[2] outlooked for RF power amplification and power switching. Defect control has enabled creation of 2-dimensional hole gases at $LaAlO_3/SrTiO_3$ interfaces, opening an avenue to new architectures for complex oxide electronics. Depth-resolved defect measurements in V_2O_5 battery electrode films reveal how lithiation introduces degenerate doping and secondary phase formation, integral to ion and charge transport inside next-generation nanoscale battery architectures.[3] Direct, localized optical, and electrical measurements of ZnO nanowires – envisioned for wearable electronics and displays - show that native point defects inside the nanowire bulk and created at metal-semiconductor interfaces are electrically active[4,5] and play a dominant role

electronically, altering the doping, carrier density along the wire length, and the injection of charge into the wire.[6] Defects in all these materials can now be manipulated by ion beams, electric fields, remote oxygen plasmas, and nanoscale design, opening new avenues to control charge injection, transport, and storage.

1. G. M. Foster et al., "Direct Measurement of Defect and Dopant Abruptness at High Electron Mobility ZnO Homojunctions," Appl. Phys. Lett. **109**, 143506 (2016).

2. H. Gao et al., " Optical Signatures of Deep Level Defects in Ga_2O_3," Appl. Phys. Lett. **112**, 242102 (2018).

3. H. Lee et al., "Direct observation of a two-dimensional hole gas at oxide interfaces," Nature Materials **17**, 231-236 (2018).

4. W.T. Ruane et al., "Defect Segregation and Optical Emission In ZnO Nanowiresand Microwires," Nanoscale **8**, 7631-7637 (2016).

5. A. Jarjour et al., Single Metal Ohmic and Rectifying Contacts to ZnO Nanowires: A Defect Based Approach," Ann. Phys. (Berlin), **530**, 1700335 (2018).

6. J.W. Cox et al., "Defect Manipulation to Control ZnO Micro-/Nanowire-Metal Contacts," Nano Letters **18**, 6974 (2018). **DOI:** 10.1021/acs.nanolett.8b02892

2D Materials
Room Union Station AB - Session 2D-TuP

2D Poster Session

2D-TuP-1 Enhancement of Solid Solubility in 2D Alloys by Selective Orbital Coupling, *Bing Huang,* Beijing Computational Science Research Center, China

Solid solubility (SS) is one of the most important features of alloys, which is extremely difficult to be largely tuned in the entire alloy concentrations by external approaches. As a result, some alloys, which were supposed to have promising physical properties, turn out to be much less useful because of their poor SS, e.g., the case for monolayer BNC alloys. The unavoidable phase separation in BNC alloys, caused by the unstable C-B and C-N wrong-bonds, has severely restricted their promising optoelectronic applications. In this talk, a mechanism of selective orbital coupling between wrong-bond states and surface states mediated by the substrate has been proposed to stabilize the wrong-bonds and in turn significantly enhance the SS of BNC alloys. Surprisingly, we demonstrate that the miscibility temperature of BNC grown on some specific substrates can be largely reduced, accompanied by the appearance of well-ordered ground-states. Interestingly, the homogenous BNC with fully tunable band gaps between 0 and 6 eV can be achieved under a low growth temperature of 1000 K. Our discovery provides a general concept to enhance the SS in monolayer alloys by selective orbital coupling.

2D-TuP-2 Black Phosphorus and Endohedral-Graphene Hybrids for Novel Optoelectronic Devices, *M Min, Srishti Chugh, A Kaul,* University of North Texas

Among the various two-dimensional (2D) materials, graphene is a material of immense technological importance given its ballistic transport which provides opportunities for high-speed field-effect transistors (FETs). Other mono-elemental 2D materials such as black phosphorus (BP) provide a thickness-dependent, direct band gap ranging from ~ 0.3 eV in the bulk to ~1.5 eV in the monolayer limit. Here, in the first part of the work, we report on the integration of zero-dimensional materials with 2D graphene membranes to enhance the optoelectronic properties of the photodetectors. Quantum dot-graphene optoelectronic devices are discussed where mechanically exfoliated graphene flakes are used in a two-terminal device configuration. The zero-dimensional materials used in this work were cluster endohedral fullerenes, $Sc_3N@C_{80}$, and monometallic endohedral fullerene, $La@C_{82}$, based on their electron-accepting and electron-donating abilities, respectively. Temperature-dependent and wavelength-dependent optoelectronic properties of the 0D-2D graphene-based hybrids will be presented. In the second part of the work, we will also show the chemical exfoliation of BP to form optoelectronic devices with protecting layers to enhance the stability of the BP. Here, we present liquid exfoliation approaches to obtain BP by sonication in organic solvent such as 1-cyclohexyl-2-pyrrolidone (CHP), *N*-methyl-2-pyrrolidone (NMP) at ambient conditions. We compare the structural properties of black phosphorus through Raman Spectroscopy analysis, Photoluminescence (PL) and two-terminal electronic device measurements to demonstrate its enhanced device stability.

2D-TuP-3 Nitrogen-Doped Graphene on Cu(111): Edge-Guided Doping Process and Doping-Induced Variation of Local Work Function, *J Neilson, H Chinkezian, H Phirke, A Osei-Twumasi,* California State University, Northridge*; Y Li,* Peking University, China*; C Chichiri,* California State University, Northridge*; J Cho,* Myongji University, Korea*; K Palotás,* Hungarian Academy of Sciences, Hungary*; L Gan,* Peking University, China*; S Garrett, K Lau,* California State University, Northridge*; Li Gao,* California State University Northridge

The nitrogen-containing sole precursor azafullerene has been used for the synthesis of nitrogen-doped graphene on the Cu(111) surface. The synthesis process, doping properties, and doping-induced variation of local work function of graphene have been studied on the atomic scale by combing scanning tunneling microscopy/spectroscopy, X-ray photoelectron spectroscopy, and density functional theory calculations. Most nitrogen dopants are at the edges of graphene islands and the graphene domain boundaries with the pyridinic configuration. Graphitic nitrogen dopants arrange into curved lines within graphene islands after multiple growth cycles, which results from a doping process guided by the edges of graphene islands. The doping-induced variation of local work function of the graphene surface has been measured on the atomic scale by recording spatially resolved field emission resonances. We find that the local work function strongly depends on the atomic bonding configuration and concentration of nitrogen dopants. The local work function decreases for graphitic nitrogen doping but increases for pyridinic nitrogen doping. This work provides new atomic-scale insights into the process for incorporating nitrogen atoms into the graphene lattice as well as the correlations between the type of nitrogen doping and the variation of local work function.

2D-TuP-4 Vibrational Progression of a Single Hydrocarbon Molecule on Graphene and Hexagonal Boron Nitride, *Alexander Mehler, N Néel, J Halle,* Technische Universität Ilmenau, Germany*; M Bocquet,* École normale supérieure, PSL University, Sorbonne Université, CNRS, France*; J Kröger,* Technische Universität Ilmenau, Germany

Probing genuine molecular properties even after adsorption on a surface requires the efficient reduction of the molecule-surface hybridization. Two-dimensional materials, such as graphene, hexagonal Boron Nitride (hBN) and stackings thereof, are promising buffer layers to this end. Scanning tunneling microscopy and spectroscopy at low temperature is used to explore molecular orbitals and vibrational quanta of the hydrocarbon molecule DBP (Dibenzotetraphenylperiflanthen) on graphene and hBN with submolecular resolution. Independent of the metal substrate, Ir(111), Pt(111) and Ru(0001), vibrational progression in both DBP frontier orbitals is observed for graphene and hBN, albeit with different numbers of vibrational quanta involved. Density functional calculations unveil that symmetry matching of electronic and vibrational excitations supports the observation of vibrational progression. The lifetime of the vibronic levels can be tuned by the molecular environment of a single DBP as well as by using different kinds and numbers of buffer layers.

2D-TuP-5 Synthesis of Layered PdS₂ Film and Homo-junction Device Fabrication, *C Jong,* TSRI/NARL, Taiwan, Republic of China*; Y Yang,* NTNU, Taiwan, Republic of China*; M Le,* NTHU, Taiwan, Republic of China*; P Chen,* MUST, Taiwan, Republic of China*; Chien-Bao Lin, P Chiu, C Hsiao,* TIRI/NARL, Taiwan, Republic of China

Lots of TMDs materials with fantastic properties have been widely discovered for electrical and optical device application. In order to replace current Si-based device several challenges should be overcame, including the 2D synthesis and patterning technique; heterojunction control between TMDs to TMDs, TMDs to dielectric film and TMDs to metallic film, doping technique and so on. Among them, MoS_2 and WSe_2 have shown their excellent electron and hole mobility in NFET and PFET evaluation. For electronic and photonic applications, a material existing air-stable, high carrier mobility, high on/off ratio, as well as a tunable band gap is far more desirable. Recent theoretical and experimental data show some noble chalcogenides can also form layered structures with S or Se atoms, like PdS_2 and $PdSe_2$[1-3]. Each Pd atom can bond to four S or Se atoms, respectively. Puckered $PdSe_2$ exhibit a widely tunable band gap that varies from metallic (bulk) to ~1.3 eV (monolayer) and the field-effect transistors made from $PdSe_2$ reveal high electron field-effect mobility of ~158 cm²/Vs are presented [4]. Recently, Mahdi et al., [5] proposed a unique alternative to reduce contact resistance through the single material junction device scheme, that is, using a single material (PdS_2) in channel and S/D region. Monolayer PdS_2 was found to be semiconducting with a bandgap of 1.1 eV and became semi-metallic as bilayer. PdS_2 was also reported with a high electron mobility than MoS_2. However, not too much experimental works has been published yet in PdS_2 synthesis. To realize the reported device integration, the thickness control and sulfurization process are important. In our previous works [6-7], a possible approach in untra-thin and uniform 2D layer film synthesis was demonstrated combined with proposed ALE and sulfurization process.

In this study, the PdS_2 film synthesis and single material junction device fabrication will be performed. Pd film was sputtered onto SiO2/Si substrate for sulfurization. The PdS_2 film was obtained after sulfurization and the structure is verified [8]. The XRD, XPS and Raman spectrum are measured for microstructure evaluation. A lift -off process in channel and source and drain patterning was achieved. With the help of anisotropic etch in Pd film thin down, the desired thickness and wafer scale flatness was controlled. The etched thickness and surface roughness are monitored by AFM. Followed by the etch process, the etched samples were sulfurized for PdS_2 formation. After the sulfurization process the homo-junction device using a single material was fabricated and the electrical properties was characterization.

2D-TuP-6 NanoESCA III: Momentum Microscopy on 2D Materials, *Marten Patt,* Scienta Omicron GmbH, Germany; *N Weber, M Escher, T Kuehn, M Merkel,* FOCUS GmbH, Germany

New 2D material classes including graphene, transition metal dichalcogenides (TMDCs) or 2D heterostructures based on TMDCs or graphene are nowadays a promising candidate to be used in future electronic devices. They are chemically versatile and thus predestined to tune their electronic structure for various applications (e.g. electronic, optoelectronic and spintronic).

To examine these materials, a fast band structure mapping in combination with a high lateral resolution in real-space and live view microscopy becomes essential. The band structure mapping is used to understand the electronic structure of new material combinations, while the real-space microscopy is needed to localize the crystals on the specimen, especially if they were produced by mechanical exfoliation or intercalation techniques [1].

The NanoESCA microscope allows to easily switch between the imaging of the real- and the momentum- space of photoemission electrons and is therefore predestined to examine novel 2D materials. In the so-called momentum microscopy mode, the NanoESCA acquires the band structure from a microscopic sample region of interest, which was beforehand defined in real-space.

We will show recent band-structure measurements of several TMDCs (see e.g. [2]) acquired with the instrument and discuss the latest technical improvements of the momentum microscopy technique with respect to 2D material characterization.

References

[1] Mattia Cattelan and Neil Fox, NanoMaterials 2018, 8, 284; doi:10.3390/nano8050284

[2] Ming-Wie Chen et al., npj 2D Materials and Applications (2018) 2:2 ; doi:10.1038/s41699-017-0047-x

2D-TuP-7 Shifting of Electronic States of Meso-tetrakis(pentafluorophenyl) Porphyrin Self-assembled Monolayers Due to Internal Molecular Structure, *Jose Ortiz-Garcia, M Wolf, M Guberman-Pfeffer, J Gascon, D Thuita, C Brückner, R Quardokus,* University of Connecticut

Meso-tetrakis(pentafluorophenyl) porphyrin (T^{F}PP) self-assembled islands were imaged on Au (111) using an ultra-high vacuum scanning tunneling microscope (LT-UHV STM). A pulse-solenoid valve was used to deposit submonolayer coverage of T^{F}PP porphyrins on Au(111). A range of bias voltages were used to image occupied and unoccupied electronic states of T^{F}PP. Density functional theory (DFT) was used to calculate the spread in energy levels of both occupied and unoccupied molecular orbitals. We found that the spacing of the energy levels of electronic states shifts depending on the presence and location of hydrogens bonded to the inner nitrogens (locants 21-24).

2D-TuP-8 Reproducibility and Replicability in Science and Engineering: A Report by the National Academies, *T Winters, Jennifer Heimberg,* National Academies of Sciences, Engineering, and Medicine

One of the pathways by which scientists confirm the validity of a new finding or discovery is by repeating the research that produced it. When a scientific effort fails to independently confirm the computations or results of a previous study, some argue that the observed inconsistency may be an important precursor to new discovery while others fear it may be a symptom of a lack of rigor in science. When a newly reported scientific study has far-reaching implications for science or a major, potential impact on the public, the question of its reliability takes on heightened importance. Concerns over reproducibility and replicability have been expressed in both scientific and popular media.

As these concerns increased in recent years, Congress directed the National Science Foundation to contract with the National Academies of Science, Engineering, and Medicine to undertake a study to assess reproducibility and replicability in scientific and engineering research and to provide findings and recommendations for improving rigor and transparency in research.

The committee appointed by the National Academies to carry out this task included individuals representing a wide range of expertise: methodology and statistics, philosophy of science, science communication, behavioral and social sciences, earth and life sciences, physical sciences, computational science, engineering, academic leadership, journal editors, and industry expertise in quality control. Individuals with expertise

pertaining to reproducibility and replicability of research results across a variety of fields were included as well.

This poster will present the committee's approach to the task and highlights from its findings, conclusions, and recommendations related to factors that influence reproducibility, sources of replicability, strategies for supporting reproducibility and replicability, and how reproducibility and replicability fit into the broader framework of scientific quality and rigor.

2D-TuP-9 Structural and Electronic Properties of Native Point Defects in MoTe$_2$, *Ziling Deng, S Mueller, W Windl, J Gupta,* The Ohio State University

We performed density functional theory(DFT) calculation to studied the structural and electronic properties of native point defects in MoTe$_2$. Various kinds of defects, e.g., vacancies, antisites with different charge states will be considered. With DFT, we will predict the constitutional defects with the lowest formation energies for all systems in Mo-rich, Te-rich and stoichiometric conditions as well as their dominated charge states. Additionally, the resulting output of our theoretical atomic scale model based on DFT-calculation will be used to simulate Scanning Tunneling Microscopy [https://en.wikipedia.org/wiki/Scanning_tunneling_microscope](STM) images to allow for comparison with experimental STM images. This study will provide an effective method to study the defects in MoTe$_2$ systems, with the comparison with experiments, the results will shed new light on the defect studying in MoTe$_2$.

MoTe2, a two-dimensional(2D) layered material has recently attracted much attention due to its excellent electronic properties. Intrinsic defects are commonly observed in MoTe2 growth, which would have a significant impact on the physical, optical, thermal, and electrical properties of the material. However, studying the atomic structure of intrinsic defects in this 2D materials is difficult since they damage quickly under the intense electron irradiation in TEM. To overcome this, we have performed a joint study between STM measurements and DFT calculations to identify the atomic structure and electronic nature of native point defects in MoTe2. We constructed analytical model from DFT and studied the structural and electronic properties of those defects. In order to understand the formation of defects and their atom-scale dynamics in MoTe2, we will use DFT to predict the constitutional defects with the lowest formation energies as well as their dominated charge states in Mo-rich, Te-rich and stoichiometric conditions to determine the necessary chemical potentials for all systems of MoTe2. Additionally, theoretically simulated STM images generated by density functional theory were used to compare with experimental STM data to enable us to assign structure of a number of defects observed during experiments.

This study provides an effective method to study the defects in MoTe$_2$ systems by presenting results for the energetics of native point defects in MoTe2. Base on our calculation, the formation energies and charged states of the vacancies and antisites will be determined, moreover, the simulated simulated STM images allow for the identification of structural defects of MoTe2 observed in the experiment.

2D-TuP-10 A Role of Au Atoms on Oxidized Black Phosphorus; Study using Scanning Photoelectron Microscopy, *D Kim, H Choi, Jaeyoon Baik,* Pohang Accelerator Laboratory, Republic of Korea

We investigated oxygen reduction of black phosphorus(BP) using scanning photoemission electron spectroscopy. In spite of many effort of realizing ultra-thin film transistor of 2-dimensional atomic material of BP, inherent limitation in the transfer method such as oxidation, has not allowed application in real devices. Therefore, it is necessary to study the development of methods to prevent oxidation or reduction through the post-processing. However, such studies are very important to observe chemical composition changes using XPS, but there are other limitations in investigating based on flakes of the BP in um-size using general XPS . In this work, we observed Au atom, which deposited on BP, could play a role of catalyst reducing the oxidation on the top layers of BP. Using SPEM analysis method with 200nm spatial resolution, we verified the reduction mechanism of the um-size flake BP. As a result, we could observe that oxygen in the BP oxide disappeared through the Au atoms. Therefore, this can be applied to BP's Oxide Removal and Thickness Control technology and is expected to provide useful information for future application of the element.

References

[1] Zehua Hu et al., Nanoscale (2018) 10, 21575 ; doi:10.1039/c8nr07395c.

[2] Hao Huang et al., npj 2D Materials and Applications (2017) 1:20 ; doi:10.1038/s41699-017-0022-6.

2D-TuP-11 Growth and Electrical, Nano-Optical Characterization of semiconducting MoS₂/WS₂ in-plane Heterostructures, *Sourav Garg, P Kung, S Kim,* The University of Alabama*; A Krayev,* Horiba Scientific, Novato

In-plane heterojunctions of atomic-thick (2D) semiconductors (MoS_2/WS_2) are novel structures that can potentially pave the way for efficient ultrathin and flexible optoelectronics, such as light sources and photovoltaics. Such heterostructures (HS) are very rare and not much is known about their characteristics. They can only be achieved through a synthetic growth process such as chemical vapor deposition (CVD). This is unlike vertical heterostructures, for which the materials can be mechanically stacked one layer on top of the other. The CVD growth of in-plane heterostructure is a thermodynamically driven process and presents a number of challenges to control the vapor pressure of the precursors. Additionally, new analytical tools need to be developed in order to gain access to and understand the physical properties of these HS.

Here, we report a one-step CVD growth of monolayer (1 nm) thick MoS_2/WS_2 in-plane heterostructures. We have characterized their morphological and optical properties using micro-Raman and photoluminescence spectroscopy. Kelvin probe force microscope was used to extract the surface potential profile across the MoS_2/WS_2 heterojunction boundary, which was then used to gain access to fundamental semiconductor heterostructure parameters such as depletion layer width and built-in field across the MoS_2-WS_2 interface. In-addition more rigorous study of heterostructures interface by tip enhanced PL (TEPL) had been performed.

2D-TuP-12 Identifying Key Parameters for the Uniformity of Nanopatterning on 2D Highly Oriented Pyrolytic Graphite Layers, *James Su,* Taiwan Instrument Research Institute, National Applied Research Laboratories, Taiwan, Republic of China

Demonstrations of local anodic oxidation nanopatterning on 2D highly oriented pyrolytic graphite (HOPG) layers were performed by adopting a conductive atomic force microscope (CAFM). Parameters such as environmental humidity, temperature, tip bias, tip velocity, set-point and apex curvature were evaluated for the uniformity of nanopatterning on HOPG. The patterns created by this method varied as the tip bias increases up to 6.8 V or tip force over 96 nN.

Biomaterial Interfaces Division
Room Union Station AB - Session BI-TuP

Biomaterial Interfaces Posters/Flash Session

BI-TuP-1 Combining Geometry of Folded Paper with Liquid-Infused Polymer Surfaces to Concentrate and Localize Complex Solutions, *Daniel Regan, C Lilly, A Weigang, L White, E LeClair, C Howell,* University of Maine

Diagnostic devices which can provide information relevant to health and safety on-site without the requirement for a fully-equipped laboratory are of great interest for medical, military, and disaster relief applications. However, most research and development work on such devices focuses on detection rather than the preliminary sample handling and preparation. In this work, we demonstrate how low-cost paper materials coated with liquid-infused polymer surfaces can be fabricated and folded to produce shapes which result in functional sample preparation; namely, the simultaneous localization and concentration of a liquid sample. Surfaces were fabricated by infusing commercially-available silicone-release paper with a compatible polydimethylsiloxane oil to create a liquid overlayer. Adhesion tests with *Escherichia coli* on these surfaces showed no remaining bacterial cells after exposure to a sliding droplet containing 10^8 cells/mL, compared to the macro- and micro-scale bacterial residues remaining on the controls. Folding of the paper substrates into several 3D engineered arrays enabled clean separation of dye-containing liquids into discreet, pre-defined localized points, whereas the use of uninfused controls resulted in the retention of dye on the sides. When used with a bacterial solution, the combined features of low bacterial adhesion and liquid separation via geometry resulted in the localization of a solution of *E. coli* and simultaneous concentration by 23.1 (±6.5) times, compared to only 6.78 (±3.6) times for uninfused controls (P= 0.004). This work demonstrates the potential of paper-based materials with liquid-infused polymer surfaces for the manipulation and handling of complex samples which may help in the future design of on-site diagnostics.

BI-TuP-2 Photoinduced Amphiphilic Zwitterionic Carboxybetaine Polymer Coatings with Marine Antifouling Properties, *Florian Victor Koschitzki, A Rosenhahn,* Ruhr-University Bochum, Germany

Due to ecological and economic consequences, the prevention of undesirable settlement of biomass on surfaces in the marine environment is of key interest. Thus, research on effective surface-modification and application of antifouling coatings is demanded. Zwitterion containing hydrogels with stable hydration have shown promising results for ultra-low fouling materials. The spectrum of application ranges from protein and plasma resistance[1], studies of bacterial adhesion[2], biomedical purposes[3] to settlement experiments with marine biofoulers.[4] Although understanding the influence of anionic and cationic groups, charge distribution and charge neutrality can be discussed using self-assembled monolayers[5] (SAM), zwitterionic moieties must eventually be applied in the form of polymer coatings for technical purposes. To combine mechanical and antifouling properties of several materials, amphiphilic polymers are increasingly being explored.[6] To demonstrate the advantage of random copolymers over homopolymers regarding antifouling [7], polymer coatings with varying hydrophilicity were prepared. Therefore, a carboxybetaine methacrylate was incorporated into a hydrophobic matrix via «grafting to» photoinduced radical polymerisation. Monomer solutions were applied on glass substrates, functionalized by 3-trimethoxysilyl propyl methacrylate. The samples were characterized by AFM, CA, IR and SEM. For further investigations concerning the antifouling properties, microfluidic experiments with the diatom genus *Navicula perminuta* were carried out. The results display severe enhancement of fouling prevention at small zwitterionic content of only (5 wt%).

[1] – W. Yang, H. Xue, W. Li, J. Zhang, S. Jiang, Langmuir **2009**, *25*, 11911-11916.

[2] – G. Cheng, G. Z. Li, H. Xue, S. F. Chen, J. D. Bryers, S. Y. Jiang, Biomaterials **2009**, *30*, 5234-5240.

[3] – L. Zhang, Z. Cao, T. Bai, L. Carr, J.-R. Ella-Menye, C. Irvin, B. D. Ratner, S. Jiang, Nat Biotech **2013**, *31*, 553-556.

[4] – S. Y. Jiang, Z. Cao, Advanced Materials **2009**, *21*, 1-13.

[5] – S. Bauer, J.A. Finlay, I. Thome, K. Nolte, S. C. Franco, E. Ralston, G. E. Swain, A. S. Clare, and A.

Rosenhahn, Langmuir **2016**, *32*, 5663.

[6] – C. Ventura, A. J. Guerin, O. El-Zubir, A. J. Ruiz-Sanchez, L. I. Dixon, K. J. Reynolds, M. L. Dale, J. Ferguson, A. Houlton, B. R. Horrocks, A. S. Clare, D. A. Fulton, Biofouling **2017**, *33*, 892-903.

[7] - A. L. Hook, C.-Y. Chang, J. Yang, J. Luckett, A. Cockayne, S. Atkinson, Y. Mei, R. Bayston, D.J. Irvine, R. Langer *et al.*, Nature biotechnology **2012**, *30*, 868.

BI-TuP-3 Peptide sequences with Ultra-Low Nonspecific Protein Adsorption and Resistance Against Marine Biofouling, *Cindy Denise Beyer, M Reback,* Ruhr-University Bochum, Germany*; J Finlay,* Newcastle University, UK*; S Gopal,* Ruhr-University Bochum, Germany*; A Clare,* Newcastle University, UK*; L Schäfer, N Metzler-Nolte, A Rosenhahn,* Ruhr-University Bochum, Germany

Efficient fouling-release coatings frequently consist of a silicone network modified by additional chemical compounds that reduce adhesion of marine fouling organisms. We explored the fouling-release potential of several oligopeptide sequences and tested them as self-assembled monolayers. The design motif of the peptide sequences considered inherent properties such as conformation and hydrophilicity. Different sequences were synthesized, and well-hydrated peptide coatings were assembled. All surfaces were characterized with respect to their wettability, layer thickness, and surface structure by contact angle goniometry, spectroscopic ellipsometry, and FTIR-spectroscopy. Protein adsorption of fibrinogen and lysozyme was very low on the oligopeptide SAMs. The assembled monolayers show remarkable fouling-release behavior against Navicula perminuta which was tested in a microfluidic assay. Also, the settlement of zoospores of the green algae Ulva linza was investigated. Besides the good antifouling behavior, the inclusion of Aib and D amino acids helped to create peptides that were 100% resistant against enzymatic degradation by trypsin. Due to their diversity, easy synthesis and biocompatibility, peptides could be used as active, hydrophilic components in fouling-release technologies.

BI-TuP-4 The Effect of Surface Charge and Film Hydration on the Antifouling Performance of Polyelectrolyte Multilayers, *Thuvarakhan Gnanasampanthan,* Ruhr University Bochum, Germany*; A Rosenhahn,* Ruhr-University Bochum, Germany

Marine biofouling, which describes the accumulation of animals, plants, and microorganisms on surfaces in the aqueous environment, causes tremendous economic and ecological concerns.[1][2] Since commonly used antifouling coatings were banned and restricted because of their toxicity, new non–toxic alternatives must be developed and established.[3] Polyelectrolyte multilayers are widely applied when protein resistance[4] and antibacterial properties[5] are required and provide a suitable platform to test the antifouling capabilities of promising compounds such as alginic acid (AA)[6], chitosan (CH)[7] and polyethylenimine (PEI)[8]. The physicochemical and marine antifouling properties of chemically cross-linked alginic acid/chitosan- and alginic acid/polyethylenimine-multilayers where investigated with a focus on the influence of surface charge and film hydration. Surface plasmon resonance spectroscopy revealed that all multilayers exhibit high protein resistance. Both, positively and negatively terminated AA/PEI–multilayers did not show any differences regarding the amount of irreversibly bound protein, neither for negatively charged nor for positively charged proteins. However, for the AA/CH–coatings the charge of the terminating layer had an effect on the protein adsorption. Besides, the type of polymer within the multilayers had a strong influence on the protein resistance. Microfluidic diatom accumulation assays[9] demonstrated that all multilayers present relatively low diatom settlement and that especially for AA/PEI–multilayers the charge of the terminating layer has a significant influence on the attachment.

References

[1] M. P. Schultz, *Biofouling* **2007**, *23*, 331.

[2] I. B. Beech, J. Sunner, *Curr. Opin. Biotechnol.* **2004**, *15*, 181.

[3] D. M. Yebra, S. Kiil, K. Dam-Johansen, *Prog. Org. Coat.* **2004**, *50*, 75.

[4] J. H. H. Bongaerts, J. J. Cooper-White, J. R. Stokes, *Biomacromolecules* **2009**, *10*, 1287.

[5] P.-H. Chua, K.-G. Neoh, E.-T. Kang, W. Wang, *Biomaterials* **2008**, *29*, 1412.

[6] Y. Li, J. Rodrigues, H. Tomás, *Chemical Society reviews* **2012**, *41*, 2193.

[7] O. Yemul, T. Imae, *Colloid Polym Sci* **2008**, *286*, 747.

[8] M. N.V. Ravi Kumar, *React. Funct. Polym.* **2000**, *46*, 1.

[9] K. A. Nolte, J. Schwarze, C. D. Beyer, O. Özcan, A. Rosenhahn, *Biointerphases* **2018**, *13*, 41007.

BI-TuP-5 Mass Spectrometric Determination of Active Adsorption sites of soil organic Carbon on Clay Mineral Surface, *Zihua Zhu, L Huang,* Pacific Northwest National Laboratory*; W Liu,* China University of Geosciences, Wuhan

The heterogenic active adsorption sites on mineral surfaces may harbor critical determination on the protecting capability, preference and efficiency on soil organic carbon (SOC) components. Molecular evidence to show organic behaviors during mineral-microbe-organic interactions is urgently needed to reveal the underlying protecting-releasing mechanism for better prediction on the SOC dynamics. However, such information has been hard to obtain in the complex soil systems. Time-of-flight secondary ion mass spectrometry (ToF-SIMS) is a powerful surface analysis tool with unique advantages to reveal systematical changes of both SOC and mineral surfaces during mineral-microbe-organic interactions. In this work, ToF-SIMS and principle component analysis (PCA) were used to study the molecular mechanisms of organic preference (e.g., humic substances vs. microbial carbon) by Fe-rich clay mineral (e.g., nontronite NAu-2) during microbial Fe redox processes. Active adsorption sites, which have only been hypothesized or computationally investigated in previous research, were successfully determined by ToF-SIMS data. Such a success indicates a bright future of extensive application of ToF-SIMS and PCA on this field.

BI-TuP-6 Blood Compatible Coating using Tethered Heparin to Reduce Coagulation in Microfluidic Devices, *Ryan Faase, W Prusinski, K Schilke, A Higgins, J Baio,* Oregon State University

Hyperbilirubinemia, a condition characterized by excessive bilirubin levels, affects over half of newborn babies and can lead to serious complications including brain damage or death. Absorption of light by bilirubin leads to isomerization reactions that convert bilirubin into more readily excreted compounds (e.g. lumirubin). Here, an extracorporeal microfluidic device has been developed and optimized to isomerize bilirubin in neonates, with an efficiency that exceeds the current treatment, exchange blood transfusions. The microfluidic devices are formed from cyclic olefin copolymer and the main design challenge for this device is hemocompatibility. Our approach is to modify the blood contacting channels by tethering heparin, a powerful anti-coagulant, to the surface. This is achieved by first coating the surfaces with poly(dopamine) (PDA) and then adsorbing silver nanoparticles onto the PDA layer followed by a thiol based amine terminated self-assembled monolayer (SAM). PDA provides a route for coating virtually any surface and along with silver nanoparticles the PDA-silver interface becomes antimicrobial. The SAM formed on the PDA-silver surface can be tailored for covalent linkage of the desired molecule. For this device, heparin is chemically modified, while retaining the active site, and covalently attached to the SAM with an end-on orientation to preserve activity. Heparin's potency, in terms of anti-coagulative power, comes from a heavily sulfated penta-saccharide sequence. This sequence selectively binds precursors that produce fibrinogen, the basis of a clot. Therefore, the heparin must be covalently bound in an end-on orientation to expose this penta-saccharide sequence as opposed to allowing it to adsorb to the surface. Fluorescent microscopy provides the relative coverage of available sites for heparin attachment. Fluorescein isothiocyanate is selective to primary amines and demonstrate the density of amines that can be covalently bonded with heparin. Additionally, surface density of these amine groups was confirmed by X-ray photoelectron spectroscopy. Finally, the activity of surface bound heparin is dependent on orientation with respect to the channel surface. Thus, sum frequency generation vibrational spectroscopy provides information on the tilt angle of heparin at an interface by probing S=O, C-H and O-H vibrational modes at the modified surface.

BI-TuP-7 Analysing the Sequestration of Pro-inflammatory Chemokines into Immuno-modulating Hydrogels using ToF SIMS, *Nicholas Dennison, R Zimmermann, M Nitschke, V Magno, U Freudenberg, C Werner,* Leibniz Institute of Polymer Research Dresden, Germany

Chemokines are a class of signalling molecules that play a crucial role in the wound healing process by recruiting immune cells to the affected tissue. In chronic inflammations, this physiological response is prolonged and exacerbated, ultimately causing the destruction of the inflamed tissue and, consequently, the production of more pro-inflammatory chemokines.

One way of interrupting this vicious cycle of chronic inflammations is to remove chemokines from the tissue. Our group has previously demonstrated that hydrogels based on star-shaped polyethylene glycol (starPEG) and desulfated heparin show a promising sequestration pattern of pro-inflammatory chemokines including interleukin-8 (IL-8) and macrophage inflammatory protein-1a (MCP-1) [Lohmann et al. *Sci. Transl. Med.* **9** (2017)].

Analysis of chemokine-loaded hydrogels with time-of-flight secondary ion mass spectrometry (ToF-SIMS) and principle component analysis (PCA) of the obtained spectra allowed for further characterisation of the scavenging process. The results obtained through this methodology were integrated with the enzyme-linked immunosorbent assay (ELISA) detection technique to further optimise the immune-modulating hydrogel.

MEMS and NEMS Group
Room Union Station AB - Session MN-TuP
MEMS and NEMS Poster Session

MN-TuP-1 Multimodal & Multifunctional Soft Sensors for Electronic Textiles, *Ashish Kapoor, T Ghosh, A Bozkurt,* North Carolina State University

Soft polymer-based sensors as an integral part of textile structures have attracted considerable scientific and commercial interest recently because of their potential use in healthcare, security systems, and other areas. While electronic sensing functionalities can be incorporated into textiles at one or more of the hierarchical levels of molecules, fibers, yarns, or fabrics, arguably a more practical and inconspicuous means to introduce the desired electrical characteristics is at the fiber level, using processes that are compatible to textiles. In this research, a prototype multimodal and multifunctional sensor array formed within a woven fabric structure using bicomponent fibers with ordered insulating and conducting segments is reported. The conducting segments are extruded from a percolating conducting composite made by dispersing carbon fillers in an elastomer. The multifunctional characteristics of the sensors are successfully demonstrated by measuring tactile, tensile, and shear deformations, as well as wetness and biopotential (heart rate). While the unobtrusive

integration of sensing capabilities offer possibilities to preserve all desirable textile qualities, this approach demonstrates the potential for scalable and facile manufacturability of practical e-textile products. The capability of these fiber-based sensors is further being explored for objective monitoring of the inner socket environment (i.e. pressure, temperature, and humidity) and residual muscle activity during daily prosthesis use in lower limb amputees.

Complex Oxides: Fundamental Properties and Applications Focus Topic
Room Union Station AB - Session OX-TuP

Complex Oxides: Fundamental Properties and Applications Poster Session

OX-TuP-1 Electrical and Structural Properties of p-type Transparent Conducting La$_{2/3}$Sr$_{1/3}$VO$_3$ Thin Films Grown Using RF Sputtering Deposition, *D Jung, Y Oh, H So, **Hosun Lee**,* Kyung Hee University, Republic of Korea

The development of efficient p-type transparent conducting oxides (TCOs) remains a global material challenge. Converting oxides from n-type to p-type via acceptor doping is extremely difficult and these materials exhibit low conductivity due to the localized nature of the O $2p$ -derived valence band, which leads to difficulty in introducing shallow acceptors and small hole effective masses. High-quality perovskite oxide (ABO$_3$) thin film p-n junctions have significant potential for electronic devices with multifunctional properties. The p-type perovskites currently in use are not sufficiently transparent in the visible region. Alloying Sr and La at the A-sites of perovskite SrVO$_3$, i.e. La$_{2/3}$Sr$_{1/3}$VO$_3$ (LSVO), can introduce holes at the top of the valence band (VB), resulting in p-type conductivity while maintaining reasonable transparency.

In this work, p-type LSVO thin films were grown on various substrates using RF magnetron co-sputtering deposition with SrVO$_3$ (actually Sr$_2$V$_2$O$_7$) and La$_2$O$_3$ targets between 400 and 500 °C with a mixed gas of H$_2$ (35%) and Ar. The generator powers were 60 and 30 W, respectively. Film thicknesses varied between 120 and 150 nm. The growth temperature and sputtering gas ambient were optimized and precisely controlled. The chamber pressure was set at . We used LSAT, LaAlO$_3$, TiO$_2$/Si, Si, SiO$_2$/Si as substrates. The structural and morphological properties of LSVO films were studied using grazing angle incidence X-ray diffraction (GIXRD), scanning electron microscopy (SEM), transmission electron microscopy (TEM), spectroscopic ellipsometry, and X-ray photoemission spectroscopy (XPS). The electrical properties of all samples were measured using Keithley 4200. Hall effect measurements provided the Hall carrier concentration and Hall mobility as 3.0×10^{20} cm^{-3} and 5.15 cm^2/(V·s), respectively. The resistivity was measured to be 4.1 mΩ·cm. In comparison, Hu et al. reported the resistivity, carrier concentration, and mobilities as 1.15 mΩ·cm, 1.69×10^{21} cm^{-3}, and 3.2 cm^2/(V·s), respectively for LSVO grown by using pulsed layer deposition [1]. GIXRD measurements showed 2Θ = 32.36˚, which arose from (112) plane of tetragonal crystal structure of LSVO films. We discuss the substrate dependence of the electrical and optical properties of LSVO thin films in detail. We plan to develop all perovskite La$_{2/3}$Sr$_{1/3}$VO$_3$/SrVO$_3$ p-n junctions.

[1] L. Hu et al., Adv. Elect. Mater. **4**, 1700476 (2018).

OX-TuP-2 van der Waals Heterostructures of Graphene and β-Ga$_2$O$_3$ Nanoflake for Enhancement Mode MESFETs and Logic Applications, ***Janghyuk Kim**, J Kim,* Korea University, Republic of Korea

β-gallium oxide (β-Ga$_2$O$_3$) is a promising material for next-generation power electronics due to its wide band gap of ~4.9 eV and excellent productivity. Interestingly, a single crystalline β-Ga$_2$O$_3$ with a monoclinic structure can be exfoliated into ultra-thin flakes along the (100) plane due to its strong in-plane force and weak out-of-plane force. The exfoliated β-Ga$_2$O$_3$ flakes can be easily integrated with 2D materials (h-BN, TMDCs) to form van der Waals heterostructures for a down-scaled novel (opto)electronic devices as well. Most of the fabricated β-Ga$_2$O$_3$ transistors exhibit n-type characteristics with a negative threshold voltage (V$_{th}$) due to oxygen vacancy or donor like impurities in β-Ga$_2$O$_3$. The negative threshold voltage of n-type β-Ga$_2$O$_3$ transistors allows only a depletion mode (D-mode) operation, which limits their implementation in the circuit design. However, an enhancement mode (E-mode) operation, allowing simple circuit designs and fail-safe operation under high voltage conditions, is preferred for power transistors.

We have demonstrated a method to control V$_{th}$ of β-Ga$_2$O$_3$ Metal-Semiconductor Field Effect Transistor (MESFET) by using various morphology of van der Waals heterostructure of β-Ga$_2$O$_3$ and graphene to achieve an E-mode operation. The junction of β-Ga$_2$O$_3$ and graphene forms a Schottky barrier due to the difference of their work functions. In the same β-Ga$_2$O$_3$ nanoflake, the β-Ga$_2$O$_3$ MESFET with a double gate of the sandwich structure of graphene/β-Ga$_2$O$_3$/graphene showed positive V$_{th}$ (E-mode operation) while the bottom gate only MESFET showed negative V$_{th}$ (D-mode operation). Furthermore, a β-Ga$_2$O$_3$/graphene van der Waals heterostructure based monolithic Direct Coupled FET Logic (DCFL) inverter was demonstrated by integrating E-mode and D-mode MESFETs on single β-Ga$_2$O$_3$ nanoflake and exhibited good inverter characteristics. These results show a great potential of van der Waals heterostructure of β-Ga$_2$O$_3$/2D materials on future nanoscale smart power integrated circuit (IC) applications. The details of our results and discussions will be presented .

OX-TuP-3 Structure and Reactitvity of a Magnetite-Terminated Hematite Surface with Oxygen Adatoms Formed by Self-Oxidation, *Constantin Walenta, F Xu, W Chen, C O'Connor, C Friend,* Harvard University

The surface composition and structure of reducible oxides, including oxides of Fe, are complex and difficult to control because of the mobility and multiple oxidation states of cations. The magnetite phase of iron oxide is a material with a complex structure and controversial surface terminations that is widely used in heterogeneous catalysis, including the water gas shift reaction and formaldehyde synthesis.

A new, unique termination of oxygen adatoms forms on top of Fe$_3$O$_4$(111) film on a α-Fe$_2$O$_3$(0001) single crystal in oxygen-deficient environments. By using a combination of chemical and activity analysis (XPS and TPRS), structure analysis (STM and LEED) and DFT calculations, we identify the atomic structure of the as-prepared Fe$_3$O$_4$(111) surface and distinguish electronic structure of oxygen adatom and uncovered iron sites. The latter is an active Lewis site for alcohol dissociation at room temperature. Further oxidation of the alkoxy intermediate to the aldehyde occurs at 700 K, and the surface fully recovers after product desorption.

The work establishes a clear understanding of a unique magnetite surface and provides insights in the selective oxidation of alcohols on iron oxide-based catalysts and a rare direct observation of oxygen mobility in iron-oxide based materials.

Plasma Science and Technology Division
Room Union Station AB - Session PS-TuP

Plasma Science and Technology Poster Session

PS-TuP-2 Low-temperature Atmospheric Plasma Deposition of Photocatalytic Doped Anatase TiO$_2$ Coatings on Polymer Substrates, *K Baba, M Quesada-Gonzalez, S Bulou, P Choquet, **Nicolas Boscher**,* Luxembourg Institute of Science and Technology, Luxembourg

Anatase titanium dioxide (TiO$_2$), one of the most important photocatalytic materials, has met a wide range of applications, including self-cleaning surfaces, environmental purification, water splitting and photovoltaic applications. Many attempts, including doping and noble-metal nanoparticles loading, have been proposed to extend the photocatalytic activity of anatase TiO$_2$ to the visible range as well as reduce the photo-induced electron-hole pair recombination probability. On the other hand, tremendous efforts have targeted a decrease of the temperature formation and deposition of anatase TiO$_2$-based thin films.

Due to their undeniable industrial advantages, such as low temperature, low cost, easy implementation and in-line process capabilities, low-temperature atmospheric-pressure plasma processes provide a promising alternative for the low-temperature deposition of functional coatings. In this work, we reported the simultaneous formation and deposition of photocatalytic anatase TiO$_2$ thin films on polymer substrates using a microwave (MW) plasma source operated at atmospheric-pressure.

We further demonstrate our approach as suitable for the formation of doped anatase TiO$_2$ thin films. Boron-doped anatase TiO$_2$ were readily deposited on different substrate such as glass, silicon and polymeric optical fibers in a one-step process. The careful selection of the titanium and boron precursors allows the deposition of well adherent, dense and crystalline B-TiO$_2$ with a visible light activity. The photocatalytic activity of the deposited films was demonstrated by monitoring de degradation of stearic acid or methylene blue under UV and visible light by FTIR and related to the narrowing of the band gap observed by UV-Vis

spectrophotometry. Finally, light-diffusing polymer optical fibers were coated using the developed method for the elaboration of a water decontamination reactor for the removal of organics and antibiotics.

PS-TuP-3 Radical Nitriding of Silicon Surface Promoted by Surface Plasmon Resonance of Gold Nanoparticle Catalyst, *Machiko Miyake, T Kitajima, T Nakano,* National Defense Academy, Japan

In recent years, the catalytic effect of gold nanoparticles has attracted attention[1, 2]. We have applied the catalytic property of gold nanoparticles to plasma surface reaction, and aim at the formation of a high-quality ultra-thin film by low damage nitriding by radical (R). This time, we compare the degree of nitridation by the presence or absence of ion irradiation (I), light irradiation (L), and the gold nanoparticle catalyst (C), respectively, and discovered the radical nitriding phenomenon by surface plasmon resonance of gold nanoparticles.

Gold is deposited for two minutes by electron beam evaporation on a SiO_2/Si(100) substrate in an ultra-high vacuum chamber.

Next, 30 mTorr of nitrogen plasma was generated in the attached chamber, and radicals (R) that had passed through a 30 line/inch SUS304 single mesh were irradiated to the sample for 5 minutes. When no light was applied, the sample surface was rotated 90 °.

The AFM images of gold nanoparticles produced by evaporation were compared under irradiation conditions of radicals, light, and ions.

The effect on the shape of gold nanoparticles increased in the order of RILC> RLC> RC.

It is clear that it is necessary to remove the ion irradiation in order to make the effect of the gold nanoparticles.

Next, surface atomic compositions by XPS were compared. The nitrogen ratio was not largely dependent on the irradiation conditions, but was relatively high in RI and RILC conditions where radical and ion irradiation occur simultaneously.

Comparing the XPS N1s spectrum, a peak near 398 eV of SiN is obtained strongly under the RLC condition where surface plasmon resonance can occur, and it can be imagined that a Si-N bond could be formed with the aid of the catalytic activity of Au nanoparticles.

When there is no light irradiation, the signal intensity of the Si-N bond is weak.

Also in the Si2p spectrum of XPS, the chemical shift between SiON and Si is small (3.6 eV) under the RLC conditions, which reflects the formation of the Si-N bond.

From the above, in the presence of light irradiation, it is considered that the catalytic activity of the Au nanoparticles is expressed by the effect of surface plasmon excitation, and the formation of the Si-N bond is promoted.

1. X. Chen, H.-Y. Zhu, J.-C. Zhao, Z.-F. Zheng, and X.-P. Gao, Angew. Chem. 120, 5433 (2008).

2. S. Bhaviripudi, E. Mile, S.A. Steiner, A.T. Zare, M.S. Dresselhaus, A.M. Belcher, and J. Kong, J. Am. Chem. Soc. 129, 1516 (2007).

PS-TuP-4 Development and Characterization of a Small-Scale Helical Dielectric Barrier Discharge for Studying Plasma-Surface Interactions, *Nazli Turan, P Barboun, W Schneider, J Hicks, D Go,* University of Notre Dame

The study of plasma-surface interactions is an emerging field for a wide variety applications, including sustainable energy (catalytic H2 production), environmental remediation (water purification), medicine (sterilization), and high-value manufacturing (nanomaterial synthesis). These applications are driven by species created in the plasma or at a plasma-surface interface, such as free electrons, gaseous ions, excited molecules and radicals, driving chemistry at a surface. Here, we develop a new dielectric barrier discharge (DBD) configuration to produce surface DBDs over a three-dimensional geometry. The motivation for this geometry was to embed the plasma source inside a packed bed (e.g., catalyst) reactor that had tight spatial restrictions so that it could be implemented in a commercial Fourier transform infrared (FTIR) spectrometer instrument.

The design, which we term a helical DBD, was inspired by surface DBD configurations often employed in plasma actuators for fluid dynamics applications. However, rather than using a 2D surface common in plasma actuators, the helical DBD uses the 3D surface of a cylinder as its dielectric, allowing for greater plasma coverage and in this case, greater interaction with a packed bed. This study characterizes the electrical properties of the helical DBD in both free space and within a packed bed reactor. Various electrical parameters, including energy, deposited power, and plasma current are measured as a function of frequency and voltage. Visual properties are presented to show how the DBD spreads along the dielectric surface or into the packed bed. The effect of being immersed in a packed bed is quantified and the potential future prospects of this type of DBD geometry are discussed.

PS-TuP-5 Characteristics of Magnetized High Density Plasma and its Applications, *Jung-Hyung Kim, H Lee, D Seong,* Korea Research Institute of Standards and Science, Republic of Korea

We developed high density plasmas in a very uniform magnetic field. To maximize the electron density and efficiency, aspect ratio of discharge cylinder is varied. The discharge pressure is about mTorr or sub-mTorr. Characterization of fully ionized high density helicon plasma is made with probes and optical emission spectra. A helicon plasma with 10^{13} cm^{-3} density is produced in a diameter of 10 cm and length of 70 cm, and the preliminary results of plasma properties are briefly described. The electron temperature is relatively high and the ions are highly ionized. These low pressure plasmas emit short wavelength lights. We inject Xe gas and/or Sn in this system to see the possibility for EUV light sources as one of applications. Weak EUV emission can be detected in low pressure high density magnetized plasma with Sn injection. We could see the possibility for EUV source with this magnetized plasma system. Hereafter, we need more RF power and higher magnetic field to more confine the high density plasma column. We need also to stabilize the plasma for stable strong EUV source at low pressure and high magnetic field.

PS-TuP-6 The Effect of Ionic Strength on the Absorption Spectrum of Plasma-Injected Solvated Electrons, *Daniel Martin, H Delgado, D Bartels, P Rumbach, D Go,* University of Notre Dame

The study of plasma-liquid interactions is an emerging field with multifarious applications that are driven by chemical species created in the plasma or at the plasma-liquid interface, such as the hydroxyl radical (OH), hydrogen peroxide (H_2O_2), and, in particular, solvated electrons (e_{aq}^-). The solvated electron is an electron in a polar solution, loosely confined in a potential well formed by the solvent molecules, and notable for being a powerful reductant. Historically, solvated electrons have been studied by using pulse radiolysis and laser photolysis. However, recently we confirmed their presence in a direct current (DC), atmospheric pressure, liquid anode discharge using phase-locked, total internal reflection absorption spectroscopy (TIRAS). The measured absorption spectrum appeared to be blue shifted from the well-established dilute solution spectrum, and one possible explanation is that the local ionic strength in the double layer at the plasma-liquid interface alters the solvation potential well via increased Coulombic interactions. In this work, we use TIRAS to measure the absorption spectrum as a function of the solution ionic strength and compare the results to measurements produced using pulse radiolysis in order to resolve any differences in the spectra of plasma-injected and bulk-produced solvated electrons.

PS-TuP-7 Inductively Coupled Plasma Reactive Ion Etching of Copper Thin Film using Organic Chemicals and Alcohols, *Moon Hwan Cha, E Lim, J Ryu, C Chung,* Inha University, Republic of Korea

To improve the performance of Semiconductor memory device, it is important to reduce RC delay. Copper is widely used as interconnect material because it has lower resistivity and higher electromigration resistance than aluminum. However, the conventional dry etching of copper is very difficult due to low vapor pressures of copper compounds and/or low reactivity of copper . As an alternative to dry etching for copper interconnect, a damascene process has been developed in the early 1990s and has been used until now. However, as the device critical dimension continues to shrink, especially below about tens of nanometers, the resistance of the device increases and the performance of the device is deteriorated. As a result, the development of a conventional dry etch process is inevitable.

In this study, new copper etching process which utilizes organic chemicals and alcohols are studied. The etch characteristics of copper under these gases are investigated using inductively coupled plasma reactive ion etching (ICPRIE) as a function of gas concentration and the effects of main etch parameters such as ICP power, dc-bias voltage to substrate, and process pressure are also examined. The etch profiles are observed using FESEM and the etch products formed during etching are analyzed using X-ray photoelectron spectroscopy (XPS), Energy dispersive X-ray spectroscopy (EDS) is also carried out to indentify the etch residues. Plasma characteristics are analyzed using optical emission spectroscopy (OES) and Langmuir probes.

PS-TuP-8 High Resolution Quadrupole Mass Spectrometry Analysis for Fusion Reactor and Plasma Facing Materials, *G Thier*, **Brian Regel**, *L Kephart,* Extrel CMS

Fusion reactions break down gaseous hydrogen electrically, forming a plasma. Plasma particles heat up to fusion temperatures and create fusion reactions, releasing huge amounts of energy. Fusion reactors such as tokamaks use tiles made of Tungsten for the interior section exposed to the highest heat and particle fluxes. A major goal of research into fusion materials testing involves exploring material performance in deuterium, helium, or mixed plasmas. The ability to effectively measure helium and deuterium in plasmas simulating fusion plasmas or the effect on plasma facing materials after exposure to such plasmas through techniques such as TDS and TPD is critical to developing our understanding proposed materials' suitability for long-term use in fusion and other plasma facing applications. An Extrel VeraSpec HRQ (High Resolution Quadrupole) Mass Spectrometer was used for the analysis of gas phase components expected in fusion reactions. A certified cylinder containing helium and deuterium was leaked into the vacuum chamber to characterize the long term mass stability of the system under high resolution conditions. This gas was then diluted to determine the low detection limits of these species under the same conditions. A certified cylinder containing carbon monoxide and nitrogen was also leaked into the vacuum chamber to assess the system's ability to resolve the spectrum of this mixture. Spectra at six hour time intervals were taken of the helium and deuterium mixture over 24 hours. The experiment demonstrated that, under high resolution conditions, no detectable mass spectral changes were observed. Diluting the mixture, detection limits of approximately 10ppm (parts per million) were calculated for helium and deuterium. Quadrupole mass spectrometry provides a low cost, simple experimental setup to monitor the effects of fusion reactions on reactor materials.

PS-TuP-9 Controlled Layer-by-Layer Etching of Copper Thin Films, *Eun Taek Lim*, *J Ryu, M Cha, C Chung,* Inha University, Republic of Korea

As the critical dimensions of semiconductor devices are reduced for their high performance, fast operating speeds and low operating power, aluminum interconnects are no longer used as a suitable electrode material, but instead of aluminum, the use of copper is increasing. Copper is known as an excellent interconnect material compared to aluminum due to its very low resistance and less electromigration phenomena that cause wire deformation and breakage. However, the damascene process presents some limitations in delineating fine patterns below tens of nanometers. To solve these fatal issues related with the damascene process, intensive researches about copper patterning has been performed using conventional dry etching. Currently, one promising way to etch copper films is cyclic etching. Cyclic etching, including surface modification and its removal, can effectively provide a good etch performance of silicon material. This etching technique is proceeded by inducing surface reactions and precise removal of the modified surfaces, resulting in the accurate control of the etch depth. These results are due to the nature of the self-limiting process and the removal of layers by layer. Various combinations of gases are possible for cyclic etching of the films

In this study, a two-step sequential cyclic etching of surface modification and ion bombardment are investigated. Surface modification and etch depth of the copper film are confirmed using a surface profilometer, a scanning probe microscope and a field emission scanning electron microscope (FESEM) as a function of various parameters such as the conditions of surface modification and bombardment energy of ions. In addition, etch profiles and etch mechanism of copper films in cyclic etching have been studied by FESEM, FETEM and X-ray photoelectron spectroscopy.

PS-TuP-10 Effects of Bias on Quasi-Atomic Layer Etching of Silicon Dioxide by Cyclic Ar/C$_4$F$_8$/O$_2$ and Ar Plasmas, *Xifeng Wang*, University of Michigan; *M Wang, A Mosden, P Biolsi,* TEL Technology Center, America, LLC; *M Kushner,* University of Michigan

With the reduction in feature size in microelectronics fabrication, the process flow in plasma etching includes several steps that are devoted to producing the mask that is ultimately used to define the semiconductor (or dielectric) critical dimension (CD). These processes include tight pitch/space and multi-layer structures composed of several materials which, in turn, require a sequence of recipes steps to etch. In this regard, atomic layer etching (ALE) is being employed in several steps of the process flow to improve CD tunability and resist selectivity.

In this work, we report on a computational investigation of the ALE plasma etching of dielectric (silicon dioxide) layers in multi-layer structures using a

cyclic fluorocarbon mixture deposition and Ar etching process. Reactor scale modeling was performed using the Hybrid Plasma Equipment Model (HPEM) and feature scale modeling was performed by Monte Carlo Feature Profile Model (MCFPM). The first step in the process largely deposits fluorocarbon polymer. The second step activates the etch. The reactor is a multi-frequency capacitively coupled plasma (CCP) augmented by a DC bias to the top electrode. During the deposition step where ion energies should be low, 40 MHz source power is applied to the bottom electrode and a 900 V negative DC bias is applied to the top electrode. For the etch step where moderately energetic ions are desired, only a 10 MHz bias is applied to the bottom electrode.

During the deposition step, ion energies to the wafer are typically lower than 40 eV. These low energy ions activate surface sites (but typically do not sputter), which then enables deposition of a controllable thickness of polymer. During the etch step, the flux of Ar$^+$ at the surface is at about 1.4 10^{15} cm^{-2}s^{-1}, when then requires several to ten of seconds to remove a monolayer or several monolayers of dielectric. Since the layers being removed are at the bottom of a high-aspect-ratio feature, it is desirable to narrow the angular distribution of the ions by increasing bias power which then also increases ion energy. The narrower distribution works towards maintaining the CD, however the higher ion energy works against maintaining the quasi-ALE character of the etch. Tradeoffs between simultaneously maintaining CD and quasi-ALE performance will be discussed .

* Work supported by Tokyo Electron Ltd. and the US Department of Energy Office of Fusion Energy Science.

PS-TuP-11 Electron Beam Generated Produced Plasmas Produced in Oxygen: Measurements and Simulations, *Scott Walton*, *D Boris,* U.S. Naval Research Laboratory; *S Rauf,* Applied Materials, Inc.

The U.S. Naval Research Laboratory (NRL) has developed a processing system based on an electron beam-generated plasma. Unlike conventional discharges produced by electric fields (DC, RF, microwave, etc.), ionization is driven by a high-energy (1-3 keV) electron beam, an approach that can yield very different plasma properties than conventional plasma processing systems. Electron beam-generated plasmas are broadly characterized by high charged particle densities (10^{10}- 10^{12} cm^{-3}), low electron temperatures (0.3 - 1.0 eV), and in reactive gas backgrounds, a relatively low radical production rate compared to discharges. When produced in oxygen backgrounds, this combination of features leads to a surprisingly large density of O$^+$ ions. In this work, we combine plasma diagnostics and modeling to characterize the spatial evolution of electron beam generated plasmas produced in oxygen as a function of operating parameters such as beam energy, beam current and pressure. Measurements of ion fluxes at adjacent surfaces indicate the large O$^+$ ion densities can lead to O$^+$/O$_2^+$ flux ratios that far exceed one. The modeling results capture salient features of the plasma and provide a better understanding of plasma kinetics that lead to the measured ion flux ratios. This work is partially supported by the Naval Research Laboratory base program.

PS-TuP-12 Silicon Micro-Channel Definition Via ICP Plasma Etching Process Using Different Hard Masks, *Hugo da Silva Alvarez*, *J Diniz, C Ruiz, A Silva, F Cioldin, V Junior,* UNICAMP, Brazil

Alumina, pieces of silicon wafers, lithographed aluminum (Al) and aluminum nitride (AlN) were used as mechanical hard masks materials for micro-channel etching in silicon (Si) using a high-density inductively coupled plasma - Reactive Ion Etching (ICP-RIE) reactor. The mechanical masks of alumina and silicon, with thickness of 1 mm and 0.35 mm, respectively, were positioned manually on the Si substrates, where the silicon micro-channels (SiMCs) were etched. In the case of Alumina, two rectangular masks were spaced 0.7 mm between them in the Si substrate, resulting in only one micro-channel. For Si mask, six Si pieces with rectangular shapes were positioned in the Si substrate with different spacing between them. The Al films with thickness of 500 nm were evaporated and wet etched using a two lithographed masks patterns: i) parallel lines with width of 0.8 mm and 0.2 mm spaced ; ii) parallel lines with width of 0.2 mm and 0.8 mm spaced. This second sample was carried out to an ICP plasma nitridation (for 30 minutes) to result an AlN/Al structure. AlN material is considered a hard mask especially for the RIE plasma etching based on SF6 gas. The ICP-RIE processes to fabricate the SiMC and to characterize the mask resistance under the plasma etching were carried out using these fixed parameters: 10 sccm of SF$_6$ + 15sccm of Ar, 15 mTorr of process pressure, 1200W of ICP and 40W of RIE powers. The SiMC profiles, obtained by scan profiler system. indicate that: (i) with alumina mechanical masks, SiMC was obtained the maximum depth value

of 108 µm, for the width of 0.7 mm. As in this case, it has only one channel, the unprotected silicon region was small when this sample is compared with others. Small silicon region to etch, highest etch rate can be obtained; (ii) with silicon mechanical masks, it was obtained the depth values between 53 and 87 µm. Furthermore, it can be observed that there is a dependence between the width and the depth of channel. (iii) with Al mask defined by lithography and etching, the SiMC profiles are uniform, with the same width and depth of about 0.24 mm and 80 µm, respectively. The spacing regions with width of 0.76 mm are with surface roughness (up to 5 µm), indicating that the Al mask has not supported the plasma etching for 2 hours; (v) with AlN/Al mask defined by lithography, etching and plasma nitridation, the SiMC profiles are uniform, with the same width and depth of about 0.33 mm and 90 µm, respectively. The spacing regions with width of 0.66 mm have not presented the surface roughness, indicating that the Al mask has supported the plasma etching for 2 hours. However, at the end of plasma etching, this mask was very thinner.

PS-TuP-13 Corrosion Barrier Coatings for Aerospace Materials Deposited by Atmospheric Pressure CVD, *Dhruval Patel*, Z Jeckell, T Choi, D Barlaz, L Bonova, D Krogstad, D Ruzic, University of Illinois at Urbana-Champaign; S Chaudhuri, University of Illinois at Chicago
Rigorous performance standards for tactical vehicles and aircrafts demand the use of chemical

processes to apply a galvanic corrosion barrier coating. Current processes are often hazardous and

environmentally unsafe as they involve chemicals such as hexavalent chromium. The handling and

disposal of the waste products of these wet chemical processes puts a significant financial burden on the

Department of Defense. This work aims to design and develop a process which employs an atmospheric

pressure plasma jet to substitute the wet chemical processes. The proposed project focuses on

depositing zirconia-silica conversion coatings on aluminum surfaces as a corrosion barrier. The process

utilizes existing chemical vapor deposition precursors with a much smaller chemical foot print. The

process is capable of depositing 100 – 300 nm zirconia-silica layers with relatively low carbon content

as observed under XPS. Initial tactical testing showed reduced water intrusion for painted silica coated

substrates.

PS-TuP-14 Atmospheric Pressure Plasma: An Alternative Tool for the Synthesis of Efficient Photocatalytic Materials, *S Ptasinska, Amal Sebastian*, University of Notre Dame
Photocatalytic splitting of water into hydrogen and oxygen is a method to convert solar energy into storable chemical energy directly, and it has received significant attention for its high potential for low cost and clean energy production. Developing efficient and cost-effective photocatalysts for water splitting is a growing need for solar energy research. In this work, we propose an alternative method to deposit photocatalytic materials with atmospheric pressure plasma (APP). The design and experimental approach for depositing the visible light photoelectrode TaOxNy using APP with a suitable solution precursor are explained in detail. The effect of plasma parameters on the composition of films is investigated by monitoring the surface chemistry changes with X-ray photoelectron spectroscopy. The observed changes in the composition of films with modulation of plasma parameters hint towards alternative processing routes to deposit photocatalytic materials efficiently

PS-TuP-15 Synthesis of Functional Polydopamine using Atmospheric Pressure Plasmas, *Yun Jong Jang*, M Mun, J Kim, D Kim, G Yeom, Sungkyunkwan University, Republic of Korea
Dopamine, known as a monoamine neurotransmitter, has functional groups such as catechol and amine. Under the state of oxidant and alkaline, the dopamine go through self-polymerization and creates polydopamine. This polymer is known to exhibit excellent adhesion (known as a mussel-inspired adhesive) to most of all organic and inorganic material surfaces. In this study, by using atmospheric pressure plasmas (dielectric barrier discharges; DBDs) with a low electron energy and a dopamine solution mist formed by piezoelectric module, a possibility of depositing functional polymer films showing the physical and chemical characteristics of

polydopamine without breaking the functional group of the dopamine has been investigated for different plasma voltages. By using the lower DBD voltage of 1.5 kV, the partial dissociation of dopamine molecule for polymerization without breaking the catechol/amine functional groups of dopamine could be achieved while the use of the higher DBD voltage to 3.0 kV tends to break more functional groups of dopamine into atoms which leads to the decreased physical and chemical characteristics of polydopamine. It is believed that this atmospheric pressure plasma polymerization method of dopamine can be applied to various areas which require surface modifications instantly by forming a polydopamine film similar to the wet methods.

PS-TuP-16 Effect of $C_x(x=4\sim7)F_8$ on the Etch Properties in Inductively Coupled Plasmas, *Hyun Woo Tak*, D Sung, Y Shin, D Kim, G Yeom, Sungkyunkwan University, Republic of Korea
In semiconductor industries, the trend of scaling down is ongoing in ultra large scale integrated (ULSI) devices such as logic devices or 3D NAND devices. To achieve the scaling down of the devices, multiple patterning technologies such as double patterning technology (DPT) and quadruple patterning technology(QPT) have become essential technologies and require a high selective SiO_2 etch process. In this study, three types of perfluorocarbon (PFC) precursors(C_4F_8, C_5F_8 and C_7F_8)were used and the effects of these PFCs on the etch characteristics of SiO_2, Si_3N_4, and ACL and their etch selectivities were investigated by using $C_x(x=4\sim7)F_8/Ar/O_2$ plasmas. Among these, C_5F_8 and C_7F_8 are liquid phase at room temperature and, to deliver these liquid precursors to the process chamber,the inductively coupled plasma (ICP) system was equipped with a constant temperature heated canister and heated gas lines. The etch results showed that the selectivities of SiO_2/Si_3N_4 and SiO_2/ACL with $C_7F_8/Ar/O_2$ plasmas were much higher than those with $C_4F_8/Ar/O_2$ and $C_5F_8/Ar/O_2$ at the optimized etch conditions. It is found that, with $C_7F_8/Ar/O_2$ plasmas, lower F radicals in plasmas and thicker fluorocarbon polymers on material surfaces were formed. Furthermore, $C_7F_8/Ar/O_2$ plasmas exhibited more anisotropic SiO_2 etch profiles than the plasmas generated with $C_4F_8/Ar/O_2$ and $C_5F_8/Ar/O_2$.

PS-TuP-17 Effect of Surface Charge Accumulation on Ion Current Distribution in Radio-frequency Magnetron Discharges, *Bocong Zheng*, K Wang, T Schuelke, Fraunhofer USA; Q Fan, Michigan State University
In radio-frequency magnetron sputtering discharges with a dielectric target, the etching profile of the target is significantly different from that obtained on a metal target. In this work, a two-dimensional electrostatic particle-in-cell/Monte Carlo collision (PIC/MCC) code, named ASTRA, is used to investigate this phenomenon. It is found that the charge accumulation on the target surface can significantly influence the ion current distribution. The transverse magnetic field significantly inhibits the motion of electrons across the magnetic field line, resulting in the accumulation of positive charges here. The positive surface charge reduces the ion current to the target surface and results in the abnormal etching profile.

PS-TuP-18 The Research of a Oxide Thin Films to be Etched Process Under Cryogenic Conditions, *Sang-Beom Han*, Samsung Electronic Company, Republic of Korea
In semiconductor fabrication, silicon oxide etching process has been more shrink and critical process for microelectronic devices. We have a tons of trouble to occur in etching deep and dense pattern. In the past, many studies have developed a further sophisticated and deeply oxide etching layer through high power, low pressure, and chemical gas mixtures. As a result we want to new approaching and trying it in terms of process temperature. Especially studies on poly-styrene films at cryogenic temperatures have been developed extensively, however there was not much research on etching of silicon oxide films at cryogenic temperatures. This experiment shows the results of investigating variations in etch rate and characteristics of oxide films at cryogenic temperatures.

PS-TuP-19 Plasma Etching High Aspect Ratio Carbon Nanotube Structures for a Neural Probe, *Spencer Roberts*, G Chen, Brigham Young University
A new approach to neural probe arrays using Carbon Nanotube Templated Microfabrication produces probes that would be smaller and more compliant than existing technologies. To achieve tall, straight probes, a sacrificial hedge is grown connecting adjacent probes and then is removed with a series of plasma etching conditions. These etches are challenging due a number a factors, including the variability in samples, the density function of the probes, and high aspect characteristics of the structure. Previously we developed a process that allowed us to selectively remove

the hedges and leave the probes intact. We have now quantified and refined that process.

PS-TuP-20 NOₓ Fixation by Atmospheric Pressure N₂/O₂ Filamentary DBD Plasma over Water: Physicochemical Mechanisms of Plasma-Liquid interactions, *Nepal Roy, C Pattyn,* Université libre de Bruxelles, Belgium; *A Remy, N Maira, F Reniers,* Université Libre de Bruxelles, Belgium

NO_x formation from N_2/O_2 gas or air through nonthermal plasmas has become an important research topic for researchers in the last decades, considering both environmental and industrial importance. In this study, an atmospheric pressure filamentary dielectric barrier discharge (DBD) plasma has been produced over the water surface by a sinusoidal20-30 kV, 24.5 kHz power supply. In order to study the physicochemical mechanism of plasma-liquid surface interaction for NO_x production, the characterization of the plasma has been performed using optical emission spectroscopy (OES) and by recording voltage-current curves (with a high voltage probe, a Rogowski coil and a digital oscilloscope). The concentration of nitrates and nitrites ions in water was determined by ion chromatography. The power absorbed by the plasma discharge has been determined by Volt-Charge (V-Q) Lissajous curves in different experimental conditions. It is shown that the absorbed power increases sharply with increasing applied voltage and with the content of N_2 in the gas mixture. OES diagnostics allows identifying the exited species, to study the relative emission intensity of NO (A-X) while varying the plasma gas composition, and to determine the rotational ($T_{rot} \approx 320\text{-}380$ K) and vibrational ($T_{vib} \approx 2600\text{-}3800$ K) temperatures under different experimental conditions. The Boltzmann plot method has been employed for the estimation of T_{rot} and T_{vib} by using the OH (A-X) and the N_2 (C-B) bands respectively. Both Trot and T_{vib} increase with increasing applied voltage and with increasing the O_2 content in the gas mixture. In the liquid phase, the concentration of NO_2^- is maximum at low applied voltages, treatment times and with pure N_2 discharges, whereas in these conditions the concentration of NO_3^- is minimum. The concentration of NO_3^- increases with increasing treatment times, applied voltages and O_2 content in the gas mixture. It is shown that the nitrites formed during the plasma treatment transform rapidly, and completely into nitrates. From the total amount of nitrites and nitrates synthesized in solution (named NO_x below), the energy yield for the conversion was estimated. Depending on the starting gas composition and applied powers, yields of ~180 W/mg NO_x to ~ 9.5 W/mg NO_x were obtained.

PS-TuP-21 Simulation Study of Capacitively Coupled Radio Frequency Silane/Hydrogen Plasma Discharges - Effect of Tailored Voltage Waveforms, *S Huang, Keh-Chyang Leou,* National Tsing Hua University, Taiwan, Republic of China

Capacitively coupled plasma discharges (CCP) have been widely employed for material processing, such as etching and deposition. The purpose of this study is to investigate the effect of tailored voltage waveforms (TVWs) on the plasma characteristics of SiH_4/H_2 plasmas, typically, for Si film deposition. A fluid model based numerical simulation analysis (CFD-ACE+) is employed to investigate the basic discharge characteristics and corresponding basic physical and chemical mechanisms occurring in the plasma reactor. The TVWs adopted in this study are formed by four harmonics of 13.56 MHz sinusoidal voltages. Different voltage waveforms can be generated by tuning the relative phase between the four frequencies. A peak or valley voltage waveform is obtained when the "phase" is 0 or π, respectively. Simulation results show that the "peak" waveform results in a lower sheath voltage, and the SiH_2/SiH_3 flux ratio reaching the substrate is 40% lower than that for CCP with single frequency of 13.56 MHz. Thus, by using TVWs, it is possible to fine tune the structure and/or property of the deposited Si film. The detailed results of the simulation analysis of CCPs with TVWs will be presented.

Surface Science Division
Room Union Station AB - Session SS-TuP

Surface Science Poster Session

SS-TuP-1 Mechanistic Studies of Thermal Dry Etching of Cobalt and Iron Thin Films, *Mahsa Konh, A Teplyakov,* University of Delaware

Thermal dry etching of cobalt and iron thin films were investigated using diketones. Two diketones (1,1,1,5,5,5-hexafluoro-2,4- pentanedione (hfacH) and 2,4-pentanedione (acacH)) were used to show their reactivity toward cobalt and iron thin films with the results being relevant to etching of CoFe alloys. To understand the mechanism of etching process, possible surface reaction pathways were followed with temperature programmed desorption (TPD). Resulting surfaces were characterized using X-ray photoelectron spectroscopy (XPS) supplemented with microscopic investigations. Starting with oxidized or halogenated surfaces was found to be necessary to form volatile products that would make etching possible. However, halogenation makes the mechanism more complicated. It was shown that several products were desorbing from the halogenated metal surfaces containing M^{2+} and M^{3+}. These products may also contain both the organic ligands and halogens. The effect of dosing temperature on the etching process was also investigated.

SS-TuP-2 Reaction of ZnO Nanomaterial with a Mixture of Gas-phase Prop-2-ynoic acid and Acetic Acid to Control Surface Coverage of Reactive Functional Groups, *Dhamelyz Silva-Quinones, A Teplyakov,* University of Delaware

Sensitization of oxide nanomaterials with a two-step process involving the reaction with gas-phase prop-2-ynoic acid followed by "click" attachment of functionalized azides to the resulting alkyne functionality has been recently reported by our group. One advantage of the first modification step being a gas phase reaction with a nanomaterial is in the ability to control surface concentration of alkyne functionality by dosing predetermined mixtures of prop-2-ynoic acid with another compound (in this case acetic acid) that reacts with the oxide surface in exactly the same way as prop-2-ynoic acid but does not lead to the formation of a reactive functionality to be utilized in the second step of sensitization. This approach is demonstrated for the mixture of these acids reacting with ZnO nanomaterial, and the concentration of surface alkyne functional groups is determined by the concentration of the prop-2-ynoic acid in the mixture with acetic acid. The resulting functionalized surface is interrogated by infrared spectroscopy to demonstrate that both acids co-adsorb on ZnO. Vibrational signatures of the CH_3 group at 1453 cm^{-1} and that of the alkyne group at 2110 cm^{-1} allow for quantification of the co-adsorbed species. This assessment is confirmed by the XPS investigation utilizing different ratios of the C 1s features corresponding to carboxylates compared to the methyl/alkyne carbon atoms in mixtures of pro-2ynoic and acetic acids. Solid state NMR spectroscopy is used to further confirm the formation and to quantify the concentration of two components in the mixed monolayer.

SS-TuP-3 Platinum Deposition onto OH-terminated Si (100) and Boron-impregnated Si (100) Substrates, *Sana Rani, C Byron, A Teplyakov,* University of Delaware

Trimethyl(methylcyclopentadienyl)platinum(IV) was used as a precursor to deposit platinum on silicon surfaces using wet chemistry method. The deposition was performed on silicon based substrates including oxidized (OH-terminated) Si(100) and boron-impregnated oxidized Si(100) surface. Fourier-transform infrared spectroscopy (FTIR) was used to confirm the purity of the precursor. The deposition process was performed at room temperature after activation of substrates at 200°C. The successful deposition resulted in formation of nanoparticles as confirmed by atomic force microscopy (AFM) with PtO_x being the majority deposited species as confirmed by X-ray photoelectron spectroscopy (XPS). These substrates were later calcined at 400°C followed by an activation at 550°C under H_2 gas environment. This activation procedure resulted in a reduction process that led the formation of metallic Pt particles as confirmed by XPS. The reactivity of precursor and dispersion of Pt nanoparticles on OH-terminated Si(100) surface was compared to that of B-impregnated surface. Calcination and activation under high temperature resulted in highly dispersed Pt nanoparticles on B-impregnated substrates.

SS-TuP-4 Barium Adsorption and De-wetting on W(112), *Michael Mroz,* Ohio University; *S Tenney, C Eads,* Brookhaven National Laboratory; *M Kordesch,* Ohio University

The tungsten (112) surface has been observed with adsorbed barium in emission microscopy. The barium metal is deposited from a filament filled with a piece of metallic barium. When the barium layer on the W(112) surface is heated, the barium de-wets, forming a "wetting layer" and droplets of barium. The de-wetting is solid-solid de-wetting, because the rupture of the film into droplets occurs at about 1/3 of the barium melting temperature (727 C). At low coverage, about 20 nm barium, the droplets are sparse, and the wetting layer uses most of the available barium. Two 2x1 domains and weak centered 2x2 low energy electron diffraction (LEED) pattern are observed. At high coverage, about 200 nm, in addition to the wetting layer, and a dense coverage of droplets (250 nm diameter), there are also larger scale networks of barium drops spread over micron scale distances.

SS-TuP-5 Self-Catalyzed Gas-Phase Cycloaddition on "Clickable" Nanostructured CuO Surface, *Chuan He*, *A Teplyakov*, University of Delaware

The surface functionalization of nanostructured metal oxides (CuO, ZnO, TiO$_2$, CeO$_2$) has attracted substantial attention due to their extensive applications in sensing, photo-catalysis, electronics, and energy conversion. A number of studies have been reported to achieve the surface sensitization of these metal oxides with organic or organometallic compounds in order to expand their versatile properties by introducing designated functionality. However, the most common approach to achieve this functionality utilizes sensitizer molecules reacting with oxide surfaces via carboxylic (COOH) or phosphonic (P(O)(OH)$_2$) anchor groups or by silylation (such as with R-Si(X)$_3$, where the X could be Cl or -OCH$_3$), which potentially leads to agglomeration, multilayer growth, or surface etching. Our recent research developed a two-step functionalization approach utilizing exposure of the oxide materials to prop-2-ynoic acid (HC≡C-COOH, prop-2-ynoic acid) in the gas phase as a first step, followed by second step of post-modification exploiting the created C≡C to introduce any pre-designed functionality to the surface via Cu(I)-catalyzed "click" chemistry with azides (R-N$_3$). More importantly, this approach requires no additional presence of the copper catalyst for nanostructured CuO due to the reduction of surface copper from prop-2-ynoic acid modification. As a result, the second step of this functionalization can be achieved through self-catalyzed cycloaddition with gas-phase species. The morphology preservation and selective covalent attachment of the carboxylic acid onto the metal oxide surfaces have been confirmed by the combination of microscopic and spectroscopic investigations including scanning electron microscopy (SEM), X-ray photoelectron spectroscopy (XPS), and solid-state nuclear magnetic resonance spectroscopy (ss-NMR) that were used to follow the process and to compare with the traditional liquid-phase modification schemes. Vienna Ab Initio Simulation Package (VASP) calculations were used to explore the reaction mechanism and key intermediates.

SS-TuP-6 XPS Study of the Gas Cluster Ion Beam Sputtering of PTFE and Oxygen-treated PTFE, *Bing Luo*, University of Minnesota

The XPS depth profiling results of polytetrafluoroethylene (PTFE) and oxygen-treated PTFE using monoatomic argon sputtering and gas cluster ion beam (GCIB) sputtering are reported. We evaluated the degrees of surface damage using these two sputtering methods. We found a mild surface damage under GCIB sputtering. On the non-sputtered PTFE surface, only CF$_2$ was present. After GCIB sputtering, CF$_3$ and CF groups were detected. Consistent with the results in the literature, monoatomic Ar sputtering induced a higher degree of damage; the CF$_3$ and CF levels were much higher than those obtained in the GCIB sputtering. The GCIB sputtering of the oxygen-treated PTFE samples revealed that the oxidation layer was mainly located in the top 10 nm. Below 10 nm, the oxygen content became insignificant. Analyzing the distribution of various carbon-fluorine species and comparing to the untreated samples indicated that in the layer from 10 to 60 nm, the PTFE composition or structure was altered by the oxygen treatment, and even at the depth of 120 nm, the property of the PTFE was affected by the oxygen treatment.

SS-TuP-7 Ultra-high Resolution Imaging of Polymers using Atomic Force Microscopy: Structure and Property at Nanoscale, *V Korolkov*, Oxford Instruments-Asylum Research; *A Summerfield*, University of Manchester, UK; *A Murphy, D Amabilino*, University of Nottingham, UK; *P Beton*, The University of Nottingham, UK; *M Kocun, **Roger Proksch***, Oxford Instruments-Asylum Research

Polymers, both synthetic and natural, are ubiquitous materials whose properties are strongly influenced by packing, conformation, and monomer composition of individual macromolecules. The ability to acquire real-space images of the microstructure of these materials with molecular-scale resolution is required to advance the understanding and control of their local ordering, a key element in the precise engineering of polymer properties. Real-space images of polymers with sub-molecular resolution could provide valuable insights into the relationship between morphology and functionality of polymers, but their acquisition is problematic due to perceived limitations in atomic force microscopy (AFM).

Here we show that individual polymer chains and sub-molecular resolution may be achieved using AFM under ambient conditions through the low-amplitude (≤ 1 nm) excitation of higher eigenmodes[1] of a cantilever on a range of commercial polymers (polythiophenes (PTs), polytetrafluoroethylene (PTFE), polyethylene(PE)). We have used this new approach to characterize both single strands of polymers adsorbed on surfaces as well as bulk semi-crystalline samples with Angstrom resolution. For example, on the surface of a spin-coated PT thin film, in which the thiophene groups are perpendicular to the interface, we resolve terminal CH3-groups in a square arrangement with a lattice constant 5.5A from which we can identify abrupt boundaries and also regions with more slowly varying disorder, which allow comparison with proposed models of PT domains. At the same time, bimodal tapping or AM-FM imaging[2] enables modulus mapping on a wide range of polymer materials. Furthermore, molecular-level spatial resolution was achieved with AM-FM imaging on polymer chains in ambient conditions and revealed chain spacing and conformation predicted by theory and other experimental methods.

Our results highlight the important role for high-resolution AFM in determining the properties of polymer strands and thin films of technological relevance, and we anticipate future progress in correlating device performance with structural properties at the sub-molecular scale based on this technique.

[1]Korolkov et al., Nat. Comm., 2019

[2]Kocun et al., ACS Nano, 2017

SS-TuP-9 Determining the Surface Electrical Potential at the Air/Water Interface, *Tehseen Adel, S Baumler, H Allen*, The Ohio State University

Several biological and chemical processes directly relate to the organization of molecules at the liquid surface. The surface electric potential across the air/liquid interface provides insight into the molecular organization and propagation of electrical fields by these surface molecules. Using a homemade Air Ionizing Surface Electrical Potential instrument, we measure the surface electrical potential of water, several pure solvents, and inorganic electrolyte solutions without disruption to the liquid surface. Alpha particle radiation from an ionizing source reduces the resistivity of the air gap above the liquid sample, establishing a closed electrical circuit for voltage measurements. From the measured surface potential, we show (i) the orientation of interfacial solvent molecules in pure solvents, and (ii) ascertain the propensity of specific aqueous ions with respect to the air/solution boundary.

SS-TuP-10 Surface Photovoltage Studies of UV-driven Hydrophilic Flipping in Polysulfone Thin Films, *John Reeks, N Posinski*, Texas Christian University; *T Haun*, Home School High School Student; *H Hilton*, Texas Christian University; *A Dorward*, Washington and Lee University; *E Bormashenko*, Ariel University, Israel; *Y Strzhemechny*, Texas Christian University

It has been shown in previous studies that hydrophobic surfaces of polysulfone flip to become hydrophilic upon exposure to UV radiation. The exact mechanisms driving this phenomenon are not completely understood. We suggest that elucidation of the surface charge transport phenomena of the as-deposited and UV-irradiated polysulfone could explicate the conversion mechanism and thus contribute to the improved applications of polysulfone on the micro- and nanoscale for novel applications in microfluidics and biophysics. To investigate the UV-driven hydrophilic flipping we performed surface photovoltage (SPV) studies on thin polysulfone films spin-cast on silicon substrates. Since SPV is sensitive to buried interfaces, the resulting spectra are expected to be comprised of features originating not only from the polysulfone films, but also from the silicon wafer and the silicon oxide layer beneath the polymer films. Thereby, to identify the signal germane to polysulfone proper, we employed in our studies polysulfone films of varying and controllable thicknesses to be probed with SPV spectroscopy as well as SPV transient experiments. SPV measurements on Si substrates acted as a control for comparison. Our experiments revealed that SPV yield is significantly affected by the polysulfone films. In particular, we observed significant polarity reversal in the SPV transients in the samples with polysulfone films, whereas SPV spectra indicated transitions at 1.1-1.5 eV appearing in the polysulfone layers. We also report on the comparison of the SPV response in the as-deposited and UV-irradiated polysulfone samples.

SS-TuP-11 Tuning Spontaneous Supramolecular Assembly *via* Manipulation of Intermolecular Forces and Growth Environment, *Ryan Brown*, Clarkson University

This poster will detail the initial experiments attempting to exploit non-equilibrium growth conditions to manipulate the spontaneous assembly of functionalized porphyrin molecules at the solid interface. Rapid evaporation of a solution can be considered a non-equilibrium growth environment, one in which a supersaturated thin film is produced and which can result in the formation of metastable supramolecular structures. Our research program seeks to manipulate the frequency and nature of the

metastable structures produced in this process by varying the chemical functional groups on a porphyrin ring (and thus intermolecular interactions), the solid substrate (and thus molecule-substrate interactions), and the deposition conditions (varying the rpm and solvent during spin coating deposition). This research is achieved by imaging molecule-decorated surfaces with scanning tunneling microscopy to locally probe the supramolecular structures produced under a given deposition condition. Structural models are then confirmed using electronic structure theory and then applied to understand how the combination of intermolecular forces, molecule-substrate interactions, and conditions in the evaporating solvent influence spontaneous assembly behavior.

SS-TuP-12 State-Resolved Dissociative Chemisorption Dynamics with RAIRS Product Detection, *Laurin Joseph, S Shepardson-Fungairino, A Utz,* Tufts University

State-Resolved Dissociative Chemisorption Dynamics with RAIRS Product Detection

Laurin Joseph, Sally Shepardson-Fungairino, and Arthur Utz

State-resolved molecular beam molecular beam experiments use energy and quantum-state selected reactants to understand how specific molecular motions (molecular vibration, rotation, and translation) promote transition state access and chemical reactivity. They also generate experimental data that serve as rigorous benchmarks for DFT-based predictions of reaction barriers and dynamics.

We are currently updating one of our differentially pumped molecular beam reaction chambers to incorporate Reflection Absorption Infrared Spectroscopy (RAIRS) detection of surface-bound reaction products. This capability will allow for real-time, coverage-dependent studies of the reactions occurring on metal surfaces, will provide structural fingerprints of reaction products, and will open the door to the study of larger, more chemically complex, reactant molecules. This poster will survey our progress to date and present preliminary reactivity data for methanol dissociation on a Ru(0001) surface.

SS-TuP-13 The Two-faced Role of Steps in the Isotopic Scrambling of Hydrogen on Pt, *Richard van Lent, L Juurlink,* Leiden University, Netherlands

The simplest heterogeneously catalyzed reaction possible is isotopic scrambling of hydrogen:

$H_2 + D_2 \rightarrow 2\ HD$
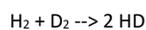
On Pt, this reaction occurs by dissociative adsorption of H_2 and D_2, mixing of H and D atoms on the surface, and recombination to form the three isotopologues, H_2, D_2, and HD. Full isotopic scrambling would lead to a product ratio of 1:1:2.

Step edges are well-known to enhance dissociative adsorption, especially at low impact energies. However, it is unknown whether subsequent diffusion and desorption only occur along the steps or involves diffusion onto terraces. We study this by combining supersonic molecular beam techniques with a curved Pt single crystal surface with straight A and B type step edges, c-Pt(111)[1-10]31^0. At a high surface temperature, we probe HD formation, spatially resolved, along the curved surface by impinging a 50:50 mixture of low energy H_2 and D_2. HD formation tracks the trend in dissociation: higher step densities yield higher HD formation. However, relatively, HD formation does not increase as rapidly as the dissociation probability. We explain why the (111) terraces are more selective toward HD formation and show that anisotropic diffusion affects isotopic scrambling.

SS-TuP-14 It's Not just the Defects - How Terrace Symmetry Impacts H_2O Adsorption at Ag Step Edges, *S Auras, Ludo Juurlink,* Leiden University, Netherlands

We investigate water desorption from hydrophobic surfaces using two curved Ag single crystals centered at (111) and (001) apices. On these types of crystals the step density gradually increases along the curvature, allowing us to probe large ranges of surface structures in between the (001), (111) and (110) planes. Subtle differences in desorption of submonolayer water coverages point toward structure dependencies in water cluster nucleation. The B-type step on hydrophobic Ag binds water structures more strongly than adjacent (111) planes, causing preferred nucleation at steps. This driving force for step-induced nucleation is smaller for A-type steps on(111) terraces. The A'-type step flanked by (001) terraces shows no indication of preferred adsorption to steps. Extrapolation to the (311) surface, not contained within either curved surface, demonstrates that both A- and A'-type steps can be regarded

chemically identical for water desorption. The different trends in desorption temperature on the two crystals can thus be attributed to stronger water adsorption at (001) planes than at (111) planes and identical to adsorption at the step. These results show that our approach to studying the structure dependence of water desorption is sensitive to variations in desorption energy smaller than 'chemical accuracy', i.e.1 kcal/mol.

SS-TuP-15 Hydration Lubrication Between Hydrophobic and Hydrophilic Surfaces, *Nir Kampf, I Rosenhek-Goldian, W Lin, J Klein,* Weizmann Institute of Science, Israel

How water rearrange above large stable, smooth, highly hydrophobic surface? We addressed this question by directly measure normal forces and sliding friction under aqueous environment between a negatively-charged hydrophilic mica surface and a fluoropolymer (AF) hydrophobic film, using a surface force balance. The roughness of the AF film was 0.3 nm determined under water by AFM. Normal-force vs. surface-separation profiles indicate that the hydrophobic surface is highly negatively-charge, in line with previous studies and attributed to adsorbed $-OH^-$ ions. Sliding of the compressed surfaces under water or salt solution reveals remarkably low friction (friction coefficient $\mu \approx 0.003 - 0.009$) up to applied pressures of at least 50 atm. Hydration lubrication by trapped hydrated counterions between the surfaces is well explained this efficient lubrication, exist in systems like artificial implants, contact lenses, etc. Moreover, molecules that are present in the biological systems were found to adsorb on the charged hydrophobic surface, contributing to reduced friction.

Reference:

Irit Rosenhek-Goldian*; Nir Kampf*; Jacob Klein (2018). Trapped Aqueous Films Lubricate Highly Hydrophobic Surfaces. ACS Nano. 12:(10)10075-10083.

*equally contributors

SS-TuP-17 Common Errors in XPS Peak Fitting, *George H. Major,* Brigham Young University*; C Easton,* CSIRO Manufacturing*; W Skinner,* Future Industries Institute*; D Baer,* Pacific Northwest National Laboratory*; M Linford,* Brigham Young University

X-ray photoelectron spectroscopy (XPS) is the most popular method for chemically analyzing surfaces, being used in many areas of research and technology. XPS spectra have layers of information that can be extracted with proper analysis. Information ranges from a basic understanding of components (elements) present in a material to advanced peak fitting and background analysis that reveal chemical states and sample morphologies. There are many examples of good XPS peak fitting in the scientific literature. However, the process of peak fitting XPS spectra is still a mixture of art and science and in many cases have no absolutely correct fits. The peak fitting process can be affected by the instrument design and components, experimental settings, and the sample. Here, we discuss a series of common errors that regularly appear in XPS peak fitting in the literature and how to avoid them. These include: (i) not plotting the data according to the international convention with binding energy increasing to the left, (ii) presenting and interpreting data that are far too noisy to be interpretable, (iii) labeling noise as chemical components, (iv) not showing the original data -- only showing the synthetic (fit) peaks and their sum, (v) not showing any background in a fit, (vi) not providing the sum of the fit components, which makes it difficult for the future reader to determine the quality of a fit, (vii) having widely varying peak widths in a fit, e.g., using extremely broad and extremely narrow peaks when there is no chemical reason for doing so, (viii) having a baseline completely miss the noise/background on either side of the peak, (ix) not collecting data over a wide enough energy window to see a reasonable amount of baseline on both sides of the peak envelope, i.e., truncating the peak, (x) in a fit to a C 1s spectrum, reversing the labeling of the C-O and C=O fit components, and other mislabeling of the components in this envelope (fitting the C 1s peak envelope is well understood so these types of errors should not be made), (xi) for the most part, higher oxidation states of elements correlate with higher binding energies; unfortunately, fit components at higher binding energies are sometimes incorrectly labeled as coming from lower oxidation states, (xii) not taking spin-orbit splitting into account when it is necessary, and/or using inappropriate ratios for these pairs of peaks, and (xiii) in a comparison of related spectra, employing widely different peak widths and positions for components that are supposed to represent the same chemical state and/or using different background types or obviously different types of synthetic peaks in these spectra.

SS-TuP-18 Exploring the Extent of Hydrogen/Deuterium Exchange on Au(111) between Molecularly-bound Surface Species, *Hasan Kaleem, E Maxwell, M DePonte, J Baker, M Gillum, D Boyle, A Baber,* James Madison University

The exchange between hydrogen and deuterium atoms in molecularly-bound surface species can occur at low temperatures on Au(111). The hypothesized mechanism for the hydrogen/deuterium exchange in ethanol-OD and water is by the Grotthuss mechanism facilitated by hydrogen-bonded molecular networks on Au(111). Therefore, the molecular orientation and packing is central to this exchange. In an effort to rationalize the hypothesized mechanism and realize the extent of hydrogen/deuterium exchange at low temperatures, the co–adsorption of fully deuterated ethanol ($EtOD_6$) and water were investigated. The fragmentation pattern for $EtOD_6$ was first monitored using temperature programmed desorption (TPD), before increasing amounts of water were added to Au(111). A broad range of masses distinct to $EtOD_6$ were monitored using a mass spectrometer and desorption areas were quantified from TPD spectra. Comparing fractional coverages for hydrogen-exchanged $EtOD_6$ products suggest that hydrogen/deuterium exchange predominantly occurs through the hydrogen-bonded network.

SS-TuP-19 First–Principles Study of on-surface and Sub-surface Oxygen in Rh(111), *Kate Fanning, W Walkosz,* Lake Forest College; *J Garcia, H Iddir,* Argonne National Laboratory; *D Killelea,* Loyola University Chicago

The interaction of oxygen with metal surfaces can directly alter their properties. On-surface and sub-surface O was shown to be a precursor for oxide formation and greatly affect the reactivity of catalytic surfaces [1-4]. Using Density Functional Theory calculations, we investigate various structures of O on the (111) surface of Rh as well as the competition between oxide formation and dissolution of oxygen into Rh to form subsurface oxygen. In particular, the work focuses on identifying pathways for surface diffusion of low-coverage adsorbed atomic O between different sites on Rh(111) as well as the surface to subsurface diffusion. The obtained results are expected to further our understanding of the chemistry of transition metal surfaces.

[1] Rose, M. K.; Borg, A.; Mitsui, T.; Ogletree, D. F.; Salmeron, M. J. Chem. Phys. 2001, 115, 10927-10934.

[2] Monine, M.; Pismen, L.; Bar, M.; Or-Guil, M. J. Chem. Phys. 2002, 117, 4473-4478.

[3] Xu, Y.; Greeley, J.; Mavrikakis, M. J. Am. Chem. Soc. 2005, 127, 12823-12827.

[4] Rotermund, H. H.; Pollmann, M.; Kevrekidis, I. G.Chaos 2002, 12, 157-163.

SS-TuP-20 STM/S Study of Domain Walls and Atomic Defects on the Surface of Iron-based Superconductors, *Zhuozhi Ge, Q Zou, M Fu, L Sanjeewa, A Sefat, Z Gai,* Oak Ridge National Laboratory

Surface defects, including domain walls and individual atomic defects, can dramatically modify the properties of iron-based superconductors. However, the nature of domain walls and atomic defects on the surface of in-situ cleaved iron-based superconductors has yet to be identified. Here, we systematically investigated the surface defects on low-temperature cleaved parent and doped $BaFe_2As_2$ superconductors by scanning tunneling microscopy/spectroscopy (STM/S). STM imaging reveals two types of domain walls on parent and Ni/Co doped $BaFe_2As_2$, one as dark trench with missing atoms and the other as straightly aligned bright blobs. Two types of point defects are also identified, one intrinsically from growth or cleaving and the other induced by scanning of the STM tip. Tunneling spectroscopy shows similar surface states at about -200 meV on domain walls and the intrinsic point defects, while on the tip-induced defects there is only one peak at about -120meV.

Vacuum Technology Division
Room Union Station AB - Session VT-TuP
Vacuum Technology Poster Session

VT-TuP-1 Dynamic High Pressure Technique for Surface Analysis of Gas Sensors in Quasi-operating Condition, *Taku Suzuki, Y Adachi, I Sakaguchi,* National Institute for Materials Science (NIMS), Japan

One of the biggest problems in surface analysis of gas sensors is the pressure gap; a conventional surface analytical tool needs high vacuum (10^{-4} Pa), while gas sensors are usually employed in atmospheric pressure (10^5 Pa).This problem has been partially overcome by recent operando techniques for surface characterization. In such a operando measurements, either effective differential pumping or a pressure separation technique, which is often called a high pressure cell, are typically utilized. With those techniques, surface analytical tool can be operated in (ultra-) high vacuum while keeping the pressure in the vicinity of a sample (near) atmospheric pressure. Those techniques are obviously useful to analyze gas sensing mechanism on surfaces. However, a high-speed evacuation system is expensive and a membrane for separating pressure limits applicable analytical techniques.

Besides above-mentioned operando measurements, a dynamic high pressure (DHP) technique has been proposed to analyze a device surface in operating condition. Briefly, it is a technique of pulsed-gas injection to a sample surface. The technique seems attractive considering economical cost and possible wide range of applicability. However, the number of reports concerning DHP is quite limited, and thus, it is not clear whether DHP is useful for surface analysis of gas sensors.

In the present study, we have developed a pulsed gas injection system of pure air combined with an ultra-high vacuum chamber and a fast pressure transducer. The pressure at the sample position reached at about 10^3 Pa and 10^4 Pa with pulse width of 10 ms and 100 ms, respectively, with the inlet pressure of 1 MPa. The background pressure was below 10^{-2} Pa with pulse width of 10 ms except for the duration of 1 s after the gas injection. We further developed a gas sensor measurement system combined with the pulsed gas injection system. In our preliminary experiment using a W-ZnO thin film gas sensor, we successfully observed substantial change of electric resistance with introducing the pulsed pure air by using a lock-in technique.

VT-TuP-2 Fundamental Study for Practical Applications of Ti-Zr-V NEG Coating to General Vacuum Systems, *Makoto Okano, A Niwata, S Kitamura,* JEOL Ltd., Japan; *Y Tanimoto, X Jin, M Yamamoto, T Honda,* High Energy Accelerator Research Organization (KEK), Tsukuba, Japan

Modifying the properties of surfaces has become essential to obtain a desired function in various ultra high vacuum (UHV) systems. Among such techniques, Ti-Zr-V non-evaporable getter (NEG) coating, originally developed at CERN[1,2] and being widely applied to particle accelerators, is one of the most promising functional coatings, as it provides high effective pumping speeds, low outgassing rates, and low secondary electron yields. Since these desirable properties are beneficial in any UHV systems, there has been an increasing demand for its widespread availability. Furthermore, NEG coating is expected to maintain UHV conditions in power-less situations; for example, its application to electron microscopes might enable long-sustained transportation and quick recovery to UHV. For these practical applications to general vacuum systems, we have started a fundamental study on NEG coatings, where the vacuum properties are measured by a build-up method and the durability of the pumping capacity is examined by repetitive cycles of air-exposure and activation. In order to establish a technique to deposit high-performance films on various vacuum chambers by magnetron sputtering, the coated surfaces are characterized by scanning electron microscope (SEM), energy dispersive X-ray spectrometry (EDS), and X-ray diffraction (XRD). The test tubes used in the build-up experiment are made of 304 stainless steel and measures 50 mm in diameter and 300 mm in length. One tube is coated with 0.7um Ti-Zr-V films and the other is uncoated. After 24 hours of stopping the sputter ion pump (SIP), the pressure in the uncoated tube increased from 2E-8Pa to 3E-6Pa, while the increase was suppressed from 6E-9 Pa to 1E-8Pa in the coated tube. Even after an additional build-up for 10 days, the coated tube was maintained under UHV conditions (7E-6Pa), and the pressure was recovered to 5E-8Pa in 5 hours after switching on the SIP. A comparison by residual gas analysis after the 24-hour build-up showed that the NEG coating improved 360-times for CO and 100-times for H_2. These results suggest a feasibility of the transportation of UHV systems without electricity. The presentation will include preliminary results of film

characterization by the surface analyses, as well as pumping properties of the NEG coating.

References

1) C. Benvenuti et al., Vacuum 60 (2001) 57.

2) P. Chiggiato and P. Costa Pinto, Thin Solid Films 515 (2006) 382.

VT-TuP-3 Fabrication and Characterization of a Variable Conductance Vacuum Valve to Control Pressure Level for a High Vacuum System, *Han Wook Song*, *S Woo*, Korea Research Institute of Standards and Science, Republic of Korea

Fabrication of a semiconductor device requires a high precision and a high degree of cleanliness. For this reason, the semiconductor device is manufactured in a state in which the contact of the foreign substances contained in the air is completely blocked, that is, in a vacuum state (approximately around 0.1 Pa.) To adjust the required vacuum level, some apparatus such as a needle valve, a gate valve, and a butterfly valve were used to control the gas flow. Recently, we developed a variable-conductance vacuum valve to control the inlet pressure for vacuum chamber, which was modified from optical iris used in optics. The present conductance variable valve is characterized in that the conductive tuck adjusting portion and the conductance operating portion employing the iris structure do not have a physically contacted or coupled structure. And the housing has no mounting holes, fastening holes, or the like for coupling the conductance operating portions, so it has a conductance variable function that can completely block the fluid leakage of the valve without any separate parts such as packing, sealing, and O-ring. The guide section of the housing will have a first magnetic body, while the conductance control unit will have a second magnetic body in the mounting hole. Therefore, when the first body and the second body are moved in a circular direction by the attraction force, the first body within the guide unit also moves in a circular direction. The cross sectional area of housing and the conductance of fluid are proportional. When using the manufactured variable valve, it showed 2% reproducibility and 0.5% repeatability in pressure generation. In the future, we will make and evaluate a large variable valve that can be applied to high vacuum systems.

VT-TuP-4 Hellum Gas Transmission Rate of Elastomer Seal with a Back-up Ring Seal, *Masaharu Miki*, EM Technical Lab Inc., Japan; *S Nowatari, H Hanada*, IIDA Co., Ltd, Japan

Hellum gas transmission rate of elastomer seal with a back-up ring seal was studied using the metal-sealed Hellum leak detector. Three kinds of samples were prepared. One is an elastomer seal (JIS B 2401 V40) without a back-up ring seal. Second is the same size elastomer seal with a back-up ring seal which adheres to the atmospheric-side surface of the elastomer seal and is made of some resin. The last is the same one with a back-up ring seal except the seal surface of the back-up ring seal is not flat but having some structure. Hellum gas transmission rate was measured and evaluated. It was found that the elastomer seal with the back-up ring seal has very low Hellum gas transmission rate, which is about less than 10% of the case without a back-up ring seal. It is like the case of a metal seal. On the other hand, the difference of the seal surface of the back-up ring seals was not found. Anyway, the elastomer seal with the back-up ring seal must be useful as seals to make vacuum chambers up-grade which structure cannot permit to use any metal seals. Pumping-down curves on total vacuum pressure and residual gas pressure (O_2, H_2O , etc.) in a vacuum chamber using the elastomer seal with the back-up ring seal are under investigation.

VT-TuP-5 Improved NEG Sputter Deposition System, *Philip Adderley*, *M Stutzman*, Jefferson Lab

Jefferson Lab been using a DC sputtering system to coat the beampipe with a Ti-Zr-V non-evaporable getter coating for 20 years. A similar system has also been used to sputter coat large diameter chambers with ultimate pressures aproaching XHV(1). The approaching upgrade of the Jefferson Lab CEBAF injector will use NEG coated beampipes of varied diameters for the first 30 meters of the machine. We describe the improvements that are being made to the sputtering system to improve stability, increase monitoring capabilities, and improve NEG film adhesion and morphology.

1) M.L. Stutzman, P.A. Adderley, A.A. Mamun and M. Poelker, J. Vac. Sci. Technol. A **36** 031603 (2018).

VT-TuP-6 Concepts for Reduced Load UHV Sealing Applications, *Ryan McCall*, Technetics Group

Designing a robust vacuum connection that can deliver UHV or XHV leak rates, withstand high temperature bake-outs and minimize hardware/bolting size can be difficult to achieve. The design process is complicated even further with Aluminum flanges or when a large diameter or shaped seal is required.

This presentation will review UHV metal sealing concepts and will detail a seal option that significantly reduces seating load by concentrating contact stress to a small area machined into the seal surface. This combination of load concentration and material selection allows for a helium tight seal with much less load than a traditional metal seal without damaging the corresponding flanges and hardware. The resilient seal loading mechanism also allows the seal to perform well in temperature cycles or bake-outs.

VT-TuP-7 Quantitative Gas Analysis with Quadrupole Mass Spectrometers - Comparison and Limitations, *Gregory Thier*, *L Kephart*, Extrel CMS; *T Whitmore*, Henniker Scientific

There are many factors to consider when comparing the overall suitability of different quadrupole-based gas analyzers for a given application. These can be categorized into two main areas, inlet/interface suitability and quadrupole mass analyzer suitability.

The suitability of the quadrupole mass spectrometer determines very important figures of merit such as precision, stability and detection limit. The quadrupole mass spectrometer includes the ionization method, the transmission characteristics, and the quality of the driving electronics.

Unfortunately, these figures of merit are often misrepresented in the commercial literature and it's this confusion which we seek to address and clarify in this document by making a direct comparison between two different classes of quadrupole analyzers; a typical 6mm rod diameter RGA type instrument typical of many currently on the market, and a higher performance 19mm rod diameter quadrupole analyzer, typical of high end analytical analyzers used in research and industry. We compare these with nominally identical inlet/transfer conditions, so that only the mass spectrometer performance is under consideration. In doing so, we present a direct comparison as it relates the various figures of merit and attempt to remove some of the mystery surrounding confusing analyzer specifications so that potential users of this powerful analytical technique may query manufacturer specifications and therefore make more informed decisions.

The specifications that we will discuss are:

- Detection Limit (minimum and maximum detectable concentration)

- Speed of Analysis (measurement speed and response time)

- Analysis Precision (repeatability of measurements)

- Analysis Stability (long-term instrument stability)

- Dynamic Range (comparison of largest and smallest detectable signals)

We will study the above by assessing and comparing the performance of two instruments, the MAX300-CAT and the MAX300-LG. The MAX300-CAT is typical of the high-end RGA based gas analyzers, based upon 6mm quadrupole rod technology, whereas the MAX300-LG is a higher performing analyzer based on 19mm quadrupole rod technology and high-performance electronics.

VT-TuP-8 Recent Developments of Home-made UHV SPM Systems and their Applications, *Qing Huan*, *Z Wu, R Ma, G He, Z Gao, L Bao, J Yuan, K Jin, H Gao*, Institute of Physics CAS, China

Scanning probe microscope (SPM) is a powerful tool for studying physical and chemical processes at single molecular/atomic level. The first part of this report will introduce our R&D progresses on UHV-SPM systems, which includes the update of a 4-probe STM, Variable-temperature STM, Low-temperature SPM combined with MBE and optical accesses, and Low-temperature SPM combined with PLD et. al. The second part will mainly introduce some research works on graphene, organic functional molecules and so on which are carried out on these home-made systems.

VT-TuP-9 An Experimentally Backed Modeling of NEG Pump Operation During Saturation, *Derek Hammar*, Coe College; *Y Lushtak*, Cornell University

Non-Evaporable Getter (NEG) pumps are increasingly common in particle accelerator applications because of their small size and their strong performance for hydrogen, the principal UHV gas.

However, these pumps present a challenge to vacuum system design because their complicated geometry results in unreasonably complicated vacuum simulations. This

project seeks to build 3D

models of NEG pumps and their environments in AutoDesk Inventor and simulate their performance

in MolFlow, creating a database to NEG performance under various installation geometries and

attempting to simplify the pump geometry without sacrificing simulation accuracy. Key results are

verified experimentally

VT-TuP-10 3D printed Mini-Channel Plates – Vacuum Compatibility and Detector Performance, *Maram Alnahhas*, J Moore, Robot Nose Corporation

Conventional production of microchannel plates (MCPs) produces linear channels. Our simulations promise a significant improvement in time resolution by changing the geometry of the channels from straight to a zig-zag (Z) configuration, which drives the electrons to land on a specific surface in each gain stage, yielding higher time resolution. The sensitivity is improved as well by controlling the outer shape of the pores; replacing the circular pore pattern with hexagon or square will increase the open area ratio for the same MCP diameter. 3D printing MCPs not only enables this Z channel approach, but is a cost-effective method to produce charged particle detectors.

3dMCPs were created using a 70-micron resolution stereolithography printer. Both linear and Z channels were printed with 30:1 length to diameter (l/d) ratio. Graphite and other dopants have been used to change the resistivity of the printed material. In principle, the 3dMCP can then be coated for secondary emissions using ALD technology. Optical microscopy of the 3dMCP and its cross-section show that good uniformity can be attained throughout once the process was optimized.

To facilitate low vacuum flow testing of the 3dMCPs, a microcontroller based multi-vacuum gauge has been constructed. This device fits on a 2.75" Conflat flange with a built-in pressure gauge and OLED display. The gauges chosen are a Pirani pressure sensor calibrated with a capacitance manometer. To digitize the signals and establish serial connections between the electrical parts, the Trinket M0 MCU was used with a built-in 12-bit ADC and a reference voltage of 3.3v. I have also designed an enclosure that could easily attach to a flange.

An apparatus was built to measure the gain and pulse output characteristics of the MCPs. TauZero (τ0) consists of an ultrahigh vacuum chamber with 2kV electron and 20kV Ga^+ guns directed at multiple test 3dMCPs. The turbo pumped vacuum system is vibrationally isolated. τ0's electronics suite includes a 6 ½ digit DMM, 16 GHz digital oscilloscope, spectrum analyzer, a time-to-digital converter with 12ps resolution, and a digitizer with pulse height analysis software.

One of the main concerns regarding 3d printed materials is whether the plastic used will contaminate a high vacuum system. 3dMCPs were outgassed in a vacuum chamber while monitoring with a residual gas analyzer to collect data during the outgassing process. Vacuum did not damage the 3dMCPs and a drop of volatiles over 24 hours was measured. We concluded that the 3dMCPs are high vacuum compatible.

2D Materials

Room A216 - Session 2D+AS+MI+NS-WeM

2D Materials Characterization by Scanning Probe Microscopy and Spectroscopy

Moderator: Ivan Oleynik, University of South Florida

8:00am 2D+AS+MI+NS-WeM-1 Plasmon Induced Excitation of Doublet Emission at the Single Molecule Level, *Alberto Martin-Jimenez, K Lauwaet,* IMDEA Nanoscience, Spain*; P Merino, J Martinez,* ICMM-CSIC, Spain*; R Miranda, R Otero,* IMDEA Nanoscience, Spain

In this contribution we report a careful investigation of the topographic, electronic, and opto-electronic properties of electronically decoupled C60 nanocrystals by means of Scanning Tunneling Microscopy (STM), Scanning Tunneling Spectroscopy (STS), STM induced Light Emission (STM-LE), and Density Functional Theory (DFT), at the single molecule level. We have observed that depending on the tunneling parameters, we are able to reversibly switch from a broad plasmonic spectrum to a series of very sharp molecular resonances of 10meV width. Based on our STS data and DFT calculations we have reached a model to explain the molecular light emission of the C60 nanocrystals. We demonstrate that the emission arises from the recombination of a doublet exciton of negatively charged molecules (anions). Our results will contribute to the general understanding of the physical mechanisms involved in the light emission of organic molecules. They may also be of importance for applications such as single photon emitters or quantum computing, since future devices may need to be able to switch chromaticity in a controlled fashion.

8:20am 2D+AS+MI+NS-WeM-2 Silicene like Domains on IrSi$_3$ Crystallites, *Nuri Oncel, D Cakir, F Fatima, D Nicholls,* University of North Dakota

Recently, silicene, the graphene equivalent of silicon, has attracted a lot of attention due to its compatibility with Si-based electronics. So far, silicene has been epitaxially grown on various crystalline surfaces such as Ag(110), Ag(111), Ir(111), ZrB$_2$(0001) and Au(110) substrates. Here, we present a new method to grow silicene via high temperature surface reconstruction of hexagonal IrSi$_3$ nanocrystals. The h-IrSi$_3$ nanocrystals are formed by annealing thin Ir layers on Si(111) surface. A detailed analysis of the STM images shows the formation of silicene like domains on the surface of some of the IrSi$_3$ crystallites. We studied both morphology and electronic properties of these domains by using both scanning tunneling microscopy/spectroscopy and first-principles calculation methods.

8:40am 2D+AS+MI+NS-WeM-3 Interfacial and Topological Superconductivity in 2D Layers Studied by Spin-Resolved Scanning Tunneling Spectroscopy, *Roland Wiesendanger,* University of Hamburg, Germany **INVITED**

In this presentation, we will first focus on interfacial superconductivity in novel types of heterostructures. In particular, we will present a low-temperature SP-STS study of ultrathin FeTe1-xSex (x = 0, 0.5) films grown on prototypical Bi-based bulk topological insulators. We observe fully developed U-shaped superconducting gaps in FeTe0.5Se0.5 layers of one unit cell (UC) thickness with a transition temperature (Tc) of ~11 K, close to the one of the corresponding bulk system (Tc ~ 14.5 K) [1]. Surprisingly, we also find clear evidence for superconductivity up to Tc ~ 6 K for one UC thick FeTe layers grown on Bi2Te3 substrates [2], in contrast to the non-superconducting FeTe bulk compound which exhibits bicollinear antiferromagnetic (AFM) order in a wide temperature range up to 70 K. Even more surprisingly, detailed investigations of the atomic-scale spin-resolved local density of states by SP-STS reveal that superconductivity in one UC layers of FeTe grown on Bi2Te3 appears to spatially coexist with bi-collinear AFM order. By using 3D-vector-resolved SP-STM techniques [3] we find an unusual reorientation of the diagonal double-stripe spin structure at Fe1+yTe thin film surfaces [4]. Moreover, variable-temperature SP-STM studies [5] reveal an enhanced Néel temperature for AFM spin ordering of the ultrathin FeTe films grown on topological insulators [6]. These findings open novel perspectives for theoretical studies of competing orders in Fe-based superconductors as well as for experimental investigations of exotic phases in heterostructures of topological insulators and superconducting layers.

In a second part, we will address experimental and theoretical studies of monolayer topological superconductivity and chiral Majorana edge modes in model-type 2D magnetic Fe islands on elemental superconducting Re [7]. In particular, we demonstrate that interface engineering by an atomically thin oxide layer is crucial for driving the studied hybrid system into a topologically non-trivial state as confirmed by theoretical calculations of the topological invariant, the Chern number.

This work is supported by the EU via the ERC Advanced Grant No. 786020 "ADMIRE".

[1] A. Kamlapure et al., Phys. Rev. B 95, 104509 (2017).

[2] S. Manna et al., Nature Commun. 8, 14074 (2017).

[3] S. Meckler et al., Rev. Sci. Instrum. 80, 023708 (2009).

[4] T. Hänke et al., Nature Commun. 8, 13939 (2017).

[5] J. Warmuth et al., NPG Quantum Materials 3, 21 (2018).

[6] U. R. Singh et al., Phys. Rev. B 97, 144513 (2018).

[7] A. Palacio-Morales, E. Mascot, S. Cocklin, H. Kim, S. Rachel, D. K. Morr, and R. Wiesendanger, arXiv:1809.04503 (2018).

9:20am 2D+AS+MI+NS-WeM-5 Geometric Imaging of Borophene Polymorphs, *Xiaolong Liu,* Northwestern University*; L Wang,* Rice University*; S Li, M Rahn,* Northwestern University*; B Yakobson,* Rice University*; M Hersam,* Northwestern University

Two-dimensional (2D) boron, known as borophene, has recently been experimentally realized[1,2] revealing a number of polymorphic structures. A common characteristic of those borophene polymorphs is the presence of hollow-hexagons (HH) in an otherwise triangular lattice. The vast number of possible HH lattices underlies the polymorphic nature of borophene. Superlattices of HHs could be further realized when borophene phases periodically intermix in the form of line defects[3]. While scanning tunneling microscopy (STM) of borophene with conventional metal probes has revealed key features of borophene, significant ambiguity of the exact atomic lattice structure exists due to the convolution of electronic and structural details. With CO-functionalized atomic force microscopy, we unambiguously resolve the HH lattice and reveal features corresponding to B-B covalent bonds[4] that are supported by numerical simulations. We further show that CO-functionalized STM is an equivalent but more accessible technique for HH imaging, allowing us to assemble a growth phase diagram of borophene involving non-rotated, 30°-rotated and randomly rotated borophene phases on Ag(111), confirming the $v_{1/5}$ and $v_{1/6}$ models as the unifying structures for all observed phases. In particular, a transition from rotationally commensurate to incommensurate phases is observed at high growth temperatures, corroborating the chemically discrete nature of borophene.

*Current affiliation of Xiaolong Liu: Kavli Postdoc Fellow, LASSP, Cornell University

1. A. J. Mannix, X.-F. Zhou, B. Kiraly, J. D. Wood, D. Alducin, B. D. Myers, X. Liu, B. L. Fisher, U. Santiago, J. R. Guest, M. J. Yacaman, A. Ponce, A. R. Oganov, M. C. Hersam, N. P. Guisinger, *Science* **350**, 1513–1516 (2015).

2. B. Feng, J. Zhang, Q. Zhong, W. Li, S. Li, H. Li, P. Cheng, S. Meng, L. Chen, K. Wu, *Nat. Chem.* **8**, 563–568 (2016).

3. X. Liu, Z. Zhang, L. Wang, B. I. Yakobson, and M. C. Hersam, *Nat. Mater.* **17**, 783–788 (2018).

4. X. Liu, L. Wang, S. Li, M. S. Rahn, B. I. Yakobson, and M. C. Hersam, *Nat. Commun.* **10**, 1642 (2019).

9:40am 2D+AS+MI+NS-WeM-6 Atomic Manipulation of Defects in the Layered Semiconductor 2H-MoTe$_2$, *Sara Mueller, S Deng,* The Ohio State University*; B St. Laurent,* University of New Hampshire*; Y Wang, W Windl,* The Ohio State University*; S Hollen,* University of New Hampshire*; J Gupta,* The Ohio State University

Here we present a charge control of native defects in the bulk transition metal dichalcogenide, MoTe$_2$ by scanning tunneling microscopy (STM). Bulk MoTe$_2$ was cleaved at room temperature in ultrahigh vacuum and imaged with a cut PtIr tip at 9K. Native defects in the MoTe$_2$ are present throughout the sample and image with complex structure. In topographic imaging, the long-range protrusion of a bright defect indicates the species is charged and we image the defects at different depths below the surface. They present with an ionization feature in tunneling spectroscopic mapping which indicates that the charge state of this defect can be manipulated by the band bending caused by the tip. Voltage pulses from the tip migrate the subsurface defects to the surface layer. The migrated defects present with the same spectroscopic signature as native surface defects. We also present DFT results that we use to clarify the identification of these native defects and energy barriers for migration between layers of 2H-MoTe$_2$.

11:00am 2D+AS+MI+NS-WeM-10 Scanning Tunneling Microscopy and Spectroscopy of a Heterotriangulene-based 2D Polymer, *Zachery Enderson, H Murali, R Dasari, T Parker, S Marder, H Li, Q Dai, S Thomas, J Brédas, P First,* Georgia Institute of Technology

Covalent Organic Frameworks (COFs) and similar materials synthesized from bottom-up procedures grant scientists a means to customize a 2D material's final properties from its initial precursors. The dimethylmethylene-bridged triphenylamine (DTPA) COF is an excellent example of the unique systems one can fabricate with these techniques[1]. The DTPA COF is initially synthesized on Au(111) or Ag(111) which facilitates crystalline growth through Ullman-type coupling. With an even number of electrons per unit cell, theory predicts a semiconducting electronic structure for the COF. Further heating in vacuum selectively cleaves the dimethyl groups but leaves the framework intact. This final COF resembles an ultra-flat covalent network of triangulene molecules with enticing proposed electronic properties, which depend on how the demethylated sites are terminated. In the case of hydrogen termination at these sites, calculations indicate that the "radical" COF on a metallic substrate will be a half-metal (fully spin-polarized density of states at the fermi energy)[2]. Using a low-temperature scanning tunneling microscope, the work outlined in this talk presents new information on the electronic structure of the DTPA COF in both its intact (methylated) and radical (demethylated) forms.

[1] Bieri, Marco, Stephan Blankenburg, Milan Kivala, Carlo A. Pignedoli, Pascal Ruffieux, Klaus Müllen, and Roman Fasel. "Surface-Supported 2D Heterotriangulene Polymers." *Chem. Commun.* 47, no. 37 (2011): 10239–41. https://doi.org/10.1039/C1CC12490K .

[2] Kan, Erjun, Wei Hu, Chuanyun Xiao, Ruifeng Lu, Kaiming Deng, Jinlong Yang, and Haibin Su. "Half-Metallicity in Organic Single Porous Sheets." *Journal of the American Chemical Society* 134, no. 13 (April 4, 2012): 5718–21. https://doi.org/10.1021/ja210822c .

11:20am 2D+AS+MI+NS-WeM-11 Scanning Tunneling Microscopy Investigations of Molecules Adsrobed on Semiconducting Graphene Nanoribbons, *Sineth Premarathna, K Latt, S Hla,* Ohio University

Unlike graphene, semiconducting graphene nanoribbons poccess a band gap and they have the capability to electronic decouple the molecules from the supporting substrate. Here, we study the structural, electronic and vibrational properties of individual para-sexiphenyl molecules adsorbed on semiconducting graphene nanoribbons. The graphene nanoribbons here are grown on the surface of Au(111) using DBBA molecules as the initial building blocks. Para-sexiphenyl molecules adsorb on the graphene naribbons with their long molecular axis positioning parallel to the long axis of the graphene nanoribbons. As expected, the tunneling spectroscopy data reveal the HOMO-LUMO gap of the molecule on graphene nanoribbons much closer to their gas phase values. Moreover, teh vibration spectroscopy measurements of the molecules further provide a strong vibration mode associate with the C=C ring stretching of the molecules. This work provide single molecule level information on the electronic, vibronic and structural properties of the molecules adsorbed on vertically stacked heterostructures formed by graphene nanoribbons on Au(111) surface.

Acknowledgement: This work is supported by the DOE-BES, DE-FG02-02ER46012 grant.

11:40am 2D+AS+MI+NS-WeM-12 Molecular Flexure and Atom Trapping with Sexiphenyl Molecules by Scanning Tunneling Microscope Manipulation, *Y Zhang, Shaoze Wang, K Braun, S Hla,* Ohio University

Molecular flexure, and molecule-metal contact of para-sexiphenyl molecules on a Ag(111) surface are investigated by using low temperature scanning tunneling microscopy, and molecular manipulations. Atom trapping with sexiphenyl molecules is realized by laterally manipulating the molecules onto individual silver atoms and up to three silver atoms have been trapped. We also demonstrate breaking of a silver dimer into individual silver atoms by atom trapping. STM manipulation experiments show that the molecule-metal complexes formed by the atom trapping are mechanically stable. Moreover, lateral manipulation of a single seziphenyl across a Ag(111) atomic step highlights how the molecule moves across step-edges; the molecule can easily conform across the step and it recovers original configuration after the manipulation.

Acknowledgement: This woek is supported by the DOE-BES, DE-FG02-02ER46012 grant.

12:00pm 2D+AS+MI+NS-WeM-13 Localized Strain Effects in Spin-Polarized Density of States for 2D-MnGaN – a Room Temperature Ferromagnetic Monolayer, *Y Ma,* Ohio University; *K Meng,* The Ohio State University; *D Hunt, M Barral, V Ferrari,* CAC-CNEA, Argentina; *F Yang,* The Ohio State University; *Arthur Smith,* Ohio University

We recently demonstrated the first observation of a 2D *room-temperature-ferromagnetic monolayer* of MnGaN (2D-MnGaN) using spin-polarized scanning tunneling microscopy and spectroscopy. The sample is grown by molecular beam epitaxy on gallium nitride substrates. We resolved ferromagnetic domains using SP-STM, demonstrated magnetic hysteresis using small *out-of-plane* magnetic fields, observed magnetic rim states, and measured magnetic DOS profiles using tunneling spectroscopy which are in excellent agreement with the predicted spin-polarized & spin-split DOS peaks obtained from first-principles theory. This work was published online in December 2017 in *Nano Letters*.[1]

More recently, we are investigating the dependence of magnetization anisotropy on *in-plane* lattice strain. First of all, we have observed from the spectroscopy measurements that the position of the spin-polarized Mn DOS peak varies from spectrum to spectrum, ranging from -1.69 eV up to -1.22 eV (relative to E_Fermi). In order to investigate if these variations could be related to structural variations, we have also carried out theoretical calculations based on first principles for both isotropic and local anisotropic lattice strains. The isotropic strain case shows that the occupied-states Mn peak can indeed shift by many tenths of an eV if the 2D-MnGaN is strained *in-plane*; for example, E = -1.58 eV for the no-strain case, whereas E = -1.33 eV for tensile strain (+9.1%) and E = -2.22 eV for compressive strain (-6.0%). On the other hand, we find an opposite behavior in the local anisotropic calculation.

Using atomic resolution STM, we have also found that significant strain variations exist within the 2D-MnGaN. As compared to an ideally periodic hexagonal lattice, the 2D-MnGaN lattice displays local spacing variations, and the spacing distribution is highly non-Gaussian and may instead be characterized as *tri-modal* with the central peak matching closely the expected average for 2D-MnGaN of 5.52 Å, but with left and right peaks centered around 5.00 Å and 5.92 Å. Therefore, the Mn atoms, centered between Ga adatoms, are under highly varying strains, ranging from tensile to compressive.

By mapping the observed Mn peak energies onto theoretical energy-strain curves, we can then estimate the expected lattice parameters corresponding to particular energies and compare with the lattice spacing distribution. These results will be discussed as well as the additional discovery of a dependence of the spin anisotropy on the lattice strain.

[1] *Yingqiao Ma, Abhijit V. Chinchore, Arthur R. Smith, María Andrea Barral, and Valeria Ferrari, Nano Letters* **18***, 158 (2018).*

2D Materials
Room A226 - Session 2D+EM+MI+MN+NS+QS-WeM
Novel 2D Materials

Moderator: Phil King, University of St Andrews

8:00am 2D+EM+MI+MN+NS+QS-WeM-1 A Safari Through Thousands of Layered Materials Guided by Data Science Techniques, *Evan Reed, G Cheon,* Stanford University INVITED

We have utilized data mining approaches to elucidate over 1000 2D materials and several hundred 3D materials consisting of van der Waals bonded 1D subcomponents, or molecular wires. We find that hundreds of these 2D materials have the potential to exhibit observable piezoelectric effects, representing a new class of piezoelectrics. A further class of layered materials consists of naturally occurring vertical hetero structures, i.e. . bulk crystals that consist of stacks of chemically dissimilar van der Waals bonded layers like a 2-D super lattice. We further combine this data set with physics-based machine learning to discover the chemical composition of an additional 1000 materials that are likely to exhibit layered and two-dimensional phases but have yet to be synthesized. This includes two materials our calculations indicate can exist in distinct structures with different band gaps, expanding the short list of two-dimensional phase change materials. We find our model performs five times better than practitioners in the field at identifying layered materials and is comparable or better than professional solid-state chemists. Finally, we find that semi-supervised learning can offer benefits for materials design where labels for some of the materials are unknown.

Wednesday Morning, October 23, 2019

8:40am 2D+EM+MI+MN+NS+QS-WeM-3 2D Ferroelectric Semiconductor α-In₂Se₃ for Non-Volatile Memory Applications, *M Si, Peide Ye,* Purdue University

α-In$_2$Se$_3$ is a novel two-dimensional (2D) ferroelectric semiconductor. It has a bandgap of ~1.39 eV, room temperature ferroelectricity, the ability to maintain ferroelectricity down to a few atomic layers and the feasibility for large-area growth. Based on the ferroelectric and semiconducting nature of the material, a ferroelectric semiconductor field-effect transistor (FeS-FET) was proposed and experimentally demonstrated [1]. In the FeS-FET, a ferroelectric semiconductor is employed as the channel material while the gate insulator is the dielectric. The two non-volatile polarization states in FeS-FETs exist in the ferroelectric semiconductor channel. Therefore, a high quality amorphous gate insulator can be used instead of the common polycrystalline ferroelectric insulator for Fe-FETs. The fabricated FeS-FETs exhibit high performance with a large memory window, a high on/off ratio over 10^8, a maximum on-current of 862 μA/μm, low supply voltage with scaled gate insulator and the potential to exceed the existing Fe-FETs for non-volatile memory applications.

[1] M. Si, S. Gao, G. Qiu, J. Qin, Y. Duan, J. Jian, H. Wang, W. Wu, and P. D. Ye, "A Ferroelectric Semiconductor Field-Effect Transistor,", arXiv:1812.02933.

9:00am 2D+EM+MI+MN+NS+QS-WeM-4 *Ab initio* Informed Theory of Axis-dependent Conduction Polarity in Goniopolar Materials, *Yaxian Wang, B He, M Arguilla, N Cultrara, M Scudder, J Goldberger, J Heremans, W Windl,* The Ohio State University

NaSn$_2$As$_2$ has recently been synthesized and was found to be an exfoliatable van der Waals Zintl phase, opening new opportunities for electronic design on the few-atom-thick scale. Although the band structure may suggest a range of metal to semi-metal, it shows strong anisotropy especially in its "polarity", characterized by its dominant carrier type, which strongly affects its electronic and thermal properties. We used DFT calculations to investigate bandstructure and Fermi surface. In addition, we employed BoltzTraP code to calculate the transport behavior in in/cross-plane directions, predicting strongly anisotropic carrier transport and directionally dependent polarity –"goniopolarity" – in this layered material. It is confirmed by experimental thermopower measurements. We show from simulations on a model band structure the Fermi surface geometry origin in a single-band toy model, and we utilize the bandwidth concept from a tight-binding model to give an insight of real space orbital contributions and nature of the bonding states in this layered crystal. Based on that, additional candidate materials for goniopolarity can be proposed, and the design space for goniopolar materials in general will be defined.

9:20am 2D+EM+MI+MN+NS+QS-WeM-5 In-Plane Mechanical Properties and Strain Engineering of 2D Hybrid Organic-Inorganic Perovskites, *Qing Tu, I Spanopoulos, S Hao, C Wolverton, M Kanatzidis, G Shekhawat, V Dravid,* Northwestern University

Two-dimensional (2D) hybrid organic-inorganic perovskites (HOIPs) are new members of the 2D materials family with wide tunability, highly dynamic structural features and excellent physical properties. Mechanical strain is inevitable in 2D-HOIP-based applications due to materials processing, thermal expansion and substrate deformation. Understanding the mechanical properties and strain engineering of such functional materials are both fundamentally and practically important to achieve high performance and mechanically stable (flexible) devices. Here the in-plane mechanical properties and the impact of in-plane uniaxial tensile strain on the electronic properties of 2D lead iodide perovskites with a general formula (CH$_3$(CH$_2$)$_3$NH$_3$)$_2$(CH$_3$-NH$_3$)$_{n-1}$Pb$_n$I$_{3n+1}$ were reported for the first time. The in-plane Young's modulus and breaking strength of ultrathin 2D HOIP flakes were measured by AFM-based nanoindentation of suspended 2D HOIP membranes.[1] The in-plane Young's moduli of 2D HOIPs are smaller than that of conventional covalently bonded 2D materials like graphene and MoS$_2$ due to the much more deformable [PbI$_6$]$^{4-}$ octahedra structure. Both the Young's modulus and breaking strength first decrease and then plateau as the thickness of 2D HOIP flake increases from monolayer to 4 layers, which is attributed to interlayer slippage during deformation. Ultrathin 2D HOIPs exhibit outstanding breaking strength/Young's Modulus ratio compared to many other widely used engineering materials and polymeric flexible substrates, which renders them suitable for application into flexible electronic devices. Furthermore, the uniaxial tensile strain was found to increase the band gap of 2D HOIPs.[2] Such strain effect on the band gap of 2D HOIPs is fully reversible and depends on the structural unit of the materials. For 2D HOIP with n = 5, the strain response of the band gap can be as high as 13.3 meV/%. First-

principles simulations show that the strain response of the band gap arises from the rotation of the inorganic [PbI$_6$]$^{4-}$ octahedra and the consequential Pb-I bond stretching and increase of Pb-I-Pb angle. The observed band gap–strain relationship can be harnessed to map the local mechanical strain in 2D HOIP-based devices and allow 2D HOIPs for sensing applications.

References

[1]. Tu Q, Spanopoulos I, Yasaei P, Stoumpos CC, Kanatzidis MG, Shekhawat GS, et al. Stretching and Breaking of Ultrathin 2D Hybrid Organic–Inorganic Perovskites. ACS Nano. 2018;12(10):10347-54.

[2]. Tu Q, Spanopoulos I, Hao S, Wolverton C, Kanatzidis MG, Shekhawat GS, et al. Probing Strain-Induced Band Gap Modulation in 2D Hybrid Organic–Inorganic Perovskites. ACS Energy Letters. 2019;4(3):796-802.

9:40am 2D+EM+MI+MN+NS+QS-WeM-6 Collective Electronic States of Epitaxial Monolayer 1T-NbSe₂, *Zhuozhi Ge,* University of Wisconsin; *H Zhang, L Liu, C Yan,* West Virginia University; *M Weinert,* University of Wisconsin; *L Li,* West Virginia University

At the single layer limit, transition metal dichalcogenides (TMDs) can adopt two different structural variants depending on the anionic environment around the metal ions: the anions are arranged in trigonal prismatic fashion in the 1H polymorph, whereas in 1T the arrangement is octahedral. While bulk 1T NbSe$_2$ doesn't exist in nature, here we show that single layer 1T NbSe$_2$ polymorph can be grown by molecular beam epitaxy on epitaxial graphene/SiC(0001) substrates. A (Ö13xÖ13) Star-of-David charge density waves is observed by *in situ* scanning tunnelling microscopy, which persists above room temperature. A gap of 0.50 eV is further observed by tunnelling spectroscopy and angle resolved photoemission spectroscopy, indicating that this monolayer 1T phase of NbSe$_2$ is also a Mott insulator, similar to that of bulk 1T TaS$_2$. Our findings indicate that the presence of epitaxial constraints can generate structural configurations that are prohibited in fully-bonded TMD crystals. These findings and their implication on the collective electronic states of single layer 1T-NbSe$_2$ will be discussed at the meeting.

11:00am 2D+EM+MI+MN+NS+QS-WeM-10 Magnetic Interfaces of MnSe2 Monolayer, *Tomas Rojas, S Ulloa,* Ohio University

Until recently, 2D magnetism was thought to occur together with defects or doping on different substrates. This situation changed drastically, as intrinsic Cr-based ferromagnetic monolayer materials were discovered, namely CrI3 and Cr2Ge2Te6. A different material, MnSe2, was predicted as stable ferromagnetic monolayer by first-principles calculations, and it has been successfully grown on several substrates. In this study, the authors confirm the intrinsic ferromagnetism of the monolayer, while for thicker samples they report an interface of the MnSe2 monolayer with bulk α-MnSe(111). This phase of the material is non-magnetic, and yet the observed magnetic moments are of up to twice the value of those in the monolayer alone. In this work, we present a detailed analysis of the interactions at this interface between the two phases, using the Heyd-Scuseria-Ernzerhof hybrid functional. We have studied the effects on the electronic and magnetic structure of both phases of the material, and the dependence on the sample thickness. We study the role that strain plays at the interface, and how it affects the magnetic moments of the structure.

Supported by NSF-DMR 1508325, and Ohio Supercomputer Center .

11:20am 2D+EM+MI+MN+NS+QS-WeM-11 Orbital Design of Topological Insulators from Two-dimensional Semiconductors, *Shixuan Du,* Institute of Physics, Chinese Academy of Sciences, China

Two-dimensional (2D) materials have attracted much recent attention because they exhibit various distinct intrinsic properties/functionalities, which are, however, usually not interchangeable. Interestingly, here we propose a generic approach to convert 2D semiconductors, which are amply abundant, to 2D topological insulators (TIs), which are less available, via selective atomic adsorption and strain engineering. The approach is underlined by an orbital design principle that involves introducing an extrinsic -orbital state into the intrinsic -bands of a 2D semiconductor, so as to induce - band inversion for a TI phase, as demonstrated by tight-binding model analyses. Remarkably, based on first-principles calculations, we apply this approach to convert the semiconducting monolayer CuS and CuTe into a TI by adsorbing Na and K respectively with a proper -level energy, and CuSe into a TI by adsorbing a mixture of Na and K with a tuned -level energy or by adsorbing either Na or K on a strained CuSe with a tuned -level valence band edge. Our findings open a new door to the discovery of TIs by a predictive materials design, beyond finding a preexisting 2D TI.

This work is in collaboration with Lei Gao and Jia-Tao Sun from IoP-CAS, Gurjyot Sethi and Feng Liu from University of Utah, Yu-Yang Zhang from UCAS.

11:40am 2D+EM+MI+MN+NS+QS-WeM-12 Rotationally Controlled van der Waals Heterostructures of 2D Materials, *Emanuel Tutuc, K Kim, G Burg, H Movva,* The University of Texas at Austin **INVITED**
Heterostructures of atomic layers such as graphene, hexagonal boron-nitride, and transition metal dichalcogenides (TMDs) can serve as testbed for novel quantum phenomena in two-dimensions, and potential device applications. A key ingredient that can add a new dimension to the atomic layer heterostructures palette is the rotational control, and alignment of different two-dimensional (2D) layers. We review here an experimental technique that enables rotationally controlled heterostructures with accurate alignment of the individual layer crystal axes [1]. We illustrate the applicability of this technique to the rotationally aligned double layers of graphene [2], or TMDs [3] separated by a tunnel barrier which display resonant, energy- and momentum-conserving tunneling in vertical transport, consistent with theoretical expectations. When two 2D layers are overlaid with a relative twist, the resulting heterostructure shows a new type of periodicity associated with the moiré superlattice, which are only beginning to be systematically investigated as platform for strongly correlated electron physics. We discuss the electron transport in tunable moiré patterns realized in twisted bilayer [4], and double bilayer graphene heterostructures.

Work done in collaboration with S. K. Banerjee, L. F, Register, B. J. LeRoy, A. H. MacDonald, T. Taniguchi, and K. Watanabe.

[1] K. Kim *et al., Nano Lett.* **16**, 1989 (2016);

[2] G. W. Burg *et al., Nano Lett.* **17**, 3919 (2017); G. W. Burg *et al., Phys. Rev. Lett.* **120**, 177702 (2018).

[3] K. Kim *et al., Nano Lett.* **18**, 5967 (2018).

[4] K. Kim *et al., Proc. Natl. Acad. Sci. USA* **114**, 3364 (2017).

Atomic Scale Processing Focus Topic
Room B130 - Session AP+BI+PS+TF-WeM

Surface Reaction Analysis and Emerging Applications of Atomic Scale Processing

Moderator: Eric A. Joseph, IBM Research Division, T.J. Watson Research Center

8:00am AP+BI+PS+TF-WeM-1 Open Spaces in Al_2O_3 Film Deposited on Widegap Semiconductors Probed by Monoenergetic Positron Beams, *Akira Uedono,* University of Tsukuba, Japan*; T Nabatame,* NIMS, Japan*; W Egger, T Koschine,* Universität der Bundeswehr München, Germany*; C Hugenschmidt, M Dickmann,* Technische Universität München, Germany*; M Sumiya,* NIMS, Japan*; S Ishibashi,* AIST, Japan **INVITED**
Positron annihilation is a useful technique for characterizing vacancy-type defects in semiconductors, and it has been successfully used to detect defects in GaN. This technique is also useful for detecting open spaces in thin amorphous films deposited on semiconductor substrates. When a positron is implanted into condensed matter, it annihilates with an electron and emits two 511-keV gamma quanta. The energy distribution of the annihilation gamma rays is broadened by the momentum component of the annihilating electron-positron pair. A freely diffusing positron may be localized in a vacancy-type defect because of Coulomb repulsion from positively charged ion cores. Because the momentum distribution of the electrons in such defects differs from that of electrons in the bulk material, these defects can be detected by measuring the Doppler broadening spectra of the annihilation radiation. Because the electron density in open spaces or vacancy-type defects is lower than that in the bulk, the lifetime of positrons trapped by such regions is longer than that of positrons in the delocalized state. Thus, the measurement of the positron lifetime also provides information of open spaces and vacancies in solid. In the present work, open spaces and defects in the Al_2O_3(25 nm)/GaN structure were probed by using monoenergetic positron beams.

Al_2O_3 films were deposited on GaN by atomic layer deposition at 300°C. Temperature treatment above 800°C leads to the introduction of vacancy-type defects in GaN due to outdiffusion of atoms from GaN into Al_2O_3. The width of the damaged region was determined to be 40-50 nm from the Al_2O_3/GaN interface, and some of the vacancies were identified to act as electron trapping centers. In the Al_2O_3 film before and after annealing treatment at 300-900°C, open spaces with three different sizes were found

to coexist. The density of medium-sized open spaces started to decrease above 800°C, which was associated with the interaction between GaN and Al_2O_3. Effects of the electron trapping/detrapping processes of interface states on the flat band voltage and the defects in GaN were also discussed.

The present research suggests that the interaction between amorphous Al_2O_3 and GaN introduces not only vacancy-type defects in GaN but also changes the matrix structure of Al_2O_3 film. We also revealed that the electron trapping/detrapping processes of interface charge states are influenced by the defects introduced in GaN.

8:40am AP+BI+PS+TF-WeM-3 Surface Reaction Analyses of Atomic-layer Etching by Controlled Beam Experiments, *Kazuhiro Karahashi, T Ito, S Hamaguchi,* Osaka University, Japan
In manufacturing of modern advanced semiconductor devices such as magnetoresistive random-access memories (MRAMs), phase-change random-access memories (PRAMs), and three-dimensional integrated circuit (3D IC) devices, damage-free high-precision etching for various materials is an indispensable process technology. Halogenation of a surface layer combined with low-energy ion bombardment or ligand-exchange of organic molecules for the formation of metal complexes is a surface reaction that may be used for such highly selective etching processes with atomic-scale precision. A better understanding of surface reactions taking place during the etching process often allows one to control and optimize the process more effectively. In this study, we have developed a new surface-reaction analysis system with highly controlled beams of various species and examined surface reaction mechanisms of plasma-assisted or thermal atomic-layer etching (ALE) processes for silicon (Si), copper (Cu), and nickel (Ni) films. The beam experiment of this system offers an experimental "simulation" of actual ALE surface reactions. The system is equipped with differentially-pumped multiple beam sources that can irradiate the sample set in an ultra-high-vacuum (UHV) chamber with different types of beams, i.e., low-energy ions, thermal molecules, metastable radicals, and atomic/molecular clusters, independently. During the beam irradiation, scattered and desorbed species may be measured by a differentially pumped quadrupole mass spectrometer (QMS). Time-resolved measurements of QMS synchronized with pulsed beam irradiation facilitate detailed analysis of the beam-surface interactions. Chemical states of adsorbed species on the sample surface may be measured by X-ray photoelectron spectroscopy (XPS). In this presentation, we discuss the mechanisms of halogenated-layer formation on the Si, Cu, or Ni surfaces by their exposure to XeF2 or Cl2 gases and the removal mechanisms of halogenated species from the surface by low-energy ion irradiation or surface heating. Thermal desorption mechanisms of Cu or Ni by the metal-complex formation with organic molecules (such as diketones) from its oxidized surface are also discussed

9:00am AP+BI+PS+TF-WeM-4 Surface Reaction Analysis of Fluorine-based Reactive Ion Etching (RIE) and Atomic Layer Etching (ALE) by Molecular Dynamics (MD) Simulation, *Erin Joy Tinacba, M Isobe, K Karahashi, S Hamaguchi,* Osaka University, Japan
Plasma etching has always been a useful process in semiconductor device fabrication. There are several ways of using plasma etching such as reactive ion etching (RIE), wherein the material surface is bombarded with energetic ions while it also exposed to chemically reactive radicals from the plasma. Because of the energy provided by bombarding ions and high chemical reactivity on the surface, the surface is etched even at a relatively low temperature due to the combination of physical and chemical sputtering effects. RIE is often suited to fast etching processes of high aspect ratio structures since it can provide high etching yields. Another application of plasma etching is plasma-assisted atomic layer etching (ALE), wherein chemical and sputtering effects of typical plasma etching are separated into two steps. In a typical ALE process, the first step is an adsorption step wherein chemically reactive molecules or radicals from a plasma are used to modify the material surface. The modified monolayer or a thin layer on the material surface is then etched during the subsequent desorption step (second step) where low-energy ions bombard the surface. The etching reaction stops when the modified layer is depleted. This cycle is repeated many times until the desired etched depth is reached. The ALE process might be slow but it can provide tight control in the etch variability for sub-10 nm technology applications.

In this paper, molecular dynamic (MD) simulation is used to understand the effects of ions and radicals of high fluorine (F) content on etching reactions of silicon (Si), silicon dioxide (SiO_2), and silicon nitride (Si_3N_4), which may be observed in RIE processes based on, e.g., SF_6, C_2F_6, or NF_3 plasmas. If such a plasma is used as a radical source and ion bombardment steps by inert gas

ions are separated from the radical exposure steps, an ALE process may be performed with similar surface reactions. In typical RIE, a supply of a large amount of fluorine to the surface by increasing the flux of energetic ions containing multiple F atoms (such as SF_5^+, $C_2F_5^+$ and NF_2^+ ions) and/or by increasing a F radical flux to the surface results in high etch rates. It has been found that the etching rates by such highly fluorinated ions obtained from MD simulations are in good agreement with experimental observations and the deep fluorination of the surface accounts for their high etch rates. Although fluorine may be considered too corrosive to be used for ALE, we also analyzed by MD simulation an ALE process by fluorine-containing radicals such as NF2 and compared the results with experimental observations.

9:20am **AP+BI+PS+TF-WeM-5 Analysis of Metal Surface during Atomic Layer Etching with Gas Cluster Ion Beam and Organic Acid**, *Noriaki Toyoda*, *K Uematsu,* University of Hyogo, Japan

Surface states of metal surface after atomic layer etchings (ALE) with gas cluster ion beam (GCIB) and organic acid were investigated using surface analysis tools (mainly X-ray photoelectron microscopy). In recent years, we have reported the usage of GCIB irradiation for the removal steps of ALE. Since GCIBs are aggregates of thousands of gas atoms or molecules, the energy/atoms or energy/molecules can be easily reduced to several eV even though the total energy of GCIB is several keV. This characteristic is beneficial for low-damage irradiation. In additions, since GCIBs induce dense energy deposition, the bombarded area experiences transient high-temperature and high-pressure conditions. As a result, chemical reactions are enhanced at low-temperature. These characteristics are suitable for the removal step in ALE.

In this study, we have investigated the surface state of metal (Ni, Cu) after ALE with GCIB and organic acid using in-situ XPS. Prior to GCIB irradiation, metal surfaces were cleaned by Ar ions. Then Ni or Cu surface were exposed to acetic acids or acetylacetones. The surface layer with adsorbed organic acid on metals were removed by subsequent GCIB irradiation. The difference of the surface states of metal between Ar and O_2-GCIB irradiation are compared with in-situ XPS results. Etching mechanism by GCIB in the presence of the adsorbed organic acid will be discussed.

9:40am **AP+BI+PS+TF-WeM-6 In-situ Characterization of Growth Kinetics of Piezoelectric Films Grown by Atomic Layer Deposition Utilizing an Ultra-high Purity Process Environment**, *Nicholas Strnad,* General Technical Services, LLC*; D Potrepka,* U.S. Army Research Laboratory*; N O'Toole, B Rayner,* Kurt J. Lesker Company*; J Pulskamp,* U.S. Army Research Laboratory

Recently, $PbZr_xTi_{1-x}O_3$ (PZT) was grown by atomic layer deposition (ALD) in a piezoelectric film stack that was micro-machined into electrically actuated cantilever beams. [1] ALD PZT is a process technology that may drive 3D PiezoMEMS that utilizes piezoelectric films deposited on micro-machined sidewall structures. AlN is also a desirable piezoelectric for 3D PiezoMEMS but integration has been hampered by its sensitivity to reactive background gases resulting in oxygen contamination of several atomic percent and above. [2] Reactive background gases can also impact oxide films by skewing the non-uniformity and growth-per-cycle (GPC). Thus, individual reactor conditions play a significant role in both the growth kinetics, and resulting quality of thin films grown by ALD. To address both of these issues there exists the need for ultra-high purity (UHP) process capability. Here, we present how the transition from non-UHP to UHP process environment affects ALD AlN and the constituent oxide films in ALD PZT. The UHP process environment also enables the rapid characterization of the reaction kinetics of ALD processes by in-situ ellipsometry. The reaction kinetics of several constituent oxides for ALD PZT are presented based on empirical in-situ observations.

References

[1] Strnad, N.A. (2019) Atomic Layer Deposition of Lead Zirconate-Titanate and Other Lead-Based Perovskites (Doctoral Dissertation) https://doi.org/10.13016/8dqx-7pev

[2] Chen, Z. (2019) Thermal atomic layer deposition of aluminum nitride thin films from AlCl3 (Master's Dissertation)

11:00am **AP+BI+PS+TF-WeM-10 Nanoscale Surface Modification of Medical Devices using Accelerated Neutral Atom Beam Technology**, *Dmitry Shashkov, J Khoury, B Phok,* Exogenesis Corp.   **INVITED**

Controlling surface properties of biomaterials is vital in improving the biocompatibility of devices by enhancing integration and reducing bacterial attachment. We use Accelerated Neutral Atom Beam (ANAB) technology, a low energy accelerated particle beam gaining acceptance as a tool for nanoscale surface modification of implantable medical devices. ANAB is created by acceleration of neutral argon atoms with very low energies under vacuum which bombard a material surface, modifying it to a shallow depth of 2-3 nm. This is a non-additive technology that results in modifications of surface topography, wettability, and chemistry. These modifications are understood to be important in cell-surface interactions on implantable medical devices. Similarly, ANAB could be used to modify surfaces of medical device coatings (small molecules and proteins)., creating a native drug elution barrier. In this study, we characterize the effects of ANAB on several materials including metals (Ti, CoCr) and polymers (PEEK, PP, PVC) and measure the differential ability of eukaryotic versus prokaryotic cell attachment on these modified surfaces. We also study the ability of ANAB to create an elution barrier on a drug coating without the use of binding polymers. We identified that eukaryotic cells including mesenchymal stem cells (MSC) and osteoblasts increase attachment and proliferation on treated surfaces as measured by MTS assay and cell visualization by microscopy. MTS assay shows that by day 14, control PEEK has 9,925±1,994 cells while ANAB-treated PEEK has 88,713±6,118 cells (n=3; p<0.0014). At the same time, we find that bacterial cells including *S.aureus* and *P.aeruginosa* have a decreased ability to bind on the ANAB-treated surface. This dichotomy of cellular attachment may be attributed to the nano-scale surface topography, favoring larger eukaryotic cells while inhibiting attachment of smaller bacterial pathogens. In studies focusing on drug elution, rapamycin was spray-coated on the surface of CoCr bare metal stents and either left as control or ANAB-treated the surface of the drug. These stents were then placed in a plasma elution assay for up to 7 days. We found that untreated stents eluted off most of the drug within 24 hours, and 100% of it by 48 hours post-elution. The ANAB-treated stents, however, showed a favorable elution profile slowly releasing the drug over the 7 day period. ANAB, therefore, has many possible uses in medical device technology in increasing integration, decreasing bacterial attachment and potentially biofilm formation, and, if desired, create an elution profile for a combination drug-device without the use of binding polymers.

11:40am **AP+BI+PS+TF-WeM-12 Chemically Enhanced Patterning of Nickel for Next Generation EUV Mask**, *Xia (Gary) Sang, E Chen,* University of California, Los Angeles*; T Tronic, C Choi,* Intel Corporation*; J Chang,* University of California, Los Angeles

The ever-increasing demand in high-precision pattern definition and high-fidelity pattern transfer in the IC manufacturing industry calls for continuous advancement in lithography technology. Extreme Ultra-Violet (EUV) lithography is being widely adopted for defining sub-10 nm nodes. Due to its ideal optical properties, Ni is under active research as the future absorbing layer material in EUV masks, the profile of which determines the quality of resulting lithographic patterns. Contemporary techniques for patterning Ni rely on noble ion beam milling, which leaves considerable amounts of re-deposition on feature sidewall. Finding chemically selective patterning technique is thus of critical importance. Due to the etch-resistant nature of Nickel, removal at an atomic level is enabled by chemical modification of the surface through plasma exposure and subsequent introduction of organic ligands. Plausible chemicals are first screened by thermodynamic assessments from available databases, experiments were then conducted to validate the theoretical predictions.

Both blanket and patterned Ni thin films were studied using this reaction scheme. Organic chemistries, such as acetic acid and formic acid were first investigated to determine the feasibility of metal-organic formation through direct exposure. The efficacy of acetic acid and formic acid etching chemistries were confirmed through solution-based studies on Ni, the formation of Ni(CH3COO)2 and Ni(HCOO)2 were confirmed through mass spectrometry. Nickel oxide formation and subsequent removal were confirmed by quantifying the change in the relative intensities of peaks of metallic Ni (852.6 eV) and oxidized Ni (853.7 eV) by X-Ray Photoelectron Spectroscopy (XPS).

The chemical reactivity difference between Ni0 and Ni2+ was quantified in the work to explore the attainable etch selectivity. Due to the decrease in radical concentration and flux, vapor phase etching of metallic Ni resulted in small thickness reduction (~ 0.4 nm/cycle). It is then tested that surface modification, particularly oxidation, is capable of promoting subsequent reactions by lowering reaction energy barrier through metal oxide formation. An oxygen plasma treatment is added prior to acid vapor exposure, and this cyclic approach results in a relatively linear etch rate of ~ 2 nm/cycle, which translates to a 50:1 etching selectivity of NiO over Ni. The same cyclic approach was then applied to patterned samples, post-

etch sidewall angle of ~ 85° is measured, which closely conserves the initial feature profile (~ 87°).

12:00pm AP+BI+PS+TF-WeM-13 Surface Reactions of Low Energy Electrons and Ions with Organometallic Precursors and their Relevance to Charged Particle Deposition Processes, *Rachel Thorman,* Johns Hopkins University; *E Bilgilisoy,* FAU Erlangen-Nürnberg, Germany; *S Matsuda, L McElwee-White,* University of Florida; *D Fairbrother,* Johns Hopkins University

Focused electron beam induced deposition (FEBID) and focused ion beam induced deposition (FIBID) are nanofabrication techniques where beams of charged particles (electrons or ions) create metal-containing nanostructures by decomposing organometallic precursors in low pressure environments. Consequently, the interactions of electrons and ions with surface-bound organometallic precursors are fundamental processes in these deposition processes. Previously performed ultra-high vacuum (UHV) studies on low energy (below 100 eV) electron interactions with adsorbed precursors (e.g. $Pt(PF_3)_4$, $MeCpPtMe_3$, and $Co(CO)_3NO$) have revealed that electron-induced reactions of surface bound precursors occurs in two sequential steps: (1) an initial step characterized by precursor decomposition/deposition and partial ligand desorption followed by (2) decomposition of the residual ligands. However, a similar level of understanding does not exist for low energy ion interactions with organometallic precursors. In this presentation, I will show that a low temperature, UHV surface science approach can serve as a platform to study the reactions of both low energy electrons (500 eV) and low energy ions (<1kV Ar^+ ions) with organometallic precursors. Results from *in situ* X-ray photoelectron spectroscopy (XPS) and mass spectroscopy (MS) clearly show that low energy electron and ion-induced reactions of several surface-adsorbed species, including $(\eta^5\text{-}Cp)Fe(CO)_2Re(CO)_5$, $Ru(CO)_4I_2$, $Fe(CO)_5$, and $Co(CO)_3NO$, are markedly different. Similarly to electron-induced reactions, low-energy ion-induced reactions proceed in a two-step process with an initial decomposition step primarily characterized by ligand loss. However, ligand loss is typically must more extensive than is observed for electron-induced reactions; for example, in the case of $(\eta^5\text{-}Cp)Fe(CO)_2Re(CO)_5$ and $Fe(CO)_5$, all CO ligands desorb in this initial step. The second step in the ion induced reactions can be described as a regime primarily characterized by physical sputtering. These contrasting results are discussed in the context of different deposition mechanisms proposed for FEBID and FIBID.

Biomaterial Interfaces Division
Room A120-121 - Session BI+AS-WeM

Microbes and Fouling at Surfaces

Moderators: David G. Castner, University of Washington, Kenan Fears, U.S. Naval Research Laboratory

8:00am BI+AS-WeM-1 Hydrophilic Polysaccharides as Building Blocks for Marine Fouling-release Coatings, *Axel Rosenhahn,* V Jakobi, X Cao, W Yu, T Gnanasampanthan, R Wanka, J Schwarze, J Koc, Ruhr-University Bochum, Germany; *M Grunze,* Heidelberg University, Germany; *J Finlay, A Clare,* Newcastle University, UK; *K Hunsucker, G Swain,* Florida Institute of Technology

Hydrophilic building blocks like polyethylene glycols are powerful ingredients in modern fouling-release coatings as they are capable to reduce the attractive hydrophobic interactions of microbes with hydrophobic matrix materials such as acrylates, silicones or polyurethanes. We explored how polysaccharides with known antiadhesive and anti-inflammatory properties in medical applications reduce the adhesion of marine fouling organisms. Among the advantages of polysaccharides is their availability, biocompatibility and degradability. Based on previous work on hydrophilic coatings [1] we focused on well hydrated hyaluronans, alginates, chitosans and chondroitin sulfate building blocks. The response of marine organisms and the ability of such components to reduce attachment and facilitate easy removal is explored on grafted monolayers of polysaccharides [2], their amphiphilic derivatives [3], and in more complex coatings such as polysaccharide containing polyelectrolyte multilayers and hybrid polymers. Lab and field experiments will be compared and discussed in the light of the previous notion that uptake of soil particles frequently challenge hydrophilic polymers when used in the real ocean environment [4].

[1] A. Rosenhahn, S. Schilp, J. Kreuzer, M. Grunze, PCCP 2010, 12, 4275

[2] X. Y. Cao, M. E. Pettit, S. L. Conlan, W. Wagner, A. D. Ho, A. S. Clare, J. A. Callow, M. E. Callow, M. Grunze, A. Rosenhahn, Biomacromol. 2009, 10, 907-915.

[3]V. Jakobi, J. Schwarze, J. A. Finlay, K. A. Nolte, S. Spöllmann, H.-W. Becker, A. S. Clare, A. Rosenhahn, Biomacromol. 2018,19, 402-408.

[4] J. Koc, T. Simovich, E. Schönemann, A. Chilkoti, H. Gardner, G.W. Swain, K. Hunsucker, A. Laschewsky, A. Rosenhahn, Biofouling 2019, DOI:10.1080/08927014.2019.1611790

8:20am BI+AS-WeM-2 A Microfluidic Assay to Test the Adhesion of the Marine Bacterium *Cobetia Marina* **Under Dynamic Shear Conditions**, *Jana Schwarze, K Nolte, R Wanka, V Jakobi, A Rosenhahn,* Ruhr-University Bochum, Germany

Microfluidic environments with laminar flow are a useful tool to quantify attachment and removal of marine biofilm formers and cells[1–3]. We present results on the microfluidic attachment of the marine bacterium *Cobetia marina* (*C. marina*), formerly named *Halomonas marina*, as it is frequently found in marine biofilms[4,5]. To identify a suitable shear stress for the microfluidic attachment assays, the attachment behavior of *C. marina* was investigated at different shear forces on hydrophobic and hydrophilic surfaces, whereby *C. marina* tends to adhere best on hydrophobic coatings. Among the optimized assay parameters are the relevance of the growth state of *C. marina*. The optimized assay parameters will be presented as well as selected examples how coating chemistries like different self-assembling monolayers, amphiphilic alginates[6] and different thicknesses of PG coatings[7] alter the attachment of the marine bacterium *C. marina* under dynamic shear conditions.

1. Christophis, C., Grunze, M. & Rosenhahn, A. Quantification of the adhesion strength of fibroblast cells on ethylene glycol terminated self-assembled monolayers by a microfluidic shear force assay. *Phys. Chem. Chem. Phys.* (2010), 12, 4498-4504. doi:10.1039/b924304f

2. Alles, M. & Rosenhahn, A. Microfluidic detachment assay to probe the adhesion strength of diatoms. *Biofouling* (2015), 31:5, 469-480. doi:10.1080/08927014.2015.1061655

3. Nolte, K. A., Schwarze, J. & Rosenhahn, A. Microfluidic accumulation assay probes attachment of biofilm forming diatom cells. *Biofouling* (2017), 33 (7): 531-543. doi:10.1080/08927014.2017.1328058

4. Ista, L. K., Fan, H., Baca, O. & López, G. P. Attachment of bacteria to model solid surfaces' oligo(ethylene glycol) surfaces inhibit bacterial attachment. *FEMS Microbiol. Lett.* (1996), 142, 59-63. doi:10.1016/0378-1097(96)00243-1

5. Arpa-Sancet, M. P., Christophis, C. & Rosenhahn, A. Microfluidic assay to quantify the adhesion of marine bacteria. *Biointerphases* (2012), 7, 26. doi:10.1007/s13758-012-0026-x

6. Jakobi, V. *et al.* Amphiphilic Alginates for Marine Antifouling Applications. *Biomacromolecules* (2018), 19, 402-408. doi:10.1021/acs.biomac.7b01498

7. Wanka, R. *et al.* Fouling-Release Properties of Dendritic Polyglycerols against Marine Diatoms. *ACS Appl. Mater. Interfaces* (2018), 10, 34965–34973. doi:10.1021/acsami.8b12017

8:40am BI+AS-WeM-3 Biofilm Mechanics as a Mechanism for Survival on Surfaces from Medical Device to Ship Hulls, *Paul Stoodley,* Ohio State University **INVITED**

Bacterial biofilms are microscopic assemblages of bacterial cells usually attached to a surface and held together by a self-produced extracellular polymeric slime (EPS) matrix. Biofilms are ubiquitous in the natural environment and are highly problematic in industry and medicine where they cause corrosion, fouling, contamination and chronic medical and dental infections. The basic biology of bacterial biofilm development and strategies evolved to survive in the environment of the ancient earth are now used by the bacteria to survive on modern man-made materials. Diffusion limitation within the EPS matrix results in sharp gradients as nutrients are consumed by respiring bacteria on the periphery faster than they can diffuse in. Similarly, cell signals (molecules used to co-ordinate behavior between individual cells) and waste products, such as fermentation acids, build up in the interior of the biofilm. Biofilms are mechanically complex showing a range of behaviors from elastic solids to viscous liquids. These viscoelastic properties can facilitate survival on surfaces exposed to high shear stresses and can explain the high pressure drop and frictional losses in pipelines and ship hull fouling. However, the mechanical response may also be exploited to drive antimicrobials into the biofilm for control. The development of microenvironments combined with

the structural versatility of the biofilm is the basis for the distinct biofilm phenotype as an emergent property of population of single cells and is a challenge to overcome in their control.

9:20am BI+AS-WeM-5 Dendritic Polyglycerols as Fouling-release Coatings Against Marine Hard- and Soft Fouler, *Robin Wanka,* Ruhr-University Bochum, Germany*; N Aldred, J Finlay,* Newcastle University, UK*; K Nolte, J Koc,* Ruhr-University Bochum, Germany*; H Gardner, K Hunsucker, G Swain,* Florida Institute of Technology*; C Anderson, A Clare,* Newcastle University, UK*; A Rosenhahn,* Ruhr-University Bochum, Germany

Polyethylene glycol (PEG) containing coatings show outstanding antifouling properties, which is commonly assigned to their hydrophilicity and their highly hydrated nature. A structurally related but hyperbranched version are polyglycerols (PGs) that increase the spatial density of non-fouling polymer units and decrease the defect density in coatings.[1,2] So far they were successfully applied in biomedicine against attachment by pathogenic bacteria. Using a surface initiated ring opening polymerization reaction[3], we grafted dendritic PGs on surfaces. The resulting samples were characterized by spectroscopic ellipsometry, contact angle goniometry, ATR-FTIR, and by degradation experiments. The prepared surfaces show excellent protein-resistance. The fouling release properties were tested in a standardized lab assay with diatoms (*Navicula incerta)* and in a dynamic field assay[4] at the FIT test site in Florida. The initial attachment of diatoms under static conditions was similar on the PGs as compared to a hydrophobic control. However, PGs show outstanding fouling release properties. Up to 94% of attached diatoms could be removed from the coatings after the exposure to a shear stress of 19 Pa. These results were confirmed in the field assays.[5] The range of testes species was also extended to macro-fouling organisms such as zoospores of green algae (*Ulva linza)* and barnacle larvae (*Balanus amphitrite*).

(1) Wyszogrodzka, M.; Haag, R. Synthesis and characterization of glycerol dendrons, self-assembled monolayers on gold: A detailed study of their protein resistance. *Biomacromolecules* **2009**, *10*, 1043–1054.

(2) Siegers, C.; Biesalski, M.; Haag, R. Self-assembled monolayers of dendritic polyglycerol derivatives on gold that resist the adsorption of proteins. *Chemistry* **2004**, *10*, 2831–2838.

(3) Weber, T.; Gies, Y.; Terfort, A. Bacteria-Repulsive Polyglycerol Surfaces by Grafting Polymerization onto Aminopropylated Surfaces. *Langmuir* **2012**, *28*, 15916–15921.

(4) Nolte, K. A.; Koc, J.; Barros, J. M.; Hunsucker, K.; Schultz, M. P.; Swain, G. E.; Rosenhahn, A. Dynamic field testing of coating chemistry candidates by a rotating disk system. *Biofouling* **2018**, *49*, 1–12.

(5) Wanka, R.; Finlay, J. A.; Nolte, K. A.; Koc, J.; Jakobi, V.; Anderson, C.; Clare, A. S.; Gardner, H.; Hunsucker, K.; Swain, G. W. *et al.* Fouling-Release Properties of Dendritic Polyglycerols against Marine Diatoms. *ACS applied materials & interfaces* **2018,** DOI: 10.1021/acsami.8b 12017 .

9:40am BI+AS-WeM-6 Nano- and Microscale ZnO with Controllable Abundance of Surface Polarity as a Platform to Study Antibacterial Action., *J Reeks, B Thach,* Texas Christian University*; W Moss,* Texas State University*; R Maheshwari,* Texas Academy of Mathematics and Science*; I Ali, S McGillivray,* **Yuri Strzhemechny,** Texas Christian University

Nano- and microcrystalline ZnO is a low-cost, easy to synthesize material employed in many current and incipient applications owing to its exceptional optoelectronic, structural and chemical characteristics as well as a broad range of production techniques. Antibacterial action of ZnO is one of these applications, with a growing field of interdisciplinary research. Despite numerous and vigorous studies of the antibacterial nature of ZnO, and, in particular, the well- documented antimicrobial action of micro- and nanoscale ZnO particles, the most fundamental physical and chemical mechanisms driving this action are still not well identified. In particular, the influence of the crystal surface polarity on the antibacterial performance is largely unknown. Normally, hexagonal (wurtzite) ZnO crystals can be terminated with either charged polar (Zn or O) or electrically neutral nonpolar surfaces. In this work, we employ a hydrothermal growth protocol to produce ZnO nano- and microcrystals with tunable morphology, in particular to obtain a dependable control of the prevalent polarity of the free surfaces. This, in turn, can serve as a platform to investigate antibacterial action mechanisms in the synthesized specimens. It is reasonable to assume that one of the key phenomena behind such action is rooted in interactions between ZnO surfaces and the extracellular layers. Thus, excess charge or lack thereof, surface electronic charge traps, as well as variations in the stoichiometry at surfaces with different polarities of ZnO particles may affect interfacial phenomena with cell surfaces. It is

possible therefore that the relative abundance of ZnO surfaces with different polarities could significantly influence their antibacterial action. In our studies, we produced ZnO crystals comparable in size with the bacteria employed in our assays, such as s. aureus. This was done intentionally in order to avoid cellular internalization of ZnO particles and thereby to address primarily the mechanisms involving ZnO/cell surface interface. These experiments were performed in conjunction with optoelectronic studies of ZnO crystals (photoluminescence, surface photovoltage) to characterize electronic structure and dominant charge transport mechanisms as fundamental phenomena governing antibacterial characteristics of our samples. We report on the results of these comparative studies relating predominant ZnO surface polarity with the antimicrobial action.

11:00am BI+AS-WeM-10 Patterning Bacteria at Interfaces with Bio-Inspired Vascularized Polymers, *K Marquis, B Chasse,* **Caitlin Howell,** University of Maine

Nearly all methods of introducing bioactive compounds to the surface of a substrate rely on application from above or fail over time due to depletion. In this work, we use a bio-inspired approach to deliver target molecules to an interface from below, making use of both theoretical modeling and experimental validation to rationally design customizable patterns and gradients. Mimicking the vascular systems of living organisms, networks of empty 3D-printed channels are filled with liquid containing the compound of interest, which flows through the vascular network and diffuses through the polymer, eventually reaching the substrate surface. In proof-of-principle experiments using *Escherichia coli* and *Staphylococcus epidermidis* as model organisms, we demonstrate both theoretically and experimentally that the concentration of antibiotic and duration over which it is delivered to the surface can be controlled by varying the location of the vascular channels and concentration of the antibiotic solution inside. The result is a well-defined and predictable patterned response from the bacteria growing on the surface, a first step toward developing new types of adaptive antifouling surfaces and cell culture tools.

11:20am BI+AS-WeM-11 Chemical Imaging of Root-Microbe Interactions, *Vaithiyalingam Shutthanandan, A Martinez, R Boiteau,* Pacific Northwest National Laboratory

Nutrient mobilization from soil minerals is critical for plant growth, particularly in marginal lands with high pH soils or low phosphate and iron availability. Rhizospheric bacteria enhance plant growth by converting root exudates such as sugars and amino acids into organic acids and chelating molecules that enhance mineral dissolution and improve the availability of nutrients such as phosphorous and iron. Hence, understanding the effect of iron availability on metabolite exchange between plant and micro-organism is crucial. The spatial proximity of bacteria to root tissue of specific composition and sites of root secretion is one key aspect of this exchange. In this work, the model grass Brachypodium and the bacteria Pseudomonas fluorescens are used as a model system for studying rhizosphere interactions that improve metal bioavailability. Brachypodium was grown under four different conditions such as: (1) + Fe, (2) − Fe, (3) + Pseudomonas + Fe, (4) + Pseudomonas − Fe. The plants were grown for 2 weeks in the hydroponic solution and removed from the system and the root samples were analyzed using Helium Ion Microscope (HIM) for spatial organization of bacteria within the rhizosphere of Brachypodium and X-ray photoelectron spectroscopy (XPS) for chemical imaging. HIM results clearly show bacteria colonies on the root surfaces. However, these colonies were populated preferentially within grooved structures along the surface of the root. We hypothesize that there are compositional differences in the surface of the root area that explain the presence of these 'hotspots'. Roots exposed with iron show larger bacteria colonies than the roots without iron content. XPS imaging measurements on these samples revealed four predominant compositional classes, lipids/lignin, protein, cellulose and uronic acid that were spatially resolved across the surface of the main root with ~10 ⬚m resolution. Carbon and oxygen concentrations were almost constant among these samples and also constant along the individual roots. On the other hand, there is a clear variation in the concentrations of nitrogen and potassium along the root as well as among the samples. Discussion on the results and their implications will be discussed in this presentation.

11:40am BI+AS-WeM-12 Biocompatible Silver Nanoparticles-loaded Chitosan Membranes with Antibacterial Activity Produced by Directed Liquid-Plasma Nanosynthesis, *Camilo Jaramillo, A Civantos, A Mesa, J Allain,* University of Illinois at Urbana-Champaign

Silver nanoparticles (Ag NPs) possess remarkable antibacterial properties that are widely recognized. The emergence of antibiotic-resistant bacteria has motivated the interest of Ag NPs as an alternative for antimicrobial protection, in a wide range of applications [1]. However, Ag NPs have also shown toxicity and low biocompatibility. In addition, their synthesis usually involves toxic compounds, further limiting their applicability as a biomaterial. Research on Ag NPs has largely focused on increasing their biocompatibility. Properties such as NPs size, dispersity, and stability have shown to play an important role on their biocompatibility [2]. Green synthesis methods that require non-toxic agents while giving control over these properties are of high interest.

Chitosan (CS) is a deacetylated derivative of chitin, a widely available polymer. Its properties include biodegradability, biocompatibility and non-toxicity, making it an attractive alternative for biomaterials. CS has been used as a bioactive coating (for proteins, drugs and antibiotics and as a stabilizing agent in the production of Ag NPs [3]. Approaches to synthesize CS-based Ag NPs include γ irradiation and sonochemical methods [4].

In this work, Directed Liquid-Plasma Nanosynthesis (DLPNS) was used to drive Ag NPs synthesis without the need of other reagents. CS membranes were used to immobilize the NPs, to explore their application as an antibacterial coating for biomaterials. The Ag NPs precursor concentration and irradiation time were used as control parameters. Surface topography and chemistry were studied by SEM, Contact Angle, XRD and EDS. Antimicrobial properties of the membranes were evaluated against gram-positive (*S. aureus*) and gram-negative (*E. coli*) bacteria. Life and death assays revealed the antibacterial activity of the membranes. To study their biocompatibility and cytotoxicity, mammalian cell cultures were used. Cell viability, adhesion and metabolism were evaluated via Alamar blue and immunostaining tests. SEM images were used to assess the presence of Ag NPs in the CS matrix, and observe the bacteria and cell morphology on the surface of the membranes.

[1] D. Wei, W. Sun, W. Qian, Y. Ye, X. Ma, Carbohydr. Res. 344 (2009) 2375–2382.

[2] E.I. Alarcon, M. Griffith, K.I. Udekwu, eds., Silver Nanoparticle Applications, Springer International Publishing, Cham, 2015.

[3] A. Civantos, E. Martínez-Campos, V. Ramos, C. Elvira, A. Gallardo, A. Abarrategi, ACS Biomater. Sci. Eng. 3 (2017) 1245–1261.

[4] N.M. Huang, S. Radiman, H.N. Lim, P.S. Khiew, W.S. Chiu, K.H. Lee, A. Syahida, R. Hashim, C.H. Chia, Chem. Eng. J. 155 (2009) 499–507.

12:00pm BI+AS-WeM-13 Multifunctional 2D MoS 2 -Based Nanoplatform for Multimodal Synergistic Inactivation of Superbugs, *Paresh Ray,* Jackson State University

Development of new antibacterial therapeutic materials is becoming increasingly urgent due to the huge threat of superbugs, which are responsible for more than half of a million deaths each year in this world. We will discuss our recent report on the development of a novel nanobiomaterial based on a melittin antimicrobial peptide (AMP)-attached transition metal dichalcogenide MoS2-based theranostic nanoplatform. The reported nanoplatform has a capability for targeted identification and synergistic inactivation of 100% multidrug-resistant superbugs by a combined photo thermal therapy (PTT), photodynamic therapy (PDT), and AMP process. A novel approach for the design of a melittin antimicrobial peptide-attached MoS2-based nanoplatform is reported, which emits a very bright and photo stable fluorescence. It also generates heat as well as reactive oxygen species (ROS) in the presence of 670 nm near-infrared light, which allows it to be used as a PTT and PDT agent. Due to the presence of AMP, multifunctional AMP exhibits a significantly improved antibacterial activity for superbugs via a multimodal synergistic killing mechanism. Reported data demonstrate that nanoplatforms are capable of identification of multidrug-resistant superbugs via luminescence imaging. Experimental results show that it is possible to kill only ~45% of superbugs via a MoS2 nanoplatform based on PTT and PDT processes together. On the other hand, killing less than 10% of superbugs is possible using melittin antimicrobial peptide alone, whereas 100% of methicillin-resistant *Staphylococcus aureus* (MRSA), drug-resistant *Escherichia coli* (*E. coli*), and drug-resistant *Klebsiella pneumoniae* (KPN) superbugs can be killed using antimicrobial peptide-attached MoS2 QDs, via a synergistic killing mechanism.

Spectroscopic Ellipsometry Focus Topic
Room A212 - Session EL+AS+EM+TF-WeM

Optical Characterization of Thin Films and Nanostructures

Moderators: Eva Bittrich, Leibniz Institute of Polymer Research Dresden, Tino Hofmann, University of North Carolina at Charlotte

8:00am EL+AS+EM+TF-WeM-1 Enhanced Strong Near Band Edge Emission from Lanththanide Doped Sputter Deposited ZnO, *C Heng,* Beijing Institutute of Technology, China; *W Xiang, T Wang,* Beijing Institutete of Technology, China; *W Su,* Beijing Instititute of Technology, China; *P Yin,* Beihang University, China; *Terje G Finstad,* University of Oslo, Norway

Research on ZnO films and nanostructures have increased steadily in the last decades being motivated by many applications including photonic applications. Incorporation of rare earth (RE) elements for the purpose utilize transition therein for conversion or manipulation of the wavelength spectrum. That was also our original motivation, however we observed the REs also can provide an enhancement of near band gap emission,NBE. This has been observed for Tb, Ce, Yb and Eu. The ZnO films were co-sputtered with RE elements onto Si wafers in an Ar+O₂ ambient yielding oxygen rich films as observed by RBS and XPS. The films were annealed in an N₂ ambient for various temperatures from 600 to 1100 °C. The luminescence behavior was studied emission and excitation spectroscopy as well luminescence decay measurements. Both undoped and RE doped films showed a large increase in emission with increasing annealing temperature, while the increase was largest for the RE doped samples. The crystallinity and microstructure of the films were studied by XPS, SEM, XRD and HRTEM. It is observed that the increase in UV NBE is correlated with crystalline improvements of ZnO. At the temperature for maximum PL emission intensity there is silicate formation due to interaction with the substrate. The maximum occurs for an annealing temperature where not all the ZnO has been consumed in the silicate reaction. This maximum appears to be 1100 °C for the thicker films and 1000 °C for thinner films. For samples having maximum NBE there seem to be random lasing occurring indicated by the intensity dependence of UV PL emission. A hypothesis for the main reason behind the increase in NBE intensity with RE doping is that the RE ions influence the film structure during nucleation early in the deposition process by influencing the mobility of atoms. The initial grain structure will have an affect on the development grain structure for the whole film and an influence on the grain growth. This influences the presence of non-radiative defect centers in the film and the grain surface and grain boundaries. As a side effect, we observe that there is very little transfer of excitation energy to the RE ions. This supports the notion that oxygen deficient centers may be necessary to have efficient energy transfer to RE ions in ZnO. Finally we remark that strong UV light from ZnO films have been sought particularly because they could offer a low temperature production for some application. The present method is still a high temperature method, but it is very simple and can be directly combined with Si technology which can be advantage for certain applications.

8:20am EL+AS+EM+TF-WeM-2 Ellipsometry Study of PLD based Temperature Controlled Thin Film Depositions of CdSe on ITO Substrates, *Flavia Inbanathan,* Ohio University; *M Ebdah,* King Saud University, Kingdom of Saudi Arabia; *P Kumar,* Gurukula Kangri Vishwavidyalaya, India; *K Dasari,* Texas State University; *R Katiyar,* University of Puerto Rico; *W Jadwisienczak,* Ohio University

Cadmium Selenide(CdSe), a n-type semiconductor with a direct bandgap of 1.73eV has been explored widely for its suitability in various applications including photovoltaics and optoelectronics, because of its optical and electrical properties. The literature presents various deposition methods for CdSe thin films out of which this work is based on pulsed laser deposition(PLD)[1]. The optoelectronic applications of CdSe thin films depend on their structural and electronic properties that depends on deposition and process parameters[2]. The stability of the thin films at various temperatures is an important factor to improve the efficiency and durability of photosensitive devices. The present work aims to fabricate the high quality CdSe thin films using PLD method and affirms the optimal deposition temperature at 250°C as validated by the films surface roughness and ellipsometry studies[3][4]. The effect of different *in-situ* deposition temperature on structural, morphological and optical properties through XRD, AFM, SEM, optical absorption/transmission and ellipsometry spectroscopy have been investigated. CdSe thin films with thickness close to 200nm were deposited on the Indium Tin Oxide (ITO) coated glass substrates at temperatures ranging from 150 to 400°C. The light absorption spectrum analysis of all the CdSe films confirmed well defined direct energy

band gap from 2.03 to 1.83eV. The ITO substrate is modelled using a two sub-layers model that consists of 130nm graded ITO on top of a 0.7mm bulk ITO layer, and the experimental ellipsometry spectra agreed very well with the fitting spectra. The ellipsometry study confirmed that CdSe thin films show an increase of 44% in refractive index(n) in the violet spectrum, and a constant value in blue-yellow spectral range but with significant changes in red spectrum for increase in temperature upto 350°C; beyond which resulted in constant value, possibly due to the stagnation in the grain growth. The extinction coefficient(k) value of CdSe approaches zero in the red spectrum region for 150°C and 300°C temperatures whereas it showed a value of 0.25 and 0.7 for 250°C and 400°C temperatures, respectively. The peaks observed around 650nm and 750nm in ellipsometry spectra are assigned to excitonic transitions. The collected data will be critically analysed in terms of CdSe optical properties engineered for optoelectronic and photovoltaic applications.

References: [1]Z.Bao *et al.,*J.Mater.Sci.:Mater Electron(2016)27,7233-7239; [2]S.Mahato, *et al.*, J.Scien.: Adv.Mater. Devices, (2017)2,165-171; [3]A.Evmenova *et al.,*Advan. Mater. Scien.Eng. (2015), ID 920421,11; [4]B.T.Diroll *et al.*, Chem. Mater.,(2015)27,6463-6469.

8:40am **EL+AS+EM+TF-WeM-3 The Application of Mueller Matrix Spectroscopic Ellipsometry to Scatterometry Measurement of Feature Dimension and Shape for Integrated Circuit Structures***, Alain C. Diebold,* SUNY Polytechnic Institute **INVITED**

One of the most difficult measurement challenges is non-destructively determining the feature dimensions and shape for complicated 3D structures. This presentation will review Mueller Matrix Spectroscopic Ellipsometry based scatterometry which uses the Rigorous Coupled Wave Approximation (RCWA) to solve Maxwell's equations for a model structure and the resulting Mueller Matrix elements are compared to experimental results. Here we use the structures used in GAA transistors fabrication as an example of challenging measurements.(1, 2, 3) In this talk, we present simulations aimed at understanding the sensitivity to changes in feature shape and dimension for the structures used to fabricate GAA transistors. Simulations of the multi-layer fins show a clear sensitivity to fin shape and Si layer thickness which is enhanced by the use of the full Mueller Matrix capability vs traditional spectroscopic ellipsometry. We also discuss experimental measurement of nanowire test structure demonstrating the ability to measure the etching of mutiple sub-surface features. [3]

References

[1] Alain C. Diebold, Anthony Antonelli, and Nick Keller, Perspective: Optical measurement of feature dimensions and shapes by scatterometry, APL Mat. **6**, (2018), 058201. doi: 10.1063/1.5018310.

[2] Sonal Dey, Alain Diebold, Nick Keller, and Madhulika Korde, Mueller matrix spectroscopic ellipsometry based scatterometry simulations of Si and Si/SixGe1-x/Si/SixGe1-x/Si fins for sub-7nm node gate-all-around transistor metrology, Proc. SPIE 10585,

Metrology, Inspection, and Process Control for Microlithography XXXII, 1058506 (6 June 2018); doi: 10.1117/12.2296988

[3] Madhulika Korde, Subhadeep Kal, Cheryl Pereira, Nick Keller, Aelan Mosden, Alain C. Diebold, Optical Characterization of multi-NST Nanowire Test Structures using Muller Matrix Spectroscopic Ellipsometry (MMSE) based scatterometry for sub 5nm nodes, Proc. SPIE Metrology, Inspection, and Process Control for Microlithography XXXIII, (2019), in press.

9:20am **EL+AS+EM+TF-WeM-5 Optical Constants and Thickness of Ultrathin Thermally Evaporated Iron Films***, Nick Allen, D Shah, R Vanfleet, M Linford, R Davis,* Brigham Young University

Carbon nanotube templated microfabrication (CNT-M) is a technique that uses a patterned iron catalyst to grow 3-D structures for device applications. Iron catalyst thickness strongly affects carbon nanotube (CNT) growth heights and the straightness of the CNT-M structures. Atomic force microscopy has been used to directly measure the thicknesses of such iron/iron oxide films, but this technique is slow and not easily scalable. A faster method is ellipsometry, but for very thin films, the optical constants and thickness are not easily separated, thus standard ellipsometry approaches are inadequate. The 2-6 nm thick iron films used as CNT growth catalysts are in this challenging region. The absorptive nature of the iron/iron oxide films adds further difficulty. In this study, a multi-sample ellipsometry analysis using iron films of various thicknesses was performed to obtain the optical constants of thermally evaporated iron. We used contrast enhancement by incorporating a silicon dioxide layer under the film being analyzed to enhance sensitivity to the optical constants.

9:40am **EL+AS+EM+TF-WeM-6 Birefringent Photonic Crystals for Polarization-discriminatingInfrared Focal Plane Arrays***, Marc Lata, Y Li, S Park, M McLamb, T Hofmann,* University of North Carolina at Charlotte

Infrared optical materials fabricated using direct laser writing have received substantial interest since the emergence

of this technology which is based on the two-photon polymerization of suitable monomers [1, 2]. We have

demonstrated that direct laser writing allows the fabrication of structured surfaces to reduce Fresnel reflection

loss in the infrared spectral range while two-dimensional photonic crystals enable optical filters with high spectral

contrast [3, 4]. In combination with the ability to fabricate large scale arrays of uniform structures, two-photon

polymerization could be a disruptive technology for enhancing focal plane arrays in IR imaging systems.

So far, photonic crystals which provide polarization selectivity have not been used for the pixel-based enhancement

of infrared focal plane arrays. Here we explore the form-birefringence found in photonic crystals composed

of arrays of subwavelength-sized slanted micro wires (Fig. 1) for this purpose. The photonic crystals investigated

here were fabricated in a single fabrication step using direct laser writing of an infrared transparent photoresist.

The lateral dimensions of the photonic crystals are comparable to the pixel size of infrared focal plane arrays which

is on the order of some tens of micrometers [5]. We observe a strong contrast under cross-polarized illumination

in the mid-infrared spectral range at w = 1550 cm-1. Finite-element-based techniques are used to optimized the

geometry of the constituents of the photonic crystals to minimize edge effects. We envision laser direct writing as

a suitable technique for the enhancement of focal plane arrays to enable focal-plane polarimeters for the infrared

spectral range.

11:00am **EL+AS+EM+TF-WeM-10 Relevance of hidden Valleys in the Dequenching of Room-temperature-emitting Ge Layers***, T Sakamoto, Y Yasutake,* University of Tokyo, Japan*; J Kanasaki,* Osaka City University, Japan*; Susumu Fukatsu,* University of Tokyo, Japan

Ge offers a unique advantage of gaining a deeper insight into the intervalley coupling of *hot* electrons [1], which is arguably of importance in the context of controlling the optoelectronic and photonic functionalities [2]. In view of the complicated valley degeneracy in the near-band-edge region, such intervalley coupling of electrons plays a pivotal part even when strain-engineering pseudomorphic Ge-based quantum structures.

The capability of direct-gap emission at room temperature is of considerable practical significance of Ge, for which an added advantage is that emission wavelengths fortuitously fall within the telecom bands. Moreover, Ge is particularly interesting from the device physics point of view as it outperforms many semiconductor allies in the sense that thermal *dequenching* occurs near room-temperature: the emitted light intensity increases with increasing temperature, which is convenient but nevertheless logic-defying.

Such a rather counterintuitive "thermal roll-up", as opposed to thermal roll-off which is usually more relevant, has been interpreted in terms of two-level electron kinetics assuming local thermal equilibrium; long-lived electrons populating the indirect conduction-band bottom, i.e., L-valleys, are excited up into the direct-gap Γ-valley by absorbing phonons, which seems to fit a fairly standard phenomenological picture reasonably well. To the contrary, this model system fails in the case of Ge layers, the quality of crystallinity of which is compromised because of a low growth temperature. In fact, they only show steady thermal roll-off, viz. *quenching*, without a trace of the anticipated dequenching.

These apparently conflicting observations can be reconciled only by considering another otherwise invisible *hidden* conduction-band valley that comes in between the L andΓ valleys to decouple them. A three-level scheme is naturally invoked thereby. Indeed, it explains not only the missing dequenching but the lost local thermal equilibrium in low-quality layers. As a proof of such a conjecture, an attempt was made to directly capture the *hidden* valleys by means of time- and angle-resolved two-

photon photoemission [3]. Preliminary results indicate the relevance of X(Δ)-valleys, which are slightly above the Γ-valley, in the dequenching of room-temperature emission as a result of ultrafast coupling of L-X(Δ)-Γ valleys by phonons taking up large crystal momenta. These are consistent with theory and luminescence study.

1. T. Sakamoto *et al.*, Appl. Phys. Lett. **105**, 042101 (2014).

2. Y. Yasutake and S. Fukatsu, Spoken at 2018 APS March Meeting (Los Angeles, 2018), P07.00012.

3. J . Kanasaki *et al.*, Phys. Rev. B **96**, 115301 (2017).

11:20am EL+AS+EM+TF-WeM-11 Spectroscopic Ellipsometry on Organic Thin Films - From in-situ Bio-sensing to Active Layers for Organic Solar Cells, *Eva Bittrich, P Uhlmann, K Eichhorn,* Leibniz Institute of Polymer Research Dresden, Germany*; M Schubert,* University of Nebraska-Lincoln, Linköping University, Sweden, Leibniz Institute of Polymer Research Dresden, Germany*; M Levichkova, K Walzer,* Heliatek GmbH, Germany
INVITED

Nanostructured surfaces and thin films of small organic molecules, polymers or hybrid materials are promising interfaces for versatile applications like sensing, water purification, nanoelectronics, energy production and energy storage devices. Ellipsometry, as non-invasive method, is well suited to contribute to the understanding of structure – property – relationships in organic thin films, but can also act as probing technique for hybrid sensing elements. Aspects from our research ranging from switchable responsive polymer brush interfaces for biosensing to thin films of small organic molecules for organic solar cells will be presented. On the one hand, swelling of polymer brushes grafted to slanted columnar thin films of silicon will be visualized by anisotropic optical contrast microscopy, as an example for a new class of hybrid sensing materials with unique sensitivity on the nanoscale. On the other hand the effect of template molecules on the morphology and optical properties of semiconducting thin films will be discussed, emphasizing the correlation of ellipsometric data with structural analysis by grazing incidence wide angle X-ray scattering (GIWAXS).

12:00pm EL+AS+EM+TF-WeM-13 Optical Dielectric Function of Si(bzimpy)2 – A Hexacoordinate Silicon Pincer Complex Determined by Spectroscopic Ellipsometry, *Yanzeng Li,* M Kocherga, S Park, M Lata, M McLamb, G Boreman, T Schmedake, T Hofmann, University of North Carolina at Charlotte

Tang and VanSlyke demonstrated light emission from the first practical electroluminescent device based on a double-organic-layer structure of tris(8-hydroxyquinoline)aluminum, Alq₃, and a diamine film in the late 80's. Since then, organic light emitting diodes (OLED) based on metal chelates such as Alq3 have been widely studied. Despite the widespread use of Alq₃, there has been a broad search for new materials with improved properties, in particular, with respect to their chemical and electrochemical stability. We have recently reported on the successful synthesis of a neutral, hexacoordinate silicon-based fluorescent complex Si(bzimpy)₂. Our results indicate that Si(bzimpy)₂ exhibits inherent advantages such as the tunability of the luminescence in the visible spectrum, greater thermal stability, and high charge mobility that is comparable to that of Alq₃. Despite the successful synthesis and encouraging electroluminescence at 560 nm the complex dielectric function of the water stable complex has not been reported yet. Here we present spectroscopic ellipsometry data which were obtained from a Si(bzimpy)2 thin-film in the spectral range from 300~nm to 1900~nm. A parameterized model dielectric function composed of a Tauc-Lorentz and Gaussian oscillators is employed to analyze the experimental ellipsometry data. We find a good agreement between the critical point energies observed experimentally and our density functional theory calculations reported recently.

Electronic Materials and Photonics Division
Room A214 - Session EM+2D+AS+MI+MN+NS+TF-WeM

Nanostructures and Nanocharacterization of Electronic and Photonic Devices

Moderators: Sang M. Han, University of New Mexico, Jason Kawasaki, University of Wisconsin - Madison

8:00am EM+2D+AS+MI+MN+NS+TF-WeM-1 Photonic Thermal Conduction in Semiconductor Nanowires, *E Tervo, M Gustafson, Z Zhang, B Cola, Michael A. Filler,* Georgia Institute of Technology

We present a practical material system—chains of infrared plasmonic resonators situated along the length of semiconductor nanowires—where near-field electromagnetic coupling between neighboring resonators enables photonic thermal transport comparable to the electronic and phononic contributions. We model the thermal conductivity of Si and InAs nanowires as a function of nanowire diameter, resonator length, aspect ratio, and separation distance by combining discrete dipolar approximation calculations, to determine the relevant dispersion relations, with thermal kinetic theory. We show that photonic thermal conductivities exceeding 1 W m^{-1} K^{-1} are possible for 10 nm diameter Si and InAs nanowires containing repeated resonators at 500 K, more than an order of magnitude higher than existing materials systems and on par with that possible with phonons and electrons. These results highlight the potential for photons in properly engineered solids to carry significant quantities of heat and suggest new ways to dynamic control thermal conductivity.

8:20am EM+2D+AS+MI+MN+NS+TF-WeM-2 Electric Field-Induced Defect Migration and Dielectric Breakdown in ZnO Nanowires, *Hantian Gao, M Haseman,* Department of Physics, The Ohio State University*; H von Wenckstern, M Grundmann,* Universität Leipzig, Felix-Bloch-Institut für Festkörperphysik*; L Brillson,* The Ohio State University

Nanowires of the II-VI compound semiconductor ZnO have generated considerable interest for next generation opto- and microelectronics . Central to nanowire electronics is understanding and controlling native point defects, which can move[1] and lead to dielectric breakdown under applied electric fields. We used nanoscale lateral and depth-resolved cathodoluminescence spectroscopy (DRCLS) with hyperspectral imaging (HSI) in a scanning electron microscope (SEM) to observe defect migration and redistribution directly under applied electric fields and after dielectric breakdown. HSI maps represent lateral intensity distributions of specific features acquired pixel by pixel across SEM-scanned areas and normalized to near band edge (NBE) emissions. A pulsed layer deposited (PLD) ZnO microwire (3 μm diameter) exhibited homogeneous distributions of common luminescence features at 2.0 eV (V_{Zn} cluster) and 2.35 eV (Cu_{Zn}) as well as 2.7 and 2.9 eV (V_{Zn}) peaks near the wire surface. With increasing electrical bias up to 3x10^5 V/cm between two Pt contacts, these defects systematically redistribute, even at room temperature, moving toward and under one of the contacts, draining the "bulk" nanowire, especially its near-surface region. Since ionized V_{Zn}-related and Cu_{Zn} antisite defects are acceptors, their removal reduces the compensation of electron density in the typically n-type ZnO and thus its resistivity.

Besides HSI lateral maps, DRCLS vs. incident beam energy yields depth profiles radially of defects at specific locations along the nanowire. These exhibit high near-surface and wire core densities that biasing reduces. Current voltage measurements with increasing field gradients show a gradual resistivity decrease until an abrupt dielectric breakdown of the microwire at 300 kV/cm (150 V/5 μm). The acceptor removal between the contacts and their accumulation under one of the contacts can both contribute to this breakdown due to the decrease in resistivity and higher current conduction between the contacts and possible defect-assisted tunneling[2] across the increased defect density under the contact, respectively. These electric field-induced defect movements may be of more general significance in understanding dielectric breakdown mechanism not only in ZnO nanostructures but also bulk semiconductors in general.

1. G. M. Foster, et al., Appl. Phys. Lett. **111**, 101604 (2017).

2. J.W.Cox, et al., Nano Lett, **18**, 6974 (2018).

8:40am EM+2D+AS+MI+MN+NS+TF-WeM-3 Characterization of SiGe/Si Multilayer FIN Structures using X-Ray Diffraction Reciprocal Space Maps, *Roopa Gowda, M Korde,* SUNY Polytechnic Institute*; M Wormington,* Jordan Valley Semiconductors Inc.*; A Diebold,* SUNY Polytechnic Institute

Nanowire and Nanosheet FET's are potential replacements for FinFET's, mainly beyond sub-10nm CMOS technology nodes, as gate-all-around (GAA) FET device architecture provides improved electrostatics in higher on current (I on) and better subthreshold swing. As GAA is one of the best promising device for logic applications for future technology nodes, there is an increased need of characterization technique for such multilayer $Si_{1-x}Ge_x$/ Si complex structures. We studied $Si_{1-x}Ge_x$/Si/$Si_{1-x}Gex$/Si/$Si_{1-x}Ge_x$/Simultilayer FIN structures using X-Ray Diffraction Reciprocal Space Maps (RSM). RSM is one of the most popular technique to study epitaxial thin-films nanostructures due to straightforward analysis of the data. We found RSM simulations showing sensitivity of nanosheet fin structures dimensions such as pitch-walk (PW), Nanosheet thickness (NST), composition and shape. RSM's provide better means to interpret more complex diffraction measurements than real space constructions. RSMs of $Si_{1-x}Ge_x$/Si multilayer structure has been simulated using Bruker JV-RADS v6.5.50/HRXRD software. 1D line profiles extracted from RSMs was also used for the analysis of nanostructures dimensions. We obtained multilayer structure dimensions from the published information. We studied the influence of nanostructure parameters PW, NST, Composition and shape on RSMs. Imperfect periodic structures impact the intensity modulation of the grating rods (GRs). We observed that satellite peaks intensity reduces and harmonics peaks intensity enhances as PW increases. Rate of intensity change in higher order peaks is much faster than the lower harmonic peaks. We observed that the spacing between adjacent interference fringes in RSMs is related to the thickness of the layers. The period of fringes is inversely proportional to the thickness of the layer, hence total FIN height can be determined. 1D line profiles along Q_z shows decreased angular width and increase in intensity of the layer peak and interference fringes as NST increases. Symmetric 004 longitudinal RSMs and their line profiles clearly show layer peak shift from substrate peak as composition increases due to increase of SiGe lattice spacing along the growth direction. Cross-shaped GR pattern in RSMs is observed which is due to trapezoidal surface grating caused by SWA. Line profiles indicate that fin shapes influence the modulation of the GRs as a function of Q_x. We demonstrate the characterization of complex $Si_{1-x}Ge_x$/ Si multilayers using RSMs and their line profiles which are relevant for lateral nanowire and nanosheet FETs. Above findings from RSM simulations clearly indicate the influence of variations in structural dimensions.

9:00am EM+2D+AS+MI+MN+NS+TF-WeM-4 Nanoscale Depth and Lithiation Dependence of V_2O_5 Band Structure by Cathodoluminescence Spectroscopy, *Mitchell Walker, N Pronin,* The Ohio State University*; A Jarry, J Ballard, G Rubloff,* University of Maryland, College Park*; L Brillson,* The Ohio State University

Vanadium pentoxide (V_2O_5) has attracted considerable interest for its potential use as a cathode for solid state lithium ion batteries. While researchers have studied the V_2O_5 lithiation charge/discharge cycle for over two decades, we are only now able to measure directly its electronic band structure from the surface to the thin film bulk and its changes with Li intercalation on a near-nanometer scale. We used depth-resolved cathodoluminescence spectroscopy (DRCLS) to monitor the changes in electronic structure from the free surface to the thin film bulk several hundred nm below. DRCLS measures optical transitions at 1.8-2, 3.1-3.2, 3.6-3.7, 4.0-4.1, and 4.6-4.7 eV between multiple conduction bands to the pristine (α) V_2O_5 valence band maximum in excellent agreement with $V_{3d}t_{2g}$ conduction band densities of states (DOS) predicted by density functional theory (DFT).[1] Triplet conduction band states at 1.8, 1.9, and 2 eV correspond to predicted V $3d_{xy}$–O_c $2p_x/2p_y$ hybridized states resulting from strong deviations of the unit cell VO_6 octahedra from cubic coordination correspond to optical absorption edges along the 3 crystallographic axes. With excitation depth increasing from < 10 to 125 nm calibrated by Monte Carlo simulations, the relative amplitudes and energies of these states change, signifying gradual changes in octahedral distortion. The band structure changes significantly with Li intercalation into $Li_xV_2O_5$ for x = 0, 1, and 2. Lithiation gradually removes the hybridized band and introduces a 2.4-2.7 eV V_{3d} t_{2g} band extending 50 nm (x=1) or 25 nm (x=2) into the surface. Higher (4.0 and 4.4 eV) features possibly related to a secondary phase dominate the spectra deep inside all V_2O_5 films near the battery electrode. Delithiation reintroduces the 1.8-2 eV split-off band although significantly narrowed by octahedral distortions. Overall, DRCLS shows that the lithiation cycle alters the V_2O_5 band structure on a scale of 10-100's of nm with lithiation. The direct measure of V_2O_5's electronic band structure as a function of lithiation level provided by DRCLS can help guide future battery engineering work as more efficient lithium ion batteries are developed. In particular, these unique electrode measurements may reveal in what ways lithiation changes V-$_2O_5$ irreversibly, as well as reveal methods to extend solid state battery life. MW and LJB acknowledge support from NSF grant DMR-18-00130. AJ and GR acknowledge Nanostructures for Electrical Energy Storage (NEES), a Department of Energy Office of Science Frontier Research Center.

1. V. Eyert and K.-H. Höck, "Electronic structure of V_2O_5: Role of octahedral deformation," Phys. Rev. B 57, 12727 (1998).

9:20am EM+2D+AS+MI+MN+NS+TF-WeM-5 Electron Microscopy of Quantum Materials: From Learning Physics to Atomic Manipulation, *Sergei Kalinin,* Oak Ridge National Laboratory **INVITED**

Atomically-resolved imaging of materials has become the mainstay of modern materials science, as enabled by advent of aberration corrected scanning transmission electron microscopy (STEM). In this talk, I will present the new opportunities enabled by physics-informed big data and machine learning technologies to extract physical information from static and dynamic STEM images. The deep learning models trained on theoretically simulated images or labeled library data demonstrate extremely high efficiency in extracting atomic coordinates and trajectories, converting massive volumes of statistical and dynamic data into structural descriptors. I further present a method to take advantage of atomic-scale observations of chemical and structural fluctuations and use them to build a generative model (including near-neghbour interactions) that can be used to predict the phase diagram of the system in a finite temperature and composition space. Similar approach is applied to probe the kinetics of solid-state reactions on a single defect level and defect formation in solids via atomic-scale observations. Finally, synergy of deep learning image analytics and real-time feedback further allows harnessing beam-induced atomic and bond dynamics to enable direct atom-by-atom fabrication. Examples of direct atomic motion over mesoscopic distances, engineered doping at selected lattice site, and assembly of multiatomic structures will be demonstrated. These advances position STEM towards transition from purely imaging tool for atomic-scale laboratory of electronic, phonon, and quantum phenomena in atomically-engineered structures.

11:00am EM+2D+AS+MI+MN+NS+TF-WeM-10 Hot Electron Emission from Waveguide Integrated Graphene, *Ragib Ahsan, F Rezaeifar, H Chae, R Kapadia,* University of Southern California

From free electron laser sources to electronic structure measurements, electron emission devices play an important role in a wide range of areas. Photoemission is one of the basic processes exploited in modern electron emission devices. However, higher-order processes like multiphoton absorption or optical field induced emission are necessary for efficient photoemission from high workfunction metallic emitters. Our work demonstrates a graphene emitter integrated on a waveguide that can evanescently couple with the photons delivered from a CW laser (405 nm) and registers photoemission at a peak power that is orders of magnitude lower than previously published results based on multiphoton and optical field induced emission processes. Coupling FDTD analysis of the waveguide to a rigorous quantum mechanical study of the scattering mechanisms and the tunneling processes in graphene, we have been able to model the emission current from the graphene emitter with good agreement to the experimental data. Our investigation reveals that the photoexcited electrons can go through three mutually competitive processes: (i) electron-electron scattering (ii) electron-phonon scattering and (iii) directly emission into the vacuum. Absorption of a photon causes a reduction in the tunnel barrier seen by the electron and the emission rate increases exponentially. Integration of graphene to the waveguide enables evanescent coupling between electrons and the photons causing almost 100% absorption of the photons. Our integrated photonics approach demonstrates an emission efficiency that is three orders of magnitude greater than free space excitation. These results suggest that integrating photonic elements with low dimensional materials such as 2D materials, nanoparticles, quantum dots, etc. can provide a new domain of efficient electron emission devices and integrated photonics.

11:20am EM+2D+AS+MI+MN+NS+TF-WeM-11 Imaging Candidate Nanoelectronic Materials with Photoemission Electron Microscopy (PEEM), *Sujitra Pookpanratana, S Robey,* National Institute of Standards and Technology (NIST)*; T Ohta,* Sandia National Laboratories

The drive to produce smaller and lower power electronic components for computing is pushing the semiconductor industry to consider novel

nanoscale device structures, not based solely on crystalline silicon. Continued innovation and progress towards novel nanoelectronic materials and devices in turn requires metrologies sensitive to electronic properties at these length scales. Tip-based imaging techniques provide electronic contrast with sub-nanometer resolution, however it is a local, scanning-based technique. Photoemission (or photoelectron spectroscopy) is the dominant technique to provide detailed electronic band structure information- level energies, dispersion, polarization dependence, etc. – but typically requires materials with millimeter, or larger, length scales. Photoemission electron microscopy (PEEM) can be employed to allow access to this vital information, providing full-field imaging capabilities sensitive to a variety of electronic contrast mechanisms at 10's of nanometers length scales. Here, we will present our results on imaging the impact of molecular dopants on multilayer tungsten disulfide (WS_2) employing the PEEM at the Center for Integrated Nanotechnologies within Sandia National Laboratories. We will also discuss the commissioning of a recently installed PEEM to perform complementary measurements at NIST-Gaithersburg.

Technological commercialization of transition metal dichalcogenides (TMDs) in nanoelectronics devices requires control of their electronic properties, such as charge carrier type and density, for specific device functionality. Conventional techniques for doping are problematic for atomically thin 2D materials. The sensitivity of mono- to few-layer (TMDs) to their local environment and interfaces can be employed *via* surface doping of molecules on TMDs to provide a promising route toward controllable doping. Investigations of surface doping for one to few layer WS_2 were performed using mechanically exfoliated WS_2 on a SiO_2/Si substrate that was then exposed to tris(4-bromophenyl)ammoniumyl hexachloroantimonate, a p-dopant molecule. PEEM was performed before and after p-dopant exposure. After doping, we find that the contrast of the surface WS_2 physical features change and valence band edge shifts about 0.8 eV away from the Fermi energy, consistent with p-doping. We will discuss the effects of molecular doping in terms of homogeneity and surface features across multiple WS_2 flakes. Lastly, we will discuss commissioning of a new PEEM instrument installed at NIST in 2019, using results of graphene to demonstrate imaging capability and energy resolution of this instrument.

11:40am EM+2D+AS+MI+MN+NS+TF-WeM-12 Comparison of Features for Au and Ir Adsorbed on the Ge (110) Surface, *Shirley Chiang,* University of California, Davis*; R Xie, H Xing,* Donghua University, China*; T Rahman,* University of Central Florida*; C Fong,* University of California, Davis
Two ad-atoms of Au and Ir adsorbed, respectively, on the Ge(110) surface are studied by a first-principles algorithm based on density functional theory. The surface is modeled by a slab consisting of 108 Ge atoms with a 10 Å vacuum region. Hydrogen atoms are used to saturate the dangling orbitals at the other side of the vacuum region. Two cases of Au adsorption and one case of Ir are reported. The case of Ir has a large binding energy because of its small atomic size compared with the Ge atom, and the partially filled d-states. The total energy for each case is given, as are the energies for removing one ad-atom at a time and also both ad-atoms. The binding energy of each case is obtained by simply taking the energy difference between these configurations; this method is more realistic because the experimental data measured by LEEM and STM indicate that the collective motions of the ad-atoms do not allow the surface to relax to its equilibrium state.[1] For a large separation in the case of two Au atoms, there is a smaller binding energy than for one ad-atom. This can relate to the fact that the collective motions seen experimentally do not happen at a full monolayer coverage of ad-atoms.[1] Additional comparisons will be made to an atomic model for Ir/Ge(111) from STM measurements.[2]

[1] B. H. Stenger et al., Ultramicroscopy, 183, 72 (2017).

[2] M. van Zijll et al., Surf. Sci. 666, 90, (2017).

12:00pm EM+2D+AS+MI+MN+NS+TF-WeM-13 Reference Materials for Localization Microscopy, *C Copeland, R Dixson, L Elliott, B Ilic,* National Institute for Science and Technology (NIST)*; D Kozak, K Liao,* FDA, National Institute for Science and Technology (NIST)*; J Liddle,* NIST Center for Nanoscale Science and Technology*; A Madison,* National Institute for Science and Technology (NIST)*; J Myung,* FDA*; A Pintar,* **Samuel Stavis***,* National Institute for Science and Technology (NIST)
As the diffraction limit fades away into the history of optical microscopy, new challenges are emerging in super-resolution measurements of diverse systems ranging from catalysts to therapeutics. In particular, due to common limitations of reference materials and microscope calibrations, many localization measurements are precise but not accurate. This can result in gross overconfidence in measurement results with statistical uncertainties that are apparently impressive but potentially meaningless, due to the unknown presence of systematic errors that are orders of magnitude larger. To solve this fundamental problem in measurement science, we are optimizing and applying nanofabrication processes to develop reference materials for localization microscopy, and demonstrating their use in quantitative methods of microscope calibration.

Our program consists of two complementary approaches. In the first, involving applied metrology, we are developing reference materials such as aperture arrays that can serve as standalone artifacts for widespread deployment. This approach will require the application of critical-dimension metrology to establish the traceability of master artifacts, and their use to calibrate a super-resolution microscope for high-throughput characterization of economical batches of reference materials. In the second approach, involving fundamental research, we are demonstrating the application of reference materials and calibration methods in our own experimental measurements. Most interestingly, achieving vertical integration of our two approaches and the unique capabilities that result, we are building reference materials into measurement devices for in situ calibration of localization measurements for nanoparticle characterization.

.

Fundamental Discoveries in Heterogeneous Catalysis Focus Topic
Room A213 - Session HC+2D+SS-WeM

Exotic Nanostructured Surfaces for Heterogeneously-Catalyzed Reactions

Moderators: Ashleigh Baber, James Madison University, Erin Iski, University of Tulsa

8:20am HC+2D+SS-WeM-2 Selective Alkane Chemistry on IrO_2(110) Surfaces, *Aravind Asthagiri, M Kim,* The Ohio State University*; J Weaver,* University of Florida
Selective conversion of alkanes to higher value species using heterogeneous catalysts is of great interest with the increasing availability of light alkanes from shale fracking. We have used a combination of temperature programmed reaction spectroscopy (TPRS) and density functional theory (DFT) to demonstrate that the stoichiometric terminated IrO_2(110) surface can activate methane and ethane below room temperatures, and furthermore, that this surface can be selective towards ethane dehydrogenation to ethylene. For ethane, DFT shows that adsorption and initial C-H bond cleavage to surface bound C_2H_4* is facile and the selectivity step occurs between further C-H bond breaking leading to complete oxidation versus ethylene desorption. The reactivity of this surface is mediated by the presence of undercoordinated Ir (Ir_{cus}) and adjacent bridge O atoms (O_{br}). Using the combination of TPRS and DFT we find that pre-hydrogenating the IrO_2(110) surface results in the formation of HO_{br} sites that increases the selectivity towards ethylene by increasing the barrier to C-H bond cleavage for C_2H_4* and decreasing the desorption energy of C_2H_4*. We will discuss efforts to use DFT and microkinetic modeling to explore doping strategies of both the Ir_{cus} and O_{br} sites to promote selectivity towards ethylene formation.

8:40am HC+2D+SS-WeM-3 Design of Nanostructured Catalysts for Better Performance, *Francisco Zaera,* University of California, Riverside **INVITED**
One of the major challenges in heterogeneous catalysis is the preparation of highly selective and robust catalysts. The goal is to be able to synthesize solids with stable surfaces containing a large number of specific surface sites designed for the promotion of a particular reaction. New synergies between surface-science studies and novel nanosynthesis methodology

promise to afford new ways to design such highly selective catalysts in a controlled way. In this presentation we will provide a progress report on a couple of projects ongoing in our laboratory based on this approach. Platinum-based catalysts have been prepared for the selective trans-to-cis conversion of olefins, with a design based on early surface-science work with model surfaces and quantum mechanical calculations that indicated a particular preference for (111) facets in promoting the formation of the cis isomers. We are currently extending this research by using the concept of "single-site catalysis" with Pt-Cu bimetallics for the selective hydrogenation of unsaturated aldehydes. In a second example, new metal@TiO_2 yolk-shell nanomaterials conceived for both regular and photo-induced catalytic applications have been used to promote CO oxidation at cryogenic temperatures and to suggest that in photocatalysis the role of the metal may not be to scavenge the excited electrons produced in the semiconductor upon absorption of light, as commonly believed, but rather to promote the recombination of the adsorbed atomic hydrogen initially produced by reduction of H^+ on the surface of that semiconductor. New mixed-oxide surfaces are being designed using atomic layer deposition (ALD) as well.

9:20am HC+2D+SS-WeM-5 Characterization of a Pd/Ag(111) Single Atom Alloy Surface Using CO as a Probing Molecule for H₂ Dissociation, *Mark Muir*, M Trenary, University of Illinois at Chicago

Tuning catalysts for selective hydrogenation reactions is ultimately determined by the nature of the active site for H_2 dissociation and the adsorption of atomic hydrogen on the surface. Several single atom alloys (SAAs) consisting of small amounts of Pd deposited onto surfaces of metals that do not activate H_2 dissociation, such as Cu(111) and Au(111), have been previously studied. In the present study, we characterize Pd/Ag(111), a possible new single atom alloy surface using reflection absorption infrared spectroscopy (RAIRS) of adsorbed CO as a probe. From 0.01 to 0.04 ML Pd/Ag(111), a v(CO) stretching peak was seen at 2050 cm^{-1} corresponding to CO adsorbed on palladium atoms at the on-top site, indicating a single atom alloy surface. By increasing the palladium coverage to approximately 0.05 ML and above, a second v(CO) stretching peak was seen at 1950 cm^{-1} corresponding to CO adsorbed on a palladium bridge site, indicating palladium dimer formation. The surface palladium coverage was determined using temperature programmed desorption (TPD) of CO and Auger electron spectroscopy (AES). By annealing these surfaces to 500 K, the palladium atoms diffuse into the subsurface, and a v(CO) stretching peak at 2150 cm^{-1} (CO adsorbed on silver atoms) is greatly enhanced in intensity due to subsurface palladium. The subsurface to surface palladium ratios on the single atom alloy surfaces were varied from capped Ag/Pd/Ag(111), to a 50:50 ratio, to approximately a 60:40 ratio. The ability of subsurface palladium on the Pd/Ag(111) SAA surfaces to facilitate hydrogen dissociation was explored using H_2 and D_2 TPD.

9:40am HC+2D+SS-WeM-6 Propyne Hydrogenation over a Pd/Cu(111) Single Atom Alloy Catalyst Studied with Infrared Spectroscopy, *Mohammed Abdel-Rahman*, M Trenary, University of Illinois at Chicago

The hydrogenation of propyne (C_3H_4) to propylene (C_3H_6) using a Pd/Cu(111) single atom alloy (SAA) has been studied using polarization dependent-reflection absorption infrared spectroscopy. This method allows for simultaneous monitoring of reactants and products in the gas-phase and species adsorbed on the surface during the reaction. The results were compared with the hydrogenation of propyne using Pd-free Cu(111) as well as previous studies on Pd/Cu SAA alumina-supported metal catalysts. Propylene production first occurs at 383 K as indicated by the presence of an infrared peak at 912 cm^{-1}, which is a uniquely characteristic of gas-phase propylene. The presence of propyne oligomers on the surface is indicated by a dramatic increase in the peak intensity at 2968 cm^{-1} at temperatures above 400 K. The progression of the peaks at 912 and 3322 cm^{-1} was used to calculate the rate of production of propylene and the rate of consumption of propyne, respectively. This reaction rate was used to determine a turnover frequency (TOF) for the reaction on the Pd/Cu SAA catalyst.

11:00am HC+2D+SS-WeM-10 "Single-Atom" Catalysis: How Structure Influences Reactivity, *Gareth S. Parkinson*, TU Wien, Austria   INVITED

The field of „single-atom" catalysis (SAC) [1-2] emerged as the ultimate limit of attempts to minimize the amount of prescious metal used in heterogeneous catalysis. Over time, it has become clear that metal adatoms behave differently to supported nanoparticles [3-4], primarily because they form chemical bonds with the support and become charged. In this sense, SAC systems resemble the mononuclear coordination complexes used in homogeneous catalysis, and there is much excitement

that SAC could achieve similar levels of selectivity, and even heterogenize problematic reactions currently performed in solution. It is important to note, however, that homogeneous catalysts are designed for purpose based on well-understood structure-function relationships, but the complexity of real SAC systems means that the structure of the active site is difficult to determine, never mind design. In this talk, I will describe how we are using precisely-defined model supports [5] to unravel the fundamentals of SAC. I will show a selection of our latest results in this area, including scanning probe microscopy, x-ray photoelectron spectroscopy (XPS) and temperature programmed desorption (TPD) data to show how the local structure of $Ir_1/Fe_3O_4(001)$ and $Rh_1/Fe_3O_4(001)$ single atom catalysts changes based on preparation and adsorption of reactants, and how the structures obtained can be rationalised by analogy to Ir(I) and Ir(IV) complexes, respectively. If time permits, I will also show that CO oxidation activity in the $Pt_1/Fe_3O_4(001)$ system is promoted by water.

[1] Qiao, B., et al., Single-atom catalysis of CO oxidation using Pt1/FeOx. Nature Chemistry **3** (2011) 634-41.

[2] Liu, J., Catalysis by supported single metal atoms. ACS Catalysis **7** (2016) 34-59.

[3] Gates, B.C., et al., Atomically dispersed supported metal catalysts: perspectives and suggestions for future research. Catalysis Science & Technology **7** (2017) 4259-4275.

[4] Parkinson GS, Catalysis Letters 149 (2019), 1137-1146

[5] Bliem, R., et al., Subsurface cation vacancy stabilization of the magnetite (001) surface. Science, 346 (2014) 1215-8.

11:40am HC+2D+SS-WeM-12 Oxidation Reactions on Rh(111), *Marie Turano*, G Hildebrandt, Loyola University Chicago; R Farber, The University of Chicago; D Killelea, Loyola University Chicago

The uptake and subsequent surface structures of oxygen on transition metal surfaces reveal much about the reactivity of the metal catalyst. On clean Rh(111) at room temperatures in ultra high vacuum (UHV), oxygen molecules (O_2) readily dissociate into two adsorbed oxygen atoms, asymptotically approaching a saturation coverage of 0.5 monolayers (ML, 1 ML= 1.5×10^{15} O atoms cm^{-2}). However, exposing Rh(111) to gas-phase oxygen atoms (atomic oxygen, AO) generated by thermally cracking molecular oxygen over a hot Ir filament, allows for higher oxygen coverages. In addition, oxygen not only adsorbs to the surface, but it may also penetrate into the subsurface region of the crystal. After atomic oxygen exposures at elevated temperatures, the Rh(111) surface is covered in a combination of oxides, adsorbed surface oxygen, and subsurface oxygen (O_{sub}). The coexistence of a variety of structures allows for the determination of which species is reactive to the oxidation of carbon monoxide (CO) on highly oxidized Rh(111) surfaces. Using scanning tunneling microscopy (STM), we have determined that CO oxidation occurs mainly at the interface between the metallic and oxidic surface phases on Rh(111) where the O_{sub}, upon emergence from the bulk, replenishes the surface oxygen. Once O_{sub} is depleted, CO consumes the oxide and the surface quickly degrades into the (2×2)-O+CO adlayer.

12:00pm HC+2D+SS-WeM-13 Adsorption and Motion of Atomic Oxygen on the Surface and Subsurface of Ag(111) and Ag(110), S Isbill, C Mize, L Crosby, *Sharani Roy*, University of Tennessee Knoxville

Silver surfaces act as important industrial catalysts for the partial oxidation of ethylene to ethylene oxide and methane to methanol. While significant strides have been taken towards understanding the mechanism of heterogeneous catalytic oxidation by silver, the role of subsurface oxygen in such catalysis has yet to be elucidated. Subsurface oxygen is adsorbed just beneath the surface of the metal and is believed to play an important role in surface reconstruction and oxidation catalysis. In the present study, density functional theory (DFT) was used to study the interactions of atomic oxygen with the surface and subsurface of the Ag(111) and Ag(110) surfaces. The goal was to investigate the adsorption of atomic oxygen at different coverages and examine its effects on the structural and catalytic properties of silver. Our study of O/Ag(111) showed that adsorption of atomic oxygen was strong at low coverage but became weaker with an increase in coverage, much more so for surface oxygen than for subsurface oxygen. Therefore, at higher and industrially relevant oxygen coverages, oxygen preferred to bind to the subsurface than to the surface. In contrast, atomic oxygen bound more strongly to the surface than to the subsurface at all studied coverages. Based on the results from DFT, we constructed analytic models for adsorption in O/Ag(111) and O/Ag(110) as well as performed kinetic Monte Carlo simulations to explain the differences in coverage dependence of surface adsorption versus subsurface adsorption

on the two surfaces. The results provide qualitative insight on why surface and subsurface oxygen might have qualitatively different effects on the electronic, geometric, and catalytic properties of silver.

Magnetic Interfaces and Nanostructures Division
Room A210 - Session MI+2D-WeM

Emerging Multifunctional Magnetic Materials I and Magnetocaloric Materials

Moderators: Greg Szulczewski, The University of Alabama, Igor Barsukov, UC Riverside

8:00am **MI+2D-WeM-1 Spin-dependent Electron Reflection at Materials with Strong Spin-orbit Interaction**, *Markus Donath, C Angrick, A Reimann, C Datzer, A Blob,* Muenster University, Germany; *J Braun,* LMU München,, Germany; *H Ebert,* LMU München, Germany

The reflection of electrons at surfaces becomes spin dependent due to exchange interaction in the case of ferromagnets or due to spin-orbit interaction in the case of heavy elements. It can be used for spin-polarization analysis, e.g., in angle-resolved photoelectron spectroscopy in a single-channel mode or in multi-channel-mode detectors by using the scattering target as a spin-polarizing mirror. In addition, the understanding of the spin-dependent scattering properties provides information about the surface barrier. We present a combined experimental and theoretical study of the spin-dependent electron reflection at surfaces with strong spin-orbit interaction. We performed spin-dependent very-low-energy electron diffraction (VLEED) experiments on Au(111), Bi_2Se_3, and W(110) over a wide range of energies and angles of incidence. We derived maps for the reflectivity, the Sherman function, and the figure of merit and compare them with *ab-initio* calculations. In addition, we discuss possible working points for the use as scattering targets in spin-polarization analyzers.

8:20am **MI+2D-WeM-2 Competitive and Cooperative Electronic States in $Ba(Fe_{1-x}T_x)_2As_2$**, *Q Zou, M Fu, Z Wu, L Li, A Li, D Parker, A Safat, Zheng Gai,* Oak Ridge National Laboratory

The electronic structure inhomogeneity in Ni, Co and Ni doped $BaFe_2As_2$ 122 single crystals are compared using scanning tunneling microscopy/spectroscopy (STM/S) at atomic level within the pure superconducting (SC) dome, coexisting of SC and antiferromagnetic (AFM) phase, and non-SC phase regions. K-means clustering statistic method is utilized to categorize the various nanometer-size inhomogeneous electronic states described here as 'in-gap', 'L-shape' and 'S-shape' states immersed into the SC matrix for Ni-and Co-doped 122, and L-shape and S-shape states into metallic matrix for Cr-doped 122. Although the relative percentages of in-gap, L-shape and S-shape states various in three samples, the total volume fraction of the three electronic states is quite similar, coincident with the electron ($Ni_{0.04}$ and $Co_{0.08}$) and hole ($Cr_{0.04}$) numbers doped into the 122 compound. By combining the volume fractions of the three states, local density of the states (LDOS), field dependent behavior and global properties in these three sets of samples, the in-gap state in SC crystals is confirmed as magnetic impurity state from Co or Ni dopants, the L-shape state is identified as the spin density wave (SDW) which competes with the SC phase, and the S-shape state is found to be another form of magnetic order which constructively cooperates with the SC phase rather than competing with it. The comparison of the vortex structures indicates that those inhomogeneous electronic states serve as pinning centers for stabilizing the hexagonal vortex lattice.

8:40am **MI+2D-WeM-3 Microscopic Origin of High Temperature Magnetism in Multiferroic Superlattices $(LuFeO_3)_m/(LuFe_2O_4)_1$**, *Janice Musfeldt, S Fan, K Smith,* University of Tennessee Knoxville; *H Das, A Rebola,* Cornell University; *B Holinsworth,* University of Tennessee Knoxville; *J Mundy,* University of California at Berkeley; *C Brooks, M Holtz,* Cornell University; *R Ramesh,* University of California at Berkeley; *D Muller, D Schlom, C Fennie,* Cornell University; *S McGill,* National High Magnetic Field Laboratory **INVITED**

Multiferroics are fascinating materials in which ferroelectric and magnetic orders coexist and spatial inversion and time-reversal symmetries are simultaneously broken. Outstanding challenges that currently prevent widespread application in memory and logic devices as well as neuromorphic computing include requirements for (i) a large coupling coefficient and (ii) room temperature operation. The development of a homologous series of superlattices with formula $(LuFeO_3)_m:(LuFe_2O_4)_n$ offers a path forward, although questions still exist about the microscopic origin of the high-temperature magnetism and the nature of the charge

ordering pattern. In order to resolve these issues and provide additional insight into how external stimuli like magnetic fields can control behavior, we combined optical spectroscopy, magnetic circular dichroism, and first principles calculations to reveal the response of the $(LuFeO_3)_m:(LuFe_2O_4)_n$ superlattice. Each of the unique iron centers has excitations at slightly different energies, so by analyzing features in the dichroic rotation - which are proportional to net magnetization - and the character of the optical hysteresis loops at these energies, we reveal the magnetic field - temperature (H - T) behavior and how spin in the $LuFe_2O_4$ layer is the most significant contributor to the overall magnetic response. We also find that trends in the coercive field can be interpreted in terms of how the exchange strength depends upon the Fe site. The techniques developed here open the door to the microscopic analysis of materials with multiple metal centers and strong charge, spin, orbital, and lattice entanglement.

9:20am **MI+2D-WeM-5 Hidden Local Spin-polarized Electronic States investigated by Spin- and Angle-resolved Photoelectron Spectroscopy**, *Taichi Okuda,* Hiroshima University, Japan **INVITED**

Spin-polarized electronic states caused by spin-orbit interaction (SOI) have been attracted much attention recently because of the potential application for next-generation spintronic devices. In order to realize spintronic devices for various applications, it is necessary to search various kinds of new materials and systems possessing spin-polarized states. Although it was believed that the breaking of structural inversion symmetry is necessary to emerge the spin-polarized electronic states by SOI, the possibility of spin-polarized states by the inversion symmetry breaking at the local structure of crystals has been suggested recently[1]. Since the spin-polarization of the local structure of the other side of the crystal is opposite to maintain the zero net spin-polarization of materials, it is difficult to observe the local spin-polarization by macroscopic measurement and the spin-polarized states are, so to speak, hidden states.

Spin- and angle-resolved photoelectron spectroscopy(spin-ARPES) is one of the most powerful tools to investigate the spin-polarized electronic states caused by SOI since it can measure directly the *k*-dependent spin-polarization of electrons in the crystal (= spin-resolved band structure). Recent realization of high-efficiency, high-resolution and three-dimensional vector analysis in spin-ARPES measurement and the characteristic of the moderate proving depth of photoemission process enabled to investigate such hidden spin-polarized states. In this talk, some examples of the observation of the hidden spin-polarized states of layered materials (MoS_2, $PtSe_2$, and $LaOBiSe_2$, etc.)[2-4] will be presented. The finding of new materials possessing hidden spin-polarized states largely expands the variety of spin-polarized materials and will contribute to the future application for the spintronic devices.

[1] X. Zhang, Q. Liu, J.-W. Luo, A. J. Freeman, and A. Zunger, Nat. Phys. **10**, 387 (2014).

[2] R. Suzuki, M. Sakano, Y. J. Zhang, R. Akashi, D. Morikawa, A. Harasawa, K. Yaji, K. Kuroda, K. Miyamoto, T. Okuda, K. Ishizaka, R. Arita, and Y. Iwasa, Nat. Nanotechnol. **9**, 611 (2014).

[3] W. Yao, E. Wang, H. Huang, K. Deng, M. Yan, K. Zhang, T. Okuda, L. Li, Y. Wang, H. Gao, C. Liu, W. Duan, and S. Zhou, Nat. Commun. **8**, 14216 (2017).

[4] S.-L. Wu, K. Sumida, K. Miyamoto, K. Taguchi, T. Yoshikawa, A. Kimura, Y. Ueda, M. Arita, M. Nagao, S. Watauchi, I. Tanaka, and T. Okuda, Nat. Commun. **8**, 1919 (2017).

11:00am **MI+2D-WeM-10 Compositional Tuning of Magnetic Exchange Interactions and Interpretation of the Pressure Dependence of the Magnetic Curie Temperature in High Entropy Alloys.**, *Michael Mchenry,* Carnegie Mellon University **INVITED**

Magnetocaloric effect (MCE) materials are of interest in a more efficient technology than conventional gas compression refrigeration.MCE cooling is environmentally friendly since ozone depleting refrigerants are not used. Critical rare earths metals (REs) and compounds have large MCE response and working temperatures near room temperature. However, their scarcity, high price and corrosion limit their use. Recently, transition metal based high entropy alloys (HEAs) are studied for MCE applications due to convenient tunability of Curie temperatures,use of inexpensive components and tuning of the breadth of the magnetic phase transformation by distributing pair-wise magnetic exchange interations on a single fcc crystalline lattice. I will present our understanding of Curie temperature, T_c, engineering in metals with direct exchange interactions as rooted in the famous Bethe-Slater curve semi-empirically derived from considerations of the chemical bond and the constraints of the Pauli exclusion principle.

The Bethe-Slater curve predicts the dependence of the magnetic exchange interactions on D/d where D is the transition metal interatomic spacing and d is the spatial extend of the magnetic d-orbitals. The Bethe-Slater curveguides alloy design to optimize T_c's through distribution of exchange interactions in MCE HEAs. I will present results for the composition and pressure dependence of the Curie temperature along with Mossbauer spectra, for which the average hyperfine field is proportional to an average pairwise exchange interaction and by inference T_c. Within this formalism, we consider J(D/d), i.e. the exchange interaction(s) as a function of D/d the variable for which the Bethe-Slater curve is parameterized. The P-dependence of $T_c$will be interpreted for FeCoNiMnCu 5-component HEAs with a room temperature T_c.

11:40am MI+2D-WeM-12 Epitaxy of Novel Co$_{1.5}$Ti$_{0.5}$FeGe Heusler Alloy Thin Films, *Shambhu KC[1], R Mahat, T Evans, S Budhathoki, G Mankey, A Gupta, P LeClair,* The University of Alabama

While the half-metallic ferromagnets are considered ideal candidates to be used for efficient spintronics devices, a single-phase microstructure with promising half-metallic character is recently reported in a bulk Co$_{1.5}$Ti$_{0.5}$FeGe Heusler alloy[1]. This alloy has Ti substitution for Co atoms in the parent Co$_2$FeTiGe alloy, where the parent alloy does not exhibit half-metallic behavior[2]. However, the Ti substitution is useful not only to stabilize single-phase behavior but also to tune half-metallicity by the Fermi level shift. In this work, successful growth of epitaxial thin films of this novel Co$_{1.5}$Ti$_{0.5}$FeGe alloy on a-plane sapphire and MgAl$_2$O$_4$(100) by using DC magnetron sputtering will be reported. In-situ reflection high energy electron diffraction shows that the films grow epitaxially with smooth surfaces. X-ray diffraction analysis confirms the epitaxial relation and lattice parameters within a few percent of the reported bulk value. Presence of finite size Laue oscillations in the XRD pattern and 0.035˚ full width at half maximum of rocking curve obtained in case of films grown on a-plane sapphire describe excellent quality of the films. The presence of superlattice peaks; (200) and (111), indicate a strong tendency to form the L2$_1$ structure. The degree of B2 ordering is estimated to be as high as 0.92 showing that intermixing between the atoms in the octahedral and tetrahedral sites is limited. Atomic force microscopy shows that the films grown on MgAl$_2$O$_4$(100) are atomically smooth with a rms roughness of 0.2 nm. Magnetic measurements of films grown at 800ºC show that the saturation magnetization is in close agreement with the bulk value. Angle-dependent magnetization measurements show the symmetry of the coercivity is consistent with a magnetocrystalline anisotropy. Temperature-dependent transport measurements show metallic behavior and an ordinary magnetoresistance as high as 1.55 % is obtained at 100 K. All the above results describe the feasibility of growing good quality epitaxial films of novel Co$_{1.5}$Ti$_{0.5}$FeGe alloy with the structural and magnetic properties consistent with reported bulk properties.

1. KC et al., Tunable Properties and Potential Half-Metallicity in (Co$_{2-x}$Ti$_x$)FeGe Heusler Alloys; an Experimental and Theoretical Investigation, submitted to Phys. Rev. Materials.

2. Kumar et al., First-principles Calculation and Experimental Investigations on Full-Heusler Alloy Co$_2$FeGe, IEEE Transactions on Magnetics 45, 3997 (2009).

12:00pm MI+2D-WeM-13 Spin Transport in NiO Measured with Ferromagnetic Resonance, *G Mankey, T Evans, S KC, Arjun Sapkota, T Mewes,* The University of Alabama

Recently, a measured spin diffusion length of approximately 22 nm was reported for spin current transmission through polycrystalline NiO.[1] The diffusion length is inferred by referencing the effective Gilbert damping constant in NiO/Fe$_{20}$Ni$_{80}$ bilayers as a function of NiO and Fe$_{20}$Ni$_{80}$ thickness. We present results using a different approach to determine the spin diffusion length, using trilayers of Fe$_{20}$Ni$_{80}$/NiO/Pt with FMR measurements covering the frequency range of 4 GHz to 50 GHz. The Pt serves as a spin sink when deposited directly on Fe$_{20}$Ni$_{80}$ and strongly increases the effective damping parameter. With NiO between the Pt spin sink and the ferromagnetic Fe$_{20}$Ni$_{80}$, the increase in damping parameter is diminished, and the decay length is extracted from measurements as a function of NiO thickness. Our preliminary measurements show that the decay length is smaller than 15 nm consistent with a decay length of approximately 4 nm determined from inverse spin hall effect measurements of Y$_3$Fe$_5$O$_{12}$/NiO/Pt structures.[2] In addition, at lower FMR frequencies (4 GHz as compared to 22 GHz) multiple resonances are observed for polycrystalline NiO,

suggesting that ferromagnetic impurities are present in the antiferromagnet.

Results for polycrystalline and epitaxial trilayers will be presented, showing the effect of processing conditions on the spin diffusion length. These measurements will be correlated with microstructural and morphological characterization of the samples.

References

1 Tetsuya Ikebuchi, Takahiro Moriyama, Hayato Mizuno, Kent Oda, and Teruo Ono, Appl Phys Express **11** (7), 073003 (2018).

2 Yu-Ming Hung, Christian Hahn, Houchen Chang, Mingzhong Wu, Hendrik Ohldag, and Andrew D. Kent, AIP Advances **7** (5), 055903 (2017).

Nanometer-scale Science and Technology Division
Room A222 - Session NS-WeM

Optics and Scattering on the Nanoscale

Moderators: Alex Belianinov, Oak Ridge National Laboratory, Nancy Burnham, Worcester Polytechnic Institute

8:00am NS-WeM-1 Semiconductor Nanowires for Optoelectronics Applications, *Chennupati Jagadish [2] ,* Australian National University, Australia **INVITED**

Semiconductors have played an important role in the development of information and communications technology, solar cells, solid state lighting. Nanowires are considered as building blocks for the next generation electronics and optoelectronics. In this talk, I will introduce the importance of nanowires and their potential applications and discuss about how these nanowires can be synthesized and how the shape, size and composition of the nanowires influence their structural and optical properties. I will present results on axial and radial heterostructures and how one can engineer the optical properties to obtain high performance lasers, THz detectors and solar cells. Future prospects of the semiconductor nanowires will be discussed.

8:40am NS-WeM-3 Photonic-Plasmonic Fiber Probe for Nanoscale Chemical Imaging, *B Birmingham, K Minn, B Ko, H Lee, Zhenrong Zhang,* Baylor University

Probing light-matter interaction in nanoscale regime requires the efficient delivery and collection of electromagnetic energy to and from the nanoscale region of interest. Metallic plasmonic nano-probes can efficiently excite and detect the near-field at nanoscale for near-field imaging and sensing applications such as tip-enhanced Raman spectroscopy (TERS). We have studied the interaction of molecules with bulk MoS$_2$, a semiconductor, using TERS. MoS$_2$, has attracted tremendous attention due to promising applications in electronics, photonics, and catalysis. Here we have compared the difference in the interaction of sub-monolayer copper phythalocyanine (CuPc) molecules with MoS$_2$ and Au. The relative Raman peak ratio and Raman peak position shift from spatial TERS mapping show the difference in the adsorbates-adsorbates interaction and the adsorbates-substrates interaction on Au and MoS$_2$ substrates.

We also propose a photonic-plasmonic probe for nanoscale confinement of light. In our device, light in a fiber couples with the surface plasmons of a nano-antenna. The coupled plasmonic mode then propagates down the conical waveguide to the narrow apex where it gets localized and strongly focused, exhibiting immense field enhancement. By changing the structures at the fiber-antenna interface, the linearly polarized fiber mode is converted to radial surface plasmon polaritons (SPP's) through asymmetric coupling. The probe can be implemented into TERS setup to obtain spectroscopic information at the nanoscale.

9:00am NS-WeM-4 Nanoscale Infrared Confinement Using Surface Phonon Polaritons, *Vanessa Breslin, A Grafton,* National Research Council Postdoctoral Fellow*; D Ratchford, A Giles, K Fears, C So, S Katzer, C Ellis, J Tischler,* U.S. Naval Research Laboratory*; J Caldwell,* Vanderbilt University*; A Dunkelberger, J Owrutsky,* U.S. Naval Research Laboratory

Plasmonic materials can be used for surface enhanced infrared absorption, a particularly useful technique for chemical sensing applications, but these materials typically suffer from high optical loss due to the fast scattering of electrons, which results in broad optical resonances. In contrast, surface phonon polaritons (SPhPs) have much lower losses because of the slower

---

scattering rates of phonons, resulting in narrower resonance bands. In particular, our group is investigating polar dielectric inorganic crystals that have mid-IR Reststrahlen bands, frequency ranges where the crystals' optical constants resemble metals and can support SPhP resonances. Currently, our efforts are focused on studying the optical properties of $W(CO)_6$ and calcite ($CaCO_3$) crystals in the mid-IR. We are also experimenting with using a helium ion microscope, a gallium focused ion beam, and other lithographic techniques to nanostructure the surface of these polar dielectric materials in order to generate SPhPs for sub-diffraction optical confinement of mid-IR incident light. The results of these studies will allow us to better understand how to tune SPhPs in a broader spectral range with different inorganic materials and provide a basis for exploring how these resonances interact with other chemical systems through enhanced spectroscopies and energy transfer.

9:20am **NS-WeM-5 Actuating and Probing a Single-molecule Switch at Femtosecond Timescales**, *D Peller, L Kastner, T Buchner, C Roelcke, F Albrecht, R Huber, Jascha Repp*, University of Regensburg, Germany **INVITED**

Accessing ultra-fast non-equilibrium phenomena is enabled by terahertz (THz) scanning tunneling microscopy [1] (THz-STM) through combining STM with lightwave electronics. In THz-STM, the electric field of a phase-stable single-cycle THz waveform acts as a transient bias voltage across an STM junction. These voltage transients may result in a net current that can be detected by time-integrating electronics. The recent development of this lightwave STM has enabled the combined femtosecond and sub-angstrom resolution in observing matter [2].

We now demonstrate the first combined femtosecond and sub-angstrom access in the control of matter. Ultrafast localized electric fields in lightwave STM enable exerting atom-scale femtosecond forces to selected atoms. By shaping atomic forces on the intrinsic timescale of molecules, coherent atomic motion can now be excited. Utilizing this coherent structural dynamics, we can modulate the quantum transitions of a single-molecule switch by up to 39%. We directly visualize the coherent excitation of the switch in the first femtosecond single-molecule movie [3].

To resolve the impact of coherent control of the single-molecule switch, alongside, we introduce single-shot action spectroscopy in lightwave STM as the first concept resolving individual path-selective reaction events of a single molecule in space and time. With this novel concept, we detect the outcome of every single laser shot and further separate the statistics of the two inverse reaction paths.

Our results open a new chapter in the control and observation of reactions of individual molecules directly on the relevant ultrafast and ultrasmall scales.

References:

[1] T. L. Cocker et al., Nature Photon. 7, 620 (2013).

[2] T. L. Cocker et al., Nature 539, 263 (2016).

[3] D. Peller et al., in preparation.

11:00am **NS-WeM-10 Nanoscale Structural Imaging through Bragg Diffraction Microscopy**, *Martin Holt,* Argonne National Laboratory **INVITED**
The development of x-ray nanobeam instrumentation at synchrotron x-ray light sources has created a wide range of opportunities in understanding nanoscale phenomena in materials science, chemistry, and condensed matter physics. Such instruments, including the Center for Nanoscale Materials/Advanced Photon Source Hard X-ray Nanoprobe (HXN) employ highly brilliant x-ray beams with focal spot sizes on the order of tens of nanometers and sufficient phase-coherent intensity to produce high-dynamic range scattering patterns from individual nanoscale objects. The far higher brilliance resulting from the APS Upgrade project promises to enable new classes of nanodiffraction experiment and to bring new challenges in the management and predictive analytic interpretation of large coherent scattering datasets. The scientific use of these instruments has required the creation of advanced x-ray analysis techniques based on combinations of coherent diffraction and ptychography with the unique optical conditions of tightly focused x-ray beams enabling correlation of structural and chemical mapping. The classes of scientific questions that are addressable by these techniques and the potential impact of diffraction limited storage rings such as the APS-Upgrade project will be explored within the context of recent results.

11:40am **NS-WeM-12 First Launch of XTIP - The World's First User Program for the Combination of Scanning Tunneling Microscopy with Synchrotron Radiation**, *Volker Rose, N Shirato, D Rosenmann, M Fisher, S Hla,* Argonne National Laboratory

The combination of the ultimate spatial resolution of scanning probe microscopy with the chemical and magnetic sensitivity of synchrotron x-rays has opened the prospect for an entirely new way of nanoscale materials' characterization. Over the last couple of years, Argonne National Laboratory has pioneered the development of synchrotron x-ray scanning tunneling microscopy (SX-STM). The technique has demonstrated imaging with direct elemental contrast down to the level of single atom height as well as imaging of nanoscale magnetic domains of thin films.

In order to open up this new capability to the entire science community, and to fully exploit the special capabilities of the technique, XTIP, a dedicated beamline for SX-STM has been construction at Argonne's Advanced Photon Source. To meet the scientific objective of the nanoscience and nanomagnetism communities most effectively, XTIP offers full polarization control over the 500-1600 eV photon energy range. The dedicated XTIP beamline, inaugurated in the summer of 2019, provides researchers access to a one-of-a-kind instrument. Among the potential breakthroughs are "designer" materials created from controlled assemblies of atoms and molecules, and the emergence of entirely new phenomena in chemistry and physics. The easy process for obtaining access to the XTIP beamline will also be covered.

This work was performed at the Advanced Photon Source and the Center for Nanoscale Materials, a U.S. Department of Energy Office of Science User Facility under Contract No. DE-AC02-06CH11357.

12:00pm **NS-WeM-13 Application of Scanning Tunneling Microscopy and Tip-Enhanced Raman Spectroscopy to the Study of Intermolecular and Molecule-Substrate Interactions**, *Jeremy Schultz[1], N Jiang,* University of Illinois at Chicago
Molecular self-assembly on surfaces is defined by the unique set of circumstances that arise from the complicated interplay of molecule-molecule and molecule-substrate interactions. These interactions are defined by their highly localized chemical environments. As a result, it becomes necessary to apply spatially resolved techniques. In this work we have applied two primary techniques to the study of intermolecular and molecule-substrate interactions. Scanning tunneling microscopy (STM) reveals local electronic effects and structure, while tip-enhanced Raman spectroscopy (TERS) defines the vibrational fingerprint of a molecule which is highly sensitive to localized chemical effects. In combination with gas phase Density Function Theory (DFT) calculations it is possible to define the effects of molecule-substrate interactions on the molecules' vibrations. Three different systems involving organic molecules on single crystals have been examined: boron subpthalocyanine, 3,6-dibromo-9,10-phenanthrenequinone, and rubrene. Through the tandem technique of STM-TERS, intermolecular interactions that result in self-assembly, specifically hydrogen bonds, halogen bonds, and van der Waals interactions have been characterized. Similarly, molecule-substrate effects on molecular configuration and binding strength have been considered through comparison with DFT simulated Raman spectra to obtain a detailed description. Ultimately, the application of complementary techniques results in highly descriptive vibrational fingerprints with spatial resolution.

Complex Oxides: Fundamental Properties and Applications Focus Topic
Room A220-221 - Session OX+EM+MI+SS-WeM

Electronic and Magnetic Properties of Complex Oxide Surfaces and Interfaces

Moderators: Yingge Du, Pacific Northwest National Laboratory, Vincent Smentkowski, GE Global Research Center

8:00am **OX+EM+MI+SS-WeM-1 Charge Transfer in Lanthanum Ferrite-Strontium Nickelate Superlattices**, *Le Wang, Z Yang, M Bowden,* Pacific Northwest National Laboratory*; J Freeland,* Argonne National Laboratory*; Y Du, S Chambers,* Pacific Northwest National Laboratory
Charge transfer at oxide interfaces can drive emergent phenomena that do not occur in the bulk, thereby significantly enriching our fundamental

---

[1] **NSTD Graduate Student Award Finalist**

understanding of these material systems and their applications. Designing oxide heterostructures and seeking new and novel interfacial phenomena has been an active area of research for some time. We have synthesized a series of $[(LaFeO_3)_m/(SrNiO_{3-d})_n]_z$ $([(LFO)_m/(SNO)_n]_z)$ superlattices (SLs) (z = 7 to 21) by oxide molecular beam epitaxy on $(LaAlO_3)_{0.3}(Sr_2AlTaO_6)_{0.7}$ (LSAT) (001) substrates. *In situ* RHEED patterns and x-ray diffraction measurements reveal a high degree of structural quality in the SLs. X-ray photoemission spectroscopy (XPS) shows that the Fe is Fe^{4+} in the $(LFO_1/SNO_1)_{21}$ SL. However, the Fe 2p binding energy shifts to lower values with increasing LFO layer thickness in $(LFO_m/SNO_1)_z$ SLs, suggesting that the volume averaged Fe valence decreases. Fe L-edge X-ray absorption spectroscopy (XAS) measurements corroborate the XPS results, indicating that Fe is 4+ for the $(LFO_1/SNO_1)_{21}$ SL and mostly 3+ for the $(LFO_5/SNO_1)_{10}$ SL. On the other hand, Ni L-edge XAS shows that Ni valence is Ni^{3+} for the $(LFO_1/SNO_1)_{21}$ SL as is also true for insulating $NdNiO_3$, suggesting that the Ni layers in this SL are insulating, which is consistent with our in-plane transport measurements. However, for the $(LFO_5/SNO_1)_{10}$ SL, the Ni valence is larger than 3+. The measured energy shifts suggest that Ni is close to 4+. The thicker LFO layer in the $(LFO_5/SNO_1)_{10}$ SL may result in a larger band offset and create a potential well to trap the holes in the Ni layer, inducing the formation of Ni^{4+}. Our ongoing studies are probing the impact of the SNO layer thickness on material structure as well as the evolution of the Fe and Ni valences in $(LFO_5/SNO_n)_z$ SLs. Additional planned experimental and theoretical investigations will address how charge transfer from Fe to Ni occurs at the LFO/SNO interface, and how to stabilize the unusual high 4+ valence in Fe^{4+} and Ni^{4+} by means of interfacial engineering.

8:20am OX+EM+MI+SS-WeM-2 Self-healing Growth of LaNiO₃ on Mixed-terminated $(LaAlO_3)_{0.3}$-$(Sr_2AlTaO_6)_{0.7}$, *Friederike Wrobel*, H Hong, S Cook, T Andersen, D Hong, C Liu, A Bhattacharya, D Fong, Argonne National Laboratory

Epitaxial $LaNiO_3$ (LNO) thin films and superlattices are known to be antiferromagnetic and weakly insulating for LNO thicknesses of 2 unit cells but paramagnetic and metallic for higher LNO thicknesses [1]. The quality of the single-crystal substrate surface, and in particular the chemical composition of the surface, is known to be a key factor governing the quality of the deposited thin film. For $SrTiO_3$ (001) substrates, there are well-established preparation methods to ensure that the surface is TiO_2-terminated and atomically smooth; the only features that appear with atomic force microscopy are the regular steps and terraces associated with crystal miscut. $SrTiO_3$ is therefore often preferred as a substrate over other materials like $(LaAlO_3)_{0.3}$-$(Sr_2AlTaO_6)_{0.7}$ (LSAT), whose surface composition is harder to control. Interestingly, for unknown reasons, the highest quality LaNiO3 thin films have been grown on mixed-terminated, untreated LSAT (001) substrates [2, 3]. At present, very few detailed studies have been conducted regarding the precise influence of the substrate on thin film growth behavior due to the need for an in-situ, atomic-scale characterization technique. Exploiting an in-situ, oxide molecular beam epitaxy (MBE) chamber at the Advanced Photon Source, we were able to monitor the deposition of thin films of LNO on LSAT (001) substrates with different surface compositions. Both non-resonant and resonant (Sr K-edge) X-ray scattering measurements were conducted at several points during the growth process. We observed the formation of atomically smooth, high-quality LNO films regardless of the initial substrate surface composition, suggesting that any excess, non-stoichiometric material on the initial LSAT substrate rises to the surface during deposition. With atomic layer-by-atomic layer MBE under the right conditions, we can therefore achieve self-healing growth behavior of complex oxides on top of mixed-terminated substrates. We will discuss details of the in-situ growth measurements and the methods used to determine the atomic and chemical structures.

1. Frano, A., et al., *Orbital Control of Noncollinear Magnetic Order in Nickel Oxide Heterostructures.* Physical Review Letters, 2013. **111**(10): p. 106804.

2. Liu, C., et al., *Counter-thermal flow of holes in high-mobility LaNiO3 thin films.* Physical Review B, 2019. **99**(4): p. 041114.

3. Wrobel, F., et al., *Comparative study of LaNiO3/LaAlO3 heterostructures grown by pulsed laser deposition and oxide molecular beam epitaxy.* Applied Physics Letters, 2017. **110**(4): p. 041606.

8:40am OX+EM+MI+SS-WeM-3 Optoelectronics with Oxides and Oxide Heterostructures, *Alexander Demkov*, University of Texas at Austin
INVITED
Si photonics is a hybrid technology combining semiconductor logic with fast broadband optical communications and optical information technologies. With the increasing bandwidth requirement in computing and signal processing, the inherent limitations in metallic interconnection are seriously threatening the future of traditional IC industry. Silicon photonics can provide a low-cost approach to overcome the bottleneck of the high data rate transmission by replacing the original electronic integrated circuits with photonic integrated circuits. The development has proceeded along several avenues including mounting optical devices based on III-V semiconductors and/or $LiNbO_3$ (LNO) on Si chips, incorporation of active optical impurities into Si, and utilization of stimulated Raman scattering in Si. All these approaches have had limited success. Recently, another path to Si photonics through epitaxial integration of transition metal oxide films was demonstrated when an effective electro-optic (Pockels) coefficient of $BaTiO_3$ (BTO) films epitaxially grown on Si *via* an $SrTiO_3$ buffer was reported to be an order of magnitude larger than that in commercially-available LNO modulators. More generally, epitaxial growth of $SrTiO_3$ on Si(001) enables monolithic integration of many functional perovskite oxides on Si, including ferroelectric BTO, ferromagnetic $LaCoO_3$, photocatalytic TiO_2 and CoO, and many others.

In this talk, I will focus on two materials systems integrated on Si (001) and well-suited for implementation in the next-generation optical technologies: $SrTiO_3/LaAlO_3$ quantum wells and Pockels-active BTO thin film heterostructures. Both materials systems are promising for use in a wide variety of optical and electro-optical devices central to integrated photonic technologies, including quantum cascade lasers, photodetectors, electro-optic modulators and switches. The resulting devices achieve refractive index tuning with power consumption many orders of magnitude less than previously reported. Taken together, these two approached will hopefully open the door for the development of new kinds of optical and electro-optical devices for use in integrated photonics technologies.

9:20am OX+EM+MI+SS-WeM-5 Medard W. Welch Award Lecture: Defect-Mediated Coupling of Built-in Potentials at Buried Interfaces Involving Epitaxial Complex Oxides, *Scott. A Chambers*[1], Pacific Northwest National Laboratory **INVITED**
Semiconductor-based devices are of broad importance, not only in electronics, but also in energy technology. Internal electric fields dictate the flow of charge that occurs both laterally and vertically. The associated potential profiles can be approximated from electronic transport data, and also calculated via Poisson-Schrodinger modeling, provided the properties of the constituent materials and interface structures are sufficiently well understood. These approaches work well for heterostructures involving, for instance, III-V semiconductors. However, when complex oxides are involved, they become unreliable because of poorly understood defects that can be present. There is, therefore, a critical need for new methods to enable the determination of band-edge profiles in heterostructures involving these materials.

The $SrTiO_3/Si(001)$ interface has been a prototypical system for understanding the materials physics and electronic structure of crystalline oxides on semiconductors. Thinner films (a few unit cells, u.c.) are known to result in flat-band heterojunctions in which the valence (conduction) band offset is large (small). However, we have recently found that thicker films (~30 u.c.) of $SrNb_xTi_{1-x}O_3$ ($0 \leq x \leq 0.2$) on intrinsic Si(001) result in completely different electronic structures. Transport data suggest sharp upward band bending in the Si, leading to hole gas formation at the interface, and a large (~2 eV) built-in potential in the SNTO, along with surface depletion. We have probed these buried interfaces using hard x-ray photoelectron spectroscopy (HAXPES). The resulting core-level spectra exhibit unusual features not seen in thinner films, and not credibly ascribed to secondary phases or many-body effects. In order to interpret these line shapes, we hypothesize that they result from large built-in potentials within the system. We have developed an algorithm to extract these potential profiles by fitting heterojunction spectra to linear combinations of spectra from phase-pure, flat-band materials, summed over layers within the probe depth, each with a binding energy characteristic of the potential at each depth. This approach leads to excellent agreement with experiment and band-edge profiles completely consistent with those from transport data. Moreover, we find that the built-in potentials extracted from HAXPES on the Si side of the interface are in quantitative agreement with those resulting from solving Poisson's equation using the SIMS profile for in-diffused oxygen from the STO. Oxygen is a shallow donor in Si, and assuming 100% donor ionization, along with the ^{18}O SIMS depth profile, leads to near-perfect agreement with HAXPES.

---

[1] **Medard W. Welch Award Winner**

11:00am OX+EM+MI+SS-WeM-10 Spin Transport Studies on Epitaxial Ultrathin SrIrO₃ Films Grown using Pulsed Laser Deposition (PLD), *M S Ramachandra Rao,* Indian Institute of Technology, India*; K Sethupathi, T Suraj, S Suresh,* Indian Institute of Technology Madras, India

Generation, transportation and detection of spin in a controlled manner are very important in spintronic devices for efficient switching mechanisms in a magnetic tunnel junction (MTJ)[1,2,3]. The conversion of charge current to spin current is known as spin Hall effect (SHE) and the inverse phenomenon is inverse SHE (ISHE). The detection of spin is usually realized by the ISHE. Spin Hall magnetoresistance (SMR) arises due to the combined effect of SHE and ISHE in a bilayer heterostructures consisting of a ferromagnetic (or ferrimagnetic) insulator (FMI) and a normal metal (NM). Magnetic Proximity Effect (MPE) observed in YIG/Pt complicates the spin transport scenario with additional effects such as Anomalous Hall effect (AHE) which attenuates the SMR signal.[4,5] Our group has successfully studied Ga: ZnO insertion on Bi: YIG/Pt and observed SMR signals[6]. Correlated metal oxide SrIrO₃ is a potential candidate which can replace Pt because of its high spin-orbit coupling.

We have deposited SrIrO₃ thin films with thickness from 3 nm to 10 nm using pulsed laser deposition on LSAT(001) substrate with LaMnO₃ as a buffer layer. Detailed structural measurements have been carried out to understand the strain induced in the bilayer system by varying oxygen partial pressure during deposition of LaMnO₃. Also, spin transport studies have been carried out since LaMnO₃ is an A-type antiferromagnet. Angle-dependent magnetic measurements performed on these bilayer samples shows SMR, as well as anisotropic magnetoresistance (AMR) and the AMR part, is dominating over SMR. A particular thickness of SrIrO₃ shows a crossover from negative magnetoresistance to positive magnetoresistance. I will be presenting our experimental observations on spin transport studies carried out in these bilayers.

References

7.   Matthias Althammer *et. al.,* Phys. Rev. B 87, 224401 (2013).
8.   T. Kikkawa *et. al.,* Phys. Rev. Lett. 110, 067207 (2013).
9.   E. Saitoh *et. al.,* Appl. Phys. Lett. 88, 182509 (2006).
10. H. Nakayama *et al.,* Phys. Rev. Lett. 110, 206601 (2013).
11. V. Castel *et al.,* Appl. Phys. Lett. 101, 132414 (2012).
12. Matthias Althammer *et.al.*Appl. Phys. Lett. 110, 052403 (2017).

11:20am OX+EM+MI+SS-WeM-11 Structural and Dielectric Characterization of Epitaxial Entropy-Stabilized Oxide Thin Films, *George Kotsonis, J Maria,* Pennsylvania State University

The emergence of entropy-stabilized oxides (ESOs) represents a new paradigm for complex oxide engineering. The large configurational entropy of ESOs facilitates mixing of chemically dissimilar cations in significant proportions. ESO research continues to intensify as the oxide community works toward a thorough understanding of structure-property-synthesis relationships. Due to inherent metastability, high energy, non-equilibrium synthesis techniques are well suited for ESO fabrication. In particular, laser ablation has excelled at producing high quality epitaxial ESO thin films, which provide a platform for fundamental characterization.

We present the growth and characterization of Ba(Ti₀.₂Sn₀.₂Zr₀.₂Hf₀.₂Nb₀.₂)O₃ and similar Barium-based perovskite structured ESO thin films grown by laser ablation. Crystal structure, surface morphology, and optical properties are characterized by X-ray diffraction, atomic force microscopy, and ellipsometry respectively. Epitaxial thin film capacitor structures were fabricated to characterize the frequency, voltage, and temperature dependence of electrical properties.

By exploiting the entropy-stabilized nature of ESOs, we demonstrate the incorporation of significant amounts of aliovalent cation pairs (*e.g.* $Sc^{3+}Ta^{5+}$) in hopes of producing nano-polar regions supporting a dispersive dielectric response similar to relaxor ferroelectrics. Additionally, we explore compositional space in search of a phase boundary between a high-symmetry ESO phase and a lower symmetry end-member. Compositions at such a boundary may exhibit phase instability and enhanced dielectric functionality similar to compositions at or near a morphotropic phase boundary. The compositional degrees of freedom available in ESO systems provide new avenues for property tuning and studying the effects of extreme chemical disorder on dielectric properties.

11:40am OX+EM+MI+SS-WeM-12 Oxygen Vacancy-Mediated Epitaxy: TiO₂(111)/Al₂O₃(0001) and Ferromagnetic Cr₂O₃(0001)/TiO₂(111), *C Ladewig, F Anwar, Jeffry Kelber,* University of North Texas*; S Shah, P Dowben,* University of Nebraska-Lincoln

The formation of all-oxide heterostructures comprising multiferroic oxides interfaced with appropriate semiconducting substrates is a promising path towards low power, voltage-switchable spintronics, including non-volatile memory and multi-functional logic devices. At the same time, the necessary scaling of film thicknesses to the nm range can induce structures and properties sharply different than those of the bulk. We report here in situ XPS, LEED, EELS and ex-situ MOKE data on the growth and properties of Cr₂O₃(0001) on TiO₁.₇(111) on Al₂O₃(0001). The data indicate that the presence of O vacancies during film growth can mediate the further growth of oxides with unusual structures and properties. These data show that (a) O vacancies during initial stages of film growth yield a TiO₂ film of an unusual crystallographic orientation and structure; and that (b) this leads to growth of an epitaxial Cr₂O₃ layer exhibiting magnetic ordering above the expected Néel temperature of thin film chromia - indicative of a strained chromia lattice due to epitaxial growth on a substrate with a lattice constant of 5.1 Å, compared to the bulk chromia lattice constant of 4.9 Å. Molecular beam epitaxy (MBE) of Ti at 500 K in 10⁻⁶ Torr O₂ on Al₂O₃(0001) initially yields TiO₁.₇(111) with the structure of corundum phase Ti₂O₃ (a = b=5.1 Å). Further deposition and annealing in O₂ results in stoichiometric TiO₂(111), but with the same lattice structure and orientation as Ti₂O₃(111), and with a total thickness of 5 nm. This is sharply different from the generally observed growth of TiO₂(001) on Al₂O₃(0001). MBE of ~ 1 monolayer of Cr on TiO₂(111) yields hexagonally-ordered Cr₂O₃ and the formation of titania oxygen vacancies. MOKE measurements confirm that this chromia layer is magnetically ordered at 280 to 315 K, likely antiferromagnetically ordered, with exchange bias coupling to the TiO₁.₇(111) substrate. O vacancies in the TiO₂(111) lattice exhibit weak ferromagnetic behavior, as is evident in the In-plane MOKE, enhancing the canting of the magnetism away from the thin film normal, which is expected for the Cr₂O₃(0001) alone. These data demonstrate that careful control of initial growth conditions and film stoichiometry during oxide MBE can template the subsequent growth of stoichiometric oxide heterostructures with non-bulk like structures and properties.

12:00pm OX+EM+MI+SS-WeM-13 Incorporation of Ti into Epitaxial Films of Magnetite, *Tiffany Kaspar, S Spurgeon, D Schreiber, S Taylor, M Bowden, S Chambers,* Pacific Northwest National Laboratory

Magnetite, Fe₃O₄, exhibits metallic conductivity via electron hopping between Fe^{2+} and Fe^{3+} occupying octahedral sites in the spinel lattice. As Ti^{4+} is doped into the octahedral sites of magnetite (the titanomagnetite series), an equal fraction of Fe^{3+} is reduced to Fe^{2+} to maintain charge neutrality. The site occupancies of Fe^{2+} and Fe^{3+} determine the transport properties of the titanomagnetite series; the end-member ulvöspinel, Fe₂TiO₄, exhibits *p*-type semiconducting transport properties. The Fe^{2+}/Fe^{3+} site occupancy remains controversial, but is likely in part a function of the lattice strain induced by doping smaller Ti^{4+} into the lattice. Here, we have deposited titanomagnetites and ulvöspinel as well-defined epitaxial thin films on MgO, MgAl₂O₄, and Al₂O₃ substrates by oxygen-plasma-assisted molecular beam epitaxy. The incorporation of Ti into the magnetite lattice is found to depend strongly on deposition conditions and substrate orientation. We have characterized the crystalline structure, phase segregation, and surface morphology with XRD, STEM/EDS, APT, and AFM, and related these to the kinetic and thermodynamic factors determined by the deposition conditions. The Fe valence state is evaluated with *in situ* XPS. The impact of film structure and Fe oxidation state on the electrical transport properties of the films will be discussed.

Plasma Science and Technology Division
Room B131 - Session PS+EM-WeM

Plasma Processing of Materials for Energy

Moderators: Ankur Agarwal, KLA-Tencor, Saravanapriyan Sriraman, Lam Research Corp

8:00am **PS+EM-WeM-1 Plasma Processes for High Efficiency Multi-Junction Solar Cells Fabrication**, *Maxime Darnon, M Volatier, P Albert, M de Lafontaine, P St-Pierre, G Hamon,* LN2, CNRS / Université de Sherbrooke, 3IT, Canada*; C Petit-Etienne, G Gay, E Pargon,* LTM, CNRS / Université Grenoble Alpes, France*; V Aimez, S Fafard, A Jaouad,* LN2, CNRS / Université de Sherbrooke, 3IT, Canada **INVITED**

Multijunction solar cells provide the highest efficiency for solar energy conversion into electricity. With record efficiency above 45%, they are used in concentrated photovoltaic systems where their cost is mitigated by the sunlight concentration. Conventional technics for such solar cells' fabrication include III-V materials epitaxy on germanium, electrodes lift off, antireflective coating deposition by physical vapor deposition and isolation by saw dicing. In this presentation, we will show how plasma processes can advantageously be used to replace some of these steps and how it could enable the fabrication of new architectures of solar cells.

A low-damage III-V plasma etching step can isolate the solar cells one to the other before the mechanical saw dicing. This reduces the density of recombination centers at the edge of the solar cells and provides therefore a higher open circuit voltage. Deep germanium plasma etching can also be used for solar cells dicing with trenches as small as 10 μm. As an alternative to physical vapor deposition, plasma enhanced chemical vapor deposition can coat high transparency silicon nitride and silicon oxide that form an excellent anti-reflective coating and passivate surface recombination centers.

In addition to their benefit for conventional solar cells fabrication, these plasma-based processes also provide opportunity for the fabrication of new kinds of multijunction solar cells, such as ultra small solar cells (<0.07 mm^2), front-side contacted solar cells, back-side contacted solar cells, and through cell via contacted solar cells.

8:40am **PS+EM-WeM-3 Combinatorial Synthesis of Ternary Oxides by Reactive Sputtering for CdTe Solar Cells**, *Yegor Samoilenko, G Yeung, C Wolden,* Colorado School of Mines

Polycrystalline CdTe-based solar cells have reached efficiencies of over 22% in the recent years. The road towards high V_{oc} and 25% devices requires a combination of low interface recombination velocity, higher lifetime, and higher carrier concentration in the CdTe absorber. It was recently demonstrated that the impact of the interface recombination on the performance of the device is more pronounced as carrier concentration and lifetime increase. Magnesium zinc oxide (MZO) has been identified as a transparent emitter that enables high efficiency in CdTe based solar cells. By controlling the alloy composition one may tune the conduction band alignment with CdTe absorber at the front interface to reduce recombination. Most previous work has employed MZO targets sputtered in Ar. However there are open questions as to what the optimal composition, its stability, and sensitivity to subsequent processing.In this work we perform a combinatorial study of MZO buffer layer prepared by co-sputtering of Zn and Mg in oxygen-containing atmosphere. Combinatorial libraries are formed with a band gap variation of more than 0.4 eV across a 2 inch substrate. These are integrated into standard CdTe to determine the optimal composition based on using J-V characteristics. In addition, the stability of these films is assessed by surface spectroscopy, and routes to stabilize performance are introduced.

9:00am **PS+EM-WeM-4 Potential Applications of TiN-based Plasmonic Nanoparticles: From Plasmon-induced Chemistry to Photothermal Absorption**, *A Alvarez Barragan, C Berrospe Rodriguez, Lorenzo Mangolini,* University of California, Riverside

The light-harvesting capacity of plasmonic nanoparticles has recently garnered attention in the synthesis of plasmon-driven photocatalysts. Gold and silver have been used to successfully drive hydrogen dissociation and CO oxidation reactions by injecting hot electrons into molecules adsorbed to their surface. However, the chemical instability of silver and the low thermal stability of both metals, in addition to their high cost, inspire the quest for alternative plasmonic materials that could potentially expand the field towards more ambitious and cost-effective applications. Titanium nitride (TiN) is a conductive ceramic with high hardness and bulk melting point (2930 °C). Its plasmon resonance located in the visible-NIR region,

low cost relative to gold and silver, and well-understood properties as a thin film in the semiconductor industry make it a strong alternative to mainstream plasmonic metals. The present work encompasses a comprehensive study of the synthesis of TiN nanoparticles via a non-thermal plasma method. It also highlights the potential of this material as an alternative in plasmonic catalysis and as a high-temperature-resistant photothermal absorber. TiN particles are synthesized via a scalable, modular, non-thermal plasma method. Titanium and nitrogen precursors are transported into a RF frequency plasma where TiN particles nucleate and grow. Platinum nanoparticles were subsequently deposited on the TiN by photo-induced reduction of an aqueous solution of chlorplatinic acid (H_2PtCl_6). The reduction of the precursor metal was driven by electron hole pair generation via plasmon decay. The addition of methanol as a hole scavenger increased the electron lifetime, leading to the obtention of metallic platinum. This reaction occurred at temperatures below 40°C under visible light illumination. In addition, a novel $TiN@SiO_xN_y$ core-shell structure is facilitated by the modular capabilities of the non-thermal plasma synthesis method. The plasmon peak of the extinction spectrum of the core-shell particles is enhanced by 60% compared to the uncoated TiN particles. The high temperature resistance of these heterostructures is also demonstrated, as their optical properties remain stable at 700 °C under vacuum and at 400 °C in air. This work strengthens the case for alternative plasmonic materials in fields dominated by precious metals, and heavily driven by materials cost.

9:20am **PS+EM-WeM-5 Plasma-induced Strain in MoS$_2$ Films for the Electrochemical Hydrogen Evolution Reaction**, *T Liu, X Liu, Souvik Bhattacharya,* Case Western Reserve University*; Z Ye, R He,* Texas Tech University*; X Gao, R Akolkar, R Sankaran,* Case Western Reserve University

There has been recent interest in growing layered materials such as molybdenum disulfide (MoS$_2$) over large areas for electronic and energy applications. One such approach is chemical vapor deposition (CVD) in which vapor precursors are thermally decomposed to nucleate a thin film at the surface of a substrate. A plasma may also be employed to assist in decomposition of the precursor molecule through gas-phase excitation, for example in plasma-enhanced CVD (PECVD) or plasma-enhanced atomic layer deposition (PEALD). Here, we report a plasma-assisted approach which is fundamentally different than these deposition techniques which we term plasma-enhanced chemical film conversion (PECFC). Precursor films are first prepared as a thin film on a substrate from liquids and subsequently converted by a combination of heating and plasma treatment. The process is additive, in that the precursor is only present where it is desired and there is little materials wastage, and substrate-independent, by circumventing the need for adsorption, allowing direct growth on application-specific substrates.

In this talk, we will present results for the synthesis of MoS$_2$ films and their application as electrocatalysts for the hydrogen evolution reaction (HER). A single-molecule precursor, ammonium tetrathiomolybdate (ATM), was first dispersed in solution with linear polyethylenimine (L-PEI) and spin-coated to produce a well-defined thin film less than 50 nm thick. The precursor film was then treated by an atmospheric-pressure dielectric barrier discharge (DBD) in a background of argon and hydrogen gas (80:20) at 500 °C. Conversion to crystalline MoS$_2$ was confirmed by X-ray diffraction and micro Raman spectroscopy. Atomic force microscopy was performed to study possible nucleation and growth mechanisms by varying the growth temperature and treatment time. The chemical composition was analyzed by X-ray photoelectron spectroscopy which showed an ideal stoichiometric ratio of 1:2 Mo:S.

A potential application of MoS$_2$ films is HER because it is composed of earth abundant elements and has been shown to be highly active through its edge sites. We carried out a systematic study of the origin of HER activity in our films, both after initial conversion and after several other post-synthesis treatments . The investigation showed that our initially-converted films have tensile strain leading to intrinsic activity that is comparable to previously reported sulfur vacancy generation by post-synthesis plasma treatment steps. In our case, the strain is induced in the initial fabrication step, providing a simpler and more scalable process to produce efficient HER electrocatalysts.

9:40am **PS+EM-WeM-6 Comparison of Pulsed and Continuous Wave Argon Plasmas for the Synthesis of Vertical Graphene Nanosheets**, *Zoe Mann, E Fisher,* Colorado State University

Vertical graphene nanosheets (VGNs) have unique structural and electronic properties that make them applicable in fields such as energy storage, electronics, and sensing. VGNs are often grown using high-power, high-

temperature processes and hazardous or unsustainable precursors such as methane. For this reason, we sought to develop a simple, efficient, and more environmentally-friendly way to synthesize VGNs. In this work, VGNs are synthesized from butter or coconut oil (sustainable, non-toxic precursors) spread on a Ni foam or Cu substrate and then treated with a high peak power pulsed plasma process. The materials formed through this process are compared to those produced with a continuous wave treatment of equivalent power and a low peak power pulsed plasma treatment, as well as to the untreated material. We used a range of characterization techniques to assess the materials, including scanning election microscopy (SEM), X-ray photoelectron spectroscopy (XPS), Raman spectroscopy, and cyclic voltammetry, providing data on the morphology, surface chemistry, bulk characteristics, and electrochemical performance, respectively. SEM imaging shows that VGNs grown by the high power pulsed PECVD technique have high surface area and abundant ultra-thin edges. XPS analysis of untreated butter and the low-power pulsed plasma treated samples reveals binding environments consistent with the chemical composition of triglycerides (the primary chemical component in butter/oil), whereas the XPS and Raman spectra of VGNs indicate the presence of sp^2-hybridized carbon. Notably, cyclic voltammograms of VGNs formed on Ni foam are characteristic of a capacitor, and these materials do not exhibit the deleterious side reactions found with VGNs formed on the Cu substrate. To better understand the underlying chemistry occurring during plasma treatment, optical emission spectroscopy data were collected, revealing key information on species important for VGN synthesis, such as atomic and molecular carbon.

Materials and Processes for Quantum Information, Computing and Science Focus Topic
Room B231-232 - Session QS+2D+EM+MN+NS+VT-WeM

Material Systems and Applications for Quantum Sciences
Moderators: Mena Gadalla, Harvard University, Kai Xiao, Oak Ridge National Laboratory

8:00am **QS+2D+EM+MN+NS+VT-WeM-1 Quantum Information at the Molecular Foundry - An Overview of New Toolsets for QIS Research**, *Adam Schwartzberg, S Cabrini, D Ogletree, A Weber-Bargioni,* Lawrence Berkeley National Laboratory (LBNL)

The fundamental unit of quantum computation and sensing is the qubit, and many physical systems have been investigated for practical realization. These include superconducting Josephson junction circuits, color centers, and isolated cold atoms or ions. Superconducting qubit circuits (SCQBs) being one of the most promising avenues to quantum computation. However, there are limitations to their practical application due to noise sources which shorten their functional lifetime.

In this talk I will introduce a suite of integrated, high-fidelity fabrication instrumentation that will allow new communities of users to investigate the fundamental limits of state-of-the-art quantum systems at the Molecular Foundry. We will enable users to understand existing systems and design new ones by creating a quantum fabrication toolset for directed growth of conventional and novel materials, advanced lithography and pattern transfer paired with in- and ex-situ surface characterization.

Three key QIS fabrication capabilities at the Molecular Foundry:

A robotic fabrication cluster system with materials deposition, including atomic layer and physical vapor depositions, plasma etching, and analytical characterization instrumentation, all automated by and contained within a vacuum sample handling robot.

A high resolution electron beam writing system will allow quantum device patterning with complete flexibility in feature shape, density and size, enabling nanoscale feature control.

A low temperature transport measurement system will allow for the investigation of novel materials for superconductors and dielectrics and "close the loop" between design and fabrication, proxy measurements such as interface characterization, and actual performance of quantum computation and sensing elements.

This instrumentation suite will enable the elucidation of chemical composition, structure, location, and size of microscopic noise sources in a superconducting quantum system, understanding the fabrication steps that introduced such noise sources, and developing fabrication approaches that minimize their presence.

I will also discuss ongoing and new research directions at the Molecular Foundry through internal staff and external user research.

8:20am **QS+2D+EM+MN+NS+VT-WeM-2 Quantum Vacuum Metrology to Advance Quantum Science Capabilities**, *Jay Hendricks, J Ricker, K Douglass,* National Institute of Standards and Technology (NIST)*; J Fedchak, J Scherschligt,* National Institute of Sandards and Technology (NIST)

NIST is developing a series of next generation pressure and vacuum standards that will serve as a basis for key vacuum technology platforms required for emerging quantum science applications. The production of quantum sensors and devices is anticipated to require extremely demanding process control with exact knowledge of background residual gas, process chamber pressure, and accurate measurement of gas pressure feedstocks.

In 2019, National Metrology Institutes around the world worked to redefine the international system of units, the SI, such that the base units are now based on fundamental constants.

Moving forward, the next generation of pressure and standards will provide a new route of SI traceability for the pascal. By taking advantage of both the properties of light interacting with a gas and that the pressure dependent refractive index of helium can be precisely predicted from fundamental, first-principles quantum-chemistry calculations, a new route of realizing the pascal has been demonstrated. This talk will briefly cover the classical methods of realizing pressure that have served the metrology community well for the past 375 years. And then will take a deeper dive into the next generation of light-based pressure standards that will enable the elimination of mercury manometers, replacing them with a smaller, lighter, faster, and higher precision standards. From a metrology stand point, the new quantum-based SI pascal will move us from the classical force/area definition, to an energy density (joules per unit volume) definition. Should the technique be further miniaturized, it will lead to a revolution in pressure metrology, enabling a photonics-based device that serves both a gas pressure sensor and a portable gas pressure standard all in one.

NOTE: this topic is appropriate for VT sessions as well but thought it would be interesting to the broader audience that is interested in emerging quantum-based technologies that are needed to advance the field of quantum science.

8:40am **QS+2D+EM+MN+NS+VT-WeM-3 Quantum Control of Spins in Silicon Carbide with Photons and Phonons**, *David Awschalom, S Whiteley, G Wolfowicz, K Miao,* University of Chicago **INVITED**

There are numerous efforts to embrace solid-state defects and construct quantum systems to enable new information technologies based on the quantum nature of the electron. Current studies include semiconductors with incorporated point defects, whose quantum mechanical spin properties allow a fundamentally different means to process information. In particular, interfacing solid-state defect electron spins to other quantum systems is an ongoing challenge. Here we demonstrate electrically driven coherent quantum interference in the optical transition of single divacancies, enabling new control of the spin-photon interface [1]. By applying microwave frequency electric fields, we coherently drive the excited-state orbitals and induce Landau-Zener-Stückelberg interference fringes in the resonant optical absorption spectrum. Furthermore, we develop a stroboscopic X-ray diffraction imaging technique that provides direct imaging and quantitative measurement of local strain at the nanometer scale. In conjunction with the fabrication of surface acoustic wave resonators, we mechanically drive coherent Rabi oscillations between arbitrary ground-state spin levels, including magnetically forbidden spin transitions, allowing for acoustic quantum control of local spins in silicon carbide and the exploration of spin-phonon coupling in the solid state [2]. These properties establish divacancies as strong candidates for quantum communication and hybrid system applications, where simultaneous control over optical and spin degrees of freedom is paramount.

[1] K. C. Miao *et al*., arxiv: 1905.12780

[2] S. J. Whiteley *et al.*, Nature Phys. **15**, 490 (2019)

Wednesday Morning, October 23, 2019

9:20am **QS+2D+EM+MN+NS+VT-WeM-5 Tunable Control over InSb(110) Surface Conductance Utilizing Charged Defects**, *Robert Walko, S Mueller, S Gant, J Repicky, S Tjung, E Lang, E Fuller, K Werner,* The Ohio State University; *F Bergmann,* Bergmann Messgeraete Entwicklung; *E Chowdhury, J Gupta,* The Ohio State University

In this work we present a scanning tunneling microscopy (STM) study of tip-induced switching of charge states in individual indium adatoms on the InSb(110) surface. These adatoms are deposited onto the surface by controlled voltage pulses between the STM tip and the surface. We observe them in two distinct charge states: positive and neutral. Adatom-induced band bending from the positively charged state has been observed to induce a tenfold increase in surface conductance relative to the charge neutral state, the effect of which can be observed >100nm away from the indium adatom. When the STM tip is brought sufficiently close to the defect, electrons can tunnel from the tip to the defect and cause the charge state to switch from positive to neutral. During imaging, this switching leads to a "crater" feature around the defect due to the lower conductance of the charge neutral state. The spatial extent of the crater can be tuned via the applied bias voltage, the tunneling set-point current, and photoillumination of the surface. We explain this phenomenon using a model of competing rates between the filling and emptying of the defect state, similar to dangling bonds on the Si(111) surface.

This work acknowledges funding from the DOE (# DE-SC0016379)

9:40am **QS+2D+EM+MN+NS+VT-WeM-6 Quantum Calligraphy: Writing Single-Photon Emitters in a Two-Dimensional Materials Platform**, *Matthew R. Rosenberger,* U.S. Naval Research Laboratory; *C Dass,* Air Force Research Laboratory; *H Chuang, S Sivaram, K McCreary,* U.S. Naval Research Laboratory; *J Hendrickson,* Air Force Research Laboratory; *B Jonker,* U.S. Naval Research Laboratory

We present a paradigm for encoding strain into two dimensional materials (2DM) to create and deterministically place single photon emitters (SPEs) in arbitrary locations with nanometer-scale precision. Our material platform consists of a 2DM placed on top of a deformable polymer film. Upon application of sufficient mechanical stress using an atomic force microscope tip, the 2DM/polymer composite deforms, resulting in formation of highly localized strain fields with excellent control and repeatability. We show that SPEs are created and localized at these nanoindents, and exhibit single photon emission up to 60K. This *quantum calligraphy* allows deterministic placement and real time design of arbitrary patterns of SPEs for facile coupling with photonic waveguides, cavities and plasmonic structures. In addition to enabling versatile placement of SPEs, these results present a general methodology for imparting strain into 2DM with nanometer-scale precision, providing an invaluable tool for further investigations and future applications of strain engineering of 2DM and 2DM devices.

Reference: Rosenberger et al., "Quantum Calligraphy: Writing Single-Photon Emitters in a Two-Dimensional Materials Platform," *ACS Nano*, 2019, https://pubs.acs.org/doi/10.1021/acsnano.8b08730

11:00am **QS+2D+EM+MN+NS+VT-WeM-10 Challenges in Topological and Quantum Materials**, *David Alan Tennant,* Oak Ridge National Laboratory **INVITED**

Quantum materials are rapidly advancing but still present great challenges. Topological quantum

materials in particular are receiving great attention as they provide potentially robust routes to

quantum information processing that are protected against decoherence processes. Among key

challenges are the prediction and realization of magnetic materials in the form of magnetic Weyl

semimetals and quantum spin liquids as ways of realizing exotic quasiparticles such as Majorana fermions

that can be used for application. These materials present new experimental challenges in terms of identifying their

quasiparticles and demonstrating quantum coherence in their ground states states. Here I will

show how we are using the integrated application of machine learning along with experiment and synthesis

to advance the discovery and understanding of these materials.

11:40am **QS+2D+EM+MN+NS+VT-WeM-12 Rare Earth Silicon Photonics Engineering for Quantum Applications**, *A Nandi, X Jiang, D Pak,* Purdue University; *D Perry, E Bielejec,* Sandia National Laboratories; *Y Xuan, Mahdi Hosseini,* Purdue University

Controlling intermodal coupling between multiple excitations within a photonic material may enable the design of novel quantum photonic metamaterials exhibiting anomalous effects. Understanding the complex mode dynamics towards the engineering of system Hamiltonian has been the subject of intensive research in recent years. Here, we design an atomic lattice composed of nearly 1000 rare earth ion segments deterministically engineered in silicon photonic structures to modify the emission properties of erbium in silicon. We observe anomalous photon emission at the telecommunication wavelength from atoms geometrically arranged to reduce the propagation loss. Moreover, we map asymmetric emission lineshapes led by intermodal Fano-type interference of the atomic and photonic resonance modes. Our observation paves the way for designing active metamaterials and novel topological photonics with engineered linear and nonlinear interactions for broad applications in quantum information. Moreover, I will result for direct integration of rare earth crystals with silicon photonic chip for implementation of quantum optical memories. The approach can impact the fields of quantum communication and computation through, for example, developing superradiant single photon sources, the study of non-equilibrium many-body quantum dynamics, and engineering quantum transport in a scalable solid-state platform.

New Challenges to Reproducible Data and Analysis Focus Topic
Room A124-125 - Session RA+AS+CA+PS+TF-WeM

Reproducibility in Science and Engineering, including materials and energy systems
Moderators: Karen Gaskell, University of Maryland, College Park, Svitlana Pylypenko, Colorado School of Mines

8:00am **RA+AS+CA+PS+TF-WeM-1 Reproducibility and Replicability in Science and Engineering: a Report by the National Academies**, *T Winters,* National Academies of Sciences, Engineering, and Medicine; *Dianne Chong,* Boeing Research and Technology (Retired) **INVITED**

One of the pathways by which scientists confirm the validity of a new finding or discovery is by repeating the research that produced it. When a scientific effort fails to independently confirm the computations or results of a previous study, some argue that the observed inconsistency may be an important precursor to new discovery while others fear it may be a symptom of a lack of rigor in science. When a newly reported scientific study has far-reaching implications for science or a major, potential impact on the public, the question of its reliability takes on heightened importance. Concerns over reproducibility and replicability have been expressed in both scientific and popular media.

As these concerns increased in recent years, Congress directed the National Science Foundation to contract with the National Academies of Science, Engineering, and Medicine to undertake a study to assess reproducibility and replicability in scientific and engineering research and to provide findings and recommendations for improving rigor and transparency in research.

The committee appointed by the National Academies to carry out this task included individuals representing a wide range of expertise: methodology and statistics, philosophy of science, science communication, behavioral and social sciences, earth and life sciences, physical sciences, computational science, engineering, academic leadership, journal editors, and industry expertise in quality control. Individuals with expertise pertaining to reproducibility and replicability of research results across a variety of fields were included as well.

This presentation will discuss the committee's approach to the task and its findings, conclusions, and recommendations related to factors that influence reproducibility, sources of replicability, strategies for supporting reproducibility and replicability, and how reproducibility and replicability fit into the broader framework of scientific quality and rigor.

8:40am RA+AS+CA+PS+TF-WeM-3 Directly Assessing Reproducibility in Materials Chemistry Research Using Literature Meta-analysis, *David Sholl,* Georgia Institute of Technology **INVITED**
While it is widely agreed that making reported research more reproducible is a desirable goal, less is known about how reproducible current work in materials chemistry is. I will discuss using literature meta-analysis as a tool to obtain quantitative insight into the reproducibility of materials chemistry experiments. Case studies will be discussed involving measurements of gas adsorption in metal-organic frameworks and the synthesis of metal-organic framework materials. These are useful examples to study because comprehensive databases of information from the open literature are available, but they share features that are common in many areas of material chemistry. Insights from these case studies suggest possible paths towards improving data reproducibility for individual researchers, for academic departments and for professional organizations.

9:20am RA+AS+CA+PS+TF-WeM-5 Reproducibility in Fundamental and Applied Science, *George Crabtree,* Argonne National Laboratory, University of Illinois at Chicago **INVITED**
The scientific enterprise operates via a few basic features, including questions, insight, hypotheses, critique, reproducibility, elaboration and revision. All contribute to the process of discovery, none can be taken as the single signature of scientific truth. Discovery science is a dynamic process informed by new observations and continuous refinement of the precision, accuracy, principals and scope of our collective scientific knowledge. History has many examples of significant revisions of previously accepted dogma based on new observations (the earth is flat, matter is infinitely divisible, the stars are fixed). New insights lead to new fundamental principles (energy is conserved, nothing can go faster than light, germs cause disease) that open new opportunities for advancing the scientific frontier and raising the quality of life. Examples of advances of the frontiers of energy science and their implications for reproducibility will be given.

11:00am RA+AS+CA+PS+TF-WeM-10 Representativeness of a TEM image for Revealing New Phenomenon in Energy Storage Materials, *Chongmin Wang,* Pacific Norththwest National Laboratory; *D Baer,* Pacific Northwest National Laboratory
Transmission electron microscopy (TEM), as a imaging technique with high spatial resolution, appears to be a routine tool for showcasing, often viewed as an enlightening figure, the structural and chemical information of materials at multiscale of down to single atomic column. One of a very common questions that raised by the viewer, not necessarily suspicious, is the representativeness of the image to the real situation as considering the sampling scale of the TEM imaging method. This question is further elevated for the case of in-situ and operando observation as which naturally couples in another dimension of "time" in addition to the "spatial" scale. In addition, beam effect can be coupled in for artifacts. In this presentation, we will check into the reproducibility of TEM imaging of both in-situ and ex-situ for revealing new phenomenon in energy storage materials, while certain cautions may also be necessary for interpreting new observations based on TEM.

11:20am RA+AS+CA+PS+TF-WeM-11 Reproducibility Issues when Developing Catalysts for Fuel Cell Applications, *M Dzara, S Zaccarine,* Colorado School of Mines; *K Artyushkova,* Physical Electronics and University of New Mexico; *Svitlana Pylypenko,* Colorado School of Mines
This talk will discuss reproducibility issues encountered during the development of novel catalysts for low temperature fuel cell performance (PEMFC) as replacements of state-of-the-art catalysts that contain Pt-based nanoparticles supported on a high surface area carbon support. Examples across several catalytic systems will be shown, including low platinum-group metal (low-PGM) catalysts with extended surfaces derived from nanowire templates, and PGM-free catalysts based on N-doped carbon with an atomically dispersed transition metal.

Reproducibility issues related to the synthesis of these catalytic materials and their impact on the performance of these catalysts will be reported first following by discussion of challenges in characterization. Specifically, the need for complementary characterization will be highlighted along with issues that arise when materials are characterized by different groups using different techniques. Another set of reproducibility issues arises when conducting characterization of catalysts under in-situ and in-operando conditions.[1] The time constraints imposed by the availability of instrumentation result in datasets that have a limited number of samples, areas per samples and replicate measurements on the same sample.

(1) Dzara, M. J.; Artyushkova, K.; Shulda, S.; Strand, M. B.; Ngo, C.; Crumlin, E. J.; Gennett, T.; Pylypenko, S. Characterization of Complex Interactions at the Gas – Solid Interface with in Situ Spectroscopy : The Case of Nitrogen-Functionalized Carbon. *J. Phys. Chem. C* **2019**, *123* (14), 9074–9086.

11:40am RA+AS+CA+PS+TF-WeM-12 Challenges in Multimodal Spectroscopic Analysis of Energy Storage Materials, *Vijayakumar Murugesan,* Pacific Norththwest National Laboratory; *K Mueller,* Joint Center for Energy Storage Research (JCESR) **INVITED**
Charge transfer across heterogeneous interfaces facilitated by redox reactions is the basis of energy storage technology. Capturing the interfacial processes over broad scales both spatially (ranging from angstroms up to 100 nm) and temporally (lasting from fs up to a few minutes) is a major challenge. This is one origin of the existing knowledge gaps in energy storage materials, which impede our ability to predict and control the emergent behaviors at electrochemical interfaces. As part of Joint Center for Energy Storage Research (JCESR) center, we developed a multi-modal in situ characterization tool set based on X-ray absorption, photoelectron and multinuclear NMR spectroscopy in combination with computational modelling that can access a range of the important complex processes. This multimodal approach helps us gain critical insights of the charge transfer process, but also presented unique challenges in data collection, analysis and reproducibility. The multitude of constituents and varying surface chemistry combined with external stimuli (applied potential and temperature) challenges the traditionally conceived time and spatial resolution limitations of the probes. For example, establishing reference systems and base line measurements for electrochemical process where combinatorial constituents react and depend on the charge state is a major challenge in spectroscopic studies and complicates subsequent corroboration with computational analysis. In this talk, we will discuss overcoming these challenges and apply the methods to critically analyzing solid-electrolyte interphase (SEI) evolution in Li-metal based batteries, multivalent ion transport across membranes and chemical stability of redox flow battery electrolytes.

Thin Films Division
Room A122-123 - Session TF1-WeM

Vapor Deposition of Functional Polymer Thin Films and Composites
Moderators: Adrienne Stiff-Roberts, Duke University, John (Jack) Lyons, U.S. Naval Research Laboratory

8:00am TF1-WeM-1 Durable Surface Energy Control with Initiated Chemical Vapor Deposited (iCVD) Polymers, *Karen Gleason,* Massachusetts Institute of Technology **INVITED**
Multiple iCVD homopolymer and co-polymer compositions have been employed for the tuning of surface energy from ultrahydrophobic to ultrahydrophilic and for fine-tuning the surface energy over much narrow ranges as well. The iCVD approach is particularly valuable for insoluble materials, including low-surface energy fluoropolymers and durable crosslinked networks. The iCVD surface modification layers can be ultrathin (<20 nm) and are able to conformally cover geometric features in the substrate. For iCVD poly(divinylbenzene) (PDVB), this combination of features enabled the controlled wetting and directed self-assembly of block co-polymers inside of confined features. Ultrathin and conformal iCVD fluoropolymers on aligned carbon nanotube stamps prevent densification of the stamp upon drying, enabling high-speed flexographic printing with nanoparticle inks.

Since film growth proceeds upwards from the substrate, iCVD offers the opportunity for interfacial engineering prior to beginning iCVD synthesis. Indeed, linker-free graftingcan be achieved in situ immediately prior to the iCVD growth on substrates from which hydrogen atoms can be abstracted. Linker-free grafted cross-linked PDVB layers display outstanding robustness and have served as a base layer for a covalent attached top layer of iCVD fluoropolymers. The grafted PDVB/fluoropolymer bilayers provide resistance against the attachment of ice and natural gas hydrates and even proved durable when sandblasted. Grafting is essential for tethering swellable hydrophilic surface modification layers. Indeed the durability of iCVD hydrogels and zwitterionic layers is greatly enhanced by grafting for the prevention of delamination.

8:40am TF1-WeM-3 Initiated Chemical Vapor Deposition of poly(N-vinylcaprolactam)-based Cross-linked Smart Hydrogel Thin Films with Tunable Temperature-responsive Swelling Behavior, *Fabian Muralter, A Perrotta, A Coclite,* Graz University of Technology, Austria

Initiated Chemical Vapor Deposition (iCVD) makes it possible to deposit smart hydrogel thin films conformally into 3D-nanostructures for sensor applications. For this contribution, cross-linked p(N-vinylcaprolactam)-based (pNVCL) thin films were synthesized by iCVD for the first time. In aqueous environment, the phase transition of these polymeric systems between a "hydrophilic" swollen state below to a "hydrophobic" shrunken state above their lower critical solution temperature (LCST) was investigated via spectroscopic ellipsometry. As previously shown for other polymers, the amount of cross-linking has been used to tune the temperature-responsive behavior of the deposited pNVCL-based systems. Interestingly, pNVCL is also reported to show decreased transition temperatures for higher molecular weight systems. Thus, by changing the filament temperature during iCVD, it was possible to lower the LCST by almost 20°C, without changing the (nominal) composition. Overall, degrees of maximum swelling of the polymer below the transition temperature of up to 250% of the dry thickness could be achieved and the LCST could be tuned in the range of 16-40°C. For probing the applicability in sensor setups, these systems were also investigated in terms of swelling in humid environment (relative humidity, RH). There, three regions could be identified: First, in rather dry environment, the systems respond by mainly filling porosity, but not showing a temperature-responsive behavior. Second, up to ~80% RH, the response in swelling is close to linear to the measured RH. Third, in very humid environment, the swelling is highly non-linear and temperature-dependent. Moreover, the film thickness approaches the value that can be observed also when the polymer is immersed in water at the respective temperature. Furthermore, the response of the polymer in water as well as in humid environment has been shown to be very fast, as, for example, it responds faster than the commercial sensor used for monitoring the RH in the measurement cell. Together with the biocompatibility reported for pNVCL, the knobs of filament-temperature and cross-linking to tune the described features of the temperature-responsive swelling behavior of these systems make them highly promising for biomedical or environmental (sensor) applications.

9:00am TF1-WeM-4 Enhancing the Key Properties of CVD Polymer Thin Films for Device Fabrication, *Xiaoxue Wang,* The Ohio State University; *K Gleason,* Massachusetts Institute of Technology

In the last decade, the rapid development of the flexible and stretchable (soft) electronics has been largely fueled by the fundamental breakthrough in soft materials synthesis and new fabrication technologies. Among the soft electronic materials, polymers stand out due to their merits of high stretchability, biocompatibility, light weight, scalability and cost-efficiency. However, despite the great prospects of electronic polymers, several critical challenges still need to be addressed: (1) Key electrical properties, such as electrical conductivity (σ) and carrier mobility (μ) of polymers are still relatively low compared with conventional rigid semiconductors, and result in higher power consumption and lower operation speed; (2) Low thermal conductivity (κ) makes heat dissipation a critical issue; (3) Conventional solution-based processing technologies may pose wettability and compatibility issues for device fabrication on flexible substrates. Here we will present a synergistic approach to combat these challenges by using Chemical Vapor Deposition (CVD) technology as an effective tool. First, record high electrical conductivity (σ) and charge carrier mobility (μ) are achieved in poly(3,4-ethylenedioxythiophene) (PEDOT), with engineered crystallization and morphology implemented by CVD. We also build wafer-scale PEDOT-Si rectifier arrays operating at 13.56 MHz for RFID readers by direct CVD synthesis. Second, record high cross-plane thermal conductivity (>10x common polymers) is demonstrated in intrinsic poly(3-hexylthiophene) (P3HT) thin films by using a self-assembling CVD growth method. This method generates an extended chain structure with π-π stacking, and thereby significantly facilitates the thermal transport. Lastly, CVD's powerful capability in device application, with gas sensors as an example, will be presented. In summary, this work establishes an innovative method to effectively tune the key physical properties of polymers by CVD-based structure-property engineering on the molecular level. In addition, this work also has the potential to facilitate novel device fabrication technologies and applications in artificial skin, bio-degradable sensors, stretchable photovoltaics and light emitting diodes (LEDs).

9:20am TF1-WeM-5 Conductive Directly Fused Poly (Porphyrin) Coatings by an Oxidative Chemical Vapour Deposition Approach, *Kamal Baba, G Bangasi, G Frache, D El Assad, J Desport,* Luxembourg Institute of Science and Technology, Luxembourg*; K Heinze,* Johannes Gutenberg University of Mainz, Germany*; N Boscher,* Luxembourg Institute of Science and Technology, Luxembourg

Thanks to their remarkable functional properties, porphyrinic compound led to the development of various technological applications, including photovoltaic[1] catalysis[2] and sensing.[3] Among this porphyrinic compounds, conjugated and directly fused porphyrins attracted strong attention.[4] Indeed, the high conjugation of these systems provides additional interesting functional properties such as two photon absorption, near infrared absorption and enhanced electro-catalytic activity.[5,6] However, while the solution-phase synthesis of directly fused porphyrin coatings has been successfully developed in recent years, the deposition of these promising compounds in thin film form has remained a challenge.

In this work, we report the simultaneous synthesis and deposition of conductive directly fused poly(porphyrin) coatings based on a substrate independent and up-scalable oxidative chemical vapor deposition (oCVD) approach. The direct fusion of nickel(II) 5,15-(diphenyl)porphyrin (NiDPP) is successfully achieved using different oxidants, such as iron(III) chloride ($FeCl_3$), copper(II) chloride ($CuCl_2$) and copper(II) perchlorate hexahydrate ($Cu(ClO_4)_2 \cdot 6H_2O$). The decisive reactions and side reactions during the oCVD process are evidenced by Lased Desorption Ionization High Resolution Mass Spectroscopy (LDI-HRMS) and UV-Vis-NIR absorption. $FeCl_3$ is demonstrated to be the most suitable oxidant, allowing the formation of singly-fused poly(NiDPP) or conductive doubly or triply-fused poly(NiDPP) that strongly absorb in the near-infrared spectral region. Owing to the highly conjugated structure of the fused tapes, the deposited coatings films exhibit electrical conductivity up to 7×10^{-1} S cm^{-1} and strong absorption in the visible to near-infrared spectral region.

The described approach is not specific to NiDPP, providing the fact that meso-position remains available, other porphyrins can be fused and deposited in thin film form. Interestingly, the developed approach is inherently scalable and readily allows the deposition and patterning of conductive fused porphyrin thin films on sensitive substrates, such as printer paper or polymer foils, paving the way to the integration of directly fused porphyrin into advanced optoelectronic devices.

References:

1. S. Mathew, A. Yella, P. Gao et al., Nat. Chem. 2014, 6(3), 242–7

2. W. Zhang, W. Lai, R. Cao, Chem. Rev. 2017, 117(4), 3717–3797

3. Y. Ding, WH. Zhu, Y. Xie, Chem. Rev. 2017, 117(4), 2203–2256

4. T. Tanaka, A. Osuka, Chem. Soc. Rev. 2015, 44, 943–969

5. H. Mori, T. Tanaka, A. Osuka, J. Mater. Chem. C. 2013, 1, 2500–2519

6. D. Khusnutdinova, B.L. Wadsworth, M. Flores et al., ACS Catal. 2018, 8, 9888–9898

9:40am TF1-WeM-6 Molecular Design and Vapor Phase Synthesis of Crown-Ether-Based Thin Film Materials, *Darrin Liau, G Rubloff, S Lee, K Gregorczyk,* University of Maryland, College Park

Ion transport in materials and at their interfaces plays a profound role in a wide spectrum of applications. These include: energy generation (solar-driven water splitting and fuel cells); energy storage (batteries and capacitors); environmental management (water desalination and purification, and nuclear waste management and remediation); solid-state ionic devices (neuromorphic computing); and a variety of biological systems (ion channels)*.* Here we present an MLD synthesis route to incorporating ion-selective moieties into a thin film, concentrating on the crown ether (CE) family of molecules for their well understood and characterized affinity to selectively bind metal cations in the electron-rich center of the molecule.

Two commercially available crown-ether materials (CE), (1), 1,4,10-Trioxa-7, 13-diazacyclopentadecane(2A15C5) and for 1,4,10,13-tetraoxa-7,16-diazacyclooctadecane (2A18C6), were measured using differential scanning calorimetry (DSC) and thermogravimetric analysis (TGA) to assess their suitability as precursors. The results for both molecules show that vaporization begins at ~100-150C in both cases, leading to evaporation of essentially all the material by ~200-250C. The DSC curves for both materials show heat flow indicative of phase changes in the range of the vaporization temperatures ~100-150°C. Malonyl chloride (MC) was used as an organic linker precursor. In-situ spectroscopic ellipsometry (SE) was used to probe the MLD process parameters, showing a wide temperature window

between 75°C-150°C with a linear growth rate ~5-6 Å/cycle. Detailed cycle-by-cycle SE show step-wise growth corresponding to the discrete precursor pulses for the CE and the MC. This allows estimates of thickness added per precursor dose, which include an increase in thickness of ~0.295 nm during the MC pulse and ~0.343 for the 2A15C5 CE pulse, for a total thickness added of ~0.622 nm for a full MLD cycle.

Chemical analysis of the as-grown MLD films was conducted by in-vacuo X-ray photoelectron spectroscopy (XPS). The presumed molecular configuration of CE and MC film is confirmed by the presence of all expected elements in the expected ratios. The O 1s spectrum indicates the presence of two species, consistent with expectations based on the presence of both C-O-C oxygen in the CE ring and C=O oxygen in the MC. The N 1s spectrum shows a single species of N in the film, as predicted from the CE moiety. The C 1s spectrum is more complex but consistent with the structure: on the higher binding energy side, we see a peak associated with N-C=O at ~290 eV, an overlapping C-N and C-O at ~288 eV, and a C-C peaks at ~285eV.

11:00am TF1-WeM-10 Chemical Insolubility of Vapor Phase Infiltrated Poly(methyl methacrylate) / AlOx Hybrid Materials, *Emily McGuinness, C Leng, M Losego,* Georgia Institute of Technology

Vapor phase infiltration (VPI) is a relatively new processing technique used for transforming polymers into organic-inorganic hybrid materials. VPI has been used to improve polymer mechanical properties, protect fabrics from UV and thermal degradation, dope conducting polymers, and act as a contrasting agent in electron microscopy for imaging phases of polymer blends. Recently, our group has explored a new application for VPI, the protection of thermoplastic polymers from solvent dissolution. In this study, poly(methyl methacrylate) (PMMA) thin films were infiltrated with trimethylaluminum (TMA) and water at different temperatures and to different depths of infiltration. The resultant AlO_x / PMMA hybrid films were then exposed to a variety of solvents to explore their stability. Chemical stability was found to vary non-linearly, with infiltration temperature. Films infiltrated at lower temperatures (70˚C and 100˚C) swelled or partially dissolved in good solvents for neat PMMA, such as toluene or chloroform, and partially dissolved in isopropanol and water, which are not good solvents for PMMA (Fig 1). In comparison, films infiltrated at higher temperatures (130˚C) showed enhanced solvent stability in most solvents, even those that dissolved neat PMMA. The increased solvent resistance is likely due to crosslinking between PMMA functional groups and TMA molecules, a reaction that has been reported to vary with temperature. Due to this variability, PMMA films infiltrated at low temperatures are only partially crosslinked while those infiltrated at high temperatures are fully crosslinked, making them more solvent resistant. The increased dissolution of hybrid films in certain alcohols and polar solvents is hypothesized to result from an interaction between the inorganic crosslinker and the solvent. We also found that complete transformation of the polymer into hybrid material was unnecessary for dissolution resistance at higher temperatures. An infiltration depth of 0.5 mm was sufficient for complete resistance to toluene dissolution at room temperature. For proof-of-concept, we applied this treatment to a quarter inch thick laser-etched PMMA sheet and then exposed it to toluene at 60˚C for 10 minutes. While the design on the neat PMMA version rapidly dissolved, the sheet with a 0.5 mm AlOx / PMMA subsurface layer showed nearly complete retention of its design (Fig 2). In this talk, we will explore these findings and discuss the differences in solvent stability of AlOx / PMMA hybrid materials as a function of temperature as well as investigate the underlying chemical and structural variations that yielded these results.

11:20am TF1-WeM-11 Atomic and Molecular Layer Deposition of Hybrid Mo-thiolate Thin Films, *Jingwei Shi, C MacIsaac, L Zeng, S Bent,* Stanford University

As a member of the two-dimensional transition-metal dichalcogenides (TMDs) family, MoS_2 has attracted great attention since it possesses unique and desirable properties for optical, electrical, and electrochemical applications. MoS_2 derives many of its interesting properties from its bonding structure, such as its direct band gap from the lack of interlayer interactions, and its good electrocatalytic performance from defect and edge Mo-S sites. Therefore, a material that contains Mo-S motifs while also lacking the long-range order found in MoS_2 may be an interesting system to study.

To this end, we recently reported the synthesis of a Mo-thiolate thin film utilizing a combination of atomic layer deposition (ALD) and molecular layer deposition (MLD) with molybdenum hexacarbonyl and 1,2-ethanedithiol as precursors. ALD and MLD are vapor deposition techniques

that may allow engineering of thickness dependent properties through its inherent angstrom-level control. The Mo-thiolate class of materials synthesized previously contained Mo-S bonding as well as aliphatic ethyl carbon chains. In this work, we extend and compare that system with the deposition of Mo-thiolate films containing butyl and benzyl organic linkers. The new process utilizes molybdenum hexacarbonyl and 1,4-butanedithiol or 1,4-benzenedithiol as precursors. The 1,4-butanedithiol and 1,4-benzenedithiol contains the S-R linkages, and the Mo-S linkages are created during each half-cycle reaction. Ellipsometry measurements of film thickness with precursor pulse time show that this system has a saturating growth rate. The measured growth rate is 1.0 Å per cycle for Mo-butanethiolate and 1.5 Å per cycle for Mo-benzenethiolate, at a deposition temperature of 170 °C. X-ray photoelectron spectroscopy (XPS) shows that the material is compositionally similar to the predicted elemental ratios. XPS analysis also shows the presence of Mo(VI) as well as oxygen contamination, suggesting some non-idealities to the process.

Key differences between the Mo-thiolate hybrids and MoS_2 are revealed when post-deposition annealing treatments are performed on the Mo-thiolate films. Due to the existence of carbon linkages in the Mo-thiolate films, the annealed films show signatures in Raman spectroscopy not only of crystalline MoS_2 but also of graphitic carbon. We further explore the differences in optical properties between the three compositionally distinct Mo-thiolates. Through this systematic comparison study, we aim to understand the role of different molecular linkages in the Mo-thiolate framework, which may be beneficial for the deliberate design of hybrid thin films based on their desired properties.

11:40am TF1-WeM-12 Electroactive Thin Films of Conjugated Polymers: Energy Conversion and Storage, *Shayan Kaviani, E Tavakoli, S Nejati,* University of Nebraska-Lincoln

Platinum group metals (PGM), transition metals, and metal oxides have been extensively studied as efficient catalysts in electrochemical energy conversion devices. Nonetheless, these catalysts have the drawbacks of susceptibility to poisoning and the high cost. To realize widespread application of cost-effective, clean and renewable energy conversion devices–based on electrocatalytic reactions, e.g. metal-air batteries–there is a need to develop alternative electrocatalysts. Conjugated polymers, as carbon-based metal-free materials possess electroactive properties with tunable optoelectronic properties. Here, we demonstrated a successful method to design and apply thin coats of these polymers on a high surface area gas diffusion layers to develop efficient air-cathode electrode for zinc-air batteries. We use oxidative chemical vapor deposition (oCVD), as a unique liquid-free and substrate-independent technique, and enable cross-coupling reaction of heterocyclic monomers and doping of the resulting films in a single step with high precision. We investigated the properties of a series of thiophene-based conjugated polymers. We used volatile liquid oxidants such as antimony pentachloride and gained control over dehydrocoupling polymerization reactions rate of thiophene derivatives. We showed that our oCVD processing conditions have a direct influence on the properties of the deposited films. By adjusting the oCVD settings, we deposited smooth (roughness factors < 1 nm) and conformal coatings of conjugated polymers on a variety of substrates. We showed that by tailoring the chemistry of monomers, we can tune the electrochemical properties of the oCVD-polymers. For instance, in the case of poly(thiophene) and poly(3,4-ethylenedioxythiophen) (PEDOT), the onsets of the oxygen reduction reaction (ORR) overpotential are measured to be 0.61 V and 0.76 V vs reversible hydrogen electrode (RHE) [1]. Populating the monomer structure with heteroatoms, we recorded an enhanced electroactivity–comparable to Pt/C–for polymeric domains of poly(3,4-ethylenedithiathiophene) (PEDTT). The electron transfer number for ORR in these polymers, follows the trend of electrocatalytic activity; the higher electroactivity, the higher number of electrons transferred. More interestingly, PEDTT shows high electroactivity toward oxygen evolution reaction (OER) with overpotential onset of 1.72 V vs RHE. This observation makes oCVD PEDTT, the first conjugated polymer with bifunctional electroactivity in oxygen reactions.

1. Kaviani, S., et al., *Electroactive and Conformal Coatings of oCVD Polymers for Oxygen Electroreduction.* ACS Applied Polymer Materials, 2019 1 (3), 552-560.

12:00pm TF1-WeM-13 Promotion of Crystalline Polyfluorene Domains in Thin Films Deposited by RIR-MAPLE, *Spencer Ferguson, B Zhang, A Stiff-Roberts,* Duke University

An important goal for functional polymer thin film deposition is to selectively deposit semi-crystalline phases to enable unique properties. As

Wednesday Morning, October 23, 2019

a specific example, semi-crystalline β-polyfluorene (β-PFO) could improve the performance of blue polymer light emitting diodes (LEDs) due to better color purity and enhanced charge conduction. However, it has been challenging to directly investigate the impact of this crystalline phase on the performance of PFO-based LEDs films deposited by spin-casting due to poor surface quality with prominent pinholes resulting from the poor solvents or additives used to promote β-PFO[1,2]. Previous work[3] has shown that emulsion-based, resonant infrared matrix-assisted pulsed laser evaporation (RIR- MAPLE) enables deposition of pinhole-free thin films containing β-PFO.

In order to further study the ability of the emulsion target used in RIR-MAPLE to promote the deposition of β-PFO, the emulsion surfactant will be investigated to study the impact of the polarity difference between the primary PFO solvent (trichlorobenzene) and the water within the emulsion. The standard surfactant used in RIR-MAPLE is sodium dodecyl sulfate, and it has a single hydrophobic tail. In a reported study on PFO, phospholipids were used to form a lamellar structure within an emulsion to drop cast films with high concentrations of β-PFO[4]. In contrast to SDS, the phospholipid surfactant has multiple hydrophobic tails, which could significantly impact the formation of β-PFO by RIR-MAPLE. In addition, sodium alkyl aryl sulfonate will be investigated as a surfactant to determine the impact of aromatic rings on the promotion of β-PFO. As a second study, the annealing of deposited films below the glass transition temperature of PFO will be investigated to determine the impact on β-PFO concentration and the overall film morphology.

For each study, UV-Vis absorbance, photoluminescence, and surface morphology will be characterized. This work will provide a path to the fabrication of thin films containing greater concentrations of β-PFO for inclusion as the active region in blue polymer LEDs.

This material is based upon work supported by the National Science Foundation under Grant No. NSF CMMI-1727572.

1. J. Peet, E. Brocker, Y. Xu, and G. C. Bazan, Adv. Mater. **20**, 1882 (2008).

2. B. Liu, T. Li, H. Zhang, T. Ma, J. Ren, B. Liu, J. Lin, M. Yu, L. Xie, and D. Lu, J. Phys. Chem. C **122**, 14814 (2018).

3. S. Ferguson, C. V. Williams, B. Mohapi, and A. D. Stiff-Roberts, J. Electron. Mater. **48**, 3388 (2019).

4. M. J. Tapia, M. Monteserín, H. D. Burrows, J. S. Seixas De Melo, J. Pina, R. A. E. Castro, S. García, and J. Estelrich, J. Phys. Chem. B **115**, 5794 (2011).

Thin Films Division
Room B131 - Session TF2-WeM

Thin Film Late News Session
Moderator: Virginia Wheeler, U.S. Naval Research Laboratory

11:00am **TF2-WeM-10 Peter Mark Memorial Award Lecture: Molecular Beam Epitaxial Growth of Novel Plasmonic Materials: Heavily-doped Semiconductors and Topological Insulators**, *Stephanie Law[1]*, University of Delaware **INVITED**
Plasmonic devices have great potential to advance the science and technology of photonics by confining light to subwavelength volumes. Traditional plasmonic devices in the visible spectral range have been made using metals like gold, silver, and aluminum. However, in order to create plasmonic devices at infrared and terahertz frequencies, we must look to alternative materials and heterostructures. In this talk, I will discuss our recent results on the molecular beam epiatxy growth of heavily-doped semiconductors for infrared plasmonics and topological insulators for terahertz plasmonics. We find that the morphology of heavily-doped semiconductors is significantly improved with the use of a bismuth surfactant. These improved materials are then incorporated into layered heterostructures that function as infrared hyperbolic metamaterials. These hyperbolic metamaterials show large mode indices and relatively high quality factor simultaneously, laying the groundwork for new infrared plasmonic devices. In addition to our work on semiconductors, I will also discuss our efforts on the growth of topological insulators (TIs) for terhertz plasmonics. We have found that the unintentional doping density can be reduced by a factor of two in TI thin films by growing a trivially-insulating lattice-matched buffer layer between the film and the substrate. These films can then be used as terahertz plasmonic films, which are then able to confine light into spaces 200 times smaller than the free space wavelength.

---
[1] **Peter Mark Memorial Award Winner**

Finally, I will discuss our recent efforts to grow self-assembled TI nanoparticles for use as quantum dots.

11:40am **TF2-WeM-12 Impact of Interface Quality on the Strength of Volume Plasmon Polaritons in Hyperbolic Metamaterials**, *Patrick Sohr, D Wei,* University of Delaware*; S Tomasulo, M Yakes,* U.S. Naval Research Laboratory*; S Law,* University of Delaware
In this work, we investigate doped and undoped semiconductors as alternative materials for hyperbolic metamaterials (HMMs) for applications in the mid to long wave infrared regimes. HMMs are artificial materials composed of subwavelength metallic and dielectric structures. In this work, we focus on layered HMMs, where the metal and dielectric layers are deposited on top of one another. These materials are highly anisotropic with a positive permittivity along one axis and a negative permittivity along the perpendicular axis. This behavior results in an open hyperbolic isofrequency surface, which is theoretically capable of supporting infinitely large wavevectors and a large photonic density of states. These materials have the potential to increase the emission rate of radiative emitters and permit for subwavelength imaging. These capabilities and others have made HMMs an interesting area of study for the fields of optics and optoelectronics.

Initially, HMMs were made using traditional metals (i.e. gold and silver) and paired with traditional dielectrics (i.e. silica and alumina). These materials have been shown to work exceptionally well in the visible to near infrared range. However, in the mid- to long wave infrared, these materials are no longer viable, and an alternative material system is required. One alternative is using doped and undoped semiconductors as the metallic and dielectric layers, respectively. Not only are semiconductors a promising material for the infrared, but also allow for easy integration with current optoelectronic devices.

In this work, we investigate three material systems for use as a semiconductor HMM: Si:InAs/AlSb, Si:InAs/GaSb, and Si:InGaAs/InAlAs. These materials are all grown by molecular beam epitaxy and characterized using Fourier Transform Infrared Spectroscopy. We show that the quality of the high wavevector modes is strongly dependent on the conduction band offset at the interface of the metal and dielectric layers. The Si:InAs/AlSb, which has the largest conduction band offset, exhibits the strongest and highest quality modes. While the Si:InGaAs/InAlAs and Si:InAs/GaSb, which have smaller conduction band offsets, exhibit weaker modes. This is due to the large wavevector modes within the HMM being comprised of coupled surface plasmon polaritons (SPPs) that exist at the interface of the metal and dielectric layers. When the electronic confinement at the interface is weak, the SPPs are less confined and do not couple as efficiently. Now that we have shown that we can grow high quality semiconductor HMMs, we can investigate some of their phenomenon in the infrared regime.

12:00pm **TF2-WeM-13 Transparent Microelectrode Arrays made by Ion Beam Assisted Deposition for Neuronal Cell *in vitro* Recordings**, *Tomi Ryynänen,* Tampere University, Finland*; R Mzezewa, E Meriläinen, T Hyvärinen, J Lekkala, S Narkilahti, P Kallio,* Tampere University
Microelectrode arrays (MEAs) are a common measurement platform in various biological *in vitro* studies where neuronal cells or cardiomyocytes are applied e.g. for drug screening, toxicity testing, cell model development or simply for increasing understanding of cell behavior. The field potential or impedimetric measurements, or stimulation performed with MEA are usually complemented with fluorescence imaging or microscopic inspection while or after the MEA recordings. The use of an inverted microscope is preferred, as imaging from the top side is often impossible because of the cell culturing medium and its reservoir placed on top of the MEA. With the inverted microscope there exists, however, another challenge. Typically, the tracks and the electrodes of the MEA are opaque and thus they prevent the full visibility of the cells from the bottom side. Partial solution is to make the tracks from transparent indium tin oxide (ITO) material. However, ITO electrodes are rare, simply because of their relatively high impedance and noise level. Instead, opaque low impedance Pt black or titanium nitride (TiN) electrodes are usually used with ITO tracks. Transparent low impedance graphene or conducting polymer electrodes have been demonstrated, but usually with challenges related to the ease of fabrication and stability. A recent approach is to use a very thin TiN layer made by atomic layer deposition (ALD) [1] or reactive sputtering [2] in the electrodes. The idea is to take benefit from TiN's columnar structure and thus capability of decreasing impedance, but still maintain the transparency, at least to some extent.

In this study, we show that ion beam assisted electron beam deposition (IBAD) is a valid alternative for sputtering and ALD in depositing both

transparent ITO tracks and very thin transparent TiN layers for the MEA electrodes. We evaluate the performance of different combinations of ITO tracks and ITO or TiN electrodes, both from imaging and impedance point of view. In the first version, both tracks and electrodes were made of ITO to guarantee full transparency and thus optimal imaging capability. In the 2nd version, ITO electrodes were coated with thin TiN layer to decrease impedance but still maintain (partial) transparency. In the third version the measurement capability was optimized by thick opaque TiN electrodes. The optical transmission and electrical impedance of these three versions were characterized and the biocompatibility of the MEAs was verified by cell experiments with human embryonic stem cell-derived (hESC) neuronal cells.

[1] Ryynänen et al. doi: 10.3389/fnins.2019.00226

[2] Mierzejewski et al. doi: 10.3389/conf.fncel.2018.38.00027

2D Materials
Room A216 - Session 2D+EM+MN+NS-WeA

2D Device Physics and Applications
Moderator: Jyoti Katoch, Carnegie Mellon University

2:20pm 2D+EM+MN+NS-WeA-1 Monolayer Electronics and Optoelectronics - Advances, Opportunities and Challenges, *Ali Javey*, University of California at Berkeley **INVITED**
Two-dimensional semiconductors exhibit excellent device characteristics, as well as novel optical, electrical, and optoelectronic characteristics. In this talk, I will present our recent advancements in surface passivation, contact engineering, surface charge transfer doping, and heterostructure devices of layered chalcogenides. We have developed a passivation technique that allows for observation of near-unity photoluminescence quantum yield in monolayer semiconductors. I will discuss the mechanism by which non-radiative recombination can be fully removed in monolayers. The work presents the first demonstration of an optoelectronically perfect monolayer, and highlights one of their unique properties. Finally, I will discuss an AC carrier injection mechanism to enable bright light emitting devices using monolayers, overcoming the problem of Schottky contacts.

3:00pm 2D+EM+MN+NS-WeA-3 Investigation on Graphene Band-gap Engineering for Graphene Transistors Applications, *Benfdila Arezki*, University M. Mammeri Tizi-Ouzou, Algeria
Graphene transistors are considered to be the successor's basic element for the next generation of advanced integrated circuits. However, graphene material suffers from the absence of bandgap to behave as semiconductor. The present paper deals with the investigation on the bandgap engineering approach aiming an increase of the switching characteristics of the graphene transistors.

The main obstacle for graphene transistor is the material zero bandgap that worsens the switching characteristics of the GFETs. Several techniques have been proposed to open a bandgap in graphene, among these engineering techniques, we can cite the Substrate induced bandgap, Bandgap engineering using h-BN/Ni (111). It is known that in theory a maximum of 0.50 to 0.53 eV can be obtained. Such bandgaps are observed on Graphene Bi-Layer (GBL) sheets grown on silicon carbide (SiC).

Other methods are the substitutional doping (SD), Nitrogen doping (NB). In any case graphene engineering should be considered in chemistry and physics view points. A high selective hydrogenation of graphene grown by lithography under the form of nanoruban showed a very interesting result of 0.7 eV. This process is part of selective chemical graphene functionalization techniques (SCGF).

In this paper we will deal with the graphene nanoruban and the opening of a bandgap capable of inducing an appreciable switching current ratio of at least $I_{ON}/I_{OFF}>10^6$.

The Graphene Nano Ribbon (GNR) structure used in the form of GNRFET for logic circuits and RF devices combines the high field, high mobility and the possibility of opening a bandgap. The higher carrier mobility of graphene is the basis of all electrical characteristics of graphene transistors.

In this paper we have used a semi-classical device model including the band to band tunneling that is described in Ref[8] to emphasize on the bandgap engineering. Device performances are studied based on the current-voltage characteristics with respective bandgap width variations. I_{OFF} current estimated and the performance ratio deduced.

3:20pm 2D+EM+MN+NS-WeA-4 Fully Inkjet Printed, High Photo-responsive, 2D WSe2-Graphene Based Flexible Photodetector, *R Hossain, A Kaul*, **Avra Bandyopadhyay**, University of North Texas
Tungsten di-selenide (WSe$_2$), a classic representative of two dimensional (2D) layered materials has recently drawn much attention due to its unique optoelectronic properties, offering a potential platform to construct hetero-structure photodetector (PD) for ultrafast optoelectronic devices on low-cost, flexible substrates [1,2]. As WSe$_2$ exhibits a weak van der Waals interlayer bonding, one of the approaches to obtain 2D WSe$_2$ is through top-down liquid phase exfoliation (LPE), where the bulk crystal is dispersed in a solvent through appropriate sonication and centrifugation conditions [1]. In this work, we report on the synthesis of WSe$_2$ via LPE and the first-ever assembly of an all inkjet printed WSe$_2$-graphene hetero-structure PD on flexible polyimide film, where the WSe$_2$ acted as a photo-active semiconductor and graphene was the carrier collector. The inkjet printed PD was photo-responsive to broadband incoming radiation in the visible regime, and exhibited a high photoresponsivity $R \sim 0.70$ A/W, and

detectivity $D \sim 3 \times 10^{10}$ Jones. The strain-dependent measurements were conducted with bending for different curvatures, indicating the feasibility of such devices for large format arrays printed on flexible substrates. The capacitance-frequency (*C-f*) measurements were performed to investigate the trap states. In conclusion, this unique all inkjet printed 2D hetero-junction photodetector formed on flexible and conformable substrate was successfully shown to be highly photo-responsive to a wide range of light intensities and strain levels, making it a promising prospect for scalable flexible electronic and optoelectronic devices and circuitry.

References:

[1] Kelly, A. G., Hallam, T., Backes, C., Harvey, A., Esmaeily, A. S., Godwin, I., ... & Kinge, S. (2017). All-printed thin-film transistors from networks of liquid-exfoliated nanosheets. Science, 356(6333), 69-73.

[2] Pradhan, N. R., Ludwig, J., Lu, Z., Rhodes, D., Bishop, M. M., Thirunavukkuarasu, K., ... & Balicas, L. (2015). High photoresponsivity and short photoresponse times in few-layered WSe2 transistors. ACS applied materials & interfaces, 7(22), 12080-12088.

4:20pm 2D+EM+MN+NS-WeA-7 Chemical Vapor Sensing with Transition Metal Dichalcogenides via Photoluminescence Modulation, *Aubrey T. Hanbicki, P Campbell, S Sivaram*, U.S. Naval Research Laboratory; *A Kusterbeck*, Nova Research, Inc.; *V Nguyen, A McGill, K McCreary, B Jonker, E Cobas, K Perkins*, U.S. Naval Research Laboratory; *A Friedman*, Laboratory for Physical Sciences
Two-dimensional transition metal dichalcogenides (TMDs) such as MoS$_2$ and MoSe$_2$ are promising materials for chemical vapor sensing applications. Their potential includes straightforward fabrication, readily available materials, and good selectivity, sensitivity, and speed of response. We previously showed [1] that monolayer TMDs are sensitive to and selective for vapors of strong electron donors and/or strong electron acceptors in concentrations as low as 1 part per million (ppm). Another attractive aspect is that TMDs have been shown to detect chemical vapors and gases in several ways, for instance via changes in electrical conductance or photoluminescence (PL) [2]. Sensors commonly have been fabricated based on the chemiresistive device properties, but here we will discuss our recent studies implementing TMD sensors using the PL as the core element of the sensor. We show that the PL intensity of monolayer CVD-grown WS$_2$ can rapidly (<< 1sec) detect triethylamine (TEA), a decomposition byproduct of the VX series of nerve agents, in concentrations <<1 ppm. The optical response is similar to the electrical response of other TMDs previously shown [1]. We shall discuss the mechanisms determining the size and shape of the optical responses. We envision suites of different TMDs using both optical and conductance sensing to rapidly and selectively detect chemical agents.

This research was performed while S.V.S held a National Research Council fellowship at NRL. This work was supported by core programs at NRL.

References

[1] A.L. Friedman et al., Sci. Reports 7, 3836 (2017)

[2] P.M. Campbell et al., Appl. Phys. Lett. 113, 163106 (2018)

4:40pm 2D+EM+MN+NS-WeA-8 Effective and Robust Graphene Immunoligical Sensors Functionalized through Non-covalent Ninding of Antibody-Conjugated Tripodal Compound, *A Hugo*, CEA-LETI, France; *C Sun*, Northwestern University; *M Kumar*, CEA-LETI, France; *R Othmen, J Renard, V Bouchiat*, CNRS-Institut Néel, France; *J Mann*, Northwestern University; *J Parpia, H Craighead*, Cornell University; *P Mailley*, CEA-LETI, France; *W Dichtel*, Northwestern University; *Thomas ALAVA*, CEA-LETI, France
Electrical detection is a very robust technique to transduce the adsorption of charged protein to a biological selective layer (i.e. biosensing). Electrolyte gated field effect transistors (EGFET) integrating graphene monolayers as the transducing element have shown outstanding electrical sensitivity in liquid compared to silicon and diamond based EGFET. In order to build graphene EGFET as effective biosensing unit it is important to attach at its surface a functional layers of biological molecules that will carry the task of enforcing specific detection of compound. Protein are widely used as specific bioreceptor for sensor biological functionalization yet it has been shown that protein lose their function when simply adsorbed on graphene. Covalent binding being out of the way for 2D dimensional crystals such as graphene (for the inherent deterioration of mechanical and electrical properties) we have shown that custom made tripodal compound attaching the graphene basal plane through Pi-stacking of aromatic moieties could be used to attach specific biomolecules to graphene while maintaining their biological function hence their specificity.

In this report we present an optimized fabrication process for graphene EGFET that includes patterning and passivation of electrical contact. The devices reproducibly show state of the art electrical performances. We demonstrate that the process can be simply transferred to different host substrates to integrate graphene EGFET ubiquitously on Silicon, glass or printed circuit board with similar performances. Finally, we implemented biological functionalization of the sensors by attaching streptavidin to the sensor thanks to the non-covalent tripodal compound. We report consistent changes in the Dirac peak of graphene due to the adsorption of tripodal compound and streptavidin as well as the binding of biotin, specifically bound to streptavidin. We show the detection to be specific and reproducible.

5:00pm 2D+EM+MN+NS-WeA-9 Electronic Properties of Ultra-Thin Na₃Bi: A Platform for a Topological Transistor, *Mark Edmonds,* Monash University, Australia **INVITED**

Na$_3$Bi in bulk form represents a zero-bandgap topological Dirac semimetal (TDS), but when confined to few-layers is predicted to be a quantum spin Hall insulator with bulk bandgap of 300 meV.[1] Furthermore, application of an electric field to few-layer Na$_3$Bi has been predicted to induce a topological phase transition from conventional to topological insulator.[2]

I will discuss our efforts to grow epitaxial few-layer Na$_3$Bi via molecular beam epitaxy, and probe its electronic structure and response to an electric field using scanning probe microscopy/spectroscopy and angle-resolved photoelectron spectroscopy. We demonstrate that monolayer and bilayer Na$_3$Bi are wide bandgap quantum spin Hall insulators (E$_G$>300 meV) that can be tuned with an electric field to semi-metallic, and at higher electric fields re-opened as a conventional insulator.[3] This is the first experimental demonstration of such an electric field tuned topological phase transition in any material. Finally, I will discuss our most recent efforts to perform transport measurements on few-layer Na$_3$Bi at doping levels corresponding to bulk conduction and edge conduction, with and without an applied magnetic field.

References

[1] C. Niu et al., Phys. Rev. B (2017) 95, 075404

[2] H. Pan et al., Scientific Reports (2015) 5, 14639

[3] J. Collins et al., Nature 564, 390 (2018)

5:40pm 2D+EM+MN+NS-WeA-11 Transparent Conductive Oxides in Contact with 2-D Materials, *Ravindra Mehta, A Bandyopadhyay, A Kaul,* University of North Texas

Combining two-dimensional materials with transparent conductive oxide can result in a fully transparent 2D electronics with outstanding device performance. It has been shown that monolayer MoS$_2$ in contact with AZO has 85% transmittance in the visible region, a low threshold voltage (0.69V) and a large switching ratio (4 × 10^8). Another study has shown that using 2D MoS$_2$ as an active channel, tin doped indium oxide as a backgated electrode and zinc doped indium oxide (IZO) as source-drain electrodes, 85% transmittance in the visible region can be obtained. The contact resistance between the IZO and MoS$_2$ was reduced after laser annealing which in turn enhances μ_{eff} and I_{on}/I_{off}. Thus, it becomes essential to study the performance of different transparent conductive oxides in contact with various 2D materials in a transistor. Black phosphorus is an interesting 2D materials since it combines unique attributes of both transition metal dichalcogenides and graphene. CVD is a preferred method compared to other techniques such as mechanical exfoliation, liquid exfoliation, and PVD to synthesize 2D materials since the materials produced are of great quality as is a scalable technique. However, CVD of black phosphorus is challenging. Thus, CVD in addition to exfoliation will be used to develop 2D materials. In this work opto-electronics performance of various transparent conductive oxides in contact with different 2D materials is evaluated with an emphasis on black phosphorus.

6:00pm 2D+EM+MN+NS-WeA-12 Negative Fermi-level Pinning Effect Induced by Graphene Interlayer in Metal/Graphene/Semiconductor Junction, *H Yoon, W Song,* Ulsan National Institute of Science and Technology (UNIST), Republic of Korea*; S Jung,* SK Hynix, Republic of Korea*; J Kim,* Ulsan National Institute of Science and Technology (UNIST)*; K Mo, G Choi, H Jeong, J Lee,* **Kibog Park,** Ulsan National Institute of Science and Technology (UNIST), Republic of Korea

We report the direct observation revealing that the electric dipole layer originating from the off-centric distribution of interacting electrons at metal/graphene interface can induce the negative Fermi-level pinning effect in metal/graphene/semiconductor junction made on a semiconductor substrate containing regions with low interface-trap density. The graphene interlayer takes a role of diffusion barrier preventing the atomic intermixing at interface and preserving the low interface-trap density region. The change of electrostatic potential across the metal/graphene interface due to the interaction dipole layer and the doping of graphene is found to cause the negative Fermi-level pinning effect, supported by the Schottky barrier decreasing as metal work-function increasing. In case of metal/graphene/GaAs junction, the local small patches with very thin or no native oxide layer are considered to be responsible for the negative Fermi-level pinning. In the prevailing region with normal native oxides surrounding the small patches, the Fermi-level pinning appears to be strong. Meanwhile, the negative Fermi-level pinning is found to occur globally in metal/graphene/SiC junction where the SiC substrate is known to produce a low density of interface traps. This work provides an experimental method to form Schottky and Ohmic-like contacts simultaneously on a semiconductor substrate covered partially with graphene by using identical metal electrodes.

Applied Surface Science Division
Room A211 - Session AS+CA+LS-WeA

Operando Characterization Techniques for In situ Surface Analysis of Energy Devices

Moderator: Svitlana Pylypenko, Colorado School of Mines

2:20pm AS+CA+LS-WeA-1 Probing the Electronic Structure of Electrocatalysts and the Formation of Reaction Intermediates, *Kelsey Stoerzinger,* Oregon State University **INVITED**

Electrocatalysts are important constituents in numerous energy conversion and storage processes. Reactants adsorb onto the electrocatalyst surface, where the interplay of electronic states results in a lower activation barrier for the transfer of electronic and ionic species in the reaction pathway to product formation. Rational design of electrocatalysts with greater activity for higher efficiency devices requires an understanding of the material's electronic structure in situ, as well as the reaction intermediates involved.

Many surface science techniques, such as X-ray photoelectron spectroscopy (XPS), collect information from inherently surface-sensitive low-energy processes, requiring operation in ultrahigh vacuum. This constraint is lifted for ambient pressure XPS, which can probe the surface in equilibrium with the gas phase at pressures up to ~a few Torr, or with thin liquid layers using a higher incident photon energy. This presentation will discuss the insights obtained with this technique regarding the electronic structure of oxide electrocatalysts in an oxidizing or humid environment, as well as the reaction intermediates of relevance to electrocatalysis.[1] I will then extend the technique to probe electrocatalysts *in operando,*[2] driving current through a thin layer of liquid electrolyte and employing a tender X-ray source.

References:

[1] Stoerzinger,K.A.Wang, L. Ye, Y. Bowden, M. Crumlin, E.J. Du, Y. Chambers, S.A. "Linking surface chemistry to photovoltage in Sr-substituted LaFeO$_3$ for water oxidation". *Journal of Materials Chemistry A* 6 (2018) 22170-22178.

[2] Stoerzinger, K.A. Wang, X.R. Hwang, J. Rao, R.R Hong, W.T Rouleau, C.M. Lee, D. Yu, Y. Crumlin, E.J. Shao-Horn, Y. "Speciation and electronic structure of La$_{1-x}$Sr$_x$CoO$_{3-\delta}$ during oxygen electrolysis". *Topics in Catalysis* 61 (2018) 2161–2174.

3:00pm AS+CA+LS-WeA-3 Surface Characterization of Battery Electrode/Electrolyte Materials Using XPS and ToF-SIMS, *Elisa Harrison, S Peczonczyk, S Simko,* Ford Motor Company*; K Wujcik,* Blue Current*; A Sharafi, A Drews,* Ford Motor Company

With a drive to develop hybrid electric and electric vehicles for improving fuel economy and lowering emissions, research of battery materials becomes necessary to increase the performance and durability of automotive batteries. Therefore, significant improvements in the energy capacity, stability, and safety of automotive batteries must be achieved. For the last two decades, traditional methods to characterize battery materials and interfaces have focused on the mechanical and electrochemical properties of the battery. There has been less emphasis on understanding chemical properties of the surface of the electrode and the chemistry that occurs at the electrode/electrolyte interface. Moving forward to develop new battery systems, gaining an understanding of the surface chemistry of battery materials is critical to improving performance.

The objective of this work is to highlight the need for surface analytical techniques and methodologies to fully characterize and improve battery materials. In this work, the surface chemistry of electrodes and electrolytes were analyzed using both X-ray photoelectron spectroscopy (XPS) and time-of-flight secondary ion mass spectrometry (ToF-SIMS). These are powerful tools to identify slight changes to the surface chemistry of battery materials with respect to factors such as electrode and electrolyte formulation, cycling conditions, air exposure, contamination, and sample replication.

3:20pm **AS+CA+LS-WeA-4 In Operando Molecular Imaging of Microbes as an Electrode**, *Xiao-Ying Yu,* Pacific Northwest National Laboratory

Metal reducing bacteria, such as *Shewanella* and *Geobacter*, has attracted attention in recent years particularly for the potential as Genome Encoded Materials. They also can function as electrodes in microbial fuel cells (MFCs). Despite the surging interest and applications of various imaging tools to understand the microbial populations, little has been explored in the *in vivo* study of MFCs using novel *in operando* electrochemical spectroscopy. We have invented a System for Analysis at the Liquid Vacuum Interface (SALVI) microfluidic cell that is suitable for culturing bacterial biofilms for *in vivo* molecular imaging. We have also illustrated that the electrochemical verison of SALVI or the E-cell is viable for *in operando* study of the electrode-electrolyte interface. We have cultured *Shewanella* and *Geobacter sulfurreducens* biofilms in SALVI and published several papers recently. In this presentation, I will show most recent *in operando* molecular imaging results using E-cell and *in situ* liquid SIMS to investigate electron transport using *Shewanella* as a model MFC electrode.

4:20pm **AS+CA+LS-WeA-7 Operando-XPS Investigation of Low-Volatile Liquids and Their Interfaces using Lab-Based Instruments**, *Sefik Suzer,* Bilkent University, Turkey **INVITED**

X-Ray based Operando Investigations have traditionally been carried out in Synchrotron facilities, due to demanding instrumentation and expertise.[1, 2] However, although sporadic, several important lab-based XPS studies have also been reported.[3] Emergence of Ionic Liquids with several promising properties, including their low volatility, has rekindled the use of XPS, especially for Operando types of measurements.[4] Our initial investigations had also concentrated on ionic-liquids and their interfaces under **dc** and **ac** electrical bias, and extended to monitoring electrochemical reactions.[5, 6] Recently, we have been investigating other low-volatile liquids and their drops on various substrates to tap into the Electrowetting phenomena.[7, 8] The common theme in all of our studies is the use of bias dependent shifts in the positions of the core-levels as reflection of the electrical potentials, recorded in a totally non-invasive and chemically resolved fashion. We use the magnitude and the frequency dependence of such potentials to extract pertinent information related to chemical and/or electrochemical properties of the materials and their interfaces. Several examples using ionic liquids, liquid poly-ethylene-glycol (PEG) and their mixtures will be presented and discussed.

References:

[1] Bluhm, H.; Andersson, K.; Araki, T.; Benzerara, K.; Brown, G. E.; Dynes, J. J.; Ghosal, S.; Gilles, M. K.; Hansen, H.-C.; Hemminger, J., J. Electron Spectrosc. Relat. Phenom. **150**, 86-104 (2006).

[2] Lichterman, M. F., Hu, S., Richter, M. H., Crumlin, E. J., Axnanda, S., Favaro, M., Drisdell, W., Hussain, Z., Mayer, T., Brunschwig, B. S., Lewis, N. S., Liu, Z. & Lewerenz, H.-J. Energy & Environmental Science **8**, 2409-2416 (2015).

[3] Foelske-Schmitz; A., Ruch; P.W., Kötz; R., J. Electron Spectrosc. Relat. Phenom. **182**, 57-62 (2010).

[4] Lovelock, K. R. J., Villar-Garcia, I. J., Maier, F., Steinrück, H.-P. & Licence, P.. Chemical Reviews **110**, 5158-5190, (2010).

[5] Camci, M.; Aydogan, P.; Ulgut, B.; Kocabas, C.; Suzer, S., Phys. Chem. Chem. Phys. **8**, 28434-28440 (2016).

[6] Camci, M. T.; Ulgut, B.; Kocabas, C.; Suzer, S., ACS Omega **2**, 478-486 (2017).

[7] Gokturk; P.A., Ulgut; B., Suzer; S., Langmuir **34**, 7301-7308 (2018).

[8] Gokturk; P.A., Ulgut; B., Suzer; S., Langmuir **35**, 3319-3326 (2019).

5:00pm **AS+CA+LS-WeA-9 Decoupling Surface and Interface Evolution in Polymer Electrolyte Membrane Systems Through In Situ X-Ray Photoelectron Spectroscopy**, *Michael Dzara*[12], Colorado School of Mines; *K Artyushkova,* Physical Electronics; *H Eskandari, K Karan,* University of Calgary, Canada; *K Neyerlin,* National Renewable Energy Laboratory; *S Pylypenko,* Colorado School of Mines

Ambient pressure X-ray photoelectron spectroscopy (AP-XPS) enables surface sensitive study of gas-solid interfaces. The fundamental knowledge obtained from such measurements provides unparalleled insight into the physicochemical processes that drive electrocatalytic devices.[1] Studies featuring AP-XPS span a broad range of materials and reactions, with many focused on thin films or other well-defined materials. In such studies, there are often clear changes in the material upon transition from ultra-high vacuum to *in situ* conditions, or there are well-defined catalyst species that participate in the relevant process.

In this work, the differing evolution of the many interfaces in polymer electrolyte membrane (PEM) electrodes in the presence of water vapor is studied through detailed analysis of AP-XP spectra. The complexity of analyzing these interfaces arises from the presence of both catalyst and ionomer species in PEM electrodes, and the subtlety of the changes induced in AP-XP spectra by interactions between the catalyst, ionomer, and gas. Adsorption of a gaseous reactant species onto a catalyst's surface results in a weak interaction and a small chemical shift in the adsorbent species, while ionomer may undergo re-orientation or degradation upon exposure to reactants, also altering the spectra. Therefore, spectral subtraction and highly-constrained curve fitting are applied to enable reliable identification of catalyst adsorbing sites and adsorption/desorption trends,[2] and ionomer changes in the presence of water vapor. Interactions between platinum-group metal-based catalysts and ionomer films with water vapor are first studied independently, and then simultaneously at the electrode scale. Such an approach allows changes in the electrode-water interface to be decoupled and assigned to either catalyst adsorption behavior, or ionomer response. This work lays the foundation for future study of different classes of electrocatalysts at the electrode scale, and *in operando* AP-XPS studies of electrocatalytic processes.

(1) Starr, D. E.; Liu, Z.; Hävecker, M.; Knop-Gericke, A.; Bluhm, H. Investigation of Solid/Vapor Interfaces Using Ambient Pressure X-Ray Photoelectron Spectroscopy. *Chem. Soc. Rev.* **2013**, *42*, 5833–5857.

(2) Dzara, M. J.; Artyushkova, K.; Shulda, S.; Strand, M. B.; Ngo, C.; Crumlin, E. J.; Gennett, T.; Pylypenko, S. Characterization of Complex Interactions at the Gas – Solid Interface with in Situ Spectroscopy : The Case of Nitrogen-Functionalized Carbon. *J. Phys. Chem. C* **2019**, *123* (14), 9074–9086.

5:20pm **AS+CA+LS-WeA-10 Low Temperature Scanning Tunneling Microscopy and Spectroscopy of Semiconductor Nanowire Device Surfaces**, *Yen-Po Liu, Y Liu, S Mousavi, L Sodergren, F Lindelöw, S Lehmann, K Dick Thelander, E Lind, R Timm, A Mikkelsen,* Lund University, Sweden

III-V semiconductor nanowires (NWs) show considerable promise as components in efficient and fast electronics as well as for quantum computing. In particular, the surfaces of the NWs play a significant role in their function due to the large surface to bulk ratio. Further, as the incorporation and activation of the nanowires in a device can affect their structure, it is relevant to study the surface structure and its influence on electronic properties in devices and during operation.

We use atomically resolved Scanning Tunneling Microscopy/Spectroscopy (STM/S) to study InAs and GaAs NWs in planar device configurations. [1-3] We use atomic hydrogen cleaning at 400°C to obtain well-defined surfaces that can be scanned with STM while the complete device is still fully functioning. [2] We study both NWs grown directly in a planar configuration as well as wires harvested from a growth substrate and placed on top of predefined metal contacts with ~100nm precision using a micro/nano probe. In our new <10K closed-cycle STM we can identify the individual device NWs simultaneously as we can apply voltages across the devices using four additional electrical contacts in the low temperature STM. We initially investigate NW device geometric structure and morphology with high precision. Then we continue to perform atomic resolution and low temperature STS mapping on top of the NWs surfaces to investigate electronic structure and potential quantum confinement effects as well as the influence of defects. These measurements can be performed while the device is actively operating by external biases applied and the I(V) characteristic across the NW is obtained. The STM tip can also

---

[1] **ASSD Student Award Finalist**

[2] **National Student Award Finalist**

act as a role as a local gate for Scanning Gate Microscopy (SGM) [4], which we can precisely locate on the operating single NWs device for SGM on the areas as STM is performed.

[1] Persson, O. et al., (2015). *Nano Letters*, 15(6), pp.3684-3691.

[2] Webb, J. et al., (2017). *Scientific Reports* 7, 12790

[3] Hjort, M. et al., (2015). *ACS Nano*, 8(12), pp.12346-12355

[4] Webb J.L. et al., (2014). Nano Research 7, 877

5:40pm AS+CA+LS-WeA-11 Work-function Estimation and In situ Measurement of Photoemission Spectroscopy of CuFeO$_2$ under Near Ambient Condition, *Soumya Banerjee, P Sapkota,* University of Notre Dame*; A Cabrera,* Pontificia Universidad Católica de Chile, Chile*; S Ptasinska,* University of Notre Dame

The quest for suitable semiconductor photoelectrodes to build efficient and stable photoelectrochemical (PEC) cells for solar water splitting is continually growing in the material sciences and solar energy community. Along with good stability in aqueous media, such photoelectrodes should have suitable band-edges and band-gap energies properly matching both the water oxidation-reduction potential and the solar spectrum, respectively. Copper-based oxide semiconductors are promising candidates fulfilling these criteria, but little is known about the interfacial properties of these compounds with H2O under operational conditions. Therefore, knowledge of their surface dynamics and interfacial reactions under realistic conditions is essential to improve our understanding of water-splitting mechanism, as well as to increase the stability and efficacy of PEC devices. The work functions of pure and Ga-doped Delafossite p-type CuFeO$_2$ semiconductor crystals with different thicknesses were measured using near ambient pressure x-ray photoemission spectroscopy (NAP-XPS) in Ar ambient. The values differ with changing thickness as well as Ga doping. The effect of water and CO$_2$ on the samples was also studied using NAP-XPS to understand the interaction between atmospheric gases and CuFeO$_2$ which may be helpful for its practical application in solar cells. No significant changes were found in XPS result obtained from CuFeO$_2$ in water ambient with and without illumination whereas CO$_2$ induced changes in oxygen XPS peak positions.

6:00pm AS+CA+LS-WeA-12 In-situ X-ray Photoelectron Spectroscopic Study of III-V Semiconductor/H$_2$O Interfaces under Light Illumination, *Pitambar Sapkota, S Ptasinska,* University of Notre Dame

A number of studies on different semiconductor materials that can be used as a photoelectrode in photoelectron-chemical (PEC) cells for solar water splitting is continually growing in material sciences and solar energy communities. III-V based compounds have been the most promising candidates because of their efficient light and carrier management properties in addition to suitable band gap and band edge energies, which properly match the solar spectrum and water redox potentials, respectively. Although most of the highly efficient PEC water splitting cells are based on III-V semiconductor, these photoelectrode materials are unstable under operational conditions. Few studies suggest oxidation leading to corrosion as a major cause of the degradation of these photoelectrodes, but it is still not completely understood and little is known about the role of the oxides formed at the interfaces. Therefore, knowledge of the interfacial reactions in realistic situations and surface dynamics are necessary to advance our understanding of water splitting mechanism, as well as to build a stable and efficient PEC solar water splitting cell. In this study, we used state of the art spectroscopic technique, ambient pressure X-ray photoelectron spectroscopy, to characterize semiconductor (GaAs and GaP) surface and to study chemical reactions occurring at the water interface in presence of secondary light source. Core level photoemission spectra from Ga2p, As3d, P2p, and O1s were collected at different water pressures in presence of secondary light source to identify the newly formed surface species, particularly oxides, and to evaluate the interaction of GaAs and GaP with water under light illumination.

Chemical Analysis and Imaging Interfaces Focus Topic
Room A120-121 - Session CA+NS+SS+VT-WeA

Chemical Analysis and Imaging of Liquid/Vapor/Solid Interfaces I

Moderators: Juan Yao, Pacific Northwest National Laboratory, Andrei Kolmakov, National Institute of Standards and Technology (NIST)

2:20pm CA+NS+SS+VT-WeA-1 Chemical Analysis and Imaging of Environmental Interfaces, *Vicki Grassian,* University of Californfornia at San Diego **INVITED**
Environmental interfaces, defined as any surface in equilibrium with its surrounding environment, are ubiquitous. From this broad definition, there are a myriad of different types of environmental interfaces that include atmospheric aerosols, nanomaterials and indoor surfaces. This talk will focus on the use of different molecular probes including various spectroscopic and imaging techniques to investigate interfaces relevant to outdoor and indoor environments.

3:00pm CA+NS+SS+VT-WeA-3 Liquid/Vapor Interfaces Investigated with Photoelectron Spectroscopy, *Hendrik Bluhm,* Fritz Haber Institute of the MPG, Germany **INVITED**
Aqueous solution/vapor interfaces govern important phenomena in the environment and atmosphere, including the uptake and release of trace gases by aerosols and CO$_2$ sequestration by the oceans.[1] A detailed understanding of these processes requires the investigation of liquid/vapor interfaces with chemical sensitivity and interface specificity under ambient conditions, *i.e.*, temperatures above 200 K and water vapour pressures in the millibar to tens of millibar pressure range. This talk will discuss opportunities and challenges for investigations of liquid/vapor interfaces using X-ray photoelectron spectroscopy and describe some recent experiments that have focused on the propensity of certain ions and the role of surfactants at the liquid/vapor interface.

[1] O. Björneholm et al., Chem. Rev. **116**, 7698 (2016).

4:20pm CA+NS+SS+VT-WeA-7 Methanol Hydration Studied by Liquid μ-jet XPS and DFT Simulations, *Jordi Fraxedas,* Catalan Institute of Nanoscience and Nanotechnology (ICN2), CSIC and BIST, Spain*; E Pellegrin, V Perez-Dieste, C Escudero,* CELLS-ALBA, Spain*; P Rejmak,* Institute of Physics PAS, Poland*; N Gonzalez, A Fontsere, J Prat, S Ferrer,* CELLS-ALBA, Spain
The advent of liquid μ-jet setups, in conjunction with X-ray Photoemission Spectroscopy (XPS), has opened up a plethora of experimental possibilities in the field of atomic and molecular physics [1]. Here, we present a combined experimental and theoretical study of the hydration of methanol at the aqueous solution/vapor interface. These are first experimental results obtained from the new liquid μ-jet setup at the Near Ambient Pressure Photoemission (NAPP) endstation of the CIRCE helical undulator beamline (100–2000 eV photon energy range) at the CELLS-ALBA synchrotron light source, using a differentially pumped SPECS PHOIBOS 150 hemispherical electron energy analyzer [2].The experimental results are compared with simulations from density functional theory (DFT) regarding the electronic structure of single molecules and cluster configurations as well as with previous experimental studies.

Methanol is the simplest amphiphilic molecule capable of hydrogen bonding due to its apolar methyl and polar hydroxyl groups. The results obtained from pure water at 600 eV photon energy emphasize the short range tetrahedral distribution as previously observed for crystalline and amorphous ice. We also find indications for ordering phenomena in water/methanol mixtures by the reduced O1s XPS liquid line width (as compared to pure water), which could be ascribed to the amphiphilic character of the methanol molecule. Regarding the C1s XPS lines, the vapor/liquid peak ratios allow for a quantitative determination of the methanol volume concentrations in both the vapor as well as in the liquid phase, that are corroborated by an analogue analysis of the valence band (VB) spectra. A detailed quantitative analysis of the water/methanol liquid VB XPS spectrum accounting for the photon energy dependence of photoemission cross sections confirms the atomic/orbital characteristics of the methanol molecular orbitals involved in the transitions and their pertinent intensities. From the decomposition of the liquid VB spectrum of the water/methanol mixture together with finite XPS probing depth we derive a methanol volume fraction of 43% for the outer liquid layers as compared to the nominal bulk liquid value of 37.5%. Finally, from the different binding energy (BE) shifts of the water/methanol liquid VB spectrum with respect to that of pure methanol, we develop a CH$_3$OH-

$(H_2O)_3$ cluster-based model that relates these different BE shifts to the different MO hybridizations within that cluster.

[1] B. Winter, M. Faubel, Chem. Rev. 106 (2006) 1176.

[2] V. Pérez-Dieste, L. Aballe, S. Ferrer, J. Nicolàs, C. Escudero, A. Milán, E. Pellegrin, J. Phys. Conf. Ser. 425 (2013) 072023.

4:40pm CA+NS+SS+VT-WeA-8 Survey of Ionic Liquid Interfaces under Vacuum and Ambient Conditions: An XPS Perspective, *Yehia Khalifa,* Ohio State University*; A Broderick, J Newberg,* University of Delaware*; Y Zhang, E Maginn,* University of Notre Dame

Properties and behavior of Ionic Liquid interfaces tend to behave differently from their bulk counterparts. In this study the preferential enhancement of the lower molar concentration anion [TFSI] in a mixture of [C2MIM][OAc] and [C2MIM][TFSI] is shown in the top 17 Å via angle-resolved X-ray photoemission spectroscopy under ultra high vacuum conditions. This is supported by molecular simulations where a quantitative relationship is also established between the two techniques. This interfacial enhancement is not only unique to mixtures but is also displayed in a pure ionic liquid with a hydrophilic anion such as [HMIM][Cl] studied via ambient pressure X-ray photoemission spectroscopy. The surface of [HMIM][Cl] under vacuum and increasing pressures of water vapor was evaluated (maximum of 5 Torr, 27% relative humidity). Our quantitative results indicate a significantly larger mole fraction of water at the interface compared to the bulk with increasing pressures when compared to previously published tandem differential mobility analysis results on [HMIM][Cl] nanodroplets. Furthermore the reverse isotherms has shown that the water uptake on the interface is a reversible process. These results highlight the unique behavior of ionic liquid interfaces that can be exploited for smart materials design and application.

5:00pm CA+NS+SS+VT-WeA-9 Ambient Pressure XPS Study of Gallium-Indium Eutectic (EGaIn) Surface under Oxygen and Water Vapor, *Meng Jia, J Newberg,* University of Delaware

Liquid metals (LMs) have a combination of high thermal/electrical conductivity and excellent deformability. The application of LMs in the field of electronics has identified many opportunities for their use as stretchable electronics, self-healing conductors and interconnects. Gallium-Indium eutectic (EGaIn) is one of the leading alternatives to toxic liquid mercury because of its low vapor pressure, low viscosity, low toxicity and high conductivity. A surface oxide layer is known to form when EGaIn is exposed to ambient conditions. However, surface sensitive measurements of this chemistry occurring under ambient conditions are strongly lacking. Herein we present results from the interaction of oxygen and water vapor with the liquid-gas interface of an EGaIn droplet deposited on an W foil using ambient pressure X-ray photoelectron spectroscopy (AP-XPS). EGaIn was examined up to a maximum of 1 Torr pressure at 550 K. Results reveal that under ambient conditions both oxygen and water vapor form a Ga(3+) oxide (Ga_2O_3) as an outer layer, while a thin layer of Ga(1+) oxide (Ga_2O) resides between metallic EGaIn and the outer Ga(3+) oxide. Both gases were unreactive towards Indium under our experimental conditions. The oxidation kinetics in the presence of water vapor were much faster compared oxygen. Proposed reaction mechanisms will be discussed.

5:20pm CA+NS+SS+VT-WeA-10 Laboratory-based Hard X-ray Photoelectron System for the study of Interfaces, *Susanna Eriksson,* Scienta Omicron

Hard X-ray photoelectron spectroscopy (HAXPES) has traditionally found its application in the core topics of condensed matter physics, but the slowly growing number of beamlines worldwide has widened its appeal to other interest groups. HAXPES uses X-rays in the 2-10 keV range to excite photoelectrons, which are used to non-destructively study the chemical environment and electronic structure of materials.

In contrast to the very surface-sensitive XPS, HAXPES is much more bulk sensitive. This makes it applicable to bulk materials and structured samples, e.g. layered samples and heterostructures. In addition, its bulk sensitivity means that realistic samples can be investigated without the need of prior surface preparation. However, the number of existing HAXPES systems is very small and they are predominantly located at synchrotrons (approx. 20 beamlines worldwide) due to low photoionization cross sections necessitating high X-ray intensities, limiting their availability to users and applications.

This work presents a new laboratory-based instrument capable of delivering monochromated hard X-rays with an energy of 9.25 keV and a focused 30x45 μm² X-ray spot, giving excellent energy resolution of <0.5 eV. Systematic reference measurements are presented outlining the

systems capability as well as the latest results from various application fields including energy related materials such as batteries.

Ultimately, this spectrometer presents an alternative to synchrotron-based endstations and will help to expand the number and range of HAXPES experiments performed in the future. HAXPES is a cutting edge characterisation method and the advancement of this technique will tremendously increase the potential to study an ever increasing range of inorganic materials and beyond.

Spectroscopic Ellipsometry Focus Topic
Room A212 - Session EL+EM-WeA

Spectroscopic Ellipsometry: Novel Applications and Theoretical Approaches

Moderators: Vanya Darakchieva, Linkoping University, Sweden, Nikolas Podraza, University of Toledo

2:20pm EL+EM-WeA-1 Optical Hall Effect in the Multi-valley Semiconductor Te-doped GaSb, *Farzin Abadizaman, C Emminger,* New Mexico State University*; S Knight,* University of Nebraska-Lincoln*; M Schubert,* University of Nebraska-Lincoln, Linköping University, Sweden, Leibniz Institute of Polymer Research Dresden, Germany*; S Zollner,* New Mexico State University

The authors conducted optical Hall effect (OHE) measurements on Te-doped GaSb (n-type) at room temperature in the far-infrared between 30 cm^{-1} and 700 cm^{-1} at magnetic fields of ±7 T and 0 T. The measurements were performed at an angle of incidence of 45 and a resolution of 2 cm^{-1}. The complex dielectric functions and Mueller Matrix (MM) elements were determined from spectroscopic ellipsometry at 0 T in the range of 300 cm^{-1} to 8000 cm^{-1} using an FTIR-VASE ellipsometer and from 30 cm^{-1} to 700 cm^{-1} using the FIR ellipsometer. Using a sum of a Lorentzian oscillator and two Drude terms, the experimental data at zero magnetic field were modeled. From the Lorentzian term, we found the transverse optical (TO) phonon energy at 226 cm^{-1} and the longitudinal optical (LO) phonon energy at 237 cm^{-1}.

Although GaSb is a direct band gap semiconductor, a calculation of the electron concentration indicates that at T = 300 K and a total electron density below 10^{18} cm^{-3}, the majority of carriers are located at the L-valley (67%) while the Γ-valley contains only 33% of the carriers. This implies that in the absence of the magnetic field, two Drude terms are needed to model the data. The surfaces of constant energy at the L-point in the Brillouin zone form eight half-ellipsoids at L, which are characterized by their anisotropic masses. However, due to the symmetry, the valleys at this point are two by two equivalent, which leads to the total number of four valleys. In the absence of a magnetic field, the contribution of all eight half-ellipsoids in the L-valley is reduced to only one Drude term, where the effective mass is the harmonic average of the transverse and longitudinal masses. As the magnetic field is turned on, each ellipsoid contributes to the anisotropic dielectric tensor, which, depending on the effective mass tensor, contributes differently to the total dielectric tensor. Therefore, in the presence of a magnetic field, the data is modeled by the sum of a Lorentzian, a Drude tensor at the Γ-valley and four Drude tensors at the L-valley.

2:40pm EL+EM-WeA-2 Study of the Temperature-dependent Optical Constants of Noble Metals based on High Temperature Spectroscopic Ellipsometry, *Jiamin Liu, H Jiang, S Liu,* Huazhong University of Science and Technology, China

Noble metals have been widely used in thermo-plasmonics field, such as thermo- photovoltaics, heat-assisted magnetic recording and photothermal therapy, thus studying the temperature-dependent optical constants of these metals are crucial for both understanding the temperature effects on optical properties and providing essential data for the plasmonic simulations.

In this work, a high temperature spectroscopic ellipsometry covering the spectral range of 200-1000nm has been built, which is able to measure the ellipsometric parameters of samples when temperature is varying from 300K to 1200K. The noble metallic samples are heated at a mixing atmosphere of 5% H_2 and 95% Ar to avoid the possible thermal oxidation. An oscillator- parametrization regression method based on the Drude-dual-TaucLorentz-Lorentz model and the B-spline model has been proposed to determine the optical constants and the roughness of the heated noble metals. Both the optical constants and the electronics parameters of noble metals heated below 900K have a temperature-dependency similar to the

recently reported results. Taking the gold film as an example, the DC resistivity is increasing from 2.273×10^{-6} to 2.414×10^{-6}Ω·cm with the temperature increasing from 300K to 800K, while the electron relaxation time is decreasing from 20.787 to 9.021fs. Additionally, it has been noticed the first absorption peak near 2.7eV first increases and then decreases, while the second absorption peak near 3.7eV shows the opposite characteristics with the temperature increasing from 300K to 800K. Besides, the optical constants of Au film heated above 900K has some similarities to that of SnTe, which might be caused by the combined effect from the possible formation of Au-Si binary phase and the possible transition of vertical columnar grains to granular grains.

3:00pm EL+EM-WeA-3 Optical Monitor for the Attitude Tracking using Polarimetry, *Song Zhang, H Gu, H Jiang, S Liu,* Huazhong University of Science and Technology, China

The attitude angles are important parameters describing the motion of the object. In the fields of precision manufacturing, robotics control, navigation of the aircraft, the accurate and real-time measurements of the attitude angles (yaw angle, pitch angle and roll angle) are very important. Due the advantages of non-contact, low cost, non-destructive and high precision, the optical methods have been popular used for measuring the attitude of the object.

In our work, we present a novel optical monitor for the attitude tracking. The proposed method utilizes the principle that polarized light incident in different directions into the birefringent crystals can produce different phase modulations. Then, the attitude angle of the object attached with a birefringent crystal can be obtained by measuring the phase change. The optical monitor is based on the division-of-amplitude polarimetry with a time resolution of several nanoseconds, which is capable of monitoring the changes in all the attitude angles simultaneously. In order to verify the correctness and the performance of the optical monitor, we performed real-time measurement experiments on the attitude angles of a zero-order quarter-wave plate and a multi-order half-wave plate. The roll angle is continuously changed within the range of 0 ~ 360°, while the pitch angle and yaw angle are varied within ±7° and ±40° respectively. The results show that not only the attitude angles, but also the angular velocities and the accelerations of the roll angle, can be extracted, and the errors of all attitude angles is less than 0.5°.

3:20pm EL+EM-WeA-4 New Progress on the Channeled Spectroscopic Ellipsometry and its Applications, *Gai Chin,* ULVAC Inc., Japan

This presentation describes a novel method for the spectroscopic measurement of the state of polarization of light. A pair of thick birefringent retarders is incorporated into the spectroscopic polarimeter, so the generated channeled spectrum is composed of three quasi-cosinusoidal components carrying the information about the state of polarization of the light that is being measured. Fourier inversion of the channeled spectrum provides the significant parameters for determination of the spectrally resolved Stokes parameters of light. No mechanical movable components for polarization control or active devices for polarization modulation are used, and all the Stokes parameters can be determined at once from only the single spectrum.

The channeled spectroscopic ellipsometry is a snapshot method for the spectrally-resolved polarization analysis. A pair of high-order retarders are utilized to generate a channeled spectrum carrying information about the wavelength-dependent multiple parameters of polarization of light. This method has a feature that it requires no mechanical or active components for polarization-control, such as a rotating compensator and electro-optic modulator.

This novel spectroscopic ellipsometry can measure the thickness and optical constants of thin films at a dramatically fast speed. Its data acquisition time is as short as 10ms. It does not require any active components for polarization-control, such as a rotating compensator or an electro-optical modulator.

It created great opportunities for new applications of the spectroscopic ellipsometry in which the compactness, the simplicity and the rapid response are extremely important. It can be integrated into the deposition tool and successfully measured thin films in-situ and ex-situ. Obviously, those from PVD, CVD and ALD are some promising applications for this novel spectroscopic ellipsometry.

This presentation describes our new progress on some key technologies for enhancing the performance of this channeled spectroscopic ellipsometry by system configuration, data analysis and other creative efforts on developing a series of new high-speed spectroscopic ellipsometers. Some novel applications will be also introduced, such as the PVD, CVD, ALD, EUV, OLED, MEMS and some excellent measurement data of thin films from the semiconductor, flat panel display and other industries.

4:20pm EL+EM-WeA-7 The Physics of Low Symmetry Metal Oxides: Applications of Ellipsometry, *Alyssa Mock,* U.S. Naval Research Laboratory; *S Knight, M Hilfiker,* University of Nebraska-Lincoln; *V Darakchieva, A Papamichail,* Linkoping University, Sweden; *R Korlacki,* University of Nebraska-Lincoln; *M Tadjer,* U.S. Naval Research Laboratory; *Z Galazka, G Wagner,* Leibniz-Institut für Kristallzüchtung, Germany; *N Blumenschein,* North Carolina State University; *A Kuramata,* Novel Crystal Technology, Inc., Japan; *K Goto, H Murakami, Y Kumagai,* Tokyo University of Agriculture and Technology, Japan; *M Higashiwaki,* National Institute of Information and Communications Technology, Japan; *A Mauze, Y Zhang, J Speck,* University of California Santa Barbara; *M Schubert,* University of Nebraska-Lincoln, Linköping University, Sweden, Leibniz Institute of Polymer Research Dresden, Germany **INVITED**

We discuss the analysis of the dielectric function tensor for monoclinic metal oxides obtained from generalized spectroscopic ellipsometry. We investigate the potential high-power device material gallium oxide and derive dispersions of transverse, longitudinal and plasmon coupled modes [M. Schubert *et al.*, Phys. Rev. B 93, 125209 (1-18) (2016); Editors' Suggestion] and the band-to-band transitions and excitons along with their eigenvectors [A. Mock *et al.*, Phys. Rev. B 96, 245205 (1-12) (2017)]. Additionally, we show that this technique can fully explain the unusual ordering of optical phonon mode pairs which is observed in beta-Ga2O3 [M. Schubert, A. Mock et al. Phys. Rev. B 99, 041201(R) (2019)] as well as their dependency on free charge carrier concentrations. [M. Schubert, A. Mock et al. Appl. Phys. Lett. 114, 102102 (2019) – Editor's Pick]. We apply this technique also for the identification of transverse and longitudinal phonons in scintillator material cadmium tungstate [A. Mock *et al.*, Phys. Rev. B 95, 165202 (1-15) (2017)], and then further extend our methodology for analysis of the dielectric and inverse dielectric tensor for transverse and longitudinal phonon mode dispersion characterization in high-power laser material yttrium orthosilicate [A. Mock *et al.*, Phys. Rev. B, 97 165203 (1-17) (2018)].

We apply our technique to investigate the effective electron mass tensor using optical Hall effect measurements [S. Knight, A. Mock *et al.*, Appl. Phys. Lett. 112, 012103 (2018); Editors' Pick], the temperature dependence of band-to-band transitions energies [A. Mock *et al.*, Appl. Phys. Lett. 112, 041905 (2018)], and the effects of aluminum alloying concentration onto the band-to-band transition energies [M. Hilfiker, A. Mock *et al.* Appl. Phys. Lett. (Under Review)]. We further apply our technique to epitaxial layers of beta-phase gallium oxide and discuss the relationship between the X-ray diffraction measured strains with respect to the optically determined shifts in transverse optical phonon modes as compared to the bulk material. Understanding of the stress and strain relationship to properties in monoclinic materials will help facilitate better control of material properties for engineering next generation power devices based on beta-Ga2O3.

5:00pm EL+EM-WeA-9 Terahertz Dielectric Anisotropy in Randomly Distributed, Spatially Coherent Polymethacrylate Microwire Arrays Fabricated by Stereolithography, *Serang Park,* University of North Carolina at Charlotte; *Y Li,* University Of North Carolina at Charlotte; *S Lee,* Harris Corp.; *S Schöche, C Herzinger,* J.A. Woollam Co., Inc.; *T Hofmann,* University Of North Carolina at Charlotte

Fabricating terahertz (THz) optical components with tailored dielectric properties including scalable anisotropies via additive manufacturing is drawing substantial interest as it potentially offers a rapid, low-cost pathway for THz optical system development. Metamaterials composed of slanted columnar structures have been reported to exhibit anisotropic behaviors at THz frequencies, which may allow the design of novel optical components including filters and sensors for the THz frequency range. Here, we report on the anisotropic THz-optical response of stereolithographically fabricated polymethacrylate slanted columnar layers. The samples are composed of randomly distributed, spatially coherent polymethacrylate wires with a diameter of 100 μm and a length of 700 μm, which are tilted by 45° with respect to the surface normal of the substrate. Generalized spectroscopic ellipsometry is employed to obtain Mueller matrix spectra of these samples in the range from 210 to 350 GHz. A simple biaxial (orthorhombic) layer homogenization approach is used to analyze the THz Mueller matrix data obtained at different azimuthal orientations. Our observations confirm that randomly distributed, spatially coherent polymethacrylate wire arrays exhibit a strong anisotropic response. In

conclusion, stereolithographic fabrication is introduced as an effective tool for fabricating metamaterials with anisotropic THz-optical properties.

5:20pm **EL+EM-WeA-10 Ultrafast Dynamics of Ge, InP and Si Proved by Time-Resolved Ellipsometry**, *Shirly Espinoza, S Richter, M Rebarz,* Institute of Physics, Academy of Sciences of the Czech Republic, Czechia*; O Herrfurth, R Schmidt,* Universität Leipzig, Felix-Bloch-Institut für Festkörperphysik, Germany*; J Andreasson,* Institute of Physics, Academy of Sciences of the Czech Republic, Czechia*; S Zollner,* New Mexico State University

Recent developments in time-resolved ellipsometry allow us to study the ultrafast behavior of single crystals of undoped Ge, InP and Si at room temperature after carriers have been excited by an ultrashort laser pulse of 1.55 eV. Information about the dynamic processes such as scattering mechanisms of the hot charge carriers and electron-phonon coupling was obtained.

With a resolution of 120 fs, and a time scale from femtoseconds to nanoseconds, the observed changes are bigger in Ge than in the other materials. Our results are in agreement with theoretical and experimental work done some years ago on the dynamics of germanium studied by time-resolved ellipsometry [1,2]. The result of our experiments could go deeper into the details of the dynamics thanks to the development of the time-resolved experimental setup using state of the art technology in the fields of ultrafast lasers, electronics, and optics.

Our current spectral range is from 1.7 to 3.5 eV. The generated carrier density is on the order of 10^{20} cm^{-3}, which allows us to compare the results with published data on doped materials [3].

References

[1] Choo H.R., Hu X.F., Downer M.C., Kesan V.P. Femtosecond ellipsometric study of nonequilibrium carrier dynamics in Ge and epitaxial Si$_{1-x}$Ge$_x$. *Appl. Phys. Lett.* 63, 1507 (1993)

[2] Zollner S., Myers K.D., Jensen K.G., Dolan J.M., Bailey D.W., Stanton C.J. Femtosecond interband hole scattering in Ge studied by pump-probe reflectivity. *Solid State Commun.* 104 (1), 51-55 (1997)

[3] Xu C., Fernando N.S., Zollner S., Kouvetaki J., Menendez J. Observation of Phase-Filling Singularities in the Optical Dielectric Function of Highly Doped n-Type Ge. *Phys. Rev. Let.* 118, 267402 (2017)

5:40pm **EL+EM-WeA-11 Optical Properties of Organic-Inorganic Lead Halide Perovskite Thin Films for Photovoltaics**, *Biwas Subedi, M Junda, K Ghimire, N Podraza,* University of Toledo

Organic-inorganic lead halide perovskite based photovoltaics (PV) exhibit high initial efficiency, can be solution processed with potentially low material costs, and material band gaps can be tuned by composition. Unfortunately, these perovskites exhibit degradation upon exposure to atmosphere, light, and heat. Spectroscopic ellipsometry over the near infrared to ultraviolet range (0.73-5.9 eV) has been applied to characterize the complex optical response of solution processed *ABX*$_3$ (*A*: methylammonium—MA, formamidinium—FA, Cs; *B*: Pb, Sn; *X*: I, Br, Cl) perovskite thin films of different compositions. A parametric optical property model has been developed which includes contributions from electronic transitions above the band gap, the direct band gap, an exponentially decaying Urbach tail, and sub-gap absorption due to defect states. Using this model, above gap critical points, band gap energies, and sub-gap absorption are compared primarily as functions of *A*- and *B*-cation compositions for thin films. In situ, real time spectroscopic ellipsometry (RTSE) of perovskite films undergoing degradation induced by controlled relative humidity is used to track optical properties changes, particularly with respect to sub-gap absorption, and morphology changes occurring at the substrate / film and film / ambient interfaces. These optical property and morphology changes are tracked by RTSE for perovskite thin films of different compositions. Optical properties characterized by spectroscopic ellipsometry are used as input for external quantum efficiency (EQE) simulations of perovskite based PV devices. Comparisons between simulated and measured EQE spectra are used to identify differences in perovskite characteristics arising from the complete solar cell device fabrication process.

6:00pm **EL+EM-WeA-12 Optical Constants of Ni at 300 K from 0.03 to 6.0 eV**, *Stefan Zollner, F Abadizaman,* New Mexico State University

The optical constants of single-crystalline, polycrystalline, and thin films of Ni from 0.06 to 6 eV are determined from spectroscopic ellipsometry at an angle of incidence of 70. The experimental data are analyzed using three alternative methods. In the first method, the dielectric function is written

as a sum of Lorentz and Drude oscillators. The second method writes the dielectric function as a product of these oscillators (Kukharskii product). In the third method, a Drude model with frequency dependent scattering rate and plasma frequency is used. We used two Drude terms in the sum model to account for d- and s-electrons. The plasma frequencies were found to be 11.9 eV and 4.86 eV for d- and s-electrons, respectively, leading to a DC conductivity of about 80,000 (1/Ωcm) at 300 K, compared to the electrical DC conductivity of 143,000 (1/Ωcm) reported previously. Furthermore, the model reveals a very large free-electron contribution to the optical constants of Ni, which disproves earlier claims about their insignificance. We also employ graphical techniques to find the plasma frequencies and free-electron scattering rates, which agree well with the parameters found from the first and the second methods.

To prepare clean samples and reduce the thickness of the overlayers, the samples were maintained in ultrahigh vacuum at a temperature of 750 K for 6 hours and then cooled down overnight. A surface roughness thickness of 1-3 nm was found using atomic force microscopy and x-ray reflectivity.

Electronic Materials and Photonics Division
Room A214 - Session EM+2D+NS+TF-WeA

THEME Session: Electronics and Photonics for a Low-Carbon Future

Moderators: Michael A. Filler, Georgia Institute of Technology, Stephen McDonnell, University of Virginia

2:20pm **EM+2D+NS+TF-WeA-1 Uncovering the Materials Paradigm for Solar Absorbers through In situ Imaging and Characterization**, *Mariana Bertoni,* Arizona State University **INVITED**

The behavior of solar cells is very often limited by inhomogeneously distributed nanoscale defects. This is the case throughout the entire lifecycle of the solar cell, from the distribution of elements and defects during solar cell growth as well as the charge-collection and recombination during operation, to degradation and failure mechanisms due to impurity diffusion, crack formation, and irradiation- and heat-induced cell damage This has been known for a while in the field of crystalline silicon, but inhomogeneities are far more abundant in polycrystalline materials, and are the limiting factor in thin-film solar cells where grain sizes are often on the order of the diffusion length.

We will show that the high penetration of hard X-rays combined with the high sensitivity to elemental distribution, structure, and spatial resolution offers a unique avenue for highly correlative studies at the nanoscale. We will present results on CdTe and Cu(In,Ga)Se$_2$ where carrier collection is directly correlated to the compositional and structural properties of the material under a large variety of synthesis and operating conditions. The segregation of copper at the grain boundaries of both solar absorbers will be discussed in detail as well as the defects impact to carrier collection efficiency. Furthermore, the kinetics of copper segregation during growth and processing will be presented.

3:00pm **EM+2D+NS+TF-WeA-3 Atomic Layer Deposition's Potential in Sustainability**, *Karen Buechler,* ALD NanoSolutions **INVITED**

Atomic layer deposition (ALD) is an exciting thin film deposition technique which holds the promise to permit enormous material innovations. These material innovations are currently enabling advanced catalysts, high capacity energy storage, advanced manufacturing technologies and many other products. Many of these products work towards reducing energy needs. This talk will highlight several examples of advanced material development through ALD which lead to advanced products which in turn are reducing the carbon footprint of consumers and manufacturers.

4:20pm **EM+2D+NS+TF-WeA-7 Challenges in Materials and Processing to Implementation of Energy Efficient SiC Technology**, *Mei-Chien Lu,* Monte Rosa Technology

Energy and sustainability have been the main driving forces for the implementation of silicon carbide technology for efficient energy conversion in recent applications in electrical vehicles, hybrid electrical vehicles, data center power management, and photovoltaic and wind power. The decades-long research and development efforts are attributed to the complexity of polytypes of crystal structures of silicon carbide. Reducing these inherent defects from crystal growth and epitaxial layer growth are crucial and continuing tasks. Device architectures are found to be more efficient along selected crystal planes. Innovative processing technologies have to be developed to make these devices built by

compound semiconductors with strong covalent bonding manufacturable. Fundamental challenges in materials, devices, and processing technologies will first be briefed. A patent landscape analysis is then conducted herein to reveal the past trends to pave the paths for future research and development. Implementations of silicon carbide devices are in its infancy with some full SiC inverter adopted by a commercial electrical vehicle manufacturer. Market shares and momentum of silicon carbide power electronics as well as the expectations from perspectives of department of energy and industry major players will be discussed. The continuous efforts to address the challenges in materials and processing are encouraged to support the full scale implementation of energy efficient silicon carbide technology.

4:40pm EM+2D+NS+TF-WeA-8 High Efficiency of Hot Electron Transfer at a Metal-Insulator-Semiconductor to Electrolyte Interface, *Hyun Uk Chae, R Ahsan, Q Lin, R Kapadia,* University of Southern California

Hot electrons generated from metal has drawn considerable interest in recent years due to the potential for lowering the high-barrier chemical reactions. The majority of hot electron controlling strategy at present have been plasmonic devices using localized surface plasmon resonance (LSPR). Several works have been done using plasmons to induce the hot electron generation to use as catalysts for chemical reactions like hydrogen evolution reaction (HER). However, the efficiency of those devices is extremely low and the mechanism behind it is quite complicated and remain unclear until now. To take advantage of hot electrons efficiently, properly and simply designed devices are required. Here, we demonstrate the different mechanisms of hot electron transfer in a thin gold film in an $Au-Al_2O_3-Si$ metal-insulator-semiconductor (MIS) junction by modulating Au film thickness, the applied voltage between Au-Si junction. Hot electron injection contributes to modifying the electron distribution inside the Au electrode, which enables HER to be driven more at same overpotential in solution. This work present that the injection of non-equilibrium electrons can shift the onset voltage of HER by ~0.6 V on the gold film in a 0.5 M H_2SO_4 solution. The efficiency of hot electron density efficiency shows ~85% at 2V of MIS junction bias and solution bias of -1.5 V vs Ag/AgCl is also presented. In addition to experimental results, we carried out the 2-D Monte Carlo simulation to track the injected hot electrons to study for the detail behaviors of thermalization mechanism inside the Au region which indicates the rate of HER. Since electrons quickly lose their energy within femtosecond by electron-electron or electron-phonon scattering, it is significant to see how they behave inside the injected medium to understand the reactions more precisely. The high-efficiency of hot electron usage reported here can be an opening towards the creation of practical hot-electron devices, which could be widely applied to the various fields.

5:00pm EM+2D+NS+TF-WeA-9 Integrated Photocathodes for Solar Driven Conversion of Carbon Dioxide to value-added Products, *Joel Ager,* Lawrence Berkeley Lab, University of California, Berkeley **INVITED**

If renewable power sources such as solar and wind could be used to produce chemical precursors and/or fuels, it would provide an alternative to mankind's unsustainable use of fossil fuels and slow the rate of CO_2 emission into the atmosphere [1,2]. Solar to chemical energy conversion by photoelectrochemical processes is a promising approach to address this challenge. Analogous to photovoltaics [3], driving the uphill redox reactions required for net solar to chemical energy conversion necessitates directional charge transport [4]. Additionally, in order to convert carbon dioxide to hydrocarbons, one must manage multi-electron transfer reactions (e.g. 12 in the case of ethylene and ethanol), and minimize potential losses in all parts of the system [5].

Charge selective contacts can be used to steer direct photo-generated carriers to catalytic sites that perform CO_2 reduction in an integrated photocathode. In contrast to conventional photocathode designs which employ p-type absorbers, we used a back illumination geometry with an n-type Si absorber to permit the use of absorbing metallic catalysts which would otherwise block the light. Back and front interfaces were configured by ion implantation and by surface passivation to achieve carrier selectivity. Surface texturing of the Si was used optimize light absorption on the illuminated side and increase the surface area available for catalysis on the electrolyte side. Selectivity to C-C coupled products was achieved by using hierarchical Au- Ag-Cu nanostructures as electrocatalysts [6].

The photovoltage, 550- 600 mV under simulated 1-sun illumination, confirms the carrier selectivity and passivation of the front and back interfaces. Compared to planar controls, textured photocathodes generate higher current densities, exceeding 30 mA cm^{-2}. Under simulated diurnal

illumination conditions, over 60% faradaic efficiency to C_{2+} hydrocarbon and oxygenate products (mainly ethylene, ethanol, propanol) is maintained for several days. By coupling photocathodes to series-connected semi-transparent halide perovskite solar cells, we demonstrated stand-alone, CO_2 reduction with a 1.5% conversion efficiency to hydrocarbons and oxygenates [7].

1. Graves,C.; Ebbesen, S. D.; Mogensen, M.; Lackner, K. S. *Renew. Sustain. Energy Rev.***2011**,*15*, 1–23.

2. Chu, S.; Cui, Y.; Liu, N. *Nat. Mater.***2016**, *16*, 16–22.

3. Wurfel, U.; Cuevas, A.; Wurfel, P. *IEEE J. Photovoltaics***2015**, *5*, 461–469.

4. Osterloh, F. E. *ACS Energy Lett.***2017**, *2*, 445–453.

5. Gurudayal et al. *Energy Environ. Sci.***2017**, *10*, 2222–2230.

6. Lum, Y.; Ager, J. W. *Energy Environ. Sci.***2018**, *11*, 2935–2944.

7. Gurudayal et al. *Energy Environ. Sci.***2019**, *12*, 1068–1077.

5:40pm EM+2D+NS+TF-WeA-11 Modeling of Optical Scattering in White Beetle Scales, *Seung Ho Lee, S Han, S Han,* University of New Mexico
Keywords: Light Scattering; Diffusion Approximation

Abstract: Extremely thin "super-white" coatings that reject solar spectrum but radiate through the transparent atmospheric window in mid-infrared have broad implications in heat management and energy savings for diverse sectors, including building construction, ship manufacturing, and space vehicle operation. In our previous work, we were able to create paint-format "super-white" coatings from microsphere-based materials.[1,2] In this work, however, we borrow our inspiration from white beetles in nature that reveal structural ingenuity at the nanometer scale to achieve such white film. White beetle scales display exceptionally strong light scattering power from a thin anisotropic random biopolymer network. While previous studies have revealed that the anisotropy plays an important role in strong light scattering, the physics of anisotropic light propagation remains less than fully understood. In particular, the studies have shown that light scattering in anisotropic random media may deviate significantly from the anisotropic diffusion approximation. This uncertainty in diffusion approximation led to a study interrogating the scale structures by fully solving Maxwell's equations. These calculations yet left questions on their accuracy, as the structural dimensions in perpendicular direction to the incident light were significantly greater than optical wavelengths. In this work, we systematically reduce the structural size in our simulations, using Fourier analysis of the white beetle scale structures. The size reduction enables fast, accurate calculations of light scattering in the biological structures. From these simulations, we find that the diffusion approximation is valid in describing light propagation in the white beetle scales. Further, we derive a light diffusion equation for anisotropic media from the radiative transfer equation and show that the equation for anisotropic diffusion derived in the past studies is inaccurate. We discuss how our newly derived equation can be used for accurate numerical calculations of light scattering and characterizing anisotropic light diffusion.

[1] S. Atiganyanun, J. Plumley, S. J. Han, K. Hsu, J. Cytrynbaum, T. L. Peng, S. M. Han, and S. E. Han, "Effective Radiative Cooling by Paint-Format Microsphere-Based Photonic Random Media," *ACS Photon.***5,** 1181-1187 (2018).

[2] J. D. Alden, S. Atiganyanun, R. Vanderburg, S. H. Lee, J. B. Plumley, O. K. Abudayyeh, S. M. Han, and S. E. Han, "Radiative Cooling by Silicone-Based Coating with Randomly Distributed Microbubble Inclusions," *J. Photon. Energy***9,** 032705-1:10 (2019).

6:00pm EM+2D+NS+TF-WeA-12 Boosting the Performance of WO₃/n-Si for Photo-electrochemical Water Splitting: From the Role of Si to Interface Engineering, *Yihui Zhao,* Electrochemical Materials and Interfaces (EMI), Dutch Institute for Fundamental Energy Research (DIFFER), The Netherlands*; A Bieberle-Hütter,* Electrochemical Materials and Interfaces (EMI), Dutch Institute for Fundamental Energy Research (DIFFER),The Netherlands, The Netherlands*; G Brocks,* Center for Computational Energy Research, Department of Applied Physics, Eindhoven University of Technology; Computational Materials Science, Faculty of Science and Technology and MESA+ Institute for Nanotechnology, University of Twente, The Netherla, The Netherlands*; H Genuit,* Dutch Institute for Fundamental Energy Research (DIFFER), The Netherlands*; R Lavrijsen,* Physics of Nanostructures and Center for NanoMaterials (cNM), Department of Applied Physics, Eindhoven University of Technology, The Netherlands

Metal oxide/Si is a promising model for designing high performing electrodes for photo-electrochemical (PEC) water splitting applications. This research provides a fundamental understanding of how and how much

the Si contributes to the PEC process in a metal oxide/Si electrode. Applying separated monochromatic UV and IR illumination as well as an Ag interface layer in a WO_3/n-Si heterostructure, we find that the band bending depth in Si, which determines the photovoltage, plays a dominant role. This discovery breaks through the existing design ideas, which focused on facilitating charge transport via interface layers within the Z-scheme, but ignored the resulting changes in the band structure of Si. Based on this discovery, we use a Pt interface layer to enlarge the extent of the n-Si band bending. The resulting WO_3/Pt/n-Si photoelectrodes exhibit a 2 times higher photocurrent density at 1.23 V vs RHE and a 10 times enhancement at 1.6 V vs RHE compared to WO_3/n-Si. In addition, we found that the native SiO_2 layer at the interface prevents Fermi level pinning in the Schottky contact between the Si and the metal. These discoveries should guide future design of metal oxide/Si electrodes for PEC applications.

Fundamental Discoveries in Heterogeneous Catalysis Focus Topic
Room A213 - Session HC+OX+SS-WeA

Metal-Support Interactions Driving Heterogeneously-Catalyzed Reactions

Moderators: Aravind Asthagiri, The Ohio State University, Jason Weaver, University of Florida

2:20pm **HC+OX+SS-WeA-1 Yittria-stabilized Zirconia (YSZ) Supports for Low Temperature Ammonia Synthesis**, *Z Zhang, S Livingston,* Colorado School of Mines*; L Fitzgerald,* University College Dublin*; D Way, **Colin Wolden**,* Colorado School of Mines

The use of renewable hydrogen for distributed synthesis of ammonia requires the development of efficient catalysts and processes that operate under mild conditions. Here we introduce yittria stabilized zirconia (YSZ) as a more active Ru catalyst support for NH_3 synthesis than traditionally used supports such as Al_2O_3. The addition of Cs promoter increased rates an order of magnitude higher by reducing the apparent activation energy from 103 kJ/mol to 65 kJ/mol. The rate enhancement is largely insensitive to the amount of promoter addition, with Cs outperforming Ba and K by a factor of 2. At 400°C under 1.0 MPa, the synthesis rate was comparable with that of most active oxide-supported Ru catalysts. The rate becomes inhibited by H_2 absorption at low temperature (< 350°C), but the use of lower H_2:N_2 ratios enables the rate to remain comparable to what is observed in stoichiometric mixtures at temperatures > 400°C. A detailed microkinetic model was developed that successfully captures the observed behavior, revealing that adsorption is coverage dependent. These results provide insight and direction into developing alternatives to Haber-Bosch for distributed synthesis of green ammonia.

2:40pm **HC+OX+SS-WeA-2 Operando PTRF-XAFS Technique for 3D Structure Determination of Active Metal Sites on a Model Catalyst Surface under Working Conditions**, *Satoru Takakusagi, L Bang, D Kido, Y Sato, K Asakura,* Hokkaido University, Japan

Polarization-dependent total reflection fluorescence (PTRF)-XAFS is a powerful technique which can determine 3D structure of highly dispersed metal species on a single-crystal surface by measuring polarization-dependent XAFS of the metal species. To obtain atomic-level understanding of metal/oxide-support interaction in heterogeneous catalysis, we have determined the precise 3D structures of single metal atoms and metal clusters deposited on single-crystal oxide surfaces such as TiO_2(110) and Al_2O_3(0001) by UHV PTRF-XAFS apparatus.[1]

Recently we have constructed a new apparatus which enables us to measure PTRF-XAFS of active metal species dispersed on a single-crystal oxide surface under working condition. A compact vacuum chamber which works both as PTRF-XAFS cell and batch-type reactor was designed and constructed. The sample can be transferred without exposure to air from another UHV chamber where the sample preparation (ion sputtering, annealing and metal deposition) and its surface characterization (LEED, XPS) are carried out. The sample in the compact chamber can be heated at high temperatures (< 700 °C) in the presence of reactant gases (typically 10~100 Pa), which makes the operando PTRF-XAFS measurements possible. Thus 3D structure-activity relationship of the active metal species on an oxide surface in heterogeneous catalysis can be obtained. We will show the details of the operando PTRF-XAFS technique and its application to CO oxidation on a Pt/Al_2O_3(0001) surface.

(References)

[1] S. Takakusagi et al., *Chem. Rec.* **18** (2018) 1, *J. Phys. Chem. C* **120** (2016) 15785, *Top. Catal.* **56**(2013*)* 1477, *Phys. Chem. Chem. Phys.* **15**(2013*)* 14080.

3:00pm **HC+OX+SS-WeA-3 Understanding and Tuning Catalytic Materials Using Nanocrystal Precursors**, *Matteo Cargnello,* Stanford University
INVITED

Catalytic processes are central to the goal of a sustainable future. A promising approach in developing catalytic materials is represented by the design of catalytic sites based on the knowledge of reaction mechanisms and structure-property relationships and aided by computation, and in the precise synthesis of these sites at the atomic and molecular level. The materials-pressure gap, however, still hinders the full realization of this strategy. Nanocrystal precursors, with tunable active sites and compositions, can help bridge this gap. The goal of this talk is to show how this approach can provide not only fundamental understanding of catalytic reactions, but also represents a way to precisely engineer catalytic sites and metal-support interactions to produce efficient catalysts that are active, stable and selective for several important catalytic transformations. Examples of the use of these building blocks as supported systems or in combination with hybrid organic materials will be shown, both to understand trends in methane and CO2 activation, and in the preparation of optimized catalytic systems combining multiple active phases. In all these examples, important efforts to obtain useful structure-property relationships will be highlighted, with this knowledge used to prepare more efficient catalysts for sustainable production of fuels and chemicals.

4:20pm **HC+OX+SS-WeA-7 CO$_2$ Hydrogenation on Supported Zirconium Oxide Clusters**, *Yilin Ma[1],* Stony Brook University*; M White,* Brookhaven National Laboratory

In this work, zirconium atoms and zirconium oxide clusters are deposited onto metal/metal oxide surfaces as model "inverse" catalysts for the study of CO_2 hydrogenation. The control over the stoichiometry of clusters and the oxidation state of the metal centers enables the study of atomic level details such as identification of active sites, interfacial electron transfer and the role of sulfur vacancies. Recent AP-XPS, AP-IR and STM results of supported zirconium oxide on Cu_2O/Cu(111) surface will be presented. Reactivity studies over Zr/Cu_2O/Cu(111) show that the formation of CO_2^- (ad)and $HCOO^-$ can be seen on regions with the presence of Zr on Cu_2O surface during the reaction condition(CO_2/H_2=1, total pressure=0.5torr), however CO_2 only binds weakly on bare Cu_2O/Cu(111) surface. Moreover, the change of zirconium oxidation state indicates the adsorption of CO_2 happens on metal or metal-support interface, where the zirconium gets oxidized when exposing to CO_2. Some DFT studies of above systems will also be shown, including the electronic structures of clusters, binding sites of CO_2 molecules, etc.

4:40pm **HC+OX+SS-WeA-8 Tuning Surface Hydrophobicity to Enhance Reaction Rate of the Lewis Acid Zeolite Nano Sn Beta for Alcohol Ring Opening of Epoxides**, *Nicholas Brunelli, A Spanos, A Parulkar, N Deshpande,* The Ohio State University

Ring opening epoxides produces compounds that are valuable in the production of fine chemicals and pharmaceuticals. Recent work[1]has demonstrated that the bulky reactants typically involved in fine chemical synthesis benefit from reducing the length scale of the materials to produce nano-zeolites (nano-Sn-Beta), which requires using a custom-synthesized structure directing agent in hydroxide conditions. While the nanozeolites can achieve higher overall conversion than Sn-Beta synthesized using fluoride conditions, the initial reaction rate is higher for Sn-Beta that tends to be hydrophobic compared to nano-Sn-Beta that is demonstrated to be hydrophilic. These results suggest that the alcohol ring opening reaction is sensitive to the reaction environment. The surface of nano-Sn-Beta can be treated to reduce the amount of defects and correspondingly increase the hydrophobicity. Interestingly, the treatment of nano-Sn-Beta materials more than doubles the observed reaction rate. Overall, this demonstrates a valuable method to tune the reaction environment that could be widely applicable to many chemical reactions.

References

(1) Parulkar, A.; Spanos, A. P.; Deshpande, N.; Brunelli, N. A. Synthesis and catalytic testing of Lewis acidic nano zeolite Beta for epoxide ring opening with alcohols. *Applied Catalysis A: General,* **2019**, *577*, 28–34.

[1] **Heterogeneous Catalysis Graduate Student Presentation Award Finalist**

5:00pm HC+OX+SS-WeA-9 Understanding Metal-Metal and Metal-Support Interactions in Bimetallic Catalysts*, Donna Chen,* Univeristy of South Carolina*; S Farzandh, D Shakya, A Brandt, T Maddumapatabandi,* University of South Carolina **INVITED**

Bimetallic catalysts are known to exhibit superior properties compared to their individual pure metal components, but in many cases the nature of these improved properties is not well understood. The main goal of this work is to understand how oxidation states, metal-support interactions, and metal-metal interactions in supported bimetallic clusters can be used to control catalytic activity. Specific catalytic reactions investigated are the water gas shift reaction (WGS)on Pt-Re and selective hydrogenation of unsaturated aldehydes on Pt-Sn. Model catalyst surfaces are prepared via vapor-deposition of metal clusters on single-crystal oxide and carbon supports. These surfaces are fully characterized by a variety ultrahigh vacuum (UHV) surface science techniques and their activities are studied in a microreactor (P~ 1 atm) coupled to the UHV chamber. Scanning tunneling microscopy investigations indicate that exclusively bimetallic clusters can be prepared by sequential deposition of metals. For the WGS reaction, the active site is determined to be Pt with subsurface Re, while Re oxide does not play a role. Density functional theory studies show that the presence of subsurface Re decreases the adsorption energy of CO on Pt, thus preventing Pt active sites from being poisoned by CO. WGS activity increases with increasing perimeter for Pt/TiO_2 clusters, and the turnover frequency is also lower in the absence of the TiO_2 support. For hydrogenation on furfural, the Pt-Sn alloy surface exhibits high selectivity to furfuryl alcohol compared to pure Pt, whereas furan and tetrahydrofuran are the main products on Pt.

Advanced Ion Microscopy and Ion Beam Nano-engineering Focus Topic
Room B231-232 - Session HI+AS+CA-WeA

Advanced Ion Microscopy and Surface Analysis Applications

Moderators: Richard Livengood, Intel Corporation, Armin Gölzhäuser, University of Bielefeld, Germany

2:20pm HI+AS+CA-WeA-1 Analytical Capabilities on FIB Instruments using SIMS: Applications, Current Developments and Prospects*, Tom Wirtz,* Luxembourg Institute of Science and Technology, Luxembourg*; J Audinot,* Luxembourg Institute of Science and Technology, Luxembourg, Luxembourg*; J Lovric, O De Castro,* Luxembourg Institute of Science and Technology, Luxembourg **INVITED**

Secondary Ion Mass Spectrometry (SIMS) is an extremely powerful technique for analyzing surfaces, owing in particular to its ability to detect all elements from H to U and to differentiate between isotopes, its excellent sensitivity and its high dynamic range. SIMS analyses can be performed in different analysis modes: acquisition of mass spectra, depth profiling, 2D and 3D imaging. Adding SIMS capability to FIB instruments offers a number of interesting possibilities, including highly sensitive analytics, in-situ process control during patterning and milling, highest resolution SIMS imaging (~10 nm), and direct correlation of SIMS data with data obtained with other analytical or imaging techniques on the same instrument, such as high resolution SE images or EDS spectra [1,2].

Past attempts of performing SIMS on FIB instruments were rather unsuccessful due to unattractive detection limits, which were due to (i) low ionization yields of sputtered particles, (ii) extraction optics with limited collection efficiency of secondary ions and (iii) mass spectrometers having low duty cycles and/or low transmission. In order to overcome these limitations, we have investigated the use of different primary ion species and of reactive gas flooding during FIB-SIMS and we have developed compact high-performance magnetic sector mass spectrometers operating in the DC mode with dedicated high-efficiency extraction optics. We installed such SIMS systems on different FIB based instruments, including the Helium Ion Microscope [3-5], a FIB-SEM DualBeam instrument and the npSCOPE instrument, which is an integrated Gas Field Ion Source enabled instrument combining SE, SIMS and STIM imaging with capabilities to analyse the sample under cryo-conditions.

Here, we will review the performance of the different instruments with a focus on new developments such as cryo-capabilities and new detectors allowing parallel detection of all masses, present a number of examples from various fields of applications (nanoparticles, battery materials, photovoltaics, micro-electronics, tissue and sub-cellular imaging in biology, geology,…) and give an outlook on new trends and prospects.

[1] T. Wirtz, P. Philipp, J.-N. Audinot, D. Dowsett, S. Eswara, Nanotechnology 26 (2015) 434001

[2] F. Vollnhals, J.-N. Audinot, T. Wirtz, M. Mercier-Bonin, I. Fourquaux, B. Schroeppel, U. Kraushaar, V. Lev-Ram, M. H. Ellisman, S. Eswara, Anal. Chem. 89 (2017) 10702

[3] D. Dowsett, T. Wirtz, Anal. Chem. 89 (2017) 8957

[4] T. Wirtz, D. Dowsett, P. Philipp, Helium Ion Microscopy, ed. by G. Hlawacek, A. Gölzhäuser, Springer, 2017

[5] T. Wirtz, O. De Castro, J.-N. Audinot, P. Philipp, Ann. Rev. Anal. Chem. 12 (2019)

3:00pm HI+AS+CA-WeA-3 Correlated Materials Characterization via Multimodal Chemical Imaging using HIM-SIMS*, A Belianinov,* Oak Ridge National Laboratory*; S Kim,* Pusan National University, South Korea*; A Trofimov,* **Olga S. Ovchinnikova,** Oak Ridge National Laboratory

Multimodal chemical imaging simultaneously offers high resolution chemical and physical information with nanoscale, and in select cases atomic, resolution. By coupling modalities that collect physical and chemical information, we can address a new set of scientific problems in biological systems, battery and fuel cell research, catalysis, pharmaceuticals, photovoltaics, medicine and many others. The combined multimodal platforms enable local correlation of material properties with chemical makeup, making fundamental questions in how chemistry and structure drive functionality approachable. The goal of multimodal imaging is to transcend the existing analytical capabilities for nanometer scale spatially resolved material characterization at interfaces through a unique merger of advanced microscopy, mass spectrometry and optical spectroscopy.Combining helium ion microscopy (HIM) and secondary ion mass spectrometry (SIMS) onto one platform has been demonstrated as a method for high resolution spot sampling and imaging of substrates. To advance this approach and to expand its capabilities I will present our results of multimodal chemical imaging using this technique on test substrates and show application of this approach for the multimodal analysis of perovskite (HOIPs) materials. I will discuss the performance metrics of the multimodal imaging system on conductive and non-conductive materials and discuss our results on understanding the chemical nature of ferroelastics twin domains in methylammonium lead triiodide (MAPbI3) perovskite using HIM-SIMS.

3:20pm HI+AS+CA-WeA-4 Compositional Characterization of Biogenic Nanoparticles using the ORION NanoFab with SIMS*, Christelle Guillermier, F Khanom,* Carl Zeiss PCS, Inc.*; D Medina,* Northeastern University*; J Audinot,* Luxembourg Institute of Science and Technology, Luxembourg

Over the past several years, the use of both nanoparticles and nanostructured surfaces have emerged as an alternative's solution to antibiotic resistant bacteria as they effectively decrease bacterial survival without being highly toxic to mammalian cells. These nanoparticles whose sizes span 10 nm to several hundred nm are composed of a variety of materials such as pure metals, metal oxides, and metalloids. Their chemical characterization however remains a challenge due to their small sizes. Scanning electron microscopy (SEM) and energy dispersive X-ray spectroscopy (EDX) are the conventional analytical techniques of choice to determine the nanoparticles' morphology, size, and elemental composition. However, although sensitive enough to detect trace elements, SEM and EDX cannot provide elemental information for the smallest features on a bulk sample, or for the lightest elements.

The ORION NanoFab is an ion microscope that allows for high resolution secondary electron (SE) imaging with a He$^+$ focused ion beam that can be focused to a 0.5 nm probe size. The same instrument offers a Ne$^+$ ion beam with a focused probe size of 2 nm. Recently, this same platform has been configured with a custom-designed magnetic sector secondary ion mass spectrometer (SIMS). It allows for the detection of all periodic table elements including H and Li which EDS cannot easily detect. Importantly, SIMS with neon provides elemental imaging with spatial resolution smaller than 20 nm. The combination of high resolution He$^+$ imaging (0.5 nm) with Ne$^+$ SIMS elemental mapping yields a direct correlative technique particularly attractive for exploring nanoparticles and nanofeatures in general.

NanoFab-SIMS has already yielded information-rich images in diverse fields of applications. We will here illustrate its potential for the characterization of biogenic nanoparticles made by bacteria and plants.

4:20pm HI+AS+CA-WeA-7 Effects of Ion Irradiation on Two-Dimensional Targets: What is Different from Bulk Materials, *Arkady V. Krasheninnikov*, Helmholtz-Zentrum Dresden-Rossendorf, Germany **INVITED**
Ion irradiation has successfully been used for introducing impurities and creating defects in two-dimensional (2D) materials in a controllable manner. Moreover, focused ion beams, especially when combined with in-situ or post-irradiation chemical treatments, can be employed for patterning and even cutting 2D systems with a high spatial resolution. The optimization of this process requires the complete microscopic understanding of the interaction of energetic ions with the low-dimensional targets.

In my presentation, I will dwell upon the multi-scale atomistic computer simulations of the impacts of ions onto free-standing (e.g., suspended on a TEM grid) and supported (deposited on various substrates) 2D materials, including graphene and transition metal dichalcogenides (TMDs), such as MoS_2 and WS_2. I will emphasize the differences between defect production under ion irradiation in 2D materials and bulk solids. The theoretical results will be augmented by the experimental data obtained by the coworkers. I will further present the results of multi-scale simulations of ion irradiation of free-standing [1] and supported [2] graphene and 2D TMDs, and demonstrate that depending on ion mass and energy, the defect production can be dominated by direct ion impacts, back scattered ions or atoms sputtered from the substrate [2]. Finally, I will touch upon the interaction of highly-charged [3] and swift heavy ions [4] with 2D systems and overview recent progress in modelling this using non-adiabatic approaches including time-dependent density functional theory and Ehrenfest dynamics [5].

1. M. Ghorbani-Asl, S. Kretschmer, D.E. Spearot, and A. V. Krasheninnikov, 2D Materials 4 (2017) 025078.

2. S. Kretschmer, M. Maslov, S. Ghaderzadeh, M. Ghorbani-Asl, G. Hlawacek, and A. V. Krasheninnikov, ACS Applied Materials & Interfaces 10 (2018) 30827.

3. R. A. Wilhelm, E. Gruber, J. Schwestka, R. Kozubek, T.I. Madeira, J.P. Marques, J. Kobus, A. V. Krasheninnikov, M. Schleberger, and F. Aumayr, Phys. Rev. Lett. 119 (2017) 103401.

4. R. Kozubek, M. Tripathi, M. Ghorbani-Asl, S. Kretschmer, L. Madauß, E. Pollmann, M. O'Brien, N. McEvoy, U. Ludacka, T. Susi, G.S. Duesberg, R.A. Wilhelm, A. V. Krasheninnikov, J. Kotakoski, and M. Schleberger J. Phys. Chem. Lett. 10 (2019) 904.

5. A. Ojanperä, A. V. Krasheninnikov, and M. Puska, Phys. Rev. B 89 (2014) 035120.

5:00pm HI+AS+CA-WeA-9 Effects of He Ion Irradiation on Gold Nanoclusters: a Molecular Dynamics Study, *Sadegh Ghaderzadeh, M Ghorbani-Asl, S Kretschmer, G Hlawacek,* Helmholtz-Zentrum Dresden Rossendorf, Germany; *A Krasheninnikov,* Helmholtz-Zentrum Dresden-Rossendorf, Germany
The interpretation of helium ion microscopy (HIM) images of crystalline metal clusters requires microscopic understanding of the effects of He ion irradiation on the system, including energy deposition and associated heating, as well as channeling patterns. While channeling in bulk metals has been studied at length, there is no quantitative data for small clusters. We carry out molecular dynamics simulations to investigate the behavior of gold nano-particles with diameters of 5-15 nmunder 30 keV He ion irradiation. We show that impacts of the ions can give rise to substantial heating of the clusters through deposition of energy into electronic degrees of freedom, but it does not affect channeling, as clusters cool down between consecutive impact of the ions under typical imaging conditions. At the same time, high temperatures and small cluster sizes should give rise to fast annealing of defects so that the system remains crystalline. Our results show that ion-channeling occurs not only in the principal low-index, but also in the intermediate directions. The strengths of different channels are specified, and their correlations with sputtering-yield and damage production is discussed, along with size-dependence of these properties. The effects of planar defects, such as stacking faults on channeling were also investigated.

Finally, we discuss the implications of our results for the analysis of HIM images of metal clusters.

5:20pm HI+AS+CA-WeA-10 Low Damage Imaging of Polymers with the Helium Ion Microscope, *Doug Wei,* Carl Zeiss, RMS, Inc.; *J Notte,* Carl Zeiss PCS, Inc.; *A Stratulat,* Carl Zeiss Microscopy, Ltd., UK
Polymers present a combination of challenges for high magnification imaging with the conventional SEM or FIB. Because they are electrically insulating, polymers are susceptible to charge accumulation and can produce imaging artifacts. Or worse, the implanted charge and surface charge can generate fields large enough to induce catastrophic dielectric breakdown. The interaction of the primary beam with the chemical bonds can cause radiolysis, cross-linking, and chain scissions which alter their morphology and other properties. Ion beams of relatively heavy species (Ga and Xe) can cause appreciable sputtering especially at high magnifications. In some cases, the sputtering can be preferential for light atoms, causing disproportionate hydrogen loss. Further difficulties include heating effects, since the typical polymers are good thermal insulators. Compounding matters, they are often temperature sensitive and can be damaged at even modest temperature rises ~ 50 deg C.

However, some of the newly available light ion beams (H, He, Li) offer unique advantages that help to circumvent the problems traditionally encountered when imaging polymers. First, the charging effects are greatly diminished compared to the SEM. In part, this is because the incident ion is likely neutralized as it enters the sample, and remains in a mostly neutral state as it penetrates deeply. This leaves only a net surface charge, which is overall positive and made more so by the ejection of secondary electrons from the surface. This is easily resolved using a collection of low energy electrons provided by a flood gun. The light ion beams also have relatively low sputtering rates compared to the heavier ions. Their interactions are primarily with the electrons of the sample. So while they can affect bonding, they are much less likely to cause sputtering. The light ions will generally be implanted deeply, often hundreds of nanometers under the surface, and helium in particular is known to diffuse out over time. Thermal effects are also much reduced with the light ion beams compared to heavier ions or the SEM. The ion's initial kinetic energy is converted to random thermal energy over a relatively large volume. And much of the transferred energy goes to the electrons in the sample, and their relatively long mean free path helps to dissipate this energy into a larger volume.

Numerous imaging examples will be provided from a variety of polymers using the helium beam from the Zeiss ORION NanoFab. These serve as representative examples of the unique sample interaction of light ions and the advantages they offer for imaging polymers.

5:40pm HI+AS+CA-WeA-11 Imaging of Biological Cells with Helium-Ion Microscopy, *Natalie Frese, A Beyer, C Kaltschmidt, B Kaltschmidt,* Bielefeld University, Germany; *A Thomas,* Institute for Metallic Materials Dresden, Germany; *W Parak,* University of Hamburg, Germany; *A Gölzhäuser,* Bielefeld University, Germany
Studies from the last decade have shown that helium-ion microscopy (HIM) is suitable for studying biological samples. In particular, cell membranes can be imaged by HIM without metallic coatings, which could lead to disturbance of the surface. In this contribution, we give two examples of biological cells imaged by HIM: (i) mouse hippocampal neurons on patterned surfaces for neuronal networks and (ii) human cells treated with colloidal nanoparticles [1, 2]. Both examples benefit from the high resolution imaging of uncoated, biological materials by HIM, as for (i) the cell adherence to patterned surfaces could be imaged and for (ii) cell morphology images indicated harmful effects of colloidal nanoparticles to cells.

[1] M. Schürmann et al., PLoS ONE 13(2), e0192647 (2018)

[2] X. Ma et al., ACS Nano 11(8), 7807-7820 (2017)

6:00pm HI+AS+CA-WeA-12 Channeling in the Helium Ion Microscope, *Hussein Hijazi, L Feldman, R Thorpe, M Li, T Gustafsson,* Rutgers University; *D Barbacci, A Schultz,* Ionwerks
The helium ion microscope (HIM) has become a unique tool for modern materials science due to its high lateral resolution for imaging, high spatial resolution and nano-scale analysis. For crystalline materials, the incident beam may undergo ion channeling, which strongly modifies all of the basic ion-solid interactions associated with these HIM functions. Here, a 30 keV He$^+$ beam was used for RBS channeling in a W(111) crystal using a novel time of flight (HIM/TOF) detector developed at Rutgers University to extract critical channeling parameters. Measurements of the minimum backscattering yield (χ_{min}), surface peak (SP), and critical angle, are compared to several theoretical estimates. The results illustrate the advantage of using channeling in a backscattering mode to characterize crystalline materials with the HIM, as the backscattering intensity modifications are far greater for scattered ions than for secondary electrons. This case of "ideal" channeling with the HIM now provides a basis for analysis of more complex materials such as polycrystalline materials and textured structures, and quantifies the role of HIM induced materials modification in crystalline materials.

Wednesday Afternoon, October 23, 2019

Magnetic Interfaces and Nanostructures Division
Room A210 - Session MI+2D-WeA

Emerging Multifunctional Magnetic Materials II

Moderators: Valeria Lauter, Oak Ridge National Laboratory, Axel Hoffmann, Technical University of Berlin

2:20pm MI+2D-WeA-1 Field and Current Control of the Electrical Conductivity of an Artificial Two-Dimensional Honeycomb Lattice, *Deepak Singh,* University of Missouri **INVITED**
Two-dimensional magnetic nanostructured geometry, such as an artificial magnetic honeycomb lattice, provides facile platform to explore many novel properties of magnetic materials in one system. Originally envisaged to explore the physics of effective magnetic monopoles and magnetic field-induced avalanche of Dirac string, artificial magnetic honeycomb lattice has emerged as a key playground to discover new and exotic magnetic phases, such as magnetic charge ordered state and the spin solid state, in disorder free environment. We have created a new artificial permalloy honeycomb lattice of ultra-small connected element, with a typical length of ~ 12 nm, in this pursuit. Using neutron scattering and complementary measurements on the newly created honeycomb lattice, we have investigated emergent phenomena of short-range quasi-spin ice and long range spin solid order. Additionally, two new properties of Wigner crystal type state of magnetic charges and magnetic diode-type rectification are discovered in the newly created artificial honeycomb lattice. The new findings create a new vista for the next generation design of spintronics devices in this two-dimensional frustrated geometry. Research at MU is supported by the U.S. Department of Energy, Office of Basic Energy Sciences under Grant No. DE-SC0014461.

3:00pm MI+2D-WeA-3 Emergence and Dynamics of Magnetic Order in Metamagnetic Nanostructures, *Vojtech Uhlir,* CEITEC BUT, Brno University of Technology, Czech Republic **INVITED**
The advantage of ferromagnetic materials is the nonvolatility of the information encoded in the internal magnetic configuration, which can be used for memory storage, logic and sensing devices. Antiferromagnets are another class of magnetic materials that features nonvolatile magnetic ordering, yet its applications have been largely overlooked until recently [1]. In materials featuring a first-order metamagnetic phase transition between the antiferromagnetic (AF) and ferromagnetic (FM) states, the nature of the phase transition can be tuned by strain, pressure, chemical doping, temperature, as well as magnetic and electric fields, potentially offering very high recording densities and huge changes in the order parameters controlled with very low power.

Moreover, metamagnetic materials are outstanding candidates for finding and exploiting new functionalities and emergent phenomena on the mesoscale [2,3]. For instance, the transition from the AF order to FM order in sub-micron-wide FeRh wires becomes greatly asymmetric when comparing the heating and cooling cycles [3,4]. This recovery of the abrupt transition in nanostructures could lead to low-energy, efficient routes to control magnetic properties, leading to potential applications, for instance, in spintronics.

Furthermore, we show the dynamic response of the electronic and magnetic order to ultrafast laser excitation can be followed by time-resolved photoemission electron spectroscopy [5], which unlike techniques probing the total magnetization in the sample provides a direct comparison to the dynamic response of the structural order.

[1] T. Jungwirth, X. Marti, P. Wadley, and J. Wunderlich, *Nature Mater.***11**, 231 (2016).

[2] F. Pressacco *et al., Sci. Rep.***6**, 22383 (2016).

[3] V. Uhlír, J. A. Arregi, and E. E. Fullerton, *Nat. Commun.***7**, 13113 (2016).

[4] J. A. Arregi *et al.,J. Phys. D: Appl. Phys.***51**, 105001 (2018).

[5] F. Pressacco *et al., Struct. Dyn. **5**, 034501 (2018).

4:20pm MI+2D-WeA-7 Time Dependence in La$_{0.7}$Sr$_{0.3}$MnO$_3$ Thin Films with Magnetic Competition, *Mikel B. Holcomb, R Trappen, N Mottaghi, S Yousefi, G Cabrera, G Bhandari, M Seehra,* West Virginia University
La$_{0.7}$Sr$_{0.3}$MnO$_3$ is a strongly correlated ferromagnetic system, commonly proposed for many magnetoresistance applications. Utilizing many techniques (bulk magnetometry, neutron reflectometry and resonant x-ray magnetic scattering), we observe magnetic competition between different magnetic phases in many samples under various growth conditions. This competition results in inverted hysteresis loops (common in superparamagnetic nanoparticles) and negative remanent magnetization.

While transmission electron microscopy images show pristine epitaxial growth, the data supports that there are regions of different magnetic order. This results in interesting magnetic measurements, that share similarities with ferrimagnets with competing magnetic lattices. In this talk, the time, field and temperature dependence of these samples will be discussed to help understand this phenomenon. Sample growth and optimization were supported by NSF (DMR-1608656), national facility measurements and theory were supported by the U.S. Department of Energy, Office of Science, Office of Basic Energy Sciences under Award Number DE-SC0016176, and optical measurements by American Chemical Society (PRF #56642-ND10). **We acknowledge the support of the National Institute of Standards and Technology, U.S. Department of Commerce, in providing the neutron research facilities used in this work.**

4:40pm MI+2D-WeA-8 Optically Induced Magnetization through Spin States at Perovskite/Ferromagnetic Interface Revealed by Neutron Magnetoreflectivity Studies, *Bin Hu,* University of Tennessee Knoxville **INVITED**
This presentation reports an optically induced magnetization at perovskite/ferromagnetic interface realized at room temperature. By using neutron magnetoreflectivity measurement, it was found that a circularly polarized light of 405 nm induces a magnetization with the thickness up to 5 nm into the surface of perovskite (MAPbBr$_3$) film underneath of ferromagnetic Co layer at room temperature. On contrast, a linearly polarized light does not generate any detectable magnetization within the perovskite surface in the MAPbBr$_3$/Co sample during the neutron magnetoreflectivity measurement. This observation provides an evidence to show optically induced magnetization on the perovskite surface in contact with Co surface. Furthermore, the MAPbBr$_3$/Co interface demonstrates a magneto-capacitance phenomenon, indicating that the electrical polarization on perovskite surface is coupled with magnetic polarization on the Co surface. On the other hand, a circularly polarized light leads to spin states in hybrid perovskites through photoexcitation. The observed magnetization indicates that circularly polarized light-generated spin states can directly interact with electric-magnetic coupling, leading to an optically induced magnetization.

5:20pm MI+2D-WeA-10 Effect of Interlayer and Underlayers on the Microstructure and Magnetic Softness in FeGa-based Ferromagnetic Composites, *Adrian Acosta, K Fitzell,* University of California, Los Angeles*; C Dong,* Northeastern University*; M Zurbuchen, N Sun, J Chang,* University of California, Los Angeles
Magnetoelectric materials provide the ability to efficiently control magnetism with electric fields, which is key to circumvent the size and efficiency limitations of traditional electric dipole antennas. Strain-mediated multiferroic antennas, composed of individual ferromagnetic and piezoelectric phases, have recently generated a lot of interest due to the potential to reduce the size of antennas by up to 5 orders of magnitude through the coupling of magnetization and electric polarization via strain at the interface. However, this requires a low-loss magnetic material with strong magnetoelastic coupling at high frequencies.

Galfenol (Fe81Ga19 or FeGa) is a promising candidate material due to its large magnetostriction (~275 ppm in polycrystalline bulk) and large piezomagnetic coefficient (>2 ppm/Oe) but is highly lossy at high microwave frequencies. Previously, nanoscale laminates were fabricated via DC magnetron sputtering of FeGa with NiFe as an interlayer material resulting in a composite with a small coercive field (<20 Oe), narrow FMR linewidth (<35 Oe), and high relative permeability (>1000) [1]. In this work, the enhancement in soft magnetic properties is correlated to the microstructure of these composites by TEM analysis where the nanolayering strategy promotes the formation smaller grain sizes. Optical magnetostriction measurements displayed an enhanced magnetostriction beyond that expected from averaging the individual FeGa and NiFe phases, indicating an interfacial contribution present leading to increase of the overall magnetostriction. The magnetostriction sensitivity peaks at a lower magnetic field (23 Oe for FeGa/NiFe multilayers vs 56 Oe for FeGa). To delineate the impact of the microstructure of FeGa on the soft and functional magnetic properties, FeGa was sputter deposited onto several materials (NiFe, Ta, Cu, and Al$_2$O$_3$) as underlayers on a Si substrate which can directly influence the polycrystalline structure and enhance its soft magnetic properties [2]. XRD and AFM are used to show the dependence of the coercivity, FMR linewidth, and magnetostriction on the texture, internal stress, grain size, and surface roughness of the FeGa film with the different underlayer materials.

Integration of these engineered composites into a strain-mediated multiferroic shear wave antenna design further demonstrates the potential of FeGa-based laminates for use in microwave communications systems for implantable medical devices.

References:

[1] Rementer, C. R., et al. (2017). *Applied Physics Letters* 110(24): 242403.

[2] Jung, H., et al. (2003). *Journal of Applied Physics* 93(10): 6462-6464.

5:40pm MI+2D-WeA-11 Tunable Spin-polarized Edge Effects in Transition Metal Dichalcogenides on FM and AFM Substrates, *N Cortes,* Universidad Tecnica Federico Santa Maria, Chile*; Oscar Avalos-Ovando,* Ohio University*; L Rosales, P Orellana,* Universidad Tecnica Federico Santa Maria, Chile*; S Ulloa,* Ohio University

We explore proximity-induced ferromagnetism (FM) and antiferromagnetism (AFM) on transition metal dichalcogenide (TMD), focusing on molybdenum ditelluride (MoTe2) ribbons with zigzag and/or armchair edges, deposited on either a FM or an AFM substrate, e.g. such as FM europium oxide and AFM manganese oxide. A three-orbital tight-binding model allows to model MoTe2 monolayer structures in real space, incorporating the exchange and Rashba fields induced by proximity to the substrate. For in-gap Fermi levels, electronic modes in the nanoribbon are strongly spin-polarized and localized along the edges, acting as 1D conducting channels with tunable spin-polarized currents. We also study the effect of atomic defects on the 1D conducting channels and on the spin-polarized currents, finding that even in the presence of either Te and/or Mo vacancies, the spin-polarized current is nonvanishing. Hybrid structures such as the MoTe2/FM-substrate and/or MoTe2/AFM- substrate configuration can serve as building blocks for spintronic devices and provide versatile platforms to further understand proximity effects in diverse materials systems.

[1] N. Cortes et al, Phys. Rev. Lett. 122, 086401 (2019).

[2] N. Cortes et al, in preparation (2019).

6:00pm MI+2D-WeA-12 Magnetocaloric Properties of Thin Film La$_{0.7}$Sr$_{0.3}$MnO$_3$: Magnetic Field Dependence and Effects of Superparamagnetism, *Navid Mottaghi*[1], *M Seehra, C Huang, S Kumari, S Yousefi Sarraf, G Cabrera, G Bhandari, R Trappen, M Holcomb,* West Virginia University

La$_{0.7}$Sr$_{0.3}$MnO$_3$ (LSMO) with Curie temperature $T_C \approx 370$ K is one of the manganites which has been of interest for applications in magnetic memory devices and spintronics.[1] The magnetic properties of LSMO thin films are also known to depend on the thickness of the films.[2] Recent magnetic investigations of a 7.6 nm LSMO film grown by pulsed laser deposition (PLD) showed it to have a $T_C \approx 290$ K with a magnetic dead layer $d \approx 1.4$ nm which demonstrated behavior consistent with containing superparamagnetic (SPM) spin clusters with blocking temperature $T_B \approx 240$ K.[3,4] Here we report magnetocaloric properties of this LSMO thin film for temperatures $T \leq T_C$ in magnetic fields H up to 4 kOe. In particular, magnetic entropy $S_M(T, H)$ is evaluated from the isothermal plots of magnetization (M) vs. H at different temperatures (Fig. 1) using the Eq. $\Delta S_M (T,H) = \sum_i [(M_{i+1} (T_{i+1}, H) - M_i (T_i, H))/(T_{i+1}-T_i)] \Delta H$. The H-dependence of $\Delta S_M (T,H)$ is analyzed using the relation $(-\Delta S_M)=aH^n$, where a is a constant and $n = 2/3$ is expected at $T = T_C$.[5] Our fit of the data to this Eq. for several $T \leq T_C$ in Fig. 2 shows $n \sim 1$ for $T < T_C$ with the magnitude of n increasing for $T > T_C$. This deviation of n from $n = 2/3$ is likely due to presence of SPM spin clusters in the dead layer for $T < T_C$. The larger magnitudes of n for $T > T_C$ is due to the Curie-Weiss variation of the magnetization in this regime.[5]

References

[1] N. Izyumskaya, Y. Alivov, and H. Morkoç, Crit. Rev. Solid State Mater. Sci. **34**, 89 (2009).

[2] M. Huijben, L.W. Martin, Y.-H. Chu, M.B. Holcomb, P. Yu, G. Rijnders, D.H.A. Blank, and R. Ramesh, Phys. Rev. B **78**, 94413 (2008).

[3] N. Mottaghi, R.B. Trappen, S. Kumari, C.Y. Huang, S. Yousefi, G.B. Cabrera, M. Aziziha, A. Haertter, M.B. Johnson, M.S. Seehra, and M.B. Holcomb, J. Phys. Condens. Matter **30**, 405804 (2018).

[4] N. Mottaghi, M.S. Seehra, R. Trappen, S. Kumari, C.-Y. Huang, S. Yousefi, G.B. Cabrera, A.H. Romero, and M.B. Holcomb, AIP Adv. **8**, 056319 (2018).

[5] M. Pękała, J. Appl. Phys. **108**, 113913 (2010).

Manufacturing Science and Technology Group
Room A226 - Session MS-WeA

Science and Technology for Manufacturing: Solid State Batteries (ALL INVITED SESSION)

Moderators: Kelsy Hatzell, Vanderbilt University, Gary Rubloff, University of Maryland, College Park

2:20pm MS-WeA-1 The Importance of Modifying the Nothing Within 3D Electrode Architectures for Solid-State Energy Storage, *Debra Rolison, M Sassin, C Chervin, J Parker, J Long,* U.S. Naval Research Laboratory **INVITED**
Our team has found that an architectural design metaphor serves as a powerful guide in re-imagining materials and electrodes in electrochemical energy science [1,2]. Key consumer and military portable power sources (e.g., batteries, fuel cells, supercapacitors) must balance multiple functions (molecular mass transport, ionic/electronic/thermal conductivity, and electron-transfer kinetics) even though these functions often require contradictory structures [2]. The design and fabrication of size- and energy-scalable three-dimensional multifunctional architectures from the appropriate nanoscale building blocks for charge storage seamlessly embodies all of the requisite functions. A critical knob to turn to amplify performance—or move to a new performance curve, such as a 3D solid-state battery with interpenetrating components [2,3]—is the ability to "paint blind," to modify interiors with functional materials that do not block the internal porosity through which reactants enter and products depart. Architecture also matters with the electrocatalysts under exploration to improve oxygen redox (higher activity and lower potential energy costs to drive the reaction) in air cathodes in aqueous metal–air batteries Expressing oxygen reduction or evolution electrocatalysts in ultraporous aerogel form allows us to extract higher activity at lower overpotentials [4–6], further underscoring the importance of nothing and the unimportance of periodicity in energy-relevant nanoarchitectures [7].

[1] J.W. Long, D.R. Rolison, *Acc. Chem. Res*. 2007, *40*, 854–862.

[2] D.R. Rolison, J.W. Long, J.C. Lytle, A.E. Fischer, C.P. Rhodes, T.M. McEvoy, M.E. Bourg, A.M. Lubers, *Chem. Soc. Rev*. 2009, *38*, 226–252.

[3] J.W. Long, B. Dunn, D.R. Rolison, and H.S. White, *Chemical Reviews* **2004**, *104*, 4463–4492.

[4] C.N. Chervin, P.A. DeSario, J.F. Parker, E.S. Nelson, D.R. Rolison, J.W. Long, *ChemElectroChem* 2016, *3*, 1369–1375.

[5] J . S. Ko, C . N. Chervin, M . N. Vila, P . A. DeSario, J . F. Parker, J . W. Long, D . R. Rolison, *Langmuir* **2017**, *33*, 9390–9397.

[6] J . S. Ko, J . F. Parker, M . N. Vila, M . A. Wolak, D . R. Rolison, and J . W. Long, *J. Electrochem. Soc.* **2018**, *165*, H777–H783.

[7] D.R. Rolison, *Science* 2003, *299*, 1698–1701.

3:00pm MS-WeA-3 Precision 3D Solid State Battery Architectures: Science, Challenges and Manufacturing Opportunity, *Sang Bok Lee Lee, G Rubloff,* University of Maryland, College Park **INVITED**
This presentation describes recent findings related to the design and architectures of thin electrode materials synthesized by thin layer deposition techniques. Throughout the presentation I will describe how these techniques enable us to synthesize electrodes of interest with precise control over the structure and composition of the material. The electrochemical response of these thin electrodes will be discussed in the aspects of structural parameters, ion storage mechanism, interfacial electrochemical issues related to electrode degradation. While it is important to identify and understand mechanisms in performance and degradation, it is even more critical to design strategies and to mitigate challenging technical hurdles for developing means to implement and validate the strategies in the aspect of future manufacturing opportunity. For example, the design and the development process of precision 3D solid state battery architectures on a Si wafer will be discussed. In a nut shell, this talk illustrates how careful design of thin materials architecture can facilitate desirable electrochemical activity, resolve or shed light on mechanistic limitations of electrochemical performance in solid electrolyte systems, and eventually try to convince audience that the thin film processes using primarily existing semiconductor fabrication facilities may

---

[1] **Falicov Student Award Finalist**

provide a new paradigm changing opportunity in solid state battery manufacturing technology.

4:20pm MS-WeA-7 Understanding the Electronic and Mechanical Properties of High Energy Density Anodes on 3D Structures, *Amy Prieto, J Ma, M Schulze,* Colorado State University **INVITED**
We are interested in mitigating mechanical failure in high energy density alloy anodes used for rechargeable Li-ion and Na-ion batteries by incorporating 3D architectures. We will present the use of direct electrodeposition of inter metallic alloys onto 3D current collectors, and their cycling in half cell and full cell batteries. A 3D architecture is critical for reasonable power densities in solid state batteries, and we will present our efforts moving toward a fully integrated solid state battery.

5:00pm MS-WeA-9 Enabling High Cycle Life Alkali Metal Anodes through Imposed Thermal Gradients, *R Atkinson III,* EXCET, Inc.*; R Carter, Corey Love,* U.S. Naval Research Laboratory **INVITED**
Solid state batteries promise a number of advantages over liquid electrolyte alternatives. The solid state battery will significantly improve safety by eliminating flammable electrolytes, enable high energy density by utilizing alkali metal anodes, and eliminate the weight and volume contribution from a host or alloying element at the anode. However, significant challenges remain in stabilizing metal anodes over many cycles and at high rates. Significant efforts in interfacial design and current collector structure have aimed to demonstrate the viability of the solid state battery, but these strategies often involve complex and costly manufacturing. Herein, we demonstrate the advantage of simply externally warming the anode (40 °C) and cooling the cathode (0°C) to stabilize charging or the plating of metal compared to isothermal controls (20 °C). This technique enables the high rate and long cycle-life desired for viability of the solid state configuration. Our results reveal remarkable stability over many hours (32% lower voltage hysteresis after 400 hr) of operation and fast charging with current densities up to 10 mA/cm^2 (competitive with 2C in conventional Li-ion). Further, a thermal gradient is easily implemented in the thermal management strategies commonly used in battery modules making the strategy commercially viable. Finally, it is likely that the thermal gradient will not only assist in realization of the metal anode but also the solid electrolyte. Solid electrolytes are challenged by low ionic conductivity which is often enhanced by heating the material up to ~80 °C. The operational benefit observed in the liquid cells and the directionality of ion movement provided suggest that application of an external thermal gradient will provide better performance than isothermal heating alone.

Carter, R.; Love, C. T., Modulation of Lithium Plating in Li-Ion Batteries with External Thermal Gradient. *ACS Applied Materials & Interfaces* **2018,***10* (31), 26328-26334.

Mistry, A.; Fear, C.; Carter, R.; Love, C. T.; Mukherjee, P. P., Electrolyte Confinement Alters Lithium Electrodeposition. *ACS Energy Letters* **2018**, 156-162.

Nanometer-scale Science and Technology Division
Room A222 - Session NS+2D+AS-WeA

Probing and Modifying Surface and Interfacial Chemistry at the Nanoscale

Moderators: Phillip First, Georgia Institute of Technology, Adina Luican-Mayer, University of Ottawa, Canada

2:20pm NS+2D+AS-WeA-1 Bitumen's Microstructures are Correlated with its Bulk Thermal and Rheological Properties, *X Yu,* Worcester Polytechnic Institute*; S Granados-Focil,* Clark University*; M Tao, Nancy Burnham,* Worcester Polytechnic Institute
Understanding of how the chemistry of asphalt binders (i.e., bitumens) affects their bulk properties is critical for development of structure-related mechanical models and performance-based specifications for asphalt binders, including mitigation of potholes and improved recycling of this non-renewable material. However, establishing the chemical-mechanical relationships that govern asphalt binders' properties remains a challenge due to binders' complex chemical makeup [1] and the intriguing dynamic molecular interactions among binders' various chemical constituents. [2] Here, we investigate the effect of chemical composition on binders'

microstructure and thermal and rheological behavior. Two virgin binders from different crude oil origins were chosen and a series of derivative binders was made by remixing different weight ratios of the asphaltenes and the maltenes obtained from the two source binders. Thermal and rheological properties of all binders were measured using modulated differential scanning calorimetry and dynamic shear rheometry, respectively. Binders' microscopic characteristics (e.g., nano- and micro-structures and their contrast in phase images) were evaluated using atomic force microscopy. In bitumens with more miscibility between the asphaltenes and maltenes, the samples appear to undergo a sol-gel transition as the asphaltene concentration increases above 25%. In less miscible bitumens, micro-scale phase segregation is readily apparent at the surface. Our results show that bitumens' characteristic microstructures, as a result of the complex molecular interactions among their various chemical components, are correlated with their bulk thermal and mechanical properties. Notably, the asphaltene/maltene ratio alone cannot predict a bitumen's bulk properties. Instead, a bitumen's distinctive microstructures and its colloidal miscibility index provide meaningful insights into the effect of chemical composition on glass transition, phase stability, and rheological properties of the bitumen, which may in turn help improve the sustainability and design of roads. [3]

1. X. Yu et al., Adv. Colloid Interface Sci. 218, 17-33 (2015).

2. X. Yu et al., Energy & Fuels 32, 67-80 (2018).

3. X. Yu et al., submitted

2:40pm NS+2D+AS-WeA-2 Energetics and Statistical Mechanical Analysis of Complexation on Metal Surfaces, *J Lee, J Evans, T Windus, P Thiel, Da-Jiang Liu,* Ames Laboratory and Iowa State University
Stabilities of metal-ligand complexes on surfaces are crucial for the process of self assembly of 2D structures. We provide a comprehensive theoretical assessment at the level of Density Functional Theory (DFT) of the stability of various coinage metal-sulfur complexes, M_mS_n, with M=Cu, Ag, and Au, both in the gas-phase and also for these complexes adsorbed on the (111) and (100) surfaces of the same coinage metal. An early influential theoretical study on S/Cu(111) proposed that the Cu-$_3$S$_3$ complex being the most stable copper containing species. Later combined low temperature STM and DFT studies suggest that a heart-shaped Cu$_2$S$_3$ and its concatenations being more stable. Larger and even more complex Ag-S complexes have being observed for S/Ag(111). No complexation have been observed for S/Cu(100) and S/Ag(100). On the other hand, a Au$_4$S$_5$ complex and its fragmentations have being observed for S/Au(100), but no complexation is observed for S/Au(111) at low S coverage. We select a set of nine types of complexes, chosen for their proposed existences, intrinsic stabilities, and affinities for adsorption on metal surfaces. For the adsorbed species, we calculate various aspects of their energetics including their formation energy from sulfur adsorbed on terraces and from metal atoms that are in thermal equilibrium with the substrate. From this perspective, our DFT analysis shows that Ag$_2$S$_3$, Ag$_3$S$_3$ and many larger complexes on Ag(111) are strongly stable, Cu-$_2$S$_3$ is stable and some larger complexes are marginally stable on Cu(111), but only Au-$_4$S$_4$ on Au(111) is stable. In contrast, no complex is stable on Cu(100) and Ag(100), but a group of complex is stable on Au(100), with Au$_4$S$_5$. DFT results are consistent with experiments with the apparent exception of Au(111). This comprehensive assessment of energetics provides key input for statistical mechanical analysis of S adlayer ordering in the absence of complexation, and of the kinetics of complex formation and associated enhanced mass transport and surface dynamics.

3:00pm NS+2D+AS-WeA-3 Adding the Chemical Dimension to Lithography at All Scales: Enabling Cellular Therapies & Other Adventures in Biology and Medicine, *Paul S. Weiss[1],* University of California, Los Angeles **INVITED**
By controlling the exposed chemical functionality of materials from the submolecular through the centimeter scales, we have enabled new capabilities in biology, medicine, and other areas. I will discuss current and upcoming advances and will pose the challenges that lie ahead in creating, developing, and applying new tools using these capabilities. These advances include using biomolecular recognition in sensor arrays to probe dynamic chemistry in the brain and microbiome systems. In other areas, we introduce biomolecular payloads into cells for gene editing at high throughput for off-the-shelf solutions targeting hemoglobinopathies, immune diseases, and cancers. These methods use specific chemical functionalization and control of surface contact and adhesion in microfluidic channels.

---

[1] **NSTD Recognition Award**

4:20pm NS+2D+AS-WeA-7 STM Directed Synthesis of Armchair Graphene Nanoribbons and Their Oxidation, *C Ma,* Oak Ridge National Laboratory*; Z Xiao,* North Carolina State University*; A Puretzky,* **Arthur Baddorf,** Oak Ridge National Laboratory*; W Lu,* North Carolina State University*; K Hong,* Oak Ridge National Laboratory*; J Bernholc,* North Carolina State University*; A Li,* Oak Ridge National Laboratory

Highly controlled synthesis of graphene nanoribbons (GNRs) can be performed on a surface by polymerization of a selected precursor. Typically, this polymerization involves surface-assisted cyclodehydrogenations during thermal activation on catalytic metal surfaces. We have shown that armchair edge GNRs can be synthesized with 7, 14, and 21 carbon atom widths by absorbing 10,10'-dibromo-9,9'-bianthryl (DBBA) precursor molecules on Au(111).[1] Synthesis follows a two-step process of which the first step is polymerization at 470 K. The second step, cyclodehydrogenation, can be promoted globally by annealing to 670 K, or locally following hole injection using a scanning tunneling microscope (STM) tip.[2] Wider 14 or 21-aGNRs were formed when two or three 7-wide GNRs were conjugated side-by-side via inter-ribbon cyclodehydrogenation at the edge sites. Scanning Tunneling Spectroscopy (STS) reveals an electronic band gap dependent on the ribbon width. Bandgaps of ~2.6, ~0.3, and ~0.7 eV are measured for 7, 14, and 21 GNRs respectively, consistent with expectations of simple models.

For practical applications, understanding the stability of GNRs to oxidation is important. We have examined the thermal stability of 7-aGNRs after exposure to air.[2] Combining STM, Raman spectroscopy, x-ray photoemission spectroscopy, and first-principles theory calculations, the armchair GNRs are found to oxidize first at the zigzag ends while the edges remain stable. Oxygen attaches to the zigzag ends at temperatures as low as 180°C. Armchair edges are stable up to 430°C and become oxidized only above 520°C. Two oxygen species are identified, one a hydroxyl (OH) and the second atomic oxygen bridging two carbons, both of which are common in oxidized graphitic lattices. The bandgap is significantly reduced from 2.6 eV to 2.3 eV in the vicinity of the hydroxyl and to 1.9 eV near bridging O. These results suggest that the oxidization will significantly affect the transport properties of GNRs and provide parameters useful for maintaining integrity of GNRs during processing for devices.

This research was conducted at the Center for Nanophase Materials Sciences, which is a DOE Office of Science User Facility.

1. C. Ma, et al., *Nano Letters* 17, 6241 (2017).

2. C. Ma, et al., *Nature Communications* 8, 14815 (2017).

3. C. Ma, et al., *Physical Review Materials* 2, 014006 (2018).

4:40pm NS+2D+AS-WeA-8 Carbon-based Two-dimensional Materials from Surface-catalyzed Reactions of Small Molecules, *M Wolf, C Gerber,* **Rebecca Quardokus,** University of Connecticut

Aryl halides undergo an Ullmann-like coupling reaction on surfaces to yield a carbon-based two-dimensional material. 1,2-dibromobenzene couples to Au(111) lifting the gold herringbone reconstruction. The reaction intermediates and coupled gold atoms are mobile on the surface at 4 K. The FCC and HCP sections of the underlying gold substrate shift to new positions. Annealing the dibromobenzene on Au(111) decouples the intermediates from the gold. The gold herringbone reconstruction returns and a covalently-bonded carbon-based network forms on the Au(111) surface.

5:00pm NS+2D+AS-WeA-9 Bottom-up Fabrication of 2D Molecular Networks via On-surface Reactions, *Sabine Maier,* University of Erlangen-Nürnberg, Germany   **INVITED**

On-surface synthesis has attracted significant attention in recent years due to its potential to fabricate novel low-dimensional nanomaterials with atomic precision. In order to understand and control the synthesis of high-quality low-dimensional nanostructures, many efforts have been made to steer the reaction pathway by the design of smart precursors and by applying templating effects from the substrate. One of the challenges is the fabrication of long-range ordered two-dimensional covalently-linked networks via on-surface reactions. In contrast to molecular self-assemblies that are constructed by non-covalent bonds, the irreversible nature of the covalent bonds limits the structural control, which results in small domains and defects.

In my presentation, I will focus on recent high-resolution scanning probe microscopy experiments in combination with density-functional theory about the bottom-up fabrication and electronic properties of atomically precise one- and two-dimensional molecular nanostructures on metals.[1-4] Thereby, the effect of the flexibility, the symmetry, and chirality of the precursor molecules on the structure formation of covalently-linked molecular structures will be discussed. In particular, I will outline how well-ordered nanoporous 1D and 2D covalent molecular structures can be fabricated by use of debromination coupling reactions. We demonstrate the narrowing of the electronic band gap by increasing the π-system in covalently-linked structures and also show delocalized electronic states in surface-supported organometallic networks. Finally, I will conclude with a comparison of the structure formation of molecular nanostructures on bulk insulators and metal surfaces.

[1] C. Steiner et al. *Nature Communications*, **2017**, 8, 14765.

[2] M. Ammon, T. Sander, S. Maier, *J. Am. Chem. Soc.*, **2017** 139 (37), 12976–12984.

[3] Z. Yang et al. *Nanoscale*, **2018**, 10, 3769-3776.

[4] X. Zhang et al., ACS Nano, **2019**, 13 (2), 1385–1393.

5:40pm NS+2D+AS-WeA-11 Determining the Jahn-Teller Stabilization Energy of Surface Vacancies on Si(111)-√3 x √3:B, *Daejin Eom,* Korea Research Institute of Standards and Science, Republic of Korea*; C Moon,* Korea Research Institute of Standards and Science*; J Koo,* Korea Research Institute of Standards and Science, Republic of Korea

The vacancy defect on the Si surface becomes increasingly important with the device scaling because it works as the charge trapping and scattering center with varying ionization states. Yet its characteristics have not been addressed as comprehensively as the bulk vacancy in Si. In fact, its behavior would be affected by the gap state evolution and the Fermi level pinning on the Si surface. On the other hand, the (111)-surfaces of Si come to have the √3 x √3 reconstruction instead of the 7 x 7 one when they are heavily B-doped [1,2]. This √3 x √3 surface does not evolve any energy state within the band gap, being contrary to the 7 x 7 one [2]. Also, the Fermi level is shifted to the valence band maximum on the √3 x √3 surface whereas it is pinned in the middle of the gap on the 7 x 7 surface [2]. Hence the vacancy defects on the two surfaces may have dissimilar characteristics from each other. Here, we generate the vacancy defects on the √3 x √3 surface via the atom manipulation technique and measure their structural and electronic properties by using the scanning tunneling microscopy and spectroscopy. We find that, unlike the 7 x 7 surface, the vacancy defects on the √3 x √3 surface are Jahn-Teller distorted in the ground state, but undergo the symmetry-restoring transition when gated by the external bias. We also determine the energy gain or stabilization energy of the Jahn-Teller transition quantitatively. These findings would extend our knowledge on the surface vacancies on Si and eventually contribute to the fabrication of better-performing nanometer-scale devices.

[1] I.-W. Lyo, E. Kaxiras, and Ph. Avouris, Phys. Rev. Lett. **63**, 1261 (1989).

[2] D. Eom, C.-Y. Moon, and J.-Y. Koo, Nano Lett. **15**, 398 (2015).

6:00pm NS+2D+AS-WeA-12 Influence of the Substrate on Self-Assembly: Terphenyl Monolayers investigated by NC-AFM and FM-KPFM, *Niklas Biere*[1], Experimental Biophysics & Applied Nanoscience, University of Bielefeld, Germany*; S Koch, P Stohmann, Y Yang, A Gölzhäuser,* Physics of Supramolecular Systems and Surfaces, University of Bielefeld, Germany*; D Anselmetti,* Experimental Biophysics & Applied Nanoscience, University of Bielefeld, Germany

Carbon Nano Membranes (CNM) are mechanical stable and homogeneous quasi-2D systems, which are formed by electron radiation induced, cross-linked self-assembled monolayers (SAM). Contrary to graphene, the CNM structural and functional properties can be tailored by the selection of precursors for the SAM formation [1]. CNMs show the capability to act as a molecular sieve to filter e.g. water molecules from impurities with extraordinary efficiency [2]. While this result promises remarkable applications, the actual process of CNM formation as well as their structure and the mechanism for water permeation is still in the focus of our investigations. Furthermore, the choice of substrate influences the self-assembly of our precursor molecules more than previously expected, even with isoelectronic surfaces like gold and silver. In this work, we will present data acquired by noncontact-AFM combined with FM-KPFM under ultra-high vacuum conditions to investigate and compare the morphology of in-situ prepared SAMs and CNMs of terphenylthiols on Au(111) and Ag(111).

[1] A. Turchanin, A. Gölzhäuser, Adv. Mater. 28 (2016) 6075-6103.

[2] Y. Yang et al., ACS Nano 12 (2018) 4695-4701.

---

[1] **NSTD Graduate Student Award Finalist**

Wednesday Afternoon, October 23, 2019

Plasma Science and Technology Division
Room B130 - Session PS-WeA

Commemorating the Career of John Coburn (ALL INVITED SESSION)

Moderators: David Graves, University of California, Berkeley, R. Mohan Sankaran, Case Western Reserve University

2:20pm PS-WeA-1 INVITED TALK: A Tribute to John W. Coburn, *David Graves*, University of California at Berkeley
Dr. John W. Coburn was one of the most influential low temperature plasma and surface scientists of the 20th century. He passed away in San Jose, California on November 28, 2018. In this talk, I will summarize some of John's many contributions and his enormous impact on both fundamental understanding and applications associated with plasma-surface interactions, thin film deposition and etching. John was born in Vancouver, British Columbia and received his BS degree in Engineering Physics and his PhD in Electrical Engineering from the University of Minnesota. After his postdoctoral work at Simon Fraser University, John joined IBM Research (Almaden, California) in 1978. He worked at IBM for 25 years, and retired in 1993. John joined the AVS while still in graduate school and he served as the National AVS Treasurer for many years and in addition served as President in 1988. In 1994, John began to collaborate with me at UC Berkeley as a Senior Research Associate in the department of Chemical Engineering. He had a tremendous impact on me and my group over a period of over 20 years. This impact was both scientific and personal. In this talk, I describe some of John's most important work in non-equilibrium plasma science and plasma-surface interactions, with a special emphasis on the work he did at UC Berkeley with me and my co-workers.

2:40pm PS-WeA-2 INVITED TALK: Interfacial Chemistry in Highly Reactive Systems, *Frances Houle*, Lawrence Berkeley National Laboratory
I joined IBM shortly after John Coburn and his close collaborator, Harold Winters, began publishing their seminal papers on use of XeF_2 to understand fundamental processes involved in plasma etching of silicon. They introduced me to the world of disordered surface reaction environments, and to the techniques they used to carry out careful experiments that shed light on how manufacturing processes work. I saw that it was possible to use well-chosen model systems to make sense of what controls interfacial chemistry in highly reactive, complex systems, and have been working on this type of problem ever since. In this talk I will describe how I have used model systems and multiscale computation to investigate the chemistry of oxidation of nanoscale organic aerosol by OH, relevant to atmospheric processes, and the photochemical generation of charge in porous photoanodes, relevant to solar energy conversion. In both cases, the interplay between transport and reactions is very sensitive to the composition of the chemical system, revealing opportunities for learning how to think more generally about rules governing interfacial reactivity.

3:00pm PS-WeA-3 INVITED TALK: Rare Gas Actinometry Turns Thirty Nine and is Still Finding Applications, *Vincent M. Donnelly*, University of Houston
Ever since the first paper on rare gas actinometry (as it would later be called), published by Coburn and Chen, this method has been widely used to measure relative and sometimes absolute number densities of atoms and small molecules. The problem originally chosen by Coburn and Chen of measuring F atom densities with Ar as the rare gas turns out to be one of the most reliable applications of this diagnostic method, for an important etchant species that is difficult to detect by other techniques. The precision of F-atom actinometry can be attributed, first, to the (apparent) match between the relative energy dependence for the electron-impact excitation cross section of F 703.7 nm emission, compared with that for Ar $2p_1$ emission at 750.4 nm. Second, the large degree of dissociation for even moderate density plasmas with typical feed gases (CF_4/O_2, SF_6, NF_3, etc.), produces high F concentrations, so dissociative excitation of F emission from other F-containing species is usually negligible. This talk will briefly review actinometry as a plasma diagnostic with an emphasis on the issues related to its quantitative application, including cases where it can be used reliably, and others that should be interpreted with caution. Recent experiments that highlight the power of this technique will be discussed, including several studies relying on other work by John Coburn.

3:20pm PS-WeA-4 INVITED TALK: A Leader In Etching (ALE): How John Coburn Paved the way for Atomic Layer Etching, *Jane P. Chang*, University of California, Los Angeles
This talk pays tributes to John Coburn's seminal contributions in the field of anisotropic etching by plasmas. John Coburn's early publication on "a system for determining the mass and energy of particles incident on a substrate in a planar diode sputtering system " set the tone for his many decades of research effort – deciphering the complex reaction mechanisms during plasma-surface interactions. Inspired by John Coburn's dedicated and outstanding contributions to the field of plasma processing, this talk highlights how the most recent development in anisotropic atomic layer etching can trace its root to John Coburn's work on delineating the reaction synergism between energetic ions and reactive neutrals. In John Coburn's words, "Today each wafer is exposed to a plasma etching environment between 10 and 20 times during its manufacture and without the highly anisotropic etching provided by this critical process, high density integrated circuit manufacturing would not be possible." This talk does not attempt to review all of John Coburn's work but focuses on the insight he provided to the research communitythat enabled the continued advances in the field where desirable etch specificity, selectivity, and anisotropy can be simultaneously achieved at the atomic scale.

4:20pm PS-WeA-7 INVITED TALK: Materials Processing Using Low Temperature Plasma Surface Interactions: Examples of the Influence of John Coburn, *Gottlieb S. Oehrlein*, University of Maryland, College Park
John Coburn's pioneering work on plasma-assisted etching reactions of materials has had a profound and lasting influence on our scientific understanding and approaches of studying mechanisms of low temperature plasma-assisted processing of materials. As a colleague at IBM Research I had the opportunity to learn from and interact with John, and his colleagues Harold Winters and Eric Kay, with whom he worked very closely for many years. In this talk I will discuss several topics that were important to John, and how they reflected in my own research and recent work performed by members of my group, including ion bombardment, ion-neutral synergies and etching directionality in pattern transfer, the fluorine/carbon ratio of fluorocarbon etching chemistries introduced by John and colleagues, and several related topics.

4:40pm PS-WeA-8 INVITED TALK: A Brief Overview on Molecular Dynamics Simulations of Plasma-surface Interaction in Reactive Ion Etching, *Emilie Despiau-Pujo*, LTM, Univ. Grenoble Alpes, CNRS, France
In the mid-70s, John Coburn and his colleague Harold Winter started to study plasma etching and reactive ion etching (RIE) processes which, at that time, were starting to be considered for pattern transfer and stripping processes in the semiconductor industry. Their research work focused on the physico-chemical mechanisms involved in this process, emphasizing surface science aspects, and continued for almost 20 years until they both retired from IBM in 1993. By designing insightful experiments, they highlighted in particular the role of energetic ion bombardment in RIE or the mechanisms responsible for a good Si/SiO_2 selectivity. 25 years later, reactive ion etching is a key process which has played a crucial role in the progress made in micro- and nano-electronics, a field which has affected every aspect of our modern lives.

Nowadays, advanced transistors feature ultrathin layered materials and must be etched with a nanometric precision and a nearly infinite selectivity to preserve the electronic properties of active layers. This challenge can no longer be addressed by conventional CW plasma processes, in which the ion-neutral synergy tends to create thick reactive layers which can compromise the etch precision. Alternative plasma technologies are thus needed and various approaches are investigated, to reduce the ion energy by decreasing the electron temperature (e.g. pulsed or low-Te plasmas), to avoid thick reactive layers using sequential and limited reaction steps (e.g. plasma-enhanced ALE), or to decouple the action of ions and radicals using sequential ion modification and chemical removal steps.

As shown by John Coburn during his entire career, the development of advanced etch processes requires a fundamental understanding of the surface reaction mechanisms involved in plasma-material interaction. Coupled with plasma diagnostics and surface characterization tools, Molecular Dynamics (MD) simulations can provide information about the reactions processes involved at the atomic scale and help to understand the phenomena governing the etch process. Since the pioneering work of Harrison et al. in the late 60s [1], atomistic simulations have been routinely used to study RIE and were shown to be a powerful tool to understand how the flux and energy of plasma species affect the structural and chemical modification of substrates. This talk will provide a brief overview of the

basics of molecular dynamics for RIE simulations (principles, accessible time and length scales, suitable force fields, etc.) as well as a review of various works performed on this topic from the 70s until very recently.

[1] D. E. Harrison et al, J. Appl. Phys. 39, 3742 (1968)

5:00pm PS-WeA-9 INVITED TALK: Plasma ALD – A Discussion of Mechanisms, *K Arts, V Vandalon,* Eindhoven University of Technology, The Netherlands, Netherlands; *H Knoops,* Eindhoven University of Technology, The Netherlands; *Erwin Kessels,* Eindhoven University of Technology, The Netherlands, Netherlands

The profound contributions of John Coburn and Harold Winters to the field of plasma etching have inspired us at the Eindhoven University of Technology to study the mechanisms of plasma deposition [1]. In the last two decades our interest has mainly focused on the surface reactions during atomic layer deposition (ALD), especially on those during plasma-enhanced ALD (also referred to as plasma ALD or radical-enhanced ALD). In his late work, John Coburn has also worked on radical-enhanced ALD, more particularly on radical-enhanced ALD of TiN as investigated by fundamental beam studies [2]. As in his work on plasma etching, a lot of attention was given to the determination of sticking and reaction probabilities as quantitative knowledge of these parameters is key to gain a detailed understanding of the ruling reaction mechanisms. Moreover, quantitative information is needed for modelling purposes. In this contribution, some of our recent work on the determination of sticking and recombination probabilities during (plasma) ALD will be presented. Data obtained from broadband sum-frequency generation [3] and thin film conformality studies [4] will be reported and mechanisms underlying the ALD processes will be discussed.

[1] https://www.atomiclimits.com/2017/11/25/surface-science-aspects-of-plasma-ald-reactions-extending-the-legacy-of-harold-winters/

[2] F. Greer, D. Fraser, J.W. Coburn, and D.B. Graves, J. Vac. Sci. Technol. A 21, 96 (2003)

[3] V. Vandalon and W. M. M. Kessels, J. Vac. Sci. Technol. A 35, 05C313 (2017).

[4] K. Arts, V. Vandalon, R.L. Puurunen, M. Utriainen, F. Gao, W.M.M. Kessels, and H.C.M. Knoops, J. Vac. Sci. Technol. A 37, 030908 (2019)

5:20pm PS-WeA-10 INVITED TALK: RF Plasmas for Material Etching, Deposition, and Surface Modification, *Dennis Hess,* Georgia Institute of Technology

For the past 40 years, rf plasmas have been used extensively for thin film etching and deposition in electronic and photonic device fabrication. However, unique surface properties on materials such as paper and other porous substrates can be generated using these low temperature reactive atmospheres. Examples of surface modification for applications in paper-based medical tests strips and microfluidic device structures through the use of fluorinated and non-fluorinated plasma treatments will be presented.

New Challenges to Reproducible Data and Analysis Focus Topic
Room A124-125 - Session RA+AS+BI-WeA

Addressing Reproducibility Challenges using Multi-Technique Approaches

Moderators: Tony Ohlhausen, Sandia National Laboratory, Vincent Smentkowski, GE Global Research Center

2:20pm RA+AS+BI-WeA-1 Responding to New and Old Challenges to Data, Analysis and Scientific Study Reproducibility, *Donald Baer,* Pacific Northwest National Laboratory; *I Gilmore,* National Physical Laboratory, UK

An increasing number of studies, surveys and editorials highlight experimental and computational reproducibility and replication issues that frequently appear in most areas of modern science. In a 2018 AVS conducted survey, 66% of those responding identified reproducibility as a significant issue. There are multiple and complex causes of what some have called a "reproducibility crisis," which can impact materials, interface/(bio)interphase, vacuum and others sciences of importance to AVS members. Reproducibility challenges are not new, but now appear in both old and new forms requiring innovative solutions. Drivers influencing reproducibility problems include the increasingly multi-discipline, multi-method nature of much advanced science, increased complexity of the problems and systems being addressed, and the large amounts and multiple types of experimental and computational data being collected and analyzed in many studies. Such issues challenge experimental teams and the review process. Systematic and sustained efforts are needed to address the causes of reproducibility problems that can hinder the rate of scientific progress and lower public and political regard for science. The Focus topic New Challenges to Reproducible Data and Analysis aims to raise awareness of the challenges, examine the causes, impacts of reproducibility problems and explore approaches that can help address both the newer and older generation of reproducibility challenges. Some problems and solutions are easy to identify, even if not readily implemented. Other drivers and causes are less obvious and therefore harder to address. This talk will introduce the focus topic sessions, review key literature on the topic of reproducibility and summarize how the presentations fit together as a way to address reproducibility challenges.

2:40pm RA+AS+BI-WeA-2 Achieving Reproducible Data: Examples from Surface Analysis in Semiconductor Technology, *Thierry Conard, P van der Heide, A Vanleenhove, C Zborowski, W Vandervorst,* IMEC, Belgium

Repeatability and reproducibility in surface analysis in the semiconductor industry are key to for supporting efficient process development as well as High Volume Manufacturing (HVM). As two examples, long term repeatability is critically important when comparing to historical data, while reproducibility is required to support technology transfers when HVM of specific devices is to be carried out at multiple sites. This however introduced a number of unique challenges for running a characterization facility.

In this presentation we will present a number of examples that can result in reproducibility issues. Particular focus will be in the areas of X-ray Photoelectron Spectroscopy (XPS) Secondary Ion Mass Spectrometry (SIMS). The first and foremost causes of repeatability and reproducibility arise from instrumental variation. A second important source arises from samples variability. We will show that assessing long-term instrumental stability is potentially hindered by long term variation of samples characteristics. We will also show that an understanding of the characterization techniques is paramount to understanding such issues.

Next to the "pure" technical causes of repeatability and reproducibility, is the human factor. This involve for instance decision making in data treatment during for example, fitting procedures, statistical treatments, etc. This will be illustrated using practical examples. And with present day characterization depending more heavily on computational support/commercial software, potential detriments to characterization repeatability will again be made evident. Finally, we will show through round-robin results, that combining all the above factors, widely varying results can be obtained on the same samples.

3:00pm RA+AS+BI-WeA-3 New Challenges in Analytical Reproducibility Illustrated with Old and New Case Studies, *Thomas Beebe Jr,* University of Delaware **INVITED**

To address the subject of this session's topic, "New Challenges to Reproducible Data and Analysis," I have chosen to select a few case studies from my research group's work over the past 30 years. My examples will therefore be drawn from the methods and techniques that I have employed: XPS, TOF-SIMS, AFM, STM, and from the surface-related fields in which we have worked: biomolecules on surfaces, molecular self-assembly, biomaterials, and perhaps some others. It has always been my goal and approach to employ careful controls, scientific statistics, and data extraction to the richest extent possible.

4:20pm RA+AS+BI-WeA-7 Challenges and Approaches to Addressing Reproducibility in Biointerface Science and Engineering, *Sally McArthur,* Swinburne University of Technology and CSIRO. Australia, Australia **INVITED**

Our publications should serve as guides to repeat our experiments/analyses and reproduce the results; however, quite often we may find ourselves not able to do so. Over the past few years, there have been many papers and editorials that have shown that issues associated with Repeatability, Reproducibility, and Replicability impact almost all areas of science, and in an AVS-conducted survey, 65% of those responding indicated that they have seen or experienced significant reproducibility issues when they have sought to recreate experiments from the literature. It is clear that the increasing demands of complex research requiring use of multiple experimental and computational research methods is a central theme. The challenge in the Biointerface Science community is compounded by the inherent variability of biology. Working at the interface between the physical and life sciences, it is often difficult for us to have in-depth knowledge of the idiosyncrasies of the many techniques we

use and we need to be aware of for our data interpretation. This talk will discuss approaches we are taking to tackle this issue within the Biointerface Science Community and the journal Biointerphases. We will look at how we can champion best practices, sharing our knowledge across our community, and seek to support researchers who are new to the field or want to explore new techniques to avoid the pitfalls and better understand both the opportunities and limitations of the techniques, methods, and approaches used in our multidisciplinary community.

Sally L McArthur, Editor Biointerphases

5:00pm RA+AS+BI-WeA-9 Complementary Measurements of Colloidal Nanoparticles and their Coatings by In-situ and Vacuum-based Methods, *Caterina Minelli,* National Physical Laboratory, UK INVITED
Engineered nanoparticles add high value to commercial products and have the potential to improve our quality of lives and boost prosperity. For example, they provide radical new approaches to cancer drug delivery, biosensing, medical imaging and catalysis. However, the effective implementation of these materials relies on the ability to measure and control their properties, such as their surface chemical identity, size and concentration. There are significant challenges in the analysis of nanomaterials due to, among other factors, the interdisciplinary nature of the field and the lack of adequate reference materials to calibrate analytical tools. The use of complementary tools provides opportunities for (1) deepening the quantitative understanding of these systems and, importantly, (2) a route to method validation. I will provide examples from our work on both these cases.

(1) We use a combination of methods to analyse nanoparticles which are employed in liquid media (*in-situ*) using techniques such as analytical centrifugation and dynamic light scattering and *ex-situ* with X-ray photoelectron spectroscopy (XPS). Sound sample preparation protocols are critical for meaningful and comparable measurements. This is especially important when using complementary methods for the analysis of the same samples. I will discuss our experience in the analysis of protein coated gold nanoparticles and polymeric core/shell nanoparticles and show how multimodal analysis is critical to the full understanding of the system.

(2) The lack of certified reference materials for nanoparticle number concentration has hindered the validation of laboratory methods, which resulted in a general distrust in commercially available instrumentation. We have led a collaborative effort to develop accurate methods based on small angle X-ray scattering (SAXS) and single particle inductively coupled plasma mass spectrometry (spICPMS) for the measurement of colloidal number concentration. We have then used these methods to assess and validate a range of laboratory methods. I will discuss the result of this work for both ideal and agglomerated nanoparticles and present the outcomes of a large VAMAS interlaboratory study which assessed four methods for the measurement of colloidal concentration.

Finally, I will look at unmet challenges in the characterisation of nanoparticles and discuss the benefits of a multimodal approach to them.

5:40pm RA+AS+BI-WeA-11 Multiple Technique Analysis of Perovskite Materials used in Battery and Fuel Cell Components, *Robin Simpson, P Mack, T Nunney,* Thermo Fisher Scientific, UK
Due to the worlds ever increasing energy needs, renewable sources, higher efficiency and energy storage have become important research areas. Therefore, full analysis of the materials used in such applications can add to our understanding of these emerging technologies. In many cases this will mean using several techniques on a single sample.

The chemical composition of the materials found in batteries or fuel cells play a huge part in the desired properties. An example of this is in the inclusion of Sr^{2+} in the A sites of lanthanum manganite. This increases the electronic conductivity of cathode material via the addition of electronic holes to the perovskite structure. XPS allows us to quantify the chemistry of the material and use that data to further improve its properties.

Chemical analysis of the surface of the material by XPS also allows us to identify diffusion or segregation effects that can occur once a battery material has been cycled. Once a build-up of surface material on an electrode becomes too thick ions cannot pass between them, preventing charging of a cell. Using XPS with other techniques like ISS allows us to characterise the surface material (~ top 10 nm) and the surface monolayer.

Here we discuss a LaSrFeCoO perovskite sample typically found in fuel cell and battery cell electrode materials. XPS is used to quantify the composition of the material and identify the La chemical bonding state to find the sample contains La_2O_3 bonding. ISS is also utilised to show no significant Fe and Co at the top surface of the sample. Comparing this to

the XPS data taken from the top 10 nm of the shows signs of Fe and Co depletion at the surface.

The perovskite materials are also found in solar cell components. These materials are often used due to their high efficiencies but also because the material band gap is tuneable therefore allowing us to optimise the material composition. Using a technique like REELS combined with XPS can enable us to measure the band gap of the material to reveal the efficiency as well as identify the composition. In this case the band gap of the sample was calculated at 6.3 eV using REELS.

We will also be discussing the use of coincident XPS/Raman to investigate the bulk and surface characteristics of the LaSrFeCoO sample without exposing it to atmosphere between analysis.

6:00pm RA+AS+BI-WeA-12 Mapping Local Physical Properties by Combining ToF-SIMS Analysis with Advanced Scanning Probe Microscopy, *Maiglid Andreina Moreno Villavicencio, N Chevalier, J Barnes,* CEA-LETI, France*; P Kermagoret, F Lorut,* ST Microelectronics, France*; B Gautier,* Université de Lyon, France
The continuous miniaturization and complexity of micro-devices have pushed existing characterization techniques to their limits. The correlation of techniques has emerged to overcome this issue and provide precise and accurate characterization. We have focused our research on combining and studying the applications of two specific techniques: time-of-flight secondary ion mass spectrometry (ToF-SIMS) and atomic force microscopy (AFM). The ToF-SIMS is a high-performance technique to chemically analyze a sample in 3-dimensions with a lateral resolution of 100 nm. On the other hand, the AFM is a high-resolution technique to obtain maps of the topography and local physical properties with a lateral resolution of 10 nm.

A ToF-SIMS / AFM methodology that combine the topographical information with the chemical composition has been established [1]. It was used to achieve a topography-corrected 3D ToF-SIMS data set and maps of local sputter rate where the effect of roughness and vertical interfaces are seen. However, the correlation of these characterization techniques is not limited to these applications. Indeed, by using advanced operation modes of the AFM, maps of diverse physical properties of the sample can be obtained at the same time as the topography.

We have explored the combination of ToF-SIMS analysis with three AFM advanced modes: piezoresponse force microcopy (PFM), scanning capacitance microscopy (SCM) and scanning spreading resistance microscopy (SSRM). These operation modes respectively allow to map ferroelectric domains, to locally measure capacitance variations and to image the sample surface resistivity.

The combined ToF-SIMS / AFM methodology was applied ex-situ per individual AFM mode on diverse samples for applications focused on micro-electronics. We will present here some promising results highlighting the strength and the perspectives of the expansion of this combination to other applications.

[1] M.A. Moreno et al, J. Vac. Sci. Technol. B 36 (2018) 03F122.

Advanced Surface Engineering Division
Room A215 - Session SE+AS+TF-WeA

Nanostructured Thin Films and Coatings

Moderators: Mehran Golizadeh, Montanuniversität Leoben, Austria, Suneel Kodambaka, University of California Los Angeles

2:20pm SE+AS+TF-WeA-1 Structural and Optical Properties of Pulsed-Laser Deposited β-Ga_2O_3 Thin Films, *Mallesham Bandi, V Zade, R Chintalapalle,* University of Texas at El Paso
In the course of demand for wide band gap semiconductors in modern electronic devices, β-Ga_2O_3 is extensively studied for the last two decades due to its wide range of applications such as field effect devices, switching memories, high temperature gas sensors, photocatalysts, deep-UV photodetector and transparent conducting electrode etc. However, fabricating device quality thin films and understanding the optical properties is an active timely research to exploit β-Ga_2O_3 into wide range of optoelectronic device applications. We report on the effect of deposition parameters on the structure and optical properties of β-Ga_2O_3 fabricated by Pulsed Laser Ablation onto a wide range of substrate materials. Polycrystalline thin films were fabricated on silicon and sapphire substrates with varying substrate temperatures and oxygen partial pressures, which resulted in various morphologies. To study the effect of morphology on

optical properties polycrystalline thin films were analyzed using spectroscopic ellipsometry. Moreover, epitaxial thin films of β-Ga_2O_3 were fabricated on C-plane sapphire and MgO (100) oriented substrates. A more detailed account of structure, growth behavior and optical properties of β-Ga_2O_3 will be presented and discussed.

2:40pm SE+AS+TF-WeA-2 Structural, Electrical, and Optical Properties of Mo-Ga Alloy Thin Films, *Nivedita Lalitha Raveendran, R Chintalapalle,* University of Texas at El Paso

Materials with thermal stability and can establish a stable contact for component layers are highly desirable for the design and development of advanced high power electronic device technologies. In this context, the present study investigates the effect of growth temperature on the structural, morphological, optical and electrical properties of the thin films of rarely investigated Mo-Ga alloy system. The objective is to understand the growth behavior, structure, electronic properties and thermal stability of Mo-Ga thin films for application in Ga_2O_3 based devices. In the present work, Mo-Ga thin films of ~350 nm thickness were fabricated on Si (100) substrates by sputter-deposition. The deposition temperature was varied in the range of 25-700°C. X-ray diffraction analysis of the deposited samples indicate the realization of nanocrystalline films at 500°C, and beyond 500°C deterioration in crystallinity was noticed. A shift in Bragg's position towards higher angle was evident with increase in substrate temperature, which could be attributed to substrate temperature induced residual stresses. Moreover, formation of non-stoichiometric thin films was observed at higher deposition temperature (>500°C). The optical properties of the deposited thin films were obtained by spectroscopic ellipsometry and a detailed analysis of the electrical properties of the thin films were also carried out. The results will be presented and discussed to establish the structure-composition-property correlation.

3:00pm SE+AS+TF-WeA-3 Metallic Glass: From Coating to First-Ever Nanotube Arrays, *Jinn P. Chu,* National Taiwan University of Science and Technology, Taiwan, Republic of China

Thin film metallic glass (TFMG) is a new class of multi-component metallic thin film with unique characteristics, including high strength, high ductility, smooth surface, absence of grain boundaries, low coefficient of friction, and corrosion resistance, though their bulk forms are already well-known for properties because of their amorphous structure. Thin films prepared by physical vapor-to-solid deposition are expected to be further from equilibrium than those prepared by liquid-to-solid melting or casting processes. This is expected to further improve the glass forming ability and widen the composition range for amorphization. In the first part of my talk, I will present some important TFMG properties and applications we have discovered in recent years. Then, the metallic glass nanotubes (MGNTs) on Si fabricated by a simple lithography and sputter deposition process for very large-scale integration is introduced. This first-ever metallic nanotube array is awarded by *American Chemical Society* (ACS) at nano tech Japan 2018 in Tokyo. Like biological nanostructured surfaces, MGNTs show some surprising water repelling and attracting properties. Nanotubes are 500-750 nm tall and 500-750 nm in diameter [1]. The MGNT surface becomes hydrophobic, repelling water. By heating/cooling the array, the surface hydrophobicity is changed. Two examples will be presented in this talk based on modifications of this scheme. First, after modification of biotin, the array acts as a waveguiding layer for an optical sensor. The MGNT sensor waveguide could readily detect the streptavidin by monitoring the shift. The detection limit of the arrays for streptavidin is estimated to be 25 nM, with a detection time of 10 min. Thus, the arrays may be used as a versatile platform for high-sensitive label-free optical biosensing [2]. Second, the array is prepared on a heating device and, with an applied electric voltage to the heating device underneath, so that the arrays are functioned as biomimetic artificial suckers for thermally adhesion response [3].

References

[1] J. K. Chen, W. T. Chen, C. C. Cheng, C. C. Yu and J. P. Chu, Metallic glass nanotube arrays: preparation and surface characterizations, Materials Today, 21 (2018), 178-185.

[2] W. T. Chen, S. S. Li, J. P. Chu, K. C. Feng, J. K. Chen, Fabrication of ordered metallic glass nanotube arrays for label-free biosensing with diffractive reflectance, Biosensors and Bioelectronics, 102 (2018), 129-135.

[3] W. T. Chen, K. Manivannan, C. C. Yu, J. P. Chu and J. K. Chen, Fabrication of an artificial nanosucker device with a large area nanotube array of metallic glass, Nanoscale, 10 (2018) 1366-1375.

3:20pm SE+AS+TF-WeA-4 Tin Oxide Nanoaggregate Fragmentation and Restructuring during Supersonic Impaction based Thin Film Deposition Processes, *Souvik Ghosh, X Chen, C Li, B Olson, C Hogan,* University of Minnesota, Minneapolis

Aerosol deposition (AD) is a versatile technique for printing thin films. During AD, gas-suspended particles are impacted inertially on a target surface at high velocities. Subsonic impaction processes often lead to highly porous, weakly bound depositions. High-speed supersonic deposition, however, can lead to denser, mechanically robust coatings of metals & metal oxides. Supersonic deposition is hence a potential low temperature route to the additive manufacturing of thin films (<1 μm to >10 μm) of a variety of materials.

However, the mechanism of film densification & consolidation remains poorly understood, particularly because AD can function with spherical or fractal-like agglomerated particles, from both dry powder feeds & aerosol synthesis processes. In an effort to better understand AD, we examined the mechanism of thin film formation via supersonic impaction of SnO_2 nanoaggregates on alumina, where we observed the formation of mechanically robust SnO_2 thin films. SnO_2 nanoaggregates were synthesized via flame spray pyrolysis (FSP) of Tin 2-Ethylhexanoate. These nanoaggregates characterized via differential mobility analysis shows a broad size distribution in the 40 nm -300 nm mobility diameter range. X-ray diffraction analysis of as-collected powders confirmed the formation of nano-crystalline SnO_2. To understand morphological changes to aggregates during high speed deposition, a differential mobility analyzer was used prior to deposition to select aggregates within a prescribed mobility diameter. The aggregates were then deposited electrostatically at low velocity (at atmospheric pressure) & supersonic speeds after passing through a 200 μm throat width, slit-type, conically contoured converging-diverging nozzle. With low speed deposition, we observed highly branched, chain like aggregates; while after supersonic deposition, we observed denser aggregates with significantly lower number of particles. Images hence suggest that the aggregates fragment & restructure during supersonic impaction.

Fragmentation & restructuring was quantified by image analysis of TEM images to determine their projected radii of gyration, perimeter, end-to-end distance, & projected area. These four parameters were then compared to those from in-silico projections of quasifractal aggregates, enabling extrapolation of the 3D architectures of deposited particles. Plots of the number of primary nanoparticles in aggregates as functions of their inferred radii of gyration confirmed that supersonic deposition leads to both (1) fewer primary particles per aggregate (fragmentation) & (2) for a given number of primary particles, smaller radii of gyration (restructuring).

4:20pm SE+AS+TF-WeA-7 From Gas-ion to Metal-ion-controlled Irradiation: A Paradigm Shift in the Thin Film Growth by Magnetron Sputtering, *Grzegorz Greczynski,* Linköping University, Sweden; *I Petrov, J Greene,* University of Illinois at Urbana-Champaign; *L Hultman,* Linköping University, Sweden **INVITED**

Ion irradiation is a key tool for controlling the nanostructure, phase content, and physical properties of refractory ceramic thin films grown at low temperatures (T_s) by magnetron sputtering. However, in contrast to gas-ion bombardment, the effects of metal-ion irradiation on properties of these films have not been extensively studied due to (i) low metal-ion concentrations during standard dc magnetron sputtering (DCMS), and (ii) difficulties in separating metal-ion from gas-ion fluxes. These issues were recently resolved with our development of high–power pulsed magnetron sputtering (HiPIMS), in which pulsed substrate bias is applied in synchronous to the metal-ion-rich portion of each pulse.[1] Careful choice of sputtering conditions allows exploitation of gas rarefaction effects such that the charge state, energy, and momentum of metal ions incident at the growing film surface can be tuned.

The results of time-resolved mass spectrometry analyses performed at the substrate position during HiPIMS and HiPIMS/DCMS co-sputtering of transition-metal (TM) targets in Ar and Ar/N atmospheres are reviewed. Knowledge of the temporal evolution of metal- and gas-ion fluxes is essential for precise control of the incident metal-ion energy and minimizing the role of gas-ion irradiation. Also, covered are the growth of TM nitride and boride alloys by metal-ion synchronized HiPIMS. In contrast to gas-ions, a fraction of which are trapped at interstitial sites, metal-ions are primarily incorporated at lattice sites resulting in much lower compressive stresses. In addition, the closer mass match with the film-forming species results in more efficient momentum transfer and provides the recoil density and energy necessary to eliminate film porosity at low T_s.

Several novel film-growth pathways are described: (i) nanostructured N-doped bcc-CrN$_{0.05}$ films combining properties of both metals and ceramics, (ii) fully-dense, hard, and stress-free Ti$_{0.39}$Al$_{0.61}$N, (iii) single-phase cubic Ti$_{1-x}$Si$_x$N with the highest reported SiN concentrations, (iv) unprecedented AlN supersaturation in single-phase NaCl-structure V$_{1-x}$Al$_x$N, (v) a dramatic increase in the hardness, due to selective heavy-metal-ion bombardment during growth, of dense Ti$_{0.92}$Ta$_{0.08}$N and Ti$_{0.41}$Al$_{0.51}$Ta$_{0.08}$N films deposited with no external heating, and (vi) simultaneous increase in both hardness and toughness of Zr$_{1-x}$Ta$_x$B$_y$ layers deposited with synchronized Ta$^+$ irradiation.

Finally, Ti$_{1-x}$Ta$_x$N alloys grown with no external heating are shown to produce high-quality Cu diffusion barriers and provide excellent corrosion protection for stainless-steel substrates.

[1] G. Greczynski, J. Lu, J. Jensen, I. Petrov, J.E. Greene, S. Bolz, W. Kölker, Ch. Schiffers, O. Lemmer and L. Hultman, J. Vac. Sci. Technol. A 30 (2012) 061504

5:00pm SE+AS+TF-WeA-9 Atomic Layer Deposition of Silver Thin Film on Polydimethylsiloxane (PDMS), *Sarah Hashemi Astaneh*, *C Sukotjo, C Takoudis,* University of Illinois at Chicago
Two types of samples were prepared in this work:

1- Silver coated PDMS

2- Silver coated PDMS with interlayer of TiO$_2$

For type 1 samples: Silver deposition was done in the costume-built ALD system. (Ag(fod) (Pet$_3$)) was used as a silver precursor and dimethyl amineborane ((BH$_3$ (NHMe$_2$)) was used as a reducing agent. Silver bubbler and dimethyl amineborane bubbler temperatures were kept at 96 °C and 50 °C, respectively. The reactor pressure and temperature was kept at 500 mtorr and 115 ˚C during deposition, respectively.

For type 2 samples: prior to silver coating, deposition of TiO$_2$ on PDMS was done in a commercial ALD system (Kurt J. Lesker 150 LE). Tetrakis (dimethylamido) titanium (IV) (TDMAT™) was used as the metal oxide precursor and maintained at 70 °C in the bubbler during all depositions. Ultra high purity N$_2$ was used as a carrier gas as well as purging gas. O$_3$ was used as an oxidizer for this ALD reaction and it was prepared using a UV-ozone generator placed immediately upstream of the deposition chamber to reduce ozone decomposition in delivery line as described in our previous studies. The reactor pressure and temperature was kept at ~1000 mtorr and 120 ˚C during TiO$_2$ deposition. This process leads to ~9 nm of TiO$_2$ interlayer on PDMS.

Right after this step, TiO$_2$ coated PDMS samples were transferred to the custom-built ALD system and silver deposition was carried on in the costume-built ALD system similar to type 1 samples.

In each of the above runs, simultaneously; same thin film was deposited on p-type Si (100) silicon wafer (University wafer Inc, USA) and used as a reference substrate to determine deposited film thickness.

The growth and composition of the silver on top of PDMS samples were analyzed with X-ray photoelectron spectroscopy (XPS) using Kratos AXIS-165 equipped with monochromatic Al Kα X-ray source operating at 15kV and 10 mA. As can be seen in figure 1, Ag 3p, Ag 3d peaks appeared clearly on Si, TiO$_2$ coated Si and TiO$_2$ coated PDMS substrates.

5:20pm SE+AS+TF-WeA-10 Fabrication of 2D Photonic Crystals using Block Copolymer Lithography on Flexible Substrates and Fibers for Wearable Technology, *Wade Ingram*, *R Spontak, J Jur,* North Carolina State University
Block copolymer lithography is a method of transferring a self-assembled pattern from the block copolymer to the substrate using vapor phase infiltration of metal or metal-organic precursors into select polymer domains. The process is able achieve sub-10 nm resolution and can be used for electronic or photonic device fabrication. In our research, we seek to use block copolymer lithography to template polymer films and textile fibers for applications in wearable electronics and advanced light absorption in garments.

Deriving inspiration from nature, 2D photonic crystals are fabricated using polystyrene-block-polymethylmethacrylate (PS-b-PMMA) copolymers. Through thermal and solvent vapor annealing, the block copolymer self-assembles into uniform domains with long-range order across the substrate. Subsequent exposure to common gas precursors like trimethylaluminum will result in a hybrid material forming from the exposed carbonyl functional groups in the PMMA domain. Etching steps in O$_2$ plasma or selective solvents results in a patterned nanostructure of the metal or metal-organic material deposited on the substrate. These structures are imaged using scanning electron microscopy before and after etching, as well as with atomic force microscopy in tapping mode to understand how robust they are. Further characterization using infrared and ultraviolet-visible spectroscopy is performed to generate plots showing how these unique nanostructures interact with light from UV through IR wavelengths. This work aims to understand how block copolymer lithography on polymeric and flexible substrates can eventually be applied to polymer fibers for functional textiles.

5:40pm SE+AS+TF-WeA-11 Use of an Einzel Lens to Enhance Electrohydrodynamic Printing Technology, *Matthew Strohmayer[1]*, *A Dhall, P Ramesh, N Tokranova, C Ventrice, Jr.,* SUNY Polytechnic Institute
Additive manufacturing (AM) shows great promise for both research and industrial applications. The main advantages of AM include limited waste and the ability to build complicated structures. The most common techniques for AM are fused deposition manufacturing, digital light printing, and ink jetting. All of these techniques suffer from resolution and material limitations. Recently, a cost-effective, versatile method of high-resolution printing called electrohydrodynamic (EHD) printing has been introduced. This method allows for spatial resolution in the hundreds of nanometers. This process works similarly to a typical ink jetting system, except instead of the ink/polymer being pushed out of a tip, it is pulled out by an applied electric field. This allows for the resultant droplet to be smaller than the needle diameter. Electrostatic repulsion of the charged droplets limits the ultimate resolution of this technique. To overcome this resolution limitation, we have incorporated an Einzel lens into the system to focus the droplets. This helps the droplets overcome the repulsive Coulomb interaction, leading to better spatial resolution. To validate this approach, simulations were performed to test for different parameters, including droplet size changes and lens optimization. This was then used to build a real system.

Surface Science Division
Room A220-221 - Session SS+AS+HC+OX-WeA

Reactions at Alloy Surfaces and Single Atom Catalysis
Moderators: Erin Iski, University of Tulsa, Bruce E. Koel, Princeton University

2:20pm SS+AS+HC+OX-WeA-1 Correlating Structure and Function for Nanoparticle Catalysts, *Graeme Henkelman,* University of Texas at Austin
INVITED
Metal nanoparticles of only 100-200 atoms are synthesized using a dendrimer encapsulation technique to facilitate a direct comparison with density functional theory (DFT) calculations in terms of both structure and catalytic function. Structural characterization is done using electron microscopy, x-ray scattering, and electrochemical methods. Combining these tools with DFT calculations is found to improve the quality of the structural models. DFT is also successfully used to predict trends between structure and composition of the nanoparticles and their catalytic function for reactions including the reduction of oxygen and selective hydrogenation. This investigation demonstrates some remarkable properties of the nanoparticles, including facile structural rearrangements and nanoscale tuning parameters which can be used to optimize catalytic rates. In this presentation I will focus on a pair of random alloy bimetallic nanoparticles which have complete different trends in hydrogenation activity as a function of composition. Pd/Au is found to be tunable as a function of composition whereas Pt/Au is not. The reason behind these different behaviors will be discussed.

3:00pm SS+AS+HC+OX-WeA-3 Surface Reactivity of PtAg and PdAg: From Single-Atom Alloys to Supported Nanoparticles, *Dipna Patel[2][3]*, Tufts University; *C O'Connor, R Madix, C Friend,* Harvard University; *E Sykes,* Tufts University
Catalytic hydrogenation reactions are important in many industrial applications. While Pt and Pd are catalytically active towards hydrogenation, they are often costly, and can suffer from poisoning by CO and coke. Previously, Ag based catalysts have been modified by alloying Pt or Pd for applications in highly selective heterogeneous catalysis. This has shown promise for catalyst design since Ag is cheaper and more resilient to poisoning. It is well known that ensemble size can dramatically change the

[1] **ASSD Student Award Finalist**
[2] **Morton S. Traum Award Finalist**
[3] **National Student Award Finalist**

catalytic pathway, however the atomic-scale structure of PtAg and PdAg alloys and their relation to catalytic activity is still unknown. Using scanning tunneling microscopy (STM) and STM-based spectroscopies, we characterized the surface structure and local geometry of Pt deposited on Ag(111) as a function of alloying temperature. At low temperatures, intermixing of PtAg is driven by a negative mixing enthalpy, resulting in different metastable states such as isolated Pt atoms in, and islands on, Ag terraces, as well as Pt rich brims located along Ag step edges. Increasing the alloying temperature results in an increased concentration of Pt atoms along Ag steps edges as well as direct exchange of Pt atoms into Ag terraces. At higher temperatures, there is sufficient thermal energy for Pt atoms to fully disperse in the Ag(111) surface layer as isolated atoms, forming single-atom alloys. STM characterization of the surface structure of PdAg alloys reveals the formation of large Pd islands on Ag(111). Using STM, we investigated H_2 activation on active Pd sites and spillover on to Ag(111). The characterization of PtAg and PdAg surface alloys enables us to correlate reaction activity and selectivity to the atomic-scale structure of the alloy and to inform catalyst design that optimizes catalytic selectivity.

3:20pm SS+AS+HC+OX-WeA-4 Single-site Catalysts by Metal-ligand Complexation at Surfaces: From Model Systems in Vacuum to High-pressure Catalysis on Oxide Supports, *Steven L. Tait,* Indiana University

A grand challenge in heterogeneous catalysis is to achieve high levels of selectivity by controlling the chemical uniformity of metal catalyst sites at surfaces. Our group is working to apply principles of on-surface metal-organic redox assembly to develop a new approach to this problem. Metal-organic coordination networks at surfaces hold promise for selective chemical function, but there is a limited understanding of the chemical reactivity of these systems. Studies of model systems in ultra-high vacuum allow for detailed characterization of the structure and chemistry of these systems. We tested chemical activity of vanadium single-site complexes that are stabilized by tetrazine-based ligands and found activity toward dioxygen activation with a high degree of selectivity compared to vanadium nanoparticles. Reaction with O_2 causes an increase in V oxidation state from V^{II} to V^{IV}, resulting in a single strongly bonded V-oxo product and spillover of O to the Au surface [1]. The metal centers are stabilized in extended, ordered metal-organic complexes that self-assemble through an on-surface redox process on the Au(100) surface and are characterized by X-ray photoelectron spectroscopy, scanning tunneling microscopy, high-resolution electron energy loss spectroscopy, and density functional theory. New results extend these chemical studies to more complex systems that include bimetallic sites and redox isomer systems [2-3], which will also be highlighted in this presentation.

We have also developed synthesis schemes to assemble quasi-square planar metal-organic complexes on high surface area powdered oxides under ambient conditions through a modified wet-impregnation method. X-ray photoelectron spectroscopy measurements demonstrate loading of metal and ligand on the surface and synchrotron-based X-ray absorption spectroscopy measurements of the coordination shell of the metal centers demonstrates single site formation rather than nanoparticle assembly [4-5]. These systems are shown to be active for the catalysis of hydrosilylation reactions at a level that is competitive with current homogeneous catalysts. They also show excellent activity for hydrogenation in flow reactor experiment.

1. Tempas, Morris, Wisman, *et al.*, *Chem. Sci.*, **9**, 1674-1685 (2018). DOI: 10.1039/C7SC04752E

2. Tempas, Skomski, Cook, *et al.*, *Chem. Eur. J.*, **24**, 15852–15858 (2018). DOI: 10.1002/chem.201802943

3. Morris, Huerfano, Wang, *et al.*, *Chem. Eur. J.*, **25**, 5565-5573 (2019). DOI: 10.1002/chem.201900002

4. Chen, Sterbinsky, and Tait, *J. Catal.*, **365**, 303-312 (2018). DOI: 10.1016/j.jcat.2018.07.004

5. Chen, Ali, Sterbinsky, *et al.*, *ChemCatChem, in press* (2019).DOI: 10.1002/cctc.201900530

4:20pm SS+AS+HC+OX-WeA-7 Controlling the Local Coordination and Reactivity of Oxide-supported Atomically Dispersed Pt-group Species, *Phillip Christopher,* University of California at Santa Barbara **INVITED**

The synthesis of oxide supported Pt-group catalysts typically produces metal particles with dimensions of a few nanometers. Recent work has shown that Pt-group species can co-exist as nanoparticles and single atoms, and that careful synthetic approaches can produce exclusively single atoms. Interest in the reactivity of supported isolated Pt-group metal atoms stems from the maximized metal utilization efficiency, unique reactivity or selectivity, connection to organometallic catalysis, and the potential for making well-defined active sites. It has proven challenging to characterize the intrinsic catalytic activity of these dispersed active sites on oxide supports at a level that relates local electronic and geometric structure to function. The difficulty arises from their atomic dispersion, heterogeneity in the local coordination of active sites on most catalysts (i.e. isolated species sit at different sites on the support), dynamic changes in local coordination under reactive environments, and often the low loading of metal that is required to achieve site isolation.

In this talk I will describe a synthetic approach to produce isolated Pt-group atoms that exhibit uniformity in their bonding environment on an oxide support and show how a combination of microscopy, spectroscopy and theory can be used to describe the local coordination of these species. Then I will describe two different approaches to control the local environment of Pt-group atoms: (1) through varied pre-treatment that tunes the local coordination and oxidation state of the single atom, and (2) through the site selective deposition of single atoms near well-defined acid sites on oxide supports. Detailed characterization by a combination of spectroscopy and microscopy is used to develop structure-function relationships for these well-defined single atom active sites in the context of CO oxidation, methanol carbonylation and ethylene hydroformylation. This work highlights the ability to tune the local environment of single Pt-group atom active sites on oxide supports in analogous ways to the engineering of organometallic catalysts.

5:00pm SS+AS+HC+OX-WeA-9 Coordination Defines Reactivity of a Model Single-atom Catalyst: Ir$_1$/Fe$_3$O$_4$(001), *Zdenek Jakub*[1]*, J Hulva, M Meier, U Diebold, G Parkinson,* TU Wien, Austria

The development of single-atom catalysts (SACs) was originally motivated by saving of the precious metal, but an equally intriguing characteristic of the ideal SAC is potentially high selectivity due to the high number of identical active sites. The coordination of the active metal center is known to play a crucial role in homogeneous catalysis, and in this talk, I will demonstrate that similar effects can be observed on a model single atom catalyst: Ir$_1$/Fe$_3$O$_4$(001). Using scanning tunneling microscopy (STM), noncontact atomic force microscopy (nc-AFM), temperature programmed desorption (TPD), x-ray photoemission spectroscopy (XPS) and DFT calculations, I will show that the coordination of single Ir$_1$ adatoms can vary depending on preparation, and that the local environment has dramatic consequences for the ability of the catalyst to adsorb CO. As deposited at room temperature, Ir atoms take 2-fold coordination to the surface oxygen atoms. Upon annealing, they incorporate into the first surface layer (5-fold coordinated Ir$_1$), and then into the first subsurface layer (6-fold coordinated Ir$_1$). The 2-fold adatoms can form both monocarbonyls and dicarbonyls, but the 5-fold Ir only binds a single CO. The structures are understood by analogy to square planar Ir(I) and octahedral Ir(III) complexes, respectively. The 6-fold Ir is coodinatively saturated, and thus deactivated for CO adsorption. These results show that control of the local coordination environment is critical to design so-called single-atom catalysts, and that incorporation into the support can be as critical a deactivation mechanism as thermal sintering.

5:20pm SS+AS+HC+OX-WeA-10 Capturing the Early Stages of Oxidation on Low-Index Ni and Ni-Cr Surfaces, *William H. Blades,* P Reinke, University of Virginia

The early stages of oxidation and corrosion of alloys control the structure and development of the oxide layer and therefore decisively influence its protective function. To this end, we have studied thenanoscale evolution of surface oxides prior to the formation of a complete layer. The oxidation of Ni(100), Ni(111), and Ni-Cr(100), Ni-Cr(111) surfaces was captured by sequential oxidization and measured with scanning tunneling microscopy/spectroscopy (STM/STS). The early-stage oxidation, and the influence of alloy composition and crystallographic orientation on surface reactivity, was studied by comparing pure Ni(100/111) and Ni-Cr(100/111) surfaces. Alloy thin films (8-18 wt.% Cr) were prepared on MgO(100/111) and exposed to oxygen up to 400 L at 773 K. Under these conditions, oxide nucleation is predicated by the development of oxygen adlayers on both the pure Ni(100/111) surfaces. The formation of a c(2x2)-O chemisorbed phase on the Ni(100) surface causes the step edges to facet into {100} segments, kinetically limiting NiO growth. However, no such faceting is observed on the Ni(111) surface and the nucleation and growth of NiO begins after only 300 L of O_2. Our experiments demonstrate that the addition of small amounts of Cr completely change the oxidation pathways.

---

[1] **Morton S. Traum Award Finalist**

On the Ni-Cr(100) surface, the nucleation and growth of NiO initiates along the step edges, forming low-angle NiO wedges with a NiO-Ni(7x8) superstructure. Terrace oxide growth commences with the nucleation of small oxide particles, driven by the presence of Cr, which grow into large oxide nodules after further oxidation. NiO growth extends into the terraces and takes a NiO-Ni(6x7) cube-on-cube interfacial relationship. Several novel surface reconstructions are observed and are tentatively attributed to Cr(100)-O reconstructions, suggesting surface segregation and phase separation of BCC Cr. Similarly, nano-sized oxide particles nucleate on the Ni-Cr(111) terrace and step edges, while single atomic NiO rows extend across the surface. Oxide nodules, similar to those found on the Ni-Cr(100) surface are observed and grow laterally along the terraces. Each of these aforementioned surface oxides present unique electronic signatures, and STS maps are used to quantify the spatial variations in their density of states and band gaps. The electronic heterogeneity of the surface underscores that the use a homogenous electric field to capture oxidation kinetics at the alloy-oxide interface should be revisited.

5:40pm SS+AS+HC+OX-WeA-11 Evolution of Steady-state Material Properties during Catalysis: Oxidative Coupling of Methanol over Nanoporous Ag$_{0.03}$Au$_{0.97}$, *Matthijs van Spronsen,* Lawrence Berkeley National Laboratory*; B Zugic,* Harvard University*; M Salmeron,* Lawrence Berkeley National Laboratory*; C Friend,* Harvard University

Activating pretreatments can be used to tune both surface composition and surface structure of bimetallic alloy catalysts. Careful selection of both gas mixtures and reaction temperatures can lead to surfaces that are able to achieve optimum selectivity and activity under steady-state reaction conditions. The activation-induced changes in material properties of a nanoporous (np) Ag$_{0.03}$Au$_{0.97}$ alloy and their subsequent evolution under steady-state conditions for CH$_3$OH oxidation are presented. Initial activation by oxidation in O$_3$ at 423 K leads to the formation of AgO and Au$_2$O$_3$ driving a strong Ag enrichment in the near-surface region, based on ambient-pressure X-ray photoelectron spectroscopy (AP XPS) and extended X-ray absorption fine structure (EXAFS) analysis. Exposing this oxidized np Ag$_{0.03}$Au$_{0.97}$ to the O$_2$/CH$_3$OH reaction mixture reduces both Ag and Au oxides and results in a surface alloy locally highly enriched in Ag. Both the oxides and the highly Ag enriched alloy unselectively oxidize methanol to CO$_2$. However, at the reaction temperature of 423 K, the Ag slowly realloys with Au. Although decreasing, the composition remains enriched in Ag in the top few nanometers under steady-state conditions. The Ag content in the surface is 29 at.% in steady state and the desired product, methyl formate, is selectively produced without significant deactivation. The activation and evolution of the active phase is not uniform: nanometer-scale patches of AgO, leading locally to Ag-rich alloys, were observed with environmental transmission electron microscopy (E TEM). These local Ag-rich AgAu alloy regions are critical for initiation of the catalytic cycle through O$_2$ dissociation. Calculations based on density-functional theory (DFT) indicate that the O on the surface assist in stabilizing the Ag. Moreover, an essential factor for retaining this local enrichment in Ag is the modest reaction temperature of 423 K. At higher temperatures, bulk diffusion induces sintering and redistribution of the Ag, leading to a loss of activity. These findings demonstrate that material properties determining catalytic activity are *dynamic* and that metastable (kinetically trapped) forms of the material may be responsible for catalysis. Hence, catalytic activity and selectivity depend on the pretreatment, reaction temperature and gas composition. These observations provide guiding principles concerning the activation of heterogeneous catalysts for selective oxidation.

6:00pm SS+AS+HC+OX-WeA-12 Reduction and Oxidation of Transition Metal Oxides: From Tailoring the Surface and Interface Properties to the New Crystalline Phases Formation*, Dominik Wrana,* Jagiellonian University, Poland*; C Rodenbücher,* Forschungszentrum Jülich GmbH, Germany*; K Cieślik, B Jany,* Jagiellonian University, Poland*; K Szot,* Forschungszentrum Jülich GmbH, Germany*; F Krok,* Jagiellonian University, Poland

In the recent years transition metal oxides have attracted tremendous interest, mostly due to the manifold real applications, ranging from (photo)catalysis, through memristive and neuromorphic device development, to energy storage and production. A specific quality which makes them so versatile is the ease by which their electronic and structural properties can be controlled by changing a cation's reduction state.

In this presentation we will present an overview of the impact that thermal reduction and oxidation have on the surface properties, which enable a precise control over the valence state of prototypical binary and ternary oxide representatives: TiO$_2$ and SrTiO$_3$. We will focus on the preparation methods under regular UHV conditions and upon additionally reduced oxygen partial pressure.

Reduction of both crystals results in the formation of oxygen vacancies and therefore d-electrons, which leads to changes in the work function and a corresponding rise in electrical conductivity, which could be tuned over many orders of magnitude [1]. A newly developed SPM-based technique, combining LC-AFM and KPFM, allows both measurements to probe the same area of the reduced TiO$_2$(110) surface [2], helping understanding of the nanoscale resistive switching . Besides the change in electrical properties, the surface structure evolves towards nonstoichiometric reconstructions [1], due to the increased oxygen deficiency. Surprisingly, not only is oxygen flow possible during UHV annealing of the oxide crystal, but also incongruent cation sublimation can be triggered, as demonstrated for the perovskite oxides like SrTiO$_3$ [3]. Extremely low oxygen partial pressure (ELOP), achieved by the use of an oxygen-getter, initiates SrTiO$_3$ crystal decomposition and the formation of stable monocrystalline cubic TiO nanowires with a c(4x4) reconstructed surface [4]. Such bottom-up growth of conductive TiO nanostructures could be an alternative to other costly methods, resulting in the creation of the TiO/SrTiO$_3$ interface, with a sharp transition between Ti^{2+} and Ti^{4+} states, proven by atomically-resolved electron microscopy. This oxide heterostructure provides an interesting metal/insulator junction with a 0.6 eV work function difference [5], opening many new possibilities for (photo)catalysis and aiding in the search for exotic interface states.

[1] Wrana, D. et al. (2018) *Applied Surface Science*, *432*, 46-52.

[2] Rodenbücher, C. et al. (2018) *APL Materials*, *6*(6), 066105.

[3] Rodenbücher, C. et al. (2017) *physica status solidi (RRL)–Rapid Research Letters*, *11*(9), 1700222.

[4] Wrana, D. et al. (2019) *Nanoscale*, *11*(1), 89-97.

[5] Wrana, D. et al. (2019) Beilstein Arch., 201912.

Thin Films Division
Room A122-123 - Session TF+EM-WeA

Emerging Thin Film Materials: Ultra-wide Bandgap and Phase Change Materials

Moderators: Cary Pint, Vanderbilt University, Brent Sperling, National Institute of Standards and Technology (NIST), Jin-Seong Park, Hanyang University, Korea

2:20pm TF+EM-WeA-1 MOCVD Growth and Characterization of ZnGeN$_2$-GaN Alloy Films*, Benthara Hewage Dinushi Jayatunga,* K Kash,* Case Western Reserve University*; K Reza, H Zhao,* The Ohio State University*; O Ohanaka, R Lalk,* Case Western Reserve University*; M Zhu, J Hwang,* The Ohio State University

ZnGeN$_2$ and GaN are almost lattice matched and both have band gaps of approximately 3.4 eV. A large conduction band offset of ~ 1.4 eV results in a type II band alignment that has great potential for novel device structures. [1,2] For the 50-50 alloy, a slightly positive mixing energy, indicating a tendency toward phase separation, has been predicted. [3] For this mixture the lowest energy configuration is predicted to be an octet-rule-preserving orthorhombic Pmn2$_1$ phase. Other compositions may in principle be made in octet-rule-preserving (and thus lower energy) phases, compared to those that break the octet rule, by random stacking of ZnGeN$_2$ and GaN layers along the orthorhombic *b* axis. [3] Whether random stacking, phase separation, or octet rule violations occur will determine whether, and by how much, the band gap may be tuned with composition, and whether the transport properties are isotropic or anisotropic. The only other work on this alloy reported to date employed a gas reduction nitridation method for synthesis of powders of different compositions, from pure ZnGeN$_2$ to a 50-50 mixture, for photocatalytic applications [4].

Here we report the results of MOCVD growth of this alloy on c-, r-, and a-plane sapphire and c-GaN/sapphire substrates, at temperatures varying from 550 ^{0}C to 700 ^{0}C. Films at the 50-50 composition exhibit better surface morphologies when grown on r-sapphire substrates. Zn incorporation increases with the increase of Ga. The highest growth rate, 3.46 µm/hr, was obtained for a film grown on r-sapphire at 670 ^{0}C and 550 torr, for which a 2θ-ω XRD measurement yielded a wurtzite (110) diffraction peak at 2θ = 57.70^0 with FWHM of 0.76^0 and an RMS surface roughness of ~ 10 nm by AFM. The Hall mobility is 8.19 cm^2/v-s with an n-type carrier concentration of 8.5 x 10^{18} cm^{-3}. Atomic-resolution HAADF-STEM revealed

the atomic arrangement of the film near the substrate interface. Introduction of a low-temperature-grown $ZnGeN_2$ buffer layer (480 ^{0}C at 600 torr with low injection of precursors compared to the film growth conditions) led to improved surface morphology and crystal quality, and yielded a room temperature photoluminescence spectrum indicating a band edge at approximately 3.5 eV, close to that predicted for the $Pmn2_1$ phase. [3]

[1] L. Han, K. Kash, H. Zhao, J Appl Phys **120**, 103102 (2016)

[2] M. R. Karim, H. Zhao, J Appl Phys **124**, 034303 (2018)

[3] B.H.D. Jayatunga, S. Lyu, S. Kumar, K. Kash, W. R. L. Lambrecht, Phys Rev Mat **2** (2018)

[4] T. Suehiro, M. Tansho, T. Shimizu, J Phys Chem **C 121**, 27590 (2017)

2:40pm TF+EM-WeA-2 Device Quality β-Ga2O3 and Related Alloys by MOCVD, *Andrei Osinsky, F Alema,* Agnitron Technology, Inc.*; Y Zhang, A Mauze, J Speck,* University of California, Santa Barbara*; P Mukhopadhyay, W Schoenfeld,* University of Central Florida

We report on the growth of device quality β-Ga_2O_3 and related alloys using MOCVD method. β-Ga_2O_3 thin films are grown using $Ga(DPM)_3$, TEGa and TMGa as Ga sources, and molecular O_2, H_2O vapor, and N_2O as an oxidizer. Films grown from each Ga source had high growth rates with up to 10 ㎛m/hr achieved using TMGa [1]. The effect of the oxidizer identity on the growth rate, electron mobility (μ_e), background carrier concentration, surface and crystalline quality of the films will be discussed. Using pure O_2 as an oxygen source, optimal growth conditions have led to the growth of smooth epitaxial UID Ga_2O_3 thin films with a RT μ_e of 176 cm^2/Vs at n~7x10^{15} 1/cm^3 [2]. The highest μ_e of ~3500 cm^2/Vs has been measured at 54 K. C and H impurities have been shown to be below the SIMS detection limit for a wide range of process conditions, whereby films with n~ 2x10^{14} cm^{-3} were demonstrated. We will also present the growth of device quality β-Ga_2O_3 layers doped with Si, Fe, and N impurities. Critical growth conditions influencing the incorporation of these dopants will be discussed. Using optimum growth conditions, controllable doping with a concentration between 10^{15} and 10^{20} 1/cm^3 were obtained for each dopant. In this work, we will also present on the MOCVD growth of (Al_x, Ga_{1-x})$_2O_3$ alloys. The MOCVD process enables the growth of AlGaO at a temperature >800 ^{o}C, improving the solubility of Al_2O_3 in β-Ga_2O_3 by preventing the formation of volatile suboxides. The MOCVD reactor used in this work has a unique feature that enables it to minimize premature reaction between the species, thereby improving the Al incorporation. AlGaO alloys with Al content of up to 43 % was obtained. The epitaxial growth of high quality strained β-(Al, Ga)$_2O_3$/Ga_2O_3 heterostructures and superlattices will be discussed. The composition homogeneity, structural quality, surface morphology and electrical properties of the heterostructures will be discussed as a function of growth conditions. Finally, the growth of alloys including β-(In, Ga)$_2O_3$ and ZnGaO using MOCVD and their application for photodetection purposes will be discussed.

[1] F. Alema et al., J. Cryst. Growth, 475, 77(2017).

[2] Y. Zhang et al., APL Materials, 7, 022506 (2019).

3:00pm TF+EM-WeA-3 Development of the β-(AlxGa1-x)2O3/β-Ga2O3 (010) Heterostructures by Plasma-assisted Molecular Beam Epitaxy, *James Speck,* University of California at Santa Barbara **INVITED**

β-Ga_2O_3 is a promising wide bandgap semiconductor for power electronics due to its ~4.8 eV bandgap, reasonable electron mobility, the availability of large area melt grown substrates, and the ability to form heterostructures by alloying on the group III site. In this presentation, we present progress in the plasma-assisted molecular beam epitaxy (PAMBE) growth of β-Ga_2O_3. The presentation will highlight the promise of β-(Al$_x$Ga$_{1-x}$)$_2O_3$/β-Ga_2O_3 heterostructures for lateral devices. We will discuss the growth of β-(Al$_x$Ga$_{1-x}$)$_2O_3$ in the context of the predicted high Al solubility in the β-phase (predicted to be up to ~60-70% for growth temperatures > 800 C). Current experiments limit the Al content to ~25% for coherent growth. We will present detailed analysis of the β-(Al$_x$Ga$_{1-x}$)$_2O_3$ alloys that show the compositions agree between atom probe tomography and high resolution x-ray diffraction. We will highlight a new growth technique, metal oxide catalyzed epitaxy (MOCATAXY), that enables higher growth temperatures due to the addition of an indium catalyst layer that serves both to react with molecular oxygen in the flux and to suppress Ga_2O_3 decomposition via the reaction Ga_2O_3 -> Ga_2O+^{1}/$_2O_2$. We will demonstrate an increase of growth temperature of ~250 C in comparison to conventional PAMBE

growth conditions. We discuss the relative merits and challenges for donor doping in MBE (Si vs. Ge vs. Sn) and options for realizing controllable semi-insulating GaN.

4:20pm TF+EM-WeA-7 Phase-Change Memory: A Quest from Material Engineering Towards the Device Performances, *Guillaume Bourgeois, G Navarro, M Cyrille, J Garrione, C Sabbione, M Bernard, E Nolot, E Nowak,* CEA-LETI, France **INVITED**

In this paper, we provide some examples of how phase–change material engineering can allow targeting specific memory applications. We present the trade-off in Phase–Change Memory between high-speed performance, required in Storage Class Memory applications, and high thermal stability of the amorphous phase at high temperature, mandatory to address automotive embedded applications.

Phase-Change Memory (PCM) is today the most mature among innovative back-end non-volatile memory technologies, thanks to a wide set of interesting features making PCM technology enough versatile to meet different applications' requirements [1]. A PCM device experiences a physical change of a chalcogenide material sandwiched between two electrodes made possible by the current induced Joule heating flowing through the cell. To achieve the amorphous phase, the PCM in the crystalline phase has to be melted, then rapidly quenched (RESET operation). Thanks to the switching phenomenon, the material in the amorphous phase changes abruptly its conductivity starting to be highly conductive, and can recover the crystalline phase thanks to a specific thermal profile during the pulse application, that provides the energy necessary to the atomic reorganization (SET operation). Thereby, PCM thermal stability relies on the magnitude of the activation energy of the crystallization that results from the combination of crystals nucleation and growth phenomena, on which also the device programming speed relies. Thus, a general trade–off exists between the time required for the SET operation and the device data retention performance [2] (Figure 1). Sb-rich GeSbTe compounds are suitable for high-speed performances with a programming time down to tens of ns still ensuring high endurance and scalability, promising for Storage Class Memory applications (SCM) [3]. Reliability at high temperature is the main requirement to target automotive embedded applications. Ge-rich compositions revealed an endurance of 10^7 cycles up to 175 °C and high temperature data retention compatible with embedded standards. We present here the device performance tuning thanks to the phase–change material stoichiometry engineering (Figure 2). Moreover, we highlight the possibility to boost the PCM performances, such as SET speed and Multi Level Cell capability, thanks to dedicated programming strategies [4].

REFERENCES

[1] F. Arnaud et al, "Truly Innovative 28nm FDSOI Technology", IEDM 2018.

[2] G. Navarro et al, "Non-Volatile Resistive Memory", ECS 2016.

[3] V. Sousa et al, "Phase Change Memory", Chapter 7, Springer 2018.

[4] J. Kluge et al, "High Operating Temperature Reliability", IMW 2016.

5:00pm TF+EM-WeA-9 Neuromorphic Materials and Architectures for Dynamic Learning and Edge Processing Applications, *Angel Yanguas-Gil,* Argonne National Laboratory

The ability to dynamically learn and adapt to changes in the environment is one of the hallmarks of biological systems. In the last years there has been a lot of research focused on exploring novel materials, such as those exhibiting memristive behavior, that could enable this type of systems. However, there are comparatively fewer studies focusing on understanding which are the ideal properties that memristive materials should have in order to optimize the performance of architectures capable of dynamic learning. This type of information is crucial to provide design targets for new materials and accelerate the integration of novel devices into architectures optimized for specific applications.

In this work, we identify the subset of the design space of memristive materials that is optimal for dynamic learning applications: in this type of application, a system, in this case a neural network, evolves dynamically and learns as it processes information in real time. This type of behavior is highly desirable for smart sensors or edge processing applications. We have implemented a benchmark architecture consisting of a discrete implementation of spiking neurons where dynamic learning takes place on a set of plastic synapses formed by memristor pairs in a crossbar array. This architecture, which is inspired on the learning center of the insect brain, is capable of dynamically learning standard machine learning datasets such as MNIST and Fashion-MNIST. We have used this model to identify the key properties that memristive materials should have to be optimal dynamic

learners, exploring the impact of the kinetics of the memristor's internal state on the system's learning ability, as well as the impact that materials and device variability and errors in tuning the memristor's internal state have on the system's performance.

The results obtained show that a fine degree of control of the memristor internal state is key to achieve high classification accuracy during dynamic learning, but that, within this optimal region, learning is extremely robust to both device variability and to errors in the writing of the internal state, in all cases allowing for 2σ variations greater than 40% without significant loss of accuracy. Moreover, the dynamics of the internal state can show distinct kinetics depending on the polarity, something that is critical for bipolar memristors. These criteria are significantly different from those required for ReRAM applications or even for neuromorphic applications based on offchip training, where the robustness of reading and writing operations are critical.

5:20pm **TF+EM-WeA-10 Atomic Layer Deposited VO₂ Thin Films Towards Modulated Infrared Optoelectronic Devices**, *Virginia Wheeler, C Ellis, M Currie, J Avila, M Meeker, A Giles,* U.S. Naval Research Laboratory*; J Caldwell,* Vanderbilt University*; J Tischler,* U.S. Naval Research Laboratory

VO₂ is a phase change material that undergoes a first order crystalline phase transition at a critical temperature (T_c = 68°C), resulting in significant changes in intrinsic electrical and optical properties, especially in the infrared. Optical changes with this phase transition are of particular interest as passive and active components of optoelectronic devices, specifically for thermal regulation and modulated signaling. Realizing this type of device often requires the integration of thin, conformal VO₂ films with complex, non-planar structures (like metamaterials). Thus, atomic layer deposition (ALD) is the ideal deposition method in these cases.

Traditional metal-based plasmonic materials suffer from high optical losses, which has promoted research towards alternative low-loss materials that can support plasmonic-like effects. One such approach employs phonon-mediated collective-charge oscillations (surface phonon polaritons, SPhPs) that are supported by nanostructured polar dielectric materials (SiC, AlN, etc), which inherently are low-loss. Geometric design of the nanostructures enables spectral tuning of resonant features between the longitudinal and tranverse optical phonons of the polar material, typically in the infrared regions. However, the spectral position and amplitude of these resonances remain fixed after fabrication. Integrating phase change materials with these structures provides a way to achieve active modulation of resonances.

In this work, nanopillar arrays were etched into SiC and AlN to create narrowband resonances in the long-wave infrared region. These structures were subsequently coated with ALD VO₂ films with different thicknesses (8-75nm). As-deposited VO₂ films are highly conformal and amorphous, and cause the resonances to shift and broaden due to the different dielectric environment. However, after annealing the films at 525°C in 6x10⁻⁵ Torr, the VO₂ films crystallize resulting in sharper resonances and spectral locations close to the initial uncoated structures. Temperature-dependence reflectance and emission measurements show that by heating through the VO₂ transition temperature, the amplitude of the resonances can be modulated. Full signal modulation (ie. on/off) requires at least a 16nm VO₂ film. This work shows the ability to actively tune surface phonon polariton resonances using ALD phase change materials.

5:40pm **TF+EM-WeA-11 Deposition Process for Vanadium Dioxide Thin Films for RF Applications**, *Mark Lust, S Chen, N Ghalichechian,* The Ohio State University

Phase change materials (PCM) are attractive due their tunability, wide range of applications, and quasi-passive actuation as compared to traditional active integrated circuits. Vanadium dioxide (VO₂) is particularly appealing because of its high contrast between dielectric and conductive states and the relatively low temperature (68 °C) at which its metal-insulator transition (MIT) occurs. This work details a process for depositing high quality VO₂ thin films on C-plane sapphire wafers as well as alumina (Al₂O₃) buffer layers using atomic layer deposition (ALD) on silicon substrates. We compare resistivity vs. temperature measurements of VO₂ on sapphire with VO₂ on the Al₂O₃ buffer layers both as-deposited and after rapid thermal annealing (RTA) at temperatures ranging from 950 to 1150°C. The VO₂ thin films yielded ratios of resistivity between conductor (heated) and dielectric (room temperature) states of 9.8×10^4 Ω-cm, 5.2×10^3 Ω-cm, and 1.5×10^4 Ω-cm when deposited on crystalline sapphire, amorphous Al₂O₃ buffer layers, and annealed Al₂O₃ buffer layers, respectively. This corresponds to an improvement by a factor of 2.9 in the annealed buffer layers over the amorphous buffer layers. Moreover, we studied various VO₂

thin films using X-ray diffraction, which showed clear indications that the films are highly pure and have a preferred crystal orientation. The deposition process we have developed will allow us to use high quality VO₂ thin films on silicon substrates, especially millimeter-wave devices such as reconfigurable antennas, sensors, and meta-surfaces.

6:00pm **TF+EM-WeA-12 Low Power, Microwave Solid State Oscillators Based on Phase Change Materials**, *Yang Liu, Z Du, B Zhao, H Wang, J Ravichandran,* University of Southern California

The information age has unleashed an exponential growth in access and quality of life for human beings, but sustaining this growth is key to our future. Currently, 10% of the world's energy is consumed for processing, communication or storage of digital media and this share is constantly increasing, which is a slowly unfolding energy crisis.[1] With the growing need for artificial intelligence, efficient use of energy for computing warrants a departure from digital logic. Brain-inspired neuromorphic computing is envisioned to be several times more efficient for associative learning problems. Phase change materials demonstrating metal to insulator transitions are suitable to realize solid state neurons in this neuromorphic framework. VO₂ undergoes a 5 order-of-magnitude change in resistivity near room temperature with minimal structural change.[2] We designed highly energy efficient, low power oscillators based on VO₂/SrRuO₃ heterostructures in the light of thermal engineering. Early simulation work has demonstrated low power consumption down to 45 μW with 3 GHz driving frequency.[3] High-quality epitaxial VO₂ thin films have been deposited on various *3m* surface symmetry substrate, SrTiO₃ and [LaAlO₃]₀.₃[Sr₂AlTaO₆]₀.₇.[4] VO₂ thin films have shown sharp 4 orders of magnitude change in resistivity around the transition temperature. The thermal boundary conductance is measured by time-domain thermoreflectance. We also present our experimental effort to achieve energy efficient and low power oscillators for neuromorphic computing.

[1]J. Nicola, Nat. Mag. 163 (2018).

[2]H.-T. Kim, B.-J. Kim, S. Choi, B.-G. Chae, Y.W. Lee, T. Driscoll, M.M. Qazilbash, and D.N. Basov, J. Appl. Phys. **107**, 023702 (2010).

[3]B. Zhao and J. Ravichandran, Phys. Rev. Appl. **11**, 014020 (2019).

[4]Y. Liu, S. Niu, T. Orvis, H. Zhang, H. Zhao, H. Wang, and J. Ravichandran, J. Vac. Sci. Technol. A **36**, 061506 (2018).

2D Materials

Room A216 - Session 2D+EM+MI+NS+QS+SS-ThM

Dopants, Defects, and Interfaces in 2D Materials

Moderator: Evan Reed, Stanford University

8:00am 2D+EM+MI+NS+QS+SS-ThM-1 Interfacial Engineering of Chemically Reactive Two-Dimensional Materials, *Mark Hersam,* Northwestern University **INVITED**

Following the success of ambient-stable two-dimensional (2D) materials such as graphene and hexagonal boron nitride, new classes of chemically reactive layered solids are being explored since their unique properties hold promise for improved device performance [1]. For example, chemically reactive 2D semiconductors (e.g., black phosphorus (BP) and indium selenide (InSe)) have shown enhanced field-effect mobilities under controlled conditions that minimize ambient degradation [2]. In addition, 2D boron (i.e., borophene) is an anisotropic metal with a diverse range of theoretically predicted phenomena including confined plasmons, charge density waves, and superconductivity [3], although its high chemical reactivity has limited experimental studies to inert ultrahigh vacuum conditions [4-7]. Therefore, to fully study and exploit the vast majority of 2D materials, methods for mitigating or exploiting their relatively high chemical reactivity are required [8]. In particular, covalent organic functionalization of BP minimizes ambient degradation, provides charge transfer doping, and enhances field-effect mobility [9]. In contrast, noncovalent organic functionalization of borophene leads to the spontaneous formation of electronically abrupt lateral organic-borophene heterostructures [10]. By combining organic and inorganic encapsulation strategies, even highly chemically reactive 2D materials (e.g., InSe) can be studied and utilized in ambient conditions [11].

[1] A. J. Mannix, *et al.*, *Nature Reviews Chemistry*, **1**, 0014 (2017).

[2] D. Jariwala, *et al.*, *Nature Materials*, **16**, 170 (2017).

[3] A. J. Mannix, *et al.*, *Nature Nanotechnology*, **13**, 444 (2018).

[4] A. J. Mannix, *et al.*, *Science*, **350**, 1513 (2015).

[5] G. P. Campbell, *et al.*, *Nano Letters*, **18**, 2816 (2018).

[6] X. Liu, *et al.*, *Nature Materials*, **17**, 783 (2018).

[7] X. Liu, *et al.*, *Nature Communications*, **10**, 1642 (2019).

[8] C. R. Ryder, *et al.*, *ACS Nano*, **10**, 3900 (2016).

[9] C. R. Ryder, *et al.*, *Nature Chemistry*, **8**, 597 (2016).

[10] X. Liu, *et al.*, *Science Advances*, **3**, e1602356 (2017).

[11] S. A. Wells, *et al.*, *Nano Letters*, **18**, 7876 (2018).

8:40am 2D+EM+MI+NS+QS+SS-ThM-3 Effects of Mn Doping on the Surface Electronic Band Structure and Bulk Magnetic Properties of ZnS and CdS Quantum Dot Thin Films, *Thilini K. Ekanayaka[1], G Gurung,* University of Nebraska-Lincoln*; G Rimal,* Rutgers University*; S Horoz,* Siirt University, Turkey*; J Tang, T Chien,* University of Wyoming*; T Paudel, A Yost,* University of Nebraska-Lincoln

Semiconducting quantum dots (QDs) are desirable for solar cells due to the ability to tune the band gap by changing the QD size without changing the underlying material or synthesis technique. Doping QDs with a transition metal is one way of further tailoring the electronic band structure and magnetic properties of QDs in order to improve overall device performance. Understanding the mechanisms causing the change in the electronic band structure and magnetic properties due to transition metal doping is important to device-by-design schemes. In this study, we measure the effects of Mn dopants on the surface electronic band structure of ZnS and CdS QDs using scanning tunneling microscopy/spectroscopy and photoemission spectroscopy. In both the ZnS and CdS systems, a decrease in band gap upon introduction of Mn is observed. Additionally, a rigid band shift was observed in ZnS upon Mn doping It is argued, using X-ray photoemission spectroscopy, that the rigid band shift is due to a hole-doping mechanism caused by the formation of Zn vacancies accompanied by a Mn^{3+} oxidation state which leads to the reduction in total S vacancies as compared to the undoped ZnS system. No band shift was observed in CdS upon Mn doping, but a strong sp-d hybridization takes place which results in a significant band gap reduction. Furthermore, induced midgap states originating from the Mn dopant appear in the surface electronic band structure of Mn: CdS. Measurements of the magnetization of Mn doped and undoped ZnS and CdS confirms the

presence of d^0 ferromagnetism. The magnetization is reduced and the coercive field is increased post Mn doping which suggests the anti-ferromagnetic alignment of Mn dopant atoms. Density Functional Theory calculations support the Mn anti-ferromagnetic alignment hypothesis and a ground state with Mn in the 3^+ valence. This study provides important information on the role of dopants and vacancies in dilute magnetic semiconductor quantum dot materials for applications in photovoltaics and spintronics.

9:00am 2D+EM+MI+NS+QS+SS-ThM-4 Interaction of Molecular O_2 with Organolead Halide Nanorods by Single-Particle Fluorescence Microscopy, *Juvinch Vicente, J Chen,* Ohio University

The photoluminescence (PL) of organolead halide perovskites (OHPs) is sensitive to its surface conditions, especially surface defect states, making the PL of small OHP crystals an effective way to report their surface states. At the ensemble level, when averaging a lot of nanocrystals, the photoexcitation of OHP nanorods under inert nitrogen (N_2) atmosphere leads to PL decline, while subsequent exposure to oxygen (O_2) results to reversible PL recovery. At the single-particle level, individual OHP nanorods photoblinks, whose probability is dependent on both the excitation intensity and the O_2 concentration. Combining the two sets of information, we are able to quantitatively evaluate the interaction between a single surface defect and a single O_2 molecule using a kinetic model. This model provides fundamental insights that could help reconcile the contradicting views on the interactions of molecular O_2 with OHP materials and help design a suitable OHP interface for a variety of applications in photovoltaics and optoelectronics.

9:20am 2D+EM+MI+NS+QS+SS-ThM-5 Complementary Growth of 2D Transition Metal Dichalcogenide Semiconductors on Metal Oxide Interfaces, *T Wickramasinghe,* **Gregory Jensen**, *R Thorat,* Nanoscale and Quantum Phenomena Institute*; S Aleithan,* Nanoscale and Quantum Phenomena Institute, Saudi Arabia*; S Khadka, E Stinaff,* Nanoscale and Quantum Phenomena Institute

A chemical vapor deposition (CVD) growth model will be presented for a technique resulting in naturally formed 2D transition metal dichalcogenide (TMD) based metal-oxide-semiconductor structures. The process is based on a standard CVD reaction involving a chalcogen and transition metal oxide-based precursor. Here however, a thin metal oxide layer, formed on lithographically defined regions of a pure bulk transition metal, serves as the precursor. X-ray diffraction and cross -sectional SEM studies show insight into the type and thickness of the metal oxide created during optimal growth conditions. The chalcogen reacts with the metal oxide, forming TMD material which migrates outward along the substrate, leading to lateral growth of highly-crystalline, mono-to-few layer, films. In addition to displaying strong luminescence, monolayer Raman signatures, and relatively large crystal domains, the material grows deterministically and selectively over large regions and remains connected to the bulk metallic patterns, offering a scalable path for producing as-grown two-dimensional materials-based devices.

9:40am 2D+EM+MI+NS+QS+SS-ThM-6 Kagome-type Lattice Instability and Insulator-metal Transition in an Alkali-doped Mott Insulator on Si(111), *Tyler Smith, H Weitering,* University of Tennessee Knoxville

The 1/3 ML monolayer (ML) 'alpha phase' of Sn on Si(111) is a remarkable platform for the study of strong correlations in a spin ½ triangular adatom lattice. In this work, we employ an adatom doping scheme by depositing potassium onto the triangular Sn lattice. The K-atoms destabilize the parent Mott insulating phase and produce a charge-ordered insulator, revealing a rare Kagome lattice at the surface. Scanning Tunneling Microscopy and Spectroscopy reveal a phase transition from an insulating kagome lattice to a metallic triangular lattice at about 200 K. DFT band structure calculations for this kagome system [J. Ortega et al., unpublished] reveal the presence of a flat-band just below the Fermi level, making this novel system a compelling platform for hole-doping studies of magnetic and/or superconducting instabilities.

11:00am 2D+EM+MI+NS+QS+SS-ThM-10 Chemical Migration and Dipole Formation at TMD/TI Interfaces, *Brenton Noesges, T Zhu,* The Ohio State University*; D O'Hara,* University of California, Riverside*; R Kawakami, L Brillson,* The Ohio State University

Proximity effects at the interface between two materials can induce physical properties not present in either material alone. Topological insulators (TIs) such as Bi_2Se_3 with non-trivial surface states are sensitive to interface proximity effects where overlayers and adsorbates can act as a dopant source, chemically interact with the TI surface, or couple across the

---

[1] **National Student Award Finalist**

TI surface states leading to novel quantum phases. Transition metal dichalcogenides (TMDs), a class of 2D van der Waals materials, are a promising candidate to control this interface given the shared general hexagonal symmetry and wide range of TMD properties. However, the interface between TMDs and Bi_2Se_3 can be more complex than the ideal van der Waals interface. Chemical species exchange like metal cation exchange and selenium migration from substrate to growing film can impact the structure and properties of either layer. Self-assembly mechanisms have also been observed where complete metal monolayers form inside the Bi_2Se_3 quintuple layer [1]. We used x-ray photoelectron spectroscopy (XPS) connected in vacuo via UHV suitcase to a molecular beam epitaxy (MBE) system to investigate chemical interaction at the interface between selenide TMDs and Bi_2Se_3. Air-free transferring is crucial to minimize contamination at the interface and prevent oxidation in the air-sensitive TMDs. We compare the effects of ultrathin pure Mn metal overlayers and monolayer $MnSe_x$ on Bi_2Se_3 to pristine Bi_2Se_3. In the case of pure Mn metal on Bi_2Se_3, Bi core levels exhibit a 1.7 eV shift toward lower binding energies while the Mn core levels also show signs of Mn-Se bonding. These core level changes indicate that, in the absence of excess Se during growth, Mn pulls Se from the substrate leaving behind Bi_2 bilayers near the surface. Depositing a monolayer of $MnSe_x$ produces very different results than the pure metal case. Bi_2Se_3 core levels measured below the monolayer $MnSe_x$ film exhibit a rigid 0.8 eV chemical shift toward higher binding energies indicative of surface/interface dipole formation. The presence of this dipole is likely due to growth of primarily α-MnSe instead of the $1T-MnSe_2$ 2D phase [2]. Scanning tunneling microscopy (STM) height maps and spectroscopy data provide further evidence of majority α-MnSe formation. XPS core level analysis combined with controlled depositions, air-free transfers and surface analysis can provide a consistent explanation of chemical diffusion and dipole formation at a TMD/TI interface. This work is supported by NSF MRSEC under award number DMR-1420451.

[1] J. A. Hagmann et al., New J. Phys. 19, 085002 (2017).

[2] D.J. O'Hara et al. Nano Lett., 18(5), 3125-3131 (2018).

11:20am 2D+EM+MI+NS+QS+SS-ThM-11 Atomically Resolved Electronic Properties of Defects in the in-plane Anisotropic Lattice of ReS$_2$, *Adina Luican-Mayer,* University of Ottawa, Canada
Among the layered transition metal dichalcogenides, the compounds that exhibit in-plane anisotropy are of particular interest as they offer an additional tuning knob for their novel properties. In this talk, we present experimental evidence of the lattice structure and properties of semiconducting ReS_2 by using scanning tunneling microscopy and spectroscopy (STM/STS). We demonstrate that rhenium atoms form diamond-shaped clusters, organized in disjointed chains and characterize the semiconducting electronic band gap by STS. When imaging the surface of ReS_2, we encounter "bright" or "dark" regions indicating the presence of charged defects that will electrostatically interact with their environment. By spatially mapping the local density of states around these defects, we explore their origin and electrostatic nature. Experimental results are compared with ab-initio theory.

11:40am 2D+EM+MI+NS+QS+SS-ThM-12 Charge Diminishing at the Si-SiO$_2$ System and its Influence on the Interface Properties, *Daniel Kropman, V Seeman,* Tartu University, Estonia*; A Medvids, P Onufrievs,* Riga Technical University, Latvia
The fact that a positive charge formation occurs in SiO_2 film during the process of Si thermal oxidation is already known, with the formation being dependent upon the oxidation conditions which involve temperature, time, and ambient conditions. This is connected by oxygen vacancies in the SiO_2 film and unsaturated $Si^{3\bullet}$ bonds at the interface. Until now this process has not been studied in depth at an atomic level. The purpose of the present work is to investigate the charge formation in the Si-SiO$_2$ system and its diminishing by means of the appropriate choice of oxidation conditions via EPR spectroscopy, IR spectroscopy, CV curves, TEM, and deflection measurements. Laser irradiation and ultrasonic treatment were used for the modification of interface properties. It has been established that, at an oxidation temperature that is within the range of 1125^0C-1130^0C in $SiO2$ film with a thickness of 0.2-0.3μ at the interface, there appears a low positive or negative charge which is connected with negatively charged acceptors that are formed by Si vacancies, and the positive charge in the SiO_2 is compensated. The results that were obtained coincide with the point defects generation kinetic model in the Si-SiO$_2$ system which was proposed in [1] and was confirmed experimentally [2]. Integral circuit technology conditions that allow the interface charge to diminish were introduced by the semiconductor plant, ALFA (Riga, Latvia) [3]. We

supposed that these results, which were obtained during long term collaboration between Estonia and Latvia, constituted a discovery that had been achieved by Si-SiO$_2$ system investigation no less than thirty years ago: the discovery of the quantum Hall effect on the Si-SiO2 structure [4].

References

1. T Y Tan, U Gösele, Appl Phys, A37,1 (1985).

2. D Kropman, S Dolgov, T Kärner, Appl Phys, A62,469 (1996).

3. D Kropman, E Mellikov, T Kärner, Ü Ugaste, T Laas, I Heinmaa, A Medvids, Material Science and Engineering B 134 (2006) 222-226.

4. K von Klitzing. Private communication (2018).

12:00pm 2D+EM+MI+NS+QS+SS-ThM-13 Size-independent "Squeezed" Shape of Metal Clusters Embedded Beneath Layered Materials, *A Lii-Rosales,* Ames Laboratory and Iowa State University*; S Julien, K Wan,* Northeastern University*; Y Han,* Ames Laboratory and Iowa State University*; K Lai,* Iowa State University*; M Tringides, J Evans,* **Patricia A. Thiel**, Ames Laboratory and Iowa State University
We have developed a continuum elasticity model for metals embedded beneath the surfaces of layered materials. The model predicts that the equilibrated cluster shape is invariant with size, manifest both by constant side slope and by constant aspect ratio (width:height ratio). This prediction is rationalized by dimensional analysis of the relevant energetic contributions. The model is consistent with experimental data for Cu and Fe clusters embedded in graphite, especially in the limit of large clusters. For comparison, we have performed a Winterbottom analysis of the equilibrium shape of an uncovered Cu cluster supported on top of graphite. The aspect ratio of the embedded cluster is about an order of magnitude higher than that of the supported cluster. Analysis of key energetics indicates that this is due to the strain energy (resistance to deformation) of the top graphene membrane, which effectively squeezes the metal cluster and forces it to adopt a relatively low, flattened shape. These insights may be useful for developing components such as metallic heat sinks or electrodes in electronic devices that use two-dimensional or layered materials.

Atomic Scale Processing Focus Topic
Room B130 - Session AP+PS+TF-ThM

Thermal Atomic Layer Etching
Moderators: Craig Huffman, Micron, Eric A. Joseph, IBM Research Division, T.J. Watson Research Center

8:00am AP+PS+TF-ThM-1 A Challenge for Selective Atomic Layer Etching of Non-volatile Materials Using Organometalic Complex, *Yoshihide Yamaguchi, S Fujisaki, K Shinoda,* Hitachi, Japan*; H Kobayashi, K Kawamura, M Izawa,* Hitachi High Technologies, Japan **INVITED**
Remarkable progress on atomic layer etching (ALE) for non-volatile materials has been made in recent years. The typical procedure for thermal ALE of non-volatile materials such as HfO_2 is cyclic repetitions of formation and desorption of the organometallic complex at a constant temperature [1]. The most significant problem in thermal ALE is formation of a volatile organometallic complex layer on the surface. The organometallic complex layer prevents diffusion of etching species into the deep at the formation step and must be easily removed at the desorption step. The thermal ALE of La_2O_3, however, is difficult to apply because the organo-lanthanum complexes are easily decomposed by mild heating (< 200 deg. C) and fail to prevent the diffusion. To solve this thermal instability, the authors have applied a thermal cycle ALE [2,3], which is a combination of a formation of the organo-lanthanum complex at a low temperature and a desorption of the complex at a high temperature. In this paper, several results of our challenge for thermal ALE of non-volatile materials using a selective organo-metallization reaction on the surface will be discussed. Some guiding principles for the organo-metallization reaction will also be explained.

A La_2O_3 thin-film sputtering deposited on a SiO_2/Si wafer was used as a sample. First, the La_2O_3 film was exposed to vapor mixture of a diketone and a stabilizer as the etchant gas at below 150 deg. C. Then the sample was annealed up to 250 deg. C. Temperature dependence in the procedure was also evaluated. After these consecutive processes, the sample was analyzed by scanning electron microscopy, X-ray photoelectron spectroscopy. Formation of the organo-lanthanum complex showed temperature dependent quasi-self-limiting characteristics. In the lower temperature range, the self-limiting characteristics enable precise control

of the organo-lanthanum complex formation. In the higher temperature range, the continuous characteristics enable a higher etch amount per cycle with high selectivity. Several differences between chemistry with and without a stabilizer in the etching gas will be discussed. The high etching selectivity of La_2O_3 to HfO_2 was also demonstrated. From these findings, we conclude that practical ALE of La_2O_3 has been successfully demonstrated.

[1] Y. Lee et al., Journal of Vacuum Science & Technology A 36, 061504 (2018).

[2] K. Shinoda et al., J. Phys. D: Appl. Phys. 50, 194001 (2017).

[3] Y. Yamaguchi et al., ALE workshop TuM4 (2018).

8:40am **AP+PS+TF-ThM-3 Characterization of Isotropic Thermal ALE of Oxide Films and Nanometer-Size Structures**, *Andreas Fischer, A Routzahn, T Lill,* Lam Research Corporation

In this work, we have characterized the reaction of aluminum oxide via the DMAC ligand exchange mechanism.

Fluorination studies of aluminum oxide were performed using NF_3, CF_4 or anhydrous HF, respectively. We also explored various methods of fluorination of the oxide surface such as thermal, in-situ or remote plasma, respectively, and found that a sufficient fluorine concentration could be obtained with either of the methods or reactants to enable atomic layer etching (ALE).

To understand reaction kinetics, we examined the interaction of aluminum fluoride (AlF_3) films with DMAC. We found that AlF_3 etched until it was completely consumed by DMAC. An analysis of its temperature-dependence allowed us to extract activation energies for the ligand exchange mechanism.

In a third part we demonstrated the utility of HF/DMAC reaction for isotropic ALE applied to nanometer-size metal oxide structures on wafers. Various metal oxides were etched and selectivities between oxides and potential mask materials were determined.

9:00am **AP+PS+TF-ThM-4 Advanced Selective Chemical Dry Etch for Oxide and Si-based Material**, *Li-Hung Chen, T Kato, K Nakahata, K Takeya,* Tokyo Electron Technology Solutions Limited, Japan

As device features continuously shrink with introducing complex structures and new materials in semiconductor manufacturing, extremely high selectivity for etch processes have become more and more important. High selective chemical dry etch is developed utilizing a separated damage-free chemical removal chamber and sublimation chamber. The required selectivity is realized by using various chemistries and quantum mechanics analysis.

Firstly, HF/NH3 chemistry is used for oxide etch with high selectivity to SiN, Si, metals and resist. On the other hand, HF mono chemistry can etch SiN with high selectivity to oxide and Si. Quantum mechanics analysis revealed that NH3 combined with HF enhances the SiO_2 reaction because of its lower activation energy. However, HF mono chemistry enhances the SiN reaction because of its lower activation energy than the oxide reaction[1]. Secondly, Gas A chemistry is introduced for etching low quality oxide with selectivity >50 to both high quality oxide and SiN. The reaction rate barrier determined by quantum mechanics shows that etch reactivity with ALD-oxide is higher than with Th-SiO2 and SiN in Gas A etch process. Furthermore, Si and SiGe etch are evaluated with different Gas B/C ratio. Etch amount of Si is increased with increasing Gas C flow which can reduce activation energy from quantum mechanics simulation. Moreover, SiGe etching amount is decreased with increasing Gas C flow. This means that selectivity between Si and SiGe can be precisely controlled by Gas flow ratio.

Various applications can be realized by utilizing chemical dry etch with specific chemistries. For oxide etch processes such as fin recess, air gap, hard mask removal and surface clean, HF/NH3 chemistry can be used to meet critical criteria such as oxide selectivity to Si, SiN, resist and metal. CIP HW is developed to enhance throughput with excellent etch selectivity and uniformity. Additionally, HF mono-gas (or F-containing treatment) can dope Fluorine (F) into oxide film which is confirmed by depth profile analysis of secondary ion mass spectrometry (SIMS), and F implantation is known for dielectric breakdown life time improvement[2]. Also, Gas A can be utilized in Silica oxide removal process, which requires high selectivity between low quality and high quality oxide. Finally, Si mandrel removal and Si or SiGe nanowire fabrication is introduced by controlling gas flow ratio. Further discussion will be presented on AVS 66th.

Reference

[1] T. Kato, et al., AVS 65th Int. Symp. & Exhibit. (2018)

[2] Y. Mitani, et al., Proc. Of IEEE P93-98 (1999)

9:20am **AP+PS+TF-ThM-5 Mechanisms of Thermal Atomic Layer Etching (ALE) of Metal by Deprotonation and Complex Formation of Hexafluoroacetylacetone (hfacH)**, *Abdulrahman Basher[1], I Hamada,* Osaka University, Japan; *M Krstic,* Karlsruhe Institute of Technology (KIT), Germany; *M Isobe, T Ito,* Osaka University, Japan; *K Fink,* Karlsruhe Institute of Technology (KIT), Germany; *K Karahashi, Y Morikawa,* Osaka University, Japan; *W Wenzel,* Karlsruhe Institute of Technology (KIT), Germany; *S Hamaguchi,* Osaka University, Japan

Thermal atomic layer etching (ALE) may be used for precise and damageless etching of difficult-to-etch materials such as Ni, Co, NiFe, MgO, and CoFeB, which can be used as materials for magnetic tunnel junction (MTJ) stacks of magnetic random access memory (MRAM) devices. The goal of this study is to understand the mechanisms of surface chemical reactions during thermal ALE of metal in general with oxidation and exposure to organic molecules. As a model case, we consider a two-step thermal ALE process of nickel (Ni) with an oxidation step and a gas exposure step at an elevated substrate temperature [1]. In the latter step, hexafluoroacetylacetone (hfacH) $CF_3C(OH)=CHC(O)CF_3$ is used as a reactive gas. In the oxidation step, a thin layer of NiO is formed on the Ni film surface and, in the gas exposure step, only (part of) this NiO layer is removed and thus self-limiting etching of Ni is achieved. Our main question is why NiO is etched but Ni is not etched by hfacH. This mechanism is studied with first-principle simulation of interaction of hfacH with Ni and NiO surfaces.

First, we examined interaction of hfacH with a metallic Ni surface, using a simulation code STATE [2,3], which is based on density functional theory (DFT) with pseudo-potentials and a plane wave basis set. Computationally, a metal surface is better represented by a plane wave basis set in general. It has been found in our simulation that, as an hfacH molecule approaches a metallic Ni surface with thermal velocity, it is more likely to be decompose and fragmented, rather than forming a hexafluoroacetylacetonate anion (hfac-) by deprotonation. This is consistent with earlier experimental observations [1,4]. The simulation clearly shows an energy threshold for deprotonation of hfacH with a metallic Ni surface.

Second, we examined interaction of enol hfacH with a NiO surface using a simulation code Turbomole [5], which is based on DFT but with Gaussian type orbitals. To better represent a NiO surface, we used the embedded cluster method (ECM) with Turbomole. It has been found that, as an hfacH molecule approaches a NiO surface, it is likely to deprotonate by transferring its hydrogen ion (H+) to an O atom of the NiO surface and the resulting hfac- tends to bond with a Ni atom of the surface because of the highly ionic nature of NiO, where Ni and O atoms are positively and negatively charged, respectively. In this way, volatile $Ni(hfac)_2$ and H_2O can be formed when hfacH molecules interact with a NiO surface. Reaction energies of such interactions have been evaluated from the simulations.

----

[1] T. Ito, et al., AVS 65th International Symposium & Exhibition (2018).

[2] Y. Morikawa, H. Ishii and K. Seki, Phys. Rev. B, **69**, 041403 (2004).

[3] I. Hamada, Physical Rev. B **89**, 121103 (2014).

[4] H. L. Nigg and R. I. Masel, J. Vac. Sci. Techol. A **17**,3477 (1999).

[5] R. Ahlrichs, M. Bär, M. Häser, H. Horn, C. Kölmel, Chem. Phys. Lett. **162**, 165 (1989).

9:40am **AP+PS+TF-ThM-6 Thermal Atomic Layer Etching of Amorphous and Crystalline Al_2O_3 Films**, *Jessica A. Murdzek, S George,* University of Colorado at Boulder

Thermal atomic layer etching (ALE) can be achieved with sequential, self-limiting surface reactions. One mechanism for thermal ALE is based on fluorination and ligand-exchange reactions. For metal oxide ALE, fluorination converts the metal oxide to a metal fluoride. The ligand-exchange reaction then removes the metal fluoride by forming volatile products. Previous studies have demonstrated the thermal ALE of amorphous Al_2O_3 films. However, no previous investigations have explored the differences between the thermal ALE of amorphous and crystalline Al_2O_3 films.

This study explored the thermal ALE of amorphous and crystalline Al_2O_3 films. HF or XeF_2 was used as the fluorination reactant. Dimethylaluminum chloride (DMAC) or trimethylaluminum (TMA) was employed as the metal

precursor for ligand-exchange. The amorphous Al_2O_3 films had a much higher etch rate per cycle than the crystalline Al_2O_3 films. When using HF and TMA at 300 °C, the amorphous Al_2O_3 was removed at 0.78 Å/cycle, whereas the crystalline Al_2O_3 showed no significant thickness removal after 250 cycles (See Supplemental Figure 1). When using XeF_2 and TMA at 300 °C, the etch rate was 0.66 Å/cycle for the amorphous Al_2O_3 film. In comparison, ALE only removed up to 10 Å of the crystalline Al_2O_3 film. XeF_2 may be able to fluorinate the near surface region of the crystalline Al_2O_3 film easier than the crystalline bulk of the film.

The differences between amorphous and crystalline Al_2O_3 are sufficient to obtain selective thermal ALE of amorphous Al_2O_3 in the presence of crystalline Al_2O_3. The investigations also examined the effect of annealing temperature on the etch rate per cycle. Amorphous Al_2O_3 was etched at approximately the same etch rate until the crystallization of amorphous Al_2O_3 at >880 °C. The thermal ALE of crystalline films is important because amorphous films may not crystallize easily when they are too thin. Consequently, amorphous films may have to be grown thicker, crystallized, and then etched back to obtain the desired ultrathin crystalline film thickness.

11:00am AP+PS+TF-ThM-10 Thermal Atomic Layer Etching (ALE) of Germanium-Rich SiGe Films, *Aziz Abdulagatov, S George,* University of Colorado at Boulder

The thermal atomic layer etching (ALE) of germanium-rich SiGe was demonstrated using an oxidation and "conversion-etch" mechanism (See Supplemental Figure 1). In this process, the SiGe surface was oxidized to a SiGe oxide layer using O_2. The SiGe oxide layer was then converted to an Al_2O_3 layer using trimethylaluminum (TMA). The Al_2O_3 layer was fluorinated by HF to an AlF_3 layer prior to the removal of the AlF_3 layer by ligand-exchange using TMA. The thermal ALE of SiGe films will be important for the fabrication of advanced MOSFET devices.

This study explored the thermal ALE of germanium-rich $Si_{0.2}Ge_{0.8}$ films. *In situ* spectroscopic ellipsometry was employed to monitor the thickness of both the $Si_{0.2}Ge_{0.8}$ and the surface oxide layer during ALE. These studies showed that the $Si_{0.2}Ge_{0.8}$ film thickness decreased linearly with number of reaction cycles while the surface oxide thickness remained constant. Using an O_2-HF-TMA reaction sequence, the $Si_{0.2}Ge_{0.8}$ ALE etch rate was 0.57 Å/cycle at 290°C. This etch rate was obtained using optimal reactant pressures of 25, 0.2 and 0.4 Torr, and dose times of 1.5, 1 and 1 s, for O_2, HF and TMA, respectively.

The $Si_{0.2}Ge_{0.8}$ ALE etch rate was lower at lower temperatures. Using an O_2-HF-TMA reaction sequence, the $Si_{0.2}Ge_{0.8}$ etch rate was reduced from 0.57 Å/cycle at 290°C to 0.07 Å/cycle at 225°C. The order of the reactant sequence also affected the $Si_{0.2}Ge_{0.8}$ etch rate. Changing the reactant sequence from O_2-HF-TMA to O_2-TMA-HF reduced the $Si_{0.2}Ge_{0.8}$ etch rate from 0.57 to 0.45 Å/cycle at 290°C. $Si_{0.2}Ge_{0.8}$ could also be etched selectively in the presence of Si and Si_3N_4. The $Si_{0.2}Ge_{0.8}$ etch rate was >10 times faster than the etch rate for Si or Si_3N_4 at 290°C (See Supplemental Figure 2).

11:20am AP+PS+TF-ThM-11 Thermal Atomic Layer Etching of GaN and Ga_2O_3 Using Sequential Fluorination and Ligand-Exchange Reactions, *Nicholas Johnson, Y Lee, S George,* University of Colorado at Boulder

Atomic layer etching (ALE) of GaN and Ga_2O_3 is important for the fabrication of power electronics devices. Thermal ALE of GaN and Ga_2O_3 was performed using sequential, self-limiting surface reactions. The thermal ALE was accomplished using fluorination and ligand-exchange reactions. XeF_2 and HF were used as the fluorination reactants. BCl_3 was the main metal precursor for ligand-exchange. Ga_2O_3 was also etched using $Al(CH_3)_3$, $AlCl(CH_3)_2$, $TiCl_4$ or $Ga(N(CH_3)_2)_3$ as the metal precursors for ligand-exchange.

Crystalline GaN samples prepared using MOCVD techniques at the US Naval Research Laboratory were etched with sequential XeF_2 and BCl_3 exposures. GaN etch rates varied from 0.18 to 0.72 Å/cycle at temperatures from 170 to 300°C, respectively (see Supplemental Figure 1). Because the GaN etch rates were self-limiting versus BCl_3 exposure and BCl_3 pressure, the GaN etching mechanism is believed to involve XeF_2 fluorination of GaN to GaF_3 and then ligand-exchange between BCl_3 and GaF_3 to yield volatile BCl_wF_x and GaF_yCl_z species. GaN fluorination using a NF_3 plasma was also successful for etching crystalline GaN at 250°C.

Ga_2O_3 samples deposited using ALD techniques were etched with sequential HF and BCl_3 exposures. Ga_2O_3 etch rates varied from 0.59 to 1.35 Å/cycle at temperatures from 150 to 200°C, respectively. The Ga_2O_3 etch rates were self-limiting versus HF and BCl_3 exposure. Ga_2O_3 ALE was also

performed using HF for fluorination and a variety of metal precursors for ligand-exchange. Ga_2O_3 etch rates at 250°C were 0.2, 0.8, 1.1 and 1.2 Å/cycle for $Ga(N(CH_3)_2)_3$, $TiCl_4$, $Al(CH_3)_3$ and $AlCl(CH_3)_2$ as the metal precursors, respectively (see Supplemental Figure 2). The wide range of metal precursors that can etch Ga_2O_3 argues that the ligand-exchange reaction with GaF_3 is facile.

11:40am AP+PS+TF-ThM-12 Mechanistic Insights into Thermal Dry Atomic Layer Processing of Metals, *Andrew Teplyakov,* University of Delaware
INVITED

The mechanisms of thermally induced reactions of atomic layer deposition (ALD) and atomic layer etching (ALE) can be sometimes viewed as proceeding in opposite directions. However, for atomic layer processing of metals, that would mean that the best designed and most efficient reaction pathways leading to metal deposition would produce insurmountable energy barriers for a reverse process. If ligand detachment, exchange, and decomposition could be desirable for ALD, the etching of the same metals would require careful consideration of the etching mechanisms at the atomic and molecular level. Given that the mechanisms of ALE can be very complex, the key concepts and approaches will be described here for thermal dry etching processing, which would allow for eliminating the role of solvents and for distinguishing thermodynamic and kinetic regimes of etching. The mechanistic investigation of thermal dry etching of cobalt will be the primary target of this work. This process will be used to illustrate the limitations of the single-reagent etching by analyzing the reaction of 1,1,1,5,5,5-hexafluoro-2,4-pentanedione (hexafluoroacetylacetone, hfacH) or 2,4-pentanedione (acetylacetone, acacH)) with a clean cobalt surface. Then the effects of surface oxidation and chlorination will be explored as a means of kinetically controlled process. Finally, a number of potential effects of the mechanisms of dry etching on the morphology of the surfaces produced and, specifically, on the "smoothing" effect of dry etching will be discussed.

Applied Surface Science Division
Room A211 - Session AS-ThM

Advances in Depth Profiling, Imaging and Time-resolved Analysis

Moderators: Jeffrey Fenton, Medtronic, Inc., Carl A. Ventrice, Jr., SUNY Polytechnic Institute

8:00am AS-ThM-1 What Really Lies Beneath the AVS Surface? Depth Profiling Can Help Provide the Answer, *Fred Stevie, C Zhou, R Garcia,* North Carolina State University **INVITED**

Scratch the surface of the AVS and you will find a lot more than semiconductors. AVS Divisions range from electronic materials to thin films to vacuum technology to biomaterials.

Depth profiles obtained using AES, XPS, or SIMS have typically been used to provide in-depth elemental analysis. SIMS excels in depth resolution and detection limit. Rotation of the sample during analysis (Zalar rotation) can maintain good depth resolution for materials that do not sputter evenly. Application of electron beams aids the study of insulators. Standards can be created to quantify the elemental components. [1]

Analysis in depth of biomaterials has shown tremendous strides as the sources used to remove material have evolved. Initial studies of depth profiles with argon, then molecular beams such as SF_5^+, larger still with C_{60}^+, and now cluster beams with argon produced ever higher secondary ion yields and made possible in-depth analysis without loss of chemical state. Continued development has resulted in three-dimensional organic analysis. [2] Some success has been achieved for quantification of organic additives, especially when the additive contains an element not present in the matrix. [3-4]

A significant limitation is the achievable depth. Profiles are typically less than 100 μm. However, some technologies need depth information on a millimeter scale. Sample preparation methods, such as etching, beveling, cross sections, and back side analysis, can be employed. Cryogenic microtome can be used to obtain a cross section of organic layers subsequently analyzed with ToF-SIMS. [5] EDS can provide in depth information on samples where material has been removed at a series of depths using FIB. [6] The emergence of plasma FIB (PFIB) instruments with microamp currents makes possible deeper profiles and exposure of larger areas for analysis by other techniques. The xenon plasma FIB can remove material as much as 50 times faster than a conventional gallium FIB. [7,8]

[1] Secondary Ion Mass Spectrometry, F. A. Stevie, Momentum Press (2016)

[2] J. Bailey, R. Havelund, A. G. Shard, I. S. Gilmore, M. R. Alexander, J. S. Sharp, D. J. Scurr, ACS Appl. Mater. Interfaces 7, 2654 (2015)

[3] Chaunzhen Zhou, Fred A. Stevie, Stephen C. Smith, J. Vac. Sci. Technol. B36, 03F115 (2018)

[4] S. C. Smith, C. Zhou, F. A. Stevie, R. Garcia PLOS ONE 13, e0209119 (2018)

[5] C. Zhou, D. Sun, R. Garcia, F. Stevie, Anal. Methods 10, 2444 (2018)

[6] R. Garcia, F. A. Stevie, L. Giannuzzi, Microscopy and Microanalysis Proceedings (2019)

[7] Noel S. Smith, John A. Notte, and Adam V. Steele, MRS Bulletin 39, 330 (2014)

[8] www.tescan.com/en-us/technology/fib-sem/

8:40am **AS-ThM-3 TOF-SIMS Tandem MS Imaging of (Sub-)Monolayer Coatings for Device Processing**, *David M. Carr*, *G Fisher,* Physical Electronics

One common objective in research, failure analysis and reverse engineering is to ascertain the 2D/3D composition and structure of molecules in devices as a result of various processing steps. Often there is insufficient background information and a lack of reference spectra to properly interpret the analytical observations. Two device processing case studies will be presented highlighting the benefits of adding MS/MS imaging to conventional TOF-SIMS experiments. The data was acquired on a PHI *nanoTOF* II designed for simultaneous TOF-SIMS (MS^1) imaging and tandem MS (MS^2) imaging [1-4].

In the first case study, a carbon residue was observed by Auger electron spectroscopy (AES) imaging on e$^-$ beam lithography-patterned and etched device structures. TOF-SIMS tandem MS imaging was applied to characterize the composition and structure of the sub-monolayer residues. In the second case study, functionalized molecules containing bipyridine and triphenylphosphine ligands were patterned by a photolithography method and loaded with metals including Au, Pd and Pt [5]. TOF-SIMS tandem MS imaging was employed to confirm the presence and elucidate the structure of metal-organic ligands.

References

[1] G.L. Fisher, *et al*, *Anal. Chem*. **88** (2016) 6433-6440.

[2] G.L. Fisher, *et al*, *Microscop. Microanal*. **23** (2017) 843-848.

[3] C.E. Chini, *et al*, *Biointerphases* **13** (2018) 03B409.

[4] T. Fu, *et al*, *Nature Sci. Rep*. (2018) accepted 06 December 2018.

[5] R. Müller and A. Welle at Karlsruhe Institute of Technology (KIT) and C. Barner-Kowollik at Queensland University of Technology (QUB) are acknowledged for providing the samples for analysis.

9:00am **AS-ThM-4 TOF-SIMS at the Edge**, *Alan Spool, D Bilich,* Western Digital Corporation

TOF-SIMS instruments are designed to extract secondary ions in the direction normal to the surface by creating a potential difference between the sample and the extraction device. The optimum geometry for getting the highest transmission is for the sample to consist of a functionally infinite flat plane. When sample topography deviates from this ideal significantly, secondary ion transmission is reduced. The effect on the yield of each secondary ion is a function of the ion mass, but also the initial ion emission angular and momentum magnitude distributions. The yields of the lightest atomic ions are least affected by topography, and the yields of heavier molecular fragments and ions most significantly affected.

To quantitatively explore these effects, two samples presenting topographic challenges were used in this study.

1. The edge of a magnetic recording disk is tightly controlled and therefore reproducible. The disk is extremely flat. The surface produces homogeneous signals for atomic species and molecular fragments of the disk lubricant and adsorbed hydrocarbons and other organic species where ion yield is not affected by topography. There is a slight bevel at the edge, much smaller in size than the edge effect on secondary ion collection. The sample height drop off past the edge in this experiment was effectively infinite.

2. A Si coupon was etched to produce a deep enough crater that ion yields from the crater bottom were affected by the topography. A lighter etch was performed over a wider area sufficient to reach dynamic equilibrium (and thus produce a surface damaged identically to that at the crater bottom). The sample was then exposed to air and allowed to oxidize and be contaminated by adventitious organics before analysis. This sample represents the condition where at a distance from the sample, the surface is essentially flat, but near to the surface the ion extraction will see non-normal fields that affect secondary ion trajectories.

With these samples, it was possible to look at the effect of the topography on the yields of a variety of secondary ions, and at a variety of instrumental conditions, both in the IonTof TOF-SIMS 5 and in the Physical Electronics NanoTof II. The analysis results of the two types of topographic challenges are shown to be differently affected by instrumental conditions. No one condition gives the ideal remediation for all topographic challenges.

The work with the edged sample promises to provide a simple test for differences in the initial angular and momentum magnitude distributions. Such distributions may provide added clues to secondary ion formation mechanisms.

9:20am **AS-ThM-5 Variation of SIMS Secondary Ion Yield of Si and Mg Dopants in GaN Grown by MOCVD**, *M. K. Indika Senevirathna,* Clark Atlanta University; *A Kozhanov, M Vernon, G Cross,* Georgia State University; *G Cooke,* Hiden Analytical Ltd, UK; *M Williams,* Clark Atlanta University

We present a study of the secondary ion yield of silicon and magnesium dopant species as a function of the primary ion beam energy in n-doped and p-doped gallium nitride, respectively. The epilayers were grown by metal organic chemical vapor deposition and depth profiled using a Hiden quadrupole secondary ion mass spectrometer. To our knowledge, this is the first such study for this matrix material system. The yields for oxygen and cesium primary beams were determined by varying the beam acceleration voltage of the primary ion beam from 0.5 kV to 5 kV at a fixed beam current. The results determine the primary beam energies for optimal species sensitivity.

9:40am **AS-ThM-6 Impact of the Molecular Weight on the Depth Profiling of Polymer Thin Films using Low Energy Cs$^+$ Sputtering**, *Amal Ben Hadj Mabrouk,* Univ. Grenoble Alpes, CEA, LETI, Grenoble; *M Veillerot,* Univ. Grenoble Alpes, CEA, LETI, Grenoble, France; *A Chateauminois,* Soft Matter Science and Engineering Laboratory (SIMM), PSL Research University, France; *C Licitra,* Univ. Grenoble Alpes, CEA, LETI, Grenoble

Organic materials have been taking an increasing role in the world of electronic systems. They provide process compatibility, flexibility and adaptability in design, and the capacity for integration of electronic functions. They can be found in thin submicronic layers in various fields such as organic photovoltaic items or organic light emitting diodes . In order to determine and control the final device properties, it is of first importance to control the organic materials structural parameters during film growth or deposition. Time of Flight Secondary Ion Mass Spectrometry (ToF-SIMS) is able to provide such depth resolved relevant molecular information. Indeed, it has recently been shown that the ToF-SIMS sputtering response was sensitive to the molecular weight of thin polymer films bombarded with Argon gas cluster ions (Ar$_n^+$) [1].

In this work, we aimed to supplement these results when depth profiling is achieved with low energy cesium ions. We present the ToF-SIMS characterization of Poly (methyl methacrylate) and Polystyrene thin films [~100nm in thickness] with varying molecular weights (from 2 to 9.9×10^5 g.mol^{-1}) spin-coated onto silicon substrates. The characterization was carried out using monoatomic cesium source at different energies for sputtering and bismuth (Bi$_3^+$) ion source for analysis.

The evolution of the sputtering yield volume (nm^3/PI) of the polymer films has been measured with the molecular weight, thickness, temperature and for different energies of sputter beam. The results are considered with respect of previous results and interpreted considering polymeric material physical parameters such as the glass transition temperature (Tg).

[1] Cristaudo V., Poleunis C., Czerwinski B. and Delcorte A. (2014) *Surf. Interface Anal.*, 46, pages 79–82, doi: 10.1002/sia.5424 .

11:00am **AS-ThM-10 Probing the Surface Structure of Au-Pt Core-Shell Nanoparticles**, *C Engelbrekt, Ich Tran, M Law,* University of California, Irvine

Au-Pt core-shell structures (Au@Pt) of atomically-thin platinum shells on gold nanoparticle (NP) cores have been developed through a mild aqueous one-pot synthesis protocol. The loading and homogeneous deposition of Pt on the starch-capped Au NPs can be finely tuned by simply adjusting concentration and the reduction rate of the Pt precursor from 0 to 30 wt% Pt. These Au@Pt NPs have shown impressive catalytic performance for a range of energy relevant reactions due to inherently improved activity of the Pt shells through synergetic interaction with the Au cores.[1,2] Details of

the core-shell interface, in particular the atomic-scale and electronic structure of the metal catalyst surface, are crucially important to understand and optimize catalytic properties of the Au@Pt NPs. Characterizing the surface of small nanoparticles with this sensitivity is challenging and most convincingly done by elemental mapping with TEM. However, for Au and Pt, which are very close in atomic mass, lattice parameters and X-ray emission lines, this approach is not sufficient. Here, we have used an array of surface sensitive spectroscopic techniques to characterize the structure of the bimetallic NP surface – specifically, detailed analysis of XPS core-level and valence band photoemission spectra, in combination with elemental analysis using ion scattering spectroscopy (ISS). ISS provides the elemental composition of the surface-exposed atoms, which is very difficult to probe with other techniques. We show that the interface structure involves surface alloying, and sub-surface Pt localization, rather than a simple formation of the Pt overlayer in Au@Pt NPs. Furthermore, time-dependent ISS can potentially be used as a gentle (mild) depth-profiling characterization technique for this kind of core-shell structure and a comparison with a depth-profiling characterization using argon cluster modes will be discussed.

(1) Engelbrekt, C.; Šešelj, N.; Poreddy, R.; Riisager, A.; Ulstrup, J.; Zhang, J. "Atomically thin Pt shells on Au nanoparticle cores: facile synthesis and efficient synergetic catalysis", *J. Mater. Chem. A* **2016**, *4* (9), 3278–3286.

(2) Seselj, N.; Engelbrekt, C.; Ding, Y.; Hjuler, H. A. H. A.; Ulstrup, J.; Zhang, J. "Tailored Electron Transfer Pathways in Au core /Pt shell -Graphene Nanocatalysts for Fuel Cells", *Adv. Energy Mater.* **2018**, *1702609*, 1702609.

11:20am AS-ThM-11 Correlating Multiple Data Streams for Valence State Identification in Transition Metal Oxide during XPS Depth Profiling, *Zhenzhong Yang, C Wang, M Engelhard, Z Zhu, Y Du,* Pacific Northwest National Laboratory

Transition metal oxides (TMO) of perovskite (ABO$_3$) structures exhibit a broad range of structural, compositional, and functional properties, which can be further tuned or even drastically transformed by means of judicious defect engineering. TMOs have a unique capability to incorporate large amount of oxygen defects owing to the multivalence nature of the transition metal cations, which can be directly probed by XPS. XPS is a surface sensitive technique. In order to study the deeper layers, depth profiling by Ar sputtering is often adopted. However, the sputtering process may change the valence state of the transition metal cations, and thus the data analysis affected by the data acquisition condition can be inaccurate or erroneous.

In this talk, using perovskite SrCrO$_3$ and its reduced structure, SrCrO$_{2.8}$, as model (SCO) materials, I will show how the XPS depth profiling data can reveal the valence state change and redox chemistry occurring in the deeper layers of the SCO thin films. In our experiments, the XPS Cr*2p* spectra suggested that a tensile strain applied by the substrate could stabilize the reduced SrCrO$_{2.8}$ structure near the interface (~10 nm) region. To examine whether the conclusion is correct, we compared SCO samples with different strain states and processing history. By correlating x-ray diffraction (XRD), transmission electron microscopy (TEM), time -of-flight secondary ion mass spectrometry (ToF-SIMS) data and density functional theory calculations, we achieved quantitative agreement and concluded that the Cr 2p spectra were not affected by the Ar beam during the XPS depth profiling process.

11:40am AS-ThM-12 Using Atom Probe Tomography for Three-dimensional Visualization of Sb Segregation in InAs/InAsSb Superlattices, *Nicole Kotulak, J Nolde, M Twigg, K Knipling,* U.S. Naval Research Laboratory*; D Lubyshev, J Fastenau, A Liu,* IQE Inc.*; E Aifer,* U.S. Naval Research Laboratory

Developing materials for mid-wavelength infrared (MWIR) photodetectors has been ongoing, with recent focus on structures that can operate at higher temperatures and across a larger portion of the MWIR range. In recent years, InAs/InAsSb strained layer superlattices (SLS) have been extensively studied and shown to achieve these performance parameters, out-performing the incumbent technologies [1]. Over the course of InAs/InAsSb SL development, as well as in similar Sb-containing device structures, it has been observed that Sb does not remain strictly within the intended layer [2-4].

The segregation of non-common-atoms at a growth interface and into the following layer leads to non-abrupt and asymmetric interfaces, which can cause changes to the optoelectronic properties of the SLS, including fundamental parameters such as band gap and effective mass [2,5,6]. For devices that rely on the precise engineering of the optoelectronic properties of the SLS in order to accomplish performance metrics, non-abrupt interfaces can, ultimately, detrimentally affect device performance, impacting suitability for specific tasks and environments [7]. Understanding the layer compositions at a near atomic-scale can enable these non-idealities to be included in bandstructure simulations to enable device design and optimization [8,9].

In this work, we use atom probe tomography (APT) to harvest 3D compositional data in an MWIR nBn T2SL photodetector consisting of 734 periods of alternating InAs and InAsSb, of which 31 total periods were analyzed. The resulting analysis shows a non-negligible concentration of Sb in the InAs layers, as well as a below-target Sb concentration in the InAsSb layers. While the background concentration of Sb stays consistent as growth of the T2SL progresses, there is an observable increase in the peak Sb concentration from the earliest-grown periods analyzed to the last-grown. These profiles demonstrate corroboration of a non-binary Sb profile observed using complementary techniques, and serve to assist in improving models of Sb-containing SLS for the development of high performance photodetectors.

[1] D. Z. Ting, et al., IEEE Photonics Journal 10, 6804106 (2018).

[2] J. Steinshnider, et al., Phys Rev Lett 85, 2953–2956 (2000).

[3] H. Haugan, et al., J Cryst Growth 436, 134–137 (2016).

[4] K. Kanedy, et al., Appl. Phys. Lett. 112, 042105 (2018).

[5] M. W. Wang, et al., Appl. Phys. Lett. 66, 2981 (1995).

[6] S. B. Rejeb, et al., J Phys D: Appl. Phys 43, 325102 (2010).

[7] K. Shiralagi, et al., J of Elec Materi 26, 1417–1421 (1997).

[8] X. Lü, et al., Appl. Phys. Lett. 104, 232106 (2014).

[9] F. Szmulowicz, et al. Phys. Rev. B, 69, 155321 (2004).

12:00pm AS-ThM-13 Multi-technique Surface Analysis of Graphenes, *Kateryna Artyushkova,* Physical Electronics and University of New Mexico*; B Schmidt, J Mann, A Ellsworth, J Newman,* Physical Electronics

Several techniques currently being used to determine the thickness of graphene films include optical contrast, Raman and scanning probe microscopy. These methods provide accurate information on thickness but limited information on other important parameters as chemical purity, homogeneity of coverage and defect density. Surface analytical techniques, such as X-ray Photoelectron Spectroscopy (XPS) and Time-of-Flight Secondary Ion Mass Spectrometry (TOF-SIMS), have the potential to fill this gap.

Surface analysis of graphene poses multiple challenges. The thickness of single-layered graphene is on the order of 0.4 nm, while even the most surface-sensitive spectroscopic techniques have on the order of 1-5 nm sampling depth. The surface carbon contamination due to adventitious carbon adds another level of complexity in trying to understand graphene chemistry and homogeneity accurately.

In this report, we will present an analysis of commercially available graphene samples prepared on several types of substrates, such as SiO2 and PET. The chemical structure and thickness of graphene samples were studied by a combination of XPS and TOF-SIMS depth profiling and angle-resolved XPS. The challenges and successes of this multi-technique analysis of graphene will be discussed.

Chemical Analysis and Imaging Interfaces Focus Topic
Room A120-121 - Session CA+2D+AS+BI+NS-ThM

Chemical Analysis and Imaging of Liquid/Vapor/Solid Interfaces II

Moderators: Utkur Mirsaidov, National University of Singapore, Xiao-Ying Yu, Pacific Northwest National Laboratory

8:00am CA+2D+AS+BI+NS-ThM-1 From Surfaces to Solid-Gas and Solid-liquid Interfaces: Ambient Pressure XPS and Beyond, *Miquel B. Salmeron,* Lawrence Berkeley Lab, University of California, Berkeley **INVITED**

The rapidly increasing field of surfaces under ambient conditions of temperature and pressure, in gas and liquid environments, reflects the importance of understanding surface properties in conditions closer to practical situations. A lot of progress has been made in the last two decades, enabled by the emergence of a number of new techniques, both spectroscopy and microscopy, that can deliver atomic scale information with the required surface/interface sensitivity. I will present recent advances with examples that illustrate the novel understanding derived from the use of new techniques. One in the gas–solid interface where two

important barriers have been bridged: the pressure gap, and the temperature gap. These gaps are very important when dealing with weakly bound molecules, where only in the presence of gas at a suitable pressure, or at low temperatures, a non-negligible coverage of adsorbed molecules can be achieved. The temperature gap manifests also in the removal of kinetic barriers. By bridging these two gaps a host of new interface structures have been unveiled that bring new understanding to catalytic phenomena. This will be illustrated with the examples of Cu and CuCo alloys in the presence of CO. In the case of solid-liquid interfaces, the introduction of new methods using well established x-ray spectroscopies is opening the way to the study of the important electrical double layer structure as a function of applied bias, as I will illustrate with the application of X-Ray absorption and IR to sulfuric acid-Pt and Ammonium Sulfate-graphene interfaces.

8:40am **CA+2D+AS+BI+NS-ThM-3 Probing Solid-liquid Interfaces with Tender X-rays**, *Zbynek Novotny*, *N Comini*, *B Tobler*, University of Zuerich, Switzerland; *D Aegerter*, *E Fabbri*, Paul Sherrer Institute, Switzerland; *U Maier*, Ferrovac GmbH, Switzerland; *L Artiglia*, *J Raabe*, *T Huthwelker*, Paul Sherrer Institute, Switzerland; *J Osterwalder*, University of Zuerich, Switzerland

Many important chemical and biological processes occur at the interface between a solid and a liquid, which is difficult to access for chemical analysis. The large inelastic scattering cross section of electrons in the condensed matter makes X-ray photoelectron spectroscopy (XPS) highly surface sensitive but less sensitive to buried interfaces. This limitation can be overcome by stabilizing an ultrathin layer of liquid with a thickness in the order of a few tens of nanometres and by employing tender X-rays (photon energy ranging between 2-8 keV) that can be used to probe the buried solid-liquid interface. We have recently built and commissioned a new instrument at the Swiss Light Source that combines ambient-pressure XPS with in-situ electrochemistry. With this new setup, we can stabilize a thin liquid layer on a solid surface by a dip&pull method [1], and by using tender X-rays (2-8 keV) from the Phoenix beamline, we can probe the properties and chemistry at the solid-liquid and liquid-gas interface while having a potential control over the ultrathin electrolyte film. The capabilities of this new instrument were demonstrated during the first commissioning beamtime, where we stabilized a thin electrolyte layer (0.1 M KOH) over the Ir(001) electrode. The dip&pull technique was used for the first time using well-defined single-crystalline surfaces (see Supplementary document). Core-level binding energy shifts following the applied potential were observed for species located within the electrolyte film. This included the oxygen 1s level from liquid water, potassium, and, interestingly, also an adventitious carbon species, while the interface was carbon-free. We will present the results from the first commissioning beamtime and outline the future directions we are going to pursue using this new instrument.

[1] S. Axnanda, E. J. Crumlin et al., Sci. Rep. 5, 09788 (2014).

9:00am **CA+2D+AS+BI+NS-ThM-4 X-ray Photoelectron Spectroscopy Insight into X-ray Induced Radiolysis at Heterogenous Liquid Electrolyte Interface**, *Christopher Arble*, National Institute of Standards and Technology (NIST); *H Guo*, Southeast University, China; *E Strelcov*, *B Hoskins*, National Institute of Standards and Technology (NIST); *M Amati*, *P Zeller*, *L Gregoratti*, Elettra-Sincrotrone Trieste, Italy; *A Kolmakov*, National Institute of Standards and Technology (NIST)

Assessing chemical processes of electrolyte interfaces under operando conditions is an aspirational goal of great importance to many industrial applications[1] that remains technically challenging to investigate. XPS is a powerful characterization tool that can probe elemental and chemical information of atoms with nanoscale depth sensitivity but has traditionally been restricted to UHV conditions. There has been a concerted effort to enable quantitative in-situ measurements of gas and liquid interfaces under realistic environments.[2-4] Recently, advances in 2D materials, i.e., graphene, have been utilized to probe heterogenous interfaces through molecularly impermeable, electron transparent membranes to maintain UHV pressure in the analysis chamber.[5]

Herein we apply photoemission spectromicroscopy to study the electrochemical dynamics of an array of several thousand individual electrolyte cells encapsulated with electron transparent bilayer graphene.[6] We monitored the chemical speciation at the electrode- aqueous $CuSO_4$ electrolyte interface as a function of potential. During the electrochemical experiments, the effects of irradiation upon the solution were observed to influence the system, and spectral deconvolution identified oxidized species of copper and oxygen as well as reduced states of sulfur that were

connected to reaction pathways tied with radiolysis. Corresponding SEM images and subsequent EDS spectral maps display spatially confided irradiated byproducts which can be associated with the species observed in with XPS.

Observations of XPS spectroscopic regions in the system were taken at varied X-ray dosages to probe the impacts of radiolysis on the liquid solution concerning the spectroscopic observation of electrochemical deposition of Cu. This experimental methodology imparts a greater understanding of the influence of X-ray induced water radiolysis processes towards the quantification of the electrode/electrolyte interfaces and the underlying dosages necessary for artifact-free data acquisition in condensed media.

References:

1. Saveant, J., *Chemical Reviews* **2008,** 108, (7), 2348-2378

2. Siegbahn, H., *J. Phys. Chem.* **1985,** 89, (6), 897-909

3. Salmeron, M.; Schlögl, R., *Surf. Sci. Rep.* **2008**, 63, (4), 169-199

4. Starr, D.; et al., *Chem. Soc. Rev.* **2013**, 42, (13), 5833-5857

5. Kraus, J.; et al., *Nanoscale* **2014** 6, (23), 14394-14403

6. Yulaev, A.; et al., *ACS Appl. Mater. Interfaces* **2017**, 9, (31) 26492-26502

9:20am **CA+2D+AS+BI+NS-ThM-5 Theoretical Investigation of Reactivity at Complex Solid-Liquid Interfaces**, *Roger Rousseau*, Pacific Northwest National Laboratory **INVITED**

Contrary to solid/gas interfaces, in solid/liquid interfaces the molecules in the liquid can be organized such that those near the surface are appreciably different from the bulk. This can be impacted by: the composition of the liquid phase, the size shape and loading of nanoparticles and the hydro/lypophilicity of the support. In this talk. we will outline the findings from our ongoing studies of both thermal and electrochemically driven hydrogenation of organic molecules. We will present both classical and ab into molecular dynamics calculations that simulate the structure and composition within the double both at the support as well as on surface of catalytic nanoparticles. The calculations explicitly identify the different roles of entropy and binding energy on the activity and selectivity of solution phase hydrogenation. A first example [1] shows how phenol/water mixtures behave on hydrophilic and lipophilic surfaces, and provides a possible explanation as to why a higher phenol hydrogenation conversion is observed [2] on Pd catalysts on hydrophilic surfaces than on lipophilic surfaces. We show how reaction rates can be manipulated by changing the concentration of phenol adjacent to the catalysts through modification of the degree of support hydrophilicity, size and loading of nanoparticles, and temperature. In a second example [3], we simulate the speciation on a Au and graphitic carbon cathodic surface of a complex solvent mixture containing organics, salts, acids, as a function of cathode charge and temperature. Here we show that the ability to transfer an electron to the organic is governed by the amount of organic in the double layer as well as its orientation with repsect to the electrode surface. While both examples included have been drawn from the upgrading of bio-oil ex pyrolysis, the principles shown are relevant to any application in heterogeneous catalysis with condensed reaction media.

References

1. Cantu DC, Wang YG, Yoon Y, Glezakou VA, Rousseau R, Weber RS. 2016, Catalysis Today, http://dx.doi.org/10.1016/j.cattod.2016.08.025

2. Perez Y, Fajardo M, Corma A. 2011, Catalysis Communications, 12, 1071-1074.

3. Padmaperuma AB, Cantu DC, Yoon Y, Nguyen MT, Wang YG, Glezakou VA, Rousseau R, Lilga MA. Manuscript in preparation, to be submitted.

11:00am **CA+2D+AS+BI+NS-ThM-10 In-situ/Operando Soft X-ray Spectroscopy for Interfacial Characterization of Energy Materials and Devices**, *Y Liu*, *X Feng*, *Jinghua Guo*, Lawrence Berkeley National Laboratory

In-situ/operando soft x-ray spectroscopy offers unique characterization in many important energy materials of energy conversion, energy storage and catalysis in regards to the functionality, complexity of material architecture, chemistry and interactions among constituents within.

It has been found that the microstructure and composition of materials as well as the microstructure evolution process have a great influence on performances in a variety of fields, e.g., energy conversion and energy storage materials, chemical and catalytic processes. In-situ/operando x-ray spectra characterization technique offers an opportunity to uncover the phase conversion, chemical environment of elements and other critical

information of solid/liquid interfaces in real time. We will present soft x-ray spectroscopy characterization techniques, e.g. soft x-ray absorption spectroscopy (XAS) and resonant inelastic soft x-ray scattering (RIXS), and the development of in situ/operando capabilities for the characterization of interfacial phenomena in energy materials and devices.

A number of the experimental studies, which revealed the catalytic and electrochemical reactions in real time, will be presented, e.g. solid (metal film)/liquid (water) electrochemical interface, Mg-ion batteries, and Li-S batteries [1-5]. The experimental results demonstrate that in-situ/operando soft x-ray spectroscopy characterization provides the unique information for understanding the real reaction mechanism.

References:

1. "Mg deposition observed by in situ electrochemical Mg K-edge X-ray absorption spectroscopy", T. S. Arthur, P.-A. Glans, M. Matsui, R. Zhang, B. Ma, J.-H. Guo, Electrochem. Commun. **24**, 43 (2012)

2. "The structure of interfacial water on gold electrodes studied by x-ray absorption spectroscopy", J. J. Velasco-Velez, C. H. Wu, T. A. Pascal, L. F. Wan, J.-H. Guo, D. Prendergast and M. Salmeron, Science **346**, 831 (2014)

3. "Nucleophilic substitution between polysulfides and binders unexpectedly stabilizing lithium sulfur battery", M. Ling, L. Zhang, T. Zheng, J. Feng, J.-H. Guo, L. Mai, G. Liu, Nano Energy **38**, 82 (2017).

4. "Interfacial insights from operando sXAS/TEM for magnesium metal deposition with borohydride electrolytes", T. Arthur, P.-A. Glans, N. Singh, O. Tutusaus, K. Nie, Y.-S. Liu, F. Mizuno, J.-H. Guo, D. H. Alsem, N. Salmon, R. Mohtadi, Chem. Mater. **29**, 7183 (2017).

"Revealing the Electrochemical Charging Mechanism of Nanosized Li2S by in Situ and Operando X-ray Absorption Spectroscopy", L. Zhang, D. Sun, J. Feng, E. Cairns, J.-H. Guo, Nano Lett. **17**, 5084 (2017).

11:20am **CA+2D+AS+BI+NS-ThM-11 The Importance of Amino Acid Adsorption on Polymer Surfaces in *P. Aeruginosa* Biofilm Formation**, *Olutoba Sanni,* University of Nottingham, UK

High throughput materials discovery screens have revealed polymers that reduce bacterial surface colonization which have progressed to currently ongoing clinical trials [Hook *et al*. Nature Biotech 2012]. These novel poly (meth)acrylate coatings reduced biofilm formation by *Pseudomonas aeruginosa, Staphylococcus aureus* and *Escherichia coli* in laboratory cultures *in vitro* and *in vivo* in a mouse foreign body infection model. These coatings are known to function by preventing biofilm formation, however why the bacterial cells respond in this way to these polymers has yet to be elucidated. The initial interaction between bacteria and surfaces has been identified as a key determining factor when bacteria decide to either irreversibly attach and colonise a surface or not.

The exposure of most materials to biological milieu is accompanied by adsorption of biomolecules. In protein containing media there is a strong relationship between the adsorbed protein layer formed on materials and mammalian cell attachment. However, in protein-free media such as used by Hook et al., this cannot be a contributor to early bacterial cell attachment. Consequently, here we carry out careful surface chemical analysis on two polymers known to exhibit drastically different biofilm formation in a standard protein-free, amino acid containing bacterial culture medium (RPMI).

Time of flight secondary ion mass spectrometry (ToF-SIMS) and X-ray photoelectron spectroscopy (XPS) analysis determined that high amino acid adsorption correlates with the surface exhibiting low *P. aeruginosa* colonisation. A total of 10 peaks characteristic of specific amino acids were identified by ToF-SIMS to be adsorbed on polymer. We successfully fitted the Freundlich and Langmuir adsorption isotherm models from which we determined adsorption capacity of polymers, calculated the on/off rate of amino acid adsorption on both anti-biofilm and pro-biofilm surfaces. With XPS, the overlayer coverage of amino acids on the polymer surface was established to be approximately 0.2 nm.

The study was extended to quantify in high throughput manner the adsorption of amino acids from RPMI media onto surfaces of 288 polymer materials printed onto a microarray. Ion fragments generated from ToF-SIMS were used to produce a regression model from which we identified polymers with cyclic moieties as major promoters of amino acid adsorption.

This is the first report suggesting adsorbed amino acids or other adsorbed nutrients may correlate with the biofilm formation tendency of materials.

Fundamental Aspects of Material Degradation Focus Topic
Room A212 - Session DM+BI+SS-ThM

Material Stabilities and Technology for Degradation Protection
Moderators: Markus Valtiner, Vienna University of Technology, Austria, Gareth S. Parkinson, TU Wien, Austria

8:00am **DM+BI+SS-ThM-1 Extremely Thin Protective Oxide Layer for Reflective Silver Thin Films**, *Midori Kawamura, E Kudo, Y Sasaki, T Kiba, Y Abe, K Kim,* Kitami Institute of Technology, Japan*; H Murotani,* Tokai University, Japan

Silver (Ag) thin films possess high electrical and optical properties, but their low stability should be resolved. We have developed a highly stable Ag thin film where thermal agglomeration can be suppressed, by utilizing nanometer thick surface Al layers. Then we have confirmed that Al surface nanolayer deposited Ag films show a high optical reflectance as well as Ag single film. Here, the Al nanolayer was oxidized to be Al oxide nanolayer, being transparent in visible region, by natural oxidation in air. In the present study, we investigate durability of the Ag films with surface nanolayers under high humidity condition.

We prepared Ag single layer (150 nm), Ti (1, 3 -nm) / Ag films and Al (1, 3 - nm) / Ag films on glass substrate by rf magnetron sputtering in Ar discharge. In addition, vacuum evaporation method was also used for the preparation of Al (1, 3 -nm) / Ag films. A difference on degradation of the films by different fabrication methods was investigated. The samples were kept for 16 hrs in a chamber where temperature and humidity was set to 55°C and 90%RH, respectively.

After the test, agglomeration occurred in Ag single layer and optical reflectance was decreased. On the other hand, Ti or Al nanolayer covered Ag films kept smooth surface even after the test. The surface roughness observed using AFM was as small as 1.0 nm. As a result, we have found that both Al and Ti surface nanolayers can play significant role as protective layer under high humidity condition. However, Ti / Ag films showed a lower reflectance due to light absorption by TiO_2 layer formed on the surface, and the samples with Al surface nanolayer showed a higher optical reflectance.

By XPS analysis, very thin Ag sulfide formation was observed in Ag single film after the humidity test, but not in Ti or Al covered Ag films. This suggests very thin Al oxide or Ti oxide nanolayer prevented contact of Ag atoms and SO_2 gas in air. However, Ag signal was detected in the surface oxide layers, which indicates onset of outward diffusion of Ag atoms.

8:20am **DM+BI+SS-ThM-2 Influence of the Electric Double Layer on Degradation of Materials**, *Dominik Dworschak, M Valtiner,* Vienna University of Technology, Austria

Corrosion and adhesion science usually focuses on the solid side of a liquid/solid or solid/adhesive interface. However, the only some nanometer thick interface itself is the complex transition region which drives many important processes in corrosion and delamination. The electric double layer (EDL) is a key part of the interfacial region but remains mostly neglected as a potential key player in degradation processes. Here, we will demonstrate that the EDL has an important influence on the corrosion mechanism of passivating materials in the transpassive region (material dissolution at potentials where the passive film breaks down).

We utilize an electrochemical flow cell combined with an inductively coupled mass spectrometer (ICP-MS) to enable the in-situ study of the time-resolved release of elements into solution. This provides detailed insights into the nature of the passive and transpassive condition. As model systems, we use nickel based alloys. These are essential to modern industry and uniquely tailored for a wide range of applications, which rely on high corrosion and heat resistance. In particular, we polarized a series of $Ni_{75}Cr_{16}Fe_9$, $Ni_{86}Cr_5Fe_9$ as well as $Ni_{74}Cr_{16}Fe_9Mo_1$ model alloys in order to understand the effect of chromium concentration and molybdenum on transpassive dissolution

In the transpassive regime we can detect the presence of protective species of chromium and molybdenum on the surface. Unexpectedly, we can demonstrate significant corrosion resistance above a critical potential where the passive film breaks down. This is traditionally known as trans passive region with bulk dissolution of metal alloys. However, we find that the EDL forms a transient passivating solution side protective layer in the transpassive region – i.e. we characterize an electric double layer induced corrosion resistance, which solely – and surprisingly - lies in the structure of the solution side. This finding has general important implications for designing degradation resistance in highly corrosive environments.

8:40am DM+BI+SS-ThM-3 Key Issues for the Stability of Protective Surface Oxides, *Philippe Marcus,* CNRS - Chimie ParisTech, France **INVITED**
This lecture will focus on a surface science approach of corrosion and protection of metals and alloys, with emphasis on the structure and growth of surface oxide layers, a central theme in corrosion science.

Understanding early stage oxidation of metal surfaces at atomic or nanometric scale is a key to a better design and an improved control of engineering metals.

The following topics will be addressed:

- Nanostructure of ultra-thin oxide layers (passive films) on metals,

- Early stage oxidation of stainless steels,

- Local electronic properties of passive films,

- Mechanisms of initiation of localized corrosion, with emphasis on the role of surface defects in localized attack leading to corrosion,

The data that will be presented are obtained by using *in situ*Scanning Tunneling Microscopy (STM), Scanning Tunneling Spectroscopy (STS), X-Ray Photoelectron Spectroscopy (XPS), Time-of-Flight Secondary Ions Mass Spectrometry (ToF-SIMS) combined with electrochemical techniques and DFT calculations.

9:20am DM+BI+SS-ThM-5 Controlling and Observing Localized Dealloying Corrosion and Dissolution via Lateral Modification of Surfactant Inhibitor Layers, *S Neupane,* Hasselt University, Belgium*; Frank Uwe Renner,* IMEC vzw. Division IMOMEC, Belgium
Corrosion processes on metals and alloys may result in substantial degradation and loss of functionality. Mitigation strategies include alloy design, to allow for passivation, or the application of inhibitors to protect materials but they are often causing irreversible damage and potential catastrophic failure at more severe corrosion conditions. The ultimate understanding of the involved fundamental processes including the initial stages of corrosion attacks is still lacking, in particular on the important atomic and molecular scale. Surfactant inhibitors protect surfaces from corrosion by forming molecular layers or so-called self-assembled monolayers separating the material from the corrosive environment. Yet, with inhibitors *localized dealloying* takes place at higher electrochemical potentials [1]. To address the fundamental nature of the site of initiation of dealloying corrosion we have recently introduced different strategies for novel surface-science approaches [2]. On the one hand the inhibitor layer can be laterally modified by using a sequential application combining different steps of micro-contact printing and solution backfilling [3]. In consequence an array of artificial defects such as patch boundaries or displacements by overprinting using foreign impurity molecules can be obtained in a well-controlled way. On the other hand the molecular stability may be locally probed by molecular-scale force measurements employing AFM techniques. In the retract force curve molecular fishing events are eventually visible which can be correlated to the inhibition efficiency. We here exemplify both aspects on noble metal model systems such as Cu-Au and more reactive surfaces including Cu-Zn and pure Cu. On Cu-Au surfaces initial dealloying pits are occurring along patch boundaries formed by sequential application of thiol inhibitors [4]. On Cu surfaces we applied different mercapto-benzimidazoles and could indeed link the observed layer stability with the actual corrosion behavior.

[1] A. Pareek et al., J. Am. Chem. Soc.133 (2011) 18264–18271. [2] B. Shresta et al., Faraday Discuss. 180 (2015), 191. [3] S. Neupane et al., Langmuir. 34 (2018) 66–72. [4] S. Neupane et al., submitted.

9:40am DM+BI+SS-ThM-6 *In Situ* Characterization of Interactions at Polymer/Metal Oxide Interfaces Under Aqueous Conditions by a Spectroelectrochemical Approach, *Sven Pletincx,* Vrije Universiteit Brussel, Belgium*; L Fockaert, A Mol,* Delft University of Technology, Netherlands*; H Terryn, T Hauffman,* Vrije Universiteit Brussel, Belgium
The mechanisms governing coating/metal oxide delamination are not yet fully understood, although strong and durable adhesive interactions at the interface are considered to be an important prerequisite for good coating durability. Achieving adequate adhesion strengths between an organic and inorganic system in various operating conditions is one of the complex challenges of interface engineering. However, obtaining local chemical information at this solid/solid interface is challenging, since common surface sensitive analysis techniques only operate under vacuum conditions, making it impossible to probe environmental effects *in situ*.[1]

The analysis of this so-called buried interfaces is achieved by characterizing ultrathin polymer films onto a metal oxide substrate by ambient-pressure photoelectron spectroscopy (APXPS).[2] Here, we show that APXPS with a conventional X-ray source can be used to study the effects of water exposure on the interaction of acrylic coatings with aluminum oxide. This is done by making the polymer layer sufficiently thin to probe the interface non-destructively.

A *spectroelectrochemical* setup of in situ ATR-FTIR Kretschmann and Odd Random Phase Electrochemical Impedance Spectroscopy (ORP-EIS) on a complementary model system is used to characterize and monitor the formed bonds at the metal oxide/polymer interface.[3] A nanometer thin aluminum layer is sputtered on an IR transparent crystal, such that the IR signal reaches the oxide/polymer interface, obtaining a near-interface spectrum. This way, we have direct access to the interface, and the influence of an above-the-polymer electrolyte (i.e. H_2O) is probed. Simultaneously the protective properties and corrosion processes of the overall hybrid system are monitored by ORP-EIS.

This work shows that by using ultrathin films in combination with a set of recently developed techniques, it is possible to non-destructively and *in situ* probe interfacial changes in hybrid systems.

1. Watts, J. F. The Interfacial Chemistry of Adhesion: Novel Routes to the Holy Grail? *Adhes. Curr. Res. Appl.* 1–16 (2006). doi:10.1002/3527607307.ch1

2. Pletincx, S. *et al.* In Situ Characterization of the Initial Effect of Water on Molecular Interactions at the Interface of Organic/Inorganic Hybrid Systems. *Sci. Rep.***7**, 45123 (2017).

3. Pletincx, S. *et al.* In Situ Methanol Adsorption on Aluminum Oxide Monitored by a Combined ORP-EIS and ATR-FTIR Kretschmann Setup. *J. Phys. Chem. C***122**, 21963–21973 (2018).

11:00am DM+BI+SS-ThM-10 Design of Corrosion Resistant High Entropy Alloys, *Gerald Frankel, C Taylor, W Windl,* The Ohio State University*; J Scully,* University of Virginia*; J Locke,* The Ohio State University*; P Lu,* Questek Innovations **INVITED**
The corrosion resistance of a metal alloy is dictated by the exposure environment as well as the alloy structure, composition, and details of the surface condition such as the presence of a passive film. The design of new alloys with improved corrosion resistance must take all of these factors into account. As a result, the degrees of freedom in alloy design are so numerous that the standard process of trial and error is extremely lengthy, even using high throughput methods. This is particularly true for emerging materials such as high entropy alloys (HEAs) and bulk metallic glasses. The complexity of the corrosion process makes integrated computational materials engineering (ICME) for corrosion resistance very challenging. In this work we describe an approach for design of corrosion resistant alloys (CRAs) using ICME. The work has focused on HEAs because of the vast, multidimensional compositional and processing space associated with HEAs. The ultimate goal of CRA design is a combination of multiscale, multiphysics models that accurately describe the details of each of the controlling mechanisms and chemical/physical interactions in the degradation process. However, progress can be made using computational approaches coupled with empiricism. Calculation of Phase Diagrams (CalPhaD) methods are extremely useful in this regard. Furthermore, a number of relevant calculable parameters, such as metal-metal and metal-oxygen bond strength or chloride ion adsorption energies, can be used to create correlations with corrosion metrics that enable prediction of corrosion properties of alloys in previously unexplored compositional space. We will present the methodology used for the design of an extremely corrosion resistant HEA as well as a series of HEAs that are less resistant, but allow for the assessment of critical parameters controlling corrosion resistance in HEAs.

11:40am DM+BI+SS-ThM-12 Determination of Hydrogen in High Strength Steels using Scanning Kelvin Probe Force Microscopy, *Ines Traxler, G Schimo-Aichhorn,* CEST Competence Centre for Electrochemical Surface Technology, Austria*; A Muhr, G Luckeneder, H Duchaczek, K Stellnberger,* voestalpine Stahl GmbH, Austria*; D Rudomilova, T Prosek,* University of Chemistry and Technology Prague, Czech Republic*; B Lutzer,* CEST Competence Centre for Electrochemical Surface Technology, Austria*; D Stifter, S Hild,* Johannes Kepler University Linz, Austria
High-strength steels are important materials for the automotive industry. Due to their good formability and high strength they are used for the manufacture of light weight and fuel-efficient automotive parts. A disadvantage of high strength steels is their proneness to hydrogen embrittlement. Even small amounts of hydrogen can cause a deterioration of mechanical properties. Therefore, the effect of hydrogen on the steel microstructure is of great interest and it is important to study and visualize

the effects and mechanisms of hydrogen in steels. For this purpose, Scanning Kelvin Probe Force Microscopy (SKPFM) is a promising technique for the investigation of hydrogen in the steel microstructure with a very good spatial resolution.

Hydrogen diffusion in different high-strength steels was investigated using SKPFM. Hydrogen entry at cut edges and coating defects was studied as well as the influence in the individual steel grains. The measurements were carried out with different salt solutions on the backside of CP1000 (complex phase), DP1000 (dual phase) and zinc coated DP1000 steels to induce corrosion and promote hydrogen entry into the steel. The permeating hydrogen was measured on the upper side of the sample by repeated surface scans and the effect on the contact potential difference (CPD) was studied. Furthermore, SKPFM measurements with different relative humidity were carried out, monitoring the effects of corrosion. Additionally, Scanning Kelvin Probe (SKP) measurements were done for comparison.

With SKPFM, the preferred diffusion pathways of hydrogen through the steel microstructure could be visualized as well as the effect of zinc coatings on hydrogen permeation.

12:00pm DM+BI+SS-ThM-13 Reflection Mode Interferometry for studying interfacial processes, *Kai Schwenzfeier, P Bilotto, M Lengauer, C Merola, H Cheng, M Valtiner,* TU Wien, Austria

Molecular level processes at electrified solid|liquid interfaces play a critical role in corrosion and degradation processes. These include adsorption of ions, evolution of electrochemical double layers, oxidation/dissolution of metals, screening effects as well as liquid properties at an interface. However those processes/effects are notoriously hard to measure due to long integration times or too small probe with many available analysis techniques.

We refined Multiple Beam Interferometry (MBI) to enable time resolved in-situ and operando measurement of processes at solid|liquid interfaces in both transmission and reflection geometry. In this presentation dynamic interfacial processes such as changes of refractive indices in small (nanometer sized gaps), a micro-to-angstrom scale view into corrosion processes and surface oxidation, as well as specific and non-specific potential driven ion adsorption in aqueous solutions will be discussed in detail. We will relate these measurements to molecular resolution AFM imaging and force spectroscopy at solid|liquid interfaces.

Electronic Materials and Photonics Division
Room A214 - Session EM+AP+MS+NS+TF-ThM

Advanced Processes for Interconnects and Devices

Moderators: Andy Antonelli, Nanometrics, Bryan Wiggins, Intel Corporation

8:00am EM+AP+MS+NS+TF-ThM-1 High-density Plasma for Soft Etching of Noble Metals, *Gerhard Franz, V Sushkov,* Munich University of Applied Sciences, Germany; *W Oberhausen, R Meyer,* Technische Universität München, Germany

During our research to define a contact which can be serve as thin hard mask in III/V semiconductor processing, we focused on the Bell contact which consists of Ti/Pt(Mo)/Au and chlorine-based plasmas generated by electron cyclotron resonance. For platinum, we identified PF_3 as main component which acts comparable to CO [1]. This fact triggered our search for suited etchants for gold and copper. For Au, the best ambient is a mixture of CH_4, Cl_2, and O_2 which is stabilized by Ar [2]. This mixture generates residual-free etching of metal films which are clearly free of "fencing" and "hear's ears."

The etching process has been established up to thicknesses of half a micron which is the typical thickness of metal films on the p-side of laser devices. With the aid of optical emission spectroscopy, the generation of CO could be proven [3]. This reagent seems to be the main component for real etching without residual fencing.

[1] G. Franz, R. Kachel, and St. Sotier, Mat. Sci. Semicond. Proc. **5**, 45 (2002)

[2] G. Franz, R. Meyer, and M.-C. Amann, Plasma Sci. Technol. **19**, 125503 (2017)

[3] G. Franz, W. Oberhausen, R. Meyer, and M.-C. Amann, AIP Advances **8**, 075026 (2018)

8:20am EM+AP+MS+NS+TF-ThM-2 Crystalline InP Growth and Device Fabrication Directly on Amorphous Dielectrics at Temperatures below 400ºC for Future 3D Integrated Circuits, *Debarghya Sarkar, Y Xu, S Weng, R Kapadia,* University of Southern California

A fundamental requirement to realize 3D integrated circuits is the ability to integrate single crystal semiconductor devices on the back-end of functional layers within a thermal budget of ~400 ºC. Present state-of-the-art methods involve wafer bonding or epitaxial growth and transfer, since directly growing on amorphous materials by traditional epitaxial growth processes like MOCVD and MBE would give polycrystalline films with submicron-scale grains. To that end, a newly introduced and actively developing growth method called Templated Liquid Phase (TLP) has demonstrated the ability to achieve single crystal compound semiconductor mesas of areal dimension ~ 10um diameter on diverse amorphous substrates. While previous demonstrations of TLP growth were at temperatures around 500-600 ºC, in this presentation we would discuss some of the recent material characteristics and device results achieved and insights obtained, for crystalline InP mesas grown on amorphous dielectrics at temperatures below 400 ºC. InP nucleation and growth was obtained for temperatures 360 ºC down to 200 ºC. Morphological variations of the grown crystals observed under different growth conditions (temperature, pressure, precursor flux) and strategies to obtain compact macro-defect free crystal growth would be presented. Contrary to general expectation of poor optoelectronic quality at these lower temperatures, the room temperature steady-state photoluminescence shows peak position and full width at half maximum comparable to that of commercial InP wafer. External quantum efficiency is within an order of magnitude of single crystal commercial wafer at optimal growth conditions. Back-gated phototransistor was fabricated using low temperature InP grown directly on the amorphous gate oxide, and with all processing steps below the thermal budget of 400 ºC. A typical device showed reasonable ON-OFF ratio of about 3 orders of magnitude, with peak responsivity of 20 A/W at V_{gs}=3.2V and V_{ds}=2.1V under an irradiance of 4 mW/cm^2 of broadband light. In summary, this technology could potentially open up a viable avenue to realize 3D integrated circuits by enabling integration of high performance electronic and optoelectronic devices on the back-end of functional layers within the acceptable thermal budget of 400^{0}C.

8:40am EM+AP+MS+NS+TF-ThM-3 The Role and Requirements of Selective Deposition in Advanced Patterning, *Charles Wallace,* Intel Corporation **INVITED**

The edge placement error (EPE) margin on features patterned at tight pitches presents a difficult integrated challenge. Area selective deposition, chemically selective etches and the design of thin films for selectivity have risen to the top priorities in advanced patterning. The EPE control requirement creates a complex interaction between many integrated modules such as thin film deposition, etch (wet and dry), chemical-mechanical polish and lithography. The introduction of EUV lithography into the semiconductor patterning process has enabled some simplification of process architecture; however, has not decreased EPE margin enough to keep up with the pitch scaling requirements. Chemical selectivity is the most effective way to avoid EPE-caused failures on devices which lead to poor yield. Some of the limits to achieving selective growth solutions include development of self-assembled monolayers (SAMs), selective ALD/CVD growth and the metrology required to prove success. The development of manufacturable deposition chambers by the industry is a key requirement in order to adequately test the capability of these new process options.

9:20am EM+AP+MS+NS+TF-ThM-5 Graphene-Template Assisted Selective Epitaxy (G-TASE) of Group IV Semiconductors, *M. Arslan Shehzad, A T. Mohabir, M Filler,* Georgia Institute of Technology

As conventional 2-D transistor scaling approaches its limits, 3-D architectures promise to increase the number of devices and reduce interconnect congestion. A process able to monolithically integrate single-crystalline group IV materials into the back-end-of-line (BEOL) may enable such designs. Here, we demonstrate the graphene-template assisted selective epitaxy (G-TASE) of single-crystal Ge on amorphous substrates at temperatures as low as 250 ˚C. This work represents a significant step forward for TASE methods, which have been largely limited to III-V and II-VI materials, bulk crystal templates, as well as higher temperatures. We specifically grow Ge nanostructures on graphene-on-oxide at the bottom of nanometer-scale oxide trenches by leveraging differences in group IV atom sticking probability between graphene and oxide surfaces. Raman mapping confirms the single crystallinity of as-grown Ge crystals. Time-dependent studies show a linear increase in Ge crystal height even after emerging

from the oxide trench, indicating Ge atoms preferentially adsorb to the top facet under our growth conditions. Our studies also reveal that G-TASE is sensitive to the plasma process used to expose graphene in the oxide trenches. This work extends TASE to a new, technologically-relevant materials system and provides fundamental insight into the underlying physicochemistry.

KEY WORDS: silicon, germanium, epitaxy, graphene, selective deposition

9:40am EM+AP+MS+NS+TF-ThM-6 Resistivity and Surface Scattering Specularity at (0001) Ru/dielectric Interfaces, *S Ezzat,* University of Central Florida*; P Mani,* View Dynamic Glass, Inc.*; A Khaniya, W Kaden,* University of Central Florida*; D Gall,* Rensselaer Polytechnic Institute*; K Barmak,* Columbia University*; Kevin Coffey,* University of Central Florida

In this work we report the variation of resistivity with film thickness and with changes in surface characteristics for ex-situ annealed single crystal (0001) Ru thin films grown on c-axis sapphire single crystal substrates. The room temperature deposition of SiO_2 on the Ru surface increased the resistivity of the annealed films and is interpreted as an increase in diffuse scattering of the upper surface from a primarily specular previous condition in the context of the Fuchs-Sondheimer model of surface scattering. The characterization of the films and upper Ru surface by low energy electron diffraction (prior to SiO_2 deposition), x-ray reflectivity, x-ray diffraction, and sheet resistance measurements is reported. The film resistivity and specularity of the Ru/SiO_2 interface is observed to reversibly transition between high resistivity (low specularity) and low resistivity (high specularity) states.

11:00am EM+AP+MS+NS+TF-ThM-10 Electrochemical Atomic Layer Deposition and Etching of Metals for Atomically-Precise Fabrication of Semiconductor Interconnects, *Y Gong, K Venkatraman, Rohan Akolkar,* Case Western Reserve University **INVITED**

Moore's law drives continued device miniaturization in nano-electronics circuits. As critical dimensions are approaching the single nanometer length scale, the semiconductor industry is seeking novel technologies for precisely tailoring materials and structures at the atomic scale. While vapor-phase, plasma-assisted techniques of atomic layer deposition (ALD) and etching (ALE) are capable of providing nano-scale control over metal deposition and etching, these processes may not provide the requisite atomic-scale precision. Additionally, ALD precursors are unstable and often expensive. Thus, alternative solution-phase electrochemical processes are being developed in our laboratory. In our electrochemical ALD (e-ALD) approach, a sacrificial monolayer of zinc is first deposited on the noble substrate via underpotential deposition (UPD). The zinc adlayer then undergoes spontaneous surface-limited redox replacement (SLRR) by the desired metal such as Cu or Co. Sequential UPD and SLRR steps enable fabrication of multi-layered deposits in a layer-by-layer fashion. An analogous approach for electrochemical ALE (e-ALE) is also being developed. In electrochemical ALE of Cu, surface-limited sulfidization of Cu forms a cuprous sulfide (Cu_2S) monolayer. The sulfidized Cu monolayer is then selectively removed through spontaneous complexation of the Cu^{+1} in a chloride-containing etchant medium. The sequence can be repeated to etch bulk metal films one atomic layer at a time. This talk will highlight numerous advantages and fundamental characteristics of e-ALD and e-ALE processes and describe opportunities for integrating them in wafer-scale metallization applications.

11:40am EM+AP+MS+NS+TF-ThM-12 Mechanical Properties of Patterned low-κ Films Measured by Brillouin Light Scattering, *Jon Zizka, H Wijesinghe,* The Ohio State University*; S King, H Yoo,* Intel Corporation, USA*; R Sooryakumar,* The Ohio State University

In order to improve device performance of interconnects, the microelectronics industry utilizes low-κ dielectric technology in place of traditional SiO_2. Integration of these materials into circuits has, however, been challenging due to poor mechanical stability as a result of the increased dielectric porosity. Large thermal stresses may also build up during successive thermal cycling due to differences in the thermal expansion of component materials. These adverse features become more prominent as smaller dimensions are sought for improvement in device performance. While titanium nitride (TiN) is currently being widely used as a hard mask to pattern low-κ materials such as SiOC:H into desired architectures with < 100 nm length scales, the high stress and stiffness of the TiN over-layer can influence the delicate underlying patterns and affect device performance.

In this study we utilize Brillouin light scattering (BLS) to probe the elastic properties of TiN/SiOC:H structures grown on Si that have been patterned

into a series of parallel wires of rectangular cross-sections with sub 200 nm pitch and depths. In studying the influence of the hard mask on the mechanical properties of SiOC:H, BLS offers a non-invasive approach to detect thermally activated acoustic excitations and to measure their mode dispersions for incident light with wave-vector components parallel or perpendicular to the TiN wires. The widely-used technique of nanoindentation (NI) to measure mechanical properties has been shown, for ultra-thin soft films, to interact with the underlying substrate, thus skewing the results. On the other hand, the inelastic light scattering approach probes ambient modes allowing for the individual acoustic behavior of the film to be distinguished from the substrate.

The results of measurements performed on samples with a range of wire dimensions (width/depth) will be presented that include the dependence of the Brillouin peak intensities on the incident and scattered light polarization as well as a model of the mode profiles. The latter include finite element modeling that simulate the different mode frequencies and associated relative vertical and horizontal displacements for the non-dispersive cantilever type modes that characterize modes with wave-vector perpendicular to the TiN wires. The modes with wave-vector parallel to the wires followed a dispersive nature similar to blanket films. The relationship of such acoustic properties will be discussed in the context of the mechanical properties of the patterned structures and the influence of processing of the nanowires.

12:00pm EM+AP+MS+NS+TF-ThM-13 Wafer-Scale Fabrication of Carbon-Based Electronic Devices, *Zhigang Xiao, J Kimbrough, J Cooper, K Hartage, Q Yuan,* Alabama A&M University

In this research, we report the wafer-scale fabrication of carbon nanotube or graphene-based electronic device such as field-effect transistors (FETs). Carbon nanotube-based devices were fabricated with the alternating electric field-directed dielectrophoresis (DEP) method, and the graphene-based devices were fabricated with the carbon films grown with plasma-enhanced atomic layer deposition (PEALD) or e-beam evaporation. Semiconducting carbon nanotubes were dispersed ultrasonically in solutions, and were deposited and aligned onto a pair of gold electrodes in the fabrication of carbon nanotube-based electronic devices using the dielectrophoresis method. The DEP-aligned tubes were further fabricated into carbon nanotube field-transistors (CNTFETs) and CNTFET-based electronic devices such as CNT-based inverters and ring oscillators using the microfabrication techniques. The fabricated devices were imaged using the scanning electron microscope (SEM) and high-resolution transmission electron microscope (HRTEM), and the electrical properties were measured from the fabricated devices using the semiconductor analyzer. The semiconducting CNTs achieved higher yield in the device fabrication, and the fabricated devices demonstrated excellent electrical properties.

Fundamental Discoveries in Heterogeneous Catalysis Focus Topic
Room A213 - Session HC+2D+SS-ThM

Nanoscale Surface Structure in Heterogeneously-Catalyzed Reactions

Moderators: Rebecca Fushimi, Idaho National Laboratory, Eric High, Tufts University

8:20am HC+2D+SS-ThM-2 Low-temperature Investigation of Propylene on $TiO_2/Au(111)$, *M Gillum, M DePonte, J Wilke, E Maxwell, V Lam, D Schlosser, Ashleigh Baber,* James Madison University

The partial oxidation of propylene creates industrially important feedstocks that are used in a multitude of chemical fields ranging from textiles to cosmetics to air sanitation. One avenue of research on propylene oxidation is being conducted using metal/oxide model catalysts, as they have shown an affinity for high selectivity oxidation reactions. To gain a comprehensive understanding of olefin intermolecular and surface interactions, temperature programmed desorption (TPD) studies were conducted using Au(111)–based model catalysts with different surface preparations. Using TPD, we were able to identify the specific adsorption sites of propylene on a $TiO_2/Au(111)$ model catalyst, differentiating between the TiO_2 nanoparticles, the $Au-TiO_2$ interface, and the gold surface. Desorption kinetics propylene were studied on pristine and titania–modified Au(111) surfaces. Desorption products were monitored using quadrupole mass spectrometry and the surface morphology was analyzed using ex-situ atomic force microscopy. The presence of titania was confirmed via X-ray photoelectron spectroscopy. By understanding the characteristic behaviors

with combined experimental techniques, active sites and reaction pathways for partial olefin oxidation over Au–based catalysts may be identified.

8:40am **HC+2D+SS-ThM-3 Structure and Reactivity of Supported Oxide and Metal Nanoparticles**, *Geoff Thornton*, University College London, UK **INVITED**

Heterogenous catalysts typically consist of metal nanoparticles on an oxide support. Model experiments involving nanoparticle growth on single crystalline oxide have been successfully employed to understand aspects of the nucleation, structure and reactivity. This contributes to catalysis design programs. Many subtleties continue to emerge, some of which will be discussed in this talk. For instance, low temperature STM experiments have allowed direct imaging of CO overlayers formed on the Pd nanoparticles themselves supported on TiO_2. The results show that the nanoparticles grow like a carpet over substrate step-edges, giving rise to a curved top facet that changes the adsorption behavior. Au nanoparticles supported on TiO_2 have been the subject of much work since the discovery by Haruta that Au is a low temperature oxidation catalyst. Despite this earlier work there has been no definitive evidence for the binding site or the direction of charge transfer associated with gold atoms and nanoparticles on the model substrate $TiO_2(110)$. We show with STM that single Au atoms are in indeed bound to oxygen vacancies on the substrate, with dimers similarly anchored. Associated DFT calculations suggest electron transfer from bridging O vacancies to Au. XPEEM in conjunction with STM have also been used to probe the electronic character of Au nanoparticles as a function of particle size and coverage. Pt and related metals on CeO_2/ZrO_2 are used for CO oxidation in autocats. The accepted mechanism is that the oxide supplies oxygen to the metal to react with CO, with the oxide being directly reoxidized. In XPEEM studies of a model inverse catalyst we show that the reoxidation can also involve the metal.

9:20am **HC+2D+SS-ThM-5 Catalysis by Well-defined Oxide Nanostructures: From Atomic-scale Properties to Rational Design**, *Fan Yang*, Dalian Institute of Chemical Physics, China

The catalytic properties of nano-oxides are increasingly recognized and currently explored for a wide range of applications. However, the nature of the active sites of these nano-oxides, as well as their catalytic chemistry, remain poorly understood, because of the difficulties to access these surface/interfacial sites at the atomic level. Using molecular beam epitaxy, we construct well-defined oxide nanostructures (NSs) on planar metal or oxide surfaces, which serve as the model systems for understanding the catalytic chemistry of the metal-oxide interface and nano-oxides. In this talk, we report our recent progress in the studies of low temperature CO oxidation and CO disproportionation reaction, using supported FeO and CeO_x NSs as the model catalysts. Overall, we wish to demonstrate that the control over supported oxide NSs could enable a wide range of catalytic properties for the rational design of highly efficient catalysts.

9:40am **HC+2D+SS-ThM-6 Structural and Chemical Effects of Cesium on the Cu(111) and $Cu_xO/Cu(111)$ Surface**, *Rebecca Hamlyn[1]*, Stony Brook University; *M Mahapatra,* Brookhaven National Laboratory; *I Orozco,* Stony Brook University; *M White, S Senanayake, J Rodriguez,* Brookhaven National Laboratory

Surface additives, particularly those of alkali metals, are commonly used for promotion of catalytic processes. These processes include carbon oxide reactions such as the water-gas shift and methanol synthesis over Cu-based catalysts. Both reactions are known to be promoted by Cs doping. Partially oxidized Cu is also understood to have a critical role in the activity of the aforementioned processes, as strictly metallic copper will not survive under redox conditions. In an effort to better understand how small additions of alkalis such as Cs act as promoters, we have carried out model studies of cesium over a metallic and oxidized copper surface using scanning tunneling microscopy and x-ray photoelectron spectroscopy. We find that the oxide structure assists in anchoring Cs over the weaker electrostatic interactions with the bare copper surface, allowing for room temperature imaging. Furthermore, with higher coverages or elevated temperature, cesium induces formation of a new ordered structure. This work provides a molecular-scale understanding of the cesiated surface, and serves as a basis for insight toward its mechanism of action in conversion of relevant gases (H_2O, CO, CO_2).

11:00am **HC+2D+SS-ThM-10 Mythbusting: From Single Crystals in UHV to Catalytic Reactors**, *Robert Madix,* Harvard University **INVITED**

For decades it has been an objective of surface science studies of chemical reactivity to make a direct connection to heterogeneous catalysis. Over these years the difficulties encountered in connecting these two areas of research gave rise to the dismissal of such possibility by the catalysis community and the invention of such shorthand terms as "pressure gap" and "materials gap" to express this view. Usually overlooked is also the fact that catalytic reactions are conducted at much higher temperatures than the related studies on single crystal surfaces, so a "temperature gap" also exists. In fact, these regimes of reactivity are directly linked by fundamental knowledge of the identity and rate constants for the operative elementary steps comprising the catalytic cycle under catalytic conditions. Further, for many catalytic materials, its state can be defined by the reaction conditions themselves in quaisi-thermodynamic terms. Connection between the reactivity observed on the single crystals with that on the catalyst surface is possible by the use of a transient pressure method which is conducted over the actual catalyst material under Knudsen flow conditions. Recently we have demonstrated this historically elusive connection between UHV-based studies and catalytic performance for the catalytic oxygen-assisted synthesis of methyl formate from methanol over a nanoporous gold catalyst. The connection is entirely based on the kinetics and mechanism determined on single crystal gold surfaces. A brief history of this development will be discussed and the specifics of how this bridge was built examined.

11:40am **HC+2D+SS-ThM-12 Cooperativity Between Pd and AgO_x Phases on Ag(111)**, *V Mehar, M Yu, Jason Weaver,* University of Florida

Metals dispersed on a reactive metal-oxide have potential to effect selective catalysis through cooperative interactions between the co-existing metal and metal-oxide phases. In this talk, I will discuss our recent investigations of the structure and reactivity of oxidized Ag(111) as well as Pd/AgO_x surfaces that are generated by depositing metallic Pd onto a single-layer AgO_x structure in ultrahigh vacuum (UHV). Scanning tunneling microscopy (STM) and low energy electron diffraction (LEED) show that the oxidation of Ag(111) with atomic oxygen mainly produces a single-layer AgO_x phase with a p(4 x 5r3) structure as well as smaller amounts of p(4 x 4) and c(3 x 5r3) structures during the initial stages of oxidation. Surface infrared spectroscopy and temperature programmed reaction spectroscopy (TPRS) demonstrate that the single-layer AgO_x structures are nearly unreactive and bind CO negligibly at temperatures down to ~100 K. In contrast, we find that CO adsorbs and oxidizes efficiently on Pd islands during TPRS, even when the AgO_x phase is the only oxidant source. STM further demonstrates that the metallic Pd islands induce partial reduction of the AgO_x support structure at 300 K. We find that the Pd/AgO_x surfaces continue to exhibit high CO oxidation activity with increasing Pd coverage up to nearly 2 ML (monolayer), suggesting that oxygen transfer from the AgO_x phase occurs at both the interior and perimeter of Pd islands. Our results reveal a cooperative mechanism for CO oxidation on Pd/AgO_x surfaces wherein O-atoms from the AgO_x support phase migrate onto metallic Pd islands and react with adsorbed CO to produce CO_2. These findings illustrate that oxygen transport across metal/metal-oxide interfaces can be highly efficient when the oxygen chemical potential is lower on the initial metal phase (Pd) compared with the metal-oxide (AgO_x) support.

12:00pm **HC+2D+SS-ThM-13 Migration Across Metal/Metal Oxide Interfaces: Enhancing the Reactivity of Ag Oxide with H_2 by the Presence of Pd/Pd Oxide**, *Christopher O'Connor[2], M van Spronsen, E Muramoto, T Egle, R Madix, C Friend,* Harvard University

An important factor in exploiting bifunctionality in dilute alloy catalysts is surface migration across interfaces separating the dissimilar materials. Herein, we demonstrate the transfer of hydrogen atoms from islands of Pd oxide onto a surrounding O/Ag(111) surface using ambient pressure X-ray photoelectron spectroscopy (APXPS) and scanning tunneling microscopy (STM). These Pd oxide islands enhance the rate of reduction of Ag oxide by more than four orders of magnitude compared to pure oxidized Ag(111). The increase in the rate of reduction of Ag oxide by H_2 is attributed to H_2 activation on Pd/Pd oxide followed by migration (spillover) to Ag/Ag oxide and rapid reaction thereafter. The oxidation and subsequent reduction processes induce significant structural changes of the catalyst surface. We further establish that the transfer of hydrogen atoms occurs from islands of metallic Pd onto a surrounding Ag(111) surface using high resolution electron energy loss spectroscopy (HREELS) and temperature programmed

---

reaction spectroscopy (TPRS). For the metallic PdAg system, hydrogen spillover is shown to be a kinetically limited process that can be controlled by temperature, pressure of H_2 and surface concentration of Pd. The highest efficiency for the amount of hydrogen spillover per surface Pd occurs for a dilute concentration of Pd in Ag. This study establishes that the migration of intermediates across interfaces can occur for oxidized PdAg alloy surfaces and specifically that hydrogen atom migration has a significant effect on the catalytic activity of this type of binary material.

Advanced Ion Microscopy and Ion Beam Nano-engineering Focus Topic
Room B231-232 - Session HI+NS-ThM

Novel Beam Induced Material Engineering and Nano-Patterning

Moderators: Olga S. Ovchinnikova, Oak Ridge National Laboratory, Shinichi Ogawa, National Institute of Advanced Industrial Science and Technology (AIST)

8:00am HI+NS-ThM-1 Tuning out-of-plane Piezoelectricity in 2D Materials using Ion Beams, *Yunseok Kim,* Sungkyunkwan University, Republic of Korea **INVITED**
Two-dimensional (2D) transition metal dichalcogenides (TMDs) have been extensively studied owing to their ultra-thin nature as well as superior material properties. In particular, after the experimental observation of intrinsic in-plane piezoelectricity in the 2D MoS_2, fundamental studies on the piezoelectricity as well as piezoelectric device applications of the 2D TMDs have attracted significant interest. However, their applications are strongly limited due to the fact that crystallographically only in-plane piezoelectricity exists in the 2D TMDs. In this presentation, I will summarize our recent effect on the realization of tunable out-of-plane piezoelectricity in the 2D TMDs using He ion beams. Among various 2D TMDs, we have chosen $MoTe_2$ because it is very sensitive to the external stimuli such as strain. We first examined the realization of the out-of-plane piezoelectriciy by local asymmtery breaking based on the surface corrugation to check its feasibility. Then, He ion irradiation as a function of dose were performed onto the $MoTe_2$ surface. It was found that the out-of-plane piezoelectricity was indeed induced by He ion beams and, further, the magnitude of the induced out-of-plane piezoelectricity was depedent on the dose level. The proposed strategy for modulation of tunable out-of-plane piezoelectricity can be easily applied to a broader class of 2D TMD materials that have not been used for applications with out-of-plane piezoelectricity. Accordingly, it can stimulate the expansion of practical energy device applications with 2D TMDs.

8:40am HI+NS-ThM-3 Defect Engineering of Ferroelectric Thin Films – Leveraging Ion Beams for Improved Function, *Lane Martin,* University of California at Berkeley **INVITED**
Modern approaches to epitaxial thin-film growth have enabled unprecedented control of ferroelectric materials including the realization of enhanced polarization and ordering temperatures, production of ordered-domain structures, and improved properties. Today we are looking beyond simple lattice mismatch control for new ways to manipulate and control ferroic response and to produce unexpected or emergent effects. In this talk, we will investigate a number of observations of such emergent or unexpected properties in epitaxial thin films made possible via innovative synthesis and processing methodologies. In particular, we will explore recent examples of how synthesis, defects, and epitaxial constraint can be combined to produce exotic effects in ferroic systems. Primary focus will be given to the *ex situ* production of defects with ion bombardment to control defect-induced electronic states that can drive dramatic changes in leakage currents and impact ferroelectric response in materials like $BaTiO_3$, $PbTiO_3$, $BiFeO_3$, and others. For example, we will explore how high-energy-ion beams (>3 MeV beams of helium ions) can induce nonequilibrium densities of intrinsic point and defect clusters that have unintended positive effects – including reducing leakage in films by as much as 3-4 orders of magnitude, tuning coercive fields for switching, and much more. At the same time, leveraging focused-helium-ion bombardment, it is possible to create nanoscale patterns of defect-engineered material where emergent function, such as multi-state switching, is accomplished. Finally, we will explore how ion-bombardment procedures can also provide a knob to tune local energy competition in materials like relaxor ferroelectrics to gain new insight into material physics. All told, we will highlight specifics about the routes to produce defect-engineered ferroelectric thin films, will explore

approaches to characterize and study the nature of defects that are produced – including application of techniques like deep-level transient spectroscopy, and will examine the implication of such defect structures for dielectric and ferroelectric properties – including studies of defect-based effects on switching processes and kinetics. We will end with an exploration of what further growth of defect-engineering approaches might enable in the way of novel function and applications in these materials.

9:20am HI+NS-ThM-5 Exploring Proximity Effects and Large Depth of Field in Helium Ion Beam Lithography: Large-area Dense Patterns and Tilted Surface Exposure, *Ranveig Flatabø,* Univeristy of Bergen, Norway; *A Agarwal,* Massachusetts Institute of Technology; *R Hobbs,* Trinity College Dublin; *M M. Greve,* Univeristy of Bergen; *B Holst,* Univeristy of Bergen, Norway; *K Berggren,* Massachusetts Institute of Technology
Helium ion beam lithography (HIL) is an emerging nanofabrication technique. It benefits from a reduced interaction volume compared to that of an electron beam of similar energy, and hence reduced long-range scattering (proximity effect), higher resist sensitivity and potentially higher resolution. Furthermore, the small angular spread of the helium ion beam gives rise to a large depth of field. This should enable patterning on tilted and curved surfaces without the need of any additional adjustments, such as laser-auto focus. So far, most work on HIL has been focused on exploiting the reduced proximity effect to reach single-digit nanometer resolution, and has thus been concentrated on single-pixel exposures over small areas. Here we explore two new areas of application. Firstly, we investigate the proximity effect in large-area exposures and demonstrate HIL's capabilities in fabricating precise high-density gratings on large planar surfaces (100 μm × 100 μm, with pitch down to 35nm) using an area dose for exposure. Secondly, we exploit the large depth of field by making the first HIL patterns on tilted surfaces (sample stage tilted 45°). We demonstrate a depth of field greater than 100 μm for an estimated resolution of 20 nm.

9:40am HI+NS-ThM-6 Fabrication of Plasmonic Nanostructures by Helium-Ion Milling, *André Beyer, M Westphal,* Bielefeld University, Germany; *S Stephan,* Oldenburg University, Germany; *D Emmrich, H Vieker,* Bielefeld University, Germany; *K Chen,* Jinan University, Guangzhou, China; *G Razinskas, H Gross, B Hecht,* Würzburg University, Germany; *M Silies,* Oldenburg University, Germany; *A Gölzhäuser,* Bielefeld University, Germany
Plasmonic nanostructures are essential for controlling and directing light on the nanoscale. While fabrication techniques like standard electron beam lithography (EBL) methods or focused ion beam (FIB) milling with Ga^+ ions are approaching their limit in the 10-nm-regime, ion beam milling with He^+ ions is capable of milling features below 6 nm [1,2]. In this contribution, we give two specific examples of helium-ion milled plasmonic nanostructures: (i) gold bowtie antennas milled from 100 nm thick polycrystalline gold films on mica substrates and (ii) nanoslit cavities in chemically-synthesized 40 nm thick single-crystalline gold flakes [2]. Both examples benefit from a combined approach using a Ga^+ FIB for milling large features and employing the fine resolution of the helium ion microscope (HIM) for milling small features. We will discuss different patterning strategies to optimize the writing speed and minimize substrate swelling. In addition, our approach to quantify the sizes of milled gaps will be shown. It is based on low dose imaging in combination with substantial line-profile averaging which we applied to few-hundred-nanometer-long homogeneous helium-ion milled lines.

[1] H. Kollmann et al., Nano Letters 14, 4778 (2014).

[2] K. Chen et al., Nanoscale 10, 17148 (2018).

11:00am HI+NS-ThM-10 Towards Atomically Precise Carbon Quantum Electronic Devices, *J Swett,* University of Oxford, UK; *O Dyck, S Jesse,* Oak Ridge National Laboratory; *Jan Mol,* Queen Mary University of London, UK **INVITED**

Towards Atomically Precise Carbon Quantum Electronic Devices

Jacob L. Swett[a], Ondrej Dyck[b], Stephen Jesse[b], Jan A. Mol[a,c]

[a] *Department of Materials, University of Oxford, Oxford, UK*

[b] *Center for Nanophase Materials Sciences, Oak Ridge National Laboratory, Oak Ridge, TN 37831, USA*

[c] *School of Physics and Astronomy, Queen Mary University of London, London, UK. Email: j.mol@qmul.ac.uk*

Graphene exhibits many unique properties that can be further enhanced through nanostructuring and atomic manipulation. Such nanostructured

devices have potential applications as molecular junctions [1], spin qubits [2], heat engines [3], and sensors [4], providing substantial motivation for their realization. Electron and ion beams provide unique and complementary tools for realizing some of these structures due to their ability to modify the graphene with atomic and nanoscale precision, respectively. Modification may take the form of direct-write patterning [5], defect production [6], dopant introduction [7], and dopant manipulation [8]. Although much progress has been realized in these areas, transport measurements of top-down fabricated atomically precise carbon nanostructures have yet to be realized. Here we present lessons learned and key findings for this emerging direction of research leveraged from years of fabrication and transport measurements of single molecules via non-covalent bonding to graphene nanoelectrodes [9]. We will present a broad overview of the challenges and progress in understanding and controlling the transport through atomic-scale devices and discuss how these lessons inform and translate to current experiments on introducing dopants and manipulating atoms on the atomic scale with electron and ion beams in graphene and other 2D materials. Finally, practical strategies for realization of these devices will be discussed, including contamination control, fabrication strategies, and transport measurements.

References:

[1] J.K. Sowa et al., J. Chem. Phys. 149, 154112 (2018)

[2] Trauzettel, Björn, et al., Nature Physics 3.3, 192 (2007).

[3] P. Gehring et al., Nano Lett. 17, 7055 (2017)

[4] P. Puczkarski et al., ACS Nano 12, 9451 (2018)

[5] Nanda, Gaurav, et al., Carbon 119, 419-425, (2017)

[6] Robertson, Alex W., et al., Nature communications 3 1144 (2012)

[7] Tripathi, Mukesh, et al., ACS nano 12.5 4641-4647 (2018)

[8] Dyck, Ondrej, et al., Small 14.38 1801771 (2018)

[9] C.S. Lau et al., Phys. Chem. Chem. Phys. 16, 20398 (2014)

11:40am HI+NS-ThM-12 Fabrication of High-Q nanofiber Bragg Cavity Using a Helium Ion Microscope, *Hideaki Takashima,* Kyoto university, Japan*; A Fukuda, H Maruya, T Tashima,* Kyoto University, Japan*; A Schell,* Central European Institute of Technology, Czech Republic*; S Takeuchi,* Kyoto University, Japan

Efficient coupling between single light emitters and photons propagating in single mode fibers has been attractive attention recently for the realization of photonic quantum information devices, such as single photon sources, and quantum phase gates. Toward the realization of these devices, we have developed nanofiber Bragg cavity (NFBC), which is an optical nanofiber embedded in a microcavity in it, using a gallium focused ion beam (FIB) milling system. The NFBC has small mode volume of wavelength size, ultra-wide tunability of the resonant wavelength, and high coupling efficiency (>80%). However, experimentally achieved quality (Q) factors have been still a few hundreds. Here, we report the development of the NFBC using a helium ion microscope (ZEISS "ORION NanoFab").

Nanofibers are fabricated by heating a single-mode fiber with a ceramic heater and stretching the end of the fiber. The diameter of the nanofibers is reduced to about 300 nm. The helium ion beam is periodically irradiated from the top side of the nanofiber to fabricate Bragg grating. The period at the center of the grating is modified for introducing a defect to be worked as a microcavity.

In order to evaluate the Q factor of the NFBC, we measure a transmission spectrum. The light of a halogen lamp is connected to the one end of the NFBC and the transmitted light is observed with a spectrometer with the resolution of 0.17 nm.

When we measure the transmission spectrum of the NFBC with the grooves of 320, a sharp resonant peak with the linewidth of 0.54 nm was observed in the center of the stop band. This agrees with the Q factor of 1260, which is more than 4 times larger than the NFBC fabricated with the Ga FIB system (Q ~ 300). Taking into account of the resolution of the spectrometer, it is expected that the real Q factor would be higher than this value.

In conclusion, we reported the fabrication of NFBC using the helium microscope. When the number of the grooves is 320, the Q factor is 1260, which is more than 4 times larger than the NFBC fabricated by the Ga FIB system.

Besides this result, we will discuss the NFBC when the number of the grooves is changed and the comparison with finite-difference time-domain (FDTD) simulation.

12:00pm HI+NS-ThM-13 Time of Flight Secondary Ion Mass Spectrometry in the Helium Ion Microscope for Battery Materials and Other Nanoscale Problems*, N Klingner,* Helmholtz Zentrum Dresden-Rossendorf, Germany*; Gregor Hlawacek,* Helmholtz-Zentrum Dresden Rossendorf, Germany*; L Wheatcroft, B Inkson,* University of Sheffield, UK*; R Heller,* Helmholtz Zentrum Dresden-Rossendorf, Germany

Helium Ion Microscopy (HIM) has become a wide spread imaging and nanofabrication technology. However, existing HIM users can currently not perform elemental analysis in an easy and cost efficient way. We present results obtained using a light weight retrofittable Time of Flight Secondary Ion Mass Spectrometer (TOF-SIMS). I will briefly give an overview on new developments in our TOF-SIMS setup which allows to obtain information on the elemental composition of the sample. The lateral resolution for the presented TOF-SIMS add-on has been measured to be 8 nm. A particular advantage of the presented TOF-SIMS implementation is that it allows for charge compensation during data acquisition and thus the elemental analysis of insulators or poorly conducting materials. In addition delayed extraction can be realized which will allow a field free application of the primary beam which reduces aberrations and the setup time. While not a dedicated high mass resolution instrument it allows to answer many scientific questions by combining the high lateral resolution of the HIM with elemental information. The examples include but are not limited to battery materials and corrosion protection of steel.

[1] Nico Klingner, Rene Heller, Gregor Hlawacek, Stefan Facsko, and Johannes von Borany. Time-of-

flight secondary ion mass spectrometry in the helium ion microscope. Ultramicroscopy, 198:10–17,

2019.

[2] Nico Klingner, René Heller, Gregor Hlawacek, J. von Borany, John A. Notte, Jason Huang, and

Stefan Facsko. Nanometer scale elemental analysis in the helium ion microscope using time of flight

spectrometry. Ultramicroscopy, 162:91–97, 2016.

Frontiers of New Light Sources Applied to Materials, Interfaces, and Processing Focus Topic
Room A124-125 - Session LS+AS+SS-ThM

Operando Methods for Unraveling Fundamental Mechanisms in Devices Towards Renewable Energies

Moderator: Olivier Renault, CEA-University Grenoble Alps, France

8:00am LS+AS+SS-ThM-1 X-Ray Insight into Fuel Cell Catalysis: Operando Studies of Model Surfaces and Working Devices*, Jakub Drnec, I Martens,* European Synchrotron Radiation Facility, France*; T Fuchs,* University of Kiel, Germany*; T Wiegmann,* European Synchrotron Radiation Facility, Germany*; A Vamvakeros,* Finden Ltd., UK*; R Chattot,* European Synchrotron Radiation Facility, France*; O Magnussen,* University of Kiel, Germany **INVITED**
Complete physico-chemical operando characterization of electrochemical devices in whole, or it's constituent materials separately, is necessary to guide the development and to improve the performance. High brilliance synchrotron X-ray sources play a crucial role in this respect as they act as a probe with relatively high penetration power and low damage potential. In this contribution the new possibilities of using using high energy, high intensity X-rays to probe model fuel cell catalysts and energy conversion devices will be presented.

HESXRD (High Energy Surface X-ray Diffraction) [1] and TDS (Transmission Surface Diffraction) [2] provide ideal tools to study structural changes during reaction conditions on single crystal model electrodes. The main advantage of both techniques is the possibility to follow the structural changes precisely with atomic resolution. While HESXRD is ideally used to determine exact atomic position, the TSD is easier to use and allows studies with high spatial resolution. For example, HESXRD can be used to follow the atomic movement of Pt atoms during electrochemical oxidation and dissolution with very high precision, explaining the different catalyst

degradation behaviors and suggesting possible routes to improve its durability [3-4]. The TSD is an excellent tool to study advanced 2D catalysts.

To study fuel cells or batteries as a whole, elastic scattering techniques, such as WAXS and SAXS, can be employed as they can provide important complementary information to more standard X-ray imaging and tomography. The advantage is that the chemical contrast and sensitivity at atomic and nm scales is superior. Coupling these technique with the tomographic reconstruction (XRD-CT and SAXS-CT) is much less common as it requires bright synchrotron sources and advanced instrumentation, but allows 3D imaging of operational devices with unprecedented chemical sensitivity. This can be demonstrated on imaging of standard 5 cm² fuel cells during operation. The change in morphology and atomic arrangement of the catalysts, PEM hydration and water distribution can be followed in one experiment as a function of operating conditions. Furthermore, the fundamental processes leading to the catalyst aging can be assessed with high temporal and spatial resolution. These advanced scattering techniques open a door to holistic investigations of operational devices, which are needed to successfully incorporate new materials at the device level.

[1] J. Gustafson et al., Science 343, 758 (2014)

[2] F. Reikowski et al., J. Phys. Chem. Lett., 5, 1067-1071 (2017)

[3] J. Drnec et al, Electrochim. Acta, 224 (2017),

[4] Chattot et al., Nature Materials, 17(2018)

8:40am **LS+AS+SS-ThM-3 Multi-scale Operando X-ray Tomography of Solid-state Li Battery Electrolytes at Elevated Temperatures and Pressures**, *Natalie Seitzman,* Colorado School of Mines*; J Nelson Weker,* SLAC National Accelerator Laboratory*; M Al-Jassim,* National Renewable Energy Laboratory*; S Pylypenko,* Colorado School of Mines

Solid state Li ion conductors are next-generation battery technologies that reap the capacitive benefits of Li metal anodes while mechanically resisting the Li interface evolution and thus prolonging lifetime. Additionally, they are not flammable, offering greater safety than liquid counterparts. However, interface evolution and Li protrusions are observed in solid state batteries despite the mechanical resistance.[1,2] There is debate as to whether these protrusions nucleate at the Li anode or within the ceramic electrolyte, and there are several factors that affect these protrusions including electrolyte density, pre-existing defects, anode/electrolyte interfacial contact, and imperfect electronic insulation within the electrolyte.[3] Understanding the influence of these variables is greatly enhanced by directly imaging the interior of the ceramic at multiple scales in conjunction with electrochemical experiments.

This talk addresses the contribution of electrolyte density and defects, interfacial contact, and conductivity to structural changes in β-Li$_3$PS$_4$ (LPS) ceramic electrolyte in operating cells via 3D X-ray imaging with sub-micron resolution. Cells of Li, LPS, and a blocking contact are constructed and studied *in operando* at 200 psi and 70°C. Because electrolyte density and initial defects depend on the composition and synthesis of the ceramic conductor, two syntheses of LPS with different particle sizes are compared. Also, pressure is a key parameter in the quality and stability of interfacial contact while temperature affects both the ionic and electronic conductivity of the ceramic.

Synchrotron micro-tomography is combined with synchrotron transmission x-ray microscopy to study the cells with spatial resolution in the hundreds of nanometers and tens of nanometers. Image analysis of these data has identified sites of Li microstructure growth[4] and now isolates variable-dependent trends such as pressure-dependent void formation in the Li anode. Linking structural changes observed *in operando* to these factors that contribute to Li evolution will guide the design of robust ceramic electrolytes with improved performance and safety.

1. L. Porz, T. Swamy, B. W. Sheldon, D. Rettenwander, T. Frömling, H. L. Thaman, S. Berendts, R. Uecker, W. C. Carter, and Y.-M. Chiang, *Adv. Energy Mater.*, **7**, 1701003 (2017).

2. E. J. Cheng, A. Sharafi, and J. Sakamoto, *Electrochim. Acta*, **223**, 85–91 (2017).

3. F. Han, A. S. Westover, J. Yue, X. Fan, F. Wang, M. Chi, D. N. Leonard, N. J. Dudney, H. Wang, and C. Wang, *Nat. Energy* (2019).

4. N. Seitzman, H. Guthrey, D. B. Sulas, H. A. S. Platt, M. Al-Jassim, and S. Pylypenko, *J. Electrochem. Soc.*, **165**, 3732–3737 (2018).

9:00am **LS+AS+SS-ThM-4 Correlating the Atomic and Electronic Structure in the Formation 2DEGs in Complex Oxides**, *Jessica McChesney, X Yan, F Wrobel, H Hong, D Fong,* Argonne National Laboratory

Using a multimodal approach, we investigate the interplay of the atomic and electronic structure of the formation of 2-D electron gas (2DEG) in complex oxide systems. Using hybrid molecular beam epitaxy for synthesis and in-situ synchrotron x-ray scattering atomic precision of the growth is obtained. The electronic structure then characterized via a combination of resonant soft x-ray angle-resolved photoemission and core level spectroscopy and compared with transport measurements.

9:20am **LS+AS+SS-ThM-5 Uncover the Mystery of Oxygen Chemistry in Batteries through High-Efficiency mRIXS and Theory**, *Wanli Yang,* Lawrence Berkeley National Laboratory **INVITED**

Energy storage through electrochemical devices (batteries) is under pressure to be greatly improved for today's sustainable energy applications, especially the electric vehicles and power grid using renewable energy sources. A battery utilizes transition-metal (TM) oxides as one of the critical electrodes, the positive electrode, which is often the bottleneck of the energy density. In general, the operation of battery cycling is based on reduction and oxidation (Redox) reactions of TMs and a recently proposed oxygen, which involve the changes on the electron occupation numbers in TM-*3d* and O-*2p* states, as well as the evolution of the electronic configuration. However, technical challenges are formidable on probing these states directly, especially for the unconventional oxygen redox states.

This presentation will start with a brief introduction of several needs and grand challenges of battery devices related with oxygen states, which is followed by soft X-ray spectroscopic experiments for providing relevant information. The focus of this presentation is on an active debate of the oxygen states in charged electrodes. We will explain the limitations on conventional soft X-ray absorption spectroscopy (sXAS) for characterizing the important oxygen states, then showcases the power of full energy-range mapping of resonant inelastic X-ray scattering (mRIXS) for clarifying the oxygen redox behaviors in batteries.

We show that mRIXS provides the ultimate probe of the intrinsic oxygen redox reactions in the lattice of battery electrodes [1], which is associated with transition-metal configurations [2]. These spectroscopic results could be quantified to decipher the electrochemical capacity [3], providing both the rationality of the device performance and evidences for understanding the fundamental mechanism of electrochemical materials for energy applications. Furthermore, the mRIXS results indicate a universal driving force of the oxygen redox reactions [4], which could be tackled through combined studies of mRIXS and theoretical calculations [5]. We show that such a spectroscopic and theoretical collaboration could deliver unprecedented information for both fundamental understanding and practical optimization on grand challenges in developing high-performance battery devices.

[1] Gent et al., Nat Comm 8, 2091 (2017)

[2] Xu et al., Nat Comm 9, 947 (2018)

[3] Dai et al., Joule 3, 518 (2019)

[4] Yang & Devereaux, J. Power Sources 389, 188 (2018)

[5] Zhuo et al., JPCL 9, 6378 (2018)

Frontiers of New Light Sources Applied to Materials, Interfaces, and Processing Focus Topic
Room A124-125 - Session LS+HC+SS-ThM

Frontiers of Time-resolved Techniques for Energy & Catalysis Highlight Session

Moderator: Jessica McChesney, Argonne National Laboratory

11:00am **LS+HC+SS-ThM-10 How to Probe Solid/Liquid Interfaces using Standing-wave Photoemission?**, *Slavomir Nemsak,* Lawrence Berkeley National Laboratory*; H Bluhm,* Fritz Haber Institute, Germany*; C Fadley,* University of California, Davis

A great efforts have been made in the development of *in-situ* and *operando* experimental methods in the last two decades, with ambient pressure photoelectron spectroscopy being one of the most profound examples [1]. In combination with advanced techniques, such as standing wave excitation, an unprecedented depth resolution across operating interfaces

can be obtained, providing valuable information on processes governing interfacial behavior.

With the excellent depth selectivity and sensitivity to chemistry and electrostatic gradients, standing wave ambient pressure photoelectron spectroscopy is exploited to probe two different solid/liquid interfaces relevant to energy research, electrochemistry, and atmospheric and environmental science [2,3]. Liquid layers are prepared either by water adsorption in a saturated vapor ambiance or using a so-called meniscus method, in which the sample is pulled out of a liquid reservoir leaving a thin liquid film on the sample's surface. The latter experimental configuration allows also for the *operando* electrochemistry [4]. The outlook and future developments of the technique will be also discussed.

[1] D.E. Starr et al., *Chem. Soc. Rev.* **42**, 5833 (2013).

[2] S. Nemšák et al., *Nat. Comm.* **5**, 5441 (2014).

[3] O. Karslıoğlu et al., *Faraday Discuss.* **180**, 35 (2015).

[4] S. Axnanda et al., *Sci. Rep.* **5**, 9788 (2015).

11:20am LS+HC+SS-ThM-11 *In situ* Spectroscopy of Synthesis of Next-Generation Cathodes for Batteries, *Feng Wang,* Brookhaven National Laboratory

There has been considerable interest in developing low-cost, high-energy electrodes for batteries. However, synthesizing materials with the desired phases and properties has proven difficult due to the complexity of the reactions involved in chemical synthesis. Additional challenge comes from the fact that synthesis is often undertaken under conditions and, hence, the process is hard to be predicted by theoretical computations. probing of synthesis reactions allows for identification of intermediates and determination of thermodynamic/kinetic parameters governing kinetic reaction pathways, thereby enabling synthetic design of materials with desired structure and properties. In this presentation, we will report our recent results from technique development and application to *in situ* probing and synthetic control of local structural ordering and stoichiometry during synthesis of next-generation cathode materials for lithium-ion batteries. Findings from this study, along with its implication to designing viable cathodes for practical use in batteries, will be discussed.

ACKNOWLEDGMENT. This work was supported by the U.S. Department of Energy (DOE) Office of Energy Efficiency and Renewable Energy, Vehicle Technologies Office, Contract No. DE-SC0012704.

11:40am LS+HC+SS-ThM-12 Structural Heterogeneity and Dynamics of 2D Materials Studied by Full-field X-ray Diffraction Microscopy and Ultrafast Surface X-ray Diffraction, *Haidan Wen,* Argonne National Laboratory
INVITED

Transition metal dichalcogenides (TMD) at the two-dimensional (2D) limit have sparked great interests in both fundamental physics and devices applications. Surfaces and interfaces play an important role in t he most common setting, i.e., a monolayer crystal on a substrate, for studying 2D phenomena and device applications. However, the structural characterization with atomic accuracy in this form has been a challenge because the crystal size is usually small and transmission electron microscopy is difficult to apply. In this talk, we show microscopic insights of structural properties can be obtained in the space or time domain using newly developed multimodal full-field x-ray imaging and ultrafast surface x-ray scattering. In the first example, we demonstrate full-field x-ray diffraction imaging of a monolayer 2D material at the Advanced Photon Source. The structural variation across a TMD monolayer or heterostructure is spatially correlated with the electronic properties characterized by the *in-situ* photoluminescence measurements. The correlation reveals mesoscale structure-property relationship in TMDs. In the second example, we report the first femtosecond surface X-ray diffraction using the free-electron laser at Linac Coherent Light Source to quantify the ultrafast structural dynamics of monolayer WSe2 crystals supported on a substrate. We found the absorbed optical photon energy is preferably coupled to the in-plane lattice vibrations within one picosecond whereas the out-of-plane lattice vibration amplitude remains unchanged during the first ten picoseconds. The observed nonequilibrium anisotropic structural dynamics agrees with first-principles modeling in both real and momentum space, marking the distinct structural dynamics of monolayer crystals from their bulk counterparts.

Magnetic Interfaces and Nanostructures Division
Room A210 - Session MI+2D+AS+EM-ThM

Novel Magnetic Materials and Device Concept for Energy efficient Information Processing and Storage
Moderators: Mikel B. Holcomb, West Virginia University, Markus Donath, Muenster University, Germany

8:00am MI+2D+AS+EM-ThM-1 Using Novel Magnonic Device Concepts for Efficient Information Processing, *Burkard Hillebrands,* Technical University Kaiserslautern, Germany **INVITED**

In the field of magnonics, wave-based logic devices are constructed and studied based on the utilization of spin waves and their quanta - magnons. The field is developing rapidly due to its potential to implement innovative ways of data processing as a CMOS complementary technology. Basic building blocks of magnonics have already been realized. Examples are linear and nonlinear spin-wave waveguide structures, magnonic logic, as well as magnonic amplifiers such as the magnon transistor and parametric amplification.

In this talk, I will give an overview about the fundamentals and the current trends in magnonics. One topic is the realization of new functionalities and devices by using novel concepts borrowed from integrated optics and combining them with the specific advantages found in magnetic systems. Examples are directional couplers and quantum-classical analogy devices, such as a magnonic Stimulated Raman Adiabatic Passage (STIRAP) device.

Another important direction is to use fundamentally new macroscopic quantum phenomena such as a Bose-Einstein condensate (BEC) at room temperature as a novel approach in the field of information processing technology. Very promising is the use of magnon supercurrents driven by a phase gradient in the magnon BEC. I will demonstrate evidence of the formation of a magnon supercurrent along with second magnonic sound, and its spatiotemporal behavior, which is revealed by means of time- and wavevector-resolved Brillouin light scattering (BLS) spectroscopy. I will conclude with an outlook.

8:40am MI+2D+AS+EM-ThM-3 Spin-Polarized Scanning Tunneling Microscopy of <10 nm Skyrmions in SrIrO3/SrRuO3 Bilayers, *Joseph Corbett, J Rowland, A Ahmed, J Repicky,* The Ohio State University; *K Meng,* The Ohio State Univesity; *F Yang, M Randeria, J Gupta,* The Ohio State University

We imaged isolated <10 nm sized skyrmions in $SrIrO_3$ on $SrRuO_3$ by spin-polarized scanning tunneling microscopy. We fabricated bilayers of 2 unit cells of $SrIrO_3$ atop of 10 unit cells of $SrRuO_3$ via off-axis sputtering. This thickness combination was selected because it showed a strong topological hall signal. We observed a granular morphology of $SrIrO_3$ mounds with rare patches of exposed $SrRuO_3$. We can distinguish $SrIrO_3$ from $SrRuO_3$ by scanning tunneling spectroscopy where, $SrIrO_3$ grains show a gap-like feature, while $SrRuO_3$ have states near the Fermi level. The height histogram of the observed granular structures is consistent with an average of 2 unit cells of $SrIrO_3$. The grains of the $SrIrO_3$ appear to act as a nucleation for skyrmion formation. Similarly, we've imaged skyrmions under applied +/- 1 T fields demonstrating their magnetic character by observing an inversion in magnetic contrast. We found that the number of $SrIrO_3$ unit cells did not determine skyrmion formation, but the size of the skymrion was linked to the grain size, i.e. the skyrmion formed roughly the size of the grain. Furthermore, we've been able to manipulate the skyrmions by utilizing the influence of the tip. On-going investigations into the mechanism of the magnetic manipulation of the skyrmion are underway, as well theoretical modeling of the isolated skyrmion to ascertain the local Dzyaloshinskii-Moriya interaction constant.

9:00am MI+2D+AS+EM-ThM-4 Relieving YIG from its Substrate Constraints - YIG Resonators on Various Crystalline Substrate Materials, *Georg Schmidt,* Martin-Luther-Universität Halle-Wittenberg, Germany **INVITED**

We have recently demonstrated the fabrication of free-standing 3D yttrium iron garnet (YIG) magnon nano-resonators with very low damping [1]. At first the resonators were fabricated on gallium gadolinium garnet (GGG) substrates which are most suitable for epitaxial deposition of YIG. The process involves room temperature deposition and subsequent annealing. Transmission electron microscopy investigation of the bridge-like structures shows that the span of the bridge is almost monocrystalline while some defects nucleate at the transitions from the span to the posts of the bridge which are epitaxially bound to the substrate. This suggests that the quality of the span may only indirectly depend on the quality of

the feet, the latter being largely determined by the lattice matching of the substrate material to the YIG. Being able to grow YIG structures on substrate materials other than GGG would not only be interesting because of availability and price but also because the high frequency properties of GGG are less than ideal while other materials like MgO or Sapphire would be preferred for high frequency applications. We have fabricated YIG bridges on various substrate materials including yttrium aluminium garnet (YAG), MgO, and sapphire. In most cases we achieve high crystalline quality of the span even for non-matching substrates. For some of the materials time resolved magneto optical Kerr microscopy even reveals magnon resonances with reasonable linewidth.

[1] F. Heyroth et al. cond-mat.1802.03176

9:40am MI+2D+AS+EM-ThM-6 Magnetic Textures in Chiral Magnet MnGe Observed with SP-STM, *Jacob Repicky, J Corbett, T Liu, R Bennett, A Ahmed,* The Ohio State University*; J Guerrero-Sanchez,* National Autonomous University of Mexico*; R Kawakami, J Gupta,* The Ohio State University

Materials with non-centrosymmetric crystal structures can host helical spin states including magnetic skyrmions. Bulk MnGe hosts a short period magnetic state (3 nm), whose structure depends strongly on atomic lattice strain, and shows a large emergent transport signature associated with the skyrmion phase. Here, we use low-temperature (5 K) spin-polarized scanning tunneling microscopy (SP-STM) to image the magnetic textures in MnGe thin films grown via molecular beam epitaxy and study the influence of the surface on those textures. Most microscopic locations show a spin spiral phase with a 6-8 nm period and a propagation direction that is influenced by step edges and surface termination. We also report the presence of isolated target skyrmions which have a triangular shape that appears to be set by the in-plane lattice vectors, and a core size of approximately 15 nm. We observe the target state is significantly more sensitive to magnetic fields than the spiral phase, and that local voltage and current pulses with the STM tip imply the texture can be 'switched' between states with different topological charge. Detailed analysis of atomic resolution STM images is used to probe the role of small lattice strain on the distinct textures. To fully understand the magnetic textures in MnGe we will expand this study by investigating films of different thicknesses to vary the magnetic anisotropy and strain.

11:00am MI+2D+AS+EM-ThM-10 Dzyaloshinskii-Moriya Interaction in Magnetic Multilayers, *Hans Nembach,* National Institute of Sandards and Technology (NIST) **INVITED**

The Dzyaloshinskii-Moriya Interaction (DMI) gives rise to chiral magnetic structures, which include chiral spin-chains and skyrmions. The latter have recently received much attention, especially for their potential application for magnetic data storage. Each skyrmion would represent a bit and would be moved along a racetrack. DMI requires broken inversion symmetry and can exist in the bulk as well as at interfaces, for example at interfaces between a ferromagnet and a material with large spin-orbit coupling like heavy metals. More recently it has been shown that interfacial DMI can also exist at interfaces with graphene and oxides.

We use Brillouin Light Scattering spectroscopy (BLS) to determine the DMI from the non-reciprocal frequency-shift Damon-Eshbach spin-waves. In order to gain deeper insight into the underlying physics of DMI, we prepared several sample series to study different aspects of the DMI. First, we prepared two samples series to study the relationship between the DMI and the Heisenberg exchange. One series was a $Ni_{80}Fe_{20}$ thickness series on a Pt layer and for the other series we introduced a Cu dusting layer at the interface between a CoFeB layer and Pt to disrupt the Heisenberg exchange directly at the interface. For both sample series, we found that the Heisenberg exchange and the DMI are proportional to each other as it has been predicted by theory. Next, we prepared a $Cu/Co_{90}Fe_{10}$ and a $Pt/Co_{90}Fe_{10}$ sample series, which were in-situ oxidized for different times and subsequently capped to prevent any further oxidation. Density functional theory calculations have shown that the hybridization and the associated charge transfer is important for the DMI and that interfaces with an oxide can have DMI. Our BLS measurements showed that oxide interfaces have DMI. Moreover, we showed that the spectroscopic splitting factor g, which we determined with ferromagnetic resonance spectroscopic, is correlated to the DMI. This is an indirect confirmation of the theory predictions regarding the role of hybridization and charge transfer.

So far, most work on DMI has been carried out for highly symmetric interfaces. Low symmetry systems can have anisotropic DMI and can potentially support anti-skyrmions. We prepared a Pt/Fe(110) sample and found that the DMI is anisotropic with the strongest DMI along the [001] direction, which coincides with the magnetic easy axis.

Finally, we studied the impact of He+ ion irradiation on DMI for the Ta/CoFeB/Pt system. We found that the DMI increases with the dose before it drops for the highest does. This is in contrast to the perpendicular anisotropy, which continuously decreases with ion-irradiation.

11:40am MI+2D+AS+EM-ThM-12 Transport in Goniopolar and (pxn) Metals, *Joseph Heremans, B He, L Zheng, Y Wang, M Arguilla, N Cultrara, M Scudder, J Goldberger, W Windl,* The Ohio State University **INVITED**

semiconductors that have *p*-type conduction along some crystallographic directions and *n*-type conduction along others due to a particular topology of their Fermi surface. The electrical and thermoelectric transport of one member of this class, $NaSn_2As_2$, will be presented. A second class of materials have similar transport properties due to different mechanisms: some, like Be and Cd, have Fermi surfaces that contain both electron and hole pockets that have partial thermopowers of opposite polarities, but very anisotropic mobilities, so that one carrier type dominates the total thermopower in one direction, and the other carrier type dominates the thermopower in the other direction. A new member of this class, the semimetal bismuth doped p-type with Sn, will be described in this talks as well. In practice, a third class of artificial materials made of separate layers of p-type and of n-type semiconductors can be made to have a similar behavior in transport as well; the last two classes are called (pxn)-materials.

The electrical conductivity and thermopower tensors in goniopolar and (pxn) materials can be made to have off-diagonal components, which cause exciting new properties like zero-field Hall and Nernst-Ettingshausen effects. These materials can be used in single-crystal transverse thermoelectrics.

[1] He, B. et al , *Nat. Mater.* (published online doi.org/10.1038/s41563-019-0309, 2019)

[2] Zhou, C. et al. *Phys. Rev. Lett.* **110**, 227701 (2013).

Manufacturing Science and Technology Group
Room A226 - Session MS+EM+QS-ThM

Science and Technology for Manufacturing: Neuromorphic and Quantum Computing (ALL INVITED SESSION)

Moderators: Nathaniel C. Cady, SUNY Polytechnic Institute, Albany, Alain C. Diebold, SUNY College of Nanoscale Science and Engineering

8:40am MS+EM+QS-ThM-3 Materials and Fabrication Challenges for Neuromorphic and Quantum Computing Devices, *S Olson, C Hobbs, H Chong, J Nalaskowski, H Stamper, J Mucci, B Martinick, M Zhu, K Beckmann, I Wells, C Johnson, V Kaushik, T Murray, S Novak, S Bennett, M Rodgers, C Borst, N Cady, M Liehr,* **Satyavolu Papa Rao,** SUNY Polytechnic Institute **INVITED**

Devices for quantum computing, quantum communications and quantum sensing share many challenges in terms of the materials, their interfaces, and fabrication technologies. This presentation will quickly review the broad swath of quantum technologies that are being actively studied, while identifying synergies among them that can be exploited for efficient development of integrated quantum computing systems. Advanced process tools capable of exquisite control of the processes, materials and interfaces at 300mm wafer scale have been utilized for the fabrication of structures for quantum computing. Examples of such efforts, including structures for superconducting transmon qubits, resonators, and superconducting nanowire single photon detectors, will be discussed – with an emphasis on the materials and process control issues that needed to be tackled, while keeping manufacturability considerations always in mind. The presentation will conclude with a discussion of how advances in the fabrication of such devices for quantum computing are being applied to 'adjacent spaces' such as neuromorphic computing using superconducting optoelectronics (in partnership with AFRL-Rome and NIST Boulder).

9:20am MS+EM+QS-ThM-5 IBM Q: Quantum Computing in the 21st Century, *Robert Sutor,* IBM Research **INVITED**
For almost 40 years, quantum computing has intrigued and amazed scientists and non-scientists in its future possibility for solving problems

that are intractable using classical computing. Over the last three years, IBM has made real quantum computers available on the cloud so that clients, students, and researchers can begin to learn and experiment with this new way of computing. We'll see what use cases are being considered in industry, the state of quantum computing today, and how you can get on the right path to make the earliest use of this rapidly evolving technology.

11:00am MS+EM+QS-ThM-10 Quantum Information Science at AFRL, *Michael Hayduk*, Air Force Research Laboratory **INVITED**
Recent advances in Quantum Information Science (QIS) indicate that future applications of quantum mechanics will lead to disruptive advances in capabilities for the US Air Force. Controlling and exploiting quantum mechanical phenomena will enable inertial sensors and atomic clocks that provide GPS-like positioning and timing accuracy for extended periods of time in degraded environments, communications networks with information security based on physics principles, unprecedented sensor resolution, and computers that may be able to provide exponential speedup in processing speed. To ensure that the future Air Force warfighter maintains a technological advantage, the AF must implement a QIS strategy that leads to robust, deployable quantum systems. This invited talk will discuss the recently developed Air Force Research Laboratory QIS strategy that covers the areas of timing, sensing, communications and networking, and computing. Capability development across these four areas will also be discussed.

11:40am MS+EM+QS-ThM-12 Neuromorphic Computing: From Emerging Devices to Neuromorphic System-on-a-Chip, *Vishal Saxena*, University of Idaho **INVITED**
Several classes of emerging non-volatile memory (NVM) devices are currently being investigated for their application in analog implementation of artificial neural networks (ANN) hardware. The device can be two- or three-terminal and employ a wide range of material systems and associated physical mechanisms to achieve two or more non-volatile memory states. ANN hardware realizations include vector matrix multipliers (VMMs) and neural-inspired or Neuromorphic computing circuits. The NVM devices are employed in the form of crossbar or crosspoint arrays with or without selectors. In order to exploit the high-density and potential low-power operation of these devices, Analog circuit designers need to accommodate non-ideal behavior of these devices. This is particularly important for optimizing transistor-level circuit design for layout area, reliability, and static and dynamic power consumption. NVM nonidealities include device variability, low resistances offered by the two-terminal devices, finite resolution, relaxation of incremental states, limited dynamic range, and read/write endurance. This talk will provide an overview of Neuromorphic System-on-a-Chip (NeuSoC) that can be realized using emerging NVM arrays, expected device characteristics, associated circuit design challenges, and potential strategies for their mitigation. The talk will also include energy-efficiency estimation and benchmarking for NeuSoCs and provide pathways for future work in this area.

Nanometer-scale Science and Technology Division
Room A222 - Session NS+2D+QS-ThM

Direct Atomic Fabrication by Electron and Particle Beams & Flash Session

Moderators: Canhui Wang, National Institute of Standards and Technology (NIST), Xiaolong Liu, Northwestern University

8:00am NS+2D+QS-ThM-1 Multiprobe Scanning Tunneling Microscopy and Spectroscopy: Atomic-level Understanding of Quantum Transport in Functional Systems, *Marek Kolmer*[1], *W Ko, A Li,* Oak Ridge National Laboratory
Techniques based on multiprobe scanning tunneling microscopy (MP-STM) allow determination of charge and spin transport in variety of systems supported on surfaces of solid materials. In classical 2- and 4-probe methods STM tips are navigated by scanning electron microscope or high-resolution optical microscope typically in micrometer scales down to hundreds of nanometers. These MP-STM methods are currently regarded as universal tools for in-situ characterization of mesoscopic transport phenomena [1,2].

Such a mesoscopic experimental paradigm has recently been changed by downscaling of 2-probe STM experiments towards the atomic level [3,4]. In this case current source and drain probes are positioned in atomically defined locations with respect to the characterized nanosystems. Our experiments rely on fully STM-based tip positioning protocol with probe-to-probe separation distances reaching tens of nm [3,4]. Such probe-to-probe lateral positioning precision is combined with about pm vertical sensitivity in probe-to-system contacts. These two factors enable realization of two-probe scanning tunneling spectroscopy (2P-STS) experiments, where transport properties can be characterized by macroscopic probes kept in atomically defined tunneling conditions [4].

Here, we will apply 2P-STS methodology to probe quantum transport properties in functional systems: graphene nanoribbons (GNRs) epitaxially grown on the sidewalls of silicon carbide (SiC) mesa structures. These GNRs display ballistic transport channels with exceptionally long mean free paths and spin-polarized transport properties as proven by mesoscopic multiprobe transport experiments [5-7]. Interestingly, the nature of these ballistic channels remains an open question. We will show that 2P-STS experiments give new insight into quantum origin of the transport behaviors.

[1] Li, A.-P. et al., Adv. Funct. Mater., 23 (20), 2509-2524 (2013)

[2] Voigtländer B. et al., Rev. Sci. Instrum., 89(10), 101101 (2018)

[3] Kolmer M. et al., J. Phys.: Condens. Matter, 29(44), 444004 (2017)

[4] Kolmer M. et al., Nat.Commun., 10, 1573 (2019)

[5] Baringhaus J., Nature, 506, 349–354 (2014)

[6] Aprojanz J. et al., Nat.Commun., 9, 4426 (2018)

[7] Miettinen A.L. et al., submitted, arXiv:1903.05185 (2019)

This work was conducted at the Center for Nanophase Materials Sciences (CNMS), which is a DOE Office of Science User Facility.

8:20am NS+2D+QS-ThM-2 Light and Heavy Ions from New Non-classical Liquid Metal Ion Sources for Advanced Nanofabrication, *Paul Mazarov*, RAITH GmbH, Germany*; T Richter, L Bruchhaus, R Jede,* Raith GmbH*; Y Yu, J Sanabia,* Raith America*; L Bischoff,* Helmholtz Zentrum Dresden-Rossendorf, Germany*; J Gierak,* CNRS—Université Paris-Sud, France **INVITED**
Nanofabrication requirements for FIB technologies are specifically demanding in terms of patterning resolution, stability and the support of new processing techniques. Moreover the type of ion defines the nature of the interaction mechanism with the sample and thus has significant consequences on the resulting nanostructures [1]. Therefore, we have extended the technology towards the stable delivery of multiple ion species selectable into a nanometer scale focused ion beam by employing a liquid metal alloy ion source (LMAIS) [2]. This provides single and multiple charged species of different masses, resulting in significantly different interaction mechanisms. Nearly half of the elements of the periodic table are made available in the FIB technology as a result of continuous research in this area [3]. This range of ion species with different mass or charge can be beneficial for various nanofabrication applications. Recent developments could make these sources to an alternative technology feasible for nanopatterning challenges. In this contribution the operation principle, the preparation and testing process as well as prospective domains for modern FIB applications will be presented. As example we will introduce a GaBiLi LMAIS [4]. It enables high resolution imaging with light Li ions and sample modification with Ga or heavy polyatomic Bi clusters, all coming from one ion source. For sub-10 nm focused ion beam nanofabrication and microscopy, the GaBiLi-FIB or the AuSiGe-FIB could benefit of providing additional ion species in a mass separated FIB without changing the ion source.

References

[1] L. Bruchhaus, P. Mazarov, L. Bischoff, J. Gierak, A. D. Wieck, and H. Hövel, *Comparison of technologies for nano device prototyping with a special focus on ion beams: A review,* Appl. Phys. Rev. 4, 011302 (2017).

[2] L. Bischoff, P. Mazarov, L. Bruchhaus, and J. Gierak, *Liquid Metal Alloy Ion Sources – An Alternative for Focused Ion Beam Technology*, Appl. Phys. Rev. **3** (2016) 021101.

[3] J. Gierak, P. Mazarov, L. Bruchhaus, R. Jede, L. Bischoff, *Review of electrohydrodynamical ion sources and their applications to focused ion beam technology,* JVSTB 36, 06J101 (2018).

[4] W. Pilz, N. Klingner, L. Bischoff, P. Mazarov, and S. Bauerdick, *Lithium ion beams from liquid metal alloy ion sources,* JVSTB 37, 021802 (2019).

---

[1] **NSTD Early Career Award Finalist**

9:00am NS+2D+QS-ThM-4 Visualizing the Interplay between Spatial and Magnetic Confinement in Graphene Quantum Dots, *Joseph Stroscio,* National Institute of Standards and Technology (NIST) **INVITED**

At the heart of the wave nature of quantum mechanics is the quantization of energy due to quantum confinement, taking place when the particle's de Broglie wavelength becomes comparable to the system's length scale. In a quantum dot (QD), electrons are confined in all lateral dimensions using geometric constraints or a combination of electric and magnetic fields. Being a tunable quantum workbench, QDs have found a ubiquity of applications. Behaving as artificial atoms they have found extensive use as qubits in quantum information technologies, and tools for emulating basic models of condensed-matter physics. QDs offer an ideal platform for studying the interplay between quantum confinement, caused by spatial constraints or by large magnetic fields via cyclotron motion, and interaction effects. Recently, the ability to apply local nanometer scale gate potentials in graphene heterostructures has enabled the creation of QDs for Dirac quasiparticles. Graphene QDs are formed inside circular p-n junctions, where one has detailed control of electron orbits by means of local gate potentials and magnetic fields. We study the interplay between spatial and magnetic confinement using scanning tunneling spectroscopy measurements of the energy spectrum of graphene QDs as a function of energy, spatial position, and magnetic field. In zero field, the Dirac quasiparticles are confined by Klein scattering at large incident angle at the p-n junction boundary. The confined carriers give rise to an intricate eigenstate spectrum, effectively creating a multi-electron artificial atom. Applying a weak magnetic field results in a sudden and giant increase in energy for certain angular momentum states of the QD, creating a discontinuity in the energy spectrum as a function of magnetic field. This behavior results from a π-Berry phase associated with the topological properties of Dirac fermions in graphene, which can be turned on and off with magnetic field. With increased applied magnetic field, the QD states are observed to condense into Landau levels, providing a direct visualization of the transition from spatial to magnetic confinement in these artificial graphene atoms. With further increase in magnetic fields, an intricate interplay between Coulomb charging of compressible Landau levels separated by incompressible rings emerges, which we map as a function of energy, spatial position, and magnetic field utilizing the exceptional capabilities of scanning tunneling spectroscopy.

9:40am NS+2D+QS-ThM-6 Using Controlled Manipulation of Molecules to Trace Potential Energy Surfaces of Adsorbed Molecules, *O Dagdeviren, C Zhou,* Yale University*; M Todorovic,* Aalto University, Finland*; Eric Altman, U Schwarz,* Yale University

The development of scanning probe microscopy techniques has enabled the manipulation of single molecules. More recently it has been demonstrated that the forces and energy barriers encountered along the manipulation path can be quantified using non-contact atomic force microscopy (AFM). To explore the practicality of using this novel approach to experimentally measure the energy barriers an adsorbed molecule encounters as it moves across a surface decorated by other molecules including potential reaction partners, we have been studying benzene molecules on Cu (100) as a model system. We first choose a specific manipulation path and then move the tip repeatedly along this path as the tip-sample distance is reduced while recording the AFM cantilever oscillation amplitude and phase. To preserve the accurancy of the recovered tip-sample interaction potentials and forces, we use oscillation amplitudes significantly larger than the decay length of the tip-sample interaction potential are used. Operating the microscopy in the tuned-oscillator mode and analyzing the resulting cantilever oscillation amplitude and phase as functions of the spatial coordinates allows recovery of the potential energy of the interaction between the tip and the sample, the force on the tip normal to the surface, and the lateral force acting on the tip along the manipulation path, all as functions of tip vertical and lateral position with 0.01 Å resolution. In over 50 distinct maniupluation events, the molecules were either pushed, pulled, jumped to the tip, or did not move depending on the chemical environment surrounding the molecule and the chemical identity of the tip. For further insight, we have compared the experimentally measured energy landscapes and manipulation outcomes with computational results obtained using a Bayesian Optimization Structure Search protocol.

11:00am NS+2D+QS-ThM-10 Direct Writing of Functional Heterostructures in Atomically Precise Single Graphene Nanoribbons, *Chuanxu Ma,* Oak Ridge National Laboratory*; Z Xiao,* North Carolina State University*; J Huang, L Liang,* Oak Ridge National Laboratory*; W Lu,* North Carolina State University*; K Hong, B Sumpter,* Oak Ridge National Laboratory*; J Bernholc,* North Carolina State University*; A Li,* Oak Ridge National Laboratory

Precision control of interfacial structures and electronic properties is the key to the realization of functional heterostructures. Here, utilizing the scanning tunneling microscope (STM) both as a manipulation and characterization tool, we demonstrate the fabrication of a heterostructure in a single atomically precise graphene nanoribbon (GNR) and report its electronic properties[1]. The heterostructure is made of a seven-carbon-wide armchair GNR (7-aGNR) and a lower band gap intermediate ribbon synthesized bottom-up from a molecular precursor on an Au substrate. The short GNR segments are directly written in the ribbon with an STM tip to form atomic precision intraribbon heterostructures. Based on STM studies combined with density functional theory calculations, we show that the heterostructure has a type-I band alignment, with manifestations of quantum confinement and orbital hybridization. We further investigate the negative differential resistance (NDR) devices using the GNR heterostructure based double-barrier models[2]. Our computational results indicate that nanoscale engineering for NDR needs to consider atomic size effect in design and atomic precision in fabrication. This combined theoretical-experimental approach opens a new avenue for the design and fabrication of nanoscale devices with atomic precision.

References

1. Ma, C.; Xiao, Z.; Huang, J.; Liang, L.; Lu, W.; Hong, K.; Sumpter, B. G.; Bernholc, J.; Li, A.-P. Direct writing of heterostructures in single atomically precise graphene nanoribbons. *Phys. Rev. Materials* **2019,** 3, 016001.

2. Xiao, Z.; Ma, C.; Huang, J.; Liang, L.; Lu, W.; Hong, K.; Sumpter, B. G.; Li, A. P.; Bernholc, J. Design of Atomically Precise Nanoscale Negative Differential Resistance Devices. *Adv. Theory Simul.* **2018,** 2, 1800172.

11:20am NS+2D+QS-ThM-11 Effects of Helium and Neon Processing on 2D Material Properties, *Alex Belianinov,* Oak Ridge National Laboratory*; S Kim,* Pusan National University, South Korea*; V Iberi, S Jesse, O Ovchinnikova,* Oak Ridge National Laboratory

Recent advances in CVD-growth consistently yield high quality 2D materials for large(er) scale fabrication. Monolayers of molybdenum and tungsten diselenide and suflide, graphene, and other exotic 2D materials are becoming routine in fabrication of functional electronic and optoelectronic devices. In order to attain novel functionalities, it is critical to tune and engineer defects in 2D materials directly with nanometer precision. Advances in ion beam-based imaging and nanofabrication techniques have offered a pathway to precisely manipulate 2D materials and offer a roadmap to create junctions, amorphized areas, and introduce dopants for new types of electronic devices. Here, we demonstrate the use of a focused helium and neon ion beams in a scanning helium ion microscope (HIM) in tailoring material functionality in MoSe2, WSe2, CuInP2S6 and graphene.

The helium ion microscope can "direct-write" capabilities, capable of both imaging and nanofabrication with Helium and Neon gases, thus making it an excellent candidate for processing a wide range of 2D, and conventional materials. We explore milling by the helium and neon ion beams of suspended and supported samples in order to control material's electronic and mechanical properties. We validate the results with other chemical imaging techniques such as Scanning Transmission Electron Microscopy, correlated band excitation (BE) scanning probe microscopy, and photoluminescence (PL) spectroscopy.

Acknowledgement

11:40am NS+2D+QS-ThM-12 Operating Molecular Propeller in Quantum Regime with Directional Control, *Y Zhang, Tolulope Ajayi,* Ohio University*; J Calupitan,* Université de Toulouse, France*; R Tumbleson,* Ohio University*; G Erbland, C kammerer,* CEMES-CNRS, France*; S Wang,* Ohio University*; L Curtiss, A Ngo,* Argonne National Laboratory*; G Rapenne,* NAIST, Japan*; S Hla,* Ohio University

Synthetic molecular machines are fascinating and have a great promise to revolutionize a large scientific adn technology fields. The immense interest to this research area is evident by the 2016 Nobel Prize in Chemistry

awarded for the design and synthesis of molecular machines. Unlike biological molecular machines, which typically have the sizes of a few microns, artificial machines operating at the nanometer scale are in the quantum regime. Here, we have developed a robust multi-component molecular propeller that enables unidirectional rotations o a materials surface when they are energized. Our propeller system is composed of a stator having a ratchet-shaped molecular gear designed to anchor on a gold surface and a rotor with three molecular blades. By means of scanning tunneling microscope imaging and manipulation, the rotation steps of individual molecular propellers are directly visualized, which confirms the unidirectional rotations of both left and right handed molecular propellers into clockwise and counterclockwise directions, respectively. Moreover, the mechanical manipulation of the molecular with the scanning probe tip further reveal detailed rotation mechanism, thereby opening a new research direction to investigate mechanical properties of the molecular machines with an atomic level precision.

Plasma Science and Technology Division
Room B131 - Session PS-ThM

Plasma Diagnostics and Sources II

Moderators: David Lishan, Plasma-Therm LLC, Geun Young Yeom, Sungkyunkwan University, Korea

8:00am **PS-ThM-1 Measurement of Plasma Neutral Densities in a Very High Frequency Ar/NH₃ Plasma with a Line-of-sight Threshold Ionization Mass Spectrometry**, *Jianping Zhao*, *P Ventzek, C Schlechte, M Burtner,* Tokyo Electron America, Inc.*; D Li, J Ekerdt,* The University of Texas at Austin*; T Iwao, K Ishibashi,* Tokyo Electron Technology Solutions Limited, Japan

Atomic precision plasma processes for logic and memory fabrication are in increasing demand due to the shrink of critical dimensions to near physical limits and increase in stack complexity. Meeting dimensionality requirements is not enough. Infinite selectivity and damage-free process with sub-angstrom control are sought to deliver high quality films with productivity worthy yields. Plasma enhanced processes, particularly plasma enhanced atomic layer deposition (ALD) rely on plasma generated radicals for much of their perceived benefit. Furthermore, low energy ions are required to mitigate damage. Large-area plasma processing systems capacitively driven at very high frequencies (VHF, e.g. 100MHz) have attracted much interest for semiconductor device and flat panel display processing. VHF has the advantage of generating plasma with more efficiency as power is coupled more into electrons and less into ions in the sheath. Depending on the film and process, benefits are reduced ion energy and high radical and ion fluxes. It remains the case that it is difficult to relate the role of the combination of species flux and energy exactly to film growth mechanisms or material properties. Ideally, both species flux and film properties would be measured simultaneously (and in real time) as the surface state from ALD is changing continuously. A significant challenge is that it is difficult to measure the absolute density of neutral species in industrially relevant plasmas reliably especially at high pressure. In order to understand the fundamental plasma chemistry property of VHF plasma, we present here the measurement of the neutral species with a line-of-sight threshold ionization mass spectrometry (LS-TIMS) technology in VHF Ar/NH₃ plasmas. Ar/NH₃ plasma has been widely used in plasma enhanced ALD and CVD. Systematic measurements were performed in a 100 MHz plasma source with a wide RF power, pressure, Ar to NH₃ flow ratio range. Plasma chemistry properties of Ar/NH₃ plasma are derived after a careful background subtraction and mass-to-charge ratio dependent sensitivity calibration. Density of NH₃ and various amine dissociation products are determined as a function of plasma discharge conditions. The LS-TIMS results are also compared to those from other optical based neutral diagnostics.

8:20am **PS-ThM-2 Radical Probe System for In-Situ Measurements of Hydrogen, Oxygen and Nitrogen Radical Densities**, *Dren Qerimi*, *G Panici, A Jain,* University of Illinois at Urbana-Champaign*; J Wagner,* Colorado State University*; D Ruzic,* University of Illinois at Urbana-Champaign

The current state-of-the-art methods to identify presence of radical species in vacuum chambers are optical methods, which suffer from the lack of spatial resolution and require expensive optical equipment. Center for Plasma Material Interactions (CPMI) at the University of Illinois developed a catalytic radical probe array to measure concentrations of reactive species in low temperature plasma with high spatial resolution. Radical probes as plasma diagnostic tool can be used to determine radical densities of hydrogen, nitrogen and oxygen in any continuous plasma source in vacuum environment. The basic principle and advantage of a probe array is the capability to distinguish between different gas species due to several sensitive elements acting as recombination catalysts [1]. The catalytic coatings cover an area of several square millimeters on the tip of a sheathed thermocouple. The catalytic probe surface provides efficient recombination of active species with subsequent energy release as a heat. All the probes are exposed to the same background plasma heating/cooling mechanisms, but the temperatures are not the same due to the fact that different catalytic materials have different recombination coefficients, therefore a temperature difference between probes is generated. The system consists of two additional probes, first to obtain the overall heat flux on probe array, and the second is a reference probe with surface chemically active to all gases.

Lifetime of radical probes, specifically catalytic surface degradation, depends highly on vacuum conditions, chamber contamination and the fact that radical species cause surface properties to change. Lifetime of radical probe system is usually three hours. However, probe surface cleaning has been achieved by applying a bias which causes contamination layer on the probe tip to sputter via ion bombardment. Argon gas is used to sputter clean probe tip. Additionally, if probe shows signs of high contamination then a long sputtering process is used to remove all the catalytic material from the probe tip and then magnetron sputtering is used to redeposit new catalytic coating. The array of several probes is capable to distinguish between different gas species with sub centimeter spatial resolution. The probes give accurate results in a broad range of reactive species concentrations from about 10^{12} to 10^{14} cm^{-3}.

Reference:

[1] M Mozetic, M Kveder, M Drobnic, A Paulin, and A Zalar. Determination of atomic

hydrogen density with catalytic probes. Vacuum, 45(10-11):1095-1097, 1994.

8:40am **PS-ThM-3 Post Charge Separation Grid Ion Flux Evaluation in Inductive Coupled Plasma Source Downstream Asher**, *Luke Zhang, S Ma,* Mattson Technology, Inc.

With semiconductor device shrink and gate dielectric thickness decrease, the potential for device damage at the photoresist strip level increase. It is desired to develop the downstream plasma asher producing high active radical concentration with low ion concentration while still maintaining excellent ash rate for different strip application. Therefore, it is critical to understand the population of charge species that can reach the wafer surface. In this study, an inductive coupled plasma (ICP) source with patented grounded Faraday shields is used [1], which offers superior resist strip capability to leading edge memory, logic and foundry applications. Faraday shield is used to reduce ion energy and electron temperature from plasma generation to obtain the better plasma damage performance. To further reduce the ion concentration on the wafer surface, charge separation conductive grid [2] is also added between the top plasma source and heated pedestal. By optimizing grid pattern, uniform gas and radical distribution can be obtained, thus the wafer uniformity can be improved. Ion flux underneath the grid are evaluated with different diagnostic tools to evaluate the grids effect including Langmuir probe and Retarding Field Energy Analyzer. The Langmuir probe with plasma detect limit 10^8 cm-3 is inserted plasma at 1cm above the pedestal is used to detect the ion flux underneath the grids. RFEA (Retarding Field Energy Analyzer) is equipped on the pedestal, which measures ion energy and ion flux directly. Both the diagnostics tools show that ion density is below the detection limit after charge separation grid. To further characterize the grid effect, one self-made thick probe with length 10mm and diameter 3.8mm inserted to the plasma with biased at negative voltage to measure ion saturation current, Pico amp accuracy ammeter is used to measure the collected current. It is found that grid dramatically reduce the ion saturation current, one thousandth of ion saturation current at Oxygen plasma detected under double grids compared to no grid condition. Different plasma chemistry and different grid are also evaluated.

[1] Stephen E. Savas, Brad S. Mattson, Martin L. Hammond, Steven C. Selbrede, Patent US 6143129

[2] Stephen E. Savas, Brad S. Mattson, Patent US 5811022

9:00am **PS-ThM-4 Development of a Novel Langmuir Probe for the Investigation of Dusty Non-thermal Plasmas**, *Austin Woodard* [1] *, L Mangolini, K Shojaei, C Berrospe,* University of California, Riverside

Dusty plasmas are characterized as plasmas containing micro- to nano-sized particles. Probing the plasma physics inherent in these systems is a daunting, but critical, task necessary for the engineering design and optimization of many common-place industrial manufacturing processes utilizing plasma, such as thin film etching and fabrication. We present the development of a test-bed for the characterization of dusty plasmas via a simple Langmuir probe. This diagnostic tool allows for the precise determination of the electron energy distribution function (EEDF) and subsequent plasma parameters but is notoriously difficult to use in dust-forming chemistries due to the inevitability of an insulating coating. To combat this, we have designed a two-stage reactor scheme that overcomes this limitation. In the first plasma reactor, the particle production cell, we synthesize graphitic carbon nanoparticles from the complete dissociation of acetylene, confirmed by a residual gas analyzer, which are then directly injected into the primary chamber volume. The quality of the measurement is minimally affected by the presence of a graphitic nanoparticle coating on the probe tip due to its high electrical conductivity, thus creating a more forgiving environment in which to employ this technique. Additionally, the approach has the advantage of decoupling the nucleation and growth-phase kinetics of the nanoparticles from the primary chamber discharge thus allowing us to study the plasma properties when varying processing parameters such as primary plasma power and chamber pressure. Due to the particle trapping induced in the primary plasma, a continues wave laser (532 nm) was used to investigate the actual particle density in the primary chamber volume, and from this, the average charge per particle. The analysis of the EEDF as a function of the plasma parameters highlights the onset of unexpected trends in plasma the properties which are not predicted by traditional OML theory; we observe secondary peaks in the EEDF that change with the processing parameters, indicating not an electronic transition, but a phenomenon directly related to the presence of dust. To investigate this theoretically, we performed simulations with a Boltzmann-solver modified to account for the effect of secondary electron emissions. These simulations also exhibited a secondary peak, at the same energy levels observed experimentally; thus, we tentatively attribute this observation to secondary emission processes directly tied to the floating potential of the particles.

9:20am **PS-ThM-5 Historical Review of Microwave Plasma Diagnostics using Plasma Cutoff Phenomenon**, *Shin-Jae You, S Kim,* Chungnam National University, Republic of Korea*; D Kim,* KIMM, Republic of Korea
INVITED

Though this paper, we present historial review of our cutoff probe research which has been performed for almost 2 decade. This paper focus on the whole progress for the cutoff probe including how to start to develop the cutoff probe in the initial period, what idea has been included during the development, how to evolve the probe during 17 years. The cutoff probe is most simple diagnostics among the plasma diagnostics tools which was made by simple intuition for the cutoff phenomenon of the plasma wave. However, the cutoff probe has been used for a long time without test of validation of probe itself. Later, EM waver simulation supported the validation for the cutoff frequency determination. Recently, by supposing the circuit modeling, the physics behind for the cut off probe spectrum (S21) was revealed and the accuracy and the application window of the probe were established. Very recently, as an extended version of the circuit model, we makes transmission line modeling to explain the cutoff spectrum in high density plasma as well as low density plasma.

Based on recent developments we also introduce a novel methodology to interpret the probe spectrum that eliminates the sheath and collisional effects and enables the use of this precise diagnostic technique in a broad range of practical processing conditions.

11:00am **PS-ThM-10 Characterization of Inductive Coupled Plasma Source RF Power Pulsing for Advanced Surface Treatment Applications**, *Shawming Ma, L Zhang, D Kohl,* Mattson Technology, Inc.

As device dimensions continue to shrink into the sub-10 nm regime, low electron temperature plasma and radicle energy control become very important factors in the fabrication of microelectronics device. A pulsing plasma reactor [1] is an efficient way to bring down the electron temperature and improve the process window by adding an additional tuning knob. Pulsed plasmas have been widely used in plasma etch tools, as high-density plasmas at low pressure demonstrate excellent plasma charge damage reduction, improved microloading and reduced mask erosion compared to traditional etchers. However, no results have thus far been reported for a high pressure, downstream pulsed plasma reactor for surface treatment and plasma ashing. For advanced surface treatment applications, radical energy control becomes necessary to control either selectivity to underlying films during resist ashing, surface film growth or surface property change. Therefore, it is desired to have radical energy control capability to improve the process window.

In this work, we explore pulsing plasma in a high pressure, downstream, grounded Faraday Shielded ICP source[2]. Source RF power of 13.56MHz frequency with pulsing frequency up to 100kHz and a vacuum capacitor automatch were used in the experiment. The pulsing window was mapped with maximum pulsing frequency 30KHz and duty cycle from 10% to 90%. A Langmuir probe is used to measure the electron energy distribution function (EEDF) developed by Plasma Sensor [3], which is inserted in the reactor 1cm above the wafer pedestal. Due to the limitations of plasma density measurement, (Langmuir probe requires plasma density above 10^8 cm-3 detection limit) the grid [4] which is used to separate high density and low density plasma, is removed from the reactor to make the measurement possible. Pulsed plasma program performs time resolved measurements of the probe V-I, the plasma parameters and EEDF. Both electropositive (e.g. Ar) and electronegative (O2/N2) plasma are used to study the pulsing plasma. The plasma impedance for the different plasma are read from the matching networks internal I-V probe. Electron temperature, density and afterglow temporal evolution at different pulsing conditions are also discussed.

[1] Pulsed plasma etching for semiconductor manufacturing, Demetre J Economou, J. Phys. D Appl. Phy. 47(2014)

[2] Stephen E. Savas, Brad S. Mattson, Martin L. Hammond, Steven C. Selbrede, Patent US 6143129

[3] Comparative analyses of plasma diagnostics techniques, V. A. Godyak and B. M. Alexandrovich, Journal of Applied Physics 118, 23302 (2015)

[4] Stephen E. Savas, Brad S. Mattson, Patent US 5811022

11:20am **PS-ThM-11 In-situ Measurement of Deposited Tilm Thickness and Electron Density by Double Curling Probe**, *Daisuke Ogawa,* Chubu University, Japan*; Y Sakiyama,* Lam Research Corporation*; K Nakamura,* Chubu University, Japan*; H Sugai,* Nagoya Industrial Science Research Institute, Japan

We developed a technique for measuring the thickness of a deposited film and electron density of a processing plasma simultaneously during a process with the use of two curling probes (CPs). As might be already known, CP is one of the microwave resonators which has a spiral-shaped slot antenna to make resonance. The resonance frequency (RF) depends on the geometry of the probe (the length and diameter of the antenna) and material of the antenna cover, etc., and the RF shifts to a higher frequency as electron density increases. Also, our recent research showed that CP can find the thickness of the film deposited after a plasma processing through the observed shift of RF when a dielectric constant of the film is known. In a deposition process operated in semiconductor industries, a film deposits not only on the processing substrate but also on a CP. The deposition shifts the RF lower, but the plasma shifts the RF higher. As a result, the observed shift in RF corresponds to a summation of the two shifts. This summation makes it difficult for us to discriminate the two shifts, but a pair of different-sized CPs (*double CP*) enables discrimination of the two shifts caused in the same plasma with the identical film thickness. We so far derived the equation giving the two shifts based on the previous theory. In order to confirm the solution of the equation, we performed a simple model experiment of deposition in an argon plasma, inserting two CPs covered with a polyimide film of known thickness (55-micrometer). We first measured the original RFs of the two probes with no polyimide film and no plasma exposure. And then, we measured the RF of each CP with a layer of the polyimide film and with plasma exposure. Finally, we derived the film thickness and electron density from the four RFs: the result revealed almost the same film thickness as the 55-micrometer polyimide film and the electron density of $2×10$ cm-3 which decently matches with the Langmuir probe data. In this presentation, we will show our latest results using the double CPs with the industrial application in mind.

11:40am PS-ThM-12 Study of Selective PECVD of Silicon on Silicon Nitride and Aluminum Oxide, *Ghewa Akiki, E Johnson, P Bulkin,* LPICM, CNRS, Ecole Polytechnique, Institut Polytechnique de Paris, France; *D Daineka,* LPICM, CNRS, Ecole Polytechnique, Institut Polytechnique de Paris

Research in the field of area selective deposition currently focuses on the use of Atomic Layer Deposition (ALD) technique, and requires an initial nucleation delay between two different substrates, as well as a "passivation" step, namely a plasma etching step that resets the nucleation delay for one surface [1]. In analogy, we aim to demonstrate a Plasma Enhanced Chemical Vapor Deposition (PECVD) based approach using a non-sinusoidal voltage waveform [2] to excite an $Ar/SiF_4/H_2$ plasma. This plasma chemistry is believed to be a key ingredient to creating a varying nucleation delay as the surface processes depend on the deposition/etching balance controlled by the H_2 flow rate [3]. As a building block for our PECVD based approach, we report on the observation of a nucleation delay for a PECVD process for microcrystalline silicon films on two different substrates, first using a standard 13.56 MHz radio frequency excitation source. The deposition selectivity on a patterned chip containing both SiN_x and AlO_x areas as well as the influence of the plasma parameters, will be presented. The analysis is performed by comparing ex-situ ellipsometry spectra before and after deposition and by Scanning Electron Microscopy (SEM) micrographs.

[1] R. Vallat, R. Gassilloud, B. Eychenne, and C. Vallée, **J. Vac. Sci. Technol. A 35,** 01B104 (2017)

[2] J. Wang and E.V. Johnson, **Plasma Sources Sci. Technol. 26** (2017) 01LT01

[3] Dornstetter JC, Bruneau B, Bulkin P, Johnson EV, Roca i Cabarrocas P, **J. Chem. Phys. 140**, 234706 (2014).

Advanced Surface Engineering Division
Room A215 - Session SE+PS-ThM

Plasma-assisted Surface Modification and Deposition Processes

Moderators: Robert Franz, Montanuniversität Leoben, Jianliang Lin, Southwest Research Institute

8:00am SE+PS-ThM-1 Core/Shell Particles using a Plasma-based Reactors, *Santiago Vargas-Giraldo, D Galeano-Osorio, C Castano,* Virginia Commonwealth University

Nano-size and micro-size manufacturing have found an invaluable tool in plasma-assisted materials deposition techniques. Primarily, plasma-assisted physical vapor deposition (PAPVD) methods are clean, reliable and flexible to develop films and coatings. Materials produced by PAPVD may lead to stable structures and stoichiometries that are not possible on other processes. On the other hand, core/shell systems have dragged high attention due to their unique properties. These structures exhibit high surface area, and the interfacial interaction between the core and the shell leads to complex chemistries and transfer phenomena. This work presents an innovative approach to synthesize shells for existing particles using sputtering equipment. It demonstrates the challenges for the direct implementation of magnetron sputtering to obtain single and double shells on glass microspheres. First, a simple flat sample stage was used to discuss the prominent structural and conformability imperfections due to shadowing effects on 3D cores. To overcome this limitation, a new sample stage to manipulate the core particles under vacuum for more uniform shell formation was designed. As proof of concept, various metals and metal oxide shells over glass micro-size spheres were obtained. Extensive materials characterization of the newly formed structures was performed. The results are the groundwork for a myriad of technological applications.

8:20am SE+PS-ThM-2 Formation Mechanisms of Converted Layer During Erosion of Composite Al-Cr Arc Cathodes, *Mehran Golizadeh, F Mendez Martin, B Rashkova,* Montanuniversität Leoben, Austria; *S Kolozsvári,* Plansee Composite Materials GmbH, Lechbruck am See, Germany; *R Franz,* Montanuniversität Leoben, Austria

Cathodic arc deposition (CAD) is a well-established physical vapor deposition technique which is characterized by a highly ionized plasma emitted from the cathode. The energy of the ions in the plasma ranges from 20 to some 100 eV, depending on the cathode material and the discharge conditions. These energetic and highly ionized plasmas significantly influence film growth mechanism and, e.g., high-temperature phases can be stabilized at typically low deposition temperatures in CAD.

The plasma properties are influenced by the properties of the converted layer which forms on the surface of composite cathodes due to local consecutive melting-solidification cycles caused by the motion of the cathode spot over the cathode surface. Therefore, a detailed understanding of the formation mechanism and properties of the converted layer is essential to understand and manipulate plasma properties.

Within the current work, composite cathodes with composition of $Al_{0.5}Cr_{0.5}$ but different grain size, namely 80 and 1200 μm, were eroded in inert Ar gas at a pressure of 1 Pa applying a current of 60 A. A short erosion time of 30 s enabled us to capture single craters left behind by a cathode spot. A cross-section of the crater prepared using focused ion beam (FIB) showed the liquid pool formed by the cathode spot was violently deformed by plasma pressure, pushing the liquid out of the crater to the rim and surrounding space (macroparticles). The leftover liquid was rapidly quenched and there was almost no heat-affected zone below the crater. This finding shows that solid-state diffusion plays a negligible rule in the formation of the converted layer.

Further, cross-sections of the cathodes eroded for 1h were prepared by conventional metallography and FIB. Detailed microstructural and phase analysis using transmission electron microscopy and transmission Kikuchi diffraction together with cross-sectional study of single craters revealed that the converted layer is formed in a way that the rim of a crater fills the neighbouring craters due to step erosion. The splashes ejected from craters by plasma pressure also contribute to forming the converted layer. The later mechanism can be dominating depending on the topography of the cathode surface, which was confirmed by the erosion of the cathodes with 1200 μm grain size.

8:40am SE+PS-ThM-3 Self-organization of Plasma in RF Magnetron Sputtering, *Matjaz Panjan,* Jozef Stefan Institute, Slovenia

Self-organization of magnetron plasma in so-called spokes has been previously reported for pulsed [1, 2] and continuous magnetron discharges [3]. In this presentation, we will demonstrate that spokes also form in oscillatory RF magnetron sputtering regime [4]. We used an ICCD camera and electrical probes to investigate the rotating plasma patterns. The spokes in RFMS were compared to the spokes in classical DCMS at similar discharge conditions. In both regimes, stable plasma patterns were observed for a wide range of discharge parameters. For similar gas pressures and discharge powers, the number of spokes in the RFMS regime was always larger than in the DCMS regime. The number of spokes changed sequentially with the increasing working gas pressure for both magnetron operations. In the DCMS regime, a single spoke was observed at the lowest argon pressure (0.25 Pa) and a second spoke was observed only at the highest pressure (2 Pa). In the same pressure range, the plasma in the RFMS regime displayed four spokes at the lowest pressure and six or seven spokes at the highest pressure. The influence of discharge power on the number of spokes was less pronounced for both magnetron regimes. Spoke patterns were analyzed by examining the inelastic collisions between electrons and argon atoms. For this purpose, we simulated the dissipation of electron energy in the drift direction and compared the calculations to the length and number of spokes for particular discharge conditions. Overall, the simulations agree well with the observed plasma patterns in DCMS and RFMS.

[1] A. Anders *et al.*, *J. Appl. Phys.*, **111** (2012) 053304

[2] A. Ehiasarian *et al.*, *Appl. Phys. Lett.*, **100** (2012) 11410

[3] M. Panjan *et al.*, *Plasma Sources Sci. Technol.*, **24** (2015) 065010

[4] M. Panjan accepted for publication in *J. Appl. Phys.* (2019)

9:00am SE+PS-ThM-4 Study of High Power Pulsed Magnetron Sputtering Discharge with Positive Bias on the Target after the Main Pulse, *Ivan Shchelkanov, T Houlahan, J McLain, I Haehnlein, B Jurczyk, R Stubbers,* Starfire Industries LLC; *D Barlaz, D Ruzic,* University of Illinois at Urbana-Champaign

Low-pressure magnetron sputtering is a well-established industry standard for high quality thin film deposition. Among different types of magnetron sputtering, High Power Pulsed Magnetron Sputtering (HPPMS), also called High Power Impulse Magnetron Sputtering (HIPIMS), offers the highest ion fraction of sputtered material, which dramatically increases the options available for thin film synthesis. The highly ionized sputtered material assists in multilayer film growth leading to more adhesive, dense, and smoother films as compared to conventional DC Magnetron Sputtering (dcMS) techniques, without the need for extra plasma-assisting elements and techniques in the process. Unfortunately, HPPMS typically suffers from

low deposition rates as compared to dcMS[1]. Various attempts have been made to overcome this drawback, among them are: more efficient magnetic field configurations [2-6], HPPMS operation with extreme target conditions [7,8], or the application of a pulsed positive bias onto the sputtered target to control the plasma potential after the main HPPMS pulse [9]. Operation with a positive voltage KICK at the end of the main HPPMS pulse allows for the deposition of multilayer coatings onto a cold, grounded substrate with better adhesion than is typical of a simple HPPMS discharge. Furthermore, for grounded substrates positioned at glancing angles with respect to the sputtered magnetron cathode, the deposited coatings exhibit a very dense structure and great adhesion to the substrate even when deposited onto the inside wall of high aspect ratio vias. To fully understand limits, effects, and drawbacks of the positive KICK, its influence on plasma parameters, deposition rate, coatings structure, and adhesion are discussed.

[1] F.Papa, et al., 2011 Thin Solid Films 520.5 1559-1563.

[2] P. Raman, et al., Journal of Vacuum Science & Technology A 33.3 (2015): 031304.

[3] P. Raman, et al., Journal of Applied Physics, Volume 120, Issue 16, Page 163301 (2016)

[4] J. McLain, et al., Vacuum, Volume 155, Page 559-565 (2018)

[5] P. Raman, et al., Vacuum, Volume 156, Page 9-19 (2018)

[6] P. Raman, et al., Journal of Applied Physics, Volume 120, Issue 16, Page 163301 (2016)

[7] A.V.Tumarkin, et al., Surface and Coatings Technology. 2016. Vol. 293. P. 42–47

[8] A.V.Kaziev et al., Surface and Coatings Technology. 2016. Vol. 293. P. 48–54

[9] B. Wu et al., Vacuum, Volume 150, Page 216-221 (2018)

9:20am SE+PS-ThM-5 Innovative PVD Strategies for the Design of Novel TiO_2-based Photoanode Utilized in Dye-sensitized Solar Cells, *Rony Snyders,* University of Mons, Belgium **INVITED**

In view of the environmental challenges that our societies face, it is accepted that the development of alternative and renewable energy sources is a must. If solar energy is recognized as one of the most promising, it is still necessary to improve the solar cell technologies. Among others, Dye Sensitized Solar Cells (DSSC) are often seen as one of the ideal technological approach if several issues are fixed. One of the key problem associated with the implementation of these cells if related to the photoanode performances, specifically in terms of charge transport. Indeed, the standard photoanode based on TiO powder often exhibit a too high electrical resistivity associated with the intrinsic properties of the material.

During the past years, we have worked on the development of alternatives TiO_2-basedmaterial in order to solve the encountered problems. More precisely we have studied the growth of (N-doped) nano-sculpted TiO_2 films by using reactive magnetron sputtering in glancing angle deposition. Concerning the doping, co-reactive deposition as well as ion implantation have been evaluated. All samples have been thoroughly characterized by state-of-the-art techniques and, for most of them, tested in DSSCs.

The results demonstrate that our approach is versatile allowing to control the morphology of the TiO_2 films at the nanoscale, and therefore to tune the capability of the material to adsorb the active dye. Specifically, we showed that a combination of our films with conventional TiO_2 nanoparticles could be a promising approach. In addition, we also demonstrate that the phase constitution of the nano-sculpted films can be optimized in the form of a core-shell anatase/rutile structure in order to improve the charge transport. On the other hand, the study of the N doping reveals that it is possible to finely control the position of the N atom (substitutional vs intersticial) as a function of the experimental parameters. In this context, we demonstrated that the O vacancies density favor the substitutional doping. Finally, w e even showed that p type TiO_2:N films presenting good electrical and optical properties can be synthesized. This last result is of particular interest for the development of "full TiO_2" tandem DSSCs.

11:00am SE+PS-ThM-10 Enhancing the Far Ultra-Violet Optical Properties of Aluminum Mirrors with a Single Step Approach to Oxide Removal and Fluorine Passivation, *David Boris,* U.S. Naval Research Laboratory*; A Kozen, S Rosenberg,* American Society for Engineering Education (residing at U.S. Naval Research Laboratory)*; J del Hoyo, G Richardson, M Quijada,* NASA Goddard Spaceflight Center*; S Walton,* U.S. Naval Research Laboratory

Astronomical measurements in the F̲ar U̲ltra-V̲iolet (FUV, 90-200nm) require the use of aluminum thin films due to aluminum's high reflectivity over this wavelength range. Unfortunately, the native aluminum oxide layer formed in atmosphere is strongly absorbing in this wavelength range, requiring that the aluminum films be passivated with a dielectric that inhibits oxidation. Due to the fast oxidation of aluminum, a simultaneous etch and deposition process is desirable to both eliminate the native aluminum oxide after growth and replace it with a different passivation coating layer. Optical measurements in the FUV range are some of the most challenging due to limited selection of low reflectivity coatings available for use on aluminum thin films. Typically magnesium fluoride (MgF_2) or lithium fluoride (LiF) coatings are used for these passivation purposes but each has its problems. MgF_2 has an absorption cutoff at 115 nm occluding a critical part of the FUV spectrum. LiF has a lower absorption cutoff at 102.5 nm, but is hygroscopic and thus susceptible to degradation in ambient conditions. A promising alternative to these coating materials is AlF_3, which theoretically can provide reflectivity greater than 50% down to 100 nm if the coating is sufficiently thin. In this work, we explore the use of electron beam generated plasmas to simultaneously etch the native oxide layer from aluminum thin films while depositing an AlF_3 capping layer to passivate the aluminum metal reflector. XPS measurements indicate that this approach is capable of producing very thin (<5 nm) AlF_3 films with some mild (<10%) oxygen contamination. We will discuss the impact of plasma power, plasma chemistry, and plasma exposure time on the composition and structure of the passivation layer and how those parameters effect the optical properties. This work is partially supported by the Office of Naval Research, the Naval Research Laboratory base program, and NASA Strategic Astrophysics Technology (SAT) grant No. NNH177ZDA001N

11:20am SE+PS-ThM-11 Improving the Crystallinity of Inorganic Coatings Synthesized by Atmospheric Plasma using a New Device for Heating the Substrate, *Antoine Remy, M Fall, F Reniers,* Université Libre de Bruxelles, Belgium

The deposition of good quality crystalline inorganic coatings by atmospheric pressure dielectric barrier discharge remains a challenge. Thanks to an original coupling of a substrate heating device based on an inductive current loop and located under the dielectric and an atmospheric pressure dielectric barrier discharge, we show that one can deposit in one step crystalline vanadium oxide and titanium oxide, with grain sizes bigger than those achieved by post-deposition annealing. As case study, vanadium oxide and titanium oxide are chosen. The respective precursors (vanadium oxytriisopropoxide - VOTP and titanium tetraisopropoxide – TTIP) are injected as vapors in a home made reactor with argon acting as carrier gas and main plasma gas. Oxygen is injected as reactant in the chamber. The DBD operates using a G10S-V AFS generator, at a frequency of 19 kHz, and with an injected power comprised between 0 and 80 W. The heating unit consists in a inductively coupled device located under the bottom electrode and dielectric and a susceptor place between the substrate and the dielectric. Thanks to a modified design of the bottom electrode, the induction loop does not heat said electrode, but the Eddy current heats only the susceptor, and the substrate. It is shown that this device allows the direct synthesis of crystalline orthorhombic V_2O_5 at 300°C, and of anatase TiO_2 at 400°C. A comparison with coatings deposited at room temperature and annealed at 300 and 400°C respectively shows that the coatings deposited on the heated substrate exhibit larger grain sizes. This original combination of an atmospheric pressure plasma DBD and a device to heat inductively the substrate shows that one can obtain good crystallinity for inorganic coatings, and opens potentially new opportunities for the deposition of such coatings by atmospheric plasma.

11:40am SE+PS-ThM-12 Improved Nitride Formation on Titanium Substrates by Femtosecond Laser Processing with Secondary Plasma, *Jeremy Mettler, D Barlaz,* University of Illinois at Urbana-Champaign*; B Jurczyk,* Starfire Industries LLC*; D Ruzic,* University of Illinois at Urbana-Champaign

We discuss the development of a plasma-enhanced, laser-induced surface conversion process for forming TiN, a common coating favored for its hardness and corrosion resistance. This process uses a pulsed femtosecond laser to provide localized energy deposition at the Ti surface, along with a

secondary plasma to supply reactive N species. This method allows the surface conversion to be conducted in a single pass, rather than requiring a pretreatment step in Ar atmosphere for oxygen removal. The nitrogen radicals react preferentially where the laser provides sufficient energy to cause conversion of the native oxide layer. The conversion efficiency was investigated for DC and RF plasmas, as well as for different plasma powers, pressures, N precursors, and sample biases. Preliminary results with no secondary plasma achieved surface conversions of up to 9% TiN, measured using XPS. The inclusion of a secondary plasma provides a marked improvement over this previous result, both in terms of oxide removal and nitride formation. Laser powers for this work were between 3-5 W. A Langmuir probe diagnostic was used to compare plasma density at different powers (on the order of 100 W) and for different compositions.

12:00pm **SE+PS-ThM-13 Characterizing the Spatially Dependent Properties of Plasma Polymerized Acrylic Acid Films**, *Karyn Jarvis, S McArthur,* Swinburne University of Technology, Australia

Plasma polymer films have been deposited on planar surfaces for a wide variety of applications, such as controlling cell growth or adding linker molecules for biosensors. They can however also be deposited onto three dimensional objects, such as tissue engineering scaffolds, biomedical implants or 3D printed devices. Coating three dimensional objects however is more complex as greater monomer fragmentation occurs closer to the electrode. It is therefore important to understand the properties of the plasma polymer films that will be deposited when a sample is different distances from the electrode. The use of plasma polymer films in biomedical applications also requires suitably stable films under physiological conditions, which will also be influenced by the distance from the electrode. Significant changes in film properties in aqueous conditions have serious implications on the incorporation of these films in biomedical devices.

Acrylic acid is a commonly used monomer for plasma polymerization to produce negatively charged carboxylic acid terminated surfaces, which have been used for a number of biomedical applications by manipulating cell growth. To gain a greater understanding of the spatially dependent behavior of plasma polymerized acrylic acid (ppAAc) films deposited in our custom-built stainless steel T-shaped reactor, ppAAc films were deposited at varying distances from the electrode (30 – 190 mm) at different deposition powers (5 – 80 W). The surface chemistry was analysed with X-ray photoelectron spectroscopy (XPS) while the film thickness was determined using spectroscopic ellipsometry. Aqueous stability was determined via immersion in Milli-Q. The film thicknesses decreased while the carboxyl group concentrations increased as the distance from the electrode increased and/or the deposition power decreased due to reduced monomer fragmentation further from the electrode and at lower powers. The aqueous stability of the films deposited further from the electrode increased as the deposition power increased. At 10 W, the film 30 mm from the electrode showed no decrease in film thickness after aqueous immersion while the films deposited 110 and 190 mm from the electrode were completely removed. Minimal film loss for the films deposited at 110 mm required a deposition power of 30 W while 60 W was required for minimal film loss for films deposited at 190 mm from the electrode. This work highlights the importance of having a spatially well characterized plasma reactor to enable the deposition of plasma polymer films with the desired properties, which has significant implications on the incorporation of these films into a number of applications.

Surface Science Division
Room A220-221 - Session SS+AS+HC+TL-ThM

Surface Science of Energy Conversion and Storage
Moderators: Steven L. Tait, Indiana University, Francisco Zaera, University of California, Riverside

8:00am **SS+AS+HC+TL-ThM-1 Chemical and Electrochemical Stability of Perovskite Oxide Surfaces in Energy Conversion: Mechanisms and Improvements**, *Bilge Yildiz,* Massachusetts Institute of Technology **INVITED**

A broad range of highly active doped ternary oxides, including perovskites, are desirable materials in electrochemical energy conversion, catalysis and information processing applications. At elevated temperatures related to synthesis or operation, however, the structure and chemistry of their surfaces can deviate from the bulk. This can give rise to large variations in the kinetics of reactions taking place at their surfaces, including oxygen reduction, oxygen evolution, and splitting of H_2O and CO_2. In particular,

aliovalent dopants introduced for improving the electronic and ionic conductivity enrich and phase separate at the surface perovskite oxides. This gives rise to detrimental effects on surface reaction kinetics in energy conversion devices such as fuel cells, electrolyzers and thermochemical H_2O and CO_2 splitting. This talk will have three parts. First, the mechanisms behind such near-surface chemical evolution will be discussed. Second, the dependence of surface chemistry on environmental conditions, including temperature, gas composition, electrochemical potential and crystal orientation will be described. Third, modifications of the surface chemistry that improve electrochemical stability and actvity, designed based on the governing mechanisms, will be presented. Guidelines for enabling high performance perovskite oxides in energy conversion technologies will be presented.

8:40am **SS+AS+HC+TL-ThM-3 Mechanism of Oxygen Reduction Reaction on Nitrogen-doped Carbon Catalysts**, *Junji Nakamura,* University of Tsukuba, Japan

Nitrogen-doped carbon materials are expected to be non-Pt catalysts for oxygen reduction reaction (ORR) in fuel cells. Among several types of nitrogen species in carbon materials, pyridinic nitrogen (nitrogen atom bound to two C atoms) has been found to create ORR active sites in our previous work[1]. We then try to prepare catalytically active carbon surfaces covered with pyridinic nitrogen-containing aromatic molecules with high density. Recently we have reported model catalyst studies using HOPG (highly oriented pyrolytic graphite) electrode covered with pyridinic nitrogen-containing aromatic molecules (dibenz[a,c] acridine (DA) molecule and acridine (Ac)molecule)[2]. The DA molecules form a two-dimensional ordered structure along the direction of the HOPG substrate by self-organization. Adsorbed DA on the HOPG surface shows high ORR activity in terms of specific activity per pyridinic nitrogen and is comparable to that of pyridinic-nitrogen-doped carbon catalysts. We study the mechanism of ORR taking place on the DA/HOPG model catalyst. In acidic reaction conditions, pyridinic nitrogen is protonated to pyridinium nitrogen (NH+) species. It is suggested that the adsorption of oxygen take place on a carbon atom in a DA molecule upon reduction of the NH+ species. Generally, the reduction of NH+ is difficult to proceed thermodynamically at higher potentials above 0 V vs RHE. However, in the presence of oxygen, the reduction of NH+ is possible by an energy gain due to simultaneous adsorption of oxygen. The supplied electron goes to pai system as SOMO electron upon reduction, which is responsible for the adsorption of oxygen. That is, the role of pyridinic nitrogen is to provide SOMO electron upon reduction of NH+ species.

References

Guo D, Shibuya R, Akiba C, Saji S, Kondo T, Nakamura J, (2016). Active sites of nitrogen-doped carbon materials for oxygen reduction reaction clarified using model catalysts. *Science*, 351, 361-365.

Shibuya R, Kondo T, Nakamura J, (2018). Bottom-up design of nitrogen-containing carbon catalysts for the oxygen reduction reaction. *ChemCatChem* doi.org/10.1002/cctc.201701928

9:00am **SS+AS+HC+TL-ThM-4 Copper Corrosion Inhibition Investigated on the Molecular Scale Using APXPS**, *Bo-Hong Liu,* Lawrence Berkeley National Laboratory*; O Karslıoğlu,* Lawrence Berkeley Nationa lLaboratory*; M Salmeron, S Nemšák,* Lawrence Berkeley National Laboratory*; H Bluhm,* Fritz Haber Institute of the Max Planck Society, Germany

Copper has been used in a wide variety of applications. Though relatively inert, it corrodes when in contact with aqueous solutions/water vapor and corroding agents such as chlorine.[1] Benzotriazole (BTA) is a commonly used corrosion inhibitor to protect copper surfaces. A consensus regarding the mechanism of corrosion protection is that BTA complexes with surface copper atoms, resulting in a Cu(I)-BTA protective polymer layer.[2] UHV-based surface science studies clarified the structure of the BTA layer on copper single crystal surfaces at low dosage, as demonstrated by a very recent study combining DFT and spectroscopic techniques;[3] however, the effect of environmental factors could not be well addressed by this approach. Here, we report an Ambient Pressure X-ray Photoelectron Spectroscopy (APXPS) study of the influence of water vapor and chlorine on well-defined Cu surfaces. To capture the material complexity of the corrosion phenomenon, we study copper single crystals as well as polycrystalline foils of metallic copper, cuprous oxide and cupric oxide. In this presentation, we will show that the water uptake of copper surfaces under humid condition is strongly influenced by the presence of a BTA layer. Also, a BTA layer blocks chlorine uptake in some conditions. Based on these experimental results, factors that influence the BTA inhibitory effect on copper corrosion are identified.

1. Atlas, D.; Coombs, J.; Zajicek, O. T., THE CORROSION OF COPPER BY CHLORINATED DRINKING WATERS. *Water Research* **1982,**16 (5), 693-698.

2. Finsgar, M.; Milosev, I., Inhibition of copper corrosion by 1,2,3-benzotriazole: A review. *Corrosion Science* **2010,**52 (9), 2737-2749.

3. Gattinoni, C.; Tsaousis, P.; Euaruksakul, C.; Price, R.; Duncan, D. A.; Pascal, T.; Prendergast, D.; Held, G.; Michaelides, A., Adsorption Behavior of Organic Molecules: A Study of Benzotriazole on Cu(111) with Spectroscopic and Theoretical Methods. *Langmuir* **2019,**35 (4), 882-893.

9:20am SS+AS+HC+TL-ThM-5 Analysis and Deliberate Modification of Electrochemical Interfaces, *Esther Takeuchi, K Takeuchi, A Marschilok,* Stony Brook University   **INVITED**

Interfaces in electrochemical energy storage systems are critical in the transport of electrons and ions and are significant factors in electrochemical function, yet remain a challenge to fully understand. In lithium based systems, the interfaces or interphases often form spontaneously due to reactions of the active materials and the electrolytes. The interfaces formed due to these spontaneous reactions may prove beneficial as they provide needed protection inhibiting further and continuous reaction. However, the characteristics of the interface may also contribute to decreased ion transport and the accompanying increased effective resistance.

Conversion-type materials for next generation lithium ion systems are appealing due to the opportunity for multiple electron transfer within one metal center. However, implementation of conversion materials has been hindered by the phase transformations occurring during cycling as well as formation of a resistive solid electrolyte interphase (SEI). This presentation will explore the effective implementation of combinations of characterization techniques including the use of *ex-situ* and *operando* methods to provide insight into the formation, composition and deliberate modification of the SEI.

11:00am SS+AS+HC+TL-ThM-10 An Investigation on Active Sites of La_2O_3 Catalyst for OCM Reaction: A Combined Study of *in situ* XRD, XPS and Online MS, *Yong Yang, C Guan, E Vovk, Z Liu, X Zhou, J Liu, Y Pang,* ShanghaiTech University, China

Oxidative coupling of methane (OCM) is a catalytic partial oxidation process that converts methane directly to valuable C_2 products (ethane and ethylene). Previous results suggested that the bulk structure change of the La_2O_3 catalyst was related to the performance of the reaction. In this work, a designed *in situ* XRD-MS coupled characterization setup coupled with online MS instrument are used for measuring both the reaction products and the bulk structure of the catalyst in real time and under simulated industrial conditions. This allows for the more detailed study in order to relate information from of bulk structure change vs. CO_2 related treatment and quantitative analysis of the reaction products, thus for a further connection and understanding of the conversion rate of CH_4 and the selectivity of C_2. The work presented focused on online characterization of the OCM reaction on La_2O_3 catalyst, covering different parameters including: 1. La_2O_3 pretreatment under different CO_2 concentrations, 2. Consecutive OCM reactions, comparing the behavior of a clean surface La_2O_3 catalyst with a La_2O_3 catalyst after OCM, 3. OCM performed after La_2O_3 has undergone pretreatment with pure CO_2. Results indicate that carbonates formation on La2O3 is two step, surface carbonates formation at below 500°C and bulk formation at 500-700°C. *In situ* TPD performed in a high pressure gas cell (HPGC) and XPS measurement results confirm the above.

The results showed that bulk CO_3^{2-} formation under CO_2 exposure, results in higher light-off temperature of CO_2 and C_2 than the clean surface during OCM reaction. There is carbonate formation on commercial La_2O_3 during OCM reaction and CO_2 desorption after OCM reaction by in situ XRD-MS, and it influences the light-off temperature of CO_2 and C_2 up to 65°C higher than the clean surface. It is proposed that CO_3^{2-} may perform as a catalyst poison in this reaction. This result provides an important insight of the active site for OCM reaction. Based on this result, a brief XPS study of the carbonate free sample surface, which may be only preppared from the HPGC vacuum connected further reveals an oxide feature related with methane activation. Additional DFT calculations based upon the experimental data indicates a carbonation mechanism which occurs in the subsurface, which in turn could be related to La_2O_3 activity.

11:20am SS+AS+HC+TL-ThM-11 Interaction of Amino Acids on Au(111) as Studied with EC-STM: From Islands to Magic Fingers, *J Phillips, K Boyd, I Baljak, L Harville,* ***Erin Iski,*** University of Tulsa

With growing interest into origin of life studies as well as the advancement of medical research using nanostructured architectures, investigations into amino acid interactions have increased heavily in the field of surface science. Amino acid assembly on metallic surfaces is typically investigated with Scanning Tunneling Microscopy (STM) at low temperatures (LT) and under ultra-high vacuum (UHV), which can achieve the necessary resolution to study detailed molecular interactions and chiral templating. However, in only studying these systems at LT and UHV, results often tend to be uncertain when moving to more relevant temperatures and pressures. This investigation focuses on the Electrochemical STM (EC-STM) study of five simple amino acids (L-Valine, L-threonine, L-Isoleucine, L-Phenylalanine, and L-Tyrosine) as well as two modifications of a single amino acid (L-Isoleucine Ethyl Ester and N-Boc-L-Isoleucine), and the means by which these molecules interact with a Au(111) surface. Using EC-STM under relevant experimental conditions, the amino acids were shown to have a considerable interaction with the underlying surface. In some cases, the amino acids trapped diffusing adatoms to form Au islands and in other cases, they assisted in the formation of magic gold fingers. Importantly, these findings have also been observed under UHV conditions, but this is the first demonstration of the correlation *in situ* and was controlled via an applied external potential. Results indicate that an increase in the molecular weight of the amino acid had a subsequent increase in the area of the islands formed. Furthermore, by shifting from a nonpolar to polar side chain, island area also increased. By analyzing the results gathered via EC-STM at ambient conditions, fundamental insight can be gained into not only the behavior of these amino acids with varied side chains and the underlying surface, but also into the relevance of LT-UHV STM data as it compares to data taken in more realistic scenarios.

11:40am SS+AS+HC+TL-ThM-12 Deposition and Structure of MoO_3 Clusters on Anatase TiO_2 (101), *Nassar Doudin, Z Dohnálek,* Pacific Northwest National Laboratory

Oxide clusters supported on metal oxide substrates are of great interest due to their importance in heterogeneous catalysis [1]. The nature and strength of the interactions between the metal oxide clusters and the support materials not only govern their structure and stability but also control the energetics of elementary steps that are critical for the overall activity [1]. Understanding the nature of the interactions is therefore important to tailor the supported metal oxide cluster systems to achieve the desired reactivity and selectivity. Here, we present a scanning tunneling microscopy (STM) and X-ray photoelectron spectroscopy (XPS) study of the monodispersed MoO_3 clusters deposited by the sublimation of MoO_3 powder on anatase TiO_2(101) surface at 300 K. After the deposition, the STM images of the lowest concentration of MoO_3 show that the clusters initially migrate over the surface and preferentially anchor at step edges before they start to aggregate on the terraces. Interestingly, the aggregates are mostly composed of three adjacent clusters, with a small concentration of monomers and dimers. Further exposures to MoO_3 increase the cluster coverage until a fully saturated over-layer is created with each clusters being are centered on top of the Ti sites. The adsorbed clusters appear as bright protrusions, with an apparent cluster height of approximately 1.5 Å and diameter of about 8.5 Å. Since the cyclic $(MoO_3)_3$ trimers are known to be a dominant gas phase species resulting from the sublimation of MoO_3 [1], we propose that each cluster on the surface is a trimer. Annealing to 550 K results in a better-order of the $(MoO_3)_3$ layer, but further annealing to 650 K leads to three-dimensional clusters. The XPS results indicate that the $Mo(3d_{5/2})$ binding energy in as-deposited $(MoO_3)_3$ is characteristic of Mo^{6+}, and the oxidation state of Mo remains (+6) upon heating to 600 K. As such, this system may offers great promise as an ideal platform for reactivity studies on well-defined supported model transition-metal oxide catalysts.

[1] Zdenek Dohnálek et al. Royal Society of Chemistry 43, 7664–7680 (2014).

12:00pm SS+AS+HC+TL-ThM-13 Ionic Conducting Nanostructures Tailored on Porous Mixed Conduction Composite Electrodes for Enhancement of Oxygen Reduction Reaction, *Jong-Eun Hong, D Joh, S Kim, H Ishfaq,* Korea Institute of Energy Research, Republic of Korea*; C Jung, J Park,* DGIST, Republic of Korea*; S Lee, H Kim, T Lim, S Park, R Song,* Korea Institute of Energy Research, Republic of Korea*; K Lee,* DGIST, Republic of Korea

With decrease in the operation temperature of solid oxide fuel cells, the oxygen reduction reaction (ORR) in the cathodes, which is sluggish, plays an important role in improving the electrochemical performance. Much effort has given to facilitate the ORR by the applications of cathode surface modification using active catalysts, nano-particle cathodes, and advanced cathode materials. In particular, the cathode surface modification with a reactive electro-catalyst has been appeared to increase the electrode

reactivity and thus to decrease the polarization resistance to the oxygen reduction reaction. Infiltration of electro-catalysts has been widely utilized to tailor the cathode microstructures as it is a facile method. In this study, one-step infiltration using an in-situ sol–gel process was applied to modify porous mixed conducting composite cathodes, and the impact of surface microstructure tailoring on the electrochemical performances was investigated. The precursors of Sm- and Nd-doped ceria (SNDC), whose ionic conductivity is even higher than that of Gd-doped CeO_2 (GDC), were infiltrated into the cathode by using an ultrasonic spray nozzle to produce fine and uniform droplets. The infiltrated samples then experienced an in-situ heat-treatment after repeating the ultrasonic spraying and drying processes and were submitted for electrochemical measurements. The detailed results on the microstructure evolution and electrochemical properties of the specimens prepared using the ultrasonic spraying infiltration are presented, and the elucidation of the results are discussed.

Thin Films Division
Room A122-123 - Session TF+EM+NS+SS-ThM

Thin Films for Energy Harvesting and Conversion
Moderators: Siamak Nejati, University of Nebraska-Lincoln, Xinwei Wang, Shenzhen Graduate School, Peking University

8:00am **TF+EM+NS+SS-ThM-1 Redesigning Batteries into Efficient Energy Harvesters and Sensors for Wearable Applications**, *Cary Pint,* Vanderbilt University **INVITED**
Here I will discuss the research efforts of my team demonstrating how active materials utilized in batteries can be reconfigured into an electrochemical framework to harvest, rather than store, energy. This new functionality of battery materials arises from the fundamental coupling between mechanical stresses and electrochemistry that my group has demonstrated while investigating the "strain-engineering" of battery materials. By exploiting this coupling in a symmetric cell device configuration, we are able to construct devices that convert mechanical energy to electrical energy by mechanical modulation of the electrochemical reaction potential. I will discuss the development of this device platform from proof-of-concept device fabrication using 2D materials to our most recent demonstration of textile-integrated biocompatible fibers integrated into fabrics for harvesting/sensing of human motion. Most notably, I will discuss how the sluggish diffusion kinetics of ions between two electrodes – whereas a challenge for emerging battery applications, enables these devices to measure a continuous response from the whole broad range of frequencies associated with human motion. This allows these wearable harvesters to provide real-time sensing data that can be directly correlated with dynamic human motion models. This new approach leverages the efficient nature of electrochemistry, the wide range of materials selection and chemistries relevant for batteries, and without any of the safety concerns of batteries due to the symmetric electrode configuration.

8:40am **TF+EM+NS+SS-ThM-3 Engineering Effective Back Contact Barrier by interfacial $MoSe_2$ defect states for CZTSe: nanolayer Ge solar cells.**, *Sanghyun Lee,* Indiana State University
The steadily emerging $Cu_2ZnSnSSe_4$ (CZTSSe) devices are alternative thin film solar cells with abundant elements in earth's crust for the past several years. Despite several advantagessuch as high absorption coefficient (>10^4 cm^{-1}) and a tunable direct band gap energy (1 to 1.4 eV), the improvement and understanding have been stagnant in the past several years. Recently, CZTSe: nanolayer Ge solar cells have shown significantly improved pseudo-mono grain toward the depth direction.

Due to the improvement and the similarity between CZTSe and $Cu(In,Ga)Se_2$ (CIGS) thin film solar cells, the CZTSe/ Molybdenum (Mo) back contact interface was often misinterpreted by expecting the similar back contact property to CIGS. However, unlike the stable CISe ($CuInSe_2$)/Mo interface, the CZTSe/Mo interface is thermodynamically unstable due to the higher oxidation states of Sn. Although the presence of an interfacial $MoSe_2$ layer at Mo/absorber is always confirmed, properties of the back contact-interface such as structure and electrical behaviors are convoluted.

Following our empirical results about the back contact barrier of CZTSe: nanolayer Ge devices, we perform analytical and numerical modeling to explain the back contact improvement theoretically. The device modeling are carried out with the simulator, developed at Indiana State University. The tool is run in MATLAB environment, connected to other external tools (Sentaurus TCAD). Based on our result, defects in $MoSe_2$ interfacial layer

dominate the back contact property of CZTSe: nanolayer Ge devices by increasing of the effective back contact barrier, which consists of two different back contact barriers, thereby increasing series resistance as well. The reduction of $MoSe_2$ defect concentration from 1×10^{17} to 1×10^{15} cm^{-3} decreases the effective barrier height by 51 meV, which results in approximately 34 % decrease in the series resistance (See supporting data). Conversely, as the defect concentration increases, the benefit from the back contact barrier lowering by the valence bands offset between $MoSe_2$ and CZTSe absorber is reduced and essentially eliminated. However, the back contact barrier between $MoSe_2$ and Mo metal contact remains the same even with increased $MoSe_2$ defect concentration. Incorporating thin Ge nanolayer at the interface between the absorber and $MoSe_2$ positively influences and possibly reduces the defect states, lowering the effective barrier. The exponential fitting of the effective barrier and series resistance agrees well with the experimental results. The improvement of the back contact barrier for CZTSe: nanolayer Ge devices is calculated as 23.8 meV than CZTSe without nanolayer Ge devices.

9:00am **TF+EM+NS+SS-ThM-4 Development of Low-Cost, Crack-Tolerant Metallization Using Screen Printing for Increased Durability of Silicon Solar Cell Modules**, *O Abudayyeh,* Osazda Energy; *A Chavez,* University of New Mexico; *J Chavez,* Osazda Energy; **Sang M. Han,** University of New Mexico; *F Zimbardi, B Rounsaville, V Upadhyaya, A Rohatgi,* Georgia Institute of Technology; *B McDanold, T Silverman,* National Renewable Energy Laboratory
One of the ways to reduce the cost of solar electricity to 3¢/kWh, thus reaching parity with fossil-fuel-based generation, is to reduce the degradation rate of solar modules and extend their lifetime well beyond 30 years. The extended module lifetime in turn can positively influence the financial model and the bankability of utility-scale PV projects. Today, the highest-risk-priority solar module degradation mechanism is what is known as hot spots, often induced by cell cracks. In order to address this degradation mechanism, we make use of low-cost, multi-walled carbon nanotubes embedded in commercial screen-printable silver pastes, also known as metal matrix composites. When the carbon nanotubes are properly functionalized and appropriately incorporated into commercial silver pastes, the resulting metal contacts on solar cells, after screen-printing and firing, show exceptional fracture toughness. These composite metal contacts possess increased ductility, electrical gap-bridging capability up to 50 μm, and "self-healing" to regain electrical continuity even after cycles of complete electrical failure under extreme strain [1]. Accelerated thermal cycling tests on mini-modules constructed from aluminum back surface field (Al-BSF) cells show a slower degradation rate for the cells integrated with the composite grid fingers and busbars for the front surface metallization compared to the cells with conventional metallization.

[1] O. K. Abudayyeh, A. Chavez, J. Chavez, S. M. Han, F. Zimbardi, B. Rounsaville, V. Upadhyaya, A. Rohatgi, B. McDanold, T. J. Silverman, and N. Bosco, in "Low-Cost Advanced Metallization to Reduce Cell-Crack-Induced Degradation for Increased Module Reliability," 2019 NREL PV Reliability Workshop, Lakewood, CO, 2019.

9:20am **TF+EM+NS+SS-ThM-5 Fabrication of Optical Test Structures for Enhanced Absorption in Thin Multi-junction Solar Cells**, *Erin Cleveland, N Kotulak, S Tomasulo, P Jenkins,* U.S. Naval Research Laboratory; *A Mellor, P Pearce,* Imperial College London, UK; *N Ekins-Daukes,* University of New South Wales, Australia; *M Yakes,* U.S. Naval Research Laboratory
In space applications, a key figure of merit is conversion efficiency at end-of-life, which combines both beginning–of-life efficiency with degradation due to radiation exposure on orbit. In currently used InGaP/GaAs/Ge triple junctions, the GaAs middle cell has the most pronounced degradation, which limits the total current generation at the end-of-life. Recently, we demonstrated that as the thickness of the GaAs cell decreases, the tolerance to radiation damage increases. [1] However, because the cell absorbs less light as the thickness of the active region is reduced, the beginning-of-life performance suffers as compared to optically thick cells. To realize the benefits of both structures, light trapping architectures may be used to increase absorption within the cell while still maintaining the increased radiation tolerance of the thinner geometry.

Designing a wavelength selective light trapping structure positioned interstitially between two of the subcells of a multi-junction device is a new challenge which prohibits many of the well-known light trapping techniques. Recently, we have proposed a structure which combines a distributed Bragg reflector (DBR) with a textured diffraction grating. [2] Such a structure would provide substantial absorption of light in the middle

subcell of a multi-junction device, while still allowing enough low-energy light to pass through the structure so the bottom cell remains well current matched with the other junctions. This structure is proposed to have over an order of magnitude increase in overall radiation tolerance while maintaining comparable beginning of life performance to the current technology.

In this presentation, we present a first experimental demonstration of this structure. The design combines a diffraction grating fabricated via nanosphere natural lithography [3], a low-index transparent spacer layer, and a DBR, which synergistically traps light inside the targeted subcell. This presentation will highlight processing techniques and challenges associated with fabricating a textured ultra-thin solar cell, while illustrating the effectiveness of integrating light trapping structures within an ultra-thin solar cell as an effort towards realizing high efficiency ultra-thin photovoltaic devices.

[1] L. C. Hirst, *et.al*, "Intrinsic radiation tolerance of ultra-thin GaAs solar cells", *APL*, 109 (2016)

[2] A. Mellor, N.P. Hylton, S.A. Maier, N. Ekins-Daukes, "Interstitial light-trapping design for multi-junction solar cells", *Solar Energy Materials & Solar Cells*, 159, (2017)

[3] H.W. Deckman and J.H. Dunsmuir, "Natural lithography", *Applied Physics Letters*, 41(4) (1982)

9:40am TF+EM+NS+SS-ThM-6 Phosphorus as a *p*-Dopant in Pyrite FeS$_2$, a Potential Low-cost earth-abundant Thin Film Solar Absorber, *Bryan Voigt[1], W Moore, D Ray, M Manno,* University of Minnesota, Minneapolis*; J Jeremiason,* Gustavus Adolphus College*; L Gagliardi, E Aydil, C Leighton,* University of Minnesota, Minneapolis

Pyrite FeS$_2$ has long been considered an ideal absorber material for low-cost and sustainable thin film solar cells because it is composed of earth-abundant, non-toxic, inexpensive elements, has a suitable band gap (0.95 eV), and absorbs light so strongly that a 100-nm-thick film absorbs >90 % of photons with energies above the band gap. Lack of doping control, however, has presented a barrier to realization of the *p-n* pyrite homojunction, *i.e.,* the simplest route to a pyrite solar cell. *Heterojunction* pyrite solar cells have proven to have disappointingly low efficiencies (~3%), surface conduction and leaky surface inversion layers being implicated as the culprit. While mitigation of pyrite surface conduction remains a challenge, doping has begun to yield to understanding, renewing optimism for a *p-n* pyrite homojunction solar cell. In particular, we have shown that rigorously phase-pure pyrite single crystals and thin films are exclusively *n*-type, due to a common dopant. Most recently, we have identified sulfur vacancies as this unintentional *n*-dopant, enabling robust control over *n*-doping levels in single crystals grown by chemical vapor transport (CVT). Progressing towards a *p-n* pyrite homojunction, here we demonstrate effective *p*-type doping in crystals by introducing phosphorus in the vapor phase during CVT growth. Increasing the phosphorus concentration from <0.1 ppm to 30 ppm evolves electronic conduction from *n*-type to *p*-type, with a clear and reproducible majority carrier inversion for concentrations >10 ppm. Typical transport properties of phosphorus-doped, *p*-type pyrite crystals include a hole thermal activation energy, room temperature resistivity, hole density, and mobility of ~170 meV, 3 Ω cm, 2 × 10^{18} cm^{-3}, and 1 cm^2 V^{-1}s^{-1}, respectively. Density functional theory calculations confirm that phosphorus substituted on the S site is an acceptor, predicting a defect level at 200 meV above the valence band maximum, in good agreement with experiment. With both *n*- and *p*-type doping control achieved, attempts at *p-n* pyrite homojunction solar cells become possible.

11:00am TF+EM+NS+SS-ThM-10 Relaxor-ferroelectric Thin Films for Energy Harvesting from Low-grade Waste-heat, *Amrit Sharma, B Xiao, S Pradhan, M Bahoura,* Norfolk State University

The need for efficient energy utilization is driving research into ways to harvest waste-heat which is ubiquitous, abundant and free. Thermal harvesting is a promising method for capturing freely available heat and converting it to a more usable form, such as electrical energy. Thermal harvesting for low power electronic devices using ferroelectric materials is one of the emerging areas of research because they possess spontaneous polarization and exhibit excellent piezoelectric as well as excellent pyroelectric coefficients. These materials are unique as they only sense time-dependent temperature change to generate electric power. We have grown lead-free BaZr$_{0.2}$Ti$_{0.8}$O$_3$ (BZT)/ Ba$_{0.7}$Ca$_{0.3}$TiO$_3$ (BCT) multilayer heterostructures and studied the structural, dielectric, ferroelectric, pyroelectric and energy density characteristics. The BZT/BCT multilayer epitaxial heterostructures were grown on SrRuO (SRO) buffered SrTiO (STO) single crystal substrate by optimized pulsed laser deposition technique. The large angle x-ray scans showed only diffraction peaks from the substrate and pseudocubic reflections (00*l*) from the multilayer heterostructure, confirming that these films are phase pure and epitaxial in nature. The atomic force microscopy (AFM) studies indicate that the surface roughness is low and that film growth is of high quality. The ferroelectric phase transitions have been probed above room temperature with relaxor behavior. The polarization versus electric field (P-E) measurement exhibits well-saturated hysteresis loop with maximum and remnant polarization of 138 and 64 μC/cm^2, respectively. Solid-state, thin-film devices, that convert low-grade heat into electrical energy, are demonstrated using pyroelectric Ericsson cycles, and their performance is optimized by independently enhancing pyroelectric coefficient and suppressing dielectric permittivity in compositionally graded heterostructures. Our findings suggest that pyroelectric devices may be competitive with thermoelectric devices for low-grade thermal harvesting.

11:20am TF+EM+NS+SS-ThM-11 Thermal Treatment Effects on the Thermoelectric Devices from Sn/Sn+SnO$_2$ Thin Films, *Satilmis Budak, E McGhee, Z Xiao, E Barnes, R Norwood,* Alabama A&M University

Approximately two-thirds of energy is lost as waste heat; the direct harvest of this waste heat using thermoelectric (TE) materials has attracted worldwide interest. TE materials can convert waste heat from industrial processes, furnaces, and engine exhaust streams into useful electricity by the Seebeck effect. The energy conversion efficiency is shown by the dimensionless figure of merit, ZT, and ZT=S^{2}σT/K, where S is the Seebeck coefficient, σ is the electrical conductivity, K is the total thermal conductivity, and T is the absolute temperature. The numerator S^{2}σ defines the power factor (PF), which primarily relates to the electric properties [1]. When operating as an energy-generating device, the TE device is termed a thermoelectric generator (TEG). The source of thermal energy manifests itself as a temperature difference across the TEG. When operating in a cooling or heating mode the TE device is termed a thermoelectric cooler (TEC). Similarly, the TE device produces heating or cooling that takes the form a heat flux which then induces a temperature difference across the TEC. TE devices are solid-state mechanisms that are capable of producing these three effects without any intermediary fluids or processes. For power generation applications TE devices are used in automobiles as exhaust gas waste heat recovery devices where thermal energy is scavenged along the exhaust line of a vehicle and converted into useful electricity [2]. The TE devices from 50 alternating layers of Sn/Sn+SnO$_2$ thin films were prepared using DC/RF Magnetron Sputtering. They were heat treated at different temperatures to form nanostructures to increase the Seebeck coefficients and electrical conductivity and decrease thermal conductivity. Seebeck coefficient, van der Pauw resistivity, and thermal conductivity were used for the characterization. SEM/EDS was used to characterize the surface morphology of the films.

[1] Hongchao Wang, Wenbin Su, Jian Liu, Chunlei Wang, "Recent development of n-type perovskite thermoelectrics", J Materiomics 2 (2016) 225-236

[2] Chetan Jangonda, Ketan Patil, Avinash Kinikar, Raviraj Bhokare, M.D.Gavali, "Review of Various Application of Thermoelectric Module", International Journal of Innovative Research in Science, Engineering and Technology Vol. 5, Issue 3, (March 2016), 3393-3400.

Acknowledgement

11:40am TF+EM+NS+SS-ThM-12 Thermoelectric Properties of Efficient Thermoelectric Devices from Sb/Sb+SnO$_2$ Thin Films, *Eshirdanya McGhee, S Budak, Z Xiao, N Caver, B McNeal,* Alabama A&M University

The thermoelectric (TE) concept could be seen as a perfect solution for recovering waste heat from engine exhaust and converts in to electric energy. TE generators are all solid-state devices that convert heat into electricity. Unlike traditional dynamic heat engines, TE generators contain

[1] **TFD James Harper Award Finalist**

no moving parts and are completely silent. Such generators have been used reliably for over 30 years of maintenance-free operation in deep space probes such as the Voyager missions of NASA. TE systems can be easily designed to operate with small heat sources and small temperature differences [1]. An ideal TE material behaves like an electron crystal and phonon glass, allowing a large temperature gradient across it while conducting electricity efficiently to generate a TE voltage. Significant progress in the TE performance of materials has been made by exploring ultra low thermal conductivity at high temperature and reducing thermal conductivity by nano-structuring, as well as by resonant doping and energy-dependent scattering of electrons [2]. The figure of merit ZT describes material performance. ZT depends on the thermoelectric material properties of Seebeck coefficient S, electrical conductivity σ, and thermal conductivity K, and $ZT = S^2\sigma T/K$ where T is the temperature of the material [3]. TE devices from 50 alternating layers of $Sb/Sb+SnO_2$ thin films were prepared by DC/RF Magnetron Sputtering. TE devices were annealed at different temperatures to form nano-structures to increase the Seebeck coefficients and electrical conductivity and decrease thermal conductivity. For the characterization, Seebeck coefficient, van der Pauw resistivity, and thermal conductivity were used. The surface morphology was characterized using SEM/EDS.

[1] Krishna Purohit, Sheetal Kumar Jain, Dr. P M Meena, Khushaboo Singh, Manish Dadhich,

"Review Paper on Optimizations of Thermoelectric System", International Journal of Innovative Research in Engineering & Management (IJIREM), ISSN: 2350-0557, Volume-3, Issue-4, (July-2016), 259-263.

[2] Kedar Hippalgaonkar, Ying Wang, Yu Ye, Diana Y. Qiu, Hanyu Zhu, Yuan Wang, Joel Moore, Steven G. Louie, and Xiang Zhang, "High thermoelectric power factor in two-dimensional crystals of MoS_2", PHYSICAL REVIEW B 95, 115407 (2017) 1-9.

[3] Saniya LeBlanc, Sustainable Materials and Technologies 1–2 (2014) 26–35.

12:00pm **TF+EM+NS+SS-ThM-13 3D Printed Triboelectric Nanogenerator**, *I Fattah, E Utterback, **Naga Srinivas Korivi**, V Rangari,* Tuskegee University

We report on the development of polymer nanocomposite layers made by 3D printing. The nanocomposite is composed of polydimethylsiloxane (PDMS), barium titanate nanoparticles, and multi-walled carbon nanotubes. Flexible layers of this composite have been 3D printed using a commercial 3D printer, and function as triboelectric energy generators. To the best of our knowledge, this is the first report of a PDMS based triboelectric nanogenerator fabricated by 3D printing. The nanogenerators have been evaluated in contact and separation mode and produce a maximum of 2.6 Volts under pressure from a human finger.

The fabrication procedure involves sonicating barium titanate ($BaTiO_3$, Skyspring Nanomaterials) and multi walled carbon nanotubes (MWCNT, Skyspring Nanomaterials) together in ethyl alcohol. This is followed by removing the excess ethyl alcohol, and manually grinding the nanoparticle powder to break any clusters. This is followed by mechanically blending liquid PDMS pre-polymer and its curing agent (~10:1 ratio by weight) with the nanoparticle powder in one beaker. Finally, the blend is filled into a dual plastic syringe, which is loaded onto an extrusion printing head of a commercial 3D printer (Hydra 16A, Hyrel LLC, USA). The printer reads a software file that defines the pattern or shape to be printed and dispenses the material from the syringe accordingly onto a base plate. For printing this composite, the base plate temperature was maintained between 75 – 90 °C, to allow curing within a few minutes. Once cured, the solid composite layers (270 μm thickness) can be peeled off the base plate.

The 3D printed PDMS-BaTiO3-MWCNT layers have been evaluated as triboelectric energy generation. In one embodiment, the 3D printed functions as the negatively charged layer in a contact-separation scheme. A polyimide sheet is used as positively charged layer. Carbon tapes are used as current collectors on both positive and negative charged layers. When these two layers are brought in contact with some pressure applied by a human finger, and then released, characteristic negative and positive voltage spikes are respectively observed. Peak voltages as high as 2.6 Volts have been obtained with the present 3D printed PDMS-BaTiO3-MWCNT layers. These observations indicate the applicability of this 3D printed composite in triboelectric energy generation.

2D Materials

Room A216 - Session 2D+AS+BI+HC+MN+NS+PS+SS+TL-ThA

Surface Chemistry, Functionalization, Bio, Energy and Sensor Applications

Moderator: Mark Edmonds, Monash University, Australia

2:20pm 2D+AS+BI+HC+MN+NS+PS+SS+TL-ThA-1 Molecular Layers on Nanoporous Gold Electrodes, *Elizabeth Landis,* College of the Holy Cross
Nanoporous gold presents a surface with high conductivity and surface area, which makes it an interesting platform for surface chemistry. However, the nanoporous gold surface lacks the functionality necessary for many applications including sensing. We have investigated self-assembled thiol-based monolayers and the electroreduction of diazonium-based salts to form aryl molecular layers on nanoporous gold. We use infrared spectroscopy and cyclic voltammetry to show that the molecular layer ordering and density depends on the functionalization method, and the underlying nanoporous surface impacts molecular ordering and electron transfer properties.

2:40pm 2D+AS+BI+HC+MN+NS+PS+SS+TL-ThA-2 Thermotropic Liquid Crystal (5CB) on Two-dimensional Materials, *Paul Brown,* American Society for Engineering Education*; S Fischer, J Kołacz, C Spillmann, D Gunlycke,* U.S. Naval Research Laboratory
Current means of redirecting light often rely on either bulky mechanical gimbals or non-mechanical diffractive elements. The former often suffer from wear and are susceptible to failure, while the latter may have significant optical power confined within side lobes. One promising non-mechanical approach that can overcome present limitations in beam redirection incorporates liquid crystal (LC) for continuous, refractive steering. Nematogens, the molecules comprising the LC in a nematic phase, support inherent anisotropic optical and dielectric properties that result from local ordering of single molecules. Recent research suggests the possibility of including two-dimensional materials to act as both an alignment layer and electrode to LC. This offers the possibility of further reducing device dimensions and device response time. Yet little research has focused on the ground state properties of a nematogen interfacing with the two-dimensional substrate. In this talk, we present density functional theory results of the electronic properties of a well-known nematogen (5CB) interacting with graphene, boron nitride, and phosphorene. We also discuss the influence of an introduced single vacancy on the electronic properties of the composite system. We find that 5CB on phosphorene offers the strongest binding of the considered nanosheets. Moreover, we observe qualitatively different band alignments, and focus in particular on type I, which prohibits free carrier transfer between the substrate and nematic LC. Lastly, we discuss the impact of single vacancies on the performance of two-dimensional materials to operate as both an alignment layer and electrode for LC-based applications.

This work has been supported by the Office of Naval Research, directly and through the U.S. Naval Research Laboratory.

3:00pm 2D+AS+BI+HC+MN+NS+PS+SS+TL-ThA-3 Is it Possible to Achieve Intra-molecular Resolution with Ambient AFM?, *Vladimir Korolkov,* Oxford Instruments-Asylum Research*; S Chulkov, M Watkins,* University of Lincoln, UK*; P Beton,* The University of Nottingham, UK
Although achieving molecular resolution is now almost a routine across various SPM imaging modes, resolving the actual molecular structure at the atomic level has only been accomplished with NC-AFM in UHV often at low temperatures and with a functionalized probe. Of course, the ultimate goal in SPM is to resolve the chemical structure of a molecule identifying each atom.

In this work we are presenting an approach to achieve intra-molecular resolution on adsorbed molecules in the ambient at room temperatures with a standard AFM cantilever with unmodified tip. We have discovered that using a combination of higher eigenmodes and low oscillation amplitudes (~3-5Å) of a standard Si-cantilever routinely provides ultra-high resolution on adsorbed molecules on surfaces[1,2] and bulk polymers[3].

With this approach we have been able to observe both intra-molecular features and inter-molecular contrast in thin films of coronene and melem molecules on the surface of hexagonal boron nitride (hBN). In case of coronene, all six benzene rings have been resolved as well as underlying atomic lattice of hBN. Unlike coronene, melem forms molecular assemblies with square symmetry stabilized with in-plane strong hydrogen bonds between amino groups. We have observed a strong inter-molecular

contrast where the hydrogen bonds are expected to be. Similar to coronene, the observed intra-molecular contrast was associated with three triazine rings. We have used Probe particle model[4] to simulate our experimental AFM images and found very good agreement between them. In fact, PPM allowed us a correct interpretation of melem square phase assembly.

Both systems were studied at room and elevated temperatures where we observed phase transitions leading to thermodynamically stable systems. The experimental results are in excellent agreement with density functional theory calculations.

We believe the proposed approach, yet still in its infancy, could potentially provide a pathway to unambiguous identification of molecules on surfaces in the ambient on standard AFM systems.

_____

[1] Korolkov et al., Nat. Chem., 2017

[2] Korolkov et al., Nat. Comm., 2017

[3] Korolkov et al., Nat. Comm., 2019

[4] Hapala et al., Phys. Rev. B 90, 085421

3:20pm 2D+AS+BI+HC+MN+NS+PS+SS+TL-ThA-4 Tailoring Surface Properties via Functionalized Hydrofluorinated Graphene Compounds, *Jangyup Son,* University of Illinois at Urbana-Champaign*; N Buzov,* University of California at Santa Barbara*; S Chen,* University of Illinois at Urbana-Champaign*; D Sung,* Sejong University, Republic of Korea*; H Ryu,* Seoul National University, Republic of Korea*; J Kwon,* Yonsei University, Republic of Korea*; S Kim, J Xu,* University of Illinois at Urbana-Champaign*; S Hong,* Sejong University, Republic of Korea*; W King,* University of Illinois at Urbana-Champaign*; G Lee,* Seoul National University, Republic of Korea*; A van der Zande,* University of Illinois at Urbana-Champaign
Mixing compounds or alloys is an important process to tailor or enhance the intrinsic properties of materials such as chemical reactivity, mechanical strength, and electronic structure. In nanosystems, such as two-dimensional (2D) materials like graphene, transition metal dichalcogenides (TMDCs), and hexagonal boron nitride (hBN), where there is no distinction between the surface and the bulk, mixing of elements is also an important tool for tailoring the interaction of the material with its environment. A successful strategy for manipulating the chemical structures of 2D materials is the chemical functionalization of graphene with single elements such as H, O, N, and F. Yet, an even wider parameter space is possible by combining these functionalization species to produce ternary functionalized graphene compounds.

Here we present a new strategy for producing functionalized graphene compounds through the systematic control of the ratio between adatoms. We demonstrate tailored hydrofluorinated graphene (HFG) compounds via the sequential exposure of graphene to low-energy hydrogen plasma and xenon difluoride (XeF_2) gas. We demonstrate reversible switching of the surface between completely hydrogenated graphene (HG) and fluorinated graphene (FG) as well as the intermediate ratio between two extremes. Moreover, we demonstrate pattern the surface functionalization on a single chip into chemically distinct materials (graphene, FG, HG, and HFG compounds).

Finally, with these patterned structures, we demonstrated tailoring of the surface and electronic properties of the 2D materials. First, the patterned structures enable direct comparisons of the relative surface properties such as wettability and surface friction. Additionally, the electrical properties of functionalized graphene compounds showed unusual recovery of electrical conductance during the partial transformation of FG to HFG, due to initial removal of existing F adatoms when exposed to hydrogen plasma. This study opens a new class of 2D compound materials and innovative chemical patterning that can lead to atomically thin 2D circuits consisting of chemically/electrically modulated regions.

4:00pm 2D+AS+BI+HC+MN+NS+PS+SS+TL-ThA-6 Functionalization of MoS_2 with Halogens, *G Copetti,* IF-UFRGS, Brazil*; E Nunes,* IQ-UFRGS, Brazil*; G Soares,* IF-UFRGS, Brazil*; Cláudio Radtke,* IQ-UFRGS, Brazil
Transition metal dichalcogenides (TMDs) with lamellar structures similar to that of graphite have received significant attention because some of them are semiconductors with sizable bandgaps and are naturally abundant. This offers opportunities for fundamental and technological research in a variety of fields including catalysis, energy storage, sensing, and electronic devices. In order to TMDs fulfill their potential, a precise control i) of surface functionalization and ii) of the number of stacked TMD monolayers are mandatory. Surface functionalization was shown to play a key role in

tuning photoluminescence properties of MoS_2, formation of controllable and low defect density dielectric/MoS_2 interfaces obtained by atomic layer deposition, and etching of MoS_2 layers. Halogenation is one of the most promising functionalization techniques of TMDs. MoS_2 etching with atomic layer control was already achieved by chlorine adsorption associated with Ar^+ sputtering. Moreover, doping techniques to tune the conductivity and photoemission properties of MoS_2 are essential. Previous works have already shown that incorporation of F-containing species in MoS_2 leads to doping, as well as other interesting properties such as tunable ferromagnetic ordering. In this work, we performed first principal calculations with the density functional theory (DFT) to gain insight into the effect of MoS_2 exposure to halogens. Results evidenced different reactivities while comparing F and Cl, as well as MoS_2 surfaces with variable amounts of defects. These results were explored experimentally. Bulk exfoliated MoS_2 as well as CVD-grown monolayer MoS_2 samples were used. Chlorination was achieved by irradiating the samples with UV light in Cl_2 flux. Prior to chlorination, sputtering of the MoS_2 with Ar ions is performed to induce S removal. X-ray Photoemission Spectroscopy measurements and Rutherford Backscattering Spectrometry showed that S vacancies play a fundamental role in the chlorination process, with vacancy concentration dictating the balance between etching of the MoS_2 layer and Cl incorporation. Fluorination was performed by exposing the samples to pulses of XeF_2. Different degrees of fluorination are achieved by varying exposure time. S is removed and F is incorporated without any loss of Mo. Chemical displacement on the Mo 3d and S 2p XPS peaks was observed after both halogenations processes. These results can clarify the mechanisms of Cl and F incorporation. Finally, the halogenation techniques proposed can be simple and useful methods to adapt the MoS_{---2} properties for future applications.

4:20pm 2D+AS+BI+HC+MN+NS+PS+SS+TL-ThA-7 Towards Higher Alcohol Synthesis from Syngas on 2D material-based catalysts: A First-Principles Study*, *Tao Jiang, D Le, T Rahman,* University of Central Florida
Synthesis of higher alcohol from syngas has been of great interest owing to the limited petroleum resources and environmental concerns. Rational designing of cheap and efficient catalyst material for such synthesis is in great demand because of diminishing supply of the current state-of-the-art catalysts. Two dimensional (2D) materials are emerging with far-reaching potential for technical and industrial applications thanks to their unique properties, recent developments and improvement of production technologies. In this talk, we will discuss our recent work, based on first principles calculations, towards the unitization of 2D materials as catalysts for higher alcohol synthesis. In particular, defect laden hexagonal boron nitride (*dh*-BN) with N vacancies is excellent catalyst for hydrogenation of CO_2 towards ethanol formation, in the reaction pathway of which thecrucial step for forming C_2 bond, i.e. reaction of adsorbed species CH_3^* and CO^* to form CH_3CO^*, is exothermic with reasonably low activation barrier (0.68 eV). On the other hand, we also find single layer of MoS_2 functionalized with small Au nanoparticle to catalyze CO hydrogenation reaction towards ethanol formation. Among all the elementary reactions, the important steps are the reaction of an adsorbed CH_3^* and a CO^* molecule and the hydrogenation of acetyl to acetaldehyde (both are exothermic with activation barriers of 0.69 and 0.47 eV, respectively) to form C_2 species.[1] The results suggest that 2D materials are suitable candidates for higher alcohol synthesis. Full reaction pathways will be discussed together with results of Kinetic Monte Carlo simulations to shed light on the selectivity of the catalysts. Contact will be made with experimental data that validate our theoretical predictions.

[1] K. Almeida, K. Chagoya,A. Felix, T. Jiang et al, "Towards Higher Alcohol Formation using a single-layer MoS_2 activated Au on Silica: Methanol Carbonylation to Acetaldehyde", submitted

4:40pm 2D+AS+BI+HC+MN+NS+PS+SS+TL-ThA-8 Proton Conductivity Properties of Electrospun Chitosan Nanofibers, *Woo-Kyung Lee, J Pietron, D Kidwell, J Robinson, C McGann, S Mulvaney,* U.S. Naval Research Laboratory
A major challenge of the 21st century will be to establish meaningful two-way communication between biology and electronics. The study of protonics, devices that mimic electronics but pass protons instead of electrons, seeks to bridge this gap. Protonic conductive materials (PCMs) are essential elements of these devices and we have demonstrated significant improvement in conductivity for chitosan PCMs when deposited as electrospun nanofibers. The observed improvements stem from both enhanced molecular alignment and from chemical doping due to the electrospinning carrier fluid, trifluoroacetic acid (TFA). We deposited electrospun chitosan nanofibers over palladium protodes and then used the helium ion microscope to isolate single nanofibers for detailed study. We observed that single chitosan nanofibers are strongly doped by TFA with x-ray photoelectron spectroscopy demonstrating extensively protonated nitrogen functionality. With the isolated, single chitosan nanofibers we observed that water uptake, fiber/electrode contact area, and doping concentration are critical parameters of protonic device performance and lead to increased conductivity (*i.e.* low resistivity). The average resistivity of single chitosan nanofibers is 6.2×10^4 $\Omega \cdot cm$, approximately two orders of magnitude lower than the resistivity of cast chitosan PCMs (cast from acetic acid solutions not TFA).We have observed excellent agreement between theoretical models and experiment results that explore each of the contributions to the improved conductivity. In addition, the fabrication and measurement of ionic field-effect transistor of single chitosan fiber using conductive atomic force microscope will be discussed.

5:00pm 2D+AS+BI+HC+MN+NS+PS+SS+TL-ThA-9 Sensor for Breath and Skin Diagnostics, *Pelagia I Gouma,* The Ohio State University
Resistive gas sensors have received a bad reputation of being largely non-selective.

Our work has produced a crystallo-chemical model for selective gas sensing by polymorphic

metal oxides. The reaction-based and ferro-electric poling sensing mechanisms are discussed

in detail. Novel processing methods to produce the respective nano sensors are presented along

with the device fabrication for the non-invasive diagnosis of gaseous biomarkers in human

and animal breath or skin. This sensor technology is expected to revolutionize medical diagnostics.

5:20pm 2D+AS+BI+HC+MN+NS+PS+SS+TL-ThA-10 Symmetry Controlled Ddsorption of Diodobenzene on MoS₂, *Zahra Hooshmand,* University of Central Florida*; P Evans, P Dowben,* University of Nebraska - Lincoln*; T Rahman,* University of Central Florida
In a joint experimental and theoretical study, we have uncovered evidence of the importance of symmetry in the adsorption of the isomers of diiodobenzene on $MoS_2(0001)$. The intensity ratio of iodine to molybdenum measured, as a function of exposure for different isomers of the diiodobenzene, show that while for ortho (1,2-) and para (1,4-) diiodobenzene the rate of adsorption at 100 K is very low, that for meta (1,3-) diiodobenzene is considerably more facile. We have applied dispersion corrected density functional theory-based calculations to understand the subtleties in the electronic structure and geometry of adsorption of these diiodobenzene isomers on $MoS_2(0001)$. All three isomers are found to weakly chemisorb with the same binding strength as well as adopt similar configurations. The calculated electron affinity of the three molecules also do not show a specific trend that would verify experimental data. However, analysis of the frontier orbitals indicate that those of 1,3-diiodobenzene are strongly affected by interactions with MoS_2, while that of the other two isomers remain unchanged. Our results show that symmetry is the identifying factor in these adsorption characteristics. The results of frontier orbitals analysis confirm that for adsorption of (1,2-) and (1,4-) diiodobenzene a reduction in the symmetry of the adsorbent is needed. To further validate our conclusions, we compare the above results with that of the adsorption of the diiodobenzene isomers on defect-laden $MoS_2(0001)$.

5:40pm 2D+AS+BI+HC+MN+NS+PS+SS+TL-ThA-11 Mechanistic Understanding of the CO Hydrogenation Reaction on Defect Engineered 2D-TaS₂ and 2D-MoS₂ Catalysts, *Mihai Vaida,* University of Central Florida
Due to global energy demands, investigation of catalytic reaction mechanisms on novel catalytic materials that can lead to efficient production of storable fuels from sustainable inputs is of central importance. In this contribution the adsorption of CO and H_2 molecules, as well as the CO hydrogenation reaction are investigated on defect engineered two dimensional (2D) TaS_2 and MoS_2. Crystalline 2D-TaS_2 and 2D-MoS_2 with surface area of 1 cm^2 are synthesized via a multistep process based physical vapor deposition on Cu(111). The surface composition, morphology, and electronic structure are investigated via Auger electron spectroscopy, low energy electron diffraction, scanning tunneling

microscopy, scanning tunneling spectroscopy, and photoemission spectroscopy. The interaction of the molecules with the surface and the catalytic reaction mechanisms are investigated via temperature programmed desorption/reaction. No catalytic reactions have been observed on crystalline 2D materials. However, an enhanced catalytic activity is observed after the generation of sulfur vacancies via Ar sputtering. The CO hydrogenation on TaS_2 occurs on low coordinated Ta atoms through the formation of formyl radical (HCO) and formaldehyde (HCOH). On 2D-MoS_2, the CO hydrogenation also occurs on low coordinated Mo atoms. However, in this case the formyl radical splits to form methyldyne radical (CH), which subsequently react with other CH radical to produce acetylene (C_2H_2).

Applied Surface Science Division
Room A211 - Session AS-ThA

Role of Surfaces and Interfaces in Energy Material and Industrial Problems

Moderators: David M. Carr, Physical Electronics, Alan Spool, Western Digital Corporation

2:20pm **AS-ThA-1 Characterization of Glass and Durable Optical Surfaces and Their Modes of Failure**, *Albert Fahey, D Baker, T Dimond,* Corning Inc.
INVITED

Glass has become the all-important interface between human users and information and communications in our daily lives. People not only want to look at bright, high-definition information-displays but also want to interact with and touch the displays. This has placed new requirements on the performance and durability of the surfaces we interact with.

Just below the outer boundaries of glass, the composition makes a transition from the surface that we interact with, defining the spatial limits of the solid, to the "bulk"-material that exhibits most of the macroscopic properties we experience that allow us to use it as building materials to construct displays, hand-held devices, smart-watches, etc.

The composition of the near-surface region, from a few nanometers to several micrometers generally governs the appearance and durability of these surfaces. It also is a critical component in the adhesion of thin films deposited to improve scratch resistance, cleanability, and optical performance.

We will review some compositional profiles of glass, thin films and other materials to understand how some of these surfaces appear, compositionally, and how this can inform us of chemistries and mechanical properties. I will review Secondary Ion Mass Spectrometry (SIMS) depth-profile data and its combination with data acquired by other methods that give us a more complete understanding of the optical surfaces we interact with.

3:00pm **AS-ThA-3 Determination of Liquid Laundry Additives Across Fabric Surfaces**, *Michael Clark, Jr., A Peera, S Donovan, R Pulukkody,* The Dow Chemical Company

Products that offer sensorial benefits in addition to cleaning are increasingly popular among consumers in the fabric care market. Such sensorial attributes are typically related to touch and smell and help provide a more enjoyable experience to the consumer both during and after the laundering process. This presentation will focus on the XPS and SIMS characterization of fabrics before and after washing with different liquid laundry formulations to determine the amount and distribution of different components on the fabric's surface.

3:20pm **AS-ThA-4 Depth Profiling of Silicones with GCIB, Do They Behave like Organic or Inorganic Molecules?**, *Michaeleen Pacholski, M Clark, Jr., P Vlasak, C McMillan,* The Dow Chemical Company

Surface analysts have a love-hate relationship with silicones. Silicones are widely used industrially for lowering surface energy, improving slip, coefficient of friction, mar and many other surface lubricity properties. Due to their low surface energies, and sometimes low viscosity or molecular weight, there is a tendency for them to spread over surfaces or be present as surface contaminants. In these cases a surface analyst may wish to remove them using a gas cluster ion beam source (GCIB). In other instances it may be desirable to understand the chemistry of a silicone coating as a function of depth. Unfortunately, GCIB profiling of silicones is not as straightforward as it is with other organic polymers.

Examples of depth profiles under different GCIB conditions from some reference silicones and silicone-containing coatings will be discussed in this presentation.

4:00pm **AS-ThA-6 Active Control of Interfacial Chemistry for Thin Film Solar Cells**, *Alexandra Koziel, K Montiel, L Wilson, J Carter, I Martin,* Case Western Reserve University

Global energy demand requires the development of efficient and reliable thin film photovoltaics with inexpensive processing. As the efficiency of hybrid perovskite solar cells has skyrocketed, practical constraints of the technology have put the scalability and durability into scientific focus. The development of inorganic interfacial layers, such as metal oxides, is a potential pathway to overcoming the stability and cost limitations associated with organic interlayers in perovskite solar cells. Thin films are sensitive to both the growth conditions, and the composition and morphology of the previously deposited layer. Interfacial engineering of metal oxides using molecular modifiers provides a powerful tool to tune interlayer properties, which can result in improved performance and stability.

This work details the effect of underlying layers on the growth of $CsGeI_3$, a novel all-inorganic perovskite absorber. The hole-transport layer (HTL) and the underlying substrate were systematically varied. Surface and bulk properties of the film stack were characterized at every growth step. The choice of HTL affects the absorber film morphology, and resulting device efficiency. Further, this approach reveals that the choice of substrate can affect the properties of layers through the entire device.

Two common HTLs, PEDOT:PSS and MoO_3, were deposited on substrates with differing surfaces. Glass, ITO (indium tin oxide, a common thin film solar cell transparent electrode), and Si substrates were selected to explore how a range of surface structures, from amorphous to polycrystalline to crystalline, affects the subsequent layers. The vapor-deposited MoO_3 was further modified with gas-phase treatments (UV-ozone and O_2 plasma exposure) and small molecules (silanization). Specifically, an IPTMS ((3-iodopropyl) trimethoxysilane) silanization procedure was developed to produce an iodine-terminated surface, for improved adhesion of the $CsGeI_3$ absorber layer. A suite of materials characterization methods were applied to the samples after each step of device fabrication to assess the evolution of morphology and composition. Bulk, surface, and interface characteristics were probed using UV-Vis absorption measurements, X-ray photoelectron spectroscopy, scanning electron microscopy, optical profilometry, and spectroscopic ellipsometry. Notably, the absorber film morphology and ultimately the stability of the film stack is sensitive to not only the HTL, but the nature of the material under the HTL (ITO vs. glass), demonstrating the influence of surface/interface properties across multiple layers in a device.

4:20pm **AS-ThA-7 Solar Energy From a Big-Picture Perspective to Nanoscale Insights via TOF-SIMS**, *Steven Harvey,* National Renewable Energy Laboratory **INVITED**

We have used time-of-flight secondary-ion mass spectrometry (TOF-SIMS) at the National Renewable Energy Laboratory to investigate the performance and reliability of solar cell materials and devices, and we will present some recent work that highlights the versatility of TOF-SIMS. This work includes: 1) Multi-scale, multi-technique investigations of photovoltaic module failure including TOF-SIMS to enable insights into the root-cause mechanisms of module degradation at the nanoscale that are observed at the length scale of meters; 2) Investigations into the performance and stability of hybrid perovskite solar cell devices and 3) Using a combination of 1-D profiling and 3-D tomography to elucidate the fundamentals of incorporating dopants in CdTe solar cells.

5:00pm **AS-ThA-9 Investigation of Surface and Bulk Properties of Extended Surface PtNi and PtNiCo Catalysts**, *Sarah Zaccarine,* Colorado School of Mines; *W McNeary,* CU Boulder; *S Shulda, S Mauger, K Hurst,* National Renewable Energy Laboratory; *A Weimer,* CU Boulder; *S Alia, B Pivovar,* National Renewable Energy Laboratory; *S Pylypenko,* Colorado School of Mines

Polymer electrolyte membrane fuel cells (PEMFCs) produce electricity with only heat and water as byproducts, but sluggish kinetics of the oxygen reduction reaction (ORR) at the cathode restrict widespread commercialization, motivating development of advanced catalysts such as the extended surface platinum nickel (PtNi) and platinum nickel cobalt (PtNiCo) nanowires investigated in this work.

These catalysts were synthesized using atomic layer deposition (ALD), a scalable route that allows controlled deposition of Pt on Ni or Co nanowires. Surface and bulk composition and structure of the PtNi and

PtNiCo nanowires was investigated as a function of synthesis conditions and a series of post-synthesis modifications. A variety of characterization techniques was used to gain a comprehensive understanding of structure-property-performance relationships. The catalyst was first studied using a combination of x-ray absorption near-edge structure (XANES) spectroscopy, extended x-ray absorption fine structure (EXAFS) spectroscopy, x-ray photoelectron spectroscopy (XPS), and scanning transmission electron microscopy (STEM) coupled with energy dispersive x-ray spectroscopy (EDS) hypermapping to obtain detailed complementary information about speciation and distribution of Pt and Ni, distinguishing differences between surface and bulk. Rotating disk electrode (RDE) testing was conducted to assess activity and stability of the catalysts. Differences between ALD-derived PtNi and PtNiCo samples will be discussed and compared to previously reported catalysts synthesized via spontaneous galvanic displacement (SGD). Catalysts were then integrated into membrane electrode assemblies (MEAs) and properties of the fabricated catalyst layers were investigated using STEM/EDS and transmission x-ray microscopy (TXM) to better understand the interfaces between catalyst and ionomer, with and without addition of carbon into the structure of the electrode. Our results demonstrate important advances in the performance of this class of materials achieved through optimization of surfaces and interfaces of the catalyst and catalyst layer.

5:20pm AS-ThA-10 Interfaces in Electrodeposited Li-Ion Battery Electrodes, *Paul Braun,* University of Illinois at Urbana-Champaign **INVITED**
Electrodeposition of electrode materials has the potential to enhance secondary battery performance and broaden the scope of available electrode form factors. For example, as we have shown, electrodeposited electrodes provide energy densities not achievable via conventional slurry-cast electrode processing methodologies. I will present our work on the electrodeposition of high performance silicon and tin-based Na and Li-ion anodes and $LiCoO_2$, $NaCoO_2$, $LiMn_2O_4$, and related Na and Li-ion cathodes. The electrolytically active materials were formed either as solid films, or where significant volume changes upon cycling are present, as a 3D mesostructured film. The capacities are near-theoretical, and in the case of the electroplated oxides, the crystallinities and electrochemical capacities are comparable to powders synthesized at much higher temperatures. What we have found, is that the interfaces, and interphases that may form during cycling, have significant impacts on the properties of the resulting electrodes. Understanding the properties of these interfaces/interphases is critical to understanding, and ultimately improving, overall cell performance.

Chemical Analysis and Imaging Interfaces Focus Topic
Room A120-121 - Session CA+NS+SS+VT-ThA

Progress in Instrumentation and Methods for Spectro-microscopy of Interfaces

Moderators: Jinghua Guo, Lawrence Berkeley National Laboratory, Andrei Kolmakov, National Institute of Standards and Technology (NIST)

2:20pm CA+NS+SS+VT-ThA-1 Helium and Neon Ion Beams for the Imaging and Analysis of Interfaces, *John A. Notte, C Guillermier, F Khanom, B Lewis,* Carl Zeiss PCS, Inc. **INVITED**
The recently developed ORION NanoFab instrument provides a single platform with He⁺, Ne⁺, and Ga⁺ focused ion beams. The gallium beam is a conventional FIB and offers high currents and high sputter yields for material removal applications such as sample preparation or exposing sub-surface features. The He and Ne ion beams originate from a sub-nanometer ionization volume of the gas field ion source (GFIS) and because of this, can be focused to remarkable small probe sizes, 0.5 nm and 1.9 nm respectively. The He beam is now well established for high resolution imaging with surface sensitivity, long depth of focus, and the ability to image insulating surfaces without a conductive overcoating. The helium beam has also been used successfully in a variety of nanofabrication tasks such as lithographic exposure of resist, fine sputtering, beam chemistry, and precision modification of materials. The neon beam with its intermediate mass provides a higher sputtering yield, and with that, the ability to perform SIMS analysis with an unprecedented small focused probe size. A newly integrated magnetic spectrometer enables analytical capabilities on this same platform, with a lateral resolution limited only by the collision cascade. Features smaller than 15 nm have been detected. Together these complementary imaging modes can be combined to provide insights of morphology and composition at the smallest length scales.

In this talk the underlying technology of the NanoFab-SIMS will be introduced, as will the physics of the beam-sample interactions. The bulk of the presentation will provide a survey of results, both published and new, demonstrating how this instrument can serve in a variety of applications related to interfaces.

3:00pm CA+NS+SS+VT-ThA-3 Interfacial Studies using Ambient Pressure XPS, *Paul Dietrich, A Thissen,* SPECS Surface Nano Analysis GmbH, Germany **INVITED**
Over the last decades XPS under Near Ambient Pressure (NAP) conditions has demonstrated its promising potential in a wide variety of applications. Starting from operando studies of surface reactions in catalysis, the applications soon have been enhanced towards studies of processes at liquid surfaces, mainly using freezing/melting cycles, liquid jets or liquid films on rotation disks or wheels. Since more than 15 years, the need for basic studies off fundamental solid-liquid interface chemistry has attracted growing interest. Dip-and-pull experiments at synchrotron sources finally also demonstrated, that in-situ and operando XPS in electrochemical experiments can be realized, significantly contributing to the basic understanding of modern energy converting or storing devices, like batteries, fuel cells, etc.

The development of pure laboratory NAP-XPS systems with optimized sample environments, like special sample holders, Peltier coolers and operando liquid cells combined with full automation and process control provides possibilities for preparation and analysis of a multitude of liquid samples or solid-liquid interfaces on a reliable daily base.

Interfaces of semiconductors with organic solvents are important for production processes and device operation. The first example presented shows the simplicity of obtaining relevant results on Silicon in different organic solvents without the need of highly sophisticated set-ups or special excitation sources beyond Al K_a.

Another example shows an operando study of metal corrosion in acetic acid. Moreover a versatile set-up is presented, allowing for studies of solid-electrolyte interfaces for example in Lithium ion batteries as a simple laboratory experiment.

Finally an outlook is given on the future perspective of applications and scientific contributions of routine operando XPS.

4:00pm CA+NS+SS+VT-ThA-6 Operando Spectroscopy and Microscopy of the Electrode-Electrolyte Interface in Batteries, *Feng Wang,* Brookhaven National Laboratory **INVITED**
Real-time tracking structural/chemical changes of electrodes in batteries is crucial to understanding how they function and why they fail. However, in real battery systems electrochemical/chemical reaction occurs at varying length scales, leading to changes not only in the bulk but often locally at electrolyte/electrode interface. *In situ* X-ray techniques are typically employed for studying structural changes in the bulk electrodes and often limited by their poor spatial resolution in probing local changes at interface. Herein, we present our recent results from developing new *operando* spectroscopy and microscopy techniques, specialized for studying electrochemical/chemical reaction and structural modification of the solid-electrode surface and interface, *in the presence of the electrolyte and during battery operation*. Examples will be given to show how interfacial reaction during battery operation is visualized directly, allowing gaining insights into electrode/electrolyte design for practical use in batteries. New opportunities for combining *first principles* simulation and deep machine learning to complement and guide experiments will also be discussed.

4:40pm CA+NS+SS+VT-ThA-8 Ultrasensitive Combined Tip- and Antenna-Enhanced Infrared Nanoscopy of Protein Complexes, *B O'Callahan,* Pacific Northwest National Laboratory*; M Hentschel,* University of Stuttgart, Germany*; M Raschke,* University of Colorado Boulder*; P El-Khoury,* Pacific Northwest National Laboratory*; Scott Lea,* Pacific Norththwest National Laboratory
Surface enhanced infrared absorption (SEIRA) using resonant plasmonic nanoantennas enables zeptomolar detection sensitivity of (bio)analytes, although with diffraction limited spatial resolution. In contrast, infrared scattering-scanning near-field optical microscopy (IR s-SNOM) allows simultaneous imaging and spectroscopy with nanometer spatial resolution through vibrational coupling to the antenna mode of a probe tip. In this presentation, we discuss our approach combining these two methods to image both continuous and sparse distributions of ferritin protein

complexes adsorbed onto IR-resonant Au nanoantennas. The joint tip- and antenna-enhancement yields single protein complex sensitivity due to coupling with the vibrational modes of the bioanalytes. The coupling is revealed through IR s- SNOM spectra in the form of Fano lineshapes, which can be modelled using coupled harmonic oscillators. Through simulations of the recorded hyperspectral images, we extract the optical signatures of protein complex monolayers. This work paves the way for single protein identification and imaging through a combination of tip and antenna-enhanced IR nanoscopy.

5:00pm CA+NS+SS+VT-ThA-9 Imaging and Processing in Liquid Gel Solutions with Focused Electron and X-ray Beams, *T Gupta,* National Institute of Standards and Technology (NIST)*; P Zeller, M Amati, L Gregoratti,* Elettra - Sincrotrone Trieste, Trieste, Italy*; Andrei Kolmakov,* National Institute of Standards and Technology (NIST)

Gels are porous polymeric scaffolds that can retain high volume fraction of liquids, can be easily functionalized for a specific need, can be made biocompatible and therefore, found numerous applications in drugs devilry, tissue engineering, soft robotics, sensorics, energy storage, etc. We have recently proposed a technique for micro-patterning and high-resolution additive fabrication of 3D gel structures in natural liquid solutions using electron and soft X-ray scanning microscopes [1]. The core of the technology is the employment of ultrathin electron (X-ray) transparent molecularly impermeable membranes that separate high vacuum of the microscopes from a high-pressure fluidic sample. In this communication, we report on effects of the beam and exposure conditions on to the degree of crosslinking of pristine and composite PEGDA hydrogels. We found that cross-linking occurs at very low irradiation doses. The size of the crosslinked area saturates with the dose and bond scission occurs at elevated radiation doses what has been supported with O 1s and C 1s XPS spectra evolution and prior research [2]. These chemically modified regions can be selectively etched what enables an additional partnering option for the gelated features with a spatial resolution of ca 20 nm. Finally, we defined the imaging conditions for guest particles in composite hydrogels in its liquid state during the crosslinking process. We were able to observe the electrophoretic migration of sub 100 nm Au nanoparticles inside the gel matrix.

References

[1] T. Gupta *et al.*, "Focused Electron and X-ray Beam Crosslinking in Liquids for Nanoscale Hydrogels 3D Printing and Encapsulation," *arXiv preprint arXiv:1904.01652,* 2019.

[2] N. Meyerbröker and M. Zharnikov, "Modification and Patterning of Nanometer-Thin Poly (ethylene glycol) Films by Electron Irradiation," *ACS applied materials & interfaces,* vol. 5, no. 11, pp. 5129-5138, 2013.

5:20pm CA+NS+SS+VT-ThA-10 In Situ TEM Visualization of Solution-based Nanofabrication Processes: Chemical Wet-etching and Capillary Forces, *Utkur Mirsaidov,* National University of Singapore, Singapore **INVITED**

Controlled fabrication of 3D nanoscale materials from semiconductors is important for many technologies. For example, scaling up the density of the transistors per chip requires the fabrication of smaller and smaller vertical nanowires as channel materials [1]. Two key processes essential to the fabrication of these devices is a precise etching of the nanostructures and the damage-free solution based cleaning (damage occurs during post-clean drying due to capillary forces). However, very little is known about both of these processes because it is extremely challenging to visualize etching and cleaning with solutions directly at the nanoscale. Here, using in situ liquid phase dynamic TEM imaging [2-4], we first describe the detailed mechanisms of etching of vertical Si nanopillars in alkaline solutions [5]. Our design of liquid cells includes a periodic array of patterned nanopillars at a density of 1.2×10^{10} cm^{-2}. We show that the nanoscale chemical wet-etch of Si occurs in three stages: 1) intermediates generated during alkaline wet etching aggregate as nanoclusters on the Si surface, 2) then the intermediates detach from the surface before 3) dissolving in the etchant.

Next, we describe the capillary damage of these high-aspect-ratio Si nanopillars during drying after the solution-phase cleaning. Our results reveal that drying induced damage to nanopillars occurs in three distinct steps. First, as water evaporates from the surface patterned with nanopillars, water film thins down non-uniformly leaving small water nanodroplets trapped between the nanopillars. Second, the capillary forces induced by these droplets bend and bring the nanopillars into contact with each other at which point they bond together. Third, droplets trapped between the nanopillars evaporate leaving the nanopillars bonded to each other. We show that even after the nanodroplets finally evaporate,

interfacial water covering the nanopillars act as a glue and holds the pillars together.

Our findings highlight the importance of being able to visualize the processes relevant to nanofabrication in order to resolve the failure modes that will occur more frequently as the device sizes get even smaller in the future.

[1] C. Thelander et al, Mater. Today 9 (2006), 28–35.

[2] M. J. Williamson et al, Nature Materials 2 (2003), p. 532.

[3] H. Zheng et al, Science 324 (2009), p. 1309.

[4] U. Mirsaidov et al, Proc. Natl. Acad. Sci. U.S.A. 109 (2012), p. 7187.

[5] Z. Aabdin et al, Nano Letters 17 (2017), p.2953.

[6] This work was supported by Singapore National Research (NRF-CRP16-2015-05).

Fundamental Aspects of Material Degradation Focus Topic
Room A212 - Session DM1+BI+SS-ThA

Low Fouling Interfaces and Environmental Degradation
Moderator: Axel Rosenhahn, Ruhr-University Bochum

2:20pm DM1+BI+SS-ThA-1 Utilizing Experimental and MD Simulation Approaches in the Understanding and Design of Low Fouling Interfaces, *Paul Molino,* University of Wollongong, Australia **INVITED**

Biofouling is a ubiquitous problem for a diverse suite of industries, impacting the functionality of materials and devices. Diverse approaches taken in the design of materials and interfaces to prevent microbial fouling often rely on atomic and molecular scale processes, however the fundamental mechanism/s underlying these processes, and their mode of action, in many cases continue to elude researchers. Highly hydrophilic chemistries such as polyethylene glycol and zwitterion-based chemistries, have long been used to generate interfaces that prevent biological interactions at surfaces. Such surface chemistries have been proposed to function through a combination of molecular water organisation and steric repulsion at the interface. Experimental approaches have confirmed the presence of hydration layers associated with hydrophilic polymer-based surfaces, yet the fundamental mechanisms underlying their capacity to inhibit surface fouling, and how such hydration layers differ from equally hydrophilic interfaces that do not prevent surface fouling is still unclear. Molecular dynamic (MD) simulations have gone some way to provide critical insights into their respective mechanism/s of action, however experimental approaches capable of adequately resolving features at a suitable spatial resolution to corroborate and build on these models have been lacking. Herein I will present a highly biofouling resistant coating composed of silica nanoparticles functionalised with a short chain hydrophilic silane. To understand the interfacial environment at the hydrated nanoparticle surface, frequency modulation – atomic force microscopy was used to provide sub-atomic resolution of the water structuring about the nanoparticle interface, which we validate using all-atom molecular dynamic simulations that strikingly predict similar structures of water layers on the original and ultralow fouling surfaces. The convergence of experimental and modelling data reveals that suitably spaced, flexible chains with hydrophilic groups interact with water molecules to produce a connective, *quasi-stable* layer, consisting of dynamic interfacial water, that provides a basis for antifouling performance of ultrathin, hydrophilic surface chemistries. This approach provides a road map for the future development and optimisation of interfacial chemistries and materials designed to combat biofouling and biodegradation.

3:00pm DM1+BI+SS-ThA-3 Study of Environmental Exposure Effects on Pristine and DC Magnetron Sputtering Metallic Coated 3D Printed Polymers, *D Mihut, Arash Afshar, P Chen,* Mercer University

Three dimensional printing is a promising technique for producing complex geometries and high precision structures from different types of materials. The technique is particularly attractive for polymeric materials due to the cost effectiveness; however when compared to other manufacturing techniques the resulting structures have low mechanical properties and low performance as exposed to harsh environmental conditions. ABS (acrylonitrile butadiene styrene) and PLA (polylactic acid) are common thermoplastic polymers used for many applications (e.g. electrical and electronic assemblies, medical devices, implants, toys). For this research, the ABS and PLA specimens for tensile and flexural testing were 3D manufactured according to standards and their mechanical properties were tested using hardness tester, and Mark-10 tensile testing equipment.

In order to simulate outdoor environmental conditions while avoiding the uncertainties associated with it, specimens were exposed to controlled environmental chamber. Accelerated exposure was performed using a UV radiation/condensation (Q-Lab QUV/basic) accelerated weathering tester. ABS and PLA samples were exposed to UV radiation, high temperature and moisture cycles for different time intervals. Some ABS samples were coated with optically thick metallic materials (silver and copper) using high vacuum DC magnetron sputtering deposition system and were later exposed to UV radiation, high temperature and moisture cycles using same conditions as for un-coated samples. The surface and cross section morphology of samples and the adhesion of metallic layers to the polymer substrates were examined using scanning electron microscopy and laser scanning microscopy. The crystalline structure of the metallic coatings was analyzed using X-ray Diffraction technique. The mechanical properties were characterized using flexural and hardness tests over the exposure time. The metallic thin films improved the surface resistance of the substrate materials and enhanced the mechanical behavior of samples exposed to harsh environmental conditions.

3:20pm DM1+BI+SS-ThA-4 Reaction Mechanism of Chloride-induced Depassivation of Oxide Films: a Density Functional Theory Study, *Q Pang, H DorMohammadi, K Oware Sarfo, P Murkute, Y Zhang, O Isgor, J Tucker, Líney Árnadóttir,* Oregon State University

A protective iron oxide film (passive film) forms on the surface of iron in alkaline environment, such as in reinforced concrete. Chloride and other aggressive ions can cause the breakdown of the passive film (depassivation) in the same environment, leading to active corrosion. The mechanism of the Cl-induced depassivation is studied on flat and stepped α-Fe_2O_3 (0001) surfaces because α-Fe_2O_3 has been suggested to be one of the dominant oxides in the outer layer of the passive film.

The oxidation state of the surface metal atoms plays an important role in Cl-surface interactions and depassivation. Cl binds more strongly to metal atoms at lower oxidation state and these adsorption sites can facilitate higher local coverage. Defect sites, such as on a step edge or next to a O vacancy have lower oxidation states, suggesting an important role of defects in the depassivation process. Two main mechanisms of depassivation have been proposed in the literature, the point defect model that proposes a depassivation through Cl enhanced Fe vacancy formation on the surface and void formation at the metal oxide/metal interface, and the ion exchange model, which proposes a depassivation mechanism through subsurface Cl. Our studies of the thermodynamics of Cl ingress into the passive film, Fe vacancy formation, and bulk vacancy stability all support the point defect model for iron oxide. The initial stages of Cl-induced depassivation are proposed through a combination of reactive force field molecular dynamics simulations and DFT calculations.

Fundamental Aspects of Material Degradation Focus Topic
Room A212 - Session DM2+BI+SS-ThA

Fundamentals of Catalyst Degradation: Dissolution, Oxidation and Sintering

Moderator: Gareth S. Parkinson, TU Wien, Austria

4:00pm DM2+BI+SS-ThA-6 Stability Challenges in Electrocatalysis, *Serhiy Cherevko,* Forschungszentrum Jülich GmbH, Germany   **INVITED**
Many industrially important electrochemical energy conversion technologies, such as electrolysis and fuel cells, rely on expensive noble metal electrocatalysts to accelerate reactions, and thus, improve energy conversion efficiency. Despite their relatively high stability, even noble metals are not completely immune. Indeed, the latter fact represents a considerable challenge in the wide-spread commercialization of electrolysers and fuel cells. Electrocatalyst or support corrosion, particle agglomeration and detachment, Ostwald ripening, structural and morphological changes are just a few examples of possible degradation processes.[1] These processes clearly illustrate the level of complexity one has to deal with in order to understand and circumvent degradation in real devices. Thus, it is difficult to imagine modern electrocatalysis research without advanced analytical tools. In this talk I will demonstrate that the application of on-line inductively coupled plasma mass spectrometry, on-line electrochemical mass spectrometry, and identical location transmission electron microscopy in electrocatalysis research can assist in clarifying the mechanisms leading to degradation. As some representative examples I will show degradation of the state-of-the-art and advanced platinum based catalysts in fuel cells and iridium based catalyst in water

electrolysis.[2-4] Time will also be devoted to discussing application of alternative non-noble metal catalysts in the energy conversion technologies and their stability. Finally, stability in other electrocatalytic systems, e.g. photo-electrochemical water splitting or carbon dioxide reduction will be touched.

Literature:

1 Cherevko, S. *Current Opinion in Electrochemistry***8**, 118-125 (2018).

2 Cherevko, S. *et al. Nano Energy***29**, 275-298, (2016).

3 Kasian, O. *et al. Angewandte Chemie***57**, 2488-2491 (2018).

4 Geiger, S. *et al. Nature Catalysis***1**, 508-515 (2018).

4:40pm DM2+BI+SS-ThA-8 Self-limited Growth of an Oxyhydroxide Phase at the Fe_3O_4(001) Surface in Liquid and Ambient Pressure Water, *Florian Kraushofer,* TU Wien, Austria*; F Mirabella,* TU Wien, Austria, Germany*; J Xu, J Pavelec, J Balajka, M Müllner, N Resch, Z Jakub, J Hulva, M Meier, M Schmid, U Diebold, G Parkinson,* TU Wien, Austria
Atomic-scale investigations of metal oxide surfaces exposed to aqueous environments are vital to understand degradation phenomena (e.g. dissolution and corrosion) as well as the performance of these materials in applications. Here, we utilize a new experimental setup for the UHV-compatible dosing of liquids to explore the stability of the Fe_3O_4(001)-($\sqrt{2} \times \sqrt{2}$)R45° surface following exposure to liquid and ambient pressure water, using low energy electron diffraction (LEED), x-ray photoemission spectroscopy (XPS) and scanning tunnelling microscopy (STM).

Short-time exposure of the surface to clean H_2O results in hydroxylation of the surface, which is not observed in UHV. After longer exposure times, we observe lifting of the ($\sqrt{2} \times \sqrt{2}$)R45° reconstruction with LEED and stronger hydroxylation of the surface with XPS, in agreement with previous reports. However, scanning tunnelling microscopy (STM) images reveal a more complex situation than simply reverting to a bulk-truncation, with the slow growth of an oxyhydroxide phase, which ultimately saturates at approximately 40% coverage. We conclude that the new material contains OH groups from dissociated water coordinated to Fe cations extracted from subsurface layers, and that the surface passivates once the surface oxygen lattice is saturated with H because no further dissociation can take place.

5:00pm DM2+BI+SS-ThA-9 The Impact of W on the Early Stages of Oxide Evolution for Ni-Cr Alloys, *Cameron Volders, V Avincola,* University of Virginia*; I Waluyo,* Brookhaven National Laboratory*; J Perepezko,* University of Wisconsin - Madison*; P Reinke,* University of Virginia
Ni-Cr alloys are highly coveted as they exhibit superior corrosion resistance due to the formation of a passive chromia film which helps protect the underlying alloy from degradation. The properties of this system are further enhanced through the addition of minor alloying elements such as Mo or W. For example, Mo is known to reduce catastrophic events such as pitting and crevice corrosion, thereby enhancing overall corrosion resistance. The ideal composition for technical Ni-Cr alloys has been optimized over many decades, however, the mechanistic understanding for the role of alloying elements such as Mo and W has not been fully developed. The primary objective of this work is to formulate a better mechanistic understanding of how the addition of W impacts the early stages of oxidation for this system and eventually use this information for further improvement of Ni-Cr alloys.

To achieve our goal, a series of oxidation experiments with the direct comparison between Ni-15Cr and Ni-15Cr-6W (weight percent) samples were performed and analyzed with the use of X-ray photoelectron spectroscopy (XPS). The first set of experiments employed an *in-operando* XPS approach where the modulation of alloy and oxide composition and bonding was observed over an extended period of time delivering a detailed view of the reaction pathways. The key results from this work include the observation of Cr surface segregation in the alloys prior to oxidation, which contributes to a rapid nucleation of Cr oxide species in the first reaction steps. The more intriuing result was the addition of W to the alloy resulted in a near complete suppression in the formation of Ni oxide, while further enhancing the formation of a pure chromia phase, which has been attributed to the addition of W increasing the supply of Cr to the surface and will be discussed.

A second series of XPS experiments focus on oxidation as function of crystallographic orientation of individual, large grains for Ni-15Cr and Ni-15Cr-6W. The differences in atom density and surface energies as a function of orientation lead us to expect significant differences in reactivity which will impact passivation and oxide performance. This has been

demonstrated for aqueous corrosion of NiCr and NiCrMo alloys by Scully et al. *J. Phys. Chem. C*, **2018**, 122 (34), 19499-19513, and our work is complementary for thermal oxidation studies. In this work, Ni-15Cr and Ni-15Cr-6W samples were thermally oxidized and we will present and discuss the difference in oxidation products for various grain orientations for both samples.

5:20pm DM2+BI+SS-ThA-10 The Stability of Platinum in Non-aqueous Media, *J Ranninger, S Wachs, J Möller, K Mayrhofer, **Balázs Berkes**,* Forschungszentrum Jülich GmbH, Germany

Many basic reactions in electrochemistry, like the hydrogen oxidation reaction, oxygen reduction reaction, water oxidation or CO2 reduction reaction has been thoroughly studied in aqueous electrolytes. To these fundamental studies well defined experimental conditions have been chosen: smooth or single crystal electrodes with known surface structures, ultrapure electrolytes and very clean experimental apparatus. In many respects electrocatalysis in organic solvents is much less advanced than its understanding in aqueous systems.

The example of LIBs shows us, however, clearly how much potential of non-aqueous electrochemistry holds, in this particular example for the development of energy storage devices. Other important and possible technical applications are new type of batteries, electro-organic synthesis including electrochemical reduction of CO2, electrodeposition, supercapacitors or electrochemiluminescence.

Stability of electrochemical systems is a particularly important question in electrocatalysis. No matter if it is a fuel cell, a battery, a supercapacitor, a construction subject to corrosion or an electrode used for synthesis, economic considerations require a certain lifetime of these systems. Therefore, it is also important to understand electrocatalysis especially the aspect of stability in non-aqueous electrolytes. To this end very sophisticated, often in situ and real-time analysis methods are required. In this work we show a powerful approach to study dissolution phenomena in non-aqueous electrochemical systems on the example of platinum.

Platinum is often considered to be a model electrode and catalyst material. This metal is probably the most thoroughly studied one in electrochemistry, however, it still shows many interesting yet not well understood features. This is also true for the stability of the metal during potential cycling. The electrochemical stability window of organic electrolytes is usually much higher than that of water enabling the simultaneous cycling and downstream analysis of dissolution in a higher potential range. As a result, even the electrochemistry of platinum shows hitherto unveiled phenomena regarding its dissolution mechanism especially when using electrolytes with ultra-low (1 ppm) water content. In this work, we focus on the effect of water, anions, cations and organic solvent molecules on the anodic and cathodic dissolution behavior of platinum. To demonstrate the benefits of this novel method on the field of non-aqueous electrochemistry the stability of other non-aqueous systems will be discussed shortly, too.

5:40pm DM2+BI+SS-ThA-11 Stabilizing Transparent Conductive Oxides as a Route to Long-Lived Thin Film Photovoltaics: A Case Study in CIGS, *N Kovach,* Colorado School of Mines*; R Matthews, E Pentzer,* Case Western Reserve University*; L Mansfield,* National Renewable Energy Laboratory*; T Peshek,* NASA Glenn Research Center*; **Ina Martin**,* Case Western Reserve University

Degradation of the aluminum-doped zinc oxide (AZO) top contact is a known failure mode in Cu(In,Ga)Se$_2$ (CIGS) solar cells. The degradation of the AZO can be observed in device and module current-voltage characteristics as an increase in series resistance and decrease in fill factor. Due to its low cost and earth abundance, AZO is a good choice for the TCO in thin-film solar cells. However, it has one of the higher degradation rates of TCOs under damp heat stress. 3-aminopropyltriethoxysilane (APTES) was used to modify the AZO top contacts in CIGS solar cells. Results demonstrate that the application of the nm-scale modifier mitigates AZO degradation in damp-heat exposure, and further, arrests the degradation of the full CIGS device.

APTES modification of thick (~0.8 μm) AZO films significantly impedes the electrical degradation of the material caused by DH exposure, without significantly affecting the initial optical, electrical, or structural properties of the AZO films. Upon 1000 h of DH exposure, resistivity of both systems increased and can be attributed only to decreased mobility, as carrier concentration was consistent. APTES modification slowed the increase in AZO resistivity over 1000 h of DH exposure; however, the protective nature of APTES modification became critical after 1500 h. At this extended exposure time, macroscopic degradation was observed only for bare AZO

including pitting and delamination and was accompanied by an increase in resistivity and decrease in carrier concentration. X-ray photoelectron spectroscopy (XPS) data show that the APTES layer stabilizes the oxygen binding environment of the AZO surface, suggesting that covalent passivation of AZO surface sites by silanization essentially "caps" reactive moieties, thereby improving the stability of the material.

Spectroscopic Ellipsometry Focus Topic
Room A215 - Session EL-ThA

Spectroscopic Ellipsometry Late New Session
Moderator: Tino Hofmann, University of North Carolina at Charlotte

5:00pm EL-ThA-9 Far-infrared Dielectric Functions of Hg$_{1-x}$Cd$_x$Se Thin Films Determined via Ellipsometry and Reflectivity, *Frank Peiris, J Lyons,* Kenyon College*; G Brill,* U.S. Army Research Laboratory

The dielectric functions of molecular beam epitaxy-grown Hg$_{1-x}$Cd$_x$Se thin films were determined using a combination of ellipsometry and reflectivity. While we have reported the dielectric functions for this alloy system above 400 cm^{-1}, in the present study, by incorporating reflectivity measurements, we are able to recover the dielectric functions in a much wider spectral region (i.e., 85 cm^{-1} and 50,000 cm^{-1}). Initially, spectroscopic ellipsometry, performed between 400 cm^{-1} and 8000 cm^{-1}, determined the dielectric function and the thickness of Hg$_{1-x}$Cd$_x$Se films. Ellipsometry results were then used to model the reflectivity data, which allowed us to obtain the absolute reflectance values and to map the dielectric function from the reflectivity spectra, obtained between 85 cm^{-1} and 8,000 cm^{-1}. By representing the dielectric function as a collection of classical oscillators, we were able to recover the details of absorption due to free electrons, phonons, and band electrons in the Hg$_{1-x}$Cd$_x$Se alloy system. Specifically, our models find two transverse phonon modes for Hg$_{1-x}$Cd$_x$Se, where the HgSe-like mode blue-shifts and the CdTe-like mode red-shifts with increasing Cd concentration.

5:20pm EL-ThA-10 Tunable Giant Circular Dichroism in Spatially-coherent Si-Au/Ag Nano-plasmonic Chiral Heterostructures, *Ufuk Kilic, M Hilfiker,* University of Nebraska-Lincoln*; R Feder,* The Fraunhofer Institute for Microstructure of Materials and Systems (IMWS), Germany*; R Korlacki, E Schubert, C Argyropoulos, M Schubert,* University of Nebraska-Lincoln

The differential absorption of left-and right-handed circularly polarized light so-called circular dichroism (CD) has recently gained enormous interest in optics, chemistry, pharmacology and biotechnology fields. [1] Particularly, the subwavelength scale periodic arrangement of nano-plasmonic structures is predicted to be a facile enhancement method of CD response and offers a great potential for chiral opto-electronics. [2,3]

In this study, by using the ultra-high vacuum, electron beam evaporated glancing angle deposition system, we successfully fabricated optically active, spatially coherent, and highly porous chiral hetero-structures (CHS).

Subsequent and repeated depositions of silicon (Si) and gold (Au)/silver (Ag) lead to nanometer-dimension sub-chiral segments which enables to tailor the circular dichroism induced by size, shape and material choice.

The incorporation of transmission mode Mueller matrix spectroscopic ellipsometry technique with finite element modeling(FEM) provides an excellent framework for optical characterization of this new type plasmonic metamaterials within the spectral range from 0.6 eV to 4.5 eV. We systematically studied the influence of geometrical parameters (such as handedness of the structure (left or right), pitch size, minor and major radius of fabricated CHS, and also number of turns) on CD phenomenon.

Interestingly, Au/Ag sub-chiral segments in CHS result in the emergence of multiple plasmonic modes which can be tunable depending on the Au/Ag-Si ratio in a single turn. In addition, the effects of both azimuthal rotation and angle of incidence on CD are also investigated as a part of this study. According to the FEM calculations, as compared with Si chiral structures, we observed a significant enhancement in the circular dichroism of Si-Au/Ag CHS which can be attributed to plasmonic resonance effect [2]. We also calculated Kuhn's dis-symmetry (g) factor (g≈(A$_+$-A$_-$)/(A$_+$+A$_-$), where A$_-$, A$_+$ are the absorbance coefficients for left and right circularly polarized light, respectively), which is useful for quantitative comparisons of chiro-optical properties of different structures. Unlike the other studies [4,5] which employs periodic nanostructures made up of single type material, we observed a very pronounced g-factor in our fabricated CHSs around 3-4 eV range.

References:

[1] de Dios, Carolina, et al. Optics Express 27.15, 21142-21152, (2019).

[2] Kneer, Luisa M., et al., ACS nano 12.9 :9110-9115(2018).

[3] Hentschel, Mario, et al., Science advances3.5, e1602735, (2017).

[4] Schulz, Matthias, et al., Nature communications 9.1, 2413, (2018).

[5] Lee, Hye-Eun, et al., Nature 556.7701, 360, (2018).

5:40pm EL-ThA-11 Numerical Ellipsometry: Methods for Selecting Measurements and Techniques for Advanced Analysis Applied to β - Gallium Oxide, *Frank Urban,* Florida International University*; D Barton,* retired*; M Schubert,* University of Nebraska-Lincoln

Ellipsometry is an optical technique through which properties of materials may be determined from measurements of light reflecting from or transmitting through a sample. Usually the measurements require data processing and a key issue is determining which measurements to make. Previously two of us (Urban and Barton)[1] have addressed this for orthorhombic, anisotropic films on substrates and here we treat the case of reflection from a single anisotropic, monoclinic β-Ga$_2$O$_3$ crystal which is non-depolarizing and has a smooth, flat surface. Prior work on Ga$_2$O$_3$ by one author (Schubert)[2] used a very large dataset containing measurements at each wavenumber for three angles of incidence and 5 azimuth angles for each of 2 crystal orientations. Step 1 in that process was to determine the best-fit permittivity tensor, ε, using Levenberg-Marquardt least squares regression. Here we present methods to determine practically the same ε using a substantially reduced subset of the same data. We exclude measurements which are less useful due to large instrument-reported estimated experimental errors (σ), noise (low intensity), and mathematical insensitivity to the desired solutions. From 10 to 30 numerical solutions to the model equations are found at each wavenumber using the reduced data set as these allow an analysis of measurement accuracy. Solutions are found using each crystal independently. The number of measurements is reduced by a factor of 25 or so depending on the options selected with further reductions expected in future works. Examples using two β-Ga$_2$O$_3$ crystals, (010) and (-201) are presented.

1. F.K. Urban III and D. Barton, Thin Solid Films, 663, pp 116-1251, (2018)

2. M. Schubert, R. Korlacki, S. Knight, T. Hofmann, S. Schöche, V. Darakchieva, E. Janzén, B. Monemar, D. Gogova, Q.-T. Thieu et al., Phys.Rev.B 93, 125209 (2016).

Fundamental Discoveries in Heterogeneous Catalysis Focus Topic
Room A213 - Session HC+SS+TL-ThA

Reaction Pathways and Addressing Challenges for Energy Production in the 21st Century & Heterogeneous Catalysis Graduate Student Award Presentation

Moderators: Sanjaya Senanayake, Brookhaven National Laboratory, Arthur Utz, Tufts University

2:20pm HC+SS+TL-ThA-1 High Resolution XPS to Identify C$_x$H$_y$ Surface Species on a Cobalt Model Catalyst: New Experimental Evidence for the Importance of Alkylidynes as Growth Intermediates in Fischer-Trospch Synthesis, *Kees-Jan Weststrate,* Syngaschem BV, Netherlands*; D Sharma, D Garcia Rodriguez, M Gleeson,* DIFFER, Eindhoven University, The Netherlands, Netherlands*; H Fredriksson, H Niemantsverdriet,* Syngaschem BV, Netherlands

Supported cobalt catalysts find their most widespread application in low temperature Fischer-Tropsch synthesis (FTS), a process in which C-C bond forming reactions produce long chain saturated hydrocarbon chains from synthesis gas, a mixture of CO and H$_2$. The versatile FTS process may very well continue to play a role in future energy scenarios: synthesis gas can be derived from any carbon-containing source, e.g. biomass or even CO$_2$ may be used. These renewable carbon sources offer a sustainable alternative to replace petroleum as the principal feedstock of chemicals and liquid transportation fuels.

The FTS reaction mechanism can be ranked among the most complex in the chemical industry. CO and H$_2$ are converted into long chain hydrocarbons in a sequence of bond-breaking and bond-making steps that are catalyzed by metals such as cobalt, ruthenium and iron (the latter is active in the carbide form). As the steady state concentration of chain growth intermediates is below the detection limits of in-situ spectroscopies simplified model studies are needed to elucidate the mechanism by which long hydrocarbon

chains grow on the cobalt catalyst surface. Since chains grow on a surface that is packed with CO, it is of crucial importance to consider how CO spectators influence the reactivity of hydrocarbon adsorbates. We use a Co(0001) single crystal surface as a model system to study how C$_2$H$_x$ adsorbates react on a cobalt surface, both in ultrahigh vacuum (~10^{-10} -10^{-7} mbar) as well as at near-ambient pressure (~0.1 mbar). By using the high resolution available of x-ray photoemission spectroscopy at the SuperESCA beamline of ELETTRA (Trieste, Italy), and the unique opportunity to combine these qualities with measurements at near-ambient pressure at the HIPPIE beamline of MAX IV (Lund, Sweden), we were able to elucidate the reaction mechanism by which carbon-carbon bonds form on a cobalt surface. We find that CO's presence is of essential importance: It promotes hydrogenation of acetylene, HC≡CH [the most stable C$_2$H$_{xad}$ without CO] to ethylidyne, ≡C-CH$_3$, a facile reaction that occurs around 250 K. Ethylidyne dimerization around 310 K produces 2-butyne (H$_3$C-C≡C-CH$_3$), a strongly bound alkyne adsorbate that hydrogenates to 2-butene (g) above 400 K. Extrapolated to FTS, the findings speak in favour of the alkylidyne chain growth mechanism: long chain alkylidynes (≡C-R), stabilized by the presence of CO spectators, react with a methylidyne (≡CH$_{ad}$) monomer to produce a 1-alkyne (R-C-CH) adsorbate. Partial hydrogenation of the 1-alkyne product is promoted by CO$_{ad}$ and produces the alkylidyne species needed for the next CH insertion step.

2:40pm HC+SS+TL-ThA-2 Beam Reflectivity Measurements of Carbon Dissolution on Nickel Single Crystal Catalysts, *Eric High, D Tinney, A Utz,* Tufts University

The interaction of carbon with metal catalysts is of significant interest. In methane steam reforming, the build-up of carbon in the nickel subsurface leads to a gradual reduction in reactivity on the surface and ultimately results in deactivation of the metal catalyst. Additionally, the initial dissolution and subsequent reemergence of carbon from the subsurface are key steps in the growth of well-ordered graphene on nickel substrates via chemical vapor deposition (CVD). Researchers have previously used Auger and X-ray photoelectron spectroscopy to investigate the dynamics of carbon dissolution into nickel surfaces. We instead employ beam reflectivity measurements to monitor the process of carbon diffusion into the nickel subsurface in real-time. We will present data collected via exposure of a Ni(997) single crystal to supersonically expanded CH$_4$ molecules at surface temperatures above 600 K. We observe significant changes in the reaction profile by increasing surface temperature as the rate of dissolution approaches the reactive flux of the high energy gas molecules. We use these results to further develop kinetic models for methane reactivity as a function of surface coverage as well as carbon diffusion into the stepped nickel crystal. The major parameters from these models include the site-blocking coverage and its subsequent dependence on surface temperature as well as an updated measure of the barrier to diffusion for the C/Ni system.

3:00pm HC+SS+TL-ThA-3 Fundamental Research Opportunities to Advance Energy Technologies, *Bruce Garrett,* Department of Energy
INVITED

The U. S. Department of Energy (DOE), Office of Science, Office of Basic Energy Sciences (BES) supports fundamental research in chemical and materials sciences to provide the foundations for new energy technologies and to support DOE missions in energy, environment, and national security. This presentation will discuss opportunities for fundamental research to impact DOE's energy mission "to catalyze the timely, material, and efficient transformation of the nation's energy system and secure U.S. leadership in energy technologies" with a focus on the way we generate, store and use energy nationally. I will provide an overview of BES strategic planning over the past decade that identified priority research directions for advancing energy applications, highlight key scientific advances in these areas, and discuss some future opportunities for modern science, particularly studies of interfacial processes, to accelerate the transformation of the U. S. energy portfolio.

4:00pm HC+SS+TL-ThA-6 Oxidation and Redox-Mediated Transformation of a Tb2O3 Thin Film from the Cubic Fluorite to Bixbyite Structure, *Christopher Lee, J Weaver,* University of Florida

The terbium oxides, a member of the rare earth oxide family, exhibit favorable properties in selective oxidation catalysis due to the high mobility of oxygen stored and released within the lattice. Of particular note is the ease of structural rearrangement into highly stable, well-ordered intermediates between the Tb$_2$O$_3$ and TbO$_2$ stoichiometries in addition to a continuum of nonstoichiometric states. As opposed to ceria, which stabilizes strongly in the CeO$_2$ stoichiometry, thin film terbia is very stable

in the Tb_2O_3 stoichiometry and can exist in an oxygen deficient cubic fluorite arrangement (CF-Tb_2O_3) as well as the bixbyite structure (c-Tb_2O_3).

We discovered a redox-mediated mechanism for the transformation of thin film CF-Tb_2O_3(111)/Pt(111) to c-Tb_2O_3(111)/Pt(111) in ultrahigh vacuum (UHV). Low energy electron diffraction (LEED) and temperature programmed desorption (TPD) shows that repeated oxidation and thermal reduction to 1000 K transforms an oxygen deficient cubic fluorite Tb_2O_3(111) thin film to the well-defined bixbyite, or c-Tb_2O_3(111) structure. In addition, TPD measurements show the development of several distinct O_2 desorption peaks arising from the oxidation of c-Tb_2O_3 domains to the stoichiometrically-invariant ι-Tb_7O_{12} and δ-$Tb_{11}O_{20}$ phases and demonstrates the more facile oxidation of c-Tb_2O_3 relative to CF-Tb_2O_3. We present evidence that nucleation and growth of c-Tb_2O_3 domains occurs at the buried TbO_x/CF-Tb_2O_3 interface, and that conversion of the interfacial CF-Tb_2O_3 to bixbyite takes place mainly during thermal reduction of TbO_x above ~900 K and causes newly-formed c-Tb_2O_3 to advance deeper into the film. The avoidance of low Tb oxidation states may facilitate the CF to bixbyite transformation via this redox-mechanism.

Further oxidation of a well-ordered c-Tb_2O_3 film provides evidence of the sequential phase stabilization of ι-Tb_7O_{12}, δ-$Tb_{11}O_{20}$, and α-TbO_{2-x} stoichiometric structures along with lower temperature peaks corresponding with more weakly-bound surface oxygen. Oxidation at temperatures between 300-500 K reveals an apparent Arrhenius activation barrier of ~7.4 kJ/mol for the initial conversion of c-Tb_2O_3 to ι-Tb_7O_{12}. Furthermore, oxidation at 100 K creates an additional oxygen species stable at lower temperatures that has a much more pronounced effect on oxidation of the film surface over the bulk of the film . The ability to control the surface termination of the TbO_x(111) thin films along with selectively creating surface bound oxygen species provides the structural basis necessary to clarify the partial oxidation mechanisms associated with terbia-based catalysis.

4:20pm HC+SS+TL-ThA-7 Discrimination of Surface Storage and Mechanistic Pathways Using Dynamic Pulse Response Experiments, *Y Wang, M Kunz,* Idaho National Laboratory*; G Yablonsky,* Washington University in Saint Louis*; Rebecca Fushimi,* Idaho National Laboratory

Pulse response experiments in a pure diffusion reactor significantly increase the number of gas/solid collisions for probing kinetic interactions but maintain straightforward transport modeling by avoiding gas phase dynamics. Using inverse-diffusion methods [1] the millisecond time-dependence of the reaction rate can be calculated as it responds to the forced concentration dynamic. More importantly, in this experiment the gas and surface concentrations are decoupled and their influence on the transformation rates of reactants and products can be studied.

Vacuum pulse response studies of ammonia decomposition on polycrystalline Fe, Co and a CoFe bimetallic preparation were conducted to investigate the microkinetic features that lead to very distinct global performance [2]. We present dynamic atomic accumulation; a new measure used to characterize the ability of a complex surface to regulate adsorbed species. We find Fe can support hydrogenated species with a longer surface lifetime that either CoFe or Co. From the time-dependence of the rate we find Co can support two mechanistic pathways for H_2 production. The quantitative rate, gas and surface concentration data of microkinetic reaction steps explain why materials with cobalt perform better at a global level.

1. Redekop, E.A., et al., *The Y-Procedure methodology for the interpretation of transient kinetic data: Analysis of irreversible adsorption.* Chem. Eng. Sci., 2011. **66**(24): p. 6441-6452.

2. Wang, Y., et al., *Transient Kinetic Experiments within the High Conversion Domain: The Case of Ammonia Decomposition.* Catalysts, 2019. **9**(1): p. 104.

4:40pm HC+SS+TL-ThA-8 Nuclearity Effects in Supported Zinc and Gallium Catalysts for Alkane Dehydrogenation, *Susannah Scott,* University of California at Santa Barbara   **INVITED**

The selective dehydrogenation of alkanes to alkenes is an important process in the valorization of shale gas liquids and in the production of on-demand olefins. Ga- and Zn-modified aluminosilicates have been extensively studied as catalysts for these reactions. In the presence of Brønsted acid sites (BAS), the olefins undergo subsequent aromatization to more valuable BTX. The nuclearity of the metal active sites, the proximity between the metal sites and the BAS, and the nature of the support, may influence the catalytic activity but detailed structure-property relationships are difficult to ascertain in conventional catalysts with many types of sites. The reactions of $GaMe_3$ and $ZnMe_2$ with the hydroxyl-terminated surfaces

of dehydrated silica and alumina, as well as with the internal and external surfaces of H-ZSM-5, are particularly simple. They generate methane and isolated dimethylgallium and methylzinc sites. K-edge X-ray absorption spectra, analyzed via inspection of the wavelet transform EXAFS (WT-EXAFS) and curvefitting of the Fourier transform EXAFS (FT-EXAFS), reveal that the silica and zeolite materials contain dinuclear grafted sites, regardless of the thermal pretreatment of the support, while alumina gives dispersed mononuclear grafted sites. Differences in reactivity and stability appear to originate in these structural variations.

5:20pm HC+SS+TL-ThA-10 Fundamental Insights into Hydrocarbon Conversion Mechanisms in Lewis and Brønsted Acid Zeolites using Temporal Analysis of Products, *Hari Thirumalai*[1], *J Rimer, L Grabow,* University of Houston

The surge in natural gas production has incentivized the search for processes that can utilize methane and light olefin derivatives in the manufacture of useful products such as benzene, toluene and xylene (BTX). These are important commodity chemicals that are used as fuel additives and as raw materials in the synthesis of specialty chemicals. Industrial demand is met through processes such as the synthesis of BTX through dehydroaromatization of light olefins or through alkylation of aromatics, typically with the use of zeolites as catalysts. Complex reaction mechanisms determined by the presence of a hydrocarbon pool dominate hydrocarbon chemistry and are challenging to study. These challenges hinder the in-depth understanding of the role of the catalyst and its eventual design for tailored applications.[1]

In this work, we use the transient kinetics technique, temporal analysis of products (TAP), to probe hydrocarbon conversion and upgrade in the transient regime of reaction. TAP experiments help probe the intrinsic kinetics of reactant conversion in a well-defined Knudsen transport regime under high-vacuum conditions. We studied the dehydroaromatization of ethylene and the methylation of toluene as case-studies for hydrocarbon conversion reactions. The precise control of reactant molecules entering the reactor and responses recorded by a high-resolution mass spectrometer at the reactor outlet in the dehydroaromatization of ethylene suggest that a Lewis acid such as Ag^+ or Ga^{3+} in the zeolite accelerate the retention of long lived carbonaceous species in the zeolite, thus attaining the autocatalytic arene cycle more rapidly. Pulse responses provide qualitative evidence that olefins are strongly bound to the metal-exchanged zeolite samples with delayed desorption, enhancing the rate of hydrocarbon conversion and carbon retention. Finally, experiments investigating the methylation of toluene to xylene provide valuable information on competitive binding of reactants to the zeolite acid sites and the ensuing primary reactions that drive the reaction.

Overall, our experiments under semi-idealized conditions help provide insight into the crucial primary reactions that initiate the hydrocarbon pool mechanism, thus elucidating the role of extra-framework species such as Ag^+ or Ga^{3+} and their synergy with the Brønsted acid sites in hydrocarbon conversion. The fundamental understanding gained from these experiments will be crucial in deciphering the role of the different zeolitic active sites in model hydrocarbon conversion reactions.

References

1. Hsieh, M. F., Zhou, Y., Thirumalai, H., Grabow, L. C., & Rimer, J. D. ChemCatChem, (2017), 9(9), 1675-1682.

Advanced Ion Microscopy and Ion Beam Nano-engineering Focus Topic
Room B231-232 - Session HI+NS-ThA

Emerging Ion Sources, Optics, and Applications & Flash Session
Moderators: Gregor Hlawacek, Helmholtz-Zentrum Dresden - Rossendorf, Shida Tan, Intel Corporation

2:20pm HI+NS-ThA-1 Cold Atom Ion Sources, *Jabez McClelland, J Gardner, W McGehee,* National Institute of Standards and Technology (NIST)*; A Schwarzkopf, B Knuffman, A Steele,* zeroK NanoTech Corp.   **INVITED**

Ionization of laser-cooled atoms has emerged as a new approach to creating high brightness ion sources for applications such as focused ion beam (FIB) microscopy, milling, and secondary-ion mass spectrometry (SIMS). Conventional sources, such as the Ga liquid metal ion source (LMIS)

---

[1] **Morton S. Traum Award Finalist**

or the gas field ionization source (GFIS), attain brightness by emitting from a very sharp tip. In contrast, cold atom sources attain high brightness through reducing the transverse velocity spread of the ions. With the ultracold, microkelvin-range temperatures achievable with laser cooling, the corresponding velocity spread can lead to a brightness significantly higher than typical LMIS values. Moreover, the phase-space shape of the emittance of the source – narrow in velocity, wide in space – brings new opportunities for ion optical design. For example, high currents can be obtained without the high current density present in sharp tip sources. This can result in reduced Coulomb effects, such as increased emittance and broadened energy spread (Boersch effect). Other advantages of this type of source include insensitivity to contamination, access to new ionic species, inherent isotopic purity, and fine control over emission, down to the single ion level. To date, sources have been demonstrated with Cr,[1] Li,[2] Rb,[3] and Cs[4,5] ions, realizing novel species and nanometer-scale spot sizes. In this talk I will review progress in the field and discuss recent developments in Li ion sources and applications.

_____

[1]A.V. Steele, B. Knuffman, J.J. McClelland, and J. Orloff, J. Vac. Sci. Technol. B **28**, C6F1 (2010).

[2]B. Knuffman, A.V. Steele, J. Orloff, and J.J. McClelland, New J. Phys. **13**, 103035 (2011).

[3]G. ten Haaf, T.C.H. de Raadt, G.P. Offermans, J.F.M. van Rens, P.H.A. Mutsaers, E.J.D. Vredenbregt, and S.H.W. Wouters, Phys. Rev. Applied **7**, 054013 (2017).

[4]A.V. Steele, A. Schwarzkopf, J.J. McClelland, and B. Knuffman, Nano Futures **1**, 015005 (2017).

[5]M. Viteau, M. Reveillard, L. Kime, B. Rasser, P. Sudraud, Y. Bruneau, G. Khalili, P. Pillet, D. Comparat, I. Guerri, A. Fioretti, D. Ciampini, M. Allegrini, and F. Fuso, Ultramicroscopy **164**, 70 (2016).

3:00pm HI+NS-ThA-3 Silicon Lithiation by Direct-writing with a Focused Li⁺-ion Beam, *W McGehee, Evgheni Strelcov, V Oleshko, C Soles, N Zhitenev, J McClelland,* National Institute of Standards and Technology (NIST)

Improving the performance of Li-ion batteries requires understanding and controlling nanoscale ion transport at the level of interfaces, grain boundaries and defects. While in the last decades a range of electron and scanning probe microscopy techniques have been developed for probing local transport, no reliable method exists for quantitative and controllable nanoscale lithiation. Moreover, wet-cell electrochemical lithiation is significantly complicated by electrolyte decomposition, formation of solid-electrolyte interfacial (SEI) layer and parasitic reactions running in parallel to lithium insertion.

Building on our previous work,[1] here we introduce a new method of direct-write quantitative lithiation of battery-relevant materials in vacuo, in the absence of SEI or liquid electrolyte. To benchmark the technique, we use a focused, several keV Li⁺-ion beam to inject lithium into 35-nm thick crystalline Si membranes with a sub-micron lateral precision. The lithiated regions, undergoing morphological, structural, chemical and functional transformations, were characterized with a combination of electron and scanning probe microscopy techniques. We observed saturation of interstitial lithium in the silicon membrane at ≈ 10 % dopant number density and spill-over of excess lithium onto the membrane's surface. The implanted Li⁺ remains electrochemically active, and the spill-over effect can possibly be avoided by cooling the sample. The presented method is especially useful for probing non-equilibrium and low-concentration phases of lithiated materials that form because of incomplete lithium extraction or during initial states of pristine anode lithiation. Focused ion beam lithiation will enable controlled studies and improved understanding of Li⁺ ion interaction with local defect structures and interfaces in electrode and solid-electrolyte materials.

W.R.M. and E.S. contributed equally.

1. Takeuchi, S.; McGehee, W. R.; Schaefer, J. L.; Wilson, T. M.; Twedt, K. A.; Chang, E. H.; Soles, C. L.; Oleshko, V. P.; McClelland, J. J. *Journal of The Electrochemical Society* **2016,** 163, (6), A1010-A1012.

3:20pm HI+NS-ThA-4 A New FIB for Deterministic Single Ion Implantation, *Nathan Cassidy,* UK National Ion Beam Centre, University of Surrey, UK*; D Cox,* Advanced Technology Institute, University of Surrey, UK*; R Webb,* UK National Ion Beam Centre, University of Surrey, UK*; B Murdin,* Advanced Technology Institute, University of Surrey, UK*; P Blenkinsopp, I Brown,* Ionoptika Ltd., UK*; R Curry,* The Photon Science Institute, University of Manchester, UK

Single isolated dopant atoms implanted into solid state devices have been shown to be a viable architecture for quantum technologies. Ion implantation provides many advantages as a manufacturing method for such devices, such as speed and scalability, however controlling the number of implanted ions with single-ion precision poses a significant challenge. In this paper we will present a new instrument designed for the deterministic implantation of single ions with high precision.

The SIMPLE (Single Ion Multi-species Positioning at Low Energy) tool, is a new focused ion beam tool in operation designed for the manufacture of quantum technologies. The tool has a 25kV LMIG set up for femtoAmp sample currents, with ultra-fast beam blanking, neutral blocking and a highly efficient secondary electron detection system. Deterministic ion implantation is achieved through extraction of single ions through fast beam blanking with low currents, ion implant detection through collection of secondary electron (SE) signal from the target and high spatial precision in ion placement.

To date we have demonstrated > 85% probability of implanting a single Bi+ ion into silicon without error, with a 20nm beam determining dopant placement precision. This surface secondary electron detection efficiency has been validated through simultaneous measurements of a transmitted electron signal, achieved by implanting through thin lamellae. The ion placement precision has been determined through imaging of ion induced damage on highly oriented pyrolytic graphite (HOPG) surfaces. Much work has taken place maximizing the detection efficiency for secondary electrons and investigating the factors which affect the SE yield.

Currently the system is running with Bi source, and there are In sources available. Alongside the development of the instrument there is also research into developing a series of liquid-metal ion sources for elements with optical and quantum applications including P, Te, Se and Cd. A second SIMPLE tool has also been installed at the UK National Ion Beam Centre, which operates with a 20kV duoplasmatron arc source, capable of 50nm spot sizes. SIMPLE #2 will initially operate with nitrogen source for the fabrication of NV centres in diamond.

4:00pm HI+NS-ThA-6 Technology and Applications of a Plasma Ion Source with User-selectable Ion Species, *Gregory Schwind, S Kellogg, J Stiller, M Doud, C Rue, B Van Leer,* Thermo Fisher Scientific   **INVITED**

The focused ion beam (FIB) has become an indispensable tool for micro- and nano-machining applications. Due to its high brightness and ease of use, the gallium liquid metal ion source (LMIS) has been the source of choice over much of the nearly four decades of FIB history. At the beginning of this decade, a new generation FIB system based on the inductively coupled plasma (ICP) ion source was brought to market, offering beam current and throughput 20 times greater than LMIS-based systems. A next generation plasma source has been developed [1], offering the option to change the ion beam species by switching the feed gas supplied to the plasma source. The ability to dynamically change ion species—for example from a noble gas such as argon to an electronegative species such as oxygen—creates new design challenges for the source, the FIB optical subsystem, and the platform as a whole. Both empirical measurements and numerical simulations were used to better understand the species-specific performance of the source design. Results show that the emission properties depend on both the ion species and the plasma density, which lead to orienting the system design around specific modes of operation optimally suited to each species, FIB current and landing energy [2].

Several new and exciting application areas are enabled by the ability to switch FIB ion species dynamically. Ion-surface interactions such as sputtering, implantation, and the creation of an amorphous damage layer depend on the ion's momentum [3], which in turn depends on ion mass. Furthermore, chemical reactivity between the incoming ion and the target surface seems to play a role in the surface modification process in some instances. Several FIB application examples illustrating these interdependencies will be shown.

[1] Sergey Gorelick and Alex De Marco, "Fabrication of glass microlenses using focused Xe beam," Opt. Express 26, 13647-13655 (2018)

[2] United States patent 8,253,118

[3] Jon Orloff, Mark Utlaut, and Lynwood Swanson, *High Resolution Focused Ion Beams,* Kluwer/Plenum: New York, (2003)

4:40pm HI+NS-ThA-8 Neutral Helium Microscopy, *Bodil Holst,* University of Bergen, Norway

Neutral helium microscopy is a new imaging technique currently under development. In a neutral helium microscope a beam of neutral helium atoms is created through supersonic expansion from a nozzle and focussed onto the surface to create a scanning instrument. The resolution is determined by the beam spotsize on the surface. The neutral helium microscope has several advantages: the very low energy of the beam (less than 0.02 eV compared to several keV for helium ion or electron microscope) , charge neutrality, and inertness of the helium atoms, a potential large depth of field, and the fact that at thermal energies the helium atoms do not penetrate into any solid material. This opens the possibility, among others, for the creation of an instrument that can measure surface topology on the nanoscale, even on surfaces with high aspect ratios. The helium microscope currently exist in two configurations: The pinhole microscope and the zone plate microscope, both are covered in this paper. We begin with a series of images which demonstrate and explores the unique contrast mechanisms of the new instrument. This is followed by a general discussion of helium microscope designs and resolution.

5:00pm HI+NS-ThA-9 GaBiLi Liquid Metal Alloy Ion Sources for Advanced Nanofabrication, *P Mazarov,* RAITH GmbH, Germany*; T Richter, L Bruchhaus, W Pilz, R Jede,* Raith GmbH, Germany*; Yang Yu, R Schmid, J Sanabia,* Raith America, Inc.*; L Bischoff,* Helmholtz Zentrum Dresden-Rossendorf, Germany*; G Hlawacek,* Helmholtz-Zentrum Dresden Rossendorf, Germany

Nanofabrication requirements for FIB technologies are specifically demanding in terms of patterning resolution, stability and the support of new processing techniques. Additionally, the type of ion defines the nature of the interaction mechanism with the sample and thus has significant consequences on the resulting nanostructures [1]. Therefore, we have extended the technology towards the stable delivery of multiple ion species selectable into a nanometer scale focused ion beam by employing a liquid metal alloy ion source (LMAIS) [2]. This LMAIS provides single and multiple charged mono- as well as polyatomic ion species of different masses, resulting in significantly different interaction mechanisms. Nearly half of the elements of the periodic table are thus made available in the FIB technology as a result of continuous research in this area [3]. This range of ion species with different mass or charge can be beneficial for various nanofabrication applications. Recent developments could make these sources to an alternative technology feasible for nanopatterning challenges. In this contribution, the operation principle, the preparation and testing process as well as prospective domains for modern FIB applications will be presented. As an example we will introduce the GaBiLi LMAIS [4]. It enables high resolution imaging with light Li ions and sample modification with Ga or heavy polyatomic Bi clusters, all coming from one ion source. For sub-10 nm focused ion beam nanofabrication and microscopy, the GaBiLi-FIB or the AuSiGe-FIB could benefit of providing additional ion species in a mass separated FIB without changing the ion source.

References

[1] L. Bruchhaus, P. Mazarov, L. Bischoff, J. Gierak, A. D. Wieck, and H. Hövel, *Comparison of technologies for nano device prototyping with a special focus on ion beams: A review,* Appl. Phys. Rev. 4, 011302 (2017).

[2] L. Bischoff, P. Mazarov, L. Bruchhaus, and J. Gierak, *Liquid Metal Alloy Ion Sources – An Alternative for Focused Ion Beam Technology*, Appl. Phys. Rev. **3** (2016) 021101.

[3] J. Gierak, P. Mazarov, L. Bruchhaus, R. Jede, L. Bischoff, *Review of electrohydrodynamical ion sources and their applications to focused ion beam technology,* JVSTB **36** (2018).

[4] W. Pilz, N. Klingner, L. Bischoff, P. Mazarov, and S. Bauerdick, *Lithium ion beams from liquid metal alloy ion sources,* JVSTB 37(2), Mar/Apr (2019).

5:20pm HI+NS-ThA-10 Focused Ion Beams in Biology: How the Helium Ion Microscope and FIB/SEMs Help Reveal Nature's Tiniest Structures, *Annalena Wolff,* Central Analytical Research Facility, Institute for Future Environments, Queensland University of Technology (QUT), Brisbane QLD 4000, Australia*; N Klingner,* Helmholtz Zentrum Dresden-Rossendorf, Germany*; W Thompson,* HeelionicsLLC*; Y Zhou,* Queensland University of Technology (QUT), Australia*; J Lin,* Affiliated Stomatological Hospital of Xiamen Medical College, China*; Y Peng,* CSIRO Manufacturing, Australia*; J Ramshaw,* St. Vincent's Hospital, University of Melbourne, Australia*; Y Xiao,* The Australia-China Centre for Tissue Engineering and Regenerative Medicine (ACCTERM), Queensland University of Technology, Australia

Focused Ion Beam (FIB) devices such as the Helium Ion Microscope (HIM) as well as FIB/SEMs are increasingly popular within the biological sciences in recent years. High resolution imaging of uncoated non-conductive samples with the HIM helps reveal nature's tiniest structures while the FIB/SEM allows to prepare TEM lamellae, 3D reconstruct the sample or reveal sub surface structures with nanometre precision.

This presentation shows how the HIM as well as FIB/SEMs can be used in biological sciences to reveal nature's tiniest structures. The presented work then focuses on the underlying ion-solid interactions and the effect of ion beam parameters on heating induced by ion beams. The work presented here deals with gallium ion solid interactions, however the broader results are applicable to any type of FIB including the helium ion microscope (HIM) and plasma FIBs. The interactions of gallium ions in skin were simulated using Monte Carlo methods, finite element simulations and numerical modelling for different beam parameters. The program SRIM [4] was used to obtain theoretical results which permit estimation of the ion beam induced temperature increases, using the physical principles of Fourier's law of conductive heat transfer.

The technique was tested on collagen, a soft biological material which is commonly used in biomedical applications. Collagen was chosen as a suitable test sample as it loses its fibrillar structure when denatured by heat, permitting damage to easily be recognized. Cross-sections and TEM lamellas were prepared from non-embedded collagen with conventional FIB processing parameters as well as heat reducing FIB parameters.

The results also show that heat damage can be prevented by reducing the local dose rate and area underneath the ion beam. Using lower acceleration voltages allows the operator to select higher local dose rates (ion beam currents) and minimized processing times. A TEM comparison of a microtome prepared lamella and a FIB prepared lamella (using different heat reducing parameters) shows that the fibrillar structures can be maintained, and heat damage avoided. The approach described here can be used to determine suitable parameters for other soft materials.

The authors acknowledge scientific and technical assistance of Peter Hines, Jamie Riches, Rachel Hancock, and Ning Liu and the facilities at the Australian Microscopy & Microanalysis Research Facility (AMMRF) at the Central Analytical Research Facility (CARF), Queensland University of Technology, Brisbane, Australia.

Frontiers of New Light Sources Applied to Materials, Interfaces, and Processing Focus Topic
Room A210 - Session LS+AC+HC+SS-ThA

Emerging Methods with New Coherent Light Sources
Moderator: Germán Rafael Castro, Spanich CRG BM25-SpLine Beamline at the ESRF

4:00pm LS+AC+HC+SS-ThA-6 Resolving X-ray Based Spectroscopies in the Sub-nanometer Regime: Enabling Atomic Scale Insights into CO Adsorption on Thin Film Surfaces, *Heath Kersell, B Eren, C Wu,* Lawrence Berkeley National Laboratory*; I Waluyo, A Hunt,* Brookhaven National Laboratory*; G Somorjai, M Salmeron,* Lawrence Berkeley National Laboratory

X-ray based spectroscopies routinely yield detailed elemental, chemical, electronic, and magnetic information on a wide array of physically and chemically diverse samples. However, the spatial resolution of these techniques is limited, frequently by the size of the X-ray spot. Conversely,

certain structural probes readily resolve sample topography with nanoscale- or even atomic-resolution. The union of X-ray based spectroscopies with nanoscale structural probes enables the acquisition of spectroscopic information at unprecedented length scales. We will demonstrate the combination of X-ray based spectroscopies (e.g. X-ray photoelectron spectroscopy {XPS}) with scanning tunneling microscopy (STM), and its application to CO adsorption and oxidation on model catalyst surfaces.

CO adsorption on various crystal surfaces plays a critical role in numerous chemical processes, including for example CO oxidation, the water gas shift reaction, and methanol oxidation. CO oxidation is widely used as a prototype reaction for studies of fundamental catalytic phenomena and is crucial in exhaust gas processing for automobiles and stationary CO sources. Recent studies demonstrate strikingly high activity for CO oxidation by Pt nanoparticles supported on cobalt oxide (CoO_x) as compared to either of the constituent materials. In the further development of these catalysts, a deeper understanding of the active sites and their deactivation is crucial. Using a combination of *operando* high pressure STM (HP-STM) and ambient pressure XPS (AP-XPS), we investigate the nature of catalytically active sites for CO oxidation on CoO-Pt catalysts at CO and O_2 pressures up to 130 mTorr. Our experiments showed very different behavior for the lattice oxygen ($O_{lat\cdots}$) in CoO between fully oxidized and sub-stoichiometric cobalt oxides. At RT, fully oxidized Co films adsorbed CO in the form of stable surface carbonate species, poisoning the reaction until reaching higher temperatures where they decomposed. On sub-stoichiometric CoO_x the CO oxidation reaction proceeded at RT, reducing the oxide to the metallic state. We discuss these results in the context of structural transformations observed *in-situ-* via HP-STM, and demonstrate the behavior of surface sites under relevant gas mixtures.

As an outlook, we will discuss various *in-situ* multi-modal approaches which enhance the spatial resolution of X-ray based spectroscopies toward the nano- or even single atom scales. Such a union of spectroscopic and structural probes will provide a more accurate and complete picture of operating devices in the near future.

4:20pm **LS+AC+HC+SS-ThA-7 Imaging with XPS: Advanced Characterization for Advanced Materials and Devices**, *Tatyana Bendikov, H Kaslasi, E Sanders, E Joselevich, D Cahen,* Weizmann Institute of Science, Israel

X-ray Photoelectron Spectroscopy (XPS), as a surface sensitive technique with the sensitivity down to single atomic layer, provides unique information about elemental composition and chemical and electronic states of elements in the material. For some research goals, however, this knowledge is not sufficient as it does not provide the entire information required for a comprehensive characterization of the investigated system. In addition to the basic functions of standard XPS, our instrument is equipped with advanced capabilities such as XPS imaging, which is particularly valuable in the analysis of patterned or inhomogeneus specimens. Following image acquisition, specific areas can thus be chosen and small spot XP spectra acquired at sites of particular interest. This information is useful in the characterization of patterned surfaces or inhomogeneous samples with surface features between several to hundreds of micrometers.

We present here two examples where XPS imaging is successfully used providing crucial information for understanding the investigated systems.

In the first example bunches of GaN nanowires (50-100 nm each) randomly spread on Si substrate were monitored with XPS imaging. Then, focusing on the GaN bunch itself, small area XP spectra were obtained. This allowed to get precise top surface composition of the bunches significantly consuming the analysis time.

In the second example variations in chemical composition though dimensions of the $Cs_xMa_{1-x}PbBr_3$ (MA = CH_3NH_3)

crystal were studied using XPS imaging. Significant changes in the N/Cs ratio, depending on the distance from the crystal edge/center, were observed on the top surface. Variations in the N/Cs and Pb/(N+Cs) ratios were also observed along the crystal bulk.

4:40pm **LS+AC+HC+SS-ThA-8 Time-Resolved Photoemission with Free-Electron Lasers**, *Kai Rossnagel,* CAU Kiel / DESY, Germany **INVITED**
Photoelectron spectroscopy is an essential analytical tool for learning about the properties and workings of quantum materials and functional interfaces, in which electrons are the main actors. In practice, photoelectron spectroscopy is a toolbox comprising three major techniques, where the momentum selectivity and atomic-site specificity of

valence and core electron emissions are exploited, respectively: Angle-resolved photoelectron spectroscopy (ARPES) is the most powerful imaging technique for the energy-momentum space of the active electrons near the Fermi level, while x-ray photoelectron spectroscopy (XPS) is a universal tool for chemical analysis and x-ray photoelectron diffraction (XPD) an established surface structural probe. A dream is to combine all three techniques into a single experiment, make it complete by adding spin and femtosecond time resolution, and thus be able to shoot femto-stroboscopic movies of intertwined electronic, magnetic, chemical, and geometric structure dynamics and gain previously unachievable, direct "in operando" insight into dynamic structure-function relationships of materials and interfaces. Here, we aim to realize this dream by combining the soft x-ray SASE3 free-electron-laser (FEL) beam at the European XFEL with the most advanced photoelectron detection scheme currently available: the time-of-flight momentum microscope with efficient 3D energy-momentum detection and 2D spin filtering. The status of the project and of FEL-based photoelectron spectroscopy in general will be presented.

5:20pm **LS+AC+HC+SS-ThA-10 Ultrafast Magnetization Dynamics on the Nanoscale***, Bastian Pfau,* Max Born Institute, Germany **INVITED**
Nanometer-scale spin configurations are attractive as information entities for spintronic applications to realize nonvolatile and energy-efficient data storage and processing. In recent years, this research field was stimulated by the discovery that the spin can be effectively manipulated using ultra-short light pulses exciting suitably designed magnetic materials. Scattering and imaging methods based on sources delivering ultra-short x-ray pulses are particularly successful in revealing the magnetization dynamics on the relevant time and length scales. I will present research results on optically induced demagnetization and formation of nanoscale magnetic domains and skyrmions in Co-based multilayer systems. We investigate these processes using small-angle scattering signals or direct imaging via holography with femtosecond x-ray pulses delivered by free-electron laser sources. These methods additionally allow to address the influence of lateral nanoscale inhomogeneity and to work with laterally localized or structured excitation.

Frontiers of New Light Sources Applied to Materials, Interfaces, and Processing Focus Topic
Room A210 - Session LS+AC+NS-ThA

Photon Science for Imaging Materials from the Meso- to the Nanoscale
Moderator: Maya Kiskinova, Elettra-Sincrotrone Trieste, Italy

2:20pm **LS+AC+NS-ThA-1 Triplet Dynamics in Photovoltaic Materials Measured with Time Resolved X-Ray Spectroscopies**, *R Costantini,* University of Trieste*; R Faber,* Technical University of Denmark*; A Cossaro, A Verdini, L Floreano,* CNR - Istituto Officine Materiali*; C Haettig,* Ruhr-University Bochum, Germany*; A Morgante,* University of Trieste, Italy*; S Coriani,* Technical University of Denmark*; Martina Dell'Angela,* CNR - Istituto Officine Materiali, Italy **INVITED**
Singlet exciton fission (SF) is a multiexciton generation process in organic molecules, where an optically excited singlet exciton is converted into two triplet excitons. The exploitation of this mechanism has been shown capable of boosting the efficiency of solar energy conversion, and it has been proposed as a mean for exceeding the Shockley-Queisser limit of efficiency of solar cells. In the last decade, several studies have investigated different chromophores to identify the ones suitable to produce high yield SF and long living triplets. Such studies spanned from the fundamental to the applicative approach, also dealing with the optimization of the interfaces with the other materials in the device in order to achieve an overall increased efficiency of the charge transport. In particular, the study of the dynamics of the triplet states, when formed and transported across all the interfaces, is crucial for modelling the charge transport properties in a working device. Here we present a new experimental approach to measure the triplet dynamics at the picosecond timescale, that uses the advantage of chemical sensitivity with respect to conventional optical techniques, thus offering the possibility of tracking the dynamics of the triplet states across different materials. We exploit the chemical selectivity of X-ray absorption spectroscopy (XAS) in an optical pump/X-ray probe experiment at a pump-probe setup that we developed at the Elettra synchrotron and with the support of novel implemented calculation

methodologies. We studied triplet dynamics in pentacene thin films (the prototypical singlet fission material) with lifetime of about 300ps.

3:00pm LS+AC+NS-ThA-3 Synchrotron X-Ray Tomography to Understand Structure and Physical Transformations in Solid State Batteries, *Kelsy Hatzell, M Dixit,* Vanderbilt University **INVITED**
The increasing demand for portable electronics, stationary storage, and electric vehicles is driving innovation in high-energy density batteries. Solid electrolytes that are strong enough to impede lithium dendrite growth may enable energy dense lithium metal anodes. Currently, the power densities of all-solid state batteries is limited because of ineffective ion transport and chemical and physical decomposition at solid|solid interfaces. The nature of ionic transport at intrinsic and extrinsic interfaces is important for mitigating chemical and structural instabilities. Extrinsic interface instabilities are responsible for high interfacial resistances. In order to displace liquid electrolytes, new materials and engineering strategies need to be developed to negate these degradation pathways. New insight into the governing physics that occurs at these interfaces are critical for developing engineering strategies for the next generation of energy dense batteries [1,2]. However, buried solid|solid interfaces are notoriously difficult to observe with traditional bench-top and lab-scale experiments. In this talk I discuss opportunities for tracking phenomena and mechanisms in all solid state batteries *in-situ* using advanced synchrotron techniques. Synchrotron techniques that combine reciprocal and real space techniques are best equipped to track relevant phenomena with adequate spatial and temporal resolutions.

Nanometer-scale Science and Technology Division
Room A222 - Session NS-ThA

SPM for Functional Characterization
Moderators: Volker Rose, Argonne National Laboratory, Renu Sharma, NIST Center for Nanoscale Science and Technology

2:20pm NS-ThA-1 Interatomic Force Laws That Evade Dynamic Measurement, *John Sader,* University of Melbourne, Australia **INVITED**
Atomically-resolved imaging and force measurements using the atomic force microscope (AFM) are performed most commonly in a frequency-modulation (FM) mode. This is achieved by configuring the AFM cantilever as an oscillator, enabling highly sensitive frequency detection with quasi real-time readout. Use of FM-AFM has led to spectacular results, including direct observation of the atomic structure of complex molecules and quantification of chemical and frictional forces at the atomic scale.

In this talk, I will briefly review the theory underpinning FM-AFM force measurements that allows conversion of the measured frequency shift to the interaction force law experienced by the cantilever tip. This will be following by new research [1] showing that this force conversion capability is directly regulated by the shape of the interaction force law – an effect that depends critically on the oscillation amplitude used. Rapidly varying interatomic force laws, which are common in nature, can lead to unphysical results. A mathematical theory is derived that enables reliable force measurements in practice. The validity of this theory is demonstrated by comparison to atomically-resolved measurements.

Reference:

1. J. E. Sader, B. D. Hughes, F. Huber and F. J. Giessibl, *Nature Nanotechnology*, 13, 1088 (2018).

3:00pm NS-ThA-3 Intermittent Contact Resonance Atomic Force Microscopy (icr-Afm) for Nanoscale Mechanical Property Characterization, *Gheorghe Stan,* National Institute of Standards and Technology **INVITED**
In the last two decades, significant progress has been made on developing new dynamic atomic force microscopy-based methods for nanoscale mechanical properties measurements. The changes in the tip-sample contact mechanics during scanning uniquely modify the high-frequency response of the AFM cantilever and much effort is dedicated to correctly retrieve the sample mechanical properties from the measured signal. Recently in a newly proposed dynamic AFM method, namely the intermittent-contact resonance atomic force microscopy (ICR-AFM), the contact stiffness measurement capability of the conventional contact resonance AFM (CR-AFM) was paired with the less-invasive surface probing of a force-controlled intermittent AFM mode. As an AFM tip goes in and out of contact with the sample during scanning, the change in the tip-sample contact stiffness is observed in the change of the eigenmode

frequencies of the cantilever and a fast detection is required to measure the frequency changes during each tap. By collecting the depth dependence of the contact resonance frequency at each point in the scan, a three-dimensional (3D) data volume is generated. This data can be used to obtain nanoscale tomographic views of the sub-surface elastic properties of a material. The involved tip-sample contact mechanics also poses some challenges for samples with edge geometries. A very convenient and robust method to address these types of contact geometries was found in the form of the conjugate gradient method applied to contact mechanics. In this talk, ICR-AFM implementation, measurements, and necessary contact mechanics models will be discussed for mechanical property characterization of thin films and nanostructures.

4:00pm NS-ThA-6 Novel Approaches Towards Cantilevers for Functional Multiparametric AFM Characterization, *Georg Ernest Fantner, N Hosseini, M Neuenschwander, B Ghadiani,* École Polytechnique Fédéral de Lausanne, Switzerland
The cantilever is arguably the most important part in the measurement chain of an atomic force microscope (AFM), because it transduces the interaction with the sample to a measurable quantity. While a large variety of different cantilevers are available for different AFM modes, most of these cantilevers use the same concepts as the first AFM cantilevers developed 30 years ago. The progress in AFM towards techniques such as high-speed AFM and multiparametric imaging puts new demands on the AFM cantilevers. In this talk I will discuss several ways we are exploring to increase the performance of AFM cantilevers by using non-standard materials, fabrication processes and actuation schemes. Applications of these new cantilevers are high-speed AFM multi-parametric imaging, and correlated microscopy.

4:20pm NS-ThA-7 Fluid Handling using Scanning Probe Lithography for Nanocombinatorics, *V Saygin, N Alsharif,* **Keith A. Brown**, Boston University
Scanning probes have been widely applied as characterization tools due to their high resolution and versatility. In parallel with the development of these capabilities, scanning probe lithography (SPL) has been advanced such that it is now capable of directly writing nanoscale domains of soft materials such as polymers, a capability that can be massively parallelized across centimeter scales through the use of cantilever-free scanning probe arrays. In this talk, we will discuss recent advances in the development of nanoscale fluid handling using scanning probes and describe how these advances allow for the realization of libraries for nanocombinatorial studies. Despite the utility of these approaches, operating with nanoscale domains of fluid raises interesting challenges in terms of managing capillary phenomena, evaporation, and deterministically directing fluid transfer. In order address these, we have performed a series of studies using atomic force microscopy to explore nanoscale fluid dynamics. After being written, polymer features can function as reactors for subsequent chemistry or as samples for further characterization. We explore the opportunities and challenges inherent to this class of experiment and highlight recent discoveries made using such libraries. While the majority of functional explorations using scanning probes center around use these instruments as characterization tools, the concept that scanning probes can also prepare combinatorial libraries is becoming increasingly common and providing new avenues for nanoscale science.

4:40pm NS-ThA-8 Accuracy of Tip-sample Interaction Measurements Using Dynamic Atomic Force Microscopy Techniques, *O Dagdeviren,* **Udo D. Schwarz**, Yale University
Atomic force microscopy (AFM) is a versatile surface characterization method that can map a sample's topography with high spatial resolution while simultaneously interrogating its surface chemistry through the site-specific high-resolution quantification of the forces acting between the sample and the probe tip. Thanks to considerable advances in AFM measurement technology, such local measurements of chemical properties have gained much popularity in recent years. To this end, dynamic AFM methodologies are implemented where either the oscillation frequency or the oscillation amplitude and phase of the vibrating cantilever are recorded as a function of tip-sample distance and subsequently converted to reflect tip-sample forces or interaction potentials. Such conversion has, however, been shown to produce non-negligible errors when applying the most commonly used mathematical conversion procedures if oscillation amplitudes are of the order of the decay length of the interaction [1]. The degree of divergence from actual values may also critically depend on both the overall strength of tip-sample interaction and the distance at which the interaction is obtained [2]. These systematic errors can, however, be

effectively eliminated by using oscillation amplitudes that are sufficiently larger than the decay length of the interaction potential.

[1] O. E. Dagdeviren et al., Physical Review Applied **9**, 044040 (2018).

[2] O. E. Dagdeviren et al., Review of Scientific Instruments **90**,033707 (2019).

5:00pm NS-ThA-9 Utilizing AFM to Study the Effect *of* Malaria-derived EVs on the Mechanical and Morphological Properties of Red Blood Cells, *Irit Rosenhek-Goldian, E Dekel, Y Ohana, S Maihib, S Cohen, N Regev-Rudzkib,* Weizmann Institute of Science, Israel

The deformability of Red Blood Cells (RBCs) is critical for the function of the cell and its viability. RBCs deform substantially and repeatedly when passing through narrow capillaries. There is growing evidence that RBC deformability is impaired in some pathological conditions. This is the case when the human malaria parasite invades these cells, leading to the secretion of Extracellular Vesicles (EVs) whose mechanistic effect on healthy RBCs is unknown.

We have applied atomic force microscopy (AFM) to study the mechanical changes occurring in cells treated with malaria-derived EVs, as well as morphological transformations in the cellular cytoskeleton. Mechanical measurements were made at physiological temperature without covalent linkage of the cells to the substrate to allow closest approximation to their natural state. Indentations were performed using a colloidal tip at applied forces kept sufficiently low to avoid damage to the cells as verified by comparing images taken before and after the mechanical test. Young's modulus values computed by Herzian analysis were achieved with sensitivity of 100 Pa. The results revealed a significant drop in compliance of the infected cells, with the mean value falling by a factor of approximately three for the infected ones. Furthermore, high-resolution images of dried cells with exposed cytoskeleton show distinct morphological differences associated with the breakdown and softening of the cell structure.

These results will be discussed with respect to the currently unknown mechanistic role of parasite-derived EVs on the RBC host membrane.

5:20pm NS-ThA-10 Silicon Oxide for RRAM Application: The SPM Analysis Approach, *Adnan Mehonic, M Buckwell, W Ng, A Kenyon,* University College London, UK **INVITED**

Resistive Random Access Memory (RRAM) has established itself as a promising technology for the next generation of non-volatile memories due to the simple design, high scalability, fast and low-power operation. Additionally, RRAM devices are considered for the implementation of power efficient hardware in applications of artificial intelligence (AI) and machine learning (ML) implemented in non-von Neumann architectures. Redox-based RRAM (ReRAM), based on the formation of conductive filaments in thin metal oxides are particularly popular due to excellent CMOS compatibility. However, significant challenges still exist for the full utilisation of the technology; such as device variability and yield. To better design and optimise the devices it is crucial to understand the physics that underlies the resistance switching processes. Here we present how SPM techniques can be used to characterise silicon oxide-based ReRAM devices. We find these techniques to be invaluable for developing a better sense of the oxide microstructure and the link with resistance switching processes. We also use the method of conductance tomography to directly visualise the shapes and sizes of conductive filaments in three dimensions - this is typically extremely challenging to obtain using conventional microscopy techniques.

Plasma Science and Technology Division
Room B130 - Session PS+2D+EM+SS+TF-ThA

Plasma-Enhanced Atomic Layer Etching

Moderators: Steven Vitale, MIT Lincoln Laboratory, Mingmei Wang, TEL Technology Center, America, LLC

2:20pm PS+2D+EM+SS+TF-ThA-1 Atomic Layer Etch: Real World Utilization of an Idealized Solution, *Peter Biolsi,* TEL Technology Center, America, LLC **INVITED**
Atomic Layer Etch: Real World Utilization of an Idealized Solution

Critical dimensions (CD) continue to shrink driven by the quest for cheaper, faster and less power-consuming devices. If simple shrink was not enough, all of the back end, middle and front end of line (BEOL, MOL and MOL) also have introduced structural complexity and stringent topographic

dimension, material property integrity and fundamental integration yield requirements. Atomic layer etching (ALE) has gained favor as an approach to extract more control over the fabrication of small CD complex topographic structures, atomic later etching. The idea is that alternating steps of self-limiting processes (e.g., passivation layer formation) and desorption (e.g., the removal of a passivation layer) mitigate aspect ratio dependence effects that lead to the aforementioned problems. The problem is that not all passivation processes are self-limiting. For the etching of dielectric materials, a self-limiting precursor step is not available as etch processes relies on cyclic process (fluorocarbon deposition and ion bombardment steps). Fluorocarbon based processes are not self-limiting rendering them quasi-atomic layer etch. Without special consideration, quasi-ALE has the same problems that continuous processes possess with additional burden of throughput.

Even though ALE can be difficult to be utilized in real-word scenarios, the learning from ALE finds its use in many etch applications. An etch chamber which can provide wide range of radical to ion flux ratios and precise ion energy control (using pulsing techniques) is suitable for ALE or utilizing ALE learnings. Currently, new ALE techniques based on surface modification by ions (Hydrogen plasma treatment of Silicon Nitride) followed by removal of modified layer by F radicals (High pressure NF3 or SF6 plasma) or surface modification by NH3/HF (to create a quasi-self-limiting diffusion barrier layer) followed by removal of modified layer by thermal means, are employed to etch critical layers where requirements are stringent. New frontier of etch technology will be the ability to achieve area selective etch without compromising etch rate of the process. Examples of such activities will be presented in this presentation.

3:00pm PS+2D+EM+SS+TF-ThA-3 Mechanism of SiN Etching Rate Fluctuation in Atomic Layer Etching, *Akiko Hirata, M Fukasawa, K Kugimiya, K Nagaoka,* Sony Semiconductor Solutions Corporation, Japan*; K Karahashi, S Hamaguchi,* Osaka University, Japan

Atomic layer etching (ALE) enables atomic-precision control of the surface reaction and low damage etching of the underlying layer for device fabrication. In this study, we investigated SiN ALE with process optimization of the surface adsorption and desorption steps, and we clarified the rate fluctuation mechanism.

A dual frequency CCP reactor (60 MHz/2 MHz) was used in this study. A SiN (50 nm) was deposited on the Si substrate by LPCVD. One etching cycle consisted of two steps. CH_3F/Ar plasma was applied to deposit the hydrofluorocarbon (HFC) polymer as the adsorption step. Then, Ar plasma was used in the desorption step. The thicknesses of SiN and the HFC polymer were measured by spectroscopic ellipsometry. The chemical bonding was analyzed by XPS.

A 1.2-nm-thick HFC polymer was deposited on SiN as the adsorption step. Next, we investigated the desorption step by using Ar plasma. The etched amount for 1 cycle was 0.58 nm. However, we found the etch-stop of SiN after 10 cycles of ALE, owing to the deposition (>6 nm) of a protective film on the surface. The etch-stop could be caused by sputtering of the Si upper electrode and/or re-deposition of the HFC film. To investigate the etch rate fluctuation, the SiN surface after ALE was analyzed. C-C and C-N bonds were detected after 1 cycle, and C-C bonds increased after 10 cycles. It was clear that the excess HFC polymer deposition suppressed the ALE reactions. Ar^+ ion bombardment during the desorption step selectively eliminated the H and F in the HFC polymer, because the bonding energies of C-H and C-F were low. As the bonding energies of C-C (6.4 eV) and C-N (7.8 eV) are relatively high, these bonds remained after the desorption step. We speculated that excess C-rich polymer deposition after ALE started from the residual C-C bond. Residual Si-C bond is also possible reason, since the MD simulation revealed that the formation of Si-C bond was promoted in the fluorocarbon layer during SiO_2 ALE. [1] These results clearly showed that the initial adsorption kinetics of HFC polymer was strongly affected by the residual carbon on the SiN surface. To suppress the C-rich polymer deposition, we studied stable SiN ALE using the desorption step of Ar/O plasma (0.36 nm/cycle) and the two-step sequential desorption step of Ar and O plasma (0.6 nm/cycle). Although the effect of O adsorption in SiO ALE has been studied previously,[2] few studies have been reported for the case of SiN. Because the surface condition is able to fluctuate with the number of cycles, precise surface control is strongly required to achieve stable ALE.

[1] S. Hamaguchi et al., 2018 AVS, PS-FrM6. [2]T. Tsutsumi et al., JVST A 35 (2017) 01A103.

Thursday Afternoon, October 24, 2019

3:20pm **PS+2D+EM+SS+TF-ThA-4 Effect of Polymerization on Ar+ Bombardment Modification of SiO₂ and Si₃N₄ Substrates: Molecular Dynamics Simulation Study**, *Hojin Kim, Y Shi, Y Tsai, D Zhang, Y Han,* TEL Technology Center, America, LLC*; K Taniguchi,* TEL Miyagi Limited, Japan*; S Morikita,* TEL Miyagi Limited*; M Wang, A Mosden, A Metz, P Biolsi,* TEL Technology Center, America, LLC

To understand the selective removal of silicon oxide (SiO_2) against silicon nitride (Si_3N_4) with gaseous reactants for advanced etch process, we have studied the surface modification of both SiO_2 and Si_3N_4 substrates with Ar+ bombardment by using molecular dynamics (MD) simulation. The substrate samples was prepared with and without carbon (C) and hydrogen (H) polymerization to investigate the effect of polymerization on surface modification. C and H atoms were deposited with low ion energy not to disrupt the surface much. After preparation of substrate, Ar+ bombardment with various ion energy (IE) were performed. We obtained a damage depth with a wigner-seitz defect analysis as a function of IE and compared the cases with and without polymerization to check the role of the added polymer layer on surface modification. In pristine Si_3N_4 and SiO_2 case, at IE=25eV, both substrates starts to show the damage with penetration of Ar+ and follows with an exponential raise as the IE increases. Damage depth at Si_3N_4 is deeper than that at SiO_2. In polymerization, simulations show that H is more deposited than C on Si_3N_4 while on SiO_2, C is more deposited than H. no silicon-hydrogen bonds appear on both substrates and in Si_3N_4, nitrogen-hydrogen bond is dominated while oxygen-carbon bond is popular in SiO_2. For damage analysis, in Si_3N_4 case, CH polymerization helps to lower about 30% in the damage depth with exponential behavior. However, SiO_2 case shows the opposite effect of CH polymerization in the damage depth. Formed polymer layer leads to increase the damage depth by comparing with pristine SiO_2 and helps more clear exponential behavior as a function of IE. Finally, analyzed results using XPS and/or SIMS from blanket SiO_2 and Si_3N_4 films etched in a Capacitively Coupled Plasma (CCP) chamber are compared with the MD simulation results.

4:00pm **PS+2D+EM+SS+TF-ThA-6 Advanced Cyclic Plasma Etch Approaches for Metal Patterning: Synergy and Surface Modification Effects**, *Nathan Marchack,* IBM T.J. Watson Research Center*; K Hernandez,* University of Texas at Dallas*; J Innocent-Dolor, M Hopstaken, S Engelmann,* IBM T.J. Watson Research Center **INVITED**

Atomic layer etching or ALE is a burgeoning research area of plasma processing that offers critical advantages needed for future advancements in semiconductor devices, namely lower damage and enhanced selectivity, through its self-limited reaction cycles separated by purge steps.[1] ALE processes offer a significantly higher degree of tunability over traditional continuous-wave (CW) plasma etching, due to the fact that parameters such as gas flows, pressure, and bias power can be adjusted on a step-specific basis rather than as a global setting for the length of the process.

Our previous work investigated the effect of varying the purge step times in a quasi-ALE process using alternating Cl_2/H_2 exposures on the etched profiles of titanium and tantalum nitride.[2] Titanium and tantalum-based conductive films have been previously evaluated as gate materials for CMOS devices but more recently have been incorporated as top electrodes for novel technologies such as magnetoresistive RAM (MRAM) and hard masks for carbon electrodes utilized in biological sensing. As the trend of downscaling device size continues, the ability to pattern these films at tight pitches with minimal redeposition becomes highly important.

Sub-surface modification of films such as Si_3N_4 and indium-doped tin oxide (ITO) by low atomic weight (LAW) ions such as H^+ has been discussed in literature as facilitating self-limited etch behavior.[3,4] We present new data exploring the incorporation of LAW species into cyclic etch processes, namely penetration depth into these metal nitride films and their role in surface oxide formation, the latter of which can contribute to novel pitch multiplication schemes.[5] SIMS measurements reveal that the depth of penetration of H^+ for TaN films can be >40 nm and can occur through a native oxide layer that inhibits etching by Cl species. Pressure variation is a significant factor in tuning this effect, which can potentially modify the etch resistance of these films and enable novel integration schemes.

[1] K. J. Kanarik, T. Lill, E. A. Hudson, S. Sriraman, S. Tan, J. Marks, V. Vahedi, R. A. Gottscho, J. Vac. Sci. Technol. A. 2015, 33, 020802.

[2] N. Marchack, J. M. Papalia, S. U. Engelmann, E. A. Joseph, J. Vac. Sci. Technol. A. 2017, 35, 05C314.

[3] S. D. Sherpa, A. Ranjan, J. Vac. Sci. Technol. A. 2017, 35, 01A102.

[4] A. Hirata, M. Fukasawa, K. Nagahata, H. Li, K. Karahashi, S. Hamaguchi, T. Tatsumi, Jpn. J. Appl. Phys. 2018, 57, 06JB02.

[5] N. Marchack, K. Hernandez, B. Walusiak, J-I. Innocent-Dolor, S. U. Engelmann, Plasma Process Polym. 2019, e1900008.

4:40pm **PS+2D+EM+SS+TF-ThA-8 Surface Modification and Stability of Plasma-assisted Atomic-layer Etching (ALE) of Si based Materials; Analysis by Molecular Dynamics (MD) Simulation**, *Satoshi Hamaguchi, M Isobe, E Tinacba, S Shigeno, Y Okada, T Ito, K Karahashi,* Osaka University, Japan

A plasma-assisted atomic-layer etching (ALE) process typically consists of alternating application of chemically reactive species (adsorption step) and Ar ion bombardment with low bias energy (desorption step) to the surface to be etched. In the adsorption step, a modified layer is formed on the material surface and, in the desorption step, the modified layer is removed with the original material underneath being intact. In this presentation, using the results of MD simulation of ALE for Si, SiO2, and SiN, together with experimental observations, physical mechanisms of the formation and removal of surface modified layers in typical ALE processes will be discussed.

Our molecular dynamics (MD) simulation of SiO2 ALE by fluorocarbon adsorption and Ar+ ion bombardment shows that preferential sputtering of oxygen takes place by Ar+ ion bombardment and a Si rich layer mixed with fluorine and carbon atoms is formed on the SiO2 surface. Ideally this modified layer should be removed completely in the subsequent desorption step, but in general it is not. In such a layer, the atomic number ratio of Si to O can be as high as unity and carbon provided in the subsequent adsorption step tends be deposited rather than removing O atoms from the surface by forming CO molecules. Therefore as the ALE cycles proceed, the adsorbed fluorocarbon layer thickens and eventually an etch stop may occur. With fine tuning of incident Ar+ ion energy, an etch stop may be avoided but the process window to achieve both continuous ALE cycles (by sufficiently high Ar+ ion energy) and ideal self-limit in each cycle (by sufficiently low Ar+ ion energy) may still be small or even nonexistent. The incompleteness of the modified surface removal in each ALE cycle seems universal phenomena for plasma-assisted ALE for most materials. For other plasma-assisted ALE processes that we examined by MD simulation, the surface modified layer formed during the adsorption step could not be removed completely by low-energy Ar+ ion bombardment, either. Indeed low-energy Ar+ ion bombardment contributes to the formation of a deeper modified layer by pushing down adsorbed species into the bulk, rather than simply removing it.

5:00pm **PS+2D+EM+SS+TF-ThA-9 Innovative Future Etch Technology by Atomic-order Control**, *Yoshihide Kihara, T Katsunuma, S Kumakura, T Hisamatsu, M Honda,* Tokyo Electron Miyagi Ltd., Japan **INVITED**

In recent years, with the progress of device miniaturization and increased challenges in the scale of integration of semiconductor devices, ultra-high selectivity and atomic layer-level critical dimension (CD) control techniques are required in the fabrication processes.

In the conventional etching, using a fluorocarbon (FC) gas, the high selectivity is obtained by taking advantage of the difference of the FC protective film thickness due to the difference of materials.[1] However, adopting the conventional approach to cutting-edge pattern structure becomes difficult due to the excessive FC film clogging the micro slit facet. To meet the highly complex requirements, alternative process was developed by using ion modification and chemical dry removal.[2] We have made several improvements on this new approach and applied it to SiN and SiC etching. The improved new approach achieves ultra-high selectivity without FC protective film and we also confirmed this process has the characteristics of a self-limiting reaction based on ion depth profile as well as ALE.

In the patterning processes, lower pattern densities have a larger CD shrinking due to micro-loading. Hence, we developed the new process flow that combines atomic layer deposition (ALD) technique and etching. With this method, we achieved CD shrinking at atomic-layer level precision for various patterns, without causing CD loading.[3]

Moreover, Quasi-ALE can etch the pattern while maintaining the mask CD for different pattern density. This is because Quasi-ALE precisely controls the surface reaction by controlling the radical flux and ion flux independently.[3] Also, it was necessary to control oval CD size between X and Y respectively. We found that X-Y CD control can be easily performed by changing the balance of FC adsorption and Ar desorption in Quasi-ALE. However, there are concerns about mask selectivity and ion damage in this approach. To solve these problems, we introduce the Advanced Quasi-ALE technique which combines mask protection together with Quasi-ALE. The Advanced Quasi-ALE achieves wider X-Y CD control margin.

On the other hand, as aspect ratio is increased in the memory fabrication process, the occurrence of bowing profile is a serious problem. To address the issue, the new improvement technique has been developed that combines the concept of ALD and etching. With this method, we are able to etch profile more vertically in high A/R feature.

Reference

[1] M. Matsui et al., J. Vac. Sci. Technol. A 19 1282 (2001)

[2] N. Posseme et al., Applied Physics Letters105 051605 (2014)

[3] M. Honda et al., J. Phys. D: Appl. Phys., Vol.50, No.23 (2017)

Plasma Science and Technology Division
Room B131 - Session PS+SS-ThA

Plasma Conversion and Enhanced Catalysis for Chemical Synthesis

Moderator: R. Mohan Sankaran, Case Western Reserve University

2:20pm **PS+SS-ThA-1 Rate Limiting Factors of Low Pressure Plasma-catalytic CO₂ Methanation Process**, *Kazunori Koga, A Yamamoto, K Kamataki, N Itagaki, M Shiratani,* Kyushu University, Japan

The methanation of CO_2 attracts attention as the ways of CO_2 reduction and energy storage as well as space exploration. It is expected to produce rocket propellant fuels at Mars and CO_2 conversion in space stations. The Sabatier reaction has been employed to generate CH_4 from CO_2 and H_2. Using catalysts realizes a high conversion efficiency. However, the conventional catalytic reaction starts at about 200 ^{o}C but thermal runaway occurs above 250 ^{o}C. The heat management is an important problem. A method using non-thermal plasma with catalyst allows methanation under low-temperature condition [1, 2]. Here, we studied rate-limiting steps of CO_2 methanation and their important parameters in the plasma-catalytic process. Experiments were carried out using a capacitively coupled plasma reactor. The electrode diameter was 50 mm and the distance between the electrodes was 6.1 mm. The Cu electrodes were employed as catalyst. We set a CO_2 gas flow rate between 1.0 sccm and 5.0 sccm and an H_2 gas flow rate between 1.0 sccm and 30 sccm. The pressure was 750 Pa. The discharge power was set in a range of 10 to 100 W. Gas composition in the discharge plasmas was measured with a quadrupole mass spectrometer. CH_4 yield rapidly increases with time after plasma initiation. It tends to be saturated after 200 s. From time dependence of catalyst temperature, the saturation occurs between 350 K and 370 K. The temperature shows the threshold temperature at which the rate-limiting step change from gas-phase reactions in plasma to surface reactions on the catalyst. The CH_4 yield increases with increasing the gas residence time. From optical emission spectroscopy, emission intensity related with CO angstrom band increase with the gas residence time but hydrogen-related emission is irrelevant to the residence time. It suggests that CO excited by plasma is responsible to the CH_4 yield increase. The results of H_2 gas flow rate dependence suggest that electron temperature is an important factor in the rate-limiting step of the gas phase reaction. I will discuss the detail mechanisms at the conference.

Work supported partly by JAXA and JST.

[1] S. Toko, et al., Sci. Adv. Mater. **10** (2018) 655.

[2] S. Toko, et al., Sci. Adv. Mater. **10** (2018) 1087.

2:40pm **PS+SS-ThA-2 Radical Nitriding of Graphene Promoted by Surface Plasmon Resonance of Gold Nanoparticle Catalyst**, *Takeshi Kitajima, T Nakano,* National Defense Academy, Japan

In recent years, catalyst activity[1] of graphene nitride including fuel cell catalysts has attracted attention. We apply the catalytic property[2] of gold nanoparticles to the surface reaction of graphene, and investigate a process that can nitride graphene while reducing the damage caused by plasma irradiation.

In this study, we compared the degree of nitridation according to the presence or absence of ion irradiation (I), light irradiation from plasma (L) and the presence or absence of gold nanoparticle catalyst (C), respectively, and discovered the presence of radical nitriding by surface plasmon resonance of gold nanoparticles.

Gold is deposited for 2 minutes by electron beam evaporation on graphite crystals in an ultra-high vacuum chamber.

It was found by AFM measurement that gold nanoparticles with a diameter of about 20 nm were formed on the graphite crystal surface by aggregation.

Next, NH₃-Ar (1: 3) mixed plasma (ICP, 70 MHz, 100 W) at a pressure of 10 Pa was generated in the plasma chamber. The sample was irradiated for 10 minutes with radicals and light that passed directly or through a 30 line/inch SUS304 single mesh.

The atomic composition by XPS was examined for each irradiation condition. It was found that in the condition RLC where gold nanoparticles were generated and irradiated with radicals and light, nitridation was promoted about twice as much as plasma irradiation.

It is speculated that irradiation of gold nanoparticles with light excites plasmons to promote the nitridation reaction.

Next, Raman scattering analysis of graphene nitride was performed. Islands found on graphite were considered as graphene. Among the Raman scattering spectra, the component intensities of 2D (2690 cm -1), G (1580 cm -1) and D (1350 cm -1) were measured to evaluate the intensity ratio.

Under RLC conditions, the I2D / IG ratio has not dropped significantly. It can be seen that the structural change of the graphene island due to ion bombardment is prevented. Furthermore, the ID / IG ratio is higher than in plasma irradiation (RIL), and it can be confirmed that nitrogen doping has progressed more. From the above, it is considered that the catalytic activity of the gold nanoparticles is expressed by the effect of surface plasmon excitation, and the formation of graphene nitride with low damage by radicals becomes possible.

1. Haibo Wang, Thandavarayan Maiyalagan, and Xin Wang, ACS Catalysis 2, 781 (2012).

2. Marie-Christine Daniel and Didier Astruc, Chemical Reviews 104, 293 (2004).

3:00pm **PS+SS-ThA-3 Plasma-assisted Catalysis: Exploring the Effects of Plasma Stimulation on Catalyst Performance**, *Jason C. Hicks,* University of Notre Dame **INVITED**

Plasmas create incredibly reactive chemical environments and have a long history in chemical synthesis and removal of volatile organic compounds.[1-2] Plasmas can be generated in the presence of a catalyst (plasma-assisted catalysis) to increase conversions and improve the selectivity to desired products. Our research in the area of plasma-assisted catalysis is focused on the ability to control the catalyst performance by tuning the plasma environment or plasma-catalyst interactions.[3-4] We have been particularly interested in the use of non-thermal plasmas for C-H and N_2 activation via dry reforming of methane and ammonia synthesis reactions, respectively. Specifically, this presentation will focus on 1) the reaction regime where catalyst-plasma interactions are observed for these reactions, 2) the various catalyst-plasma interactions observed, and 3) the role of the plasma in enhancing reaction efficiency. This presentation will highlight our recent progress in controlling plasma-catalyst interactions to enhance reaction efficiency.

(1) Neyts, E. C.; Ostrikov, K.; Sunkara, M. K.; Bogaerts, A. *Chem. Rev.***2015**, *115* (24)

(2) Mehta, P.; Barboun, P.; Go, D. B.; Hicks, J. C.; Schneider, W. F. ACS Energy Lett. **2019** 5, (4)

(3) Mehta, P.; Barboun, P.; Herrera, F. A.; Kim, J.; Rumbach, P.; Go, D. B.; Hicks, J. C.; Schneider, W. F. *Nat. Catal.***2018**, No. 4.

(4) Barboun, P. Mehta, P. Herrera, F.A. Go, D.B. Schneider, W.F. Hicks, J.C. ACS Sus Chem & Eng, **2019**, accepted.

4:00pm **PS+SS-ThA-6 A Plasma-aerosol Droplet Reactor for the Synthesis of Ammonia from Nitrogen and Water**, *Joseph Toth, D Lacks, J Renner, M Sankaran,* Case Western Reserve University

Alternative approaches are sought to the high-pressure, high-temperature Haber-Bosch (H-B) process for nitrogen fixation in order to enable distributed synthesis from renewable feedstocks. A potentially promising reactive strategy is plasma excitation which was historically the first method to fix nitrogen by reacting nitrogen and oxygen in air. More recently, plasmas have been combined with solid catalyst materials to synthesize ammonia at atmospheric pressure and lower temperatures than the H-B process. However, most of these reactions still require hydrogen gas which remains linked to fossil fuels and leads to both high cost and environmental consequences.

Here, we present a novel plasma-aerosol droplet reactor to synthesize ammonia from nitrogen and water at atmospheric pressure and near room

temperature. Introducing the water as droplets instead of water vapor increases the throughput that can be achieved and also simplifies the system, eliminating the need for heated lines to avoid condensation on the walls. The plasma was formed as a dielectric barrier discharge inside a quartz tube with an outer ring electrode and an inner wire electrode. The water droplets were generated using a commercial nebulizer via a high nitrogen flow rate causing a Venturi effect which siphoned the water into the gas stream. The products were collected by bubbling the gas effluent leaving the reactor through a concentrated sulfuric acid bath and condensing in a second trap chilled to -40 $^{\circ}$C. The ammonia was then measured by the *o*-phthalaldehyde colometric assay technique. The ammonia production rate was found to be a function of the power and flow rate with production rates up to 600 μg/hr at 70 W. Controls were run with an argon plasma and with no water droplets to verify that no ammonia was produced without both nitrogen and water. In addition to ammonia, we also tested for nitrites/nitrates (NO_x) and measured up to 3000 μg/hr total production rate. The efficiency, power consumption, and potential reaction mechanisms will also be discussed.

4:20pm PS+SS-ThA-7 Plasma-assisted Nitrogen Fixation by Water: Development and Evaluation of Hybrid Membrane Based Plasma-Electrochemical Reactor, *R Sharma, Richard M.C.M. van de Sanden, H Patel, V Kyriakou, U Mushtaq,* Dutch Institute for Fundamental Energy, Netherlands*; A Pandiyan,* Dutch Institute for Fundamental Energy*; S Welzel, M Tsampas,* Dutch Institute for Fundamental Energy, Netherlands

The worldwide energy crisis and environmental issues have greatly driven the current research on exploring and efficiently utilizing the environmentally-friendly and sustainable energy sources[1]. Most sustainable sources such as solar and wind energy are in principle able to meet the global energy demand. Nevertheless, they are intermittent and require new concepts of conversion and storage of electricity. Storing energy in form of chemical bonds is considered as an effective option for long term storage. Thus there is quest of developing effective processes for converting electrical energy into molecules.

In this context, nitrogen fixation is unquestionably one of the most important chemical conversion process since it converts N_2 into molecules of high energy (e.g. NH_3, NO)[2]. However, contemporary chemical industry for nitrogen fixation imposes great concerns about the environmental sustainability in terms of immense energy consumption and burdened emissions profile. Nevertheless, plasma-technology has been receiving renewed attention as an alternative "green" approach for N_2 activation which is one of the fundamental requirement for nitrogen fixation.

Up to now solutions were mainly sought on material axis, however recent theoretical studies have revealed that there are intrinsic limitations of catalysis (i.e. scaling relationships) which keep the processes far from the optimum performance. In this work, we will present a unique solution to the aforementioned limitations by employing a hybrid type reactor consisting of a plasma reactor and solid state water electrolysers with oxygen ion[3] or proton conducting membranes. Unlike conventional plasma catalysis that requires the co-activation of reactants, in the proposed alternative approach, electrolysers provide reacting species on catalysts with a controllable manner while a radiofrequency plasma is used to increase the reactivity of N_2. Such spatial separation of N_2 dissociation and catalytic formation of the target molecules provides truely independent parameters to optimise the nitrogen fixation process. One aided benefit of the proposed approach is that both technologies, i.e. water electrolyser and plasma activation, utilize base molecules (N_2 and H_2O) and can be directly powered by renewable electricity. Such a scheme may be a stepping stone to zero carbon footprint processes. Moreover, the advantages of proposed approach will be also compared to conventional plasma catalysis or pure plasma processes.

References

[1] Chu et al, Nat. Mater., 16 (2017), 16

[2] Patil et al, Catal. Today, 256 (2015), 49

[3] Tsampas et al, Catal. Sci. Technol., 5 (2015) 4884

4:40pm PS+SS-ThA-8 Plasma-Assisted Ammonia Synthesis in Hybrid Plasma-Catalysis DBD Reactors, *Z Chen, X Yang, Y Ju, S Sundaresan, Bruce E. Koel,* Princeton University   **INVITED**
Solar and wind power are creating increasingly large amounts of electricity, and an important question is how can we take advantage of the expanding increase of renewable electricity for catalysis? One approach is plasma-assisted catalysis, which utilizes excited gaseous molecules or new reactive species formed in a (non-equilibrium, low temperature) gas discharge

plasma, along with a catalyst to enable increases in the activity and selectivity for carrying out desirable chemical reactions. A significant challenge in plasma-catalysis hybrid systems is to achieve the strongest synergistic interactions between the plasma and catalyst to increase performance and overall energy efficiency. We report on two types of dielectric barrier discharge (DBD) reactors (with a coaxial tube and parallel plates) that have been used to screen catalytic effects of different metal surfaces and supported catalysts in plasma-catalysis hybrid systems at near atmospheric pressure, utilizing both AC and nanosecond pulsed discharges. We observed strong synergistic effects between non-equilibrium plasma and catalysts for both NH_3 synthesis and methane coupling reactions. We compared the performance for ammonia synthesis of catalysts using active metals (Pd, Pt, and Fe) or less active metals (Au, Ag, and Cu) or their alloys. We found that the metal-nitrogen (M-N) bond energy was not the only parameter governing the catalytic activity for NH_3 synthesis in plasma. Better catalytic activity could be achieved by bimetallic catalysts that contained catalytic sites for both N_2* dissociation and hydrogenation of M-N bonds, leading to our observations of a highly active PdFe catalyst for NH_3 synthesis in plasma. In addition, we will also report briefly about results in CO_2 reforming of methane in the coaxial reactor, where we found that under thermal only conditions, $PtFe/Al_2O_3$ catalyzed mainly the formation of CO and H_2, but with the plasma on, the selectivity shifted to methane coupling reactions. Interestingly, an Ag/Al_2O_3 catalyst with an AC discharge demonstrated 100% selectivity to CH_4 coupling reactions at 350 $^{\circ}$C. Methane coupling using the plasma-catalysis reactor at low temperatures and pressures mainly produced higher hydrocarbons, suggesting a potential route for converting cheap and abundant methane gas into high value hydrocarbons and fuels.

5:20pm PS+SS-ThA-10 Efforts towards Plasma-assisted Catalysis: Elucidating Gas-phase Energetics, Kinetics, and Surface Interactions, *Angela Hanna, E Fisher,* Colorado State University
With increasing concern about environmental health and climate change, there is a greater need to investigate fundamental reactivity of pollutant species. Improving the effectiveness of substrates used in vehicular emissions abatement hinges on the ability to discern the contributions of gas-phase species in surface reactions. A fundamental understanding of interactions between plasma species is essential to characterizing complex plasma chemistry phenomena. Inductively-coupled N_XO_Y plasma systems were investigated to determine possible synergisms between precursor chemistry and gas-surface interface reactions with a variety of catalytic substrates (i.e., Pt substrates and zeolites). The impact of adding dilute amounts of water vapor to the gas feed was also systematically explored. Precursor chemistry was probed via gas-phase diagnostics; time-resolved optical emission data elucidated NO (g) and N_2(g) production kinetics from N_XO_Y source gases, whereas steady-state emission and absorbance data provide information regarding energy partitioning between rotational and vibrational degrees of freedom. The presence of micro-structured catalysts within the plasma significantly decreases excited N_2 vibrational temperature, suggesting these materials promote vibrational relaxation within the discharge. Our unique Imaging of Radicals Interacting with Surfaces (IRIS) allows us to probe the gas-surface interface and provides evidence of how plasma species synergistically interact with catalytic substrates. In addition to evaluating the spectroscopic characteristics of the discharge (N_XO_Y), we have assessed material morphology and chemical composition before and after plasma exposure. The porous network of zeolite substrates was maintained after prolonged plasma exposure, although surface etching of oxygen or N-doping occurred at different plasma operating conditions. This holistic experimental approach, combining gas-phase diagnostics, IRIS, and robust materials characterization will be essential to realizing the potential of plasma assisted catalysis for pollution remediation.

Advanced Surface Engineering Division
Room A215 - Session SE-ThA

New Challenges and Opportunities in Surface Engineering

Moderators: Jolanta Klemberg-Sapieha, Ecole Polytechnique de Montreal, Canada, Matjaz Panjan, Jozef Stefan Institute, Slovenia

2:20pm SE-ThA-1 Evaluating Electro-Mechanical Reliability using In-Situ Methods, *Megan J. Cordill, O Glushko,* Erich Schmid Institute of Materials Science, Austrian Academy of Sciences, Austria   **INVITED**
Electrical, mechanical and interfacial properties of thin metal films on compliant polymer substrates are important to understand in order to

design reliable flexible electronic devices. Thin films of Cu and Au on polyimide and polyethylene terephthalate substrates were examined for their use as interconnects in flexible electronic devices. Using in-situ tensile straining with atomic force microscopy (AFM), X-ray diffraction (XRD), and confocal laser scanning microscopy (CLSM) mechanical and interfacial behavior can be examined. AFM and CLSM can provide information about crack spacing and film delamination, while XRD experiments are utilized to determine the lattice strains and stresses present in the films. If these in-situ techniques are combined with in-situ 4-point-probe (4PP) resistance measurements, the influence of the mechanical damage on the electrical properties can be correlated. This combination of multiple in-situ investigations are particularly useful when studying the electro-mechanical behavior under cyclic loading conditions where some materials can have an improvement of the electrical conductivity after a few hundred cycles. Mechanism behind these phenomena as well as methods to measure the adhesion of metal-polymer interfaces found in flexible electronic devices will be discussed.

3:00pm SE-ThA-3 Surface Engineering for Bearing Applications: Present Status and (Near)-Future Needs, *Esteban Broitman*, SKF - RTD - Research & Technology Development Center, Netherlands **INVITED**
Machines with rotating components usually rely on bearings to reduce friction in moving its parts around a fixed axis. The increasing demand for more precise bearings to lower power consumption and heat generation, while simultaneously support increasing applied loads and/or higher speeds, has given place to the use of surface engineering processes.

In the case of bearings, it is widely accepted the advantages of using coatings as the surface process to improve its performance. During the last three decades, advanced coatings have enjoyed a growing interest in several industrial applications because they can be engineered to provide different properties like electrical insulation, low friction, and resistance to corrosion, surface initiated rolling contact fatigue, abrasive wear, and plastic deformation. The main surface engineering processes to deposit these coatings include traditional technologies such as dipping and liquid spraying, chemical conversion, galvanizing and electroless processes, as well as more sophisticated technologies such as thermal spraying, physical vapor deposition, diffusion, and ion implantation. However, the special characteristics of the bearing steel and the need to limit the deposition costs reduce the number of methods that can be practically used.

In this talk I will first introduce the four main areas where coatings can contribute to improve the performance of bearings made of standard bearing steel: lower friction, decreased wear, corrosion resistance, and electrical insulation. For each area I will review which coatings are industrially used, their possible industrial deposition methods, and their main mechanical and tribological properties. Examples of SKF coatings used to extend maintenance and life expectancy of specialized bearings will be described, like NoWear® (carbon-based nanostructured coating), Black Oxide (iron oxide conversion film), INSOCOAT® (aluminum oxide coating), and manganese phosphate films. I will finish the presentation visioning which the (near)-future needs of specialty surface-treatment coatings are in response to bearing application challenges, including a novel fifth area of sensorized coatings.

4:00pm SE-ThA-6 *In situ* Scanning Electron Microscopy based Uniaxial Compression of sub-micrometer-size NbC(100) Single-crystalline Pillars, *A Aleman, K Tanaka, H Zaid, J Yang, **Suneel Kodambaka***, University of California, Los Angeles
Cubic group 4 and 5 transition-metal carbides (TMCs), such as HfC and TaC, are hard (>20 GPa) and strong (moduli >270 GPa) solids with high melting points (> 2900 K) that exhibit superior strengths at elevated temperatures and excellent resistance to wear, ablation, and corrosion. They are attractive for applications in cutting tools, hard protective coatings, advanced propulsion systems, spacecrafts, rockets, and hypersonic jets that operate under extreme environments, e.g. at ultra-high temperatures (> 2000 K) and highly corrosive atmospheres. The realization of enhanced ductility, especially at low temperatures could potentially enable new applications for this class of materials. Our recent efforts have focused on understanding the mechanical behavior of group 5 TMC single-crystals, VC, NbC, and TaC.

Here, we report on the room-temperature mechanical behavior of 100-oriented NbC single-crystalline pillars of diameters between 330 and 830 nm. We prepared the pillars via focused ion beam milling of bulk, commercially-available, NbC single-crystals. We carried out uniaxial compression of the pillars using Hysitron PI-85 picoindenter *in situ* in a scanning electron microscope . We find that all the pillars exhibit plastic

deformation with strains up to 26%. Load-displacement curves obtained during the compression tests reveal multiple displacement bursts, indicative of sustained slip. Interestingly, yield strengths vary non-monotonically with pillar diameter between 8 GPa and 12 GPa and by up to 40% among the pillars of the same diameter. From the post-compression images of the pillars, we identify {110}<110> and {111}<110> as the two likely slip systems operating within these pillars. We suggest that the observed size-dependence in NbC(100) pillars is a consequence of the activation of these two slip systems. We observe a similar size-dependence in VC(100) pillars based upon which we suggest that the observed mechanical behavior is characteristic of group 5 TMCs.

4:20pm SE-ThA-7 Thermal Stability of MoNbTaVW High Entropy Alloys Thin Films Deposited by Cathodic Arc, *A Xia, **Robert Franz***, Montanuniversität Leoben, Austria
High entropy alloys (HEAs) are a new emerging class of materials typically consisting of 5 to 13 metallic elements in an approximately equimolar ratio. Studies conducted on HEA bulk materials revealed promising combinations of properties, such as high strength, ductility, corrosion resistance, wear resistance, hardness, low diffusion and thermodynamic stability. While research on bulk high entropy alloys has seen quite a boost over the past years, investigations on thin films are still a relatively unexplored area.

Within the current work, the thermal stability of refractory MoNbTaVW HEA thin films was studied up to an annealing temperature of 1600 °C. The thin films with a thickness of about 1 µm were synthesized on sapphire substrates by cathodic arc deposition. The samples were annealed in a vacuum furnace for 1 hour at temperatures ranging from 1000 to 1600 °C in steps of 100 °C. After annealing, scanning electron microscopy images were recorded indicating changes in the film morphology at 1200 °C and above. Analysis by X-ray diffraction revealed the formation of new phases at 1500 °C. Nanoindentation tests were performed to assess possible changes in the mechanical properties of the films. A decrease from about 20 GPa for the as-deposited films to about 9 GPa after annealing at 1600 °C was noticed. The electrical conductivity of the MoNbTaVW thin film slightly decreased due to annealing as the measured resistivity increased from $5 \cdot 10^{-7}$ Ωm to $1.5 \cdot 10^{-6}$ Ωm.

4:40pm SE-ThA-8 Erosion Resistant Coatings Inside Narrow Tubes to Protect Aircraft Engine Components, *A Kilicaslan, O Zabeida, E Bousser, M Martinu, **Jolanta Klemberg-Sapieha***, Polytechnique Montreal, Canada
There is an ever-growing interest in the use of functional coatings to protect surfaces of materials and workpieces against harsh environments such as corrosion, abrasion or solid particle erosion (SPE), making surface engineering solutions a very attractive balance between performance and cost. Numerous vapor-based fabrication techniques have been developed, namely PVD, CVD and PECVD, that can be used to achieve high hardness and high wear resistance, while being compatible with substrate materials such as metals, and different substrate shapes. This is increasingly important in the case where there is a need for protective coating solutions for inner surfaces of tubular components, such as parts of aircraft engines, oil pipelines, mining components, and numerous others. Specifically, certain aircraft diffusers are designed to conduct the air to the combustion chamber by means of many narrow gas inlets arranged around a circular frame. In such case, SPE arising from dust particles and volcanic ashes present in the air can result in an increase of the gas inlets diameter, leading to back streaming of air into the compressor (known as the compressor surge), which can give rise to significant aircraft engine damage and catastrophic consequences.

In response, we propose a novel Non-Line-Of-Sight (NLOS) technique to coat the inner parts of non-linear surfaces and cavities with hard, wear- and erosion-resistant coatings possessing high erosion resistance, hardness significantly higher than the hardness of the particles impacting the surface, as well as a large thickness (preferably 8 µm and more).

Specifically, we review, study and demonstrate the fabrication process of hard SPE-resistant TiN protective coatings on the inner surfaces of narrow tubes using a non-obvious NLOS approach yielding a uniform film thickness and properties along the tube axis (better than 20%). The deposition process indicates the importance of applying pulsed-DC PECVD, when uniform hard TiN films are prepared at low-frequency in the several kHz range. The TiN films (about 12 µm thick), exhibit high hardness and Young's modulus (25 and 225 GPa, respectively), corresponding to the (111) preferred crystallographic orientation. We show that the SPE resistance on the inner surface decreased by a factor of more than 15 compared to the bare substrate, and that the process is well suited for the protection of

aerospace, manufacturing, 3D printed and other critical components with a complex shape of inner surfaces.

Surface Science Division
Room A220-221 - Session SS+2D+AP+AS+OX+SE-ThA

Dynamics at Surfaces/Reactions and Imaging of Oxide Surfaces

Moderators: Irene Groot, Leiden University, The Netherlands, William E. Kaden, University of Central Florida

2:20pm SS+2D+AP+AS+OX+SE-ThA-1 Adsorption, Reaction, and Diffusion of Energetic Reagents on Morphologically Diverse Thin Films, *Rebecca Thompson[12], M Brann, S Sibener,* The University of Chicago

I present work from two studies illustrating the impact of condensed-phase film morphology on reaction kinetics and surface adsorption. To begin, I will discuss the **oxidative reactivity of condensed propene films**. This work is conducted in a state-of-the-art ultra-high vacuum chamber equipped for operation at cryogenic substrate temperatures. Time-resolved reflection absorption infrared spectroscopy (RAIRS) is used to track propene reactivity when films are exposed to a supersonic expansion of ground state oxygen atoms, $O(^3P)$. I demonstrate that propene reacts significantly on exposure, producing primarily propylene oxide and propanal. Oxide production is significant; partial oxidation products are rarely observed in gas phase studies and olefin oxides are incredibly important chemical intermediates in a variety of industrial processes. Regardless of initial film thickness, the reaction follows zero order kinetics, with a calculated activation energy of 0.5 kcal mol^{-1}. This low barrier closely matches that reported in gas phase studies, suggesting that the condensed-phase reaction is likely diffusion-limited. I also highlight that the propene deposition temperature has a substantial impact on reactivity. Films deposited below 50 K produce dramatically different RAIR spectra that correspond to a more amorphous film composition. These films are nearly unreactive with $O(^3P)$, indicating that oxygen diffusion is directly tied to the density and ordering in the more crystalline film.

This dependence on film structure is also observed in the second study, which explores **embedding in and adsorption on crystalline, non-porous amorphous, and porous-amorphous water ice films**. Using a combination of supersonic molecular beams, RAIRS and King and Wells mass spectrometry techniques, I demonstrate that direct embedding into the bulk is remarkably insensitive to film structure; the momentum barrier is identical between amorphous and porous-amorphous ice films. Below this barrier, however, sticking probabilities differ considerably between the different films, suggesting that the pore structure is more efficient at dissipating incident energy. These discoveries are critical for the accurate quantitative modeling of molecular uptake and reactivity on icy astrophysical bodies such as comets and planetismals. When taken together, these two studies provide fundamental mechanistic insight into the sticking, diffusion, and reactivity of small molecules on complex films, with a specific emphasis on the impact of film morphology and organization.

2:40pm SS+2D+AP+AS+OX+SE-ThA-2 Oxidation of Semiconductors and Semimetals by Supersonic Beams of O_2 with Scanning Tunneling Microscopy Visualization, *Ross Edel[3], T Grabnic, B Wiggins, S Sibener,* The University of Chicago

Our research examines the oxidation of semiconductor and semimetal surfaces using a novel, one-of-a-kind instrument that combines a supersonic molecular beam with an in-line scanning tunneling microscope (STM) in ultra-high vacuum. This new approach to surface reaction dynamics provides spatiotemporal information on surface oxidation over nanoscopic and mesoscopic length scales. We have uncovered the kinetic and morphological effects of oxidation conditions on three technologically relevant surfaces: Si(111)-7×7, highly oriented pyrolytic graphite (HOPG), and GaAs(110). A complete understanding of the oxidation mechanism of these surfaces is critical due to their technological applications and roles as model systems. Samples were exposed to O_2 with kinetic energies from 0.4-1.2 eV and impingement angles 0-45° from normal, with STM characterization between exposures. In some cases, we were able to monitor the evolution of specific features by revisiting the same

nanoscopic locations. Our study of Si(111)-7×7 revealed two oxidation channels, leading to the formation of dark and bright reacted sites. The dark sites dominated the surface and exhibited almost no site selectivity while the bright sites preferred the corner sites of the 7×7 unit cell. Our observations suggest that two adsorption pathways, trapping-mediated and direct chemisorption, occur simultaneously. On HOPG, we found that different oxygen energies, incident angles, and surface temperatures produce morphologically distinct etching features: Anisotropic channels, circular pits, and hexagonal pits. Reaction probability increased with beam energy and demonstrated non-Arrhenius behavior with respect to surface temperature, peaking at around 1375 K. Finally, oxidation of GaAs(110) was found to proceed by two morphologically distinct, competing mechanisms: a homogeneous process leading to layer-by-layer oxide growth, and a heterogeneous process with oxide islands nucleating from surface defects. The rates of both mechanisms change with O_2 kinetic energy, with homogeneous oxidation dominating at lower energies (<0.7 eV) and heterogeneous oxidation with higher energies (≥1.0 eV). The results obtained in this work provide vital information about the morphological evolution and kinetics of semiconductor and semimetals, offering a comprehensive overview of the spatiotemporal correlations that govern oxidation dynamics on surfaces.

3:00pm SS+2D+AP+AS+OX+SE-ThA-3 Studying Molecule-Surface Interactions using Rotational Orientation Control of Ground-State Molecular Beams, *Gil Alexandrowicz,* Swansea University, UK **INVITED**

Performing quantum state selective experiments of molecule-surface collisions provides unique insight into the interaction potential. One particularly tricky molecular property to control and measure is the rotational projection states, i.e. the orientation of the rotational plane of the molecule. Previous data was mostly restricted to photo-excited/paramagnetic species. In this talk, I will describe the molecular beam apparatus which allows to control and measure the rotational orientation of ground state molecules [1], present new experimental results for H_2 colliding with ionic surfaces and discuss the future of this new technique in terms of studying molecule-surface interaction-potentials and modifying the outcome of reactive molecule-surface collisions.

[1] Nature Communications, 8, 15357 (2017).

4:00pm SS+2D+AP+AS+OX+SE-ThA-6 Diffusion of (100)-epitaxially Supported 3D fcc Nanoclusters: Complex Size-dependence on the Nanoscale, *King Chun Lai, J Evans,* Iowa State University

Diffusion of supported 3D nanoclusters (NCs) followed by coalescence leads to coarsening of ensembles of supported NCs via Smoluchowski Ripening (SR) which is a key pathway for degradation of supported metal catalysts. The dependence of the NC diffusion coefficient, D_N, on size N (in atoms) is the key factor controlling SR kinetics, and traditional treatments assumed simple monotonic decrease with increasing size. We analyze a stochastic model for diffusion of (100)-epitaxially supported fcc NCs mediated by diffusion of atoms around the surface of the NC. Multiple barriers for surface diffusion across and between facets, along step edges, etc. are chosen to accurately describe Ag [Lai and Evans, Phy. Rev. Materials 3 (2019) 026001]. KMC simulations reveal a complex oscillatory variation of D_N with N. Local minima D_N sometimes but not always correspond to N = N_c where the equilibrium Winterbottom NC structure is a closed-shell. Local maximum generally correspond to N = N_c + 3. The oscillatory behavior is expected to disappear for larger N above $O(10^2)$. Behavior has similarities to but also basic differences from that for 2D supported NCs [Lai et al Phys. Rev. B 96 (2017) 235406]. Through detailed analysis of the energetics of the 3D NC diffusion pathway (which involves dissolving and reforming facets), we can elucidate the above behavior as well as observed trends in effective diffusion barrier.

4:20pm SS+2D+AP+AS+OX+SE-ThA-7 Oxide Surface Formation on Rh Nanoparticle during O_2 Exposures Observed by Atom Probe Microscopy, *Sten Lambeets,* Pacific Northwest National Laboratory*; T Visart de Bocarmé,* Université Libre de Bruxelles, Belgium*; N Kruse,* Washington State University*; D Perea,* Pacific Northwest National Laboratory

Metallic surfaces may undergo a series of surface and subsurface structural and chemical transformations while exposed to reactive gases that inevitably change the surface properties. Understanding such dynamics from a fundamental science point of view is an important requirement to build rational links between chemical/structural surface properties and design new catalysts with desired performance or new materials with enhanced resistance to corrosion. The research presented here addresses the early oxide formation dynamics on a rhodium (Rh) single nanoparticle during O_2 exposures and reveals the inter-facet cooperation between

---

[1] **Morton S. Traum Award Finalist**
[2] **National Student Award Finalist**
[3] **National Student Award Finalist**

Rh{012} and Rh{113} facets, as well as the important role that the subsurface plays.

Field Ion and Field Emission Microscopies (FIM and FEM) enable correlative atomic to nanoscale imaging of the surface of a very sharp Rh needle, the apex size and shape of which models that of a Rh nanoparticle. FIM is used to map, with atomic lateral resolution, the Rh surface revealing a complex network of crystallographic facets, while FEM is used to observe and record O_2 dissociative adsorption and subsequent reaction with H_2 over this same surface of Rh in real-time with nano-scale lateral resolution. Since FEM imaging relies on local work function variations, it notably can be used to follow the fate of adsorbed oxygen atoms (O(ads)) on the Rh surface. As a result, we directly observe that the O_2 dissociative adsorption is mainly active on the Rh{012} regions. The application of Atom Probe Tomography (APT) provided a means to map the fate of the absorbed oxygen leading to bulk oxide formation through Rh{113} facets. Thus the correlative combination of FIM, FEM, and APT provides unique insight into the mechanism of bulk oxide formation starting from the dissociative oxygen absorption occurring at {012} facets and subsurface penetration of the adsorbed oxygen occurring through {113} facets. leading to a preferential accumulation of the oxygen within the bulk along the [111] direction. This work offers a unique methodology to explore the interactions between the different crystal facets of a complex surface, to explore the complex dynamics linking the surface and the bulk, and finally, offers exciting perspectives leading to a better understanding of heterogeneous catalysis and corrosion dynamics.

4:40pm SS+2D+AP+AS+OX+SE-ThA-8 Noncontact AFM on Oxide Surfaces: Challenges and Opportunities, *Martin Setvin,* TU Wien, Austria **INVITED**
Recent development of the noncontact atomic force microscopy (nc-AFM) has opened new possibilities in different fields – imaging of organic molecules [1], controlling the charge state of adsorbed species [2], or enhanced chemical resolution of surface atoms [3]. I will focus on the emerging possibilities and opportunities in the field of oxide surfaces and their surface chemistry.

The limits of atomic resolution will be illustrated on clean and water-exposed binary oxides like TiO_2, In_2O_3 or iron oxides. The enhanced chemical resolution of nc-AFM offers a unique opportunity for approaching complex materials with ternary chemical composition. This will be demonstrated on bulk-terminated perovskites $SrTiO_3$ and $KTaO_3$. A dedicated cleaving procedure [4,5] allows preparing flat regions terminated by domains of SrO/TiO_2 (or KO/TaO_2) with a well-defined atomic structure. The surface stability, point defects, electronic structure, and chemical properties of such surfaces will be discussed and linked to the incipient-ferroelectric character of these materials.

[1] Gross, L.; Mohn, F.; Moll, N.; Liljeroth, P.; Meyer, G., *Science* 2009, *325*, 1110

[2] Gross, L.; Mohn, F.; Liljeroth, P.; Repp, J.; Giessibl, F. J.; Meyer, G., *Science* **2009,***324*, 1428

[3] Sugimoto, Y.; Pou, P.; Abe, M.; Jelinek, P.; Perez, R.; Morita, S.; Custance, O., *Nature* **2007,***446*, 64

[4] I. Sokolovic, M. Schmid, U. Diebold, M. Setvin, *Phys. Rev. Materials* 3, 034407 (2019)

[5] M. Setvin, M. Reticcioli, F. Poelzleitner, J. Hulva, M. Schmid, L. A. Boatner, C. Franchini, U. Diebold, *Science* 359, 572-575 (2018)

5:20pm SS+2D+AP+AS+OX+SE-ThA-10 Edge-Enhanced Oxygen Evolution Reactivity at Au-Supported, Ultrathin Fe2O3 Electrocatalysts, *Xingyi Deng, D Kauffman, D Sorescu,* National Energy Technology Laboratory
Transition metal oxides have been emerging as promising candidates to replace the state-of-the-art IrO_2 electrocatalysts for oxygen evolution reaction (OER) in alkaline electrolyte, but their key structure-property relationships are often shadowed by heterogeneities in the typical catalyst samples. To circumvent this challenge, we have combined ultrahigh vacuum surface science techniques, electrochemical measurements, and density functional theory (DFT) to study the structure-dependent activity of well-defined OER electrocatalysts. We present direct evidence that the population of hydroxylated Fe edge-site atoms correlates with the OER activity of ultrathin Fe_2O_3 nanostructures (~0.5 nm apparent height) grown on Au(111) substrates, and the Fe_2O_3/Au catalysts with a high density of edge sites can outperform an ultrathin IrO_x/Au OER catalyst at moderate overpotentials. DFT calculations support the experimental results, showing more favorable OER at the edge sites along the Fe_2O_3/Au interface with lower predicted overpotentials resulted from beneficial modification of intermediate binding. Our study demonstrates how the combination of surface science, electrochemistry, and computational modeling can be used to identify key structure-property relationships in a well-defined electrocatalytic system .

5:40pm SS+2D+AP+AS+OX+SE-ThA-11 Adsorption and Reaction of Methanol on the Magnetite Fe₃O₄(001) Surface*, Matthew Marcinkowski,* Pacific Northwest National Laboratory*; K Adamsen,* Aarhus University, Denmark*; N Doudin, Y Yang Wang, S Smith, B Kay, Z Dohnalek,* Pacific Northwest National Laboratory
Methanol's interaction with iron oxide surfaces is of interest due to its potential as a hydrogen storage molecule, and from a fundamental perspective as a chemical probe for the reactivity of an oxide surface. We present here a study examining the adsorption and reaction of methanol on magnetite Fe_3O_4(001) at cryogenic temperatures using a combination of temperature programmed desorption (TPD), simulations, x-ray photoelectron spectroscopy (XPS), and scanning tunneling microscopy (STM). Methanol's desorption profile from Fe_3O_4(001) is complicated, exhibiting peaks at 145, 175, 238, and 273 K corresponding to the desorption of intact methanol, as well as peaks at 350 and 516 K due to the reaction of methoxy intermediates. The saturation of a monolayer of methanol corresponds to 4 molecules/ unit cell, equivalent to the number of surface octahedral iron atoms. We probe the kinetics and thermodynamics of the desorption of molecular methanol using inversion analysis. Deconvolution of the complex desorption profile into individual peaks allows for calculation of both the desorption barrier and pre-factor of each feature. Low temperature scanning tunneling microscopy is used to observe the structure corresponding to each of the molecular desorption features. 20% of the adsorbed methanol reacts to form a methxoy intermediate by 180 K, which remains on the surface above room temperature after intact methanol has desorbed. This methoxy reacts via one of two channels, a recombination reaction with surface hydroxyls to form additional methanol at 350 K, and a disproportionation reaction to form methanol and formaldehyde at 516 K. Only 20% of the methoxy species undergo the disproportionation reaction, with most of them reacting via the 350 K pathway. Our study provides a detailed view of the adsorption and reaction of methanol and its surface intermediate methoxy on Fe_3O_4(001).

Thin Films Division
Room A124-125 - Session TF+AS+EL+PS+RA-ThA

Characterization of Thin Film Processes and Properties
Moderators: Richard Vanfleet, Brigham Young University, Virginia Wheeler, U.S. Naval Research Laboratory

2:20pm TF+AS+EL+PS+RA-ThA-1 Phase Separation in III-V Semiconductor Thin Films*, Mark Twigg, N Mahadik, N Kotulak, S Tomasulo, M Yakes,* U.S. Naval Research Laboratory **INVITED**
Phase separation in III-V semiconductor alloys remains a problem that limits the performance of electronic materials. As the first stage in a comprehensive program addressing this issue, we have begun investigating an alloy system in which only the group III elements differ: InGaAs. Lattice-matched InGaAs alloy films were deposited at three temperatures (400, 450, and 500C) by molecular beam epitaxy on a (001) InP substrate.

According to kinetic instability theory, the critical temperature for spinodal phase separation in InGaAs is 814C, a temperature well above the growth temperatures used in this study [1,2]. Dark-field (DF) cross-sectional transmission electron microscopy (XTEM), using the composition sensitive g=002 reflection, was used to determine the amplitude of composition modulations averaged over the thickness of the XTEM sample. The amplitude of composition modulation was found to decrease with increasing growth temperature, yielding values of 0.6, 0.4, and 0.3 atomic percent for the growth temperatures 400, 450, and 500C, respectively, a trend in accord with kinetic instability theory. X-ray reflectivity and 2-dimensional small angle x-ray measurements also indicate that the 400C growth shows significantly greater phase separation than the 450 and 500C growths. Atom probe tomography indicates that the amplitude of composition modulation for the 400C growth is approximately 1 atomic percent, a value that compares favorably with the 0.6 atomic percent measured by DF XTEM.

The range of wavelengths for lateral composition modulation is found to extend from approximately 3 to 30 nm. According to the literature, such wavelengths have been found to depend on growth temperature for a number of III-V semiconductor alloys, in agreement with predictions based

on surface diffusion. Measurements of the composition modulation wavelength as a function of temperature have been performed by analyzing DF XTEM images recorded using the g=220 diffraction vector, from XTEM samples with the glue line along the rapidly-diffusing [110] direction. Fast Fourier Transform (FFT) power spectra recorded from each image allowed the dominant composition modulation wavelengths to be determined. Analyzing these wavelengths as a function of temperature yields the same activation energy (0.55 eV) as that found in surface diffusion measurements for In adatoms on the (001) InGaAs surface [3]; thereby confirming the role of surface diffusion in phase separation driven composition modulations.

[1] F. Glas, Phys. Rev.B, 62, 7393 (2000).

[2] I. P. Ipatova, V. G. Malyshkin, and V. A. Shchukin, J. Appl. Phys. 7198 (1993).

[3] Stevens et al., J. Appl. Phys. 121, 195302 (2017).

3:00pm TF+AS+EL+PS+RA-ThA-3 In-Situ Spectroscopic Monitoring of Methylamine-Induced Hybrid Perovskite Phase Transitions, *Jonathan Meyers*[1], *L Serafin, J Cahoon,* University of North Carolina at Chapel Hill
Lead halide perovskites have shown remarkable promise for use in thin film optoelectronic devices such as photodetectors, light-emitting diodes, and solar cells. Methods for casting thin films of perovskite have been extensively studied, and great improvements have been made in an effort to improve device efficiency and stability. A few reports have suggested some benefits to processing or post-processing techniques in a methylamine (MA) atmosphere, including healing grain boundary defects to create pinhole free films with grains on the order of tens of microns and improving crystallinity. The process can be observed spectroscopically as the MA induces a reversible phase change which bleaches the dark perovskite film. In this work, we perform the MA-treatment in a vacuum reactor while monitoring in-situ the UV-visible spectral response correlated with temperature and MA partial pressure. Clear evidence is found for the existence of a solid intermediate phase in transitioning from $MAPbI_3(s)$ to $MAPbI_3 \cdot xMA(l)$ and back again. We construct a phase diagram and demonstrate that the critical partial pressure of the phase transition changes from 10 to 500 torr between 25 and 120 °C. By tuning the kinetics of film crystallization, compact films with domains up to 80 µm can be produced.

3:20pm TF+AS+EL+PS+RA-ThA-4 Angle-Resolved HAXPES Analysis of Al_xO_y and Cu_xO_y Layers formed by Metal Salt Diffusion into a poly 2-vinylpyridine (P2vP) Polymer Layer, *Pierre Mani,* Universidad Autonoma de Ciudad Juarez, México*; M Snelgrove,* Dublin City University, Ireland*; P Rueff,* Synchrotron SOLEIL, France*; R Lundy,* Trinity College Dublin, Ireland*; J Bogan, R O´Connor,* Dublin City University, Ireland*; J Enríquez,* Universidad Autonoma de Ciudad Juarez, México*; M Morris,* Trinity College Dublin, Ireland*; G Hughes,* Dublin City University, Ireland
This work is motivated by the desire to develop a semiconductor device patterning technology based on precursor infiltration into block copolymer materials. Developing an understanding of the preferential infiltration of metal precursors into one of the polymer blocks is of critical importance to advance this patterning approach. In this study, metal salts were used as a means to diffuse metal ions into poly 2-vinylpyridine (P2VP) polymer brush layers (~4 nm), which had been deposited by spin coating onto silicon substrates. Thin P2VP films infused with aluminum nitrate and copper nitrate by a wet chemical process were analyzed with angle resolved hard x-ray photoelectron spectroscopy (AR HAXPES). This photoemission based technique gives a lot information about a variety of core levels.[1] The large sampling depth of HAXPES measurements (20-30nm) enabled details of the chemical composition of the thin film to be characterized and subsequent angle-resolved HAXPES measurements offered a robust analysis of the interfaces and discrete layers that are present in the films. These measurements displayed evidence of bonding interactions between the elements in the polymer film and the infiltrated salts, which assists in developing an understanding of the infiltration process which needs to be optimized for device fabrication applications.[2]

[1] P. G. Mani-Gonzalez, M. O. Vazquez-Lepe, F. Espinosa-Magaña, and A. Herrera-Gomez J. Vac. Sci. Technol., A 31, 010601 (2013).

[2] C. Cummins and M. A. Morris. Using block copolymers as infiltration sites for development of future nanoelectronic devices: Achievements, barriers, and opportunities. Microelectron Eng., 195:74–85, 2018.

4:00pm TF+AS+EL+PS+RA-ThA-6 Obtaining Smooth Surfaces and Measuring Surface Roughness, *Steven M. George,* University of Colorado at Boulder **INVITED**
Smooth surfaces are important in many areas including friction, adhesion, optics and film growth. Smooth surfaces can be obtained from rough surfaces using chemical mechanical polishing (CMP). Rough surfaces can also be smoothed using atomic layer deposition (ALD) if the conformal ALD film thickness is comparable with the lateral length scale of the roughness. In addition, rough surfaces can be smoothed using isotropic thermal atomic layer etching (ALE) if the ALE etch depth is comparable with the width of the surface asperities. Quantifying the degree of surface roughness after CMP, ALD or ALE is challenging. Surface roughness can be obtained using atomic force microscope (AFM) or x-ray reflectivity (XRR) measurements. However, the AFM and XRR techniques do not always agree. Some of the inconsistencies are attributed to the different lateral length scales for the AFM and XRR measurements. Using both AFM and XRR to characterize surface roughness is recommended for reliable measurements. In addition, XRR measurements for surface roughness should include both specular and diffuse off-specular scattering.

4:40pm TF+AS+EL+PS+RA-ThA-8 Characterizing Ultra-thin Layer Growth and Area Selective Deposition using High Resolution Low Energy Ion Scattering (LEIS), *Thomas Grehl,* IONTOF GmbH, Germany*; P Brüner,* ION-TOF GmbH, Germany*; V Pesce, B Pelissier, R Gassilloud, C Vallée,* Laboratoire des Technologies de la Microélectronique (LTM), France
When depositing ultra thin films of only very few nm of thickness, the characterization of the early stages of film growth is crucial for the quality of the film. For example, the initial thickness distribution before layer closure, created by the nucleation mechanism, will often remain after the film is complete. To analyze these early stages of growth requires very surface sensitive analytical techniques with good detection limits.

Specifically for area selective deposition, the demand for characterization increases even further. The deposition processes get more complex, involving atomic layer or plasma etching to remove nucleation on blocked areas. This also requires means of characterization, determining the effects of etching steps on the film being created, possible contamination and the level of success of the blocking.

One technique specifically suited for this application is Low Energy Ion Scattering (LEIS). By scattering noble gas ions from the surface of the sample, the mass of the atoms in the outer atomic layer is determined non-destructively. Due to specific charge exchange processes, the peaks in the scattering spectrum correspond only to the outer atomic layer, making LEIS the most surface sensitive technique to determine the elemental composition of a surface.

In addition, information from deeper layers is available in two ways: First of all, features in the spectrum contain information about the first few nm of the sample – especially for heavier elements, the in-depth distribution can be determined non-destructively. For more complex systems or light elements, sputter depth profiling can be applied as well.

In this presentation, we will illustrate the main features of LEIS on ALD films. The main part will be on an area selective deposition (ASD) process for Ta_2O_5 films on TiN or Si. Here, plasma-enhanced ALD (PE-ALD) and various plasma or ALE like etching processes, all using fluorine-containing compounds, are used to develop a super-cycle scheme for ASD. We show the effect of the different etching methods and use sputter depth profiling to determine the distribution of F – a light element not accessible to non-destructive depth profiling in LEIS. An important result is the distribution of F close to the surface, in the bulk of the film, or at the interface.

Besides this, some further sample systems will be used to highlight the use of LEIS for ultra-thin film characterization.

5:00pm TF+AS+EL+PS+RA-ThA-9 Real-Time Monitoring of Aluminum Oxidation Through Wide Band Gap MgF_2 Layers for Protection of Space Mirrors, *B Johnson, T Avval, G Hodges, K Membreno, D Allred, Matthew Linford,* Brigham Young University
Because of its extraordinary and broad reflectivity, aluminum is the only logical candidate for advanced space mirrors that operate deep into the UV. However, aluminum oxidizes rapidly in the air, and even a small amount of oxide (as little as a nanometer) can have a noticeable, detrimental impact on its reflectivity at short wavelengths. Thin films of wide band gap materials like MgF_2 have previously been used to protect aluminum surfaces. Here we report the first real-time, spectroscopic ellipsometry (SE) study of aluminum oxidation as a function of MgF_2 over layer thickness, which ranged from 0 – 6 nm. SE data analysis was

Thursday Afternoon, October 24, 2019

performed vis-à-vis a multilayer optical model that included a thick silicon nitride layer. The optical constants for evaporated aluminum were initially determined using a multi-sample analysis (MSA) of SE data from MgF_2 protected and bare Al surfaces. Two models were then considered for analyzing the real-time data obtained from Al/MgF_2 stacks. The first used the optical constants of aluminum obtained in the MSA with two adjustable parameters: the thicknesses of the aluminum and aluminum oxide layers. The thicknesses obtained from this model showed the expected trends (increasing Al_2O_3 layer thickness and decreasing Al layer thickness with time), but some of the Al_2O_3 thicknesses were unphysical (negative). Because the optical constants of very thin metals films depend strongly on their structures and deposition conditions, a second, more advanced model was employed that fit the optical constants for Al, and also the Al and Al_2O_3 thicknesses, for each data set. In particular, the Al and Al_2O_3 thicknesses and optical constants of Al were determined in an MSA for each of 50 evenly spaced analyses in each four-hour dynamic run performed. The resulting optical constants for Al were then fixed for that sample and the thicknesses of the Al and Al_2O_3 layers were determined. While the first and second models yielded similar Al and Al_2O_3 thickness vs. time trends, the film thicknesses obtained in this manner were more physically reasonable. Thicker MgF_2 layers slow the oxidation rate of aluminum. The results from this work should prove useful in protecting space mirrors prior to launch. Detailed surface/material analysis by X-ray photoelectron spectroscopy will also be shown, as well as more advanced SE modeling.

5:20pm TF+AS+EL+PS+RA-ThA-10 Visualization of Ultrafast Charge Motion in Thin Films via THz Emission Spectroscopy, *Aaron Lindenberg,* Stanford University **INVITED**
We describe a method for probing ultrafast time-dependent currents in thin films and heterostructures by recording the associated emitted electromagnetic fields. This detection scheme offers direct sensitivity to the flow of charges at the atomic-scale and enables a real-time probe for investigating ultrafast charge transfer processes at molecular interfaces. Applied to transition metal dichalcogenide heterostructures having a staggered (Type-II) band alignment, we observe a burst of electromagnetic radiation at terahertz frequencies following above gap excitation. The emitted electric field transients encode information about the charge transfer within the heterostructure. The polarity of the emitted field reflects the direction of the charge transfer and the polarity is reversed as the order of the bilayer within the heterostructure is altered. We find that the charge transfer proceeds at an ultrafast rate (~100 fs) indicating a remarkable efficiency for the charge separation across these atomic-scale bilayers.

We will also describe initial experiments and coupled theoretical efforts probing charge separation and ultrafast photovoltaic responses in multiferroic BFO periodic domain structures. We show that charge separation occurs dominantly at the domain walls and provide a quantitative estimate of the efficiency of this process.

Thin Films Division
Room A122-123 - Session TF+SS-ThA

Metal Halide Perovskites, Other Organic/Inorganic Hybrid Thin Films & Flash Session

Moderators: Mark Losego, Georgia Institute of Technology, Greg Szulczewski, The University of Alabama

2:20pm TF+SS-ThA-1 Tailoring Electrode-electrolyte Interfaces in Lithium-ion Batteries using Molecularly Engineered Functional Polymers, *Laisuo Su,* Carnegie Mellon University; *J Weaver,* National Institute of Standards and Technology (NIST); *M Groenenboom,* National Institute of Sandards and Technology (NIST); *B Jayan,* Carnegie Mellon University **INVITED**
The performance and stability of lithium ion batteries (LIBs) depend on charge transfer and reactions at electrode-electrolyte interfaces (EEI), making interfaces design a key issue. Here we molecularly engineer this interface using conformal, functional polymer nanolayers via a novel vapor-based deposition technique. We demonstrate that poly(3,4-ethylenedioxythiophene) (PEDOT) nanolayer doubles the capacities of $LiCoO_2$ at high rates and extends its 4.5 V cycling life by 260%. The improved rate performance is enabled by high diffusion coefficient of Li^+ in PEDOT measured from neutron depth profiling. Such behavior is further understood by density functional theory (DFT) simulation. The extended cycling stability comes from strong interactions between PEDOT and Co atoms, as suggested from X-ray photoelectron spectroscopy and DFT

simulations. Additionally, in-situ synchrotron X-ray diffraction reveals that PEDOT uniformizes current distribution and improves $LiCoO_2$ structural stability during cycling tests. This work adds understanding and provides guidelines for designing the EEI for advanced LIBs.

3:00pm TF+SS-ThA-3 Chemoselective Adsorption of Alkyne-functionalized Cyclooctynes for the Formation of Si/organic Interfaces, *C Laenger, Julian Heep,* Justus-Liebig-University, Giessen, Germany; *P Nikodemiak, T Bohamud,* Philipps-University, Marburg, Germany; *P Kirsten,* Justus-Liebig-University, Giessen, Germany; *U Hoefer, U Koert,* Philipps-University, Marburg, Germany; *M Duerr,* Justus-Liebig-University, Giessen, Germany
Controlled organic functionalization of the Si(001) surface may play an important role in the efforts towards further miniaturization of silicon based electronic devices. The first step of such an organic functionalization in terms of organic molecular layer deposition on Si(001) would be the chemoselective adsorption of bifunctional molecules on silicon: whereas one functionality binds to the surface, the other stays intact for the attachment of further layers. This task, however, is complicated by the high reactivity of the dangling bonds with respect to almost all organic functional groups. As a consequence, bifunctional organic molecules typically react via both functional groups on the silicon surface. We solved this problem using cyclooctyne as the main building block of our strategy. The strained triple bond of cyclooctyne reacts via a direct reaction channel, in contrast to most other organic functional groups, which react on Si(001) via a metastable intermediate. This makes the latter ones effectively unreactive in competition with the direct pathway of cyclooctyne's strained triple bond [1].

In this work, we focus on the preparation of a functionalized organic layer on Si(001) using an alkyne-functionalized cyclooctyne, i.e., ethynyl-cyclopropyl-cyclooctyne (ECCO). If the ECCO molecule binds chemoselectively to the silicon substrate via cyclooctyne's strained triple bond, the terminal, linear triple bond of the ECCO molecule can be employed for the attachment of the second layer of molecules, e.g., via alkyne-azide coupling. We first show that the linear triple bond follows an indirect reaction pathway via a weakly bound intermediate. XPS and STM results then clearly indicate that ECCO adsorbs selectively on Si(001) via a [2+2] cycloaddition of cyclooctyne's strained triple bond. No indication for a reaction via the ethynyl group was detected. This chemoselectivity was observed for all coverages, starting from the isolated molecules up to saturation coverage of one monolayer [2]. The ECCO molecules can thus form an organic functionalization of the Si(001) surface which can be used for controlled attachment of further molecular layers.

[1] Reutzel, et al., J. Phys. Chem. C **120** 26284 (2016).

[2] C. Länger, et al., J. Phys.: Condens. Matter **31** 034001 (2019).

3:20pm TF+SS-ThA-4 Durability of Property Changes in Polyester Fabrics Infused with Inorganics via Vapor Phase Infiltration, *Kira Pyronneau, E McGuinness, M Losego,* Georgia Institute of Technology
Vapor Phase Infiltration (VPI) is a processing method for transforming polymers into organic-inorganic hybrid materials. During VPI, a polymer is exposed to vapor-phase metalorganic precursors that sorb, diffuse, and react within the bulk of the polymer to create new hybrid materials. VPI has been shown to modify properties such as the mechanical strength of spider silk, the thermal and UV degradation resistance of Kevlar, and the fluorescence of polyester. This study aims to better understand how VPI can change textile properties for industrial applications and the durability of these changes. To this end, polyester fabrics were treated with trimethylaluminum (TMA) and co-reacted with water in a custom-built vacuum chamber. The temperature of the treatment process was varied from 60˚C to 140˚C to establish a relationship between processing temperature, physiochemical structure, and material properties. Using thermogravimetric analysis (TGA), these infiltrated fabrics were found to have inorganic loadings between 5 and 8 weight percent, with a maximum inorganic loading at 100 °C (Figure 1). These results are consistent with our current understanding of precursor / polymer sorption thermodynamics and indicate that processing temperature can be used to control the loading of inorganics through both the diffusion rate and the sorption equilibrium. To examine the durability of this inorganic loading, wash fastness testing at 100˚C for 90 minutes followed by TGA and SEM/EDX was used to determine the effects of high temperature wash cycles. These tests demonstrated that the inorganic loading remains even after intense laundering (Figure 2). To further characterize the durability of VPI treatment, known changes due to the VPI process were compared before and after washing. In particular, mechanical properties, fluorescence, and thermal degradation behavior were investigated. This talk will explore the

wash-fastness of VPI treatments of polyester at different processing temperatures and the retention of enhanced properties relevant to the textile industry.

4:00pm TF+SS-ThA-6 Materials Synthesis and Device Fabrication for Novel Inorganic Perovskites, *Mingzhen Liu,* UESTC, China   **INVITED**

In recent years, organic lead halide perovskite materials have attracted much attention due to their outstanding optoelectric properties and low manufacturing cost. To improve the stability of perovskite solar cells, inorganic $CsPbI_3$ perovskite has been demonstrated as promising material for solar cells owing to the superb photoelectronic property and composition stability. However, the low stability of perovskite phase $CsPbI_3$ (α-phase) with an appropriate band gap under ambient environment hinders its practical application.

Here, we investigate new ways of synthesizing inorganic perovskite materials and optimizing the device stability through dimensional engineering. we tailor the three-dimension $CsPbI_3$ perovskite into quasi-two-dimensional $Cs_xPEA_{1-x}PbI_3$ perovskite, where an optimal $Cs_xPEA_{1-x}PbI_3$ film remains stable in α phase up to 250℃. Moreover, we further present an in-depth investigation of the so-called stable 'α-$CsPbI_3$,' especially the starting material hydrogen lead trihalide ($HPbI_3$, also known as $PbI_2 \cdot xHI$) that is usually used for synthesizing α-$CsPbI_3$. We notice that the "mythical" $HPbI_3$, the often-assumed reaction product of HI and PbI_2, does not actually exist. Instead, adding acid to DMF is known to generate a weak base dimethylamine (DMA) through hydrolysis, and with the presence of PbI_2 the actual final product is believed to be a compound of $DMAPbI_3$. Our findings offer new insights into producing inorganic perovskite materials, and lead to further understanding in perovskite materials for solar cells with improved efficiency and stability.

4:40pm TF+SS-ThA-8 Carrier-Gas Assisted Vapor Deposition of Metal Halide Perovskite Thin Films, *Catherine Clark,* University of Minnesota*; E Aydil,* New York University*; R Holmes,* University of Minnesota

Hybrid organic-inorganic halide perovskites have emerged as an important class of optoelectronic materials with potential applications in photovoltaics and light emitting devices. One of the challenges in forming thin films of halide perovskites is controlling stoichiometry and morphology. We have designed and built a carrier-gas assisted vapor deposition (CGAVD) system capable of depositing halide perovskite thin films (*e.g.,* $CH_3NH_3SnI_xBr_{3-x}$) with independent control over their stoichiometry and morphology. In our CGAVD system, an inert carrier gas (N_2) transports sublimed material vapors through a hot-walled chamber to a cooled substrate where they selectively condense and/or react. By separately controlling the precursor sublimation rate, *via* source temperature, and the transport rate to the substrate, *via* carrier gas flow rate, we realize fine control of species flux at the substrate and successfully co-deposit materials with very different vapor pressures (*e.g.* $CH_3NH_3Br, SnBr_2$). Four additional independent parameters (dilution gas flow, chamber pressure, gas temperature, and substrate temperature) can be varied to access a wide range of deposition conditions and film morphologies with controlled stoichiometry. To navigate the vast parameter space of CGAVD, we use an experimentally validated transport and reaction model, which informs the deposition parameter selections. We find that repeatable and spatially uniform deposition requires operating in a regime where solid source material is at equilibrium with its vapor and convective transport determines the flux of species arriving at the substrate. Importantly, we find that films grown using CGAVD have a stoichiometric "self-correcting" and robust operation window, wherein excess precursor flux during co-deposition is rejected from the film and a phase-pure perovskite film results. This is practically advantageous as it relaxes the need for balancing precursor fluxes exactly during co-deposition. We demonstrate the growth of $CH_3NH_3SnI_xBr_{3-x}$ thin films with a wide range of stoichiometries and morphologies. Specifically, by tuning the source material temperature (140 °C – 290 °C), the carrier gas flow rate (2 sccm – 100 sccm), the substrate temperature (8 °C – 70 °C), and the chamber pressure (350 mTorr – 10 Torr), we realize corresponding changes in grain orientation and grain size from <100 nm to over 1 μm. CGAVD is a promising approach to deposition of other halide perovskites and can potentially enable the growth of previously inaccessible morphologies and multi-layer perovskite films.

5:00pm TF+SS-ThA-9 Synthesis and Optical Properties of Organo-halide 2D Perovskites, *Misook Min, A Kaul,* University of North Texas

Organic-inorganic halide perovskite materials have attracted interest in recent years due to their excellent optoelectronic properties, such as high absorption coefficient, tunable band gap, small exciton binding energy.

These advantages combined with the extremely low fabrication coat make this kind material suitable as a light absorber for solar cells, light emitting diodes, field-effect transistors and photo-detectors [1]. Hybrid organic-inorganic perovskite described by the formula ABX_3 (A = organic ammonium cation, B = inorganic compounds, X = halide anion). Specifically, the iodide and bromide versions of $CH_3NH_3PbX_3$ have led to a breakthrough in various research field. We report the scalable synthesis and properties of the 2D series of lead iodide $(CH_3(CH_2)_3NH_3)_2(CH_3NH_3)_{n-1}Pb_nI_{3n+1}$($n$ = 2, 3, and 4) perovskites [2]. The 2D $(CH_3(CH_2)_3NH_3)_2(CH_3NH_3)_{n-1}Pb_nI_{3n+1}$ were synthesized and materials characterization was conducted using atomic force microscopy (AFM), X-ray diffraction (XRD), and Photoluminescence (PL) spectroscopy. The crystal structure and surface morphology for n = 2, 3, and 4 perovskites was validated using XRD and AFM, and the peak optical absorption was consistent with the composition-tunable bandgap for these formulations occurring at ~ 2.18 eV, 2.06 eV, and 2.03 eV. Our results show that hybrid organic-inorganic perovskites can be easily and efficiently prepared. Also, the hybrid organic-inorganic perovskites define a promising class of stable and efficient light absorbing materials for photo-detectors and other applications.

5:20pm TF+SS-ThA-10 Encapsulation of Perovskite Nanocrystal Solids using Metal Oxides - A Closer Look into Optical Properties, *Riya Bose, Y Zheng, T Guo, Y Garstein, A Malko,* University of Texas at Dallas

The performance (i.e., light harvesting, optical gain or emission outputs) of many optoelectronics devices (i.e., lasers, photovoltaics (PVs), light emitting diodes (LEDs), etc.) critically depends on the ability to deposit solution processed nanocrystals (NCs) into well-organized, close-packed solids with high photoluminescence quantum yields (PL QYs) and the long term stability of NC films. However, irrespective of the high quality of NCs or the passivation techniques used in solution, the deposition of NC multilayers as well as the exposure to the environment during solid state device fabrication often require or lead to changes in the NCs chemical environment, such as exchange/loss of ligands, which eventually lead to formation of trap states that decrease the PL QYs of NCs and are often detrimental to device performances. An attractive approach to protect the NCs' integrity is the use of atomic layer deposition (ALD) in which self-limiting surface reactions of the precursors allows conformal growth of the metal oxide layer with precise thickness control to encapsulate NCs. This process, though prevents the deterioration of NCs, is observed to decrease their PLQY significantly. To mitigate this issue, we recently developed an alternate gas phase deposition technique where a pulsed co-deposition of both metal and oxidant precursors at room temperature (RT) (reminiscent of chemical vapor deposition, CVD) is able to deposit uniform metal oxide (AlO_x) films, originating from gas-phase reactions in the immediate vicinity of the NC layer. Unlike conventional ALD, this method is observed to preserve the optical properties, e.g., PLQY and lifetime of metal chalcogenide NCs film. With this new approach, we investigate the encapsulation of hybrid metal halide perovskite NCs, which have been at the forefront of recent optoelectronic materials research due to their high absorption coefficients, high charge carrier mobilities, balanced ambipolar transport properties, and easy solution processability. However, in spite of the exceptional upsurge in the lab scale device efficiency of perovskites in a remarkably short time frame, the practical application of the same in real world is restricted by their inherent instability. AlO_x deposition on perovskite nanocrystals with our modified approach not only retains the optical properties of the NCs, but also improves them, even at a single particle level, which paves the way for unique optoelectronic opportunities.

Atomic Scale Processing Focus Topic
Room Union Station AB - Session AP-ThP

Atomic Scale Processing Poster Session

AP-ThP-1 Atomic Resolution Characterization of Atomic Layer Etching Normally-off AlGaN/GaN Hetrostructure Device by Using Aberration-corrected STEM, *Chien-Nan Hsiao,* Taiwan Instrument Research Institute, National Applied Research Laboratories, Taiwan, Republic of China; *C Lin, C Chen, M Chan, W Chen, F Chen,* National Applied Research Laboratories, Taiwan, Republic of China

An in-situ plasma enhanced atomic layer etching system has been design and fabricated. N_2O , BCl_3 and Ar plasma were used as the precursor for III-group epitaxy layer at various temperature. The optical detector was used to in-situ monitor the plasma spectrum during the step by step etching process. The AlGaN/GaN hetrostructure of normally-off high power GaN device (150 V) and etching per cycle of ALE were investigated using an aberration-corrected scanning transmission electron microscope with energy distribution spectrometer. It is found that the layer by layer etching feature shows the process is a controlled self-limited reaction. In addition, the influence of various aberration coefficients such as defocus, astigmatism, coma, spherical aberration and star aberration on the shape of the probe and more importantly on the electron intensity distribution within the probe was calculated. The accuracy required for compensation of the various aberration coefficients to achieve sub-angstrom resolution (0.078 nm) with the electron optics system was evaluated by the calculation of phase shift. Furthermore, the saturation curve of atomic etching rate and precursor pulsed time has been established. The etching per cycle of AlGaN is around 0.33 nm.

AP-ThP-2 Programmable Radical-Assisted Sputtering Enabling Designed Deposition Processes with Atomic Layer Accuracy, *Hideo Isshiki, Y Tanaka,* The University of Electro-Communications, Japan; *S Saisho,* Shincron Co. LTD., Japan

A programmable multi-cathode plasma generator (PMCPG), which consists of a high voltage DC power supply, a multichannel digital pattern generator (DPG), and a high voltage switch (HV-SW) attached to each cathode, was developed. We have applied PMCPG to radical-assisted sputtering (RAS) process, and called it "Programmable RAS (PRAS) ". The RAS system provided by Shincron has been widely used for mass production on the optical thin film coating of metal oxide compounds. RAS process is a process alternating metal ultra-thin layer deposition and radical reaction on the metal surface deposited just before. Conventional RAS system needs a large space to spatially separate above two steps. RAS process has a possibility to realize functional materials controlled with atomic layer accuracy. Therefore, the laboratory size RAS system is required to advance the development of functional material devices. We noticed that RAS process can be performed by switching between the metallic mode and the reactive mode found in reactive sputtering. So we have developed PMCPG to enable the time-separated RAS process.

DC pulse plasma on each cathode is generated by direct drive of DC power supply using DPG and the attached HV-SW, and a certain metal sputter is performed selectively under the metallic mode. On the other hand, radical source gasses are fed into the chamber synchronized with the plasma generation on the other cathode, generating the radicals. At the same time, the deposition rate decreases abruptly because of shift to the reactive mode with skipping over the hysteresis region. In this way, the radical reactions on a deposited metal surface proceed preferentially, and then RAS process is complete. The process cycle corresponding to a metal oxide monolayer was estimated to be a few seconds. We also confirmed that the plasma generation using the electronic switching system follows the pulse train more than 50kHz. From the fact that DPG can generate various pulse train for the plasma generation, it is suggested that PRAS enables designed deposition processes with atomic layer accuracy. In this work, YSZ and cubic $(Er_{0.1}Y_{0.9})_2Zr_2O_7$ were successfully synthesized by PRAS. Typical deposition rate of transparent YSZ was more than 1.5µm/hour, indicating the reproduction of RAS process. Layer-by-layer deposition of cubic $(Er_{0.1}Y_{0.9})_2Zr_2O_7$ was also confirmed through X-ray diffraction. This system has four cathodes and can meet the requirements for plasma generation on each cathode independently. We expect that PRAS system enables an artificial material synthesis driving "the materials informatics".

You can find the demo of PMCPG at http://www.flex.es.uec.ac.jp/?page_id=243.

Applied Surface Science Division
Room Union Station AB - Session AS-ThP

Applied Surface Science Poster Session

AS-ThP-1 Hydrogen Generation Eases Safety and Infrastructure Requirements for Efficient and Productive Vacuum Deposition Processes, *David Wolff,* Nel Hydrogen

Hydrogen is frequently employed as a backfill gas during various vacuum coating processes involving metals. Hydrogen plays several roles and provides multiple benefits:

- As a carrier gas and diluent for active gases used to modify substrate surfaces

- As a cleaning and protective agent to clean deposition surfaces and prevent oxidation at high temperatures

- High purity hydrogen is relatively inexpensive, safe and effective in this application when used properly

The major challenge with hydrogen is the storage of hydrogen often required to have a source of pure hydrogen gas. Hydrogen gas for small and medium scale applications is generally delivered from far-away generating facilities and stored at the customer's site in the form of a compressed gas. Storage of hydrogen is closely controlled by national and international code guidelines and local Authorities Having Jurisdiction.

Proton Exchange Membrane (PEM fuel cell technology) hydrogen generation makes it possible to generate hydrogen at production rates and purity levels suitable for scientific and production applications. Most importantly, PEM hydrogen generation produces pure, pressurized, dry hydrogen in a load-following fashion without the need for hydrogen storage.

Poster will outline the code and cost advantages that PEM hydrogen generation can provide for scientific and production hydrogen use in vacuum applications.

AS-ThP-2 Progress in Understanding SIMS Spectra from Silicones, *Paul Vlasak, M Pacholski,* The Dow Chemical Company

The unique properties of poly(dimethylsiloxane), also known as PDMS or silicone, have allowed PDMS-based materials to proliferate in modern industry. A huge variety of applications using PDMS have been developed including structural adhesives, release agents, optical components, lubricants, anti-foam agents, and potting agents to name a few. Considering the omnipresence of PDMS in industrial settings along with its low surface energy and tendency to migrate, it comes as no surprise that PDMS is frequently encountered in industrial surface analysis laboratories. Because PDMS is readily detected and easily recognized by its characteristic fragmentation pattern, SIMS is well suited to identifying the presence of silicones on a wide range of materials.

Over the years we have observed variation in the fragmentation patterns and relative intensities of characteristic ions in the SIMS spectra from assorted PDMS-containing materials, however, the structural details that may influence the observed spectra remain poorly understood. In the past, we confirmed that endgroup type and molecular weight of PDMS fluids have a systematic influence on negative ion spectra. In addition, we determined that substrate type and thickness of the PDMS layer also greatly influence the spectra obtained, allowing us to hypothesize that the differing energy distributions and collisional cascades within the films and substrates strongly influence ion yields [1].

Using well-characterized PDMS reference materials spin-coated on a variety of substrates, the effects of cluster ion versus monoatomic ion sputtering will be presented as an extension of our past work. In addition, we previously demonstrated that spectra from a particular PDMS fluid became independent of substrate type as film thickness increased beyond the penetration depth of the primary ions, while current work further explores the sub-monolayer regime. Lastly, using thin films of various PDMS mixtures, investigation of potential layering of PDMS as a function of molecular weight or endgroup type will be presented.

[1] Vlasak, P.R.; Pacholski, M.L. (2018, October) *Differentiating Silicones Using SIMS*; presented at AVS 65th International Symposium & Exhibition, Long Beach, CA.

AS-ThP-3 Silicon Wet Etching Using NH4OH Solution For Texturing of Silicon Micro-Channels, *José Alexandre Diniz, A Silva,* UNICAMP, Brazil

This work presents the surface texturing of the horizontal wall of silicon micro-channels (SiMCs) using the NH4OH solution. The micro-channels are obtained on the backside of Si substrates, where the solar cells are fabricated. The micro-channels are used as heat sinks through which fluid will flow, such as water or alcohol. The texturing results in the micro-channels with roughness (in micro-pyramid shape) on horizontal surface. The roughness assists in the dilution of bubbles that can occur inside the fluid, because if the bubble excess occurs into the fluid, this can difficult the transport into the SiMC. The texturing is based on the formation of micro-pyramids with the use of NH4OH (ammonium hydroxide) alkaline solution etching, which is anisotropic. Our NH4OH solution etching can control the size of micro-pyramids on the surface into the SiMC This occurs because the etch rates are different for three [100], [110] and [111] Si crystal planes. The Si etching is due to the presence of the OH- (hydroxyl) in the NH4OH solution that reacts with Si. The micro-pyramids occurs because the (100) mono-crystalline substrates have a lower Si surface density of the plane than the (110) plane. The difference in density causes the etch rate for (100) plane to be greater than (110), which in turn, is greater than for (111). Thus, since it is a surface with lower density is easier penetration of the solution, which facilitates the Si reaction with hydroxyl (OH -). Anisotropic etching is obtained by alkaline solution of monocrystalline Si substrate, with (100) surface orientation. Exposure of [111] crystal plans occurred, forming the micro-pyramids. The obtained values of micro-pyramid height of 770 nm and 920 nm, when compared with a desired micro-channel depth of 200 μm, represent a ratio (between roughness and channel depth) lower than 5%. This ratio is considered suitable to reduce a significant impact on micro-channel performances.

AS-ThP-4 Ionic Liquids: Advanced Oil Additives for Lubricating Case-Hardened Titanium Alloys (OD-Ti64), *Harry Meyer III, H Duan, W Li, C Kumara, Y Jin, H Luo, J Qu,* Oak Ridge National Laboratory

Titanium alloys possess many excellent characteristics (corrosion resistance, high fatigue strength and high strength-to-weight ratio) that has led to many important applications in several field (aerospace, bioengineering, automotive, etc.). However, these same alloys have only limited use as tribological materials due to abrasion and adhesion resistance. We previously investigated the use of oxygen-diffused Ti64 (OD-Ti64) and found that, in dry sliding conditions, the oxygen diffusion treatment improved the wear resistance compared to untreated Ti64. OD-Ti64 performed better than untreated Ti64, with respect to wear resistance when a lubricant containing ZDDP because of the formation of a ZDDP-based protective triobfilm.

This study extends these previous investigations by evaluating the use of ionic liquids (ILs) as oil additives to lubricate oxygen-diffusion (OD) case-hardened titanium for improved friction and wear behavior. A base oil for boundary lubrication of an OD-treated Ti-6Al-4V sliding against a steel ball was tested using four oil-soluble ILs used as additives. This poster will present data that will show (1) the ILs improved the friction behavior to various extents; (2) two phosphate ILs clearly outperformed conventional ZDDP; (3) ILs exhibited excellent wear protection suggesting good material-chemical compatibility; and (4) the carboxylate IL protected the OD-Ti surface from any measurable wear. The morphology and chemical composition of the worn surfaces and tribofilms were examined using a combination SEM, TEM, EDS, and XPS.

AS-ThP-5 Controlling Surfaced-catalyzed Coupling of Aryl Halides for Preparation of Two-dimensional Covalent Networks, *Margaret Wolf, C Gerber, R Quardokus,* University of Connecticut

Formation and design of two-dimensional carbon-based materials can be controlled through surface-catalyzed reactions of small molecules. We use low-temperature scanning tunneling microscopy (LT-UHV STM) to monitor and characterize the surface-catalyzed reaction of dibromobenzene and dibromobithiophene. The Ullmann-like and Yamamoto-like coupling on Au(111) lifts the gold herringbone reconstruction and the gold atoms and coupled adsorbate are mobile at 4 K. Annealing results in two-dimensional covalent networks and restores the gold herringbone reconstruction.

AS-ThP-6 Characterization of Mineral Associated Organic Matter in Alkaline Soil, *Mark Engelhard, R Kukkadapu, T Varga, R Boiteau, L Kovarik, J Cliff, M Wirth, A Dohnalkova, C Smallwood, D Perea, J Moran, K Hofmockel,* Pacific Northwest National Laboratory

Warden Soil (alkaline, fine sandy loam) from Prosser, WA was characterized by a suite of spectroscopic and microscopic techniques to gain insights into the nature of mineral-associated soil organic matter (SOM) and its stability under environmental perturbations (e.g., after spiking the soil with siderophores, fluctuating redox conditions, etc.). This approach was undertaken since: a) SOM associated with minerals has been recognized to be relatively stable with respect to biological degradation compared with particulate organic matter (POM), and b) the stability of mineral-OM moieties is primarily a function of interaction between the mineral and OM type, and their physical accessibilities by organisms, oxidants, etc.

Coupled Mössbauer spectroscopy and XRD measurements revealed that ~60-65% of total Fe (5.5 wt.%) in the soil was present in feldspars. The balance of the Fe was primarily partitioned as magnetite, ilmenite, and a suite of nano-Fe(III)-oxides. Various forms of Ca were evident in TEM as: a) "Ca-OM polymers", b) $CaCO_3$ coated with Ca-OM (consistent with XPS results), and c) Ca feldspar. OM-coated magnetite particles were also evident in TEM results. XPS measurements also demonstrated various types of surface organic C (20-25× that of bulk): a) aliphatic and aromatic C-(C-H), such as C-C, C=C, C-H, b) C-(O,N) bonds as in carbohydrates and amines, c) C displaying bonds to oxygen as in aldehydes, ketones, and amides (C=O, O-C-O, O=C-N), and iv) carboxylic C (O-C=O. NanoSIMS results of ^{13}C- and ^{15}N-labeled siderophore-spiked soils showed that Ca-OM phases rather than Fe-OM phases were preferential hosts for siderophores implying weaker but quickly forming interactions were preferentially established and stable enough to exist in calcareous environments. This provides a potential explanation of the lack of pyoverdines/catechols (siderophores) observed in grassland soils, and more broadly demonstrates the importance of adsorption kinetics rather than thermodynamic equilibrium on the fate and preservation of SOM.

AS-ThP-7 Atomic Structure Simulation of Nitrogen Supersaturated Austenitic Stainless Steel, *Honglong Che, M Lei,* Dalian University of Technology, China

Low temperature nitriding of Fe-Cr-Ni austenitic stainless-steel forms a nitrogen supersaturated layer that owns a composite property of wear and corrosion resistance. It is widely used in the industry, and nuclear power plant is a very important application for its stringent performance requirements. To understand the nature of this nitrogen supersaturated layer, a serial systematically composition changed Fe-Cr-Ni austenitic stainless steel in three groups are prepared, nitrided and investigated. It is confirmed that the nitrided layers on all the Fe-Cr-Ni austenitic alloys are consistent of duplex structure of outer γ -Fe N like ordered$γ'_N$ and inner $γ_N$, althougha featureless continuous layer is observed with light-optical microscopy and a gradual decrease in nitrogen content is measured with EPMA when the alloys with a Cr-content over 12 wt. %. Cell model based on Cr-N and Fe-N interaction that considered the atomic construction of octahedral interstice is built that can explain the composition and structure evolution during the alloy composition change. The Cell Model is also used to calculated the average nearest neighbor nitrogen atoms (ANNNA) around Cr and Fe, which well explained the extended X-ray absorption fine structure (EXAFS) experiment results in both as nitrided and denitrided of 304 and 316 stainless steel. It further confirmed the reasonability of Cell Model and revealed the atomic structure of the $γ'_N$ and $γ_N$ phase.

AS-ThP-8 Determination of the Number of Layers of a 2D Material by Angle-Resolved Photoelectron Spectroscopy, *P Tyagi,* University at Albany - SUNY*; Carl A. Ventrice, Jr.,* SUNY Polytechnic Institute

The electronic structure of most 2D materials depends on the number of molecular layers and the stacking sequence between the layers. Therefore, it is important to have a non-destructive technique for analyzing the overlayer coverage of a 2D material directly on the growth substrate. A technique for determining the number of molecular layers using angle-resolved XPS has been developed. The system that will be presented is graphene growth on CuNi substrates, where controlled growth of multilayer graphene films can be performed. Since single atomic layer graphene films can be grown on Cu substrates, these samples are used as a standard reference for a monolayer of graphene. HOPG is used as a standard reference for bulk graphite. The electron mean free path of the C-

1s photoelectron can be determined by analyzing the areas under the C-1s peaks of monolayer graphene/Cu and bulk graphite. With the electron mean free path, the graphene coverage of a film of arbitrary thickness can be determined by analyzing the area under the C-1s of that sample. In principle, this technique can be used to determine the thickness of other 2D materials if a sample with a single molecular layer can be prepared.

AS-ThP-9 Effect in Core Level Binding Energy Spectra of Phthalocyanine (MePcs) Functionalized Carbon Nanotubes Studied by XPS and DFT, *Lázaro Huerta,* Instituto de Investigaciones en Materiales, México; *E Basiuk, V Basiuk,* Universidad Nacional Autonoma de México, México; *R Escamilla,* Universidad Nacional Autónoma de México, México; *M Flores,* Universidad de Guadalajara, México, Mexico

In this work was studied single-walled carbon nanotubes (SWNT) functionalized with noncovalently bonded hybrids of 3d transition metal (Me) phthalocyanines MePcs by X-ray photoelectron spectroscopy (XPS) and density functional theory (DFT).

The transition metal Me 2p core level spectra exhibit a series of details, specifically shake-up and multiplet splitting. This latter can affect BE values for an electron from any orbital, as occurs in the links of the phthalocyanines under study, before and after interacting with the surface of the wall single-walled carbon nanotubes, in which not only the splitting occurs but, literally, bonds disappear, although its physical-chemical meaning is that its energy becomes indistinguishable.

The approximate XPS spectra measurements for neat MePcs (where Me=Co, Ni, Cu and Zn). and MePc+SWNT hybrids show very strong interactions between macrocyclic complexes and carbon nanotube sidewalls and found the existence of one N 1s component for noncovalent MePc+SWNT complexes versus three components for neat phthalocyanine β-polymorphs. As well the decrease of multiplet splitting and the increase of spectral resolution, observed for both N 1s, C 1s and Me 2p peaks as a result of phthalocyanine deposition onto SWNTs.

Density functional theory (DFT) studies, showed high absolute values of binding energies and show that the macrocycles (of MePcs) suffer strong bending distortion in order to increase the area of their contact with nanotube sidewall. The combination of XPS and DFT helps the final explanation.

AS-ThP-10 Probing the Electrical Double Layer by *in situ* X-ray Photoelectron Spectroscopy through a Carbon Nanotube-Strengthened Graphene Window, *P Wang, Yunfeng Li, L Wang, J Klos, Z Peng, N Kim,* University of Maryland, College Park; *H Bluhm,* Lawrence Berkeley National Laboratory; *K Gaskell, S Lee, B Eichhorn, Y Wang,* University of Maryland, College Park

A detailed description of the electrical double layer structure formed at the electrode-electrolyte interface is very important for both fundamental understanding in many electrochemical processes and further advancements in energy storage devices. However, the electrical double layer is deeply "buried" by the bulk electrolyte solution, leading to significant signal loss and low detection resolution when measuring the interface structure from the electrolyte side. Here, we report the fabrication of a novel transparent electrode made of a graphene-carbon nanotube hybrid membrane that allows us to detect the electrical double layer from the solid side of the electrode using X-ray photoelectron spectroscopy. The robust and ultrathin nature of the hybrid membrane enables the detection of different elements with excellent photoelectron signals. By *in situ* monitoring the concentration changes of cations and anions under different local electrical potentials, we experimentally decipher the chemical structure of the electrical double layer, which is consistent with theoretical predictions.

AS-ThP-11 Antibacterial Performance of Electrically Activated Conductive Water Filter Papers, *Dorina Mihut, A Afshar, L Lackey,* Mercer University

Silver and copper thin films were coated on commercially available 3 M water filter papers using DC high vacuum magnetron sputtering technique. The filter papers (10 X 7 cm size) are flexible structures consisting of nonconductive fibers and metallic nanoparticles were deposited with 300 nm and 1 µm thicknesses resulting in a complete coverage of the fibers surface. Both silver and copper thin films deposited on water filter paper are effectively working against common types of harmful bacteria that are found in waste water. The research is investigating the possibility of creating electrically conductive structures and the synergistic antibacterial effect obtained by using metallic thin films deposited on water filter paper and an electrical current applied to the structures. The antibacterial activity of electrically conductive structures was tested by applying an increased

electrical potential. The morphology of the coatings and their adherence to the water filter paper was examined using the digital optical microscopy and Scanning Electron Microscopy and their chemical composition was investigated using the X-ray diffraction technique. A ll thin films showed good adhesion to water filter fibers and ensured a high area of exposure to contaminated water. The antibacterial effect of different conductive thin films was characterized by using the standardized membrane filtering technique for water and wastewater examination. The testing media (i.e. contaminated water) containing bacterial samples were collected from local wastewater basins. Water was tested for the bacterial content before and after the exposure to conductive thin films coated filters.

AS-ThP-12 Biocompatible and Robust Non-wetting Surface Inspired by Three Natural Organisms: Lotus Leaf, Mussel, and Sandcastle Worm, *Kiduk Han,* POSTECH, Republic of Korea; *T Park,* POSTEC, Republic of Korea; *H Cha, K Yong,* POSTECH, Republic of Korea

When the contact angle of water to a specific surface exceeds 150°, the surface is referred to as superhydrophobic (SH) surface. This SH surface has been developed by mimicking the Lotus leaf structure and it is useful for preventing structural deformation, oxidation and contamination of materials that can be affected by water. However, the SH surface has a limitation in practical use due to its poor physical durability, and there has been a great difficulty in applying it to research fields such as medical and tissue engineering due to the biohazard of its components. To overcome these problems, we have developed a technique for producing biocompatible and robust SH surfaces using mussel adhesive-protein adhesive (iMglue), and have applied this technology to catheters and patches to confirm its biomedical utility. The nanoparticles were deposited on the iMglue by dip coating and spray coating method, and the surface energy of the particles was lowered through chemical reaction to produce a water repellent surface. This surface is expected to play an important role in biomedical field due to its antibacterial and wound closure capabilities.

AS-ThP-13 In-situ ToF-SIMS Analysis of FIB Prepared Li Ion Battery Anodes, *Vincent Smentkowski, R Hart, H Cao,* GE-Research; *F Kollmer, J Zakel, H Arlinghaus,* IONTOF GmbH, Germany

Depth profiling (1D or 3D) is often used to determine the depth distribution of species in a material. Depth profiling works well when the surface of a sample is smooth and when the depth(s) are in the nm to micron thickness range. For thicker layers, one can mount the material in epoxy and generate a cross section which can be imaged. Unfortunately, cutting and polishing often damages (or at least smears) fragile materials such Li ion batteries. Over the two past decades, Focused Ion Beam (FIB) has proven to be a viable approach to expose sub surface layers 10s of microns thick which is often analyzed by SEM or TEM in conjunction with EDS [1]. Unfortunately, most EDS detectors are not able to detect light species such as Li and C (especially at the degraded vacuum which most SEM's operate under), and definitely can not detect H. ToF-SIMS not only detects all elements (and their isotopes), it also allows for the analysis of molecular fragments which is often critical for understanding the material. FIB/ToF-SIMS has been used to analyze other material systems [2, 3].

In this late breaking poster, we will provide preliminary in-situ FIB/ToF-SIMS results which were generated on an anode taken from a Li ion battery. In order to simultaneously obtain high lateral resolution images at high mass resolution, the delayed extraction data collection mode was utilized [4]. The advantages of multivariate statistical analysis (MVSA) for these complex data sets will be demonstrated.

[1] Lucille A. Giannuzzi, and Fred A. Stevie, Eds., "Introduction to Focused Ion Beams", Springer-Verlag US (2005) DOI: https://doi.org/10.1007/b101190.

[2] Felix Kollmer, D. Rading, R. Moellers, H.-G. Cramer, Wolfgang Paul, Ewald Niehuis, "Novel Cluster Ion Beams For Secondary Ion Generation, Sputtering And FIB/SIMS Application", Microscopy and Microanalysis 18(S2) (2012) 904-905; DOI: 10.1017/S143192761200637X.

[3] John S. Hammond, Gregory L. Fisher, Scott R. Bryan, Rait Kanarbik and Pritt Möller "FIB-TOF Tomography of Solid Oxide Fuel Cells", Microscopy and Microanalysis 19 (suppl 2) (2013) 672-673, DOI:10.1017/S1431927613005357.

[4] Quentin P. Vanbellingen, Nicolas Elie, Michael J. Eller, Serge Della-Negra, David Touboul, Alain Brunelle, "Time-of-flight secondary ion mass spectrometry imaging of biological samples with delayed extraction for high mass and high spatial resolutions" Rapid Commun. Mass Spectrom. 29 (2015) 1187–1195, DOI: 10.1002/rcm.7210

AS-ThP-14 Characterization of Surface-Immobilized Aptamers for Electrochemical Biosensing, *Ramya Vishnubhotla*, National Institute of Sandards and Technology (NIST); *S Robinson, J Giddens,* University of Maryland, College Park; *S Semancik,* National Institute of Standards and Technology (NIST)

Electrochemical measurements have shown promise for detecting biomolecules such as DNA and proteins. In this presentation, we focus on surface-immobilized DNA aptamers that can be used to bind certain species and thereby produce electrochemical signals indicating detection of desired targets. Our sensing approach is based on monitoring binding events and conformation changes that occur on reusable, temperature-controlled electrochemical microdevices. We present our findings on two "model" aptamers that bind streptavidin and platelet-derived growth factor (PDGF), respectively. The commercially-purchased aptamers were bound to the Au working electrodes of the devices through a thiol group that was synthesized at the 5' end of the DNA. Changes in temperature caused folding and unfolding of the aptamer, altering the average distance between a terminal redox-active methylene blue moiety (at the 3' end) and the Au surface. The resulting change in current (due to electron transfer between each methylene blue molecule and the Au surface) was monitored over a temperature range of ~10 °C – 60 °C. Initial studies included surface characterization using XPS and AFM in order to better understand the behavior of the aptamers under environmental stressing, such as changes in the chemical environment and temperature. Surface plasmon resonance (SPR) studies were also performed to provide instrumental analyses of the aptamer-protein binding events, to compare to results obtained with the electrochemical microdevices.

Chemical Analysis and Imaging Interfaces Focus Topic
Room Union Station AB - Session CA-ThP
Chemical Analysis and Imaging at Interfaces Poster Session

CA-ThP-1 Probing Solid-liquid Interfaces with Tender X-rays, *Nicolò Comini, Z Novotny, B Tobler,* University of Zuerich, Switzerland; *D Aegerter, E Fabbri,* Paul Sherrer Institute, Switzerland; *U Maier,* Ferrovac GmbH, Switzerland; *L Artiglia, J Raabe, T Huthwelker,* Paul Sherrer Institute, Switzerland; *J Osterwalder,* University of Zuerich, Switzerland

Many important chemical and biological processes occur at the interface between a solid and a liquid. Despite its importance, it is very difficult to collect meaningful signals from this buried interface. We recently built a new instrument at the Swiss Light Source that combines ambient-pressure X-ray photoelectron spectroscopy with in-situ electrochemistry. With this new setup, we can stabilize a thin liquid film by a dip&pull method [1] and using tender X-rays, we can probe the solid-liquid interface while having potential control over the electrolyte film. We will present results from the first commissioning beamtime and outline the future direction we are going to pursue.

[1] S. Axnanda, E. J. Crumlin et al., Sci. Rep. 5, 09788 (2014).

CA-ThP-2 Using AES, EDS, and FIB to Detect, Identify, and Image Buried Metallic Particles, *Ashley Ellsworth, D Paul, J Newman,* Physical Electronics Auger Electron Spectroscopy (AES) is a powerful analytical tool that provides quantitative elemental information from surfaces of solid materials. The average depth of analysis for an AES measurement is approximately 5 nm with lateral spatial resolution as small as 8 nm. The information AES provides about surface layers or thin film structures is important for many industrial and research applications where surface or thin film composition plays a critical role in performance including: nanomaterials, photovoltaics, catalysis, corrosion, adhesion, semiconductor devices and packaging, magnetic media, display technology, and thin film coatings used for numerous applications.

In this work, we demonstrate the use of AES in conjunction with a focused ion beam (FIB) to produce site specific imaging of microscale features beneath a sample surface. The combination of the two techniques allows for high spatial resolution analysis of buried particles and defects. This information can be very useful in helping to determine important parameters such as the origin of defects, corrosion mechanisms, coating problems, etc. We will highlight the advantages of FIB milling compared to traditional depth profiling. Energy dispersive x-ray spectroscopy (EDS) is also a powerful complementary technique to Auger analysis as it provides information from much deeper in the sample surface (few μm). With the combination of AES, FIB, and EDS, we show that buried metal particles can be first located and characterized with EDS, followed by the subsequent FIB

milling and high spatial resolution Auger spectroscopy and imaging of the particles.

CA-ThP-3 Secondary Ion Mass Spectrometry Designed for Ultra-sensitive Molecular Analysis of Solids and Liquids, *Stanislav Verkhoturov, D Verkhoturov, E Schweikert,* Texas A&M University

SIMS is a method of choice for elemental and molecular surface thin layer analysis. We present here significant enhancements in SIMS capability with regards to a) detection sensitivity, and b) applicability to liquid samples.

Detection of atto to zeptomole amounts of analyte is demonstrated with deposits of fractional monolayers of organics on double layer graphene. Three innovations make ultrasensitive analysis possible. The graphene support minimizes interference between analyte and substrate signals. Secondly, the analysis is run in a unique experimental setup. The sample on graphene is bombarded with 50 keV C_{60}^+ in transmission mode, i.e. the ejecta are mostly in the forward direction where they are collected in a time-of-flight mass spectrometer, ToF MS. Thirdly, the bombardment is reduced to a series of single C_{60} impacts, each coupled with ToF measurement. This event-by-event bombardment-detection mode allows the selection of specific impacts on analyte at the exclusion of signals from supporting materials. In this approach, unusually high ionization of analyte molecules (e.g. ~10%) was observed. A distinct ejection-ionization mechanism operates here. The molecules "trampoline" off the graphene following a C_{60} impact. The mass spectra contain abundant peaks of molecular ions. The proposed mechanism of ionization involves tunneling of electrons from the vibrationally exited area around the hole to the molecules⁻. Another proposed mechanism is a direct proton transfer exchange.

Liquid samples are inherently incompatible with SIMS, which operates under vacuum. We demonstrate the feasibility of storing liquids in carbon nanotube, CNT, sponges. We found that within a practical experimental time of 30 min, liquids with vapor pressure of < 1 torr can be analyzed. The CNT sponge (97% porosity) was made from multiwall carbon nanotubes (CNT cross-section ~6 layers). Hydrophilic and hydrophobic sponges were examined. For the hydrophobic case, we examined the lubricant fluids (vapor pressure ~100 millitorr). The mass spectra of pure fluids were used as a blank for comparison with mass spectra of wear tracks on metals. For the hydrophilic case, pure glycerol and the glycerol-water mixture have been examined. Glycerol evaporates slowly from the sponge. The method allows to investigate the organic molecules dissolved in glycerol and glycerol water mixture. Thus, the event-by-event technique applied on CNT sponges is a promising method for analysis of liquid and soft materials by Cluster SIMS.

Spectroscopic Ellipsometry Focus Topic
Room Union Station AB - Session EL-ThP
Spectroscopic Ellipsometry Focus Topic Poster Session
Moderator: Tino Hofmann, University of North Carolina at Charlotte

EL-ThP-1 Teaching Ellipsometry to Undergraduates, *John Woollam,* University of Nebraska-Lincoln

Ellipsometry is taught at universities at different levels. This class is a beginning course at the undergraduate level for students who have not had classes in optics or solid-state physics. We use Fujiwara's *Spectroscopic Ellipsometry*[1], Collett's *Field Guide to Polarization*[2], and other sources for basic theory. We have simple in-class experiments to demonstrate basic concepts. The most unique aspect of our class is the use of a 1960s Gaertner model L119 manual null ellipsometer. The instrument is ideal to demonstrate alignment of light source, rotation axis of instrument, and sample to rotation axis of instrument. In addition, students "calibrate" Ps and As, the azimuth offset positions of the polarizer and analyzer. They learn practical aspects of polarizers, retarders, and multiple reflections from optical elements. They measure P- and S-reflectance vs. angle of incidence and compare to predictions by Fresnel equations.

Students measure polarization state of light by null ellipsometry, rotating analyzer ellipsometry (by hand!), and Stokes parameter methods. They compare results of all three methods and explain sources of systematic and random errors. They are then shown how modern ellipsometry instruments drastically reduce both types of errors. The course generally has 6 to 8 students, making laboratory aspects practical and educational.

The combination of classroom demonstrations, theory, and hands-on experiments is both fun and an effective learning process.

1. H. Fujiwara, *Spectroscopic Ellipsometry* (Wiley, West Sussex, England, 2007).

2. E. Collett, *Field Guide to Polarization* (SPIE Press, Bellingham, Washington, 2005).

Electronic Materials and Photonics Division
Room Union Station AB - Session EM-ThP

Electronic Materials and Photonics Poster Session

EM-ThP-1 Synthesis and Characterization of Fluorenone Derivatives as Organic Semiconductors for Organic Thin-Film Transistors, *Sung Yong Seo, J Jeong, K Lim, B Choi, Y Yun, M Son, G Kim,* Pukyong National University, Republic of Korea

Solution-processable 2,7-bis(5'-(2-ethylhexyl)-[2,2'-bithiophen]-5-yl)-*9H*-fluoren-9-one, 2-(2,7-bis(5'-(2-ethylhexyl)-[2,2'-bithiophen]-5-yl)-*9H*-fluoren-9-ylidene)malononitrile, 2,7-bis(5'-octyl-[2,2'-bithiophen]-5-yl)-*9H*-fluoren-9-one, and 2-(2,7-bis(5'-octyl-[2,2'-bithiophen]-5-yl)-*9H*-fluoren-9-ylidene)malononitrile were synthesized and characterized as solution-processable organic semiconductors for organic thin-film transistors (OTFTs). Thermal, optical, and electrochemical properties of the fluorenone-based semiconductors were investigated. The solution-sheared thin films based on fluorenone derivatives exhibited n and p-channel characteristics as an active layer in organic thin-film transistors according to the structure. The highest electron mobility was 0.085 cm^2 $V^{-1}s^{-1}$.

EM-ThP-2 Beryllium Oxide Band Alignment with Wide Bandgap Semiconductors, *Donghyi Koh, S Banerjee,* University of Texas at Austin; *J Brockman, M Kuhn, S King,* Intel Corporation

Beryllium oxide (BeO) is a large band gap (> 8 eV) dielectric with extreme properties that makes it ideal for pairing with other wide bandgap semiconductors with similar extreme properties for various high-power, -temperature, and -frequency device applications. For such devices to be succesful, large (> 1 eV) valence and conduction band offsets are needed at the interface between BeO and the wide bandgap semiconductor. However, relatively little is known regarding the band alignment between BeO and other materials. In this regard, we have utilized x-ray photoemission spectroscopy (XPS) to determine the valence band offset (VBO) between atomic layer deposited (ALD) BeO and epilayers of diamond and the cubic form of silicon carbide (3C-SiC) grown on silicon substrates. Using the valence band alignment rules of transitivity and commutativity, we are able to combine these results with previously reported values for the band alignment of BN, AlN, GaN, and InN to diamond and SiC to further deduce the alignment of these wide bandgap semiconductors to BeO. We will show that all BeO/wide band semiconductor combinations examined exhibit a type I band alignment with > 1 eV valence and conduction band offsets that are ideally suited for high-power, -temperature, and -frequency device applications.

EM-ThP-3 Thermal Conductivity of Nano-porous Low-k Dielectrics, *Hari Harikrishna, S Huxtable,* Virginia Tech; *S King,* Intel Corporation

We have investigated the influence of growth conditions, post deposition curing, and nano-porosity on the thermal conductivity for a series of organo-silicate (SiOCH) low-k dielectric thin films. Time-domain thermoreflectance (TDTR) was specifically utilized to meaure thermal conductivity while the influence of growth conditions and post deposition curing on mass density, network bond structure, percent porosity, pore size and pore interconnectivity were examined using techniques including nuclear reaction analysis (NRA), Rutherford backscattering spectroscopy (RBS), transmission Fourier-transform infrared (FTIR) spectroscopy, nuclear magnetic resonance (NMR), ellipsometric porosimetry (EP), and positronim annihilation lifetime spectroscopy (PALS). Analytical models describing the dependence of thermal conductivity on mass density and volume % porosity were found to generally over-predict the experimentally measured thermal conductivity, but improved agreement was obtained when considering only the density of heat carrying network bonds experimentally measured by FTIR. Ashby's semi-empirical relation, which assumes that only 1/3 of the heat carrying bonds are aligned to the heat transport direction, was also found to reasonably describe the observed trends relating thermal conductivity and mass density. However, the thermal conductivity results were found to be best described via a model proposed by Sumirat (*J. Porous Mater. 9, 439 (2006)*) which considers the effect of both the volume percent porosity and phonon scattering by nanometer sized pores.

EM-ThP-4 Characterization of Textile Yarn Coated with Polypyrrole/Carbon Black Electronic Material, *R Villaneuva, Deepak Ganta, C Guzman,* TAMIU

Electronic textiles combine the advantages of flexibility in textiles and the performance of electronics in a wearable form for sensing applications. We report an inexpensive and straightforward coating method of pre-treatment, dipping, and drying the cotton yarn, combining the advantages of polypyrrole/carbon black, while investigating the mechanical, in situ electrical properties, and thermal conductivity of polypyrrole/carbon black composite coated cellulose (cotton) yarn. The coated yarn is mechanically stable with the tensile strength of~11.6 N. The resistivity and conductivity properties of the yarn are measured from the linear response of the I–V curve, showing an ohmic behavior. Further, the coated surface was tested using scanning electron microscopy for uniformity in the surface coating. Thermal conductivity for the coated fabric was measured using Transient-hot-bridge method and measured to be 0.12 Wm−1 K–1 at ambient temperature.

EM-ThP-5 Optical and Nonlinear Optical Properties of (1-x)Pb(Mg$_{1/3}$Nb$_{2/3}$)O$_3$-xPbTiO$_3$ Thin Films Grown by Pulsed Laser Deposition, *Da-Ren Liu,* Taiwan Instrument Research Institute, Taiwan, Republic of Korea

Thin film optical devices have been especially attractive because of their potential for the integration with electronic and optoelectronic systems. Owing to its ferroelectricity, pyroelectricity, high dielectric constant and large electro-optic coefficients, lead magnesium niobate-lead titanate (PMN-PT) can be used in many applications that include pyroelectric detectors, actuators, integrated capacitors, and nonlinear optical devices. In this study, highly textured thin films of lead magnesium niobate-lead titanate were grown by pulsed laser deposition (PLD). The measurement of glancing-angle x-ray powder diffraction (GAXRD) was used to determine the structure of the PMN-PT films. The thickness and roughness of the films were characterized by grazing-incidence x-ray reflectivity (GIXR), and the complex refractive indices were measured in the range from 1.5 to 4.1 eV by spectroscopic ellipsometry (SE). The average oscillator strength and its associated wavelength were estimated by using a Sellmeier-type dispersion equation. Z-scan measurements were performed to study the third-order optical nonlinearity. It was found that the PMN-PT films exhibited strong nonlinear optical effect. The results show that PMN-PT thin films are promising materials for nonlinear optics.

EM-ThP-6 Toward Selective Deposition of Boron Carbide Layers, *Raja Sekhar Bale, R Thapa, L Dorsett, S Wagner, D Bailey, A Caruso,* University of Missouri-Kansas City; *J Bielefeld, S King,* Intel Corporation; *M Paquette,* University of Missouri-Kansas City

The semiconductor industry is pushing its boundaries in device scaling technology by way of novel processing methods and increasingly complex patterning schemes. This requires a variety of functional and patterning-assist materials as well as advanced deposition techniques. For years, Si-based materials have been used to meet these needs; however, these alone cannot fulfill the range of material requirements moving forward. Boron carbide has shown promise due to compelling dielectric, thermal, mechanical, chemical, and etch properties. Toward applying this material to next-generation integration schemes, we have been exploring the potential of going beyond traditional growth processes (e.g., plasma-enhanced chemical vapor deposition) and investigating innovative area-selective atomic layer deposition (AS-ALD) strategies. Herein we explore schemes for the selective metal/dielectric deposition of boron carbide using layer-by-layer methods. X-ray photoemission spectroscopy (XPS) and atomic force microscopy (AFM) techniques are employed for characterization and imaging of the resulting surfaces.

EM-ThP-7 The Effect of Processing Conditions on the Growth of Transition Metal Dichalcogenides by Molecular Beam Epitaxy, *Peter Litwin, S McDonnell,* University of Virginia

The synthesis of high-quality transition metal dichalcogenides films is of significant interest for potential applications in nanoelectronic and thermoelectric devices. Molecular beam epitaxy is a promising route towards this aim, providing fine control over growth conditions. To further the present understanding of growth conditions on the quality of transition metal dichalcogenide thin films, we study the effect of growth temperature, chalcogen to metal flux ratio, and the use of a ripening step on the stoichiometry and surface morphology of grown WSe$_2$ thin films. In-

situ X-ray photoelectron spectroscopy is performed to analyze the intrinsic chemical composition of the grown material prior to atmospheric exposure, and ex-situ atomic force microscopy is employed to study the surface morphology of grown, sub-monolayer films. We find that both low and high growth temperature ranges can be detrimental to the chemical makeup of the grown material and that these results are echoed in the resulting grain morphology. An intermediate growth temperature produced chemically superior films over a wide range of chalcogen to metal flux ratios. The chalcogen to metal flux ratio was seen to provide some control of the film morphology, with high fluxes producing films with cleaner grain boundaries. Lastly, we show that the use of a ripening step in the early stages of growth results in a chemically superior material. This ripening step has the added benefit of producing films which are chemically more consistent than those grown in the absence of this step. There is also evidence to suggest that utilizing a ripening step may expand the processing window for film growth, allowing the use of higher processing temperatures and consequently better control over film quality.

EM-ThP-8 Co-sputtered and Rapid Thermal Annealed ZnS:Cu Thin Films for Photovoltaic Applications, *Y Jun,* EM Co., Inc., Republic of Korea; *Sakal Pech, M Yoo, G Cho, N Kim,* Chosun University, Republic of Korea

ZnS is one of the attractive II-VI semiconductors because of their potential applications in the novel electronics and optoelectronics devices. ZnS is an n-type semiconductor with relatively high transparency, large Bohr exciton radius (2.5 nm), large exciton binding energy (40 meV), high index of refraction (2.27) [1], and wide bandgap showing different bandgaps of 3.68 eV and 3.91 eV for cubic zinc blende (ZB) phase and hexagonal wurtzite (WZ) phase, respectively [2]. ZnS is considered one of the prospective candidates for the CIGS photovoltaic (PV) applications, compared to CdS, it has non-toxic handling, wide bandgap, and better lattice matching to CIGS absorber with bandgaps of 1.3–1.5 eV [2]. Some dopant metals, such as Al, Cu, Ag, Mn, and Tb, are widely doped into ZnS lattice. Some researchers have studied the effect of Cu doping on the emission of light in ZnS, in this study, ZnS:Cu thin films were deposited by using a co-puttering method for photovoltaic applications. Effect of doping content on morphological, optical and electrical properties of ZnS thin films after rapid thermal annealing (RTA) treatment was investigated with the structural properties of the different phases of ZB, WZ, and the mixture of them in X-ray diffraction studies . Optical and electrical characteristics of the thin films were analyzed by using an UV-Visible spectrophotometer and a Hall effect measurement system for optical transmittance, bandgap, resistivity, and carrier concentration. Acknowledgement: This work was supported by the Korea Institute of Energy Technology Evaluation and Planning (KETEP) and the Ministry of Trade, Industry & Energy (MOTIE) of the Republic of Korea (No. 20184010201650). [1] Sanjeev Kumar, C.L. Chen, C.L. Dong, Y.K. Ho, J.F. Lee, T.S. Chan, R. Thangavel, T.K. Chen, B.H. Mok, S.M. Rao, M.K. Wub, Room temperature ferromagnetism in Ni doped ZnS nanoparticles, J. Alloy Compd. 554, 357 (2013). [2] Md. Anisuzzaman Shakil, Sangita Das, Md. Ashiqur Rahman, Umma Salma Akther, Md. Kamrul Hassan Majumdar, Md. Khalilur Rahman, A Review on Zinc Sulphide Thin Film Fabrication for Various Applications Based on Doping Elements, Mater. Sci. Appl. 9, 751 (2018).

EM-ThP-9 Biomimetic Electrospun Polyethylene Fabrics for Effective Radiative Cooling Under Sunlight, *Bokyung Park, S Han, S Han,* University of New Mexico

Clothing fabrics normally show high absorptivity for the mid-infrared radiation from human body. This high absorptivity, compared to transparency in the same spectral region, makes heat removal from the body relatively inefficient in hot weather conditions. In addition, the microstructures of typical fabrics are far from optimum for effective light scattering in the visible range, and the absorbed sunlight can significantly heat up the skin under the fabric. In this work, we borrow our inspiration from nature to optimize the fabric design. Biological species, such as white beetles, ingeniously regulate their body temperature using their scales. These scales consist of anisotropic fibrillar network structures to achieve extraordinary light scattering that is far superior to man-made optical diffusers. Based on the random photonic structures found in beetle scales, we have electrospun biomimetic fabrics using polyethylene, which is minimally absorptive in the mid-infrared range. By manipulating the fabric microstructures (e.g., anisotropy, porosity, and fibril diameter), we were able to increase the sunlight scattering strength. Optical scattering strength of our fabrics was characterized, using the optical diffusion model where the minimum photon transport mean free path – a length over which light propagation is no longer correlated to its original direction – represents the maximum scattering strength . We have discovered that the scattering

strength can be enhanced by almost a factor of two by increasing the anisotropy of threads in the fabric. Our results suggest that fabrics for efficient heat removal from human body can be fabricated by simple electrospinning techniques that are low-cost, scalable, and high-throughput.

EM-ThP-10 Suppression of the Spectral Weight ofTopological Surface States on the Nanoscale via Local Symmetry BreakingviaLocal Symmetry Breaking, *Omur E. Dagdeviren, S Mandal, K Zou, C Zhou, G Simon, S Albright, X Zhu, S Ismail-Beigi, F Walker, C Ahn, U Schwarz, E Altman,* Yale University

In topological crystalline insulators, the topological conducting surface states are protected by crystal symmetry. Here, we show using scanning tunneling microscopy/spectroscopy that defects that break local mirror symmetry of SnTe suppress electron tunneling over an energy range as large as the bulk band gap, an order of magnitude larger than that produced globally via magnetic fields or uniform structural perturbations [1]. The results reveal the influence of various defects on the electronic properties, including screw dislocations, point defects, and tilt boundaries that lead to dislocation arrays that serve as periodic nucleation sites for pits grown on SrTiOinsulators the topological conducting surface states are protected by crystal symmetry. Here, we show using scanning tunneling microscopy/spectroscopy that defects that break local mirror symmetry of SnTe suppress electron tunneling over an energy range as large as the bulk band gap, an order of magnitude larger than that produced globally via magnetic fields or uniform structural perturbations [1]. The results reveal the influence of various defects on the electronic properties, including screw dislocations, point defects, and tilt boundaries that lead to dislocation arrays that serve as periodic nucleation sites for pits grown on SrTiO$_3$ [2,3]. Complementary ab initio calculations show how local symmetry breaking obstructs topological surface states as shown by a threefold reduction of the spectral weight of the topological surface states. The findings highlight the potential benefits of manipulating the surface morphology to create devices that take advantage of the unique properties of surface states and can operate at practical temperatures.

[1] O.E. Dagdeviren et al., Physical Review Materials **2**, 114205 (2018).

[2] O.E. Dagdeviren et al., Advanced Materials and Interfaces **4**, 1601011 (2017).

[3] O.E. Dagdeviren et al., Physical Review B **93**, 195303 (2016).

EM-ThP-11 Optical and Electrical Properties of Layer-by-layered and Mixed ZnS/CdS Structures with a Decrease in Cd-content by Co-sputtering Method, *S Pech,* Chosun University, Republic of Korea; *Y Jun,* EM Co., Inc., Republic of Korea; *Geum-Bae Cho, N Kim,* Chosun University, Republic of Korea

CdS is one of the most attractive n-type II–VI semiconductor materials for window layers or buffer layer in heterojunction thin film solar cells because of its high transmitivity, low resistivity, and excellent permeability with a bandgap of 2.42 eV [1]. However, the use of cadmium would be deleterious for the environment because of carcinogenic and toxic nature. To reduce the use of cadmium ZnS/CdS structures were investigated in this study. ZnS is an n-type semiconductor with relatively high transparency, large Bohr exciton radius (2.5 nm), large exciton binding energy (40 meV), high index of refraction (2.27) [2]. Two types of structure were fabricated with the same thickness: layer-by-layered and mixed structures were fabricated by co-sputtering method with each ZnS and CdS target as a function of Cd-content. Cd-content was adjusted by a sputtering time for CdS target. All samples were annealed in a rapid thermal annealing system at 400°C for 10 min. Structural properties of two-types of structure with the different Cd-content by X-ray diffraction studies. Optical and electrical properties of them were analyzed by using an UV-Visible spectrophotometer and a Hall effect measurement system for optical transmittance, bandgap, resistivity, carrier mobility, and carrier concentration. Acknowledgement: This work was supported by the Korea Institute of Energy Technology Evaluation and Planning (KETEP) and the Ministry of Trade, Industry & Energy (MOTIE) of the Republic of Korea (No. 20184010201650). [1] Nam-Hoon Kim, Seung-Han Ryu, Hyo-Sup Noh, Woo-Sun Lee, Electrical and optical properties of sputter-deposited cadmium sulfide thin films optimized by annealing temperature, Mater. Sci. Semicond. Process. 15, 125 (2012). [2] Sanjeev Kumar, C.L. Chen, C.L. Dong, Y.K. Ho, J.F. Lee, T.S. Chan, R. Thangavel, T.K. Chen, B.H. Mok, S.M. Rao, M.K. Wub, Room temperature ferromagnetism in Ni doped ZnS nanoparticles, J. Alloy Compd. 554, 357 (2013).

Thursday Evening Poster Sessions, October 24, 2019

EM-ThP-12 Design and Simulation of a Leaf-like Antenna on Thin Kapton Sustrate for the 915MHz Frequency, *Felipe Frazatto*, *L Manera, L Perissinotto,* UNICAMP, Brazil

When launching a satellite into orbit, every gram reduced from its total weight counts toward cheaper missions, with this in mind and inspired by the wide range of applications allowed by flexible electronics, this work presents the study and simulation of a leaf-like coplanar microstrip antenna on an one mil thick Kapton substrate centered in the 915MHz frequency to be used with a LoRa communication module in Low Earth Orbit (LEO) CubeSats.

Ring resonators and coplanar transmission lines (CPW) were also simulated to be used in the substrate's material characterization and help understand the various challenges poused by the thin thickness. Comparing the simulations of the CPW and characteristic impedance equations found in the literature, it was possible to notice divergences between the simulated model impedance and the theoretical calculated value when dealing with the thin substrate, witch indicates that the equation's models may not consider effects that appear with the reduced thickness, making it difficult to obtain a good impedance matching.

The designed antenna is presented alongside a impedance matching semi flexible circuit, a coplanar waveguide, ring resonator and the study of the impedance matching hardships when using thin substrates for radio frequency applications.

EM-ThP-13 Atom Probe Tomography Analysis of the Composition of GaAsNBi, *Jared W. Mitchell*, *R Goldman,* University of Michigan, Ann Arbor

We use atom probe tomography (APT) to develop an understanding of the composition of our $GaAs_{1-x-y}N_xBi_y$ samples. These alloys are of interest because of the significant bandgap narrowing that can be generated by incorporation of dilute concentrations of N and Bi. Notably lattice-matching with a GaAs substrate has also been demonstrated, yielding a bandgap of ~1 eV with a ratio of x_N/y_{Bi} = 083. The distribution of these alloys in the sample is of marked interest because of the observation of localized states generated by their incorporation, notably in the case of interstitial complexes developing in the As sublattice, which are important contributors to the electronic structure of these materials. We use APT to demonstrate the presence of As cluster states and to evaluate the composition and distribution of impurities of our sample.

EM-ThP-14 Silicon Nanowire P-N Junction Photovoltaic Device, *Michael Small*, *S Collins, R Smith,* University of Maine

This paper presents the fabrication and testing of a low cost, silicon nanowire photovoltaic device. The silicon nanowires are etched into the surface of a silicon wafer, via metal assisted chemical etching (MACE). This method of nanowire fabrication does not require photolithographic patterning, thereby reducing manufacturing complexity and related costs. Vertically aligned nanowire p-n junctions have the potential to increase the optical bandwidth of a silicon photovoltaic device by allowing a greater amount of short wavelength light to reach the depletion region near the junction, resulting in improved conversion efficiency. When compared to a planar analog, the nanowire device produced an order of magnitude higher power in response to blue light (405 nm), attributed to increased collection at the exposed p-n junctions. Power conversion efficiency is eight times better than previously reported with a similar construct.

EM-ThP-15 Effect of N_2/H_2 Plasma on the Epitaxial Growth of InN by Hollow Cathode Plasma Assisted Atomic Layer Deposition, *Mustafa Alevli*, *N Gungor,* Marmara University, Turkey

The high electron saturation velocity, small effective electron mass and high electron mobility of indium nitride (InN) makes it a suitable material for high frequency electronics. The possibility of InN in the existing high electron mobility transistors (HEMTs), currently based on other group III-nitrides. However, InN decomposes to In metal and N_2 gas at around 500°C, making deposition of the InN films challenging with conventional methods such as metal organic chemical vapor deposition (MOCVD) and Molecular Beam Epitaxy (MBE). Nevertheless, Hollow cathode plasma assisted atomic layer epitaxy (HCPA-ALD) is a layer-by-layer crystalline growth technique that is based on a pair of self-terminating and self-limiting gas-surface half-reactions, in which at least one half-reaction involves species from plasma. The inclusion of plasma generally offers the benefit of substantially reduced growth temperatures and greater flexibility in tailoring the gas-phase chemistry to produce varying film characteristics. The benefits of plasma come at the cost of a complex array of process variables that often challenge the ability to predict, a priori, the influence of any one input parameter. This work focuses on a variety of gas input flow fractions (N_2

and N_2/H_2) used in the HCPA-ALD growth of InN films. Changes in plasma parameters are then linked with changes in film characteristics. To evaluate the optical properties of the InN films, we use spectroscopic ellipsometer to measure the dielectric function and a complex refractive index. Data were fitted using a fitting based analysis program, and the results show our films have a bandgap of about 1.4 eV, which is bigger than the previously reported values. The Raman spectra showed two Raman active modes of E_2 and $A_1(LO)$ of the wurtzite InN for all InN samples. For InN, we found out that addition of H_2 plasma with N_2 plasma resulted in InN films with poor crystalline quality showing high level of impurities with significant voids in the films, resulting in low-density films with poor adhesion properties. Our results indicate that higher N_2 plasma exposure time is necessary to obtain InN films with minimum amount of carbon incorporation. The presence of C impurities was observed in all films grown with N_2 plasma only and suggests that the N_2 plasma without H_2 is not efficient in terms of effectively removing the ligands of the chemisorbed organometallic trimethyl-metal precursors.

EM-ThP-16 Atomic Layer Deposition of Functional Films for Transparent and Flexible Organic Electronic Devices, *Yu Duan,* Jilin University, China

Among the advanced electronic devices, transparent flexible organic electronic devices with rapid development are the most promising technologies to customers and industries. However, thin-film encapsulation (TFE) and the transparent oxide conductive (TOC) of organic devices still remain a big challenge, because of the difficulty in low temperature and low plasma power fabricating process. Atomic layer deposition (ALD) is increasingly used in the field of organic electronics. However, the deposition of ALD outside the temperature window still cannot be stably implemented. In this study, transient steric hindrance caused by gas-phase molecules at low-temperature (80℃) was investigated. In order to mitigate the effect of this transient hindrance, a process of consecutive short-pulses was adopted in fabricating TFE and TOC. Overall, the proposed idea would help low-temperature ALD for organic electronics become mature and be widely promoted.

EM-ThP-18 Incredibly Simple Synthesis of a Zinc Oxide / Graphene Hybrid Nano Material, *Daniel Little,* Ohio Dominican University; *J Pfund, A McLain, S Lantvit, S King,* University of Wisconsin - La Crosse

Hybrid materials of zinc (II) oxide (ZnO) nanocrystals and graphene are of current interest due to their cheap, Earth-abundant composition, low toxicity, and varied applications in photocatalysis, sensing, and electronics among others. We have developed a novel methodology for the synthesis of such materials utilizing the thermal decomposition of zinc (II) oxalate in solid-state solution with graphene nanoplatelets. Although the procedure involves simply precursor mixing and heating, electronic interaction between the ZnO and graphitic phases is spectroscopically observed in the hybrid material – beyond that of a homogeneous mixture of ZnO and graphene – via powder XRD, XPS, and ATR-IR spectroscopy. The synthetic method employed can be easily tuned for the desired hybrid product stoichiometry, and is easily industrially scalable with minimal chemical waste products. The method can also be adapted for the creation of thin film composite materials.

EM-ThP-19 Metal Oxide-based Heterojunction Thin Films for Solar Cell Applications, *Zainuriah Hassan*, *M Mohamed Saheed, A Yusof,* Institute of Nano Optoelectronics Research and Technology (INOR), Universiti Sains Malaysia, 11800 USM, Penang, Malaysia

Hello Everyone,

I'm writing on behalf of Pete Sheldon and Joe Greene to advise you that we will have a brief Executive Session on Monday, July 29th, from 7:30 – 8:15 a.m. just prior to the Board Meeting, in the New York Office—the agenda is attached. Please plan accordingly!

We look forward to seeing you in New York!

Yvonne

Thursday Evening Poster Sessions, October 24, 2019

Fundamental Discoveries in Heterogeneous Catalysis Focus Topic
Room Union Station AB - Session HC-ThP

Fundamental Discoveries in Heterogeneous Catalysis Poster Session

HC-ThP-1 The Role of Boron in Supported Platinum Dry Reforming Catalysts, *Carly Byron, S Bai, A Teplyakov,* University of Delaware

Dry reforming of methane (DRM) has been proposed as an alternative to coal or natural gas production of synthesis gas, and the process has been optimized with various metal catalysts to enhance catalytic activity and reduce surface carbon contamination. In this work, boron was paired with platinum, a highly active DRM catalyst, on a silica support material, and surface characterization techniques were used to determine how the presence of boron affected the metal catalyst and the catalytic performance. X-ray photoelectron spectroscopy (XPS) revealed the existence of trigonal (BO_3 structures) and tetrahedral (BO_4 structures) B-containing surface species, which agreed with solid-state ^{11}B NMR results. Density functional theory (DFT) calculations were performed to determine the thermodynamically stable configuration of the B/SiO_2 species, as well as the most favorable species for platinum adsorption. Tetrahedrally coordinated boron was found to be the most favorable species for platinum adsorption. A butane dehydrogenation reaction was utilized to produce fully deactivated $Pt/B/SiO_2$ catalysts samples for further analysis. After complete catalyst deactivation, ^{11}B NMR combined with theoretically-predicted isotropic chemical shifts calculated by Amsterdam Density Functional (ADF) revealed that, in addition to BO_3 and BO_4 fragments, a boron-carbon surface species had been formed during butane dehydrogenation, but this was only observed on catalysts containing platinum. From this observation, it has been concluded that platinum causes carbon contamination during this reaction, but it is mitigated by the presence of boron.

HC-ThP-2 Spectroscopic Characterization of Ethylidyne formed from Acetylene on Pd(111), *Ravi Ranjan, M Trenary,* University of Illinois at Chicago

The surface species formed following the adsorption and hydrogenation of acetylene (C_2H_2) on Pd(111) in the temperature range of 90-450 K are identified and characterized. The techniques used to detect the species are reflection absorption infrared spectroscopy (RAIRS) and temperature programmed desorption (TPD). Acetylene was adsorbed at low temperature and then heated to 300 K where it converts to ethylidyne (CCH_3), which is identified by its $\delta(CH_3)$ bending mode at 1327 cm^{-1}. The reaction mechanism for this conversion is quite complex; in the literature there are discrepancies in the identification of the intermediates with both vinyl ($CHCH_2$) and vinylidene (CCH_2) having been proposed. The experimental data available to date favors the formation of vinylidene as an intermediate in the conversion of acetylene to ethylidyne (CCH_3). Evidence for vinylidene is seen in the appearance of its bending mode ($\delta(HCH)$) at 1425 cm^{-1}. The possible mechanism of ethylidyne (CCH_3) formation is through isomerization of acetylene to vinylidene (CCH_2) followed by hydrogenation of vinylidene. In the temperature range of 400 to 450 K, C_2H_2 decomposes and forms a C_xH_y species as verified by TPD spectra showing an H_2 peak at 440 K following C_2H_2 adsorption at low temperature. The low energy electron diffraction (LEED) pattern of acetylene adsorbed at 95 K gives rise to a ($\sqrt{3}\times\sqrt{3}$)R30° pattern. The experimental result is also supported by quantum mechanical computational calculations based on density functional theory.

HC-ThP-3 XPS, TOF-SIMS, and AES Analysis of Fresh and Aged Alumina-Supported Silver Catalysts, *John Newman, D Carr, D Paul, L Swartz,* Physical Electronics; *M Di Mare, W Suchanek,* Scientific Design Company, Inc.

Alumina supported silver catalysts have been used for decades for the direct oxidative conversion of ethylene to ethylene oxide. Ethylene oxide is used in many cleaning and sterilizing products; however, its major industrial application is in the production of ethylene glycol used in the generation of antifreeze, polyesters, liquid coolants and solvents. Global production of ethylene oxide is estimated to grow to 28 million metric tons in 2019 at an estimated market value of over $48 billion (1, 2).

Due to the huge size of this market, incremental improvements in the efficiency and longevity of the catalyst can be very beneficial. Many companies continuously explore ways in which to improve the various aspects of the catalyst system – the physical and chemical properties of the catalyst, the preparation technology, and the reaction conditions.

In this investigation, three surface sensitive (outermost ≤ 5 nm) techniques, X-ray Photoelectron Spectroscopy (XPS), Time-of-Flight Secondary Ion Mass Spectrometry (TOF-SIMS), and Auger Electron Spectroscopy (AES) were used to study the changes that occur between fresh and aged Cs-promoted, alumina-supported Ag catalyst samples. XPS provided insights into the overall surface concentrations of the elements present as well as chemical state changes that occurred during aging. TOF-SIMS was used to detect and spatially locate elements at concentrations often too low to detect with XPS or AES, and AES high magnification elemental mapping and small area spectroscopy were used to study the localized elemental changes that occurred between fresh and aged catalyst samples. Information gained from these experiments provides valuable insights on the physical and chemical transformations taking place during aging of the catalyst. This information can then be used to suggest further modifications to improve the performance of the catalyst system.

References

1. PR Newswire, *Global Ethylene Oxide Market Report 2018 - Forecast to 2023: The Growing Demand for PET Bottles from the Packaging Industry*, Nov 26, 2018

2. Business Wire, *Global Ethylene Oxide Market Report By Application*, April 24, 2018

HC-ThP-4 Infrared Spectroscopy of Carbon Dioxide Hydrogenation over the Cu(111) and Pd/Cu(111) Single Atom Alloy Surfaces under Ambient Pressure Conditions, *Arephin Islam, M Trenary,* University of Illinois at Chicago

Copper catalysts are used in the water gas shift reaction to convert mixtures of carbon monoxide and water to hydrogen and carbon dioxide. Conversely, the reverse water gas shift reaction utilizes carbon dioxide as a resource. Related to the reverse water gas shift reaction is the synthesis of methanol from carbon dioxide and hydrogen. The mechanisms of these reactions involve several possible surface intermediates, each of which should be identifiable by their vibrational spectra. We have used reflection absorption infrared spectroscopy (RAIRS) to study these reactions under ambient pressures in the range of 0.1 to 150 Torr. In the presence of ambient pressures of carbon dioxide, a peak is observed at 1295 cm^{-1}, which is assigned to the symmetric stretch of an adsorbed CO_2 molecule that is bent through its interaction with the surface. Upon addition of $H_2(g)$ at 300 K, the spectra change and new peaks due to surface species appear. By performing the experiment with polarized infrared radiation, the gas phase and surface species are easily distinguished. The results demonstrate that CO_2 hydrogenation is readily achieved over a Cu(111) model catalyst and that surface intermediates can be detected with RAIRS.

HC-ThP-5 Morphology of an Oxide Formed on Au(111) at High Temperatures under Ambient Pressure Conditions, *Jordon Baker, H Kaleem, E Maxwell, A Baber,* James Madison University

The deactivation of heterogeneous catalysts occurs via several mechanisms such as poisoning, coking, and sintering, among others. In order to maintain the high chemical reactivity of heterogeneous catalysts, the process for catalyst deactivation must be well understood and avoided. The effect of high temperature annealing cycles on the morphology of TiO_2/Au(111) model catalysts has been studied. When modified with TiO_2 nanoparticles, the morphology of the model catalyst can vary based on differences in the annealing cycle parameters. Atomic force microscopy (AFM) was used to image the morphology of the surface before and after annealing TiO_2/Au(111) to 1000 K. TiO_2 nanoparticles sintered and Au(111) step edges smoothed, but surprisingly a new surface feature was observed with AFM under ambient conditions, resembling mixed metal oxides formed under UHV conditions. X-ray photoelectron spectroscopy was used to characterize the surface species remaining after the high temperature exposure. The stabilization of a mixed metal oxide on Au(111) has not previously been observed, and future work will investigate the chemical reactivity of these materials.

HC-ThP-6 Machine-Learning Enabled Search for The Next-Generation Catalyst for Hydrogen Evolution Reaction, *Sichen Wei, S Baek, K Reyes, F Yao,* University at Buffalo

As a zero-emission, eco-friendly fuel, hydrogen gas can be generated via electrochemical (EC) water splitting. Achieving high-efficiency water splitting requires the use of a catalyst to minimize the overpotential to drive the hydrogen evolution reaction (HER). Noble metals such as platinum (Pt) can provide an excellent catalytic activity for HER but are too

expensive and scarce for broad applications. Therefore, the development of active HER catalysts made from low-cost materials constitutes a crucial challenge in the utilization of hydrogen energy.

Earth-abundant transition metal dichalcogenides (TMDs), such as molybdenum disulfide (MoS$_2$), have been discovered recently, which exhibit good activity and stability for electrocatalytic reactions. In order to fully explore the untapped potential of MoS$_2$, the synthesis recipe for MoS$_2$ needs to be optimized. Such an optimization process needs scientists to search through a combinatorially large space of experimental parameters, which will be time-consuming and costly if using conventional trial-and-error approaches.

In this report, MoS$_2$ HER catalytic activity optimization is performed by examining different combinations of synthesis parameters during the hydrothermal process. To investigate the structure-activity relationship, scanning electron microscope (SEM), X-ray diffraction (XRD), Raman spectroscopy and various electrochemical characterizations have been conducted. A strong correlation between hydrothermal conditions and HER performance matrix has been observed. In order to accelerate the search for the best synthesis recipe, machine-learning (ML) techniques have been introduced to help identify the optimal parameter combinations for producing MoS$_2$. The hydrothermal parameters with the corresponding onset potentials and Tafel slopes are adopted as prior knowledge and are incorporated into the Bayesian Optimization model. The model will be able to guide the wet chemical synthesis of MoS$_2$and yield the most effective HER catalyst eventually.

HC-ThP-7 Intermolecular Interactions of Small Alcohols on Au(111), Eric Maxwell, J Baker, H Kaleem, A Baber, James Madison University

Metal oxide nanoparticles supported on Au(111) are active catalysts for the oxidation of small alcohols to form industrially significant products and intermediates such as aldehydes. In a systematic study to better understand the adsorption behavior of these small alcohols, coverage studies of methanol, ethanol, and 1-propanol have been conducted on Au(111) using ultrahigh vacuum temperature-programmed desorption (TPD). These three alcohols molecularly adsorb to distinct terrace, step edge, kink, and multilayer sites, for which desorption energies are calculated by Redhead's peak maximum method. The use of complete analysis as a more accurate method for the calculation of desorption energies is also explored for the case of methanol. TPD experiments and subsequent analysis uniquely allow for the investigation of both adsorbate-surface interactions and adsorbate-adsorbate intermolecular interactions. This provides a more robust understanding of surface phenomena and affords valuable data for modelling and predicting the adsorption behavior of small alcohols on Au(111)-based catalysts. It is shown that, for all adsorption sites, desorption energy is directly proportional to carbon chain length. However, the rate at which desorption energy increases varies distinctly between adsorption sites. This study indicates that the role of intermolecular interactions in the adsorption behavior of small alcohols varies between adsorption sites, and can be predicted for other small alcohols.

Advanced Ion Microscopy and Ion Beam Nano-engineering Focus Topic
Room Union Station AB - Session HI-ThP
Advanced Ion Microscopy Poster Session

HI-ThP-1 Fabrication of a Single Atom Ir/W(111) Tip by a Simple Sputtering Method, Kwang-Il Kim, University of Science and Technology, Republic of Korea; J Hwang, Chungbuk National University, Republic of Korea; T Ogawa, Korea Research Institute of Standards and Science, Republic of Korea; B Cho, Korea Research Institute of Standards and Science (KRISS), Republic of Korea; I Park, Korea Research Institute of Standards and Science, Republic of Korea

Atomically defined tip, which is widely used as a gas field ion source (GFIS) for ion microscopes or a coherent electron source for electron microscopes, has been of importance in various fields, such as biology and material science, because its high brightness and angular current density can realize microscopes with high spatial resolution [1]. Single Atom Tips(SATs) can be typically fabricated by a build-up method or field-assisted reactive gas etching method with oxygen and nitrogen [2,3]. Tungsten (W) is a typical material for a tip because of the high melting point and mechanical stability. These characteristics of W are preferred especially to produce helium ion beams because it is easier to generate larger currents

at higher electric fields. In recent years, the oxygen GFIS using SAT has attracted more attention in the field of Secondary Ion Mass Spectroscopy. However, W tips have limitation because they are corrosive in oxygen environments [4]. Thus, fabrication of SAT with a cover layer of inert FCC noble metals on tungsten tips with BCC structure has been proposed. The metals were deposited by the electroplating method [5]. Among FCC noble metals, Iridium has the possibility to achieve the highest brightness and stability among various BCC-FCC metal systems because it has the strongest bonding with tungsten and high resistibility against corrosion of oxygen [6]. In this study, we show that SAT can be fabricated by field evaporation effect in ultra-high vacuum system using a native tungsten tip that was not heated in the initial process to remove an oxide layer, which is generated with electrochemical etching. Additionally, the iridium was deposited by a conventional simple sputtering method. As a result of this study, we can fabricate an SAT of Ir(211) on W(111) using field ion microscopy by field evaporation and build-up process without pre-heating for removing initial oxidized layers. We also analyzed how the shape of the pyramid changes depending on the number of the build-up process and the electric field intensity applied in the faceting process. Since this method uses a conventional sputtering coater, the complexity of the equipment configuration could be eliminated compared to that in previous studies.

[1] N.Economou et al., Scanning 34(2): 83-89, 2012

[2] M. Rezeq et al., The Journal of chemical physics, 124(20), 204716, 2006

[3] VT Binh et al., Surface Science, 202(1-2), L539-L549, 1988

[4] Wood, John A., et al. Applied Surface Science 367 (2016): 277-280.

[5] Kuo, Hong-Shi, et al. nano letters 4.12 (2004): 2379-2382.

[6] Oshima, Chuhei, et al. e-Journal of Surface Science and Nanotechnology 16 (2018): 294-297.

Preference: Poster

HI-ThP-2 Morphology Modification of Si Nanopillars under Ion Irradiation at Elevated Temperatures, Xiaomo Xu, K Heinig, Helmholtz Zentrum Dresden-Rossendorf, Germany; W Möller, Helmholtz-Zentrum Dresden-Rossendorf, Germany; H Engelmann, N Klingner, Helmholtz Zentrum Dresden-Rossendorf, Germany; A Gharbi, R Tiron, CEA-LETI, France; J von Borany, Helmholtz Zentrum Dresden-Rossendorf, Germany; G Hlawacek, Helmholtz-Zentrum Dresden Rossendorf, Germany

Ion beam irradiation of vertical nanopillar structures can be utilized to fabricate a vertical gate-all-around (GAA) single electron transistor (SET) device in a CMOS-compatible way. After irradiation of Si nanopillars (with a diameter of 35 nm and a height of 70 nm) by either 50 keV broad beam Si$^+$ or 25 keV focused Ne$^+$ beam from a helium ion microscope (HIM) at room temperature and a fluence of 2e16 ions/cm^2, strong deformation of the nanopillars has been observed which hinders further device integration. This is attributed to ion beam induced amorphization of Si allowing plastic flow due to the ion hammering effect, which, in connection with surface capillary forces, dictates the final shape. However, plastic deformation can be suppressed under irradiation at elevated temperatures (investigated up to 672 K). Then, as confirmed by bright-field transmission electron microscopy, the substrate and the nanopillars remain crystalline, and are continuously thinned radially with increasing fluence down to a diameter of 10 nm. This is attributed to enhanced forward sputtering through the sidewalls of the pillar, and found in reasonable quantitative agreement with the predictions from 3D ballistic computer simulation using the TRI3DYN program.

Frontiers of New Light Sources Applied to Materials, Interfaces, and Processing Focus Topic
Room Union Station AB - Session LS-ThP
Frontiers of New Light Sources Applied to Materials, Interfaces, and Processing Poster Session

LS-ThP-1 Bringing Synchrotron Capabilities to a Local X-ray Facility: the Lyncean Compact Light Source, Benjamin Hornberger, J Kasahara, M Gifford, Lyncean Technologies, Inc.

Synchrotron facilities around the globe are the supercomputers of X-ray science, contributing to many areas of materials science. There are more than fifty synchrotrons worldwide serving more than ten thousand researchers. The light generated by these sources is typically high flux,

monochromatic, energy-tunable and, in some cases, coherent. They serve a myriad of applications and thousands of researchers, but they come at a high construction and operating cost and generally require government support. Furthermore, these facilities are oversubscribed by an ever-expanding user base.

Consequently, there is an increasing need for small, locally owned and operated, multi-discipline, X-ray facilities that provide the flux and energy tunability that is required for experiments such as diffraction, spectroscopy, or dynamic imaging.

The Lyncean Compact Light Source (CLS) is the cornerstone of this kind of modern, multi-discipline, and high-performance laboratory. The Lyncean CLS is the first commercially developed X-ray source in its class; it was specifically created to deliver a true home laboratory alternative to many experiments performed today at the large synchrotrons. X-rays are produced in the CLS via inverse Compton scattering through the interaction of low energy electrons (25 to 45 MeV) in a miniature storage ring with a micrometer-period, high powered laser pulse (laser-undulator). Tunable, monochromatic, and high flux undulator synchrotron radiation is generated in the CLS "mini-synchrotron" as a result of the high repetition rate (~65MHz) of this interaction. Characteristics of the CLS X-ray beam are similar to those of a bending magnet synchrotron in terms of flux and coherence, and as such, similar synchrotron quality applications can be performed: imaging/tomography, diffraction, scattering, and spectroscopy.

In this presentation we describe the technology behind the Lyncean Compact Light Source and provide examples of the various measurements that are possible with the system. The broad range of applications served by the Lyncean Compact Light Source illustrates our vision for a new kind of multi-discipline X-ray facility.

LS-ThP-2 Observing Formation of Detonation Nanodiamond at Sub-Microsecond Timescales at the Advanced Photon Source, *Trevor Willey, J Hammons, M Bagge-Hansen, M Nielsen, L Lauderbach, R Hodgin, W Shaw, W Bassett, E Stavrou, S Bastea, L Fried, L Leininger,* Lawrence Livermore National Laboratory

Over the past few years, we have developed a capability to perform small-angle x-ray scattering (SAXS) and wide-angle x-ray scattering (WAXS) during high explosive detonation. We can acquire a SAXS or WAXS pattern from individual 80 ps x-ray pulses, which at the APS in 24-bunch mode, arrive every 153.4 ns. We can acquire up to eight frames, from sequential pulses, per event. Various morphologies of carbon condensates appear during detonation, dependent upon the pressure and temperature attained, and liquid, diamond, and graphitic phases can be inferred from the SAXS and WAXS. Transmission electron microscopy of recovered nanoparticles confirms these phases. Nanoparticles, including detonation nanodiamond, form over a few hundred nanoseconds. Here, we present an overview of the capability and a few select results.

Magnetic Interfaces and Nanostructures Division
Room Union Station AB - Session MI-ThP

Magnetic Interfaces and Nanostructures Poster Session

MI-ThP-1 Room Temperature Skyrmion in Alternative Layer Molecular Beam Epitaxial Grown B20 Fe-rich Fe$_{1.2}$Ge Films, *Tao Liu, R Bennett, S Chen, A Ahmed, R Kawakami,* The Ohio State University

Magnetic Skyrmions are localized, topological spin textures that arise from competition between exchange interaction and Dzyaloshinskii-Moriya interaction (DMI) in magnetic materials with broken inversion symmetry. Their topological stability, small size, and the ability to be very energy efficiently written, read and manipulated, put them at the forefront of candidates for next generation storage technology. However, it is still challenging to find a material which can achieve skyrmion at room temperature with size no more than 10 nm, which has already become a major bottleneck of their developments. In order to realize this goal, it requires strong exchange interaction strength J, which sets the temperature scale, and a large DMI strength D that determines skyrmion stability and size, Ja/D (a is the atomic lattice spacing). Current skyrmion research is focused on two classes of materials: metallic multilayers and B20 crystals. Neither of them can meet this challenge. Metallic multilayers can meet the criteria of room temperature operations, but with small DMI arising from surface inversion symmetry broken. B20 crystals have a large bulk DMI and nanoscale skyrmions with sizes down to 3 nm, but cannot achieve room temperature operations.

In this work, we successfully synthesized Fe-rich Fe$_{1.2}$Ge films by alternative layer molecular beam epitaxy at room temperature and adding extra Fe atoms at the Fe-sparse atomic layers. As shown in figure 1, the cross sectional TEM result indicated that the Fe-rich Fe$_{1.2}$Ge film is B20 structure. Its XRD peak position shift to a lower angle relative to FeGe film, which might be good evidence indicating the extra Fe atoms went into the B20 structure rather than formed another stucture phase. The Curie Temperature of the Fe-rich Fe$_{1.2}$Ge film has been pushed above room temperature (RT), and the observing of clear topological Hall resistance with maximum value around $H=\pm1.5$ kOe could be the result of stabilization of RT skymrmion.

MI-ThP-2 Investigation of Exchange Bias in L1$_0$- MnGa/ θ-MnN/MgO Bilayers, *Sneha Upadhyay,* Ohio University; *K Meng, F Yang,* The Ohio State University; *D Ingram, A Smith,* Ohio University

Exchange bias, a shift in the center for the magnetic hysteresis loop of a magnetic material, has gained a lot of attention due to its application in spintronics. Generally, exchange bias is observed in layered magnetic structure like antiferromagnetic/ferromagnetic bilayers. In this work, the L1$_0$ MnGa (T_c= 590K) / θ-MnN (T_N= 660K) bilayer on MgO substrate was studied for the investigation of exchange bias motivated by the recent report of giant exchange bias using MnN as the antiferromagnet.[1]

These bilayers were prepared using molecular beam epitaxy, and the growth was monitored by *in-situ* RHEED. Three samples were grown with MnN thickness of 47 nm while L1$_0$ MnGa thicknesses were varied from 15nm, 3nm and 1 nm. During the growth, RHEED images were taken which showed some disorder and roughness on the surfaces especially for thinner ones. In order to observe exchange bias, these samples were field cooled through the Néel temperature and the hysteresis was taken at a specific applied field using SQUID. The measurements showed the presence of a small but finite exchange bias in the case of the 3 nm L10 MnGa/θ-MnN sample in the *in-plane* direction only, and the amount of loop shift from the origin was estimated to be 300 Oersted. The results were compared with the recent publication for the case of CoFeB/ θ-MnN which showed giant exchange bias (3600 Oersted).

Although the field cooling procedure is important to observe exchange bias, in our previous measurements, we were unable to field cool through the high Néel temperature of MnN. Currently, we are working on a new field cooling capability in our MBE chamber and further plan to study the sample using *in-situ* spin-polarized scanning tunneling microscopy under an applied magnetic field. We also plan to repeat the SQUID measurements as well with the high-temperature, field-cooled sample.

[1] P. Zilske, D. Graulich, M. Dunz, and M. Meinert, "Giant perpendicular exchange bias with antiferromagnetic MnN," *Appl. Phys. Lett.* **110**, 192402 (2017).

MI-ThP-3 Investigating a Possible Kondo Resonance for Iron-induced Islands on Chromium Nitride (001), *K Alam, Y Ma, Shyam Chauhan, S Upadhyay, A Smith,* Ohio University

Chromium and iron surfaces have been of intense interest due to their high technological importance. Stroscio *et al.* investigated the electronic states of Fe(001) and Cr(001) surfaces using room temperature scanning tunneling spectroscopy, finding surface state peaks at +170 meV and -50 meV, respectively, relative to the Fermi level and enabling a chemical identification of surface elemental species in FeCr alloys.[1] Later, Hanke *et al.* measured the temperature-dependent spectroscopy on Cr(001) surfaces and found that both orbital Kondo effect and single-particle models could be used to reasonably interpret the observed temperature-dependent Cr(001) surface peak seen at 20 meV above E_F.[2]

Recently, we have carried out a study of Fe on CrN(001) surfaces exhibiting a step-terrace morphology as grown by molecular beam epitaxy. These CrN samples are antiferromagnetic below 270 K.[3] We performed STS spectroscopy on, and between, nanometer-sized islands resulting from sub-ML Fe deposition. Spectroscopy on the clean CrN regions displays a broad dip near E_F and a peak at 125 meV, similar to the oxygenated Cr surface reported by Hanke et al. Whereas spectroscopy on the islands displays sharp spectral features exactly at, or within a few meV of, E_F. We make a case for interpreting these spectra in terms of a Kondo resonance.

[1] Stroscio et al., Phys. Rev. Lett. **75**, 2960 (1995).

[2] Hanke et al., Phys. Rev. B **72**, 085453 (2005).

[3] Alam et al., Phys. Rev. B **96**, 104433 (2017).

MI-ThP-5 Characteristics of a Single Molecule Magnet on Graphene: A DFT Study, *Rainier Berkley*, Z Hooshmand, T Rahman, University of Central Florida

Single-molecular magnets (SMMs) are molecules that function as nanoscale magnets below their blocking temperature. These systems have become of increasing interest due to their potential applications for magnetic technologies, since they display many unique quantum phenomena and their structures can be tuned to modify their magnetic and quantum properties. However, in order for SMMs to be applicable for magnetic technology they must retain stability both in their structures and their magnetic moments during and after the deposition process. Due to the complicated nature of magnetic interactions with substrates, the effects of magnetic materials on substrates are not fully understood. Therefore, in order to fully understand these systems a study of the interactions between a well-characterized SMM and substrate at the most fundamental level is required. For this purpose, we have studied the interactions of a [Mn3]2 dimer1 with graphene using Density Functional Theory (DFT) calculations. The [Mn3]2 dimer can exhibit two different ground states: ferromagnetic (FM) and anti-ferromagnetic (AFM). Our calculations for the spin of both the FM and AFM configurations of the isolated [Mn3]2 dimers in gas phase, agree with experimental results (S=12 and 0 respectively)1 only when the dimers are charged (+2). More importantly, our calculations reveal that graphene is inert; thus, hardly affecting the magnetic properties of the FM and AFM dimers and that both dimers display the same spin as in their isolated gas phase structures after deposition. These results are further confirmed by charge redistribution analysis in which there are no strong charge distribution from/to molecules to/from graphene and the spin density remains almost intact after interactions of molecules with substrate. Our results provide insights into the design of coupled SMM/substrate systems, namely [Mn3]2 dimer on graphene.

1 Nguyen et al. J. Am. Chem. Soc. 2015, 137, 7160–7168.

* This work is supported by DOE-DE-SC0019330

MI-ThP-6 Molecular Conductivity Switching via Voltage Controlled Spin Crossover at a Ferroelectric Interface, *Aaron Mosey*, Indiana University-Purdue University Indianapolis; *G Hao,* University of Nebraska-Lincoln; *A N'Diaye,* Lawrence Berkeley National Laboratory; *A Dale,* Indiana University-Purdue University Indianapolis; *U Manna,* Illinois State University; *P Dowben,* University of Nebraska-Lincoln; *R Cheng,* Indiana University-Purdue University Indianapolis

The scale of new micro and nano magneto-electronic devices is bounded by thermal and quantum constraints as predicted by Moore's Relation. This necessitates a push into the limits of harnessable natural phenomena to facilitate a post-Moore's era of design. Thermodynamic stability at room temperature, fast (Ghz) switching, and low energy cost narrow the list of candidates. Molecular electronic frontier orbital structure of Fe ions in octahedral fields will split in response to the local energetic environment, giving rise to the e_g and t_{2g} suborbitals. The energetic scale between these two orbitals as a result of this deformation yields a low spin diamagnetic state or an S=2 high spin paramagnetic state. Spin crossover complex [Fe(II)(H$_2$B(pyz)$_2$(bipy))$_2$] will show locking of its spin state well above the transition temperature, with an accompanied change of conductivity, when placed in a polar environment. Here we show voltage controllable, room temperature, stable locking of the spin state, and the corresponding conductivity change, when molecular thin films of [Fe(II)(H$_2$B(pyz)$_2$(bipy))$_2$] are deposited on a ferroelectric polyvinylidene fluoride hexafluropropylene substrate. This opens the door to the creation of a thermodynamically stable, room temperature, multiferroic gated voltage device.

Manufacturing Science and Technology Group
Room Union Station AB - Session MS-ThP

Manufacturing Science and Technology Poster Session

MS-ThP-1 Evaluation of Mechanical Properties of Infill Structures Change during 3D Modeling, *Seita Ogawa*, A Matsumuro, Aichi Institute of Technology, Japan

By products with a 3D printer, modeling of complex shapes is possible based on the data obtained by 3D CAD and 3D scanner. In recently, 3D printers are actively used for products from the stage of being used for prototyping. Therefore, we have focused on the filling rates and infill structures for 3D printing products. There are cavities in the shaped object, and the mechanical properties of the object change depending on infill structures and filling rates. Our purpose of this study is to evaluate

mechanical characteristics for infill formation conditions due to create an important database in future. we considered it to be important creating a database of their mechanical properties for products used 3D printer.Conventional tensile test and three-point bending test were performed using typical types of materials, ABS resin, PLA resin, and Primalloy（Mitsubishi Chemical Co., Ltd.）. In this research, the infill structures of several kinds of default set with slicer software used, i.e. hatching, zigzag, honeycomb and 3D honeycomb. The filling rates were increased to 50% every 10%. The test pieces used the dumbbell shape based on JIS.K7161. I used a MUTOH 3D printer MF-2200D as a device, and used an Imada measuring stand and a force gauge for a tensile test and a three-point bending test. In the three-point bending test, we tested from both side of flat surface and edge side to the stacking direction.As a result, the ABS test piece of the filling rate 30% and 50% increased 60% and 70% higher than the filling rate 10% and 50% respectively in the tensile strength. It was found that an increasing of the filling rates leads to an increasing of mechanical properties. Summarizing results of all test conditions, it was cleared that the tendency of the mechanical properties of bending from two directions was different in the all materials. The tendency of mechanical properties was different depending on different kinds of material.From our results, we considered it to these databases will be great important for products of large field using 3D printers. Furthermore, we try to investigate several kinds of infill structures that have higher strength. Finally, we hope that our study contributes to innovative industry in the near future.

MS-ThP-2 Development of Innovative CNT/Extra Super Duralumin Composite Materials, *Chihiro Fujiwara*, Aichi institute of Technology; *A Matsumuro,* Aichi Institute of Technology, Japan

Current science and technology should serve as it overcoming the issues of global environment and realization of the new industrial revolution immediately. To solve these important problems, drastic challenge from every field is accomplished. We focus on materials development with innovative characteristics in this study. In late years technology development about the space utilization become much active. Importance of the aerospace apparatus will increase more and more. Due to contribute to current technological development, we should design creatively an innovative high specific strength material. As our research objective, we came up with the idea of the development of an Extra Super Duralumin (ESD) based composite material with Carbon Nanotube (CNT), which has been well known as unprecedented excellent characteristics. ESD is an aluminum base alloy with high tensile strength and pressure resistance. The basic fabrication process of metal based composite material with nano-carbon materials have been established in various materials system. We established original successful uniform dispersion of CNT with in Al based materials, and we demonstrated already that Vickers hardness of CNT/Al composite pellet-formed sintered materials showed several times up in comparison with that of conventional Al bulk material.

In this study, pellet-plate type specimens consisted of our CNT/ESD composite materials were fabricated using compression sintering method with commercial single wall carbon nanotube and ESD powder of dozens of micrometers of particle size powder. The heat-treatment after sintering specimen was done under the conventional method. The obtained main optimum conditions as follows: CNT composite ratio of 1wt. %, ultrasonic dispersion time of 4 h and sintered temperature of 723 K for 4 h.

It has already been demonstrated that Vickers hardness of CNT/ESD composite showed about 6 % increase in comparison with sintered ESD bulk material, and the density decreased down to 1.5 %. So, the specific strength improved up to 10 % just as expected. This result shows clearly possibility to develop a product with innovative characteristic by the effect of composition with nano-carbon materials. These results would suggest bringing a change in the concept of manufacturing process. From now on, we will estimate tensile and bending characteristics with quantity evaluation. Furthermore we would intend challenge to develop CNT/ESD and graphene/ESD composites bulk materials made using the melting process due to lead the innovative materials to practical use. We would like to present charming results at the conference.

MS-ThP-3 Development of Composite Resin Materials with High Dispersion Cellulose Nanofibers, *Naoki Iwanaga*, A Matsumuro, Aichi Institute of Technology, Japan; *K Osawa,* Aichi Institute of Technology, Japn, Japan

Progress of science and technology should serve as it overcoming the problem of global environment immediately. The challenge from every field is accomplished to solve this important problem. In terms of material

issues, high strength and environmentally friendly objects are required. So, we strongly focused on cellulose nanofibers(CNF).

CNF show extraordinary mechanical, physical and chemical properties. Furthermore, CNF is a biodegradable material with low environmental impact and excellent recyclability. Therefore, it is possible to suppress the occurrence of micro plastics, which is a problem in global issues.

In addition, development of the advanced composite resin filaments with CNF for uses 3D printing leads to extend especially application field, due to excellent environmental problem and mechanical properties as one of core of current technology Industry revolution.

In this study, we try to development an innovative high strength resin based composite materials reinforced by CNF with characteristics of eco-friendly and material characteristics.

At first, we researched the possibility of the application of CNF composite materials with ABS base resin, in order to investigate possibility of fabrication of composite material with CNF and improvement of characteristics in comparison with conventional resin materials. The fabrication method with uniform dispensation of CNF in ABS resin powder was applied with the ultrasonic method established on our own. Specimen were made by the die molding method at 250K for 30minutes.

In our results, the optimum dispersion time was determined 6 hours by surface observation.

FT-IR measurement showed that CNF and ABS resin could be dispersed while maintaining its structure. We should remarkable results of representative mechanical property. Tensile strength and young's modulus for specimen excellently increased up to about 70 % for 1.0 wt% CNF and 97 % for 0.5 wt% CNF in comparison with the value of pure ABS resin specimen. Furthermore, strength improvement using nylon 6 was clarified as the same trend in the case of ABS resin.

These results described above should clarified the development important guidelines for fabrication process, of an innovative composite resin materials with enough specific characteristics of CNF.

Furthermore, in order to expand the possibility of practical realization, we are now challenging, to apply to biodegradable PLA resin.

MS-ThP-4 Improvement of Laminated Interface Strength of Printed Objects by FDM 3D Printer, *Li Song,* Aichi institute of technology, Japan

Indispensable 3D printing technique in manufacturing has made us an important unavoidable problem until now. It is unquestionably laminated interfacial existence in molded products. The problem become obviously that the strength of printed products in a vertical direction for printing direction is extremely weaker than the strength with along direction about almost same strength of original filament. The reason is absolutely clear for existence of laminated interfaces with a heterogeneous structure.

In this study, we tried to chanllenge an innovative improvement method of the excellent laminated interface strength which is the ultimate purpose to obtaine conventional products with strength of the bonding force with uniformization of the upper layer and the structure. We tried to create a new 3D printer by installing a compact halogen spot heater attached to one direction at the extruder of the FDM 3D printer with commercially black PLA filament as our first step. We consructed our original system in conjunction with the extruder with spot optical heating on fabricating lower layer interfaces due to change semi-melted state of already fabricated solid satate molded object during modeling. This effect contributes to the homogenization of the interface organization that is improvement of the interface strength.

In this study, it is great important to optimize optical radiation conditions of halogen spot heater due to change lower layer state to semi-melt again while maintaining the shape of the solidified lower layer part, while maintaining the shape of a product. Through trial and error, Optimum conditions of geometric placement of the devices and the irradiation temperature of 393 K estimated using a thermocouple. In order to evaluate a change of the interface strength by a tension test more definitely, we loaded perpendicularly in the laminated direction.

We showed great results that the tensile strength of typical specimen increased from 27 MPa to 34 MPa, and the surface smoothness drastic increase from Ra of 24 to 11 simultaneously by a mild fusion effect by the heat. Both surprisingly results was supported by the fracture surface observations. Using laser microscope, the microstructure of the unheated fracture surface was broken at the specific layer, but that of of heated product was observed at complex layers. These results were attributed to

the interfacial texture homonigetion because of optimal semi-meltrized under layers.

The above-mentioned result makes the great effectiveness of the laminate spot heating method at the same time of molding heating remarkable clear.

MS-ThP-5 Investigation of Multi-Level ReRAM in 65nm CMOS for Logic-in-Memory Applications, *Sarah Rafiq, K Beckmann, J Hazra, M Liehr,* SUNY Polytechnic Institute*; S Jha,* University of Central Florida*; N Cady,* SUNY Polytechnic Institute

Resistive Random Access Memory (ReRAM) has been extensively investigated as a non-volatile memory due to its low energy consumption and scalability. Bipolar ReRAM devices integrated in array architectures with selector devices is a prime candidate for high density memory arrays, novel logic-in-memory applications, and neuromorphic computation. Using a 65nm CMOS process technology, we have integrated 100×100 nm^2 HfO$_2$-based ReRAM devices at the metal 1 / via 1 (M1/V1) interface in a 1 transistor – 1 ReRAM (1T1R) configuration. Arrays of 1T1R cells were evaluated for binary switching between high resistance states (HRS) and low resistance states (LRS), exhibiting excellent yield and performance across a full 300mm wafer. Multi-level switching of 1T1R cells was then investigated by adjusting the gate voltage of the control transistor, which in turn, modulates the current compliance during programming (set operation) of the ReRAM device. Individual 1T1R cells within 8×8 arrays were programmed using increasing compliance current from 20 uA to 0.14 mA , which resulted in a 5-fold change in resistance level from 36 kOhm to 6.6 kOhm respectively. Multiple arrays from multiple 300 mm wafers have been evaluated to determine the variability within arrays, and the effects of changing processing conditions between wafers. Our results show that within a single wafer, 1T1R performance is consistent, but that variation in processing conditions for the HfO$_2$ switching layer can dramatically affect resistance levels and endurance of 1T1R. When comparing arrays on a single wafer, the standard deviation of the resistance state (for 100 switching cycles) decreased from 15 kOhm when programmed with current compliance of 20uA , to less than 500 Ohm at higher current compliance. Therefore, multiple distinguishable resistance states were achieved with higher current compliance. Using the two states (LRS and HRS), a 2×2 sub-array of 1T1R cells was then used to implement XOR logic functionality in a logic-in-memory configuration. Despite one of the cells having a low HRS not exceeding 20 kOhm, the output of the XOR logic was still unaffected. This demonstrates the robustness of logic-in-memory applications. The distinct binary state based logical computations, enabled by the appropriate selection of current compliance, also paves the way for ternary state logic and memory. Ongoing efforts are focused on higher precision control of the multi-level memory performance for 1T1R arrays up to 512×512 cells, and understanding the effects of wafer processing conditions on stochasticity of multi-level memory states, with the ultimate goal of full analog operation.

MS-ThP-6 III-V NanoWires for Junctionless Transistors Fabricated by Focused Ion Beam (FIB) System with Silicon Nitride Passivation, *Cássio Almeida,* University of Campinas, Brazil*; P Souza,* PUC-Rio, Brazil*; M Pires,* Federal University of Rio de Janeiro, Brazil*; J Diniz,* University of Campinas, Brazil

III-V Junctionless semiconductors devices were fabricated on InGaP and GaAs substrates using Gallium (Ga$^+$) Focused Ion Beam (FIB) System. Two groups of samples, with n$^+$-InGaP (10nm)/GaAs-buffer layer (300nm) and n$^+$-GaAs (10nm)/GaAs-buffer layer (300nm), both on semi-insulating GaAs (001) nominal orientation substrates, were studied. The samples were grown by Metalorganic Vapor Phase Epitaxy (MOCVD) in an Aixtron AIX 200 horizontal reactor at 100mbar, where the samples are heated by infra-red (IR) lamps. The total hydrogen carrier gas flow rate was 8L/min. The precursors used for the GaAs growth were trimethylgallium (TMGa) and arsine (AsH$_3$). Silane (SiH$_4$) was used for the n doping. The layers were grown at 630°C with a growth rate of 0,36nm/s and a V/III ratio of 70 for the n doped layer. A pre-growth treatment for de-oxidation at 700°C was applied to the GaAs substrates for 15minutes under AsH$_3$ over pressure. Furthermore, for the first time, the silicon nitride layer (SiN$_x$), thickness of 10nm, deposited by ECR-CVD, was used as gate dielectric of Junctionless and as passivation layer of the surfaces of structures. The morphology of the samples was observed by Atomic Force Microscopy (AFM). X-Ray diffraction (XRD) analysis was used in order to determine the InGaP lattice parameter and mismatch to the GaAs substrate. Hall measurements provided silicon doping levels of 10^{+19}cm^{-3} for both groups of samples, indicating the formation of n$^+$-type layers. These samples were used for

MOS Junctionless (JL) Transistors applications, since III-V semiconductors present higher electron mobility values than silicon. These JL transistors (with three terminals: gate, source and drain) are fabricated using a Focused Ion Beam (FIB) System. Thus, Gallium (Ga^+) Focused Ion Beam (FIB) is used to define the III-V (InGaP or GaAs) nanowires (III-V NWs), which are the electron conduction channel between source and drain and Pt deposition (as gate, drain and source electrodes) layers. Finally, drain-source current (I_{DS}) versus drain-source voltage (V_{DS}) and drain-source current (I_{DS}) versus gate-source voltage (V_{GS}) measurements of JL devices will be extracted and will be able to indicate if these InGaP or GaAs nanowires and the passivation, with the SiN_x deposited by ECR-CVD are of high quality and suitable for Junctionless technology.

MS-ThP-7 The Development of High Efficiency X-ray Tube with Carbon Nanotube Yarn based-cold Cathode, *Hyun Suk Kim, C Lee,* Wonkwang University, Korea

It is development high-efficiency X-ray rube using carbon nanotube yarn as an electronic source of field emission. It is inevitable to secure durability for uniform electronic emission characteristics of materials and to improve the stable structure of the emitter due to the miniaturization of the X-ray tube. Aimed at a high-efficiency X-ray generator with a new concept of cold-polar emission e-meter structure that can control the gap of uneven field discharge by a Chaos of uncontrolled faults in the process. The effects of various structures on the beam focusing performances and emission currents were simulated and fabricated. In the design of the X-ray sources, it is important to ensure that the fine beam focus and efficient electron emission can be simultaneously obtained. Therefore, the geometrical parameters, such as electrode shape and the gaps between parts should optimized. Owing to the unique design of the cathode, the electron beam emitted from the cathode was focused onto the anode without using electric lenses or extra biased electrodes. It was indicated that the beam spot sizes on the anode plate different with the changing electrode shape design. It will be studied that the optimum x-ray yield condition and focusing electrical shape effect in the CNT micro-focus CNT x-ray tube.

MS-ThP-8 High Aspect Ratio Carbon Nanotube Optical Collimator, *Tyler Westover, R Davis, R Vanfleet,* Brigham Young University

Patterned carbon nanotube forests are finding an increasing number of applications due to their high aspect ratios and the characteristics of the nanotubes themselves. For example carbon nanotubes are highly absorptive of light in various wavelengths including visible and near infrared. Due to the high absorption of light that comes into contact with a carbon nanotube forest these structures work as sidewalls for an optical collimator. Here we will present our results using a carbon nanotube collimator in the visible and the IR.

MS-ThP-9 Development of a Fabrication Process for Integrated inductors on Flexible Substrate, *Wilson Freitas,* State University of Campinas, Brasil; *M Oliveira Piazzetta,* Brazilian Nanotechnology National Laboratory, Brazil; *L Manera,* UNICAMP, Brazil; *A Gobbi,* Brazilian Nanotechnology National Laboratory, Brazil

This paper presents the development of a fabrication process for integrated inductors on flexible substrate. The process consists of two metal and one dielectric layer on a polyimide flexible substrate. Kapton was the choice for the substrate due to its attractive characteristics such as high dimensional stability and thermal and electrical insulation. The first metal layer was 0.5 µm thick gold deposited by electroplating on a nickel film. Nickel was deposited by sputtering and used both as a seed for the electroplating deposition process and to improve the adhesion of gold to the substrate. Gold lines were patterned by lift-off and serve as mask for nickel wet etching. The second metal layer was made through the same process, with thickness of 1 µm. Silicon dioxide was selected as dielectric, also patterned by lift-off and preceded by a chrome e-beam deposition step to enhance adhesion. Structures were formed by conventional photolithography process, with minimum line and space dimensions of 10 µm. With the use of intermediate layers of nickel there was no need for substrate modification to improve metal layers adhesion. The first metal layer thickness was optimized to improve dielectric step coverage, and the second layer was made thicker to reduce series resistance and provide better performance in both quality factor and frequency response. With this technology, it was possible to fabricate integrated inductors with 1 to 5 nH, maximum quality factor of 8, and self-resonant frequency in excess of 20 GHz, with values compatible with those from simulation with Keysight ADS, allowing for the implementation of VCOs and others RF circuits for hybrid flexible electronic structures.

Nanometer-scale Science and Technology Division
Room Union Station AB - Session NS-ThP

Nanometer-scale Science and Technology Poster Session

NS-ThP-1 Probing Intermolecular and Molecule-Substrate Interactions at Angstrom Scale by Ultrahigh Vacuum Tip-Enhanced Raman Spectroscopy, *Sayantan Mahapatra, J Schultz, N Jiang,* University of Illinois at Chicago

Conventional spectroscopic techniques are limited by the optical diffraction limit to about half wavelength and therefore offers about 200 nm x 200 nm microscopic zone for working in the visible light range. Tip-enhanced Raman spectroscopy (TERS) emerges as an advanced analytical technique, where the plasmonically active probe is not only used to detect the tunneling current but also to interrogate the local chemical environment of surface adsorbed molecules with angstrom scale precision. In this work, we studied two regioisomers (positional isomers), *trans-* and *cis-*tetrakispentafluorophenylporphodilactone (*trans-* and *cis-*H_2F_{20}TPPDL) using scanning tunneling microscopy (STM), ultrahigh vacuum (UHV) TERS on Ag(100) with the spatial resolution down to 8 Å, which has wide range of applications in various field of surface science & nanotechnology such as regioselective catalysis reaction, chemical reactions, molecular electronics etc. We have shown, it is possible to distinguish these two structurally very similar forms with high accuracy & precision. The two-component molecular junction has been identified using high resolution two-dimensional (2D) Raman mapping. Furthermore, these new class of porphyrinoids i.e. porphodilactones (PDL) have been studied on different single crystals [Ag(100), Cu(100) and Au(100)] to probe the intermolecular and molecule-substrate interactions. This work demonstrates, STM combined with TERS is a complementary technique to characterize a system completely at angstrom scale.

NS-ThP-2 Cobalt Nanoparticles Supported on Multiwalled Carbon Nanotubes for Catalysts in Hydrogen Generation , *Brian Price,* Christopher Newport University

With the threat of fossil fuels running out in the near distant future coupled with an increased concern over the environment, a large amount of focus has been dedicated towards green forms of energy. One such source could come from hydrogen through the reduction of sodium borohydride, but this reaction is slow and needs a low cost catalyst. Using abundant metals to make nanoparticles supported by carbon nanotubes would create a globally producible catalyst. The catalytic effect of cobalt metal boride carbon nanotube composites was observed through its reaction with sodium borohydride. The metal boride carbon nanotube composites were synthesized through reduction of metal organic frameworks in the presence of carbon nanotubes. The composites were characterized through scanning electron microscope (SEM), transition electron microscope (TEM), x-ray diffraction (XRD), infrared spectroscopy (IR).

NS-ThP-3 Advanced Hybrid Metrology for Measuring Pattern Fidelity for Nano Technology--Combining Massive metrology using Full Contour based Data Extraction and Analysis, *Allen H. Rasafar,* GLOBALFOUNDRIES Inc.

Objectives:

This paper will present a new method for Pattern Fidelity assessment using an advanced holistic/hybrid metrology solution for sub 7nm technology nodes. Adopting this structured approach will enable a holistic metrology solution to close the gap on illusive yield losses and open the opportunities for a new metrology work space.

Methods:

Current state of metrology methods is not fully meeting voice of the customer. Metrology tools are not capable to deliver advanced algorithm for extraction and analysis of the data embedded in SEM images. Most of the metrology tools are collecting very basic measurement and spend more time handling and measuring the wafer. Tools are not designed to go over throughput specs. Innovation is lost in between generation based approach. An innovation in metrology was long overdue for delivering a metrology solution that is not solely based on older technology.Thus, the new metrology space sets a new standard for extracting critical pattern fidelity data for CD/OV, OPC measurement and offer unmatched analysis using high resolution wide field SEM images. The sophisticated application of advanced contour extraction methods is redefining the opportunities embedded in SEM image for better process analysis.This work will highlight advantages of this method over OCD, and simple contour measurement techniques that is used by some SEM and eBeam tools. With this method

we will pull massive amount of data related to pattern shape, size, Line edge roughness, Line width variations, and dense contact uniformity achieved by Big data analysis expertise.

Conclusions:

A structured approach is demonstrated and compared to existing pattern fidelity assessment solutions in an actual sub-14nm and 7nm Fab settings. This method overlays design(physical layout)to image of pattern captured by high resolution SEM tools and collected across all dies, and wafers. A large volume of images is analyzed and comprehensive results are reported including full statistical distribution of image variations by location, image to image (die to die), distribution of overall measurements, outliers, defect distribution, and representation of weak points in physical design and OPC feedback. We invite wider adoption of this method by the industry to to enable Fabs, and engineers to achieve better process improvement, debug and enhancing design for manufacturing. The Big Data approach provides new opportunities for full stack analysis of the layers at each step, make predictions for the stacked layers at subsequent process steps. Big Data method will enable sharing data within functional team and all stakeholders in a secure server work space.

NS-ThP-4 A Nanoscopic View of Photo-induced Charge Transfer in Organic Nano-crystalline Heterojunctions, *Qian Zhang, S Cohen, B Rybtchinski,* Weizmann Institute of Science, Israel

Organic photovoltaics are promising as cost-efficient, tunable, and flexible platforms for solar energy conversion, yet their performance and stability are still far from optimal. Here we present a study of photo-induced charge transfer processes between electron donor and acceptor organic nanocrystals, as part of our path-finding effort to develop robust and efficient organic nanocrystalline materials for photovoltaic applications. We produced sub-micron to microns-long nanocrystals of perylenediimides (PDIs) as electron acceptors, and with Copper Phthalocyanine (CuPc) as the electron donor. Three different configurations of donor-acceptor heterojunctions were prepared. Charge transfer in the heterojunctions was studied with Kelvin-probe force microscopy (KPFM) under laser or white light excitation. We also conducted theoretical calculations and time-resolved photo-luminescence measurements to understand the differences in the photovoltaic processes of these organic nanocrystals. Our work demonstrates that excitonic properties can be tuned by controlling the crystal and interface structures in the nanocrystalline heterojunctions, in order to minimize photo-voltaic losses.

NS-ThP-5 Ferroic-ionic Interaction in Hybrid Organic Inorganic Perovskites, *Yongtao Liu[1][2], L Collins, A Ievlev, A Belianinov,* Oak Ridge National Laboratory; *M Ahmadi,* University of Tennessee Knoxville; *S Jesse, S Kalinin,* Oak Ridge National Laboratory; *B Hu,* University of Tennessee Knoxville; *O Ovchinnikova,* Oak Ridge National Laboratory

Hybrid organic-inorganic perovskites (HOIPs) such as methylammonium lead iodide ($CH_3NH_3PbI_3$) have attracted broad research interest due to their outstanding photovoltaic performance. However, fundamental understandings of the origin of the high performance and the anomalous current-voltage (I-V) hysteresis of HOIPs solar cells still lag. Although ferroelectricity is proposed to be a reason of the related behavior, the convincing evidence supporting ferroelectricity in HOIPs is missing because the strong ion motion in HOIPs complicates the ferroic characterization. A clear understanding of the interplay between ferroic behavior and ion motion in HOIPs will be helpful for clarifying this question.

In this work, using multi-modal functional and chemical imaging methods, we unveil a ferroic-ionic interaction in $CH_3NH_3PbI_3$. In piezoresponse force microscopy (PFM) experiments, we observed ferroelastic twin domain structures in $CH_3NH_3PbI_3$. Although PFM shows 'piezoelectric-like' contrast of thetwin domains,our studies—including band excitation (BE) PFM, laser Doppler vibrometer (LDV) PFM, and BE contact resonance atomic force microscopy (BE-AFM)—unambiguously reveal the mechanical origin rather than the electromechanical origin of the 'piezoelectric-like' contrast. This ferroelastic domain was accompanied by ion segregation due to the strain-driven ion redistribution, which was observed using helium ion microscopy secondary ion mass spectrometry (HIM-SIMS) and atomic force microscopy infrared spectroscopy (AFM-IR). To further address how ion distribution affects the ferroic behavior of $CH_3NH_3PbI_3$, we studied the interaction of the ion distribution and the fields (elastic field and electric field) distribution in $CH_3NH_3PbI_3$. It is shown that the ion redistribution is accompanied by a reversible change in lattice strain, suggesting the

dependence of the elastic field on ion distribution. Furthermore, we found that the local ion distribution could manipulate the formation of ferroelastic twin domain. The electric field was studied by Kelvin probe force microscopy (KPFM), which indicates that the ion distribution affects local electric field intensity and the electric field distribution. By combining KPFM and time-of-flight secondary ion mass spectroscopy (ToF-SIMS), we observed a screen effect of ion migration on the electric field in $CH_3NH_3PbI_3$. The remainder of the field is very small due to the compensation of ion migration. These results suggest that the ion motion can alter local field and hence local ferroic behavior of HOIPs. Overall, this work offers an understanding of ferroic-ionic interplay in HOIPs, providing a pathway to develop novel devices.

NS-ThP-6 Processing of Nanoscale Lamellae in Bulk Al-Cu Eutectic Samples Through Selective Laser Melting, *Jonathan Skelton, J Floro, J Fitz-Gerald,* University of Virginia

Eutectic alloys with nanoscale lamellar spacing may have a wide range of applications in functional materials such as thermoelectrics and photovoltaics, as well as in enhanced mechanical properties. This is due to an intimate interleaving of two or more phases where the length scales are controlled in part by the solidification rate. Utilization of nanoscale eutectics remains limited as a result of the lack of methods available to readily produce them in bulk materials. Rapid solidification through laser irradiation has been shown to create these structures on the surface of model eutectic materials, such as Al-Cu, with an interphase spacing dependent on the scanning velocity of the laser, but the limited absorption depth of the laser frustrates formation of bulk nanostructured samples. Selective laser melting (SLM) presents an innovative solution to this problem by building 3D samples via a layer-by-layer method, where each pass is rapidly cooled by the bulk material. In this research, the relationship between the SLM processing parameters and the resulting microstructure of bulk Al-Cu eutectic samples is investigated, with a focus on controlling the interphase spacing and directionality of the lamellar microstructure. An SLM Solutions GmbH 125 system was used to process the samples in this study, operating at scan velocities ranging from 50 to 150 mm/s at a CW laser power of 100 W. Cross-sections of samples exhibited lamellar spacing of 40 to 100 nm within narrow eutectic colonies of approximately 3 μm width that extended the height of the individual scan layers (50 μm). The solidification mechanism that produced these colonies is investigated, and the fine lamellar spacing is analyzed in accordance to the Jackson-Hunt theory. Samples in this study were characterized by scanning electron microscopy (SEM), focused ion beam (FIB), and energy dispersive X-ray spectroscopy (EDS). Support for this research from the National Science Foundation grant #CMMI-1663085 is gratefully acknowledged.

NS-ThP-7 Precision Nanometer-scale Scanning Probe Microscopy Data Recalculation for Diamond Tool Cutting Edge Structures, *J Su, Nian-Nan Chu, C Hsiao,* Taiwan Instrument Research Institute, National Applied Research Laboratories, Taiwan, Republic of China

Ultra-high precision diamond tool machining demands for high resolution three-dimensional inspection. Scanning Probe Microscopy (SPM) fulfills these needs through high resolution 3D measurements, non-destructive examination and a variety of probes for specific structural measurements. Moreover, recalculation of SPM data in respect to probe effect will improve data accuracy, especially for small angle structures. Here we present an algorithm method to evaluate probe effect and improve the resulted accuracy based on the scanning probe mechanism. This work is valuable to ultra-high precision diamond tool machining where other methods are incompatible.

Advanced Surface Engineering Division
Room Union Station AB - Session SE-ThP

Advanced Surface Engineering Poster Session

SE-ThP-2 Plasma and Heat Treatment Response of Carborane Self-Assembled Monolayer on Copper, *Rupak Thapa, L Dorsett, S Malik, R Bale, S Wagner, D Bailey, A Caruso,* University of Missouri-Kansas City; *J Bielefeld, S King,* Intel Corporation; *M Paquette,* University of Missouri-Kansas City

Self-assembled monolayers (SAMs) have a wide variety of applications. These include modifying the properties of metal surfaces to act as protective layers or to enable molecular recognition for sensors. Here, we investigate copper surfaces modified by thiol-carborane SAMs. We use carborane-based boron carbide due to its excellent chemical, thermal, and

---

mechanical properties along with its symmetrical icosahedral shape and capacity to cross-link under the influence of heat or plasma. It has been shown that carborane-based SAMs provide better corrosion resistance on silver and have the ability to change the electronic properties (e.g., work function) of gold and silver. Here, we investigate the influence of plasma and heat on carborane SAMs on copper using in situ ellipsometry, in situ x-ray photoelectron spectroscopy, and water contact angle measurements. We use various plasmas (N_2, O_2, and Ar) at different conditions (power, pressure, and time) to determine how these stabilize, degrade, and/or otherwise modify the SAMs. We also heat the samples to various temperatures and investigate their growth properties and thermal stability. Results suggest that SAMs based on 1,2-dithiol-o-carborane containing two thiol groups are more stable than those based on 9-thiol-m-carborane containing one thiol group.

Thin Films Division
Room Union Station AB - Session TF-ThP

Thin Films Poster Session

TF-ThP-1 Oxygen Partial Pressure Dependence of Structural and Photoluminescence Properties in Eu^{3+} doped Tantalum based Double-perovskite Thin Film, *Jung Hyun Jeong, J Oh, B Choi, J Kim, S Seo,* Pukyong National University, Republic of Korea*; K Jang,* Changwon National University, Republic of Korea
In this study, we investigated the structural and photoluminescence properties of Eu^{3+} doped $SrLaMgTaO_6$ (SLMTOE) double-perovskite thin films depending on the oxygen partial pressure. The X-ray diffraction patterns were examined to determine the growth behaviors of the SLMTOE films on the $SrTiO_3$ (100) substrates. In the oxygen partial pressure range of 10-200 mTorr, the SLMTOE thin films were aligned with the $SrTiO_3$ (001) substrate. The SLMTOE films grown at 100 mTorr have a low crystallinity but emitted the strongest red light corresponding to $^5D_0$-$^7F_2$ transition (Eu^{3+}). Based on this sample, the behavior of PL intensity was different at low oxygen partial pressure (10-100 mTorr) and high oxygen partial pressure (100-200 mTorr). To figure out the different PL intensity behavior, we performed the x-ray photoelectron spectroscopy (XPS). Our XPS result implies that the enhancement of PL intensity at low partial pressures is associated with defects in the thin film lattice, and the weakening of PL intensity at high partial pressures is due to the change in the ratio of Eu^{3+} to Eu^{2+} by the self-reduction process.

TF-ThP-2 Influence of the Crystal Structure on Photoluminescence Properties of Dy^{3+} and Pr^{3+} Doped Rare-earth Oxyorthosilicates (R_2SiO_5) (R = La, Gd, Y) Thin Film Phosphors, *S Ogugua, H Swart,* University of the Free State, South Africa*; O. Martin Ntwaeaborwa,* University of the Witwatersrand, South Africa
Phosphors have many technological uses in applications such as solid-state lighting, optical laser, data storage, medicine, quantity control, scintillation, advertising, solar cells, theft prevention, etc. We have prepared a series of praseodymium (Pr^{3+}) and dysprosium (Dy^{3+}) doped mixed rare-earths oxyorthosilicate phosphors with a general formula R_2SiO_5 hosts (R = La, Gd or Y) using the solution combustion method. By varying the molar ratio of La to Y and Gd to Y, we modified the unit cells and the crystal field strengths of the host lattices. This modification of the crystal field of the host lattice can lead to the shifting of the emission wavelengths, increase of the rate of radiative transitions, and minimization of energy loss by non-radiative transitions. We evaluated the crystal structure and photoluminescence properties of Pr^{3+}/Dy^{3+} doped R_2SiO_5 (R = La, Gd or Y) in powder and laser ablation deposited thin film forms. We varied several deposition parameters including partial pressure of gas (O_2 and Ar), type of laser pulse, and substrate temperature using the 1064 nm Nd:YAG solid state laser. The effects of varying the La to Y/Gd ratios on the field strengths of the host lattices and the influence of the various deposition conditions on the emission colour and photoluminescent intensities will be discussed.

TF-ThP-3 Transparent Hybrid Thin-Films of Copper-Mesh and Conductive Polymers for ITO-Free Organic Light-Emitting Diodes, *K Lim, Y Kim,* Pukyong National University, Republic of Korea*; S Jeong,* Pusan National University, Republic of Korea*; Min Kyo Jeong, S Seo, J Jeong,* Pukyong National University, Republic of Korea
We report on highly transparent conductive electrodes based on copper (Cu)-mesh structures combined with conductive polymer films. The hybrid transparent electrodes show outstanding optical and electrical properties

(transmittance of 81.7 % at a wavelength of 550 nm, sheet resistance of 100.7 ohm/sq). The effective current collecting property of metal mesh structures as well as the excellent current spreading property of the conducting polymer enables the high performance of the hybrid transparent electrodes. Organic light-emitting diodes (OLEDs) employing the hybrid transparent electrodes results in 2.0-fold enhanced current and power efficiencies, compared to the control polymer electrode-based OLED without current collecting metal mesh structures. The results present that Cu-mesh structures combined with conductive polymer films can be a promising transparent conductive electrode for highly efficient low-cost, flexible indium tin oxide-free OLEDs.

TF-ThP-4 Fabrication of IrO_2/Pt Composite Films by Pulsed-dc Magnetron Sputtering and Plasma-enhanced Atomic Layer Deposition, *Chao-Te Lee, Y Yu, W Cho,* Taiwan Instrument Research Institute, Taiwan*; W Chen,* Taiwan Instrument Research Institute, Taiwan, Taiwan, Republic of China*; H Chen,* Taiwan Instrument Research Institute, Taiwan
The IrO_2/Pt films were prepared on Si substrate by pulsed-dc magnetron sputtering and plasma-enhanced atomic layer deposition (PEALD), respectively. The IrO_2 film was prepared from a high purity Ir target and deposited on Si substrate at room temperature with various working pressure, gas ratio (Ar/O_2 ratio) and pulse frequencies (10~100 kHz) by a pulsed-dc magnetron sputtering. Effects of process parameters on the film composition, microstructure, surface roughness, and electrical properties were investigated by field emission scanning electron microscopy with energy dispersive X-ray spectroscopy (FESEM-EDX), X-ray diffraction (XRD), high resolution transmission electron microscopy (HRTEM), atomic force microscopy (AFM), and cyclic voltammetry (CV) measurement, respectively. The nanoblade structure of the IrO_2 film was prepared at a working pressure was 20×10^{-3} Torr, and Ar/O_2 rate was 10. The Pt film was prepared on the nanoblade structure of IrO_2 film by PEALD. Effects of plasma power, and thickness on the microstructure, and electrical properties of the IrO_2/Pt films were investigated. The research goal is to obtain high charge delivery capacity (CDC) of the film. It is expected that the high quality IrO_2/Pt film can be explicated in biomedical technology.

TF-ThP-5 The Effect of Deposition Parameters on the Optical and Electrical Properties of MoO_3/Ag/Mo/ MoO_3 Films by Reactive rf Magnetron Sputtering, *C Lee,* Taiwan Instrument Research Institute, Taiwan*; Wei-Chun Chen,* Taiwan Instrument Research Institute, Taiwan, Taiwan, Republic of China*; H Chen,* Taiwan Instrument Research Institute, Taiwan*; C Jaing,* Minghsin University of Science and Technology, Japan
Stacked MoO_3/Ag/Mo/MoO_3 (MAMM) films were deposited on glass substrate as ITO-free and electrochromic applications. The effects of the thickness of Mo layer on the electrical and optical properties of the MAMM films were examined by the four-point probe system and a spectrophotometer. The resistivity of MAMM films was decreased with increasing the thickness of Mo layer. The resistivity of the films were 5000 and $3X10^{-5}$ Ω/cm when the thickness of Mo layer was 1 and 2 nm, respectability. It was found that the ITO-free MAMM film as the Mo layer is over 2 nm. The luminous transmittance of MAMM films was decreased with increased the thickness of Mo layer. After the optical simulated, and prepared the electrochromic MAMM films, the MAMM films for hot-mirror and electrocromic applications was also investigated.

TF-ThP-6 Effect of Sintering Conditions on Characteristic of $BaFe_2(PO_4)_2$ and Ceramic Target Production for Thin Films, *Jung Hwan Kim, B Jung, J Jeong, S Seo,* Pukyong National University, Republic of Korea*; K Jang,* Changwon National University, Republic of Korea
Inorganic compounds composed of low-dimensional ferromagnets exhibit fascinating properties and provide a rich opportunity to investigate the ferromagnetic states, phase transitions, magnetic transitions and magnetization phases. Among them, $BaFe_2(PO_4)_2$ (BFPO), which is a two-dimensional ferromagnetic material, has a special structural and magnetic structure at low temperature. Anomalous distortion at about 150K causes a structural phase transition from rhombohedral(R) to triclinic(P). However, further cooling results in a magnetic phase transition from paramagnetic to ferromagnetic at about 80K, and at the same time, it returns to the original rhombohedral(P →R). The change of structural phase transition and the change of band gap in the sintering process of BFPO. This study could be a preliminary study on the fabrication of ceramic targets for thin film deposition of BFPO.

TF-ThP-7 Development of Thin Film of Ferric Hydroxide Dispersed in Polymer Matrix Doped with Ethylenediamine, *S Fernandes, Leandro Tiago Manera, H Ceragioli,* UNICAMP, Brazil

The present work presents the development of a thin film based on ferric hydroxide ($Fe(OH)_3$) dispersed in a polymer matrix of polyvinyl acetate (PVA) containing ethylenediamine ($H_2N-(CH_2)_2-NH_2$) to form a membrane phosphate in solution. Ferric hydroxide was obtained from the stoichiometric reaction of iron ($FeCl_3$) perchloride with ammonium hydroxide (NH_4OH), and after washing, filtration and drying the $Fe(OH)_3$ was diluted with ethyl alcohol to add to ethylenediamine doped PVA. The thin film for the formation of the membrane was obtained by the spin-coating method. For the selectivity tests, the membrane was applied in a semiconductor insulating electrolyte (EIS) device to be used as hydrogen phosphate sensor. The EIS device is formed by the selective membrane deposited on a structure composed of a thin layer of silicon oxide on the silicon substrate, and a gold-plated tungsten micro tip as the reference electrode. The thin film composing the selective membrane was characterized structurally by elliptiometry, Raman spectroscopy, X-ray diffraction, and atomic force microscopy (AFM). In order to evaluate the selectivity of the thin film of the membrane, the electrical characterization of the EIS device was carried out, obtaining the voltage capacitance curves for the pH variation and for the variation of the hydrogen phosphate concentration in solution, which showed a result in the sensitivity of 143 mV/pH and sensibility in the measurement of the hydrogen phosphate concentration of 42 mV/mg/dL.

Keywords— ferric hydroxide; hydrogen phosphate; thin films; selective membrane

TF-ThP-8 Dual-temperature Atomic Layer Deposition of HfO$_2$/Al$_2$O$_3$ on In$_{0.53}$Ga$_{0.47}$As, *Changmin Lee, S Choi, Y An, W Lee, W Oh, D Eom, J Lee, H Kim,* Sungkyunkwan University, Republic of Korea

$In_{1-x}Ga_xAs$ has been considered to be one of the promising candidates for future n-channel metal-oxide-semiconductor field-effect transistors (MOSFETs) [1]. However, due to its poor interface quality with the high-k gate dielectrics (e.g., high interface state density, D_{it}), Al_2O_3 has been used preferably as an interface passivation layer under the HfO_2 gate dielectric with a higher k value [2-5]. Most recently, Choi *et al.* [6] reported that low-temperature atomic layer deposition (ALD) of a HfO_2 (4 nm)/Al_2O_3 (1 nm) stacked structure at 100 °C was effective in reducing both D_{it} and leakage current density. However, because they used an identical ALD temperature for both HfO_2 and Al_2O_3 layers, the capacitance equivalent thickness (CET) of the HfO_2/Al_2O_3 gate dielectric stack was significantly increased [6].

In this presentation, we will introduce a dual-temperature ALD process for the HfO_2/Al_2O_3 stacked gate dielectric to decrease the CET values while maintaining low D_{it} and leakage current density values. While the ALD temperature for the Al_2O_3 passivation layer (~1 nm) on a n-type $In_{0.53}Ga_{0.47}As$ substrate was fixed at 100 °C, the following ALD temperature for the HfO_2 layer (~4 nm) was varied from 100 to 300 °C to decrease the CET values. After the fabrication of MOS capacitors with a stacked gate dielectric structure, the effects of the ALD temperature for the overlaid HfO_2 film on various electrical parameters and characteristics, such as CET, D_{it}, bulk trap density, and static/dynamic leakage currents, were studied.

[1] Shinichi Takagi, Rui Zhang, Junkyo Suh, Sang-Hyeon Kim, Masafumi Yokoyama, Koichi Nishi, and Mitsuru Takenaka, 2015, 545, 06FA01.

[2] A. O'Mahony, S. Monaghan, R. Chiodo, I.M. Povey, K. Cherkaoui, R. E. Nagle, É. O'Connor, R. D. Long, V. Djara, D. O'Connell, F. Crupi, M. E. Pemble, and P. K. Hurley, 2010, 33, 69.

[3] S. Monaghan, A. O'Mahony, K. Cherkaoui, É. O'Connor, I. M. Povey, M. G. Nolan, D. O'Connell, M. E. Pemble, P. K. Hurley, G. Provenzano, F. Crupi, and S. B. Newcomb, J. Vac. Sci. Techno. B, 2011, 29, 01A807.

[4] R. Suzuki, N. Taoka, M. Yokoyama, S. Lee, S. H. Kim, T. Hoshii, T. Yasuda, W. Jevasuwan, T. Maeda, O. Ichikawa, N. Fukuhara, M. Hata, M. Takenaka, and S. Takagi, Appl. Phys. Lett., 2012, 100, 132906.

[5] K. Ohsawa, S. Netsu, N. Kise, S. Noguchi, and Y. Miyamoto, Jpn. J. Appl. Phys., 2017, 56, 04CG05.

[6] S. Choi, J. Song, Y. An, C. Lee, and H. Kim, J. Korean Phys. Soc., 2018, 72, 283.

TF-ThP-9 Conformal CVD of Hf$_{1-x}$V$_x$B$_2$ from Two Precursors: Control of Composition x in Deep Trenches, *Kinsey Canova, G Girolami, J Abelson,* University of Illinois at Urbana-Champaign

Fabrication of device interconnects in the high aspect ratio features of modern electronics requires highly conformal, electrically conductive films.

HfB_2 is a metallic ceramic which can be deposited with excellent conformality at low temperatures using the single-source CVD precursor $Hf(BH_4)_4$; conformality is due to the kinetic saturation of growth rate at precursor pressures of a few mTorr. Here we report the conformal growth of $Hf_{1-x}V_xB_2$ alloys by adding a co-flow of the vanadium precursor $V[N(CH_3)_2]_4$. This alloy is of special interest for its reported superconducting transition near 7 K.

Alloy compositions previously investigated were limited to the solubility limit of ~ 4 % V in HfB_2. In our low-temperature process, however, metastable compositions with excess V can be obtained, and the film stoichiometry x is controlled by relative reaction rates of the two precursors. We report the compositional variation versus precursor flux, which is then used to develop a kinetic model of growth based on the adsorption and reaction rates for both precursors. This model is extended to estimate compositional variation vs. depth z in a deep trench and tested by coating macro-trenched substrates. We also report the electrical resistivity from ambient to cryogenic temperatures.

TF-ThP-10 Catalyst-enhanced Chemical Vapor Deposition of Titanium-doped MgB$_2$ Thin Films, *Xiaoqing Chu, Y Yang, C Caroff, G Girolami, J Abelson,* University of Illinois at Urbana-Champaign

We report a CVD process to deposit titanium-doped polycrystalline MgB_2 films at low temperatures (≤ 400 °C) using Mg (DMADB)$_2$, a highly volatile Mg precursor. The low growth temperature assures that the film does not lose Mg by evaporation, which occurs above 400 °C. When used alone, however, this precursor requires higher temperatures in order to react (it is slightly too stable chemically). We show that CVD proceeds at temperatures as low as 300 °C upon addition of the analogous Ti precursor, Ti(DMADB)$_2$. We identify Ti(DMADB)$_2$ as a catalyst because each Ti molecule drives the decomposition of up to 4 Mg(DMADB)$_2$ molecules. With a high precursor to catalyst pressure ratio, the films are stoichiometric (metal : boron = 1 : 2), and the concentration of oxygen, carbon, and nitrogen is each below the detection limit of ~ 1 at. %. For a film grown at 350 °C, the stoichiometry determined by RBS is $Mg_{0.82}Ti_{0.18}B_2$; it is well crystallized; and the room temperature resistivity is a few hundred $\mu\Omega\cdot cm$. Literature reports suggest the possibility of superconductivity at T = 10-33 K depending on the doping levels of Ti.

TF-ThP-11 Computational Simulation of Novel Pyroelectric Infrared Detectors and Their Integration with Silicon, *A Batra, George Taylor, J Sampson,* Alabama A&M University

Pyroelectric infrared detectors (PIR) of are fast-response thermal sensors operating at ambient temperature unlike semiconductor detectors, which require cooling. Their spectral response is uniform in a wide range of wavelengths, including the main band of IR transmission within the earth's atmosphere. A further increase in pyroelectric response is possible by integrating pyroelectric sensors with silicon technology. The unique structures of PIR can the most sensitive among known structures. Effective sensitivity and performance depend not only on the pyroelectric sensor element material characteristics, but also on the thermal performance of the complete structure of a detector, such as substrate material (Si), absorbing layer, and isolation layers including associated electronics. Thus, we have calculated the thermal transfer function by solving a one-dimensional thermal diffusion equation for a single element n-layer structure. From which the performance of any number of layers detector structure can be derived, predicted, and optimized; the calculated and predicted responsivity and other parameters of integrated detector system will be presented.icon Technology

TF-ThP-12 Kinetically Stabilized Growth of InN by MEPA-MOCVD, *G. Brendan Cross, Z Ahmad,* Georgia State University*; D Seidlitz,* Technische Universität Berlin, Germany*; M Vernon, A Kozhanov,* Georgia State University

We report on kinetically stabilized indium nitride grown on sapphire and gallium nitride, by migration enhanced plasma assisted metal organic chemical vapor deposition (MEPA-MOCVD). Deposition is studied over a range of temperatures, pressures, flows and plasma power, outside the range of indium nitride grown in conventional MOCVD. Raman and FTIR spectroscopy, XRD and atomic force microscopy are used to explore the crystalline quality, growth rate, and surface morphology change with these parameters.

TF-ThP-13 Structure Characterization of PECVD a-SiCN:H Thin Films: Toward Machine Learning Algorithms for Modeling of Complex Disordered Solids, *Sai Siva Kumar Pinnepalli, C Burkett,* University of Missouri-Kansas City; *J Hwang,* Ohio State University; *N Oyler, M Paquette,* University of Missouri-Kansas City

Plasma-enhanced chemical vapor deposition (PECVD) is a routinely employed process in thin-film technologies. Despite its array of advantages and affordability, it suffers from the lack of systematic principles to define growth conditions for an intended output. A deeper understanding of plasma processes is necessary for rational design and strategic synthesis of robust materials spanning a broad spectrum of applications. The properties of these materials are highly dependent on structure; and the structure varies as a function of growth conditions. Interpreting or predicting the effects of PECVD process variables such as temperature, pressure, flow rate and plasma power density on structural features of thin-films is a formidable task. The traditional 'cook and quench' molecular dynamics approach is incapable of replicating the relatively longer time scales and non-thermodynamic nature of the actual experiment. An alternative approach entails advanced machine learning algorithms applied not to reproduce, but rather to map the process-structure-property correlations. However, this requires training data in the form of empirically determined chemical models obtained under known process conditions. Here, PECVD grown amorphous hydrogenated SiCN thin films obtained from structurally different molecular precursors are studied to compile such a data set due to their stability, scope for precursor synthesis, and compatibility with various characterization techniques: FT-IR, solid-state NMR, fluctuation electron microscopy (FEM), as well as X-ray and neutron diffraction. We present the effects of process parameters on a-SiCN:H thin films, extensive structure and property characterization, and propose chemical structure models.

TF-ThP-14 Growth of Hafnium Oxide and Zirconium Oxide for the Fabrication of Electronic Devices Using Plasma-Enhanced Atomic Layer Deposition, *Samuel Banks, K Bell, S Chance III, B Rodgers, Z Xiao,* Alabama A&M University

Hafnium dioxide (HfO_2) and zirconium oxide (ZrO_2) have been used widely as the gate oxide in the fabrication of integrated circuits (ICs) because of their high dielectric constants. In this research, we report the growth of hafnium dioxide (HfO_2) and zirconium oxide (ZrO_2) thin film using plasma-enhanced atomic layer deposition (PEALD), and the fabrication of complementary metal-oxide semiconductor (CMOS) integrated circuits using the PEALD-grown HfO and ZrO thin films as the gate oxide. The PE-ALD-grown films were analyzed using high-resolution transmission electron microscopy (HRTEM) and energy dispersive X-ray spectroscopy (EDS). MOSFETs, CMOS inverters, and CMOS ring oscillator were fabricated, and the electrical properties of the fabricated devices were measured. The measurement results on the devices fabricated with the two films were compared.

TF-ThP-15 Nanoscale Multilayered Thin-Film Thermoelectric Materials and Devices, *Joevonte Kimbrough, A Glenn, A Henderson, S Budak, Z Xiao,* Alabama A&M University

In this research, we report the growth of nanoscale multilayered thermoelectric thin films and fabrication of integrated thermoelectric devices for high-efficiency energy conversion and solid-state cooling. Nanoscale multilayered thin films such as Sb/Sb_2Te_3 and Te/Bi_2Te_3 thin films were grown using the e-beam evaporation. Integrated thermoelectric devices were fabricated with the nanoscale multilayered thin films using the clean room-based microfabrication techniques such as UV lithography. X-ray diffraction and reflection and high-resolution tunneling electron micrograph (HR-TEM) were used to analyzed the e-beam-grown nanoscale multilayered thin films. SEM was used to image and analyze the fabricated devices. The thermoelectric characteristics of the fabricated devices were measured and analyzed.

TF-ThP-16 Microstructural Evolution in Sputter-deposited 316L Stainless Steel / Si (100) Thin Films, *Christopher Bansah, C Solomon,* Youngstown State University

This study investigates effect of substrate temperature on the phase and microstructural evolution of 316L stainless steel thin film. The 316L SS thin film were prepared on a Si (100) substrate by using dc magnetron sputtering in an argon atmosphere. The substrate temperature was increased from 293 K to 673 K. X-ray diffraction (XRD), scanning electron microscopy (SEM), atomic force microscopy (AFM), focused ion beam (FIB), and transmission electron microscopy (TEM) and were used to investigate the phases and microstructure of the thin films. The phase and microstructural analysis reveal that films deposited at room temperature showed amorphous or disordered structure. The disordered structure was attributed to the insufficient thermal activation energy for atom mobility during low temperature deposition. By increasing the substrate temperature the thin film become crystalline and the grain size increased with the temperature.

TF-ThP-18 Characterization of Fluorine-doped SiO_2 Films Deposited by Magnetron Sputtering, *Bohuei Liao,* Taiwan Instrument Research Institute; *C Hsiao,* Taiwan Instrument Research Institute, Taiwan, Republic of China

Fluorine-doped SiO_2 films were deposited by magnetron sputtering with a Si metal target at room temperature. In order to obtain better optical and mechanical properties, films were investigated under different ratios of O_2 to CF_4 gas. The optical properties, microstructure, surface roughness, and crystalline structure, of fluorine-doped SiO_2 films have been studied. The transmittance increased as increasing the CF_4 gas in the ultraviolet range. The refractive index decreased as increasing the CF_4 gas.

TF-ThP-19 MOCVD Growth and Characterization of Wide Bandgap $ZnGeN_2$ Thin Films, *Md Rezaul Karim,* The Ohio State University; *B Jayatunga,* Case Western Reserve University; *Z Feng, M Zhu, J Hwang,* The Ohio State University; *K Kash,* Case Western Reserve University; *H Zhao,* The Ohio State University

$ZnGeN_2$ is a wide bandgap material having less than 0.1% lattice mismatch and similar bandgap as GaN [1]. Based on first principles calculations, the valence band maximum of $ZnGeN_2$ is ~1.4 eV above that of GaN at the heterointerface [2]. Such a staggered band alignment between two closely lattice-matched materials has promising applications for novel optoelectronic device designs, for example, high efficiency blue and green light emitting diodes [3]. However, the thin film synthesis of $ZnGeN_2$ is still at an early stage, in contrast to the mature GaN.

Here, we study the growth of $ZnGeN_2$ thin films using metalorganic chemical vapor deposition (MOCVD) and characterization of the crystalline, optical, and electrical properties. Diethylzinc (DEZn), germane (GeH_4) and ammonia were used as the precursors for Zn, Ge and N, respectively, and GaN templates and sapphire were used as substrates. The Zn/Ge atomic ratios in $ZnGeN_2$ were determined from energy dispersive X-ray spectroscopy. They were found to decrease with increase in growth temperature (from 600 to 700 °C) but to increase with increase in pressure (from 300 to 500 Torr) and $DEZn/GeH_4$ molar flow rate ratio. The X-ray diffraction 2θ-ω spectra of the $ZnGeN_2$ films are consistent with orthorhombic (perfectly ordered cations) or distorted wurtzite (disordered cations) polymorphs. High resolution scanning transmission electron microscopy imaging was used to investigate the crystalline quality and crystalline structure of the films. The $ZnGeN_2$ films grown on c-sapphire and GaN substrates have planar surfaces from scanning electron micrographs while those on r-sapphire substrate have stepped surface morphologies. A broad peak at ~2.05 eV was observed from room temperature photoluminescence (PL) spectra and is was attributed to transitions involving deep level defects. The PL excitation spectra peaked around 3.4 eV, and is attributed to excitonic enhancement of the absorption near the band gap. The as-grown films were found to be n-type with 10^{18} -10^{19} cm^{-3} carrier concentrations and room temperature mobilities up to 17 cm^2/V·s.

In summary, the studies from this work on the MOCVD growth of $ZnGeN_2$ thin films are a step towards the better understanding of this material and thus, towards the implementation of $ZnGeN_2$ for device applications.

Acknowledgements

References

1. A. Punya, T. R. Paudel, and W. R. L. Lambrecht, Phys. Status Solidi C, 8, 2492 (2011).

2. A. P. Jaroenjittichai, S. Lyu, and W. R. L. Lambrecht, Phys. Rev. B., 96, 079907(E) (2017).

3. L. Han, K. Kash, and H. Zhao, J. Appl. Phys., 120, 103102 (2016).

TF-ThP-20 Low Temperature Charging Dynamics of Ionic Liquid and Its Gating Effect on FeSe$_{0.5}$Te$_{0.5}$ Superconducting Films, *Cheng Zhang*, University of Tennessee Knoxville; *W Zhao, S Bi*, Huazhong University of Science and Technology, China; *C Rouleau, J Fowlkes*, Oak Ridge National Laboratory; *W Boldman*, University of Tennessee Knoxville; *G Gu, Q Li*, Brookhaven National Laboratory; *G Feng*, Huazhong University of Science and Technology; *P Rack*, University of Tennessee Knoxville

Ionic liquids (ILs) have been investigated extensively due to its unique ability to form the electric double layer (EDL) which induces high electrical field. For certain materials low temperature IL charging is needed to limit the electrochemical etching. Here we report our investigation of the low temperature charging dynamics in two widely used ILs – DEME-TF$_2$N and C$_4$mim-TF$_2$N. Results show that the formation of the EDL at ~220 K requires several hours relative to milliseconds at room temperature, and an equivalent voltage V_e is introduced as a measure of the EDL formation during the biasing process. The experimental observation is supported by molecular dynamic simulation, which shows that the dynamics are logically a function of gate voltage, time and temperature. To demonstrate the importance of understanding the charging dynamics, a 140 nm thick FeSe$_{0.5}$Te$_{0.5}$ film was biased using the DEME IL, showing a tunable Tc between 18 and 35 K. Notably, this is the first observation of the tunability of the T_c in thick film FeSe$_{0.5}$Te$_{0.5}$ superconductors.

TF-ThP-21 Design and Characterization of Nanomaterials using PREVAC's Research Platforms, *Lukasz Walczak*, PREVAC sp. z o.o., Poland

Magnetics, optoelectronics, energy storage and renewables, catalysis and nanoelectronics, semiconductors, new graphene-type materials and their surface are under intensive investigation of many research groups [1-3]. The wide variety of novel technologies and materials available, precise, well defined scientific problems or proprietary production recipes demand customized analysis and deposition systems.

Innovative and compact PREVAC surface analysis platform as part of multi-technique surface analysis system will be presented, in order to permit complete characterization of nanomaterials in the UHV and ambient pressure conditions. We will report some results from these systems.

Also we introduced PREVAC deposition platforms, based on well tested MBE system technology, offering a high quality and stable UHV performance. Compact construction allows the connection of different deposition sources at versatile configurations as well as the incorporation of RHEED, inventive alternative GIFAD [4] and other analysis techniques.

As the next deposition platform the sputtering systems for depositing metal and dielectric thin films on substrates at the different temperature will be shown. A range of magnetron sputtering sources, using RF, DC, or pulsed DC power, can be operated in the multimode by SYNTHESIUM software for producing thin films.

Finally we describe PREVAC's PLD systems. Typically it is used with a focused pulsed excimer laser to vaporize a small section of a solid target material in a vacuum chamber in order to produce thin-films. Standalone configuration or as part of a larger integrated research system, system is fully automated. The transfer system features a six position target manipulator which allows transfer of both target and substrate holders for simple and efficient operation.

References:

1. L. K. Preethi, et al., Sci. Rep. , 14314 (2017)

2. M. Weis, et al., Sci. Rep. **7**, 13782 (2017)

3. N. M. Freitag et al., Nature Nanotechn. **13**, 392-397 (2018)

4. A. Momeni et al. J. Phys. Chem. Lett., **9**, 908–913 (2018)

TF-ThP-22 Deposition of the Porous Film on the Reactive Liquid Substrate via Metal-organic Precursors, *Haoming Yan, Q Peng,* University of Alabama

Solid on liquid deposition (SOLID) has been achieved and reported for a few times. It has potential in many applications, such as gas sensors, optical lens, selective deposition and etc. SOLID can also take the advantages of the nature of the liquid substrate, like the atomically smooth surface and the naturally formed shape of the liquid. However, the materials that can be deposited onto the liquid substrate are very limited. The reported material that can be deposited on a liquid substrate is mainly poly-para-xylylene via CVD and metals via sputtering. There is no report of using a reactive liquid as a substrate for the solid film deposition. In this work, the metal oxide film can be deposited onto the liquid substrate using the metal-organic precursors and the liquid that can react with them. This method creates more possibilities of the materials that can be deposited

on the liquid substrate and potentially broaden the application of the SOLID.

TF-ThP-23 Self-Limited Surface Reaction between Trimethyl Aluminum and Formamidinium Lead Iodide Perovskite, *Qing Peng, X Yu, H Yan,* University of Alabama

Surface site-limited reaction is critical to modifying hybrid halide perovskites without destroying their bulk properties. However, no surface site-limited reaction on hybrid halide perovskites has been demonstrated and confirmed. Herein, we report one surface-site limited reaction on FA lead iodide with tri-methyl aluminum. The strong coordination between organic cations FA$^+$and trimethyl aluminum, a very strong Lewis acid, is found to be the key for this self-limited reaction behavior. Our results provide a model system to understand the effect of surface species on surface reaction behavior on hybrid halide perovskites.

TF-ThP-24 The Evolution of Atomic Layer Processing as a Field: Atomic Layer Etching,and its Connections with Atomic Layer Deposition, *Elsa Alvaro,* Northwestern University; *A Yanguas-Gil,* Argonne National Laboratory

Atomic layer processing, with its ability to manipulate materials with atomic layer precision, is becoming increasingly relevant for a wide range of applications. A counterpart to Atomic Layer Deposition (ALD), Atomic Layer Etching (ALE) allows controlled layer-by-layer removal of material by using self-limiting, sequential steps. This technique, which appeared in the 1990s, has garnered the interest of the semiconductor industry, where the ability to remove material selectively and in a self limiting way could help fabricate structures and devices at increasingly smaller dimensions. In this paper, we describe the trajectory of ALE, and its connection and overlap with ALD and other research fields. Using citation, network and text analysis methods, we have studied trends in topics, authors and publications. In addition, we have examined the overlap between ALD and ALE, using cocitations as a way of identifying papers that may draw from both fields. The ultimate goal is to understand not only the evolution of ALE, but whether ALD and ALE are effectively merging into a larger, atomic layer processing community.

TF-ThP-25 Electrical Properties of In$_2$O$_3$ Thin-film Transistors under Vacuum and Inert Environments, *Keisuke Nakamura, K Sasaki, Y Shibata, K Oe, S Aikawa,* Kogakuin University, Japan

Indium oxide (In$_2$O$_3$)-based thin-film transistor (TFT) have attractive much attention because high field-effect mobility (> 10 cm^2/Vs) can be obtained even room temperature deposition. However, a high-temperature post-annealing is necessary for typical fabrication processes. This sacrifices the merit of In$_2$O$_3$-based TFTs that can be fabricated at low temperature. One reason for high-temperature treatment is that an In$_2$O$_3$ surface might be sensitive to ambient gases, thus, the electrical properties of the film is changed in various environmental conditions. In order to clarify such instability, we investigate the electrical properties of In$_2$O$_3$ TFT in ambient, vacuum and N$_2$ environments.

The In$_2$O$_3$ TFT was fabricated on a Si substrate with a thermally-grown oxide layer (SiO$_2$ thickness: 200 nm). Before deposition of In$_2$O$_3$ active channels, the substrate was ultrasonically cleaned in acetone and isopropyl alcohol, and was irradiated by an excimer lamp (wavelength: 172 nm) for 5 min to remove the organic residue. The In$_2$O$_3$ film was then deposited at room temperature by RF magnetron sputtering. The O$_2$/(Ar + O$_2$) ratio, RF power and total pressure during sputtering deposition were fixed at 25 %, 100 W and 0.24 Pa, respectively. The background pressure was below ~5 × 10^{-4} Pa. The thickness of the active channel formed through a stencil shadow mask was 20 nm by optimizing the deposition time. Source and drain electrodes (Cu: 100 nm) were then formed by an electron beam evaporation through a stencil shadow mask. The In$_2$O$_3$ TFT was characterized in a vacuum probe station with a semiconductor parameter analyzer (Agilent 4156A) at room temperature in the dark condition. The electrical measurement of the TFTs was performed in ambient at first, then the chamber was evacuated to ~4 × 10^{-2} Pa for vacuum measurement. A N$_2$ gas was subsequently introduced into the chamber to be N$_2$ environmental condition.

The In$_2$O$_3$ TFT properties were drastically changed between ambient and vacuum conditions. This might be caused by desorption of excess oxygen in the film. To investigate a measurement environmental sensitivity in In$_2$O$_3$ TFT, a sequential *I-V* measurement was performed. The result showed that the transfer characteristics between 1st and 2nd measurement is obviously different. The degradation of the sensitivity after the 2nd measurement might be due to N$_2$ molecule passivation. However, the sensitivity tended

to slight recover with increasing the number of measurements. We will discuss the N_2 passivation effect, and the relationship between the sensitivity and number of measurements.

TF-ThP-26 Toward Ultra-fast Switching Speed Electrochromic Supercapacitor, *Weimin Jiao, S Wei, C Chang, F Yao,* University at Buffalo

As one of the most promising energy storage devices, supercapacitors have been widely adopted in different fields due to their high power density and long service life. However, with the rapid development of intelligent electronic products, there is an urgent need to construct multifunctional supercapacitors to broaden the range of applications. Integration of electrochromism into supercapacitors is one of the innovative approaches to achieve device multifunctionality. An electrochromic supercapacitor can change color reversibly in response to different applied voltages. The instant capacity of the devices can be simply recognized by naked eyes. Implementation of electrochromism to supercapacitors can also prevent device overcharging, leading to a longer device lifetime. Nevertheless, the performance of previously reported electrochromic supercapacitor devices suffers from a slow switch mechanism as well as a low power density, which highlights the need for the electrode structures optimization.

In this report, an electrochromic asymmetrical supercapacitor device (EASD) is developed, which successfully achieves the multifunctional combination of electrochromism and energy storage by adopting polyaniline and tungsten trioxide as the positive and negative electrodes, respectively. In order to improve the device performance, a facile electrochemical activation process is applied to the electrode. The optimized EASD shows a high volumetric energy density of 35.3 mWh/cm^3 at a high power density of 1.02 W/cm^3 with excellent cycling stability. More importantly, it exhibits a high coloration efficiency of 123.4 cm^2/C with an ultra-fast switching speed of 1.4 s / 0.4 s for colored / bleached states, which is one of the fastest switching devices reported so far. Such an EASD shows great potential in the applications of smart windows, smart electronics, and intelligent energy storage.

TF-ThP-27 Growth and Structure of Cr-doped ZnO Thin Films, *Gabrielle Pasternak,* Washington and Jefferson College*; A Gardill,* Lawrence University*; S Chamberlin,* Washington and Jefferson College

There is a constant search for more efficient materials for use in electronics. Zinc Oxide (ZnO) is a well-known semiconductor used in numerous applications. However, the effects of doping ZnO with chromium (Cr) are less documented. Using spray pyrolysis – a robust and industrially relevant technique – an aqueous solution of Zn and Cr nitrates is sprayed onto a heated substrate to create thin films of polycrystalline $(Zn_{1-x}Cr_x)O$ with various Cr concentrations below x = 0.05.

X-ray diffraction (XRD) is used to verify the retention of ZnO's structure, confirming that Cr substitutes for Zn in the crystal lattice. XRD can also give detailed information about the crystal lattice parameters and crystallite size – both important in understanding the effectiveness of our growth process. Verifying with XRD that we have grown good crystalline material is the first step to increasing the understanding of $(Zn_{1-x}Cr_x)O$. We have also begun to investigate the optical and chemical properties of this material.

TF-ThP-28 Developing an Approach to Improve the Beta-phase in Ferroelectric PVDF-HFP Thin Films, *Ashley S. Dale, A Mosey, J Soruco, R Cheng,* Indiana University Purdue University Indianapolis

Improved fabrication of poly(vinylindene fluoride)-hexafluoropropylene (PVDF-HFP) thin films is of particular interest due to the high electric coercivity found in the beta-phase structure of the thin film. For example, ongoing studies of ferroelectric-spin crossover coupling using x-ray spectroscopy imply the ferroelectric-spin coupling would benefit from a better ferroelectric response. Langmuir-Blodgett (LB) deposition and Langmuir-Schaffer (LS) deposition methods create a beta-phase dominant PVDF-HFP thin film when the deposition is followed by annealing. However, applications for PVDF-HFP thin films exist in organic spintronic devices where annealing is prohibited by other materials in the device heterostructure. We show that it is possible to obtain high-quality, beta-phase dominant PVDF-HFP thin films using a modified approach to LB deposition and without the use of annealing or additives. Samples implement a unique step design with a bottom electrode of copper and aluminum and a top electrode of gold or aluminum. This design allows a single thin film sample to be characterized using scanning electron microscopy, atomic force microscopy, X-ray diffraction, and electrical hysteresis measurements.

TF-ThP-29 Ternary Thin Film Alloys for Varistor Application, *Ajit Dhamdhere, S Rathi, N Mukherjee, J Heo, S Lee, J Mack, B Nie,* Eugenus, Inc.

In this work we propose to employ atomic layer deposition (ALD) grown thin films of $Ti_xSi_yN_z$ as a universal heating electrode for integrated electronic devices. In this work the Ti:Si ratio and film thickness were varied, and corresponding structural and physical analysis was performed using multiple characterization techniques. By varying the Si fraction in the film, wide range of resistivity was achieved. Atomic level control of Ti:Si fraction in the films enabled fine tuning of the morphology from polycrystalline to fully amorphous with optimum resistivity. The $Ti_xSi_yN_z$ films were grown using Eugenus 300 mm QXP commercial mini-batch ALD reactor. X-Ray diffraction (XRD), high resolution transmission electron microscopy (HRTEM), and selected area electron diffraction (SAED) of these films corroborated transition from nano-crystalline to pure amorphous phase with increase in Si concentration. $Ti_xSi_yN_z$ films processed in our labs have already exhibited superior diffusion barrier properties and stability of the resistivity of the films. Our recent work on the in-situ high temperature XRD studies of the $Ti_xSi_yN_z$ films showed superior phase stability of the $Ti_xSi_yN_z$ films at high temperatures of 800°C with negligible alteration in recrystallization (Figure 1). Nanoindention based hardness studies of these films indicated the change in mechanical properties with varying Si% in the TiN matrix. The sub-nanometer level of surface roughness of these $Ti_xSi_yN_z$ films as established by Atomic Force Microscopy would also benefit adhesion of our $Ti_xSi_yN_z$ films with other electronic materials yielding coherent interfaces.

TF-ThP-30 Plasma Study and Fretting Corrosion of Zr/ZrN/CNx Multilayers Deposited by HIPIMS on Ti6Al4V, *Martín Flores, L Flores, J Perez, M Flores, O Jimenez,* Universidad de Guadalajara, Mexico

Multilayers of ceramic-metallic hard coatings can improve the the tribocorrosion resistance of biomedical alloys as Ti6Al4V. The coatings deposited by HIPIMS have a more compact growth respect to films deposited by DC magnetron sputtering; this diminish the presence of pinholes and defects that permit to predict a reduction in permeability. The design of the multilayer was made with a top layer of CNx in order to reduce the friction coefficient. In this work we study the fretting corrosion behavior of Ti6Al4V biomedical alloys coated with multilayers of Zr/ZrN/CNx deposited by HIPIMS (High Power Impulse Magnetron Sputtering). The used plasmas was characterized by OES, also the ions and neutral species were studied by means of a mass and energy analyzer. The fretting corrosion tests were made in fetal bovine serum (BFS), the geometry used was a cylinder of coated Ti alloy on a flat CoCrMo sample. The worn surface at wear track was analyzed by SEM and Raman spectroscopy. We report the results of composition of tribolayer and removed material of the wear tracks. The friction coefficient and the fretting damages were reduced by the coating.

TF-ThP-31 Size Dependent Strengthening in High Strength Nanotwinned Al/Ti Multilayers, *Yifan Zhang, S Xue, Q Li, J Li, J Ding, T Niu, R Su, H Wang, X Zhang,* Purdue University

Here we report on the study of magnetron-sputtered highly textured Al/Ti multilayers with various layer thicknesses (h = 1 - 90 nm). The hardness of Al/Ti multilayers increases monotonically with decreasing layer thickness without softening and exceeds 7 GPa, making it one of the strongest light-weight multilayer systems reported to date. High resolution transmission electron microscopy (TEM) and X-ray diffraction pole figure analyses confirm the formation of high-density nanotwins and 9R phase in Al layers. The density of nanotwins and stacking faults scales inversely with individual layer thickness. In addition, there is an HCP-to-FCC phase transformation of Ti when h ≤ 4.5 nm. And the post-indentation TEM analysis reveals deformation induced phase transformation in Ti layer. The high strength of Al/Ti multilayers primarily originates from incoherent interface, high-density twin boundaries, as well as stacking faults. Our findings have general implication for the design of high-strength and light-weight heterogeneous nanocomposite materials.

2D Materials

Room A215 - Session 2D-FrM

2D Late News Session

Moderators: Daniel Gunlycke, Naval Research Laboratory, Ivan Oleynik, University of South Florida

10:40am 2D-FrM-8 Mechanistic Insights into a Modified ALD Process to Achieve Crystalline MoS₂ Thin Films, *Nathaniel Richey, L Zeng, M Yasheng, J Shi, I Oh, S Bent,* Stanford University

Stimulated by the discovery of two-dimensional (2D) graphene, 2D transition metal chalcogenides (TMDs) are attracting much attention owing to their similar layered structure and graphene-analogous properties. Numerous research efforts are under way to explore their potential applications, such as optoelectronics, electrochemical cells, and energy harvesting devices. However, challenges remain in the development of controllable growth methods for TMDs with large-scale conformality at moderate growth temperatures. There has been an increasing trend toward resolving these issues by employing atomic layer deposition (ALD) due to its promise of layer-by-layer growth.

Despite the promise brought by ALD, further effort is needed as the TMD films grown using low temperature ALD often show non-ideal stoichiometry and require high-temperature post-annealing to improve the film quality. As an example, the known ALD processes that use $Mo(CO)_6$ and H_2S as the precursors have shown an ALD window of 150 ~ 175 °C. However, results from both literature and our laboratory show that the S-to-Mo ratio is close to 1.5:1, relatively far from the ideal value of 2:1, with the presence of undesired MoO_x species. We performed an investigation into the mechanisms of this ALD process. Based on understanding that ligand loss is a rate limiting step in the ALD process, a new methodology was developed that produces higher-quality MoS_2 films from these same precursors. These results were achieved by using a slightly elevated growth temperature and enhancing the chemical vapor deposition component of $Mo(CO)_6$ for better CO removal. A series of MoS_2 films were synthesized on Si substrates by this modified process, resulting in controllable linear growth behavior, a S-to-Mo ratio of 2:1, and strong characteristic MoS_2 Raman peaks. Additional characterization tools, including grazing incident X-ray diffraction (GIXRD), X-ray reflectivity (XRR) and atomic force microscopy (AFM), were also used to examine the film crystallinity, density, and surface morphology. By characterizing the material as a function of process conditions, we are able to elucidate fundamental mechanisms and key kinetic factors behind the MoS_2 growth process using $Mo(CO)_6$ and H_2S. This study may help shed some light on future design of ALD processes for 2D TMDs.

11:00am 2D-FrM-9 The Electronic Properties of Quasi-One-Dimensional TiS₃ and ZrS₃, *Simeon Gilbert,* University of Nebraska-Lincoln; *H Yi,* Synchrotron SOLEIL; *A Lipatov, T Komesu,* University of Nebraska-Lincoln; *A Yost,* Oklahoma State University; *A Sinitskii,* University of Nebraska-Lincoln; *J Avila,* Synchrotron SOLEIL, France; *M Asensio,* Madrid Institute of Materials Science; *P Dowben,* University of Nebraska-Lincoln

The transition metal trichalcogenides (TMTs) are an emerging class of 2D materials in which 2D sheets are formed by the van der Waals-like bonding of quasi-1D chains. Here we present our work on the electronic properties of two TMTs, TiS_3 and ZrS_3, including the experimental band structure from nanospot angle resolved photoemission spectroscopy (nanoARPES). The band structures of both TMTs exhibit strong in-plane anisotropy due to their quasi-1D structure. The extracted effective hole mass for both materials is doubled along the chain direction, giving rise to a preferential charge transport direction. Additionally, high resolution nanoARPES measurements show a spin-orbit coupling splitting at the top of the valence band in TiS_3. This spin-orbit coupling splitting is expected to increase for heavier TMTs such as ZrS_3. We also show that metals such as Au and Pt can form Ohmic contacts with TMTs rather than Schottky barriers using X-ray photoemission spectroscopy at the metal-semiconductor interface. Other advantages of TMTs include clean edge termination, band gaps of ~1eV and high predicted electron mobilities. Combined with their anisotropic electron transport, strong spin-orbit coupling and Ohmic contacts, these advantages make the TMTs strong candidates for use in nanoscale electronics, optoelectronics and spintronics.

11:20am 2D-FrM-10 Single Asperity Sliding Friction across the Superconducting Phase Transition, *Wen Wang, D Dietzel, A Schirmeisen,* Institute of Applied Physics, University of Giessen, Germany

In sliding friction, different energy dissipation channels have been proposed, including phonon and electron systems, plastic deformation, and crack formation. However, the details of how energy is coupled into these channels is heavily debated, and especially the relevance of electronic dissipation remains elusive. Here, we present friction experiments of a single asperity sliding on a high Tc superconductor in a wide temperature range from 40 K to 300 K. Overall, friction decreases with temperature as expected for the case of nanoscale energy dissipation in the framework of the Prandtl-Tomlinson-model. But at the same time, we also find an unexpected large peak around T_c of 95 K. We model these results by a superposition of phononic and electronic friction, where the electronic energy dissipation channel vanishes when cooling below the superconducting phase transition T_c. In particular, we find that the friction contribution linked to the electron system constitutes a constant offset above T_c, which decreases to zero below Tc with a power law in agreement with BCS theory. While current point contact friction models usually neglect such friction contributions, our study shows that electronic and phononic friction contributions can be of equal size.

11:40am 2D-FrM-11 Definition of CVD Graphene Micro Ribbons with Lithography and Oxygen Plasma Ashing, *Fernando Cesar Rufino, A Pascon,* UNICAMP, Brazil; *D Larrudé,* Mackenzie Presbyterian University, Brazil; *L Espindola, F Cioldin, J Diniz,* UNICAMP, Brazil

The excellent physical properties of graphene [1], such as transport (high electron mobility 250000 cm^2/Vs), elasticity (in the order of TPa) and mechanical strength (in the order of GPa), make this 2D material a strong candidate in electronic devices development, especially in the area of radiofrequency and applications in sensors. In researches related to electronic devices, graphene can be a great ally in the development and miniaturization of Field Effect Transistors, FET. Concerns related to the miniaturization process are the equipment and the materials necessary to achieve this objective, since the repeatability and the cost of the manufacturing process are two essential variables to ensure the viability of the proposed project.

In this work, we present the union of conventional techniques in the fabrication of microdevices and the application of graphene obtained by chemical vapor deposition (CVD), in the development of Field Effect Transistors based on Graphene, GFET [2]. In the fabricated GFETs, the conduction channel is formed by parallel micro ribbons of graphene, with the smallest dimension of 250 nm of width. This dimension was obtained by Photolithography and oxygen plasma ashing. Through these two techniques we can ensure the repeatability of the fabrication process and these are low cost techniques when compared to what is commonly found in the literature, which is the definition of graphene patterns by Electron Beam Lithography (high cost and low repeatability technique). In addition, the characteristics of good quality graphene remain at the end of the fabrication process, as proven by Raman spectroscopy.

The GFETs were fabricated on two different substrates. One on Si/SiO_2 and another on glass. In both materials, the same structures with the same parameters were fabricated and were able to reach dimensions in the order of 360 nm, for comparisons we used Atomic Force Microscope (AFM) to verify the roughness and Scanning Electronics Microscope (SEM) for detection and measurement of the structures. The graphene used in the fabrication of the devices was the last material to be transferred to the sample by fishing and using PMMA [3], ensuring the least possible handling of the material and therefore possible contaminations.

References:

[1] K. S. Novolselov et al, Science **306**, 666 (2004).

[2] F. C. Rufino et al, SBMicro 2018.

[3] L. Jiao et al., Am. Chem. Soc., 12612 (2008).

12:00pm 2D-FrM-12 Reactivity of Metal Contacts with Monolayer Tungsten Disulfide, *Ama Agyapong, K Cooley, S Mohney,* The Pennsylvania State University

Using two-dimensional transition metal dichalcogenides (TMD) for electronics, optoelectronics, and catalysis often requires integration with a metal, motivating fundamental studies of metal-TMD interactions. We previously published predictions on the reactivity of metals with tungsten disulfide based on thermodynamics. [1] Our current work employs an easy approach to test these predictions on reactivity of metal contacts with monolayer (1L) WS_2 using Raman spectroscopy performed through the backside of the contact. Au, Cu, Pd, Al, and Ti were deposited by electron beam evaporation onto 1L WS_2 grown on a sapphire substrate and capped with a thin film of silica to avoid agglomeration of the metal during annealing. Samples were annealed at 100, 200, and 300 °C under Ar for 1 hour. The results from Raman spectroscopy are in excellent agreement

with the predictions from thermodynamics. Au, Cu, and Pd did not react with 1L WS_2 upon deposition or annealing. Reaction of Al with 1L WS_2 occurred upon annealing, while Ti reacted upon deposition, as indicated by loss of the characteristic peaks in the Raman spectrum for WS_2. We will also describe interesting changes in the Raman spectrum for WS_2 from Au/WS_2 samples and present transmission electron microscopy of these samples.

[1] Yitian Zeng, Anna C. Domask, Suzanne E. Mohney, Condensed phase diagrams for the metal–W–S systems and their relevance for contacts to WS_2, Materials Science and Engineering: B, Volume 212, October 2016, Pages 78- 88: http://dx.doi.org/10.1016/j.mseb.2016.07.005.

Chemical Analysis and Imaging Interfaces Focus Topic
Room A226 - Session CA+AS+NS+SE+SS-FrM

Novel Applications and Approaches in Interfacial Analysis

Moderators: Paul Dietrich, SPECS Surface Nano Analysis GmbH, Germany, Jeong Young Park, Korea Advanced Institute of Science and Technology (KAIST), Republic of Korea

8:20am **CA+AS+NS+SE+SS-FrM-1 Chemical Reactions on Bimetal Surfaces with Operando Surface Techniques**, *Jeong Young Park,* Korea Advanced Institute of Science and Technology (KAIST), Republic of Korea **INVITED**
The origin of the synergistic catalytic effect between metal catalysts and reducible oxide has been debated for decades. Clarification of this effect, namely the strong metal–support interaction (SMSI), requires an understanding of the geometric and electronic structures of metal–metal oxide interfaces under operando conditions.[1] A bimetallic platinum (Pt) alloy catalyst is an excellent platform to uncover the contentious role of the metal–metal oxide interface because the alloyed transition metal can coexist with the Pt surface layer in the form of an oxidized species on the bimetal surface during catalytic reactions.

 In this talk, I present in-situ observation results of structural modulation on Pt-Ni metastable and Ni (111) surfaces at 0.1 Torr pressure of CO, O_2, and CO oxidation conditions with ambient-pressure scanning tunneling microscopy (AP-STM) and ambient-pressure X-ray photoelectron spectroscopy (AP-XPS).[2] We show that the stable Pt-skin covered $Pt_3Ni(111)$ surface is broken by segregation of dissociative oxygen-induced Ni oxides under elevated oxygen pressure environment, which evolved clusters could have a crucial relation with enhanced catalytic activity. We show that NiO1-x/Pt-Ni nanostructures are on the $Pt_3Ni(111)$ surface under CO oxidation and these metal-oxide interfaces provide more efficient reaction path for CO oxidation [2]. Furthermore, I will **show the research efforts for understand the catalytic behavior of bimetal PtCo and PtNi nanocatalysts using in-situ surface techniques including catalytic nanodiode and transmission electron microscopy. The catalytic nanodiode that consists of metal catalyst film, semiconductor layers, and Ohmic contact pads revealed the strong correlation between the hot electron flux (chemicurrent) and catalytic activity under CO oxidation and hydrogen oxidation. Using this approach, the catalytic activity and hot electron generation on PtCo bimetal nanoparticles were investigated. In-situ transmission electron microscopy reveals the formation of metal oxide layers on bimetal nanoparticle surfaces under oxygen conditions. We show that formation of interface between Pt and CoO enhances both of catalytic activity and chemicurrent yield [3].**

[1] J. Y. Park et al. Chemical Reviews 115, 2781-2817 (2015)

[2] J. Kim et al. Science Advances 4, eaat3151 (2018).

[3] H. Lee et al. Nature Communications 9, 2235 (2018).

9:00am **CA+AS+NS+SE+SS-FrM-3 Principal Component Analysis to Reveal Camouflaged Information in Spectromicroscopy of (complex) Oxides**, *David Mueller, M Giesen,* Forschungszentrum Juelich GmbH, Germany; *D Stadler,* University of Cologne, Germany; *T Duchon, F Gunkel, V Feyer,* Forschungszentrum Juelich GmbH, Germany; *S Mathur,* University of Cologne, Germany; *C Schneider,* Forschungszentrum Juelich GmbH, Germany
Spectroscopic imaging techniques are becoming more and more accurate and available, which results in an increase of data to handle and analyze.

Near Edge X-Ray absorption spectroscopy, especially in the soft X-Ray regime, has the ability to identify inhomogeneities in chemistry and electronic structure, which is mostly done by fingerprinting or using internal standards. In a spectromicroscopic image, each pixel contains such a spectrum, and by the lack of rigorous fitting routines that are for example present in XPS, reduction and preevaluation of data is needed. Principal Component Analysis (PCA) of X-PEEM data affords this in an unambiguous and unbiased way by identifying and highlighting spectroscopic features which contribute to a spectrum.[1]

Two cases where PCA revealed information that might have been missed otherwise are presented here: Firstly, iron oxide thin films grown by CVD showed a considerable influence of an external magnetic field on chemistry and crystallinity. Combination of O-K- and Fe-L-Edge X-PEEM unambiguously identified different iron oxide polymorphs (Fe_3O_4 and α-Fe_2O_3) depending on field strength during deposition. The former XAS Edge showed subtle spatial variations in the EXAFS regime that could be identified as the breakdown of long-range ordering, pointing to incomplete crystallization when films are deposited without magnetic field assistance.[2]

The second example is the surface decomposition of $Pr_{0.5}Ba_{0.5}CoO_{3-\delta}$ (PBCO), a promising material for the use as water splitting catalyst and solid oxide electrochemical cell electrode. Using spatially resolved O-K-, Co-L-, and Ba- and Pr-M-Edge XAS, changes in surface chemical composition upon annealing and its impact on the electronic structure were observed. Laterally resolved by X-PEEM, PCA could reveal that exposing thin films of the material to technologically relevant conditions (1073 K, 20 mbar of O_2) leads to a more complex decomposition pathway than simple spinodal unmixing to the end members $BaCoO_3$ and $PrCoO_3$ as the spectromicroscopic dataset could only be described satisfactory by a linear combination of three components.

9:20am **CA+AS+NS+SE+SS-FrM-4 *In situ* Electron Microscopy of Catalysts with Atomic Resolution under Atmospheric Pressure**, *Xiaoqing Pan,* University of California Irvine **INVITED**
Understanding the atomic structures of catalysts under realistic conditions with atomic precision is crucial to design better materials for challenging transformations. For example, under reducing conditions, certain reducible supports migrate onto supported metallic particles and create strong metal–support states that drastically change the reactivity of the systems. The details of this process are still unclear and preclude its thorough exploitation. In the past decade, most of atomic-scale transmission electron microscopy (TEM) studies involving gas-solid interactions were conducted in an environmental TEM, where the gas pressure is typically limited to less than 1/100 of atmosphere. Recently, it has become possible to overcome this limitation through a MEMS-based, electron-transparent closed cell with a heating stage.

In this talk, I will present our recent results using this device (the Protochips Atmosphere™system) in selected catalyst systems. In a palladium/titania (Pd/ TiO_2) catalyst, we directly observed the formation of the oxide overlayers on the supported Pd particles with atomic resolution under atmospheric pressure and high temperature. It shows that an amorphous reduced titania layer is formed at low temperatures, and that crystallization of the layer into either mono- or bilayer structures is dictated by the reaction environment. This transition occurs in combination with a dramatic reshaping of the metallic surface facets. *In-situ*TEM observations of a modular Pd-ceria core-shell nanostructured catalyst (Pd@CeO_2) showed that an unexpected structural transformation occurs upon heating at high temperatures. The system reaches to a stable state with the mixture of nanoparticles with two different sizes, which accounts for the exceptional catalytic properties that have been reported. Using the similar techniques, we also studied the core-shell platinum-metal (Pt-M) nanoparticles which show a catalytic performance in the oxygen reduction reaction (ORR) superior to that of pure Pt nanoparticles. To understand the formation mechanism of the Pt shell, we studied thermally activated core-shell formation in Pt_3Co nanoparticles via *in-situ*electron microscopy with the gas cell. The disordered Pt_3Co nanoparticle was found to transform into an ordered intermetallic structure after annealing at high temperature (725°C) in 760 Torr O_2, followed by layer-by-layer Pt shell growth on (100) surfaces at low temperature (300°C). The apparent'anti-oxidation'phenomenon promoted by the ordered Pt_3Co phase is favorable to the ORR catalyst, which operates in an oxidizing environment.

10:00am CA+AS+NS+SE+SS-FrM-6 Exposing Buried Interfaces in Thin Film Photovoltaics through Thermo-mechanical Cleaving, *Deborah McGott*, Colorado School of Mines*; C Perkins, W Metzger,* National Renewable Energy Laboratory*; C Wolden,* Colorado School of Mines*; M Reese,* National Renewable Energy Laboratory

Thin film solar cells, such as cadmium telluride (CdTe) and Cu(In,Ga)Se$_2$ (CIGS), contain buried interfaces that are critical to carrier transport, recombination, and device performance, yet are poorly understood due to their inaccessibility within the device stack. In particular, accessing the interface in a way that preserves the chemical structure has historically been extremely difficult. Here, we describe an innovative technique to expose buried interfaces through a two-step thermo-mechanical cleaving process. First, a stressor layer (typically an epoxy or commercially available polymeric backsheet) is applied to the solar cell. Then, the stack is submerged in a cold bath (T ≤ -30°C) to thermally shock the system. This causes the stressor to contract quickly and pull the polycrystalline film cleanly off of its substrate at an interface that is weakened by a monolayer accumulation of 2-D material (CdCl$_2$ in CdTe and MoS$_2$ in CIGS) .

Focusing on CdTe solar cells, we then use X-ray photoelectron spectroscopy to probe the oxidation states at the newly exposed SnO$_2$ interface. We show that the tin oxide front electrode promotes the formation of nanometer-scale oxides of tellurium and sulfur. Most oxidation occurs during CdCl$_2$/O$_2$ activation. Surprisingly, we show that relatively low-temperature anneals (180–260°C) used to diffuse and activate copper acceptors in a doping/back contact process also cause significant changes in oxidation at the front of the cell, providing a heretofore missing aspect of how back contact processes can modify device transport, recombination, and performance. Device performance is shown to correlate with the extent of tellurium and sulfur oxidation within this nanometer-scale region. Mechanisms responsible for these beneficial effects are proposed.

10:20am CA+AS+NS+SE+SS-FrM-7 Switchable Dopants on Percolation Networks of 2D Materials for Chemiresistive Sensing Applications in Aqueous Environments, *Peter Kruse,* McMaster University, Canada

Permanent doping of semiconductors and low-dimensional structures to modulate their electronic properties is a well-established concept. Even in cases where doping of thin films by analytes (e.g. carbon nanotubes by ammonia) is applied in sensors, it is only reversed by physical removal of dopant molecules, e.g. heating. We have introduced the concept of molecular switches as chemical dopants for thin nanocarbon (or other 2D-materials) films. These molecules can be switched between doping and non-doping states in the presence or absence of a particular analyte. They impart selectivity not only due to their change in doping behavior, but also by physically blocking other potential dopants in the analyte solution from interacting with the conductive film. The resulting structures can act as chemiresistive films. Chemiresistive sensors are a well-established technology for gas-phase sensing applications. They are simple and economical to manufacture, and can operate reagent-free and with low or no maintenance. Unlike electrochemical sensors they do not require reference electrodes. While in principle they can be made compatible with aqueous environments, only a few such examples have been demonstrated. Challenges include the need to prevent electrical shorts through the aqueous medium and the need to keep the sensing voltage low enough to avoid electrochemical reactions at the sensor. We have built a chemiresistive sensing platform for aqueous media. The active sensor element consists of a percolation network of low-dimensional materials particles that form a conducting film, e.g. from carbon nanotubes, pencil trace, exfoliated graphene or MoS$_2$. The first member of that platform was a free chlorine sensor. We are currently working to expand the applicability of our platform to other relevant species, in particular anions and cations that are commonly present as pollutants in surface and drinking water. Our sensors can be incorporated into a variety of systems and will also be suitable for online monitoring in remote and resource-poor locations.

10:40am CA+AS+NS+SE+SS-FrM-8 Analysis Of Radioactive Materials In Liquid Using In Situ Sem And Tof-Sims, *Jennifer Yao, X Yu, Z Zhu, E Buck,* Pacific Northwest National Laboratory

Characterization of nuclear materials in solid particles or particles in liquid slurry, particularly in high level waste, can establish the elemental, organic, and isotopic compositions that effect the properties of the materials during nuclear fuel cycle activities and processes. Techniques to evaluate such detailed information, even at small concentrations, can support nuclear materials and science programs by increasing our ability to manage and control nuclear materials. However, radioactive materials analysis in liquids and slurries can be challenging using bulk approaches. We have developed

a vacuum compatible microfluidic interface, system for analysis at the liquid vacuum interface (SALVI), to enable surface analysis of liquids and liquid-solid interactions using scanning electron microscopy (SEM) and time-of-flight secondary ion mass spectrometry (ToF-SIMS). In this work, we illustrate the initial results from the analysis of liquid samples of importance in the geologic disposal of UO2 spent nuclear fuel in a repository environment using in situ liquid SEM and SIMS. Our results demonstrate that multimodal analysis of UO2 materials is possible using SALVI. Both in situ liquid SEM and SIMS can be used as new approaches to analyze radioactive materials in liquid and slurry forms of high level nuclear waste.

11:00am CA+AS+NS+SE+SS-FrM-9 Interactions between Synthetic Bilgewater Emulsion and Biofilms, *Jiyoung Son,* Earth and Biological Sciences Directorate*; J Yao,* Earth & Biological Sciences Directorate*; X Yu,* Pacific Northwest National Laboratory

Presentation Summary:

This presentation will showcase our latest results of the interaction between biofilms and synthetic bilgewater using a surface chemical imaging technique.

Abstract

Bilgewater, an oil-in-water (O/W) emulsion, is a persistent pollutant released to the ocean from the lowest part of ships. Microbes play an important role in the ocean. It is hypothesized that microbes release organics that can act as surfactants that affect bilgewater formation or weakening. We present the first systematic study of emulsions and biofilms and investigate the effects of biofilms on bilgewater emulsions. Three strains were selected *Pseudomonas*, *Arthrobacter*, and *Cobetia marina*. A Navy O/W emulsion consisting of three oils and a detergent mixture was used as the synthetic bilgewater model [1]. Biofilms were cultured in a microchannel to allow healthy culture [2]. Once a thick layer of biofilms was formed, the medium solution was changed to a mixture consisting of 50 % bilgewater emulsion. Dispersed biofilms were collected at 24 hrs. and 48 hrs. after emulsions were introduced into the channel. Bilgewater emulsions, biofilms, and mixtures of bilgewater emulsions and biofilms were analyzed using multiple *in situ* and *ex situ* techniques including time-of-flight secondary ion mass spectrometry (ToF-SIMS), scanning electron microscopy (SEM), and optical microscopy. Our findings indicate that biofilms change the chemical makeup of the emulsion surface compositions and emulsion droplet size distribution, confirming the hypothesis that extracellular polymeric substance (EPS) related components released from biofilms can function as surfactants and change the oil-in-water interfaces.

Key words: bilgewater emulsion, oil-in-water, microfluidics, biofilm, EPS, surfactant

Reference

1. Church, J., D.M. Paynter, and W.H. Lee, *In Situ Characterization of Oil-in-Water Emulsions Stabilized by Surfactant and Salt Using Microsensors.* Langmuir, 2017. **33**(38): p. 9731-9739.

2. Yao, J., et al., *In Situ Characterization of Boehmite Particles in Water Using Liquid SEM.* J Vis Exp, 2017(127).

11:20am CA+AS+NS+SE+SS-FrM-10 Mechanistic Insights into the Study of γ -Al$_2$O$_3$ Surface and its Interface with Pt, *Kofi Oware Sarfo, A Clauser, M Santala, L Árnadóttir,* Oregon State University

Metal/metal oxide interfaces occur in heterogeneous catalysis where metal catalyst nanoparticles are dispersed on highly porous metal oxide supports to increase the surface area for reactions. The interactions between catalyst nanoparticles and the catalyst support has previously been shown to affect the extent of dispersion of the active metal catalyst, particle sintering and the electronic properties of the catalyst. The capability to describe and predict the structure of the catalyst, the catalyst support and the interface between the two is therefore a critical step towards understanding the catalyst-support interactions. γ-Al$_2$O$_3$, a polymorph of Al$_2$O$_3$ is a commonly used catalyst support due to its durability at operation conditions and high surface area. Here we combine theoretical and experimental methods to investigate and predict the structure and thermodynamic stability of the interface between γ-Al$_2$O$_3$ and Pt nanoparticles. The experimental approach involves the fabrication of the embedded Pt nanoparticles and the use of high resolution transmission electron microscopy (HRTEM) to image the atomic structure for the embedded interfaces. The theoretical approach utilizes density functional theory (DFT) and thermodynamic models to calculate surface energies of γ-Al$_2$O$_3$ (111) and interfacial energies between Pt(111) and γ-Al$_2$O$_3$ (111) to

describe the stabilities of the surfaces and interfaces. Of the three interfacial terminations, Pt atoms interacting with oxygen terminated γ-Al_2O_3 (111) are the most stable interfaces at atmospheric conditions. The stability of this interface is based on the strong electrostatic interaction between the Pt atoms and the oxygen atoms at the oxygen terminated interface. This work therefore, provides the complement to experimental study of the atomic structure of the interface between γ-Al_2O_3 and Pt nanoparticles.

11:40am CA+AS+NS+SE+SS-FrM-11 Artificial Intelligence--An Autonomous TEM for In-situ Studies, *Huolin Xin,* University of California Irvine **INVITED**
Deep learning schemes have already impacted areas such as cognitive game theory (e.g., computer chess and the game of Go), pattern (e.g., facial or fingerprint) recognition, event forecasting, and bioinformatics. They are beginning to make major inroads within materials science and hold considerable promise for materials research and discovery. In this talk, I will introduce deep convolutional neural networks and how they can be applied to the computer vision problems in transmission electron microscopy. I will also discuss the development and application of liquid TEM to the study of solid/liquid interfaces at the nanoscale.

Fundamental Discoveries in Heterogeneous Catalysis Focus Topic
Room A213 - Session HC+SS-FrM

Catalysis at Complex Interfaces
Moderators: Elizabeth Landis, College of the Holy Cros, Fan Yang, Dalian Institute of Chemical Physics, China

8:20am HC+SS-FrM-1 Pd Nanoparticles on Alumina Nanofibers by Electrospinning for Heterogeneous Catalysis, *Miguel Angel Rodriguez Olguin, M Enes da Silva, J Faria, A Susarrey Arce, H Gardeniers,* University of Twente, Netherlands
The pressing transition from unsustainable fossil fuels to a sustainable economy based on renewables with minimal chemical waste is one of the grand challenges for the twenty-first century. To mitigate these challenges, it is crucial that improved synthetic catalytic methods are developed, that increase conversion and selectivity of existing chemical transformation processes. For example, *alumina* is a widely used catalyst support owing to its excellent thermal stability and inherent chemical acidity. Technologies like three-way catalytic converters rely on well-defined alumina-based structured monoliths of about hundred of micrometers to millimeters dimensions without spatial control on the allocation of the metal catalyst. The latter is considered essential to derive at more stable catalysts, it may prevent sintering for instance. Additive manufacturing of catalyst materials can pave the path to control the distribution of catalytic nanoparticles, and mass transport modulation by optimized 3-dimensional support designs. In this work, we present co-axial electrospinning to control the distribution of Pd nanoparticles (Pd NPs) over synthetic fibrous-like Al_2O_3 structures. First, our approach involved several synthetic routes for the fine tuning of the Al_2O_3 fibers by varying the formulation of $Al(NO_3)_3 \cdot 9H_2O$, $Al(OH)_3$, $C_{14}H_{27}AlO_5$ precursors and Al_2O_3 nanoparticles additives. Thermal stability and chemical properties of the nanofibers have been tested. The Al_2O_3 fibers morphology is visualized with Scanning Electron Microscopy (SEM), and the fiber diameter is estimated between 81 nm to 107 nm depending on aluminum precursor. Furthermore, X-ray Diffraction (XRD) is utilized to confirm the crystalline phase of the Al_2O_3 used as support. Second, the Al_2O_3 that performs best in terms of morphology, crystallinity, surface area and acidity is loaded with Pd NPs. The location of Pd NPs is varied by tuning the Pd concentration of the precursor suspension. Finally, the Al_2O_3-Pd fibrous catalyst is tested by chemisorbing CO species. CO chemisorption in liquid phase is performed with *in-situ* Attenuated Total Reflectance Infrared Spectroscopy (ATR-IR). Further, liquid phase catalytic reactions will be explored.

8:40am HC+SS-FrM-2 Multi-Layered TiO₂ Nanofibrous Structures Decorated with Catalytic Nanoparticles for Photoelectrocatalytic Applications, *Cristian Deenen, C Eyövge, A Susarrey-Arce, H Gardeniers,* University of Twente, Netherlands
Electrospinning is a technique to fabricate nanofibers by applying a high potential between a nozzle and a collector. As a solution is pumped through the nozzle, a jet is ejected from the nozzle that solidifies as it moves towards the collector, resulting in nanofiber deposition on the collector.

A drawback in conventional electrospinning setups consisting of a singular electrified nozzle is the difficulty in depositing multiple material combinations due to the time and labor required to either manually replace the nozzle or to flush the fluidic elements of the electrospinning setup. A novel multi-nozzle approach will be demonstrated to reduce the time required for the switching of precursor materials from minutes to seconds. The proposed concept opens up new possibilities for the fabrication of complex devices with a variety of material formulations, such as alternating functional layers of interest to the fields of catalysis, electrochemistry and photovoltaics.

Mounting multiple nozzles on a rotating disc allows the inactive nozzles to be rotated out-of-plane, away from the electric field between the active nozzle and the collector, which at the same time reduces the risks of dripping from the inactive nozzles. Combining this concept with appropriate control of electrical voltages and fluidic flow through the different nozzles, allows the engineering of a flexible platform for fast and reliable manufacturing of multi-component materials using electrospinning. In this work, we will demonstrate the instrumental concept and apply it to the fabrication of catalytic layers composed of TiO2, decorated with three different metal catalyst nanoparticles (Au, Pd, Pt) which function in concert for light harvesting and efficient hydrogen production during photoelectrocatalysis.

9:00am HC+SS-FrM-3 Water Oxidation Reaction in Natural Photosynthesis, *Junko Yano,* Lawrence Berkeley National Laboratory **INVITED**
Many of the catalytic reactions in inorganic systems and natural enzymes involve multiple electrons, and proceed through several intermediate steps. For example, photosynthetic water oxidation in nature is catalyzed by the metal center that consists of oxo-bridged four Mn and one Ca atoms, which is located in multi-subunit membrane protein, Photosystem II (PSII). This is one of the most important, life-sustaining chemical processes occurring in the biosphere. The oxygen-evolving complex (OEC) in PSII, which contains the heteronuclear Mn_4CaO_5 cluster, catalyses the reaction

$$2H_2O \rightarrow O_2 + 4e- + 4H+$$
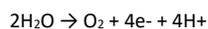
that couples the four-electron oxidation of water with the one-electron photochemistry occurring at the PSII reaction center. The OEC cycles through five intermediate S-states (S_0 to S_4) that corresponds to the abstraction of four successive electrons from the OEC (Fig. 1). Once four oxidizing equivalents are accumulated (S_4-state), a spontaneous reaction occurs that results in the release of O_2 and the formation of the S_0-state.

Recently, the development of X-ray Free Electron Lasers (XFELs) has opened up opportunities for studying the dynamics of biological systems. Intense XFEL pulses enable us to apply both X-ray diffraction and X-ray spectroscopic techniques to dilute systems or small protein crystals. By taking advantage of ultra-bright femtosecond X-ray pulses, one can also collect the data under functional conditions of temperature and pressure, in a time-resolved manner, after initiating reactions, and follow the chemical dynamics during catalytic reactions and electron transfer. Such an approach is particularly beneficial for biological materials and aqueous solution samples that are susceptible to X-ray radiation damage.

We have developed spectroscopy and diffraction techniques necessary to fully utilize the capability of the XFEL x-rays for a wide-variety of metalloenzymes, like Photosystem II, and to study their chemistry under functional conditions. One of such methods is simultaneous data collection for x-ray crystallography and x-ray spectroscopy, to look at overall structural changes of proteins and chemical changes at metal catalytic sites. We have used the above techniques to study the water oxidation reaction of Photosystem II, in which the Mn_4CaO_5 cluster catalyzes the reaction. The current status of this research and the mechanistic understanding of the water oxidation reaction based on the X-ray techniques is presented.

9:40am HC+SS-FrM-5 Synthesis and Characterization of Carbon-supported PdCu Nanoparticles for the Water Electrolysis in Acid Medium, *Jonder Morais, D Lima, M Castegnaro, M Alves,* Universidade Federal do Rio Grande do Sul, Brazil
Hydrogen is an important option for an energetic vector due to its high energy density, high heat of combustion and it can be produced in different ways, such as water electrolysis, which is a clean and efficient process. It generates pure H_2 and the required energy for the process can be obtained from renewable sources. However, it is essential to find efficient catalytic materials to be applied as the electrodes for the water electrolysis that usually involves the use of noble metals. An important alternative to lower

the production costs for the electrode material is the development of bimetallic nanoparticles supported on amorphous conducting carbon. Recently, a catalyst composed by carbon-suported bimetallic PdCu alloy nanoparticles presented significant activity in the oxygen oxidation reaction [1]. In this sense, PdCu based electrocatalysts were synthesized accordingly and the morphology, composition and structure of PdCu nanoparticles were characterized by TEM, EDS and XRD, respectively. Cathodes were prepared by the brushing technique with the electrocatalyst [2] and tested in the hydrogen evolution reaction (HER) employing 0.5 M H_2SO_4 aqueous sol ution as the electrolyte. Cyclic voltammetry, chronoamperometry and Tafel analysis were carried out to evaluate the stability, reaction mechanism determination and efficiency of HER. Moreover, XPS measurements were performed on the PdCu cathodes before and after the electrochemical measurements in order to monitor the modifications on the electronic structure of the electrocatalyst. Cyclic voltammetry analysis of the cathode showed that the system rapidly becomes highly stable. Tafel analysis indicated that for this system, the mechanism of the reaction is that of Volmer-Heyrovsky, where the H^+ desorption is the determining step. The reaction exchange current density of HER for PdCu was around 0.8 mA cm^{-2}, in the equilibrium potential of -270 mV_{SCE}. Moreover, the current density observed in the chronoamperometry analyzes at -2 V_{SCE} was around 340 mA cm^{-2}. XPS analysis showed a significant change in the copper structure after the hydrogen evolution reaction, indicating that it assumed a more metallic character after the reaction. The obtained results indicate that the PdCu carbon-supported bimetallic nanoparticles are a very promising electrocatalysts and should be further studied.

Financial support from CAPES and CNPq is acknowledged.

[1] M. V. Castegnaro, J. Morais et al, *Langmuir* 33 (2017) 2734-2743

[2] D. W. Lima, E. M. A. Martini et al, *J. Int. J. Hydrogen Energy* 42 (2017) 5676-5683

10:00am HC+SS-FrM-6 Nanoscale Spectromicroscopy and Chemical Activity of Bilayer Silicate Films on Pd(100) and Pd(111), *Samuel Tenney, C Eads,* Brookhaven National Laboratory; *L Mark,* University of Colorado at Boulder; *V Lee,* University of North Texas; *M Wang,* Brookhaven National Laboratory; *J Medlin,* University of Colorado at Boulder; *J Kelber,* University of North Texas; *D Stacchiola,* Brookhaven National Laboratory
In this talk we present the first reported photothermal infrad (PTIR) spectra and hyperspectral images of ultrathin bilayer silicate films with a spatial resolution better than 10nm and compare this with traditional infrared reflection absorption spectroscopy (IRRAS) of the same surface. The growth of the ultrathin bilayer silicates on Pd(100) and Pd(111) surfaces was observed in real-time with an in-situ low energy electron microscope (LEEM) capable of selected area low energy electron diffraction (μ-LEED). The samples were further probed with ambient pressure X-ray photoelectron spectroscopy (AP-XPS), temperature programmed desorption (TPD) and high resolution electron energy loss spectroscopy (HREELS). The chemical activity and enhanced selectivity of these model silicate/Pd catalysts will be discussed.

10:20am HC+SS-FrM-7 Formation and Properties of Mirror Twin Grain Boundary Networks in Molybdenum Dichalcogenides, *Matthias Batzill,* University of South Florida **INVITED**
Edges, defects, and dopants in 2D transition metal dichalcogenides have been shown to give rise to special chemical, electronic, and magnetic properties in these materials. To utilize the potential of these modifications a detailed understanding of their controlled formation and atomic scale properties is needed. In this talk we present our studies on the controlled formation of metallic mirror twin grain boundaries (MTBs) in $MoSe_2$ [1] or $MoTe_2$ [2] by incorporation of excess Mo into the lattice. Very high density of MTB networks can be obtained in $MoTe_2$ that effectively metallizes the material and thus may act as a metallic contact patch [3]. Such line defects may also increase electrocatalytic properties for hydrogen evolution reactions [4]. On a more fundamental level, we show that these 1D metallic grain boundaries host one dimensional electron gas and we present the first angle resolved photoemission (ARPES) studies of such line defects. These studies show evidence for the presence of Tomonaga-Luttinger Liquid behavior of 1D electron systems [5]. Finally, we show that other transition metals may also be incorporated into $MoTe_2$ and the incorporation of vanadium induces room temperature ferromagnetic ordering and thus is an example of a 2D dilute ferromagnetic semiconductor [6].

[1] Y Ma, S Kolekar, H Coy Diaz, J Aprojanz, I Miccoli, C Tegenkamp, M Batzill. Metallic Twin Grain Boundaries Embedded in $MoSe_2$ Monolayers Grown by Molecular Beam Epitaxy. *ACS Nano* 11, 5130-5139 (2017)

[2] HC Diaz, Y Ma, R Chaghi, M Batzill. High density of (pseudo) periodic twin-grain boundaries in molecular beam epitaxy-grown van der Waals heterostructure: $MoTe_2/MoS_2$. *Appl. Phys. Lett.* 108, 191606 (2016)

[3] PM Coelho, HP Komsa, H Coy Diaz, Y Ma, AV Krasheninnikov, M Batzill. Post-Synthesis Modifications of Two-Dimensional MoSe2 or MoTe2 by Incorporation of Excess Metal Atoms into the Crystal Structure. *ACS Nano* 12, 3975-3984 (2018).

[4] T Kosmala, H Coy Diaz, HP Komsa, Y Ma, AV Krasheninnikov, M Batzill, S Agnoli. Metallic Twin Boundaries Boost the Hydrogen Evolution Reaction on the Basal Plane of Molybdenum Selenotellurides. *Adv. Energy Mat.*, 1800031 (2018).

[5] Y Ma, et al. Angle resolved photoemission spectroscopy reveals spin charge separation in metallic MoSe2 grain boundary. *Nature Commun.* 8, 14231 (2017).

[6] PM Coelho, et al. Room temperature ferromagnetism in MoTe2 by post-growth incorporation of vanadium impurities. *Adv. Electr. Mat.* in press.

11:00am HC+SS-FrM-9 Selectable Catalytic Reduction of Carbon Dioxide to Formic Acid or Methanol over Defect Hexagonal Boron Nitride*, *K Chagoya, T Jiang, D Nash, D Le,* **Talat S. Rahman***, R Blair,* University of Central Florida
Finding effective heterogeneous catalysts, consisting of abundant elements, for the hydrogenation of waste gas carbon dioxide into value added molecules is a challenging task for global energy and sustainability solutions. In a closely coupled computational and experimental effort, we find that vacancies induced in defect-laden hexagonal boron nitride (*dh-BN*) can effectively activate the CO_2 molecule for hydrogenation. Computationally, we demonstrate that activation occurs through back-donation to the π* orbitals of CO_2 from frontier orbitals (defect state) of the *h-BN* sheet localized near a nitrogen vacancy (V_N). Subsequent hydrogenation to formic acid (HCOOH) and methanol (CH_3OH) occurs through vacancy facilitated co-adsorption of hydrogen and CO_2. More importantly, we find that *dh*-BN is a temperature-driven switchable catalyst with formic acid formation observable at reaction temperatures above 160 ˚C and pressures of 583 kPa, while methanol formation was observed at lower temperatures (as low as 20 ˚C), which are in great agreement with thermodynamics and kinetics of our calculated reaction pathways.

*Work supported in part by DOE grant DE-FG02-07ER15842

Nanometer-scale Science and Technology Division
Room A222 - Session NS+AS-FrM

Electron-Beam Promoted Nanoscience
Moderators: Omur E. Dagdeviren, Yale University, Qing Tu, Northwestern University

8:20am NS+AS-FrM-1 Vibrational Spectroscopy in the Electron Microscope, *Ondrej Krivanek, N Dellby, C Meyer, A Mitelberger, T Lovejoy,* Nion Co. **INVITED**
Vibrational (phonon) spectroscopy using an electron microscope's primary beam was introduced in 2014, and it has now progressed very significantly. The attainable energy resolution stands at ~5 meV (at 30 keV primary energy), our understanding of the electron-matter interaction has deepened, and several types of new applications have been explored.

Phonons can be excited by fast electrons in two fundamentally different ways: by dipole scattering, which is similar to exciting the sample by infrared light, and by impact scattering, which bears a closer resemblance to neutron scattering. Dipole scattering occurs only in polar materials, and it is characterized by small scattering angles (~0.1 mrad) and interaction distances of tens of nanometers. Impact scattering involves a direct interaction between the fast electron and an atomic nucleus, and it leads to large scattering angles. Selecting the impact scattering (with an aperture in the diffraction plane) allows the vibrational signal in h-BN to be imaged with atomic (0.2 nm) resolution [1,2]. In elemental Si, impact scattering is dominant, and it allows atomic resolution to be reached without angular selection [3].

The angular (momentum) distribution of vibrational scattering has also been explored [4-6]. Attainable spatial resolution is then inversely related to the angular resolution. Optical and acoustic branches of vibrational scattering have been mapped in hexagonal and cubic BN, and in graphene and graphite.

Friday Morning, October 25, 2019

Dipole scattering provides another exciting possibility: probing the sample from a small distance, by "aloof spectroscopy". This approach limits the maximum energy that can be transferred to the sample with significant probability as 1/b, where b is the distance of the confined electron beam from the sample. In this way, vibrational properties of biological and other "fragile" materials can be probed without significant radiation damage [7], and this may well revolutionize analysis in the electron microscope. The technique has recently been used to detect isotopic substitution: ^{13}C vs. ^{12}C at a specific site in an amino acid (L-alanine), and to map the distribution of the two species [8].

[1] C. Dwyer et al., Phys. Rev. Letts **117** (2016) 256101

[2] F.S. Hage et al., Phys. Rev. Letts **122** (2019) 016103

[3] K. Venkatraman et al., arXiv:1812.08895 (2018)

[4] F.S. Hage et al., Sci. Adv. 2018;4:eaar7495 1-5

[5] R. Senga et al., arXiv:1812.08294 (2018), Nature (2019, in print)

[6] Lovejoy et al. Proceedings 2019 M&M Conference (in print)

[7] P. Rez et al., Nature Comms **7** (2016) 10945, doi: 10.1038/ncomms10945

[8] J. Hachtel et al., Science **363** (2019) 525–528

9:00am NS+AS-FrM-3 In-situ Electron Microscopy of Localized Surface Plasmon Initiated Reactions, *Canhui Wang, W Yang, A Bruma,* UMD/NIST; *R Sharma,* National Institute of Sandards and Technology (NIST) **INVITED**
Excitation of localized surface plasmon (LSP) resonance on metal nanoparticles has been shown to overcome the reduced the energy barrier for photochemical reactions, even allowing certain reactions to occur at room temperature. (1-2) Understanding the reactions promoted by LSP resonance at the nanoscale is important for designing efficient photocatalytic systems for a wide range of energy and environmental applications. However, many important questions related to this type of reaction process remain unclear due to the complexity of the reaction kinetics, and lack of spatial resolution available with optical methods. Details such as the location of gas adsorption sites, how the energy is being absorbed and released, and how those details are correlated to the structure of the catalyst nanoparticles, remain elusive and are only hinted by theoretical calculations.

Here we use *in-situ* electron microscopy and combine an ensemble of data acquisition and processing techniques to characterize LSP-initiated chemical reactions at high spatial resolution using an aberration-corrected environmental scanning transmission electron microscope. Electron energy loss spectrum (EELS) imaging is used to acquire both elemental and LSP resonance maps from the same area that contains the plasmonic nanoparticles. The elemental maps allow us to locate the gas adsorption sites, the elemental distribution of the reactants and plasmonic nanostructures, as well as the spatial distribution of the solid reaction products, with nanometer resolution. The LSP-EELS maps provide insight into how the energy is channeled from the fast electron to the plasmonic nanostructure. Localized reactant consumption (mass loss) distribution is mapped in terms of thickness changes by subtracting the thickness map acquired after the reaction from the thickness map acquired before the reaction. This allows us to pinpoint the reaction hotspot near the nanoparticle surface. The LSP induced electric field distribution near the nanoparticle surface is simulated using the metallic nanoparticles boundary element method(MNBPEM) (3) and compared with the reactant mass loss map. These techniques allow us to explore and study previously unknown LSP initiated reactions with unprecedented details on the sub-particle level. (4) The results improved the understanding of the dynamics of LSP initiated reactions and give insights into nanoparticle engineering for optimizing reaction efficiency.

1. Mukherjee S, et al. (2012) Nano letters 13(1):240-247.

2. Thomann I, et al. (2011) Nano letters 11(8):3440-3446.

3. Waxenegger. J, et al. (2015) Comp. Phys. Commun. 193, 138.

4. Yang, W.C.D, et al. (2019) Nature Mater. 1.

9:40am NS+AS-FrM-5 Nanoscale Manipulation of Redox of Ag by Electron Beam, *Jianguo Wen, H Sheng,* Argonne National Laboratory; *J Wang,* Wuhan University, China **INVITED**
Employing electrons for direct control of nanoscale reaction is highly desirable since it provides fabrication of nanostructures with different properties at atomic resolution and with flexibility of dimension and location. In 2016, Kalinin et al summarized past experiments of manipulating atoms with scanning transmission electron microscopy (STEM) and proposed to utilize the imaging tool to create structures atom by atom (1). Here, applying *in situ* transmission electron microscopy, we show nanoscale oxidation and reduction of Ag can be manipulated by electron beam. We demonstrated fabrication of an array of 3 nm Ag_2O nanodots in an Ag matrix.

Under high vacuum environment (~10^{-7} Torr pressure), oxygen in a TEM can be ionized by high-energy electron beam and causes oxidization of Ag. After enough e-beam illumination, a growth of Ag_2O on the surface is observed when electron beam flux is below ~$5x10^5$ $e^-/Å^2s$. Ag_2O islands epitaxially grow on Ag surface with orientation relationship of $<110>_{Ag}$ // $<110>_{Ag2O}$ and $\{111\}_{Ag}$ // $\{002\}_{Ag2O}$ in most cases. In-situ high-resolution transmission electron microscopy (HRTEM) imaging shows that Ag_2O nucleates at atomic steps on Ag surfaces.

With the increase of electron-beam intensity above ~$5x10^5$ $e^-/Å^2s$, the formed Ag_2O islands can be fully reduced back to Ag, such that a fully reversible oxidation and reduction of Ag is achieved by varying electron beam intensity. The growth and reduction of Ag2O island is electron-beam dose rate dependent, a near equilibrium state has been achieved at the dose rate of ~$5x10^5$ $e^-/Å^2s$. A brief explanation for this electron-beam dose rate dependence is the competition between the electron-beam ionization induced oxidation of Ag and electron stimulated desorption induced reduction of Ag_2O. Aberration-corrected HRTEM observation reveals that O atoms are preferably inserted and extracted along the $\{111\}$ close-packed planes of Ag, leading to the nucleation and decomposition of nanoscale Ag2O islands on the Ag substrate.

Taking another step further, patterned oxidation has also been tested to verify the reliability of the electron-beam irradiation as a nanofabrication technique. By controlling probe size, electron flux, and dwell time, we demonstrated fabrication of an array of 3 nm Ag_2O nanodots in an Ag matrix. These findings do not only facilitate the basic understanding of oxidation/reduction kinetics in Ag-Ag_2O, but also open up a promising approach for precise fabrication of nanostructures with metal or semiconductor properties in devices.

1) Kalinin, Sergei V., Albina Borisevich, and Stephen Jesse. "Fire up the atom forge." *Nature News* 539.7630 (2016): 485.

10:20am NS+AS-FrM-7 Dynamics of Material Surfaces and Interfaces – The Good, the Bad and the Electron Beam, *Jakob Birkedal Wagner,* DTU Nanolab, Technical University of Denmark, Denmark **INVITED**
A good understanding of the dynamics and formation mechanisms of surfaces and interfaces at the nanometer scale is of great importance in order to exploit the controllability of nanostructures and their applications in photovoltaics, electronics, sensors, *etc.* on an industrial scale.

In situ electron microscopy serves a unique platform for monitoring and studying structural dynamics at length scales from micrometer down to atomic scale and temporal resolution approaching millisecond range. In addition, elemental and chemical information is gained from spectroscopic techniques with spatial resolution approaching the atomic scale.

Here, I will present a few cases of the surface and interface dynamics studied at the microscopy facility at Technical University of Denmark. This includes surface dynamics of supported nanoparticles (catalyst) [1] under harsh environment (elevated temperature, gas and electron beam), as well as interface dynamics of grain boundaries in metal thin films [2], growth of nanostructures from bottom-up processes [3-6] and volatility of soot oxidation catalysts. [7]

The influence of the high-energetic electron beam will also be discussed in terms of sample damage and controlled reaction enhancement.

References

[1] P. Liu, PhD thesis (2018), Technical Unity of Denmark

[2] A. Bastos Fanta *et al.* Materials Characterization 139, 452 (2018)

[3] J. Kling *et al.* Carbon 99, 261 (2016)

[4] L.. Zhang *et al.* ACS Nano 11, 4483 (2017)

[5] S. Rackauskas *et al.,* Scientific Reports 7, 12310 (2017)

[6] W. F. van Dorp *et al.*, Nanotechnology 24, 345301 (2013)

[7] D. Gardini *et al.*, Appl. Catal. B, 183, 28 (2016)

11:00am NS+AS-FrM-9 Atomic-Scale Mechanism of Unidirectional Oxide Growth, *Xianhu Sun, W Zhu, D Wu,* SUNY Binghamton University; *Z Liu,* University of Pittsburgh; *X Chen, L Yuan,* SUNY Binghamton University; *G Wang,* University of Pittsburgh; *R Sharma,* National Institute of Standards and Technology (NIST); *G Zhou,* SUNY Binghamton University

A fundamental knowledge of the unidirectional growth mechanisms is required for precise control on size, shape, and thereby functionalities of nanostructures. Using transmission electron microscopy that spatially and temporally resolves CuO nanowire growth during the oxidation of copper, here we provide direct evidence of the correlation between unidirectional crystal growth and bicrystal boundary diffusion. Based on atomic scale observations of the upward growth at the nanowire tip and oscillatory downward growth of atomic layers on the nanowire sidewall, we clearly show that bicrystal boundary diffusion is the mechanism by which Cu atoms are delivered from the nanowire root to the tip. Together with density-functional theory calculations, we further show that the asymmetry in the corner-crossing barriers promotes the unidirectional oxide growth by hindering the transport of Cu atoms from the nanowire tip to the sidewall facets. We expect broader applicability of our results in manipulating the growth of nanostructured oxides by controlling the bicrystal boundary structure that favors anisotropic diffusion for unidirectional, one-dimensional crystal growth for nanowires or isotropic diffusion for two-dimensional platelet growth.

11:20am NS+AS-FrM-10 Application of Electron-beam-excited Localized Surface Plasmon Resonance to Provide Guidelines for Plasmonic Catalysts, *Wei-Chang Yang*[1]*, C Wang, L Fredin, H Lezec, R Sharma,* National Institute of Standards and Technology (NIST)

Optically-excited localized surface plasmon (LSP) resonances have been used to induce chemical reactions, such as hydrogen dissociation and ethylene epoxidation. Energy harnessed by plasmonic nanostructures and transferred to adsorbed reactants is theorized to initiate these chemical processes by compensating for the heat required otherwise. As we know, there are three important steps for designing a plasmonic catalyst system: (1) adsorption of reactants; (2) adequate resonance energy to overcome the reaction barrier; and (3) desorption of products. However, they have not been resolved at a sub-nanoparticle scale using optical methods. Herein, we demonstrate that the sub-particle information, gained from electron energy-loss spectroscopy (EELS) and cathodoluminescence (CL), can be used to measure these steps for selected reactions.

LSP resonances, excited by electrons, on shape-controlled Au nanoparticles, were exploited to drive CO disproportionation: $2CO_{(g)}$ --> $CO_{2(g)}$ + $C_{(s)}$, at room temperature (commonly initiated by heat above 400 ˚C) in an environmental scanning transmission electron microscope equipped with a monochromated electron gun. Triangular Au nanoprisms were synthesized and loaded on TiO_2 support in a cantilevered configuration. *In situ* core-loss EELS was used to detect CO adsorption on the Au surfaces, for the first time, revealing the preferential adsorption sites at selective edges but not on the entire surfaces. Low-loss EELS maps of the Au nanoprisms showed that the electron beam was most efficiently coupled with the LSP dipole mode, indicated by the maximum EELS intensity, when placed at the cantilevered corner, suggesting a strong electric field caused by this specific mode at the same corner. *In situ* EELS showed that energy shifts occurred to the LSP resonance in CO environment and disappeared after CO evacuation, indicating a change in electron density of the Au particle as CO was adsorbed and desorbed, respectively. Energy transferred to the adsorbed CO was identified based on the spectral difference between EELS and CL. Carbon deposits, resulting from room-temperature CO disproportionation mediated by the LSP resonance, were detected by core-loss EELS at the cantilevered corner edge after evacuating CO. This shows that the active sites on the nanoprisms are where the preferable CO adsorption sites and the locations of maximum field amplitude superimpose.

Our findings provide unprecedented information on an LSP-induced chemical reaction with nanometer precision, shedding light on the design principles for new plasmonic catalysts that enable low-temperature reactions.

Plasma Science and Technology Division
Room B130 - Session PS+2D+SE+TF-FrM

Plasma Deposition and Plasma-Enhanced Atomic Layer Deposition

Moderators: Scott Walton, Naval Research Laboratory, David Boris, U.S. Naval Research Laboratory

8:20am PS+2D+SE+TF-FrM-1 Plasma-based Synthesis of 2D Materials for Devices on Flexible Substrates, *N Glavin,* Air Force Research Laboratory; *Christopher Muratore,* Department of Chemical and Materials Engineering, University of Dayton **INVITED**

Synthesis of flexible two-dimensional electronic devices using low-cost, naturally abundant materials (e.g., MoS_2) directly onto inexpensive polymeric materials at economically viable scales enables use of their unique characteristics in grand challenge areas of energy, healthcare, and national security. Recently-proven approaches for low temperature, plasma-based 2D synthesis suitable for flexible substrates developed by the authors include growth of amorphous materials with subsequent photonic annealing to access crystalline domain sizes up to several microns. This approach has been demonstrated for synthesis of large area ultrathin monolithic layers as well as $MoS_2/WS_2/BN$ multilayers with pristine interfaces, allowing interrogation of intrinsic properties of 2D materials and their heterostructures as they apply to diverse optoelectronic devices, with a current focus on molecular sensing. Advantages of plasma-based approaches will be discussed in terms of detailed kinetic studies of crystal formation and compositional evolution on the substrate surface. Correlations of structure, especially defect densities, to materials properties and device performance will be discussed in the context of diverse device applications including photodetectors and molecular sensors.

9:00am PS+2D+SE+TF-FrM-3 Homogeneous Ternary Oxides of Aluminum with Silicon, Molybdenum, and Niobium by Plasma Enhanced ALD by Sequential Precursor Pulses, *Steven Vitale,* MIT Lincoln Laboratory

Deposition of ternary oxide films by ALD is well known. In the vast majority of cases ternary films are deposited by sequential deposition of thin layers of the constituent binary oxides, such as Al_2O_3 / SiO_2. This nanolaminate approach allows for precise control of the global film stoichiometry and is a good solution for many applications, including optical coatings where the wavelength of light is much greater than the nanolaminate thickness thus the film appears quasi-uniform. The nanolaminate approach is less desirable for electronic applications which are sensitive to surface defect sites in the material which may acts as charge traps. For these applications a truly homogenous film which does not possess internal interface states is preferred. True homogenous ternary oxide growth by sequential precursor pulses before the oxidation step is much less well explored. In this work we grow homogeneous ternary oxides of $Al_xSi_yO_z$, $Al_xNb_yO_z$, $Al_xMo_yO_z$ by plasma enhanced ALD using sequential precursor pulses. The stoichiometry of the films is measured by XPS. Using this data we propose models of how the precursors interact with the surface under competitive adsorption. It is found that trimethyl aluminum (TMA) is so strongly adsorbed to the surface at unity surface coverage that ternary oxide growth is not possible if the surface is first exposed to TMA. However if the surface is exposed to the Si, Nb, or Mo precursor first, ternary oxide growth is achieved. The growth kinetics for the three films are markedly different, however, and we explain this through models of the adsorption energy of each precursor.

9:20am PS+2D+SE+TF-FrM-4 Piezoelectric Response of ZnO Thin Films Grown by Plasma-Enhanced Atomic Layer Deposition, *Julian Pilz, T Abu Ali,* Graz University of Technology, Austria; *P Schäffner, B Stadlober,* Joanneum Research Forschungsgesellschaft mbH, Austria; *A Coclite,* Graz University of Technology, Austria

ZnO is a direct band gap semiconductor with attractive piezoelectrical, optical, and electrical properties, particularly appealing for a variety of functional devices. Especially the utilization of piezoelectric properties of ZnO nanostructures for transforming mechanical to electrical energy has attracted much research interest. For most of these so called nanogenerators, solution based deposition methods have been applied to create the desired nanostructures, often lacking a precise control of the deposition parameters. Atomic layer deposition, on the other hand, allows conformal and uniform deposition on high aspect ratio structures with Å-level thickness control.

In this study, we investigate the piezoelectric response of ZnO thin films on flexible substrates as a starting point for piezoelectric nanostructures. The

---

films are grown by plasma-enhanced atomic layer deposition (PE-ALD) to thicknesses below 100 nm by adapting diethylzinc and O_2-plasma as reactants. In comparison to thermal ALD (where diethylzinc and water are used as reactants), PE-ALD allows the deposition of films with higher resistivity, an important property to minimize the leakage of piezoelectric charges. Commercially available Polyethylenterephthalat (PET) coated with Indium Tin Oxide (ITO) serves as the flexible substrate and bottom electrode, respectively. The deposition of ZnO thin films is carried out at substrate temperatures between room temperature and 100 °C, as a change in preferential crystal orientation from (100) to (002) can be observed in this temperature range. The macroscopic piezoelectric characterization is performed in a home-built stamp station, in which a defined periodic force is exerted onto the samples and the generated piezoelectric charges are measured. Out of this, the longitudinal piezoelectric coefficient d_{33} can be obtained. Preliminary results show d_{33} coefficients > 7 pC/N, which is comparable to literature results. The piezoelectric characterization is made for the different samples to understand how the d_{33} coefficient changes for films deposited at different substrate temperatures and thus having different crystal orientation. Since the [002] is the polar axis in the ZnO wurtzite crystal structure, films with preferred orientation in this direction are therefore expected to show higher d_{33} coefficients.

The work lays the basis for developing functional piezoelectric generators and sensors in thin film form. However, the concepts can be easily transferred to depositions on lithographically defined templates in order to create nanostructured ZnO, which exhibits increased piezo response.

10:00am PS+2D+SE+TF-FrM-6 Plasma-enhanced Molecular Layer Deposition of Boron Carbide from Carboranes, *Michelle M. Paquette, R Thapa, L Dorsett, R Bale, S Malik, D Bailey, A Caruso,* University of Missouri-Kansas City; *J Bielefeld, S King,* Intel Corporation
Atomic layer deposition (ALD) research has exploded in this era of electronic miniaturization, smart materials, and nanomanufacturing. To live up to its potential, however, ALD must be adaptable to many types of materials growth. To extend the reach of this layer-by-layer deposition framework, researchers have begun to explore molecule based processes. Still relatively rare, existing molecular layer deposition (MLD) processes are limited and typically based on the condensation of "linear" 2D or "brush-type" organic polymer chains. To this end, icosahedral carborane ($C_2B_{10}H_{12}$) molecules provide an interesting target. Carboranes have been used in the plasma-enhanced chemical vapor deposition of boron carbide films for low-*k* interlayer dielectrics, neutron detection, and a variety of protective coatings. These are symmetric twelve-vertex molecules, known to form close-packed monolayers and to possess labile H atoms at each of the vertices capable of cross-linking in the presence of heat, plasma, or other energy source. As such, the carborane molecule is particularly intriguing as a novel MLD precursor for 3D growth, possessing unique symmetry, reactivity, and volatility properties not commonly encountered in traditional organic molecules. However, a challenge in developing a layer-by-layer process lies in achieving the selective coupling chemistry required, which in the case of molecular reagents requires typically exotic bis-functional derivatives. Herein we describe progress in developing a plasma-enhanced molecular layer deposition process based on carborane derivatives, where the plasma is exploited to create the surface functionalization necessary for selective coupling and to cross-link carborane layers. We investigate the deposition of several carborane derivatives on different functionalized surfaces with the application of various types of plasmas toward achieving controlled layer-by-layer growth of thin boron carbide films.

10:20am PS+2D+SE+TF-FrM-7 Gas Phase Kinetics Optimization Study for Scaling-up Atmospheric Pressure Plasma Enhanced Spatial ALD, *Yves Creyghton,* Holst Centre / TNO, The Netherlands, Netherlands
DBD plasma sources have been successfully integrated in spatial ALD equipment for low-temperature ALD (<120 °C) of metal-oxides. Applications involving (semi)conductive substrates require remote plasma operation. Radical losses during transport from remote plasma limit substrate speeds or demand excessive plasma flow rates. Proximity remote plasma sources were developed with sufficient radical flux even at low gas flow rates. The sources were demonstrated for ALD of InZnO for high mobility thin film transistors. Further optimization asks for deeper understanding of radical kinetics. In this contribution experimental and calculated data will be presented which allow insight in the radical gain and loss processes. A reference temperature of 100 °C and gas flows in the range 2-10 slm (for a 4 cm wide source) were applied. Alumina depositions

were carried out using TMA and 2% O_2-N_2 plasma gas. Deposited layers obtained for different relative height positions of the plasma source were analyzed. Growth per cycle (GPC) values indicate a strong decay of plasma reactivity for gaps > 0.5 mm. As O_3 --should not decay over such small distance, this indicates that the process is radical based. Surprisingly the GPC also shows a peak value at 0.1 mm (Fig. 1). O_3 and NO_x were measured in the plasma exhaust gas as a function of % O_2 (Fig. 2). The 1-2% O_2 for maximum NO appears to correspond with the optimal gas composition for both high GPC values and refractive index values close to 1.58 indicating high layer quality. This result suggests NO plays a role in downstream plasma radical formation. Further understanding of the role of plasma species such as N, metastable N_2(A) and NO has been obtained by modelling. Kinetic data sets for optimization of O_3 production have been implemented in a CFD model for the transport of plasma species from the remote plasma. For the analysis of modelling results, the reaction volume has been divided in 3 parts (1) the plasma ionization zone itself, (2) the flow dominated plasma source aperture and (3) the diffusional transport dominated surface reaction zone. The dominating reactions for gain and loss of O radicals differ much between zones (Fig. 3). As the main O radical formation in zone (2) is due to metastable excited N_2(A), in zone (3) reactions between N radicals and NO are the main source of O radical generation. In both zones, the main O radical loss process is due to generation of O_3. The experimentally validated model has been used for finding improved plasma process settings (source geometry, frequency, flow) allowing the further optimization of high-throughput plasma enhanced spatial ALD of metal oxides.

10:40am PS+2D+SE+TF-FrM-8 Taking Plasma ALD to the Next Level: From Fundamental Understanding to Selective 3D Processing, *T Faraz, K Arts,* Eindhoven University of Technology, The Netherlands, Netherlands; *L Martini, R Engeln, H Knoops,* Eindhoven University of Technology, The Netherlands; *Erwin Kessels,* Eindhoven University of Technology, The Netherlands, Netherlands **INVITED**
Current trends in semiconductor device manufacturing impose extremely stringent requirements on nanoscale processing techniques, both in terms of accurately controlling material properties and in terms of precisely controlling nanometer dimensions. Plasma-based processing remains key in next-generation device manufacturing with plasma-enhanced atomic layer deposition (PE-ALD or plasma ALD) being a method that has obtained a very prominent position in obtaining ultrathin films with atomic scale precision [1]. In this contribution the state-of-the-art of PE-ALD will be presented including latest insights into reaction mechanisms as well as some developments in plasma ALD equipment and emerging applications. Aspects such as the role of (energetic) ions, conformality in high aspect ratio structures, and selective processing will be discussed [2].

[1] H.C.M. Knoops, T. Faraz, K. Arts, and W.M.M. Kessels, J. Vac. Sci. Technol. A 37, 030902 (2019)

[2] T. Faraz, K. Arts, S. Karwal, H.C.M. Knoops, and W.M.M. Kessels, Plasma Sources Sci. Technol. 28, 024002 (2019).

11:20am PS+2D+SE+TF-FrM-10 Computational Investigation of Plasma Enhanced ALD of SiO₂, *C Qu,* University of Michigan; *P Agarwal, Y Sakiyama, A LaVoie,* Lam Research Corporation; *Mark J. Kushner,* University of Michigan
Plasma enhanced atomic layer deposition (PE- ALD) of dielectric films typically consists of two steps – precursor deposition and oxidation. For example, in a SiO_2 PE-ALD process, the Si-containing precursor is often deposited in the feature without use of plasma while the oxidation step is performed by an oxygen containing plasma. In principle, the surface kinetics of both steps are self-terminating. Although the plasma step is performed using gas pressures of several to 10 Torr, in addition to O-atoms the fluxes onto the wafer contain energetic particles in the form of ions, photons, hot-neutrals and excited states. When performing PE-ALD in high aspect ratio (HAR) features, transport of these species into the feature determine the quality of the deposition. Optimizing the PE-ALD depends on control of these fluxes.

In this work, results from a computational investigation of reactor and feature scale processes in idealized PE-ALD of SiO_2 will be discussed. Reactor scale simulations of a capacitively coupled plasma sustained in Ar/O_2 mixtures were performed using the Hybrid Plasma Equipment Model (HPEM); and provided fluxes and energy distributions of radicals, ions, excited states and photons onto the wafer. Feature scale simulations were performed with the Monte Carlo Feature Profile Model (MCFPM). The idealized ALD process consists of a non-plasma first step using an Si-R (R indicates organic) precursor. The second step uses fluxes from the Ar/O_2

plasma to remove the organic and oxidize the Si site. The base-case features are moderate to high aspect ratio (AR = 7-20) vias and trenches. The metrics to evaluate the process are surface coverage of Si, O, R, stoichiometry, defect density, surface roughness and deposition rate.

In self-terminating processes, many of these metrics should scale with pt, where p is the probability of reaction and t is the step length. For example, a given surface coverage of Si-R or Si-O should depend on first order on pt. However, as deposition proceeds and a feature fills, the effective AR increases. When coupled with conductance limited transport into the feature, with increasing AR the value of pt to produce a given surface coverage increases. As the deposition proceeds and AR increases, stoichiometry and defect density begins to have a dependence on height inside the feature, as surfaces deep in the feature receive less exposure to the reactive fluxes. The consequences of ion- and photon-induced damages will also be discussed.

* Work supported by LAM Research Corp. and the DOE Office of Fusion Energy Science.

11:40am PS+2D+SE+TF-FrM-11 Analyzing Self-limiting Surface Reaction Mechanisms of Metal Alkyl Precursors and Nitrogen Plasma Species: Real-time In-situ Ellipsometric Monitoring of III-nitride Plasma-ALD Processes, *Ali Okyay*, OkyayTech Inc., Turkey; *A Mohammad, D Shukla, S Ilhom,* University of Connecticut; *B Johs,* Film Sense LLC; *B Willis, N Biyikli,* University of Connecticut

ALD-grown films are vastly characterized via ex-situ measurements to quantify various material properties. However, gaining insight into the saturating surface reactions and growth mechanisms is only possible with real-time in-situ process monitoring of individual ALD cycles. While several in-situ measurement techniques have been employed in ALD research, in-situ ellipsometry stands out as one of the best options for real-time monitoring surface reactions. The promising potential of in-situ spectroscopic ellipsometry has already been demonstrated for a number of materials grown by remote plasma-ALD. Here, we verify that cost-effective multi-wavelength ellipsometer (MWE) can also be used effectively for real-time in-situ analysis of plasma-ALD growth cycles. We demonstrate for the first time that real-time dynamic in-situ MWE measurements convey not only accurate film deposition rate, but as well resolve single chemisorption, ligand removal, and nitrogen incorporation events with remarkable clarity. Moreover, forcing the limits for fitting the acquired in-situ MWE data, we were able to track the evolution of the optical constants of III-nitride films along the ALD cycles which indeed showed thickness-dependent behavior.

Our main motivation behind this study was twofold: (i) Analyze and compare the self-limiting growth characteristics of binary III-nitride (AlN, GaN, and InN) thin films via real-time in-situ ellipsometry and to gain insight into the ALD surface reaction mechanisms including chemical adsorption, ligand removal, and nitrogen incorporation steps. (ii) Performance evaluation of our custom designed ALD reactor featuring improved hollow-cathode plasma source by comparing our results with previous plasma-ALD grown III-nitrides.

Despite using the conventional alkyl metal precursors (trimethylaluminum, trimethyl/ethylgallium, trimethylindium) utilized also widely in MOCVD epitaxial growth, their solid-gas surface interactions with nitrogen plasma species shows notable differences, particularly with respect to substrate temperature, plasma power, plasma exposure time, and plasma gas composition. In terms of substrate temperature, AlN exhibited crystallinity at lower temperatures when compared to GaN and InN. Even at 100 °C, AlN showed crystalline behavior whereas GaN displayed amorphous character up to 200 °C. While $Ar/N_2/H_2$ composition is optimal for AlN, N_2/H_2 and Ar/N_2 mixtures proved to be better for GaN and InN. InN experiments revealed that the inclusion of H_2 gas led to mixed phase growth with substantial $c\text{-}In_2O_3$ phase. The possible surface reaction mechanisms that lead to these different growth behaviors will be discussed in detail.

12:00pm PS+2D+SE+TF-FrM-12 Tribological Properties of Plasma Enhanced Atomic Layer Deposition TiMoN with Substrate Bias, *Mark Sowa*, Veeco ALD; *A Kozen,* University of Maryland; *N Strandwitz, T Babuska, B Krick,* Lehigh University

In our previous study, we demonstrated a tertiary plasma enhanced atomic layer deposited transition metal nitride (TiVN) with exceptional wear rates and friction coefficients. We have extended that work with an investigation of another tertiary transition metal nitride system, $Ti_xMo_yN_z$. For films deposited at 250°C and 300W on a Veeco CNT G2 Fiji PEALD system, we have demonstrated how the ratio of TiN:MoN cycles (1:0, 2:1, 1:1, 1:2, 0:1) provides linear control of the Ti:Mo in the resulting film. Through application of an 13.56MHz RF substrate bias (0-188V) during the plasma

step, ion bombardment energy of the substrate can be varied, providing a means for tweaking the films physical and chemical characteristics which in turn are shown to impact the resulting film's tribological properties. As PEALD metal nitrides have broader interest than wear layers and to gain insights on the interrelationships of the mechanical properties, the processing details, and other film properties, we also report on the resulting film composition/impurities, density, crystallinity, optical properties, resistivity, and morphology.

Advanced Surface Engineering Division
Room A215 - Session SE+AS+SS-FrM

Tribology: From Nano to Macro-scale
Moderators: Robert Franz, Montanuniversität Leoben, Andrey Voevodin, University of North Texas

8:20am SE+AS+SS-FrM-1 The Scaling of Tribological Effects from Nano- to Macro-scale, *Peter Lee,* Southwest Research Institute **INVITED**
The last few decades has seen the advancement of technologies such as atomic force microscopes (AFM), scanning force microscopes (SFM) and friction force microscopes (FFM) to measure friction, wear and adhesions at the nano- and micro-scale, leading to the study of nano- and micro-tribology. The study of two surfaces at the nano- and micro-meter scale has led to the advancement of small scale engineering devices such as nano- and micro-electromechanical systems (NEMS and MEMES). However, it has also led to the study of materials used in macro-engineering in an attempt to understand the fundamentals of lubrication, friction and wear at the asperity scale in macro-systems.

Macro-tribology involves large apparent areas of contact where only a fraction of the asperity tips are in contact, whereas nano-tribology usually involves studying a single asperity contact where the actual contact is the same as the apparent contact. Consequently, roughness and actual contact shape plays a more significant role in the tribological behavior, which in turn means significant effects on forces such as friction, adhesion and surface tension. Tribology at the macro-scale is governed by complex phenomena such as ploughing, abrasive, and adhesive wear. Friction at the nano-scale is often studied purely in the wearless (interfacial) regime, where adhesion is substantial but wear is minimal.

This presentation will explore current research at the nano-scale and discuss how this has the potential to help in understanding and modeling at the macro-scale.

9:00am SE+AS+SS-FrM-3 Nanotribology of Graphene in Organic Solvents, *Prathima Nalam, B Sattari Baboukani,* University at Buffalo, State University of New York; *Z Ye,* Miami University
Two-dimensional (2D) materials such as graphene, *etc.* are emerging as friction-reducing additives for transmission fluids and lubricating oils to enhance the service life of sliding metallic components. Here in this work, we investigate the dissipative mechanism for a supported (on silica substrate), monolayer of graphene when immersed in organic solvents such as *n*-hexadecane and cyclohexane. Nanoscale friction measurements on graphene conducted using atomic force microscope showed a non-monotonic variation *i.e.* a decrease and then an increase in friction forces as a function of immersion time in organic solvents. This behavior was attributed to the re-arrangement of organic molecules at the 2D confinement formed between the graphene and the underlying substrate. The oscillatory forces measured at the interface showed an increased packing order of the solvent molecules under 2D confinement and with equilibration time lead to a higher dissipative interface. The diffusion of organic molecules to the 2D confinement also results in a partially-suspended graphene layer and the interfacial friction is discussed by understanding the quality (local pinning states of individual atoms) of the contact made by the AFM probe while sliding on graphene.

9:20am SE+AS+SS-FrM-4 Measuring Atomicscale Surface Friction of a Molecular Vehicle on Au(111), *K Latt, Sanjoy Sarkar, K Kottur, M Raeis,* Ohio University; *A Ngo,* Argonne National Laboratory; *R Tumbleson, Y Zhang, E Masson, S Hla,* Ohio University
Designing molecules with technomimetic properties has been actively pursued in the past decade. Among these, molecules specially designed for translational motion, dubbed as nanocars or molecular vehicles, are particularly appealing as they could ultimately be used to transport a molecular cargo or some specific chemical information from a start to an end point on a surface and on demand. Here, we have designed and

assembled an electric nanovehicle using four molecular wheels and a molecular chassis as separate modules. An 'H' shape chasis is formed by two benzimidazolium groups linking the front and the rear axles to a terphenyl drive shaft. Final assembly of the nanovehicle is realized by attaching four pumpkin shaped cucurbituril molecular wheels. The chassis of the nanovehicle includes positive charges, which are used for the controlled lateral movement of the vehicle by scanning tunneling microscope tip induced electric field manipulation. The threshold voltage required to drive the nanovehicle is determined from the Vaussian-fit of the data. Moreover, we have determined lateral force to move the nanovehicle on a Au(111) surface at 5K and it is found to be in superlubricity regime.

9:40am SE+AS+SS-FrM-5 The Use of the Nanocomposite Concept in Hard Coatings for Improving the Frictional Performance, *Albano Cavaleiro,* University of Coimbra, Portugal INVITED

Nanocomposite thin films based on a structural arrangement consisting of grains of a transition metal nitride enrobed in a thin layer of silicon nitride, have been developed in last decades with the final aim of maximizing the mechanical strength. This specific arrangement was proved to be efficient regarding the oxidation resistance and the structural stability at high temperatures as well as the wear resistance, reason why these coatings are commercially available in the market. However, their performance in applications requiring low friction, against specific materials, is very inefficient. On the other hand, in last years the addition of elements, able to provide low friction, such as Ag or V, to traditional hard coatings (TiN, TiAlN, TiCrN,…) has been deeply studied. Results were very successful from the lubrication point of view but the wear resistance was clearly reduced, due to either a decrease of the global mechanical strength of the coatings or the rapid depletion of the lubricant element from the coating by out diffusion to the contact zone.

In this talk an overview of the influence of the addition of lubricant elements to Ti-Si-N system will be presented. The coatings were deposited by conventional magnetron sputtering as well as by using HiPIMS power supplies. The importance of the type of the structure of the deposited coatings (nanocomposite or supersaturated solid solution) on their thermal stability, including oxidation resistance, will be discussed based on the diffusion of the lubricant elements. A comparison of the mechanical properties of the coatings deposited by both methods will be performed and the results will be interpreted based on the (micro)structure and residual stresses. Results on the tribological behaviour achieved by tests at room and high temperatures (up to 900 ºC) against different balls (steel, alumina and Ti-alloy) will be presented and commented. Generally, results show that a decrease of the mechanical performance of the coatings is obtained with that elements addition. However, in relation to tribological performance, significant improvements could be reached although under specific testing conditions (type of ball, temperature, …). In many cases, no improvements were observed.

10:20am SE+AS+SS-FrM-7 Development of Ultra-thick CrAlAgN Coatings by HiPIMS for Self-lubrication at Elevated Temperatures, *Jianliang Lin,* Southwest Research Institute*; X Zhang,* Southeast University, China

The pursuit of advanced coating systems to provide sufficient oxidation resistance and self-lubrication for high temperature tribological application continues. One of the approaches is to dope traditional hard transition metal nitride coatings with solid lubricants, e.g. Ag, Au, which diffuses towards coating surface to provide lubrication at elevated temperatures. However, the long term performance of these self-lubricating coatings at high temperatures in ambient air is limited by the rapid out diffusion of Ag, which is strongly affected by many factors, e.g. the volume fraction of the dopant and the density of the coating. It is expected that dense coating structure combined with increased coating thickness is helpful for achieving long term lubrication performance. In this paper, ultra-thick CrAlAgN coatings (50 µm) are deposited on steel and cement carbide substrates using high power impulse magnetron sputtering (HiPIMS) by carefully control the processing parameters. The structure and composition of the coatings were first tailored to achieve a combination of good adhesion, high density and good mechanical strength with HiPIMS deposition. The Ag concentration in the coatings is varied in the range of 3-10 at.%. For the coating performance, the oxidation resistance of the coating were studied in ambient air using isothermal test. The high temperature wear resistance of the coating was measured using a high temperature pin-on-disc tribometer in the ambient air from 500 °C to 900 °C. It was found that Ag doping degrades the mechanical strength and

oxidation resistance of the CrAlN coatings, but the ultra-thick CrAlAgN coating show robust self-lubricating performance at high temperatures.

Surface Science Division
Room A220-221 - Session SS+HC+PS-FrM

Planetary, Ambient, and Operando Environments

Moderators: Catherine Dukes, University of Virginia, Petra Reinke, University of Virginia

8:20am SS+HC+PS-FrM-1 Seeing is Believing: Atomic-scale Imaging of Catalysts under Reaction Conditions, *Irene Groot,* Leiden University, The Netherlands, Netherlands INVITED

The atomic-scale structure of a catalyst under reaction conditions determines its activity, selectivity, and stability. Recently it has become clear that essential differences can exist between the behavior of catalysts under industrial conditions (high pressure and temperature) and the (ultra)high vacuum conditions of traditional laboratory experiments. Differences in structure, composition, reaction mechanism, activity, and selectivity have been observed. These observations indicated the presence of the so-called pressure gap, and made it clear that meaningful results can only be obtained at high pressures and temperatures. However, most of the techniques traditionally used to study catalysts and their reactions were designed to operate under (ultra)high vacuum conditions. To bridge the pressure gap, the last years have seen a tremendous effort in designing new instruments and adapting existing ones to be able to investigate catalysts in situ under industrially relevant conditions.

In this talk, I will give an overview of the in situ imaging techniques we use to study the structure of model catalysts under industrial conditions of atmospheric pressures and elevated temperatures. We have developed set-ups that combine an ultrahigh vacuum environment for model catalyst preparation and characterization with a high-pressure flow reactor cell, integrated with either a scanning tunneling microscope or an atomic force microscope. With these set-ups we are able to perform atomic-scale investigations of well-defined model catalysts under industrial conditions. Additionally, we combine the structural information from scanning probe microscopy with time-resolved mass spectrometry measurements on the gas mixture that leaves the reactor. In this way, we can correlate structural changes of the catalyst due to the gas composition with its catalytic performance. Furthermore, we use other in situ imaging techniques such as transmission electron microscopy, surface X-ray diffraction, and optical microscopy, all combined with mass spectrometry.

This talk highlights a short overview of the instruments we developed and illustrates their performance with results obtained for different model catalysts and reactions. Results for reactions such as NO oxidation and hydrodesulfurization will be discussed.

9:00am SS+HC+PS-FrM-3 *Operando* NAP-XPS and NAP-STM Investigation of CO Oxidation on CoO Nanoislands on Noble Metal Surfaces, *Jonathan Rodríguez-Fernández, Z Sun, E Rattigan,* Aarhus University, Denmark*; C Martín, E Carrasco,* IMDEA Nanoscience, Spain*; E Pellegrin, C Escudero,* ALBA Synchrotron Light Source, Spain*; D Ecija,* IMDEA Nanoscience, Spain*; J Lauritsen,* Aarhus University, Denmark

Nanostructured cobalt oxides (CoOx) have proven to be interesting low temperature oxidation catalysts, for example for preferential oxidation (PROX) of carbon monoxide (CO). CoOx has been identified as one of the most active materials for CO oxidation showing activity down to temperatures as low as -80^0C^1. However, the pure oxide catalyst seems to be strongly poisoned by water. Some studies indicate that combining CoOx with gold synergistically improves the catalytic performance and poisoning resistance[2-3], but an understanding of this metal-oxide effect is lacking. To obtain an atomic scale understanding of the improved catalytic performance of combined Au-CoOx catalysts we have designed a model system where cobalt oxide nanoparticles are synthesized on an Au single crystal surface by physical vapor deposition in an oxygen environment [4-5].

Here, we significantly advance the mechanistic understanding of cobalt oxide nanocatalysts for CO oxidation by studying the surface chemistry of the model catalyst under *operando* conditions. We use powerful near ambient pressure techniques such as scanning tunneling microscopy (NAP-STM) and synchrotron X-ray photoelectron spectroscopy (NAP-XPS) to study CoO_x nanoislands on Au(111) at mbar pressure in a CO/O_2 gas mixture. From STM results, we find that the structure of the ~20nm wide monolayer cobalt oxide nanoislands is static during exposure to a mixture of CO and O_2 gases at a pressure of 1.5 mbar. Under these conditions at

room temperature, the nanoislands seem to exhibit activity towards CO oxidation, and we can detect CO, CO_2 surface species by NAP-STM experiments and by analysis of the corresponding O1s and C1s core level NAP-XPS spectra. In addition, we study the morphological evolution by NAP-STM and the reactivity of the CoO nanoislands from RT to 300^0C under *operando* conditions. At around 200^0C, CO_2 is found in gas phase and decreasing at the surface. Furthermore, to observe the influence of the substrate, we repeated the CoO nanoislands on Pt(111), obtaining similar reactivity results.

References:

1. Xie, X., et al., Nature 458 (2009): 746-749.

2. Cunningham, D. A. H., et al., Catal. Lett. 25 (1994): 257-264.

3. Liu, Y., et al., J. Catal. 309 (2014): 408-418.

4. Fester, J., et al., Nature Communications 8 (2017): 14169.

5. Walton, Alex S., et al., ACS Nano 9.3 (2015): 2445-2453.

9:20am SS+HC+PS-FrM-4 Reaction of 2-Propanol on SnO2(110) Studied with Ambient-Pressure X-ray Photoelectron Spectroscopy, *J Diulus, R Addou, **Gregory Herman**,* Oregon State University

Tin dioxide (SnO_2) has a wide range of applications, including gas sensors, transparent conductors, and oxidation catalysts. The surface chemistries for each of these applications can be strongly influenced by the surface structure and cation oxidation states. The oxidation of volatile organic compounds (VOC) has recently been demonstrated using SnO_2, where 2-propanol was used as the probe molecule. More recently it was observed that the surface Sn^{2+}/Sn^{4+}ratio strongly influenced the activity of carbon monoxide oxidation. In this study, we have used ambient pressure X-ray photoelectron spectroscopy (AP-XPS) to characterize the surface chemistry of 2-propanol on well-defined SnO_2(110) surfaces. We have prepared stoichiometric and reduced surfaces which were characterized with both AP-XPS and low energy electron diffraction. AP-XPS was performed on these surfaces for 2-propanol pressures up to 1 mbar, various 2-propanol/O_2ratios, and a range of temperatures. These studies allowed us to evaluate the chemical states of 2-propanol on the SnO_2(110) surface under a wide range of experimental conditions. The effect of surface preparation, 2-propanol/O_2ratios, and sample temperature was evaluated using AP-XPS and mass spectrometry. Using valence-band spectra, we have found that the surface was reduced from $Sn^{4+}$to $Sn^{2+}$when the sample was heated in 2-propanol and that the main reaction product in the gas phase was acetone. This suggests that the reaction occurs through a mechanism where bridging oxygens are hydroxylated upon adsorption of 2-propanol. These bridging hydroxyl groups can react and result in water desorption. This process leads to the reduction of the SnO_2(110) surface. We have found that the low temperature AP-XPS spectra (300-400 K) was nearly identical for 2-propanol and 2-propanol/O_2mixtures. After running the reactions at higher temperatures we found that the surface remained oxidized. Several oxidation products were also observed in the gas phase. Based on the experimental results we find that the surface was inactive for the oxidation of 2-propanol for temperatures below 500 K. With 2-propanol/O_2mixtures the reactivity increased substantially at lower temperatures. Furthermore, we propose that in 2-propanol/O_2mixtures the reaction occurs through a Mars–van Krevelen mechanism.

9:40am SS+HC+PS-FrM-5 Chemical Speciation and Structural Evolution of Rhodium and Silver Surfaces with High Oxygen Coverages, *Daniel Killelea, M Turano,* Loyola University Chicago*; R Farber, K Gibson, S Sibener,* The University of Chicago*; W Walkosz,* Lake Forest College*; R Rosenberg,* Argonne National Laboratory

Understanding the interaction of oxygen with transition metal surfaces is important in many areas including corrosion and catalysis. Of interest to us is the formation and chemistry of subsurface oxygen (O_{sub}); oxygen atoms dissolved in the near-surface region of catalytically active metals. The goal of these studies is to understand how incorporation of O_{sub}into the selvedge alters the surface structure and chemistry. The oxygen – Ag system, in particular, has been studied extensively both experimentally and theoretically because of its role in two important heterogeneously catalyzed industrial reactions: the epoxidation of ethylene to produce ethylene oxide and the partial oxidation of methanol to produce formaldehyde. In addition, the O/Rh and O/Ag systems serve as models for the dissociative chemisorption of diatomic molecules on close packed metal surfaces. Despite extensive research, there remain questions about the fundamental chemistry of the O/Ag system. Rh is also used in partial oxidation reactions, and its response to adsorbed oxygen provides an interesting complement to Ag. Where Ag extensively reconstructs, Rh does

not. In particular, the structure of the catalytically active surface remains poorly understood under conditions of high oxygen coverages or subsurface oxygen. To improve our understanding of this system, we use ultra-high vacuum (UHV) surface science techniques to characterize Ag and Rh surfaces after exposure to atomic oxygen (AO) to obtain O coverages in excess of 1 ML. AO is generated by thermally cracking molecular O_2. We then use low-energy electron diffraction (LEED) and UHV Scanning Tunneling Microscopy (UHV-STM) to further characterize the various oxygenaceous structures produced, and quantify the amount of oxygen with temperature programmed desorption (TPD). We have found that the surface temperature during deposition is an important factor for the formation of $O_{sub}$and the consequent surface structures. Finally, we have recently found that Rh surfaces are significantly more reactive towards CO oxidation when O_{sub} is present. This enhanced reactivity is located at the interface between the less reactive RhO_2oxide and O-covered metallic Rh. These results reveal the conditions under which $O_{sub}$is formed and stable, and show that O_{sub}also leads to enhanced reactivity of oxidized metal surfaces.

10:00am SS+HC+PS-FrM-6 Molecular Processes on Icy Surfaces in the Interstellar Medium and the Outer Solar System, *Edith Fayolle, R Hodyss, P Johnson,* Jet Propulsion Laboratory, California Institute of Technology*; K Oberg,* Harvard University*; J Fillion, M Bertin,* Sorbonne Université **INVITED**

Molecular ices have been observed in various planetary and astrophysical environments: from patches in permanently shadowed regions on Mercury and the Moon, to the ice crust of outer Solar System bodies, and onto dust grains in prestellar cores, protostellar envelopes, and protoplanetary disks. Interstellar and planetary ices are mostly composed of H_2O, and more volatile molecules, e.g. N_2, CO, CH_4, CO_2, H_2S, SO_2, NH_3, held together as a solid through van Der Waals forces and dipole-dipole interactions, such as hydrogen bonding. They are found as mixtures or pure layers and display crystalline or amorphous structures.

Understanding ice formation, sublimation, and composition is crucial to interpret both gas phase and solid state observations, constrain the physical conditions encountered in space, and test for the likely chemical inheritance from star-forming environments to planetary systems. Vacuum and cryogenic techniques are used to reproduce astrophysical conditions and grow ice analogues. Analytical techniques, including IR- UV-spectroscopy, mass spectrometry, and microgravimetry, are employed to measure fundamental parameters such as desorption, diffusion energies, and reactions products & rates in the solid phase.

In this talk, I will show several examples of astrochemical experiments relevant to icy environments. The fundamental parameters derived from these experiments are further used as inputs for astrochemical models simulating the formation and evolution of ices on various bodies. In some cases, these experiments can directly explain recent observations, for e.g., the unexpected variety of molecules detected in lunar cold traps by the Lunar Crater Observation and Sensing Satellite mission or the location of snowlines in protostellar and protoplanetary environments probed by radio-interferometers like the Atacama Large Millimeter Array.

10:40am SS+HC+PS-FrM-8 Bilayer Silicates as Models for Space-weather-mediated Water-cycling Processes at the Interface of Airless Bodies, *B Dhar, **William E. Kaden**,* University of Central Florida

Following recent observations indicating the presence of water and/or hydroxyl groups inhomogeneously distributed across the surface of the moon, many groups have worked to put forwarded feasible models necessary to rationalize both effects. From those models, there seems to be reasonable agreement that a solar-wind mediated, H^+ implantation-based mechanism is responsible for initial hydration/hydroxylation at the lunar surface. How and why the OH-group concentration varies with both latitude and longitude, however, remains debated in the literature. A recently reported kinetics model provided a plausible temperature-dependent recombinative desorption/dissociative readsorption pathway, which accurately predicts observed systematic trends in the concentration of OH groups as a function of latitude when also accounting for daily oscillations in photon and proton flux vs. latitude over long periods of time. Key to the postulated OH-group migration pathway is the presence of mineral surfaces with atypically low barriers to recombinative water desorption; something that varies with both surface composition/structure and OH group concentration. To account for the effects of the average lunar mineralogical surface composition, the author's simply modeled the moon as a homogenous distribution of simple binary oxides present at concentrations corresponding those associated with each of the corresponding metals.

In the work presented in this this talk, we have used recently developed recipes allowing for the growth of extremely well-defined, atomically-planar, and crystalline silicate sheets to serve as tailor-designed anologues of mineralogically relevant structures containing deliberately varied surface sites expected to be present at the surface of the moon and elsewhere. More specifically, we have grown and fully characterized two bilayer films; one consisting of pure silica (SiO_2) and the other present as a two-dimensional alumino-silicate ($Al_{0.33}Si_{0.67}O_2$). Using temperature programmed desorption, we have then characterized differences in the OH-silicate interactions as a function of one deliberately varied surface-site's coordination, and then link our observations to help provide a more nuanced insight into how and why water may evolve and cycle into and out of the surface of airless bodies in the presence of the solar wind.

11:00am **SS+HC+PS-FrM-9 Unraveling the Evolution of the Solid-Electrolyte Interphase Layer at Li-Metal Anodes**, *Venkateshkumar Prabhakaran, S Roy, G Johnson,* Pacific Northwest National Laboratory, Joint Center for Energy Storage Research*; M Engelhard, V Shutthanandan, A Martinez, S Thevuthasan,* Pacific Northwest National Laboratory*; K Mueller, V Murugesan,* Pacific Northwest National Laboratory, Joint Center for Energy Storage Research

Chemical transformations of electrolyte constituents (such as solvent and solvated electroactive ions) at the Li-metal electrode determine the evolution of the solid-electrolyte interphase (SEI). The ability to rationally design an SEI layer that will provide efficient charge transfer processes will improve the performance of Li-batteries. The main challenge is to unravel the complex set of interfacial reactions that occur during charge transfer processes and subsequently delineate the pathways of various decomposition reactions and phase formation. Herein, we report progress in understanding such complex interfaces using bottom-up assembly of solvated cations and bare anions of selected composition on Li-metal anodes. Soft landing of mass-selected ions, a versatile approach to surface modification, is ideally suited for building the interface with selected electroactive ions which will help unravel the complexity associated with the multitude of interfacial processes occurring during evolution of the SEI layer.[1,2] Ion soft landing combined with operando infrared reflection-absorption spectroscopy (IRRAS) and in-situ x-ray photoelectron spectroscopy (XPS) were used to characterize the decomposition of counter anions and solvent molecules on bare Li metal surfaces. Specifically, we soft-landed isolated electrolyte anions (*e.g.,* bis(trifluoromethane)sulfonimide, $TFSI^-$, polysulfides, S_x^-) and solvated Li solvent cluster cations (e.g. Li-(dimethoxyethane)$_x$) on bare Li metal surfaces without their corresponding counter ions, and monitored their spontaneous decomposition using IRRAS and XPS. Our in-situ multimodal measurements captured the spectroscopic signatures of reaction pathways of the electrolyte anions and solvent molecules on the reactive Li surface. We will discuss the evolution of the SEI layer based on multimodal spectroscopic analysis of electrochemical interfaces prepared using the ion soft landing approach. In particular, the chemical signatures of transient species that evolve during decomposition at well-defined interfaces will be discussed.

References:

1. Johnson, G. E.; Hu, Q.; Laskin, J., Soft landing of complex molecules on surfaces. *Annual Review of Analytical Chemistry* **2011,***4*, 83-104.

2. Prabhakaran, V.; Johnson, G. E.; Wang, B.; Laskin, J., *In situ* solid-state electrochemistry of mass-selected ions at well-defined electrode–electrolyte interfaces. *Proceedings of the National Academy of Sciences* **2016,***113*, 13324-13329.

Thin Films Division
Room A216 - Session TF-FrM

Theory and Characterization of Thin Film Properties

Moderators: Angel Yanguas-Gil, Argonne National Lab, Gerben van Straaten, Eindhoven University of Technology, The Netherlands

8:20am **TF-FrM-1 Incorporation Mechanisms and Electronic Properties of Impurities in Wide-Band-Gap Semiconductors**, *John (Jack) Lyons, S Erwin,* U.S. Naval Research Laboratory **INVITED**

The management of unwanted impurities as well as the controlled introduction of dopant species continue to be challenges in wide-band-gap (WBG) semiconductors such as AlN and Ga_2O_3. In these materials, contaminants such as carbon often incorporate during growth and subsequently act as trapping centers, which can have a detrimental impact on device performance. Moreover, establishing hole conductivity through the introduction of acceptor impurities has proven to be especially difficult in these compounds. In this talk, I will discuss the use of first-principles calculations to understand the incorporation and electronic properties of impurities in WBG semiconductors.

In many growth techniques carbon-containing precursors, such as trimethylaluminum (TMA) for AlN, are often employed. These precursors are thought to be a major source of carbon contamination during growth. Focusing on atomic-layer deposition, we have developed a model to elucidate the decomposition of TMA at the AlN surface, and subsequent incorporation of carbon into the AlN film during growth. We find that the use of H-containing plasma is crucial for scrubbing methyl species from the surface. However, the plasma also leads to atomic carbon, which opens a channel for trapping carbon impurities into the film. In light of this dual role, we propose a solution for minimizing carbon contamination into AlN.

Quantitative determination of the electrical role of particular impurity species present within WBG semiconductors has long been a challenge for theoretical calculations. However, using hybrid density functional theory we are now able to accurately predict the role of impurities such as carbon. We find that carbon acts predominantly as a deep acceptor trap in AlN, as it does for GaN. In contrast, carbon is found to act as a donor species in WBG oxides such as Ga_2O_3. Other potential acceptor dopants, such as magnesium, are also found to act as deep acceptors, due to their propensity to trap localized holes. In fact, no acceptors are found to be effective *p*-type dopants in either Ga_2O_3 or AlN. However, acceptor dopants are still found to be useful for producing semi-insulating material.

9:00am **TF-FrM-3 Review and Demonstration of Feature Scale Simulations**, *Paul Moroz,* TEL Technology Center, America, LLC

Feature-scale simulations (FSS) represent an important tool for modeling of etching, deposition, and implantation processes routinely applied during semiconductor materials processing and device fabrication. Traditionally, FSS uses a combination of Monte Carlo methods with special algorithms for modeling gaseous and solid (in volume and at the surface) species, as well as algorithms for advancing feature profiles and materials composition as a result of reactive interactions of incoming species with solid materials. The mentioned FSS approach, at least at present time, seems to be the only feasible approach to simulate materials processing at the feature-scale level ranging from tens of nanometers to tens of micrometers, while applications of such advanced methods as quantum chemistry or molecular dynamics are still too expensive computationally in spite of highly efficient code parallelization to run on multi-processor computers. Phenomenological description of reactions (chemical and physical) represents a weakness of FSS, as it is very difficult to implement proper sets of reactions valid at different conditions. Here, we discuss an approach used in the FPS3D code [1-5], for simulation of etching, deposition, and implantation with the present focus given to simulation of ALD/CVD processes. Examples include such difficult topics as HAR etching, as well as CVD and ALD. For ALD examples we consider silicon nitride deposition [5] for different chemistries, some of them allowing deposition of a single monolayer per cycle, while others allowing only a fraction of a monolayer to be deposited per cycle.

References:

[1] P. Moroz, IEEE Trans. on Plasma Science, 39 2804 (2011).

[2] P. Moroz, D. J. Moroz, ECS Transactions, 50 61 (2013).

[3] P. Moroz, D. J. Moroz, J. Physics: CS 550 012030 (2014).

[4] P. Moroz, 15th Int. Conf. on Atomic Layer Deposition, Portland, OR (2015).

[5] P. Moroz, D. J. Moroz, Japan. J. Appl. Phys. **56**, 06HE07 (2017).

9:20am **TF-FrM-4 Process Optimization in Atomic Layer Deposition Using Machine Learning**, *A Yanguas-Gil, S Letourneau, A Mane, Noah Paulson, A Lancaster, J Elam,* Argonne National Laboratory

Process development and process optimization are ubiquitous, resource-intensive tasks in thin film research and development. The goal of these activities is to find the set of process parameters (e.g. temperature, pressure, and flow) that maximize film quality at minimal cost. Typically, this is accomplished by coating a substrate (e.g. a silicon wafer) under a given set of conditions, measuring the film properties ex situ, and adjusting the conditions to improve the film quality. This activity can consume significant time and resources, especially if an additional goal is to achieve uniform films across a large substrate. Process development can be accelerated and economized using in situ measurements. For instance,

quartz crystal microbalance (QCM) measurements can be employed to monitor film thickness in real time as the deposition conditions are varied. However, this still requires the careful attention of a skilled operator to make informed choices based on experience and intuition. An alternative strategy is to use machine learning (ML) to analyze the QCM data and adjust the growth conditions based on an algorithm. To explore this possibility, we used ML to optimize the atomic layer deposition (ALD) of Al_2O_3 with trimethyl aluminum (TMA) and H_2O in a viscous-flow tubular reactor using in situ QCM measurements. We initially developed the ML code using simulated QCM data generated by a 1-D model of ALD transport and reaction. This allowed us to tailor the algorithm to ensure saturation of the TMA and H_2O ALD reactions and to converge efficiently on the optimal dose and purge times. An additional benefit of these simulations was that we could explore the effects of non-ideal behavior such as a CVD component to the surface reactions and strong interaction between the reaction products and the surface. Next, we interfaced the ML code to our ALD system and allowed the algorithm to optimize the TMA and H_2O timings. We observed rapid convergence, as predicted by our simulations, and found that the ML algorithm was capable of adapting to large variations in the initial conditions such as the precursor partial pressures and the carrier gas flow rate. We are now building an array of QCM sensors to measure the thickness simultaneously at 10 locations along our flow tube, and we hope to report on ML opimization of thickness and uniformity using this array.

9:40am TF-FrM-5 Electroless Deposition of Cobalt Metal on a Palladium Layer on an Amine-modified Surface, *A Ng, Anthony Muscat,* University of Arizona

Solution-deposited palladium on amine-terminated self-assembled monolayers (SAMs) is a well-characterized catalyst and adhesion layer combination for solution-based electroless metallization of dielectric films. A reducing agent is typically added to the deposition bath or a sensitizer such as tin is co-deposited producing relatively thick Pd layers. Thinner Pd deposits would enable barrier seed layers for filling < 10 nm wide gaps in patterned dielectric films with metal. In this work, we eliminated the reducing agent from the deposition bath and worked at pH < 2 to deposit monomeric Pd(2+) species and show that the amine groups terminating the SAM reduce Pd(2+) to Pd(0). The amount of Pd deposited depended on the coverage of the two types of amines on the SAM. The adsorption of $PdCl_4^{2-}$ ions in solution on protonated amine groups ($-NH_3^+$) is well known. Our data suggest that the nonprotonated amine groups ($-NH_2$), which coexist with $-NH_3^+$, chemically reduce the Pd(2+) ion to Pd metal by oxidizing to the amine radical cation ($-NH_2\bullet^+$). Pd bonds to and covers the $-NH_2\bullet^+$groups in the process depositing around a monolayer of Pd from solution on the SAM-covered silicon oxide surface. The Pd layer served as a catalyst for solution deposition of cobalt films on the surface using a reducing agent under oxygen-free conditions. The cobalt deposited initially as islands that grew together into a closed film with good adhesion.

10:00am TF-FrM-6 The Origins of Condensation-Driven Degradation of Hydrophobic Thin Films, *Jingcheng Ma, N Miljkovic,* University of Illinois at Urbana-Champaign

Dropwise condensation of steam on metallic surfaces coated with thin (~ 1μm) functional hydrophobic films has the potential to achieve remarkable heat transfer coefficients approaching ~100 kW/m²K. However, the long-term durability of these thin films has limited the application of functional coatings for the past century. Although degradation due to steam condensation has been qualitatively described as 'blistering', no satisfactory insight exists capable of answering two key questions: what is the mechanism of water vapor mass transfer, and what is the driving force for film delamination. Hence, scientists have been forced to abandon rational thin film development in favor of ad-hoc trial-and-error approaches. Here, we demonstrate that pinholes on hydrophobic coatings are the source of blisters so commonly seen during degradation. By creating shape-controlled pinhole-blister structures in thin deposited films, we show that blisters form in a spatially-controlled order during water vapor condensation from the ambient. The shape, initiation, and growth of the blisters was systematically investigated. Our experiments demonstrate that water vapor is mainly transferred to the blister through spatially-random pinholes which exist in the film after deposition, and the driving force for film delamination is capillary force. Based on the new insights developed here, we propose a non-dimensional pressure to determine the threshold when blistering will be initiated by a pinhole, or when discrete droplets grow up and above pinholes. To the best of our knowledge, our work represents the first quantitative description of blistering initiation. The techniques and insights presented here will inform future work on

polymeric thin films to enable their rational and durable design for a variety of applications.

10:20am TF-FrM-7 Structural and Electrical Properties of Sputtered HEA Thin Films of CrFeCoNiCu and their Oxidation Studies, *Jeyanthinath Mayandi,* SMN, Department of Physics,University of Oslo, Norway; *M Stange, E Sagvolden, M Sunding, Ø Dahl,* SINTEF Materials and Chemistry, Norway; *M Schrade,* SINTEF, Materials and Chemistry, Norway; *J Deuermeier, E Fortunato,* Universidade Nova de Lisboa, Portugal; *O Løvvik, S Diplas,* SINTEF Materials and Chemistry, Norway and University of Oslo, Norway; *P Carvalho,* SINTEF Materials and Chemistry, Norway and Universidade de Lisboa, Portugal; *T Finstad,* SMN, Department of Physics, University of Oslo, Norway

High-entropy alloys (HEAs) represent a class of materials that is intensively investigated for a range of possible applications. They generally show a high degree of phase stability by the high entropy while the structure is a random atom position disorder unlike other alloys which can influence physical properties differently than regular alloys. In general, there are few studies on oxidation of HEA and studies on adding oxygen during the fabrication of HEA. In this study we have sputtered thin films of CrFeCoNiCu onto insulating and optically transparent substrates in order to measure structural, electrical and optical functional properties. We have varied the oxygen pressure in the sputtering environment as well as oxidizing the samples at elevated temperatures after deposition. Optical and electrical characterization was performed on films sputter deposited on fused quartz wafers. The films were characterized by TEM, XRD and XPS. The films with no intentional oxygen had an FCC structure with a texture showing strong (111) preferred orientation as seen by XRD. TEM analysis showed columnar morphology with twins parallel to (111) planes. Samples sputtered under high oxygen content showed a simple NaCl structure(FeO). The samples were annealed in air and O_2 ambient in the temperature range of 300 to 500 °C. This caused an oxide layer growing on top of the FCC structure. XPS was utilized to find the atomic compositions and chemical stated of the elements. Hall measurements and Seebeck measurements were performed on the as prepared and oxidized films from 10 K to 600K. For the FCC structure the resistivity was a factor 10^4 higher than the elemental metals while can be satisfactory described by electron phonon scattering by the Bloch-Grüneisen description and the low temperature negative temperature effect by the Kondo effect. The sign of the Hall coefficient was positive while the Seebeck coefficient was negative, indicating the Fermi surface containing pockets of electrons and holes and an energy dependent scattering time. A detailed comparison of the as prepared and the oxidized thin films will be discussed in terms of the structural chemical and electrical properties of the grown films. In addition the electric properties will be discussed in terms of a model considering electronic structure and scattering.

10:40am TF-FrM-8 Observation of Topological Hall and Curie Temperature above Room Temperature in Strain-engineered FeGe Thin Films, *Adam Hauser, S Budhathoki, K Law, S Ranjit, A Sapkota,* The University of Alabama; *A Thind, R Mishra,* Washington University in St. Louis; *D Heiman,* Northeastern University; *M Jamer,* United States Naval Acadamy; *A Borisevich,* Oak Ridge National Laboratory; *T Mewes,* The University of Alabama; *J Gallagher,* U.S. Naval Research Laboratory

The need to control and manipulate magnetic spin in nonvolatile memory applications drives exploration of new magnetic materials with non-uniformly ordered magnetic phases. Of particular interest are materials with inversion asymmetry, most commonly found in non-centrosymmetric space groups. Our group has successfully grown epitaxial B20 FeGe films with 4% tensile strain on a Ge(111) substrate by Sputter Beam Epitaxy, an off-axis magnetron sputtering technique in which beam-shaping, shutter control, and QCM-guided flux control of off-axis, direct-current (DC) magnetron sputter sources are employed upon high-purity elemental Fe and Ge targets in ultra-high vacuum. QCM control is modified to relative atomic ratios, and film compositions are confirmed by energy dispersive x-ray spectroscopy (EDS) and Rutherford Backscattering (RBS). X-ray diffractometry has confirmed that the films are single-crystal and phase pure, with near-substrate-limited rocking curve (FWHM 0.07º) and strong Keissig fringes in x-ray reflectometry. We find no evidence of strain relaxation up to 110nm, and off-axis XRD and HAADF STEM confirm the B20 phase necessary for the Skyrmionic phase. A strain-enhanced T_C = 350K by SQUID magnetometry and a clear Topological Hall effect (THE) signature observed at 330K suggest potential for Skyrmionic behavior at or above room temperature in a single layer thin film. Direct observation is required for confirmation of a Skyrmion lattice phase.

11:00am TF-FrM-9 Infrared Absorption Oscillator Strength Factors in SiNx Thin Films, *Sara DiGregorio, S Habermehl,* Sandia National Laboratories

The oscillator strength factor of the Si-N asymmetric stretch mode of SiN films was studied for films of varying composition and thickness. Thin films were deposited by low pressure chemical vapor deposition at 850°C from mixtures of dichlorosilane and ammonia. The oscillator strength factor for each film was determined from Fourier Transform infrared spectroscopy and ellipsometric measurements. We found that the oscillator strength factor systematically decreases with increasing silicon volume fraction from 2.10×10 cm to 1.44×10 cm for compositions ranging from 0% to 25% volume fraction amorphous silicon. We believe this trend is related to charge transfer induced structural changes in the basal SiN_x tetrahedron as the volume fraction of amorphous silicon increases. For stoichiometric silicon nitride the oscillator strength factor was found to be $2.01 \times 10^{19} \pm 7.25 \times 10^{17}$ cm^{-2}, which is consistent with a reported value of 2.07×10^{19} cm^{-2} and a theoretical value of 1.99×10^{19} cm^{-2}. Additionally, in the composition range investigated, we found that the oscillator strength values agree favorably with trends observed in films deposited by plasma enhanced chemical vapor deposition. This work was selected as the best graduate student presentation at the 2019 NMAVS symposium (Albuquerque-June2019).

11:20am TF-FrM-10 Computer Aided Molecular Design of novel precursor materials for Atomic Layer Deposition, *Mina Shahmohammadi,* University of Illinois at Chicago; *R Mukherjee,* Vishwamitra Research Institute; *C Takoudis,* University of Illinois at Chicago; *U Diwekar,* Vishwamitra Research Institute

Atomic Layer Deposition (ALD) is a vapor phase technique to deposit thin films of various metals and metal oxides on a substrate. Due to sequential and self-limiting reactions, conformal and pinhole-free thin films can be produced which have widespread applications. In this process, a precursor, which is often a metal surrounded by organic functional groups, chemisorbs on the substrate and part of the molecule subsequently desorbs from the surface after completion of the reaction. Precursor chemisorption on the substrate leads to a self-limiting process and it eventually results in films with desired thickness at the Ångström length scale. To design and conduct an ALD experiment, the precursor(s) should be chosen based on the ALD conditions (i.e., bubbler and reactor temperatures, pressure, gas flow, etc.) and likely applications of the final film. It is practically impossible to carry out a huge number of ALD experiments using numerous precursors and deposition conditions in order to find the optimum one depending on the applications of interest. In addition, only existing precursors can be tested experimentally. This study focuses on developing a computational tool for the design of novel precursor materials with enhanced properties for the ALD of metal oxides and metals.

Computer-Aided Molecular Design (CAMD) is a methodology where materials with optimal desired properties are generated from the combination of functional groups. This approach is the reverse of Group Contribution Method (GCM) in which the thermodynamic properties of a compound are estimated from the structural and functional groups comprising the molecule. For CAMD, we need the properties of the functional groups. In our previous work, we have redeveloped a new GCM for ALD effectively to predict the growth rate curve using Adsorbate Solid Solution Theory (ASST). In this work, novel precursor molecules for ALD are generated using properties of the functional groups. In order to do that, we will be using a combinatorial optimization method called Efficient Ant Colony Optimization (EACO). This is the first time CAMD is being applied to design precursor materials for ALD. In the future, novel designed precursors will be synthesized and their properties will be tested experimentally using a Kurt J. Lesker ALD150LE™ system. Characterization of the deposited films with designed precursors will validate the proposed simulation technique and help us to optimize materials in the best possible way.

11:40am TF-FrM-11 The Use of Molecular Oxygen for a Low Cost and Low Temperature ALD of Amorphous Titania, *Harshdeep S. Bhatia, C Takoudis,* University of Illinois at Chicago

The interest in Titania films has been increasing in the past few decades. This increase can be attributed to the various applications of ultrathin films of Titanium dioxide. The thin film deposition of Amorphous Titania can be performed using a low temperature precursor, Tetrakis(dimethylamido) Titanium (TDMAT) along with the use of ozone however with oxygen, comparable growth rates have only been reported at temperatures greater than 150 C. For use with organic substrates, it is important that the reaction is performed at low temperatures to prevent denaturation and degradation. The use of Ozone has also been reported to cause degradation in some polymers, mainly elastomers. Ozone cracking, along with the high cost of manufacturing a high concentration of ozone, does not make ozone the most suitable choice and could easily be replaced by using pure molecular oxygen. In this study, growth temperatures below 160 C were used to uniformly deposit amorphous Titania using TDMAT and oxygen. The as-deposited films were characterized using Spectroscopic Ellipsometry (SE), X-ray Photoelectron Spectroscopy (XPS). The application of this reaction could lead to low temperature deposition of Titanium oxide on organic substrates for the use in biomedical implants as a protective coating, seed layer to deposit other conductive metals on organic substrates. One of the most interesting phenomena observed using SE was the appearance of a very small but non-zero extinction coefficient in the visible range. This extinction coefficient was similar to Urbach tail absorption usually observed in the UV range. This also points towards slight absorption of Visible light by the deposited Titania films which opens new avenues for research in photocatalytic activity of Titania films within visible light spectrum.

12:00pm TF-FrM-12 Ultra-High Purity Process Capability for High-Performance Atomic layer Deposition, *Noel O'Toole, G Rayner, Jr.,* Kurt J. Lesker Company; *N Strnad,* General Technical Services, LLC; *D Potrepka,* U.S. Army Research Laboratory

Ultra-high purity (UHP) process capability is motivated by the need to produce superior, high-quality thin films and interfaces by atomic layer deposition (ALD) techniques. In particular, UHP equipment design reduces background impurity levels, including oxygen, to limit incorporation during film growth. Creating and maintaining a UHP process environment are also essential for ALD process reproducibility. This presentation will address the potential sources of background contamination, as well as system design requirements to obtain a controlled UHP process environment. Results will be presented that demonstrate the effectiveness of this technology to obtain high-quality titanium nitride thin films by plasma-enhanced ALD (PEALD) techniques.

Author Index

Bold page numbers indicate presenter

Author Index

Bang, L: HC+OX+SS-WeA-2, 151
Bangasi, G: TF1-WeM-5, 139
Banks, H: QS+2D+EM+MN+NS-TuA-7, 95
Banks, S: TF-ThP-14, **234**
Banks, T: BI+AS+NS-MoM-8, 10
Banniard, L: MN-MoM-10, 13
Bansah, C: TF-ThP-16, **234**
Bao, L: VT-TuP-8, 115
Baraldi, A: 2D+AS+MI+NS-TuM-10, 51
Barbacci, D: HI+AS+CA-WeA-12, 153
Barboun, P: PS-TuP-4, 108
Barlaz, D: PS1+SE-MoM-6, 15; PS-TuM-2, 66;
  PS-TuP-13, 110; SE+PS-ThM-12, 189;
  SE+PS-ThM-4, 188
Barletta, F: PS1+SE-MoM-1, 14
Barmak, K: EM+AP+MS+NS+TF-ThM-6, 177
Barnes, E: TF+EM+NS+SS-ThM-11, 193
Barnes, J: RA+AS+BI-WeA-12, 160
Barnola, S: PS+AS+EM+SS+TF-MoA-1, 35;
  PS+EM-TuM-3, 64
Barral, M: 2D+AS+MI+NS-WeM-13, 118
Barraza-Lopez, S: 2D+EM+MI+MN+NS+QS-
  TuM-6, 53
Bartels, D: PS1-MoA-3, 37; PS-TuP-6, 108
Barton, D: EL-ThA-11, 202
Basaldua, I: TF+EM+MI-TuM-6, 73
Basher, A: AP+PS+TF-ThM-5, **169**
Basiuk, E: AS-ThP-9, 220
Basiuk, V: AS-ThP-9, 220
Basker, V: TF+EM+MI-TuM-11, 74
Bassett, W: LS-ThP-2, 227
Bassiri-Gharb, N: TF+EM+MI+MN+OX+PS-
  MoM-8, **20**
Bastea, S: LS-ThP-2, 227
Basu, P: PS+EM-TuM-11, 65
Batista, E: AC+AS+LS-TuM-5, 54
Batra, A: TF-ThP-11, 233
Batzill, M: 2D+EM+MI+NS-TuA-11, 80;
  HC+SS-FrM-7, **241**
Bauer, E: AC+LS+MI-MoM-9, 5
Baumbach, R: AC+LS+MI-MoM-1, **4**
Baumgartner, Y: TF+EM+MI-TuM-1, 72
Baumler, S: SS-TuP-9, 112
Beach, G: TF+EM+MI+MN+OX+PS-MoM-5,
  20
Bechtel, H: 2D+AS+MI+NS-TuM-1, 50
Beckmann, K: EM+2D+AP+NS+PS-TuM-3, 60;
  MS+EM+QS-ThM-3, 183; MS-ThP-5, 229;
  TF-TuA-11, 99
Beebe Jr, T: RA+AS+BI-WeA-3, **159**
Béjanin, J: QS+EM+MN+NS+VT-MoA-1, 38
belahcen, S: AP+EL+MS+PS+SS+TF-TuA-9, 82;
  TF+2D+AP+EL+SS-MoA-4, 43
Belianinov, A: HI+AS+CA-WeA-3, 152;
  NS+2D+QS-ThM-11, **185**; NS-ThP-5, 231
Bell, K: TF-ThP-14, 234
Bell, T: QS-TuM-5, 68
Bellissimo, A: 2D+AS+MI+NS-TuM-2, **50**
Belyansky, M: TF+EM+MI-TuM-11, 74
Ben Hadj Mabrouk, A: AS-ThM-6, **171**
Ben Sedrine, N: EM+OX+TF-TuA-9, 87
Bender, T: VT-TuM-4, 76
Bendikov, T: LS+AC+HC+SS-ThA-7, **206**
Benjamin, A: QS+2D+EM+MN+NS-TuA-2, 94
Bennett, R: MI+2D+AS+EM-ThM-6, 183; MI-
  ThP-1, 227
Bennett, S: MS+EM+QS-ThM-3, 183
Benoit, D: AS+BI+RA-TuM-13, 57
Benotmane, K: PS+EM-TuM-3, 64
Bent, S: 2D-FrM-8, 237; TF1-WeM-11, 140
Bera, K: PS2-MoM-5, 17; PS-TuM-6, 67
Berggren, K: HI+NS-ThM-5, 179
Berghuis, W: TF+EM+MI-TuM-10, **74**
Bergmann, F: QS+2D+EM+MN+NS+VT-WeM-
  5, 137

Bergsman, D: TF-TuA-12, **99**
Berkes, B: DM2+BI+SS-ThA-10, **201**
Berkley, R: MI-ThP-5, **228**
Bernard, M: TF+EM-WeA-7, 165
Bernholc, J: NS+2D+AS-WeA-7, 157;
  NS+2D+QS-ThM-10, 185
Berrospe Rodriguez, C: PS+EM-WeM-4, 135
Berrospe, C: PS-ThM-4, 187
Bertin, M: SS+HC+PS-FrM-6, 247
Bertolini, G: 2D+AS+MI+NS-TuM-2, 50
Bertoni, M: EM+2D+NS+TF-WeA-1, **149**
Bertram, F: TF+PS-TuA-1, 96
Beton, P: 2D+AS+BI+HC+MN+NS+PS+SS+TL-
  ThA-3, 195; SS-TuP-7, 112
Beverstock, D: VT-MoA-6, **48**
Beyer, A: HI+AS+CA-WeA-11, 153; HI+NS-
  ThM-6, **179**
Beyer, C: BI-TuP-3, **105**
Bhandari, G: MI+2D-WeA-12, 155; MI+2D-
  WeA-7, 155
Bhatia, H: TF-FrM-11, **250**
Bhattacharya, A: OX+EM+MI+SS-WeM-2,
  133
Bhattacharya, S: PS+EM-WeM-5, **135**
Bi, S: TF-ThP-20, 235
Bianchi, M: 2D+AS+MI+NS-TuM-10, 51
Bieberle-Hütter, A: EM+2D+NS+TF-WeA-12,
  150
Bielefeld, J: EM-ThP-6, 222; PS+2D+SE+TF-
  FrM-6, 244; SE-ThP-2, 231
Bielejec, E: QS+2D+EM+MN+NS+VT-WeM-
  12, 137; QS+2D+EM+MN+NS-TuA-7, 95
Biere, N: NS+2D+AS-WeA-12, **157**
Bignardi, L: 2D+AP+EM+MI+MN+NS+PS+TF-
  MoA-3, 26; 2D+AS+MI+NS-TuM-10, 51
Bilgilisoy, E: AP+BI+PS+TF-WeM-13, 122
Bilich, D: AS-ThM-4, 171
Bilotto, P: DM+BI+SS-ThM-13, 176
Binek, C: OX+EM+HC+MI+NS+SS+TF-TuA-1,
  91
Biolsi, P: PS+2D+EM+SS+TF-ThA-1, **208**;
  PS+2D+EM+SS+TF-ThA-4, 209; PS+EM-TuA-
  1, 92; PS+EM-TuA-3, 93; PS+EM-TuA-4, 93;
  PS+EM-TuM-5, 65; PS-TuP-10, 109
Bird, L: BP-SuA-3, 1
Birmingham, B: NS-WeM-3, 131
Bisag, A: PS1+SE-MoM-1, 14
Bischoff, L: HI+NS-ThA-9, 205; NS+2D+QS-
  ThM-2, 184
Bittrich, E: EL+AS+EM+TF-WeM-11, **126**
Biyikli, N: EM+OX+TF-TuA-8, **87**;
  PS+2D+SE+TF-FrM-11, 245
Blades, W: SS+AS+HC+OX-WeA-10, **163**
Blain, M: MN+QS-TuA-11, **89**
Blair, R: HC+SS-FrM-9, 241
Blanchard, P: AS+BI+RA-TuM-10, 56
Blenkinsopp, P: HI+NS-ThA-4, 204
Bligaard, T: HC+SS-MoM-8, 12; HC+SS-MoM-
  9, 12
Blob, A: MI+2D-WeM-1, 130
Blomfield, C: 2D+AS+MI+NS-TuM-12, 51;
  AS+BI+RA-MoM-10, 9; AS+BI+RA-MoM-9,
  8; AS+BI+RA-TuM-11, 57; EW-TuL-6, **78**
Bluhm, H: AS-ThP-10, 220; CA+NS+SS+VT-
  WeA-3, **146**; LS+HC+SS-ThM-10, 181;
  SS+AS+HC+TL-ThM-4, 190
Blumenschein, N: EL+EM-WeA-7, 148
Bobba, F: NS-TuA-10, 90
Bocquet, M: 2D-TuP-4, 103
Boeder, P: VT-MoA-11, 49
Bogan, J: TF+AS+EL+PS+RA-ThA-4, 215
Bohamud, T: TF+SS-ThA-3, 216
Boiteau, R: AS-ThP-6, 219; BI+AS-WeM-11,
  123
Bol, A: 2D+AP+EM+MI+NS+PS+TF-MoA-5, 28

Boldman, W: TF-ThP-20, 235
Bonova, L: PS-TuP-13, 110
Bónová, L: PS1+SE-MoM-6, 15
Bonvalot, M: AP+EL+MS+PS+SS+TF-TuA-9,
  82; TF+2D+AP+EL+SS-MoA-4, **43**
Booth, C: AC+AS+LS-TuM-11, 55; AC+AS+LS-
  TuM-5, 54; AC+LS+MI-MoM-9, 5
Borchers, J: TF+EM+MI+MN+OX+PS-MoM-3,
  19
Boreman, G: EL+AS+EM+TF-WeM-13, 126
Boris, D: PS1+SE-MoM-9, 16; PS-TuP-11, 109;
  SE+PS-ThM-10, **189**
Borisevich, A: TF-FrM-8, 249
Borman, T: TF+SE-MoA-5, **46**
Bormashenko, E: SS-TuP-10, 112
Borodinov, N: BI+AS-TuM-4, 58
Borst, C: MS+EM+QS-ThM-3, 183
Bose, R: TF+SS-ThA-10, **217**
Bouchiat, V: 2D+EM+MN+NS-WeA-8, 143
Bourgeois, G: TF+EM-WeA-7, **165**
Bournel, F: TF+2D+AP+EL+SS-MoA-8, 44
Bousser, E: SE-ThA-8, 212
Bouyer, P: QS-TuM-1, **67**
Bowden, M: OX+EM+MI+SS-WeM-1, 132;
  OX+EM+MI+SS-WeM-13, 134
Boyd, K: SS+AS+HC+TL-ThM-11, 191
Boyle, D: SS-TuP-18, 114
Bozkurt, A: MN-TuP-1, 106
Bracher, D: QS+2D+EM+MN+NS-TuA-8, 95
Brandon, J: PS-TuM-1, 66
Brandt, A: HC+OX+SS-WeA-9, 152
Brann, M: SS+2D+AP+AS+OX+SE-ThA-1, 213
Braun, A: AC+AS+LS-TuM-5, 54
Braun, J: MI+2D-WeM-1, 130
Braun, K: 2D+AS+MI+NS-WeM-12, 118
Braun, P: AS-ThA-10, **198**
Brédas, J: 2D+AS+MI+NS-WeM-10, 118
Bregliozzi, G: VT-TuM-1, **76**
Brehm, J: TF+EM+MI+MN+OX+PS-MoM-10,
  21
Brena, B: TF+2D+AP+EL+SS-MoA-8, 44
Brenac, A: MN-MoM-10, 13
Brenner, M: 2D+EM+MI+MN+NS+QS-TuM-5,
  52
Brenning, N: TF+SE-MoA-1, 45
Breslin, V: NS-WeM-4, **131**
Brill, G: EL-ThA-9, 201
Brillson, L: 2D+EM+MI+MN+NS+QS-TuM-5,
  52; 2D+EM+MI+NS+QS+SS-ThM-10, 167;
  EM+2D+AS+MI+MN+NS+TF-WeM-2, 126;
  EM+2D+AS+MI+MN+NS+TF-WeM-4, 127;
  EM+OX+TF-TuA-7, 87; TF-MoM-5, 22; VT-
  TuA-11, **101**
Brockman, J: EM-ThP-2, 222
Brocks, G: EM+2D+NS+TF-WeA-12, 150
Broderick, A: CA+NS+SS+VT-WeA-8, 147
Broitman, E: SE-ThA-3, **212**
Brongersma, H: AS+BI+RA-TuM-6, **56**
Brooks, C: MI+2D-WeM-3, 130
Bröskamp, S: BI+AS-TuA-10, **86**
Brostow, W: 2D+EM+MI+NS-MoM-3, 2
Brounstein, Z: AC-MoA-6, **30**
Brown, I: HI+NS-ThA-4, 204
Brown, K: NS-ThA-7, **207**
Brown, P: 2D+AS+BI+HC+MN+NS+PS+SS+TL-
  ThA-2, **195**
Brown, R: SS+HC-MoA-10, 43; SS-TuP-11,
  112
Bruchhaus, L: HI+NS-ThA-9, 205; NS+2D+QS-
  ThM-2, 184
Brückner, C: 2D-TuP-7, 104
Bruhwiler, D: VT-MoA-3, 48
Bruma, A: NS+AS-FrM-3, 242
Brundle, C: AS+BI+RA-MoM-1, **7**

Author Index

Author Index

Author Index

Author Index

Author Index

Author Index

Author Index

Author Index

Author Index

Author Index

Author Index

Author Index

Author Index

Author Index

Author Index

Yuk, S: SS+HC-MoA-3, 42
Yun, Y: EM-ThP-1, 222
Yusof, A: EM-ThP-19, 224

— Z —

Zabeida, O: SE-ThA-8, 212
Zaccarine, S: AS-ThA-9, **197**; RA+AS+CA+PS+TF-WeM-11, 138
Zade, V: SE+AS+TF-WeA-1, 160
Zaera, F: HC+2D+SS-WeM-3, **128**
Zaid, H: SE-ThA-6, 212; TF+PS-TuA-2, 96
Zakel, J: AS-ThP-13, 220
Zapien, J: AC-MoA-9, 31
Zauscher, S: BI+AS+NS-MoM-1, 9; BI+AS+NS-MoM-6, **10**
Zborowski, C: RA+AS+BI-WeA-2, 159
Zeller, P: CA+2D+AS+BI+NS-ThM-4, 173; CA+NS+SS+VT-ThA-9, 199
Zellers, E: MN-MoA-3, **34**
Zeng, L: 2D-FrM-8, 237; TF1-WeM-11, 140
Zepeda, T: 2D+AS+MI+NS-TuM-13, 52
Zhai, D: 2D+EM+MI+MN+NS+QS-TuM-3, 52
Zhan, C: MN-MoA-3, 34
Zhang, B: TF1-WeM-13, 140
Zhang, C: SS+HC-MoA-5, 42; TF+EM+MI+MN+OX+PS-MoM-11, 21; TF-ThP-20, **235**
Zhang, D: PS+2D+EM+SS+TF-ThA-4, 209; PS+EM-TuA-4, 93
Zhang, H: 2D+EM+MI+MN+NS+QS-TuM-10, **53**; 2D+EM+MI+MN+NS+QS-TuM-11, 53; 2D+EM+MI+MN+NS+QS-WeM-6, 119
Zhang, K: OX+EM+HC+MI+NS+SS+TF-TuA-9, **92**
Zhang, L: EM+PS+TF-MoA-6, 33; PS-ThM-10, 187; PS-ThM-3, **186**
Zhang, Q: NS-ThP-4, **231**; SS+HC-MoA-3, 42

Zhang, S: EL+EM-WeA-3, **148**; QS-TuM-5, 68
Zhang, W: 2D+AP+EM+MI+NS+PS+TF-MoA-3, 28
Zhang, X: AC+AS+LS-TuM-5, 54; QS+2D+EM+MN+NS-TuA-8, 95; SE+AS+SS-FrM-7, 246; TF+EM+MI-TuM-13, 74; TF-ThP-31, 236
Zhang, Y: 2D+AS+MI+NS-WeM-12, 118; AS+BI+CA+LS-TuA-11, **84**; BI+AS-TuM-3, **58**; CA+NS+SS+VT-WeA-8, 147; DM1+BI+SS-ThA-4, 200; EL+EM-WeA-7, 148; NS+2D+QS-ThM-12, 185; NS-TuA-10, 90; SE+AS+SS-FrM-4, 245; TF+EM-WeA-2, 165; TF-ThP-31, **236**
Zhang, Z: AP+2D+EM+PS+TF-MoM-2, 5; EM+2D+AS+MI+MN+NS+TF-WeM-1, 126; HC+OX+SS-WeA-1, 151; NS-WeM-3, **131**; TF+2D+AP+EL+SS-MoA-5, **44**
Zhao, B: TF+EM-WeA-12, 166
Zhao, H: EM+OX+TF-TuA-7, 87; TF+EM-WeA-1, 164; TF-ThP-19, 234
Zhao, J: PS-ThM-1, **186**
Zhao, R: QS+EM+MN+NS+VT-MoA-10, 40; QS+EM+MN+NS-MoM-10, **19**
Zhao, S: BI+AS+NS-MoM-6, 10
Zhao, W: TF-ThP-20, 235
Zhao, Y: EM+2D+NS+TF-WeA-12, **150**; TF-MoM-10, **23**
Zheng, B: PS-TuP-17, **110**
Zheng, L: MI+2D+AS+EM-ThM-12, 183
Zheng, Y: TF+SS-ThA-10, 217
Zhitenev, N: HI+NS-ThA-3, 204
Zhou, C: AS-ThM-1, 170; EM+OX+TF-TuA-9, 87; EM-ThP-10, 223; NS+2D+QS-ThM-6, 185
Zhou, G: NS+AS-FrM-9, 243

Zhou, T: 2D+AP+EM+MI+MN+NS+PS+TF-MoA-5, 26
Zhou, X: SS+AS+HC+TL-ThM-10, 191
Zhou, Y: HI+NS-ThA-10, 205; PS-TuM-10, 67
Zhu, M: 2D+EM+MI+MN+NS+QS-TuM-5, 52; MS+EM+QS-ThM-3, 183; TF+EM-WeA-1, 164; TF-ThP-19, 234
Zhu, T: 2D+EM+MI+MN+NS+QS-TuM-5, **52**; 2D+EM+MI+NS+QS+SS-ThM-10, 167
Zhu, W: NS+AS-FrM-9, 243
Zhu, X: EM-ThP-10, 223
Zhu, Z: AS+BI+CA+LS-TuA-11, 84; AS+BI+CA+LS-TuA-4, 83; AS-ThM-11, 172; BI-TuP-5, **106**; CA+AS+NS+SE+SS-FrM-8, 239
Zieve, R: AC+LS+MI-MoM-5, **4**
Zimbardi, F: TF+EM+NS+SS-ThM-4, 192
Zimmermann, R: BI+AS-TuM-6, 59; BI-TuP-7, 106
Zizka, J: EM+AP+MS+NS+TF-ThM-12, **177**
Zollner, S: EL+EM-WeA-1, 147; EL+EM-WeA-10, 149; EL+EM-WeA-12, **149**
Zorman, C: MN-TuM-13, 64; MN-TuM-3, **62**
Zou, K: EM-ThP-10, 223
Zou, Q: 2D+EM+MI+MN+NS+QS-TuM-11, **53**; MI+2D-WeM-2, 130; SS-TuP-20, 114
Zucker, M: VT-MoA-8, 49
Zugic, B: SS+AS+HC+OX-WeA-11, 164
Zurbuchen, M: MI+2D-WeA-10, 154
Zutic, I: 2D+AP+EM+MI+MN+NS+PS+TF-MoA-5, 26
Zwicknagl, G: AC+LS+MI-MoM-8, **4**